V 1

PREDICTION OF IN SITU CONSOLIDATION PARAMETERS OF BOSTON BLUE CLAY

by

IMAD BOTROS GHANTOUS

B.Sc., University of London, King's College
London, England (1979)

SUBMITTED IN PARTIAL FULFILLMENT
OF THE REQUIREMENTS FOR THE
DEGREES OF

MASTER OF SCIENCE

and

CIVIL ENGINEER

at the

MASSACHUSETTS INSTITUTE OF TECHNOLOGY

June 1982

[i.e. Sept. 82]

Signature of Author _____
Department of Civil Engineering
March , 1982

Certified by _____
Monsen M. Baligh
Thesis Supervisor

Certified by _____
Amr S. Azzouz
Thesis Co-Supervisor

Accepted by _____
Francois M.M. Morel
Chairman, Department Committee

PREDICTION OF IN SITU CONSOLIDATION
PARAMETERS OF BOSTON BLUE CLAY

by

IMAD BOTROS GHANTOUS

Submitted to the Department of Civil Engineering in March, 1982 in partial fulfillment of the requirements for the degree of Master of Science and Civil Engineer.

ABSTRACT

Predictions of permeability (k_v and k_h) and consolidation parameters (c_v and c_h) of fine grained soils are of crucial importance in determining the dissipation rates of "excess" pore water pressures and the associated soil settlements. The current state of the art employs laboratory and in situ methods involving significant uncertainties in measurements, e.g., sample disturbance, size effects, stress strain and stress strain rates, apparatus induced error, and interpretation techniques tend to interfere with the measured parameters. Published case studies show that existing methods for determining k_v and c_v can, at best, predict those parameters within a factor of two or three, although factors of five to ten are not unusual.

Significant efforts at MIT were devoted to predict the pore pressure distribution induced by quasi-static cone penetration and their subsequent dissipation. Techniques to infer soil parameters namely, c_h and k_h, were developed.

The predicted c_h (probe) profile was compared to results of an extensive laboratory testing program consisting of conventional oedometer and constant rate of strain tests. Reasonable agreement was achieved in soft to medium clays with OCR < 3 (elevation ≃ 42 ft.) at the I-95 test site. For the upper stiffer clays, with OCR > 3, c_h(probe) significantly exceeded c_h (O.C.) from laboratory tests.

Furthermore the predicted k_h (probe) profile was also compared to the profile inferred from constant head tests on undisturbed samples. The agreement was very reasonable.

The predicted c_h(probe) profile at the I-95 test site was further evaluated by executing a consolidation analysis using a finite element computer program, ADINAT, using the c_h(probe) profile as input parameters. Comparison of predicted induced excess negative pore pressure isocrones with observed measurements revealed excellent agreement.

Additional interesting aspects of this study include: the use of X-Radiography in planning and scheduling laboratory testing programs, behavioral aspects of Boston Blue Clay exhibiting normalized behavior of the coefficient of swelling, $c_{vs(O.C.)}$ and coefficient of volume change, $m_{vs(O.C.)}$ in the overconsolidated range. A method for the determination of the coefficient of consolidation, k_h or k_v, at the in situ stress from constant rate of strain tests is suggested.

Thesis Supervisor: Mohsen M. Baligh
Title: Associate Professor of Civil Engineering

Thesis Co-Supervisor: Amr. S. Azzouz
Assistant Professor of Civil Engineering

ACKNOWLEDGEMENTS

The author wishes to express his deepest gratitude to his supervisor, Professor Mohsen M. Baligh, for his guidance during the progress of this research. His discussions with the author were highly inspiring and indeed very motivating in which he shared with the author his immense knowledge in the field of soil mechanics.

The author is deeply indebted to his co-supervisor, Professor Amr S. Azzouz, for his meticulous review of each chapter in this thesis and his constructive criticism. While acknowledging his guidance as being the author's academic advisor, the author acknowledges his friendship which is valued immensely.

The author is deeply greatful to Mr. Adnan Ghantous for his encouragement and financial support during the author's graduate study at M.I.T. His academic advice proved to be most rewarding.

The author would like to thank his parents for their patience, support and encouragement and to Miss Denise Fudala whose love and perseverance were generously offered.

The author acknowledges the friendship of Dr. Mike Kavvadas, Messers, Michael Morrison, Aziz Malek, Alain Goulouis, Jack Germaine and Miss Deirdre O'Neill who provided support when mostly needed.

The professional skills of Ms. Terri Demeris and Mrs. Stephanie George in deciphering my manuscripts are deeply appreciated.

Two people provided the author with immense support and unequalled understanding. Their encouragement provided the author with the motivation and patience required to overcome several barriers. Their generosity was overwhelming and perhaps words are poor tools to express the author's gratitude. So to you Dr. and Mrs. Walid Ghantous this work is dedicated.

TABLE OF CONTENTS

LIST OF TABLES

LIST OF TABLES (continued)

LIST OF TABLES (continued)

LIST OF TABLES (continued)

LIST OF FIGURES

LIST OF FIGURES (continued)

LIST OF FIGURES (continued)

LIST OF FIGURES (continued)

LIST OF FIGURES (continued)

LIST OF FIGURES (continued)

LIST OF FIGURES (continued)

LIST OF FIGURES (continued)

LIST OF FIGURES (continued)

LIST OF FIGURES (continued)

LIST OF FIGURES (continued)

LIST OF FIGURES (continued)

LIST OF FIGURES (continued)

LIST OF FIGURES (continued)

LIST OF FIGURES (continued)

LIST OF FIGURES (continued)

LIST OF FIGURES (continued)

LIST OF FIGURES (continued)

LIST OF FIGURES (continued)

LIST OF FIGURES (continued)

LIST OF FIGURES (continued)

LIST OF FIGURES (continued)

LIST OF FIGURES (continued)

LIST OF FIGURES (continued)

LIST OF FIGURES (continued)

LIST OF FIGURES (continued)

LIST OF FIGURES (continued)

CHAPTER I

INTRODUCTION

Geotechnical problems involving fine grained soils almost always require considerations of transient water flow, or consolidation. The rates of consolidation are governed by the coefficient of consolidation, c_v or c_h, which is a function of the coefficient of permeability, k_h or k_v, and the coefficient of compressibility, m_h or m_v. Predictions of the coefficient of consolidation, or permeability, from laboratory tests are severely affected by the magnitude of sample disturbance, interpretation techniques, size effects, degree of representativeness (e.g., degree to which field stress-strain and stress-strain rates are simulated) and the magnitude of apparatus induced errors.

Predictions of the coefficient of consolidation, or permeability, from in situ testing, on the other hand although affected by some of the aforementioned problems, their magnitudes are greatly attenuated. However, in situ testing has its own problems. The absence of the ideal conditions enjoyed by laboratory testing procedures such as the knowledge of boundary conditions and the relatively simple stress or strain fields, pose problems concerning interpretation of the compiled data.

Recognizing the great potential of in situ tests in soil

exploration, an extensive research effort has been underway at M.I.T. for the last five years to evaluate several in situ devices. One such device is the piezometer probe. Several theories have been proposed for the interpretation of dissipation records and the derivation of soil parameters, namely, k_v, k_h, c_v and c_h.

This research is involved with the evaluation of the predictions of the piezometer probe data using the interpretation techniques developed by Baligh and Levadoux (1980) and a general evaluation of the current state of the art techniques for predicting values of the coefficient of consolidation, c_v or c_h, and permeability, k_v or k_h.

The study can be divided into four parts: the first (Chapter 2) provides a general evaluation of the current state of the art predictions of c_v or c_h, and k_v or k_h; the second (Chapters 3 through 6) reviews the techniques available for the interpretation of the piezometer probe dissipation records; the third (Chapters 7 through 9) applies the predictions of the piezometer probe of in situ parameters in a case study format; the fourth (Chapters 10 through 12) considers a comparative study of the predictions of in situ soil parameters offered by an extensive laboratory testing program and the parameters offered by Baligh and Levadoux's (1980) piezometer probe pore pressure decay interpretation techniques.

Chapter 2 presents a general overall appraisal of the ability of the current state of the art methods in predicting the coefficient of consolidation, c_v or c_h, and the coefficient of permeability, k_v or k_h. Laboratory as well as in situ methods are appraised by evaluating their predictions in eleven case studies. Conclusions based on general trends are drawn and the necessity for a better measurement tool is emphasized.

Chapter 3 suggests a well defined systematic approach for solving problems characterized by multiplicity of interactions; gaps in our knowledge of the situation and computational limitation. The procedure basically consists of: (1) defining the problem; (2) alternative solutions are generated; (3) solutions are evaluated; (4) an iterative procedure is followed. In all four parts modelling expertise is called upon. A thorough investigation of the modelling procedure is presented. Attributes of a good model and the resulting accrued benefits are listed. Finally, guide lines for structuring the system objectives are presented.

Chapter 4 invokes the first step of our systematic approach; system definition and description. Definition of the problem involves acknowledgement of the difficulties and limitations encountered by geotechnical engineers of which consolidation and permeability characteristics are of significant importance in performing accurate consolidation analysis and aid in decision

making in foundation engineering. The limitations of conventional and in situ testing procedures are evaluated and the need for a new in situ testing device is emphasized.

System hardware, the piezometer probe, is described and the importance of system flexibility is accentuated. System output records consisting of steady penetration and dissipation records are described and their importance in identifying stratigraphy is highlighted. The constraints and difficulties in predicting initial excess pore pressure distribution and interpreting dissipation records are presented. Finally, the value system is defined.

Chapter 5 invokes the second step of our systematic approach: alternative generation. Several existing theories of cone penetration are based on either a bearing capacity approach or cavity expansion approach. Disqualifying bearing capacity approaches a priori, the comparison reduces to that of comparing cavity expansion approaches, of which Torstenson's method is representative, with Baligh and Levadoux's method (1980). Torstenson's method for predicting initial pore pressure distribution and subsequent derivation of soil's coefficient of consolidation, c_v, is presented in detail. Baligh & Levadoux's method is then discussed. The methodology (the strain path method) and approximations involved with predictions of initial (penetration) pore pressures are reviewed and the sensitivity of the model to those approximations is

tested. Subsequent pore pressure decay is obtained through use of ADINAT computer program that utilizes the uncoupled Terzaghi Rednulic governing equation. Sensitivity to this assumption was checked by comparison with dissipation solutions obtained from CONSOL computer program that utilizes Biot's coupled solution.

Chapter 6 invokes the final step of our systematic approach: alternative evaluation. The value system involved considers how close to reality the models of each alternative are. Torstenson's method for evaluating initial distribution of the pore pressures is highly questionable as it raises serious theoretical and practical problems caused by the severe over-simplifications he introduces. It does not provide the necessary insight into cone penetration mechanism. Evaluation of Baligh & Levadoux's dissipation solutions in Boston Blue Clay had the following main objectives: (1) Evaluate the capability of simple linear solutions in predicting in situ dissipation measurements in Boston Blue Clay; (2) Investigate effect of various practical factors on reliability (practicability) of estimated profiles of c_v, c_h, k_v and k_h; (3) Compare estimated coefficients of consolidation and permeability with laboratory measurements and field performance data. Comparison of steady state penetration and dissipation records in B.B.C. and Connecticut Valley Vared Clay (C.V.V.C.) with

predicted intral pore pressure distribution and subsequent dissipation records justifys several of the assumptions made and lead to a specific methodology for estimating the horizontal coefficient of consolidation, c_h, and the coefficient of permeability. The use of such parameters in practice is investigated.

Chapter 7 describes the activities involved in the Construction of the Julius Adams Stratton Building (Student Center). The site history and geology is concisely presented. A brief account of the instrumentation installed in the foundation soils involves their location and description. Description of the construction activities involves a brief account of the two stages of excavation and the foundation mat pours. Earth and concrete quantities are tabulated and their locations schemetically presented from contractor's records.

Chapter 8 reviews the previous analysis performed on the Student Center foundations. Analyses extended from qualitative discussions of field data to quantitative evaluation of engineering properties. Predictions of pore pressure dissipation isocrones in the underlying clay layer due to initial excavation and subsequent reloading are evaluated. This chapter attempts to exhibit the errors involved in the use of the traditional Terzaghi soil model coupled with non-representative soil parameters.

Chapter 9 is an extension of the last step of our systems approach methodology, alternative evaluation. Avoiding an ordinal evaluation of the piezometer probe predictions by comparing deduced soil parameters with laboratory inferred parameters, a cardinal evaluation is attempted. Using the soil parameters, infered from the pore pressure decay records due to cone penetration at the I-95 test site, coupled with a new finite element program, ADINAT, the pore pressure dissipation isocrones in the foundation clay is predicted. Consequently the predicted pore pressure isocrones are compared to field observed values at discrete locations derived from the field instrumentation.

Chapter 10 describes the scope of the extensive laboratory testing program. The laboratory testing procedures involving traditional Oedometer tests, Constant Rate of Strain tests, and permeability determination tests in triaxial cells under constant head conditions are also described.

Chapter 11 describes the role of x-radiography in the planning phase of the laboratory testing procedure. The M.I.T. x-radiography facility is described and image interpretation and procedures briefly examined. Several examples pertaining to the identification of anomalies and zones of gross sample disturbance are presented. The use of x-radiography as a tool for qualitative identification of soil stratification is investigated.

Chapter 12 involves the use of laboratory test data on undisturbed soil specimens retrieved from the I-95 test site to verify predictions derived from dissipation records of the piezometer probe. Verification involves the comparison of the variation of $c_{h(probe)}$ versus depth, reference profile, with laboratory derived $c_{h(0.C)}$ at the in situ overburden stress $\bar{\sigma}_{vo}$. The verification procedure also involves comparison of the variation of $k_{h(probe)}$ with laboratory $k_{h(0.C)}$. The severity of the assumptions used in interpreting the $c_{vs(0.C)}$ profile for the foundation clay under the Student Center is assessed. Interesting soil behavioral aspects are derived and applied to the aforementioned investigation.

Finally, Chapter 13 summarizes the main conclusions reached in this study.

CHAPTER 2

LABORATORY TESTING, IN SITU TESTING AND FIELD PERFORMANCE COMPARISONS

2.1 INTRODUCTION

Lambe (1973) reviewed the types of predictions soils engineers attempt, Table 2.1. Of interest is type A predictions. The soil's engineer is usually forced to work with insufficient and inaccurate data as he attempts to verify a type A prediction as to the probable behavior of a certain project at hand. Lambe (1973) portrays a cognitive model the soils engineer implements to arrive at a type A prediction, Fig. 2.1. A quick glance at such a model easily reveals it's vulnerability. Each of it's constituent phases is as good as the mechanism or the data it involves. Hence if the data regarding the soil parameters are erroneous the further away would our prediction be from the actual field performance.

Although some of the constituent submodels of the aforementioned cognitive model could be improved through the endownment of more sophisticated stress or deformation fields, such sophistication, in the author's opinion, is not fully warranted. It turns out that the selection of the soil parameters is of critical importance and in some instances highly dominant.

Perhaps the most efficient way of introducing the importance of such input data would be to carry out a series of type C predictions on several case histories. Ten case histories were collected, summarized and later collectively presented in tabular form to facilitate identification of trends.

2.2 CASE 1: SELSET RESERVOIR EMBANKMENT

2.2.1 General

Kennard and Kennard (1962) and Bishop and Vaughan (1962) provide an accurate description of the dam and its performance. In short, the 30 ft. high reservoir embankment is constructed of boulder clay fill with drainage blankets, on a foundation of boulder clay having a low shear strength over large areas. We shall concern ourselves solely with laboratory and field testing for the determination of soil parameters of interest, namely, the coefficient of permeability and consolidation, k and c_v, in the three main parts of the earth structure:

(a) Foundation,

(b) Fill, and

(c) Puddle Core.

The relevent index properties are shown in Table 2.2.

2.2.2 Foundation

1. Coefficient of Consolidation

Two methods could be utilized for measuring the coefficient of consolidation, c_v, in the laboratory:

(a) Direct method, obtained by direct measurement of the rate of dissipation of pore water pressure which could be carried out most conveniently in a triaxial apparatus (Bishop & Vaughn 1962). Bishop and Gibson (1963) have shown that anomalies in the values of c_v could result due to the reduced shear stresses set up by the end restraints. Yet, there is no evidence to date that shows that this results in a significant error in c_v value.

(b) Indirect methods, based on volume change measurements which depends largely on the method of calculation, Ladd (1973). Such an indirect method could prove to be cumbersome and even hard to calculate with partially saturated soils.

Fig. 2.2.a shows values of c_v from laboratory dissipation* tests on samples cut with their axis horizontal. It is interesting to notice that there is a clear increasing trend of c_v with increasing effective stress which could be

*See later foot note.

attributed to the nonsaturated nature of the foundation clay.

The field performance values of c_v were calculated using the Terzaghi one dimensional uncoupled linear theory of consolidation with the qualification that where the data is sufficiently complete, c_v is made to vary with average effective stress to give the best fit.

Figure 2.2.b shows results of c_v as obtained from field performance evaluation. Again, a clear increasing trend of c_v with increasing effective stress, $\bar{\sigma}$, is noted. Comparing Figs. 2.2.a and 2.2.b at a specific value of effective stress, at 30 psi say, the value of c_v obtained from field tests is approximately 3 times the laboratory value.

Field tests on hydraulic piezometers were performed using the constant head technique only, with positive induced excess pore pressures. If sufficient time is allowed to elapse for the steady state to be approached, the permeability can be evaluated by the simple expression, Hvorslev (1951):

$$k = \frac{q_\infty}{F \cdot \Delta h}$$

where q_∞ denotes the steady state flow which is theoretically only attained at time $t = \infty$, Δh denotes the applied change in head and F denotes the intake factor, which is $4\pi r$ for a spherical piezometer of radius r in an isotropic medium.

Gibson's (1963) solution presented a linear relationship between q_t, the flow into or out of the piezometer at any time t and the dimensionless parameter $1/\sqrt{T}$ where $T = \frac{ct}{r^2}$ and c denotes some average of the consolidation and swelling coefficient. The relationship reads:

$$q_t = 4\pi r \cdot k \cdot \Delta h \left[1 + \frac{1}{\sqrt{\pi T}}\right]$$

Means of interpreting field data using the above equation were discussed by Gibson (1963). Values of c_s thus obtained are equal, on average, to 400 ft^2/year, which reflect the low coefficient of swelling of the boulder clay.

2. Coefficient of Permeability

Laboratory values of the coefficient of permeability, k, were obtained using the constant head permeability test in the triaxial cell under steady conditions*. The average value from four tests run under low effective stress was 1.3×10^{-8} cm/sec. or omitting one high value, 0.84×10^{-8} cm/sec. The value of k by direct measurement in laboratory on a remodeled sample, at the same effective stress, was 0.43×10^{-8} cm/sec.

*Laboratory and field procedures remain identical unless stated otherwise.

2.2.3 Fill

1. Coefficient of Consolidation

The fill was formed of the same boulder clay. Laboratory and field performance values of c_v are compared in Figs. 2.3.aand 2.3.b. The average value from the laboratory dissipation tests was 24 ft^2/year at 40 p.s.i. effective stress and from field performance 30 ft^2/year at 40 p.s.i. The value of c_s from the q vs. $1/\sqrt{t}$ line gives a c_s value of 14 ft^2/year.

2. Coefficient of Permeability

Two constant head tests in the fill gave an average value of $k = 1.2 \times 10^{-8}$ cm/sec, in an area placed about 1% of the optimum water content. The directly measured laboratory value on remolded clay in this stress range is approximately 1.1×10^{-8} cm/sec, but may correspond to a slightly different voids ratio.

2.2.4 Puddle Core

Here again, the material is boulder clay, placed at a higher water content and with some of the larger stone content removed or crushed.

1. Coefficient of Consolidation

The field performance c_v could not be obtained, as the boundary pore pressures were not known in detail. The increase in laboratory c_v with effective stress is illustrated in Fig. 2. 4 . The slope of the q vs. $1/\sqrt{t}$

line gave a c_v value of 84 ft^2/year (this value to be compared with 15 ft^2/year obtained from laboratory tests in the same effective stress range.

2. Coefficient of Permeability

Two constant head tests gave an average value of 0.74×10^{-8} cm/sec (consolidating) and 0.84×10^{-8} cm/sec (swelling), the average effective stress being lower in the latter case. The directly measured k value from a laboratory test in the relevant stress range is about 0.77×10^{-8} cm/sec.

2.2.5 Summary

1. Foundation

(a) Soil reasonably uniform with possible macro structure.

(b) Values of c_v from laboratory test and back figured from field performance exhibit an increasing trend with effective stress, probably attributed to partial saturation.

(c) Values of c_v from the laboratory dissipation tests at a particular value of effective stress are approximately three times less than the values of c_v obtained from field performance calculations.

(d) Values of c_s obtained from constant head tests averaged 400 ft^2/year.

(e) The values of permeability obtained from in situ tests were approximately double the values obtained from laboratory tests on a remolded sample at the same effective stress.

2. Fill

(a) Soil reasonably uniform.

(b) Values of c_v from field performance were approximately 1.25 times the values obtained from laboratory dissipation tests.

(c) Values of c_s from constant head tests were approximately 14 ft^2/year.

(d) Value of permeability deduced from constant head tests was approximately equal to that obtained from laboratory tests.

3. Puddle core

(a) Soil is reasonably uniform.

(b) Values of coefficient of consolidation, c_v, obtained from in situ tests were approximately 5.6 times the values obtained from laboratory dissipation tests.

(c) The values of coefficient of permeability obtained from in situ tests were approximately equal to those obtained from laboratory tests.

2.3 CASE 2: BALDERHEAD DAM

2.3.1 General

Kennard, Penman and Vaughan (1967) have described the embankment. In short, the rolled core of the 160 ft. high Balderhead dam is constructed of boulder clay very similar to that at Selset but more variable in character. The relevent index properties are shown in Table 2.2. The study herein envolves only the core section of the dam.

2.3.2 Coefficient of Consolidation

The field performance value of c_v from three piezometers in the lower third of the core was 128 ft^2/year at an average vertical effective stress of 47 p.s.i. Laboratory dissipation tests on samples from the more clayey and more sandy (but less common) boulder clay gave values of 25 ft^2/year and 170 ft^2/year at effective stresses of 47 and 45 p.s.i., respectively. The field value thus lies a little above the mean laboratory value.

Two of the piezometers used for measuring the field performance gave c_v values from the constant head test averaging 75 ft^2/year in the relevant stress range, but throughout the core the values varied widely.

2.3.3 Coefficient of Permeability

Values of k from constant head permeability tests in the core are plotted in Fig. 2.5. There is a clear

tendency for k to decrease with increase in effective stress. The average value is 0.73 x 10^{-8} cm/sec at 53 p.s.i. effective stress. This may be compared with the directly measured laboratory value of 0.64 x 10^{-8} cm/sec and 4.3 x 10^{-8} cm/sec at 5 p.s.i. on the more clayey and more sandy laboratory samples. Tests ran on samples with similar index properties gave values of permeability approximately .56 x 10^{-8} cm/sec at an effective stress of 53 p.s.i.

2.3.4 Summary

1. Field performance value of c_v at an average vertical stress of 47 p.s.i. were approximately 1.3 times values obtained from laboratory dissipation tests and 1.7 times the value obtained from in situ piezometer tests.

2. Values of coefficient of permeability k from constant head tests were approximately 1.3 times the values obtained from laboratory tests at the same effective stress.

2.4 CASE 3: DIDDINGTON DAM

2.4.1 General

Hammon and Winder (1967) described the design and the construction of Diddington dam. In short, the 70 ft. high embankment forming the reservoir is constructed mainly of a boulder clay of high plasticity derived from Oxford clay. The foundation consists of Oxford clay overlain by up to

20 feet of boulder clay. The relevent index properties are shown in Table 2.2. The study, herein, involves the two parts of the earth structure, namely:

(a) Foundation, and;

(b) Fill.

2.4.2 Foundation

The boundary between the boulder clay and the Oxford clay was not well defined. In retrospect, it is difficult to be certain of the correct geological description of some of the samples.

1. Coefficient of Consolidation

Dissipation tests on 4" diameter samples from depths of 6 ft. and 11 ft. gave average values of c_v of 12 ft^2/year and 4.3 ft^2/year, respectively, in the effective stress range of 20-60 p.s.i., with c_v showing some increase with effective stress. Values calculated from the volume changes during the consolidation stage of drained triaxial tests gave 9.0 ft^2/year and 5.0 ft^2/year, respectively, for the same cores. The average value of oedometer tests on the boulder clay in the effective stress range 16-125 p.s.i. is 17 ft^2/year.

The field performance value of c_v, based on piezometers at 5 and 10 feet below stripped level, averaged 11 ft^2/year at an average vertical effective stress of 15 p.s.i. Field constant head tests performed on a piezometer at a

depth of 8 feet below stripped level gave a value of c_s equal to 7.5 ft^2/year.

2. Coefficient of Permeability

A constant head field permeability test on the same piezometer mentioned above gave a value of k = 0.33×10^{-8} cm/sec. Directly measured values of k are not available, but those calculated from the dissipation tests gave average values of 2.15×10^{-8} cm/sec for the shallow sample and 0.17×10^{-8} for the deeper sample.

2.4.3 Fill

Fill is primarily of rolled boulder clay from the same strata as the foundation. The core was placed wet of optimum, but dryer placement was permitted in the shoulders. Owing to the prevailing dry weather, the pore pressures were negative.

1. Coefficient of Consolidation

The laboratory value of c_v for remoulded boulder clay average 6.0 ft^2/year at an average effective stress of 30 p.s.i. In this fill, two tests gave an average value of c_v = 1.4 ft^2/year. A value of c_v is available from one constant head test on the core, and this also give 1.4 ft^2/year.

2. Coefficient of Permeability

Constant head permeability tests in the fill gave a value of k = 0.87×10^{-8} cm/sec (two values only) and

in the rolled core k = 0.18 x 10^{-8} cm/sec (three values only), if high values are neglected. Laboratory values calculated from dissipation tests on remoulded clay averaged 0.4 x 10^{-8} cm/sec.

2.4.4 Summary

1. Foundation
   - (a) Fewer tests results.
   - (b) Soil has higher clay content.
   - (c) Values of c_v obtained form field performance are approximately 1.5 times the values obtained from laboratory tests in the same effective stress range and 1.5 times the values obtained from in situ tests.

2. Fill
   - (a) Fewer test results.
   - (b) Good agreement between values of c_v derived from field performance and laboratory tests.
   - (c) Values of c_v derived from field performance are approximately twice the values derived from in situ tests.
   - (d) The value of coefficient of permeability derived from in situ tests is much less than that derived from laboratory tests.

2.5 CASE 4: M.6 MOTORWAY TRIAL EMBANKMENT

2.5.1 General

Bishop and Al Dahahir (1969) examined the M.6 Motorway trial embankment. One of the purposes of the M.6 Motorway Trial Embankment was to examine the effectiveness of drainage blankets in reducing the excess pore pressures set up in boulder clay fill placed under extremely wet conditions. The test section was divided into three areas. One has a drainage blanket at the base of the fill only. The other two sections had an intermediate blanket at heights above the base blanket of 6 ft. and 10 ft., respectively, Fig. 2.6.

2.5.2 Coefficient of Consolidation

Using a set of isochrones derived from piezometer readings, an analysis of field performance values of c_v were obtained for a range of values of average vertical effective stress, Fig. 2.7. Again, the marked increase in c_v with effective stress is obvious.

A limited number of laboratory dissipation tests are also shown in Fig. 2.7. Considering the somewhat variable character of the material and high stone content, the agreement is good. Fig.2.8 shows that the increase in c_v is a consequence of the variation of its components, k and m_v.

2.5.3 Coefficient of Permeability

Constant head permeability tests (laboratory and field) were carried out at various stages of pore pressure dissipation, Fig. 2.9. The decrease in value of k with effective stress is apparant and is in conformity with results of the laboratory tests.

2.5.4 Summary

1. Reasonably uniform soil conditions.
2. Field performance values of c_v are approximately 1.5 times the values of c_v obtained for laboratory dissipation tests.
3. Field performance values of c_v are approximately 0.4 times the values of c_v obtained from in situ tests.
4. Values of coefficient of permeability k obtained from constant head tests are approximately twice those obtained from laboratory tests.

2.6 CASE 5: FIDDLER'S FERRY EMBANKMENT

2.6.1 General

Smith and Rennie (1967) and Al-Dhahir, Kennard and Morgenstern (1969) give a good description of the scheme and the pore pressure observation. In short, Fiddler's Ferry Power station involved the construction of ash

disposal lagoons, formed by 35 feet high embankments, 13,500 feet long, on marsh ground adjacent to the River Mersey. The soft clay foundation, overlying peat and sand was instrumented with piezometers and pore pressure observations were recorded over a span of 5 years. Fig. 2.10 shows a plan of the embankments. Fig. 2.11 shows cross sections along the dam and the pertinent stratification. Pertinent index tests are shown in Table 2.2 . The stratigraphy, classification tests and undrained strenths are summarized in Table 2.3 .

2.6.2 Coefficient of Consolidation

Constant head tests were performed on three separate occasions over a period of two years. Observations obtained at P19 are given in Figure 2.12. These displays the ideal linearity and are readily interpreted within the framework of the Tergaghi theory of consolidation. Results of comparable quality were obtained at P22 and P25. Test carried out at P20, P23, and P26 display a persistant upward curvature in the relationship between q vs. $\frac{1}{\sqrt{t}}$. The data are given in Fig. 2.13. However, it should be noted here that all three tips are located close to the peat layer and thus the aforementioned curvature could be attriubted to the possible creep in the peat. The coefficient of consolidation found from the constant head tests are plotted

in Figure 2.14 against the average effective stress during the test.

Oedometer tests carried out in a routine manner on specimens cut from block samples gave on average a coefficient of consolidation of 6 ft^2/year in the vertical direction and 9 ft^2/year in the horizontal direction. These values were supported by coefficients of consolidation computed from the consolidation stage of triaxial tests which generally range between 4 and 10 ft^2/year. A study into the anisotropic consolidation properties at another location on the site showed no significant difference between coefficients of consolidation in the horizontal and vertical direction. Results of the aforementioned oedometer tests are also shown in Fig. 2.15 versus the effective stress.

The field performance values of c_v are subject to some uncertainty, as drainage in the upward direction was partly restricted by the presence of the embankment, where an increase in pore pressure was noted during the period of consolidation. Lateral drainage was neglected. The average value of field performance in low effective stress range was 63 ft^2/year, which may be compared to an oedometer derived value of 6.9 ft^2/year. In the higher effective stress range the corresponding values are 37 ft^2/year and 5.4 ft^2/year. Value of c_v obtained from constant head tests

averaged 200 ft^2/year compared to field performance value of 39 ft^2/year at the same effective stress level.

2.6.3 Coefficient of Permeability

Field constant head permeability tests yield values that range from 3.2×10^{-8} cm/sec to 46×10^{-8} cm/sec. Omitting the two high values, an average of 6.6×10^{-8} cm/sec is obtained at 12.7 p.s.i. effective stress. The latter is to be compared with a laboratory derived value of 0.72×10^{-8} (vertical flow) and 1.03×10^{-8} (horizontal flow). Fig. 2.14 shows the values of the permeability, k, obtained from in situ constant head test and as calculated from oedometer tests, plotted versus effective stress.

2.6.4 Summary

1. Variable shallow alluvial strata and marked macro structure.
2. The relationship between q and $\frac{1}{\sqrt{t}}$ for the in situ constant head tests exhibits an upward curvature probably due to presence of the porous element in the close proximity of the peat layer.
3. Values of coefficient of consolidation, c_v, derived from field performance observation is approximately 9 to 7 times the values given from laboratory tests and approximately 0.3 times the value obtained from in situ tests.

4. Values of the coefficient of permeability derived from field constant head tests were approximately 6.0 - 9.0 times the values obtained from laboratory tests.

2.7 CASE 6: BACKWATER DAM

2.7.1 General

Scrimgeour and Rocke (1966) present a general description of the retention scheme. The Backwater dam near Dundee in Scotland is a 140 ft. high embankment made of boulder clay. The boulder clay in the borrow pits contains occasional large boulders and cobbles. Stones in excess of 9 inches (shoulders) and 6 inches (core) were removed from the boulder clay prior to placing on the main embankment. Particle size distribution is shown in Table 2.4 . To assist in the design, and also to gain information on the most suitable method of compaction, an instrumented trial embankment some 20 ft. high was constructed. Fig. 2.16 shows the main and the trial embankment.

2.7.2 Coefficient of Consolidation

Field performance values of c_v were obtained by using lumbe's extension of Terzaghi's theory (1963) for the case of a gradually applied load. The fitted c_v values are shown in Fig. 2.17 and are also plotted as a frequency

distribution in curve Fig. 2.17 and whose dominant value may be taken in the region of c_v = 65-70 ft^2/year. Values of c_v obtained by the same technique from the trial embankment yield a value of c_v = 40 ft^2/year. This is believed to be due to the incompatable effective stress levels in the trial and main embankment and is strongly supported by evidence shown in Fig. 2.18. Laboratory tests done on undistrubed samples were carried out in a Row cell* occasionally including stones up to 3 inches in diamter. A total of 20 undisturbed samples were tested for m_v and c_v. Following these undisturbed tests, the material was air dried and stones greater than 3/4 inch removed. It was remixed to a water content 2% greater than the placement value. Material was recompacted using Proctor effort and tested. Few 4 inch triaxial dissipation tests were run. Step load tests were performed using a pressure increment ratio of unity. c_v values were deduced by fitting the pore pressure dissipation curves at 50% using Terzaghi's theory.

Figure 2.17 shows results from undistrubed laboratory tests from the main and the trial banks and from recompacted samples from both banks (curves 2, 3 and 4, respectively). Curves 2 and 3 are in good agreement with curve 1, while curve 4 clearly underestimates the value of c_v.

*Rowe and Barden (1966)

2.7.3 Coefficient of Permeability

The constant head swelling-type permeability tests will be discussed in the next section. In the case of the in situ permeability tests of the consolidation type conducted on piezometers in the main embankment, the values of k are listed in Table 2.5 .

2.7.4 Indirectly Obtained Coefficients of Consolidation

The constant head swelling type permeability tests on the piezometers in the trial bank gave values of permeability which, when combined with the relevant value of compressibility from laboratory tests on undisturbed samples from the trial embankment gave a c_v in the region of 20 ft^2/year. This value is appreciably lower than the c_v = 40 ft^2/year found from field performance analysis.

Using relevant values of m_v (with respect to effective stress) shown in Fig. 2.19 deduced from settlement gauges, the resulting indirect c_v obtained from the in situ obtained value of k for contant head consolidation type permeability tests discussed earlier, the resulting "indirect" c_v (= $\frac{k}{m_v \gamma_w}$) are shown in Table 2.5 . Also shown in Table 2.5 are values of c_v obtained from the slope of Q(t) versus $\frac{1}{\sqrt{t}}$ * ("direct" c_v).

---

*Gibson R.E. (1963)

2.7.5 Summary

1. Reasonably uniform soil conditions.
2. Values of coefficient of consolidation for the main embankment backfigured for a gradually applied load were approximately 1.7 times the values backfigured for test embankment and was attributed to the difference in the effective stress level.
3. Value field performance coefficient of consolidation for the main embankment and the trial embankment was approximately equal to the value obtained from laboratory tests.
4. When the values of constant head swelling type permeability tests on piezometers in trial embankment were combined with laboratory obtained values of the coefficient of compressibility, m_v, the derived values of c_v were approximately one half the values of the field performance values.

2.8 CASE 7: LYNDHURST EMBANKMENT

2.8.1 General

Raymond (1968) gives a detailed description of the method of construction and performance of Lyndhurst Embankment. In short, Stage 1 of construction consisted of 4 ft. of

fill placed on sawdust between 3 ft. high berms constructed over a one month period. Stage 2 consisted of 2 ft. of fill placed quite rapidly. The foundation consists of muskeg deposit whose profile is shown in Table 2.6. Comparisons of the performance of muskeg deposit is complicated by their high permeabilities causing rapid consolidation settlements.

2.8.2 Coefficient of Permeability

In situ measurements if the coefficient of permeability were conducted using push type piezometers. When steady state flow condition is reached within a homogeneous, isotropic soil, the coefficient of permeability, k, may be calculated using Gibson's (1963) equation:

$$k = \frac{Q_\infty}{F \cdot \Delta h} = \frac{Q_\infty}{4\pi r \Delta h}$$

In order to calculate the coefficient of permeability, k, the equivalent radius, r, of the tip must be calculated. Hvorslev (1951) suggests the following transformation equation for an ellipsoidal tip:

$$r = \frac{L}{2} \left\{ \sinh^{-1} \left(G \frac{L}{D} \right) \right\}^{-1}$$

where L is the length of the tip, D is its maximum diameter and G is an imperial constant. Using an alternative analysis Raymond et al. (1970) used a finite difference solution whose results together with Hvorslev's relationship appear in Fig. 2.20. The equation:

$$\frac{Q_s}{Q_e} = \frac{r_s}{r_e} = 0.6 + 0.204 \frac{L}{D}$$

as an adequate simplified equation in which Q_s and Q_e and the steady state flow for a spherical and an ellisoidal (or cylindrical) tips respectively, and r_s and r_e are the radii of a spherical and an ellipsoidal (or cylindrical) tip and $r_e = D/2$. Remembering that soils are nonhomogenous and using the idealization that cross-anisotropy suffices the description of the nonhomogenous characteristic, the above equation could be written in transformed dimensions as follows:

$$\frac{Q_s}{Q_e} = \frac{r_s}{r_e} = 0.6 + 0.204 \frac{L}{D} \sqrt{\frac{k_h}{k_v}}$$

Ideally, therefore, a series of tests in cross-anisotropic soil using different piezometers tips with various L/D ratios would reveal the values of k_h and k_v. The results

of a series of tests plotted as $Q/\Delta h$ against L/D are shown in Fig. 2.21. In order to interpret these results, a family of lines representing the case of $k_h = k_r$ was first drawn, after which a best fit straight line was selected. Only constant head increase type results of in situ tests on the muskeg deposit are shown in Table 2.6.

Laboratory tests were performed on specimens taken vertically and horizontally from the soil deposit from the soil deposit and on soil remoulded at the in situ moisture content. Tests were carried out in an oedometer modified to perform falling head permeability tests. Permeability tests were conducted well after primary consolidation was complete. The effect of leaching was also investigated.

Two methods for obtaining the coefficient of permeability were utilized:

a. Direct Method: Obtained from falling head tests.

b. Indirect Method: Obtained from rates of settlement, assuming Terzaghi's consolidation theory is valid.

For the purposes of illustration, a set of typical laboratory results on Leda clay according to the well-known semi-logarithmic relationships are shown in Fig. 2.22. Attention is drawn to the fact that indirect methods tend to lower the values of k at any one value of void ratio and that

there is little variation in the directly measured permeability until the consolidation loads exceed the preconsolidation pressure. Table 2.6 shows collectively the values of the vertical and horizontal permeabilities as obtained from laboratory and in situ tests.

After the second stage of construction, 50% of the settlement in the muskeg occured in about 5 days. This 5-day 50% settlement is comparable with that predicted using field in situ permeability results with laboratory compressibility results over a similar load increment. Laboratory tests gave a compressibility value for the peat and marl of 0.44 and 0.53 cm^2/kg respectively, or an average of 0.48 cm^2/kg. The average in situ vertical permeability in the upper 20 feet is 13900 x 10^{-6} cm/min. Since the underlying clay is impermeable relative to the muskeg, the drainage path length is 610 cms., resulting in a predicted 50% settlement time of 1.8 days. This compares as favorably with the observed value as can generally be expected. Similar comparisons were observed for the other two muskeg deposits. Only if the secondary settlement is included can the amount of settlement be predicted from the laboratory tests. Nevertheless, the large difference between the laboratory directly measured permeability and the in situ permeability leaves little doubt that the latter value should be used when predicting rates of consolidation of muskeg deposits.

2.8.3 Coefficient of Compressibility

In situ interpretation of dessipation record according to Gibson's (1963) method were deemed totally unsatisfactory. No laboratory derived values were reported either.

2.8.4 Summary

1. Soil conditions are erratic.
2. In situ interpretation of dessipation record according to Gibson's (1963) method were deemed unsatisfactory.
3. Laboratory falling head tests and indirect methods using rates of settlement and Terzaghi's consolidation theory for providing estimates of the coefficient of permeability, k, that are approximately 68 to 47 times the values obtained from in situ tests in the upper 24 feet and 2.8 → 0.3 times in the lower 24 feet.
4. The time required for 50% settlement as deduced from field performance data is approximately 2.5 told that deduced by combining in situ values of the coefficient of permeability, k, and laboratory coefficient of compressibility, m_v.
5. Ratio of k_v to k_h ≈ unity.

2.9 CASE 8: ARLINGTON DAM

2.9.1 General

Beavan and Strouts (1970) report some observations of field tests, laboratory tests and field performance of Arlington Dam foundation. In short, the dam is constructed of Weald clay founded on comparatively recent alluvium of gravel, sand, silt and clay overlying Weald Clay. Beavan et al. describe the instrumentation and method of installation to which the reader is referred to for further information. The relevant index properties are shown in Table 2.2 .

2.9.2 Coefficient of Consolidation

In situ values of the coefficient of consolidation were deduced from constant head tests (consolidation type) on four piezometers beneath a low part of the dam. Only 2% fluctuation in the applied constant head after the first hour was allowed. Using Gibson's* Method for interpreting the in situ values of c_v and the coefficient of permeability k from the straight line relationship between the quantity of flow and the reciprocal of square root time, the values thus infered are listed in Table 2.7 .

*Gibson (1963)

Field performance values of c_v were estimated approximately from the dissipation records shown by each piezometer in conjunction with the use of Terzaghi's one-dimensional consolidation theory.

No laboratory tests were done on Weald clay from the same locations as the piezometers. However, conventional oedometer tests on vertical samples were done on sample of Weald in the close proximity*. Values of c_v thus derived are shown in Table 2.7 .

2.9.3 Coefficient of Permeability

In situ values of the coefficient of permeability were obtained from constant head tests (consolidation type) as mentioned above. Values of this in situ permeabilities are listed in Table 2.7 .

Laboratory values of k were derived from $c_{v(lab)}$ and $m_{v(lab)}$ deduced from consolidation tests mentioned above and whose values appear in Table 2.7 .

2.9.4 Summary

1. Marked vertical variation, stiff and fissured.
2. Values of field performance coefficient of consolidation, c_v, was approximately 0.4 times less than the values derived from laboratory tests and 0.01 times

*Within 400 yd horizontally and 30 ft vertically.

the value deduced from in situ constant head tests.

3. Values of coefficient of permeability, k, derived from in situ tests was 7.0 times the value derived from laboratory consolidation tests.

2.10 CASE 9: JULIUS ADAMS BUILDING (STUDENT CENTER, M.I.T.)

Bromwell et al.(1968),Gass (1964) and DeFries (1967) describe the wide excavation and the construction process of the Student Center. In short, the M.I.T. Student Center is a five story reinforced concrete frame structure. It was constructed on the west side of the M.I.T. Campus during 1963-1964. The building has a floating foundation and rests on a 3 to 10 foot thick concrete mat constructed on a sand-gravel layer overlying a 60 to 75 feet thick stratum of Boston Blue Clay, Fig. 7.3 . The foundation was extensively instrumented and monitored. Average index properties for the Boston Blue Clay stratum is shown in Table 2.2 .

1. Coefficient of Consolidation

An extensive laboratory testing program was initiated in 19 in which over 40 oedometer tests were conducted. Values of c_s which one averages of values computed by both log time and square root of time fitting methods from the aforementioned tests are shown in Fig. 8.1 . Average c_s values for the first stress decrement from maximum past

pressure, $\bar{\sigma}_{vm}$, is 60 ± 30 x 10^{-4} cm^2/sec. Also, c_s decreases with increasing OCR.

Field performance values of c_s were determined using Terzaghi's one dimensional linear unlinked theory coupled with the piezometer dissipation records. Computed field performance value of c_s was equal to 360 ± 60 x 10^{-4} cm^2/sec, approximately six times the value obtained from laboratory tests.

This case is further discussed and analysed in Chapters 7-12 to which the reader is referred for more information.

2.11 CASE 10: NATIONAL MUSEUM IN OTTAWA

Crawford (1953) provide an accurate record of the settlement under the heavily loaded National Museum in Ottawa. The soil underlying the Museum is generally considered a marine deposit, but recent geological work has cast doubt on earlier interpretation (Gadd, N.R., 1963). It's engineering properties are similar to those of the extensive deposits of "Leda" clay in the St. Lawrence and Ottawa River Valleys. Uniform block samples of clay were cut from a small tunnel in the city of Ottawa, at a depth of 33 ft. The soil on which the tests were made had a natural water content averaging 58.4%, a liquid limit of 54% and a plastic limit of 25%. The sensitivity was approximately 50%.

Further laboratory consolidation tests performed by Crawford (1964) are also reported and finally we shall pursue a comparison between field and laboratory observations.

2.11.1 Test Procedures and Apparatus

Most of the tests were made with vertical pressures of 0.5, 1, 2, 4, 8 and 16 KSC. Departures from this loading schedule were slight and had no apparant effect on the results. Variations in procedure included daily load increments (Series A) weekly increments (Series B) and increments at the end of primary consolidation (Series C). A fourth set of tests involved controlled rate of loading (Series D).

All specimens were tested in "teflon" coated stainless stell consolidation rings with an area of 20 sq. cm and either 1 cm or 2 cm high. All tests except those of Series B were done with the ring sealed to a base plate in the center of which a 1/2 in diameter Alundum disc was flush mounted and corrected to a no flow pressure measuring system. The top surface of the specimen was covered with a free-draining Alundum disc. In Series B tests, pore pressures were not measured, the consolidation ring was floated between two free-draining discs. Therefore, only in Series B was the maximum length of drainage path equal to one-half the height.

Incremental loading tests were conducted in the normal manner, with an 11 to 1 lever ratio consolidation press and a load increment ratio of 1.0. The controlled rate of loading tests were made in a standard gear driven soil compression machine with proving ring to measure the vertical load. Full precautions were exercised to reduce system flexibility to a minimum, Table 2.8.

2.11.2 Rate of Compression

It is difficult to compare rates of compression for specimens loaded in increments, because the rate varies greatly during the test. The virgin compression of a specimen from group B, for example, occured during a 28-day period, or at an average rate of approximately 1% per day, but the actual rate varied from approximately 1% per min, during the first minute of each load application to approximately 1% per week at the end of such loading period.

The rates of compression for the various types of tests during loading from 2 to 4 kg per sq. cm are shown in Fig. 2.23. The 1 cm thick specimen (96-1-23) has the highest rate, averaging more than 3% per min during first loading and approximately 40% per hr. during the complete loading period. This high forced-rate of consolidation probably leads to an unusually high degree of disturbance. Specimen 96-1-27 was loaded at the slowest rate, a constant 7.4% per hr.

The laboratory rates of compression are all considerably faster than known field rates. Under the heavily loaded National Museum in Ottawa, the rate of compression was only 1/2% per yr. When specimen 96-1-23 was loaded from 2 to 4 ksc it compressed 1% in one tenth of a minute or approximately 10 million times faster. The maximum field rate is only approximately 1/50 of the rate of secondary compression.

2.12 CONCLUSIONS

Referring to Table 2.9 the following conclusions could be drawn:

1. A consistent increasing trend in the ratio of $(c_v)_{\text{performance}}/(c_v)_{\text{lab}}$ is identified when going from remoulded to undisturbed soil (puddle core to foundation). This is to be intuitively yet in no way quantitatively expected since the macrostructure becomes more dominant factor in undistrubed soils. Similarly the trend is more prominent with an increase in sensitivity (puddle core to Leda clay).
2. No one identifiable trend could be detected in the ratio of $(c_v)_{\text{performance}}/(c_v)_{\text{in situ}}$. It is evident that $(c_v)_{\text{in situ}}$ is totally irratic and not much relevance should be attached to it.
3. $(k_v)_{\text{in situ}}/(k_v)_{\text{lab}}$ has a consistent increasing trend when going from remoulded to undisturbed soil.

Although the zone surrounding the piezometer is disturbed yet it has the advantage of measuring the average permeability over a larger area of influence hence in comparing the macrostructure in the surrounding soil mass. Thus the increasing trend should be expected.

4. A better measurement tool is required to identify soil parameter so that a more consistant (less guess work) approach could be followed.

Prediction type	When prediction made	Results at time prediction made
A	Before event	-
B	During event	Not known
B1	During event	Known
C	After event	Not known
C1	After event	Known

Table 2.1 Classification of predictions, (Lambe, 1973).

SITE	ZONE	DESCRIPTION	INDEX VALUES LL	PL	CF	LABORATORY TEST VALUES C_v ft²/year	k cm/sec	IN SITU TEST VALUES C_v ft²/year	k cm/sec	FIELD PERFORMANCE C_v ft²/year
SELSET (ENGLAND)	FOUNDATION	BOULDER CLAY	32	13	24	25.0 d,h (40)	0.67*3 (40) 0.43*3 (80) x0.38 h (77)	460.0 C_s (80)	0.84 (80)	64.0 (30)
	FILL	BOULDER CLAY	29	15	20	24.0 d (40)	0.67*3 (40) 1.10*3 (12)	14.0 C_s (12)*2	1.2 (12)*2	30.0 (40)
	PUDDLE CORE	BOULDER CLAY	29	15	20	7.0 d (8) 16.0 d (40) 13.0 d (30)	0.67 (40) 0.77 (30)	84.0 C_v (30)	0.79 (30)	44.0 (8)*2
BALDERHEAD (ENGLAND)	FILL	BOULDER CLAY	28	14	18	25-170 d (46)	0.56*4 (53) 0.64-4.3 (5)	75.0 C_v (53)	0.7 (53)	128.0 (47) 100.0 (45)*5
DIDDINGTON (ENGLAND)	FOUNDATION	BOULDER CLAY AND OXFORD CLAY	58	20	38	12.0-4.3 d (40) 17.0 o (70) 9-5 t (20)	x2.2-0.17 (40)	7.5 C_s (9.4)	0.33 (9.4)	11.0 (15)
	FILL	BOULDER CLAY	58	20	38	6.0 d 1½" (30)	x0.4 (30)	1.4 C_s (16) 1.4 C_v (21)	0.87 (16) 0.18 (21)	5.0 C_s (34)
(ENGLAND) M.6 (KENDAL)	FILL	BOULDER CLAY	26	19	7	15.0 d (3) 30.0 d (9)	2.1 (5) 1.6 (11)	50.0 C_v (3)	4.9 (5) 2.8 (11)	20.0 (3) 50.0 (9)
FIDDLER'S FERRY (ENGLAND)	FOUNDATION	ESTUARINE CLAY	46	25	30	6.9 o (5.1) 8.2 o,h (5.1) 5.4 o (12.6) 9.2 o,h (12.6)	x0.72 (12.7) x1.03 (12.7)	200.0 C_v (11.8)	6.6 (12.7)	63.0 (5.1) 39.0 (12.6)
BACK WATER (DUNDEE) (SCOTLAND)	TRIAL EMBANKMENT	BOULDER CLAY	++ 27	10	-	60-80 r (1.50-30) 25-35*3r(12.5-20)				65-70.0 (25)
	MAIN EMBANKMENT	BOULDER CLAY	++ 27	10	-	65-75 r (1.50-30) 25-35*3r (12.5-20) 20.0 ir (10)		254.0 C_z (30)	6.50 (30)	70.0 (30)

x DENOTES k value calculated from C_v and m_v.

o DENOTES test on 3" diameter oedometer.

*3 Test on remoulded material.

*4 From test on remoulded material of similar index properties from Selset.

*5 Allowing for the decrease in total stress during consolidation as measured on a total stress cell.

( ) Denotes effective stress value to which test result applies, in psi.

d Denotes dissipation test on 4" diameter sample except where otherwise stated.

*2 Upper part of fill was slightly more sandy.

r Denotes tests performed in a Rowe consolidation cell.

ir Indirect method of obtaining C_v from k obtained from in situ tests (swelling type) and m_v values from consolidation tests in a Rowe cell.

*7 See sec. for details on how permeability data was obtained.

io Denotes indirectly obtained permeability from oedometer tests.

t From volume changes in consolidation stage of 1½" diameter triaxial test with side drains.

CF Denotes % less than 0.002 mm.

Table 2.2 Comparison of laboratory tests, in situ tests and field performance for 10 case studies.

SITE	ZONE	DESCRIPTION	INDEX VALUES LL	PL	CF	LABORATORY TEST VALUES C_v ft²/year	k cm/sec	IN SITU TEST VALUES C_v ft²/year	k cm/sec	FIELD PERFORMANCE C_v ft²/year
LYNDHURST (ENGLAND)	6 ft (Depth)	PEAT					*7 12.5 V 50.0 H		295 V 295 H	
	12 ft	MARL					*7 3.30 V 3.30 H		208 V 208 H	
	18 ft	ALGAE					*7 0.40 V 0.50 H		190 H	
	24 ft	A and C					*7 0.50 V 0.50 H		1.4 V 1.4 H	
	30 ft	CLAY					*7 0.45 V 0.42 H		0.50 V 0.50 H	
	36 ft	CLAY					*7 0.36 V 0.36 H		0.170 V 0.17 H	
	42 ft	CLAY					*7 0.25 V 0.27 H		0.09 V 0.09 H	
	48 ft	CLAY					*7 0.1 V 0.1 H		0.10 V 0.10 H	
ARLINGTON (ENGLAND)	5 ft (Depth)	WEALD CLAY	65	32	-	18*o (sq ft/yr)	5.0 io			
	8 ft		58	27	-	6*o	3.0 io			
	11 ft		59	26	-	16*o	4.0 io			
	20 ft		58	30	-	5*o	5.0 io	404* C_v (25)	21 (25)	4.0* C_v (25)
	23 ft		59	26	-	9*o	1.0 io			
	25 ft		42	20	-	5*o	2.0 io			
M.I.T. CAMPUS (CAMBRIDGE U.S.A.)	STIFF TO MEDIUM BOSTON BLUE CLAY ELEV. -12.5 → -45.0	BOSTON BLUE CLAY	50	25	-	cm/sec 30×10^{-6} C_{vs} o				350×10^{-6} C_{vs}
	SOFT BOSTON BLUE CLAY ELEV. -45.0 – -78.5		50	25	-	60×10^{-6} C_{vs} o				350×10^{-6} C_{vs}

x DENOTES k value calculated from C_v and m_v.

o DENOTES test on 3" diameter oedometer.

*1 Test on remoulded material.

*6 From test on remoulded material of similar index properties from Selset.

*5 Allowing for the decrease in total stress during consolidation as measured on a total stress cell.

( ) Denotes effective stress value to which test result applies, in psi.

d Denotes dissipation test on 4" diameter sample except where otherwise stated.

*2 Upper part of fill was slightly more sandy.

r Denotes tests performed in a Rowe consolidation cell.

ir Indirect method of obtaining C_v from k obtained from in situ tests (swelling type) and m_v values from consolidation tests in a Rowe cell.

*7 See sec. for details on how permeability data was obtained.

io Denotes indirectly obtained permeability from oedometer tests.

t From volume changes in consolidation stage of 1¼" diameter triaxial test with side drains.

CF Denotes % less than 0.002 mm.

Table 2.2 (cont.) Comparison of laboratory tests, in situ tests and field performance for 10 case studies.

Depth Below Ground Level (ft.)	Description	L.L.	P.L.	W.C.	γ (pcf)	Undrained Shear Strength (psf)	Sensitivity	Remarks
0 - 1.0	Topsoil							
1.0- 6.5	Firm mottled grey and brown fissured silty clay	46.2	24.6	38.8	118	760	1.3	Undrained strengths higher towards top of layer but less sensitive; no strong anisotropy in terms of undrained strength
6.5-10.0	Soft grey clay containing some organic matter			58.5				
10.0-17.0	Woody peat containing layers of soft fat organic clay			230.0	75	1160		Peat
		51.5	28.3	60.0		585	2.0	Clay layers

Table 2.3 Average soil properties at chainage 88 On Fiddler's Ferry test embankment.
(From Al-Dhahir et al. 1969)

Size	Percent passing
Gravel	82 - 72
Silt	54 - 42
Clay	20 - 12

Table 2.4 Particle size distribution of Boulder clay used in Backwater Dam construction.

Piezometer No.	Main dissipation value c_v ft²/yr. (m^2/yr.) 1st season	2nd season	In situ Constant Head Permeability-Consolidation Test Permeability x 10^{-8} cms/sec (x 10^{-10} m/sec)	c_v ft²/yr. (m^2/yr.) direct	c_v ft²/yr. (m^2/yr) indirect
D1	118 (11.0)	150 (13.9)	3.35	1650 (153.5)	160 (14.9)
4	180 (16.7)	-	53.50	-	2550 (237.0)
5	63 (5.9)	-	1.78	216 (20.1)	51 (4.7)
6	54 (5.0)	70 (6.5)	2.30	116 (10.8)	51 (4.7)
8	58 (5.4)	-	2.70	36 (3.3)	64 (5.9)
11	66 (6.1)	-	710.0 unreliable	-	-
12	69 (6.4)	-	1.60	138 (12.8)	29 (2.7
U1	44 (4.1)	unreliable	1.50	810 (75.2)	84 (7.8)
2	61 (5.7)	80 (7.4)	0.64	115 (10.7)	36 (3.3)
4	72 (6.7)	96 (8.9)	2.95	-	155 (14.4)
5	100 (9.3)	380 (35.3) unreliable	0.50	21 (1.9)	27 (2.5)
6	58 (5.4)	-	10.10	550 (51.1,	345 (32.1)
7	50 (4.6)	-	2.78	247 (22.9)	74 (6.9)
9	54 (5.0)	-	7.00	276 (25.6)	150 (13.9)
12	unreliable	-	1.80	72 (6.7)	33 (3.1)
13	72 (6.7)	-	5.10	66 (6.1)	88 (8.2)

Table 2.5 Coefficients of permeability and consolidation from field performance and insitu tests.(Backwater Dam)
(From Wilkinson et al. 1969)

Table E1. Laboratory and field values of c_v and k for Weald Clay

	Field				Laboratory					
Borehole or piezometer	CF1	CF2	CF3	CF5	9	39A	39A	39A	50	50
Chainage, ft	2100	2080	2060	2020	1000	1700	1700	1700	900	900
Depth below o.g.l., ft	20	20	20	20	23	5	8	11	20	25
P.L.%	-	30	33	34	26	32	27	26	24	20
L.L.%	-	62	43	75	59	65	58	59	54	42
Cell pressure for 4 in. dia. triaxial dissipation, lb/sq. in.	-	-	-	-	-	-	30	-	30	-
Consolidation pressure range for 3 in. dia. oedometer, lb/sq. in	-	-	-	-	16 to 31	16 to 31	-	16 to 31	-	16 to 31
Overburden pressure, lb/sq. in.	25	25	25	25	-	-	-	-	-	-
k(lab)*, or k(in situ), 10^{-9} cm/s	22	16	35	13	1	5	3	4	5	2
c_v(lab), or c_v(in situ), sq.ft/year	600	700	15	300	9	18	6	16	5	5
Dissipation after 0.42 year, U%	4.5	0	6.7	18.3	-	-	-	-	-	-
c_v(performance), sq.ft/year, calculated from U	0.6	Small	1.4	10	-	-	-	-	-	-

* Note that k(lab) is derived from c_v(lab) and m_v(lab)

Table 2.7 Laboratory and field values of c_v and k for Weald Clay. (From Beaven et al. 1969)

Material	Depth feet	10^{-6} k_v cm/min Field	Lab	10^{-6} k_h cm/min Field	Lab
Peat	6	17700	750	17700	3000
Marl	12	12500	200	12500	200
Algae	18	11500	24	11500	30
A & C	24	83	32	83	34
Clay	30	31.3	27	31.3	25
"	36	10.4	22	10.4	22
"	42	5.2*	15	5.2*	18
"	48	6.3	6	6.3	6

*Results very scattered

Table 2.6 Vertical and horizontal coefficients of permeability from in situ tests at a site near Lyndhurst. (from Raymond et al. 1969)

Test Series	Specimen No.	Initial Height, H, in centimeters	Length of Drainage Path	Nat. Water Content, in %	Nat. Void Ratio	Preconsol. Pressure, in kilograms per square centimeter	Loading
A	96-1-12	2	H	60.1	1.71	1.80	Daily increments
	96-1-16	2	H	57.8	1.63	1.80	
	96-1-18	2	H	57.0	1.63	1.85	
	at end of primary					2.65	
	96-1-19	1	H	59.9	1.67	2.20	
	96-1-21	1	H	59.0	1.67	1.7[a]	
B	96-1-13	2	H/2	59.4	1.69	1.40	Weekly increments
	96-1-20	2	H/2	57.3	1.63	1.33	
C	96-1-22	2	H	56.1	1.60	3.00	At end of primary
	96-1-23	1	H	57.5	1.64	2.62	
D	96-1-24	1	H	58.8	1.67	2.20	Constant rate
	96-1-25	1	H	59.0	1.67	2.47	
	96-1-27	2	H	58.5	1.67	2.47	

[a] By chance, the pressure of 2 kg per sq cm was allowed to act for 4,300 min. The additional secondary compression deflected the pressure-void ratio curve more than normal, causing a lower interpretation of preconsolidation pressure.

Table 2.8 Sample nomenclature and consolidation data from tests on Leda clay. (From Crawford 1953)

SITE	ZONE	INDEX VALUES LL	PL	CF	$(C_v)^*$ performance / (C_v) lab	$(C_v)'$ performance / (C_v) ** in situ	$(k)v$ in situ / $(k)v^{**}$ lab
SELSET	FOUNDATION	32	13	24	(1) 3.0 †		2.0 †
	FILL	29	15	20	(1) 1.2 †		1.0 =
	PUDDLE CORE	29	15	20	(1) 6.0 †	0.5 ↓	1.0 =
BALDERHEAD	FILL	28	14	18	(1) 1.1 †	1.8 †	
DIDDINGTON	FOUNDATION	58	20	38	(1) 1.5 †	1.5 †	
	FILL	58	20	38	(1) 2.0 †	0.4 ↓	< 0.45 ↓
M.6	FILL	26	19	7	(1) 1.5 †	0.4 ↓	2.0 †
FIDDLER'S FERRY	FOUNDATION	46	25	30	(1) 9.0 †	0.3 ↓	9.0-6.0 †
BACKWATER	TRIAL EMBANKMENT	27	10	-	(2) 1.0 =		
	MAIN EMBANKMENT	27	10	-	(2) 1.0 =	3.5 †	
LYNDHURST	6 ft (Depth)						25.0 †
	12 ft						68.0 †
	18 ft						475.0 †
	24 ft						2.8 †
	30 ft						1.1 †
	36 ft						0.4 ↓
	42 ft						0.3 ↓
	48 ft						1.0 =
ARLINGTON	10 ft (Depth)	59	26	-	(3) 0.4 ↓	0.01 ↓	7.0 †
M.I.T. CAMPUS	-45 ft (Elevation)	50	25	-	(3) 6.0 †		
NATIONAL MUSEUM	FOUNDATION †	54	25		(3) 10^6 †		

(1) LAB VALUE OBTAINED FROM TRIAXIAL DISSIPATION TESTS.
(2) LAB VALUE OBTAINED FROM CONSOLIDATION TESTS IN A ROWE CELL.
(3) LAB VALUE OBTAINED FROM CONSOLIDATION TESTS IN AN OEDOMETER CELL.
(4) CONSTANT HEAD IN SITU TESTS. (SWELLING/CONSOLIDATION).

* $(C_v)_{performance}$ from matching piezometer records using Terzaghi's one-dimensional unlinked theory.
** $(C_v)_{in\ situ}$ & $(k)_{in\ situ}$ from constant head tests using Gibson's (1963) interpretation method.
† Sensitivity = 50

Table 2.9 Summary of laboratory, in situ and field performance comparisons.

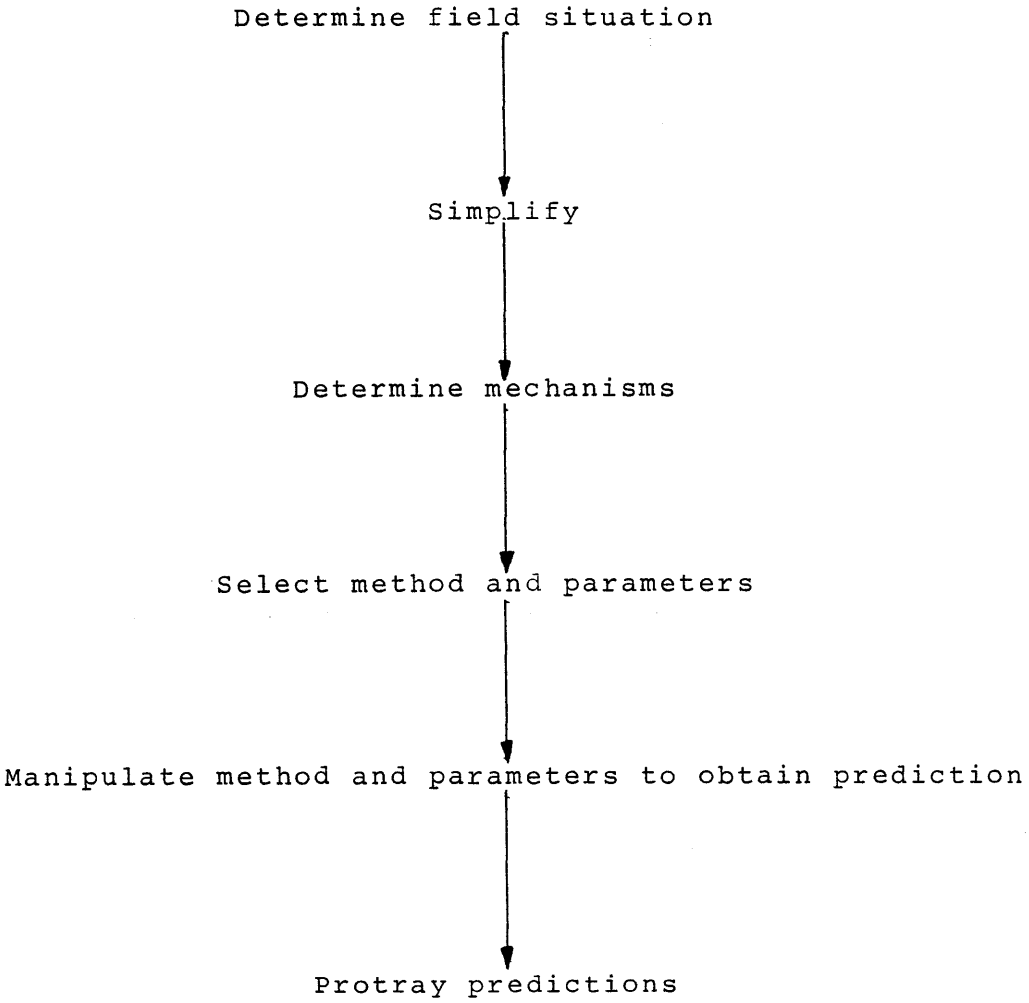

Figure 2.1 Lambe's cognitive problem solving model.

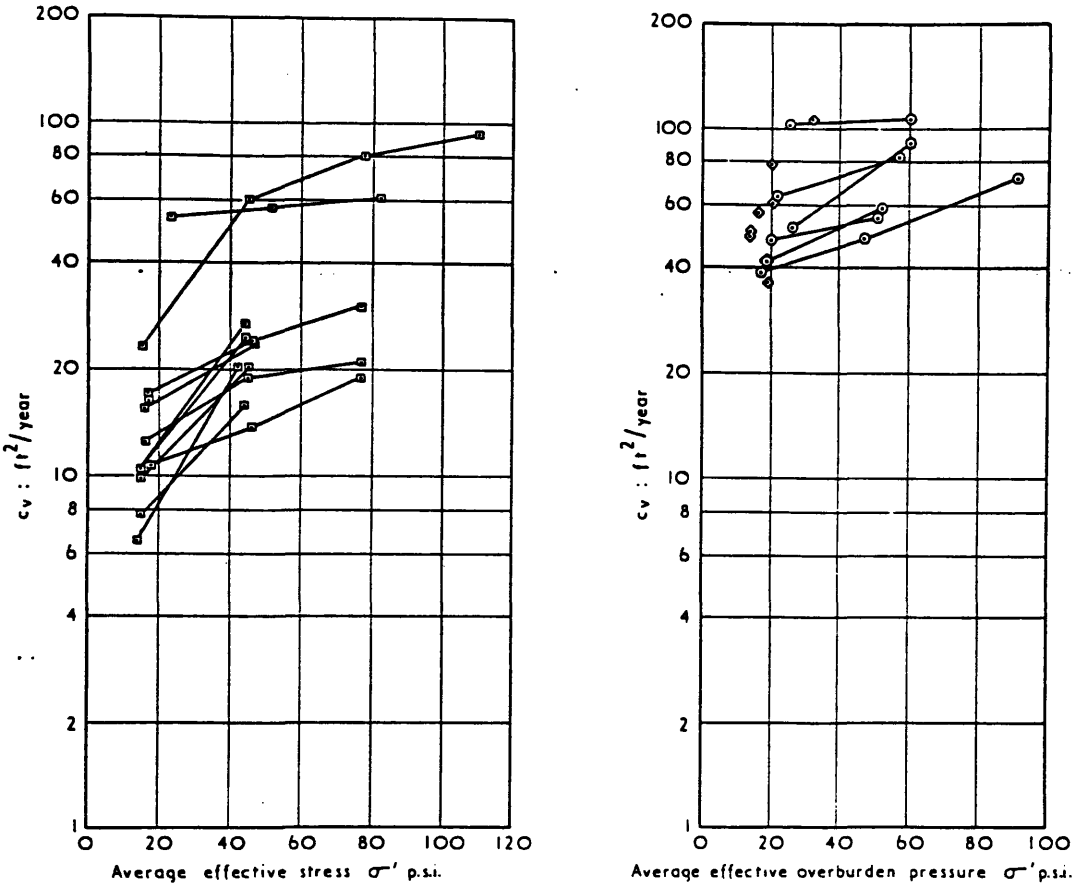

Figure 2.2

Selset boulder clay foundation: comparison of values of c_v from laboratory dissipation tests on undisturbed samples (a), with field performance values (b)

(From Bishop et al. 1969)

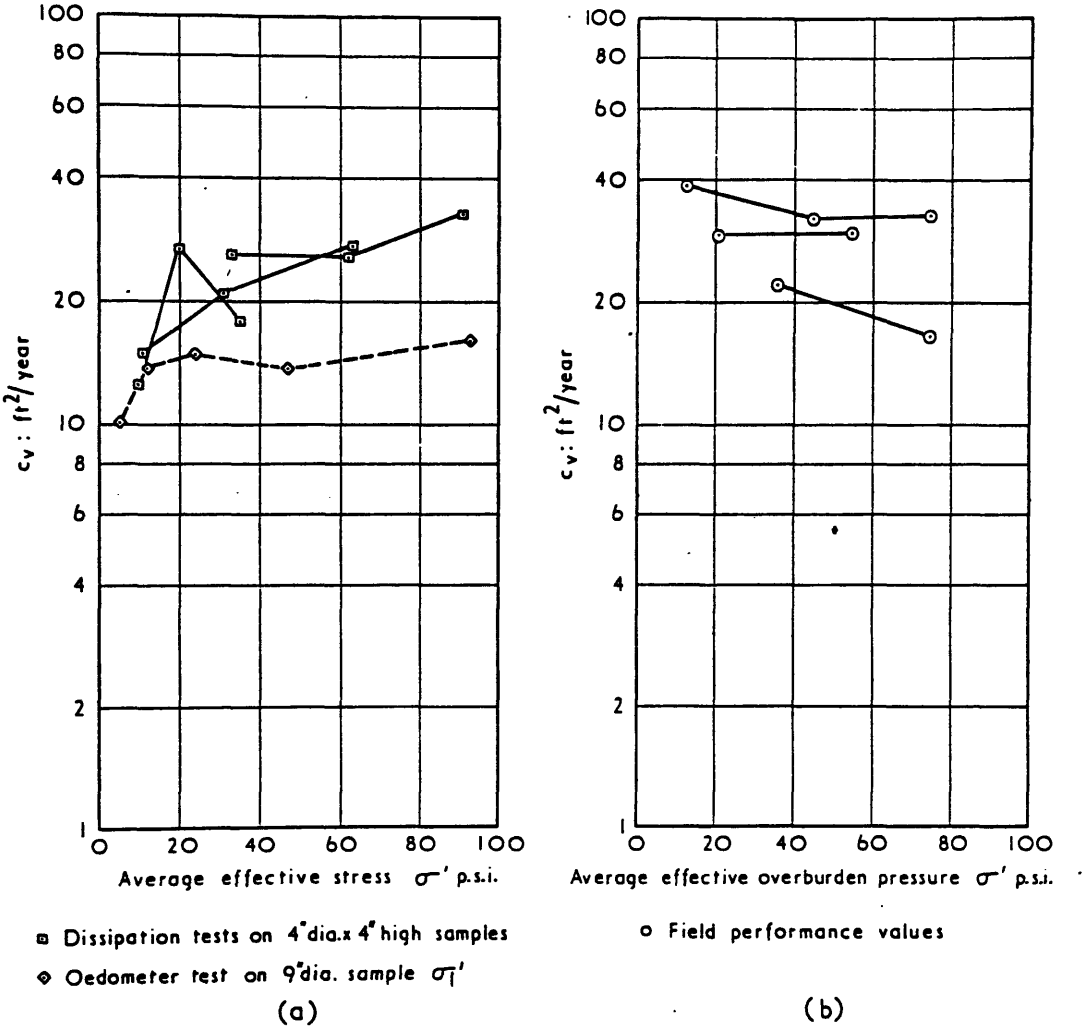

Figure 2.3

Selset boulder clay fill: comparison of values of c_v from laboratory dissipation tests on compacted samples (a), with field performance values (b)
(From Bishop et al. 1969)

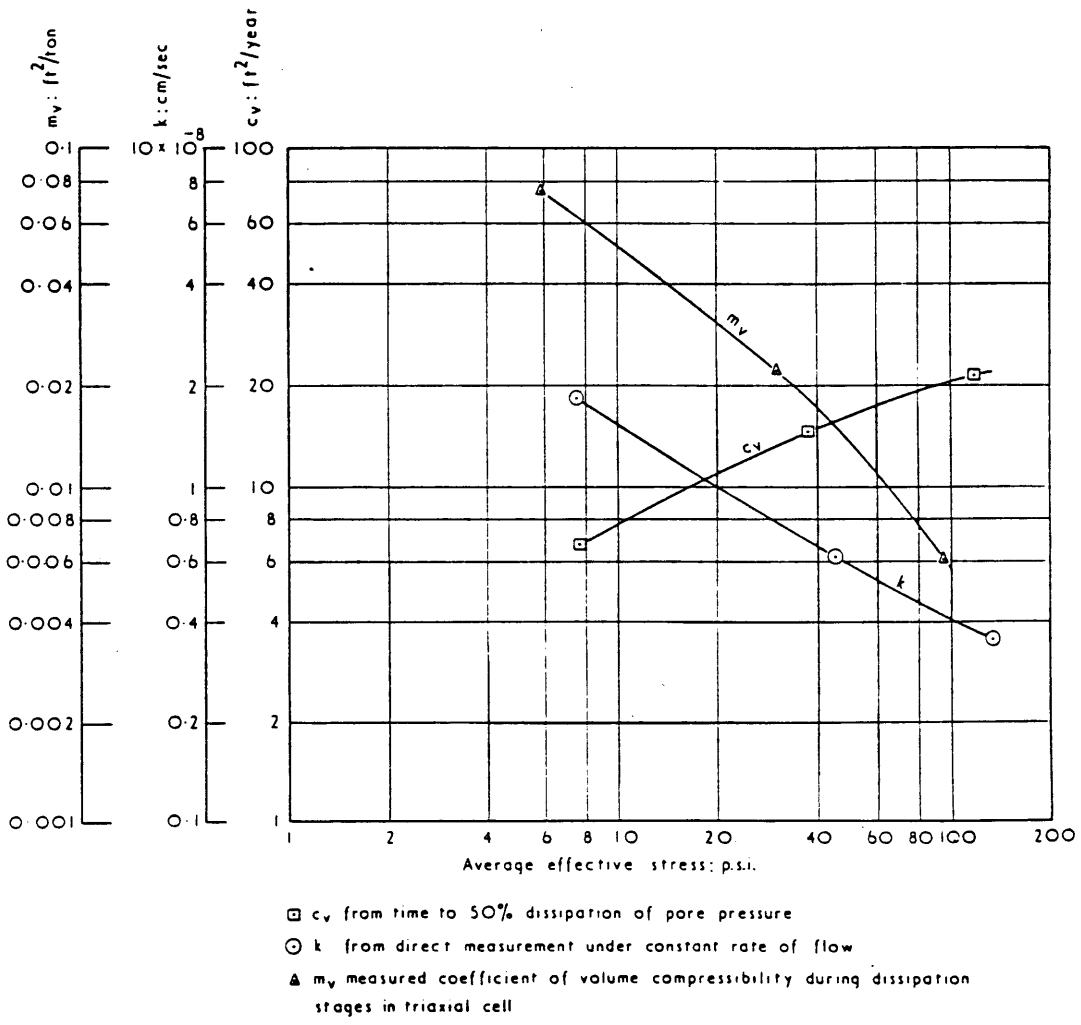

⊡ c_v from time to 50% dissipation of pore pressure

⊙ k from direct measurement under constant rate of flow

▲ m_v measured coefficient of volume compressibility during dissipation stages in triaxial cell

Figure 2.4

Selset boulder clay puddle core: values of c_v, m_v and k by direct measurement on a remoulded sample

(From Bishop et al. 1969)

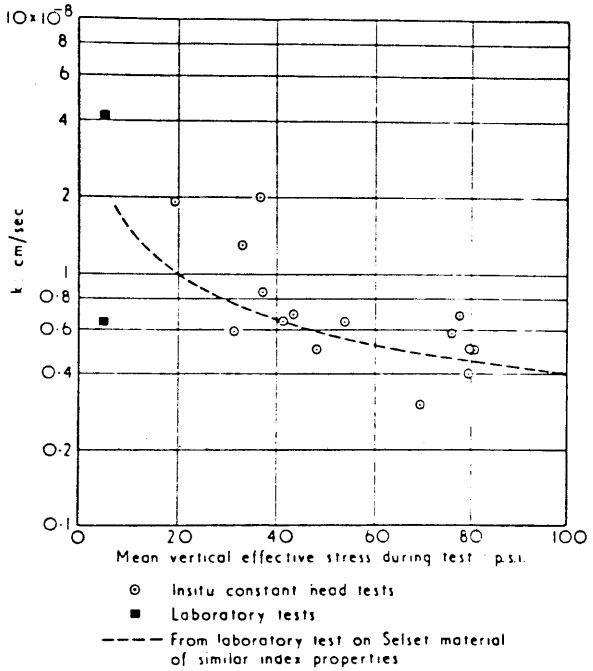

Figure 2.5

Balderhead boulder clay fill: values of k from insitu constant head tests in the rolled core compared with laboratory values on Balderhead clay and on Selset puddle core material of similar index properties

(From Bishop et al. 1969)

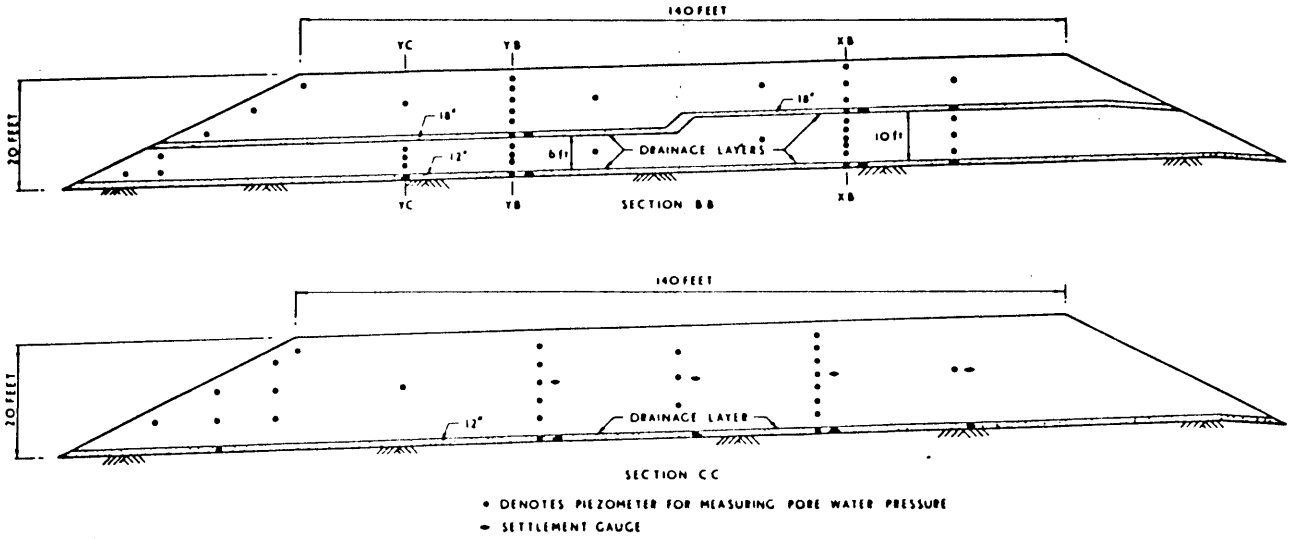

Figure 2.6

Cross sections of the M.6 Motorway Trial embankment showing positions of piezometers

(From Bishop et al. 1969)

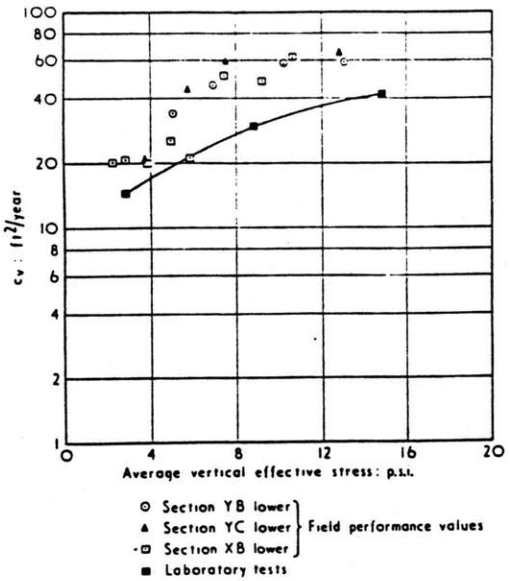

M.6 boulder clay fill: comparison of values of c_v from laboratory dissipation tests on a recompacted sample with field performance values

Figure 2.7
(From Bishop et al. 1969)

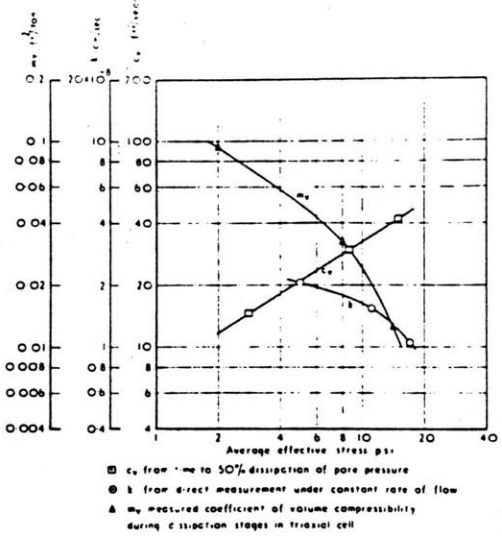

M.6 boulder clay fill: values of c_v, m_v and k by direct measurement on a recompacted sample

Figure 2.8
(From Bishop et al. 1969)

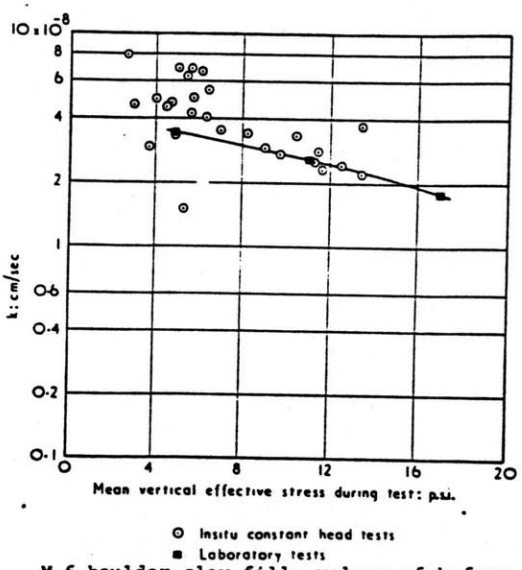

M.6 boulder clay fill: values of k from insitu constant head tests compared with laboratory values obtained by direct measurement

Figure 2.9
(From Bishop et al. 1969)

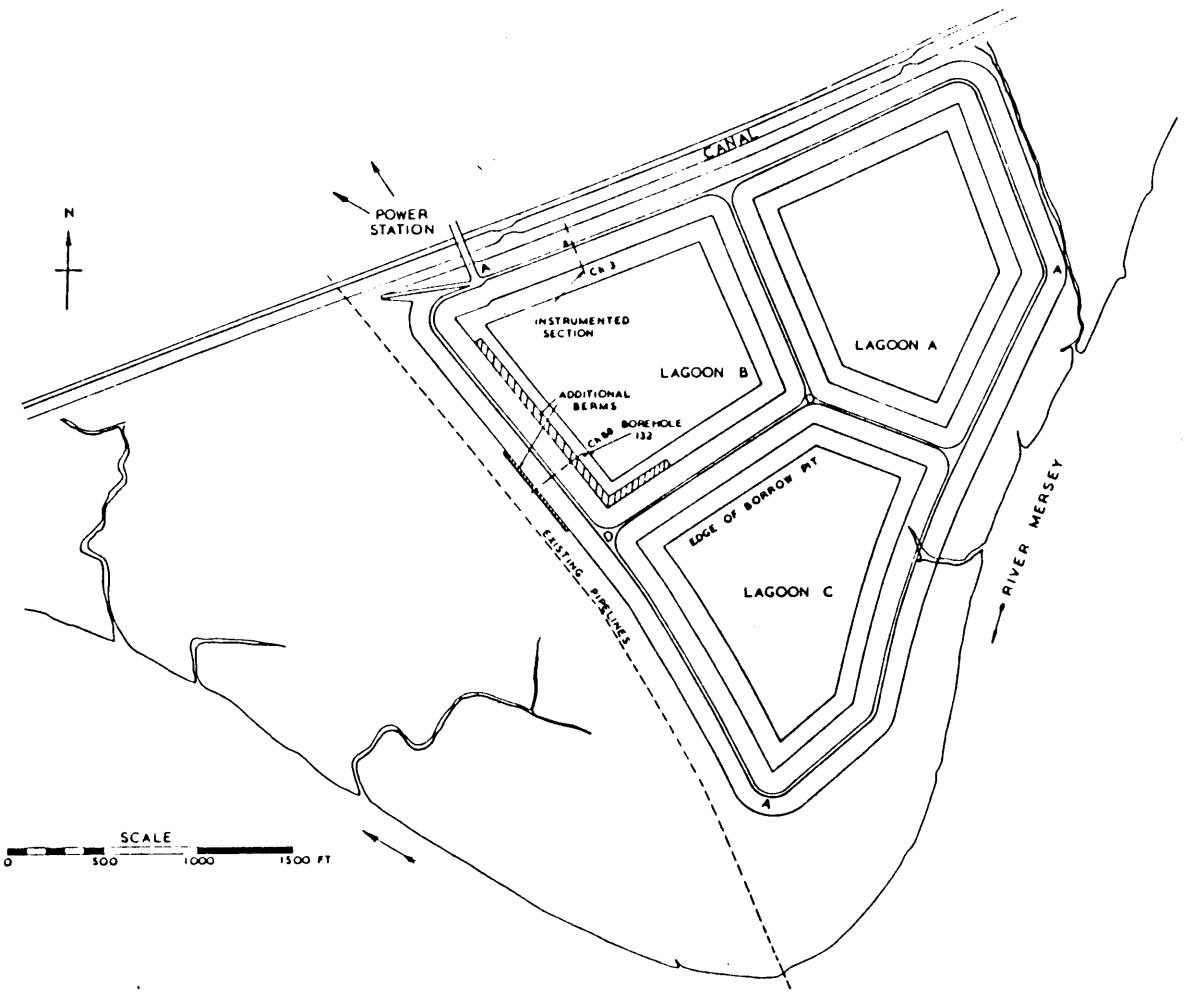

Figure 2.10 Plan view of Fiddler's Ferry power station lagoons and embankment (From Al-Dhahir 1969)

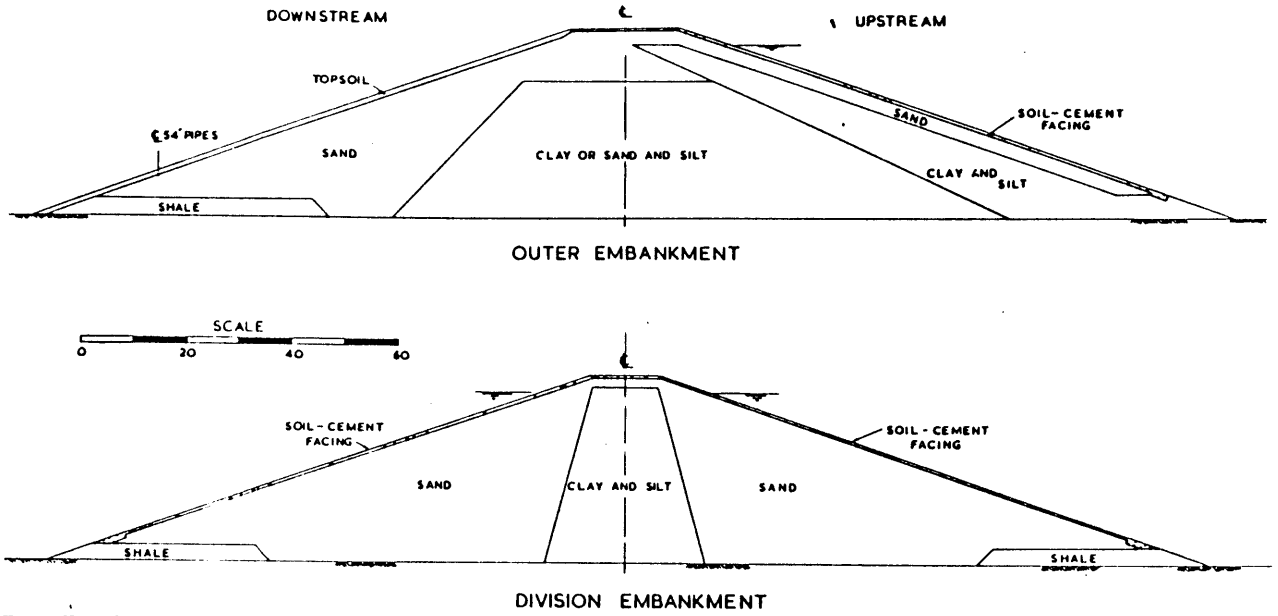

Fig. No. 2 Embankment Cross-Sections.

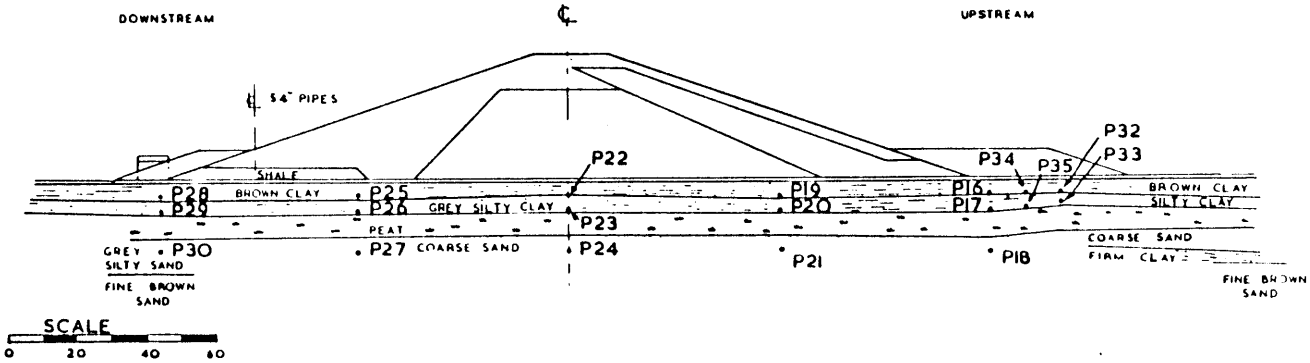

Figure 2.11 Instrumented cross section at chainage 88 on Fiddler's Ferry embankment.
(from Al-Dhahir 1969)

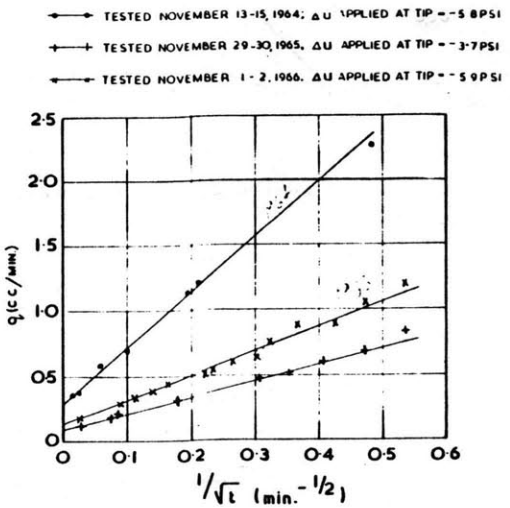

Figure 2.12 Constant head tests at P19.

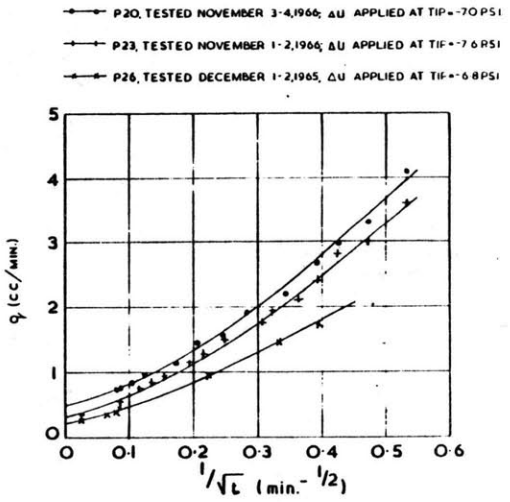

Figure 2.13 Constant head tests at P20, P23 & P26.

(From Al-Dhahir 1969)

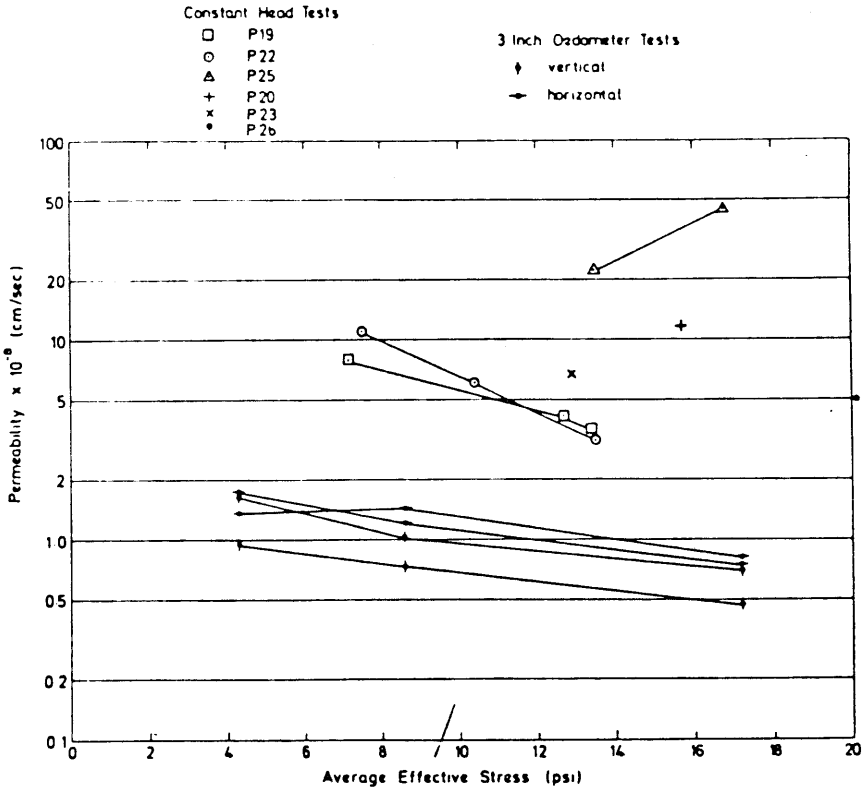

Figure 2.14 **Variation of Permeability with average effective stress.**

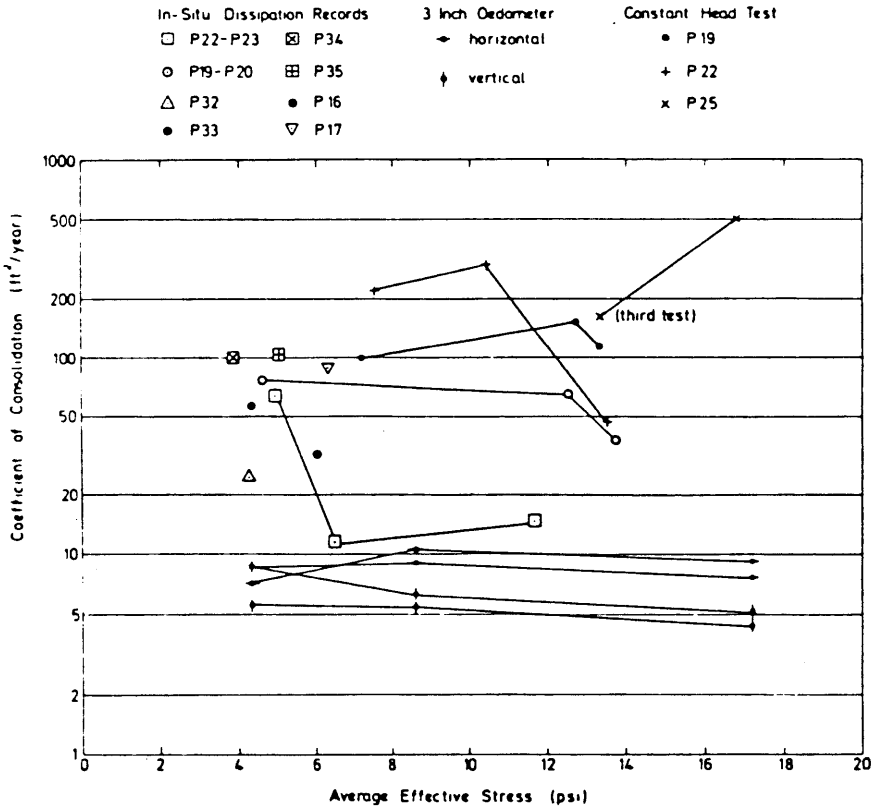

Figure 2.15 **Variation of Coefficient of Consolidation with average effective stress.**
(From Al-Dhahir et al. 1969)

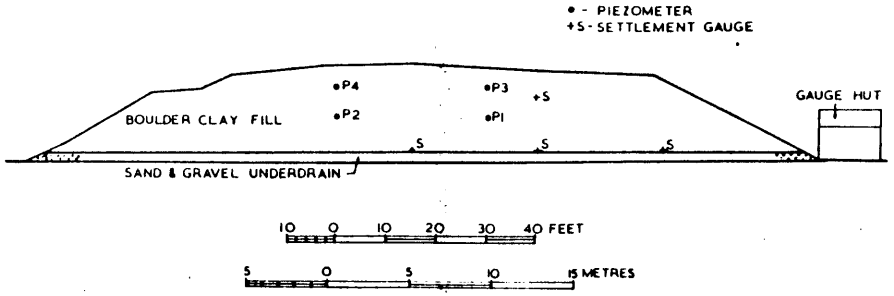

Figure 2.16 (a) Cross section of trial embankment showing positions of fill piezometers and settlement gauges.
(Backwater Dam, from Wilkinson et al. 1969)

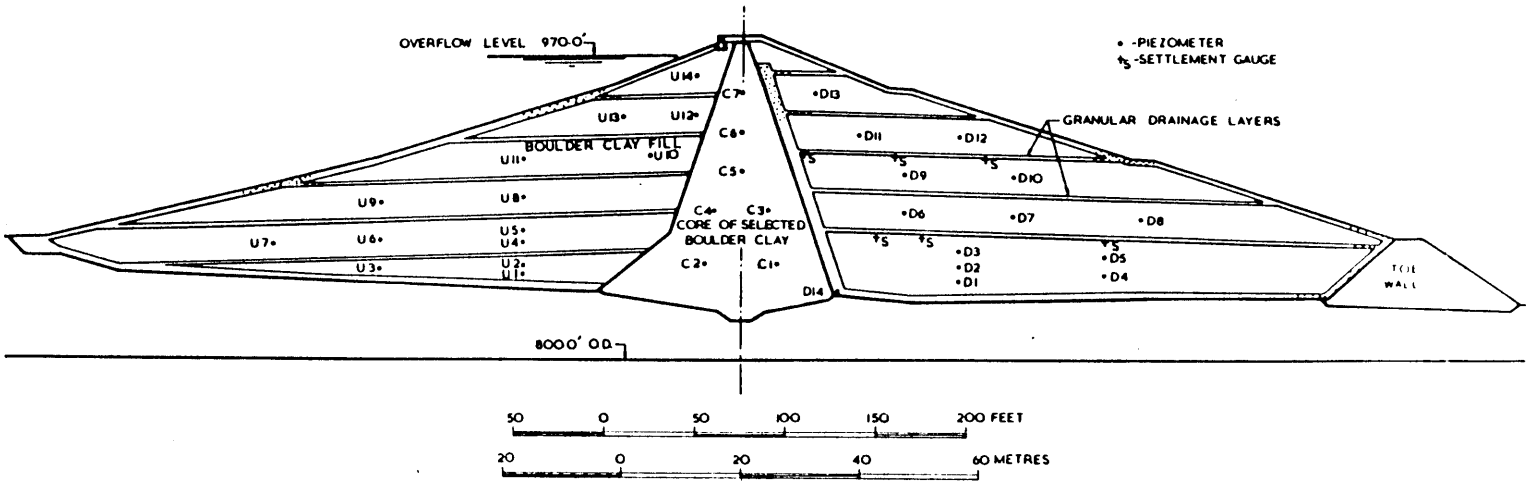

Figure 2.16 (b)
Cross section of the dam showing positions of fill piezometers and settlement gauges.
(From Wilkinson et al. 1969)

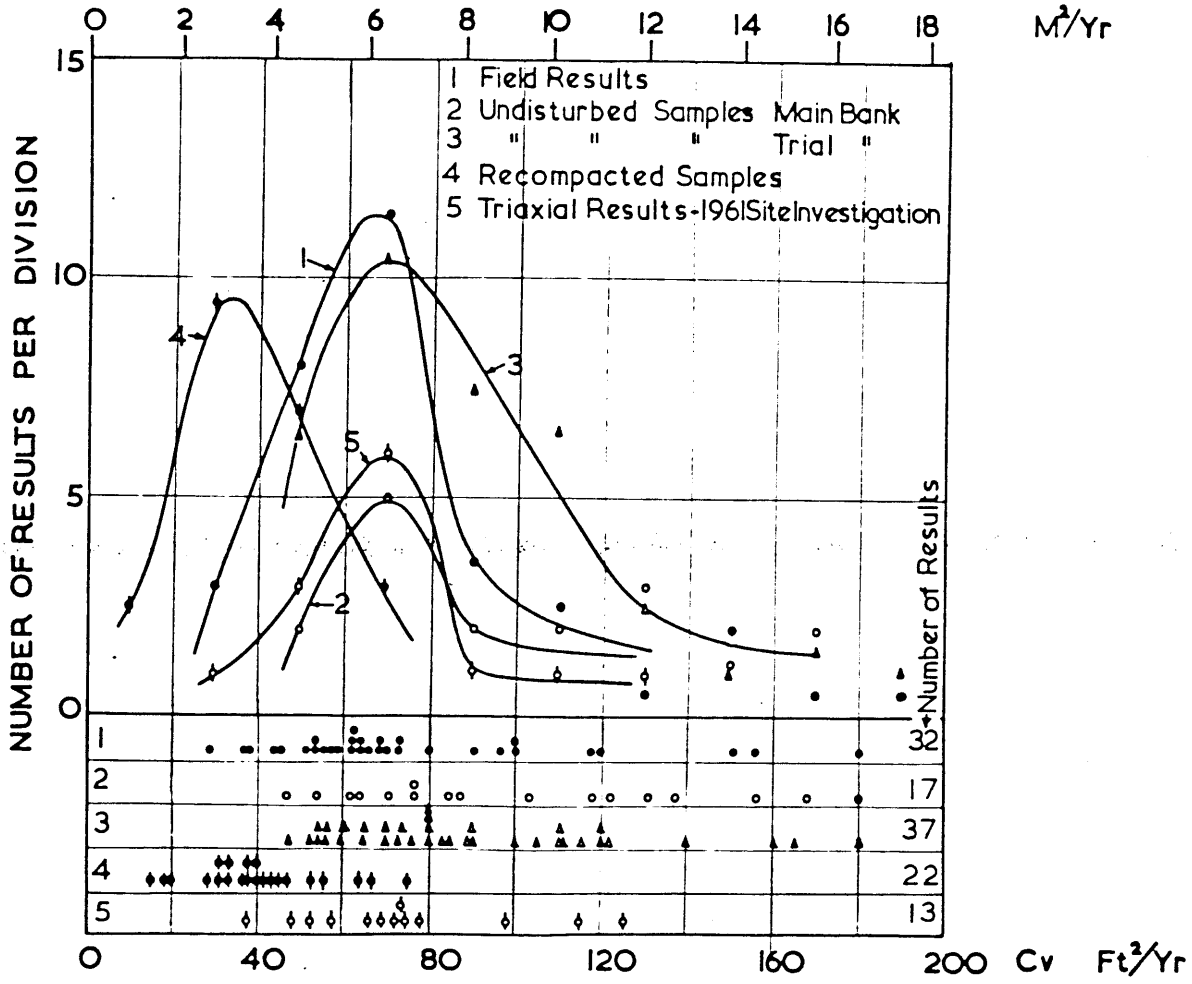

Figure 2.17 Frequency distribution curves of c_v comparing field behaviour and laboratory test results.
(From Wilkinson et al. 1969)

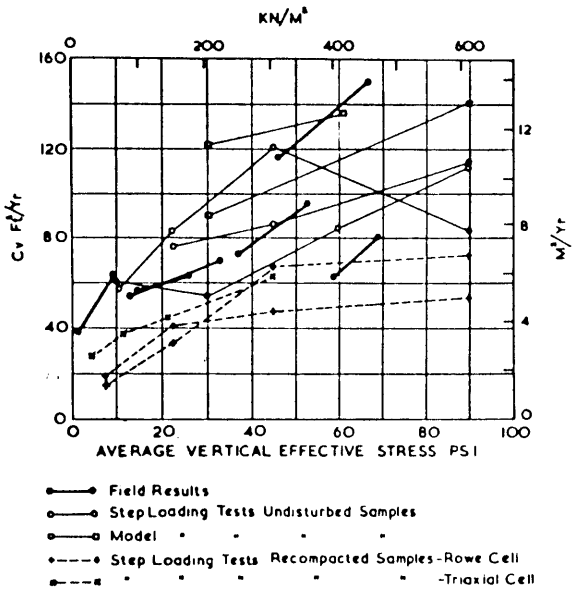

Typical relationships between c_v and average vertical effective stress for field performance and laboratory test results.

(Backwater Dam, from Wilkinson et al. 1969)

Figure 2.18

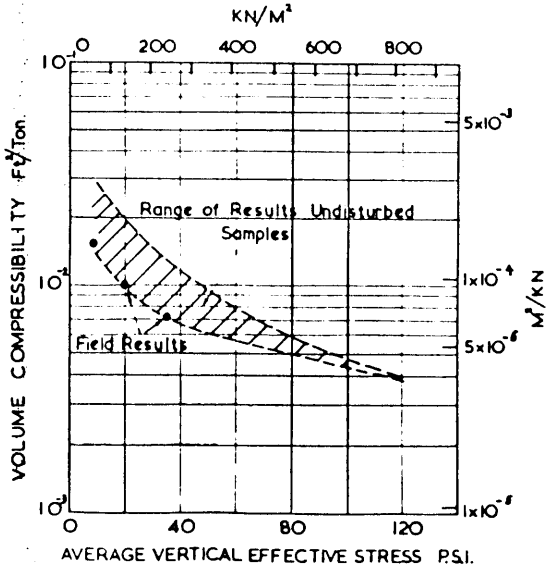

Relationship between m_v and average vertical effective stress for the main embankment performance and laboratory tests on undisturbed embankment samples.

(Backwater Dam, from Wilkinson et al. 1969)

Figure 2.19

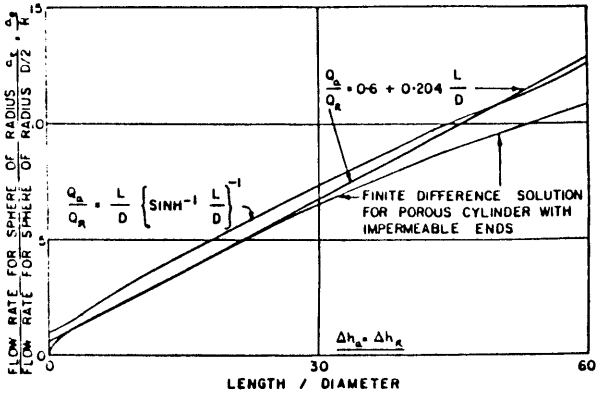

Figure 2.20 Ratio of flow rate between a spherical and a cylindrical piezometer tip
(From Raymond et al. 1969)

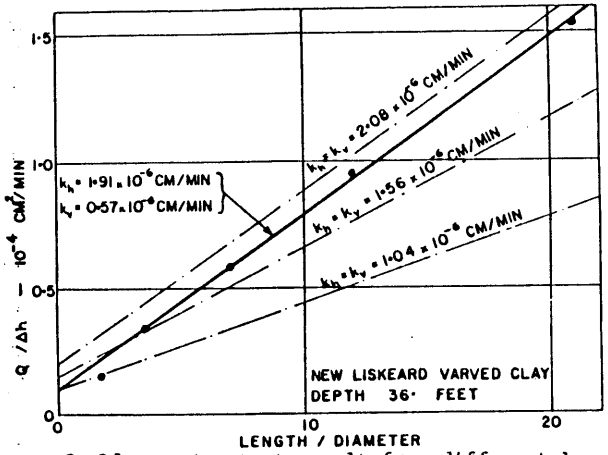

Figure 2.21 In-situ test result from different length tips
(From Raymond et al. 1969)

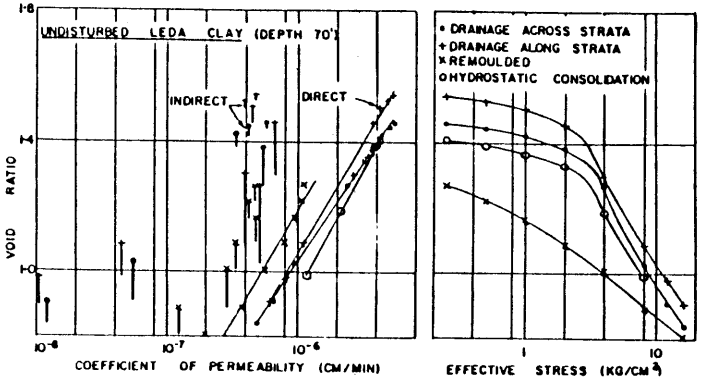

Figure 2.22 Typical laboratory results on Leda clay.
(From Raymond et al. 1969)

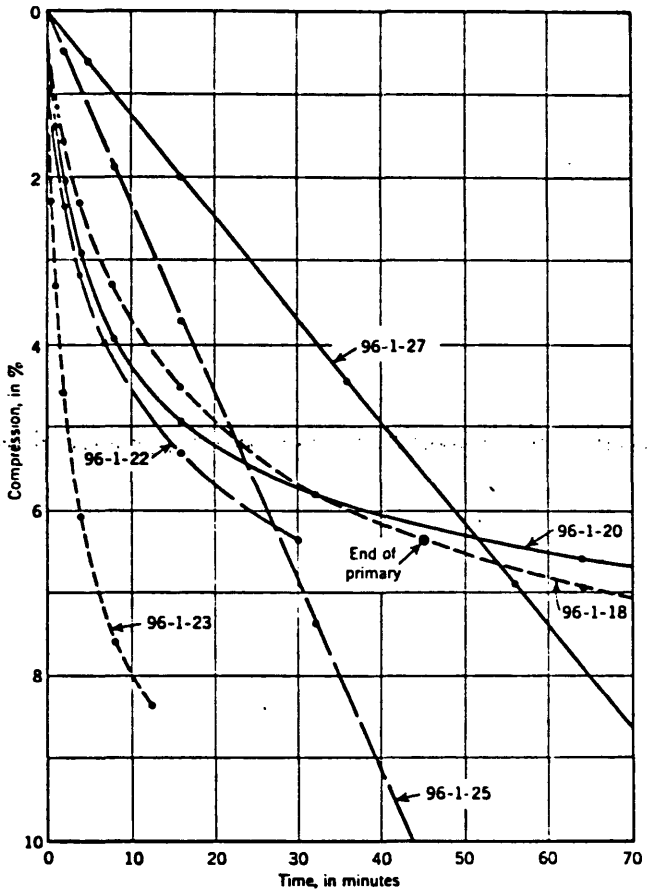

Figure 2.23 –RATE OF COMPRESSION WITH VARIOUS METHODS OF LOADING WHEN LOADED FROM 2 TO 4 KG PER SQ CM
(From Crawford et al. 1953)

CHAPTER 3

A SIMPLIFIED SYSTEMS APPROACH FOR SOLVING COMPLICATED PROBLEMS

3.1 INTRODUCTION

In our current endeavor towards achieving a better understanding of the various mechanisms involved with the problem of prediction of in situ soil properties, we are faced with problems characterized by multiplicity of interactions (the problem is complicated); gaps in our knowledge of the situation and computational limitation. We need a comprehensive, systematic attack with due consideration of multiple interactions. We need a method which accepts complexity and uncertainty as an inherent part of any problem and applies rational procedures to attack the problem.

How do we solve problems? This is a question that has no unique answer. Probably there are four dependent interacting processes which can be distinguished in problem solving process, namely:

(a) The problem is defined;

(b) Alternative solutions are generated;

(c) The solutions are evaluated; and

(d) An iterative procedure is followed.

In the definition of the problem, we consider what it is we want to do, how we will judge a solution (or part of a solution), and what constraints we must accomodate. The generation of alternative solution produces descriptions of actions which may solve our problem. Finally, we evaluate the possible solutions. However, the process is not that simple. We do not follow such a simple linear or one-way procedure, we double back and repeat ourselves many times. We usually oscillate from one function to another. We do this in an almost random manner until, finally, we exit Figure 3.1 illustrates this procedure. The result of our effort is an ordered set of solutions. There is no way to determine that we have the best possible solution. We must always admit that we have not thought of every solution and that a better one may exist.

3.2 IMPORTANT SYSTEMS CONCEPTS

The word system derives from the Greek "Systema" and means "an assemblage of objects united by some form of regular interaction or interdependence". The functional uniqueness of a system derives from the relation among its parts. A system is identified by its functions. Furthermore a system is a collection of systems.

Let's use a "set diagram" to represent some of the

things mentioned above. In Figure 3.2 (a), let each point in the area enclosed by the dashed line represent a system; then a system is a group of points or an area in this "universe of systems".

Notice in part (b) that another group of points (a system) can overlap the first group, indicating that the parts of one system may function in another system. In part (c) also notice that system 1 can be constructed from system A + system B + system C, illustrating that a system is composed of subsystems.

When we isolate an area (group or subsystems), as system 1 in the diagram, then we call the remaining area (in the "Universe of Systems") the total environment. Often in a problem-solving situation, for all practical purposes, not all elements in the universe affect the performance of the system, nor are all elements under the control of the decision maker. The environment of the system consists of these elements which affect the system performance but are not under the direct control of the decision maker. Fig. 3.2 (d) classifies this point. The striped area labeled "system" specifies the points often referred to as decision elements, i.e., elements which can be adjusted by the decision maker and can affect the performance of the system. The specification of the boundaries between the area labeled "environment" and "system" clearly is a problem.

3.3 BLACK BOX VIEW OF SYSTEMS

Systems feed on input to produce output. As the system becomes more complex, the number of inputs and outputs tends to increase. Several important points should be regarded in connection with identifying or assigning inputs and outputs.

The first important point is that system inputs and outputs are normally parts of the system, not of the environment. Figure 3.3 clearly shows that. Although an input may be drawn from the environment in the physical sense, it nevertheless is usually an element over which we have control and hence it is not part of the environment in the systems sense as defined earlier. Input elements which we choose are called decision parameters. Their values are determined by the decision maker. Elements which we cannot control are called environmental constraints.

The identity of a system lies in its output - in what it does. It is more important in systems analysis that important outputs of a system be properly determined. A guideline for determining principal system outputs is to ask a series of questions like the following:

What is being accomplished?

What is being produced?

What is the major activity?

What is the goal? Function? Objective?

Why are we trying to accomplish, produce, etc..., this or that?

In identifying system outputs, a helpful guideline is to realize that they are usually dependent parameters. That is, they are affected by other elements within the system. They tend to be effects not causes. One can observe what a system does by a so called black box approach. We observe the response or output for a given stimulus or input. If the output is simply related to the input and not affected by feedback to the input (and subsequent reprocessing by the black box), the system is said to be a feed forward system. If the output is fed back and coupled to the input, the system is a feedback system. Fig. 3.4 (a) & (b) represent schematically a feedforward and a feedback system. Control in a system is achieved by feedback, which can be positive or negative. When the output of a system is changed, e.g., goes up due to some disturbance or input, then the feedback system can either reinforce this change (positive feedback) or can counteract this change (negative feedback).

Most systems reflect an overall negative feedback influence. This is observed in their tendency toward stability. Let us quantify the concepts of feedback by introducing the notion of a transfere function for some simple systems. The transfere function of a system is that

operation which transforms input to output in a system. Figure 3.5 (a) shows a system having k as its multiplicative factor relating output), to input, I. Using this notation, Figure 3.5 (b) & (c) outline some simple procedures and results for finding the transfer function of systems.

For the system to remain stable, a change in output, ΔO, for a given change in input, ΔI, must satisfy the criterion:

$$\frac{\Delta O}{\Delta I} < 1.$$

If this condition is not satisfied, the output of the system "blows up". This situation is a positive feedback case and is depicted in the arrow diagram in Fig. 3.6 (a).

Stability is normally achieved by negative feedback. In this case an increase in I increases I_1, which increases O which decreases I_1, which decreases O which increases I_1, which increases O, etc. This is shown in Fig. 3.6 (b).

Applying the stability criteria to the relation derived in Figure 3.5 (c), we have that:

$$\frac{k}{1+k} < 1$$

In general, the stability of such a system will depend on the magnitude and sign of the gain, k, the magnitude and sign of the feedback, and on time delays in the system. Time

delays can produce instability or oscillations in systems that might otherwise be stable. The stability of a system will also depend on the character of the input. The behavior of a system for one kind of signal may be very different than that for another.

3.4 REPRESENTATIONS OF REALITY, THE SYSTEMS MODEL

In previous sections we discussed, in part, the complexity of reality. We used words to describe or perception of the real word, and associated certain mechanistic properties, e.g., input, output, and feedback. Simple diagrams helped to explain complex systems. In short, a systems description of reality - a systems model of reality, was presented.

In the general sense, a model is a description or perception of a thing in existence or being planned. A model is a representation of a real or a planned system.

In no field is the model used more widely and with greater variety than in systems analysis. The multidisciplinary nature of contemporary problems demands the use of models of all sorts that fit the particular aspect under consideration. The complexity of such problems and the philosophy of the systems approach demand the organization and simplification that models can produce. Indeed, the systems view

itself as a model of reality that has been called "the science of organized complexity". There is no way that real problems can be "solved" without understanding and representing the important facts and relationships that underlie the situation. This is the heart of the modeling process; it is the heart of the problem-solving process.

3.4.1 The Nature of Models

As a representation of a real or a planned system, a model possesses the following characteristics:

(1) It is usually simpler;

(2) Easier to understand;

(3) Easier to construct, and

(4) Easier to manipulate than the thing it represents.

Models are approximate, uncertain, and incomplete. If they were not such, they would be the real system. Often, a model is used to make a decision within the problem-solving process. This decision is sometimes made on the basis of a very crude model. A "ball park" prediction or a "limiting case" kind of consideration. We do this because the crude model is sufficient to make the decision, there is no need to spend the extra resources to construct a more refined version. The ultimate value of a model resides in its ability to help us make a decision or to answer an important question. The model is a means to an end, decision making.

information we have, uncertain as it may be, to describe the system. We should accept uncertainty as a fact of life when using system approach and use approximations abundantly. However, we should always determine the sensitivity of the model's output to the uncertainty involved and the approximations used.

The model is determined by the questions being asked and the process being represented. It is a substitute for the system. Thus, the same system can be represented by different forms of models, the forms being determined by the questions being asked. The correctness of the model is determined not only by how well it represents the process, but also by how well it answers the questions being asked. Often, the problem solver confines himself to the use of a certain type of model. He forces the problem to fit the model rather than vice versa.

3.4.2 The Systems Approach, A Model for Problem Solving

The systems approach is a model for problem solving. It consists of a non-algorithmic, iterative series of overlapping processes: defining the problem, generating alternatives, and evaluating alternatives. The three basic processes involve modeling. The models are generated by the questions associated with the basic steps of system

The object, then, is to construct a model which is good enough, just adequate to serve the intended purpose.

We often must force ourselves to quit developing a model that has already provided an answer we need. It is easy to get caught up in useless refinements in order to satisfy perfectionalism which we have been taught to strive for. We should adopt a "sufficientism" philosophy which has a theme, "precision for decision", i.e., just make the model precise enough to make the needed decision. Perfection is a costly (and unattainable) venture in model building. Approximation becomes a necessity. The relationships between important variables are so often complex that we are forced to make simple educated guesses as a beginning to a solution.

We often get a grasp on a problem by using analogy. That is, we develop a preliminary solution to a problem at hand by finding a similar or related problem for which we know the solution. Frequently, the analogous problem is in a different area, and usually the similarity is a mathematical one.

Uncertainty is inevitable in model building. Many times the model is constructed to predict future status or values of parameters of the system and its environment. Parameters and input data are uncertain. We must use the

approach. For example, questions associated with these processes include:

Defining the Problem:

What is the problem?

What is the value system?

How will we pick among alternatives?

What are the constraints?

Generating Alternatives:

What are the alternatives?

How will these alternatives operate under the conditions (constraints) of the problem?

What will they produce?

Evaluating Alternatives:

Which alternative do I pick?

What are the factors affecting the worth of each alternative?

These questions and others associated with the basic processes demand the use of models which will differ in type. We must be prepared to work with a host of different models which respond to these questions at hand.

3.4.3 Types of Models

Models are often contrasted as follows:

According to	Types
Origin	Empirical - Theoretical
Function	Prescriptive - Descriptive
Element representation	Iconic - Analogue - Symbolic
Complexity	Linear - Nonlinear
Temporal characteristics	Static - Dynamic
Nature of changes	Continuous - Discrete
Execution technique	Numerical - Analytical
Predictability	Deterministic-Probabilistic

The choice of the model is determined by the intended purpose of the model. Hence, the contrast of interest in systems analysis is between prescriptive and descriptive models. If a model describes facts and relationships, it is a descriptive model. If, on the other hand, it reflects a value system, it is prescriptive. However, more than often, models contain a bit of both prescriptive and descriptive. Thus, a prescriptive or normative model is a representation of what ought to be. It is a set of rules, procedures or instructions which reflect a series of value judgements.

The system approach is a prescriptive model. It expresses a philosophy and is based on a value judgement. Parts of the methodology require modeling of various types. For example, defining the problem requires the determination of a value system, a prescriptive model. This is perhaps

the most important model we must construct since it is required for choosing or evaluating alternatives.

Descriptive models answer "What if" questions. They allow one to observe the performance of the system under various conditions. Thus, when we ask the question "What happens to X if Y changes from two to three?" we are seeking a descriptive model. All models contain some degree of prescription and description. A demonstration of this is the observation that in what appears to be a description of fact, we choose a particular way to present the facts. We feel that one way is better than another, a prescriptive judgement.

The problem solving process involves a coordination of both descriptive and prescriptive modeling. It uses descriptive models for insight into the important relationships which display the system performance and, it uses a prescriptive approach to decide or choose among alternative solutions.

3.4.4 Constructing Models

The questions being asked should suggest the type of model and the detail needed. Model construction is a subbranch of problem solving (and vice versa) and as such is a series of overlapping iterative processes. The model is developed in stages proceeding from the qualitative to the

quantitative. The model should be intellegible to others. Documentation is important. The components of creating a formal model could be stated as follows:

(a) Based on theory

(b) Drawn from some data

(c) Theory plus data resulting in the formualtion of a methotology.

The process involved in the construction of models include:

1. Identifying the purpose of the model: What are the questions being asked? What processes are to be represented? Why are we producing the model? What would we like to come out of it?
2. Identifying the important parameters: What are the variables? Which parameters will affect our decision.
3. Identifying the relations among the variables: How are the variables related? What are the direct relations? How does a change in each variable affect the other variables?
4. Drawing diagrams: What pictures, sketches, graphs, arrow diagrams, etc. are appropriate?
5. Executing the model sufficiently enough to satisfy the purpose of the model:

What idealizations and approximations are sufficient to get a grasp on the questions asked?

6. Testing the model with reality:

   How do relations check with observation? What is the model's sensitivity to the approximations made.

7. Iterating:

   Repeat the process. What refinements of the model are necessary to satisfy the purpose of the model? In the process of the iteration we move from simple to complex, from general to specific. Figure 3.7 gives a schematic presentation of the model building process discussed. The attributes of a good model could be summarized as follows:

   (a) Simplicity
   (b) Answers the right questions
   (c) Versatility
   (d) Extendability
   (e) Validity
   (f) Provide insight into the process modelled
   (g) Clarity/understandability
   (h) Completeness
   (i) Robustness (not sensitive to assumptions)
   (j) Feasibility
   (k) Economy

3.5 DEFINITION OF THE PROBLEM

The processes of the systems approach to complex problem solving usually begin with a response to need (a problem) for which a solution(s) is sought. This initial response is an attempt to produce a definition of the problem. Definition of the problem consists of:

(1) A determination of the needed functions

(2) A statement and analysis of the constraints upon the system

(3) A definition of a value system

Before proceeding to examine the first of those three components, it is necessary to emphasize that the problem is not defined in one swoop, many iterations are necessary. As the needed functions, system constraints, and the value system are considered and we produce an initial definition of the problem, we will begin to consider the generation and/or evaluation of some alternatives. As we do so, we may find that we must redefine the problem. An improved definition may in turn lead to new alternatives which may lead to a further improvement in the definition of the problem.

As we complete a number of these iterations and improvements, we may tend to become satisfied that we have "zeroed in" on the problem, that we have completed the

definition. This satisfaction, however, will eventually be replaced with a growing sense of frustration as we realize that the problem definition, by its very nature, will always be incomplete. Our definition of the problem can only be complete if we are able to choose consistently between any two given alternatives. But we can choose consistently only if the complete set of alternative is known to us, which is rarely the case.

3.5.1 Determination of the Needed Functions - The System Objective

It is imperative that we avoid solving the wrong problem! The first and critical stage toward this end is to elicit answers to the following questions: What is it we really want to do? or What must be done? The above questions could also be phrased, What actions must the system perform? The answer to these questions is called the objective of the system. An objective is a statement of what functions we want the system to perform.

In the attempt to define the real problem and to determine the needed functions, we should seek an objective which is general (non specific). However, we must exercise care to avoid overgeneralizing the objective, while at the same time avoiding inclusion of any system variables. As the analysis progresses, the functions of the system and

subsystem will be stated in a more and more specific manner. Eventually we will be forced to a consideration of alternatives (hows) which will perform the specific sub-functions (whats). But, early in the analysis generality rather than spedificity is desirable; specificity cannot be avoided, but should be delayed.

3.5.2 Functional Analysis

As mentioned in the previous section, we must establish the needed functions of the system. A formal, documented determination of the functions of a system is called functional analysis. In this documentation a diagrammatic model of the system is prepared by breaking down the functions of the system into hierarchical array of sub-functions of the subsystems, sub-subfunctions of sub-subsys-tems, and so forth. A diagram of such hierarchical array provides us with a means of recognizing the important functions of the system. It also is an aid to generation of alternative solutions to the problem and can be used in the evaluation of how well the alternatives perform the function (meet the objective of the system).

There are three types of useful functional analysis:

(1) Subfunction-branched functional analysis specifies various subfunctions at the branching point in the array;

(2) Alternative-branched functional analysis specifies alternative ways of accomplishing the function at the branching point in the array.

(3) Sequential functional specifies in time the sequence of operations of a system.

While the alternative-branched analysis is directly related to how a function may be performed (alternative), it is only indirectly related to what (functions) the system is to perform. The types of functional analysis used, that is, the models we choose, will depend upon the nature of the problem being analyzed and the stage of the process or questions at hand. It might very well be that all three models should be used. It is also clear that the distinction as to type is somewhat artificial. For example, during functional analysis it becomes more and more difficult to break down subfunctions of subfunctions of subfunctions, etc. without entering into an alternative analysis. The deeper into the subsystems and subfunctions the analysis goes, the more difficult it becomes to avoid a branching into alternatives (how) rather than a branching into functions (what). Since it is the latter which is the central feature of the problem definition, at least in its early stages, subfunction analysis is directed toward the determination of the needed functions.

3.6 SUMMARY

A well defined systematic approach for solving complex problems has been presented. The procedure basically consists of : (1) defining the problem; (2) alternative solutions are generated; (3) solutions are evaluated; (4) an iterative procedure is followed. In all four parts modelling expertise is called upon. A thorough investigation of the modeling procedure was presented. Attributes of good models and the resulting accrued benefits were listed. Finally, guide lines for structuring the system objectives were presented.

Having established this notion of problem solving using the systems approach, we are well equipped with a methodology to persue our investigation concerning the prediction of the in situ consolidation properties of soils.

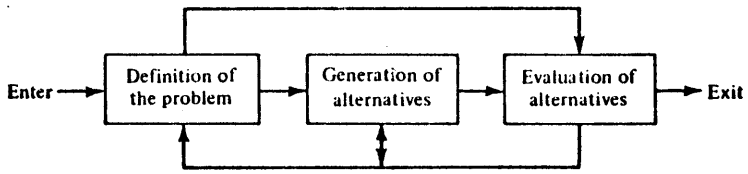

Figure 3.1 The problem-solving process—a systems approach

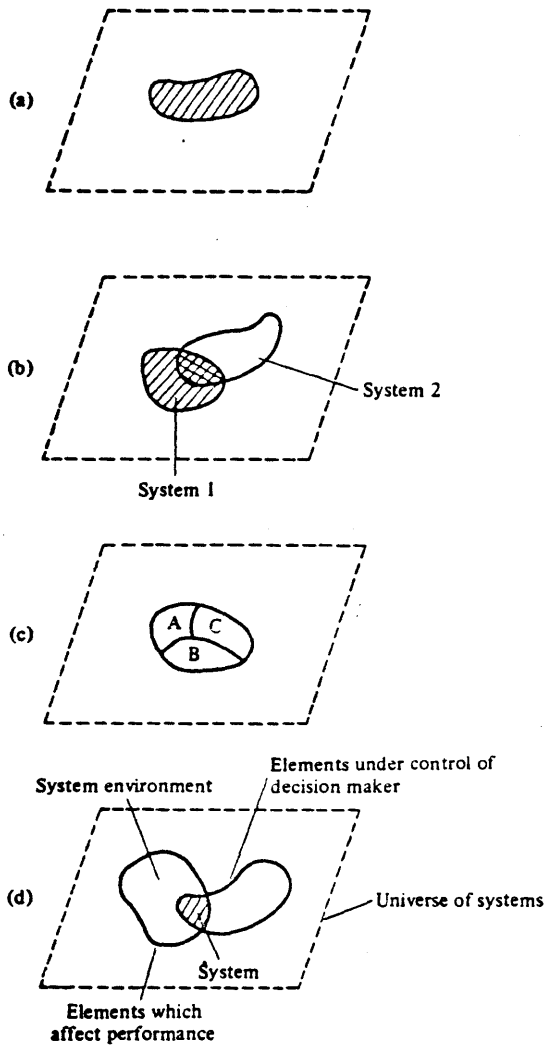

Figure 3.2

Aspects of a system illustrated with Venn diagrams. (a) A system as a group of elements (striped area) in a universe of systems (total area). (b) System 1 overlapping with system 2. Cross-hatched area represents elements of both systems. (c) A system composed of subsystems *A*, *B*, and *C*. (d) A system and its environment.

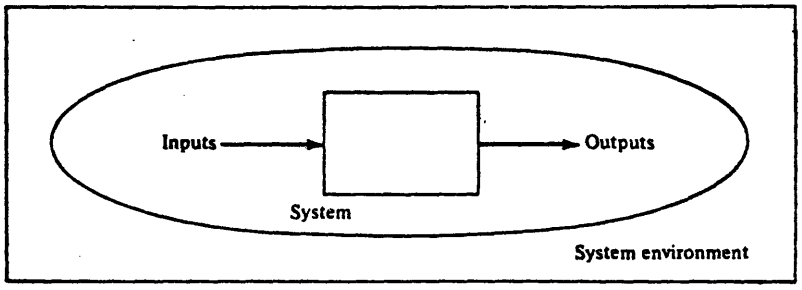

Figure 3.3 Inputs and outputs as parts (elements) of the system, not of its environment

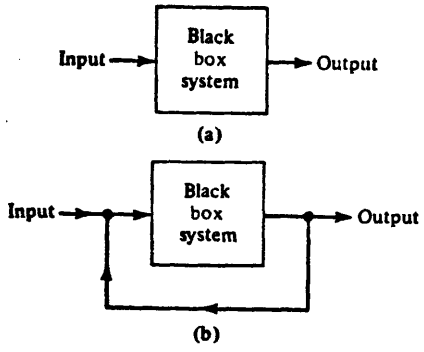

Figure 3.4
(a) A feedforward system. (b) A feedback system.

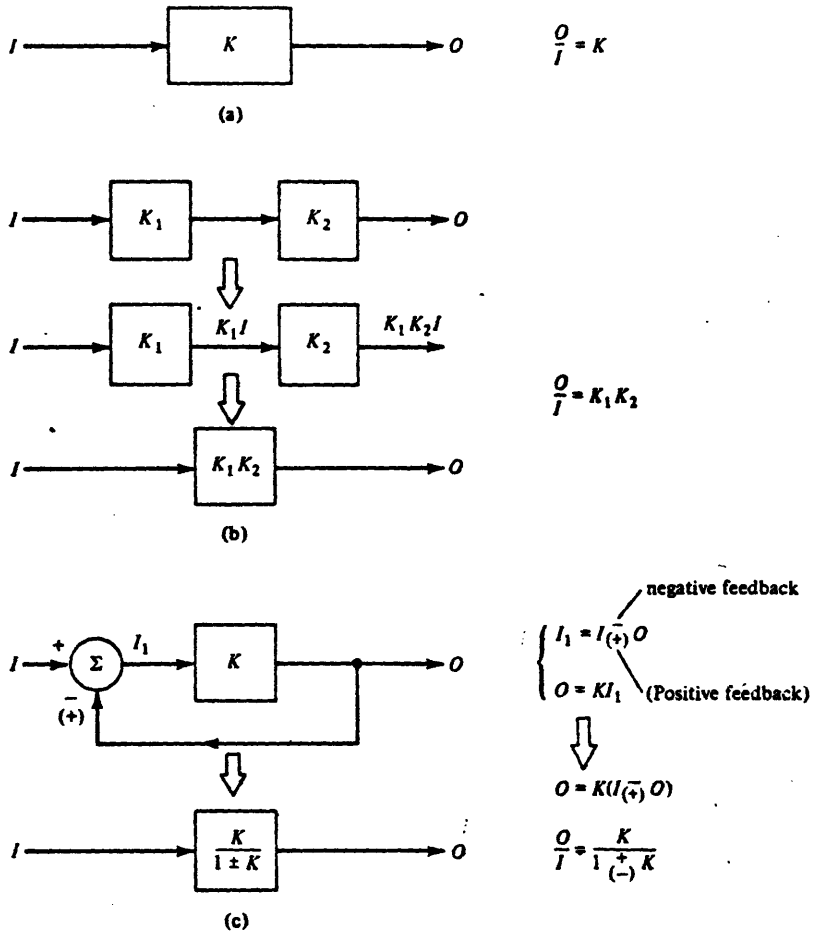

Figure 3.5 Transfer functions: (a) For a system with simple gain K. (b) For a system with elements in series. (c) For a simple feedback system.

Figure 3.6

Arrow diagrams of feedback loops. (a) Positive feedback. (b) Negative feedback.

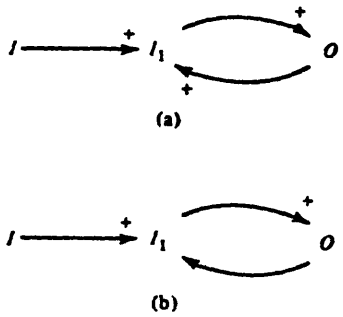

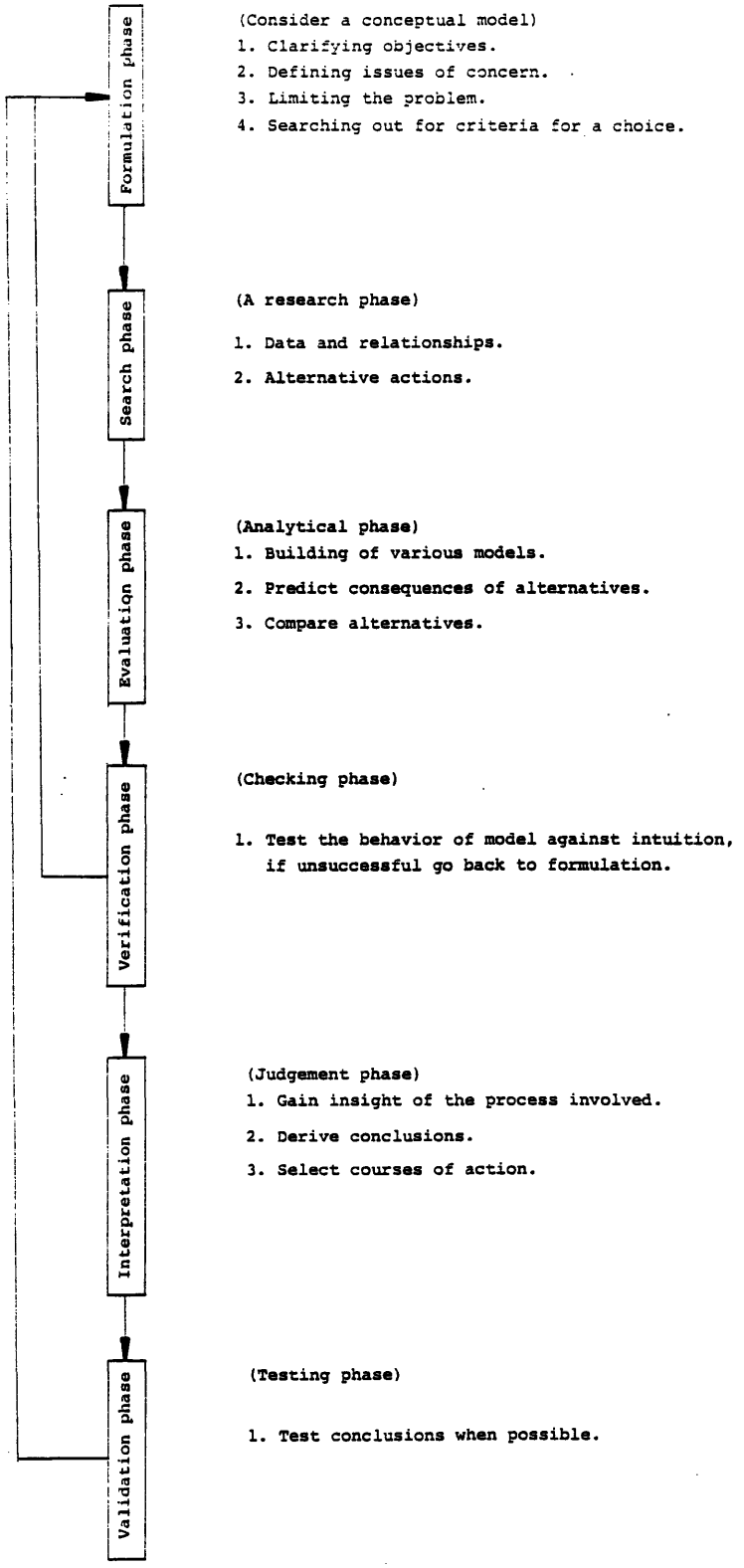

Figure 3.7 The model building procedure.

CHAPTER 4

DEFINITION OF THE PROBLEM; SYSTEM DEFINITION AND DESCRIPTION

4.1 INTRODUCTION

The previous chapter presented a prescriptive model for solving problems characterized by multiplicity of interactions, gaps in our knowledge of the situation thus pertaining and the computational limitations encountered when the boundaries of simple approaches are breeched. The systematic attack strategy was basically subdivided into three components, namely:

(1) Defining the problem,

(2) Generating alternatives, and;

(3) Evaluating alternatives.

We are now going to concentrate our efforts on attempting to utilize this model to aid our investigation concerned with evaluating the consolidation properties of soils. Dealing with the first item, defining the problem, and addressing the following questions:

What is the problem?

What must be accomplished?

What is the value system?

How will we pick among alternatives?

What are the constraints?

4.2 WHAT IS THE PROBLEM? AND WHAT MUST BE ACCOMPLISHED?

Typical problems encountered by geotechnical engineers almost always require knowledge of consolidation and/or permeability properties of the soil deposit at hand. In most practical situations involving coarse grained soils (gravels and sands; $k \simeq 10^{-4}$ cm/sec) impose "drained" conditions. Good estimates of the permeability of gravels is rarely needed since their permeability is often too large. On the other hand, estimates of the permeability of natural deposits could be established by either using empirical correlations with effective grain size, D_{10}, or by in situ testing. Improved estimates of the in situ permeability through laboratory testing is inhibited due to sample disturbance. Errors within an order of magnitude are not uncommon.

"Undrained" conditions are intimitly related to the behavior of fine grained soils and would henceforth necessitate knowledge of the coefficient of consolidation. In relatively "structureless" clays, the most experienced engineer using the best laboratory testing equipment and procedures can, at best, predict field values of k and c_v

with a factor of two or three. However, the average geotechnical engineer using routine sampling and testing methods can probably estimate k and c_v within a factor of five to ten from laboratory measurements. In "structured" fine grained soils, estimates of k and c_v from laboratory measurements can be several orders of magnitude lower than field value and thus have very limited use in designs.

Reliable in situ tests in fine grained soils are time consuming and require considerable skill and experience. Under ideal conditions, useful permeability data can be obtained. However, direct measurements of the more important coefficient of consolidation, c_v, are not sufficiently reliable.

Laboratory tests are expensive and time consuming. More importantly, they provide information at discrete locations only and thus reflect local rather than global properties of the soil deposit. Moreover, predictions based on values of the vertical coefficient of consolidation, c_v, measured in the laboratory generally under predict the rate of consolidation observed on full scale structures. On the other hand, large scale field loading tests are seldom available before construction and provide the overall consolidation behavior of the soil mass. Similarly, field pumping tests are difficult to interpret and may lead to erratic results

because of their sensitivity to soil nonhomogeneity.

Hence, the need often arises for a more economical in situ test that would provide reliable profiles of consolidation (and/or permeability) coefficients. These profiles would be especially valuable to:

(a) Identify drainage layers which are crucial in two or three-dimensional consolidation problems, dewatering and grouting operations as well as in dam foundations (uplift pressures and piping);

(b) Perform more accurate consolidation analysis for application in predicting settlement rates, monitoring earth structures, designing preloading surcharge and vertical sand drains, and;

(c) Aid for decision making in foundation engineering such as selecting adequate dewatering methods and pressure relief, planning of long term instrumentation program, tunnelling operations, etc.....

Thus, a more reliable and economical method for estimating the in situ consolidation and/or permeability characteristics of find grained soils is required.

4.3 SYSTEM DESCRIPTION: HARDWARE

Piezometer probes used at M.I.T. were developed by Wissa and simultaneously by Torstenson (1975). Originally, those first generation probes were designed to measure pore pressures at the tip of the 18° conical element. Later designs by Baligh et al. (1978) introduced a 60° conical element and pore pressure measurements at the tip and at the shaft Fig. 4.1. The pore pressure censor consists of a high air entry stainless steel porous element hydraulically connected to a pressure transducer contained in a 1.5" diameter stainless steel housing. The upper end of the steel housing screws onto a standard A or Aw drilling rod. Interruption period could be extended to observe pore pressure decay patterns. Penetration resumes at a rate of approximately 2 cm/sec (± 50%)*. During pore pressure decay, electrical signals generated by the pore pressure transducer are transmitted to the surface through an electrical wire strung through the jacking rods and recorded on a strip chart against time.

One of the most important features of any measuring

*Tests conducted by M.I.T. to investigate the effect of penetration rate on cone resistance and penetration pore pressures indicate that in clays, a ± 50% change in the "standard" penetration velocity of 2 cm/sec has no detectable effects.

device is whether or not it interfers with the actual quantity being measured. In the case of the piezometer probe, the fact that a quantity of water is exchanged between the soil and the measuring probe would sustain interference. Yet, such interference could be reduced if the "flexibility" of the system is reduced, i.e., if the amount of water required to flow into the piezometer is held at a minimum. The necessity of a "rigid" system is particularly appreciated in the case of highly pervious soils (silty sands and sands) or very impervious soil (plastic clays). In pervious soils, pore pressure dissipation might be very fast, faster than the response time of the probe. In impervious soils, the required amount of inflow might be larger than can be provided rapidly by the soil.

The key to attain a "rigid" system is through proper deairing. Inadequate deairing could result in the following symptoms:

(a) Smooth (v.s. sharp) changes of pore pressures during penetration;

(b) Prolonged rise in pore pressures after penetration has stopped, and;

(c) A slow increase in pore pressures when penetration resumes.

If one of the above mentioned features is observed, the test should be stopped and a new piezometer installed. A deairing technique at least as careful as currently adopted at M.I.T. is strongly recommended. The procedure consists of the following steps:

(a) Disassembling the probe, cleaning and thoroughly drying all parts;

(b) Placing all parts in a container under a good vacuum (less than 10 millitorrs)* for at least 12 hours.

(c) Flowing deaired water into the container (still under vacuum);

(d) Assembling the probe under water, and;

(e) Preventing the stone from drying by keeping it under water until it is used in the field.

Lunne and Lacasse (1980) using the Torstenson probe have confirmed the advantages of this method when used on Scandinavian clays.

4.4 TYPICAL SYSTEM OUTPUT RECORDS

Typical records obtained from in situ testing using the piezometer probe would aid the geotechnical engineer in two aspects:

(a) Provide information on the subsurface straigraphy

*1 Torr equals 1mm mercury, approximately .00113 atm.

(i.e., the extent, thickness location of the different soil layers, Baligh et al. (1980).

(b) Provide estimates of engineering properties of the layers pertinent to foundation design.

Accurate information on soil stratification and variability in properties is necessary to interpolate reliably between data obtained from widely-spaced boreholes, plan the final testing program, select adequate spatial distributions of soil parameters and, hopefully, reduce the risk of inadequate foundation performance.

4.4.1 Steady Penetration Records

Fig. 4.2 shows a typical record of pore pressures measurements at the tip of an 18° conical probe in a deposit of Boston Blue Clay. When steady penetration starts, e.g. at a depth of 43.5 ft., the pore pressures increase rapidly and reach the so called "penetration valve", u_i, in less than 3 inches. Steady penetration at a rate of about 2 cm/sec. continues to a depth of 47 feet (indicated by the arrow) when another push rod is required. The installation of the rod takes 45 sec. and the pore pressure during this time decreases due to soil consolidation. Penetration is then resumed and the process repeated. Note the unmistakeable sudden decrease in u_i at depths 47.2, 49.3 and 58.6 ft. which suggests the presence of a dense sandy lens.

Fig. 4.3 shows the cone resistance, q_c, and the penetration pore pressure, u_i, obtained from two separate tests 45 ft. apart in a deposit consisting of peat, sand and heavily desicated clay which contains sand lenses. Individually, q_c and u_i records detect major changes in soil strata, but jointly, they have an excellent potential for soil identification as well. For example, in the peat, q_c is low and u_i is high, whereas in the relatively clean sand, q_c is high and u_i is very close to the hydrostatic valves, u_o.

In both records we note:

(a) The cone resistance and the penetration pore pressure, u, are very consistant. This is believed to be due to the simplicity of the test procedures, the uniform nature of the shearing process during penetration, and the minor importance of human interference.

(b) Since much more data points are obtained compared to, say, the field vane test, stratification and variability in the soil properties are more clearly defined, the possibility of missing weak layers is greatly reduced, and the need to apply engineering judgement to delete or modify test results is vertually eliminated. On the other hand, the enormous volume of data requires special handling.

Baligh et al. (1980) describe the use of steady penetration record for soil profiling.

4.4.2 Dessipation Records

Figure 4.4 shows a typical dissipation record at 20, 40, 50 and 68 ft. depths in Boston Blue Clay around an 18° tip after interrupting steady cone penetration. Each dessipation record starts with a value of pore pressure equal to the so called initial penetration value and later gradually decays untill it ultimately reaches the steady state pore pressure. Due to the dependence of the penetration pore pressures on the nature of the soil penetrated, it is usually hard to estimate those values a priori in erratic deposits. Furthermore, the steady state pore pressures are practically never reached since their attainment would involve extended periods of penetration interruption which is obviously bounded by the soil investigation program's economies.

It is usually more meaningful to plot the variation of the ratio $\bar{u}(=\Delta u/\Delta u_i)$ with time. Δu is the pore pressure increment at any one time t and is equal to $u-u_o$ where u is the pore pressure at any time t and u_o is the steady state pore pressure. Δu_i is the initial pore pressure increment and is equal to u_i-u_o where u_i is the initial penetration induced pore pressure. Inspection of Figure 4.5 reveals the following:

(1) For any one value of the degree of consolidation, say, the rate of dissipation decreases with increasing depth. This persumably is due to the decrease in the

permeability with depth as will be discussed later.

(2) The shape of the dissipation curves also changes drastically with depth. Notice however, that the dissipation curve relative to 50 ft. could be derived from that relative to 68 ft. simply through horizontal linear translation of the latter, a property of dissipation curves that is discussed later.

4.5 SYSTEM OBJECTIVES

(a) Provide the measured soil parameters, e.g. vertical or horizontal coefficient of consolidation and/or permeability;

(b) The magnitude of this parameter;

(c) The magnitude of the dessipation period;

(d) The cone angle that provides the most reliable results;

(e) Location for measuring the pore pressures, on the cone, and;

(f) Insight to the mechanism of soil deformation around the cone etc...

4.6 CONSTRAINTS AND DIFFICULTIES IMPOSED ON THE SYSTEM

Basically, the difficulty in interpreting dissipation records requires the estimation of:

(a) Initial spatial distribution of the penetration pore pressures, and;

(b) The rate of subsequent dissipation of those pore

pressures.

The rest of this section will be devoted to give a brief account of the difficulties encountered.

4.6.1 Initial Excess Pore Pressure Distribution

Existing methods utilized to deduce the initial spatial variation of the pore pressure distribution around the shaft of the piezometer probe are usually inferred from solutions of pore pressure patterns around a pile which are based on solutions of cylindrical cavity expansion in an elastic perfectly plastic material. Soderberg (1962) models pile installation by the expansion of a cylindrical cavity. The excess pore pressure is assumed to be equal to the radial stress increment caused by cavity expansion
Two models were used to determine the initial pore pressure distribution, namely:

(1) The first model assumes that the soil behaves as an elastic perfectly plastic material and the solution is obtained assuming plane stress conditions (Nadai, 1959).

(2) The second model assumes the soil to behave as a "viscous substance" unable to support tensile stresses and the radial stress is evaluated from equilibrium alone

However, pore pressure spatial variation around the tip of a conical piezometer probe is by far much more complicated since the problem is clearly two dimensional.

4.6.2 Subsequent Pore Pressure Decay

Developing an interpretation theory that faithfully incorporates the behavior of a particular soil under specific loading conditions, lacks the generality required to be able to use it for other soils under more versatile loading conditions. Yet to be able to formulate such a universally applicable theory is at the present impossible due to several reasons, namely:

(a) Non-linear behavior of soils; when subjected to stresses exceeding its' maximum past pressure, soils would exhibit market non-linearities in the value of its' coefficient of consolidation. Thus any interpretation method that assumes linear behavior would, henceforth, be applicable for stresses below its' maximum past pressure. In spite of the fact that certain finite element formulations have been proposed to solve problems involving such non-linearities, yet, such solutions are restricted to simple geometries and simplified behavioral models, Small et al. (1976).

(b) Soil Remolding; deep steady core penetration causes large strains in the vicinity of the probe resulting in undrained shear failure in a zone extending to approximatly 6.5 diameters away from the probe. Figure 4.6 illustrates the effect of overconsolidation on the shear induced pore pressure (normalized with respect to the maximum past

pressure) at different axial strain levels during a plane strain compression tests on resedimented Boston Blue Clay. It is obvious that the induced pore pressures due to undrained shearing are positive* and would, henceforth, imply a decrease in the mean effective stress,
Thus we can interpret this decrease in effective stress as an artificial overconsolidation and we can thus deduce that any subsequent dissipation of the induced pore pressures would occur in a reloading mode as shown in Figure 4.7
Such limited experimental data using oversimplified stress systems cannot be assumed to simulate the field conditions. More careful testing to simulate the actual soil consolidation around cones requires complicated stress systems to be imposed on laboratory samples in order to maintain shear stresses during reconsolidation. However, this shearing is expected to vary with time and is difficult to estimate.

(c) Soil Anisotropy; behavioral anisotropy is an inherent characteristic of soils due to their mode of deposition. Anisotropy implies different directions due to a system of applied stresses. If we are to assess the anisotropy in the value of the coefficient of consolidation

*When the clay is initially overconsolidated (OCR=4, say), undrained shearing generates negative u_s and thus the mean effective stress, σ'_{av}, is increased. However, this increase in σ'_{av} is small compared to σ_{vm} (< 15%)

we should then assess the anisotropy in the two principle directions of its' components, namely, the permeability and the compressibility.

Mitchell and Gardner (1975) stipulate that the ratio of the vertical to horizontal compressibility is close to a unity. The anisotropic characteristic of the coefficient of compressibility could be, therefore, attributed to the anisotropy in the permeability.

Based on limited laboratory data, typical values of k_h/k_v for homogeneous clay deposits (i.e., clays with a uniform stratification) are given by Ladd, (1976):

	Nature of Clay	k_h/k_v
(1)	No evidence of layering	1.2 ± 0.2
(2)	Slight layering, e.g. sedimentary clays with occasional silt dustings to random lenses.	2 - 5
(3)	Varved clays in Northeastern U.S.	10 ± 5

Ladd (1976) recommends to evaluate k_v from laboratory tests and k_h from in situ permeability tests.

In view of such complicated behavioral characteristics, developing a model that could incorporate such complications would seem utopic. Existing methods rely heavily on one-dimensional linear solutions. Classical approaches to

such problems involved the use of either the Terzaghi-Rendulic* uncoupled or unlinked theory, where the total stresses and the pore pressures are assumed to be independent or the Biot (1941) coupled or linked theory, where the interaction between the skeleton and the pore water is incorporated. The coupled theory has been shown to be relatively more realistic than the uncoupled theory since it predicts the Mandel-Cryer** effect which is manifested during the early stages of consolidation process, marked by an increase in the pore pressure. Yet, the use of the coupled theory involves several computational difficulties especially when the finite element method is utilized to solve a two dimensional consolidation problem, Biot's theory requires 3 degrees of freedom (2 for displacements and 1 for the pore pressure) at each node, whereas the Terzaghi-Rendulic theory requires only one (pore pressure). Sills (1975) shows that for problems involving one-dimensional rectlinear consolidation and expansion of spherical and cylindrical cavities, both the coupled and the uncoupled theories would lead to the same governing equation. Few attempts have been made to interpret dissipation records

---

*Terzaghi (1923), Rendulic (1936)

**Mandel (1953), Cryer (1963)

around cores since rapid response piezometer probes were only lately developed.

4.7 THE VALUE SYSTEM

It is perhaps pertinent to remind the reader that empirical approaches in interpreting in situ tests represent the backbone of present geotechnical practice.* Empirically oriented approaches use engineering judgement coupled with empirical correlation relating soil response to soil type subjected to specific stress systems, to guess answers to the probable soil behavior subjected to a complicated stress system. To some extent empirical approaches are justified by the very complicated behavior of soils. However, heavy reliance on empiricism has serious and far reaching consequences. In particular, new methods and techniques are very difficult to incorporate into practice because of:

(a) The large effort required to provide convincing empirical evidence, and;

(b) The dependence of present practice on existing testing methods and techniques.

---

*See for example the use of standard penetration test or cone penetration test in practice.

A much more rational approach is intimately related to our ability of understanding the soil behavior subjected to the complicated stress systems. Conversely, granted our ability to understand the soil behavior and to create models that exactly duplicate field conditions would effectively lead to the exact in situ soil parameters we seek. However, if our model is exact then it should be reality and that can only be the case if the state of nature reveals itself. Thus our models would always tend to be incomplete and only a vague representation of reality. We, therefore, should base our judgement on how close to reality are the assumptions used in the models that constitute a specific approach. Some important guidelines to this effect are stated below:

(1) Are the complicated aspects of soil behavior as related to soil consolidation around cones accounted for in the models? Such aspects include:

(a) Soil nonlinearities

(b) Soil anisotropy

(c) Nonhomogeneities

(d) Time-dependent behavior (creep)

(2) Is the two dimensional nature of consolidation around the cone encorporated in the models? Fluid flow and soil deformations take place in radial and vertical directions.

(3) Which dissipation mechamism is used in the models? Biot's coupled or linked theory or the Terzaghi-Rendulic uncoupled or unlinked theory?

(4) Is the initial pore pressure distribution in the close proximity of the probe's tip clearly two dimensional; hence, the use of one-dimensional analysis involves severe oversimplifications.

(5) Is the choice of the model parameters easy to obtain? Are they stress dependent? The rigidity index is hard to obtain if used in a model since both the numerator and denominator manifest market nonlinearities under various stress levels and shearing modes.

(6) What is the type of the parameter estimated? For example, is it the vertical or the horizontal coefficient of consolidation?

(7) For what practical purpose is the estimated value of the model parameter useful. For example, is it useful in predicting heaves due to soil unloading.
Is it useful to predict settlements under drains during construction (cyclic loading; initial excavation and subsequent drain construction)?

(8) Finally, does the approach provide us with a systematic procedure to evaluate the parameter we seek? Would it clearly recommend the instrumentation and

confiuration and latter interpretation of results?

We could extend this list indefinitely but we should always keep in mind that we will never attain perfection but rather seen "precision for decision".

% Dissipation	$\bar{u}$	Cone Angle - Stone Location					
		18° Tip		18° Mid-cone		60° Tip	
		T*	R^2T^{**} (cm^2)	T*	R^2T^{**} (cm^2)	T*	R^2T^{**} (cm^2)
20	0.8	0.16	0.58	0.52	1.89	0.44	1.60
40	0.6	1.35	4.90	2.6	9.44	1.9	6.90
50	0.5	3.0	10.9	4.7	17.1	3.65	13.2
60	0.4	6.0	21.8	8.2	29.8	6.5	23.6
80	0.2	30.0	109	34	123	27	98

* $T = c_h\, t/R^2$

** R = 0.75 in = 1.91 cm for M.I.T. probes

Table 4.1 Recommended Time Factors for Predicting the Horizontal Coefficient of Consolidation from Dissipation Records (from Baligh and Levadoux, 1980)

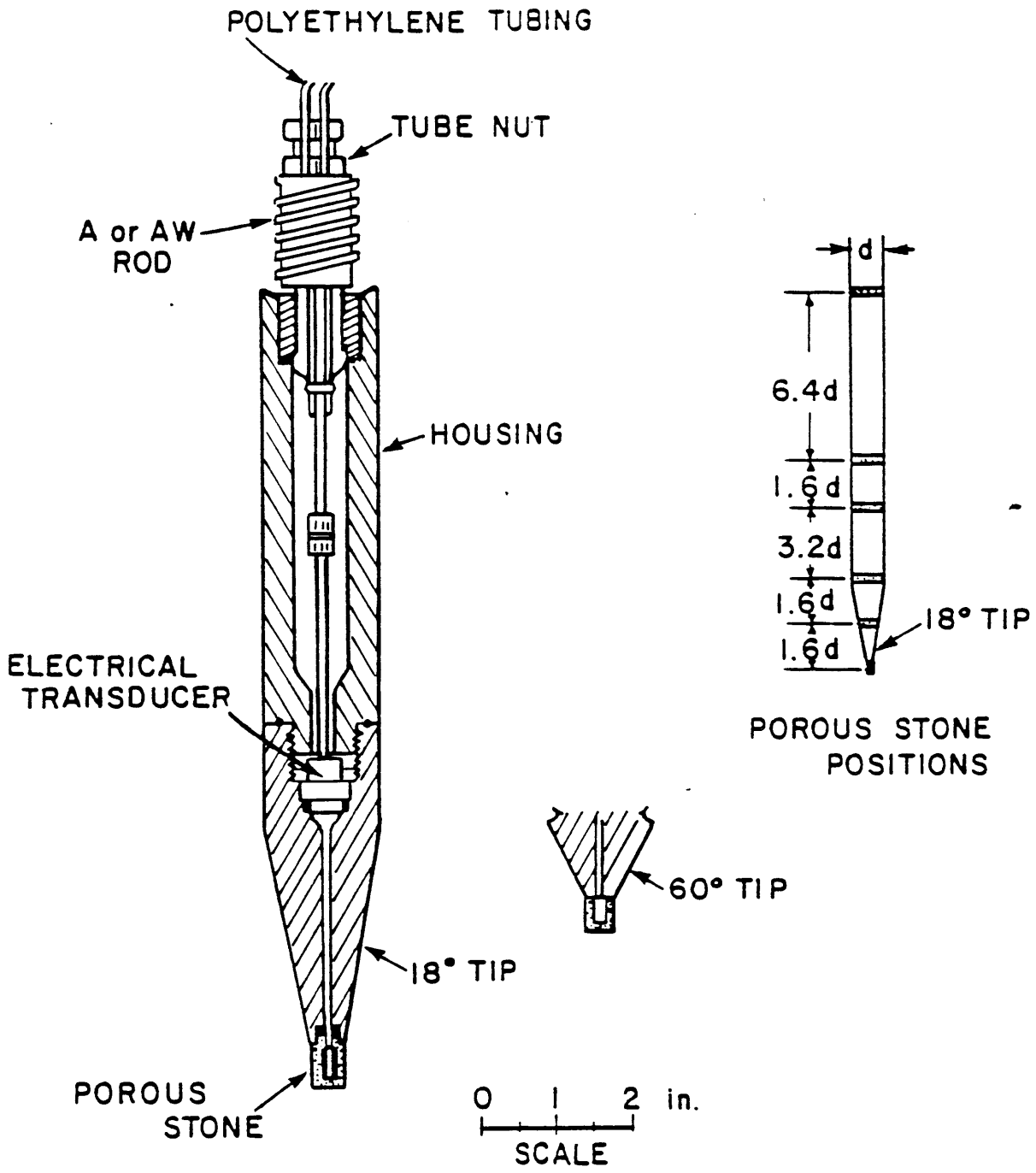

Figure 4.1 Conical piezometer probes used at MIT (after Wissa et al., 1975; Baligh et al., 1978)

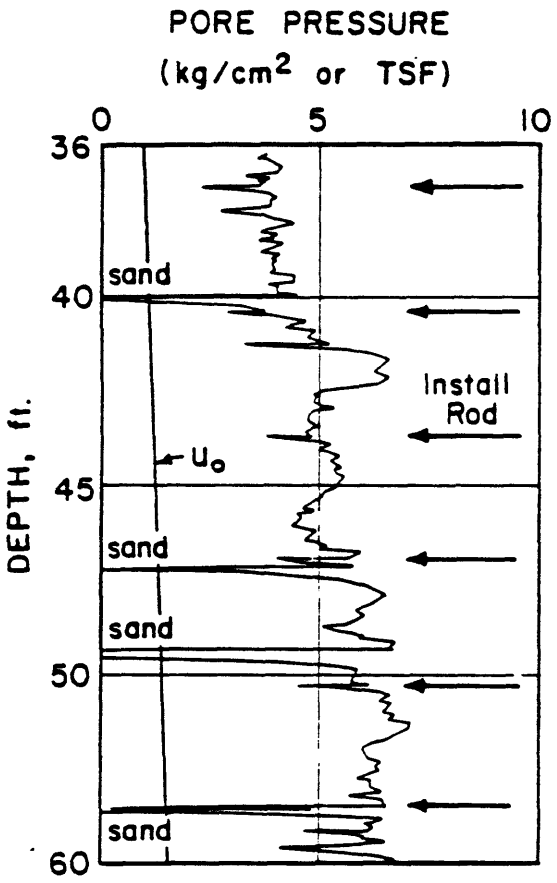

Figure 4.2 Typical pore pressures recorded at the tip of an 18° conical probe during penetration in clay (from BOSS 79)

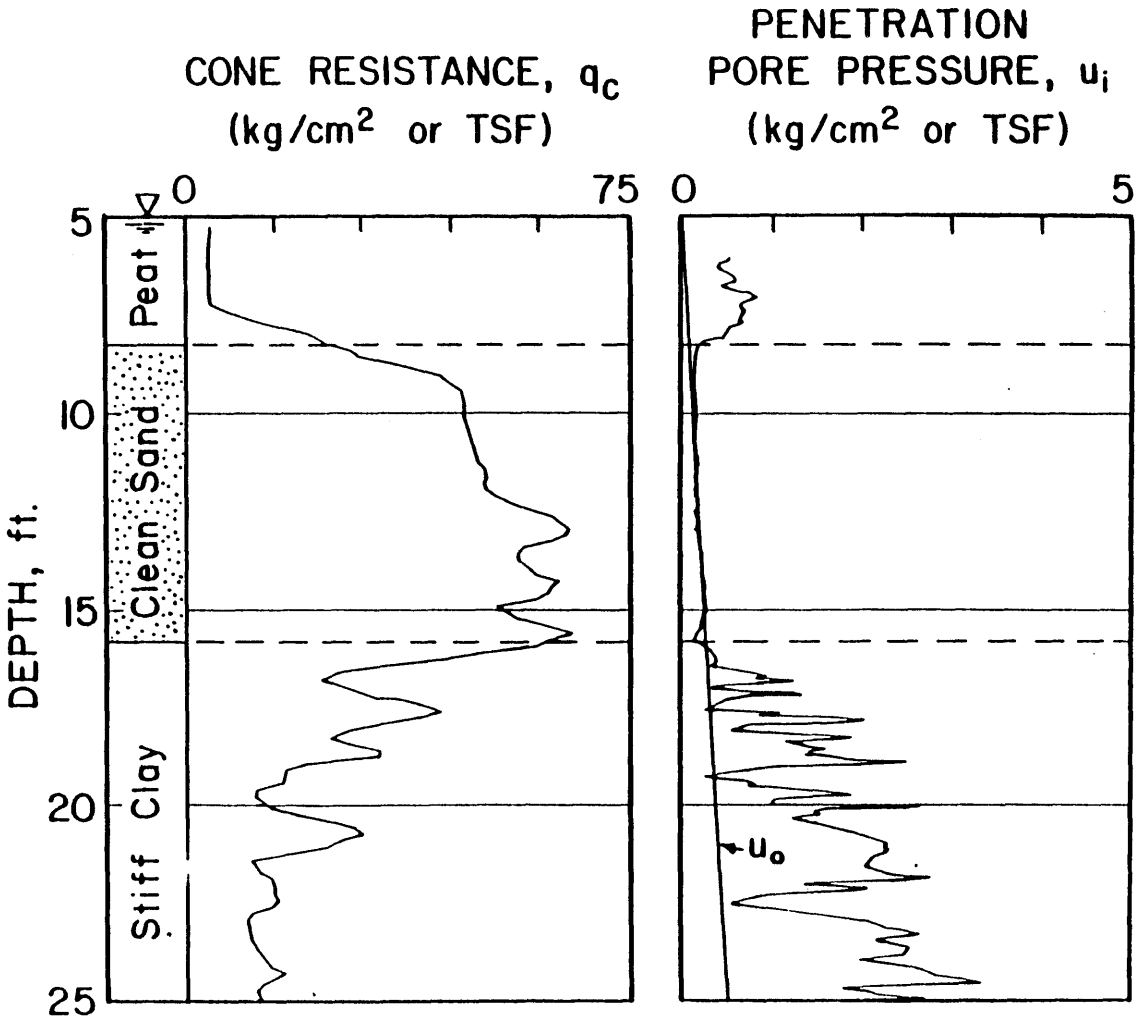

Figure 4.3 Cone penetration in soil stratification and identification (Baligh and Levadoux, 1980).

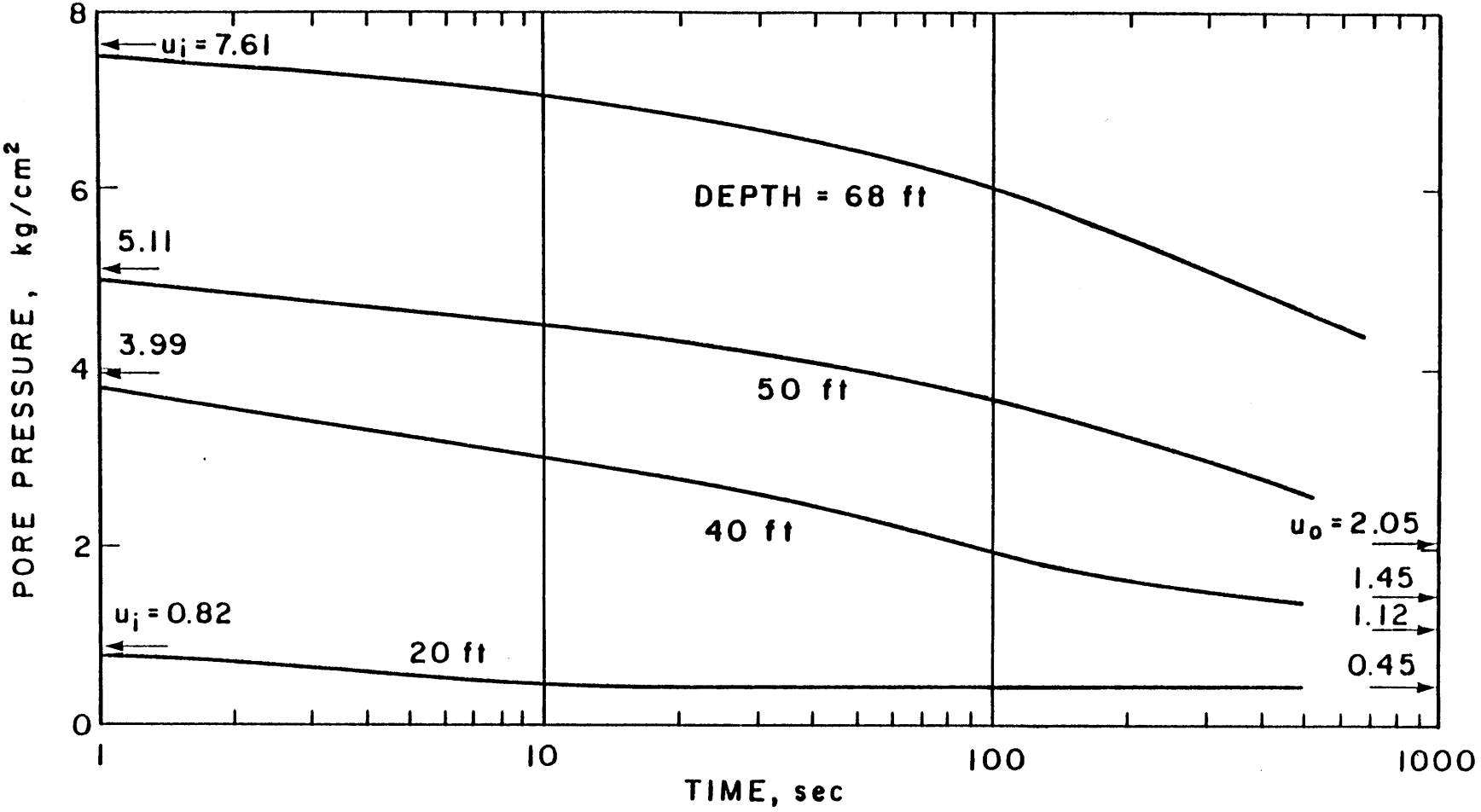

Figure 4.4 Typical dissipation records after interrupting steady cone penetration in clay (Baligh and Levadoux, 1980).

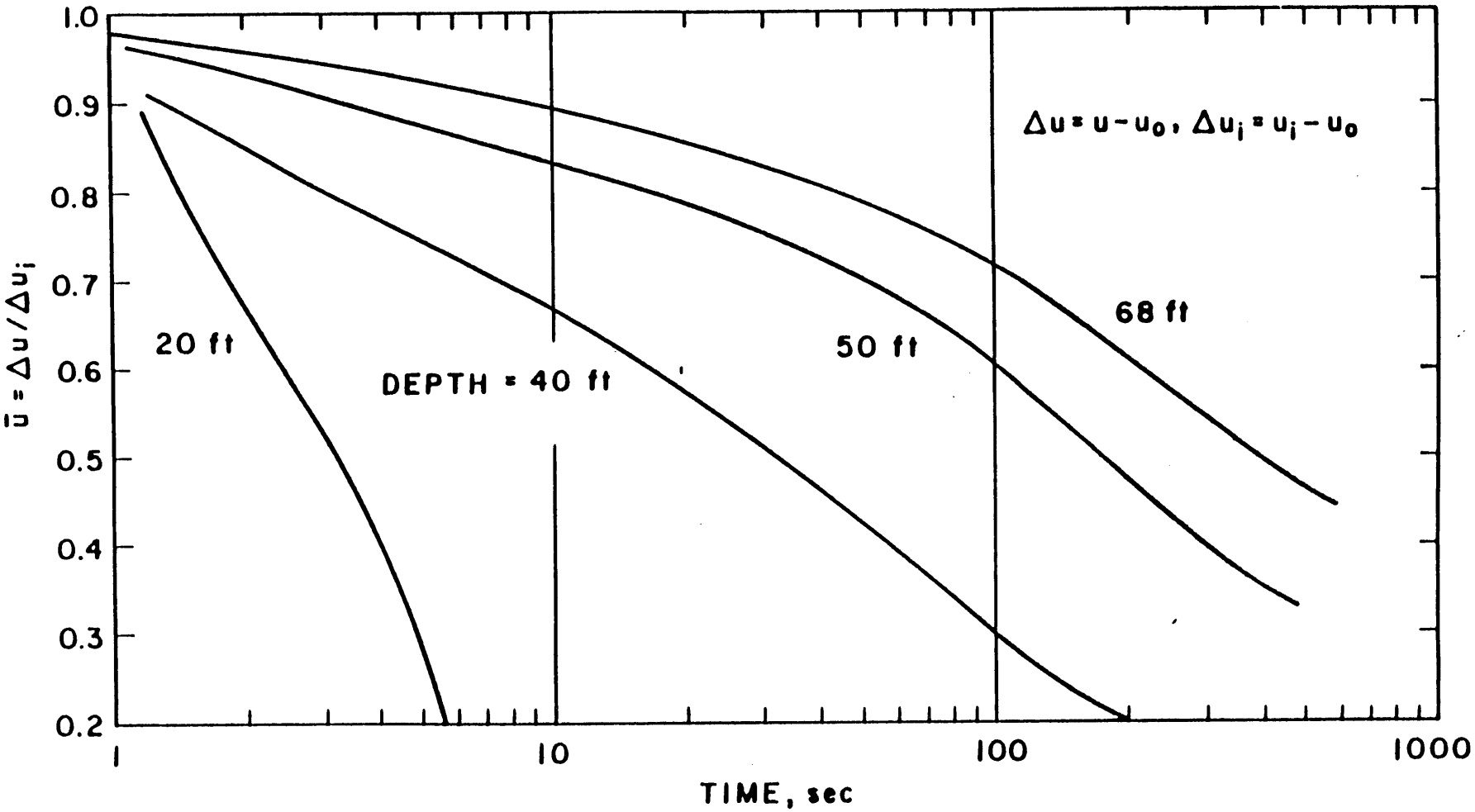

Figure 4.5 Typical normalized dissipation curves (Baligh and Levadoux, 1980).

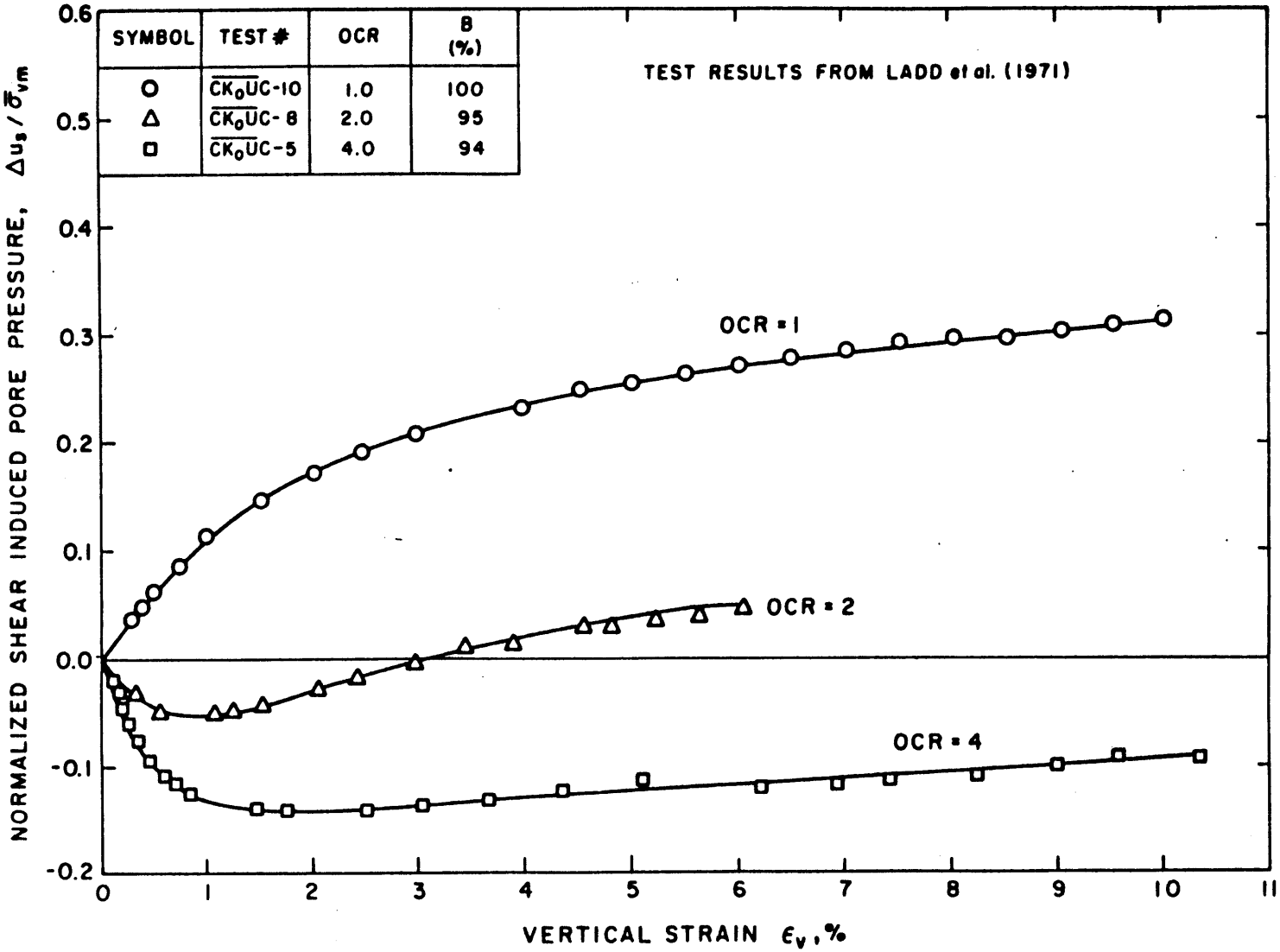

Figure 4.6 Effect of overconsolidation on the normalized shear induced pore pressure in plane strain compression tests on resedimented Boston Blue Clay (from Baligh and Levadoux, 1980)

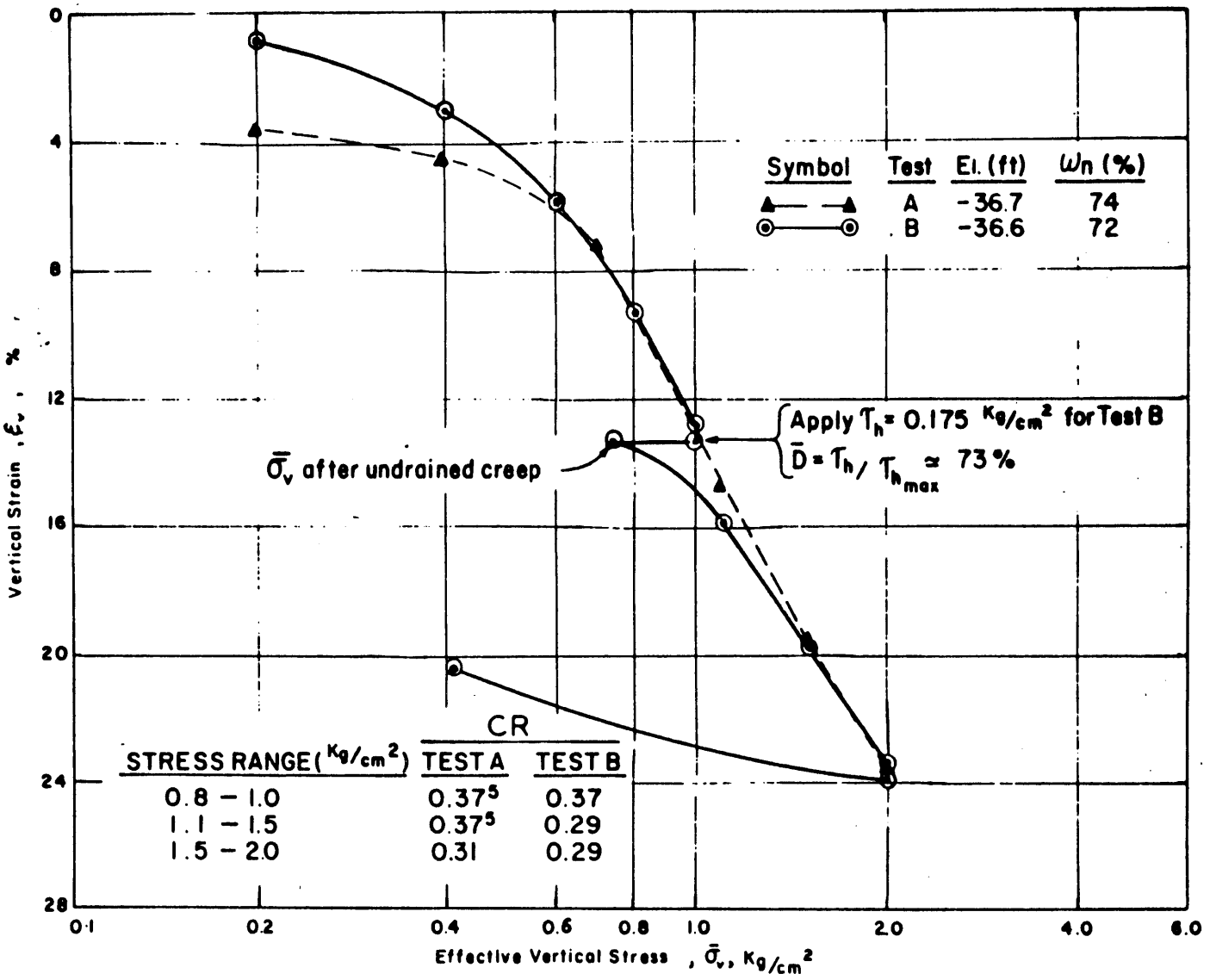

Figure 4.7 Fffect of undrained shear and creep on the compressibility of Atchafalaya clay (from Fuleihan and Ladd, 1976)

CHAPTER 5

ALTERNATIVE SOLUTIONS FOR THE INTERPRETATION OF THE SYSTEM OUTPUT

5.1 INTRODUCTION

Having defined the problem and established the system's objective and corresponding subobjectives, we can now move to the second phase of our perscriptive systems model, generating alternatives.

In order to assess the value of the coefficient of consolidation, c_v/c_h, we should be able to interpret the dissipation records using a specific methodology. Such methodologies are perscriptive models which specify how the interpretation is to be done. In turn, such prescriptive models are based on descriptive models that actually describe the behavior of the system in response to external stimula. Such descriptive models answer the "what if" question as we described in Chapter 4.

Meaningful prescriptive models can only be obtained if the associated descriptive model faithfully represent both aspects of system behavior, namely:

(1) The continuous deep penetration of a cone (or pile) in a homogeneous mass represents a two dimensional

steady state problem, i.e., to an observer moving with the cone (or pile), stresses*, strains and deformations in the soil do not change with time. In saturated clays, steady cone penetration causes undrained shearing and develops excess pore water pressures.

(2) When penetration is interrupted, subsequent pore pressure dissipation around the conical piezometer probes is two dimensional in nature and is governed by the initial distribution of excess pore pressures generated during steady state penetration.

Several existing theories of cone penetration utilize simple models and are based on one of two approaches:

(a) Bearing capacity solutions that neglect the steady state aspects of cone penetration. Examples of such solutions are listed below:

1. Terzaghi (1943)
2. Meyerhof (1951) and (1961)
3. Mitchell and Dorgunoglu (1973)

(b) Cavity expansion solutions that neglect the two dimensional aspects of cone penetration, Table 5.1.

(c) Baligh and Levadoux's method (1980) extensively discussed in this Chapter.

---

*including pore pressures

Bearing capacity solution cannot predict the distribution of excess pore pressures during cone penetration and will be discredited a priori. Torstenson's method (1975) will be considered as a representation of the second category solutions, the cavity expansion solutions.

Attempts to measure the initial penetration pore pressure and subsequent dissipation records are difficult to conduct because of:

(a) The interaction between the measuring device and the surrounding soil; and,

(b) The difficulties in estimating accurately the relative location of the moving tip with respect to the soil element where pore pressures are measured.

Thus it suffices to investigate the applicability of two alternatives, namely:

(1) Torstenson's interpretation method

(2) Baligh and Levadoux's interpretation method.

The rest of the chapter will address the following questions:

(a) What are the alternatives?

(b) How are those alternatives arrived at, the models used and how will they operate under the conditions (constraints) of the problem?

(c) What will they provide us with?

5.2 TORSTENSON'S APPROACH FOR THE EVALUATION OF THE COEFFICIENT OF CONSOLIDATION

Torstenson (1977) evaluates the pore pressure distribution due to undrained penetration of a conical piezometer probe in clays by means of a model utilizing the classical solution to the expansion of spherical and cylindrical cavities in an infinite medium initially subjected to an isotropic state of stress. The reader is referred to Hill (1950) or Ghantous (1978) for a good review of such approaches for various failure criteria.

Assuming that, due to expansion, the excess pore pressure, Δu, equals the octahedral (or isotropic) total stress change, $\Delta\sigma_{oct}$, he determines Δu in the plastic zone* ($R < r < r_p$):

$$\Delta u = 4S_u \ell n \left(\frac{r_p}{r}\right)$$

for a spherical cavity, and:

$$\Delta u = 2S_u \ell n \left(\frac{r_p}{r}\right)$$

for a cylindrical cavity and in which R is the radius of the cavity, r_p, is the radius of the interface between the elastic and the plastic zone and is given by:

---

*In the elastic zone $\Delta\sigma_{oct}=0$ and, therefore, $\Delta u = 0$

$$r_p = \sqrt[3]{I_r}\, R$$

for a spherical cavity;

$$r_p = \sqrt{I_r}\, R$$

for a cylindrical cavity; $I_r = G/Su$ is the righdity index; G, the elastic shear modulus, Su, the undrained shear strength of the clay.

When penetration stops, Torstenson assumes that the consolidation is governed by the Terzaghi-Rendulic (uncoupled) equations:

$$\frac{\partial u}{\partial t} = c\ (\frac{\partial^2 u}{\partial r^2} + \frac{2}{r}\frac{\partial u}{\partial r})$$

for a spherical cavity and,

$$\frac{\partial u}{\partial t} = c\ (\frac{\partial^2 u}{\partial r^2} + \frac{1}{r}\frac{\partial u}{\partial r})$$

for a cylindrical cavity, in which, t, is the time and c is the coefficient of consolidation. Torstenson solves these equations with the finite difference technique and provides charts of normalized excess pore pressure at the cavity wall, $\Delta u/\Delta u_i$ vs. the time factor, $T=ct/R^2$, for different values of E_u/S_u, Fig. 5. 1.

In order to evaluate the coefficient of consolidation,

c, from dissipation records obtained with the piezometer probe, Torstensson proposes the use of the formula:

$$c = \frac{T_{50}}{t_{50}} R^2$$

in which T_{50} is the predicted time factor for a selected value of E_u/S_u and t_{50} is the measured time for 50% dissipation, i.e., $\Delta u/\Delta u_i = 0.5$.

No attempt is made at the moment for evaluating this alternative, this will be thoroughly covered in Chapter 6. where we deal with the final phase of our perscriptive model, Evaluation of Alternatives.

5.3 BALIGH AND LEVADOUX'S METHOD FOR DETERMINING THE COEFFICIENT OF CONSOLIDATION (1980)

Before we attempt to investigate the models developed by Baligh et al, it would be worthwhile recalling the model construction methodology already discussed in 3.4.4 and perhaps elicit few important aspects.

The components of creating a formal model could be stated as follows:

(a) Based on Theory

(b) Drawn from some data

(c) Theory plus data resulting in the formulation of a methodology.

The construction process consists of:

(a) Identify the purpose of the model

(b) Identify important parameters

(c) Identify relations among the variables

(d) Draw diagrams, graphs, etc.

(e) Execute model sufficiently enough to satisfy purpose of model

(f) Test model's sensitivity to assumptions made

(g) Test model with reality

(h) Iterate

As mentioned earlier in this chapter, deriving a specific interpretation methodology, perscriptive model requires the use of descriptive models that actually describe the behavior of the model in sympathy to external stimula.

Henceforth, two models are investigated whose purposes are to describe the initial penetration pore pressures distribution and describe the subsequent pore pressure dissipation, respectively.

The two models are described herein in close adherence to the guidelines of the model construction process.

5.3.1 Initial Excess Pore Pressure Model

(a) Identification if important parameters

Baligh et al identified the following parameters:

1. The "size" of the soil zone affected by cone

penetration. This is conveniently expressed by the parameter $\lambda = r_p/R$; where R is the radius of the cavity*, and r_p is the smallest radius around the cavity where no excess pore pressures develop.

2. The "Spaital variation" of the initial excess pore pressures. Three types of variations with the radius, r, were considered: constant, linear and logarithmic between r=R and $r=\lambda R$, Fig. 5.2.

3. The location of boundary drainage. Two limiting situations were invisaged, namely:

   a. Dissipation in an infinite medium (as in actual situations)

   b. Drainage takes place at $r=\lambda R$.

Comparisons between these two cases provide valuable insight into the effect of the outer soil or dissipation and the importance of the drainage boundary in numerical solutions.

The relative importance of those variables was assessed through the use of a sensitivity analysis involving closed form numerical solutions obtained by Levadoux and Baligh (1980).

In essence, such closed form solutions involve pore pressure dissipation around spherical and cylindrical

* or the radius of the cone shaft

impervious cavities in a linear isotropic elastic solid.

When the soil extends to infinity, consolidation is governed by the Terzaghi-Rendulic equation involving no coupling between pore water pressures and total stresses. The Terzaghi-Rendulic equation is identical to the heat equation governing the diffusion of heat in solids and, therefore, the same solution techniques can be utilized (Carslaw and Jaeger, 1959).

The technique of solution used consists of superimposing a continuous distribution of spherical (or cylindrical) sources at time t=0 so that the desired initial pore pressure distribution is achieved. The pore pressure at point M at time t due to an instantaneous source of strength, unity, at point M' at time 0 is known as a Green's function. Carslaw and Jaeger (1959) provide these Green's functions for many geometries and boundary conditions.

Application of heat conduction equation to consolidation problems is carried out by simply substituting the temperature and the diffusivity by the pore pressure and the coefficient of consolidation respectively.

Results of this sensitivity analysis are stated herein:

1) Dissipation curves (plotted as $\bar{u}$ vs. logT) are very sensitive to the initial distribution of the normalized

excess pore pressures* $\Delta u_i(r)/(\Delta u)_{sh}$, where $\Delta u_i(r)$ is the excess pore pressure at a radius r and $(\Delta u)_{sh} = u_i(R)$ is the excess pore pressure at the cavity wall (shaft), as characterized by:

(a) The extent (or size or radius) of the soil subjected to excess pore pressures compared to the cavity radius, i.e., the parameter λ, Figs. 5.3 and 5.4 .

(b) The spatial variation in the soil, e.g., logarithmic, linear, etc., Figs. 5.5 and 5.6 .

2) Analyses performed for a given initial distribution (λ and spatial variation) assuming spherical symmetry, lead to slightly faster dissipation than cylindrical symmetry (a factor of 1.5 to 2 in the backfigured coefficient of consolidation at 50% dissipation), Fig. 5.6 .

3) Dissipation is mainly controlled by the soil properties within a radius λR and is little affected by the outer soil. Furhtermore, the soil near the cavity is predominantly subjected to a decrease in volume (compression or recompression) during dissipation, Figs. 5.3 and 5.5

*Linear solutions are not affected by the absolute value (magnitude) of the excess pore pressure.

(b) Identify relationships among variables

The following description taken from Baligh and Levadoux (1980) manifests the necessary relationships established between the various variables constituting the system under consideration.

(1) The Strain Path Method

Deep steady cone penetration in clay is essentially a "strain-controlled" problem where strains and deformations are primarily imposed by kinematic requirements. For this type of problem, Baligh (1975) proposes an approximate method of solution called the "Strain path method". This method is based on concepts similar to the more popular "stress path method" (Lambe, 1967) and consists of four basic steps: a) estimate the initial stresses; b) estimate an approximate strain field satisfying conservation of volume, compatibility and boundary velocity requirements; c) evaluate the deviatoric stresses at a selected number of elements by performing laboratory tests on samples subjected to the same strain paths or, alternatively, by using an appropriate soil behavioral model, and; d) estimate the octahedral (isotropic) stresses by integrating the equilibrium equations.

Table 5.2 compares the strain path method with the stress path method to identify their strong similarities.

As indicated in Table 5.2, the strain path method is an approximate method because the estimated stresses will not, in general, satisfy the equilibrium requirements, unless the estimated strain field is identical to the actual one.

(2) The Strain Path Method in Cone Penetration

Figure 5.7 describes the steps for evaluating stresses and pore pressures in the soil due to deep steady cone penetration in saturated clays by means of the strain path method:

1) Estimate a velocity field* satisfying the conservation of volume (or mass) requirement and the boundary conditions.
2) From the velocity field determine the soil deformations by integration along streamlines. Figure 5.8 shows the deformation of a square grid due to steady penetration of a 60° cone as determined by Levadoux and Baligh (1980) after neglecting the shearing resistance of the soil (i.e., assuming the soil to behave as an ideal fluid.
3) Compute the strain rates, $\dot{\varepsilon}_{ij}$, along the streamlines by differentiating the velocities with respect to

*The velocity field describes the velocity of soil particles as they move around the cone.

the spatial coordinates.

4) Integrate the strain rates, $\dot{\varepsilon}_{ij}$, along streamlines to determine the strain path (ε_{ij}) of different soil elements. Figure 5.9 shows the deviatoric* strain paths of three soil elements (initially located at r_o/R = 0.2, 0.3 and 1.0 from the axis) due to penetration of a 60° cone (Fig. 5.8). Clearly, the paths are complicated and involve large strains with strain reversals.

5) Estimate the initial stresses, $(\sigma_{ij})_o$, and initial pore pressures, u_o, in the soil prior to cone penetration.

6) Compute the deviatoric stresses, s_{ij}, and the shear-induced pore pressures, u_s, along streamlines. Levadoux and Baligh (1980) developed the necessary mathematical models to estimate s_{ij} and u_s due to the complicated strain paths imposed by cone penetration taking into consideration the anisotropic inelastic nonlinear behavior of clays. Using soil parameters obtained from laboratory tests on normally consolidated resedimented Boston Blue clay,

---

*No volumetric straining takes place during undrained shearing of a saturated soil.

Levadoux and Baligh (1980) predict: a) The deviatoric stress paths. Fig. 5.10 shows the stress path for an element initially located at a radius r_o=25R due to steady penetration of a 60° cone. For comparison, the paths corresponding to (idealized) Direct Simple Shear (DSS) and Presurementer (PR) modes of shearing are also shown in Fig. 5.10 Clearly, cone penetration subjects the soil to very complicated stress paths consisting of a combination of triaxial compression, DSS and PR models.

b) The shear induced pore pressures. Fig. 5.11 compares the predicted contours at Δu_s due to penetration of 18° and 60° cone with cylindrical cavity solutions.*

7) (a) From equilibrium considerations, compute the total stresses,** σ_{ij} ($=s_{ij} + \delta_{ij}\,\sigma_{oct}$), given the deviatoric stresses, s_{ij}. This requires the determination of the octahedral stresses, σ_{oct}. Since the assumed strains are not exact, the

---

*According to the same soil model.

**δ_{ij} = Kronecker delta: = 0 when $i \neq j$; = 1 when $i = j$ and, $\sigma_{oct} = 1/3\ \sigma_{ii}$.

estimated values of σ_{oct} are approximate because they depend on the integration path, i.e., on the direction where equilibrium is satisfied; radial, axial, etc.

(b) From s_{ij} and Δu_s, compute the effective stresses, $\bar{\sigma}_{ij}[=(\bar{\sigma}_{ij})_o + \Delta\bar{\sigma}_{ij};\ \Delta\bar{\sigma}_{ij} = \Delta s_{ij} - \Delta u_s\ \delta_{ij}]$

8) From σ_{oct} and u_s determine the penetration pore pressures u_i $(=u_1 + \Delta u_i;\ \Delta u_i = \Delta\sigma_{oct} + \Delta u_s)$

Finally, by estimating the shear stresses at the cone soil interface and integrating tractions along the cone face, the cone resistance, q_c, can be evaluated.

(c) Execute model sufficiently enough to satisfy purpose of models

Further simplifying assumptions had to be encorporated before a spatial distribution of the initial and shear induced pore pressures could be predicted, namely:

(1) Soil was assumed to offer no shearing resistance when penetrated

(2) Octahedral stresses were computed by satisfying equilibrium in the radial direction

(3) Following solutions using strain path method are based on soil properties derived from laboratory tests or resedimented B.B.C.

Figs. 5.11 and 5.12 represent the contour of initial and shear induced pore pressures.

(d) Test model's sensitivity to assumptions made and compare to reality

Figure 5.13shows the predicted normalized distribution of the initial pore pressures, i.e., $\Delta u_i/(\Delta u)_{dh}$, as obtained from the above model for the various locations (cone & shaft) on the probe. Also included are actual penetration pore pressures in B.B.C. as measured by the piezometer probe for various locations of the stone. The agreement is reasonable in view of the fact that soil parameters pertaining to normally consolidated resedimented were used to arrive at the predicted pore pressure distribution. In actuality, the clay stratum investigated had a variable degree of overconsolidation. However, agreement of predicted vs. measured initial normalized pore pressures deteriorated when considering elevations at which the OCR > 3. The measured pore pressures exhibited significant scatter.

In order to check the validity of spatial distribution radially away from the shaft, the analogy between the pore pressure distribution around a pile during driving and that encountered around the shaft of a penetrating piezometer probe was utilized. Results of the radial distribution of pore pressures around a cylindrical pile (21.9 cm. in diameter) jacked into Champlain clay is shown in Fig. 5.14

(Roy et al., 1979). Champlain clay has an OCR ≈ 2. Also shown in Fig. 5.14 are results of predicted initial pore pressures. The agreement is again extraordinary in view of:

(1) Approximations in strain path method

(2) Uncertainties in field measurements*

(3) Difference in behavior of B.B.C. used for prediction of pore pressures induced in Champlain Clay

Thus, the model is not sensitive to the assumptions done and agrees perfectly with measured field results. No further iterations to improve on the model are required, since the model suffices its intended purpose with sufficient accuracy.

5.3.2 Subsequent Pore Pressure Dissipation (due to cone penetration interruption) Model

a) Model components

The initial distribution of normalized excess pore pressures prior to consolidation was obtained from steady state penetration solutions in normally consolidated Boston Blue Clay. Once established, subsequent dissipation would be governed by their spatial distribution around the penetrating probe.

*Pore pressure measuring devices were small size Genor M-600 piezometers which are hoepfully less sensitive to soil piezometer interaction

Before attempting to present the model utlized by Baligh et al. (1980), perhaps totology at this stage is warranted. In view of the complicated behavioral characteristics of soil consolidation around cones involving:

(a) Non-linear behavior

(b) Soil remoulding

(c) Soil anisotropy

add to that the two dimensional nature of consolidation around the probe, developing a model that faithfully incorporates such complications would seem utopic. Classical approaches towards consolidation problems utilize the Terzaghi-Rendulic linear uncoupled/unlinked theory. More sophisticated analysis would utilize the coupled/linked Biot's theory which truely predicts the Mandel-Cryer effect. The assumption of linearity is to some extent justified on the basis that it provides valuable normalizations and hence covers a wide range of applications.

One of the advantages accruing from the use of linear consolidation analysis based on Terzaghi theory is the fact that two soils with the same normalized distribution of initial excess pore pressures (caused by steady penetration) but with different values of the coefficient of consolidation must have parallel (or horizontally shifted) dissipation curves. Furthermore, the amount of horizontal shift required

to reach one dissipation curve from another represents the ratio between the coefficient of consolidation for the two soils. This simple role is important in evaluating predictions.

Realizing that a two dimensional analysis is absolutely necessary to capture the true pore pressure distribution around the tip, Baligh et al. (1980) used a finite element program ADINAT (Bathe, 1977) to perform a two dimensional linear isotropic uncoupled consolidation analysis using the initial pore pressures described earlier. Adequate description of the computer program, constituting the dissipation model, is presented in Chapter 9 . Fig. 5.15 and 5.16 shows the spatial distribution of the pore pressures depicted at four values of the dimensionless parameters $T = \frac{ct}{r^2}$, normalized with respect to the initial in situ value of the vertical effective stresses for an 18° and 60° cone. Figs. 5.17 and 5.18 show the corresponding dissipation curves at the cone and the shaft.

A further refinement to the model was introduced when a finite element program, CONSOL*, replaced ADINAT. CONSOL utilizes Biot's coupled/linked theory to perform a two

*For further description of the formulation the reader is referred to Ghaboussi and Wilson (1971 and 1973)

dimensional linear consolidation analysis. Fig. 5.19 shows the effect of coupling on the predicted contours of excess pore pressures during isotropic consolidation around 18° cone. Fig. 5.20 shows the effect of linear coupling on dissipation curves for an 18° tip (linear isotropic analysis). Evidently, the effect of linear coupling between total stresses and pore pressures is reasonably small except at early stages of consolidation especially near the apex of an 18° cone**. This suggests that uncoupled solutions can provide reasonably accurate prediction away from apex and after sufficient dissipation has taken place.

Baligh et al. showed that a reduction in the vertical coefficient of consolidation, c_v, from c_h (isotropic case) to 0.1 c_h causes little delay in the uncoupled pore pressure dissipation at 4 selected locations along the tip and the shaft of an 18° piezometer probe in a linear elastic material, Fig. 5.21. This suggests that c_h governs consolidation around piezometer probes.

Finally, errors in the static and penetration pore pressures (u_o, u_i, respectively) can seriously affect the estimated coefficient of consolidation. Matching of measured and predicted dissipation records at small, large and

** In analyses, an ideal cone is considered with a singular apex point. This geometry is not encountered in actual probes

intermediate degrees of consolidation is recommended if effors in u_o, u_i or both, respectively, are expected.

Thus the descriptive model answered our "What if" question as was anticipated in Chapter 3.

Testing the model with reality is going to be postponed to the next chapter since it will have a dual purpose, namely: (a) test validity of the aforementioned model and simultaneously test the validity of the total approach as recommended by Baligh et al.

Author	Cavity		Material Model	Initial Stresses	Proposed Applications	Remarks
	Cyl.	Sph.				
Bishop, Hill and Mott (1945)	x	x	Elastic-plastic (Von Mises) strain hardening	Not considered (presumably isotropic)	Metal indentation	Closed form solution: experimental results of copper indentation compare well with theory: use natural strains.
Chadwick (1959)		x	Elastic-perfectly plastic (Tresca)	Isotropic	Cylindrical cavity expansion in soils and metals	Considers both loading (expansion) and unloading (contraction) of a spherical cavity.
Gibson and Anderson (1961)	x		Elastic-perfectly plastic (Tresca)	$\sigma_r = \sigma_\theta$	Interpretation of the pressuremeter test	Closed form solution
Ladanyi (1963)	x	x	Experimental stress and mean effective stress vs. strain curves determined from triaxial test	Isotropic	- Stress distribution around cavities - Bearing capacity of deep foundations - Excess por. pressure distribution around driven piles	- Numerical integration of equilibrium equations - Predicts both total stresses and pore pressures.
Butterfield and Bannerjee (1970)	x		Elastic-perfectly plastic (Von Mises)	Isotropic	- Stress and pore pressure distributions around driven piles	- Closed form solution - Consider boundary shear stresses (shaft friction) - Error in equations (do not satisfy the conservation of volume: see Appendix A for correct solution).
Baguelin et al. (1972)	x		General (non linear) stress-strain curve	$\sigma_r = \sigma_\theta$	Pressuremeter test	Provide a method of interpretation of the pressuremeter test (i.e., obtain stress-strain curve from expansion curve).
Ladanyi (1972)	x		General stress-strain curve	$\sigma_r = \sigma_\theta$	Pressuremeter test	Same as above.
Palmer (1972)	x		General stress-strain curve	$\sigma_r = \sigma_\theta$	Pressuremeter test	Same as above.
Vesic (1972)	x	x	Elastic-perfectly plastic	Isotropic	- Ultimate cavity pressure - Evaluation of pressuremeter tests - Evaluation of excess pore pressures due to pile driving	- Considers volume change for drained expansion - Evaluates pore pressures and total stresses for undrained expansion
Prevost and Hoeg (1975)	x		Elastic-plastic (Von Mises) w/ isotropic hardening or softening	Isotropic	Pressuremeter test	- Provide mathematical expressions for the yield function to obtain closed form solution - stresses.
Carter, Randolph and Wroth (1978)	x		Modified cam-clay	K_o condition	Stress distribution along the shaft of a driven pile	Finite element analysis

NOTE: All references consider a) an incompressible isotropic homogeneous non viscous material (unless otherwise indicated)

b) plane strain deformations in the cylindrical cavity expansion with $\Delta\sigma_z = \frac{1}{2}(\Delta\sigma_r + \Delta\sigma_\theta)$

Table 5.1 Summary of existing solutions for cylindrical and spherical cavity expansion (Baligh and Levadoux, 1980).

Stress Path Method	Strain Path Method
APPLICATIONS	
Surface Problems	Deep Problems
STEPS	
1. Estimate initial stresses 2. Estimate incremental stresses 3. Perform stress path tests on samples (or use adequate soil model) to obtain strains at selected locations. 4. Estimate deformations by integrating strains	1. Estimate initial stresses 2. Estimate incremental strains 3. Perform strain path tests on samples (or use adequate soil model) to obtain deviatoric stresses at selected locations. 4. Estimate octahedral (isotropic) stresses by integrating equilibrium equations.
APPROXIMATION	
In step 2, stresses are approximate thus leading to strains not satisfying compatibility requirements. i.e., deformations in step 4 depend on strain integration path.	In step 2, strains are approximate thus leading to stresses not satisfying all equilibrium conditions. i.e., octahedral stresses in step 4 depend on equilibrium integration path.

Table 5.2 Comparison of stress path and strain path methods (Baligh and Levadoux, 1980).

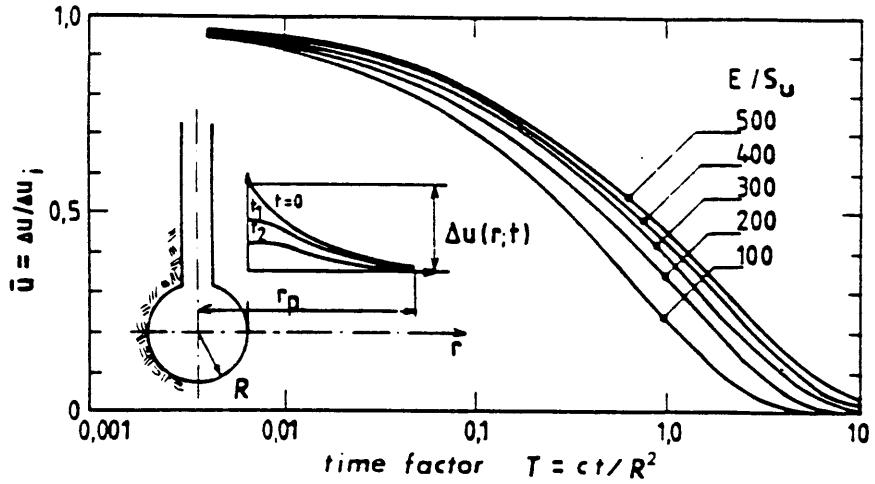

R = radius of pore pressure probe
c = coefficient of consolidation

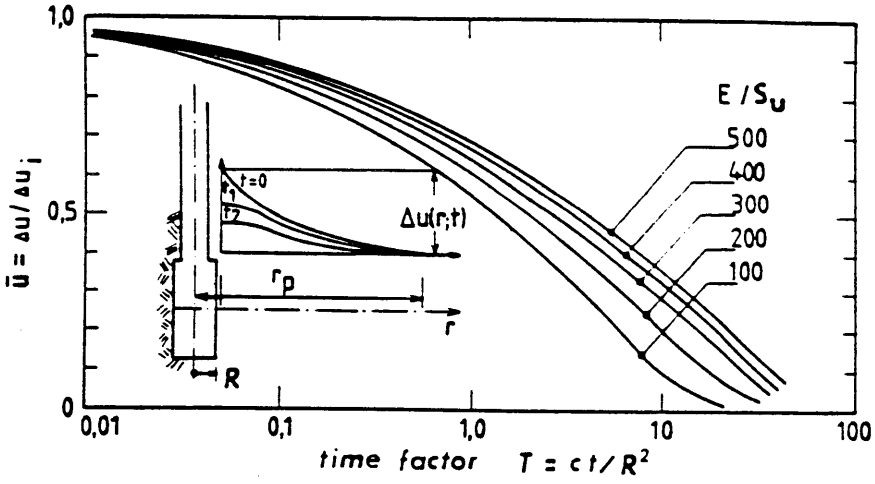

R = radius of pore pressure probe
c = coefficient of consolidation

Figure 5.1 Pore pressure dissipation around spherical and cylindrical pore pressure probes predicted by Torstenson 1977

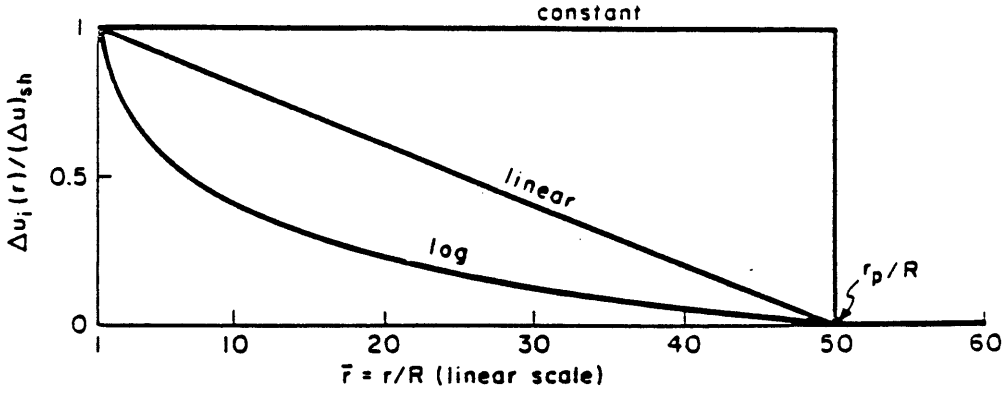

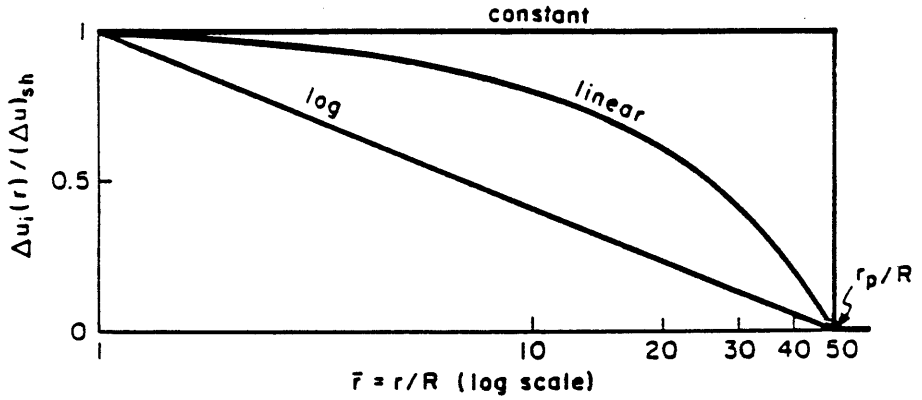

INITIAL NORMALIZED EXCESS PORE PRESSURE DISTRIBUTION	EQUATION	
	$1 < \bar{r} < \lambda$	$\bar{r} > \lambda$
CONSTANT	1	0
LINEAR	$(\lambda - \bar{r})/(\lambda - 1)$	
LOGARITHMIC	$1 - [\ell n(\bar{r})/\ell n(\lambda)]$	

Figure 5.2 Initial normalized excess pore pressures for one-dimensional consolidation analyses (Baligh and Levadoux, 1980).

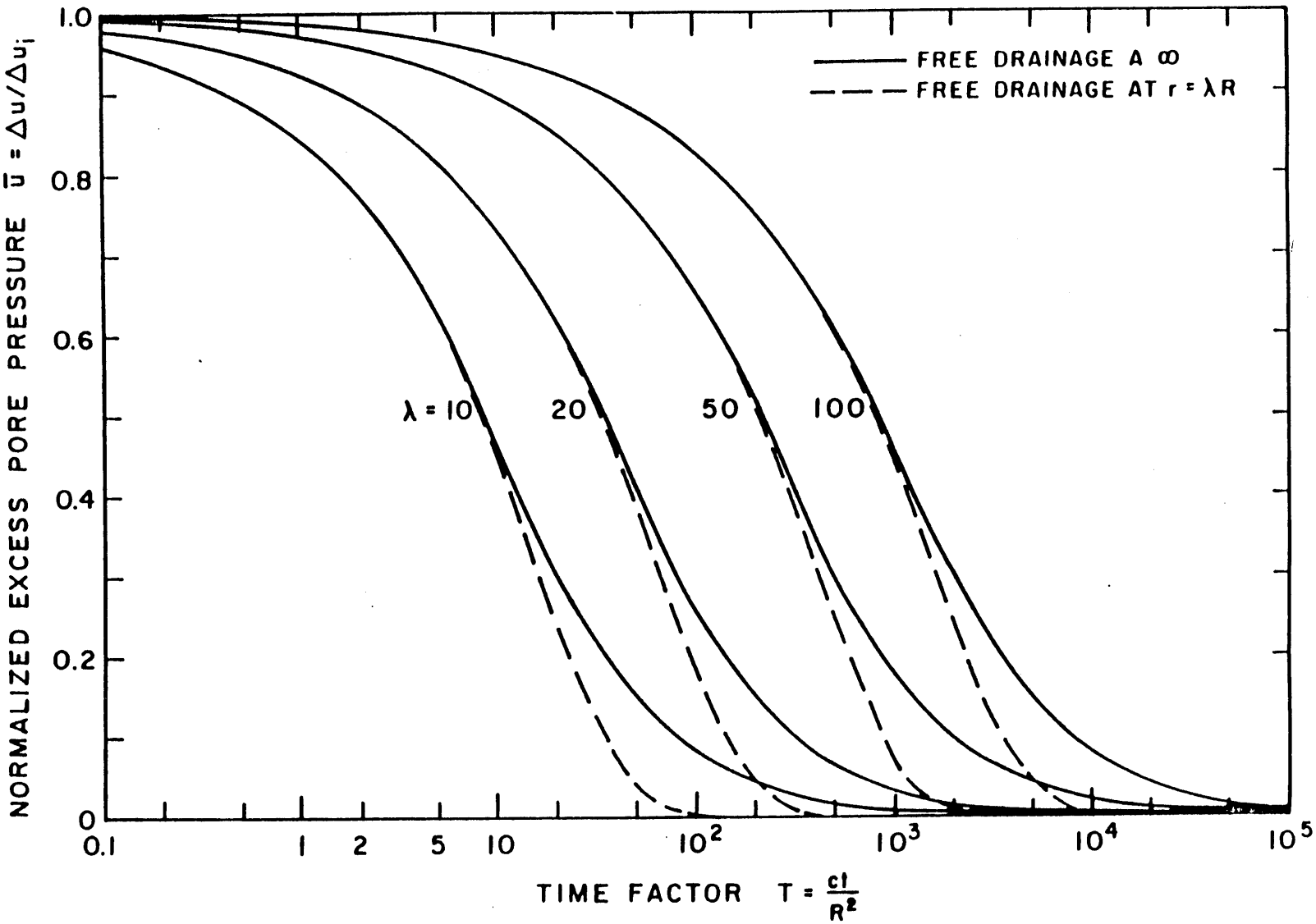

Figure 5.3 Dissipation curves at the wall of a cylindrical cavity; linear initial pore pressure distribution (Baligh and Levadoux, 1980).

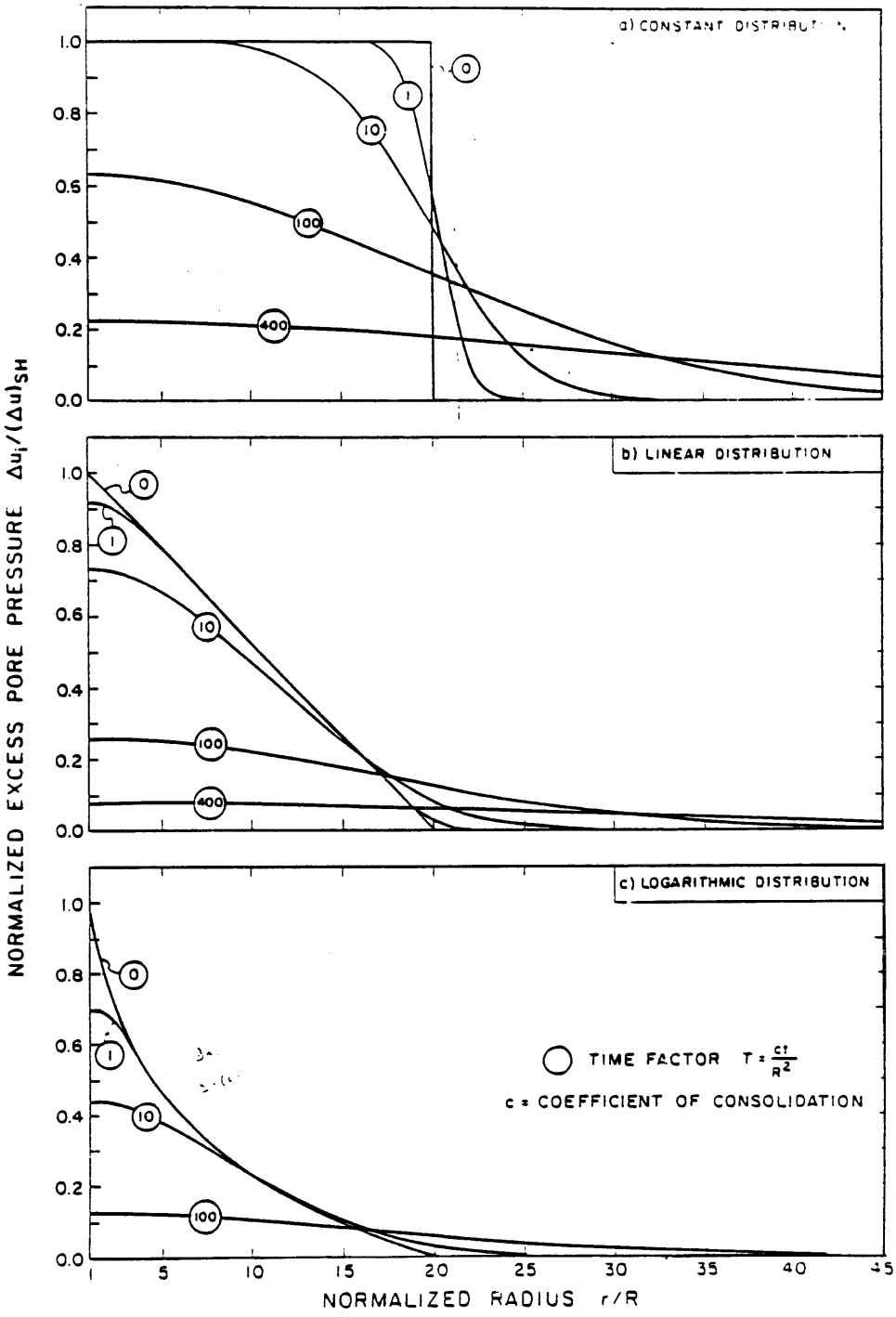

Figure 5.5 Effect of initial excess pore pressure distribution on dissipation around an impervious cylinder (λ=20) (Baligh and Levadoux, 1980).

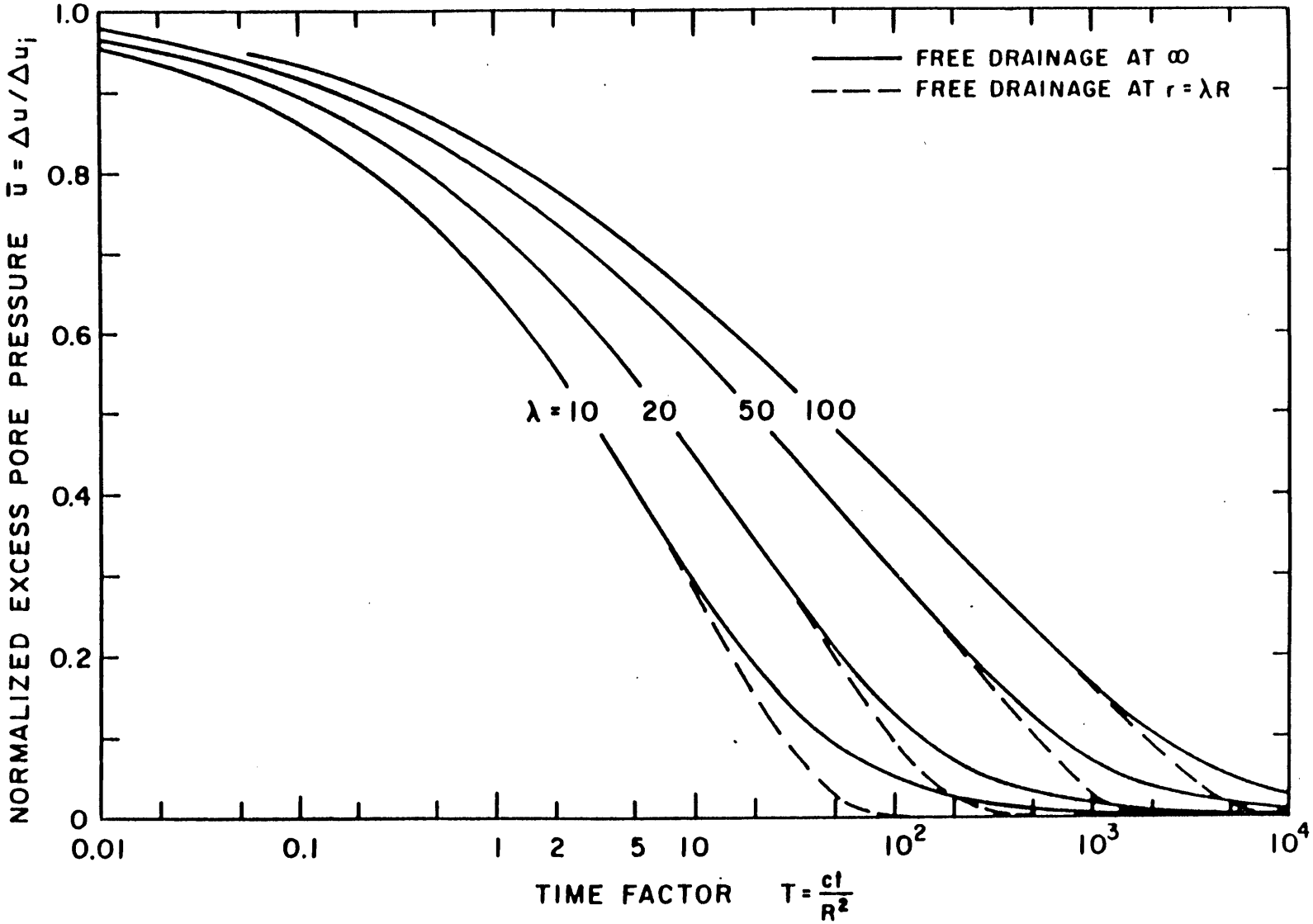

Figure 5.4 Dissipation curves at the wall of a cylindrical cavity; logarithmic initial pore pressure distribution (Baligh and Levadoux, 1980).

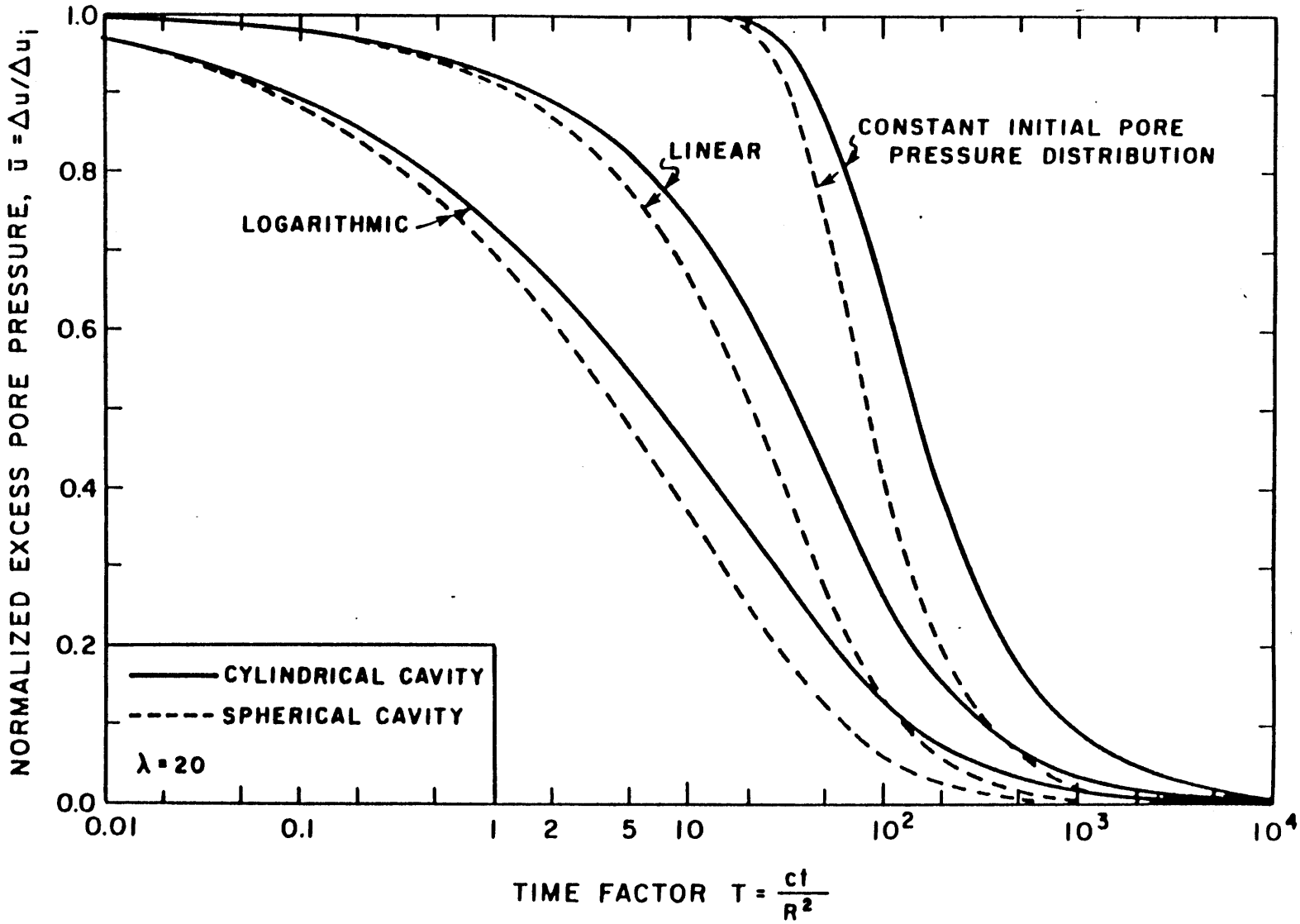

Figure 5.6 Effect of cavity type and initial distribution of excess pore pressures on dissipation at the cavity wall (Baligh and Levadoux, 1980).

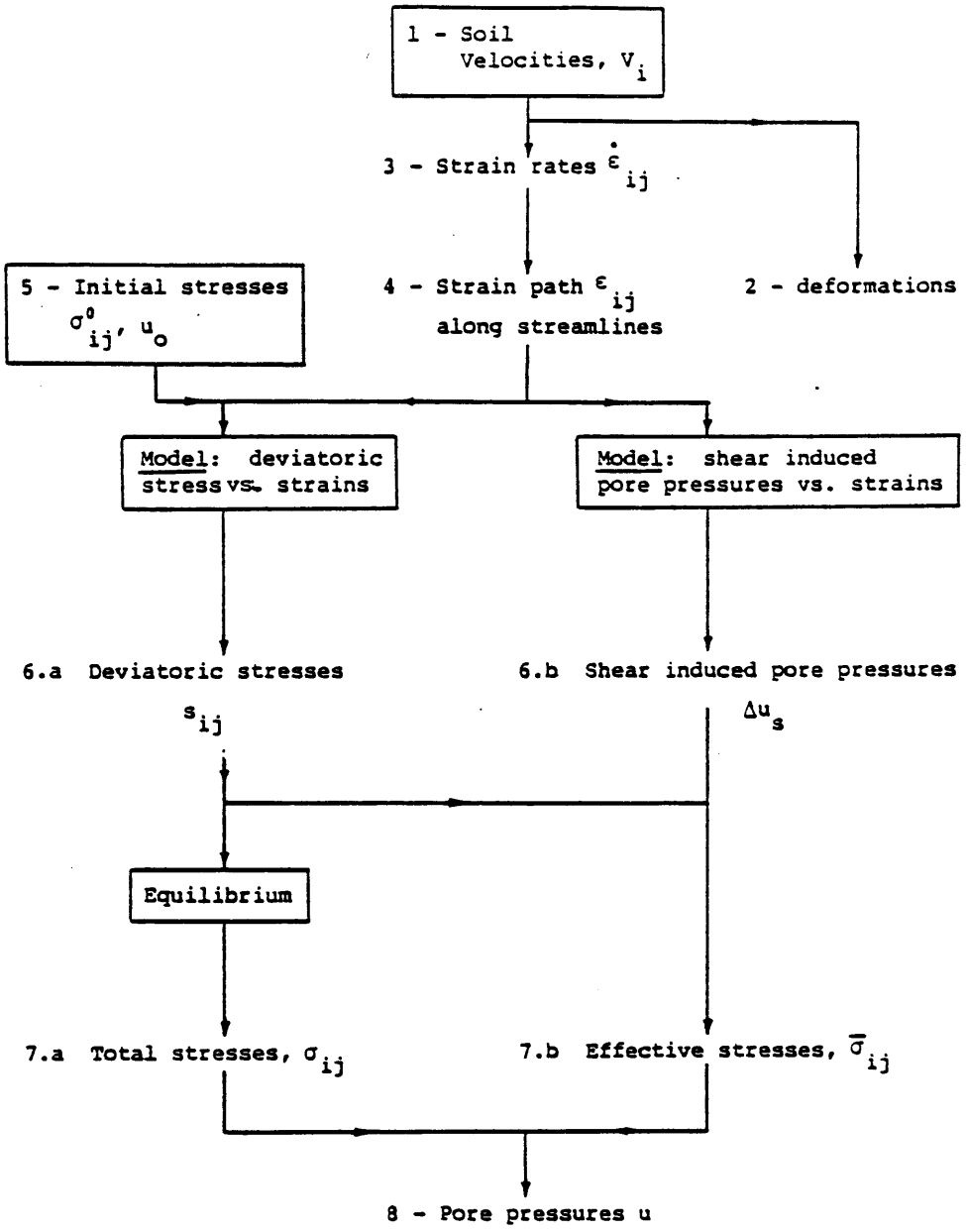

Figure 5.7 Application of the strain path method to deep steady cone penetration in clays (Baligh and Levadoux, 1980).

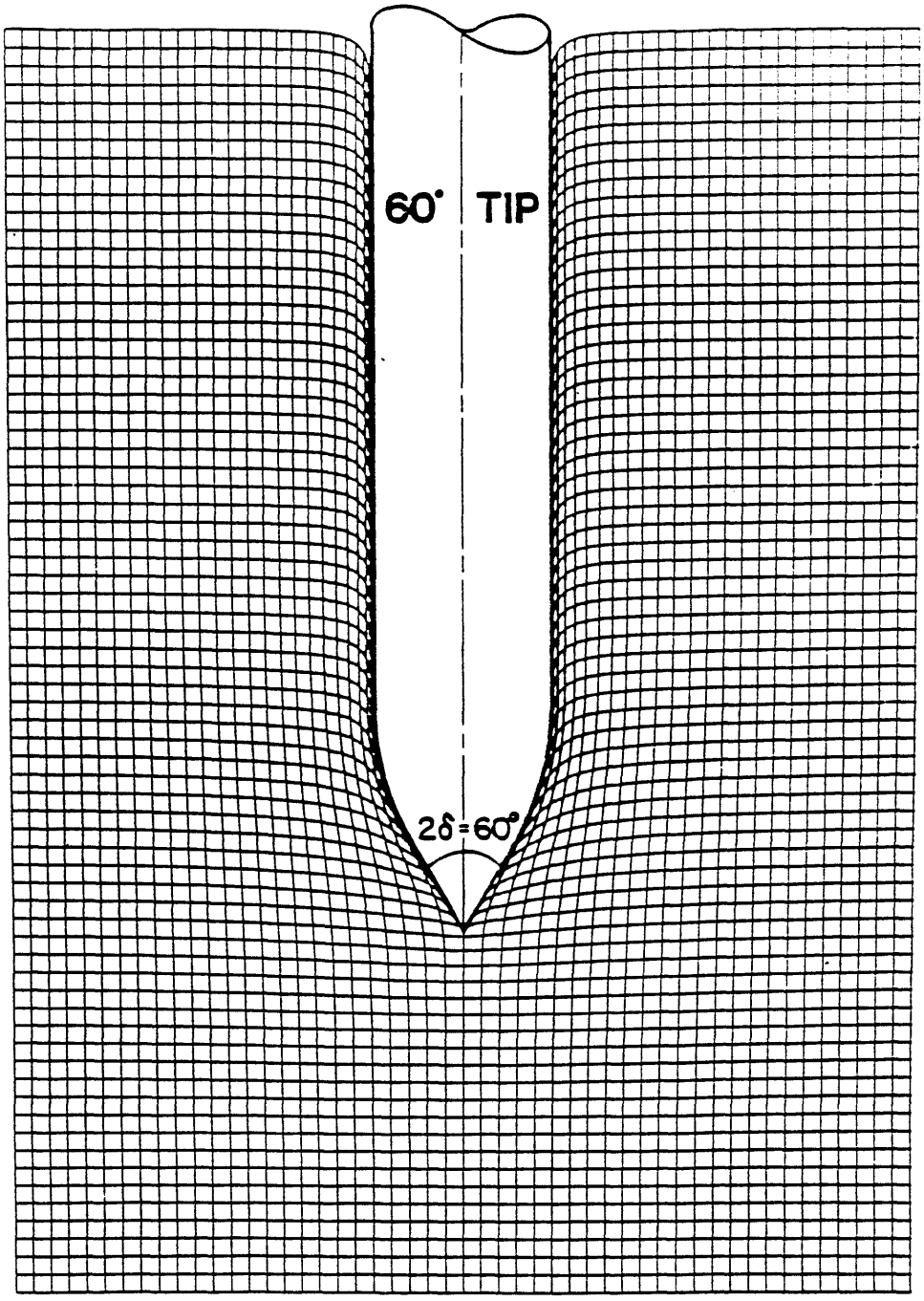

Figure 5.8 Predicted deformation pattern around a 60° cone assuming no shearing resistance of the soil (Balign and Levadoux, 1980).

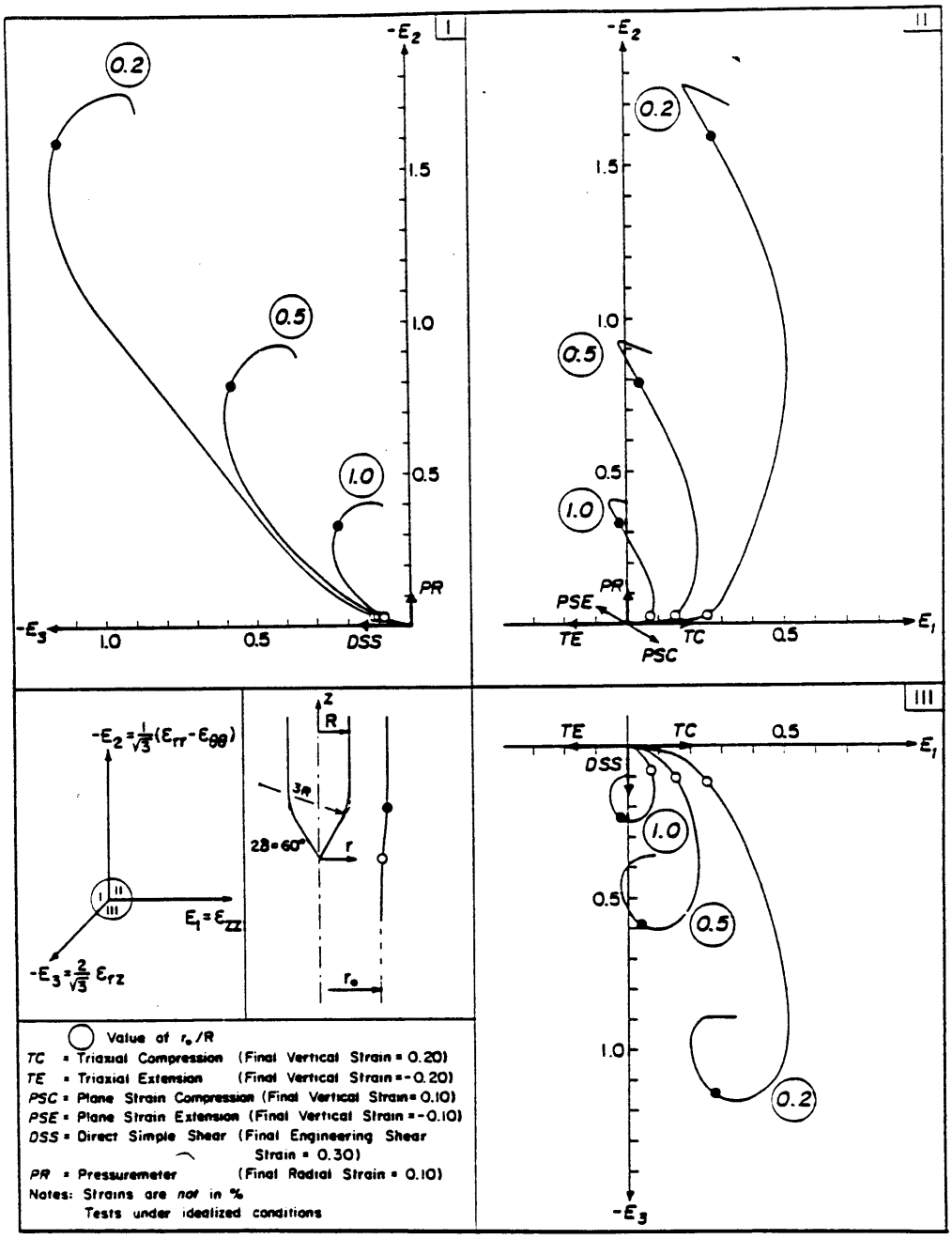

Figure 5.9 - Strain paths of selected elements during penetration of a 60° cone (Baligh and Levadoux, 1980).

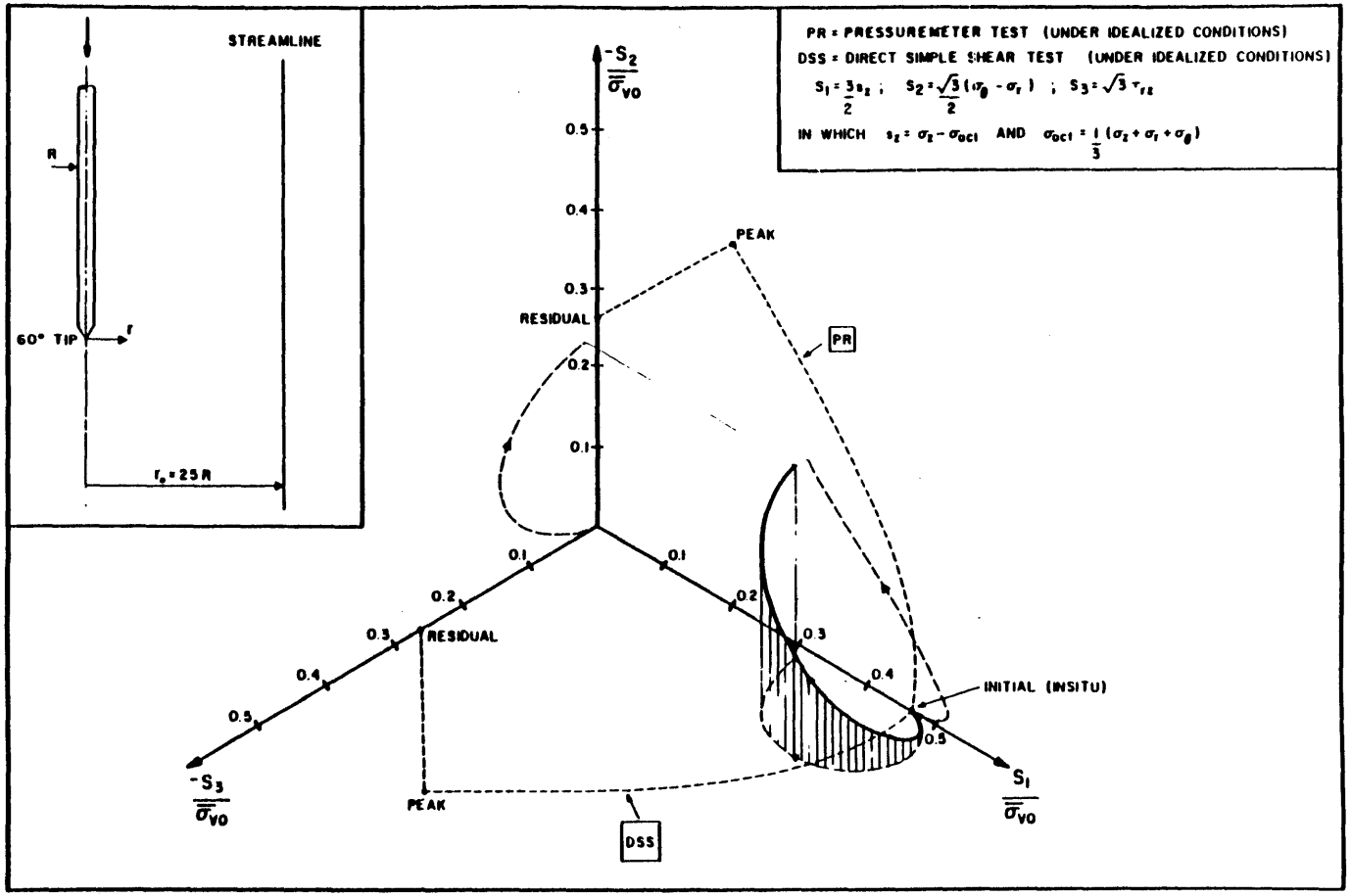

Figure 5.10 Predicted deviatoric stress path during steady penetration of a 60° cone in normally consolidated Boston Blue Clay (Baligh and Levadoux, 1980).

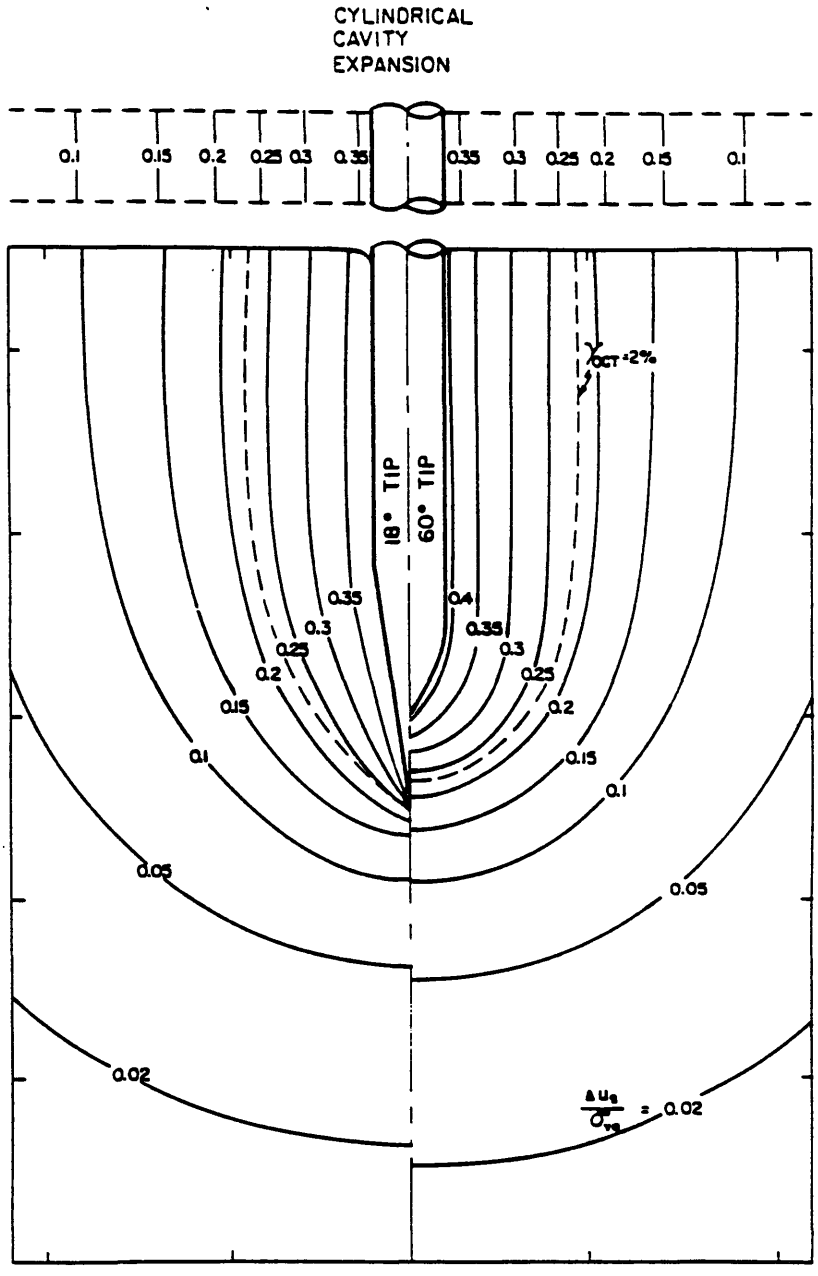

Figure 5.11 Predicted shear induced pore pressures during steady cone penetration in normally consolidated Boston Blue Clay (18° and 60° tips) (Baligh and Levadoux, 1980).

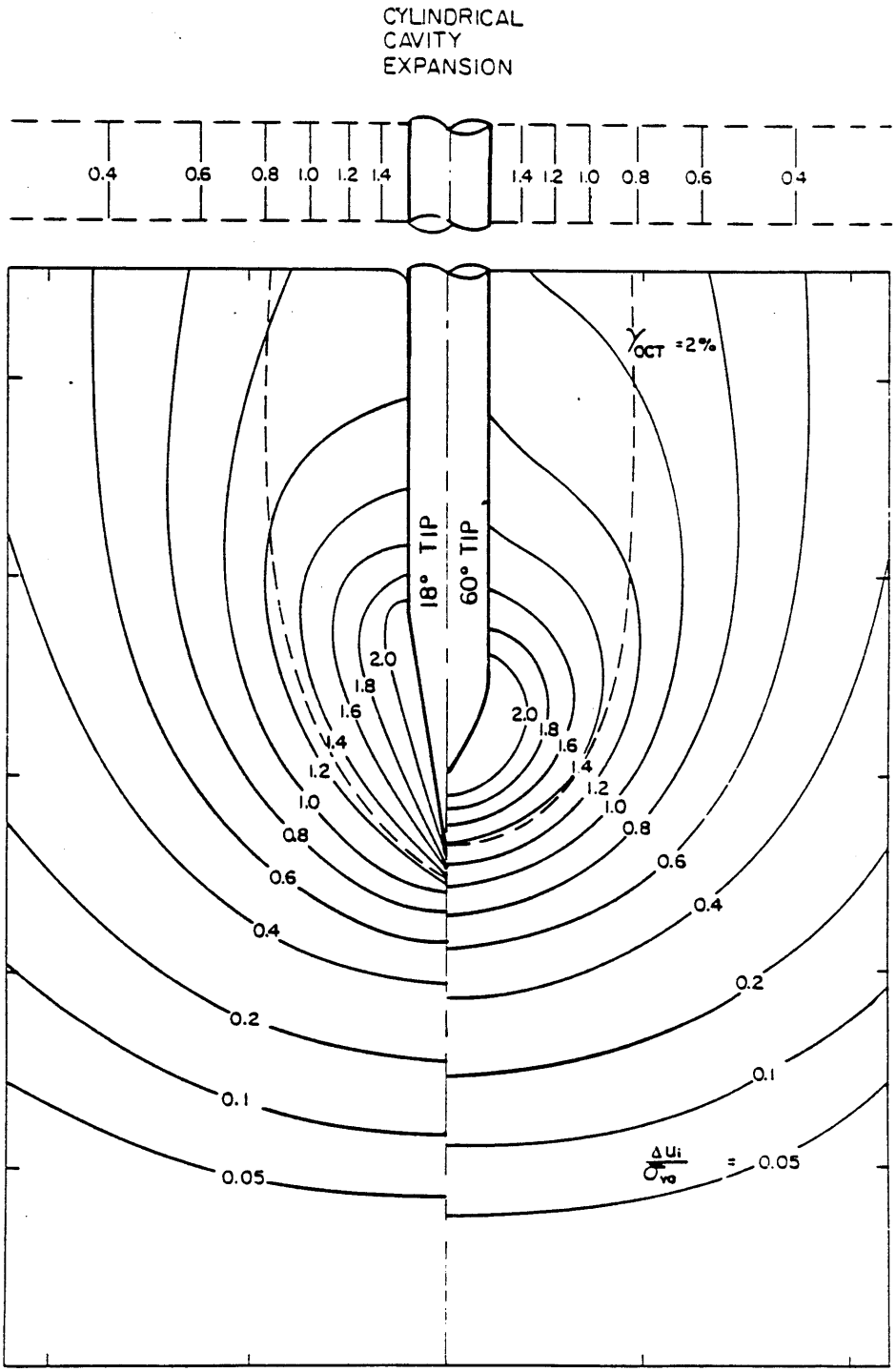

Figure 5.12 Predicted excess pore pressures during steady cone penetration in normally consolidated Boston Blue Clay (18° and 60° tips) (Baligh and Levadoux, 1980).

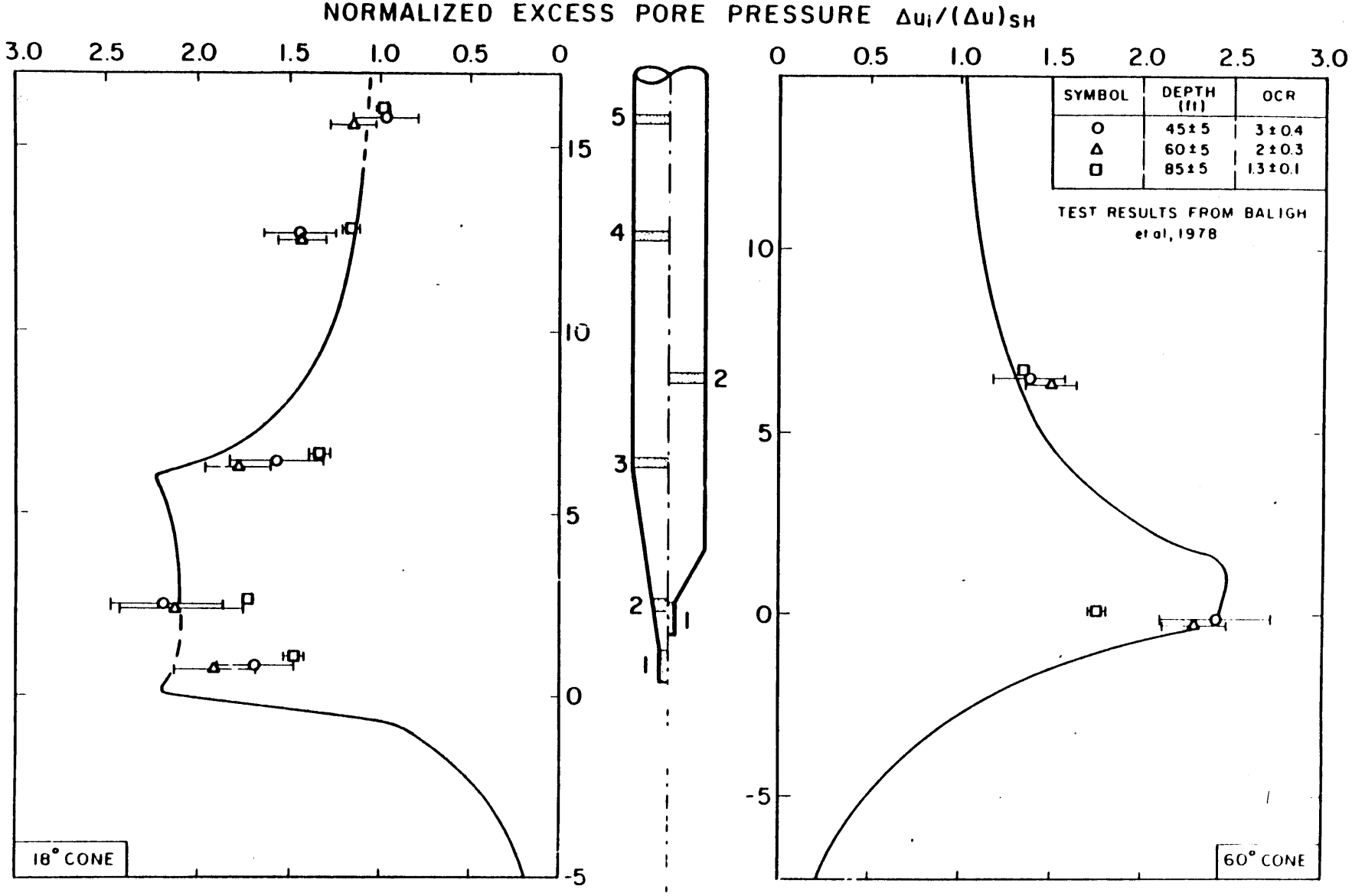

Figure 5.13 Predicted vs measured normalized excess pore pressures along the face and shaft of 18° and 60° cones during steady penetration in Boston Blue Clay (Baligh and Levadoux, 1980).

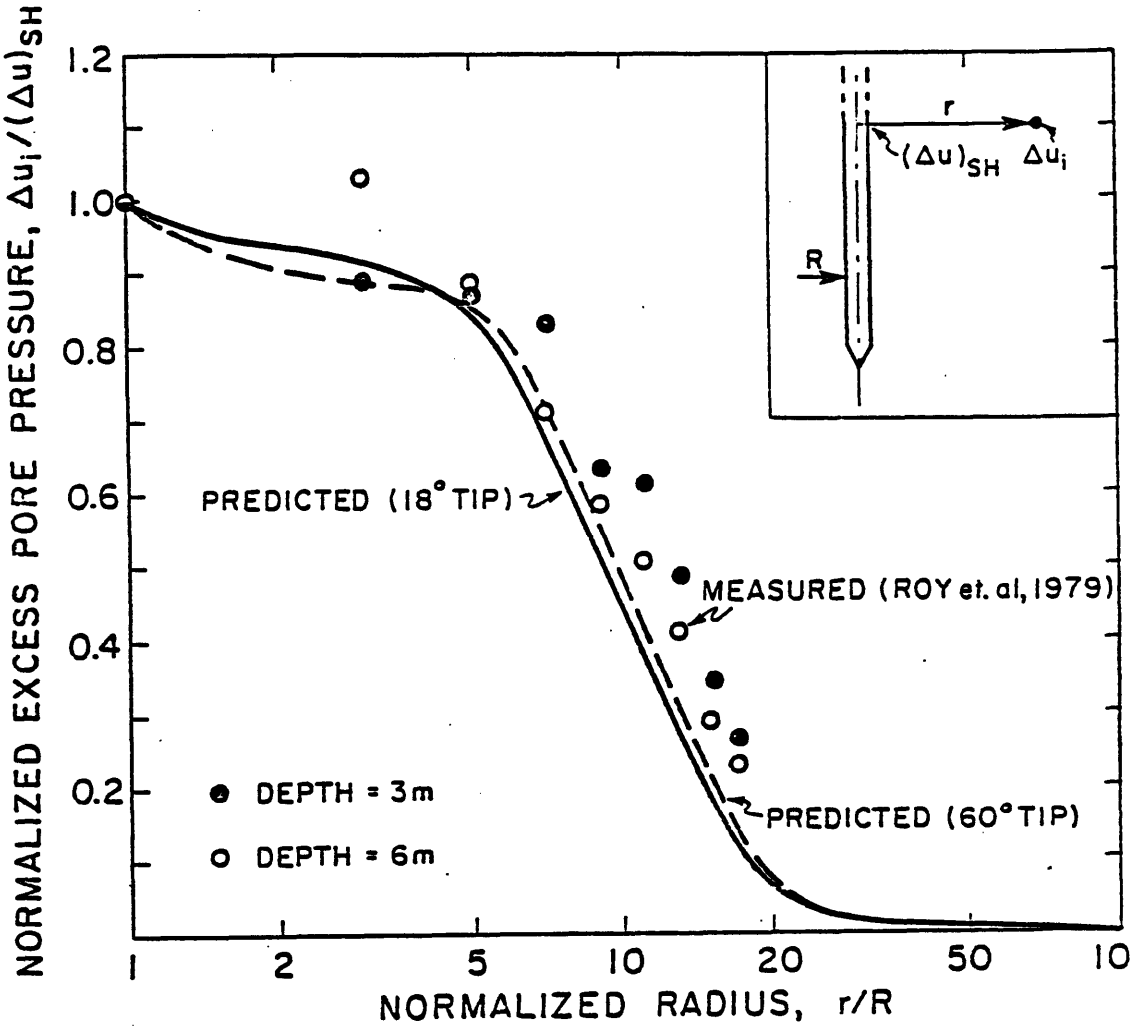

Figure 5.14 Predicted vs measured distribution of normalized excess pore pressures during penetration in clays (Baligh and Levadoux, 1980).

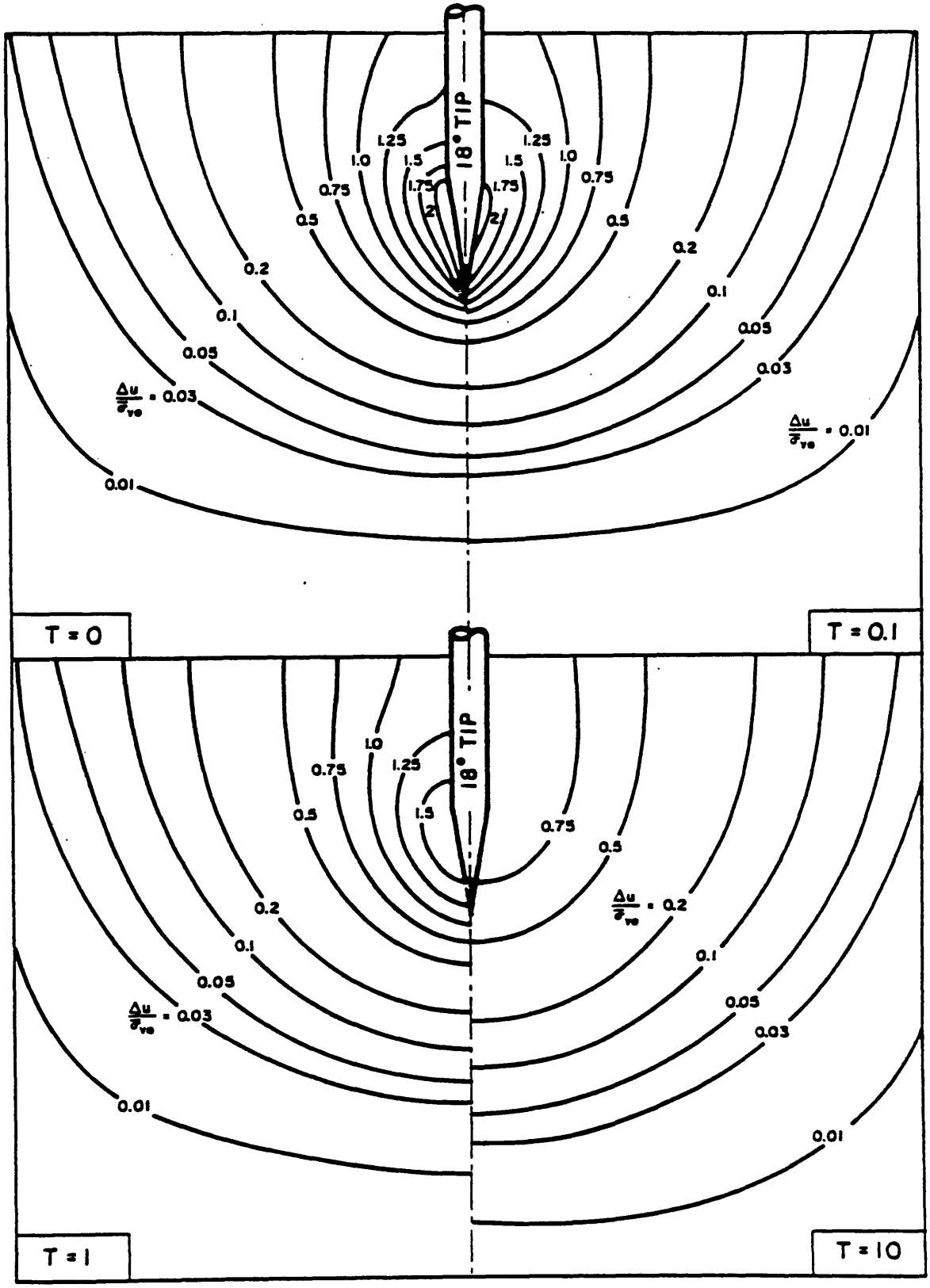

Figure 5.15 Contours of excess pore pressures during uncoupled consolidation around an 18° cone in a linear isotropic material (Baligh and Levadoux, 1980).

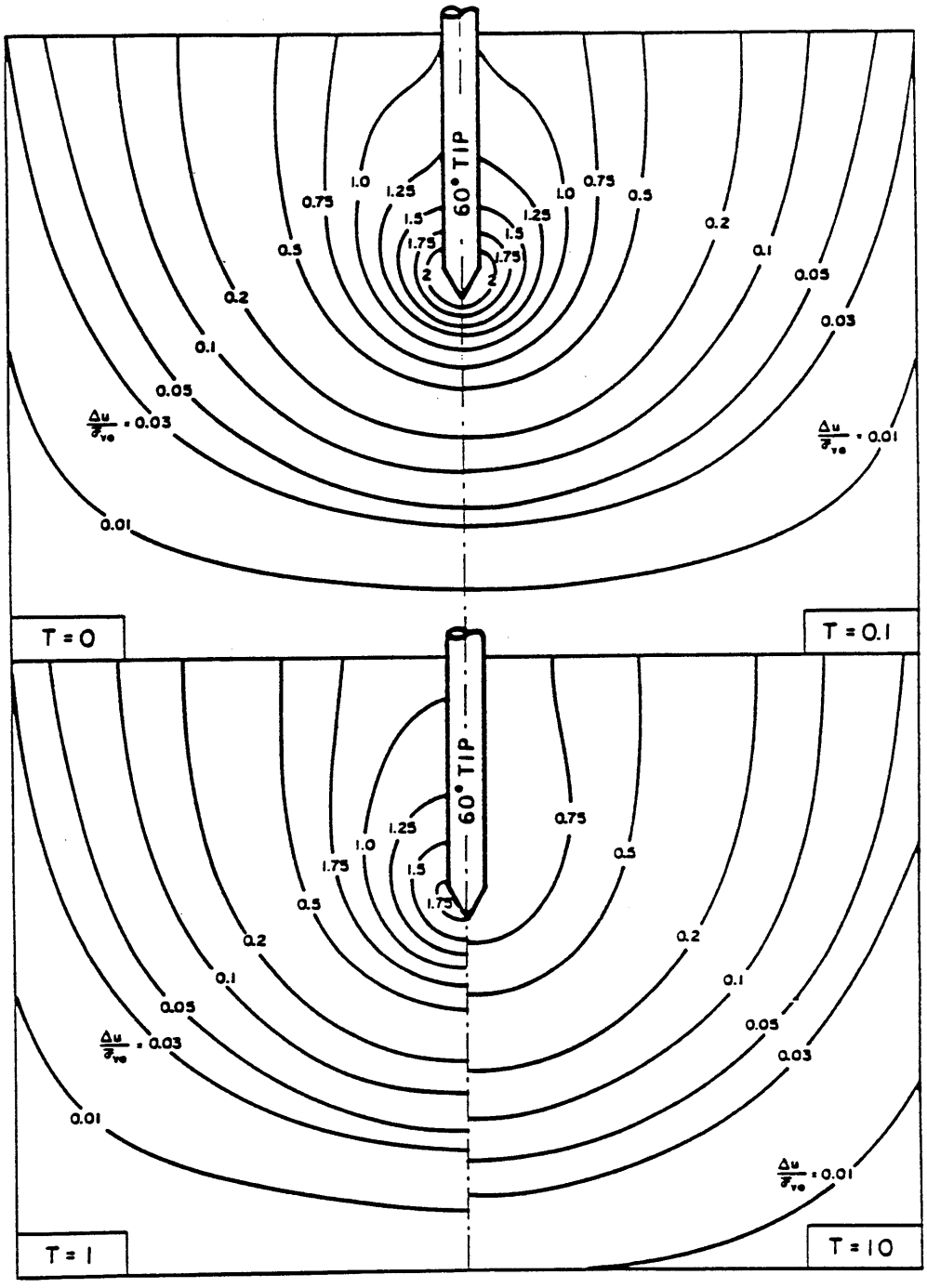

Figure 5.16 Contours of excess pore pressures during uncoupled consolidation around a 60° cone in a linear isotropic material (Baligh and Levadoux, 1980).

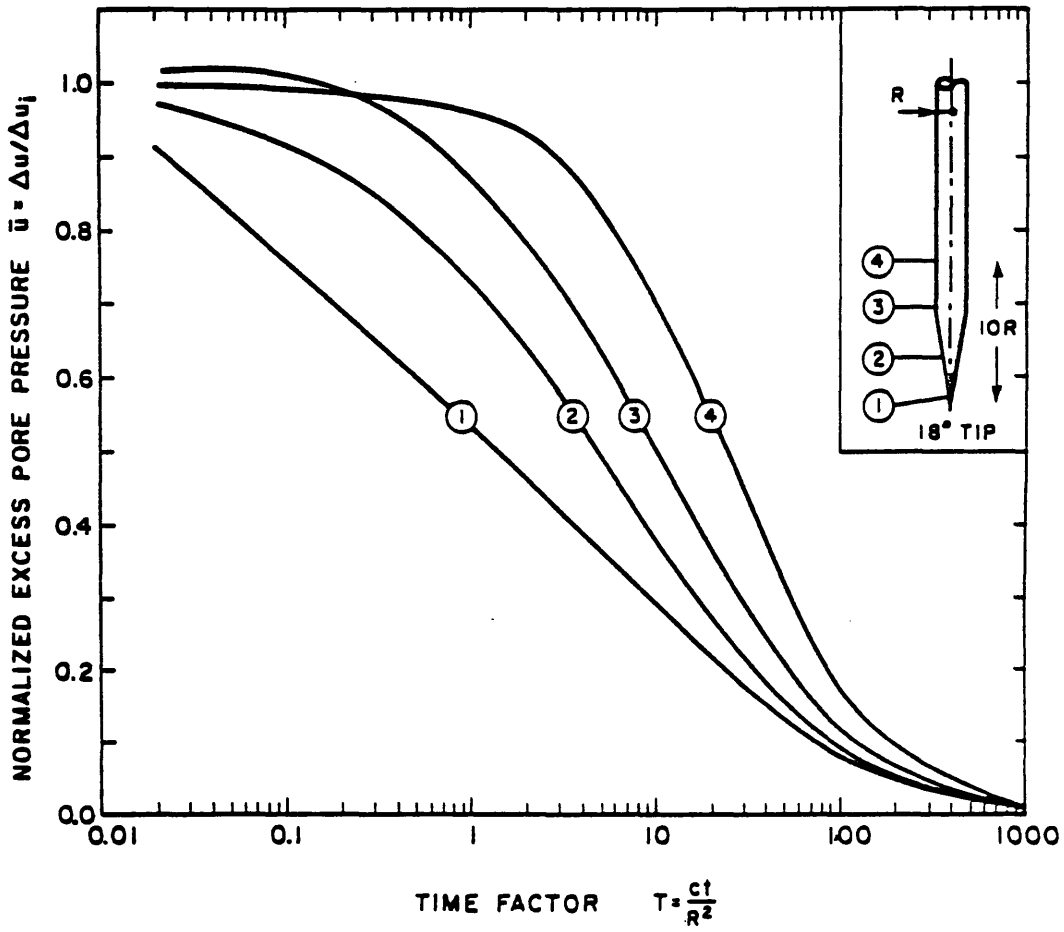

Figure 5.17 Dissipation curves for an 18° cone according to linear isotropic uncoupled solutions (Baligh and Levadoux, 1980).

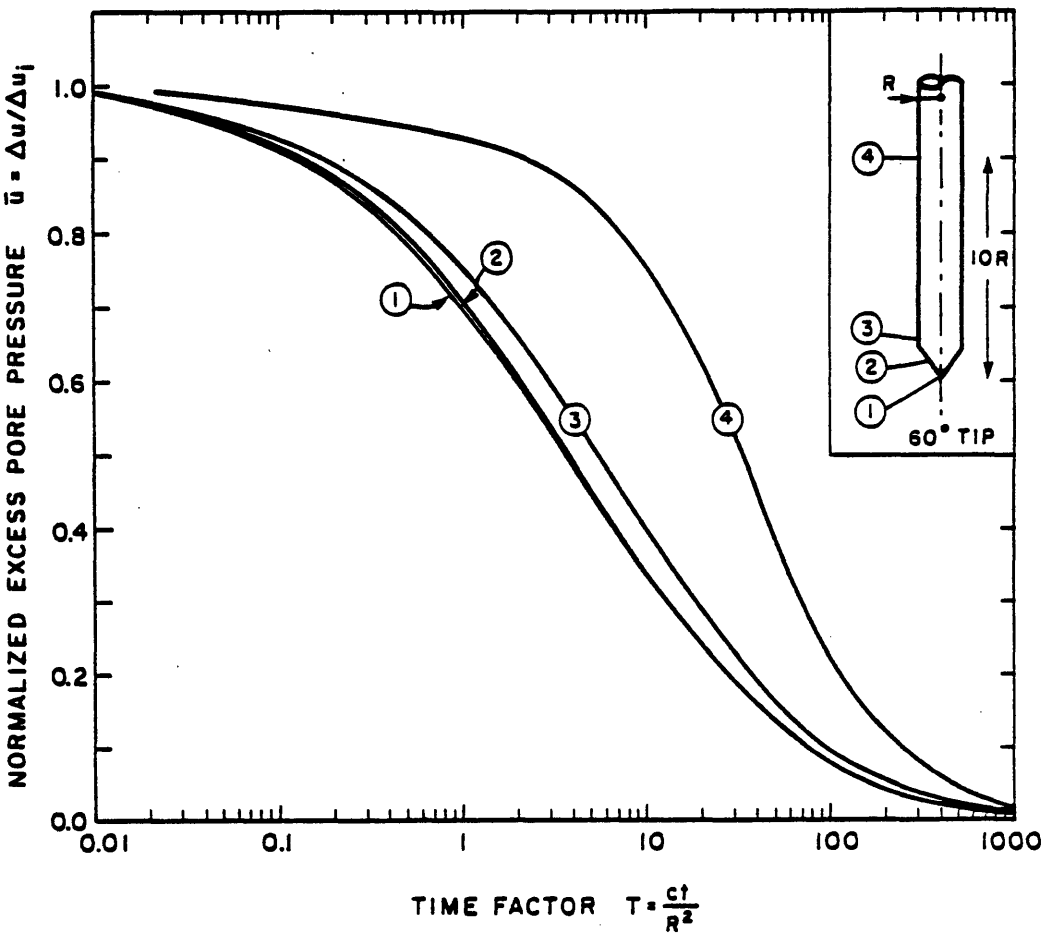

Figure 5.18 Dissipation curves for a 60° cone according to linear isotropic uncoupled solutions (Baligh and Levadoux, 1980).

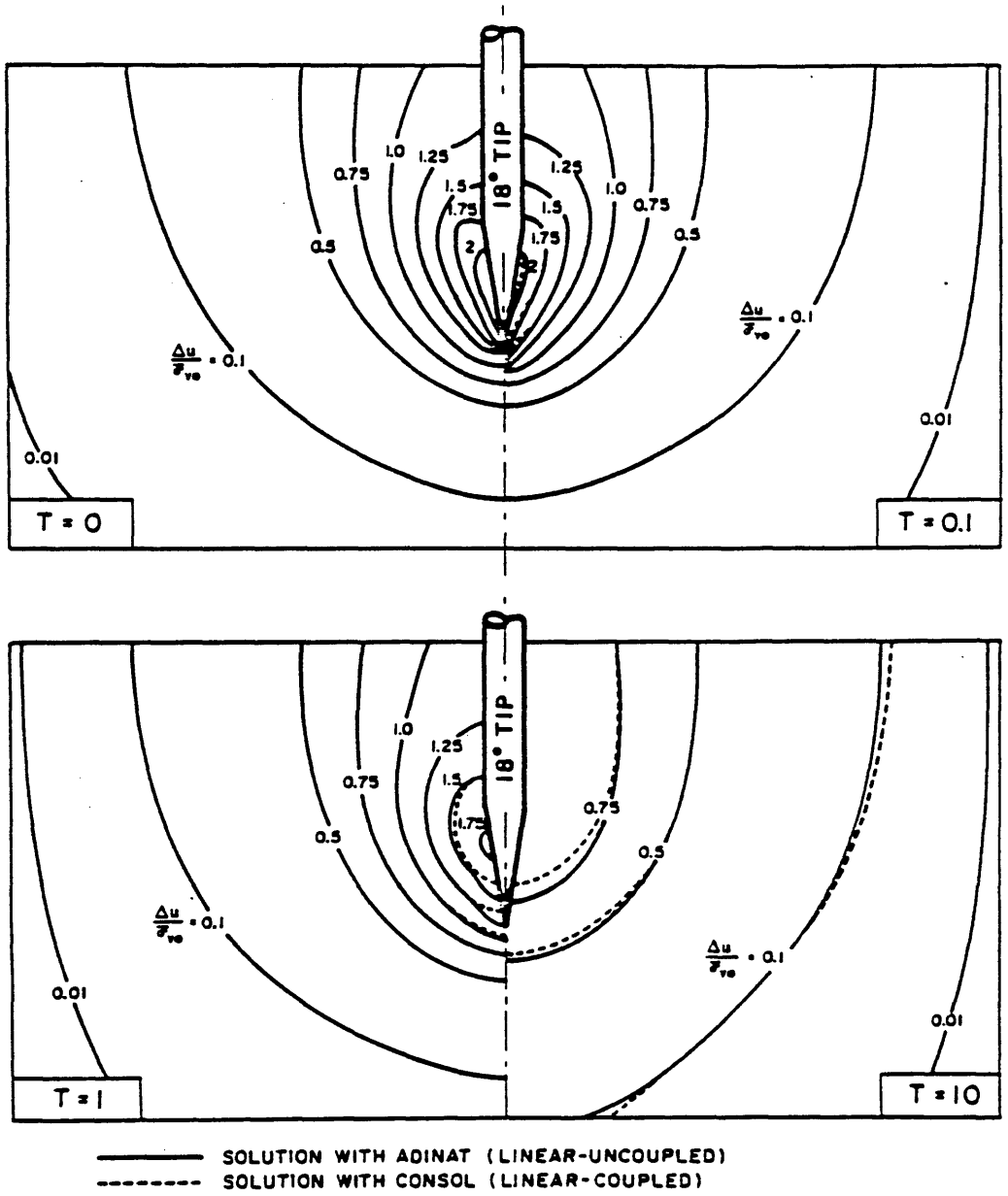

Figure 5.19 Effect of coupling on the predicted contours of excess pore pressures during isotropic consolidation around an 18° cone (Baligh and Levadoux, 1980).

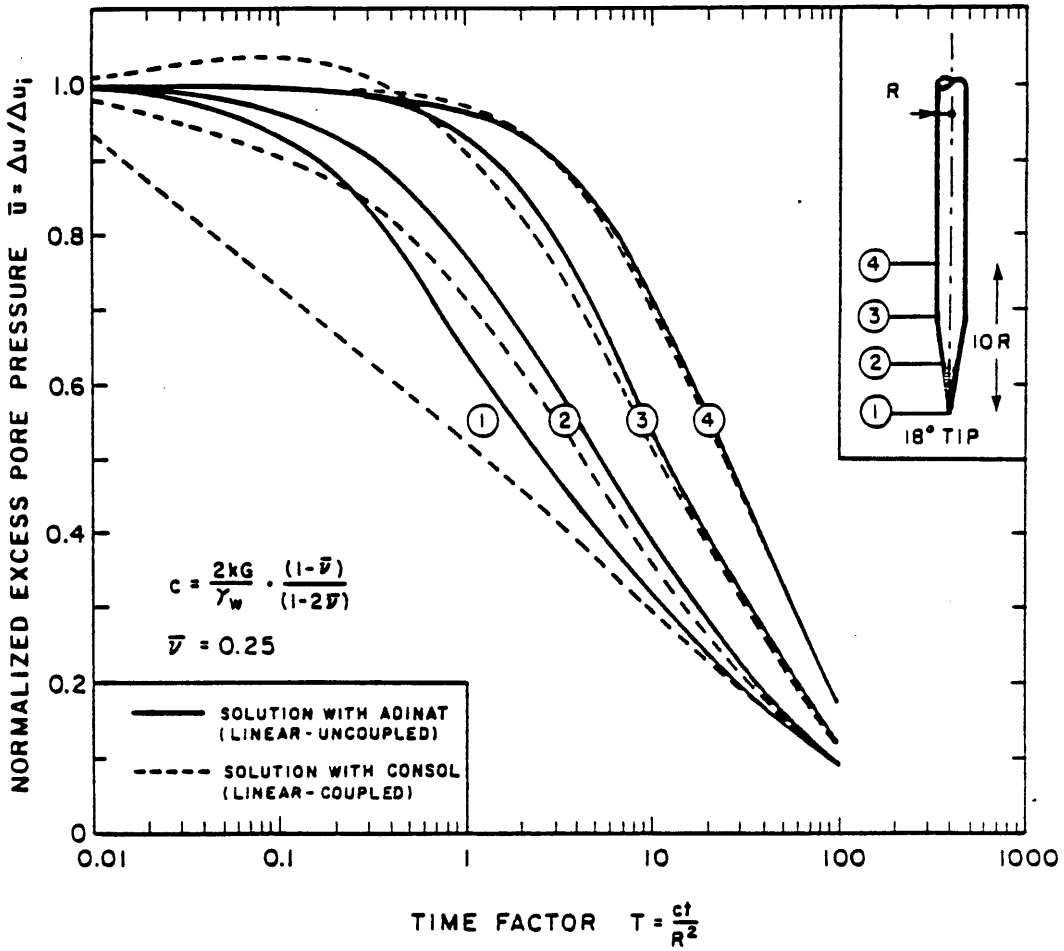

Figure 5.20 Effect of linear coupling on dissipation curves for an 18° tip (linear isotropic analyses) (Baligh and Levadoux, 1980).

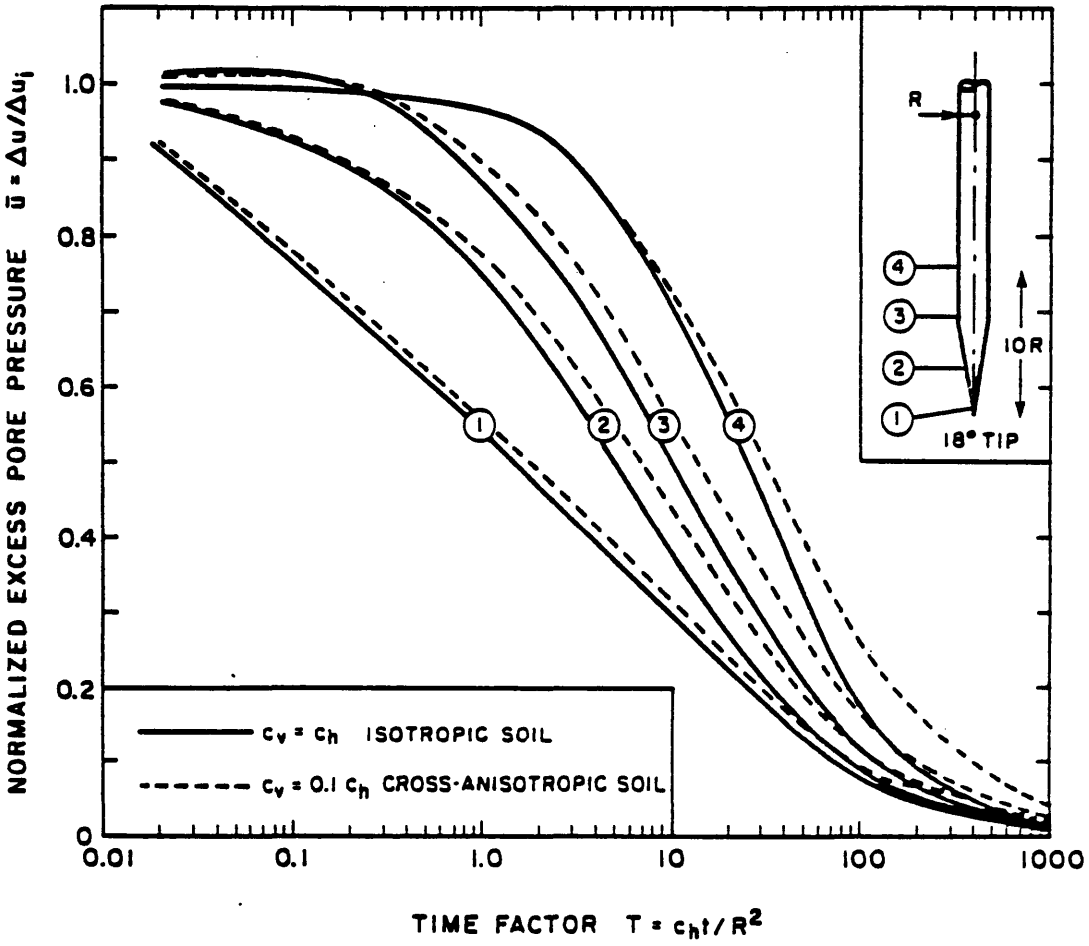

Figure 5.21 Effect of anisotropy on dissipation curves for an 18° cone (uncoupled linear analysis) (Baligh and Levadoux, 1980).

CHAPTER 6

EVALUATION OF ALTERNATIVES AND THE PERSCRIPTION OF AN INTERPRETATION METHOD

6.1 INTRODUCTION

The final step in our perscriptive system's model, alternative evaluation, is examined herein. Due to the fact that our models are consistently incomplete (since if they were complete and comprehensive they would be reality which is only achieved if the state of nature reveals itself) and are a vague representation of reality, our judgement should be based on how close to reality are the assumptions and system output of a particular approach. Few guidelines were suggested as a yardstick although the list one can generate could be infinite. The two alternatives are evaluated versus such guidelines and then compared and contrasted. It was felt that the best method of evaluating Baligh and Levadoux's method would be:

(a) Compare predicted dissipation curves, coefficients of consolidation, c_h and c_v, and coefficients of permeability, k_v and k_h, with dissipation curves obtained from in situ field tests and values of c_v, c_h, k_v and k_h obtained from lab tests.

Rembering that the distribution of the induced pore pressures during penetration of 18° and 60° cones was based on soil properties botained from laboratory tests on resedimented normally consolidated Boston Blue Clay, the generality of the interpretation method is conserved when applied to Connecticut Valley Varved Clay, CVVC, and compared to field and laboratory results.

(b) The predicted soil parameters namely the profile of the vertical coefficient of consolidation, is used to predict the performance of a wide excavation on M.I.T. campus. Verification is based on a comparison of the predicted dissipation curves vs. field piezometer data. This evaluation is treated in Chapters 7-9.

6.2 EVALUATION OF TORSTENSON'S METHOD

The use of Torstenson's method for evaluating the initial distribution of the pore pressures is highly questionable as it raises serious theoretical and practical problems caused by the severe oversimplifications he introduces. The problem thus invisaged could be summarized as follows:

1) The initial pore pressure distribution in the close proximity of the probe's tip is clearly two dimensional in nature and hence use of one-dimensional analysis involves severe oversimplifications.

2) The use of an elastic perfectly plastic behavioral model, generally underestimates the extent of the plastic zone which is very sensitive to the secant modulus at low strains (Levadoux, 1980).

3) The choice of the rigidity index E/s_u $(=3G/s_u)$ requires a good understanding of the mode and the rate of shearing of the clay. Fig. 6.1 and Table 6.1 clearly manifest the marked non linearities exhibited by undrained shearing of Boston Blue Clay. Estimates of G_s can easily vary by one order of magnitude depending on γ, the overconsolidation ratio and type of test. Similarly, s_u can easily defer by a factor of 2 in view of all the uncertainties involved.

4) Difficulty in choosing the appropriate cavity type and the associated equivalent radius R.

5) A rational justification for selecting the logarithmic initial excess pore pressure distribution corresponding to cavity expansions in an elastic-perfectly plastic material.

As mentioned earlier in this chapter with regards to Torstensson's method of predicting initial pore pressure, its applicability is highly questionable. Likewise, use of his method to predict the coefficient of consolidation is equally questionable for the following reasons:

a) What is the "type" of the estimated coefficient of consolidation c, i.e., horizontal vs. vertical and overconsolidated vs. normally consolidated?

b) What cone angle and porous stone location are considered adequate?

c) Why was the condition for 50% consolidation used to estimate the coefficient of consolidation c?

In short, Torstensson's method for prediction of initial penetration pore pressure distribution and subsequent dissipation mechanism, do not provide the necessary insight into cone penetration mechanism which is essential in understanding and hoepfully accounting for soil nonlinearities neglected in conventional consolidation analysis.

6.3 EVALUATION OF BALIGH AND LEVADOUX'S DISSIPATION SOLUTIONS IN BOSTON BLUE CLAY

The linear dissipation solutions involve significant simplification of soil behavior during consolidation by assuming that the soil skeleton is linear and exhibits no

time-dependent properties. Uncertainties in the initial excess pore pressure distribution derived by the strain path method based on properties of normally consolidated Boston Blue Clay also present significant oversimplification and loss of generality.

Simple linear solutions are attractive for applications in different soils, but can cause serious difficulties in interpreting test results for the selection of appropriate engineering parameters for design. Few comprehensive non-linear analyses were conducted to study consolidations around penetrating objects. Randolf et al (1978) investigate nonlinear consolidation around pile shafts and conclude that, in this relatively simple one-dimensional problem, pore pressure dissipation is not significantly affected by soil nonlinearities.

Predictions of $\Delta u_i/(\Delta u)_{sh}$ obtained by the strain path method on the basis of laboratory test data on normally consolidated resedimented Boston Blue Clay provide good agreement with in situ measurements (a) on the face and shaft behind 18° and 60° cones in a B.B.C. deposit having $1.3 < OCR < 3$; and (b) in the soil surrounding a jacked pile in Champlain Clay, Roy et al (1979), Fig. 5.14.

A more comprehensive evaluation of the aforementioned method is presented herein. Its main objectives are to

address the following questions.

(a) Evaluate the capability of simple linear solutions in predicting in situ dissipation measurements in Boston Blue Clay;

(b) Investigate the effect of various practical factors on the reliability (repeatability) of the estimated profiles of the coefficients of consolidation and permeability, e.g. cone angle, porous stone location, degree of consolidation (dissipation) required, etc.; and,

(c) Compare the estimated coefficients of consolidation and permeability with laboratory measurement and field performance data.

6.3.1 Site Description

(a) Geology

The Boston Blue Clay (BBC) was formed during the wane of the late Pleistocene ice age (about 14,000 years ago) under a marine environment in the Boston Basin, probably not very far from the ice margin. The clay deposit overlaid a glacial till which covered the bedrock, and had a typical thickness in excess of 50 to 125 ft. depending on the topography of the till. The clay includes numerous lenses of fine sands, isolated sand pockets and occasional stones or pebbles. Subsequent to clay deposition, movements of the

earth crust and of the sea level resulted in emergence of the clay above the sea, followed by extensive weathering, desiccation, and erosion of the upper part of the deposit. This was followed by at least two periods of submergence and deposition, of lesser significance, in which outwash sand, and peat and silt were deposited above the clay. Further geologic details are given by Kenney (1964) and Aldrich (1970).

(b) Soil Conditions at the Test Site

The test site is adjacent to the coastline in Saugus, Mass., 160 to 200 ft. (49 to 61 m) to the east of the unfinished Interstate 95 embankment centerline at Station 246, Figs. 6.2 and 6.3 . M.I.T. studied this embankment extensively in the last decade by means of laboratory and in situ tests, embankment monitoring during construction, and a planned embankment loading to failure (D'Appolonia et al., 1971; M.I.T., 1975).

Figure 6.4 shows the soil profile at the test site as determined by conventional sampling and laboratory testing methods. The upper 25 ft. consist of peat, sand and stiff clay layers which overlie 130 ft. of Boston Blue Clay (BBC). The BBC of interest is located between depths 25 and 120 ft. Typically, the visual classification, and index tests (e.g., the natural water content, w_n, the liquid limit, w_ℓ, and plastic limit, w_p) provide little reliable information regarding stratification and variability

On the other hand, laboratory estimate of the maximum past pressure, $_{vm}$, by means of conventional oedometer and constant rate of strain consolidation tests clearly indicate that the clay above a depth of 75 ft., approximately, is significantly overconsolidated (i.e., has an OCR = $\bar{\sigma}_{vm}/\bar{\sigma}_{vo}$ well above unity).

(c) Undrained Shear Strength

Fig. 6.5.(a) show the undrained shear strength, s_u, of the clay determined by means of laboratory tests on 3" and "undisturbed" fixed piston samples. Unconfined (U) and unconsolidated undrained (UU) tests are not significantly different and vary between the wide range given by 0.4 ± 0.2 TSF without a clear trend with depth. Higher quality samples obtained in 1978 give higher strengths and exhibit relatively less scatter because of the reduced effect of sample disturbance.

Fig. 6.5.(a) also shows the peak strengths, s_u, obtained by the SHANSEP procedure based on the estimated OCR profile in Fig. 6.4 for k_o- consolidated undrained plane strain compression (PSC) and plane strain extension (PSE) tests (Ladd and Foott, 1974). Direct simple shear and triaxial tests where samples are isotropically and k_o- consolidated generally give s_u between the band provided by PSC and PSE in Fig. 6.5.(a) (except for the k_o-consolidated triaxial extension tests yielding s_u 18%

lower than PSE). The SHANSEP profile in Fig. 6.5.(a) are smooth and cannot detect soil variability. because averaging is required in estimating the profile of $\bar{\sigma}_{vm}$. s_u(PSE) is significantly less than s_u(PSC) and hence indicates the significant strength anisotropy of the clay.

Azzouz and Baligh (1978) backfigured the field strength, s_u(field) required for circular arc stability analyses based on the results of a planned embankment failure that extended to a depth of 75 ft. The profile of s_u(field) above 75 ft. is based on their results and below 75 ft. is estimated from the SHANSEP strength profiles, Fig. 6.5.(a)

Figure 6.5.(b) shows the undrained shear strength, s_u, determined by means of the Geonor Field Vane (FV) at about 3 ft. intervals in four holes within 200 ft. from the test site where one notes that s_u(FV) is generally between 0.4 and 0.6 TSF throughout the profile. Looking more carefully, two distinct layers can be identified: the first is located below a depth of 75 ft. where s_u(FV) exhibits less scatter and increases with depth. The second layer is above 75 ft. where s_u(FV) varies between 0.4 and 0.6 TSF with little identifiable trend. This is the more overconsolidated part of the deposit which was probably subjected to significant dessication.

(c) Cone Penetration Data

Figure 6. 6 shows the cone penetration resistance, q_c, obtained by a standard FUGRO 60° cone and the pore pressure, u_i, measured at the tip of an 18° conical piezometer during steady penetration at a rate of 1 to 2 cm/sec in three different holes (each). Since cone penetration is continuous and largely independent of testing procedures and human interference, q_c and u_i provide consistent and reliable data for evaluating stratification and variability of the soil.

As in the case of field vane test results (Fig. 6.5.(b)) and conventional sampling and laboratory testing data (Fig. 6. 4), BBC between 25 and 120 ft. can be divided into an upper overconsolidation clay above 75 ft. and a different lower clay. In addition, q_c and u_i indicate that the upper clay can possibly be divided into two sublayers, 25 to 60; and 60 to 75 ft., or even three sublayers, 25 to 40; 40 to 60; and 60 to to 75 ft.

(d) In Situ Static Pore Pressures

Figure 6.7 shows estimated values of the total stress, σ_{vo}, and the static pore pressures, u_o, in the soil obtained by leaving conical probes in the ground for sufficient periods of time. Measurements suggest that some artesian pressure exists in the underlying glacial till. For purposes

of dissipation calculations, a 10 ft. artesian head in the till was selected.

(e) Pressuremeter Results

Ladd et al. (1979) conducted a comprehensive study of self boring pressuremeter tests in BBC. Fig. 6. 8 shows the limit pressure, p_l, obtained at Sta. 246 by means of the French PAFSOR equipment. Amongst all pressuremeter measurements, p_l was most consistent (less scatter) and relatively independent of the testing procedures and the interpretation method. Results in Fig. 6. 8 indicate that, regardless of the interpretation method, the variation of p_l with depth in the upper BBC above a depth of 75 ft. is different from the lower BBC below 75 ft.

Another interesting aspect of pressuremeter results is the ratio of peak to ultimate* strengths backfigured from PAFSOR tests at Station 246. Fig. 6. 9 indicates that:

1) In spite of significant scatter due to testing procedures and different interpretation methods, the lower BBC below 75 ft. exhibits a more pronounced strain-softening behavior; and

2) Tests performed by the British CAMKOMETER equipment at Station 263 give basically the same results.

*At relatively large strains.

(f) Clay Compressibility

Constant rate of strain tests performed by Germaine (1978) on good quality undisturbed samples at Station 246 indicate different compressibilities in the upper and lower BBC below 75 ft. Fig. 6.10 shows typical strain vs. log effective stress plots for two samples recovered from depths 41.5 and 84.5 ft. Clearly, the lower clay exhibits a very sensitive behavior with collapse in structure once the maximum past pressure is exceeded.

6.3.2 Evaluation of predictions

The underlying perscriptive model involved in the evaluation process involves the following steps:

1) Select a section (layer) of the BBC deposit where dissipation data exhibit no trend with depth.
2) Compare dissipation measurements obtained at mid-height of an 18° cone with linear uncoupled solutions in order to estimate a coefficient of consolidation for this section. The mid-height of the case is attractive because:
   (a) Solutions are based on the same cone geometry as actual piezometers. This is not the case for measurements conducted at the tip of a cone.
   (b) The analytical uncertainties are reasonably small (e.g. low level of linear coupling,

pore pressure gradients and numerical instabilities near the cone axis).

(3) Using this coefficient of consolidation and the solutions presented in Chapter 5, predict dissipation rates for 18° and 60° cones at different locations on the cone, at different locations on the cone and shaft behind it, and evaluate predictions by comparisons with measurements.

6.3.3 Results of Comparisons

Results of linear uncoupled consolidation analyses based on initial distribution of excess pore pressures determined by the strain path method are compared to dissipation measurements in soft (OCR < 2) Boston Blue Clay deposit below 60 ft. at Saugus site. The comparison (Figs 6.11 through 6.13) indicates that reasonably good dissipation predictions are achieved at four locations on a 18° cone and at the tip of a 60° cone when the horizontal coefficient of consolidation c_h=0.04 cm^2/sec. Additional results of this comparison show that:

1) Predictions of excess pore pressure dissipation based on linear uncoupled solutions lead to good agreement with measurements (at different locations on an 18° cone and

at the tip of a 60° cone) at the early stages of consolidation. This suggests that the initial distribution of excess pore pressures estimated by the strain path method is reasonably accurate.

2) Predictions at later stages of consolidation tend to overestimate dissipation rates* especially on the shaft behind the 18° cone and the tip of the 60° cone. This is believed to result from coupling, nonlinearities, and various levels of soil remoulding around the cone so far neglected in the analysis.

3) The accuracy achieved by linear uncoupled solutions in estimating c_h (within a factor of 1.5 to 2.5) is believed to provide adequate predictions for most practical purposes. More sophisticated analyses would be necessary if measurements conducted to large degrees of consolidation (say $\bar{u} < 0.1$) indicate a more significant deviation from predictions.

Table 6.2 presents the recommended factors to interpret dissipation records obtained by means of 18° probe when the stone is located at the tip and mid-height; and, for a 60° probe with the stone at the tip. The coefficient of consolidation c_h at a given degree of consolidation is

*By underestimating the time to reach a given degree of consolidation by a factor of 1.5 to 2.5

evaluated by dividing the factor R^2T (in Table 6.3) by the measured time necessary to achieve this dissipation level.

6.3.4 Predictions of the Consolidation Profiles

Profiles of c_h(probe) in the BBC deposit at Saugus are then obtained at different dissipation levels for three types of conical probes:

(a) An 18° cone with the stone at tip,

(b) An 18° cone with the stone at mid-height, and;

(c) A 60° cone with the stone at the tip.

The above results are collectively presented in Fig. 6. 14 The profiling analysis based on dissipation data indicates that:

1) At early dissipation stages ($\bar{u} > 0.8$) the scatter of the data is so high that reasonable c_h(probe) profiles cannot be established. The scatter is particularly high when the porous stone is located at the tip of the cone and less severe when the stone is at mid-height.

2) All three probes provide consistent c_h(probe) profiles after 50% consolidation ($\pm$ 10%) involving a very moderate degree of scatter.

3) Values of c_h estimated at high levels of consolidation ($\bar{u} = 0.2$) are slightly lower than obtained at 50% dissipation in the clay below 45 ft. having an OCR < 3, and higher in the more pervious clay about 45 ft.

6.3.5 Comparison with Laboratory Measurements and Field Performance

Figure 6.15 compares the predicted (reference) profile of horizontal coefficient of consolidation, c_h(probe) obtained from dissipation records of conical probes with relevant laboratory and field measurements. This comparison indicates:

1) The predicted variation of c_h(probe) with depth is consistent with the trends of c_v(Nc) measured in the laboratory in normally consolidated range and the profile of c_v(loading) backfigured by Duncan and by Davis and Poulos (MIT, 1975) on the basis of in situ pore pressure measurements conducted in the foundation clay under the I-95 embankment for a period of 7 years after construction.

2) The predicted magnitude of c_h(probe) is: (a) very close to c_v(unloading) backfigured by Bromwell and Lambe (1968) on the basis of in situ pore pressure measurements in a very similar BBC deposit due to a wide excavation; and (b) much higher (20 to 40 times) then c_v(Nc) or c_v(loading) described earlier.

3) Profiles of c_h(probe) can therefore provide good estimates of the coefficient of consolidation to be used in foundation problems involving unloading and possibly reloading of overconsolidated clays above the maximum past pressure.

4) Problems involving the compression of clays in the normally consolidated range require modification of c_h(probe) to account for the difference in clay compressibility during dissipation (as expressed by RR (probe) and the compression ratio, CR, in the normally unconsolidated range.

6.3.6 Prediction of the Coefficient of Permeability Profiles

Baligh et al propose the following approximate equations for the evaluation of the horizontal coefficient of permeability:

$$k_h(\text{probe}) \simeq \frac{\gamma_\omega}{2.3\ \bar{\sigma}_{vo}} \cdot RR^*(\text{probe}) \cdot c_h(\text{probe}) \qquad 6.1$$

Fig. 6.16 shows the predicted profile of k_h(probe) based on above equation and the reference c_h(probe) profile** estimated from dissipation studies for selected values of $RR_{(probe)} = 0.5,\ 1 \text{ and } 2 \times 10^{-2}$.

In spite of the various uncertainties in selecting adequate values of RR(probe) and the severe simplifications needed to reach EQ. 6. 1 , the predictions of k_h(probe) are considered very satisfactory especially when compared with other existing in situ permeability testing methods.

---

*Slope of the vertical strain vs. vertical effective stress.
**Basically obtained at 50% dissipation.

6.3.7 Application of the Predictive Method to a Varved Clay Deposit

In 1977, MIT conducted cone penetration and pore pressure measurements in a Connecticut Valley Varved Clay (CVVC) on the campus of the University of Massachusetts in Amherst, Massachusetts.* The soil conditions at the site are presented in Fig. 6.17 as obtained from a typical sampling and laboratory testing program. Fig. 6.18 shows the undrained shear strength of the clay, s_u, as determined by the (Geonor) field vane test and the Shansep procedure (Ladd and Foott, 1974). The SHANSEP strengths are based on plane strain compression (PSC) and direct simple shear (DSS) test results and the estimated stress history ($OCR=\bar{\sigma}_{vm}/\bar{\sigma}_{vo}$) in Fig. 6.17. Furthermore, Fig. 6.19 presents the cone resistance, q_c, from two standard Fugro cones (60° angle pushed at 1 to 2 cm/sec.

The prediction method was then applied to the results of dissipation tests performed at the site. Two sufficiently long dissipation records indicate that predictions apply surprisingly well to CVVC in spite of large differences in behavior from BBC, Fig. 6.20. This is especially important because it means that the prediction method developed for

*Refer to Baligh et al. (1978) for more detailed information on the site.

BBC can also be applied to other clays.

Profiles of c_h(probe) estimated according to the proposed method, Figs. 6.21 and 6.22, are virtually identical for 18° and 60° cones. Furthermore, c_h(probe) profiles are consistant with measurements of cone resistance and penetration pore pressures.

No (laboratory or field) tests were conducted by M.I.T. to provide direct measurements of the overconsolidated horizontal coefficient of consolidation CVVC. Therefore, the predicted values of c_h(probe) cannot, at present, be rigorously evaluated. However, a comparison of k_h(probe) with laboratory measurements of the horizontal permeability indicates very good agreement, Fig. 6.23 . Furthermore, the estimates of c_v(Nc) from c_h(probe) are very close to laboratory measurements of the coefficient of consolidation in the normally consilidated (virgin range) Fig. 6.24.

Type of Soil	Index Properties			$s_u/\bar{\sigma}_{vc}$ (1)		
	w_ℓ (%)	P.I. (%)	L.I. (2)	PSC (3)	DSS (4)	PSE (5)
Portsmouth Clay	35	15	1.8	0.350	0.200	0.155
Haney Sensitive Clay	44	18	0.75	0.296	———	0.211
Boston Blue Clay	41	21	0.81	0.340	0.200	0.190
AGS CH Clay	71	40	———	0.370	0.250	0.220
San Francisco Bay Mud	88	45	1.04	0.370	0.250	0.280
Connecticut Valley Varved Clay	35-65	12-39	1.00	0.280	0.165	0.255

(1) $s_u = q_f = 0.5(\sigma_1 - \sigma_3)_f$ except for DSS where $s_u = (\tau_h)_{max}$

(2) $L.I. = \dfrac{w_n - w_p}{w_\ell - w_p}$

(3) plane strain compression

(4) direct simple shear

(5) plane strain extension

Table 6.1 Plane strain undrained shear strength of six normally consolidated clays in different modes of failure (data from Ladd et al., 1977; table courtesy of A.S. Azzouz)

PIEZOMETER TYPE	ADVANTAGES	DISADVANTAGES
18 TIP°	-Very sensitive to local soil variability hence, very good for soil profiling -Fast dissipation hence economical to operate, especially to evaluate the in situ static pore pressures -Inexpensive design	-Stone exposed to bending damage by gravels and other obstructions -Large scatter in dissipation curves at early times and significant scatter at later times -Geometry difficult to include in theoretical analyses hence requires semi-empirical interpretation
60° TIP	-Little scatter in c_h when matching done at intermediate times ($t_{40} < t < t_{60}$, say) -Fast dissipation -Inexpensive design -Rational interpretation despite geometry -Provides insight into penetration mechanisms with dutch cone (same cone angle)	-Stone exposed to bending damage -Large scatter in dissipation curves at early times hence requires at least 40% dissipation to determine c_h.
18° Mid-Height	-Reasonable dissipation time -Reasonable scatter in dissipation curves even at early times -Rational theoretical predictions -Stone well protected from structural damages	-More expensive design (need special porous elements) -Porous stone is easily smeared during penetration in granular materials
18° or 60° With Stone on Shaft	-Close simulation of pile installation hence, useful in pile design -Very little scatter in dissipation curves -Easier to interpret -Appears to provide estimates of c_h closer to normally consolidated values -Excellent protection for the porous stone	-Very long dissipation time (i.e., expensive to operate) -Not very sensitive to small scale soil variability (i.e., tendency to average out pore pressure) -More difficult to keep the stone well drained -More expensive design

NOTES: The conclusions in this table are based on M.I.T. experience in three clay deposits. Different probe designs and/or procedures in other clays might lead to different conclusions.

Table 6.2 Evaluation of different probe designs (Baligh and Levadoux, 1980).

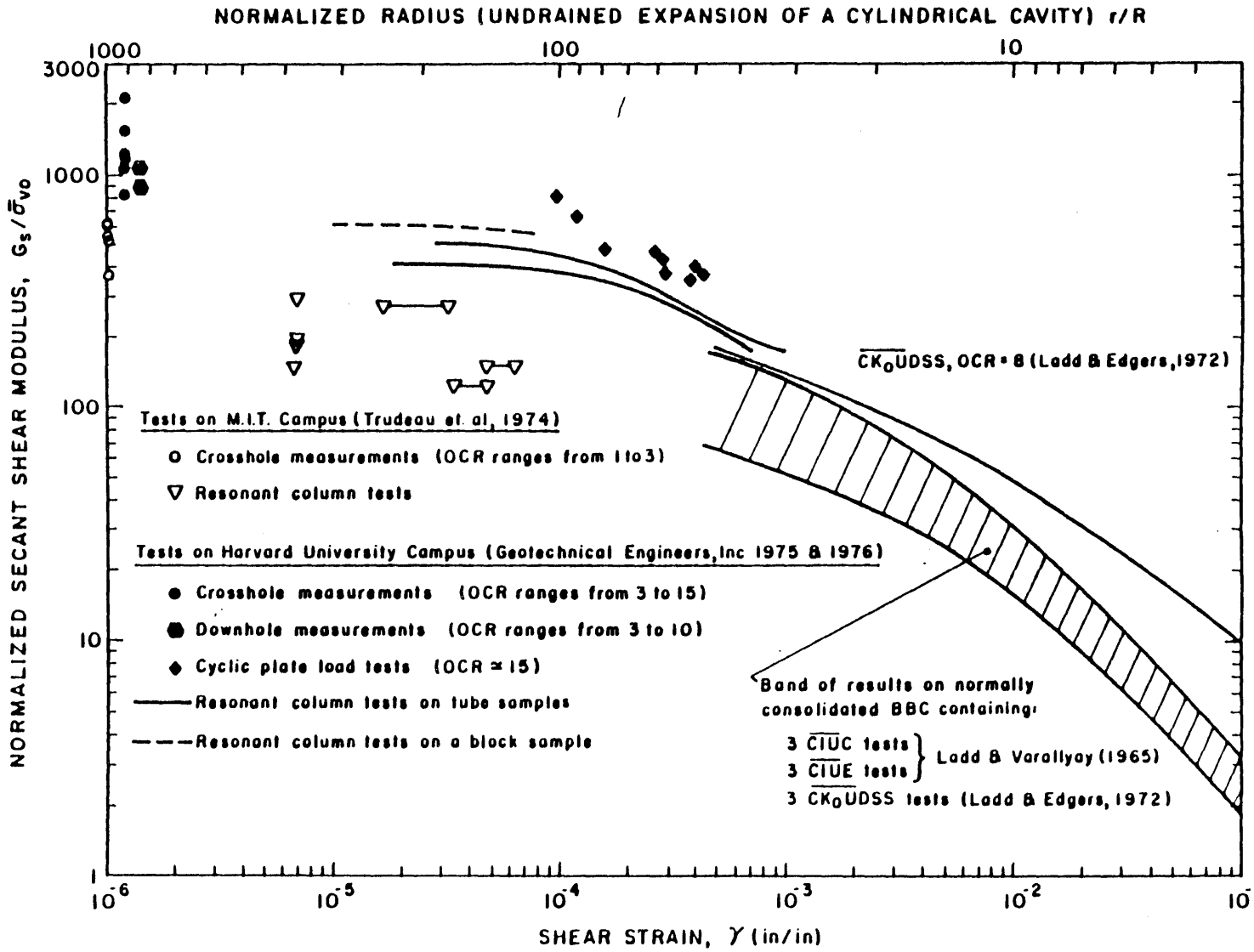

Figure 6.1 Laboratory and field measurements of the secant shear modulus, G_s, of Boston Blue Clay as a function of strain level (from Azzouz et al., 1980)

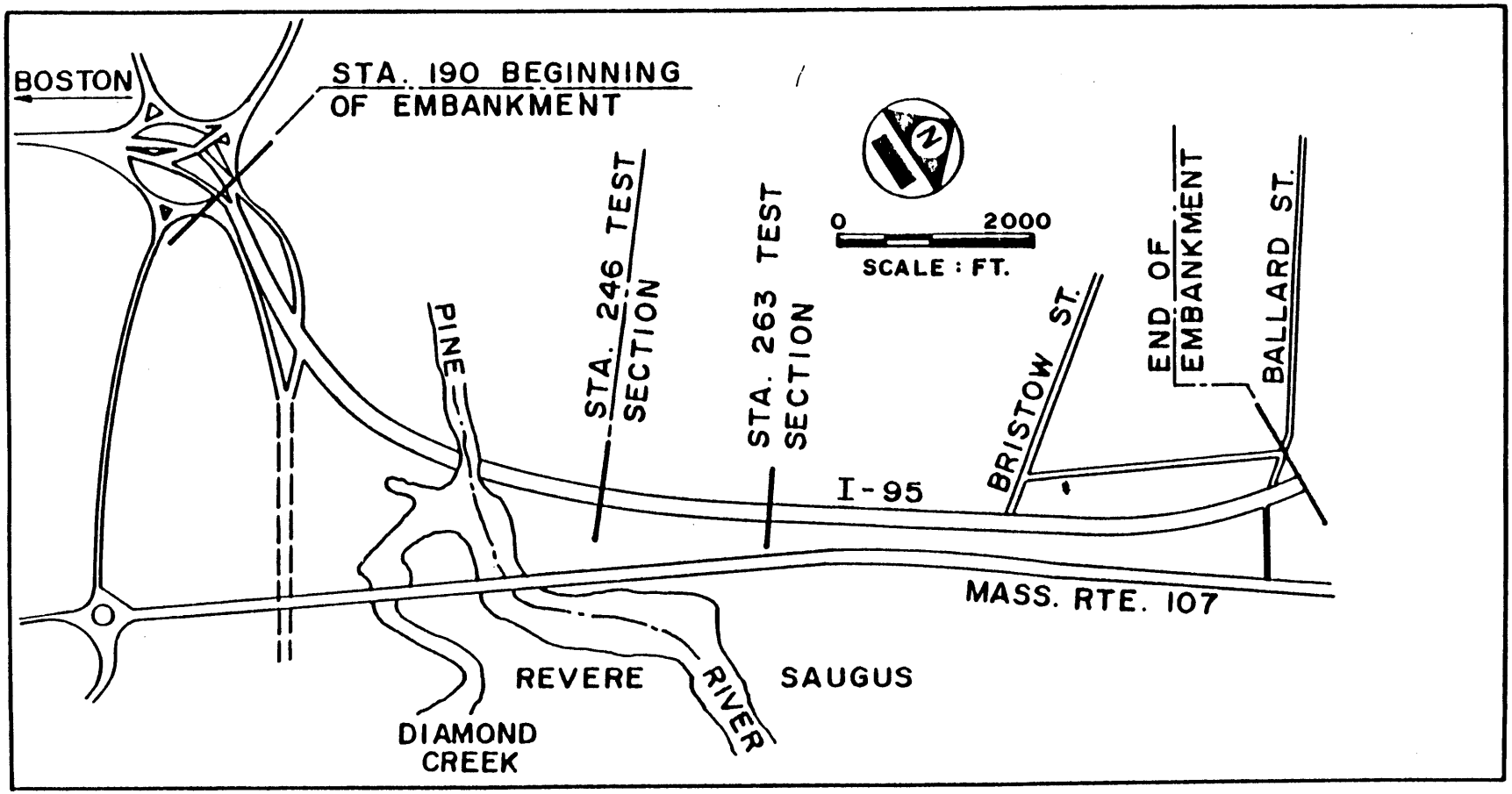

Figure 6.2 Location map of Saugus I-95 embankment (after Lacasse et al., 1978)

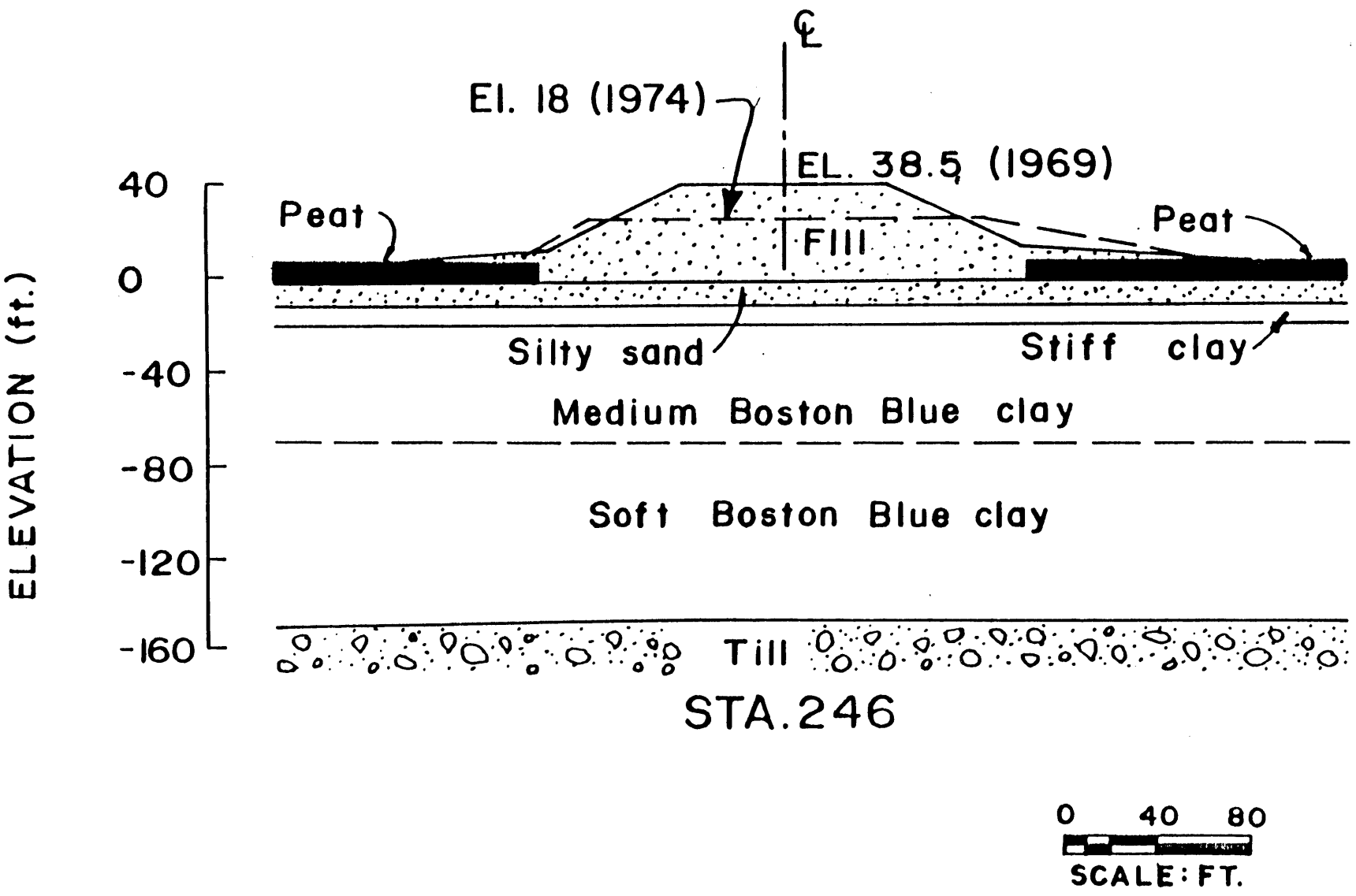

Figure 6.3 Cross section of Station 246 at Saugus I-95 embankment (after Lacasse et al., 1978)

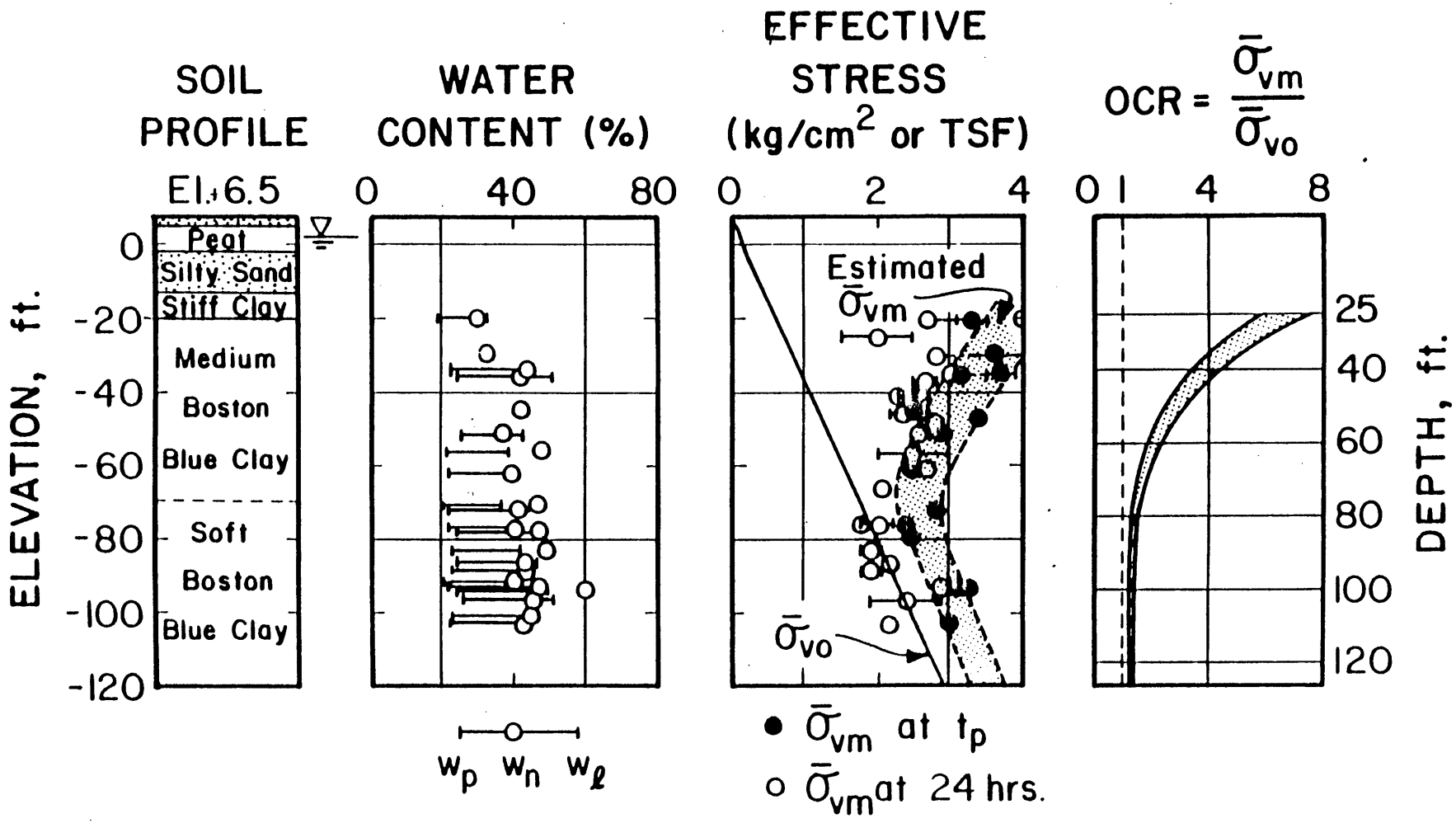

Figure 6.4 Soil profile, index properties and stress history at the Saugus site (from BOSS 79)

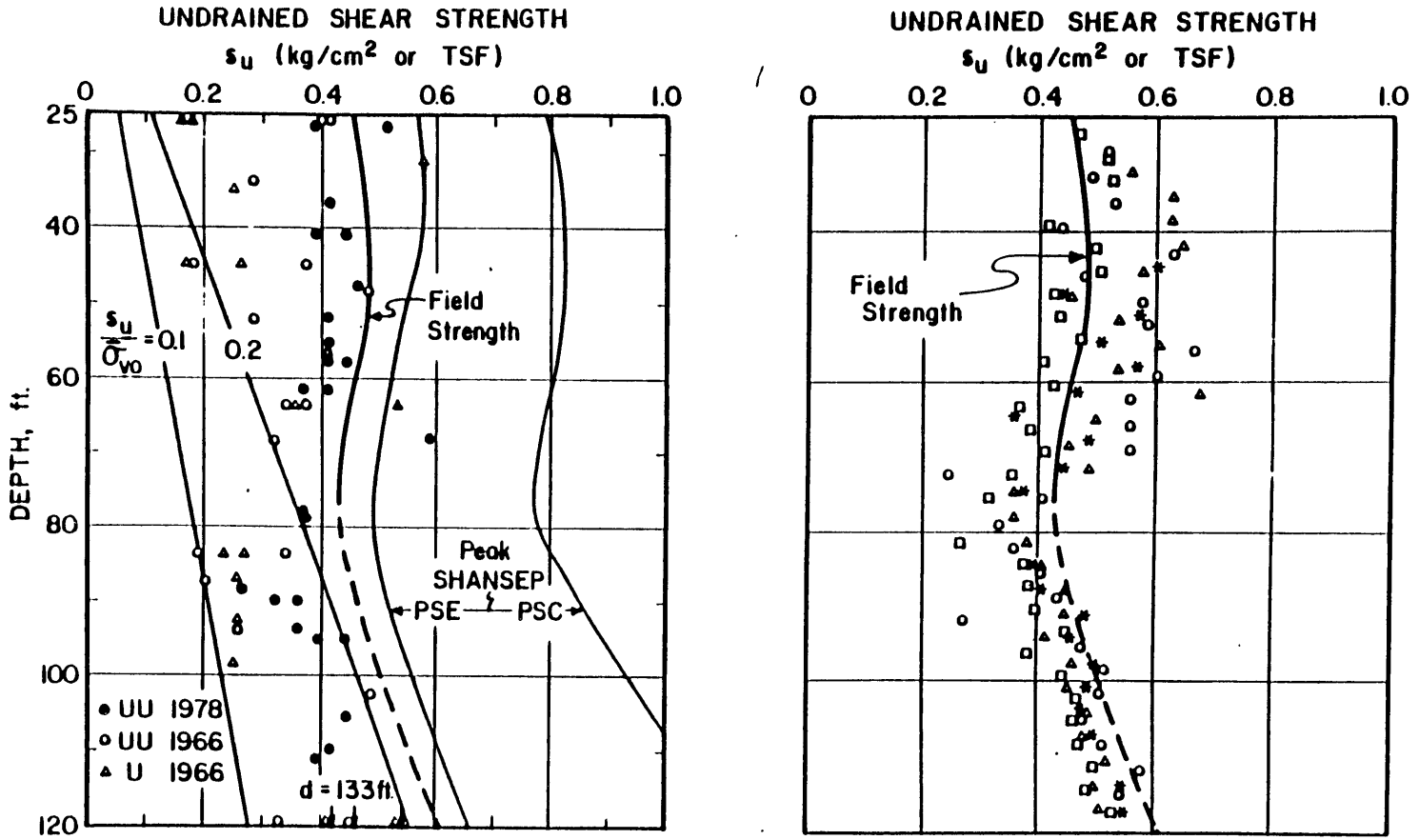

a) Laboratory tests

b) Field vane strength

Figure 6.5 Undrained shear strengths at the Saugus site (from BOSS 79)

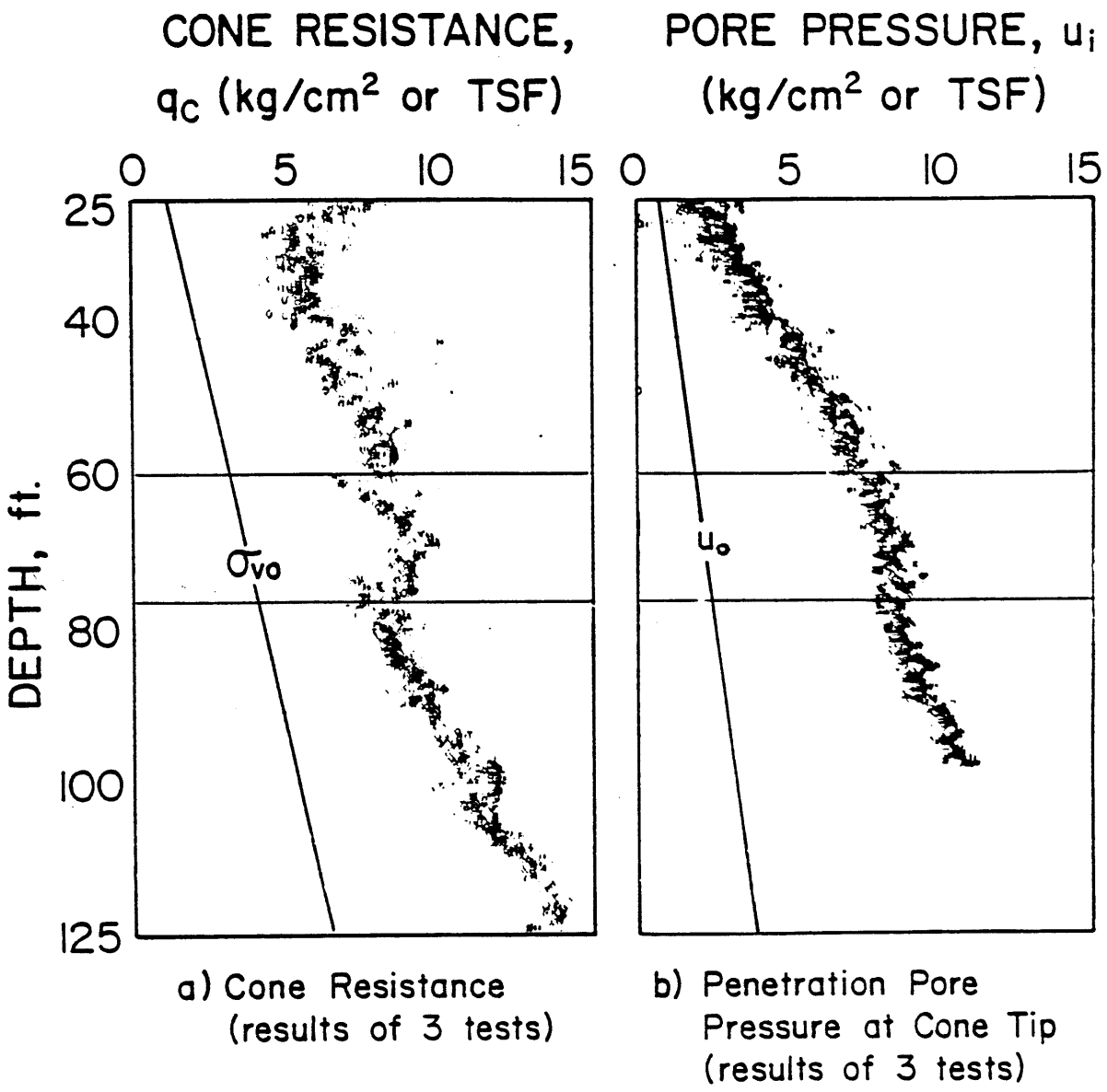

Figure 6.6 - Cone resistance and penetration pore pressures at the Saugus site (Baligh and Levadoux, 1980).

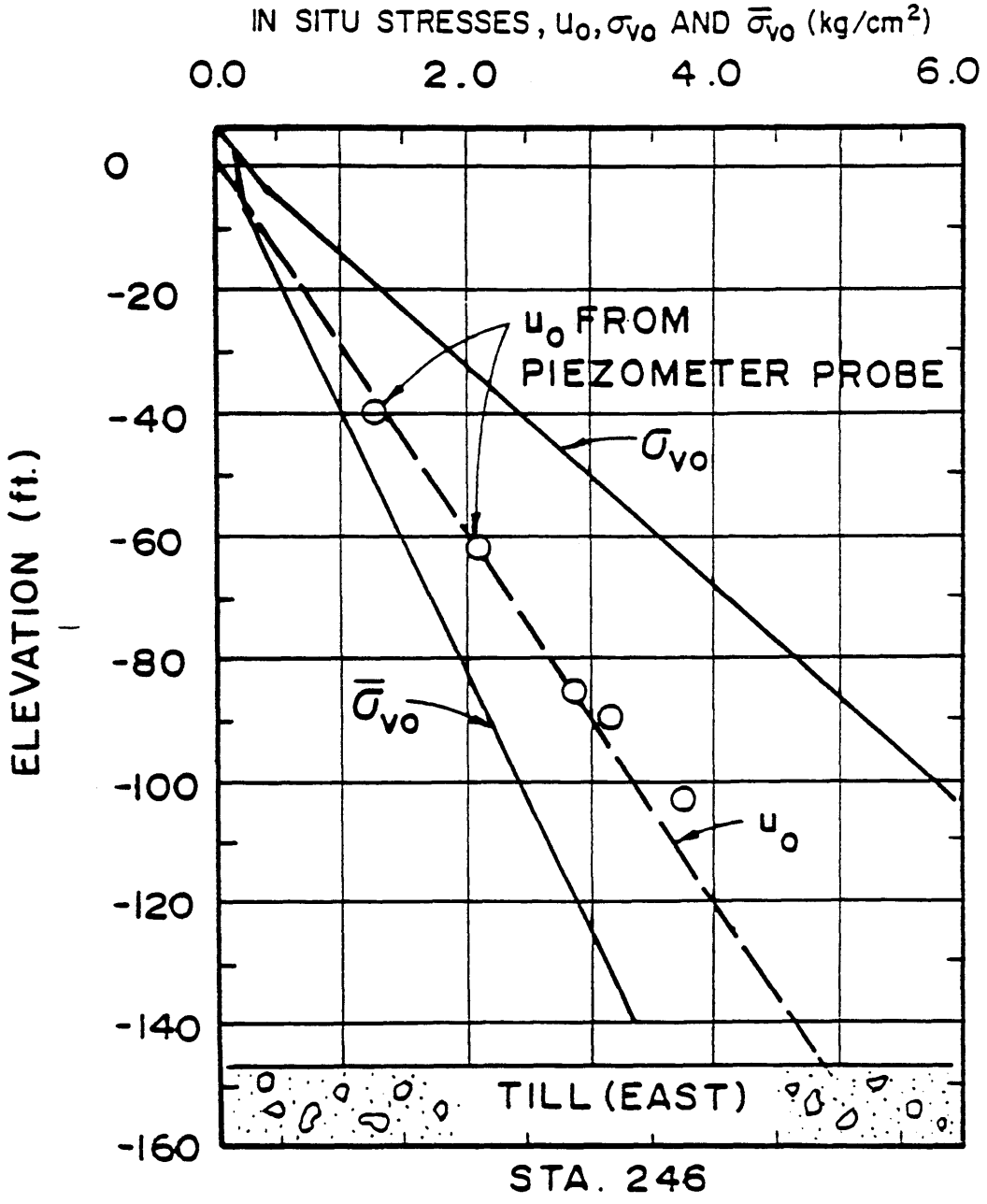

Figure 6.7 In Situ Stresses at the Saugus site (after Ladd et al., 1979)

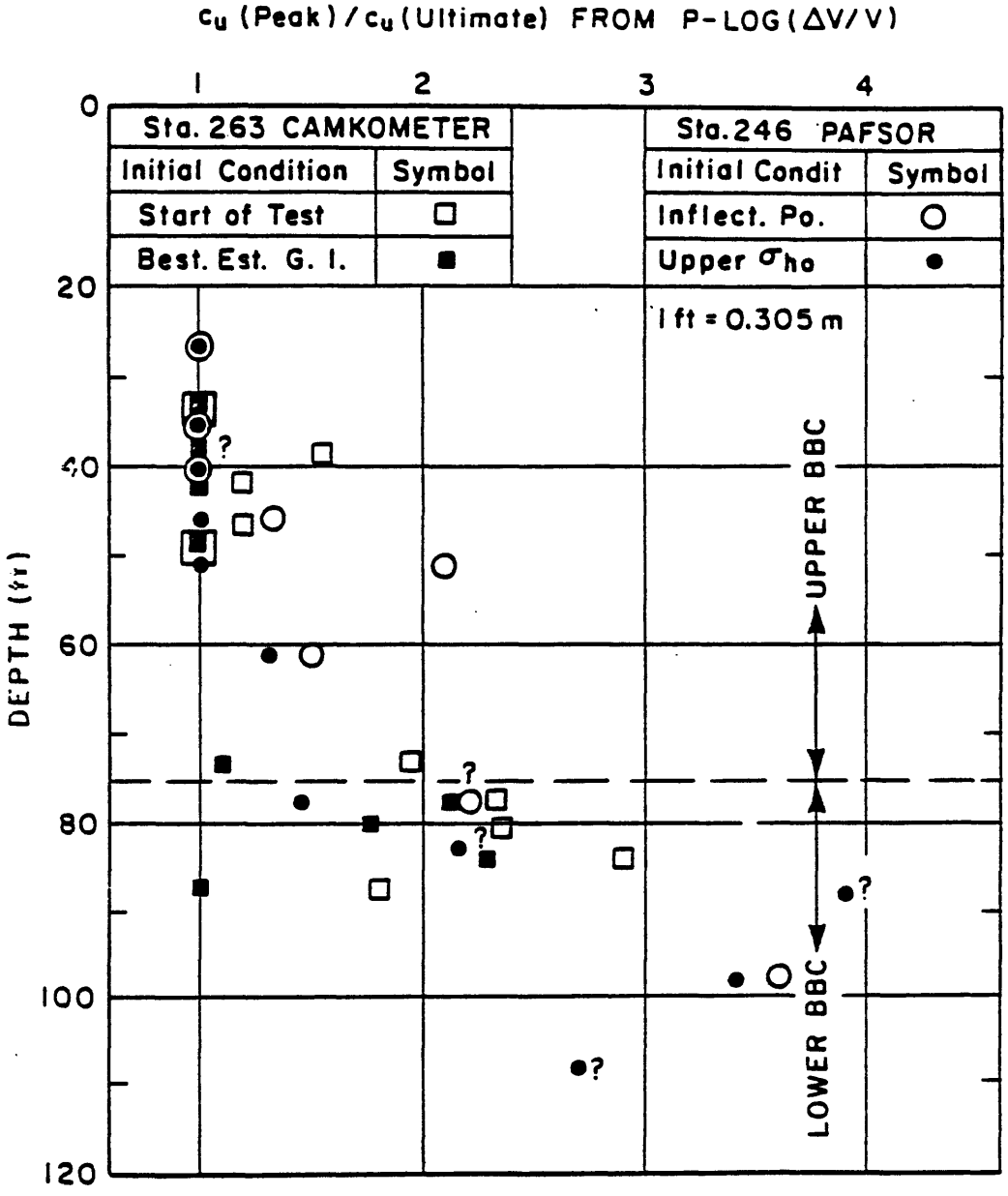

Figure 6.9 Ratio of Peak to Ultimate Strengths Measured by Pressuremeter at the Saugus Site (Baligh and Levadoux, 1980).

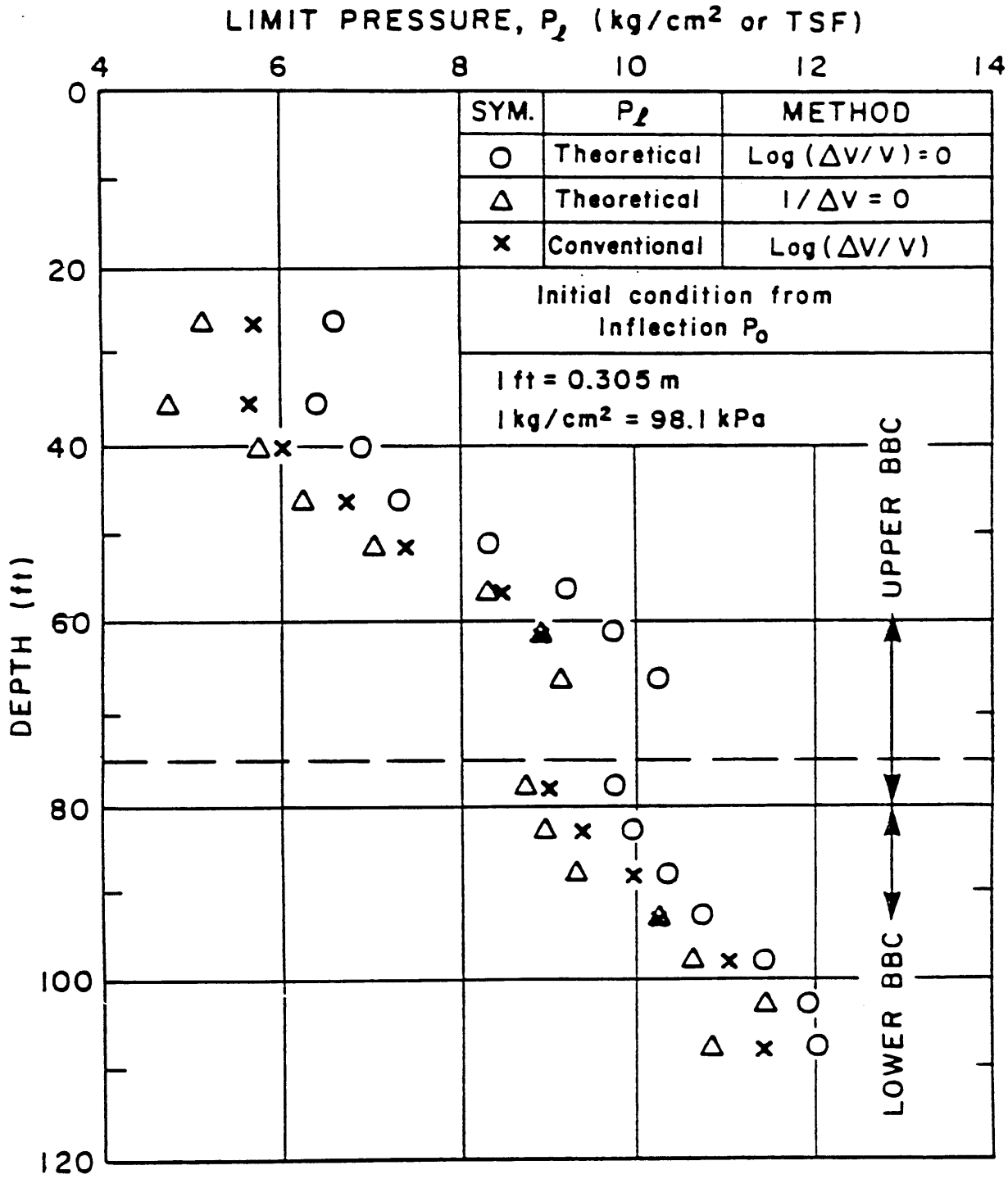

Figure 6.8 Limit Pressure Measurements at the Saugus Site (Baligh and Levadoux, 1980).

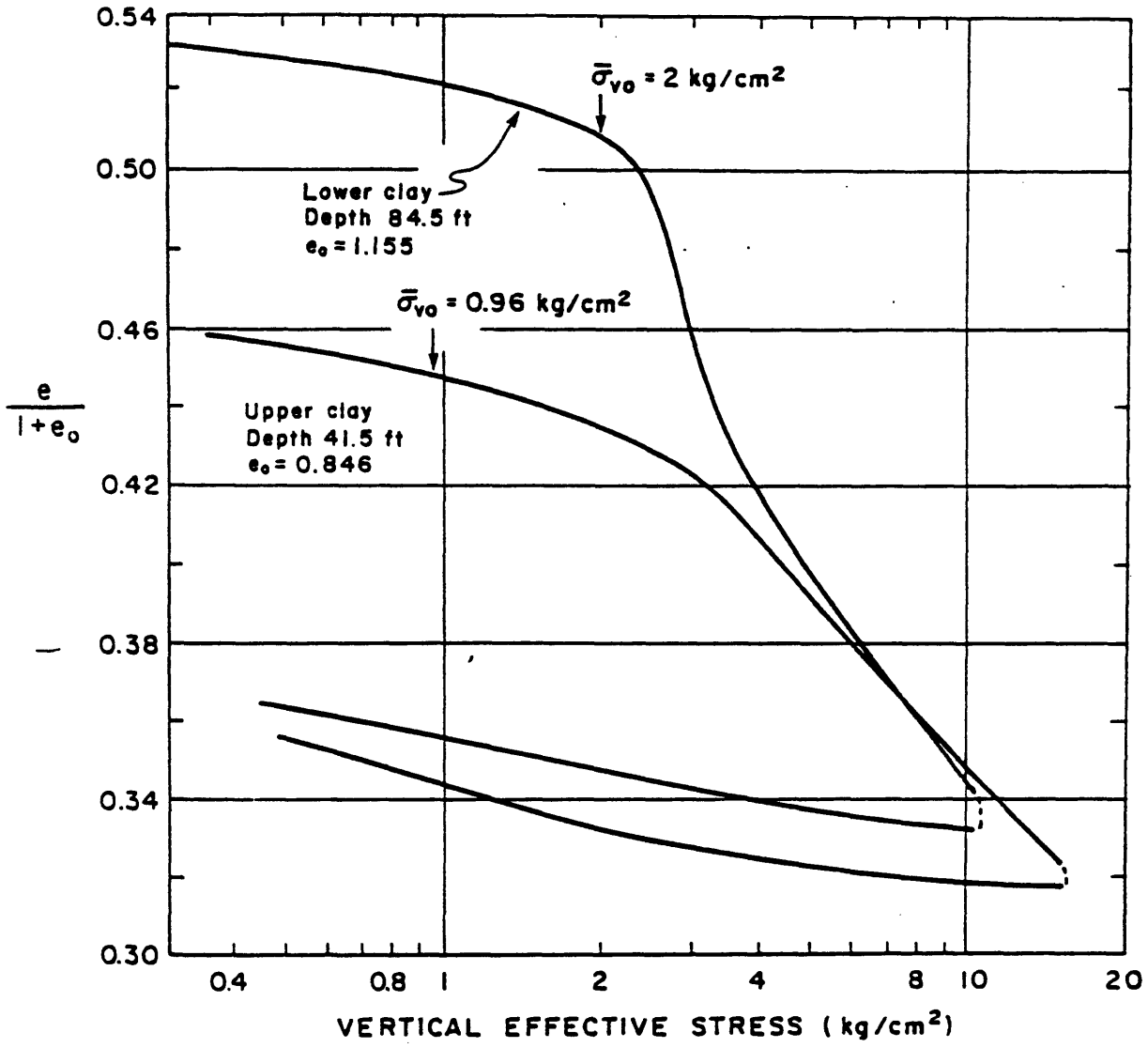

Figure 6.10 Typical Compressibility of the Upper and Lower Boston Blue Clay at the Saugus Site (CRSC tests) (Baligh and Levadoux, 1980).

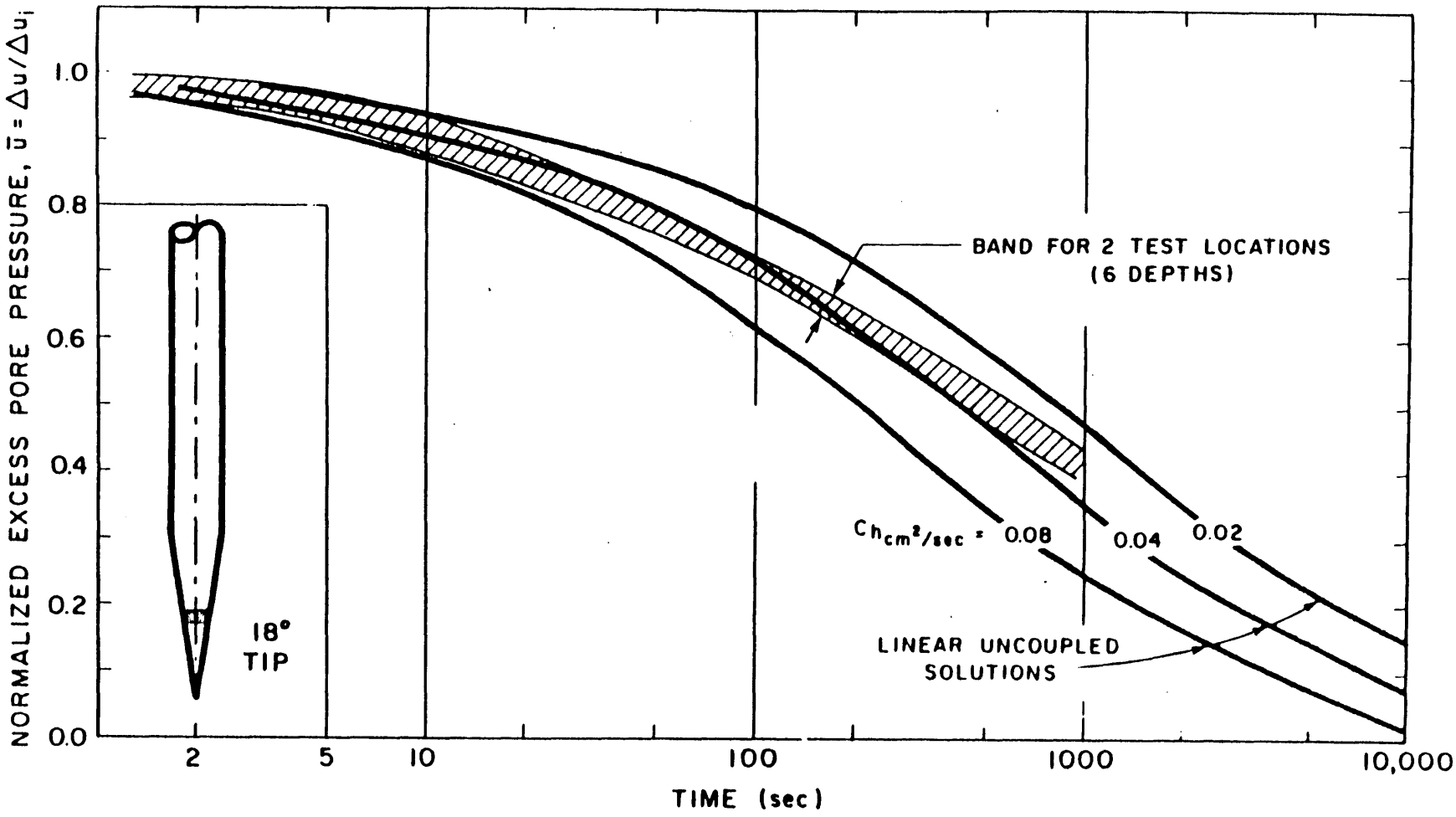

Figure 6.11 Predicted vs Measured Dissipation Curves at Mid-Height of an 18° Conical Probe Below 60 ft at the Saugus Site (Baligh and Levadoux, 1980).

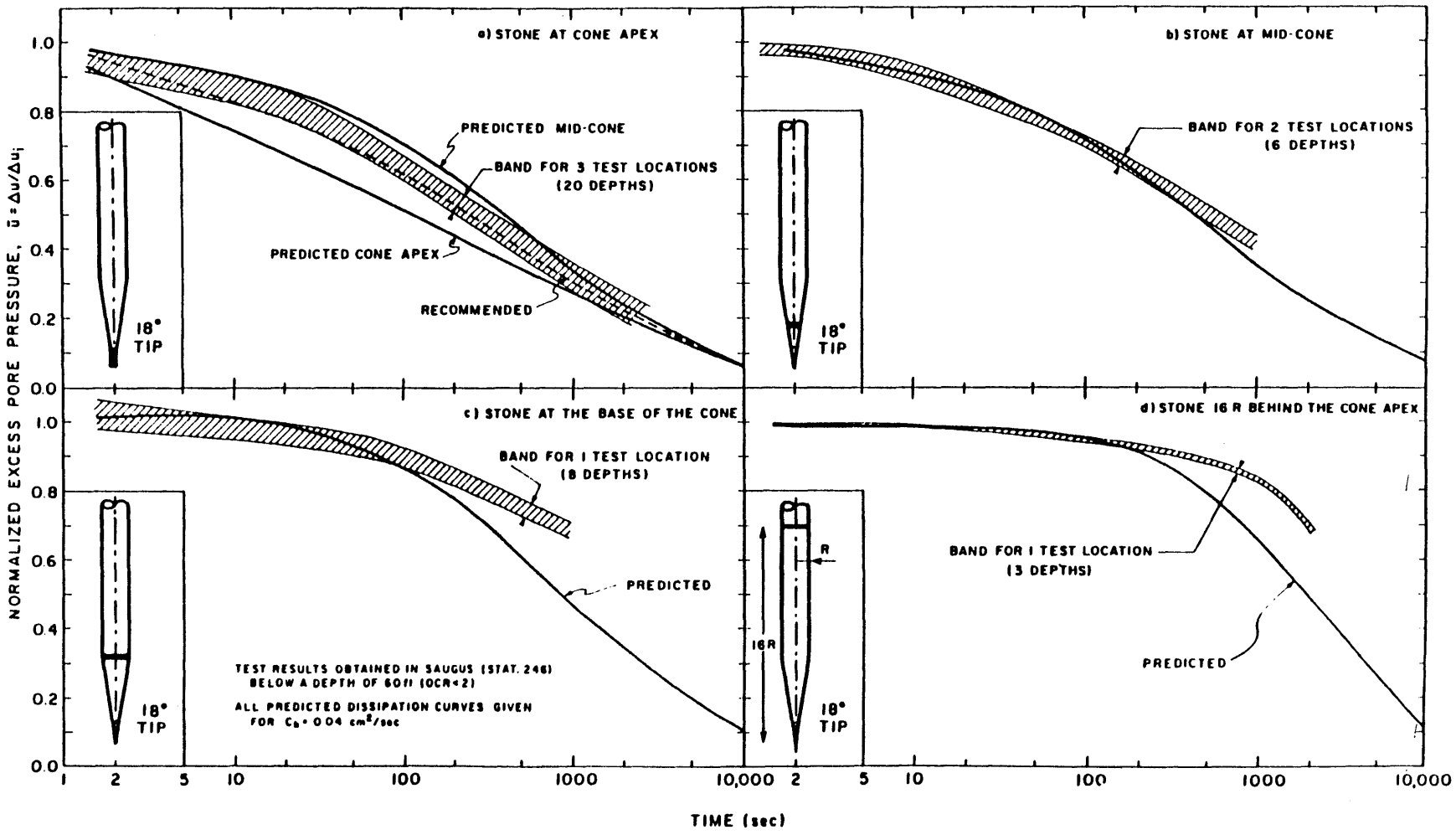

Figure 6.12 Evaluation of Linear Uncoupled Dissipation Predictions for an 18° Conical Probe in Boston Blue Clay (OCR<2) (Baligh and Levadoux, 1980).

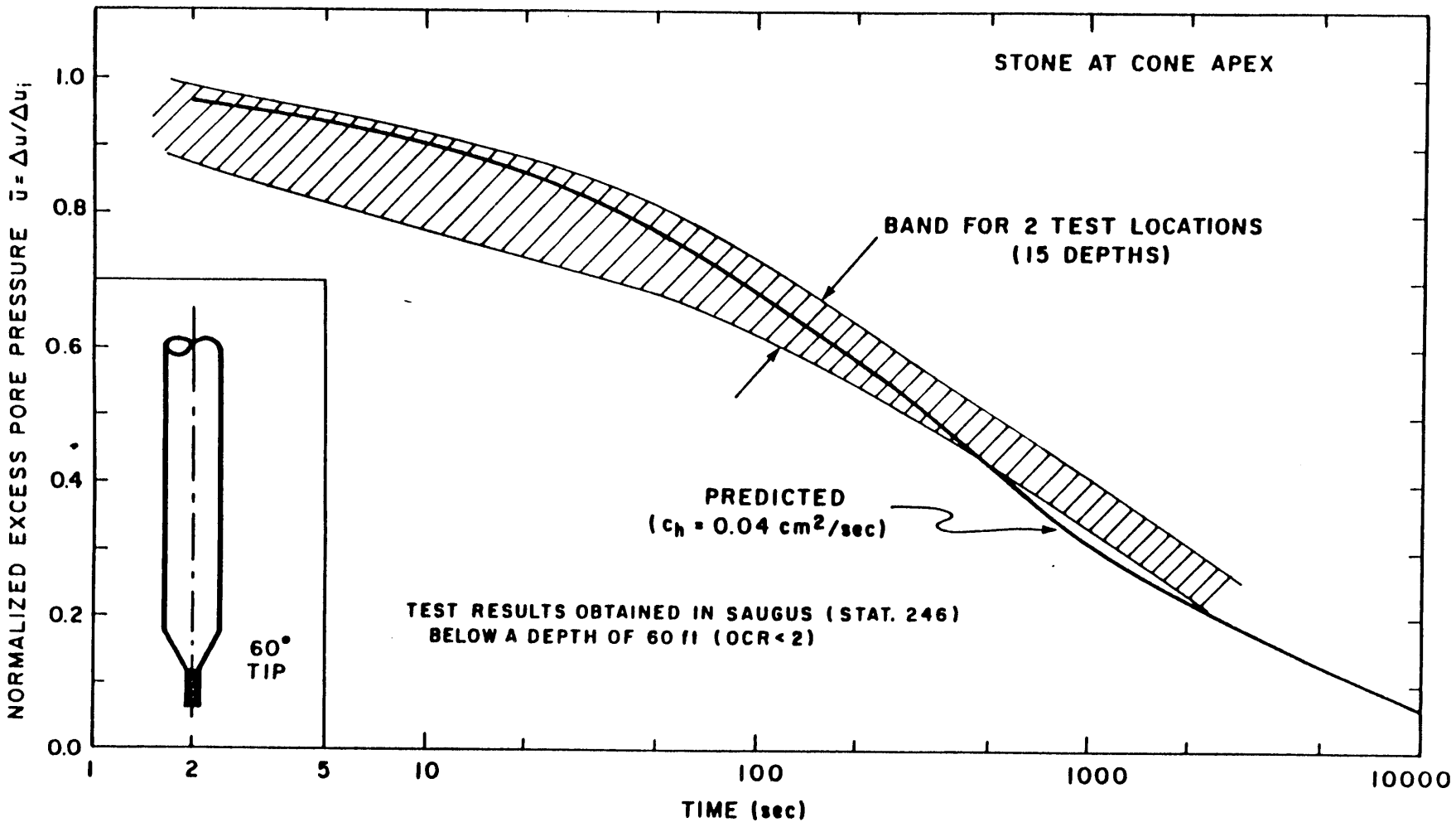

Figure 6.13 Evaluation of Linear Uncoupled Dissipation Predictions for a 60° Conical Probe in Boston Blue Clay (OCR<2) (Baligh and Levadoux, 1980).

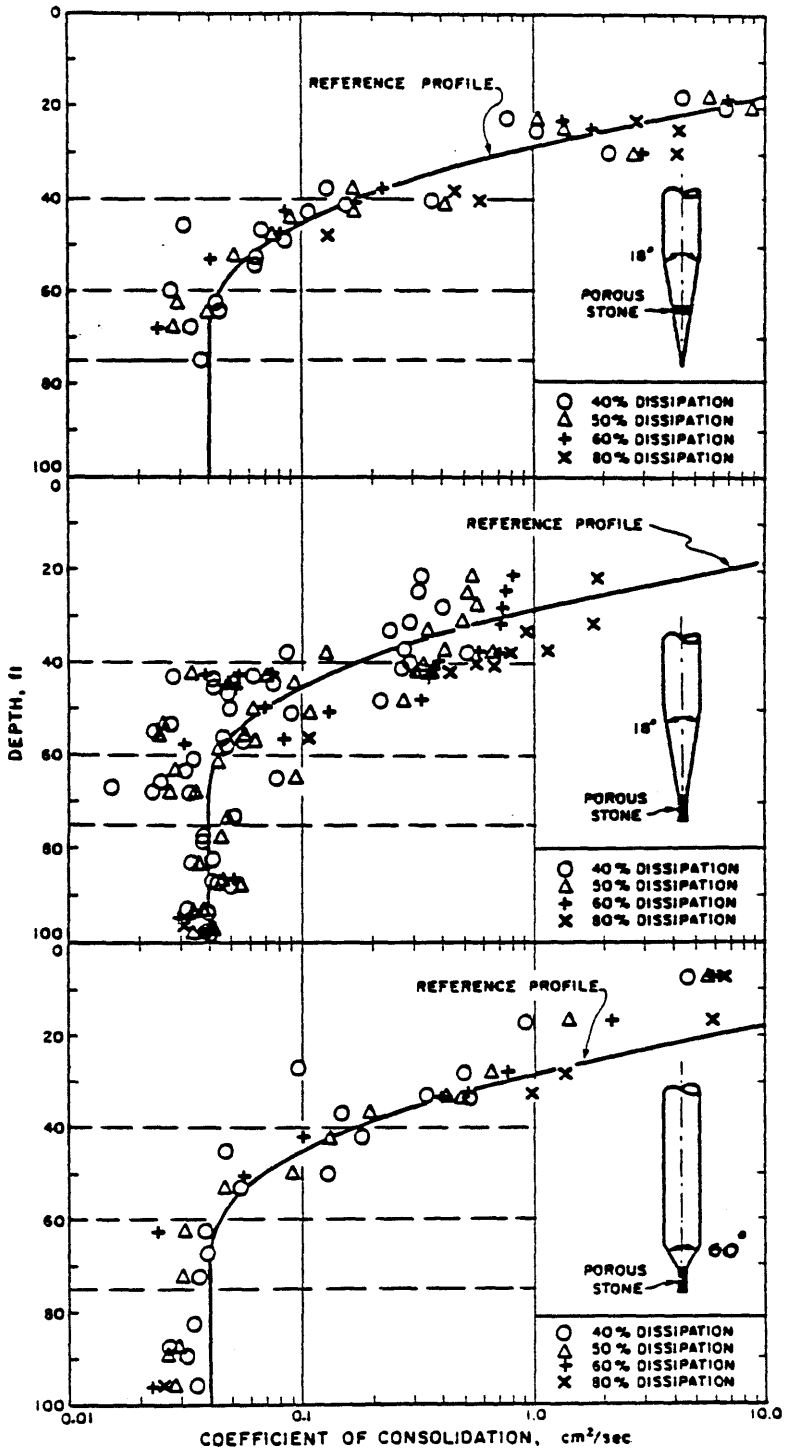

Figure 6.14 Summary of predicted c_h (probe) profile in Boston Blue Clay, Saugus site (Baligh and Levadoux, 1980).

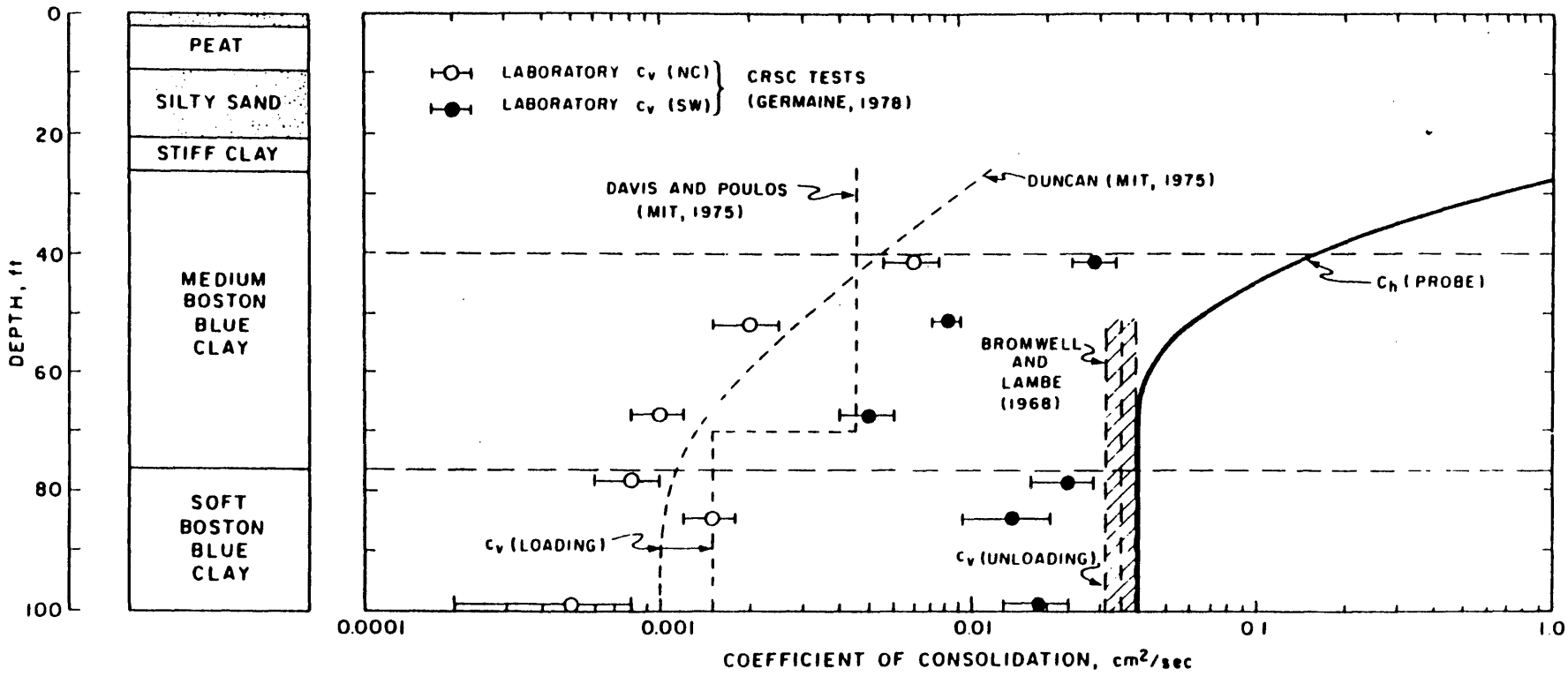

Figure 6.15 Comparison of Predicted and Measured Coefficients of Consolidation in Boston Blue Clay (Baligh and Levadoux, 1980).

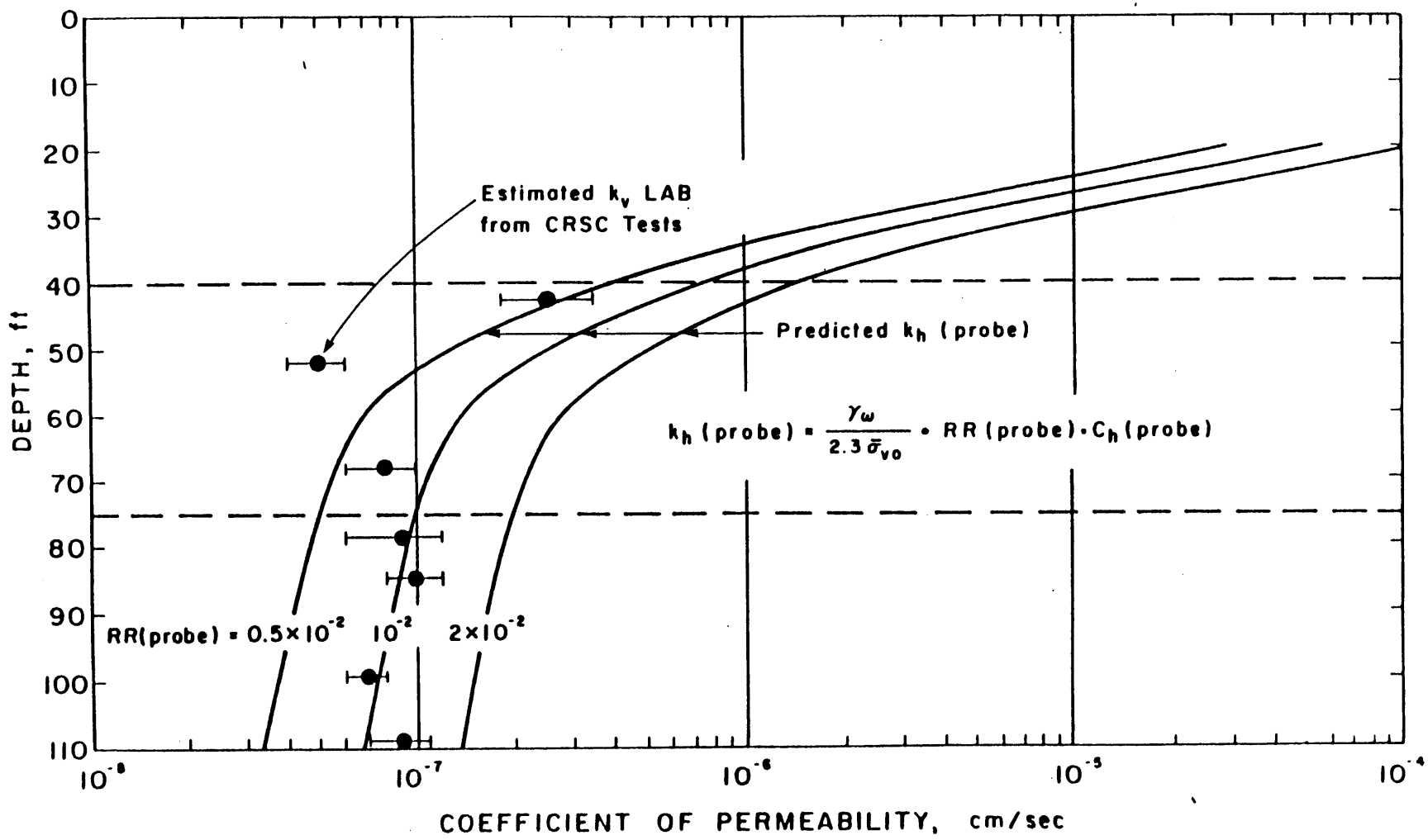

Figure 6.16 Comparison Between Estimated and Measured Coefficients of Permeability in Boston Blue Clay (Baligh and Levadoux, 1980).

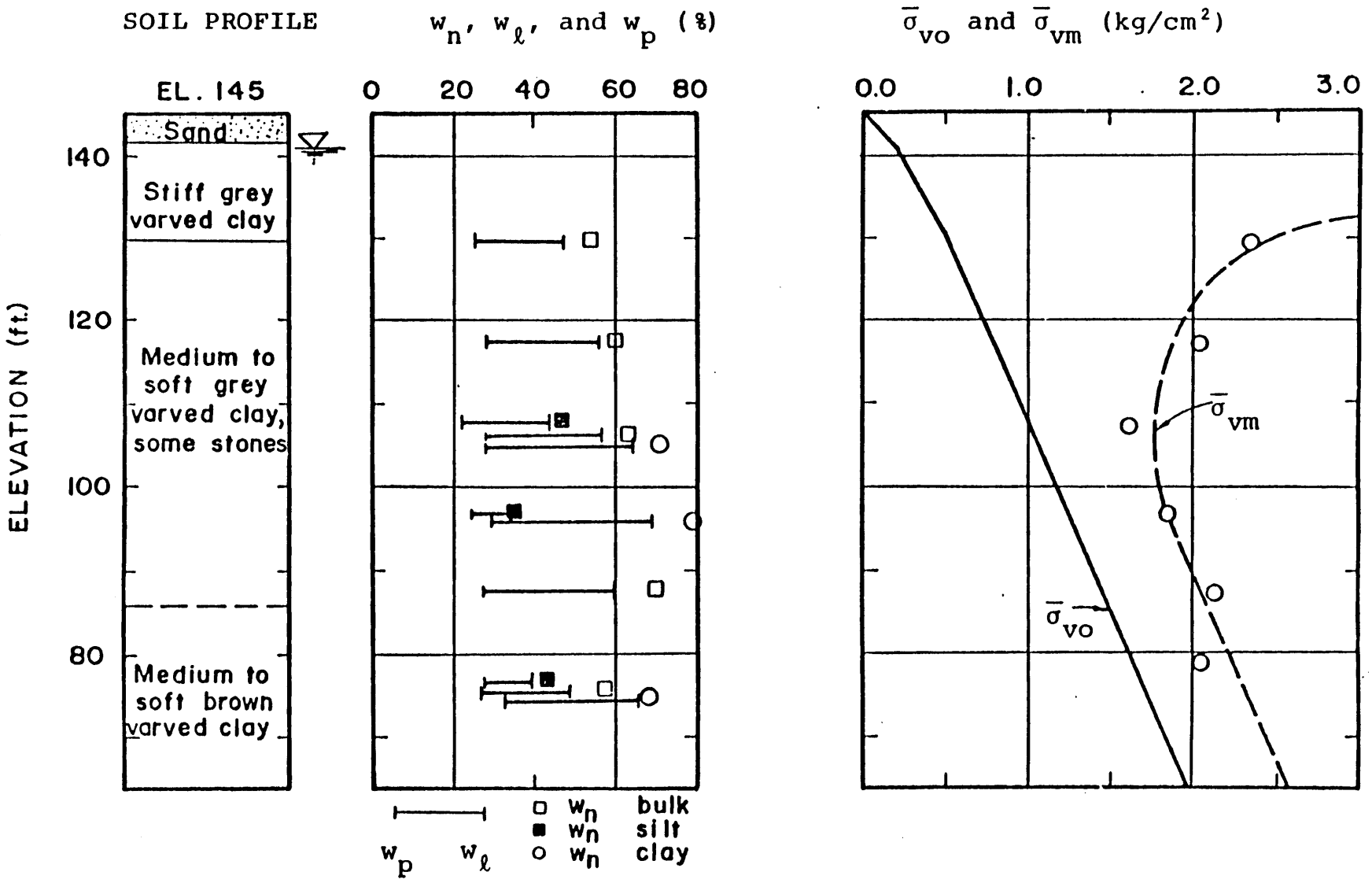

Figure 6.17 Soil conditions at the Amherst, Mass. testing site (Route 116 bypass and North Hadley Road; data from Ladd, 1975).

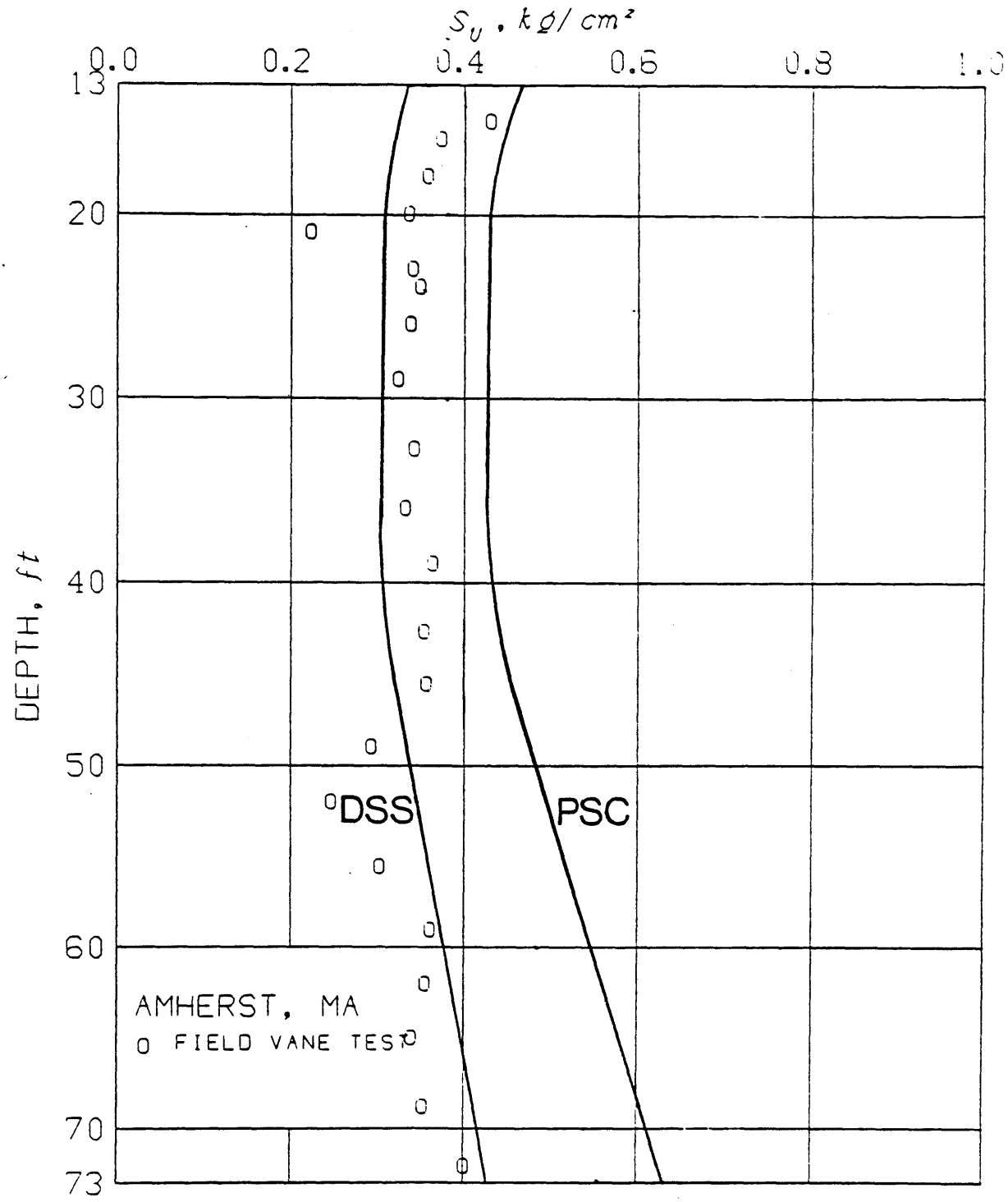

Figure 6.18 SHANSEP and field vane strength profiles for the Amherst, Mass. testing site (data from Ladd, 1975).

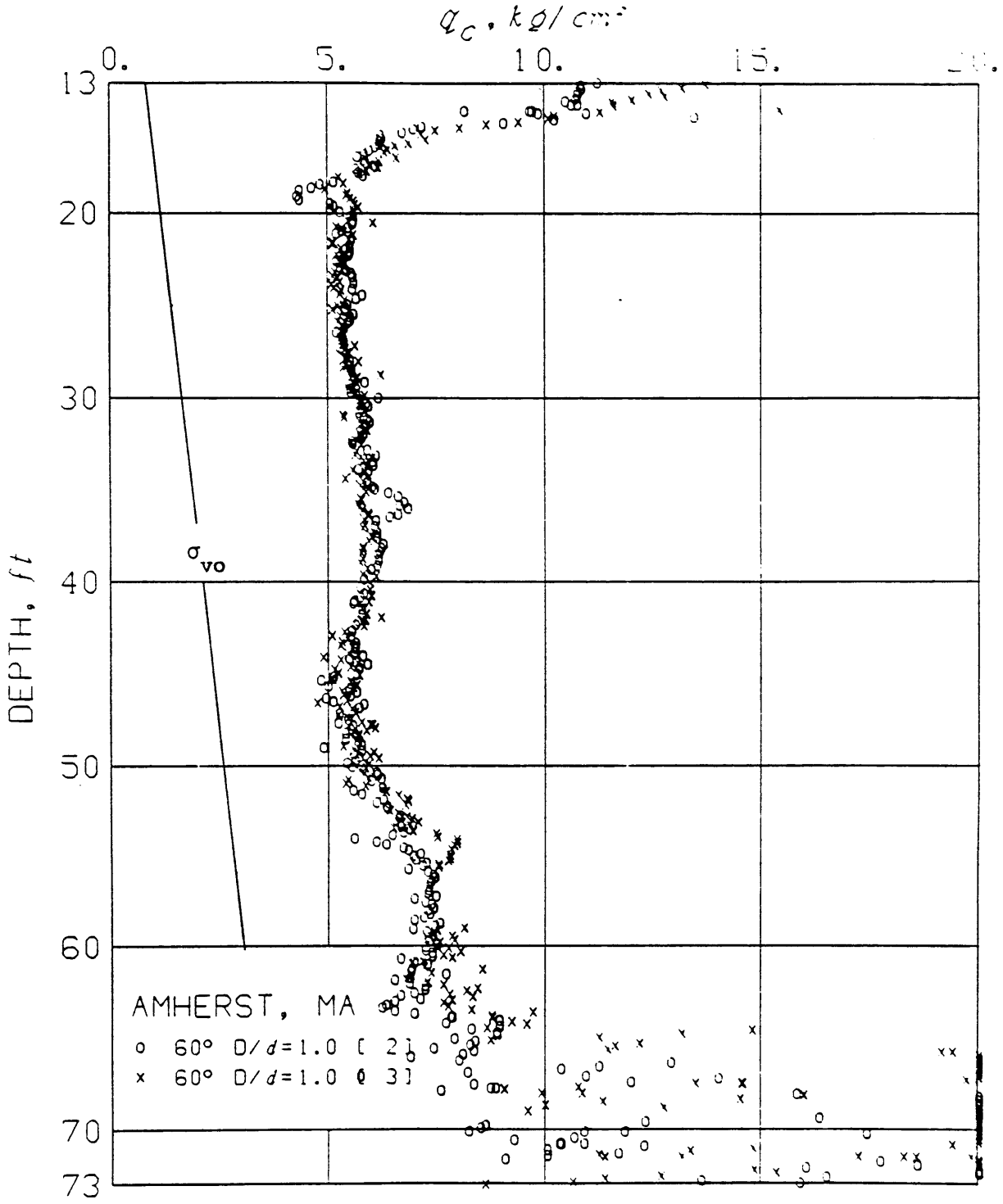

Figure 6.19 Profile of Cone Resistance, q_c, in Connecticut Valley Varved Clay at Amherst, Mass. (from Baligh et al., 1978)

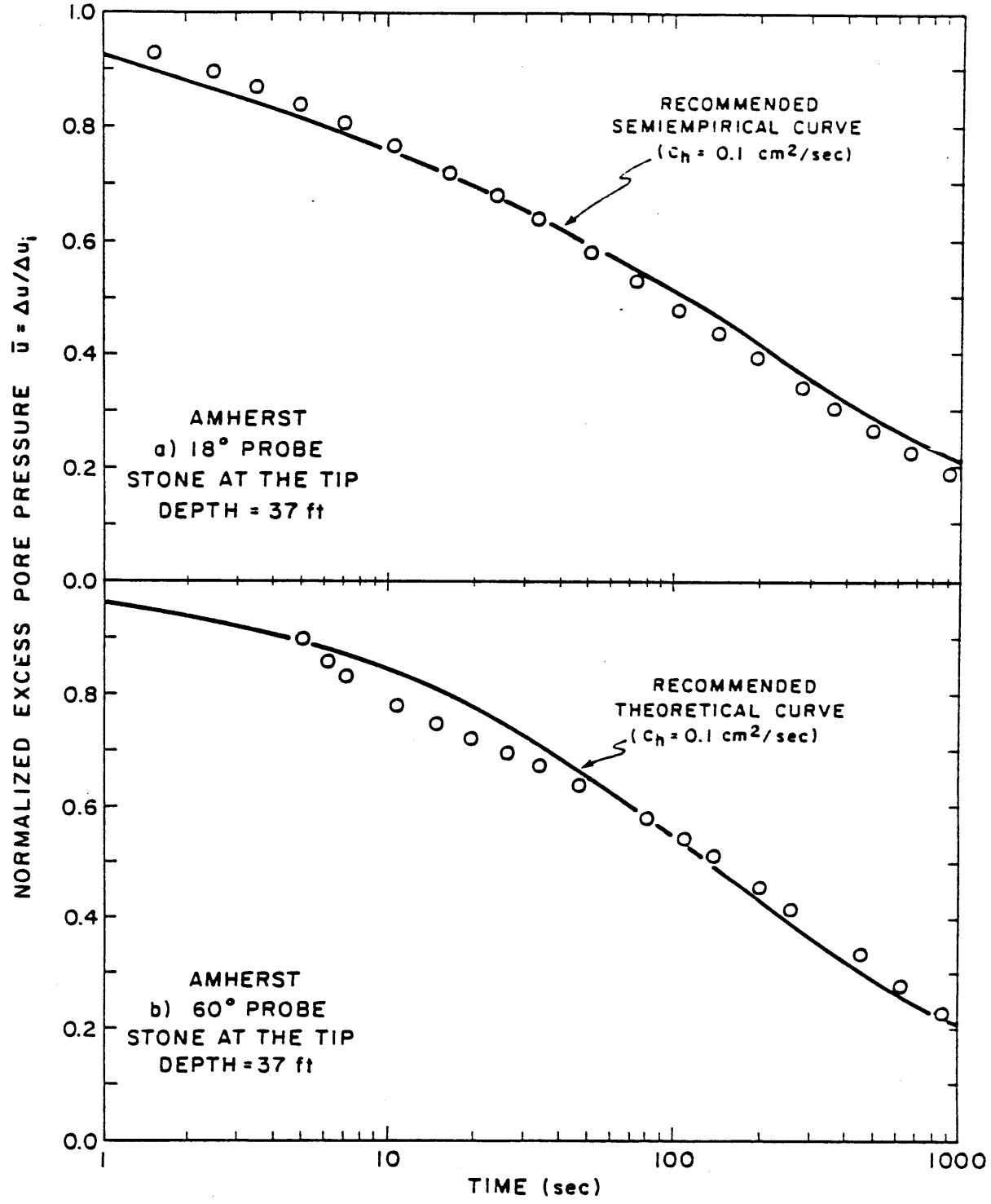

Figure 6.20 Evaluation of Predicted Dissipation Curves for 18° and 60° cones (assuming c_h = 0.1 cm²/sec) (Baligh and Levadoux, 1980).

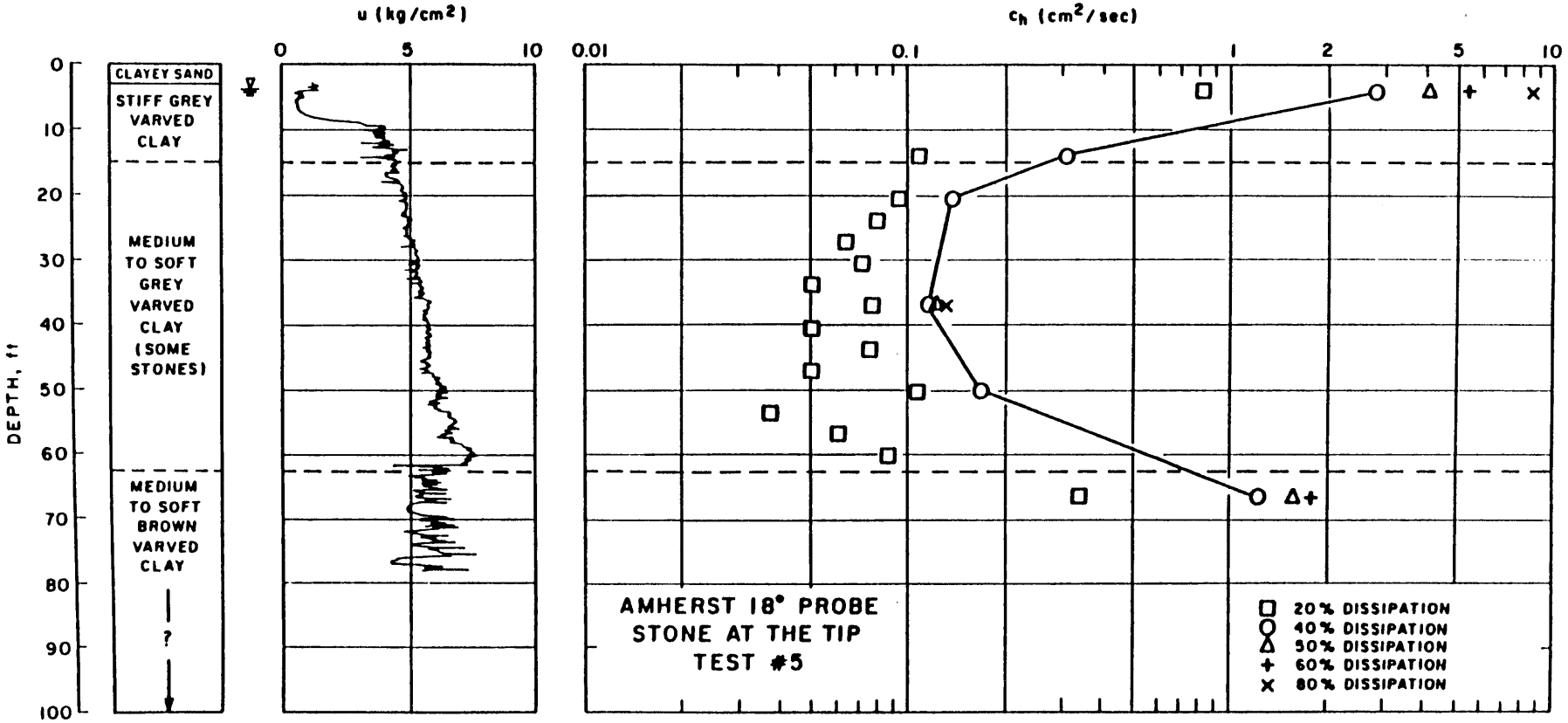

Figure 6.21 Results of 18° conical probes at the Amherst site (Baligh and Levadoux, 1980).

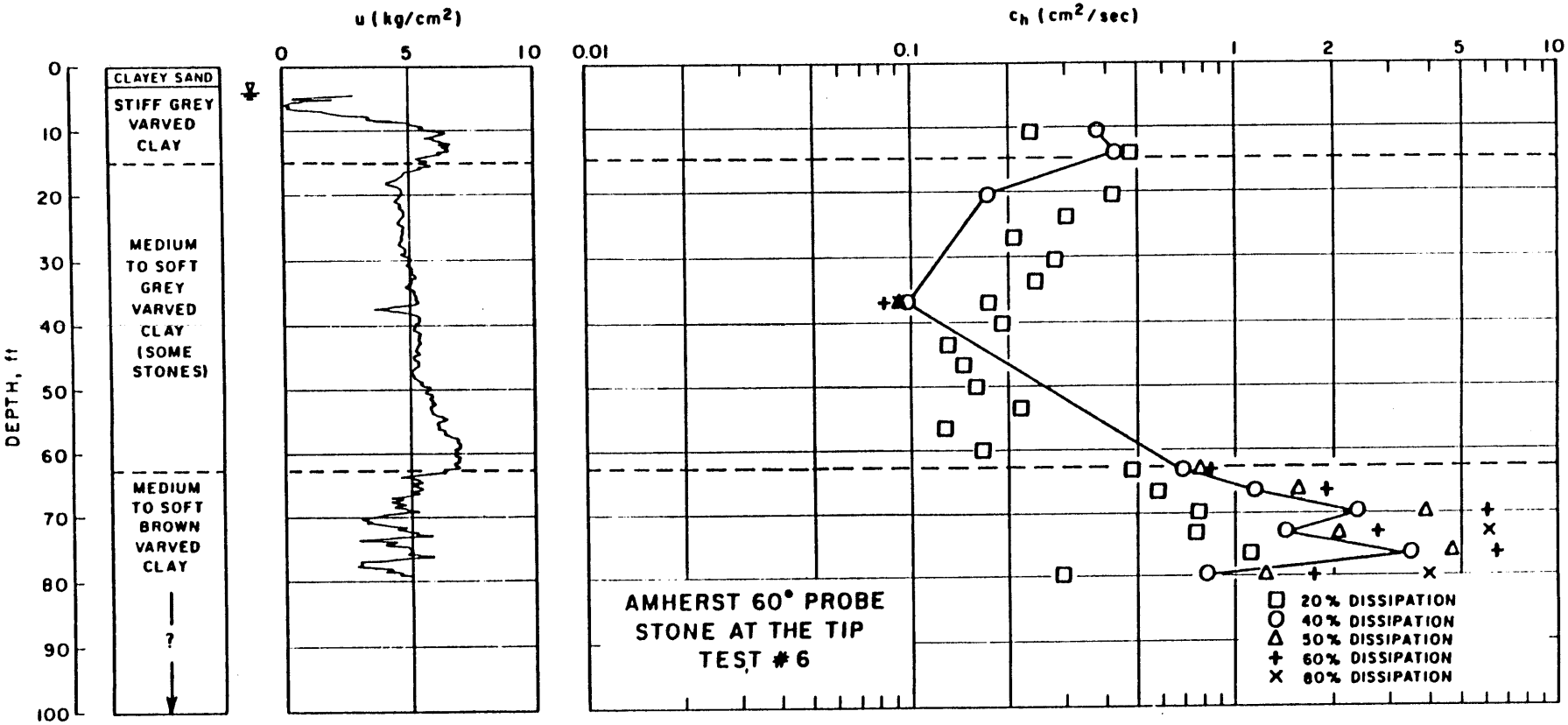

Figure 6.22 Results of 60° conical probes at the Amherst site (Baligh and Levadoux, 1980).

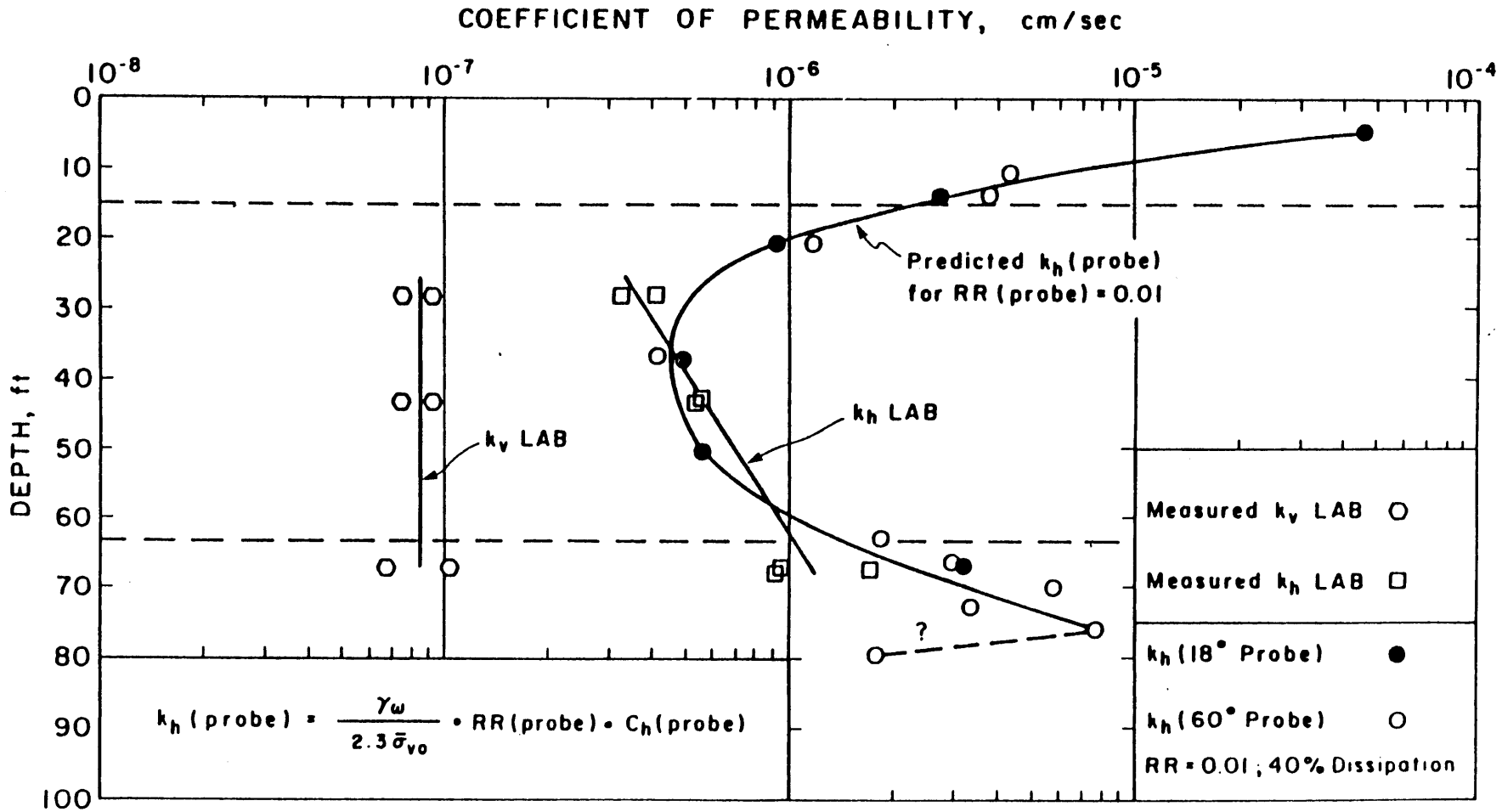

Figure 6.23 Comparison of Predicted and Measured Coefficients of Permeability at the Amherst Site (Baligh and Levadoux, 1980).

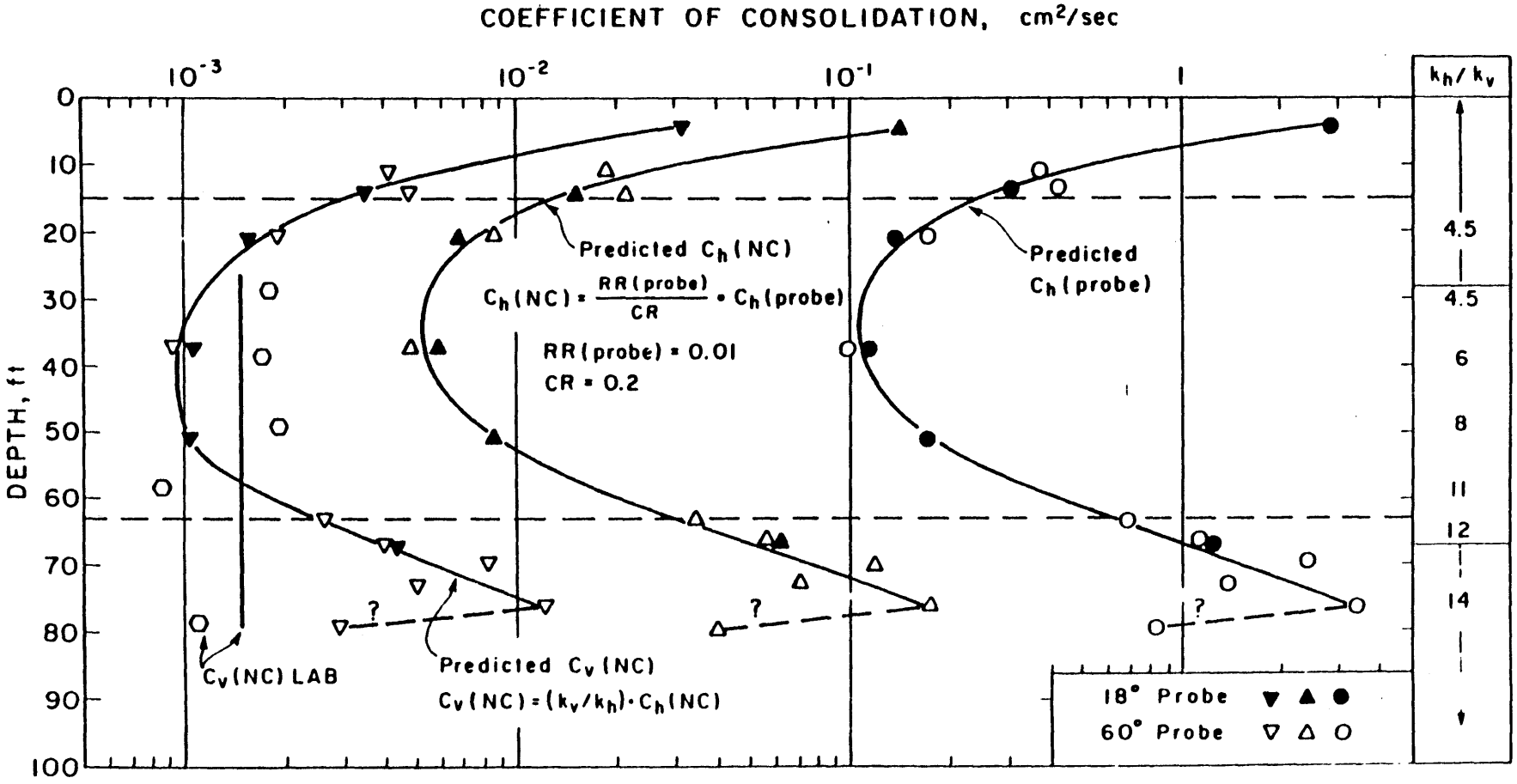

Figure 6.24 Comparison of Predicted and Measured Coefficients of Consolidation at the Amherst Site (Baligh and Levadoux, 1980).

CHAPTER 7

DESCRIPTION OF THE CONSTRUCTION OF THE STUDENT CENTER BUILDING

7.1 INTRODUCTION

In November of 1962, the Foundation Evaluation and Research-M.I.T., FERMIT, program was initiated by the Massachusetts Institute of Technology. The program was conducted by the Soil Mechanics Division of the Department of Civil Engineering and has the following objectives:

1) Insure that future building foundations constructed on the M.I.T. campus perform satisfactorily;
2) Reduce the chances of foundation construction damaging existing structures, and;
3) Build foundations at a minimum cost to the institute.

Results from the FERMIT project have been described in several publications (Gass, 1964,Ladd et al., 1965,FERMIT, 1967, etc.).

The heart of the evaluation program was the field instrumentation of several campus buildings. One of the instrumented buildings was the Julius Adams Stratton Building (Student Center) which is the focus of this study. This chapter presents the construction history of the Student Center and the pertinent field instrumentations and measurements.

7.2 SITE HISTORY AND GEOLOGY

Horn and Lambe (1964) presented a thorough study of the Boston area geology. A summary of the pertinent features concerning the M.I.T. campus is presented herein.

The soils underlying the campus are of glacial or pre-glacial origin. The Wisconsin Glaciation Era deposited a layer of till over bedrock which in the campus area is predominantly a shale of the Permian-Carboniferous Period.

Glacial clay sediments, later known as Boston Blue Clay, were probably deposited in brackish water some 14,000 years ago towards the end of the late Pleistocene Ice Age. This illitic clay is present in considerable thicknesses and represents the compressible stratum. Subsequently, during the Valder's Glacial Substage, sea level fell with respect to land causing the clay sediments to emerge from below sea level. Erosion, weathering and desiccation resulted in the formation of over consolidated medium to stiff Boston Blue Clay. During warmer climates, sea level rose rapidly, depositing sand on the clay surface. As the sea level continued to rise to its present level, organic silt, shells and peat covered the entire area.

Until approximately 1850, the area that is now the site of the M.I.T. campus was marshland in the Charles River Basin. The subsequent filling operation consisted of constructing a sea wall and hydraulically filling behind the wall with the

dredged material. Since the Charles River Dam was completed in 1910, the water level in the Charles River Basin has been maintained at a mean elevation of +13 feet Cambridge City Base, and transforming the Charles River into a fresh water basin.

In 1912, M.I.T. purchased the filled area along the Charles River and Massachusetts Avenue and Boston's and Alabany's railroad tracks. Additional filling was necessary to bring the site to its present grade. This additional fill consisted chiefly of silt, mostly sandy and often shell-bearing, pumped and dredged from the river. This was supplemented for a part of the site by hauled sand and gravel, ashes and other city waste.

A generalized soil profile of the M.I.T. campus is shown in Figure 7.1.

7.3 SOIL CONDITIONS UNDER THE STUDENT CENTER

The precise stratigraphy under the Student Center was obtained from interpolation between 14 wash borings in which 2 inch splitspoon samples were taken of the various soils encountered. An additional boring (U-1) was installed and 3 inch fixed piston "undisturbed" tube samples were taken from the clay layer. The boring logs are documented in the FERMIT Files. The locations of the basement level borings are shown in Figure 7.2.

The obtained generalized soil profile is shown in Figure 7.3. A maximum of 8 feet of stiff clayey silt and sand with gravel (till) overlying shale bedrock form the lower boundary of the clay layer. The till layer dips gently to the east. The Boston Blue Clay layer, 60 to 72 feet thick with an average of 66 feet, is overlain by an average of 11 feet of loose to compacted rubble fill, followed by 4 feet of organic silt and peat and 20 feet of compacted sand and gravel.

7.4 BUILDING DESCRIPTION

The location of the Julius Adams Stratton Building (Student Center) is shown in Figure 7.4. A plan and cross sectional representation of the building are shown in Figure 7.5. The Student Center is a five story reinforced concrete framed structure founded on a 3-5 foot thick reinforced concrete monolithic mat with plan dimensions of about 142 by 236 feet. The concrete mat contributed about a third of the total dead load (approximately 30,000 tons). The general finished grade of the basement floor is approximately elevation +10 feet, with lower areas at the east and west ends. The base of the mat therefore ranges generally between elevations +7 and 0. The building was constructed in an open excavation with a well-point system for dewatering. Based on calculations presented in the FERMIT Files, the dead weight of the building plus the time average of the live load are probably just about equal to the weight of the

excavated material. Hence, the design is based on a fully floating foundation.

7.5 INSTRUMENTATION AT THE STUDENT CENTER

Several types of instruments were installed at the site prior to construction. Special emphasis and detail will be given to the instruments that contribute to pore pressure measurement and water table location as their data will be used later in the following chapters. The field instrumentation is classified as follows:

a) Pore Pressure Measuring Devices

(1) Eight piezometers, casagrande type, denoted PSC-1 through 8, in two clusters.

b) Water Table Elevation easuring Devices

(1) Nine observation wells marked WSC-1 through 9.

c) Elevation Reference Point

(1) One bench mark, denoted BM-SC.

d) Settlement Measuring Devices

(1) Six swelling reference rods marked SSC-1 through 6.

(2) Four foundation reference rods marked FSC-1 through 4.

(3) Numerous initial settlement rods.

(4) Building settlement pins.

A plan and elevation location of the aformentioned instruments are shown in Figure 7.6, 7.5.(a) and tabulated in 7.1.

Interpretation and appreciation of the data derived from the piezometers and the wells depend on a sound understanding of the limitations, structure and method of installation. Description of such instruments was presented in Gass (1964) and is restated herein.

7.5.1 Observation Wells

A total of 8 observation wells were installed in the vicinity of the Student Center building and others have been installed at various locations on the campus to record ground water levels in the sand and gravel stratum. The locations of most of these are shown in Figure 7.5.(a).

In essence the wells are simply well points installed by driving and washing a 2 1/2 inch casing to the desired depth, placing the 1 1/4 inch well point with a 1 inch riser, and surrounding the point with a sand filter. The casing is then withdrawn leaving about a 3 foot length of casing at the top as a collar. Both the casing and the riser are provided with a vented cap. A typical installation is shown in Figure 7.7.

7.5.2 Piezometers

Two groups of four piezometers each were installed at the Student Center building to measure pore pressures at various levels in the foundation clay stratum. As shown in Figure 7.5.(a) one group was located in the central portion of the basement of the structure and the other at the west end. These are permanent installations and the choice of locations was dictated partly by the necessity of avoiding any interference with the appearance or function of the building.

The piezometers are porous plastic of the flush flow type. They are installed in a manner similar to the observation wells by driving and washing a casing to the required depth, placing the piezometer and surrounding it with a tamped sand filter as the casing is partially withdrawn. The filter is extended into the bottom of the casing and then two tamped bentonite seals each with a thickness of about 1 1/2 feet and separated by a layer of sand are placed. The upper seal is then capped by another layer of sand and the remaining annular space in the casing is left filled with water. A typical installation together with the essential details of the Student Center piezometer groups is given in Figure 7.8.

An essential point to note is that the clay seals are formed in the casing, which is left in place, and that no joints or couplings are allowed in the lower 10 feet of the casing. The latter is an attempt to ensure that there will

be no leakage along the pipe due to displacement by the couplings during driving.

Detailed diagrams of the rest of the instrumentation is presented in Figures 7. 9 through 7.16 For more information, the reader is referred to Gass (1964).

7.6 CONSTRUCTION HISTORY

The construction history of the Student Center building was directly extracted from the FERMIT Files depending largely on contractors quantities and FERMIT personnel observations.

The progress is going to be divided into two phases namely, the excavation phase and the construction phase. The description of each is given in detail below.

7.6.1 Excavation

Excavation was executed in two stages. Stage one was excavated down to elevation +16 feet. A system of well points surrounding the site was driven into the sand-gravel stratum and pumping commenced in an attempt to lower the water table in preparation for the second excavation. Which was excavated down to elevation +8. Excavation then proceeded slightly in advance of pouring the foundation mat.

After a thorough review of the conflicting evidence presented in the FERMIT Files as to the progress of the

stage one excavation, the only dependable account of the activity progress could be summarized as follows:

a) Stage one excavation commenced on the afternoon of September 17, 1963.

b) Stripping of the existing parking lot occupied the period from the 17th to the 21st of September 1963.

c) Excavation was 90% complete by September 30th.

d) An Earth ramp at the northeast corner was removed on October 4th.

The only schematic evidence that was found of stage one excavation is given in Figure 7.7.

Important foundation dewatering operations commenced on September 25, 1963. Approximately 170 well points were installed. Gass (1964) presents evidence that the dewatering operation was felt 2000 feet away from the site.
One could roughly estimate the elevation of the ground water table at the center of the excavation through observation well SC-1.

Excavation stage two was better documented. It commenced on October 7 and lasted through October 16, 1963. The progress of the activity is documented in the five sketches shown in Figs. 7.18 through 7.22. Fig. 7.23 shows a schematic representation of the limits of the two excavation stages.

7.6.2 Concrete Pours

A detailed record of the concrete pours was reasonably well kept as a list of pours in cubic yards prepared by the contractor and maintained in the FERMIT Files. Location of these pours was well documented up to the third floor (the Student Center is a five-story buidling). As mentioned earlier the largest single pours were those of the foundation mat. Figure 7.24 gives the location and quantity of concrete pours in the foundation mat and Appendix A gives a record of all concrete pours and some of their locations.

7.7 FIELD MEASUREMENTS

7.7.1 Piezometer Data

Gass (1964) presented the piezometer data in the form of plots of water elevation versus time. Those plots were checked against tabulated data in the FERMIT Files and re-plotted in a similar format after few corrections were done in Figures 7.25 through 7.29. The reason the piezometers were plotted in pairs will become evident later. Special attention should be given to Figure 7.29 which concentrates on the piezometer readings during excavation since this period will be of interest to us in later analysis. For the sake of accuracy, the piezometer readings are also tabulated and appear in Tables B.1 through B.4 in Appendix B .

Instr. No.	Type of Instr.	Date Installed	Elev. of Sensor *
WSC-1	Wells		- 6.5'
WSC-2	"		- 3.0'
WSC-3	"		- 7.0'
WSC-4	"		- 6.5'
WSC-5	"		- 3.0'
WSC-6	"		- 6.5'
WSC-7	"		- 6.5'
WSC-8	"		- 5.5'
WSC-9	"		- 3.5'
SSC1	Swelling Reference Rods	9/30 63	-14.3'
SSC2	"	9/20 63	-13.3'
SSC3	"	9/21 63	-19.6'
SSC4	"	9/20 63	-17.1'
SSC5	"	9/20 63	-16.3'
SSC6	"	9/21 63	-17.6'

* All elevations are referenced to Cambridge City Base

Table 7.1 Description of the instrumentation at the Student Center.

Instr. No.	Type of Instr.	Date Installed	Elev. of Sensor *
PSC-1	Piezometer	9/19 63	-20.3'
PSC-2	"	9/19 63	-34.3'
PSC-3	"	9/20 63	-47.4'
PSC-4	"	9/20 63	-62.6'
PSC-5	"	10/7 63	-19.3'
PSC-6	"	10/7 63	-33.2'
PSC-7	"	10/7 63	-47.2'
PSC-8	"	10/7 63	-61.6'
FSC-1	Settlement Rod	10/16 63	-30.0'
FSC-2	"	10/17 63	-51.0'
FSC-3	"	10/21 63	-30.0'
FSC-4	"	10/19 63	-57.0'
+ B.M.$_{SC}$	Bench Mark	10/18 63	

* All elevations are referenced to Cambridge City Base
+ Elevation of top of stainless steel ball = -2.731

Table 7.1 (continued) Description of the instrumentation at the Student Center.

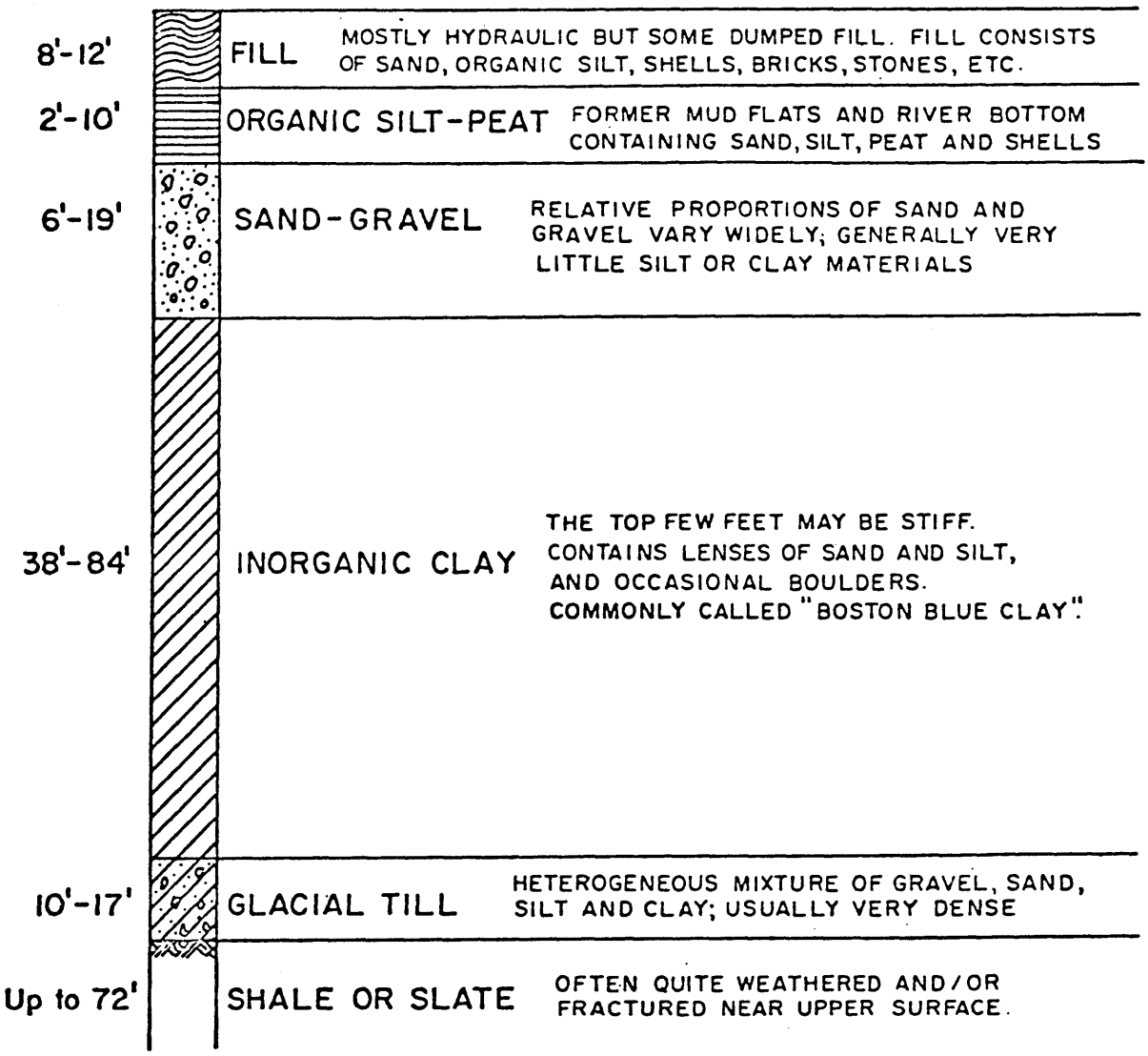

Figure 7.1 Generalized soil profile at the M.I.T. Campus.

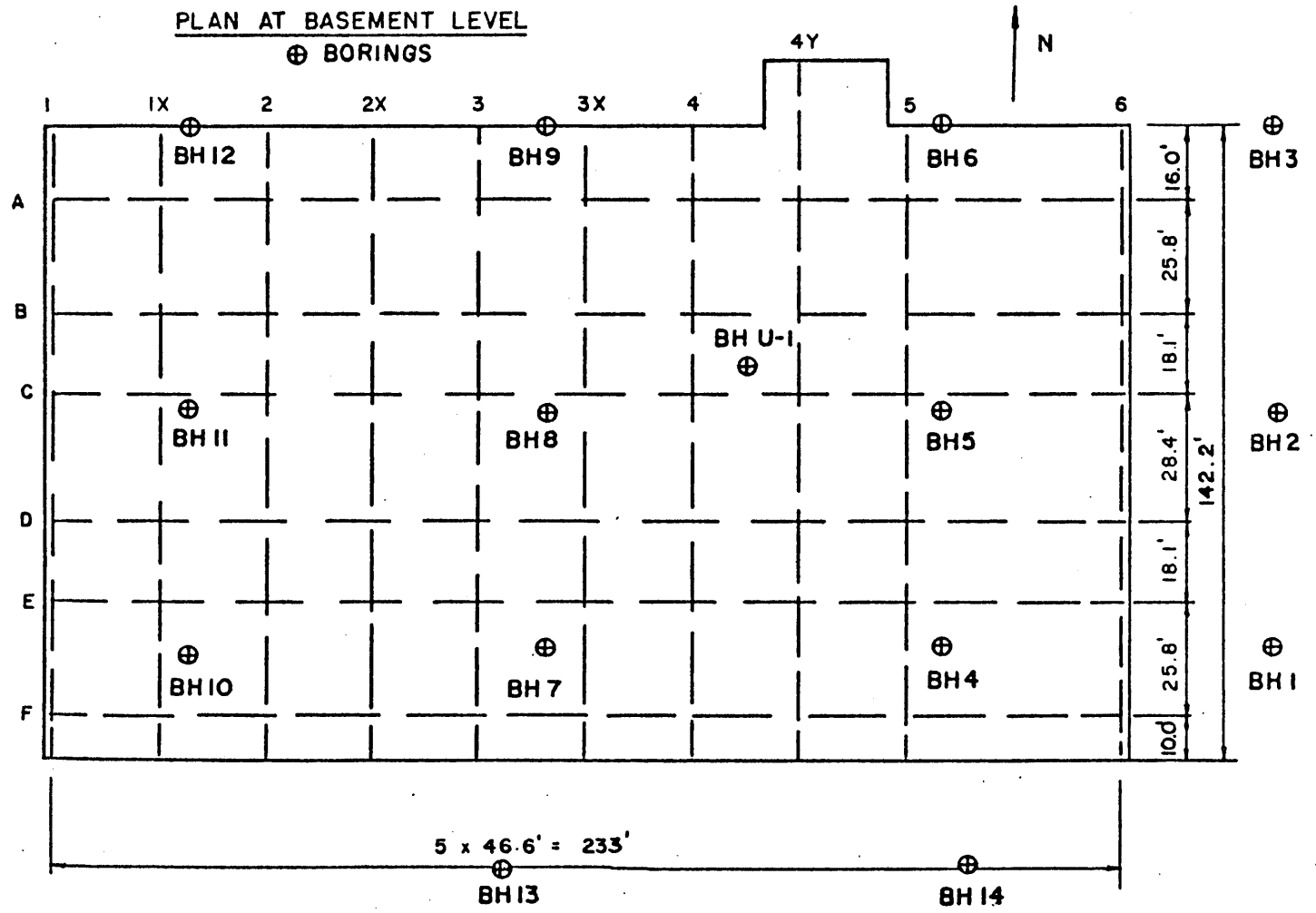

Figure 7.2 Location of the basement level borings at the Student Center.

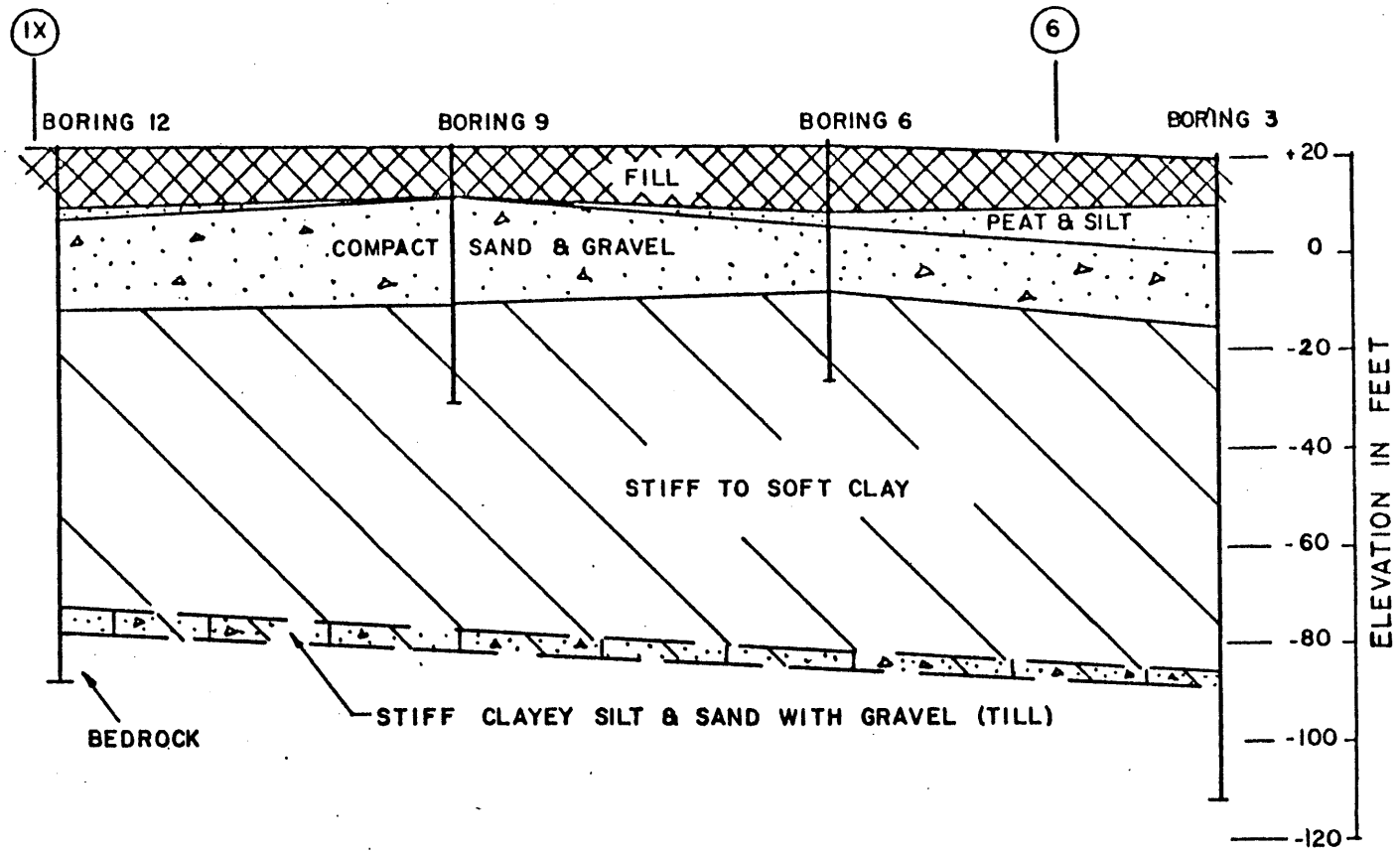

Figure 7.3 Generalized soil profile at the Student Center.

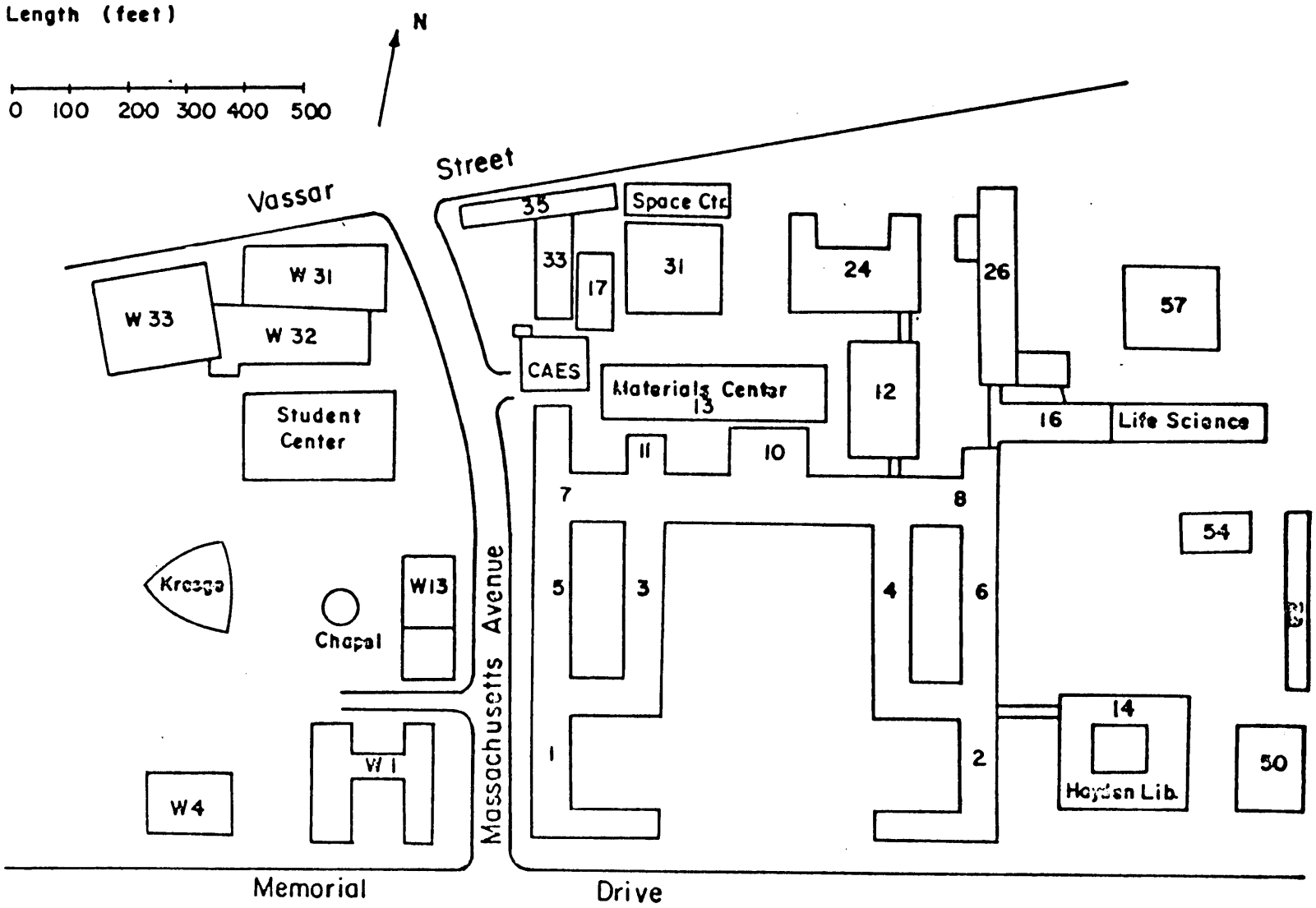

Figure 7.4 Location of the Student Center on the M.I.T. campus.

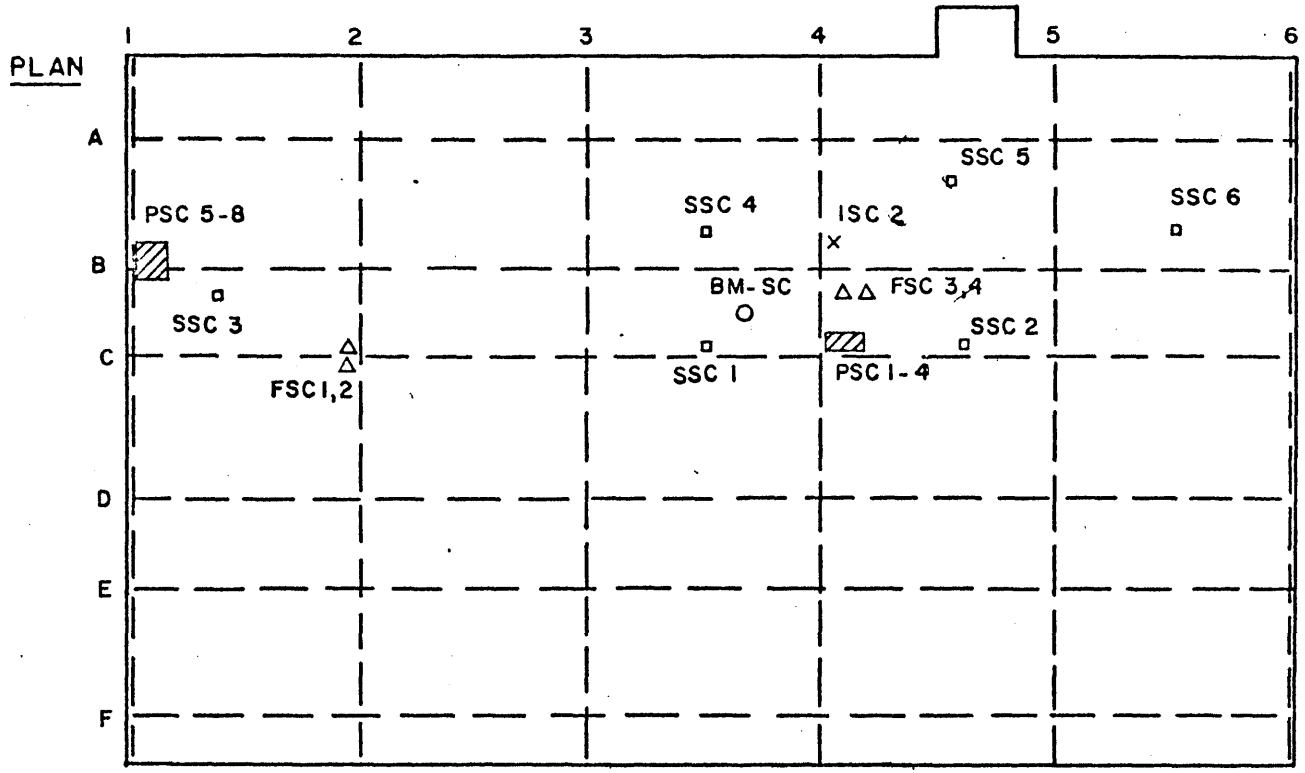

Figure 7.5.(a) Plan view of the Student Center also showing the location of the installed instrumentation.

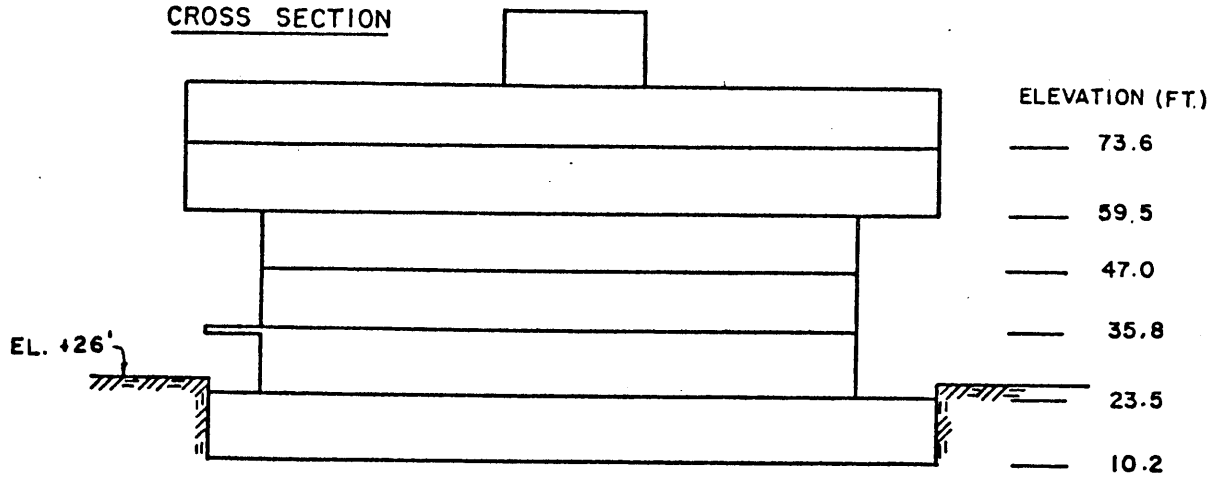

Figure 7.5.(b) Cross-sectional representation of the Student Center.

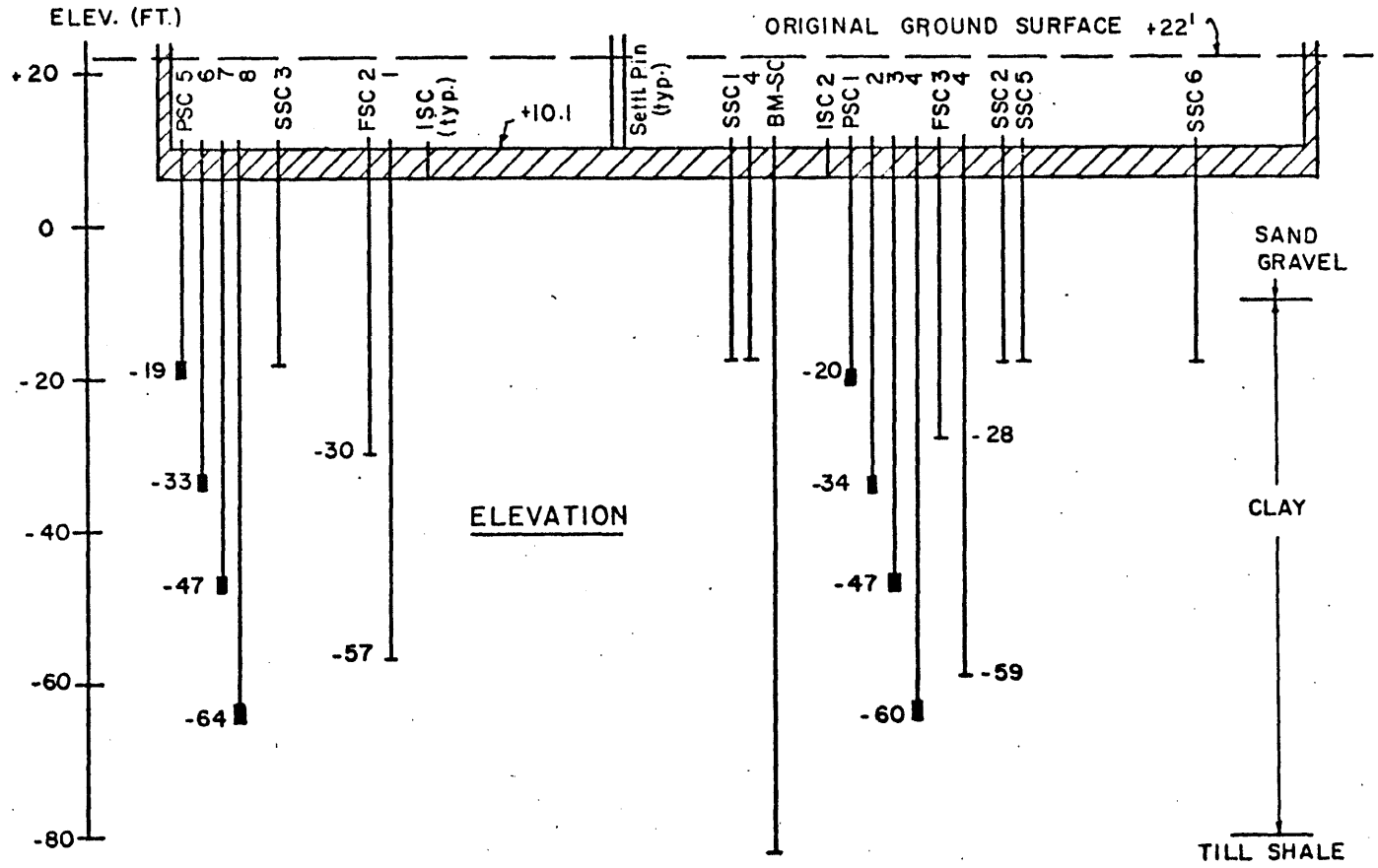

Figure 7.6 Elevation view of the instrumentation location at the Student Center.

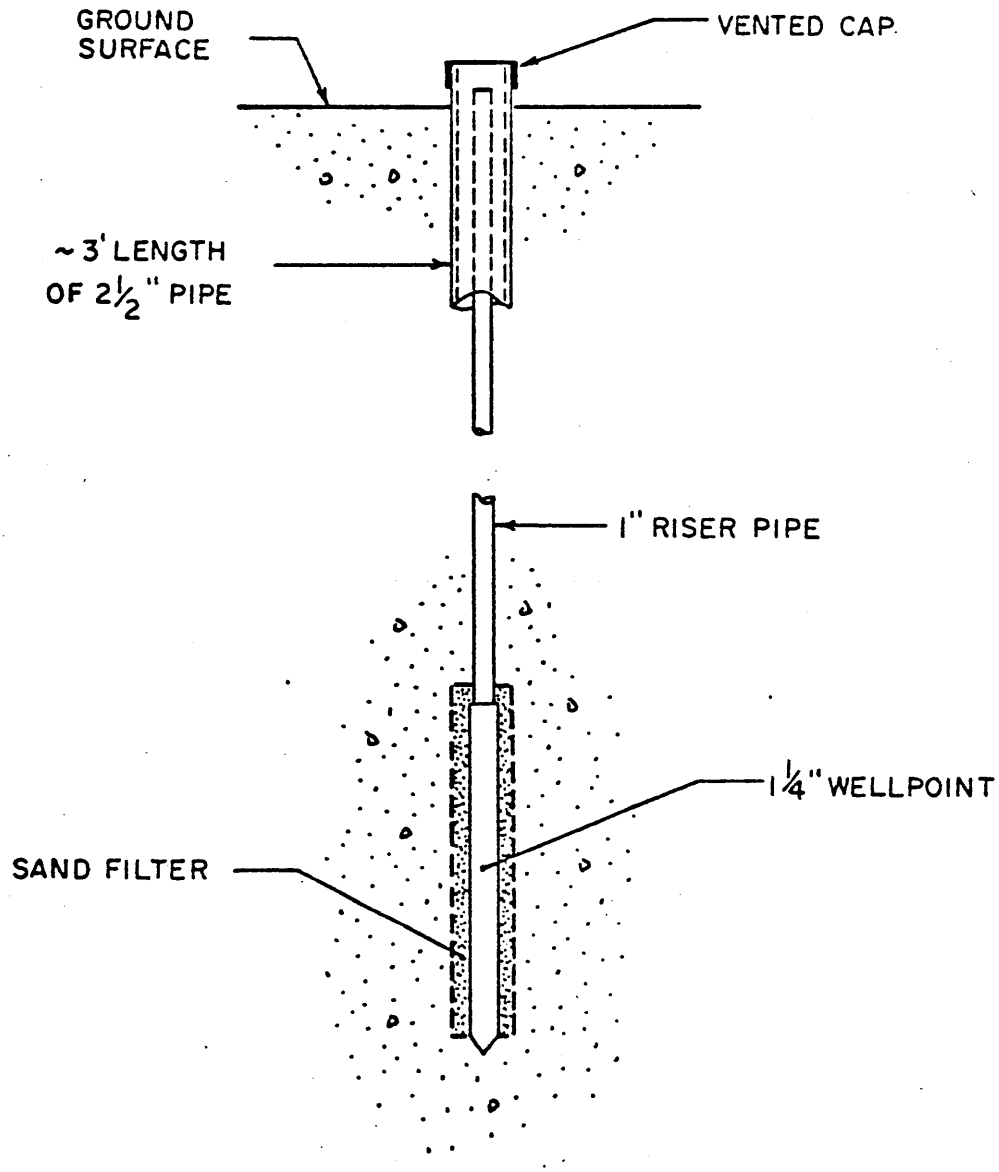

Figure 7.7 Schematic diagram of a typical observation well on M.I.T. campus.

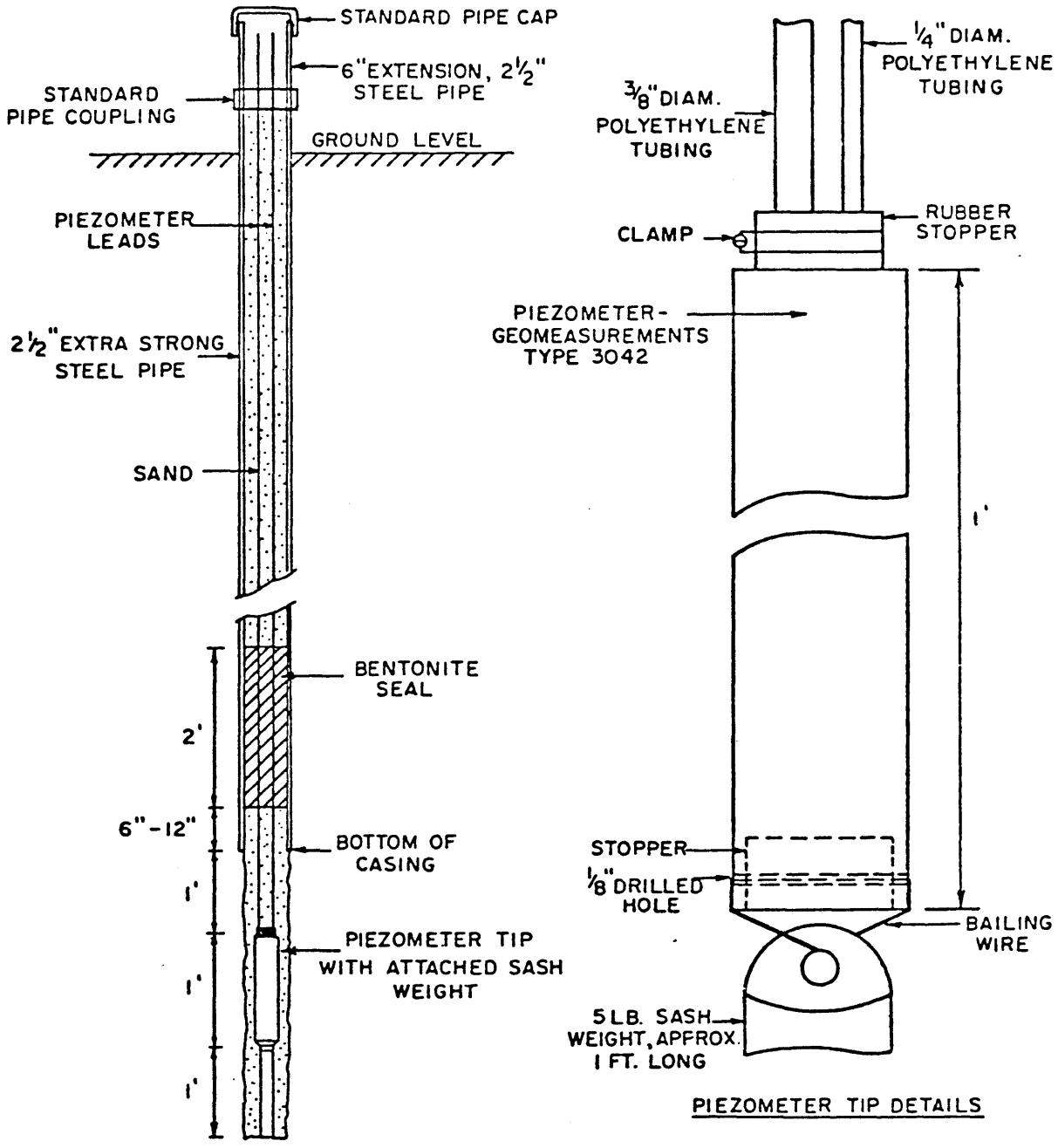

Figure 7.8 Detail of open hydraulic piezometer.

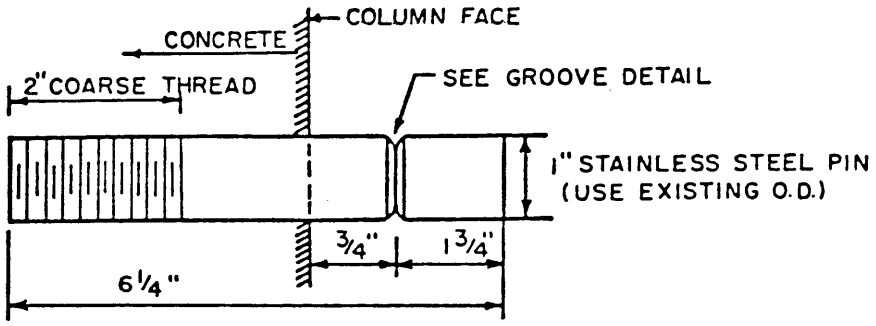

Settlement Pin Detail – August 1965

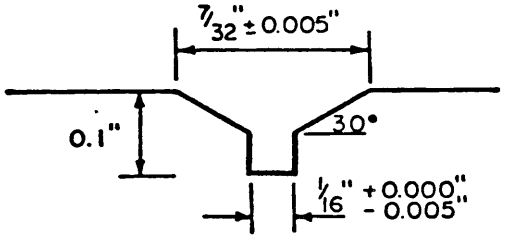

Groove Detail

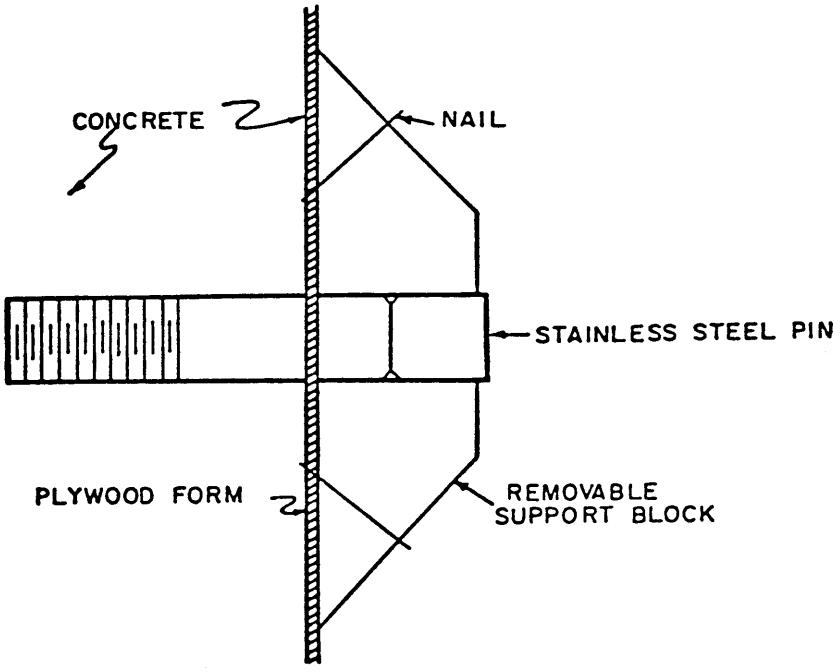

Installation Detail

Figure 7.9 Settlement pin detail.

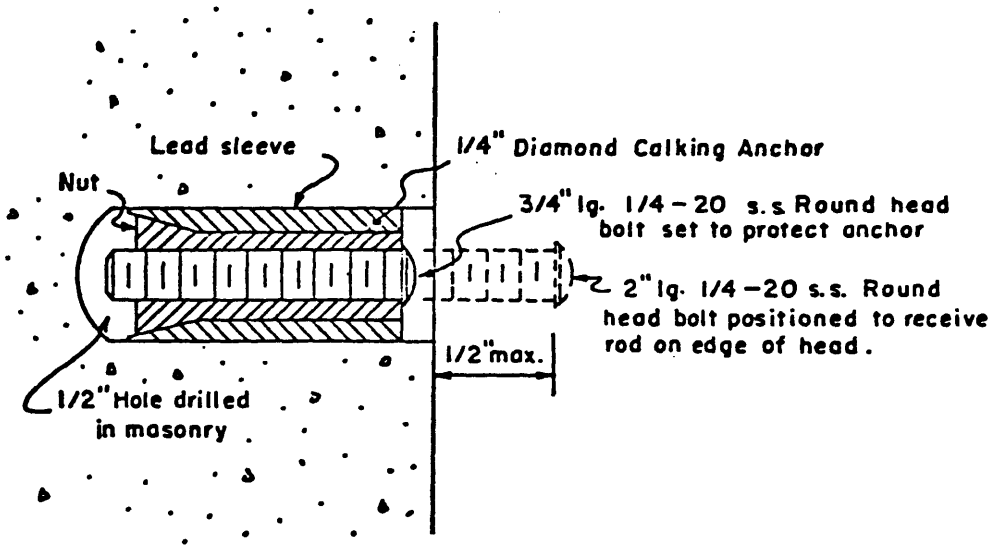

Note: When 3/4" s.s. bolt is replaced after observation is made, the 3/4" bolt should be properly lubricated and "finger-tightened" to prevent seizure.

Figure 7.10 Detail of settlement reference screw.

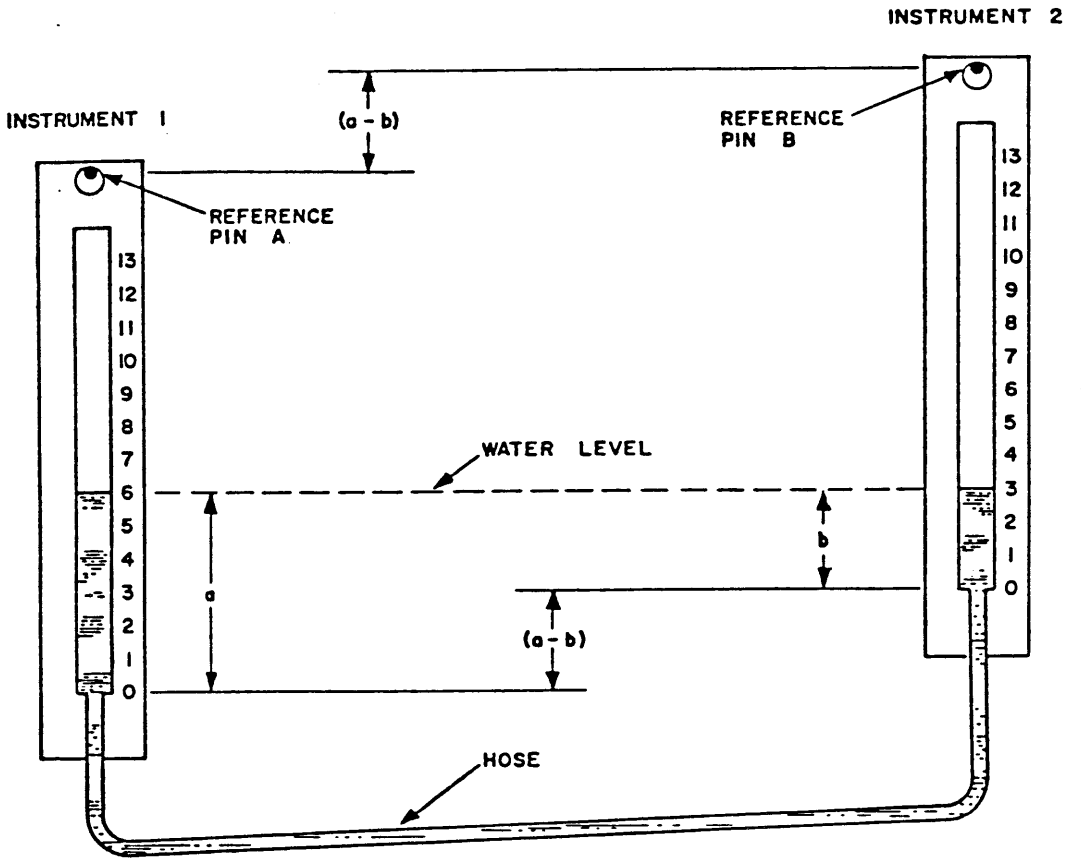

Figure 7.11 Schematic diagram of hose level.

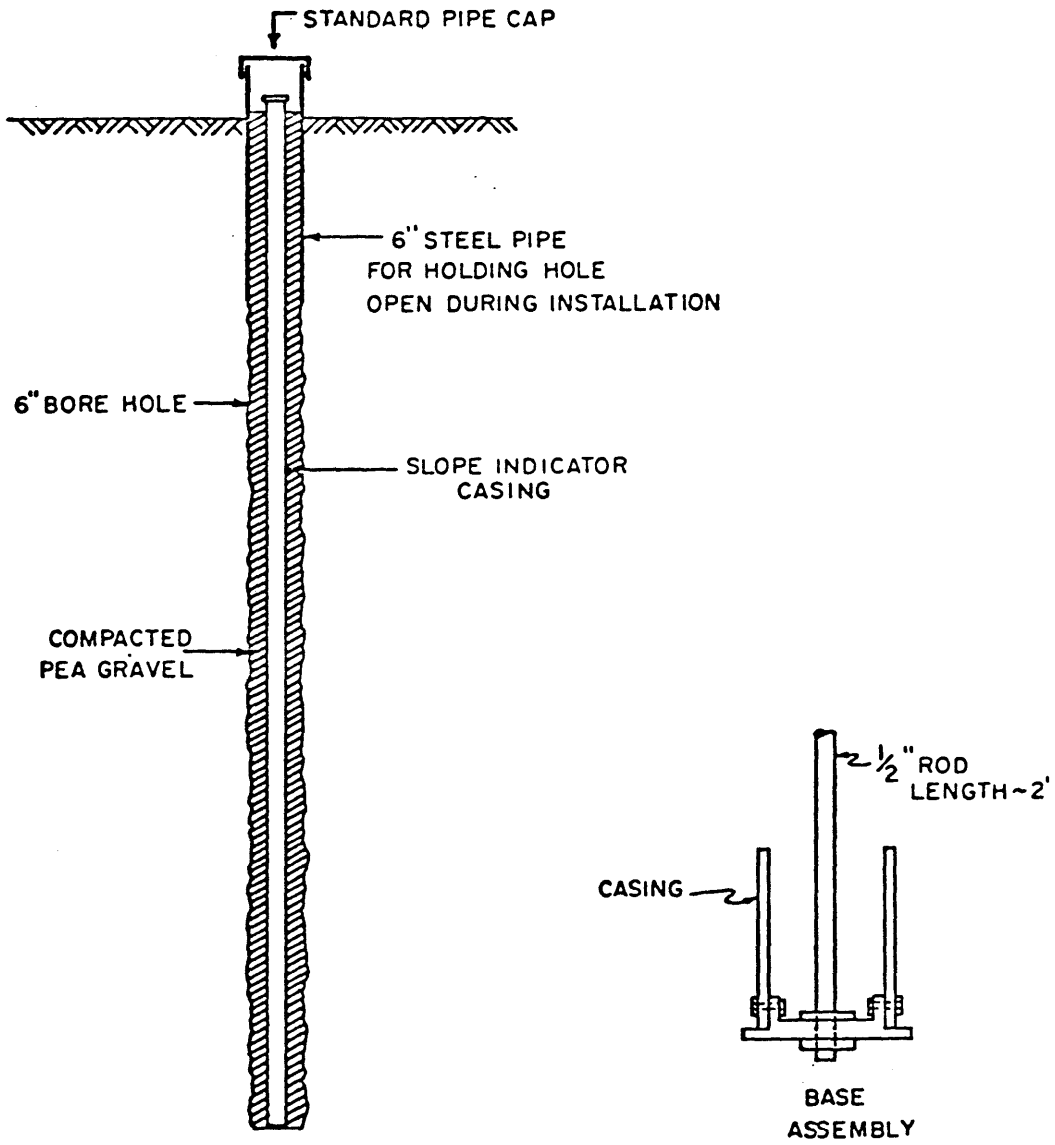

Figure 7.12 Schematic detail of slope indicator well installation.

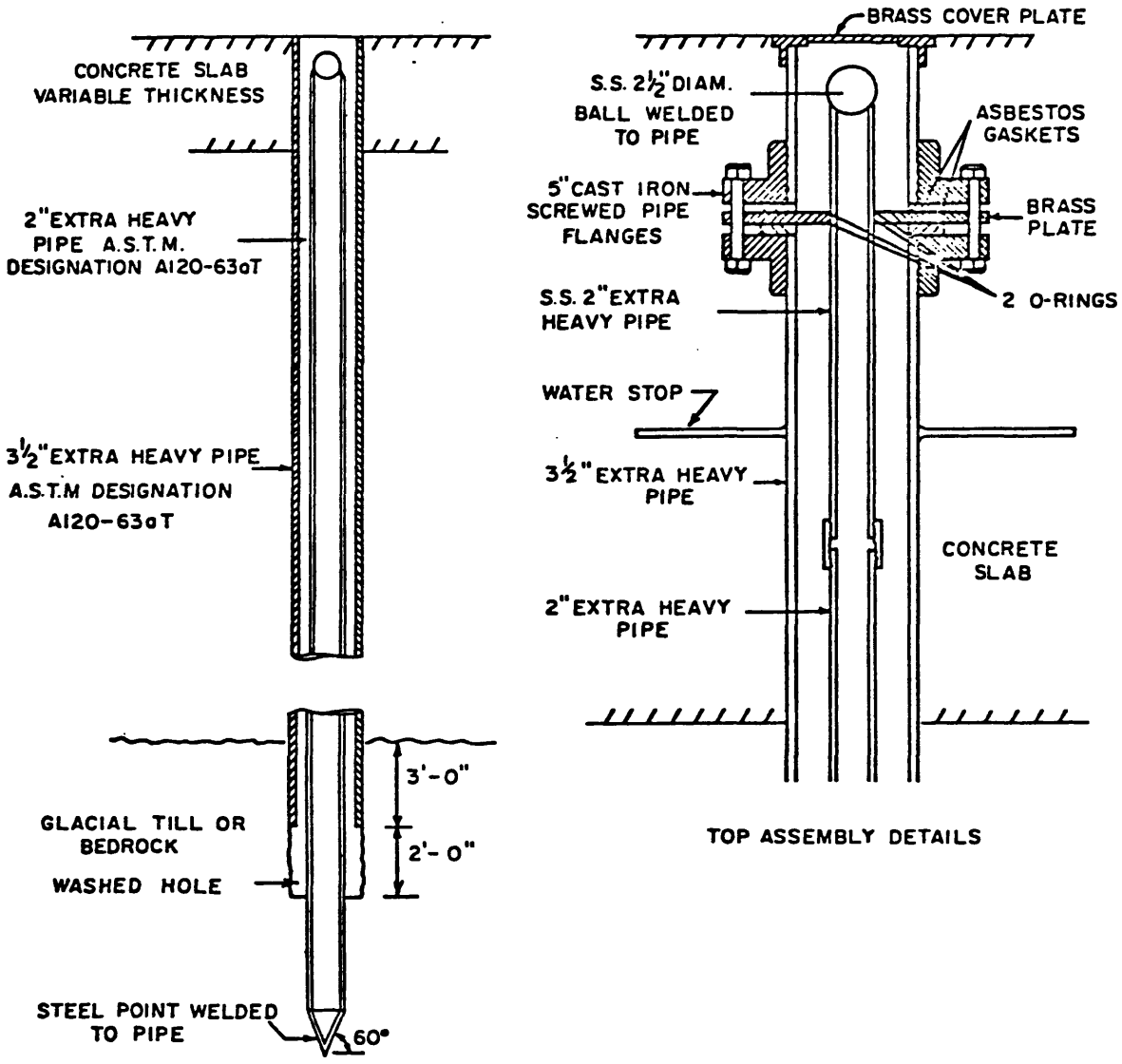

Figure 7.13 Detail of deep benchwork installation.

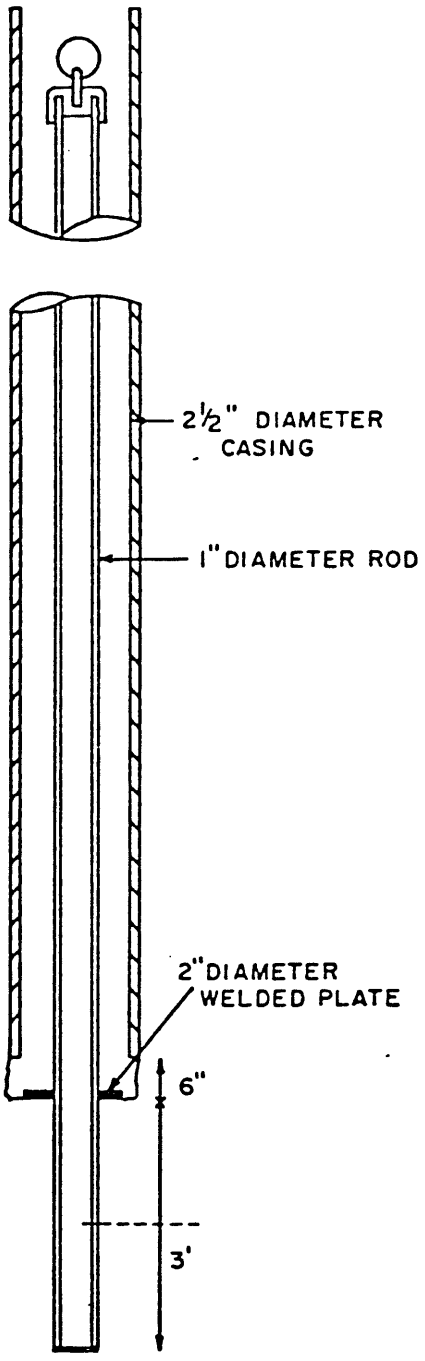

Figure 7.14 Schematic detail of settlement rod.

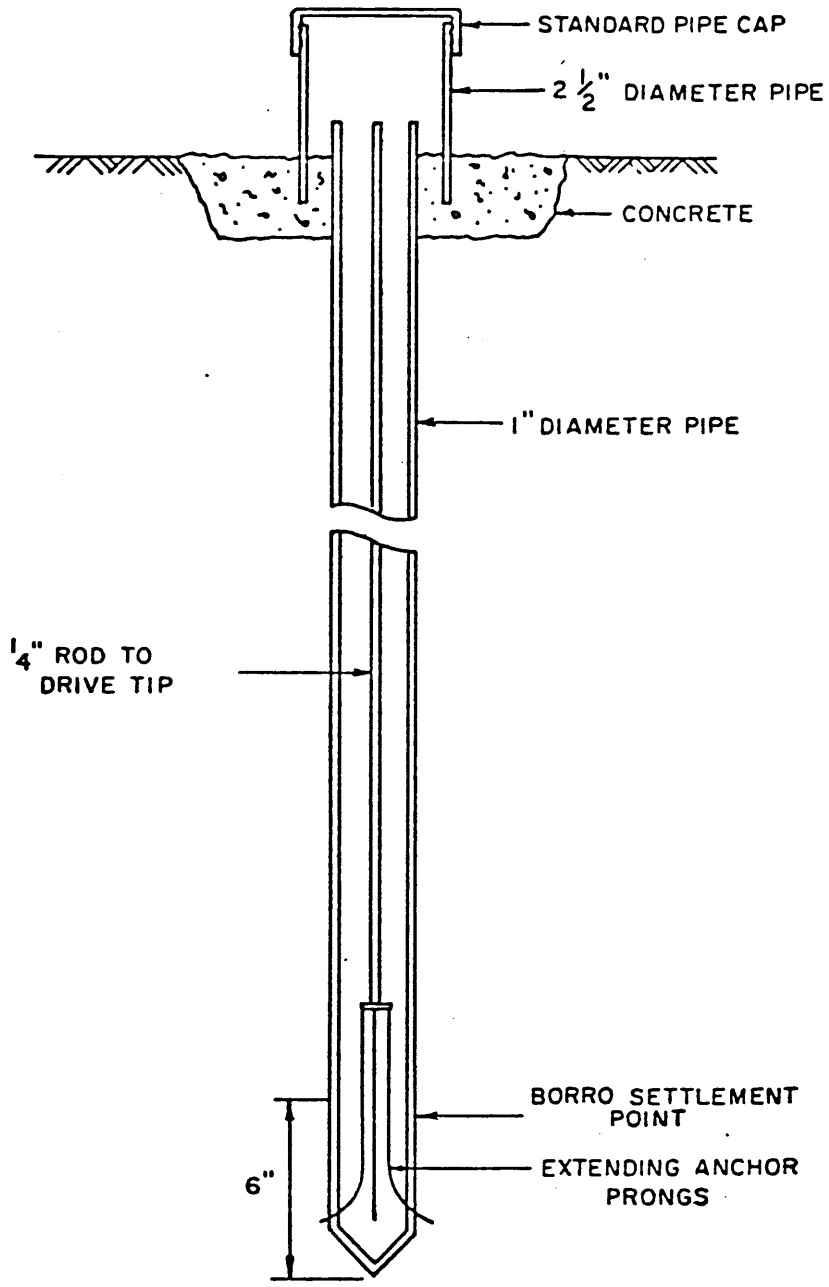

Figure 7.15 Detail of heave rod.

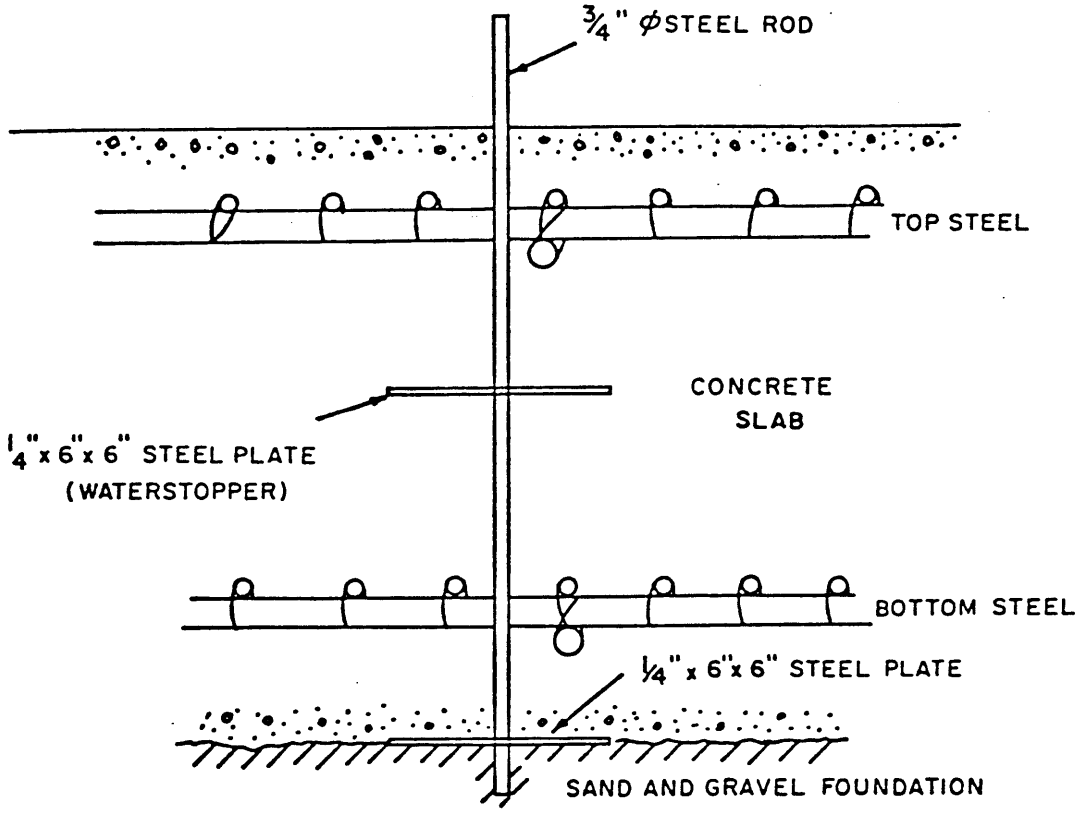

Figure 7.16 Typical initial settlement rod.

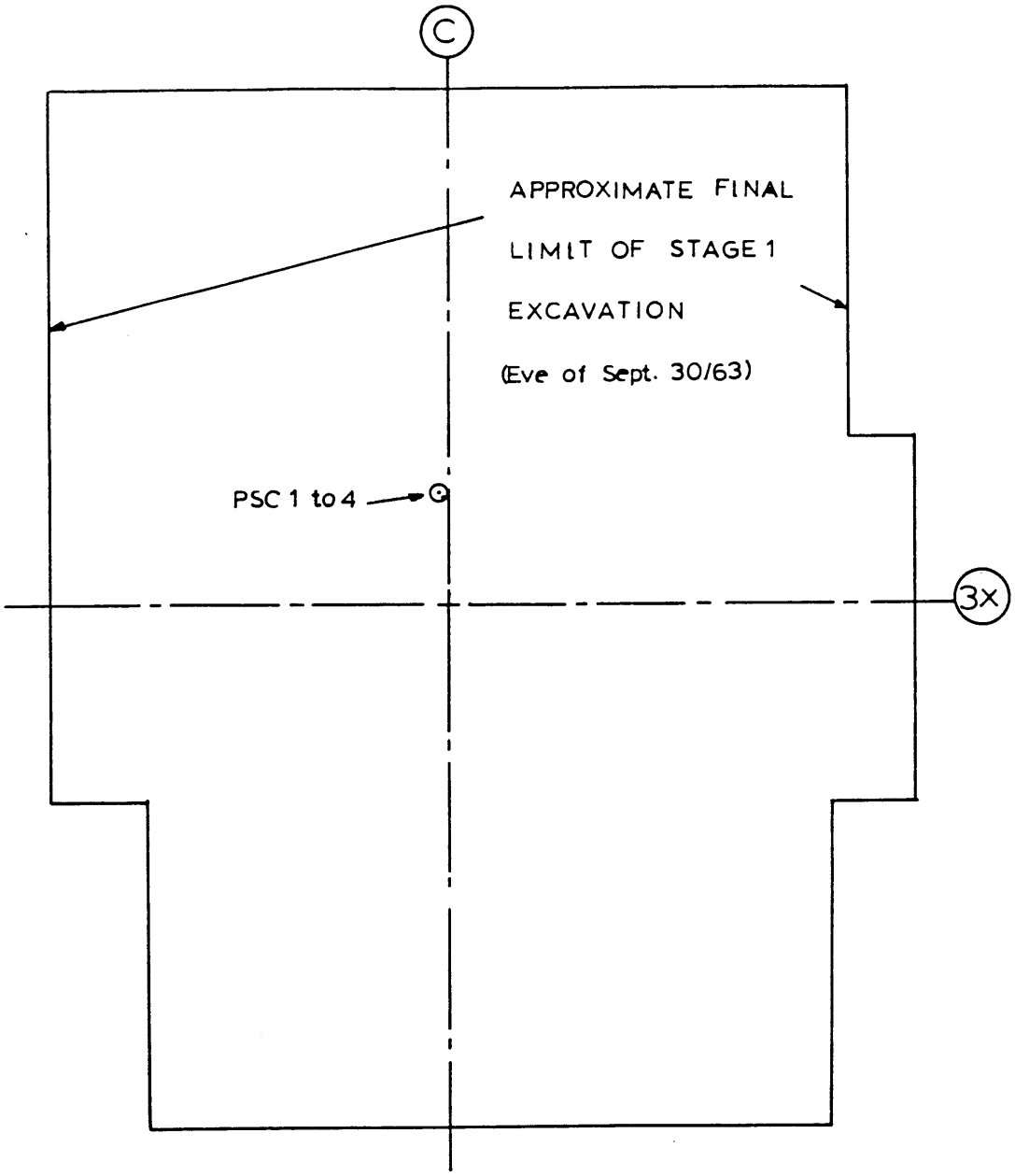

Figure 7.17 Limits of Stage 1 excavation.

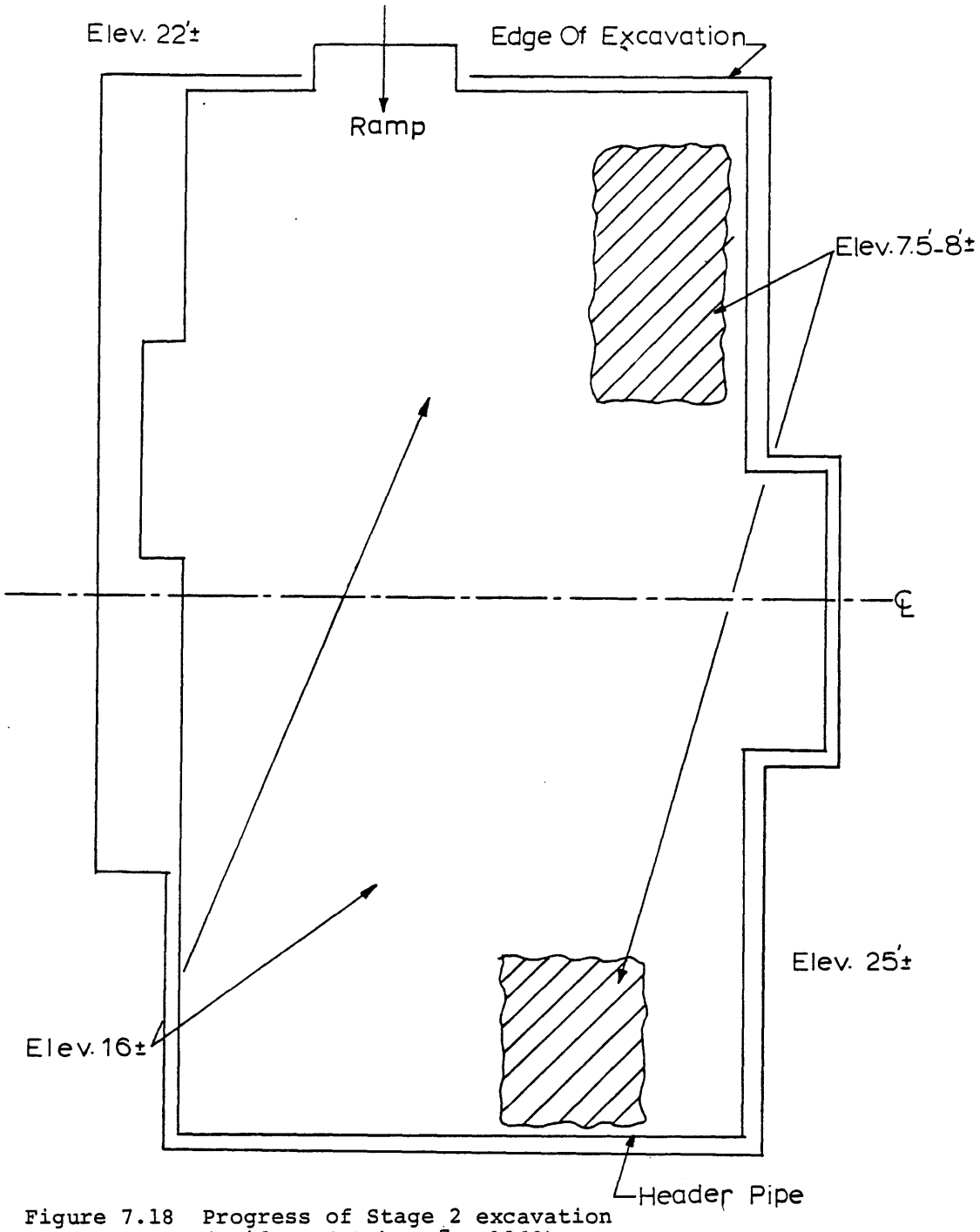

Figure 7.18 Progress of Stage 2 excavation (Friday, October 7, 1963).

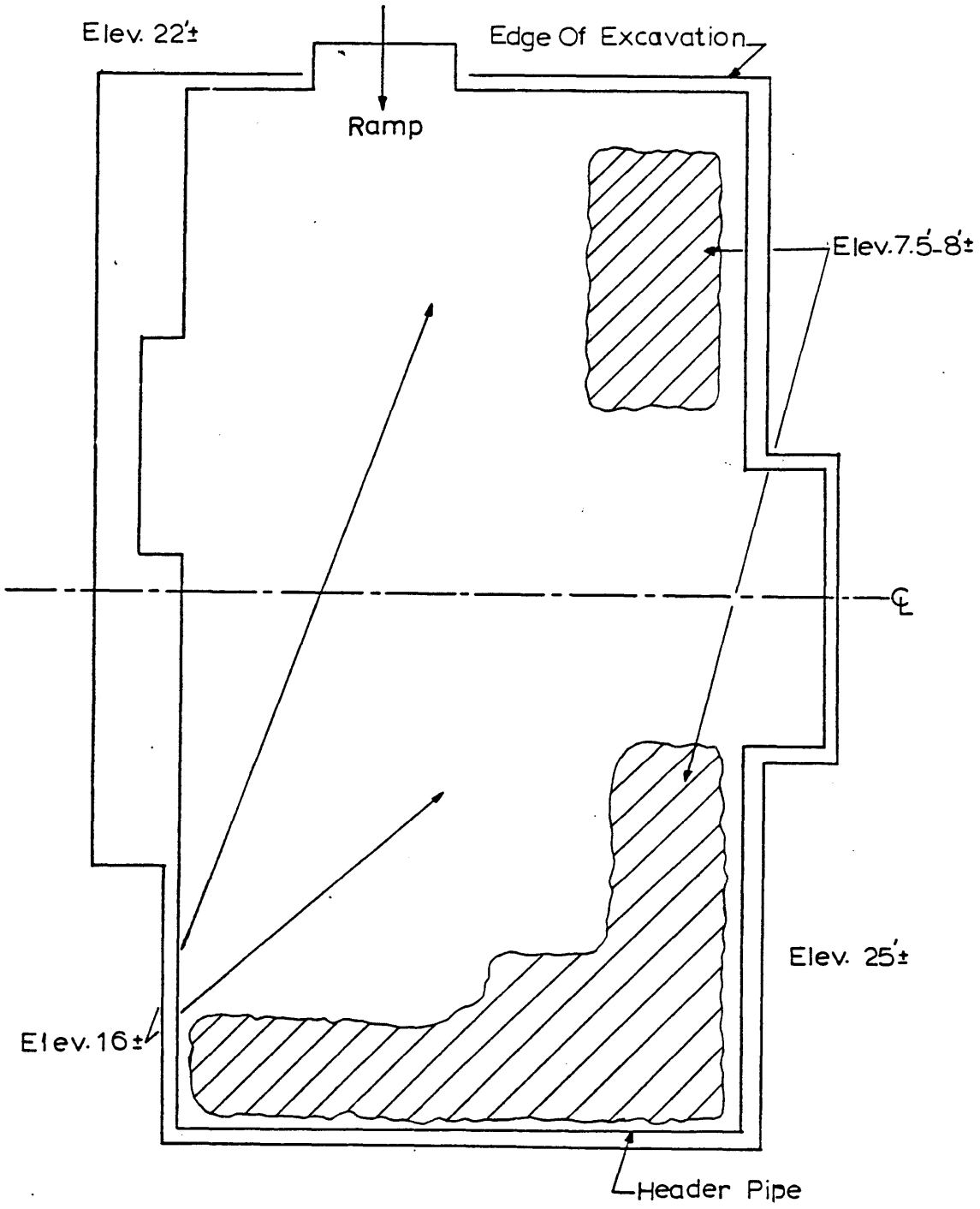

Figure 7.19 Progress of Stage 2 excavation (Wednesday, October 8 ,1963)

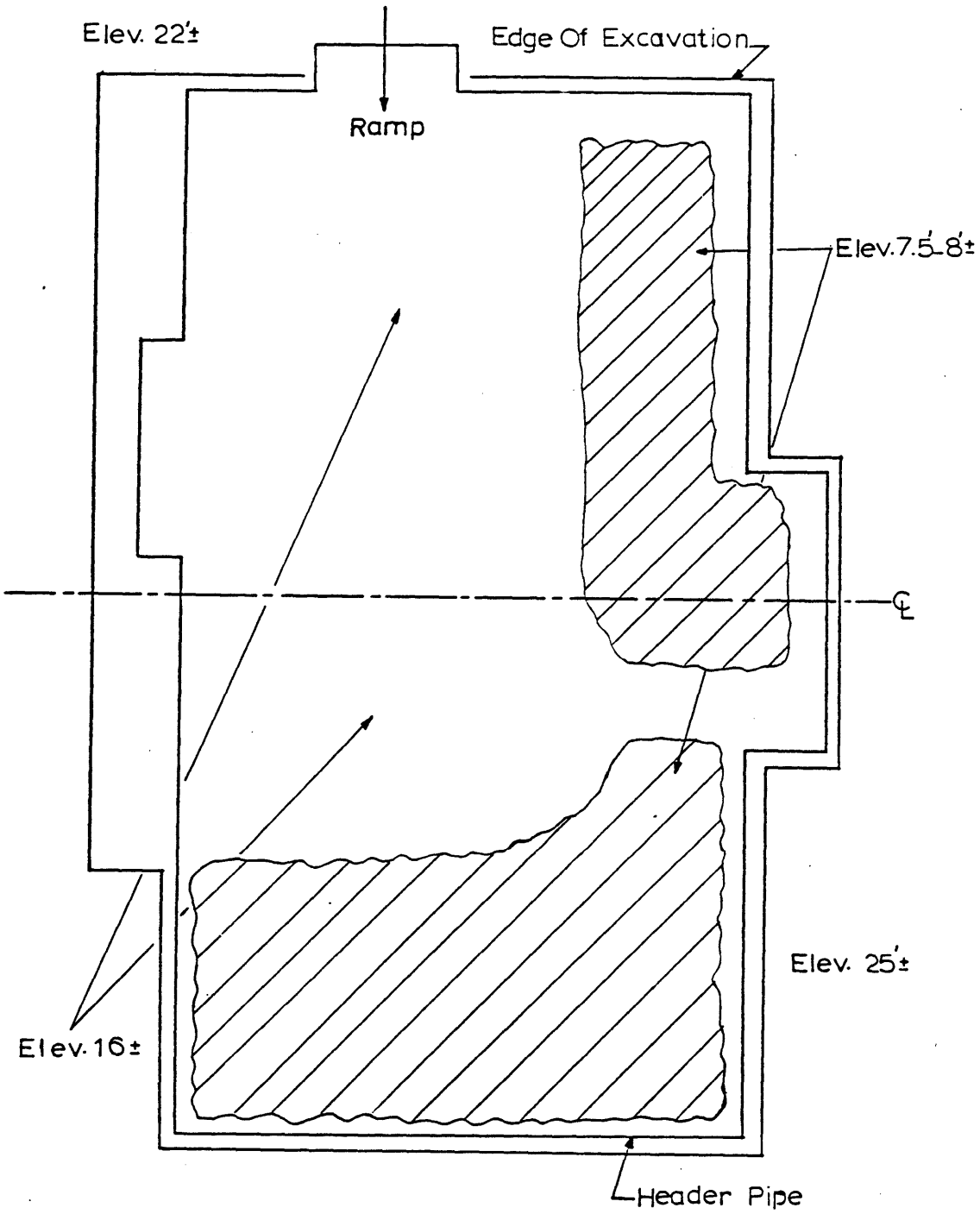

Figure 7.20 Progress of Stage 2 excavation (Wednesday, October 9, 1963)

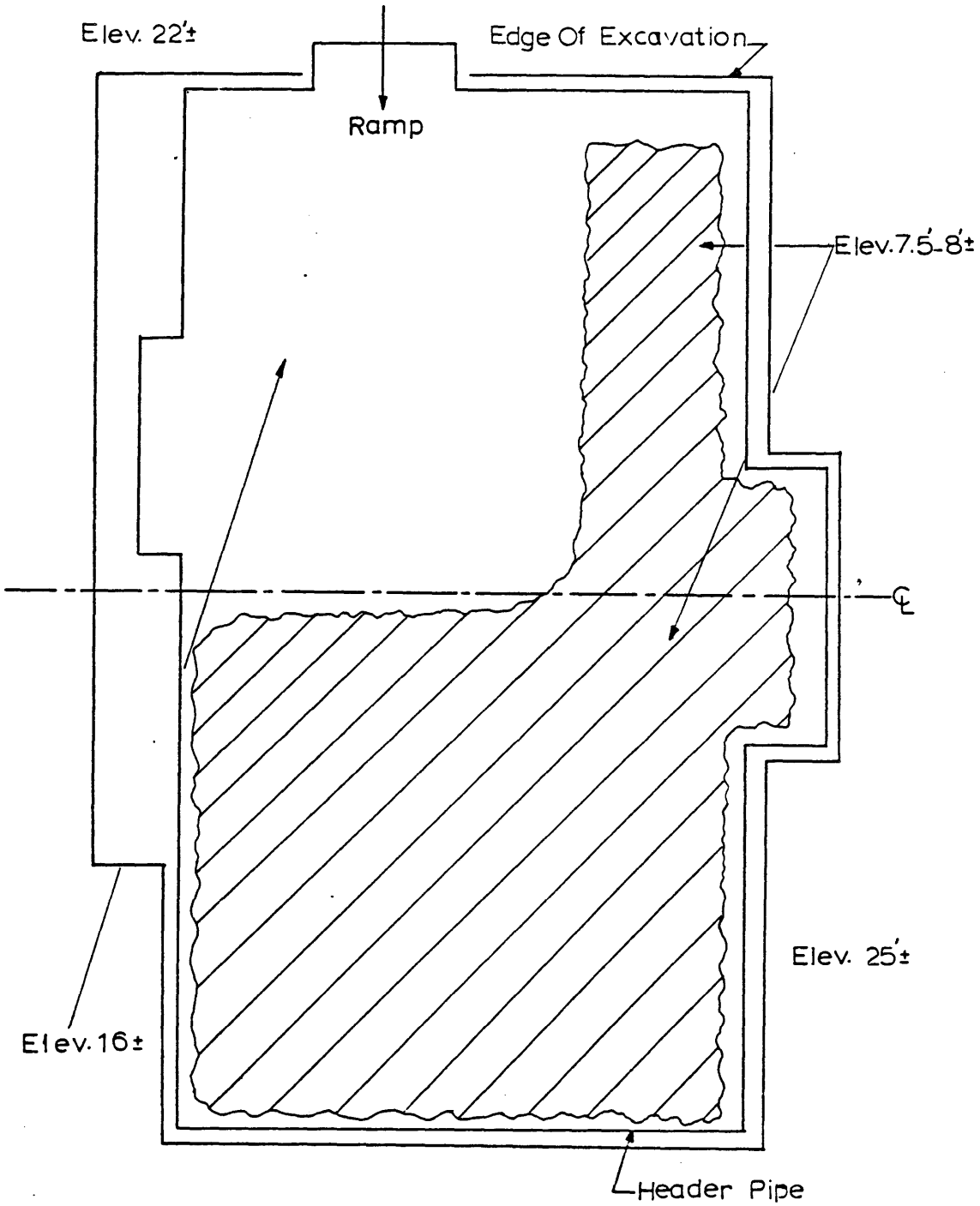

Figure 7.21 Progress of Stage 2 excavation (Thursday, October 10. 1963)

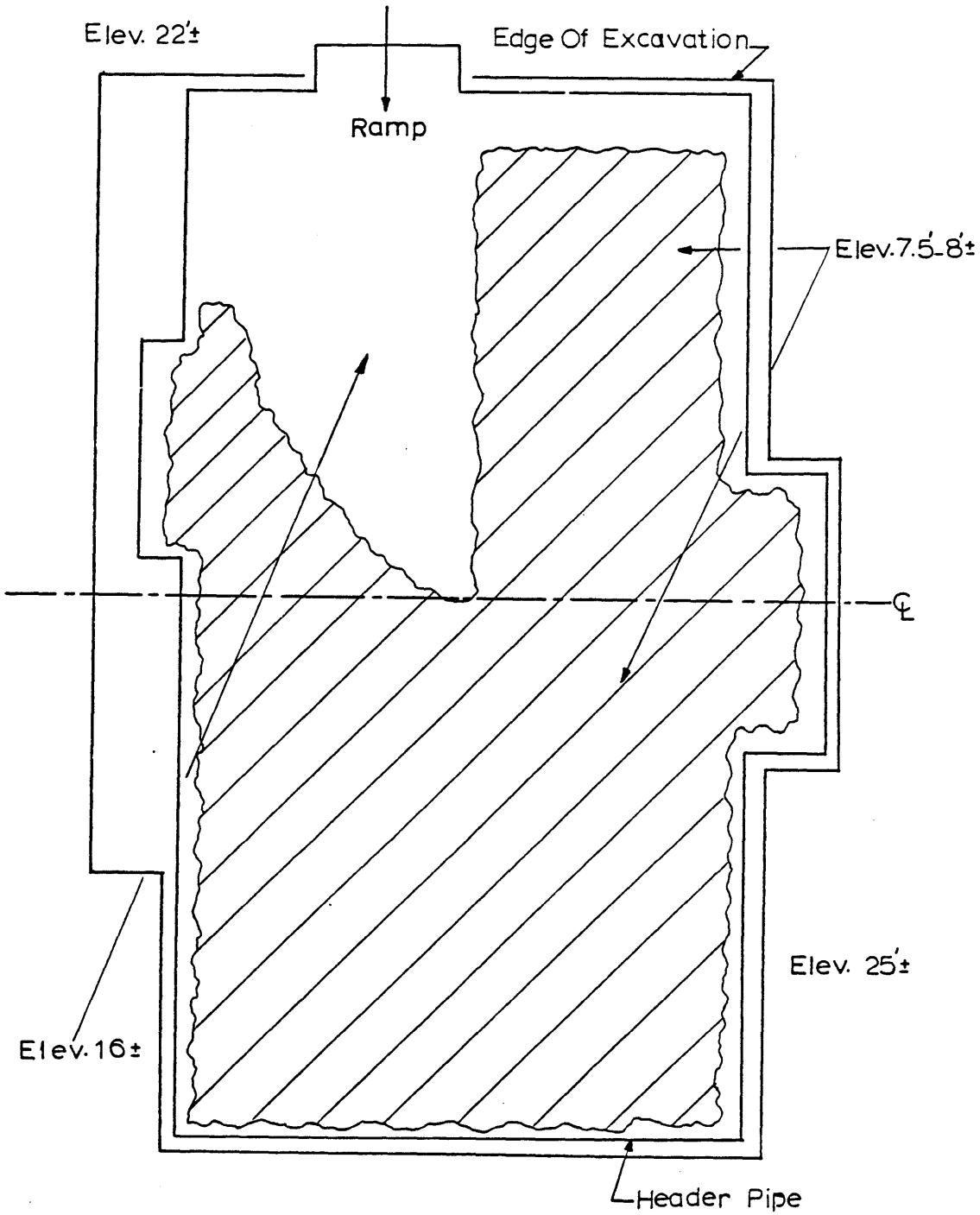

Figure 7.22 Progress of Stage 2 excavation (Friday, October 11, 1963)

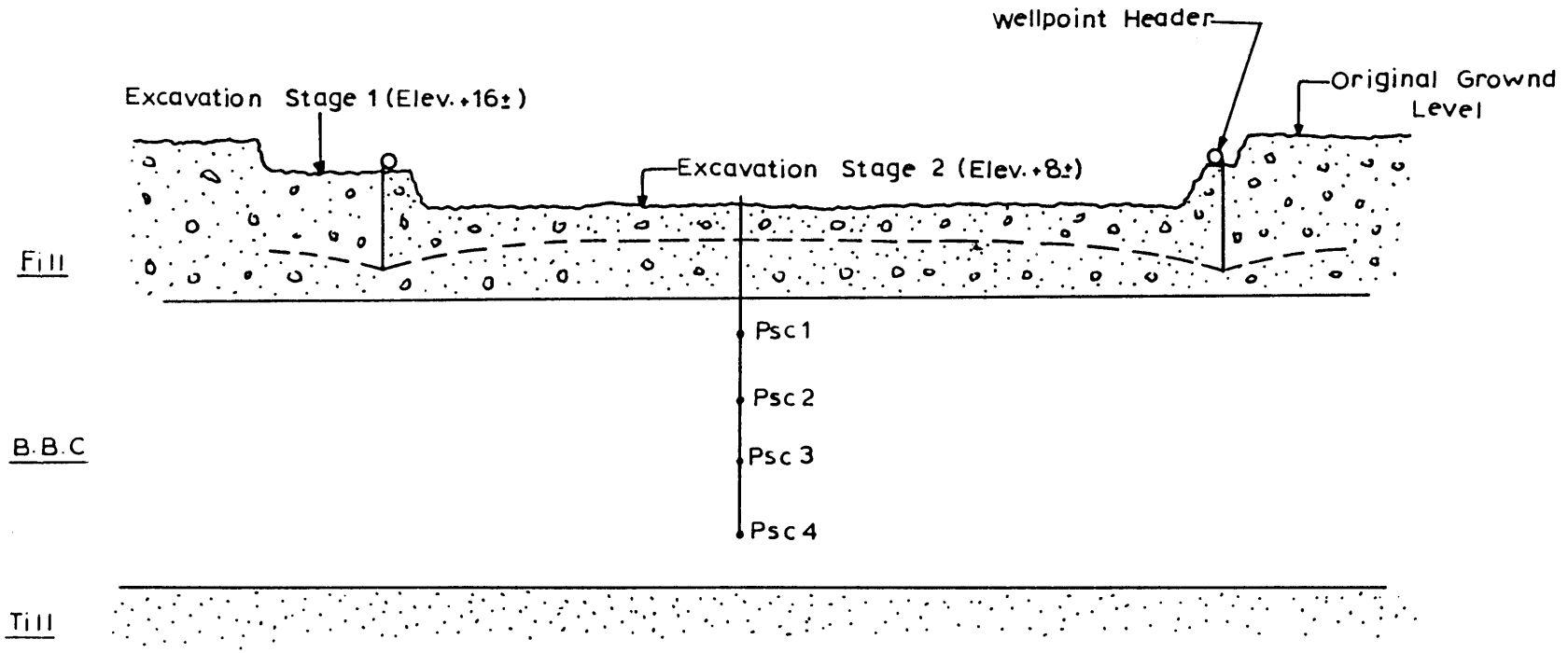

Figure 7.23 Schematic representation of the limits of the two excavation stages.

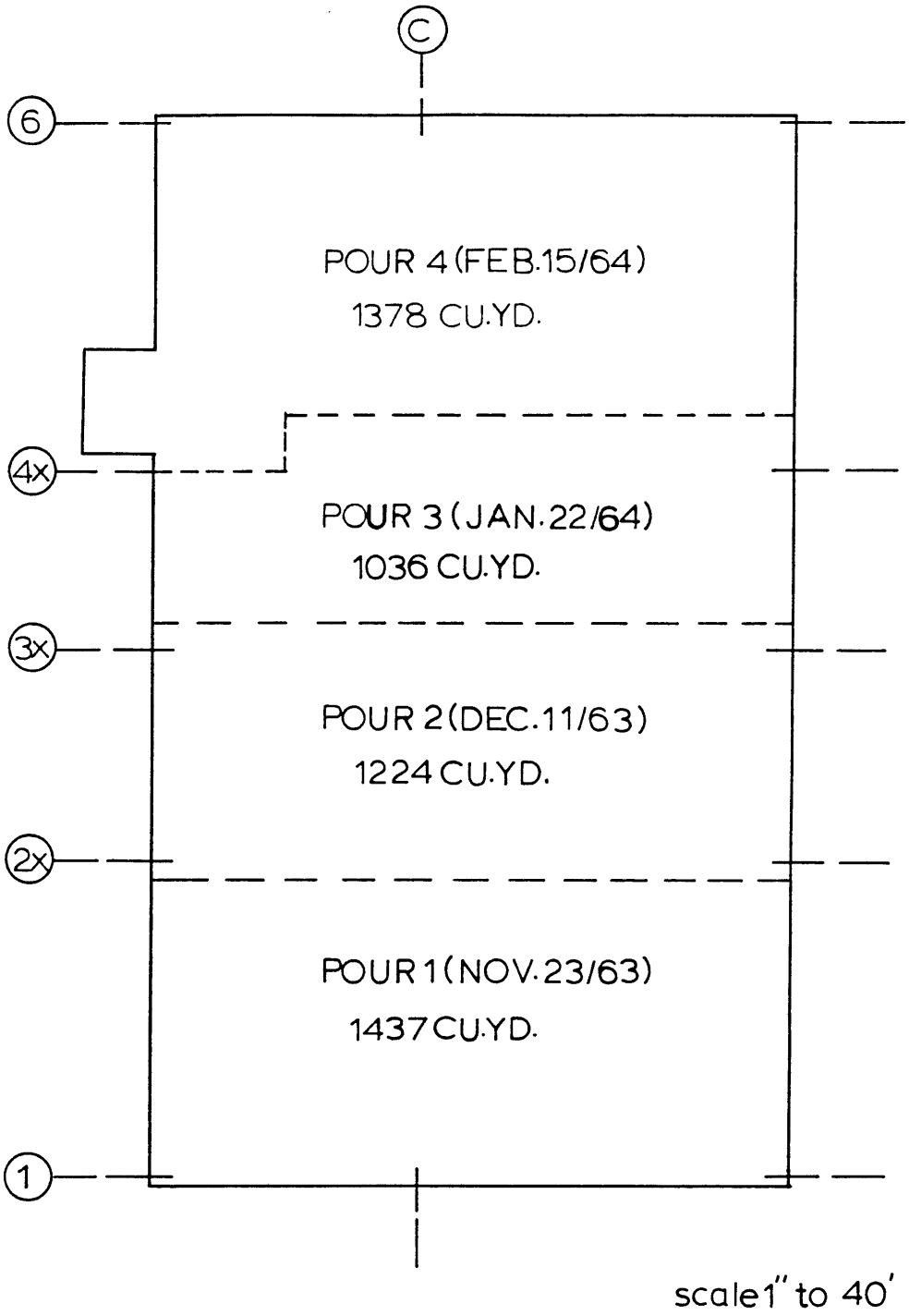

Figure 7.24 Location and quantity of concrete pours in the foundation mat.

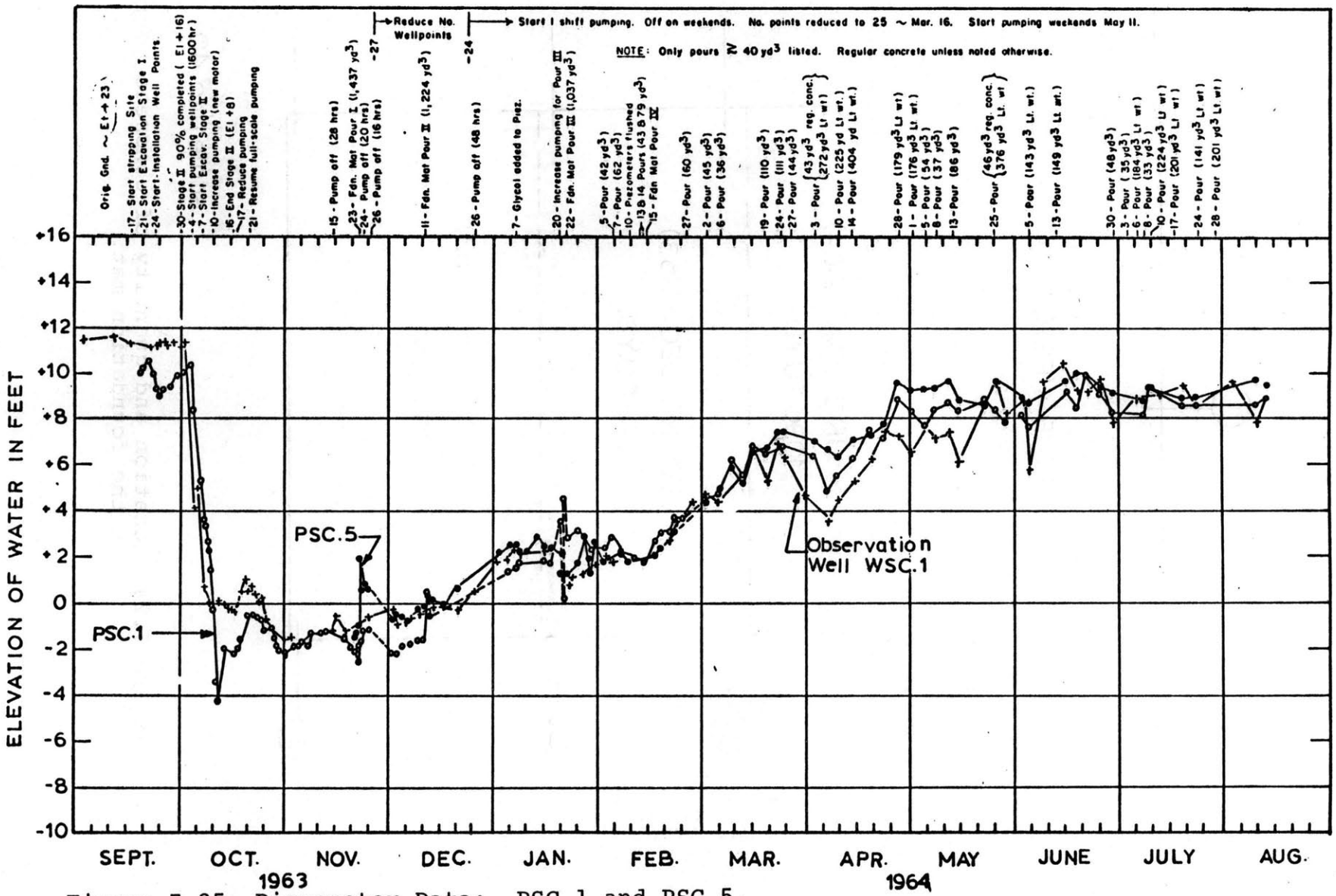

Figure 7.25 Piezometer Data: PSC 1 and PSC 5.

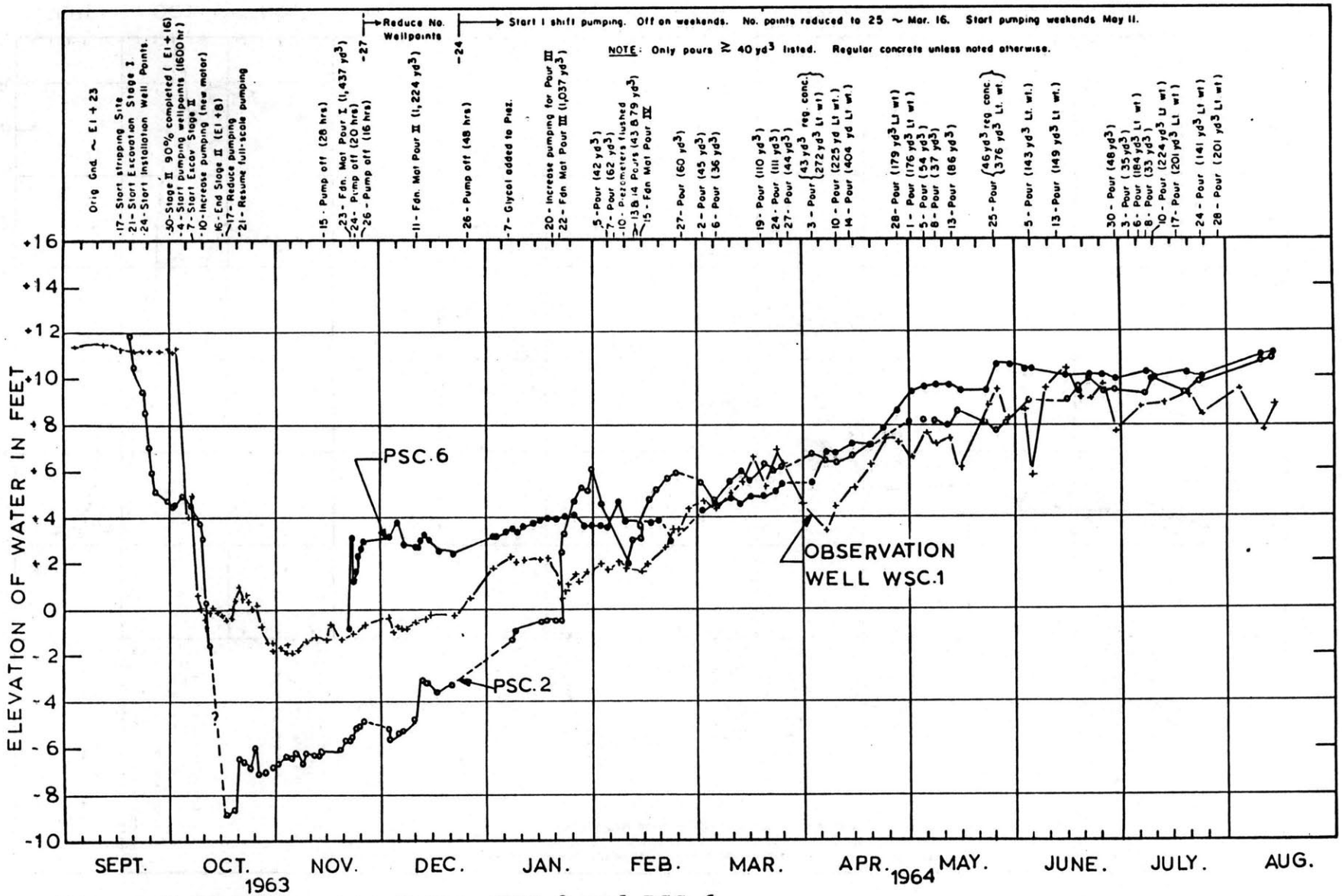

Figure 7.26 Piezometer Data: PSC 2 and PSC 6

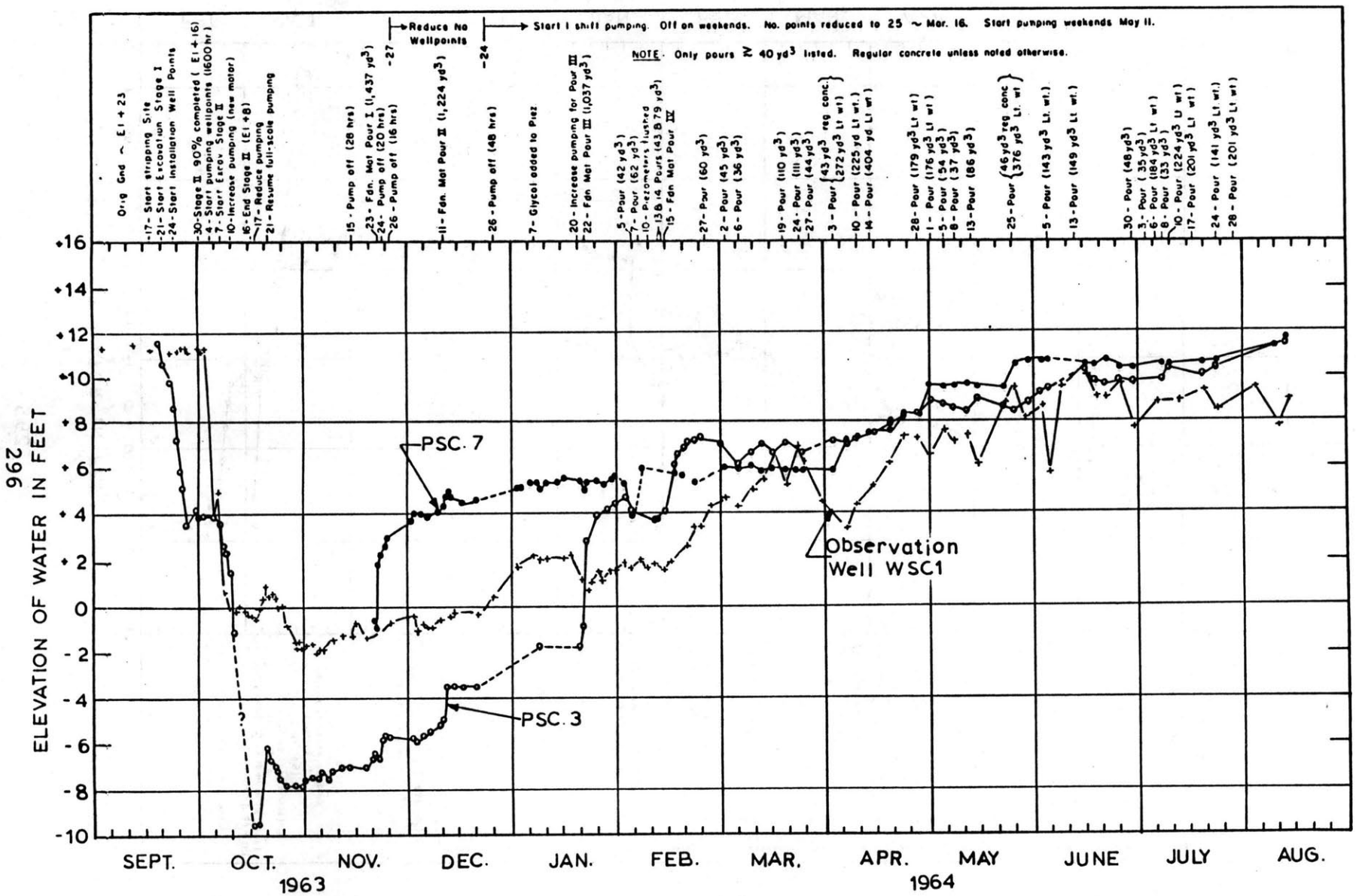

Figure 7.27 Piezometer Data: PSC 3 and PSC 7.

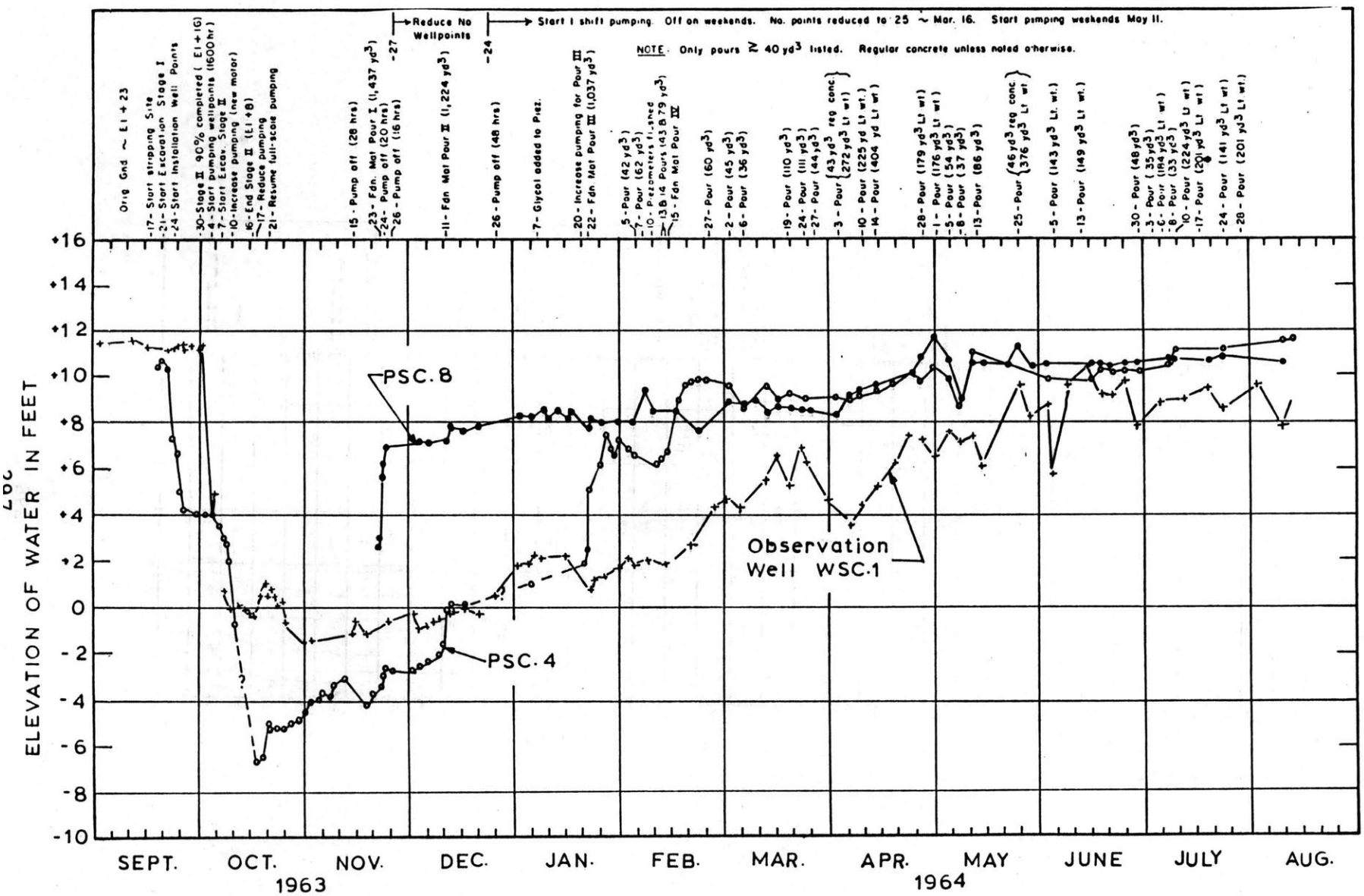

Figure 7.28 Piezometer Data: PSC 4 and PSC 8.

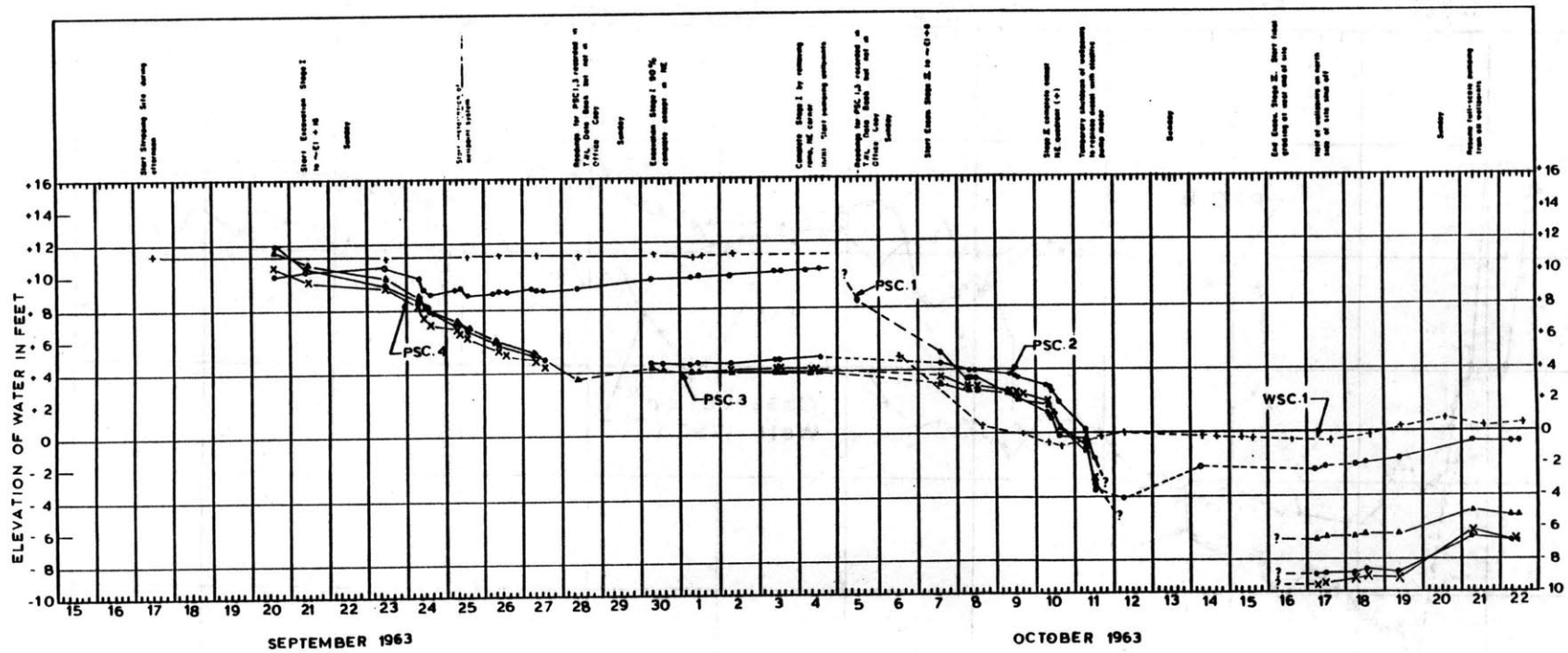

Figure 7.29 Piezometer Data: PSC 1 through PSC 4.

CHAPTER 8

PREVIOUS ANALYSIS DONE ON THE STUDENT CENTER

8.1 INTRODUCTION

The student center case study has been a popular topic for analysis due to the abundance of field observations which are well documented. Analyses extended from qualitative discussion of the field data to quantitative evaluation of engineering properties, Table 8. 1.

With the development of new and much more versatile methods of analyses and computer programs, oversimplifying assumptions on the boundary conditions and the corresponding material properties could be relaxed and much more realistic situations, as well as ones that are closer to reality, could be tackled.

This chapter presents all the previous analyses done on the student center and compares the various methods discussed; by so doing it will shed light on the pitfalls thus encountered.

8.2 SOIL TESTING PROGRAM COMPILED BY LADD AND LUSCHER (1965)

Numerous borings and laboratory soil investigatons were performed in connection with the M.I.T. campus construction in order to establish the stratigraphy and the engineering properties of the soils underlying the campus. The soil

type primarily investigated is Boston Blue Clay which, as mentioned earlier, exists in a substantial layer under the campus. Some data on an organic silt layer deposited by the Charles River, close to the present soil surface, and on the bedrock shale are also included.

8.2.1 Borings

The geological profile that was concluded from interpolation between borings retrieved from five M.I.T. campus locations was already presented in Chapter 7. The five locations are as follows:

a) Hayden Library and near vicinity

b) Materials Center

c) Life Sciences buildings

d) Student Center

e) Center for Advanced Engineering Study (C.A.E.S.).

Their locations are shown in Figure 7.4.

8.2.2 Index Properties, Unit Weights, Stress History

Information about undisturbed samples obtained at the Student Center along with the values of the in situ vertical effective stresses at each sample location are presented in Table 8.2. Also included are identification of soil types and results of index properties. Similar tables appear in the report by Ladd and Luscher(1965)for the other sites, the information being collectively summarized in Figure 8.1 and Table 8.3.

8.2.3 Consolidation Tests on Boston Blue Clay

One dimensional consolidation (oedometer) tests were run in brass fixed ring units (diameter = 2.5 inches and height = 0.6 to 1.0 inches) according to the procedure recommended by Lambe, 1951. Deviations from standard procedures included variations in the pressure increment ratio, cycles of unloading and reloading and changes in temperature. The results of twenty-one tests run on samples from different sites have been compiled in Appendix C.

8.2.4 Nomenclature

Before presenting the data obtained by Ladd and Luscher (1965), it is important to define all the paramters they used:

a) C_c - the compression index for initial loading at a stress equal to the overburden pressure and for virgin compression.

b) C_s - the swelling index for rebound from a maximum past pressure of 16 kg/cm^2 back to 1.6 kg/cm^2, i.e., over one log cycle.

c) C_r - the recompression index for cyclic rebound and recompression between a maximum past pressure of 6 to 8 kg/cm^2 and 1 kg/cm^2.

d) CR - the compression ratio. Because settlement is proportional to the compression index divided by

the initial height of specimen, a better measure of compressibility is obtained by dividing C_c by $(1+e_o)$ where e_o is the initial in situ void ratio of the sample.

e) RR - Recompression ratio equal to C_r divided by $(1+e_o)$.

f) SR - Swelling ratio equal to C_s divided by $(1+e_o)$.

8.2.5 Inferred Soil Parameters

The deduced soil paramters could be divided into three categories: Stress History, Compressibility and Rate of Consolidation.

A. Stress History

The variation of the maximum past pressure* with elevation is shown in Figure 8.1. Two important observations could be cited from this distribution.

1) The wide scatter

2) Certain results fall below the existing effective stress level.

The wide scatter could be attributed to two factors. First, remembering that the data has been aggregated from many sites, we can thus attribute this scatter to the spatial variability in the values of the maximum past pressure due to varying degrees of dessication. Second, inaccuracies

*All oedometer data plotted at 24 hr. intervals between load increments at an L.I.R=1.

induced by test procedures to determine the value of maximum past pressure. Unfortunately, the effect of each cannot be realized.

Concerning the second observation, Ladd et al. (1965) attribute this phenomenon to the possibility of soil arching and thus exhibiting lower values of the maximum past pressure, although of course, this might not be the only reason, as inaccuracies in the determination of the maximum past pressure could also be responsible for this phenomenon.

B. Compressibility

As mentioned earlier, since the settlement is proportional to the compression ratio, a better measure of compressibility is obtained by dividing the indices C_c, C_r and C_s by $(1+e_o)$. Figure 8.1 shows a summary of the results from all the sites. Table 8.2 shows the values by site location. Ladd et al. (1965) point out the fact that RR and SR obtained from a rebound cycle from a maximum past pressure of 16 kg/cm^2 are only slightly different with the former being higher. Values of CR do not exhibit consistent trend with change in depth or location and such that the average values do not differ by more than 15%.

C. Rate of Consolidation

The square root and log time methods were used to obtain the coefficient of consolidation, c_v. The load was doubled for loading and halved for unloading to keep the load increment

ratio equal to one. Values of the average between the two methods are tabulated in Table 8.2.(b) for the Student Center and the Materials Center. Due to reasons already discussed, the scatter in the values of C_s is anticipated.*

8.2.6 Oedometer Tests on Organic Soils

Curves of void ratio and coefficient of consolidation versus log pressure for four consolidation tests from CAES and Materials Science Center sites are presented in Figures C.4 through C.8 . The results show the organic soils to be slightly overconsolidated (OCR of about 1.5) while tests at Materials Center indicate normally consolidated soil. Values of $C_c/(1+e_o)$ for virgin compression averaged 0.25, those for $C_s/(1+e_o)$ about 0.02.

8.3 QUALITATIVE ANALYSIS OF FIELD DATA, GASS (1964)

Observation of piezometer data reveals that the greatest fluctuation in the pore pressures were experienced during the excavation phases I & II and mat pour II & III. The rest of the pours were too small to show significant variation.

---

*partly due to increased side friction

A good agreement was obtained in comparing the piezometer responses with construction history. Gass (1964) calculated the induced pore pressures for stage II of the excavation using influence factors derived from newmark charts and showed that, with the exception of piezometer 1, the piezometric levels change almost exactly in phase with changes in stress. Response of piezometers to the variation in water table elevation was not as simultaneous, with the exception of piezometer 1. It would appear that there is approximately a 1 day lag for 90% equalization of pore pressures.

Deep concern was expressed as to the quick, almost instantaneous response of piezometer 1 to groundwater variation which was attributed to improper sealing (Gass, 1964). A penetration of 6 to 8 feet did not seem too great a security in a relatively stiff material.

The fact that observation well SC-1 is not in the close proximity of the piezometers 1 through 4, actually 100 feet north of the northeast corner of the Student Center, further aggravates the situation, since there is no good reason why the water table under the Student Center should coincide with the level of water in the observation well. The only justification presented was that several spot checks in sumps during excavation showed that the water level in sand and gravel coincided with that in SC-1. Lack of data on the amount of pumped water at any time did not help in

improving the situation. Thus, the variation of water elevation in SC-1 remains to be the best available means of describing the variation of the elevation of water table under the student center.

Observation of swelling reference rods shown in Figure 8. 2 suggest that the top of the clay structure rose approximately 3/4 inch after excavation period. The fact that the rise continued for three months would suggest that the clay was swelling. In absolute value, over 60% of total swelling appeared to take place after 3 months excavation period that indicates that immediate elastic deformations were small, i.e., the assumption of one dimensional consolidation could be warranted.

Most of the initial settlements of the structure occurred during thepouring of the heavy concrete mat. Its magnitude ranged from 1/10 to 1/4 inch. The seat of this initial settlement is probably mostly in the sand and gravel structure. Gass (1964) verifies this assumption by pointing out the fact that the Mat Pour III, which surrounds foundation reference rods FSC3 and 4, produced settlements over 1/8 inch at initial settlement rods ISC2. However, foundation reference rods FSC3 and 4, which would indicate movements within clay structure, showed zero movement of the clay structure.

Since February 1964, there has been no clear trend of movement of foundation reference rods. Keeping in mind the

three factors, namely:

a) Excavation caused a relief in stress in the clay and hence a tendency to swell,

b) Lowering of the groundwater level in the sand and gravel probably creates a tendency for the clay to consolidate, and

c) Addition of structural bonds should cause consolidation, it might very well be that these factors are cancelling each other.

It is rather unfortunate that the foundation settlement rods were terminated at the top of the clay layer since the total swelling cannot be apportioned across the layer. However, observation of the values of c_{vs} presented by Ladd and Luscher would suggest that a considerable proportion of heave occurred in the upper part of the stratum.

8.4 EXPERIMENTAL/QUANTITATIVE ANALYSIS: VON ARNIM (1967)

Realizing that the final settlements due to construction of buildings on fully floating foundations is definitively related, and in many cases equal to the heave observed during excavation period, developing heave prediction methods is of essence, since substantial economies could be attained through optimal design of the heavily reinforced concrete mat.

Various methods could be used in the evaluation of settlements. Extrapolation of three of these methods, namely:

1) The one dimensional method,
2) The Skempton and Bjerrum method, and
3) Lambe's stress path method,

to encorporate problems involving heave and their direct application to the excavation at the Student Center is presented below.

8.4.1 Soil Properties

Analysis of data compiled by Ladd and Luscher (1965) reveals that the coefficient of consolidation during swelling of the overconsolidated material, i.e., the top silty clay, is as expected, higher than the coefficient of consolidation during swelling of the normally consolidated material and exhibits a lot of scatter. In order to quantify this variability, the variation of the coefficient of consolidation was discretized into two quantities whose absolute magnitude is not known, but such that the coefficient of consolidation of the overconsolidated material is twice that of the normally consolidated material (lower 34 ft.) and remain constant within each layer. The reason behind refraining from quantifying the values of the coefficients of consolidation using data from Ladd and Luscher is principally due to the fact that soil properties inferred from lab tests are different

than those encountered in the field due to the absence of minor geological features.

Sabga (1966) ran piezometer sensitivity tests at the Center for Advanced Engineering Studies in the close proximity of the Student Center and concluded that the permeability of the top clay is twice that of the bottom clay, a fact that is crucial in determining the pattern and magnitude of pore pressures that would act within the soil during a steady-state seepage condition.

8.4.2 Piezometer Readings

Observations of field data would suggest that the induced negative pore pressure dissipates much faster than would be predicted by lab tests. Excess pore pressures recorded by PSC-1 and 4 dissipate very fast, a fact that suggests top and bottom drainage. The fact that piezometer PSC-1 measured the lowest tensions would appear to be in disagreement with forecasts of all methods for pore pressure prediction, all of which would indicate that the largest decrease in pore pressure should occur at the top layers of the clay. The situation is further aggrevated by observing that PSC-1 readings are directly corrolated and respond instantaneously to changes in the water table, a situation that suggests improper sealing of the piezometer during installation. Von Arnim presented two reasons to justify the integrity of PSC-1 piezometer data, namely:

1) The probability of a broken seal is minized due to the fact that the personnel responsible for installing the piezometers were extremely well trained and careful, and

2) Due to its shallow location, one would expect substantial degrees of pore pressure dissipation primarily affected by the material properties and the short drainage path.

8.4.3 Assumptions and Boundary Conditions

1. The author postulates that the accuracy of the piezometers is ±1 foot.

2. The variation of the imposed stresses with time is derived by considering the average vertical stresses obtained by dividing the total weight of soil removed over the entire area of the excavation. The effect of pours I, II and IV were ignored and only pour III was considered to be significant due to its location encompassing PSC-1 through 4 cluster.

3. One dimensional drainage conditions exist, all drainage is in the vertical direction.

4. No excess pore pressures existed prior to the commencement of the construction activities.

5. Layer of glacial till underlying the Boston Blue Clay is free drainage material.

6. The ratio between the coefficients of consolidation of the overconsolidated and the normally consolidated material is 2:1.

7. The effect of the varying groundwater condition during the first 15 days after excavation is equivalent to that of a constant draw down of 12 ft., and that the corresponding effect during the period of 105 days after excavation is equivalent to that of a uniform 8 ft. drawdown.

8.4.4 One Dimensional Analysis to Backfigure the Value of Coefficient of Consolidation

Using an iterative procedure, the author attempted to backfigure the distribution of the initial induced pore pressure immediately after excavation is completed. The procedure followed the following steps:

a) Assume that the piezometer level reduction at PSC-2 and PSC-3 15 days after excavation is still similar to that manifested immediately after excavation, since their location is close to the center of the clay layer, Figure 8.3.

b) Assume that the initial induced pore pressure could be divided into a triangular and a rectangular distribution.

c) Using the following equation for the determination of the degree of consolidation at depth Z for the rectangular pore pressure distribution:

8.4.5 Prediction of the Heave and Pore Pressures at the Student Center Excavation

Having established the boundary conditions and the soil properties, the three methods of pore pressure and heave prediction were utilized in a comparative format against the field data. The results obtained are presented below.

A. One Dimensional Method

A.1 Initial Pore Pressures

Recalling that the induced pore pressures could be expressed as:

$$\Delta u = \Delta\sigma_h + A(\Delta\sigma_v - \Delta\sigma_h)$$

and since no lateral movements are permitted in this method, then the A parameter has to equal a unity and the change in pore pressures is equal to the change in the vertical stresses as derived from the elastic theory with $\nu = 0.5$.

A.2 Immediate Heave

The mechanism of heave in one-dimensional method would imply that the immediate heave is nill.

A.3 Heave Due to Swelling

The heave at the end of primary swelling is given by the equation:

$$\rho = 0.435 \sum_{1}^{n} \frac{C_s}{1+e_o} r \frac{\Delta\sigma}{\Delta\bar{\sigma}_{av}} \Delta H$$

$$U_z = 1 - \sum_{m=0}^{m=\infty} \frac{Z}{M} (\sin \frac{M.Z}{H}) \exp (-m^2 T_v)$$

where:

$M = 1/2\ (2m+1)$

H = length of drainage path

T_v = time factor = $c_v t/H^2$

and the graphical solution shown on Fig. 8.4 for the triangular distribution, an approximate value of the field coefficient of consolidation could be obtained through a trial and error procedure for the time interval under consideration, 15 days say, as shown in Fig. 8.5.

d) For the calculated value of c_v and the 15 day isocrone, the initial pore pressure distribution could be obtained, Fig. 8.6.

e) The final step in this procedure would be to close the interation loop by using the estimated initial pore pressure distribution coupled with the deduced value of c_v to figure out the 105 day isocrone and compare it to the 105 day isocrone derived from field data.

This iterative procedure yielded a value of $c_v = 3.0 \times 10^2$ cm^2/sec to the lower 32', a value much larger than that deduced from lab tests. The initial pore pressure distribution and a final back check on the 105 day isocrone are shown in Figs. 8.6 and 8.7.

The values of c_{vs} in the above equation for various depths were derived from Ladd and Luscher's oedometer tests for the appropriate stress decrements. The variation of c_{vs} with depth is shown in Fig. 8. 8. Tables 8.5 and 8.5 show the variation of heave with depth for 8 ft. drawdown and zero drawdown. Integration across the stratum would yield total heaves for the two drawdown conditions and 105 infinity time intervals shown in Tables 8.4 and 8.5.

A. Pore Pressure Distribution at 105 Days

Using the initial induced pore pressures in condjunction with the field backfigured value of the coefficient of consolidation for swelling the 105 day isocrone was obtained and is shown in Fig. 8. 7 .

B. Lambe's Stress Path Method

Seven rather sophisticated triaxial tests were performed on undisturbed Boston Blue Clay samples retrieved from the CAES* site in the close proximity of the Student Center, by means of a 3" thin-walled fixed piston sampler.

Tests were carried out in a Wykenham-Farrance triaxial cell and the pore pressures were measured by a Geonor null device whose accuracy was extensively checked. The accuracy of the system was reported to be 0.02 kg/cm^2 for pore pressure measurements and 0.009% for strain measurements. The steps

*CAES, Center for Advanced Engineering Studies

followed in a typical test are shown below:

1. Sepcimen is subjected to a backpressure of 3.0 kg/cm^2.
2. Ram friction was found to be significant and hence the specimen was reconsolidated only to its in situ state of stress to avoid large deformations. Further tendency of specimen bending increased concern as to ram friction being more important than the later applied stress decrements.
3. Undrained unloading of the specimen by decrements of deviatonic stress computed from elastic theory, (Boussinesque), while leaving the cell pressure constant. Pore pressures and deformations were carefully recorded
4. Swelling at a constant deviatoric stress carried out in stages until the final horizontal effective stress was equal to the total horizontal stress expected if the material was perfectly elastic, $\nu = .5$. Vertical and volumetric strains at the end of primary consolidation were recorded

5. Undrained loading of the soil specimen to the original stress difference. Pore pressures and deformation were recorded.

6. Consolidation at constant deviator stress until the final vertical and horizontal stresses were equal to those acting at the end of the K_o consolidation. Strains and pore pressures were carefully recorded.

B.1 Initial Pore Pressure

Replacing the excavation configuration by an equivalent circular foundation, we can, theoretically, assume that provided sample disturbance is minimal and the stress path of a soil element in the field during undrained loading could be established by using elastic theory, $\nu = 0.5$, then the induced initial pore pressures in the field would duplicate those obtained in the laboratory. These predicted pore pressures are shown in Fig. 8.9 which are exactly the distances BC on the stress path loop.

B.2 Immediate Heave

By the same token, the immediate heave exhibited by the clay structure is obtained by integrating the immediate heaves exhibited by the soil specimens at different depths after unloading. The distribution of the heave across the clay layer is shown in Fig. 8.10.

B.3 Heave Observed During Swelling

The observed strains experienced by the soil specimen when swelling under a constant deviatoric stress until the effective stresses acting on the specimen after swelling are equal to the total stresses expected in the field, have been

summarized in Fig. 8.10. Those were reported for an 8' drawdown and hydrostatic condition.

B.4 Pore Pressure Distribution at 105 Days

Having established the initial distribution of pore water tensions and using the backfigured value of c_v the 105 day isocrone was obtained and is shown in Fig. 8.11.

C. Skempton and Bjerrum Method

It is rather unfortunate that this method was totally crippled by lack of data on the "A" parameter required to calculate the change in pore pressures. The method has been further plagued by the absence of data on Young's Modulus that rendered the method totally useless.

8.5 QUANTITATIVE/DIAGNOSTIC ANALYSIS; Lambe et al. (1968)

8.5.1 Statement of Purpose

In a diagnostic attempt to try to explain the anomalies between field and laboratory values of the coefficient of consolidation, Lambe et al. (1968) postulate four possible causes, namely:

a) Sample disturbance

b) Laboratory test procedures

c) Errors in field measurements

d) Use of one-dimensional consolidation theory.

The above mentioned causes were discussed in detail in Chapter and only a brief account of the symptom/cause/remedy pertaining to each cause is listed.

A. Sample Disturbance

1. Up to 40 fold decrease in c_v.
2. Decrease in the permeability resulting from a lower void ratio at any given consolidation pressure.
3. The undisturbed c_v is approximated through use of the following equation:

$$(c_v)_u = (c_v)_d \frac{K_u}{K_d} \frac{(a_v)_d}{(a_v)_u} \quad .$$

where $a_v = -\frac{\Delta e}{\Delta \sigma_v}$

$(\ )_u$, $(\ )_d$ = disturbed and undisturbed (Shmertman's correction) properties

B. Laboratory Test Procedures

1. Up to 100 times reduction in c_{vs}
2. Values of load decrement ratio ($\Delta\bar{\sigma}/\bar{\sigma}$) are frequently less than a half in the field and vary with depth.
3. The curve fitting method used ($\sqrt{t}$, or logt method).
4. Severe data scatter due to predominant effect of side friction.
5. Corrected c_{vs} could be obtained through the use of the following equation:

$$c_{vs} = c_{vc}\left(\frac{a_{vc}}{a_{vs}}\right)$$

where all of the above parameters are measured at the same average void ratio.

C. Errors in Field Measurements

1. Decrease in value of c_{vs} as a function of experienced time lag.*†
2. Proper clearing and reduction of system flexibility.

D. Use of One-Dimensional Theory

1. Reduced values of c_{vs}.
2. Causes are chiefly due to the two assumptions.
   a. Ratio of horizontal to vertical permeability is a unity.
   b. Ratio of vertical drainage path to radius of loaded area (H/a) is very small.
3. Davis and Poulous (1965) recommend the use of an average permeability given by the equation:

$$k_{av} = \sqrt[3]{k_h^2\, k_v}$$

†Accuracy of the piezometer was estimated to be ±.25'.

*Lambe et al. (1968) assert that the time lag in piezometers installed at Student Center Excavation was 24 hrs. for 90% equalization.

to relax the assumption on the equality between horizontal and vertical permeability and hence the resulting three dimensional coefficient of consolidation could be calculated by the use of the following equation:

$$(c_{vs})_3 = 1/3 \left(\frac{1+\nu}{1-\nu}\right) \frac{k_{av}}{k_v} (c_{vs})_1$$

4. Gibson, Schiffman and Pu addressed the importance of the H/a ratio for $k_h=k_v$ case and present curves of equivalent one dimensional coefficients of consolidation for various H/a ratios.

8.5.2 Calculation of Field c_{vs} at the Student Center

To illustrate the effect of the above mentioned deficiencies, the value of the coefficient of consolidation for swelling was backfigured from piezometer observations at the Student Center Excavation. The assumptions made for this calculation are shown below.

8.5.3 Working Framework

A. The total vertical stress release from the excavation (Elevation +22 to +7.5) was 0.82 kg/cm^2.

B. Excavation and dewatering were assumed to have occurred on October 7, the middle of the actual excavation period. Figure 8.14 gives values of initial excess pore

pressures (+=0) obtained by extrapolating the measured pore pressures at the end of excavation back to the middle of excavation period.

C. The bottom shale is a drainage material.

D. One dimensional analysis is capable of predicting the behavior of the foundation soil

E. Equilibrium pore pressures at t=90 were taken as those resulting from a steady state upward seepage due to pumping. The average head due to pumping was -13 ft. for t=15 days and -10 ft. for t=105 days.

F. Effects of errors in the assumed initial pore pressure distribution can be minimized by computing $_{vs}$ using the following equation.

$$c_{vs} = \frac{T_{s2} - T_{s1}}{t_2 - t_1} H^2$$

G. Assume one value of c_{vs} for the entire clay layer.

8.5.4 Results

The back-figured value of the coefficient of consolidation for swelling was computed to be equal to $350 \pm 50 \times 10^{-4}$ cm^2/sec. A value approximately sixfold greater than the laboratory value compiled by Ladd and Luscher ($60 \pm 30 \times 10^{-4}$ cm^2/sec). The method employed was a trial and error procedure whereby the 15 day isocrone was used in conjunction with the initial induced pore water tension, as derived

from field data, to compute the field coefficient of consolidation for swelling.

The validity of this value was later checked by computing the 105 day isocrone and comparing it to the 105 day isocrone derived from field data. It was concluded that the lack of correspondence between the predicted and the field observed data at PSC-1 was due to its sensitivity to errors in the assumed steady state pore pressures, Fig. 8.15.

Finally, realizing the causes of this sixfold discrepancy, remedial measures were applied to the Laboratory value of c_{vs} and the corresponding improvements are shown in Table 8.6.

8.6 GENERAL EVALUATION

Before we attempt any critical evaluation of the previous analysis, we should always take into account the status of the technology prevailing then. The new advancements in computer technology coupled with development of new, highly sophisticated in situ testing instrumentation are responsible for improving our ability to truly predict the response of the foundation soils to boundary imposed loading. Hence what might appear to us as solution deficiencies were then required assumptions for a working hypothesis.

Limitations of oedometer testing and the deficiencies in providing accurate soil parameters have already been discussed in detail in Chapter 2 . The data from the tests run by Ladd

and Luscher however, would serve to illustrate few of the points mentioned. Attention is drawn to Tables 8.2 and 8.3. where the following facts are exhibited:

a) Virgin comp. ratio is generally constant in value once consolidation stress exceeds σ_{vm}.

b) Shape of unload reload cycle is often independent of maximum past pressure.

c) The recompression ratio decreases with smaller unload reload cycles.

d) Slope of swelling curve increases with increasing rebound but the swelling ratio is independent of maximum past pressure for a given OCR.

e) The recompression ratio is roughly equal to the swelling ratio for a change in OCR approximately equal to five.

f) The value of swelling ratio for one cycle of rebound from $\bar{\sigma}_m$ is approximately 1/5 to 1/10 of virgin compression ratio.

g) c_v for recompression is substantially larger than that for virgin compression.

h) c_v for swelling is larger initially but it decreases rapidly with rebound.

i) Sample disturbance will have minor effect on c_v in normally consolidated region.

j) Sample disturbance will have a large effect on c_v during initial loading.

k) Dependence of c_v on the method of determination employed.

l) Inability to supply continuous data.

m) Inability to duplicate field conditions which include actual stresses imposed and the minor geological features.

Gass's explanation of the low tensions and the almost instantaneous response to groundwater variation experienced by PSC-1 is totally unjustified. The high coefficient of consolidation at shallow depths coupled with the short drainage path is responsible for PSC-1's behavior. This effect would be more closely examined in the following chapter.

The methods by which Von Arnim (1967) and Lambe et al. (1968) backfigured the value of the in situ coefficient of consolidation seem to be haphazard and completely unreliable. Due to the limitations imposed by the method of analysis, the variation in the groundwater elevation could not be accounted for. Instead, an average drawdown in both analyses were estimated and employed. Von Arnim (1967) used the following approximation:

> "The effect of the varying groundwater condition during the first 15 days after excavation is equivalent to that of a 12 ft. drawdown, and the corresponding effect during the 105 day period corresponds to an 8 ft. drawdown."

Those values appear to be very dubious. A close examination of the groundwater elevation variation and using an average of all readings would yield a value of 9.6 ft. for the 105 day interval. Therefore, if the average of readings was not used, how can the author justify his assumption?

Lambe et al. (1968) used the following assumption:

> "The effect of the groundwater condition during the first 15 days after excavation is equivalent to that corresponding to a -13 ft. drawdown and the corresponding effect during the 105 day period is a 10 ft. drawdown."

Using his assumption as concerning the t=0 designation, a close examination of the groundwater elevation variation reveals that the average for the 105 day interval is 9.8 ft., which is close to what he assumed.

Several other errors have been detected in the values of the piezometer field data reported by Von Arnim when constructing the 105 day isocrone. Errors greater than 2 ft. are evidenced in Figure 8. 3 , which shows the corrected versus the reported 105 day isocrone. His method of back-figuring the value of the coefficient of consolidation seemed to be very cumbersome, in particular his prediction of the in situ initial pore pressures. There is no evident gain in predicting these values when the distribution could be assessed from field data and hence cumulative errors could be avoided. Several compensating errors were encountered in the analysis of which

a) Due to assumption that top 32' have a c_v value for swelling double that for the lower 34' and the use of the recommended transformation yields a shorter overall drainage path.

b) The value of the backfigured c_v value is low in comparison to that of Lambe et al. (1968) (and lower than the in situ value as we shall see in the next chapter).

c) The predicted initial pore pressure distribution is lower than the actual.

d) The top boundary conditions are lower than anticipated (by use of averages).

In trying to explain the discrepancy shown in Fig. 8.7 between the field and the predicted 105 day isocrone, it will be assumed that the bottom two piezometers, PSC-3 and 4 are mainly influenced by the bottom boundary conditions and the top two piezometers, PSC-1 and 2 are influenced by the top boundary conditions. Clearly, the mismatch at PSC-3 and 4 is aggrevated by (a) and (c) but compensated partially by (b) and the mismatch at PSC-1 and 2 is aggrevated by (a) and (b) but compensated by (c) and (d). Thus any apparent agreement with field data is fruitious and the analysis depends heavily on compensating errors.

The data pertaining to the analysis of heaves has been included to demonstrate erroneous conclusions based on oversimplifying assumptions. At first glance, the use of any one

dimensional analysis would be discredited since it was reported that about 50% of the heave was termed "immediate". However, a close examination of the swelling reference rods data would reveal that this "immediate" heave has occurred over a period of six days. Two reasons were put forward for the low pore water tensions experienced at PSC-1, by the same token, they could be also responsible for the termed "immediate" heaves. It will be seen later that the actual values of the coefficient of consolidation for swelling near the top boundary is actually almost four times that for the lower 32' and also possesses a much higher SR value. Thus what is termed "immediate" heave is really the value of the heave at the end of primary for the topmost layers and the assumption of one dimensional analysis is still warranted.

The use of Lambe's method to predict pore pressures was particularly included to show that not only are the soil properties derived from lab tests in error but also the response to simulated field behavior is grossly underestimated and highly effected by the laboratory instrumentation and its limitations. This is clearly evidenced in Figure 8.11.

Lambe et al.'s analysis of the problem was more careful and all of the reported values of the field 105 day isocrone are accurate. Since one can consider that PSC-3 and 4 are basically influenced by the bottom boundary condition and

since the value of the backfigured value of c_v=350x10^{-4} cm/sec is close to the field in situ value (as we shall see later) and since the initial pore water tensions are those derived from field data, then the agreement as would be expected and as is evidenced in Figure 8.13 is quite good. However, agreement with field data deteriorates for PSC-1 and 2, not only due to the fact that "the top piezometer is more sensitive to the assumed steady state pore pressures", as was reported, but also due to the fact that the c_v value is grossly underestimated for the top 32 feet.

Other miscellaneous errors in both analyses included:

a) Stress distribution - the clay structure is assumed to be a semi-infinite elastic half space when in actuality it is a finite layer.

b) Stress relief - assumed magnitude equal to 0.82 TSF when in actuality it is 0.73 TSF.

Finally, it should be stressed that when a pore pressure prediction scheme is initiated, it is of utmost importance that the assumed boundary conditions be accurate and duplicate exactly the field conditions, since the pore pressure response to the applied boundary conditions is instantaneous and is reflected in the field piezometer readings that would deviate from predicted behavior when we assume some average value of the boundary conditions. However, with regard to heave predictions, since the corresponding field behavior to

applied loads is not instantaneous and since sufficient time is available, heave predictions are not very sensitive to averaging boundary conditions.

Author	Type of Analysis	Method of Analysis	Soil Parameters Used	Treatment of Field Pumping Operation	Treatment of Loading (or Unloading) Operation	Remarks
Gass, A.A. (1964)	Qualitative evaluation of field data.	Observation of pore pressure decay from piezometer data also, heave and subsequent settlements from settlement rods' readings.	-	-	-	Consideration of possible loss of integrity of data supplied by shallowest piezometer (PSC-1). Suspicion of a broken seal.
Ladd, C.C. & Luscher, U. (1965)	Laboratory evaluation of engineering parameters of the Boston Blue Clay layer underlying the Student Center.	Conventional oedometer tests on "undisturbed" samples of Boston Blue Clay foundation soil. Routine Atterberg limits and soil profiling.	-	-	-	Values of C_v supplied by conventional oedometer tests are averages over load increments and are not representative of small load decrements. Laboratory data affected by sample disturbance, size effects, etc.
Von Arnim, K. C. (1967)	Predictions of pore pressure distribution and settlements under the Student Center.	a) One dimensional trial and error analysis using conventional Terzaghi uncoupled solution to backfigure values of C_v and use it to calculate settlements. b) Lambe's Stress Path method executed on "Undisturbed" samples of Boston Blue Clay to predict pore pressures and settlements. c) Skempton and Bjerrum's Method required determination of A parameter in the pore pressure equation.	For one dimensional analysis divide layer into two layers such that C_{vs} value corresponding to the top layer is twice that corresponding to the bottom layer. Backfigured value of $C_{vs} = 3.0 \times 10^{-2} cm^2/sec$ for the bottom soft clay.	For first 15 days after excavation, used a constant draw down of 12' of water. At 105 days effect equivalent to a constant 8' of water.	Assumed uniform stress release due to excavation and also uniform stress distribution due to pour III of foundation mat. Effects of pours I, II and IV were neglected.	Method of analysis not fully justified. Use of Lambe's Stress Path Method appears to give excellent agreement with settlement readings.
Lambe and Bromwell (1968)	Prediction of pore pressure distribution under Student Center.	Using values of C_v recommended by Ladd & Luscffer, used one dimensional analysis.	Used a constant value of C_{vs} throughout the Boston Blue Clay layer equal to $3.5 \times 10^{-2} cm^2/sec$.	Assumes an average head due to pumpint equivalent to -13 ft. for the first 15 days and -10 ft. for t=105 days.	Assume a uniform stress over entire area due to excavation and reloading	Erroneous use of stress distributions and effects of pumping. More of a prescriptive, remedy type analysis. Concern over the integrity of piezometer P_{sc}-1 expressed.

Table 8.1 Summary of previous analyses done on the Student Center

Test. No. (Fig. No.) (4)	Depth (ft.)	Elev. (ft.)	Soil Type	W_N (%)	W_L (%)	e_o	$\bar{\sigma}_{vo}$ (Kg/cm^2)	$\bar{\sigma}_{vm}$ (3) (Kg/cm^2)	Compression Index, C_c		Rebound Recompress Index C_r (1)	Swelling Index C_s (2)	Remarks
									At $\bar{\sigma}_{vo}$	Virgin			
C-(1)-1 (Fig. C-3)	39.0	-16.5	Medium Blue Clay with Some Fine Sand	32.8	48.0	0.925	1.52	4.1±0.7	0.072	0.335	0.055	0.053	Low value of $\bar{\sigma}_{cm}$ is surprising T=30±5°C
C-(2)-1 (Fig. C-3)	44.5	-22.0	"	38.7	52.5	1.06	1.66	6.1±0.5	0.063	0.45	0.075	0.080	T=20±1°C Fig. C-3
C-(2)-2 (Fig. C-3)	44.5	-22.0	"	39.7	-	1.12	1.66	6.1±0.5	0.080	0.44	0.076	0.076	T=10.3°C for first 2 cycles
C-(3)-1 (Fig. C-4)	49.0	-26.5	"	39.7	49.8	1.108	1.78	4.0±0.3	0.112	0.397	0.078	0.059	T=30±5°C Fig. C-4
C-(4)-1 (Fig. C-4)	54.0	-31.5	"	47.0	54.3	1.32	1.91	5.0±0.5	0.117	0.58	0.102	0.090	T=27±5°C
C-(6)-1 (Fig. C-5)	64.0	-41.5	Soft Blue Clay and Some Fine Sand	32.2	35.9	0.97	2.20	2.7±0.2	0.156	0.303	0.034	0.042	T=27±5°C Fig. C-5
C-(6)-2 (Fig. C-5)	4.0	-41.5	"	40.5	-	1.16	2.20	2±2	0.360	0.360	-	0.057	T=21±1°C
C-(8)-1 (Fig. C-6)	74.0	-51.5	"	36.0	42.3	0.995	2.46	2.0±0.2	-	0.282	0.033	0.035	T=29±5°C
C-(8)-2 (Fig. C-6)	74.0	-51.5	"	41.0	-	1.15	2.46	1.6±0.1	-	0.360	0.045	0.040	T=22 1°C for initial loop; then T lowered to 5±0.4°C
C-(10)-1 (Fig. C-7)	86.0	-63.5	"	41.5	42.4	1.14	2.80	Indeter-minate	-	∿0.30	0.056	0.049	Sample was very disturbed T=29±5°C

(1) Ave. swelling and recompression index between $\bar{\sigma}_{vm}$ = 6-8 kg/cm^2 and $\bar{\sigma}_c$ - 1 kg/cm^2

(2) Swelling index for $\bar{\sigma}_c = \bar{\sigma}_{vm}$ = 16 kg/cm^2 back to $\bar{\sigma}_c$ = 1.6 kg/cm^2

(3) From Cosogrande Construction

(4) The e-log $\bar{\sigma}_c$ curve is shown in that figure

Table 8.2.(a) Compression data on Boston Blue Clay--Student Center (After Ladd and Luscher, 1965)

All stresses in Kg/cm^2

Test No.	Depth (ft.)	Elev. (ft.)	$\bar{\sigma}_{vo}$	$\bar{\sigma}_{vm}$	Coef. of Consolidation c_v, 10^{-4} cm^2/sec												Remarks
					Compression at $\bar{\sigma}_{vo}$	Recompression, $\bar{\sigma}_{vm}$=6-8			Swelling, $\bar{\sigma}_{vm}$=6-8			Swelling, $\bar{\sigma}_{vm}$=16					
						1→2	2→4	4→6.8	6.8→4	4→2	2→1	16→8	8→4	4→7	2→1		
					$\sqrt{t}$ logt	$\sqrt{t}$ logt	$\sqrt{t}$ logt	$\sqrt{t}$ logt	$\sqrt{t}$ logt	$\sqrt{t}$ logt	$\sqrt{t}$ logt	$\sqrt{t}$ logt	$\sqrt{t}$ logt	$\sqrt{t}$ logt	$\sqrt{t}$ logt		
C-(1)-1	39.0	-16.5	1.52	4.1±0.7	75 30 52	87 55 71	72 62 67	87 i (58)	110 75 92	92 56 74	73 13 43	94 124 109	79 51 65	50 35 42	16 13 14		
C-(2)-1	44.5	-22.0	1.66	6.1±0.5	35 31 33	20 13 16	22 20 21	27 23 25	45 31 38	17 16 16	8 11 10	32 18 25	18 16 17	8 8 8	i i		T=2.1±2°C
C-(2)-2	44.5	-22.0	1.78	6.1±0.5	74 24 49	27 32 30	30 27 28	46 36 41	77 40 58	29 23 26	30 14 22	50 37 44	23 20 22	i i	8 3 6		T=10.3°C for $\bar{\sigma}_c$→16 Kg/cm^2
C-(3)-1	49.0	-26.5	1.91	4.0±0.3	40 33 36	38 30 34	42 32 37	29 23 26	80 70 75	25 17 21	12 8 10	122 60 91	38 26 32	14 10 12	6 4 5		
C-(4)-1	54.0	-31.5	2.20	5.0±0.3	50 20 35	17 31 24	16 18 17	22 11 16	41 27 34	14 20 17	10 6 6	33 17 25	19 13 16	6 7 7	6 4 5		
C-(6)-1	64.0	-41.5	2.46	2.7±0.2	40 i (27)	103 i (69)	152 32 92	39 i (26)	i i	126 i (84)	55 58 56	96 i (64)	33 43 38	37 22 30	21 33 27		
C-(8)-1	74.0	-51.5	2.80	2.0±0.2	27 i (18)	80 51 66	91 63 77	80 94 87	46 60 53	73 i (47)	29 16 23	136 35 85	64 44 54	39 26 33	16 10 13		
C-(10)-1	86.0	-63.5	2.20	---		28 32 30	45 32 38	72 26 49	81 41 61	30 40 35	10 8 9	27 45 36	50 30 40	15 14 14	23 2 13		Sample very disturbed
C-(6)-2	64.0	-41.5	2.46	2.2	68 i (45)	-	-	-	-	-	-	-	38 33 36	13 9 11	6 4 5		
C-(8)-2	74.0	-51.5	1.25	1.6±0.1	7 3 5	26 28 27	16 19 18	21 21 21	i 28 (42)	50 35 42	17 16 16	59 64 62	22 12 17	11 11 11	6 3 4		T=5±0.4°C for second loop
C-(BU3-4)-1	34.5	-14.8	1.55	6±1	∿130 (93)							342 82 212	144 80 112	- -	- -		
C-(BU3-6)-1	46.0	-26.3	1.9	4.8±0.3	65 (43)							60 58 59	34 21 28				
C-(BU3-8)-1	58.0	-38.3		4.0±0.3	40 (27)							116 135 126	153 38 95		9 5 7		

Note: i = value indeterminate

Table 8.2.(b) Coefficient of consolidation data for Boston Blue Clay--Student Center and Materials Center (after Ladd and Luscher 1965)

Location	Virgin Compression $C_c/(1+e_o)$			Recompression (1) $C_r/(1+e_o)$			Swelling (2) $C_s(1+e_o)$		
	No. of Tests	Ave. Value	Range	No. of Tests	Ave. Value	Range	No. of Tests	Ave. Value	Range
C.A.E.S.	4	0.180	0.163-0.201	4	0.0295	0.0240-0.0385	4	0.0285	0.0250-0.0320
Student Center	10	0.181	0.140-0.250	9	0.0290	0.0165-0.0440	10	0.0280	0.0175-0.0390
Materials Center	5	0.195	0.155-0.220	-	-	-	5	0.0255	0.0230-0.0325
Hayden Library	11	0.170	0.145-0.225	-	-	-	11	0.0250	0.0165-0.0330
All Four Locations	30	0.179	0.140-0.250	13	0.0292	0.0165-0.0440	30	0.0266	0.0165-0.0390

(1) Ave. of rebound - recompression curves between $\bar{\sigma}_{vm}$ = 6-8 kg/cm^2 and $\bar{\sigma}_{vc}$ = 1 kg/cm^2

(2) For rebound from $\bar{\sigma}_{vm}$ = 16 kg/cm^2 back to $\bar{\sigma}_{vc}$ = 1.6 kg/cm^2

Table 8.3 Summary of compressibility data on Boston Blue Clay--M.I.T. Campus (after Ladd and Luscher 1965)

PREDICTION OF HEAVE, ONE DIMENSIONAL METHOD
FOR NO DRAWDOWN (HYDROSTATIC CONDITION)

Elevation	-12.5	-26	-38	-47	-57	-60	-67
$\bar{\sigma}_{vo}$	1.40	1.778	2.110	2.343	2.560	2.716	2.900
$\Delta\sigma_v$	-0.770	-0.750	-0.726	-0.701	-0.664	-0.636	-0.632
DW	0	0	0	0	0	0	0
Δu	-0.770	-0.750	-0.726	-0.701	-0.664	-0.636	-0.632
$\bar{\sigma}_{ave}$	1.019	1.403	1.747	1.993	2.228	2.398	2.584
$\Delta u/\bar{\sigma}_{ave}$	0.760	0.532	0.416	0.352	0.298	0.265	0.244
C_s	0.09	0.072	0.039	0.033	0.020	0.020	0.020
$1+e_o$	2.13	2.13	2.11	2.00	1.90	1.87	1.88
$\varepsilon^{\infty}/100$	14.0	7.82	3.34	2.52	1.37	1.23	1.13
U_z^{105}	1.00	0.75	0.54	0.41	0.47	0.42	0.63
$\varepsilon^{105}/100$	14.0	5.86	1.81	1.03	0.644	0.516	0.711

Note: all stresses in kg/cm^2
ε in percent.

Table 8.4 Prediction of heave, one dimensional method for no drawdown (hydrostatic condition)

PREDICTION OF HEAVE, ONE DIMENSIONAL METHOD FOR 8' DRAWDOWN

Elevation	-12.5	-26	-38	-47	-57	-60	-67
$\bar{\sigma}_{vo}$	1.40	1.778	2.110	2.343	2.560	2.716	2.900
$\Delta\sigma_v$	-0.770	-0.750	-0.726	-0.701	-0.664	-0.636	-0.632
DW	0.270	0.222	0.184	0.148	0.103	0.089	0.055
Δu	-0.500	-0.538	-0.542	-0.553	-0.561	-0.547	-0.577
$\bar{\sigma}_{ave}$	1.150	1.509	1.839	2.066	2.280	2.543	2.612
$\Delta u/\bar{\sigma}_{ave}$	0.435	0.357	0.295	0.267	0.246	0.215	0.221
C_s	0.09	0.072	0.039	0.033	0.020	0.020	0.020
$1+e_o$	2.13	2.13	2.11	2.00	1.90	1.87	1.88
$\varepsilon^{\infty}/100$	8.00	5.25	2.37	1.92	1.02	0.88	0.90
U_z^{105}	1.00	0.75	0.54	0.41	0.47	0.42	0.63
$\varepsilon^{105}/100$	8.00	3.94	1.28	0.79	0.48	0.37	0.57

Note: all stresses in kg/cm^2
ε in percent.

Table 8.5 Prediction of heave,one dimensional method for 8' drawdown.

Cause	Remedial Measure	Improved C_{vs} Value	Improvement Ratio*
Sample Disturbance	$(C_v)_u = (C_v)_d \frac{K_u}{K_d} \frac{(a_v)_d}{(a_v)_u}$	No improvement; effect still within experimental error range	---
Laboratory Test Procedures	$C_{vs} = C_{vc} \frac{a_{vc}}{a_{vs}}$	$100 \pm 50 \times 10^{-4}$	42%
Errors in Field Instrumentation	Accuracy ±0.25', time lag less than 24 hrs. for 90% equalization	---	---
One-dimensional Analysis	$k_{av} = \sqrt[3]{k_h^2 k_v}$	130×10^{-4} cm^2/sec	55%
	$(C_{vs})_2 = 1/3 (\frac{1+\nu}{1-\nu}) \frac{k_{av}}{k_v} (C_{vs})_1$		
	Use Gibson, Schiffman and Pu's curves	250×10^{-4} cm^2/sec	77%

* Improvement ratio = $(\frac{B-A}{A}) \times 100$

$\frac{\text{BACKFIGURED VALUE OF } C_{vs}}{\text{Laboratory value of } C_{vs}} = A$

$\frac{\text{BACKFIGURED VALUE OF } C_{vs}}{\text{Improved value of } C_{vs}} = B$

Table 8.6 Improvement ratios expected from the use of suggested remedial measures.

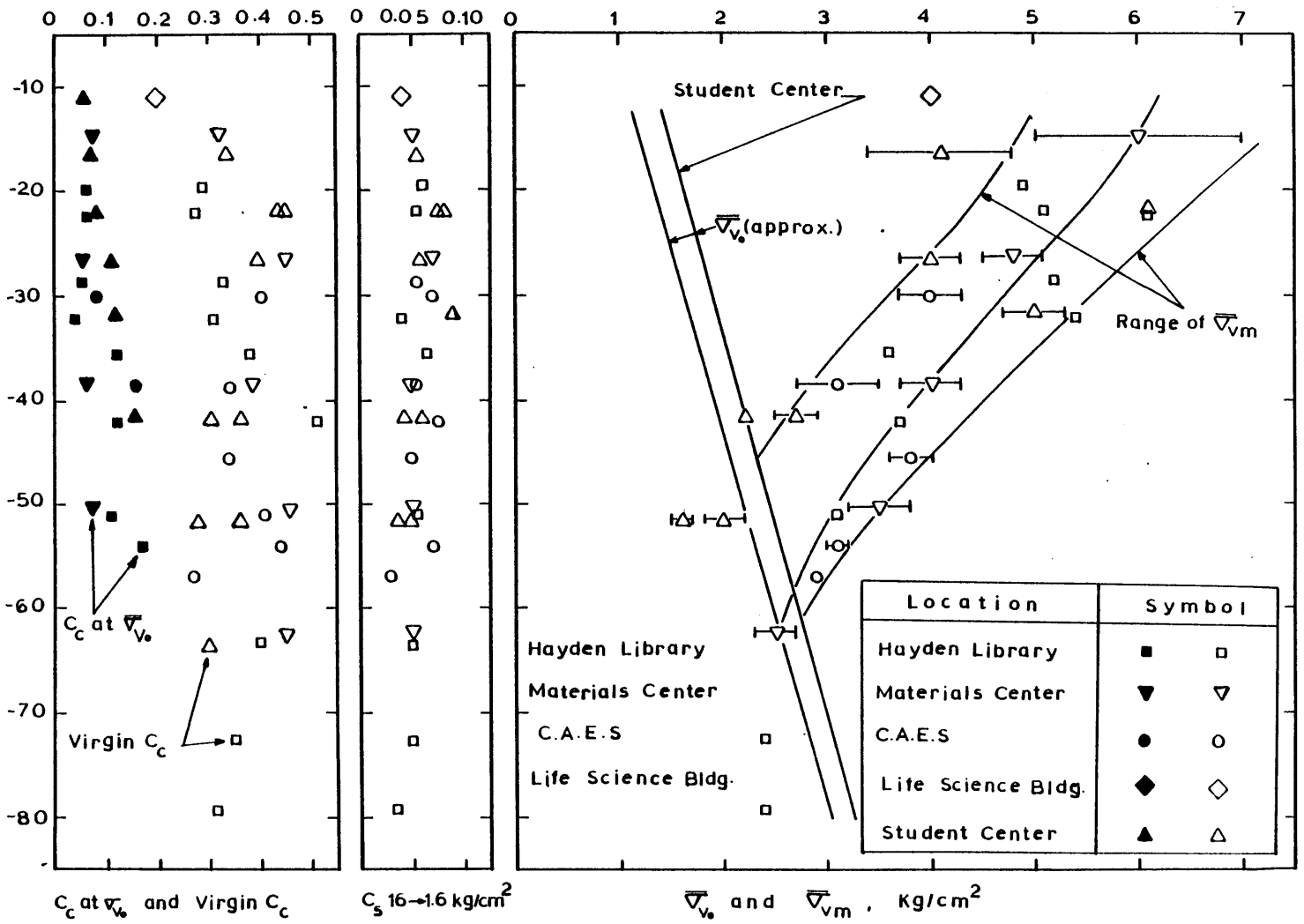

Figure 8.1 Stress history and compression, recompression and swelling indices for the B.B.C stratum at the selected locations.

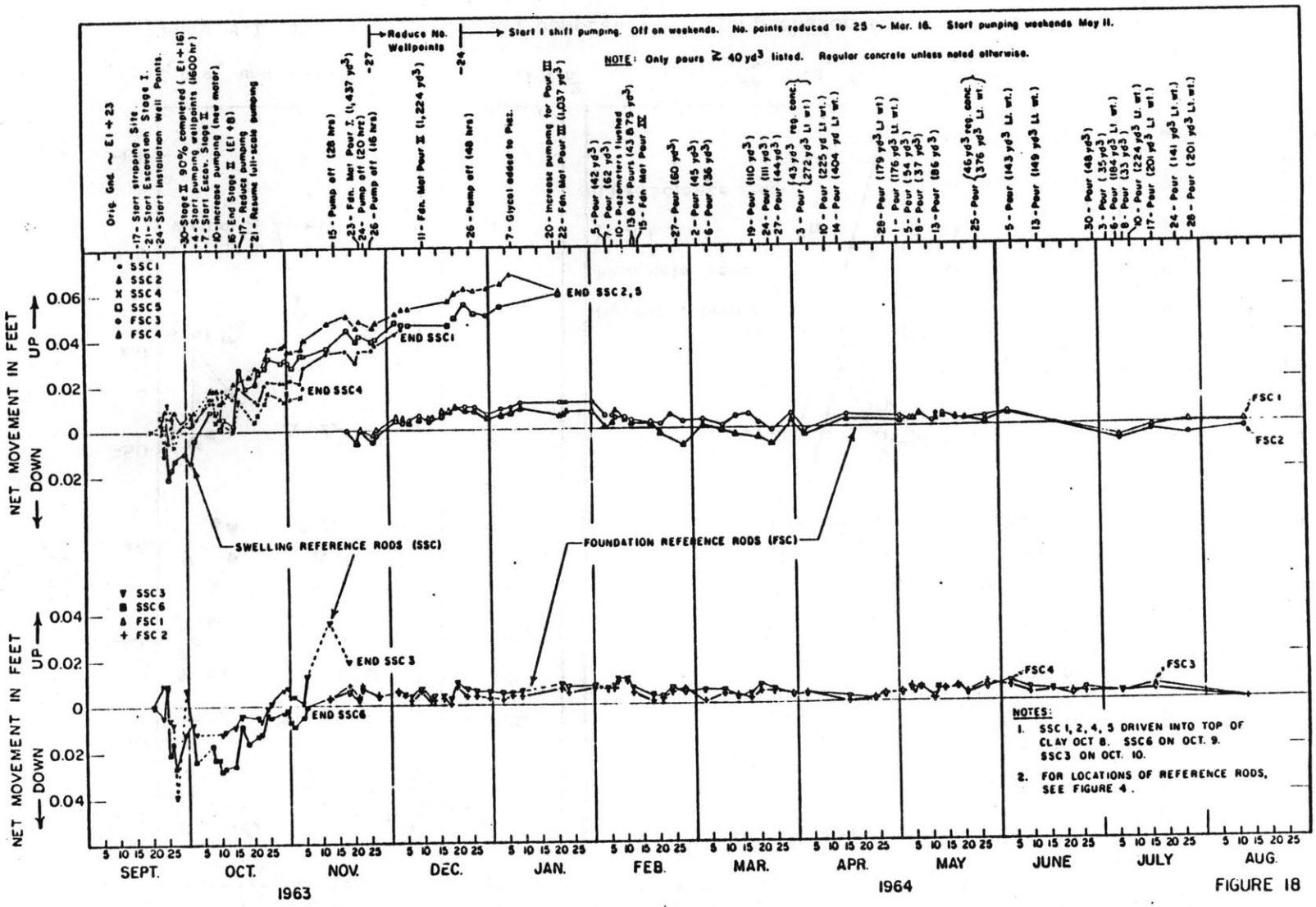

Figure 8.2 Swelling and foundation reference rod movements at M.I.T. Student Center (from Gass 1964).

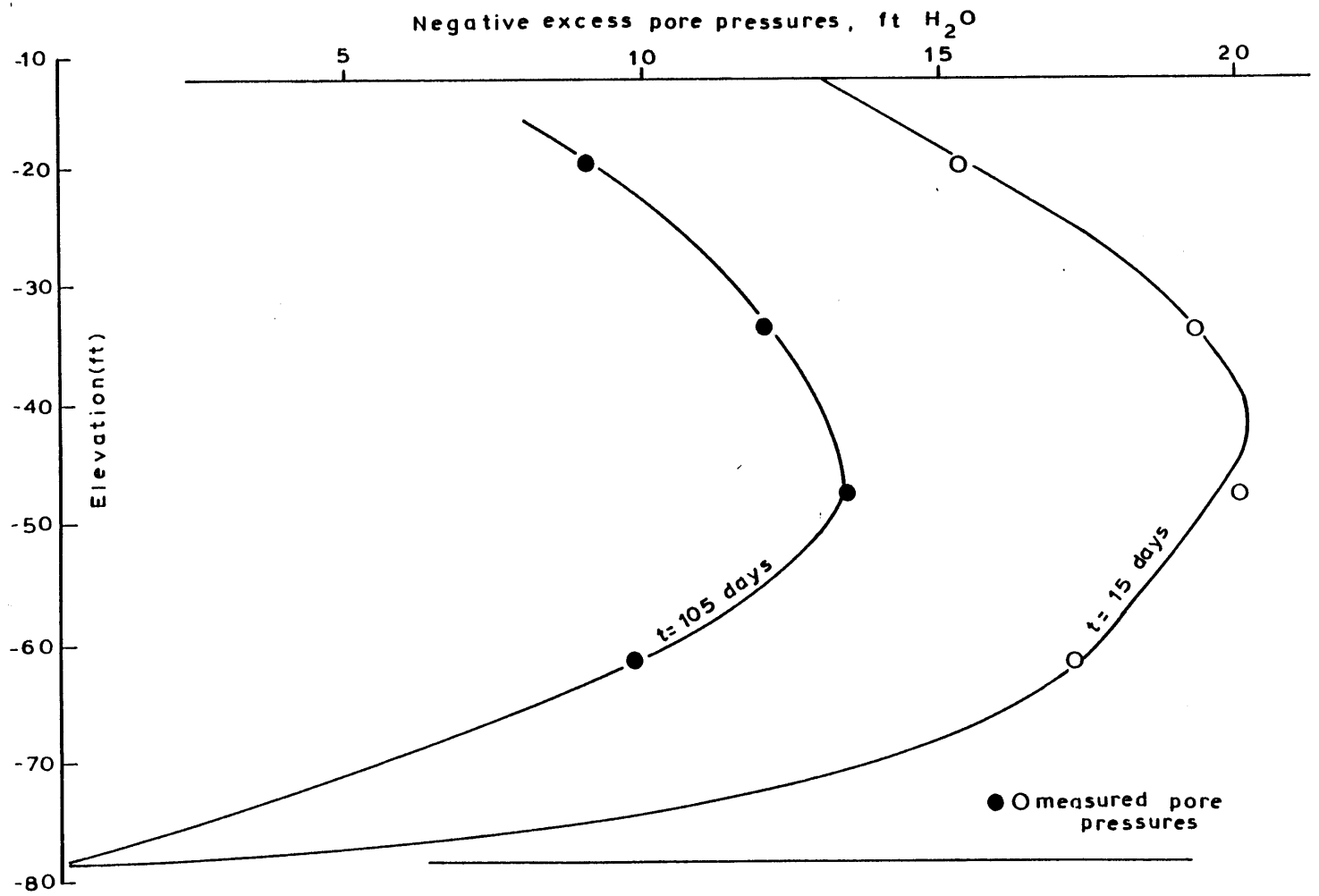

Figure 8.3 Simplified pore pressure vs. depth under the Student Center after stages 1 and 2 of excavation.

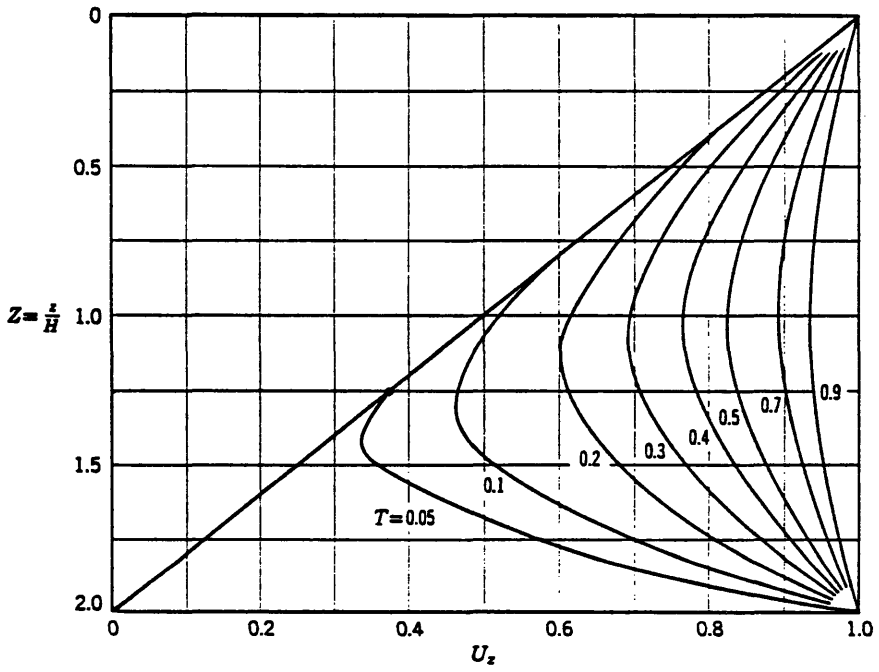

Figure 8.4 U_z versus Z for triangular initial excess pore pressure distribution.

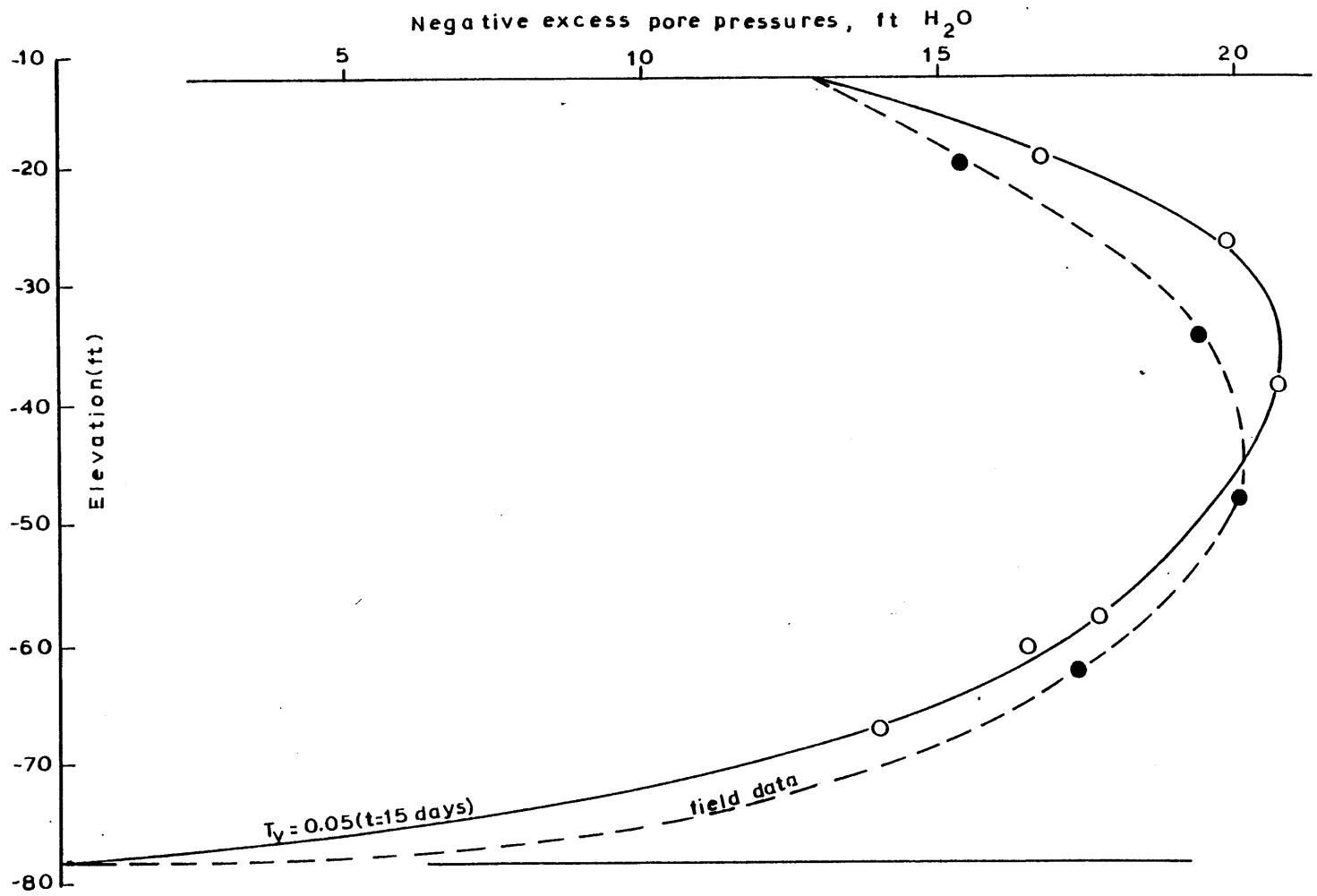

Figure 8.5 Predicted pore pressures 15 days after excavation.

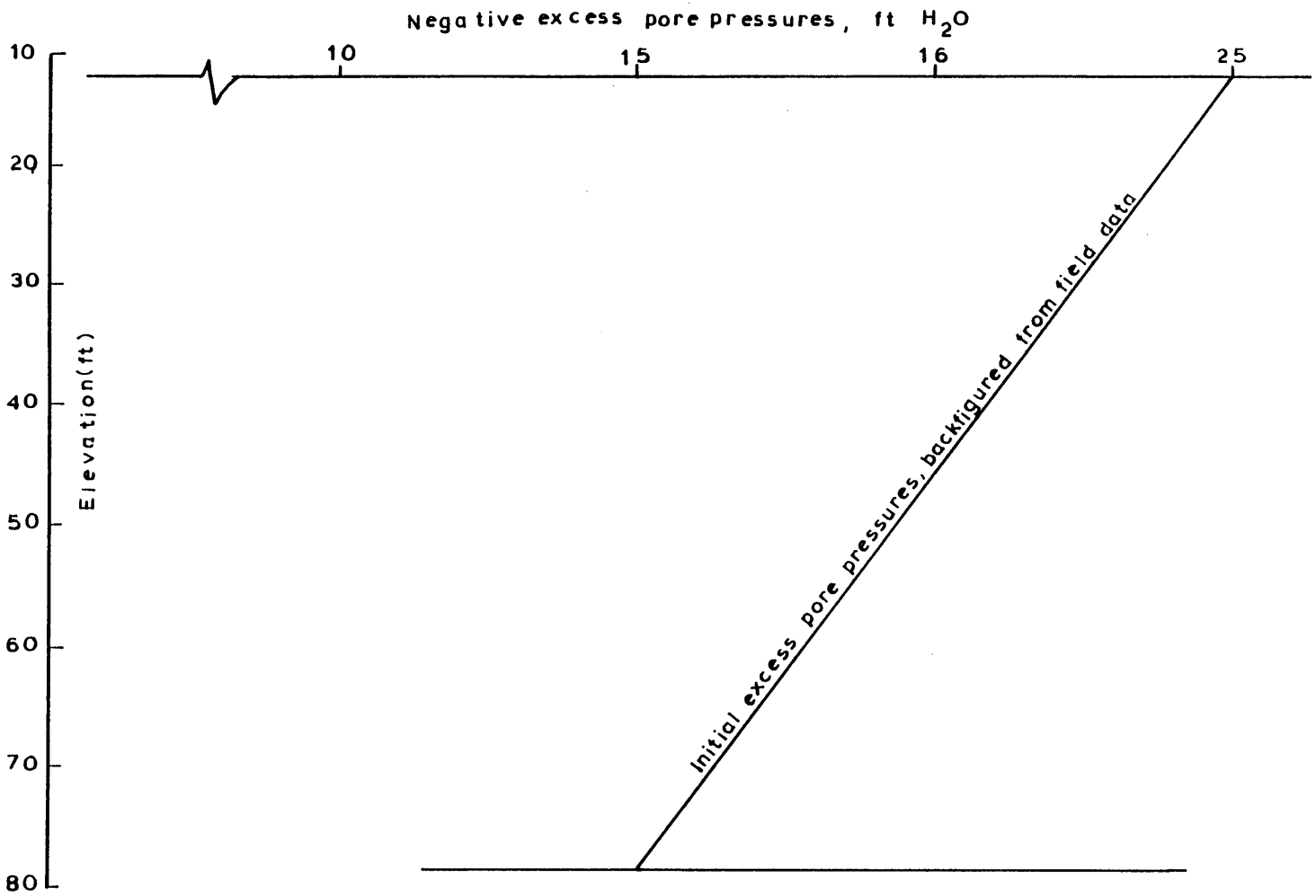

Figure 8.6 Initial pore pressure backfiggured from field data.

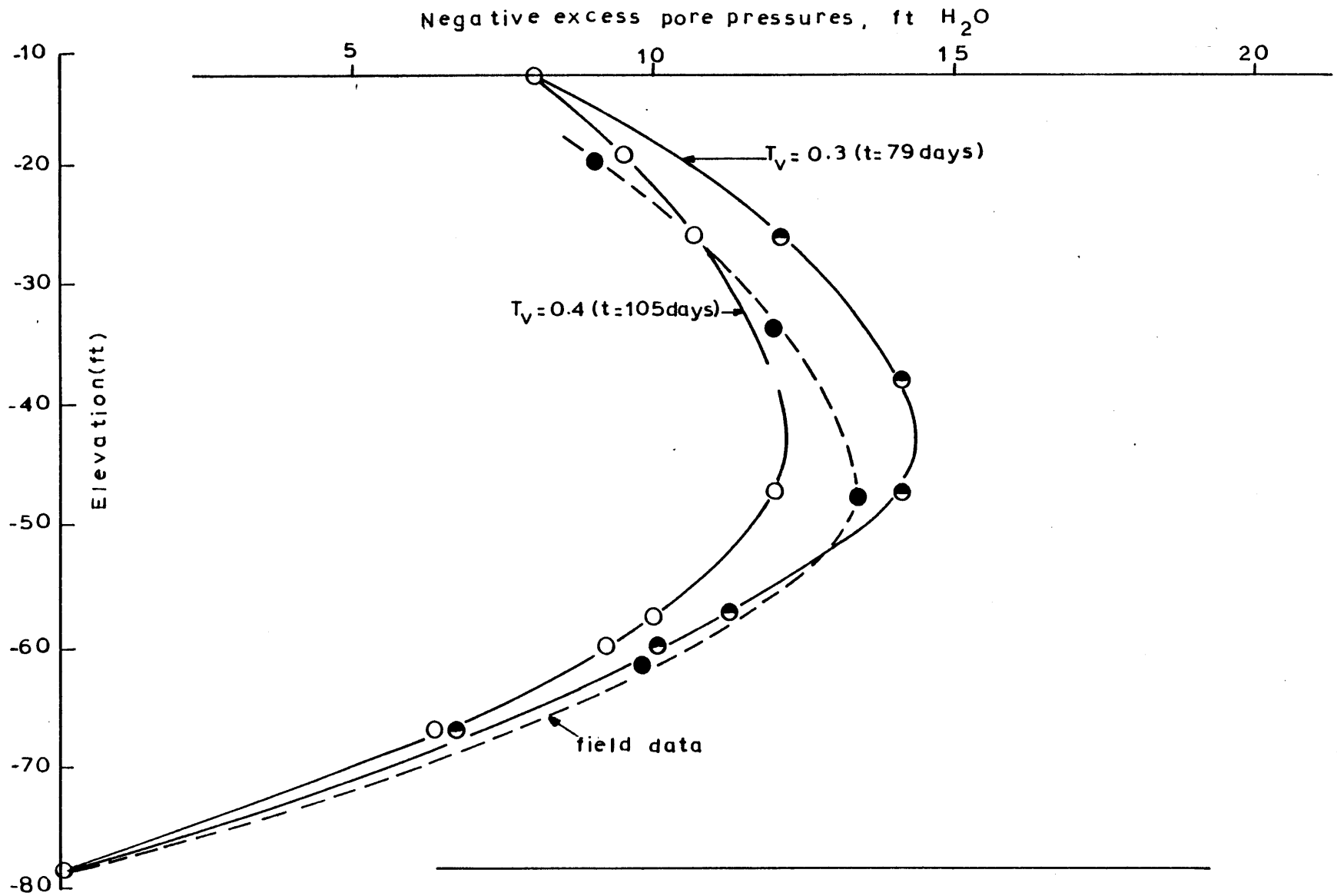

Figure 8.7 Predicted pore pressures 105 days after excavation.

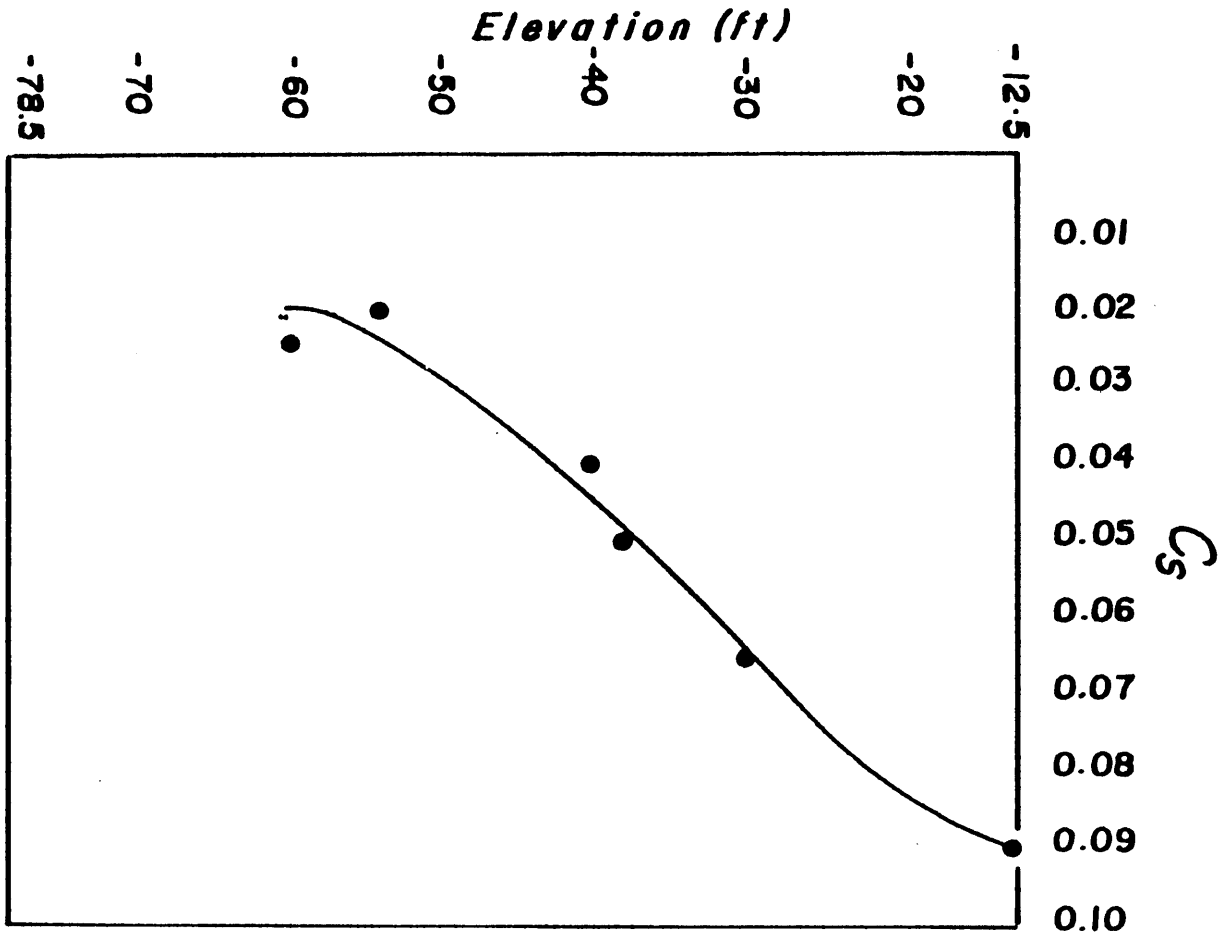

Figure 8.8 SWELLING INDEX FOR APPROPRIATE INCREMENTS VS. DEPTH

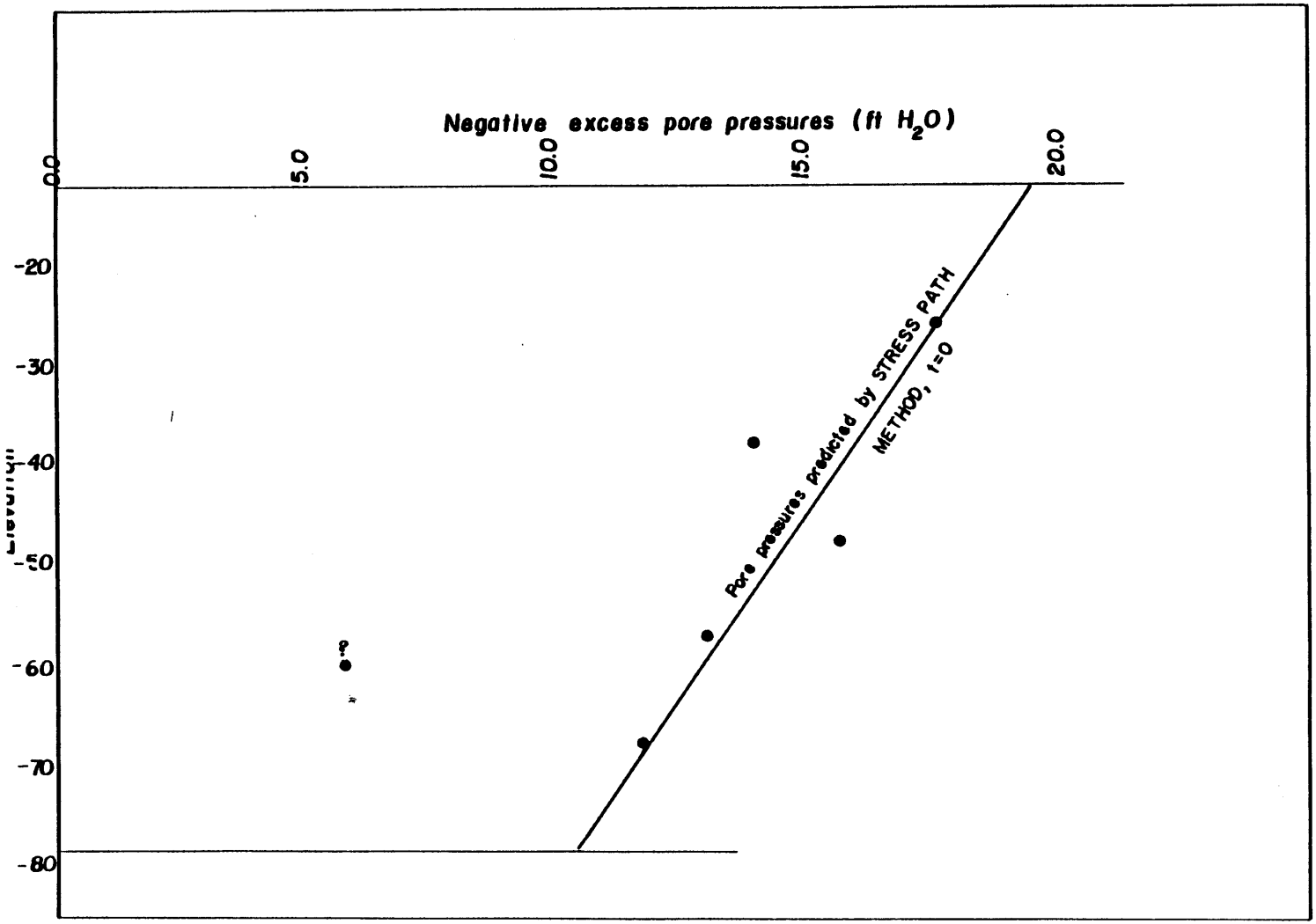

Figure 8.9 PORE PRESSURES VS. DEPTH

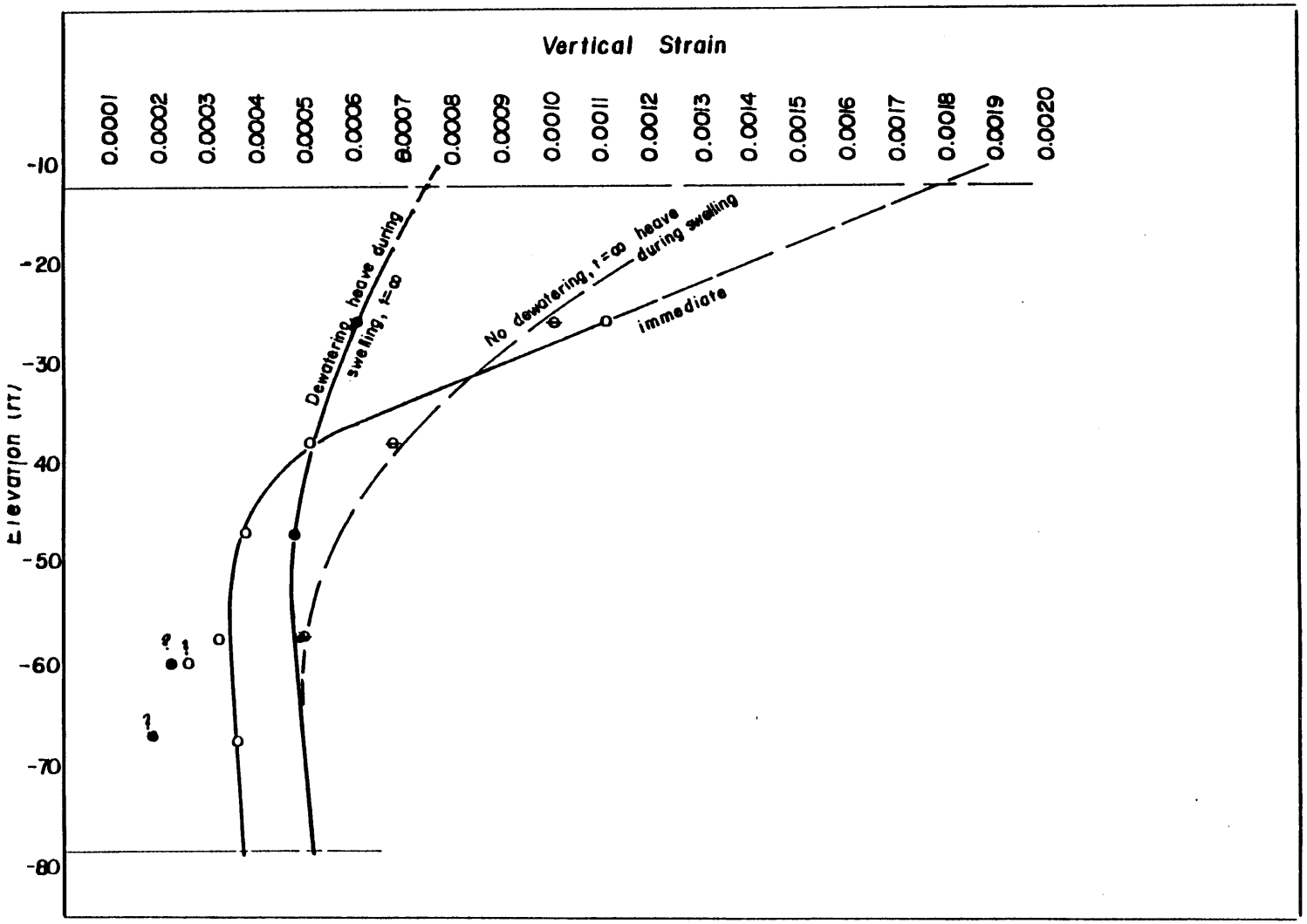

Figure 8.10 UNDRAINED UNLOADING STRAIN, AND STRAIN DUE TO SWELLING VS. DEPTH

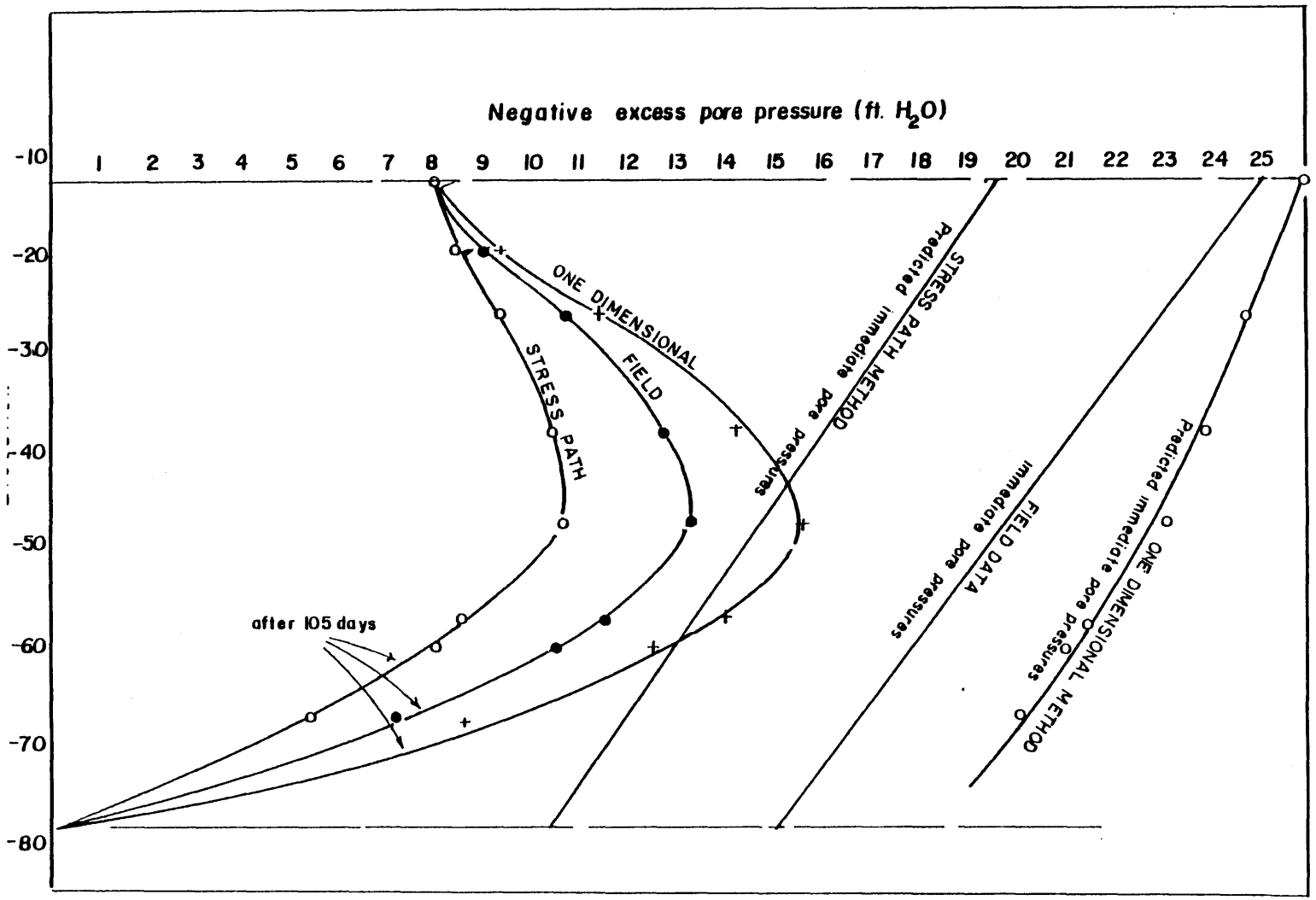

Figure 8.11 PORE PRESSURES VS. DEPTH

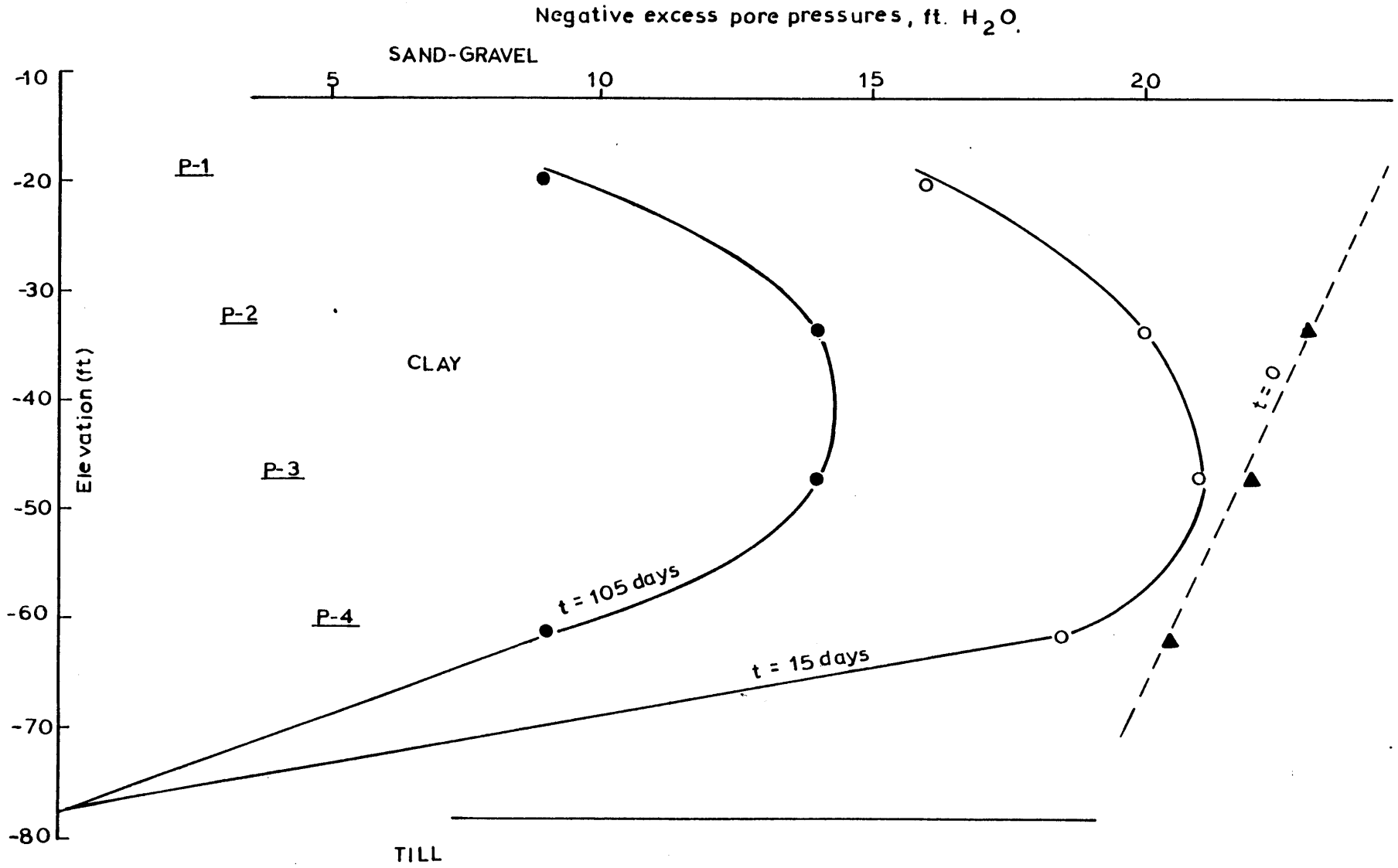

Figure 8.12 Measured pore pressures at 15 and 105 days after excavation.

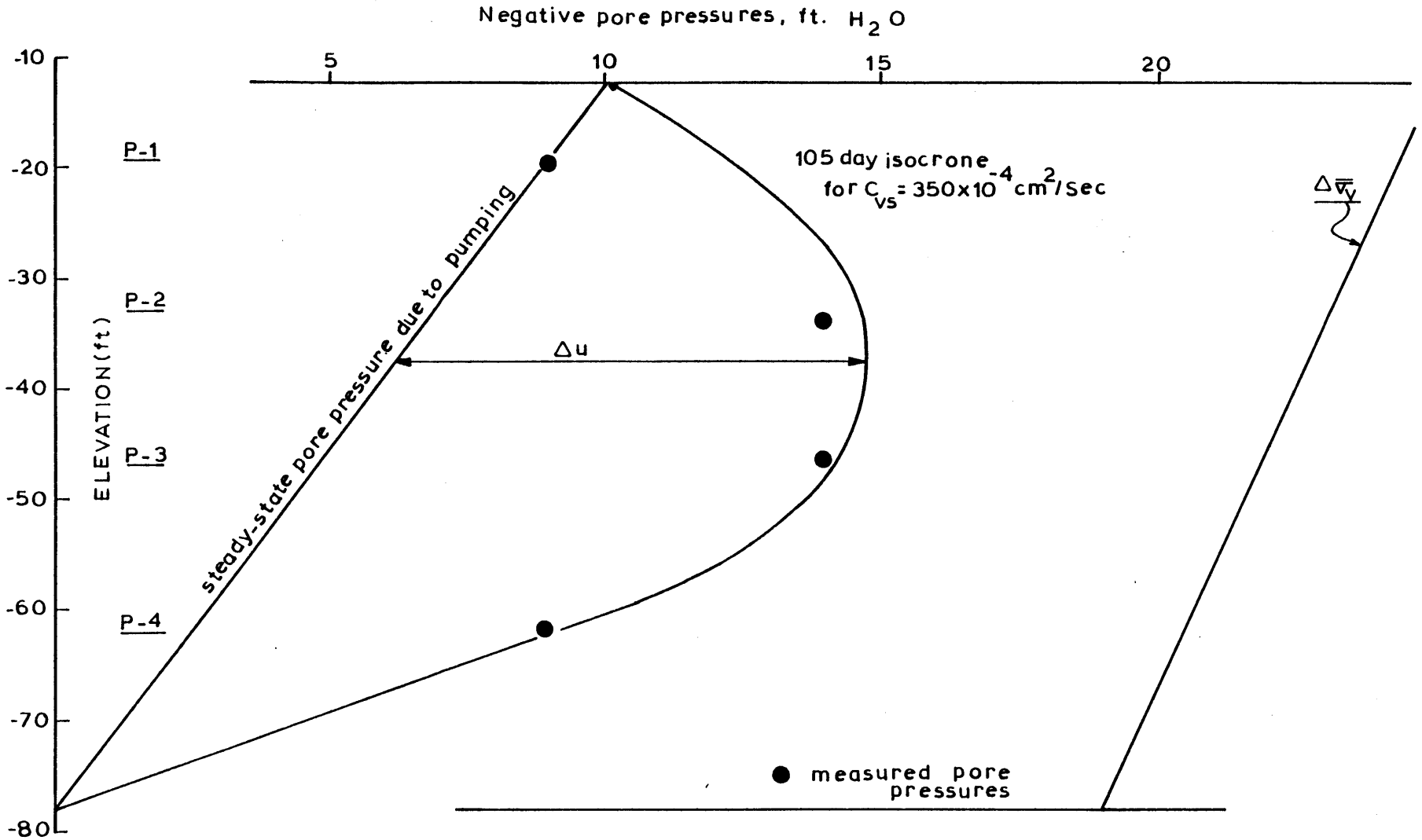

Figure 8.13 Measured and computed pore pressures after 105 days.

CHAPTER 9

PREDICTION OF INDUCED PORE PRESSURE ISOCRONES UNDER A WIDE EXCAVATION

9.1 INTRODUCTION

In the last step of our systems approach, Alternative Evaluation, we basically compared prediction of the coefficient of consolidation profiles, deduced from dessipation records and interpreted using recommendations presented by Baligh and Levadoux (1980)*, with laboratory values at discrete locations (Germaine (1978)) and with field back figured values using an average overall value of c_v for each of the over-consolidated and normally consolidated parts of the B.B.C. stratum [Bromwell and Lambe (1968), Davis and Poulos (1975) and Duncan (1975)].

Evaluation of the recommended c_h profile by comparison with laboratory values at discrete locations is fruititious since we borrow that the laboratory values themselves are not truely representative of field soil parameters due to sample disturbance, size effects, stress systems etc. We shall thus call the comparison our "ordinal" comparison as it only reveals relative ranking with respect to magnitude of the two values.

---

*Hereafter called the reference c_h profile.

"Cardinal" comparison, on the other hand, is intimately related to a comparison between a predicted value and the "actual" in situ value. Theoretically, such an in situ value can never be determined experimentally since any interferance with the soil mass, i.e., sampling operations or in situ testing, will tend to change the in situ value, by varying degrees, due to induced disturbance. The only way the state of nature can be revealed would be through the use of a type C prediction or a post mortom assessment; a full scale field performance analysis. If and only if the soil model used to perform such an analysis encorporates all the soil properties, i.e., nonlinear soil response, coupling effects, anisotropic properties etc., would the field coefficient of consolidation c_v be correctly estimated. However, as discussed in previous chapters, the formulation of such models in very difficult, if at all possible. In retrospect, we can never hope to achieve a true "Cardinal" comparison. Yet, we can state with a high degree of confidence that such back figured values are very close to the in situ values and represent the best estimate of the state of nature. We shall thus classify such comparisons as being "Quasi Cardinal" in nature and will hence forth base our value system on such a technique.

In previous chapters, the construction history of the Julius Adams Building, the Student Center, was thoroughly

presented. Efforts by several authors to back figure the values of the in situ coefficient of consolidation were investigated. Oversimplifing assumptions pertaining to the material properties and boundary conditions precludes their acceptance as a best estimate of the state of nature. The abundance of field pore pressure dissipation records in a clay stratum very similar to that present under the I-95 test embankment from which the recommended c_v profile was obtained; add to that the fact that the building rests on a floating foundation, thus implying that the soil experienced a zero net charge in effective stress and in which c_v unloading and c_v reloading are the prime consolidation parameters, would seem to offer a perfect opportunity to perform a Quasi Cardinal comparison between predicted c_v profile and the back figured values of c_v obtained from field performance data. The methods utilized to achieve this comparison and the resulting evaluation are presented herein.

9.2 PREDICTION OF EXCESS PORE PRESSURE ISOCRONES WITH VARIABLE k AND m_v PROFILES

It is pertinent at this stage to note that the description of excess pore pressure isocrones in a one dimensional transient flow problem is governed primarly by the field equation,

$$\frac{\partial^2 u}{\partial t^2} + \frac{1}{k_{(z)}} \frac{dk}{dz} \frac{\partial u}{\partial z} = \frac{1}{c_{v(z)}} \left\{ \frac{\partial u}{\partial t} - \frac{\partial \sigma}{\partial t} \right\} \qquad 9.1$$

where

$$c_{v(z)} = \frac{k_{(z)}}{\gamma_w m_{v(z)}}$$

In the traditional Terzaghi formulation of the governing field equation, it is assumed that $c_{v(z)}$ is constant and furthermore k(z) is also constant thus yielding the equation

$$\bar{c}_v \frac{\partial^2 u}{\partial z^2} = \frac{\partial u}{\partial t} - \frac{\partial \sigma}{\partial t} \qquad 9.2$$

where

$$\bar{c}_v = \frac{\bar{k}}{\bar{m}_v \gamma_w}$$

In an attempt to illustrate the effect of a variable k and m_v and to assess the error involved in neglecting the effect of their variation with depth, Gibson et al. (1964) used polynomial distributions of k and m_v given by:

$$k_{(z)} = k_o \left\{ 1 + \alpha \frac{z}{H} \right\}^p \qquad 9.3$$

$$m_v(z) = m_o \left\{1 + \beta \frac{z}{H}\right\}^q \qquad 9.4$$

in which k_o and m_o denote the permeability and compressibility at the top of a doubly drained clay layer; H indicates the thickness of the layer; and α, β, p and q stand for parameters that characterize the manner of variation of k and m_v with depth, and for the case in which $\alpha = \beta$ a closed form solution of equation 9.1 was used to analyze the following cases.

(a) Polynomial distribution of k at a constant m_v:

Figure 9.1 represents a tenfold permeability decrease and Figure 9.2 represents a tenfold permeability increase through the layer. The effect of the magnitude of permeability is indicated in Figure 9.3 which represents the excess pore pressure isocrone at 50% consolidation. Figure 9.4 represents the time settlement curves for the polynomial variation of permeability k_v.

(b) Polynomial distribution of m_v at constant k_v:

Figure 9.5 represents a tenfold variation of m_v, with k being held constant. The extreme effects is distribution of excess pore pressure occur for distribution 1k and 4k. The excess pore pressure isocrone at 50% consolidation is shown in Figure 9.6 . Figure 9.7 represents the time settlement curves for the polynomial variation of m_v.

(c) Polynomial distribution of k and m_v at constant c_v:

Figure 9.8 shows the polynomial variations of m_v and k_v, with c_v being held constant. The extreme effects in distribution of excess pore pressure occur for distributions 4c and 1c. The excess pore pressure isocrone at 50% consolidation is shown in Figure 9.9 . Figure 9.10 represents the time settlement curves for the polynomial variation of k and m_v.

Upon comparing the various aforementioned cases several conclusions could be drawn.

1. The variation of the permeability k is largely responsible for the derivation of the calculated excess pore pressure isocrone at 50% consolidation from that predicted by conventional theory.
2. The variation of the compressibility m_v is largely responsible for the deviation of the calculated time settlement curves from that predicted by conventional theory.

*Throughout this parametric study it was assumed that double drainage exists. The settlement is expressed in terms of the degree of consolidation U. The time is expressed in terms of the dimensionaless time factor, T_v, defined by

$$T_v = \frac{c_o t}{H_d^2}$$

where c_o is the coefficient of consolidation at the top of the layer.

3. It is seen from Figure 9.10 that the time-settlement curves for similar distributions are proportional to net absolute permeability.

A question of interest now arises: "Could we have reasoned, using the analysis and results presented above coupled with the stress history of the foundation soil under the student center, the deviation of the piezometer reading from that predicted by conventional theory ?"

The stress history of the foundation soils, Figure 9.11 , clearly suggests that the top half of the clay stratum is heavily over-consolidated (1<OCR<4.8). One would henceforth predict that the c_v profile might be of the 1m (Figure 9.1) type. Remembering that m_v has little effect on the actual pore pressure dessipation and as evidenced by Figure 9.6 we could safely assume that m_v could be held constant with minimal error introduction. We could thus expect that the shape of the isocrones at 50% would mimic that of the 1m case in Figure 9.6 . It is thus obvious that the piezometer reading (P-4) suggesting a lower value of the excess pore pressure is in perfect agreement with the theory and does not reflect any instrument malfunction.

As mentioned earlier, the feasibility of the analytical solution depends heavily on whether the actual variation of k_v and m_v with depth can be described with sufficient accuracy, by simple functional relationships. Quantitive evaluation of

the c_h profile involving comparison of predicted versus field pore pressure dissipation records would involve using a model that can intimately encompass the variation of the soil properties namely c_v, c_h, k_v, k_h, m_v and m_h. Since such variations are usually by no means easy to express in simple functional relationships we are compelled to use approximate numerical techniques that can accomodate such variations. A finite element program ADINAT was subsequently used and is described in the following section.

9.3 ADINAT: A FINITE ELEMENT PROGRAM FOR AUTOMATIC DYNAMIC INCREMENTAL NONLINEAR ANALYSIS OF TEMPERATURES, BATHE (1977)

9.3.1 General

The program ADINAT was developed to provide solutions for general linear and nonlinear steady-state and transient heat transfer analysis. A specific feature of a heat transfer analysis program is that the same code can also be used to solve other field problems, such as steady state seepage or transient state seepage problems. The reason for this direct applicability of ADINAT to a number of field problems is the analogy between the various field variables.

9.3.2 Governing Field Equations

Considering a three-dimensional body in a transient seepage state, the divergence theorem dictates:

$$\int_{\delta R} \underline{V} \cdot \underline{n} \, dA = \int_{R} \underline{\nabla} \cdot \underline{V} \, d \text{ vol.} \qquad 9.5$$

where $\underline{V}$ is the velocity vector, $\underline{n}$ is the normal to the surface of the body and $\underline{\nabla}$ is the operator defined by

$$\underline{\nabla} = \begin{Bmatrix} \frac{\partial}{\partial x} \\ \frac{\partial}{\partial y} \\ \frac{\partial}{\partial z} \end{Bmatrix} \qquad 9.6$$

R defines the volume of the body, and δR represents the surface of the body.

Assuming that our global frame of reference coincides with our principal frame of reference, i.e.,;

$$\underline{k} = [\underline{k}] = \begin{Bmatrix} k_1 & 0 & 0 \\ 0 & k_2 & 0 \\ 0 & 0 & k_3 \end{Bmatrix} \qquad 9.7$$

and using Dary's law for flow through porous media namely:

$$\{V\} = -[k] \{\phi\} \qquad 9.8$$

where $\{V\}$ is the velocity vector expressed in matrix notation, $[k]$ is a second order matrix given above and $\{\phi\}$ is given by:

$$\{\phi\} = \left\{ \frac{\partial h}{\partial_{x_i}} \right\} \qquad i = 1,2,3 \qquad 9.9$$

where h is the total head equal to the sum of the elevation head h_e and the pressure head h_p.

Substituting 9.9, 9.8 & 9.7 into the right hand side of 9.5 we arrive at:

$$-\int_R \nabla \cdot (k\nabla h)\, dV \qquad 9.10$$

Also,

$$\int_R \nabla \cdot (k\nabla h)\, dV = -\frac{\partial V}{\partial \tau} \qquad 9.11$$

where $\frac{\partial V}{\partial \tau}$ expresses the ratio of volume charge.

The ratio of volumetric change, d, could be expressed by the following equation:

$$d = \frac{\bar{\sigma}_{oct}}{\bar{K}} \qquad 9.12$$

where $\bar{K}$ is the bulk modulus. Thus substituting into 9.11 we arrive at

$$\frac{\partial V}{\partial t} = \int_R \frac{\partial d}{\partial t}\, dV$$

and

$$\frac{\partial V}{\partial t} = \int_R \frac{\partial}{\partial t} \left(\frac{\bar{\sigma}_{oct}}{\bar{K}} \right) dV \qquad 9.13$$

Substituting into 9.7 we arrive at

$$\int_R \left[\nabla \cdot (k \nabla h) + \frac{\partial}{\partial t} \left(\frac{\bar{\sigma}_{oct}}{\bar{K}} \right) \right] dV = 0$$

But R is arbitrary hence the integral vanishes. Thus,

$$\frac{1}{\bar{K}} \frac{\partial}{\partial t} (\bar{\sigma}_{oct}) + \nabla \cdot (k \nabla h) = 0 \qquad 9.14$$

Using only excess pore pressures and using the effective stress principal we can transform 9.14 to

$$\nabla \cdot (k \nabla u) = \frac{\gamma w}{\bar{K}} \frac{\partial}{\partial t} \left(u - \sum_{i=1}^{3} \frac{\bar{\sigma}_i}{3} \right) \qquad 9.15$$

9.3.3 Establishing the Analogy

The left hand side of equation 9.15 is exactly identical to the left hand side of the heat transfer equation given below

$$\nabla \cdot (k \nabla \theta) = -q^B \qquad 9.16$$

where θ, the temperature, is replaced by u, the excess pore pressure. We assert that $-q^B$, the rate of heat generated per unit volume, is equal to the right hand side of equation 9.15.

A simple case of one dimensional consolidation with constant values of coefficient of permeability and compressibility reduces equation 9.15 to

$$k \frac{\partial^2 u}{\partial z^2} = m_v \gamma_w \frac{\partial u}{\partial t} - m_v \gamma_w \frac{\partial \sigma_v}{\partial t} \qquad 9.17$$

In equation 9.16, q^B is given by

$$q^B = \tilde{q}^B - C\dot{\theta} \qquad 9.18$$

where the quantity $C\dot{\theta}$ is the part of the rate of heat generated, q^B, per unit volume and C is the material heat capacity. By analogy with equation 9.17

$$\tilde{q}^B = m_v \gamma_w \frac{\partial \sigma_v}{\partial t}$$

$$q^C = C\dot{\theta} = -(\gamma_w m_v) \frac{\partial u}{\partial t}$$

and $C = \gamma_w m_v$.

Thus, the two important parameters are the permeability (conductivity) k, and the product of $m_v \gamma_w$ (material heat capacity).

9.3.4 Special Problems With Input Data

All the heat flow functions are input as tables of g(t) versus t, and the loads at solution step "n" are found in

the g(t) tables by linear interpolation as in trasient analysis. This creates serious problems when the analogy with the consolidation equation is utilized. Clearly what we then need to input as g(t) is the slope of the variation of the input negative (or positive) pore pressure as a result of a change in the total stress due to excavation (or loading). However, this creates a difficulty with problems involving step loading, i.e., the slope goes to infinity at points of discontinuity. To by-pass this effect, the following procedure is suggested.

(1) No discontinuities in values of σ_v

Figure 9.12 shows a loading curve consisting of a broken line representation with no discontinuities in values of σ_v. However at points a, b, c etc., there is an abrupt change in the slope. This change should be smoothed so that for any one point in time t there exists only one value of the slope G(t). To do this, choose a small value of ε with respect to Δt_1 and Δt_2 and then the input data could be prescribed as shown in Figure 9.12.

(2) Loading curves with discontinuities in values of σ_v

Figure 9.13 shows a loading curve where the value of σ_v experiences a jump at t_{i+1}. At that point, the slope goes to infinity. Again to avoid this problem choose two values ε and ε' such that $\varepsilon << \Delta t$ and $\varepsilon' << \varepsilon$. Now we can replace the infinite slope by a finite slope through joining

points at a time $t_{i+1-\varepsilon+\varepsilon'}$ and $t_{i+1+\varepsilon-\varepsilon'}$ with a straight line and to insure compatibility with original configuration we write:

$$(t_{i+1}-\varepsilon-\varepsilon'-t_i)s_i+\frac{1}{2}(s_i+\hat{s}_i)(t_i+1-\varepsilon+\varepsilon'-t_{i+1}+\varepsilon+\varepsilon')$$

$$+\hat{s}_i(t_{i+2}+\varepsilon-\varepsilon'-t_{i+1}+\varepsilon-\varepsilon')+\frac{1}{2}(s_{i+2}+\hat{s}_i)(t_{i+2}+\varepsilon+\varepsilon'-t_{i+2}$$

$$+\varepsilon+\varepsilon'-t_{i+2}-\varepsilon+\varepsilon')+s_{i+2}(t_{i+3}-t_{i+2}-\varepsilon-\varepsilon')$$

$$= \Delta t_i s_i+\Delta t_{i+2}s_{i+2}+\Delta$$

After simplification we arrive at

$$\hat{s}_i = \frac{\Delta}{2\varepsilon} + \frac{1}{2}(s_i + s_{i+2})$$

Thus, the value of t and G(t) are input as shown in Figure 9.13.

9.4 ADINAT PROGRAM VALIDATION

Having obtained the analogy between the heat transfer and transient flow governing equations and establishing the corresponding material parameters, it is now important to actually check the program's integrity by attempting to solve a problem whose answer has been pre-determined using some other method of analysis, a closed form solution, say.

The first case investigated was that of a simple one dimensional consolidation stratum with double drainage and having the following material properties:

$$c_{(z,t)} = \text{constant} = 3.225 \text{ ft}^2/\text{day}$$

and

$$k_{(z,t)} = \text{constant} = 2.834 \text{ ft/day}$$

A simple one dimensional mesh with 21 nodes and 20 elements was used. Applying an external load of arbitrary value:

$$q_{(t)} = \text{constant} = 26.27$$

to the upper boundary was simulated by an initial pore pressure excitation of constant value distributed at each node and equal to q. The time intervals were then designated. Since the external load $q_{(t)}$ is constant, i.e.; it's slope is nill, only one loading curve whose value is zero for any time t was input that applies for all the nodes. This case is identical to that of a conventional oedometer test where a constant load is applied at the surface and the resulting total stress distribution, initially translated to an increase in pore pressure, is assumed to be uniform across the sample.

The solution to this problem was earlier presented by Carl Terzaghi (1923) in a form of a dimensionless plot, $Z = \frac{z}{H_d}$* and $\bar{U} = \frac{u}{u_o}$** of the normalized excess pore pressure variation across the sample with time. The results of the pore pressure distribution across the sample obtained from ADINAT corresponding to the dimensionless parameter $T_v = \frac{c_v t}{H_d^2} = 5\%$, & 50%, i.e.; $t = .05 \frac{H_d^2}{c_v}$ was plotted in a similar fashion to Terzaghi's solution and the two isocrones corresponding to the same $T_v = .05$ & $.5$ compared, Figure 9.14. An excellent agreement between the two solutions was observed.

In the second trial run investigated, the same problem geometry, initial and boundary conditions were retained. A constant value of $c_v = 3.225$ ft^2/day was also employed. However, RR..., the Recompression Ratio, was assumed to be constant and equal to .01. Using the following approximate equation:

$$m_{v(O.C)} = \frac{RR}{2.3\ \sigma_{vc}} \quad \text{and} \quad \sigma_{vc} = \sigma_{vo}$$

---

*$Z = \frac{z}{H_d}$ in which z is depth of any soil element from top boundary and H_d is the drainage length.

**$\bar{U} = \frac{u}{u_o}$ where u is the excess pore pressure at any time $t > t = 0^+$ and u_o is initial excess pore pressure.

and an m_v varation shown in Figure 9.15 (a), the corresponding pore pressure isocrone corresponding to T_v = 5 and 50% are shown in Figure 9.15(B). When compared to Terzaghi's solution, it appears that at T_v = 5% the agreement is very good. However, the isocrone corresponding T_v = 50% deviates slightly from the conventional solution and is further skewed in the same fashion as that predicted by Gibson et al. (1964) and shown in Figure 9. 9 , although the degree of skewness is of a less magnitude since the ratio of k and m_v at the top and bottom boundary is only 4.25 compared to 10.0 used by Gibson et al. (1964).

Finally, the solutions given by Gibson et al. for the three cases namely:

a) Constant m_v and variable k_v and c_v

b) Constant k_v and variable m_v and c_v

c) Constant c_v and variable k_v and m_v

were also checked. The two extreme polynomial variations (1) and (2), representing a tenfold increase or decrease in the appropriate variable material properties, were used to characterize the material properties. The results thus obtained plotted directly over the analytical solution obtained by Gibson et al. with no appreciable abbreviations as shown in Figures 9.16 to 9.18.

We are now clearly confident that the computer program, ADINAT, is capable of modelling consolidation behavior of soils when subjected to external loading and the analogy

drawn in section 9.5.3 holds true.

9.5 ESTABLISHING THE SOIL PROPERTIES UNDER THE STUDENT CENTER

Before we actually indulge in any analysis to establish the soil properties under the Student Center, it is perhaps helpful to review few notions that would yield some insight into the technique utilized at a later stage.

Figures 9.19 and 9.20 are representation plots of the compression curve (% strain versus log $\bar{\sigma}$) and variation of the coefficient of consolidation of swelling with effective stress (c_{vc}, c_{vs} versus log $\bar{\sigma}$). Figures 9.19 and 9.20 were obtained from a constant rate of strain test on a sample of Boston Blue Clay retrieved from a depth of 90.89 feet.

Examining Figure 9.20 that characterizes the variation of c_{vc}/c_{vs} with effective stress, we observe three important trends for the loading and reloading mode:

(1) c_{vc} decreases significantly as the consolidation stress approaches the maximum past pressure;

(2) c_{vc} is approximately constant in the normally consolidated region (some clays may show a slight increase at higher consolidation stresses);

(3) c_v from the reload cycle is much larger than that obtained from the initial loading up to the maximum past pressure.

For normally consolidated clay, both k and m_v are decreasing with increasing stress, but the ratio k_v/m_v remains essentially constant. Hence the value of $c_v = k_v/m_v\ \gamma_w$ is constant in that range. During recompression, the permeability decreases slightly while m_v increases considerably, thus the large decrease in c_v as $\bar{\sigma}_{vc}$ approaches $\bar{\sigma}_{vm}$. Finally, c_v during the initial loading to $\bar{\sigma}_{vm}$ is too small because sample disturbance has increased m_v.

Three important trends for the unloading mode could be sighted:

(1) At the instant of unloading the soil exhibits a very stiff soil skeleton response with a very small value of m_{vs}. Thus the value of C_{vs} at the instant of unloading is very large.

(2) C_{vs} decreased monotonically with continual unloading.

(3) The two curves of C_{vs} obtained from first and second rebound appear to be almost parallel.

It is crucial at this stage to actually stress a very important observation. Table 9.1 is a computer output of a program designed to reduce data obtained from the CRSC test and provide useful soil parameters and response data to the continuous loading operation. Attention is drawn to data items 56, 59, 113 and 117.

Comparing the soil parameters at points A & C one can make the following observations:

(1) The value of k_v decreased by almost 40%.

(2) The value of m_v decreased by almost 60%.

(3) The value of c_v increased by almost 50%.

Comparing the soil parameters at points B and D one can make the following observations:

(1) The value of k_v decreased by 45% (which is attributed to the change occuring during passage from A to C).

(2) The value of m_{vs} decreased by almost 30%.

(3) The value of c_{vs} decreased by almost 12%.

Within the range of stresses discussed herein it would appear as if the soil exhibits a normalized behavior with respect to c_{vs} parameter. Although it might be argued that this is by no means conclusive since only one test was used, yet it would be verified later in the experimental part of this thesis. However, for the time being we shall assume that the soil does exhibit normalized behavior that could be schemetically described as shown in Figure 9.21.

Notice that the same argument applies with respect to the recompression mode and the behavior of $c_{v\ \text{recompression}}$, mutatis mutandis*. Keeping the aforementioned assumptions in mind, we are now in a position to infer the soil parameters of interest under the Student Center.

---

*mutatis mutandis: with the respective differences having been considered.

Figures 9.11 and 9.22 illustrate the stress history of the Student Center foundation soils and the I-95 test site. The corresponding variation of the over-consolidation ratio with elevation is shown in Figures 9.23 and 9.24 . Figure 9.25 is our reference profile of c_h (c_h recompression) at I-95 test site as obtained by B&L (1982). Figure 9.26 is the k_h profile at I-95 test site principally derived from the reference profile. Using those six plots we can easily predict the c_h and k_h profile under the Student Center by simply using the normalized soil behavior developed earlier. The resulting profiles of c_h and k_h are shown in Figures 9.27 and 9.28.

One important condition must hold to validate and warrant the use of the above technique. It is essential that the variation of the soil type with elevation at the two sites be similar, otherwise the aforementioned operation would be similar to that of adding apples to oranges! This could be easily checked by comparing the atterberg limits for each site. Also the compression curves from tests done in those two sites could be compared.The soils at the two sites compared very favourablly and satisfied the above mentioned criterion.

9.6 ADINAT INPUT DATA

With the knowledge of the material characteristic properties, the general problem geometry and boundary conditions, the input data required for the program was possible.

9.6.1 Finite Element Mesh Designation

The generalized soil profile under the Student Center has already been discussed in Chapter 7. In short, it consists of a maximum of 8 feet of stiff clayey silt and sand with gravel (fill) overlying shale bedrock forming the lower boundary of the clay layer. The till layer dips gently to the east. The Boston Blue layer, 60 to 72 feet thick with an average of 66 feet, is overlain by an average of 11 feet of loose to compacted rubble fill, followed by 4 feet of organic silt and peat and 20 feet of compacted sand and gravel.

A perfect idealization of the above problem geometry would be to consider an infinitly wide 66 ft deep compressible layer with free drainage from the top and bottom direction.*

Fig. 7.5 shows the geometry of foundation mat and the location of the piezometer P1 through P4. When the dimensions of the foundation mat are compared to the depth of the clay layer and keeping in mind the location of the piezometer P1

*The bottom boundary (fill) was proved to be a perfect drainage layer 8.4.1.

through P4, a one dimensional consolidation analysis appears to be warranted. Henceforth, a 27 node finite element mesh composed of 26 linear one dimensional elements was used. Figure 9.29 and Table 9.2 give a schemetic representation of the finite element mesh.

9.6.2 Boundary Conditions

The two boundary conditions were described through two forcing functions. Recall that on September 25, 1963 important foundation dewatering operations commenced through a system of approximately 170 well points surrounding the site and extending to the top of the clay layer. The pumping schedule together with a rough estimate of the location of the ground water table are shown explicitly in the FERMIT files. Table 9.3 shows the excess negative pressures generated at the top boundary and characterizes the variation with time. The bottom boundary is characterized by a nill function since it interphases with a free draining layer (till). Thus the variation of excess pore pressures with time at nodes 1 and 27 are totally described by the aforementioned forcing function.

9.6.3 Loading Functions

The construction history of the Student Center was earlier described in 7.6 . The total stress release due to the two stages of excavation and subsequent reloading imposes a variable stress distribution with time. For

uniform vertical loading of p/unit area, a smooth rectangular area and a rough (adhesive) interface, between the compressible layer and the base, Burmister (1956) has evaluated the vertical total stress σ_z beneath the corner of the rectangular at various depths in the layer for $\nu = 0.4$. The value of ν has little influence on these vertical stresses, especially near the top of the layer. Using the load influence factors coupled with the appropriate manipulation we can easily arrive at the total stress didtribution due to excavation and the four major concrete pours corresponding to the foundation mat as shown in Table 9.4.

In section 9.3 we have argued that the analogy between the heat flow and transient water flow governing equations reguines that any external loading applied to the compressible layer he reflected through a series of loading functions whose values at any one point in time, t, be equal to the slope of the variation of total stress with time at any one particular depth d, at that time. Instantanious loading implies that total stresses could be replaced by an equivalent increase (or decrease) in pore pressures. Thus the situation could be theoretically idealized by the model described schematically in Figure 9.29. Instantanious loading requires particular attention since it would imply infinite du/dt values. Techniques developed in 9.3 should be carefully

implemented to by-pass this problem.

9.6.4 Material Properties

It is observed that the clay layer is subjected to stress increments (decrements) which are small when compared to it's in situ stress and it's maximum past pressure at any depth h. It will, henceforth, be assumed that the material properties would remain constant during such an unload-reload cycle and hence constant with time.

One element group characterizes the material properties of the 26 elements. The material properties of interest are the permeability k_v, k_h (conductivity k_v, k_h) and the product of $m_v \gamma_w$, $m_h \gamma_w$.

The choice of a one dimensional mesh reduces the problem to that of characterizing the variation of k_v and $m_v \gamma_w$ with depth. This can only be done if one assumes that $c_v = c_h$ and $k_v = k_h$. Clearly this requires justification and has initiated an extensive laboratory testing program on undisturbed samples retrieved from the I-95 test site.

An interesting observation worth mentioning concerns the possible conclusion of a reduced sensitivity of the excess pore pressure isocrones to the variation of the soil dissipation properties near the top boundary of the clay layer.

This could be due to the effect of the severe pumping experienced by the soil near the top boundary and it could very well be that the excess pore pressures near the top boundary are extensively affected by the boundary condition rather than by the actual effect of the excavation and construction. This fortunately would work to our advantage. If our assumption of $c_v/c_h = 1$ and $k_v/k_h = 1$ is not absolutely true, which we expect might be the case near the top boundary, the magnitude of the error thus induced in the resulting excess pore pressure isocrones would be attenuated by the effect of the dominating boundary condition.

The material property designations for the 26 elements could henceforth be easily deduced from Figures 9.27 and 9.28 and are tabulated in Table 9.5 .

9.7 ADINAT PREDICTED DISSIPATION CURVES

Figure 9.30 shows the predicted excess negative pore pressure dissipation curves. The loading curves are characterized by a step function that describes the various excavation and construction stages. Points a and b represent initial and final activities of stage I excavation potrayed in terms of the excess negative pore pressure induced (in feet of H_20) at the four locations of interest. Likewise, points c and d are indicative of stage II of excavation.

The remaining portion of the loading curve is concerned with the three major foundation mat pours (I,II&III) although there is no reason why the whole construction history of the Student Center cannot be specified given the exact quantity and location of the concrete pours and using the simple equilibrium equations, Figure 9.31.

$$\sum F_\sigma = 0 \Rightarrow \iint_A \sigma dxdy = P \Rightarrow \iint_A (\alpha x+\beta y+\gamma) dxdy = P$$

$$\sum M_x = 0 \Rightarrow \iint_A \sigma y dxdy = Py_o \Rightarrow \iint_A (\alpha x+\beta y+\gamma) y dxdy = Py_o$$

$$\sum M_y = 0 \Rightarrow \iint_A \sigma x dxdy = Px_o \quad \iint_A (\alpha x+\beta y+\gamma) x dxdy = Px_o$$

Solution of the system of simultaneous equations will yield values of the coefficients $\alpha,\beta\&\gamma$. By then using principal of superposition, coupled with numerical solutions developed by Poulos and Davis (1973), the stresses developed at any location of the compressible stratum could be evaluated.

The predicted dissipation curve corresponding to the variable profile of c_v appears as the solid curve on Figure 9.30. Several observations are sighted:

1. All four heading curves are minutely affected by Pour I and no appreciable stress increment is noted.
2. The effect of the stress increment induced by Pour II diminishes at shallower depths.

3. The stress increment induced by Pour III exhibits an opposite trend, i.e.; increases at shallower depths.
4. Agreement of predicted excess negative pore pressures with observed field values appears to be poor at the end of stage I of excavation. This could be primarily attributed to the in exact earth work quantities reported or sequence of removal.
5. Agreement is restored at the end of excavation stage II which would suggest that probably the distribution of earthwork removal between stage I and II is not accurate but the total stress release attributed to stages I and II is reasonable.
6. Agreement of predicted excess negative pore pressures with observed field values appears to be excellent after excavation stage II. Lack of agreement at the initial dissipation stage at the deepest piezometer (P-4) could be attributed to possible instrumentation error that has been detected in the reported values. Attention is drawn to the corresponding reported observed values of piezometer P-4 between 10/8/63 and 10/21/63 which are believed to be approximate. Perfect agreement resumes after this period which reinforces our hypothesis.

7. The predicted excess negative pore pressure dissipation curve corresponding to the shallowest piezometer agrees very well with field observed values of piezometer P-1 and also with observed values of well WSC-1. This clearly suggests that the top boundary condition dominates the pore pressure dissipation pattern for the shallow piezometer P-1. This tends to attenuate any possible errors that could be induced by assuming $c_v/c_h = 1.0$ & $k_v/k_h = 1.0$ at very shallow depths.

Figure 9.32 portrays the process of depletion of the excess negative pore pressure isocrones with time, Four snap shots of the pore pressure isocrones at t = and are superimposed. Two observations are sighted:

1. Agreement of predicted pore pressure isocrones with field values is excellent.
2. The value of predicted and observed pore pressure for shallow piezometer oscillates in sympathy with the boundary condition (effect of pumping).

A question of significance now arises: If the shallow piezometer P-1 is so dependent on the boundary condition was there any accured advantage of considering a variable C_v profile?

In order to answer this question, two additional computer runs were executed. In the first run, the value of c_v was held constant at a value of 0.04 cm^2/sec which is equal to

that of the bottom 40 feet. The corresponding excess pore pressure isocrone is shown in Figure 9.33. Another run in which the value of $\bar{c}_v$ was held at a value of .15 cm^2/sec equivalent to the value of c_v at an elevation of 12.5 ft (top boundary), was executed and the corresponding excess pore pressure isocrone shown in Figure 9.33. Several observations are sighted:

1. The error induced by using a constant value of $\bar{c}_v$ = 0.04 ft^2/sec is an increase of approximately 8% at shallow depths and increase in magnitude to approximately 20% in the vacinity of PSC-2.
2. The error induced by using a constant value of c_v = 0.04 ft^2/sec decreases to approximately 3% as we approach the bottom boundary.
3. The error induced by using a constant value of c_v = .15 cm^2/sec in a decrease of approximately 52%. The magnitude of the error reduces to approximately zero in the close vacinity of PSC-1.
4. Moving away from the center line of the compressible stratum, the pore pressure isocrone is more dependent on the local value of c_v and the boundary conditions immediately adjacent.

We can thus conclude that the boundary condition probably has a significant effect at shallow depths but there is a definite increase in the value of c_v and it's prescribed variation with depth is probably a very good representation of the state of nature.

9.8 CONCLUSIONS

1. Traditional consolidation analysis based on Terzaghi's governing field equation disregard variation of k_v and m_v.
2. Excess pore pressure isocrones are very sensitive to variations in the value of the permeability k_v and not so sensitive to the variation in the value of m_v with depth.
3. A new computer program ADINAT developed for heat transfer problems could be used to solve transient flow analysis with due regard to existing analog between the governing field equations.
4. Boston Blue Clay exhibits normalized behavior in as far as compressibility is concerned and hence is independent of maximum past pressure. Correlation of values of c_v based on equivalent values of OCR is possible.
5. Predicted dissipation records of excess negative pore pressures agree very well with observed field values.

6. Significant advantages are accrued from use of a variable c_v profile. Errors of up to 20 to 50% in the prediction of excess pore pressure isocrones could result from use of a constant value of c_v.
7. Piezometers located close to the boundary are affected by local values of c_v and boundary conditions.
8. Assumptions of $c_{vs} = c_{vc}$, $c_{vv} = c_{vh}$ and $k_h = k_v$ should be verified experimentally or otherwise.

LOCATION	VERTICAL STRESS (kg/cm^2)	PERCENT COMPRESSION (%)	m_{vc}/m_{vs}	k_v	c_{vc}/c_{vs}	DATA ITEM
A	3.923*	12.385	0.0334	0.407×10^{-7}	0.1210×10^{-2}	56
B	1.928**	12.184	0.00298	0.462×10^{-7}	0.1551×10^{-1}	59
C	8.426*	18.9670	0.01216	0.225×10^{-7}	0.1850×10^{-2}	113
D	3.75**	18.6320	0.0019	0.253×10^{-7}	0.132×10^{-1}	117

*On virgin compression prior to unloading.

**On unloading branch with OCR=2.

$$\frac{C_{vs}^{B} - C_{vs}^{D}}{C_{vsB}} \times 100 = 15\%$$

Table 9.1 C.R.S.C data on a sample of B.B.C retrieved from a depth of 90.89 feet

NODE	X	Y	ELEVATION	ELEVATION OF MID POINT OF ELEMENT	ELEMENT #
1	0	0	78.5	77.25	1
2	0	2.5	76.0	74.75	2
3	0	5.0	73.5	72.25	3
4	0	7.5	71.0	69.75	4
5	0	10	68.5	67.25	5
6	0	12.5	66.0	64.75	6
7	0	15.0	63.5	62.25	7
8	0	17.5	61.0	59.75	8
9	0	20.0	58.5	57.25	9
10	0	22.5	56.0	54.75	10
11	0	25.0	53.5	52.25	11
12	0	27.5	51.0	49.75	12
13	0	30.0	48.5	46.75	13
14	0	33.5	45.0	43.75	14
15	0	36.0	42.5	41.25	15
16	0	38.5	40.0	38.75	16
17	0	41.0	37.5	36.25	17
18	0	43.5	35.0	33.75	18
19	0	46.0	32.5	31.25	19
20	0	48.5	30.0	28.75	20
21	0	51.0	27.5	26.25	21
22	0	53.5	25.0	23.75	22
23	0	56.0	22.5	21.25	23
24	0	58.5	20.0	18.75	24
25	0	61.0	17.5	16.25	25
26	0	63.5	15.0	13.75	26
27	0	66.0	12.5	-	

Total thickness of clay layer = 66 ft

Table 9.2 The finite element mesh,nodal points and element designations

CUMULATIVE TIME (DAYS)	EXCESS NEGATIVE P.P. (FT OF H_2O)
73.00000	-0.1192D+02
74.00000	-0.1242D+02
76.00000	-0.1230D+02
77.00000	-0.1234D+02
78.00000	-0.1062D+02
81.00000	-0.1207D+02
84.00000	-0.1192D+02
9 .00000	-0.1177D+02
92.00000	-0.1182D+02
97.00000	-0.1103D+02
104.00000	-0.9730D+01
109.00000	-0.9280D+01
111.00000	-0.9490D+01
113.00000	-0.9380D+01
118.00000	-0.9340D+01
120.00000	-0.9280D+01
123.00000	-0.1040D+02
124.00000	-0.1105D+02
125.00000	-0.1074D+02
126.00000	-0.1044D+02
128.00000	-0.9980D+01
129.00000	-0.1036D+02
131.00000	-0.9920D+01
133.00000	-0.9920D+01
136.00000	-0.9610D+01
138.00000	-0.9740D+01
141.00000	-0.9510D+01
143.00000	-0.9740D+01
145.00000	-0.9630D+01
148.00000	-0.9840D+01
150.00000	-0.9550D+01
155.00000	-0.8840D+01
157.00000	-0.8110D+01
159.00000	-0.8030D+01
162.00000	-0.7150D+01
164.00000	-0.6920D+01
168.00000	-0.7170D+01

Table 9.3 (cont.) The excess negative pore pressures generated at the top boundary due to pumping.

CUMULATIVE TIME (DAYS)	EXCESS NEGATIVE P.P. (FT OF H_2O)
0.0	-0.1900D+00
1.50000	-0.2600D+00
3.00000	-0.3300D+00
5.00000	-0.2700D+00
6.00000	-0.1900D+00
7.00000	-0.1900D+00
8.00000	-0.2700D+00
10.00000	-0.1500D+00
11.00000	-0.2800D+00
12.00000	-0.1800D+00
15.00000	-0.7490D+01
16.00000	-0.6530D+01
18.00000	-0.1085D+02
19.00000	-0.1147D+02
20.00000	-0.1222D+02
21.00000	-0.1165D+02
22.00000	-0.1146D+02
24.00000	-0.1169D+02
25.00000	-0.1178D+02
26.00000	-0.1186D+02
27.00000	-0.1194D+02
28.00000	-0.1161D+02
29.00000	-0.1111D+02
30.00000	-0.1061D+02
31.00000	-0.1103D+02
32.00000	-0.1090D+02
33.00000	-0.1119D+02
34.00000	-0.1144D+02
35.00000	-0.1140D+02
36.00000	-0.1232D+02
39.00000	-0.1298D+02
40.00000	-0.1323D+02
41.00000	-0.1323D+02
42.00000	-0.1319D+02
44.00000	-0.1311D+02
45.00000	-0.1348D+02
46.00000	-0.1340D+02
47.00000	-0.1328D+02
50.00000	-0.1288D+02
53.00000	-0.1273D+02
56.00000	-0.1277D+02
57.00000	-0.1221D+02
60.00000	-0.1281D+02
64.00000	-0.1257D+02
67.00000	-0.1217D+02

Table 9.3 The excess negative pore pressures generated at the top boundary due to pumping.

ELEMENT NUMBER	POUR I (ft of H_2O)	POUR II (ft of H_2O)	POUR III (ft of H_2O)	POUR IV (ft of H_2O)
1	.1575	2.2786	4.5636	1.835
2	.1270	2.2342	4.6909	1.8174
3	.0965	2.1899	4.8181	1.7998
4	.0660	2.1456	4.9454	1.7822
5	.0355	2.10125	5.072	1.7646
6	.0050	2.0569	5.200	1.747
7	-.002	1.994	5.4509	1.67992
8	-.009	1.9313	5.6600	1.6128
9	-.016	1.8685	5.8691	1.5457
10	-.023	1.80578	6.0782	1.47868
11	-.030	1.743	6.2872	1.4116
12	-.040	1.6505	6.350	1.3247
13	-.040	1.558	6.5578	1.2379
14	-.040	1.4655	6.9144	1.15115
15	-.040	1.373	7.271	1.06433
16	-.040	1.2805	7.8650	.9775
17	-.040	1.188	8.155	.8907
18	-.0325	.9812	8.440	.7386
19	-.025	.77455	8.7361	.58649
20	-.0175	.5678	9.026	.4344
21	-.010	.3611	9.3168	.28228
22	-.008	.2888	9.404	.22582
23	-.006	.21666	9.5733	.16937
24	-.004	.1444	9.6729	.1129I2
25	-.002	.07222	9.7726	.0564
26	0.0	0.0	9.932	0.0

Table 9.4 Stress distribution for the foundation mat pours.

ELEMENT NUMBER	PERMEABILITY k(ft/day)	COEFFICIENT OF VOLUME CHANGE c_v(ft^2/day)	COEFFICIENT OF COMPRESSIBILITY $m_v \times \gamma_w$ (1/ft)
1	2.976×10^{-4}	3.72	8.0000×10^{-5}
2	3.1181×10^{-4}	3.72	8.3819×10^{-5}
3	3.401×10^{-4}	3.72	9.1425×10^{-5}
4	3.628×10^{-4}	3.72	9.75268×10^{-5}
5	3.9118×10^{-4}	3.72	1.05155×10^{-4}
6	4.2519×10^{-4}	3.72	1.14298×10^{-4}
7	4.535×10^{-4}	3.72	1.21908×10^{-4}
8	4.8189×10^{-4}	3.72	1.2954×10^{-4}
9	5.2441×10^{-4}	3.72	1.4097×10^{-4}
10	5.8110×10^{-4}	3.72	1.5621×10^{-4}
11	6.3779×10^{-4}	3.72	1.7144×10^{-4}
12	6.8031×10^{-4}	3.72	1.8288×10^{-4}
13	7.6535×10^{-4}	3.72	2.0574×10^{-4}
14	8.7023×10^{-4}	3.813	2.2827×10^{-4}
15	9.6378×10^{-4}	3.999	2.4100×10^{-4}
16	1.0771×10^{-3}	4.185	2.5737×10^{-4}
17	1.2189×10^{-3}	4.464	2.7305×10^{-4}
18	1.4173×10^{-3}	4.882	2.90311×10^{-4}
19	1.7008×10^{-3}	5.3940	3.15313×10^{-4}
20	2.1543×10^{-3}	5.952	3.6194×10^{-4}
21	2.6645×10^{-3}	6.696	3.9792×10^{-4}
22	3.4015×10^{-3}	7.626	4.4604×10^{-4}
23	4.3937×10^{-3}	8.649	5.0800×10^{-4}
24	5.2441×10^{-3}	9.765	5.3703×10^{-4}
25	7.6535×10^{-3}	11.160	6.8579×10^{-4}
26	9.9212×10^{-3}	13.02	7.61997×10^{-4}

Table 9.5 The finite element material properties.

OCR	ELEVATION UPPER LIMIT	EQUIVALENT ELEVATION UPPER LIMIT	C_h	ELEVATION MEDIAN	EQUIVALENT ELEVATION MEDIAN	C_h	ELEVATION LOWER LIMIT	EQUIVALENT ELEVATION LOWER LIMIT	C_h
1	47.5	64	.04	60	72.5	.04	65	-	
1.5	36.5	53	.044	46	60	.04	52.5	67.5	.04
2	27	46	.06	37.5	52	.047	44.5	58	.04
2.5	18	40	.09	30	45	.064	37	51	.047
3	10	35	.145	23	40.5	.09	30	45.5	.062
3.5	4	31.5	.23	16.5	36.0	.13	23.0	41.0	.084
4	0	28	.37	10	32.5	.195	17	37.0	.115

Table 9.6 Derivation of the material properties by correlating the Student Center and the I-95 test site with respect to their OCRs .

TO FIND VARIATION OF K WITH ELEVATION

(a) Correlation with respect to OCR

OCR	ELEVATION UPPER LIMIT	EQUIVALENT ELEVATION UPPER LIMIT	K	ELEVATION MEDIAN	EQUIVALENT ELEVATION MEDIAN	K	ELEVATION LOWER LIMIT	EQUIVALENT ELEVATION LOWER LIMIT	K
1	47.5	64	2.5×10^{-7}	60	72.5	2×10^{-7}	65	-	
1.5	36.5	53	4.2×10^{-7}	46	60	3×10^{-7}	52.5	67.5	2.2×10^{-7}
2	27	46	7.4×10^{-7}	37.5	52	4.3×10^{-7}	44.5	58	3.0×10^{-7}
2.5	18	40	1.5×10^{-6}	30	45	8.0×10^{-7}	37	51	5.0×10^{-7}
3	10	35	3.2×10^{-6}	23	40.5	1.5×10^{-6}	30	45.5	8.1×10^{-7}
3.5	4	31.5	6.3×10^{-6}	16.5	36.0	3.0×10^{-6}	23.0	41.0	1.3×10^{-6}
4	0	28	1.8×10^{-5}	10	32.5	6.0×10^{-6}	17.0	37.0	2.25×10^{-6}

Table 9.7 Derivation of the variation of the coefficient of permeability by correlating the Student Center and the I-95 test site with respect to their OCRs.

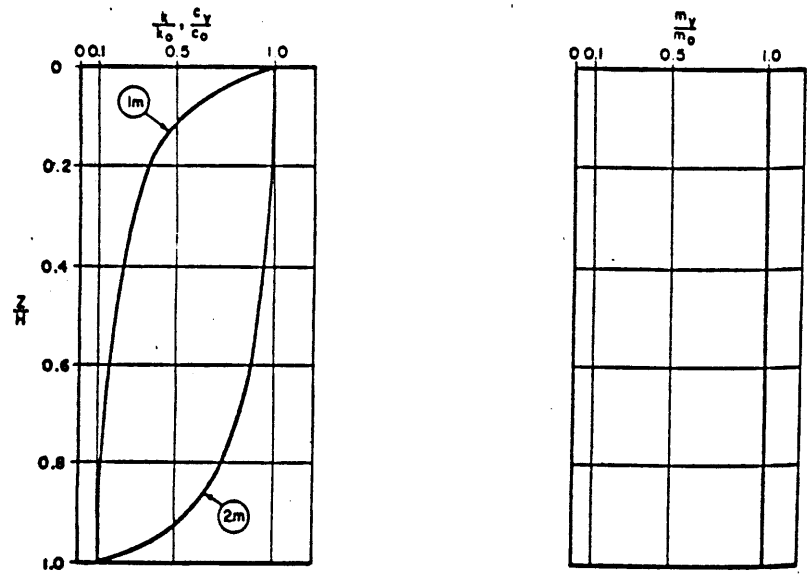

Figure 9.1 Consolidation parameters: constant compressibility, polynomial variation (tenfold decrease)

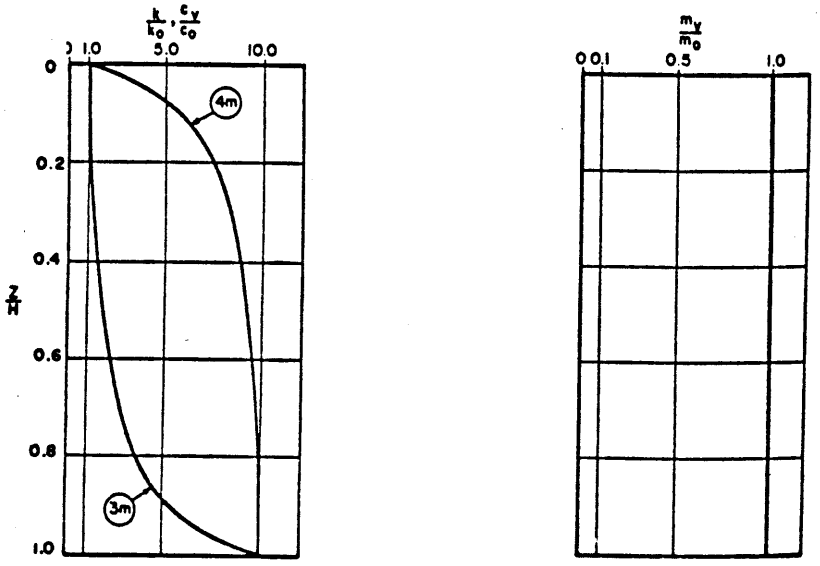

Figure 9.2 Consolidation parameters: constant copressibility,polynomial variation (tenfold increase)

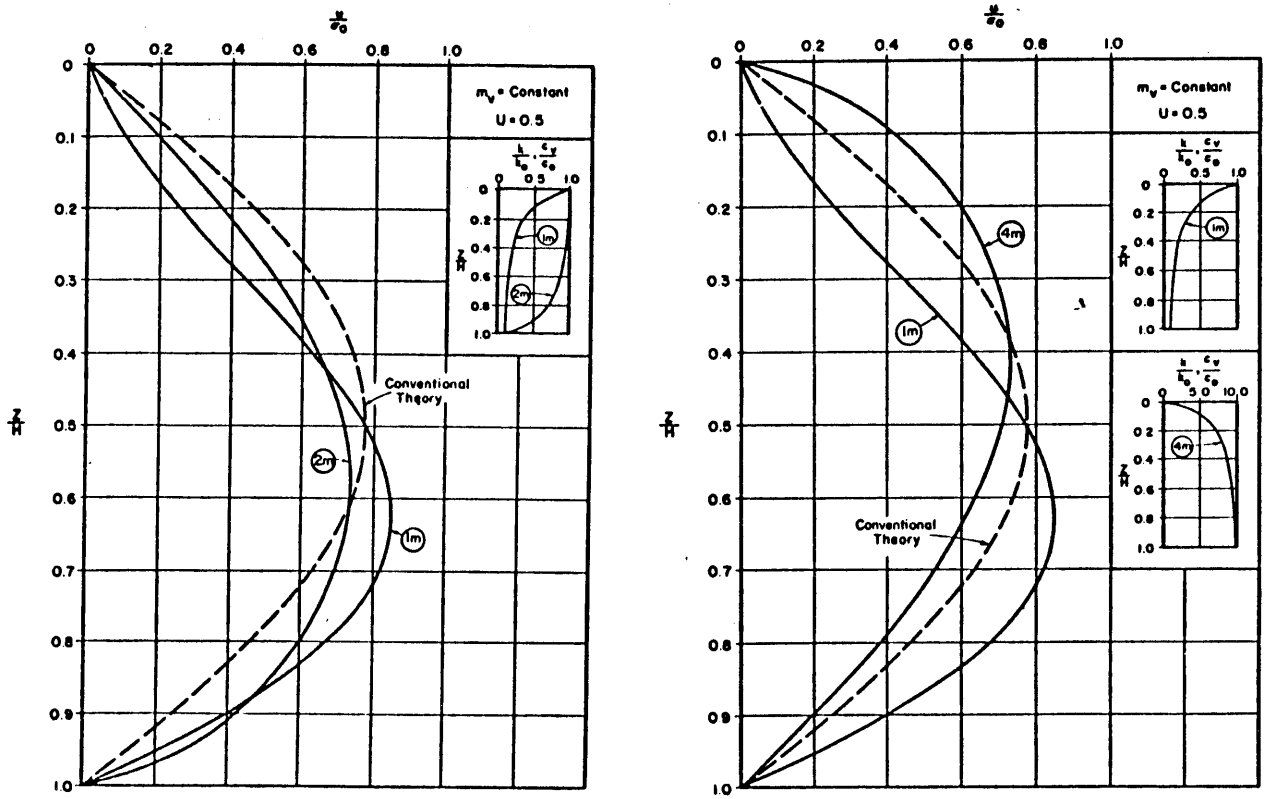

Figure 9.3 Pore pressure isocrones : constant compressibility, polynomial variation.

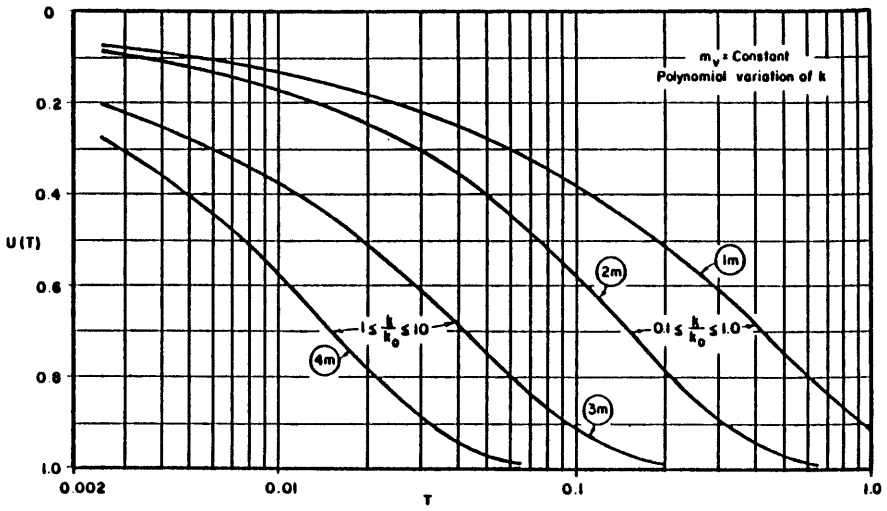

Figure 9.4 Consolidation time-settlement relations:constant compressibility, polynomial variation.

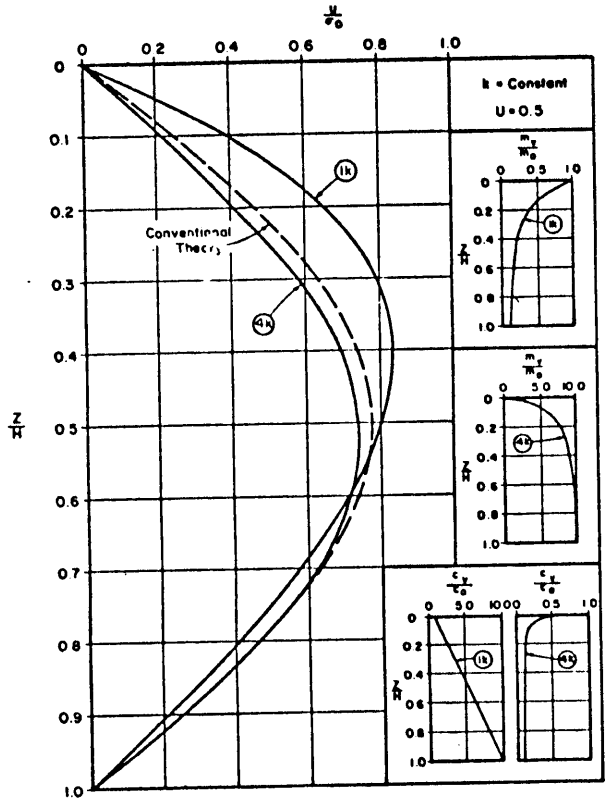

Figure 9.6 Pore pressure: constant permeability, polynomial variation.

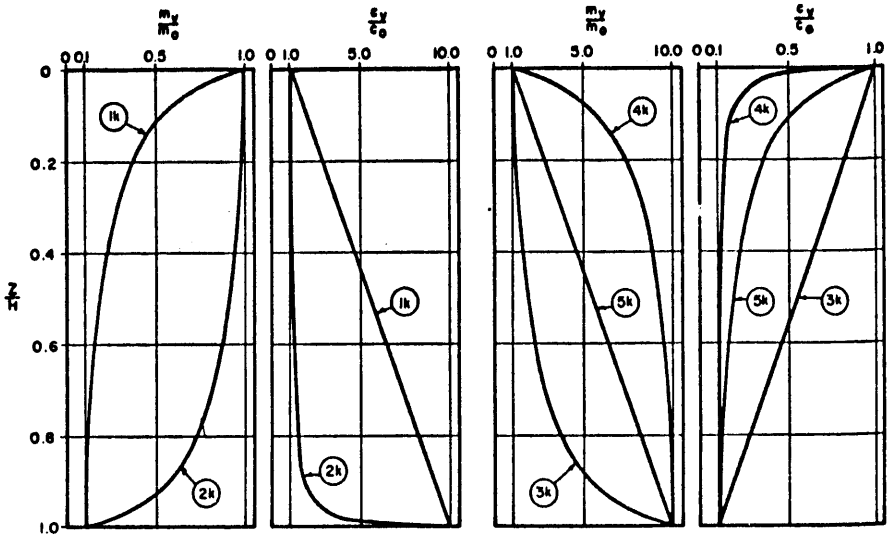

Figure 9.5 Consolidation parameters: constant permeability, polynomial variation.

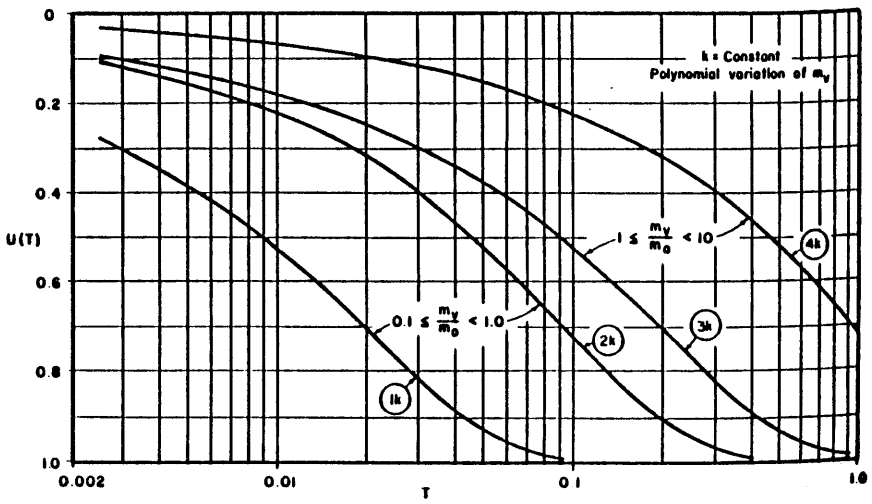

Figure 9.7 Consolidation time-settlement relations: constant permeability, polynomial variation.

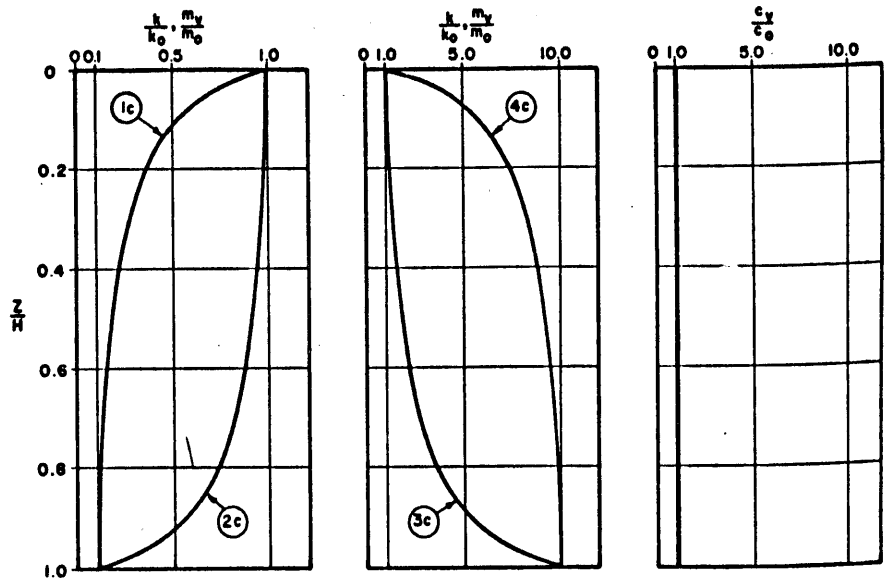

Figure 9.8 Consolidation parameters: constant coefficient of consolidation, polynomial variation.

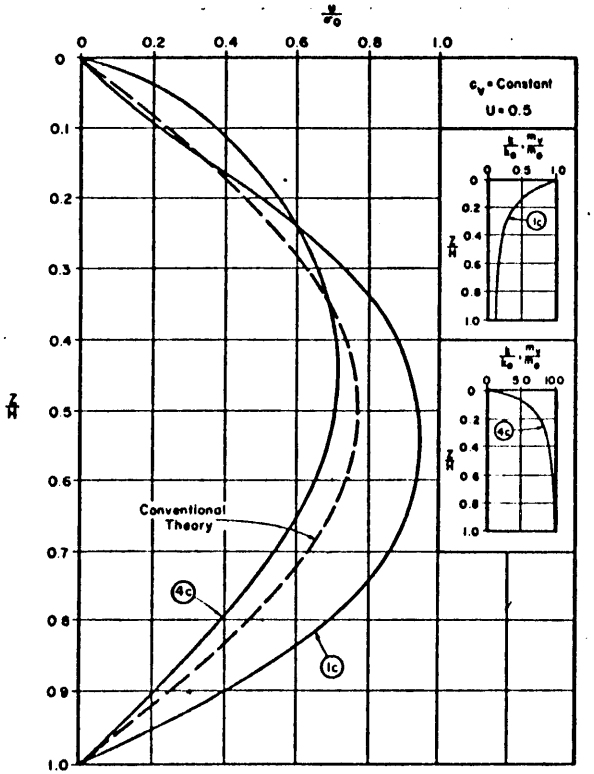

Figure 9.9 Pore pressure isocrones constant coefficient of consolidation, polynomial variation.

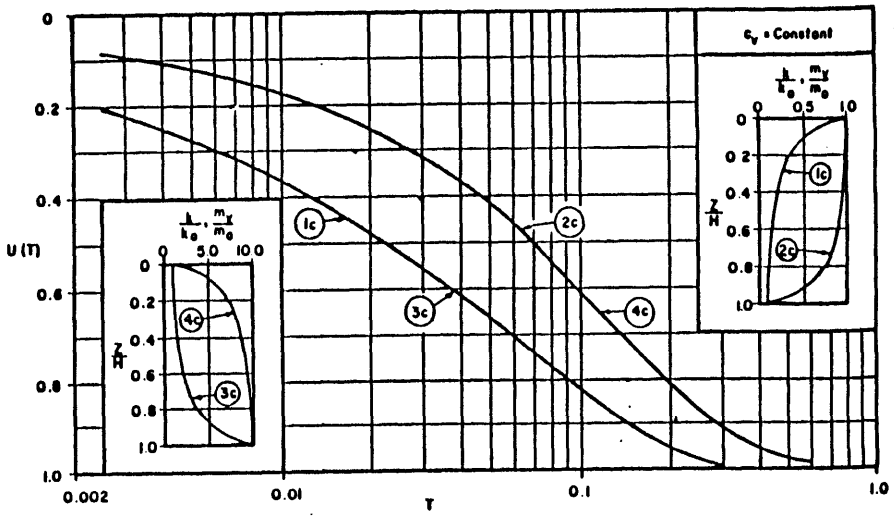

Figure 9.10 Consolidation time-settlement relations:constant coefficient of consolidation,polynomial variation.

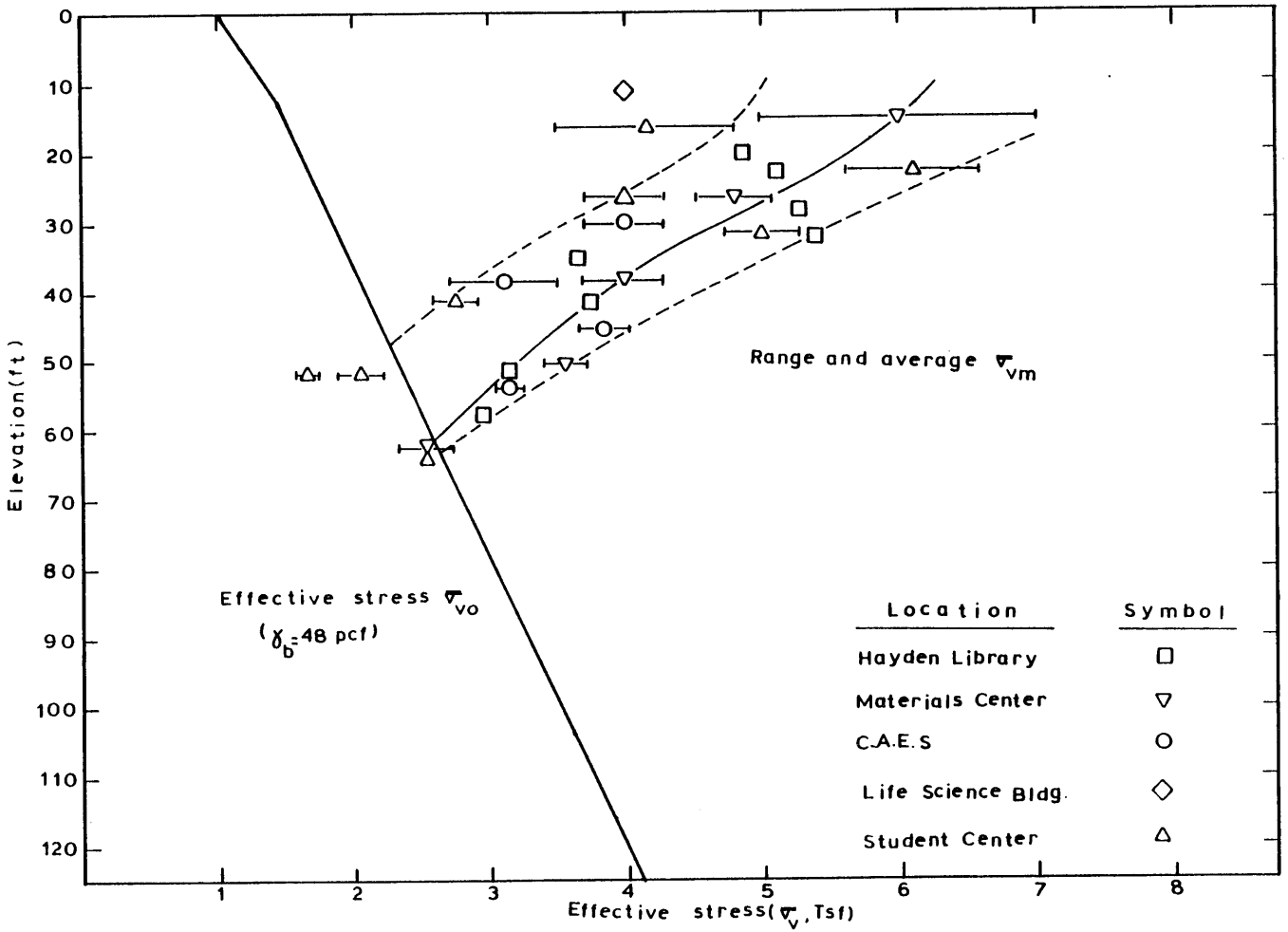

Figure 9.11 Stress history of the B.B.C stratum under the specified locations.

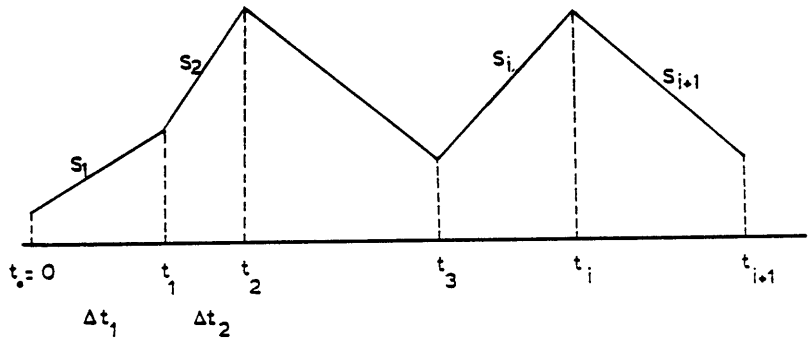

TIME	SLOPE
$t_o=0$	S_1
$t_1-\varepsilon$	S_1
$t_1+\varepsilon$	S_2
.	.
.	.
$t_i-\varepsilon$	S_i
$t_i+\varepsilon$	S_{i+1}

Choose $\varepsilon << \Delta t_i$

Figure 9.12 Modification of slope of loading curve for A.D.I.N.A.T. input purposes for for the case of a "broken line"representation of the loadig curve.

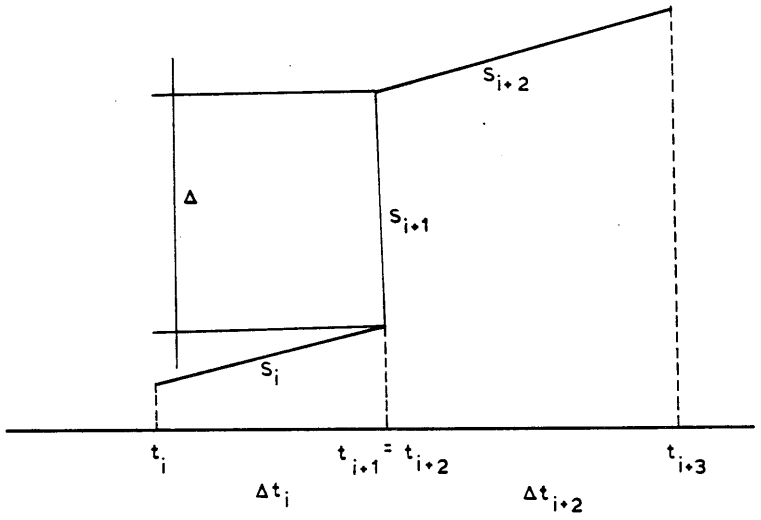

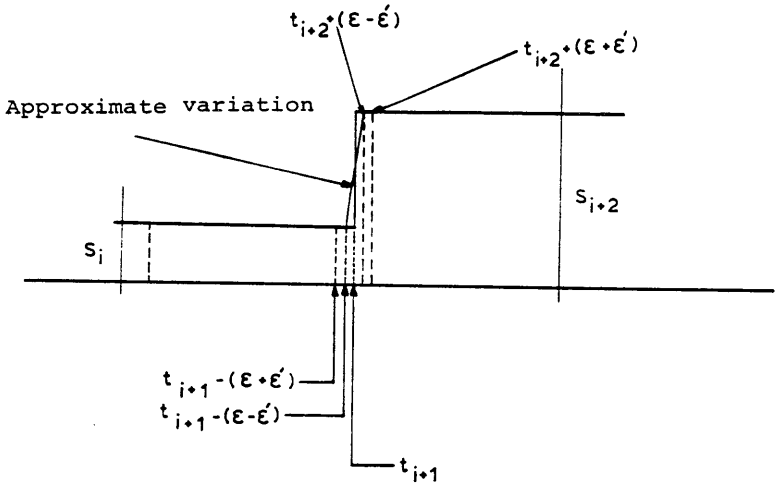

Figure 9.13 Modification of slope of loading curve for A.D.I.N.A.T. input purposes for the case of a discontinuous loading curve.

TIME	SLOPE
t_i	s_i
$t_{i+1}{}^{-\varepsilon-\varepsilon'}$	s_i
$t_{i+1}{}^{-\varepsilon+\varepsilon'}$	$\hat{s}_i$
$t_{i+2}{}^{+\varepsilon-\varepsilon'}$	$\hat{s}_i$
$t_{i+2}{}^{+\varepsilon+\varepsilon'}$	$s_i{}^{+2}$
t_{i+3}	$s_i{}^{+2}$

$$\text{if } s_i = s_{i+2} = 0 \quad \Rightarrow \quad \hat{s}_i = \frac{\Delta}{2\varepsilon} \quad \text{if } \varepsilon = .1 \quad \Rightarrow \hat{s}_i = \frac{\Delta}{.2}$$

Figure 9.13 (cont.) Modification of slope of loading curve for A.D.I.N.A.T. input purposes for the case of a discontinuous loading curve.

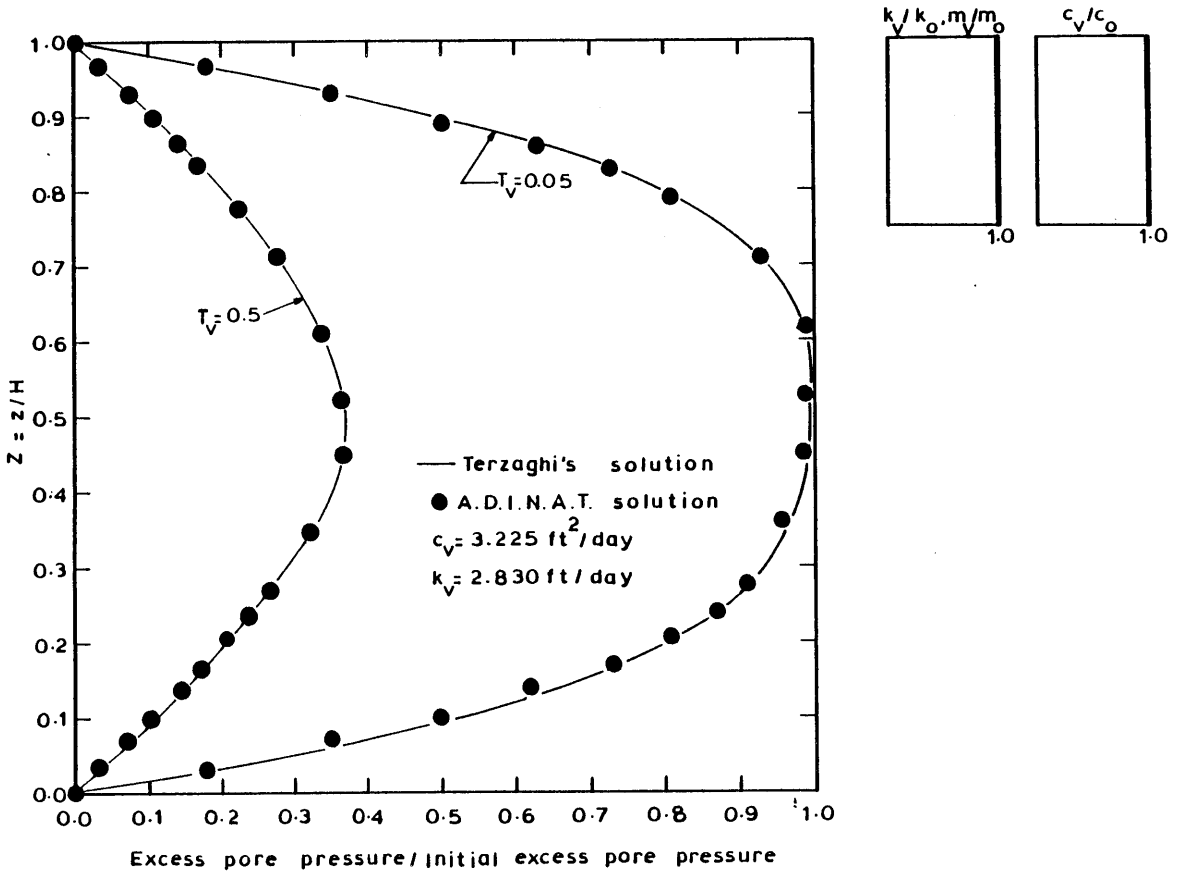

Figure 9.14 Comparison of predicted pore pressure isocrones with Terzaghi's solution for constant values of the permeability, compressibility and coefficient of consolidation.

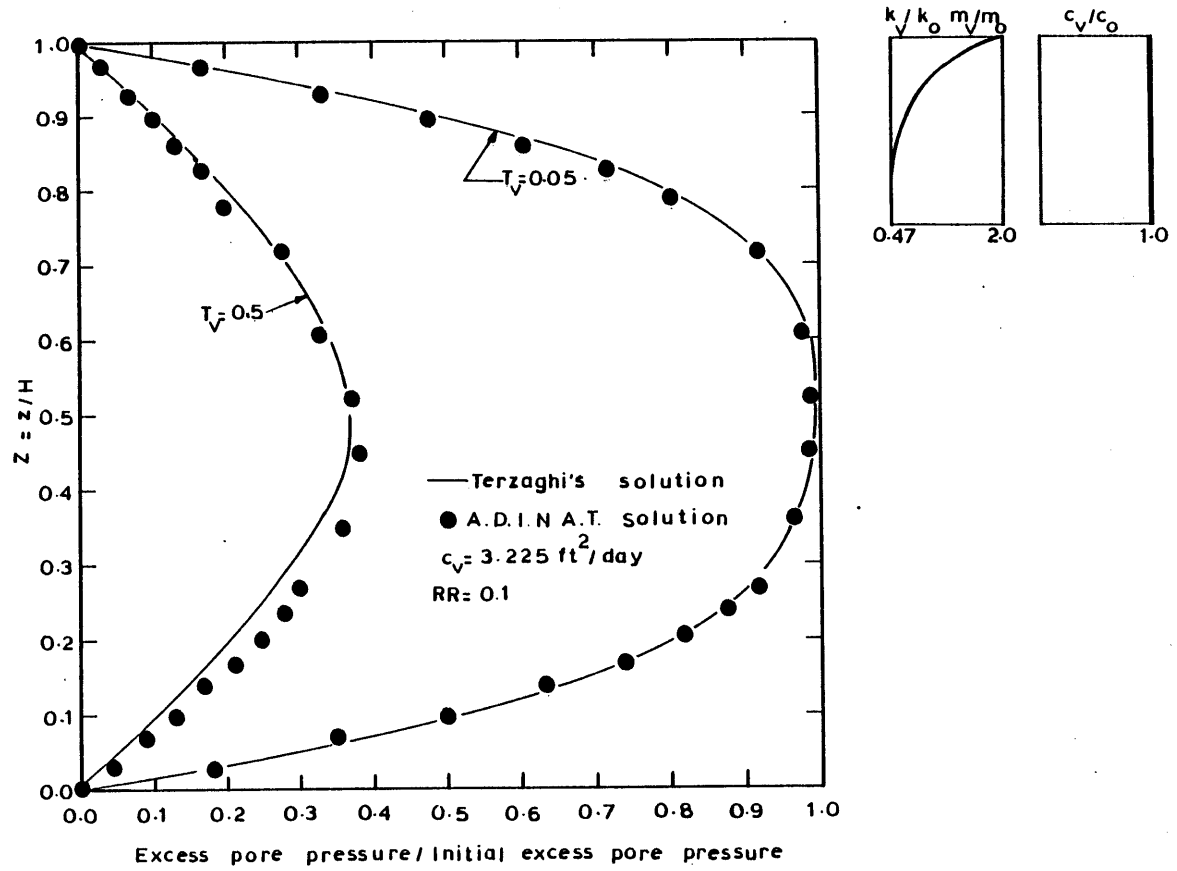

Figure 9.15 (b) Comparison of predicted pore pressures isocrones with Terzaghi's solution for a constant value of RR = 0.01 and a constant coefficient of consolidation.

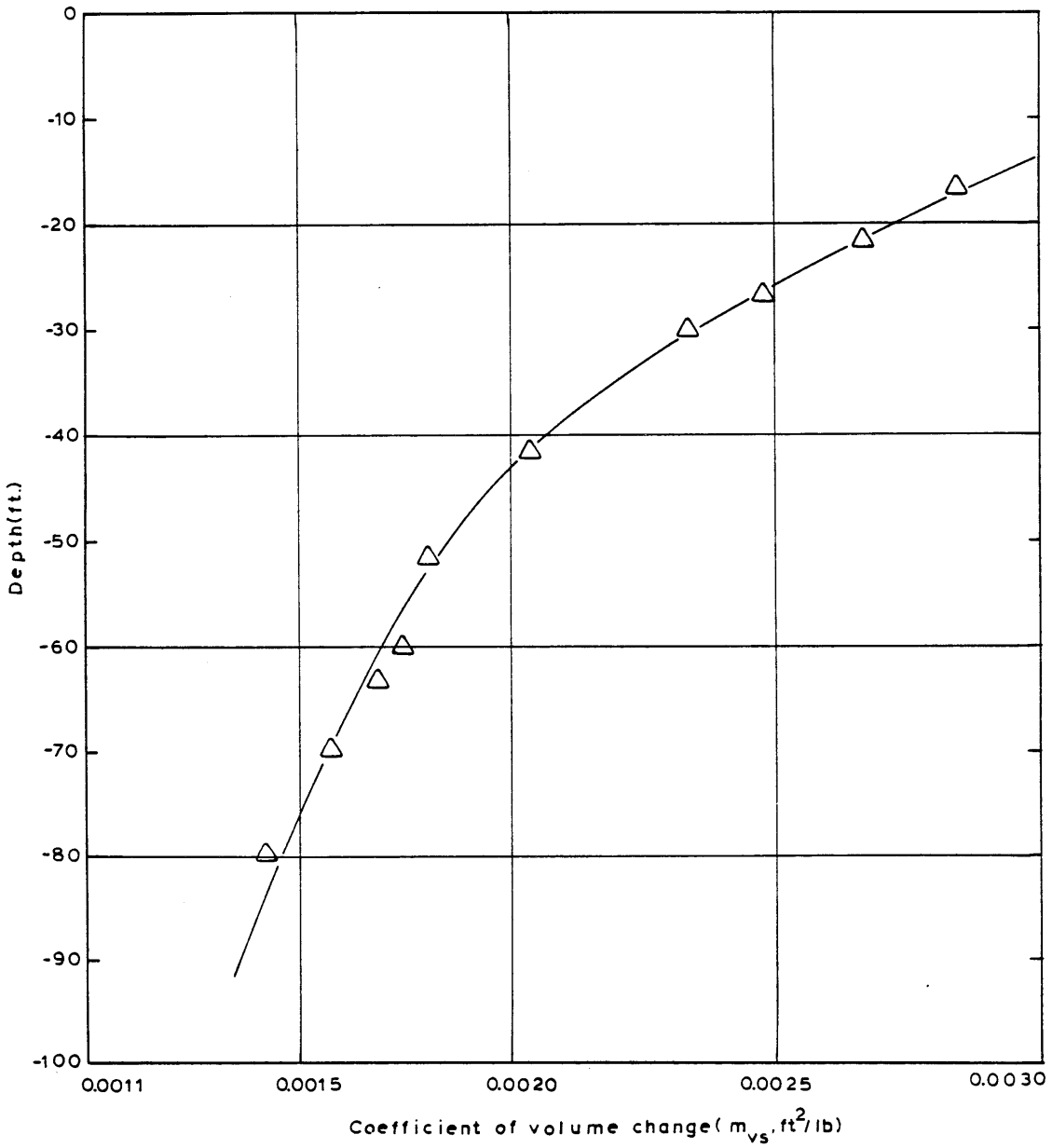

Figure 9.15 (a) Variation of coefficient of volume change with depth assuming a recompression ratio, RR = 0.01, and a coefficient of consolidation, c_v = 3.255 ft.^{2}/day.

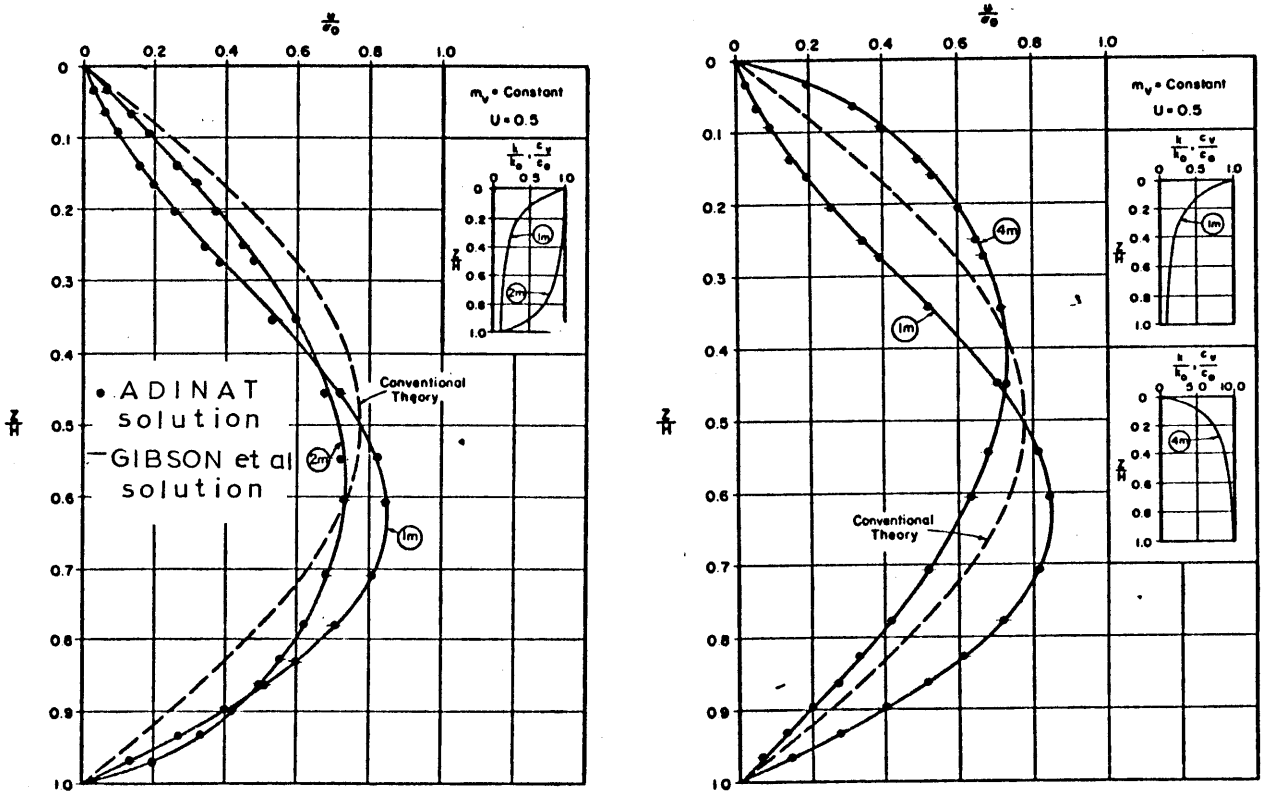

Figure 9.16 Comparison of pore pressure isocrones for T_v = 50% as predicted by A.D.I.N.A.T. computer program and closed form solution proposed by Gibson et. al. for the case of constant compressibility, polynomial variation.

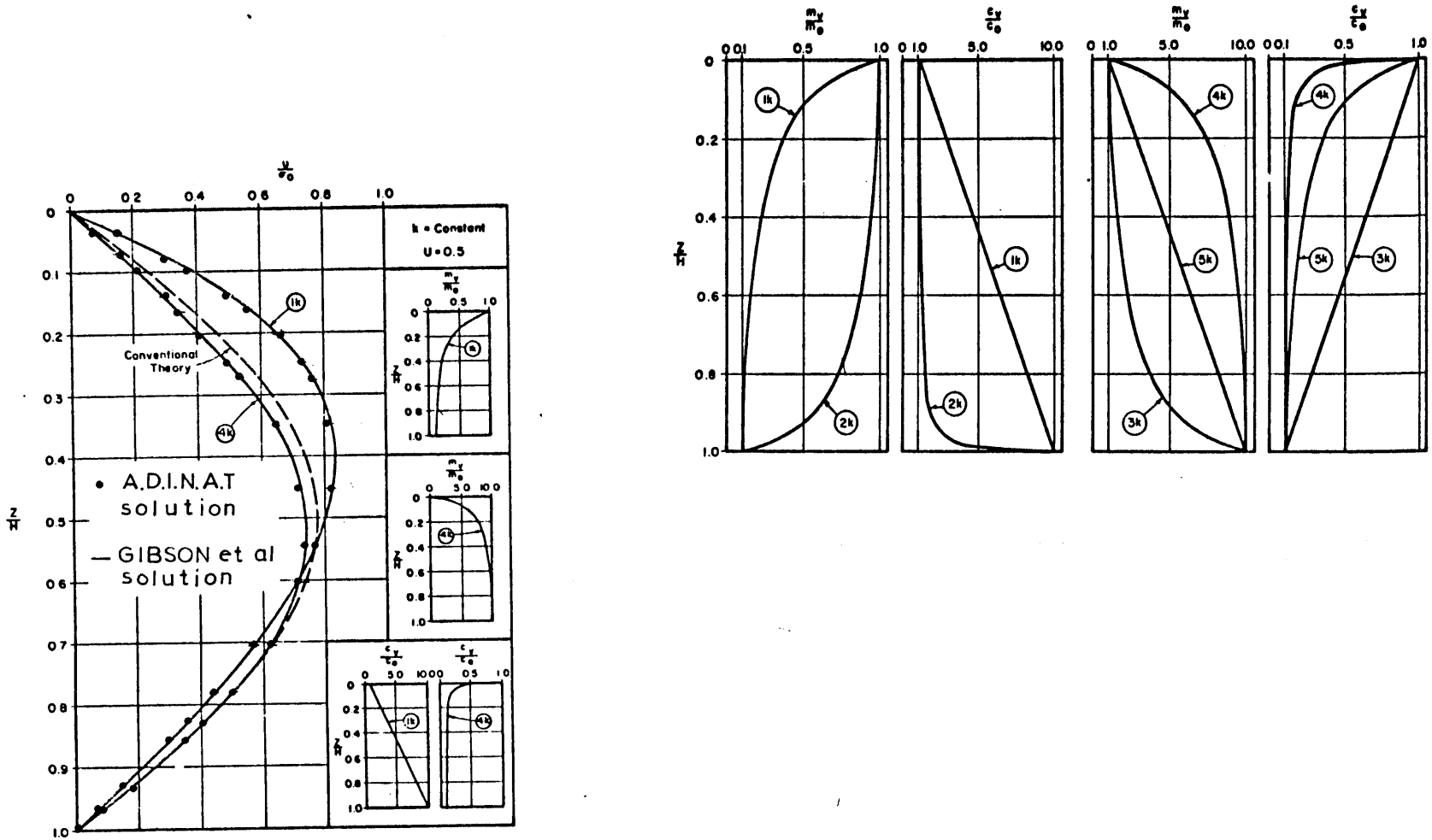

Figure 9.17 Comparison of pore pressure isocrones for T_v = 50% as predicted by A.D.I.N.A.T. computer program and the closed form solution proposed by Gibson et. al. for the case of constant permeability, polynomial variation.

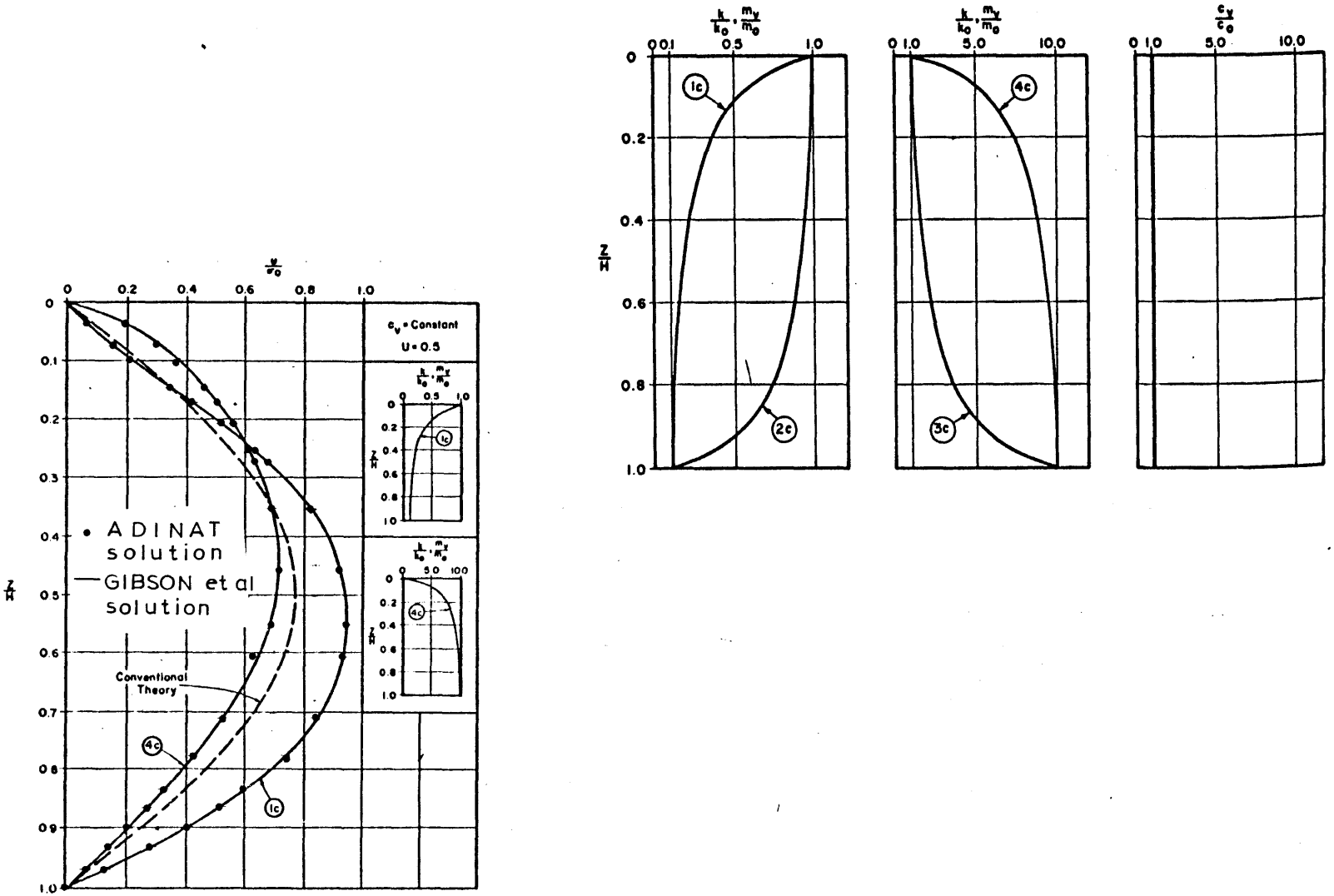

Figure 9.18 Comparison of pore pressure isocrones for T_v = 50% as predicted by A.D.I.N.A.T computer program and the closed form solution proposed by Gibson et. al. for the case of constant coefficient of consolidation, polynomial variation.

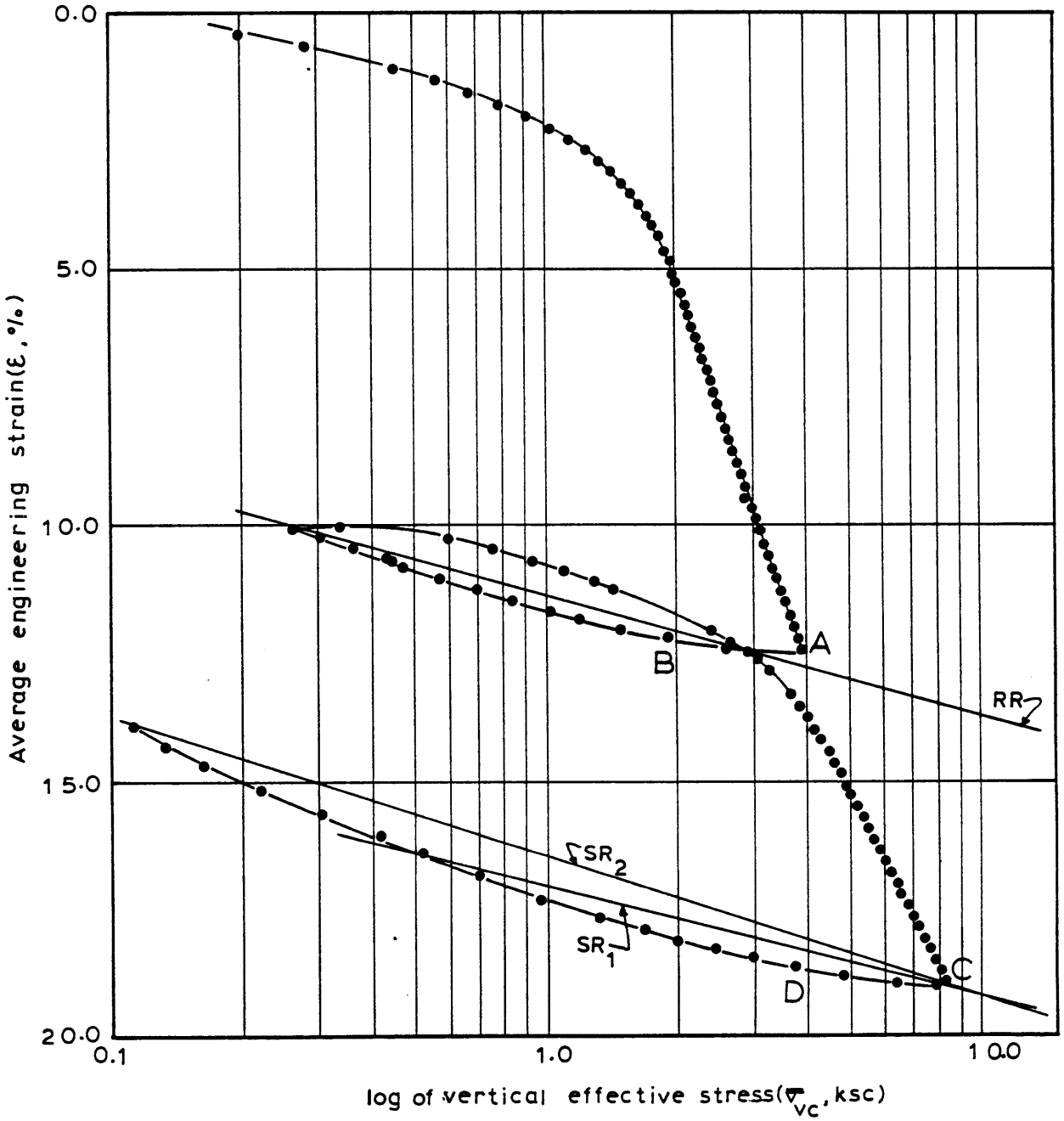

Figure 9.19 Compression curve of a sample of B.B.C retrieved from a depth of 90.89.

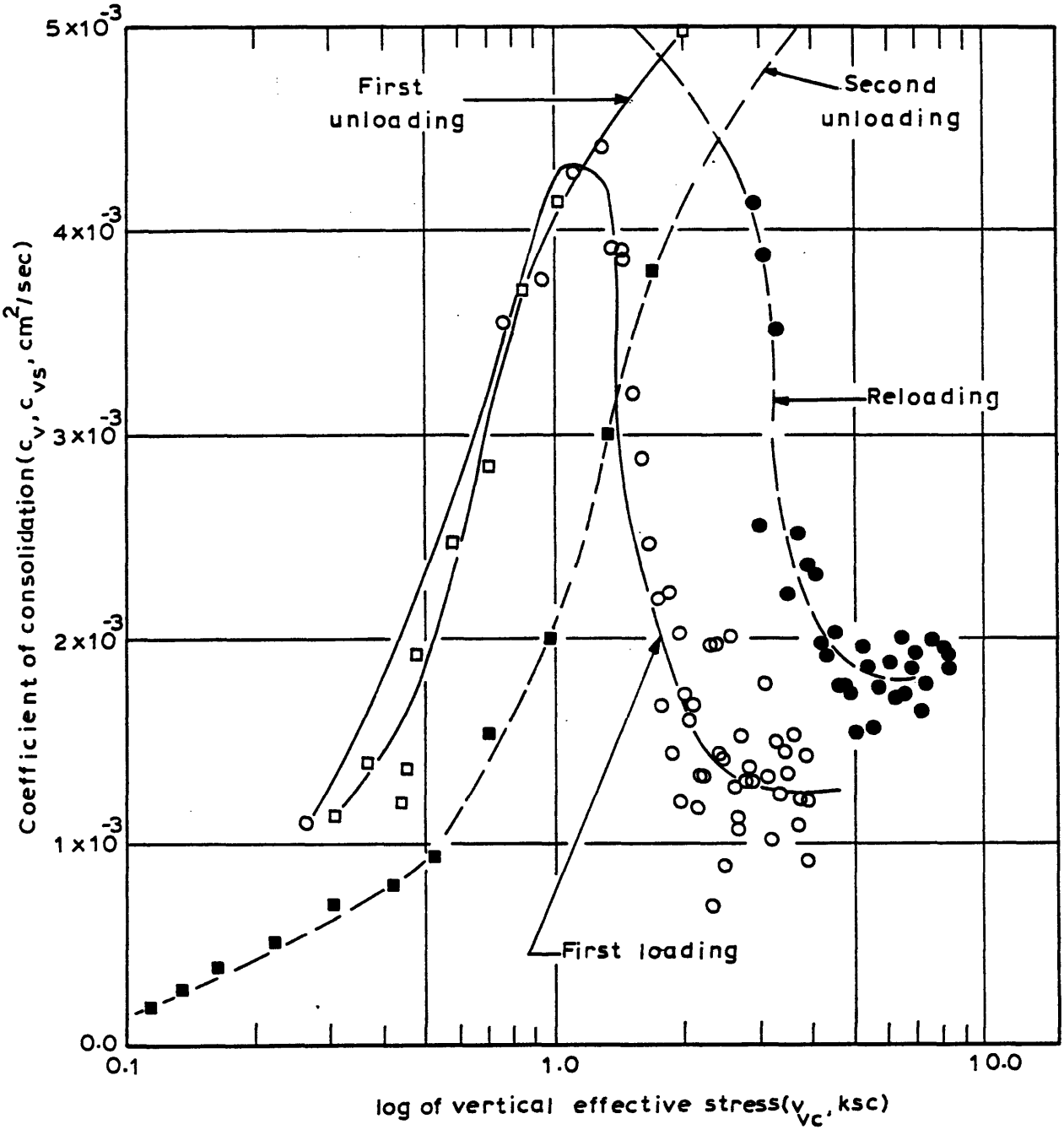

Figure 9.20 Variation of the coefficient of consolidation with the consolidation stress for a sample of B.B.C retrieved from a depth of 90.89 feet.

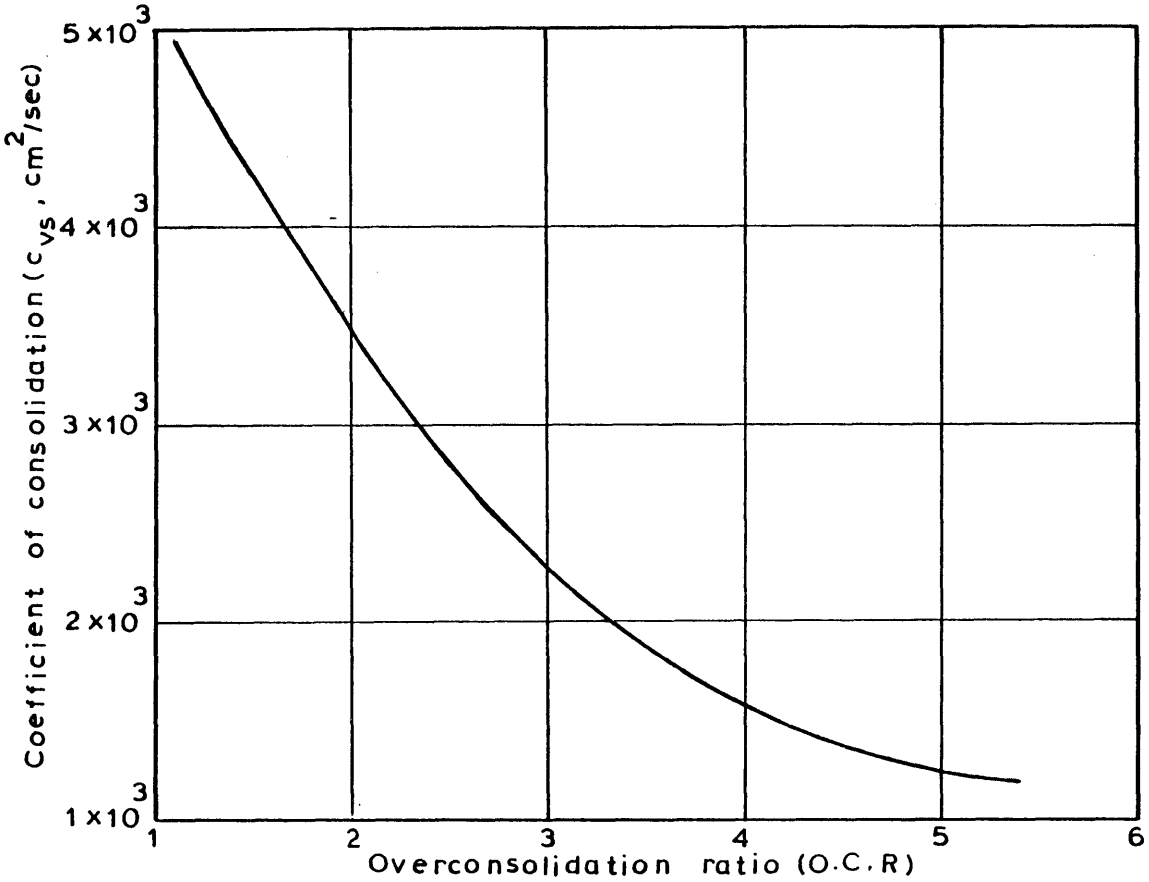

Figure 9.21 Idealized behavior of the variation of the coefficient of consolidation with the over consolidation ratio.

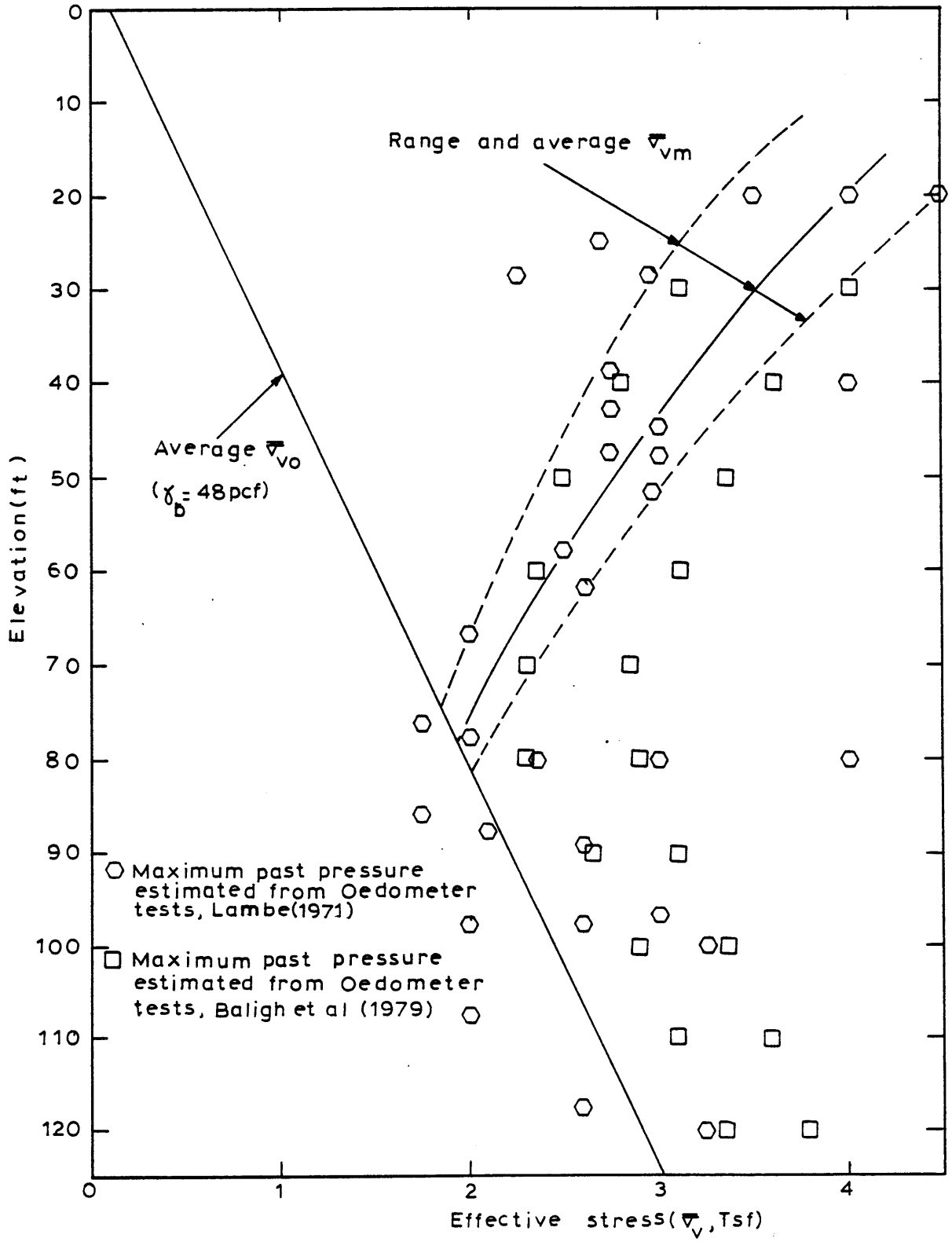

Figure 9.22 Stress history of the B.B.C stratum under the I-95 test site.

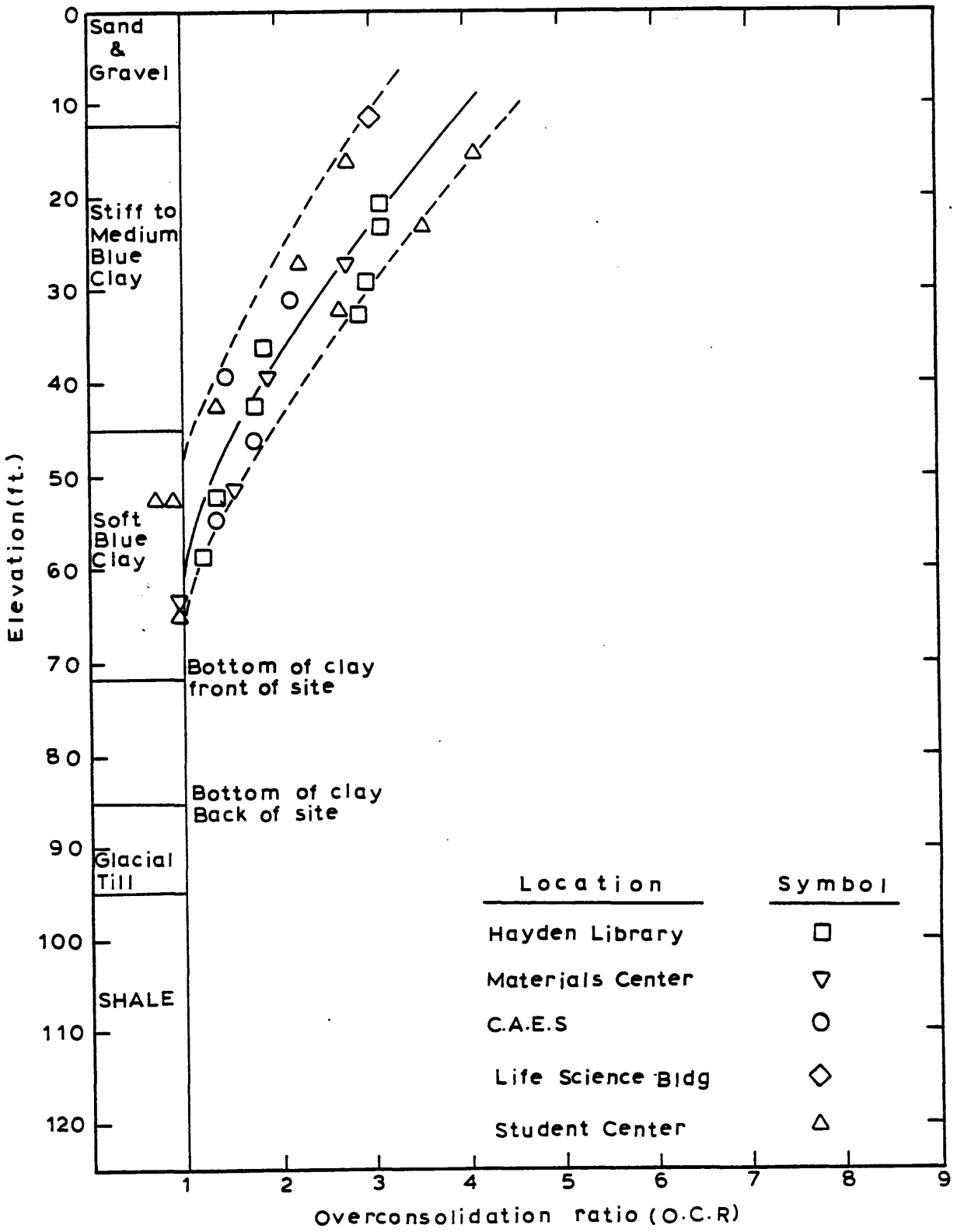

Figure 9.23 Variation of the overconsolidation ratio with elevation for the B.B.C stratum under the specified locations.

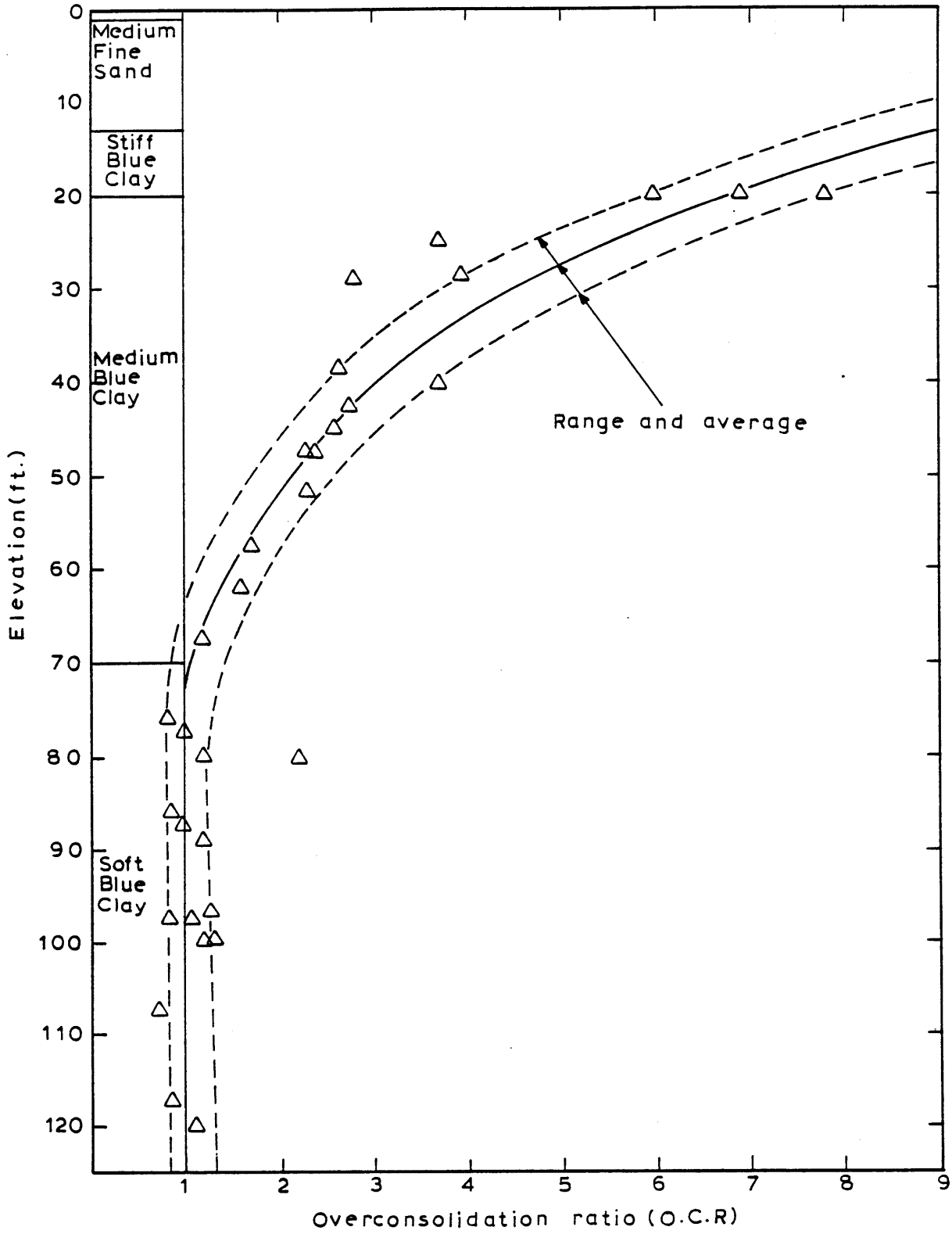

Figure 9.24 Variation of the overconsolidation ratio with elevation for the B.B.C stratum under the I-95 test site.

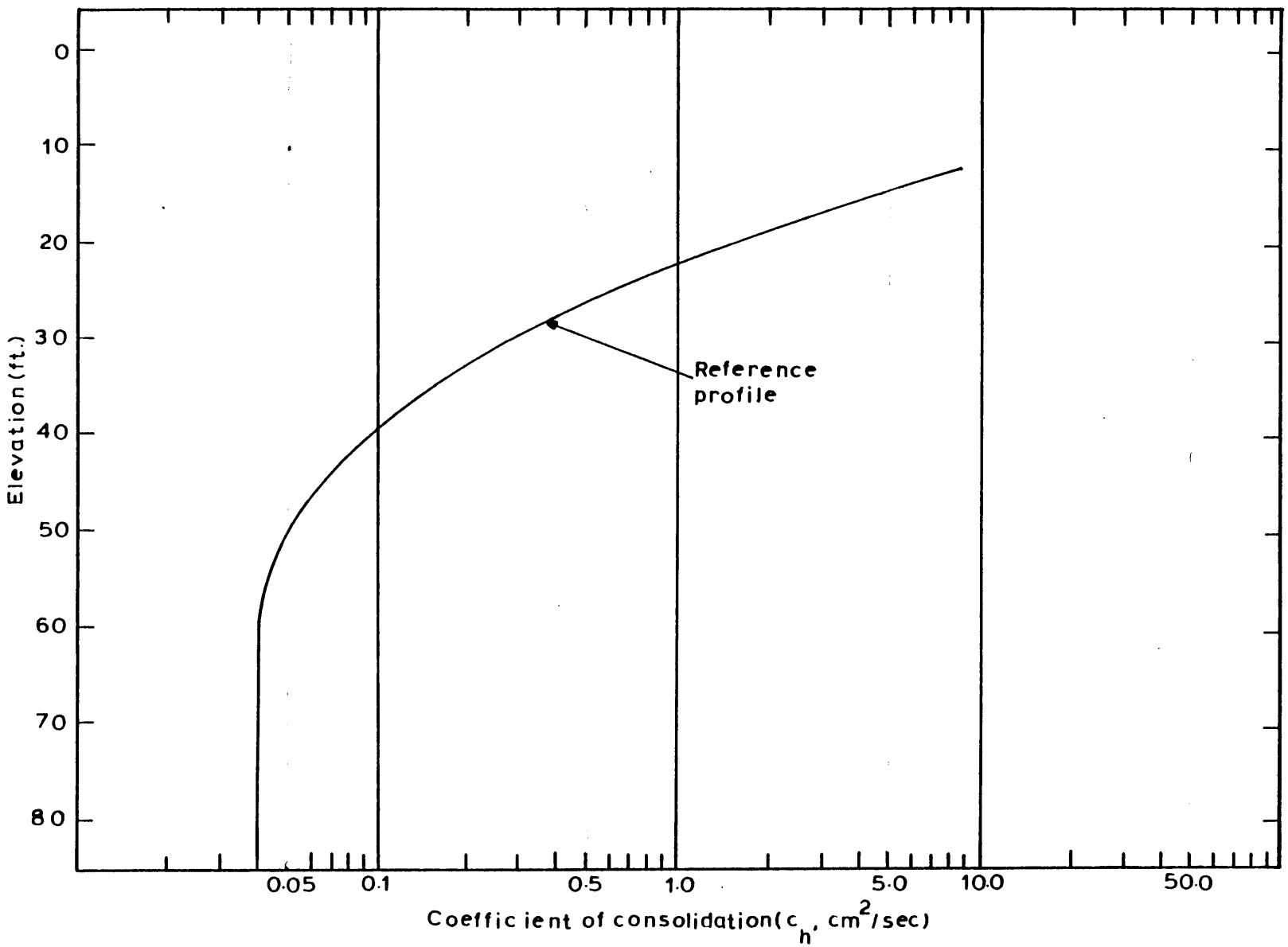

Figure 9.25 Predicted profile of the coefficient of consolidation .

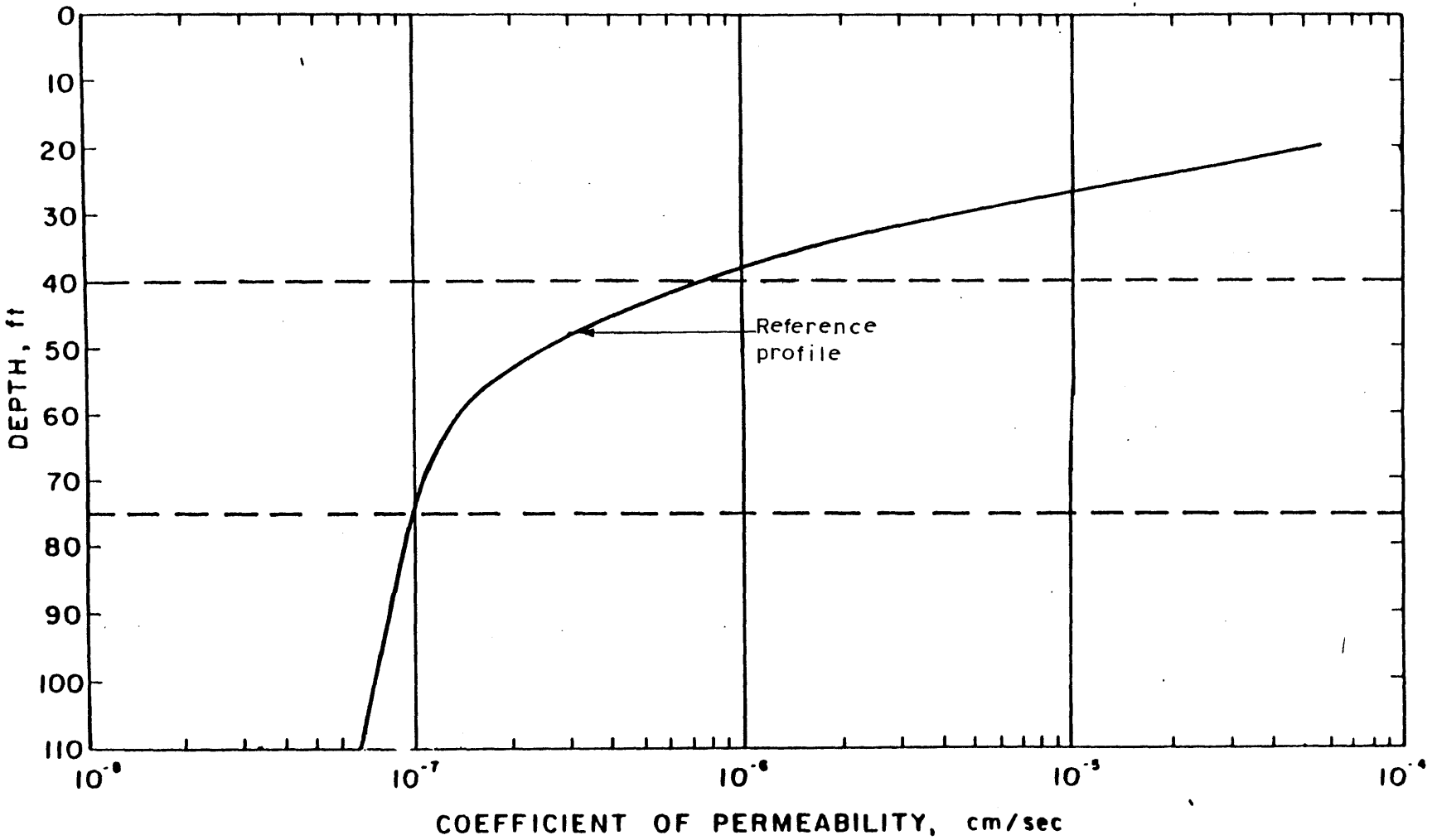

Figure 9.26 The coefficient of permeability reference profile.

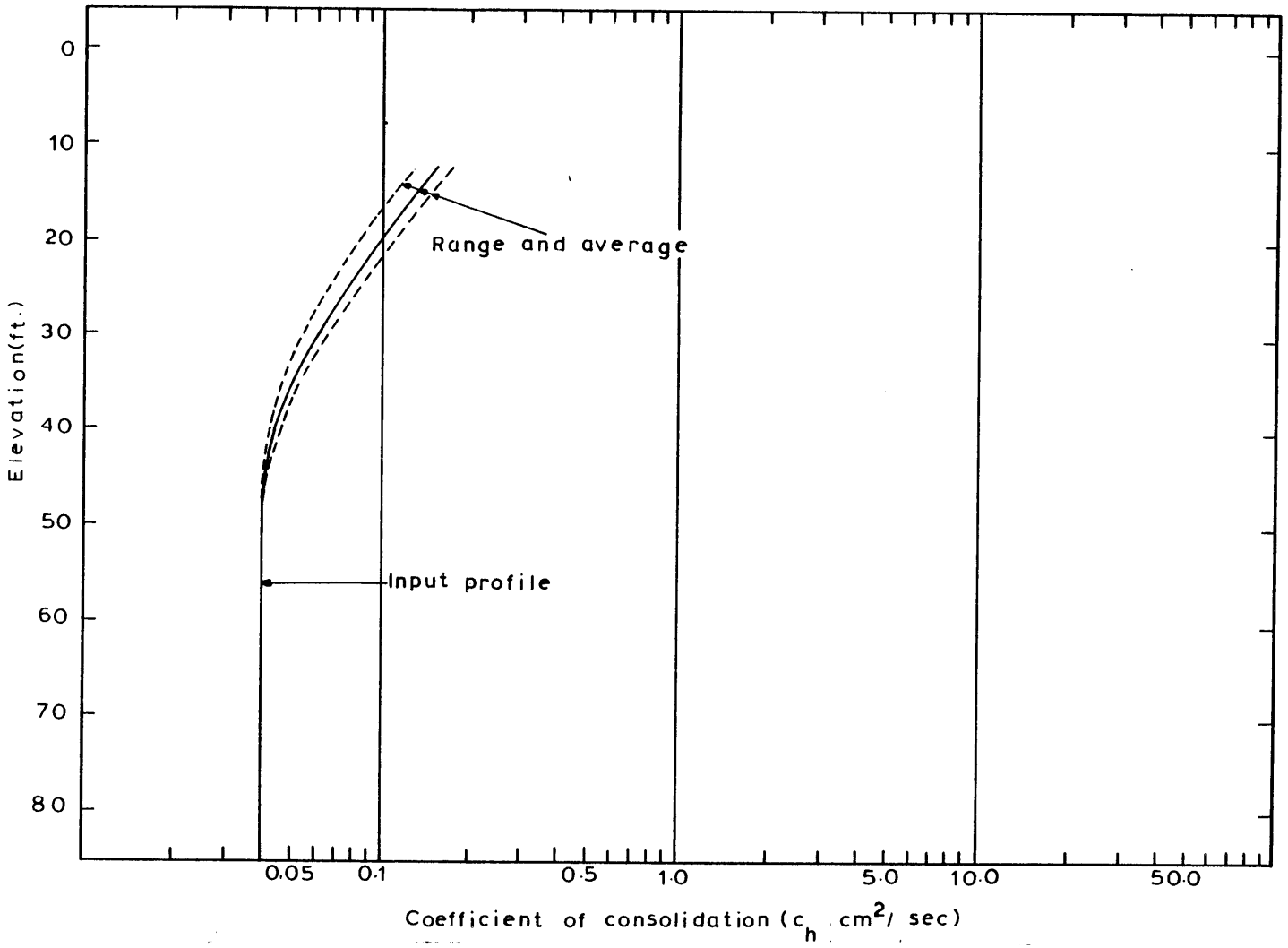

Figure 9.27 A.D.I.N.A.T. input coefficient of consolidation profile.

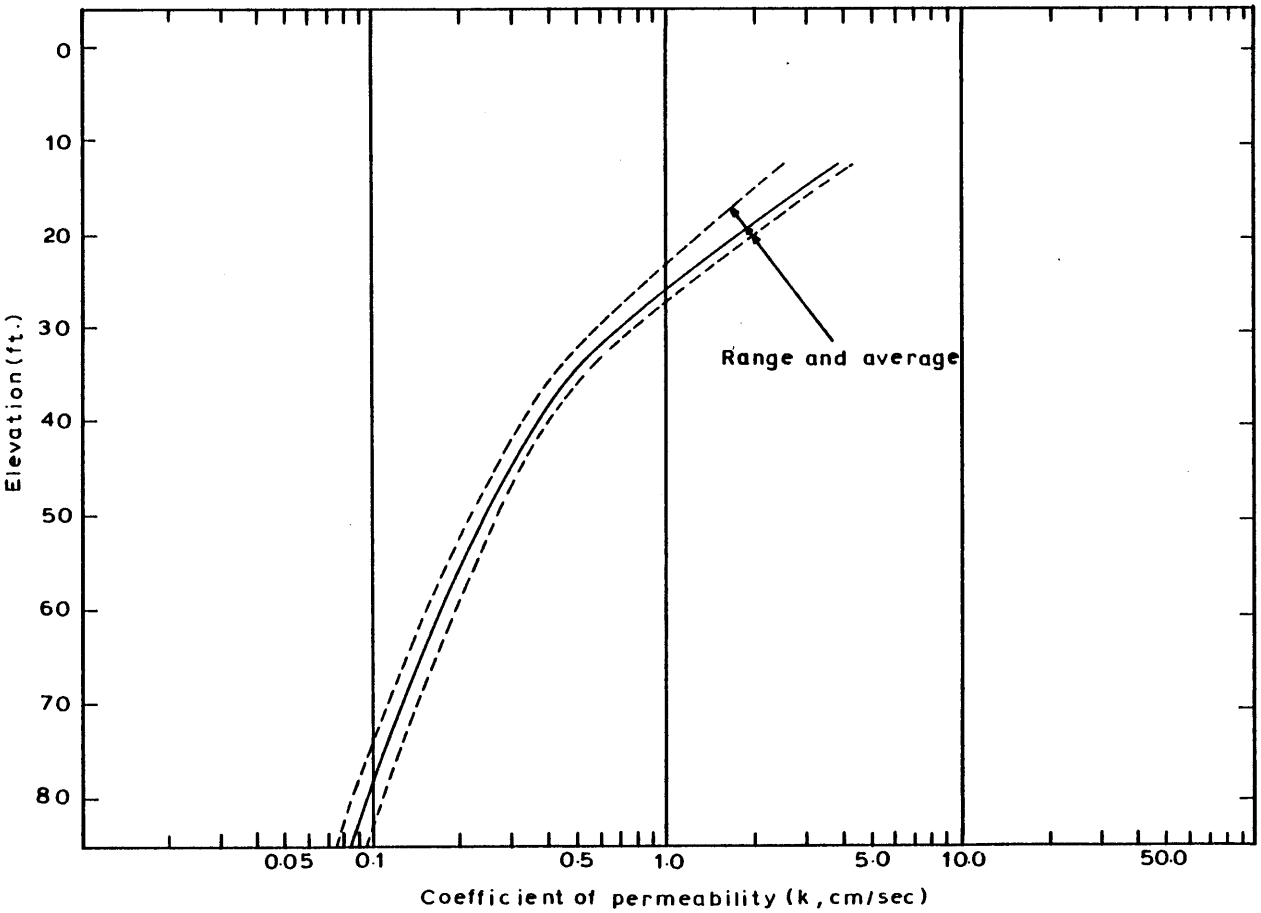

Figure 9.28 Profile of the coefficient of consolidation at the Student Center.

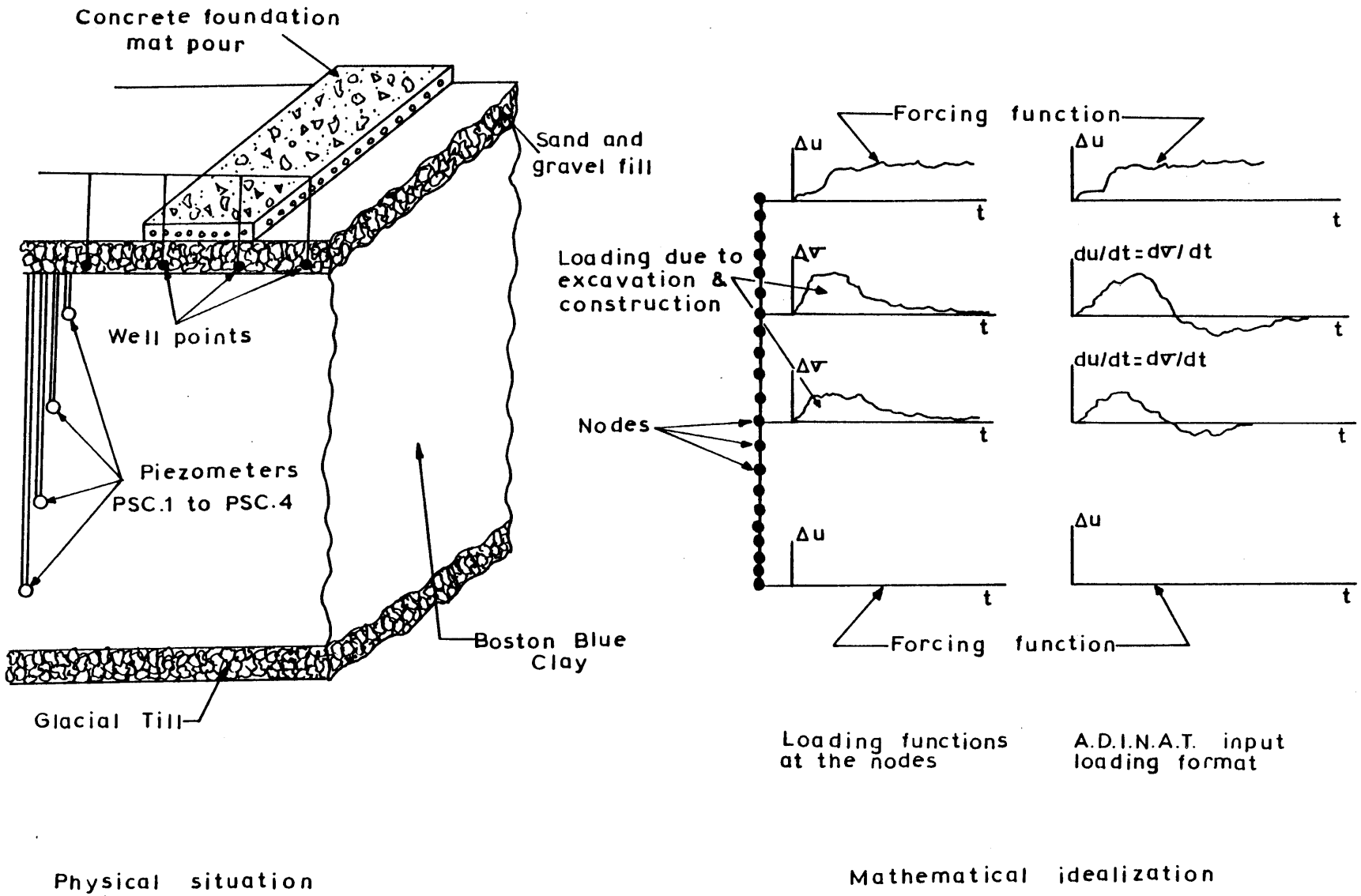

Figure 9.29 A schematic representation of the problem formulation.

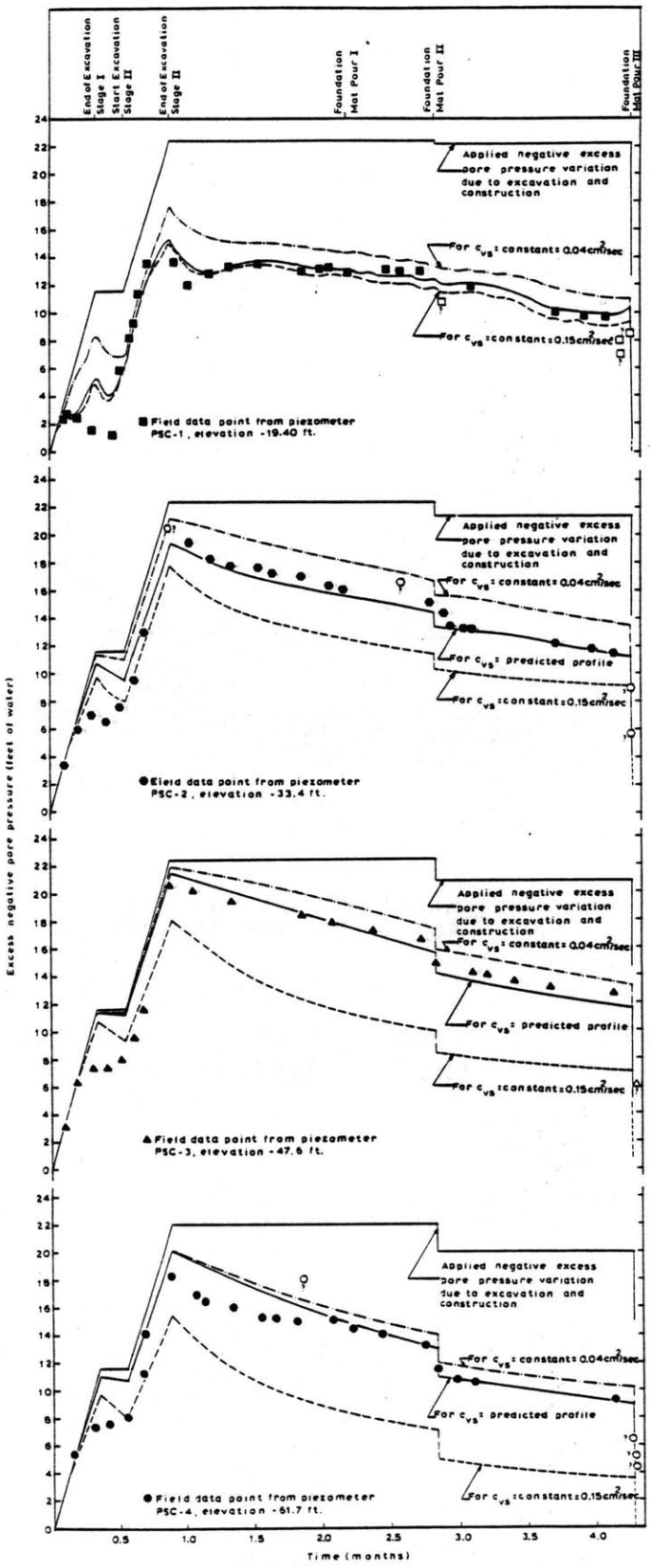

Figure 9.30 Comparison of predicted and measured pore pressure dessipation at the Student Center.

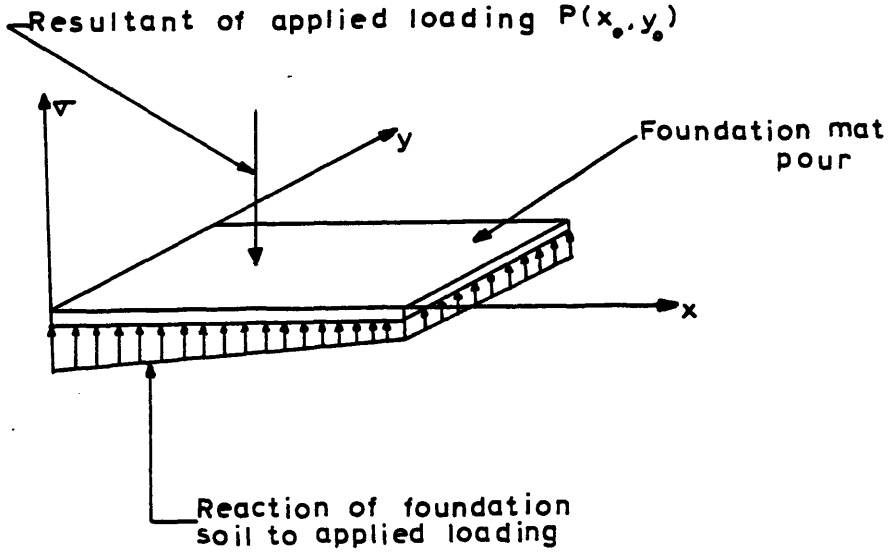

Figure 9.31 Idealized stress distribution under the foundation mat.

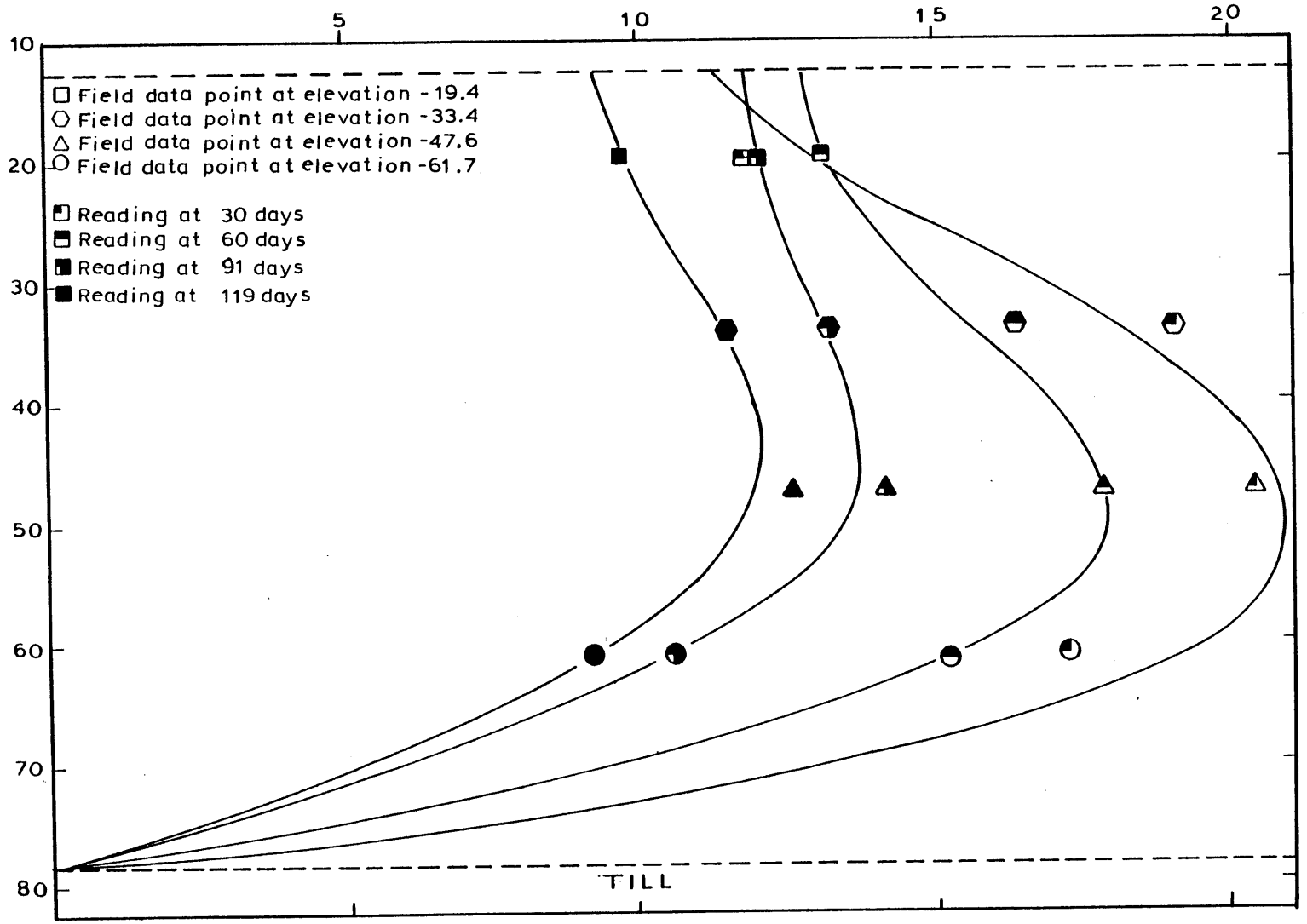

Figure 9.32 Process of depletion of the negative excess pore pressure isocrones.

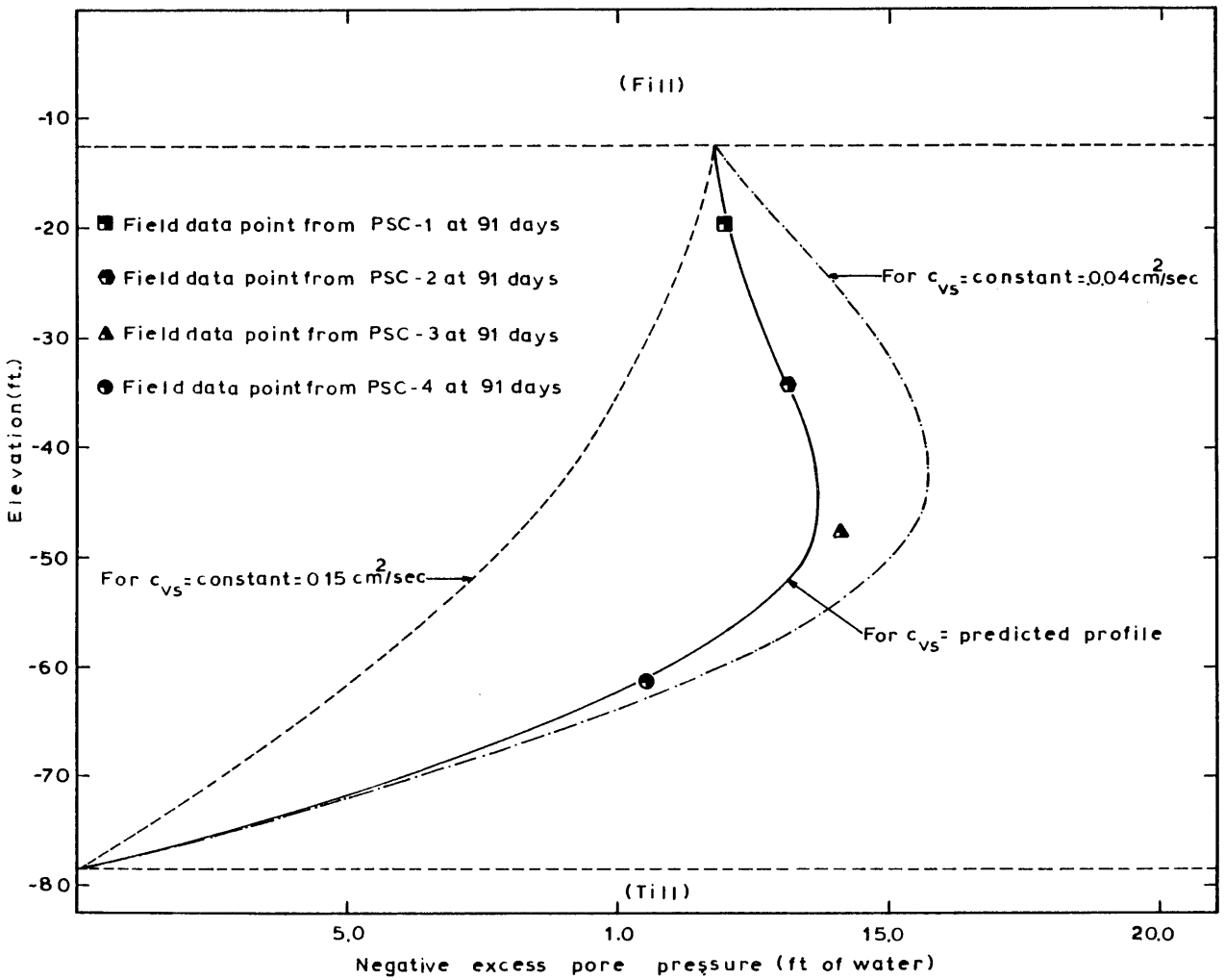

Figyre 9.33 Comparison of excess pore pressure isocrones for constant and variable c_{vs} profiles at the Student Center.

CHAPTER 10

LABORATORY ENGINEERING TESTS ON BOSTON BLUE CLAY

10.1 INTRODUCTION

At various stages along the progress of this thesis, the author has made several assumptions that fascilitated the analysis of the problem under consideration by providing the appropriate soil parameters necessary for the model then used. Such assumptions require validation.

The validation procedure took the form of an extensive laboratory testing program that was initiated on January of 1980 and extended for two years. The purpose of this testing program is twofold:

(a) Evaluation of the piezometer probe predicted soil parameters

(b) Verification of assumptions utilized in the case study involving the foundations of the Student Center building.

The testing program encompassed eight conventional oedometer tests, fourteen constant rate of strain tests (CRSC) and eighteen permeability tests. Coupled with earlier testing programs performed by Germaine (1978) and Ladd et. al. (1965), a large data base was compiled and deployed to arrive at various aspects of the soil

behavior in response to various loading modes. In what follows, a complete and detailed account of the laboratory testing procedures is presented.

10.2 SITE DESCRIPTION

10.2.1 Geology

The Boston Blue Clay was formed during the wane of the late Pleistocene ice age (about 14,000 years ago) under a marine environment in the Boston Basin, probably not very far from the ice margin. The clay deposit overlaid a glacial till which covered the bedrock, and had a typical thickness in excess of 50 to 125 ft. depending on the topography of the till. The clay includes numerous lenses of fine sands, isolated sand pockets and occasional stones or pebbles. Subsequent to clay deposition, movements of the earth crust and of the sea level resulted in emergence of the clay above the sea, followed by extensive weathering desiccation, and erosion of the upper part of the deposit. This was followed by at least two periods of submergence and deposition, of lesser significance, in which outwash sand, peat and silt were deposited above the clay. Further geologic details are given by Kenney (1964) and Aldrich (1970).

10.2.2 Soil Conditions at the Site

The test site is adjacent to the coastline in Saugus, MA, 160 to 200 ft. to the east of the unfinished Interstate 95 embankment centerline at station 246, Figs. 6.2 and 6.3 M.I.T. studied this embankment extensively in the last decade by means of laboratory and in situ tests, embankment monitoring during construction, and a planned embankment loading to failure (D'Appolonia et. al., 1971; M.I.T., 1975).

Figure 11.3 shows the soil profile at the test site as determined by conventional sampling and laboratory testing methods. The upper 25 ft. consist of peat, sand and stiff clay layers which overlie 130 ft. of Boston Blue Clay. The Boston Blue Clay of interest is located between depths of 25 and 120 ft. Typically, the visual classification, and index tests (e.g., the natural water content, w_n, the liquid limit, w_l, and plastic limit w_p) provide little reliable information regarding stratification and vaniability of the clay. On the other hand, laboratory estimates of the maximum past pressure, $\bar{\sigma}_{vm}$, by means of conventional oedometer and constant rate of strain consolidation tests clearly indicate that the clay above a depth of 75 ft., approximately, is significantly overconsolidated.

10.3 SAMPLING OPERATION

The sampling operation took place in the vicinity of station 246. One bore hole labeled M-2 was used in the sampling operation. Its approximate location is shown in Fig. 6.1.

According to the field crew, drilling was performed using a standard auguring procedure. Casing was used up to the top of the clay layer. Subsequently, a heavy drilling mud was injected to offer support to the inner lining of the hole when auguring proceeded into the clay stratum.

Samples were taken between depths of 21.5 ft. to 102.0 ft. with a fixed piston 3.5 inch diameter thin walled sampler. After retrieval of the sampler, an estimate of the shear strength of the soil was obtained using a Torvane device. This is quite valuable in immediately detecting the quality of the samples and later serve as a base line for any possible disturbance during transportation, storage and subsequent extrusion. The tubes were then sealed at both ends with hot wax, labeled and momentarily stored on site in an upright position. Upon completion of the sampling operation, the tubes were transported to M.I.T. where they were immediately logged and stored in the humid room.

Table 11.1 shows the locations of the sampled soil, the tube's serial number and the values of the shear strength obtained from the Torvane.

10.4 PLAN OF TESTING PROGRAM

The testing program invisaged consisted primarily of the following steps:

(a) Sample Radiography

(b) Planning and scheduling of testing program

(c) Phase I of testing program

(d) Phase II of testing program.

10.4.1 Sample Radiography, Planning and Scheduling of Testing Program

Chapter 11 discusses the uses of x-radiography in planning and scheduling of testing program to which the reader is refered to.

10.4.2 Phase I of Testing Program

The primary objectives of phase I of the testing program could be summarized as follows:

(a) Define the stress history as a function of depth.

(b) Identify the variation of the coefficient of consolidation, c_v and c_h^*, as a function of depth.

*Subscripts define the values of the parameters deduced from samples trimmed in the vertical and horizontal direction.

(c) Identify the value of the coefficient of consolidation, c_v and c_h, as a function of the overconsolidation ratio at discrete elevations.

(d) Define the value of the coefficient of compressibility in the virgin compression region, CR_v and CR_h, the coefficient of rebound, SR_v and SR_h, and the coefficient of recompression, RR_v and RR_h, as a function of depth.

The aformentioned objectives were achieved by running eight conventional oedometer tests and fourteen constant rate of strain tests executed on M.I.T.'s general purpose consolidation cell (Wizza et. al., 1969).

10.4.3 Conventional Oedometer Tests

The oedometer tests were conducted following the procedures described in Lambe (1951), with the following exceptions:

(1) Load increment ratios less than unity were used near the vicinity of the maximum past pressure, $\bar{\sigma}_{vm}$, in order to obtain a compression curve with a better defined minimum radius of curvature;

(2) Vertical strain, ε_v, rather than void ratio, is used since compression curves based on strain yield

more consistant and reliable estimates of compressibility and maximum past pressure (Ladd, 1973);

(3) The maximum past pressure was estimated from compression curves based on strains corresponding to the end of primary consolidation, as recommended by Ladd (1973), such strains being determined from dial readings versus log time data.

The samples were 2.5 inches in diameter and about 0.80 inches in height and were innundated with water after the first load was applied.

The loading program was basically derived from a consideration of the maximum past pressure estimated earlier by Germaine (1978) from conventional oedometer and CRSC tests. An unload-reload cycle emmanating from a consolidation stress equivalent to $2 \times \bar{\sigma}_{vm}$ was performed. Final unloading was initiated from a consolidation stress equivalent to $4 \times \bar{\sigma}_{vm}$. The inclusion of the unload-reload cycle was crucial for observing the variation of the pertinent soil parameters at various stages of overconsolidation and its dependence on the laboratory maximum past pressure.

10.4.4 Constant Rate of Strain Tests (CRSC)

(a) Apparatus Description (Wissa et. al., 197)

Figure 10.1 shows the basic parts constituting the M.I.T. general purpose consolidation cell. The cell is

basically composed of two chambers, a cell chamber and a test specimen chamber hydraulically isolated from each other by means of a rolling diaphram that seals the loading cap to the outer retaining ring. The loading piston uses a rolling diaphram seal and runs in ball bushings. It seals to the loading cap by means of an O-ring to prevent uplift on the piston by the cell pressure.

Top surface drainage from the test specimen occurs through a coarse porous stone located on the underside of the loading cap. Two drainage lines are included to allow for flushing air out from the porous stone after assembly. A back pressure is applied to the test specimen, to ensure 100% saturation, through one of those drainage lines.

The base plate of the cell contains the pore pressure measuring system which uses a high air entry ceramic porous stone, epoxied into a recess in the center of the plate. Two small bore holes connect the stone to a pressure transducer. The pore pressure measuring system was designed to have a very low volume compressibility in order to minimize hydrodynamic lag during the test.

The test specimen is mounted in a retaining ring using a removable knife-edge shoe cutter. The retaining ring in turn fits tightly into an outer heavy-walled

ring that gives it the necessary lateral support to prevent lateral movements during loading. Two O-rings seal the inner ring to the outer ring, which in turn is sealed to the cell base by another O-ring located in the base plate. The test chamber can accomodate two sample sizes, 2.5 and 1.93 in. in diamter.

Vertical deformations of the sample are determined by measuring the movement of the cell piston both with a dial gauge and with an electrical displacement transducer (DCDT). The load applied externally to the piston is monitored with a load cell. The back pressure and cell pressure are monitored with test gauges and pressure transducers and the pore pressure at the impervious surface is measured with a pressure transducer.

(b) Laboratory Procedure

The various steps involved in setting up a CRSC test are summarized as follows:

1. Device preparation
2. Specimen preparation
3. Mounting the specimen
4. Loading
5. Floating system
6. Unloading
7. Floating system
8. Reloading

9. Floating system
10. Unloading
11. Disassemblage
12. Data reduction

1. Device Preparation

It is of utmost importance that the bottom pore pressure stone be fully deaired at all times. Deairing the stone involves innundation of the bottom plate, to which the stone is epoxied, in water contained in an air tight flask. A vacuum of no less than 10 millitores is applied for a minimum period of 24 hours. From then on a thin film of water should always cover the stone at all times.

Device preparation also involves proper calibration of all the pressure transducers, the displacement transducer involved and the load cell and making sure that the loading program would not inflict pore pressures or displacements that would either exceed the capacity or shift the response into the non linear range.

Before proceeding with the testing program the pore pressure response is checked by fully assembling the cell and applying a back pressure and monitoring the pore pressure response. If the response is sluggish deairing the stone is necessary.

The range of pressure transducers, displacement transducers and load cell are set on the data aquisition system. Initial z_3 reading is determined and later used to define contact of the inner chamber with the top of the soil specimen.

2. Specimen Preparation

The soil specimen extruded from the tube is first trimmed to dimensions somewhat greater than the final dimensions by using a miter box. The assembled cutting shoe and specimen ring with a thin silicone grease coating (on inside and outside) are then pushed into the oversided sample now placed over a rotating pedastal. Successive pushes of no more than .125" of an inch with a total soil overhang of .06" are advisable. With silty samples great care should be excersized to avoid spalling and formation of gaps between soil and specimen ring. The specimen is then gently pushed into the ring, the top and bottom surfaces trimmed off and then the specimen is pushed further to allow space for top porous stone.

3. Mounting of Specimen

The specimen is then gently slid over the pedestal and onto the pore pressure stone making sure that the water film is dried off gradually in front of the sliding specimen ring. A filter paper is placed over the top

side to avoid soil extrusion into the top porous stone. The inner chamber is then gradually and carefully slid over the specimen ring making sure that it descends over the ring in a true vertical fashion with the chamber piston in the upstroke position. The chamber is then bolted down firmly. The two backpressure lines are connected and the top porous stone is flushed. Seating is then maintained and checked.

The outer cell is then lowered over the inner chamber and tightly bolted. The piston head is then lowered and contact maintained*. By continuously monitoring the pore pressures, any possible disturbance during setting up the assembly could be detected.

The assembled cell is then placed in the loading frame and the space between the inner and outer chamber is filled with deaired water. Contact with the load cell is carefully maintained and the DCDT reading corresponding to the true contact position is recorded.

A backpressure and cell pressure of approximately 4.00 Kg/cm^2 is then applied in 0.5 kg/cm^2 increments making sure that at the end of each increment pore pressure equalization is achieved and that the DCDT reading corresponding to the initial true contact position is maintained. The soil is left to saturate

*Lowering the piston requires applying a vacuum to the piston shaft.

over a period of 24 hours.

4. Loading

After proper choice of the strain rate compatible with the soil type the clutch is released and the motor is started. Readings initially at 5 to 10 min. are advisable but could be increased to 30 minutes after one hour. A rough estimate of the value of the maximum past pressure could be obtained by simply plotting the logarithm of the load cell reading versus time during first loading. As soon as the specimen is normally consolidated the logarithm of the load cell reading is linearly related to time, which allows one to predict the value of the maximum past pressure and hence schedule the unload reload cycle ($2 \times \bar{\sigma}_{vm}$) and maximum applied stress before final unloading ($4 \times \bar{\sigma}_{vm}$).

5. Floating the System

The term implies the application of a constant load, after the motor is stopped for purpose of stress reversal or final disassemblage, to dissipate the excess pore pressure under the load then applied. This is achieved by using the belofram and adjusting the air pressure so that the load cell reading remains identical to that achieved at the instant the motor was halted.

However, during the testing program it was noticed that the excess pore pressures at any one time never exceeded 0.1% of the applied load even with the samples retrieved from elevations exceeding 100 ft. Hence floating the system was not necessary at the point of stress reversal.

6., 7., 8., 9. and 10. Similar to steps 4 and 5.

11. Disassemblage

After fully unloading the sample, the backpressure and the cell pressure are lowered in increments of 0.5 kg/cm^2, again making sure that pore pressure equalization is achieved at the end of each pore pressure decrement. Then the cell is dismantled following exactly the reverse sequence of events followed in Step 3.

12. Data Reduction

The data acquisition system can provide the data in either a hard copy format or on a magnetic tape that could be used in conjunction with a computer program, CRSCX (Wissa, et. al. (1971)),that has been modified to enhance its plotting capabilities to produce the resulting compression curve and variation of coefficient of consolidation, c_v or c_h, with effective stress.

10.4.5 Phase II of Testing Program

The primary objectives of phase II of the testing programs are twofold:

(1) Define the value of the coefficient of consolidation, k_h and k_v, as a function of depth

(2) Define the relationship between the ratio of k_h/k_v as a function of depth.

The aforementioned objectives were achieved by running eighteen permeability tests conducted in conventional triaxial cells.

(a) Apparatus Description

Figure 10.2.a shows the complete set up used in running the permeability tests. Basically the set up could be subdivided into four systems.

1. Cell pressure system
2. Back pressure system
3. Manometer system
4. Triaxial cell system

1. Cell Pressure System

The Cell pressure system comprizes of two mercury pots A & B and a system of polyurethene piping shown in Fig. 10.2.b The polyurethene piping is flushed with deaired water. The system supplies a cell pressure to the two triaxial cells through values x and y. The value

of the cell pressure could be simultaneously measured mechanically by use of dial Q or electronically through use of the pressure transducer block S. The cell pressure in the two cells could be varied individually by simply changing the elevation of either of the two mercury pots.

2. Specimen Pore Pressure System

The pore pressure of the soil specimens residing in the triaxial cells could be varied by simply changing the elevations of the two mercury pots C and D. The pore pressure is supplied via valve L and M to the top and the bottom of the soil sample. The system could be used to supply a back pressure to saturate the sample or a pore pressure gradient across the sample. The value of the pressure supplied at the top and bottom of the sample could be simultaneously measured mechanically by use of the dial Q or electrically through the use of the pressure transducer blocks.

3. Manometer System

The volume of water entering or exiting the soil sample could be measured by the use of four manometers that are connected to the top and bottom end of each soil sample. Copper tubing is used to reduce the system flexibility to a minimum. Readings of the displaced volumes of water need to be taken manually.

4. Triaxial Cell System

Two Wykham Ferrence cells are used to house two soil specimens that are trimmed in either the vertical or the horizontal directions from the same elevation. The soil specimen is hydraulically insulated in two coaxially fitted prophylactics and tightly secured to the bottom pedestal and the top cap by overlapping O-rings. Drainage is allowed from the top and bottom ends of the sample via valves x and y. To keep the piston in contact with the soil sample after a cell pressure is applied, a harness is applied over the piston and any possible lift off is counterbalanced by adding the appropriate weights at the ends of the harness. This insures that an accurate measurement of the height of the specimen could be obtained at any stage by reading the displacement dial R. A transducer block L is fitted to measure the pore pressure response to an increase in cell pressure for the purpose of deriving the value of the degree of saturation of the soil sample. Use of transducer block S could lead to slightly reduced values of the degree of saturation owing to the flexibility of the connecting polythene tubing.

(b) Laboratory Procedure

The steps involved in running a permeability test could be summarized as follows:

(1) Device preparation

(2) Specimen preparation

(3) Mounting the specimen

(4) Specimen saturation

(5) Consolidation

(6) Gradient application and permeability measurement

(7) Disassemblage

(1), (2) and (3) Device preparation, Specimen preparation and Mounting

Those operations were conducted following the procedures described in Lambe (1951) and

(4) Specimen Saturation

In order to ensure a 100% degree of saturation the soil specimen is subjected to a back pressure of no less than 4 kg/cm^2. This is done by gradually increasing the cell pressure and the specimen pore pressure in a step wise fashion in that order, such that at any one time the pore pressure is less than the cell pressure by approximately .1 kg/cm^2. The back pressure is left on for a minimum of 24 hours. The degree of saturation is then checked by closing the drainage lines, top and

bottom, and increasing the cell pressure and monitoring the pore pressure response indicated by pore pressure transducer L.

(5) Consolidation

The sample is isotropically consolidated to the in situ stress by increasing the cell pressure and allowing top and bottom drainage. This will reduce the time to achieve primary consolidation by reducing the drainage path. The volume of water expelled is measured by the manometer. For horizontally trimmed samples, it was assumed that the in situ stress could be derived by assuming a $K_o = 0.55$.

(6) Gradient Application and Permeability Measurement

A minimum of three hydraulic gradients were applied across the specimen ranging the value from 10 to 100. Clearly, achieving a hydraulic gradient across the soil specimen by simply increasing or decreasing the value of the pore pressure soley at one end induces a change in the effective stress state of the soil specimens due to the application of the seepage force j. Although it cannot be totally eliminated, its effect could be reduced by simultaneously, depending on the direction of flow, increase the pore pressure at the top and decrease it at the bottom by equal amounts such that the overall

desired gradient across the sample is achieved.

Each gradient is imposed for a minimum of 24 hours during which continuous measurements of the volume of water entering and exiting the soil specimen is monitored.

(7) Disassemblage

After removal of the last applied gradient the sequence of events followed in Steps (4)(3) are followed in exactly the reverse order.

(12) Data Reduction

The value of the coefficient of permeability, k_h or k_v, could be obtained from the relationship

$$k_v(k_h) = \frac{V_v}{i} (V_h) \qquad (11.1)$$

where V is the permeant velocity and i is the hydraulic gradient.

The permeant velocity is obtained for the relationship:

$$V_v(V_h) = \frac{Q}{A \times t}$$

where Q is the total volume of water that permeated through the sample in time t and A is the current specimen cross sectional area.

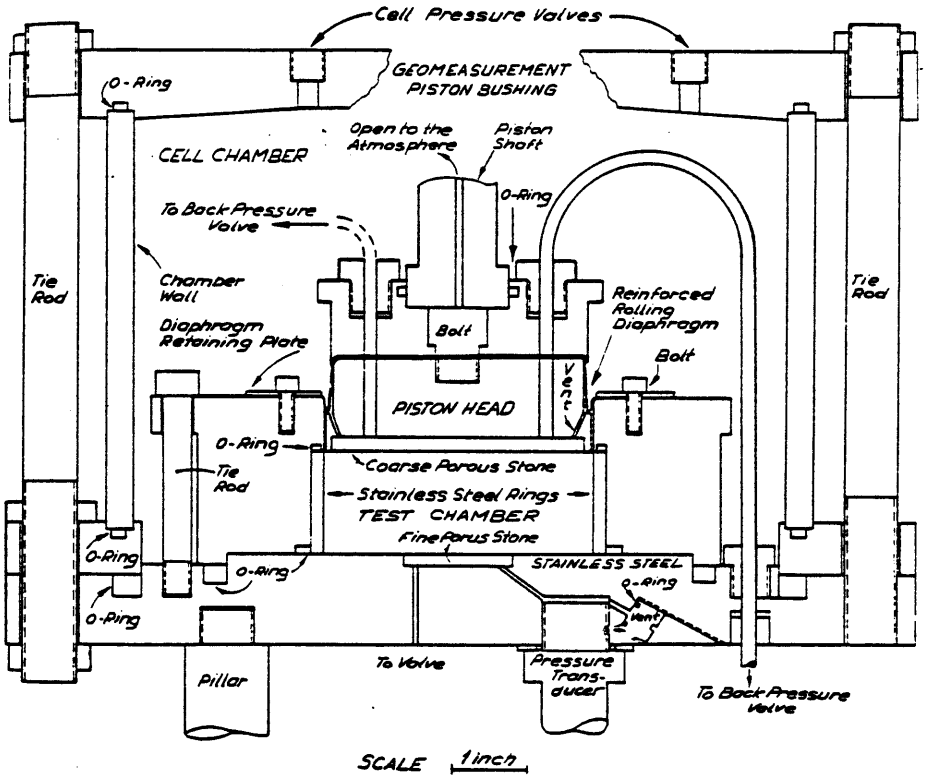

Figure 10.1 (a) M.I.T.'s general purpose consolidation cell.

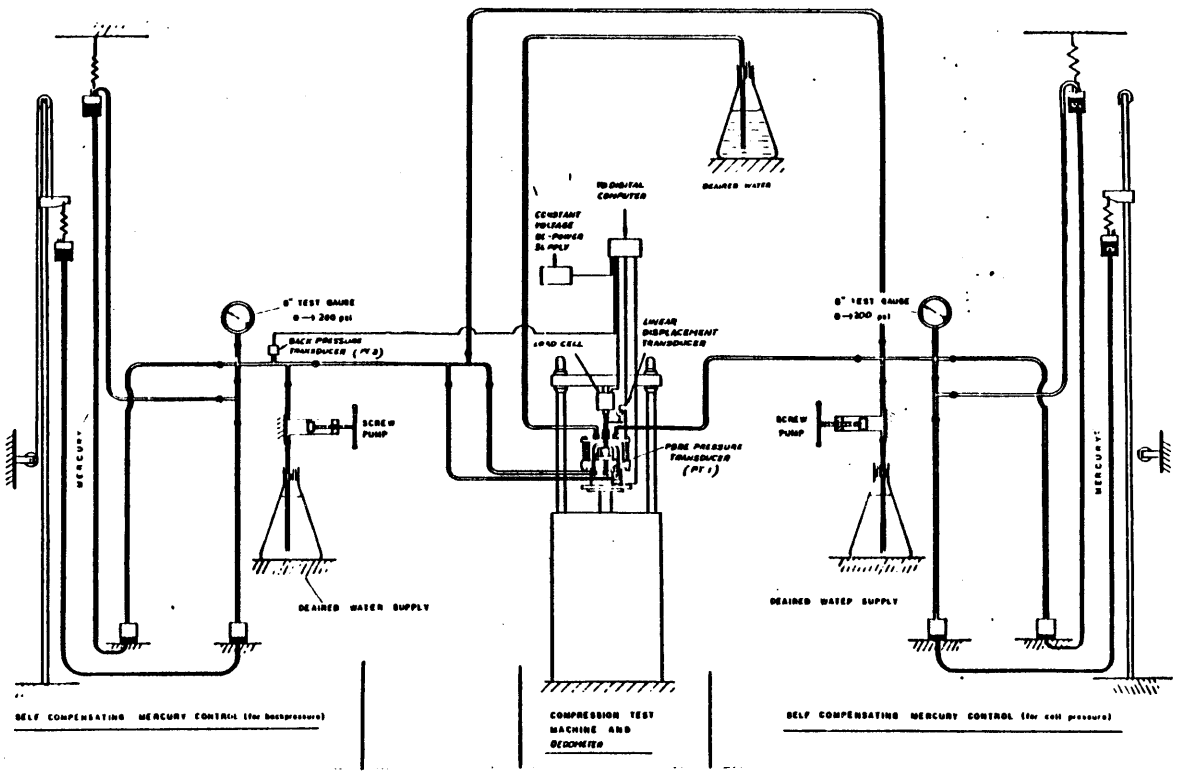

Figure 10.1 (b) M.I.T.'s general purpose consolidation cell and pressure system.

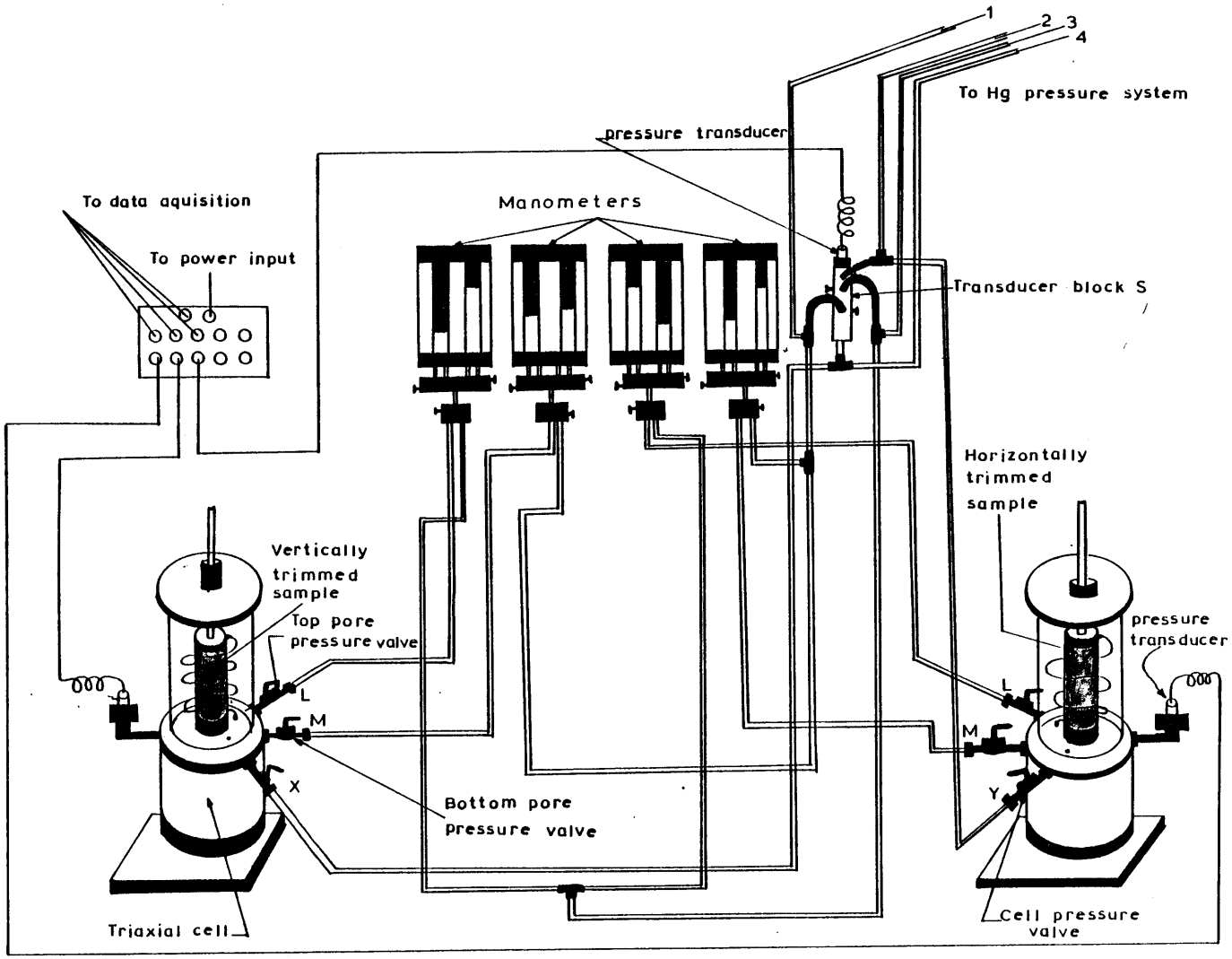

Figure 10.2 (a) General set up for permeability determination.

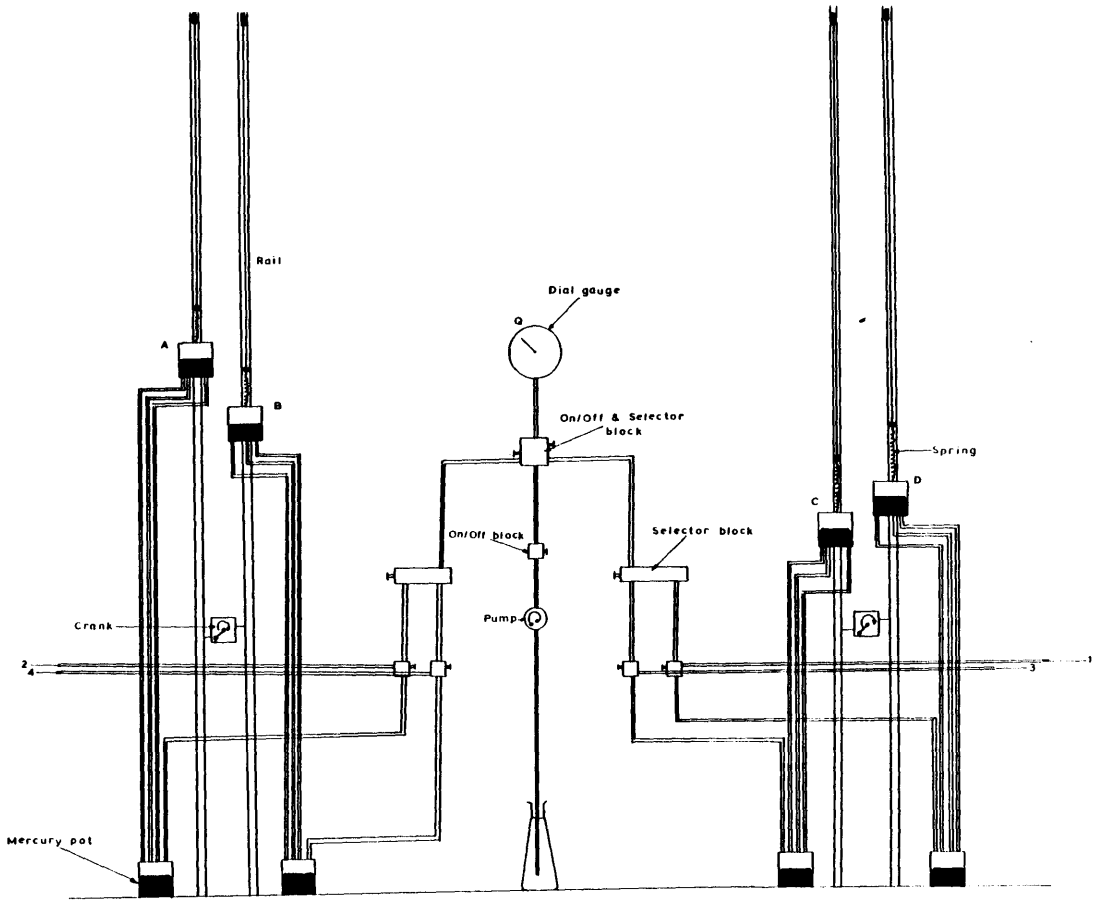
Rail
Dial gauge
Q
A
B
On/Off & Selector block
Spring
D
C
On/Off block
Selector block
Pump
Crank
2
4
1
3
Mercury pot

CHAPTER 11

X-RADIOGRAPHY

11.1 INTRODUCTION

X-rays are a form of electromagnetic energy possessing an extremely short wavelength on the order of about 10 to 0.011 angstroms. Such a characteristic enables x-rays to penetrate solid bodies that would otherwise reflect or absorb visible light.

The absorption of x-ray energy along any ray, which occurs when radiation passes through a solid body can be estimated by the exponential equation:

$$I = I_o e^{-mx}$$

where; I is the intensity of transmitted radiation,

I_o is the intensity of incident radiation,

m is the absorption coefficient of the material being penetrated by the ray, and

x is the path length of the x-ray.

Thus, depending on the absorption characteristics of a solid object, defined by m, the intensity of the emerging ray could be thought to characterize the opacity of the object to x-rays.

The intensity of the emerging x-rays could be permanently recorded by placing a photographic film behind the object.

The film consists of a transparent support, coated on both sides, to double the reaction, with an emulsion consisting of a thin layer of gelatine containing very fine grains of silver halide in suspension. When the emerging x-rays strike the film at a particular location, a chemical reaction is initiated and results in an induction of a positive charge on the silver halide crystals. When emersed in a developing agent, the exposed areas turn darker depending on the intensity of the emerging rays.

Clearly, the consistency and homogeniety of a specimen could be easily evaluated by x-radiography techniques since existing inhomogenieties possess different absorption coefficients and would henceforth cast a different shadow density on the photographic film that obstructs its path.

Thus, x-radiography techniques are important tools that could be used for nondistructive testing of materials.

11.2 GEOMETRIC CONSIDERATIONS FOR IMAGE INTERPRETATION

Before indulging in the physics of image formation it is important to define some of the common jargon used when interpreting x-ray images:

(1) Density: The degree of blackening of a particular area on a radiograph (Fig.11.1).

(2) Contrast: The degree by which an interpreter can distinguish between two different density planes, (Fig.11.2)

(3) Deffinition: Ability of a radiograph to resolve fine detail.

Consider a source "s" emitting x-rays that are intercepted by an object "o" and recorded on film "F", (Fig. 11.3). The shadow of object "o" cast on film "F" would experience an enlargement that is a function of the distance "os" and "Fo". The geometry involving similar triangles dictates the following relationship:

$$\frac{SF}{So} = \frac{O}{I}$$

where, SF is the distance between the source and the film,

So is the distance between the source and the object,

O is the size of the object defined as its normal projection on a vertical plane,

I is the size of the image on the film "F".

Sharpness of the image, deffinition, is largely governed by the size of the source and the thickness of the object. When the source is not ideally a point but a finite length, the source could be thought of as combination of an infinite number of smaller sources. Each of those sources would cast its own shadow on the film and each of those shadows are slightly displaced producing an ill defined image. This anomaly is referred to as unsharpness, Arthur et al. (1967, Fig. 11.4

Clearly the two parameters involved are the size of the source "s" and its distance from the object, S_o. A larger

focal spot for the source "S" could withstand larger voltages and exposure times that would enhance the density and the contrast attributes of a radiograph. On the other hand a large focal spot would cause unsharpness. Unsharpness could be reduced by increasing the source to object distance S_o. Thus, clearly a tradeoff exists. Obviously, the optimum would be to use the smallest focal spot and the largest possible source to object distance and maintaining the highest possible levels for the three afforementioned attributes.

Since the size of an image is the approximate* representation of the normal projected area of that image on a vertical plane then its image is a distorted representation. Spatial distortion relates to the distortion in the spatial relationship between two objects "S" and "O" due to the relative location of the focal spot. The effect of distortion could be minimized by the use of steroscopic x-ray assessment and other procedures, Allen et al. (1978), (Fig.11.5)

11.3 USE OF X-RADIOGRAPHY IN GEOTECHNICAL ENGINEERING

The earliest use of x-radiography was reported by Tschebotanioff (1950) as attributed to the work of Gerber (1929) in monitoring the deformations of lead pallets embedded

*Assessing no enlargement due to object-film separation.

in sands. Later work by Davis et al. (1949) on deformations under footings and by Bernhand et al. (1950) on effectiveness of soil compaction, all used the same technique. However, their efforts went unappreciated.

A revival in interest in x-radiography in geotechnical engineering research came about in the early 1960's with the growing interest of developing a "generalized" soil behavior model. X-radiography was reintroduced in soil mechanics research at Cambridge University, by the late Professor Roscoe in 1960. Using the same technique of monitoring movements of embedded lead pallets, the recorded movements were translated into strains and the description of a strain field, within a specimen subjected to external stresses was now possible.

The later extension of the traditional use of x-radiography in geotechnical research spawned various uses that have helped in broadening our understanding of soil behavior. Some of those uses are listed herein:

(1) The influence of inherent anisotropy due to soil's depositional history and the effect of inhomogeneities such as layering or pre-existing rupture layers on the stress strain response, Arthur et al. (1972, 1977, 1975) and Ladd et al. (1978).

(2) The distribution of strains caused by various loading modes could be investigated. This modeling technique can lead to behavioral aspects that are hard, if not impossible,

to predict. Strain distributions caused by cyclic wave loadings on a model of an experimental sand island for offshore oil prospecting was investigated by Arthur, (1977). Deformation around self boring pressure meters was investigated by Ladd et al. (1978).

(3) Density measurements are possible since the intensity of an emerging x-ray bundle is dependent, in part, on the voids ratio of the penetrated medium. Absolute density measurements are difficult to obtain, Krimitzky (1972). Relative density measurements are easily detected from a radiograph and can convey variations in soil type, Ladd et al (1978).

(4) Orientation of rapture surfaces could be detected during the early stages of their formation since density changes accompany dialating rupture layer, Ladd et al. (1978).

(5) The ability of observing the spatial movement of particles of low capacity to penetrating x-rays could help in the inference of soil behavior from the interrelationship of individual soil particles, Sharma (1976).

(6) Radiography could also be used to help in diagnosing problems that could occur during the development phase of new testing apparatus such as its use in the development of the directional shear cell, or for verifying the validity of old shear devices, Arthur et al. (1977).

(7) Radiography could aid in assessing the uniformity of laboratory constituted samples. This procedure is currently being used at M.I.T. to test uniformity and homogeneity of constituted samples of granular soils for directional shear apparatus (Bekenstein (1980).

(8) Assessing the integrity and representativeness of undisturbed samples and preliminary scheduling of laboratory testing programs, Ladd et al. (1980, 1981), Allen (1978).

11.4 USE OF X-RADIOGRAPHY IN PLANNING AND SCHEDULING LABORATORY TESTING PROGRAMS

In spite of the long strides that offshore and onshore insitu testing has undergone, frequently it is felt necessary to retrieve "undisturbed" soil specimens for laboratory testing to act as either the primary source of data, or, as a guideline in interpreting data obtained from insitu testing. Moreover, soil behavioral models developed in geotechnical engineering research more than often rely on data obtained from laboratory tests on "undisturbed" samples, Ladd (1964) and Baligh et al. (1980).

Offshore soil samples obtained during foundation investigations are difficult to obtain requiring expensive sophisticated techniques. With the persisting need for energy resources prospecting in deeper waters, the costs are expected to escalate dramatically. It is henceforth, of great importance

that any testing program be very carefully planned and scheduled to reduce waste to a minimum and maximuze the volume of reliable data.

In retrospect, development of soil behavioral models that are intimately related to the development of interpretation methods of insitu testing require laboratory testing for providing essential model parameters to develop interpretation criteria, Baligh et al (1980) and Levadoux (1981).

Internal features of a sample, such as the presence of gravel, shells, cracks, worm and root holes, gas patches and other anomalies will affect and at worse could invalidate the data obtained from routine tests run on such samples.

An obvious need arises when having to plan the location of test samples to obtain a spatial view of the interior of the soil sample. A non-destructive technique is desirable to retain the integrity by avoiding the introduction of disturbance. X-radiography techniques appear to be very desirable in that respect. Simplicity, expediancy and relatively low cost enhance its use as a powerful planning and scheduling technique that increases the reliability of laboratory data..

Realizing the importance in planning and scheduling test programs, the geotechnical group at M.I.T. now considers it standard practice. In what follows is a brief description of M.I.T.'s x-radiography facility and a brief account of the use

of x-radiography as a planning tool in a few research projects.

11.5 M.I.T.'S RADIOGRAPH FACILITY

Figure 11.6 shows a plan view of M.I.T.'s radiograph facility located in the geotechnical research laboratory. The facility features a Philips MG 151-160kv constant potential high voltage generator that can supply energy levels of up to 160kv to a Philips MCN 161-160kv metal ceramic double-focus (0.4mm and 3.0mm), thin Beryllium window (1mm), x-ray tube.

The tube is water-cooled, very small and light in weight that facilitates its movement and inspection.

To reduce the amount of radiation emanating from the focal spot and direct the x-ray beam to the specified object, a lead diaphragm is attached to the focal spot opening. A special x-ray tube stand is constructed for vertical shooting for the purposes of a directional shear apparatus.

The emission, intensity, duration and size of focal spot could be selected from a control panel that resides outside the shell. Special circuit breakers and alarm devices are installed to enhance safety of x-ray operators and other persons in the vicinity.

The films are developed in a specially constructed darkroom adjacent to the shell provided with the necessary chemicals and other equipment. Taverna (1979) presents a more rigorous description of the facility to which the reader is referred to

for more details.

11.6 PROCEDURES FOR X-RADIOGRAPHY

Figure 11.7 shows the general set up used in performing quality radiographs of soil samples retained in steel liners. Typically, the set up consists of a four legged, rigidly braced frame made up of angular steel elements. A wooden flat base, whose elevation could be changed by simply anchoring its steel frame to the main risers, provides support to steel sampling tubes. A wooden front panel has a rectangular opening the size of the x-ray film, 10 in. square, and is placed around the sample and anchored to the corresponding risers. A wooden back panel houses the film cassette and provides support to the identification tag and the density gradient indicator, and together with the front panel provide support to the steel sampling tube.

In spite of the measures taken to reduce scattered radiation such as placing a lead screen diaphragm directly in front of the focal spot to limit the area covered by the x-ray beam, scattered radiation can never be eliminated totally. The soil specimen itself is a source of scattered radiation.

Preventive measures to reduce scattered radiation from matter outside the soil specimen consisted of placing a 1/8 inch thick lead frame around the 10 inch square opening

in the front panel. Lead sheets 1/8 inch thick placed around the specimen for areas inside the frame. A 1/8 inch thick lead shield is also placed behind the film cassette to inhibit reflected radiation from walls and floor. A 1/16 inch aluminum plate is placed in front of the 10 inch square window to reduce radiation from all sources.

The curvature of the sample liner produces an apparent change in density, thickness or minorological composition of the soil sample. A film exposure gradient results with lighter areas towards the outer edge of the sample liner. This effect could be compensated for in several ways. Film development techniques, computer corrections (Chavez, 1975) or by the use of a filter gradient. The latter was used at M.I.T. and basically consists of vertical aluminum plates of varying thickness positioned in front of the sample such that all x-rays will penetrate an approximately uniform mass.

To provide a frame of reference for the radiographs, lead markers and letters were attached at 1 inch intervals along a wooden stake placed alongside the tube.

Successive shots along the lengths of the tube are easily achieved by moving the wooden base to predetermined locations. An overlap of at least 1 inch is advisable between successive shots. Numerous trials are necessary to determine the most appropriate values of the voltage, the current, the exposure time and the developing particulars.

room. Table 11.1 shows the locations of the sampled soil, the tube serial number and the values of the shear strength obtained from the Torvane.

11.7 RADIOGRAPHS OF BOSTON BLUE CLAY TUBE SAMPLES

This section presents radiographs (reproduced herein as positives made from x-ray negatives) to illustrate various features detected in Boston Blue Clay Samples.

(a) Examples of Sample Disturbance

Figure 11.16 summarizes permeability and CRSC test data obtained from middle and bottom of the tube retrieved from a depth of 41.5-42.5 ft. The pictures and test results show the following (Fig.11.9):

(1) White color next to marking 0 at the top of the tube indicates a very low density material, which is the top wax seal.

(2) The large black area immediately in contact with the wax seal indicates a high density material. Later, the suspicions were confirmed by visual identification of a relatively large stone shown in the inset on Figure 11.10.

(3) The radiograph shows very good quality clay with identifiable bedding planes. Three specimens were extruded and permeability tests were conducted. In retrospect this proved to be a poor choice.

Figure 12.16 shows that the obtained values are much lower than those obtained from laboratory tests on samples in the immediate vicinity. The values of the torvane increased from an average of .190 TSF to .280 TSF immediately below the sample location indicating a definite disturbance zone between markings O and H, Figure 11.8 and 11.10.

Figure 11.11 is another example of a large stone confirmed upon extrusion from a tube sampler retrieved from 82-84 ft., Fig.12.12.

(b) Examples of Non-Homogeneous Soil Type

Figure 11.13 shows a clear indication of the presence of numerous bedding planes and a totally heterogeneous composition of the soil specimen. This could be traced to the geologic history of the deposit. Subsequent to clay deposition, movements of the earth crust and sea level resulted in the emergence of the clay above the sea, followed by extensive weathering, dessication, and erosion of the upper part of the deposit. This was followed by at least two periods of submergence and deposition, of lesser significance, in which outwash sand, peat and silt were deposited above the clay. Further geologic details are given by Kenny (1964) and Aldrich (1970). The inset in Figure 11.14 is a visual representation of the layered non-homogeneous clay. The heterogenous layers are basically composed of very fine silt and sand. Figure 11.15 clearly exhibits a band of high density material in the bottom portion

of the tube sampler retrieved from a depth of 82-84 ft. This was visually confirmed upon extrusion from the sampler and indicated the presence of a layer of gravel. The inset in Figure 11.16 confirms the suspicion.

(c) Example of a Good Quality Sample

Figure 11.17 shows a good quality sample between markings A and I with the exception of a silt seam at F. The values of shear strength obtained by the Torvane were very consistant, approximately .22 TSF. The values of the maximum past pressure agreed with previous stress history derived from earlier tests on the same deposit. Likewise the values of the permeability agreed very favorably with the predicted profile and with laboratory values obtained from previous tests on the same deposit by Germain (1978).

11.8 FURTHER SOIL SAMPLING AT M.I.T. CAMPUS

11.8.1 General

M.I.T. has developed several new theories which provide the geotechnical engineer with a framework for analyzing and interpreting the piezocone penetrometer data. Additional testing is needed to further evaluate the device and establish correlations between the penetrometer measurements and the engineering properties of the soil as determined by means of laboratory testing techniques.

One of the requirements for evaluating new devices is a site having a known and established soil profile and properties. The foundation soils under the M.I.T. campus were extrusively evaluated and their stress history and soil properties are well established, Ladd et al. (1965). Horn et al. (1964), Lambe et al. (1964), Gass (1964), Davis (1965), Sabga (1966). A test site on the western side of the campus was proposed. Insitu testing was performed on 10/30/81 through 11/12/81.Soil samples were also retrieved for laboratory testing using the same procedures vollowed in the previous sampling operation at I-95.

Figure 11.18 shows the generalized soil profile at the site and Fig.11.19, the corresponding stress history.

11.8.2 Radiographs of Boston Blue Clay Samples

This section presents radiographs (reproduced herein as positives made from x-ray negatives) to illustrate various features detected in the Boston Blue Clay samples:

(a) Gross Sample Disturbance

Figure 11.20 shows the effect of disturbance on the bottom part of the tube sampler retrieved from a depth of 58-60 ft. The contorted bedding planes between markings 7 and 4 could be caused by tube side friction or mishandling of the tube after retrieval. Obviously this section of the tube is disqualified from being representative of the insitu soils and cannot be used for testing purposes. Figure 11.21 also shows

the effect of disturbance in the middle section of the tube sampler retrieved from a depth of 95-97 ft. The disturbance manifests itself in the formation of two shear planes AA and BB. The effect of disturbance is most prominant between markings "J" and "H". At "I" a plug of soil is displaced vertically downwards. The bedding planes immediately adjacent to it have remained horizontal. The cause of this disturbance is not well understood, it could be due to sampler side friction or due to a shock, etc. However, it is evident that the portion of the sampling tube should be avoided.

(b) Examples of Good Quality Samples

Figure 11.22 shows a good quality sample retrieved from a depth of 58-60 ft. Again, the soil appears to be homogeneous and uniform in consistency with the exception of an isolated sand patch shown as a dark plane close to mark "H".

(c) Stratification Identification

Figure 11.23 shows a clear change in the nature of soils retrieved from a depth of 74-76 ft. Beginning at mark denoted by "H" the soil below which appears to be of a higher density than the one on top of it. Assuming no change in the minerology, which is safe to assume in this case, it would appear that this part of the tube sampler contains a higher portion of sand or

silt etc. This is in agreement with the soil profile shown in Figure 11.28. Silt or sand seams are also evident in the top and bottom portion and further verify the afforementioned soil profile.

Figure 11.24 shows an unexpected anomaly. Contrary to the soil profile given in Figure 11.28, the radiograph of the middle portion of the tube retrieved from 84-86 ft. shows that at marking "I" there is a definite change in the soil composition suggesting a lower density soil underlying the clay with the high silt or sand content. This anomaly persists for approximately one foot and then the original consistency prodominates, Figure 11.25.

Finally, Figures 11.26 and 11.27 show a marked change in the soil composition. Figure 11.26 representing the bottom portion of the sampler tube retrieved from a depth of 95-97 ft., exhibits the abundance of silt or sand seams in clayey metrix. Figure 11.27 representing the middle portion of the sampler tube retrieved from a depth of 100-102 ft. clearly indicates the presence of a much denser material and becomes progressively denser with depth. This indicates a much higher silt or sand content and is in agreement with the soil profile shown in Figure 11.28. A horizontal crack appears at "G", presumably due to progressive loss of adhesion as the silt or sand content increases with

depth. The expansion of a gas pocket at "G" after retrieval could also provide an explanation to the presence of the horizontal crack.

11.9 SUMMARY

With the current need for high quality representative soil specimens characterized by a high cost of retrieval, a reliable method for planning and location of each specimen in the sampling liner is of essence. X-radiography provides an excellent non-destructive method that provides a spatial view of the interior of the soil sample.

X-radiography is successful in identifying:

(1) Zones of excessive disturbance;
   (a) Possible presence of remolded soil, (Figure 11.20)
   (b) Zones in the vicinity of foreign objects; stones, shells, etc., (Figure 11.9)
   (c) Zones experiencing shock due to mishandling, (Figure 11.21)

(2) Zones containing large horizontal cracks, possibly due to gas or difficulty in retrieval, especially when sand or silt seams are experienced. (Figure 11.27)

(3) Location of good to excellent quality samples with little or no evidence of disturbance. (Figure 11.22)

(4) Identifying location of foreign objects; stones, shells, gravel layers, etc.. (Figure 11.9,11.12 11.15)

(5) Differences in macroscopic structures, e.g., very uniform and homogeneous to slightly layered. (Figure 11.13)

(6) An estimate of the possible soil profile in the location.

It is therefore of essence that x-radiography of such samples be executed prior to the initiation of any testing program to:

(1) Minimize the amount of wasted material

(2) Maximize the reliability of test data

(3) Ensure representativeness

(4) Reduce the number of tests run on poor quality material

(5) Identify the exact location of the soil specimen to be tested.

Preliminary identification of possible locations of good quality samples should be continuously updated, guided by the values of shear strength obtained by the Torvane.

The increased reliability of the laboratory data improves the basis for making engineering judgements regarding design of foundations for public facilities and enhances our ability to perform a proper evaluation of newly developed insitu testing.

Tube No.[1] (Depth)	Sample No.	Depth (ft.)	$s_u(TV)$ Field (TSF)[2]	$s_u(TV)$ Lab (TSF)	w_n (%)	Sample Orientation[3]	Test[4]	$\frac{s_u(TV)_{lab}}{s_u(TV)_{field}}$[5]	Sample Quality	Sample Visual Description
M-2 (21.5'-23.5')	21.5-23.5-C.V	22.24	-	.600	19.61	Vertical	CRSC	-	Fair-Poor	Excessive presence of sand patches (yellowish in color) Very poor cohesion lead to difficult handling procedures. Large stone removed from first two inches of sampler. Stiff nature coupled with abundance of large sand and silt patches necessitated patching operation as sample crumbles when trimmed.
	21.5-23.5-C-H	22.43	-	.600	22.09	Horizontal	CRSC	-	Fair-Poor	
	21.5-23.5-P-V	22.70	-	.650	29.25	Vertical	Permeability	-	Fair-Poor	
	21.5-23.5-P-H	22.95	-	.650	26.56	Horizontal	Permeability	-	Fair-Poor	
M-2 (26.5'-28.5')	26.5-28.5-O-V	26.59	-	.350	30.85	Vertical	Oedometer	-	Fair	Presence of sand patches and silt seams attenuated. Poor cohesion lead to difficult handling procedures. Values of $s_u(TV)_{lab}$ were consistent throughout sampler Presence of contacted layering suggest probable disturbance
	26.5-28.5-O-H	26.77	-	.350	26.92	Horizontal	Oedometer	-	Fair	
	26.5-28.5-P-V	27.04	-	.375	25.42	Vertical	Permeability	-	Fair	
	26.5-28.5-P-H	27.25	-	.375	25.88	Horizontal	Permeability	-	Fair	
	26.5-28.5-C-V	27.43	-	.370	21.12	Vertical	CRSC	-	Fair	
	26.5-28.5-C-H	27.63	-	.370	21.46	Horizontal	CRSC	-	Fair	

1. Fixed Piston 3.5" diameter thin walled sampler
2. $s_u(TV)$ field values taken immediately after sampling operation in the field before waxing tube sampler.
3. Reader referred to Fig. 12.8 for sample orientation.
4. CRSC tests carried out in M.I.T.'s general purpose consolidation cell on 1.94" diameter samples, WISSA (1969). Oedometer Tests carried out in fixed ring oedometer cells Lambe (1951). Constant heat permeability tests carried out on 1'5" diameter samples in triaxial cells.
5. Values close to unity indicate good quality samples. Here disturbance introduced due to sampling, transportation and handling.

Table 11.1 Laboratory testing program, sample designation, quality and visual description.

Tube No.[1] (Depth)	Sample No.	Depth (ft.)	$s_u(TV)$ [2] Field (TSF)	$s_u(TV)$ Lab (TSF)	w_n (%)	Sample Orientation[3]	Test [4]	$\frac{s_u(TV)_{lab}}{s_u(TV)_{field}}$ [5]	Sample Quality	Sample Visual Description
M-2 (36.5'-38.5')	36.5-38.5-C-V	36.59	-	.390	50.07	Vertical	CRSC	-	Good	Excessive presence of layering less silt content. Improved cohesion and easier handling procedures. Consistent values of $s_u(TV)_{lab}$.
	36.5-38.5-P-V	37.06	-	.380	35.09	Vertical	Permeability	-	Good	
	36.5-38.5-P-H	37.06	-	.380	35.09	Horizontal	Permeability	-	Good	
	36.5-38.5-C-H	37.18	-	.385	31.15	Horizontal	CRSC	-	Good	
G (40'-42')	SP 03 VERT	41.00	-	-	30.53	Vertical	CRSC	-	Good	-
M-2 (41.5'-43.5')	41.5-43.5-P-V	42.25	0.30-0.15	.189	34.52	Vertical	Permeability	0.63	Poor	Presence of silt seams (continuous and isilated). Presence of silt seams causing occasional spalling. At 41.59 a large stone removed causing disturbance in its vicinity evidenced by low values of $s_v(lab)$
	41.5-43.5-P-H	42.47	0.30-0.15	.196	42.87	Horizontal	Permeability	0.653	Poor	
	41.5-43.5-C-V	43.12	0.30-0.15	.416	27.69	Vertical	CRSC	1.38	Good	
	41.5-45.3-C-H	43.31	0.30-0.15	.416	29.15	Horizontal	CRSC	1.38	Good	
G (51'-52')	SP 05 VERT	51.95	-	-	43.50	Vertital	CRSC	-	Good	-

1. Fixed Piston 3.5" diameter thin walled sampler
2. $s_u(TV)_{field}$ values taken immediately after sampling operation in the field before waxing tube sampler.
3. Reader referred to Fig.12.8 for sample orientation.
4. CRSC tests carried out in MIT's general purpose consolidation cell on 1.94"diameter samples, WISSA (1969). Oedometer Tests carried out in fixed oedometer cells, Lambe (1951). Constant head permeability tests carried out on 1.5" diameter samples in triaxial cells.
5. Values close to unity indicate good quality samples. Here disturbance introduced due to sampling, transportation and handling.

Table 11.1 (cont.) Laboratory testing program, sample designation, quality and visual description.

Tube No.[1] (Depth)	Sample No.	Depth (ft.)	$s_u(TV)$[2] Field (TSF)	$s_u(TV)$ Lab (TSF)	w_n (%)	Sample Orientation[3]	Test[4]	$\frac{s_u(TV)_{lab}}{s_u(TV)_{field}}$[5]	Sample Quality	Sample Visual Description
G (61'-62')	SPO 7 VERT	62.31	-	-	41.61	Vertical	CRSC	-	Good	-
M-2 (60'-62')	60-62-P-V	60.53	-	.325	40.79	Vertical	Permeability	-	Good	Layered clay with reduced frequency to no layering. Clay soft and plastic. Relatively easy to trim.
	60-62-P-H	60.53	-	.325	40.12	Horizontal	Permeability	-	Good	
	60-62-C-V	61.47	-	.352	43.20	Vertical	CRSC	-	Good	
	60-62-C-H	61.47	-	.352	40.18	Horizontal	CRSC	-	Good	
G (66'-67')	SP 08 VERT	67.48	-	-	47.10	Vertical	CRSC	-	Good	Layered clay with reduced frequency. Soft plastic clay. Occasional isolated sand or silt pockets.
G (72'-73')	SP 16 VERT	73.48	-	-	42.70	Vertical	CRSC	-	Good	Layered clay with greatly attenuated frequency. Soft and plastic
M-2 (75'-77')	75-77-P-V	75.17	0.15	0.200	38.81	Vertical	Permeability	1.33	Good	Layered clay with greatly attenuated frequency. Soft and plastic.
	75-77-P-H	75.50	0.15	0.245	36.87	Horizontal	Permeability	1.633	Good	
G (77'-79')	SP 09 VERT	78.48	-	-	42.00	Vertical	CRSC	-	Good	Homogeneous soft plastic clay.

1. Fixed Piston 3.5" diameter thin walled sampler.
2. $s_u(TV)_{field}$ values taken immediately after sampling operation in the field before waxing tube sampler.
3. Reader referred to Fig. 12.8 for sample orientation.
4. CRSC tests carried out in MIT's general purpose consolidation cell on 1.94" diameter samples, WISSA (1969). Oedometer Tests carried out in fixed ring oedometer cells, Lambe (1951). Constant heat permeability tests carried out on 1.5" diameter samples in triaxial cells.
5. Values close to unity indicate good quality samples. Here disturbance introduced due to sampling, transportation, and handling.

Table 11.1 (cont.) Laboratory testing program, sample designation, quality and visual description.

Tube No.[1] (Depth)	Sample No.	Depth (ft.)	$s_u(TV)$[2] Field (TSF)	$s_u(TV)$ Lab (TSF)	w_n(%)	Sample Orientation[3]	Test[4]	$\frac{s_u(TV)_{lab}}{s_u(TV)_{field}}$[5]	Sample Quality	Sample Visual Description
M-2 (82'-84')	82-84-O-V	82.19	0.24	0.250	45.35	Vertical	Oedometer	1.04	Good	Homogeneous soft plastic clay, a layer of gravel initially identified in the Xradiogram was confirmed upon visual identification.
	82-84-O-H	82.58	0.24	0.250	40.39	Horizontal	Oedometer	1.04	Good	
	82-84-P-V	83.77	0.24	0.230	45.89	Vertical	Permeability	.958	Good	
	82-84-P-H	83.77	0.24	0.230	41.12	Horizontal	Permeability	.958	Good	
G (82'-83')	SP 17 VERT	83.49	-	-	41.10	Vertical	CRSC	-	Good-Fair	Homogeneous soft clay Blue/Gray
G (83'-84')	SP 10 VERT	84.49	-	-	44.50	Vertical	CRSC	-	Good	Homogeneous soft plastic clay. Blue/Gray
G (87'-88')	SP 18 VERT	88.49	-	-	50.00	Vertical	CRSC	-	Good	Homogeneous soft plastic clay. Blue/Gray
M-2 (90'-92')	90-92-O-V	90.07	0.227	0.250	47.67	Vertical	Oedometer	1.098	Good	Homogeneous soft clay. A layer of shells and stones was earlier detected on Xradiograph and later confirmed visually. Blue/Gray Frequency of layering increases near bottom end of tube.
	90-92-O-H	90.25	0.227	0.250	45.06	Horizontal	Oedometer	1.098	Good	
	90-92-P-V	90.50	0.227	0.245	48.70	Vertical	Permeability	1.076	Good	
	90-92-P-H	90.50	0.227	0.245	48.80	Horizontal	Permeability	1.076	Good	
	90-92-C-V	90.89	0.227	0.266	45.80	Vertical	CRSC	1.17	Good	
	90-92-C-H	90.25	0.227	0.250	43.05	Horizontal	CRSC	1.10	Good	

1. Fixed Piston 3.5" diameter thin walled sampler.
2. $s_u(TV)_{field}$ values taken immediately after sampling operation in the field before waxing tube sampler.
3. Reader referred to Fig. 12.8 for sample orientation.
4. CRSC tests carried out in MIT's general purpose consolidation cell on 1.94" diameter samples, WISSA (1969). Oedometer tests carried out in fixed ring oedometer cells, Lambe (19). Constant heat permeability tests carried out on 1.5" diameter samples in triaxial cells.
5. Values close to unity indicate good quality samples. Here disturbance introduced due to sampling, transportation and handling.

Table 11.1 (cont.) Laboratory testing program, sample designation, quality and visual description.

Tube No.[1] (Depth)	Sample No.	Depth (ft.)	$s_u(TV)$[2] Field (TSF)	$s_u(TV)$ Lab (TSF)	w_n(%)	Sample Orientation[3]	Test[4]	$\frac{s_u(TV)_{lab}}{s_u(TV)_{field}}$[5]	Sample Quality	Sample Visual Description
G (92'-93')	SP 19 VERT	93.12	-	-	48.90	Vertical	CRSC	-	Good	Homogeneous soft plastic clay. Blue/Gray
G (97'-98')	SP 20 VERT	97.83	-	-	42.90	Vertical	CRSC	-	Good	Homogeneous soft plastic clay. Blue/Gray
G (98'-99')	SP 13 VERT	99.48	-	-	38.70	Vertical	CRSC	-	Good	Homogeneous soft plastic clay. Blue/Gray
M-2 (100'-102')	100-102-O-V	100.19	0.225	0.275	40.63	Vertical	Oedometer	1.22	Good	Uniform & Homogeneous plastic soft clay. Blue/Gray. Occasional presence of gravel and isolated sand patches. Frequency of laying increases close to bottom end of tube.
	100-102-O-H	100.22		0.289	44.10	Horizontal	Oedometer	1.24	Good	
	100-102-P-V	100.64		0.270	42.87	Vertical	Permeability	1.20	Good	
	100-102-P-H	100.72		0.250	40.42	Horizontal	Permeability	1.11	Good	
G (109'-110')	SP 15 VERT	109.48	-	-	40.70	Vertical	CRSC	-	Good	Homogeneous and uniform plastic soft clay. Blue/Gray

1. Fixed Piston 3.5" diameter thin walled sampler.
2. $s_u(TV)_{field}$ values taken immediately after sampling operation in the field before waxing tube sampler.
3. Reader referred to Fig. 12.8 for sample orientation.
4. CRSC tests carried out in MIT's general purpose consolidation cell on 1.94" diameter samples, WISSA (1969). Oedometer Tests carried out in fixed ring oedometer cells, Lambe (1951). Constant heat permeability tests carried out on 1.5" diameter samples in triaxial cells.
5. Values close to unity indicate good quality samples. Here disturbance introduced due to sampling, transportation and handling.

Table 11.1 (cont.) Laboratory testing program, sample designation, quality and visual description.

A. B.

Figure 11.1 Two areas of different density. Area A has a greater density than area B.

A. B.

Figure 11.2 Two diagrams of different contrast. Diagram A has higher contrast than diagram B.

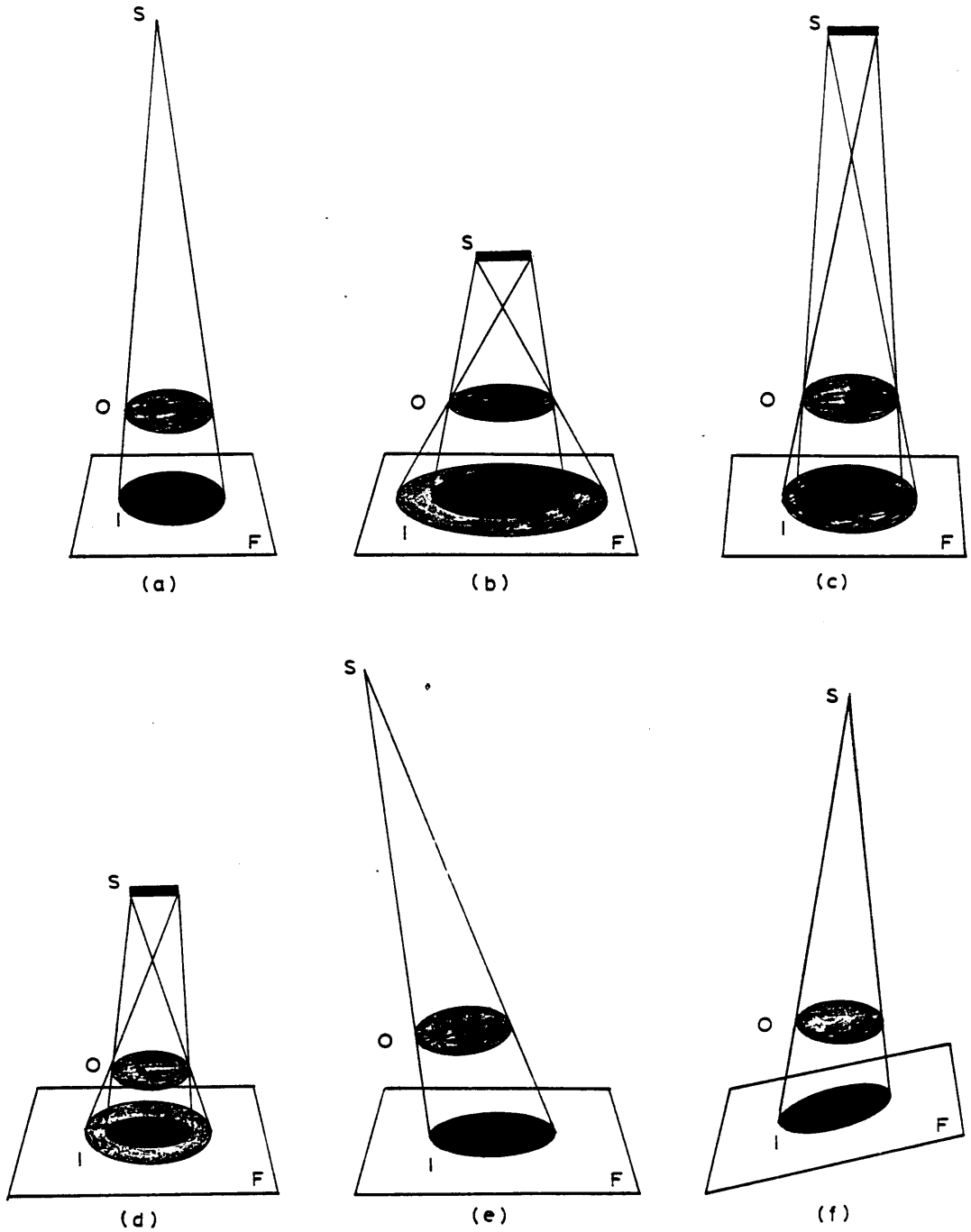

Figure 11.3 Geometric principals of image formation.(From Kodak,1969,Fig.13)

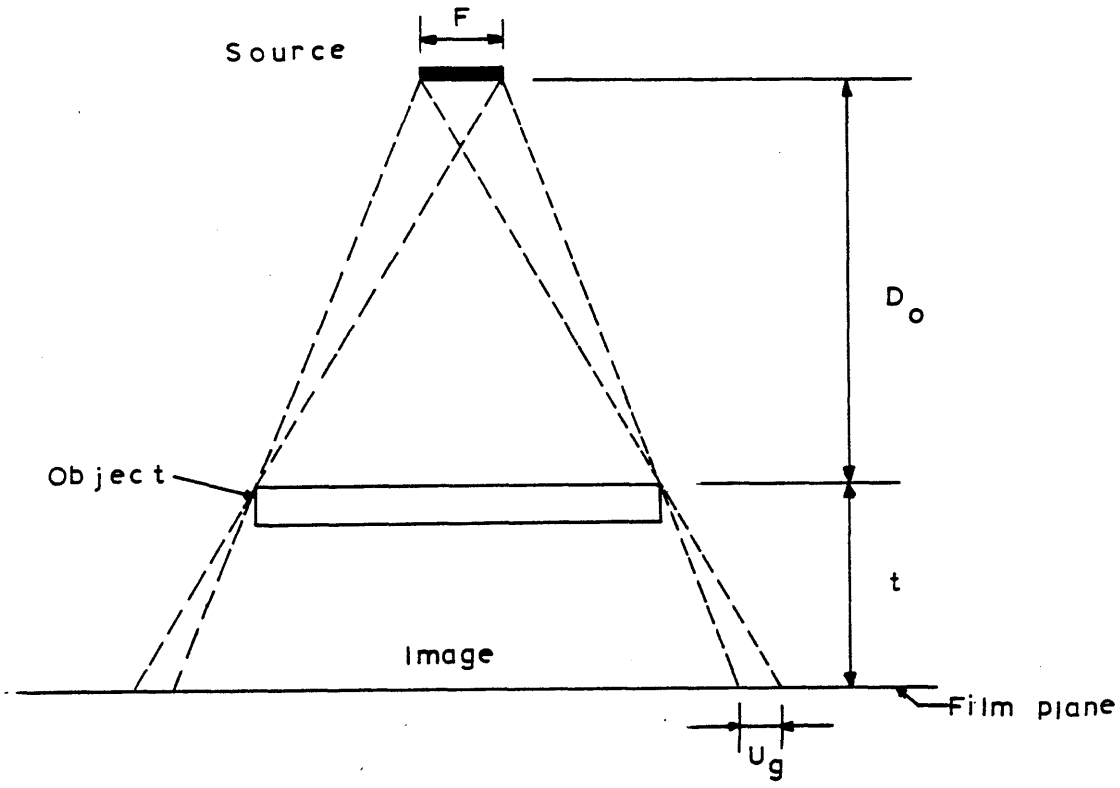

Figure 11.4 Geometric construction for determining Geometric Unsharpness (U_g).

$$U_g = F\ (t/D\ )$$

(From Kodak, 1969, Fig. 16)

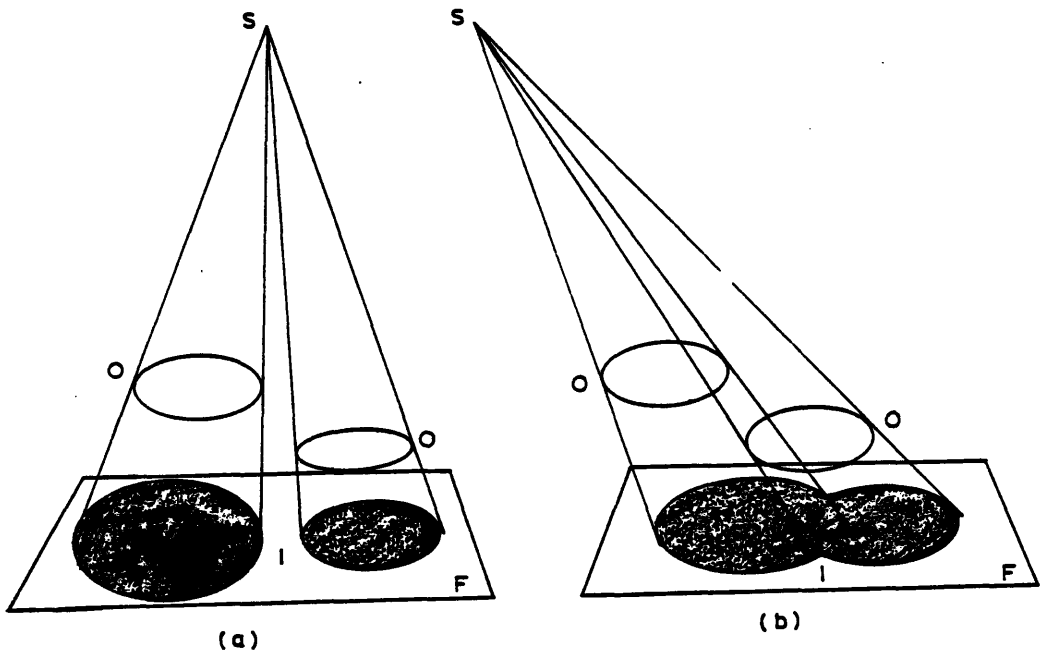

Figure 11.5 Two circular objects can be rendered as two separate circles (A),or as two overlapping circles (B), depending upon the direction of radiation.
(From Kodak,1969,Fig.14)

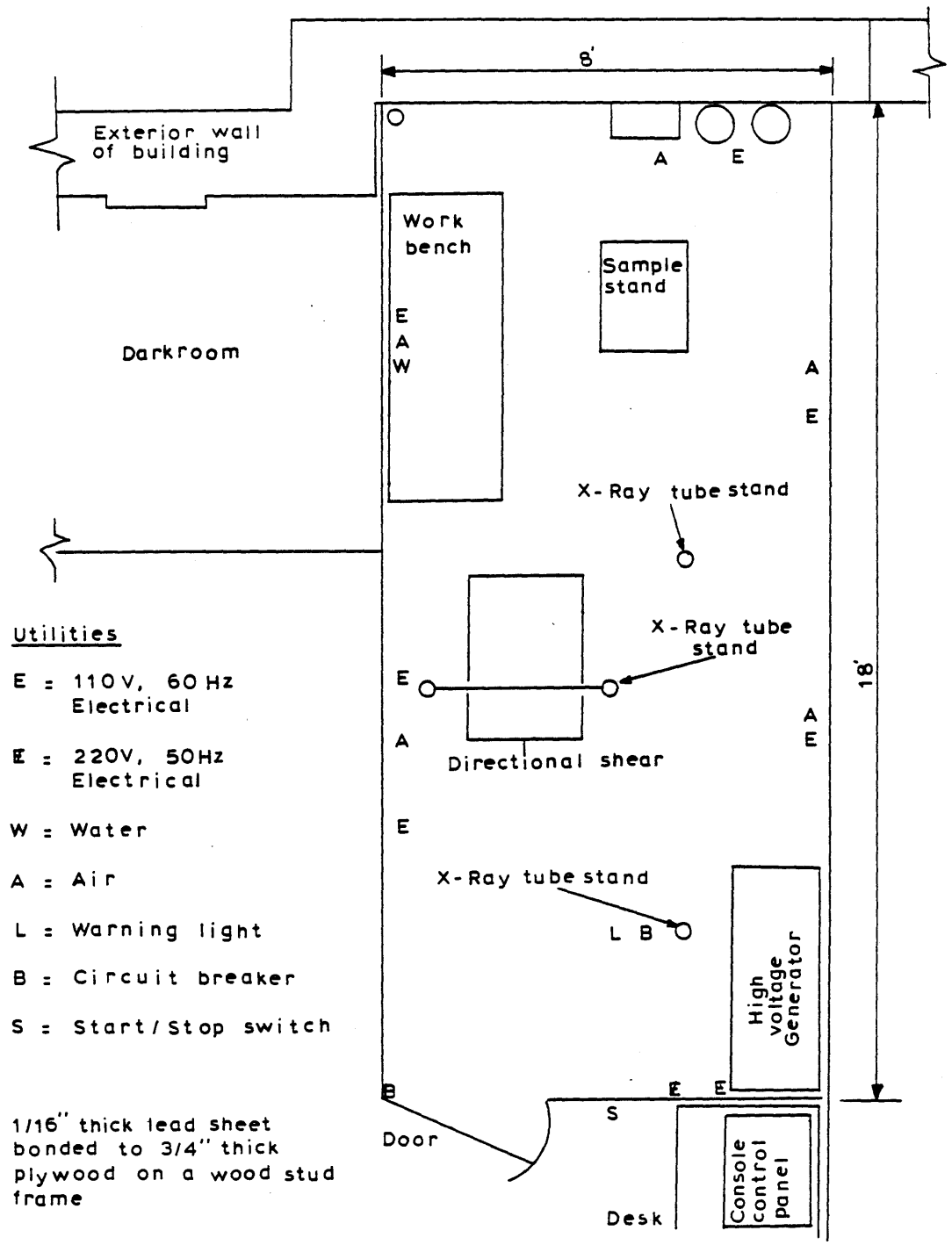

Figure 11.6 M.I.T.'s X-Radiography Facility
(Taverna Fig.2-3)

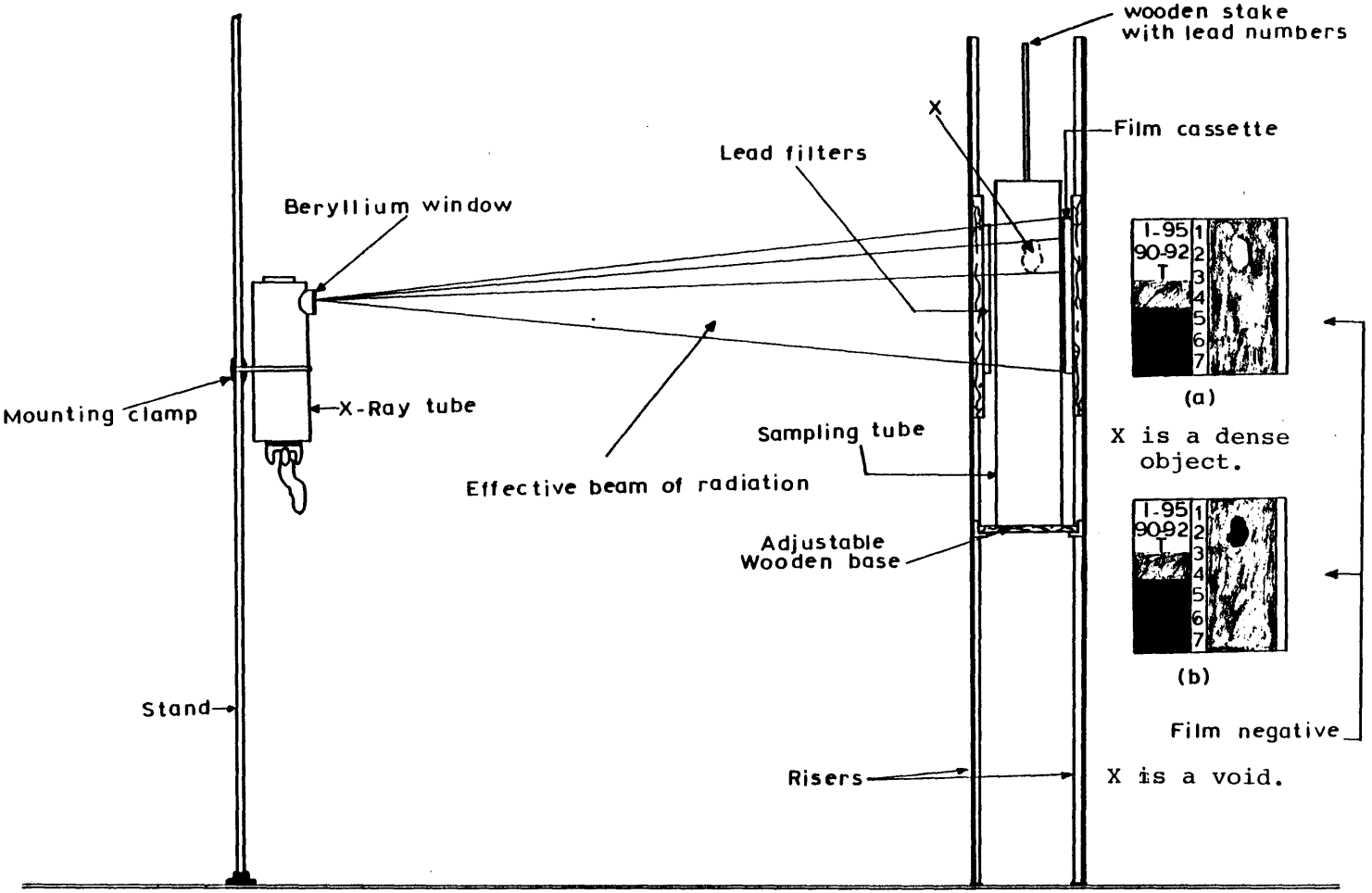

Figure 11.7 (b) General set up used to perform quality radiographs of soil samples retained in steel samplers.

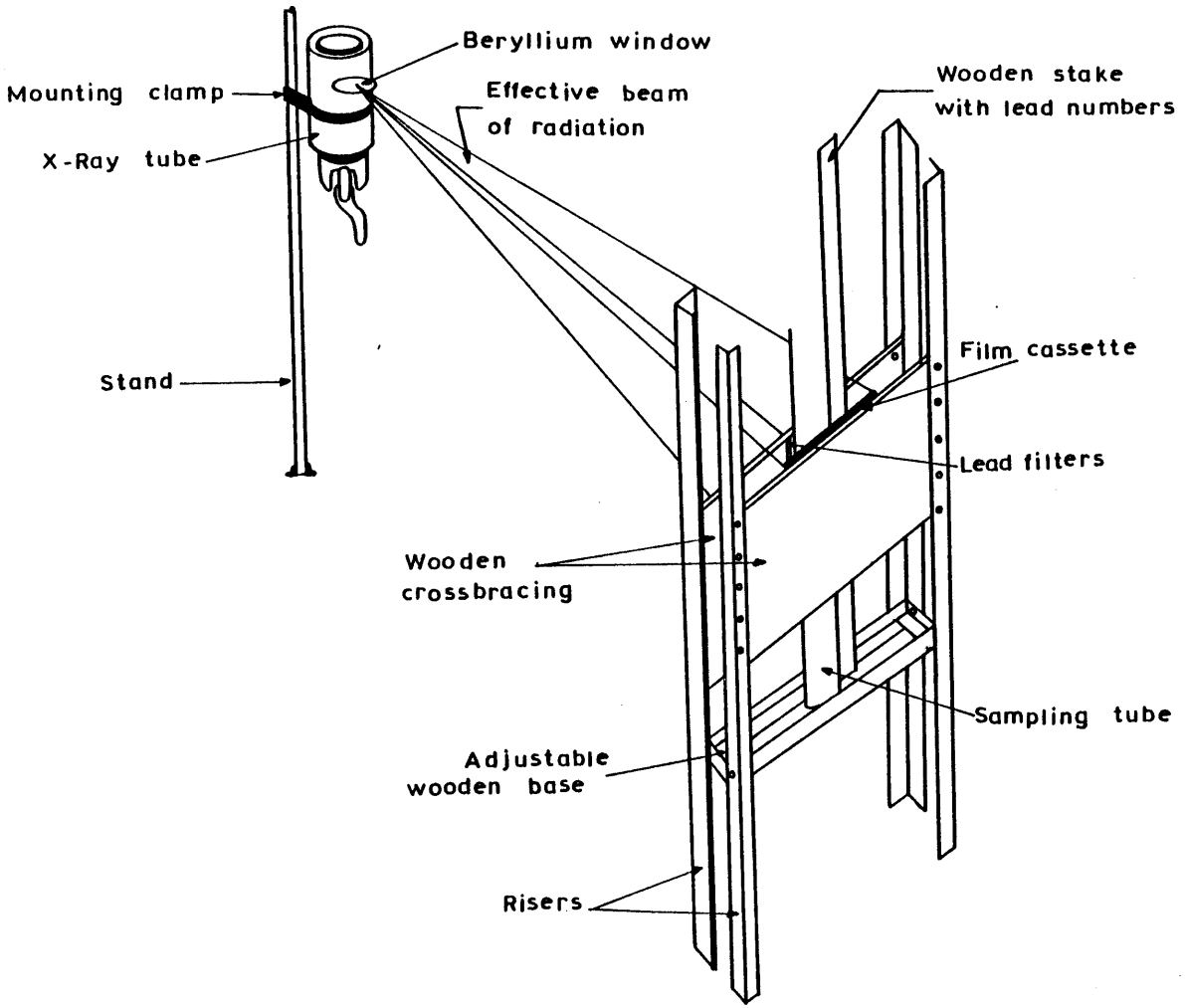

Figure 11.7 (a) General set up used to perform quality radiographs of soil samples retained in steel samplers.

(M-2)

SAMPLE NO. 41.5 - 43.5 **DEPTH** 41.5 - 43.5 ft.

Soil Type Boston Blue Clay. **Description** Interlayered with silt seams

Sample Type 3.5" Fixed piston w_N(%) 33.557 γ_t(pcf) 102.42

Testing Dates 5/8/81 - 10/23/81 s_u(TSF) Average of T.V. = 0.275

DEPTH (ft)	Description – Remarks	TV (TSF)	w_N (%)	w_L (%)	w_P (%)	P.I. (%)	L.I. (%)	G_s	Salt (g/ℓ)	Composition – Engr. Tests
41.5	1 1/8" Stone removed from top of tube	0.25								
		0.13								Visual inspection
		0.17								
	Blue / gray clay with a high content of silt and sand discontinuous seams	0.19								Aborted
			34.52					2.77		41.5-43.5-P-V
		0.19								
42.5		0.28	42.87					2.77		41.5-43.5-P-H
		0.26								Aborted
		0.33								
	Blue / gray clay with a reduced content of silt and sand discontinuous seams	0.42	27.69	48.91	23.52	25.39		2.77		41.5-43.5-C-V
		0.42	29.15	48.82	23.53	25.29		2.77		41.5-43.5-C-H
43.5										

Figure 11.8 Log of sampler tube (M-2) 41.5 -43.5

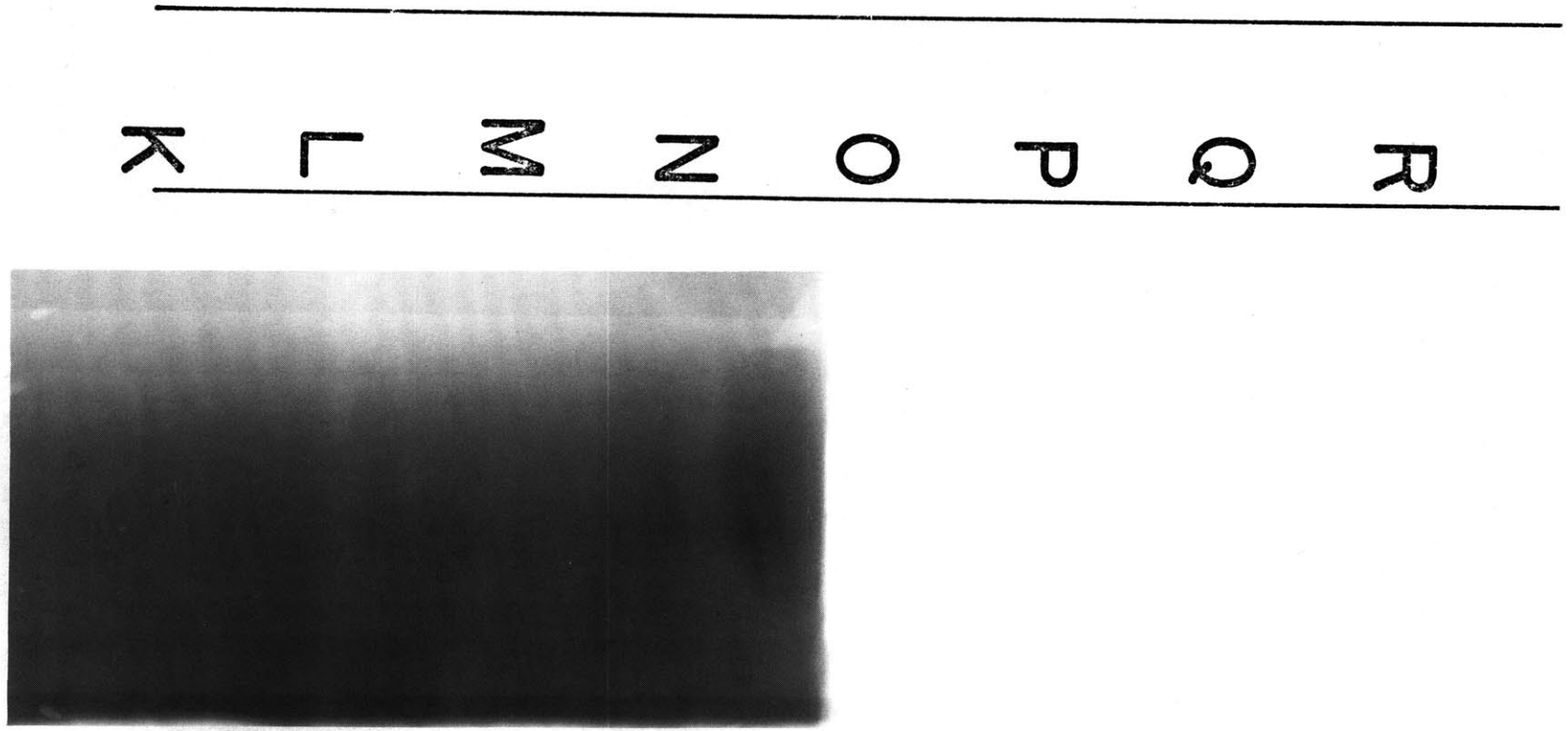

Figure 11.9 Radiograph print: Sample M2-41.5-43.5 (Top).

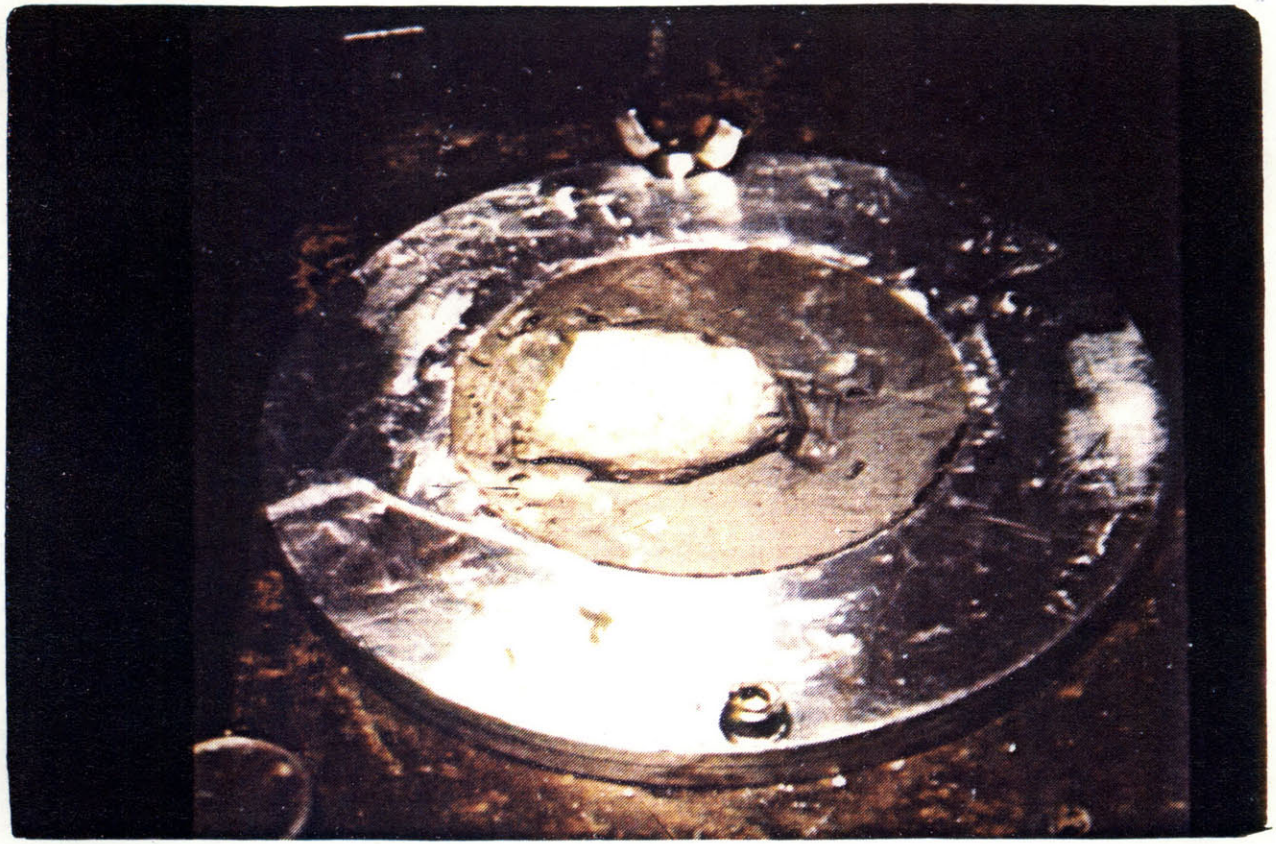

Figure 11.10 A large stone identified upon extrusion.

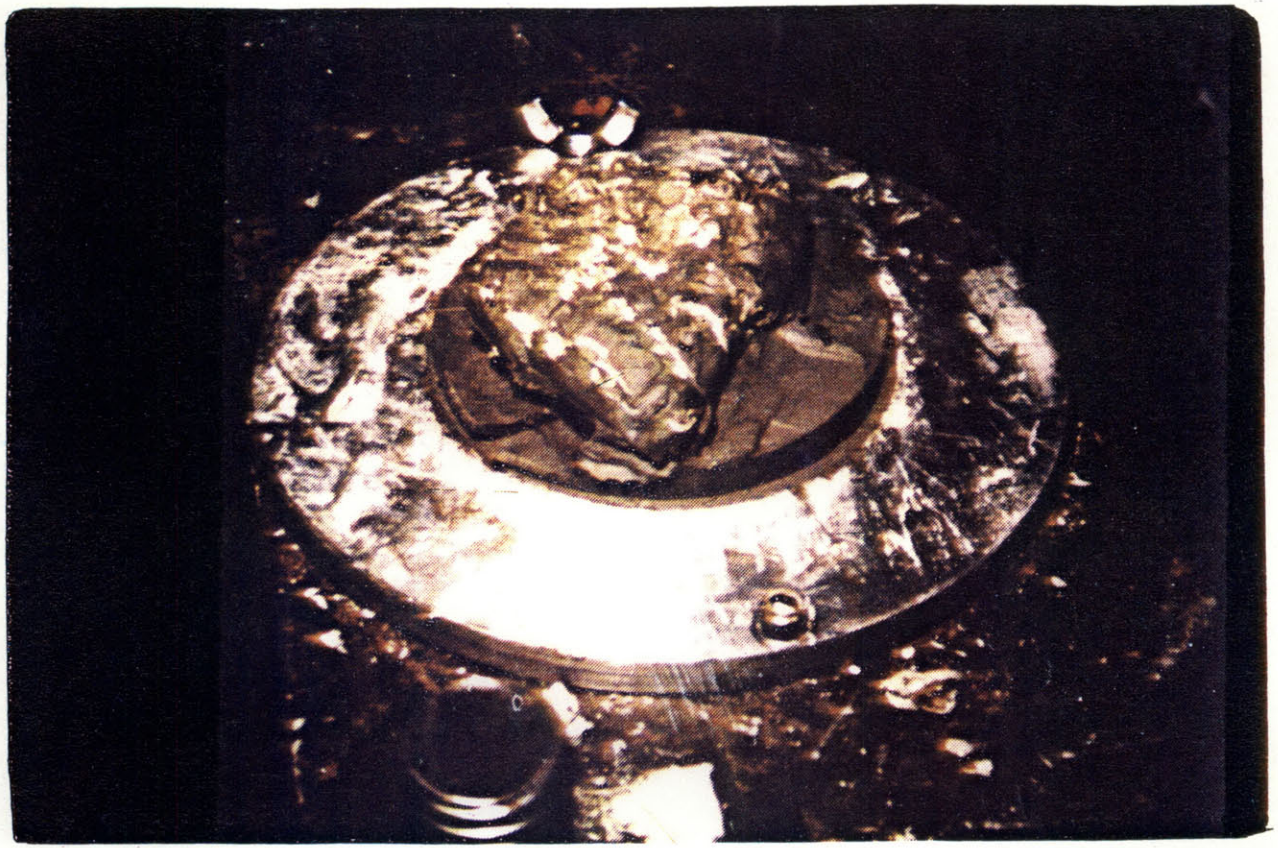

Figure 11.11 A large stone identified up extrusion.
(M2-82-84 Top)

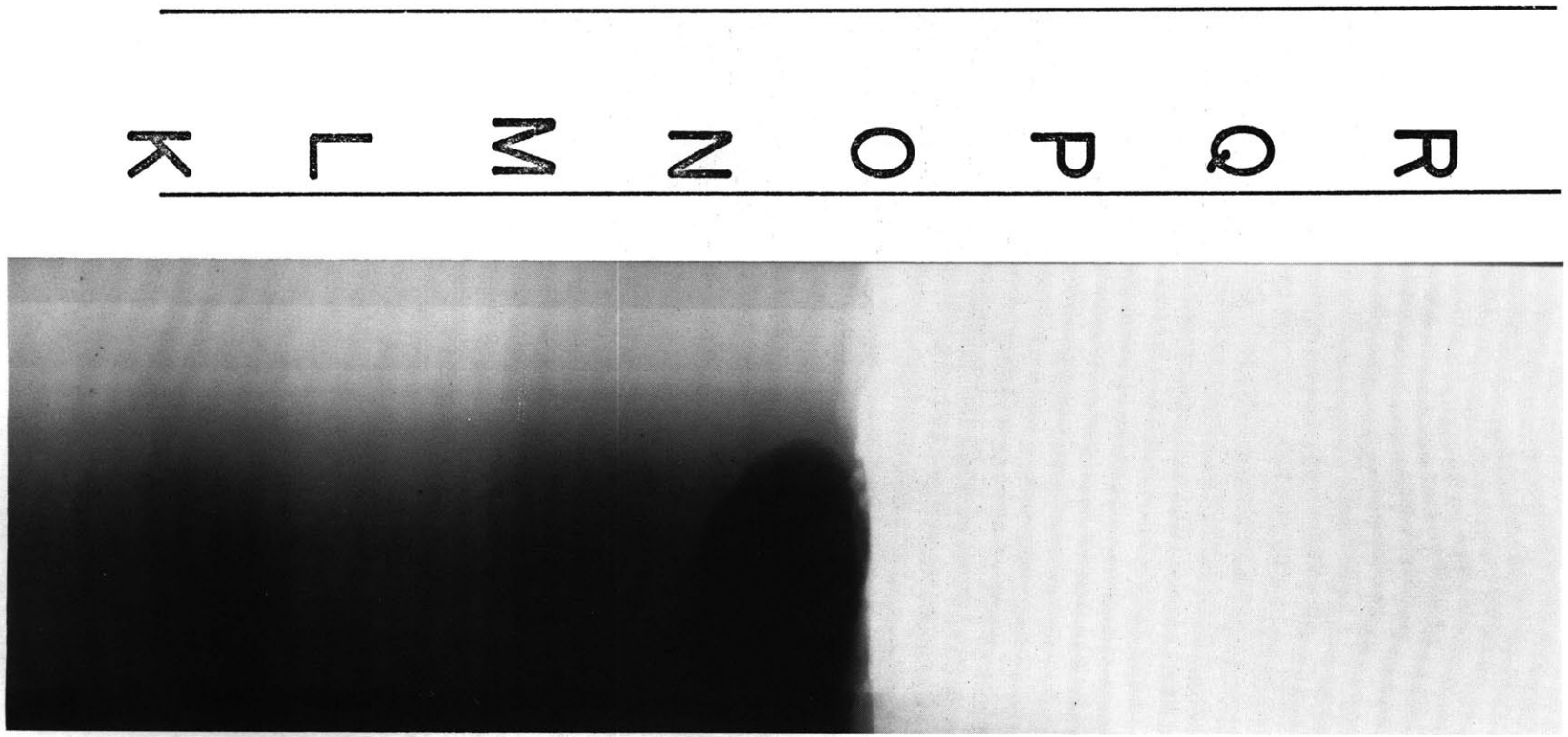

Figure 11.12 Radiograph print: Sample M2-82-84 (Top).

Figure 11.13 Radiograph print: Sample M2-41.5-43.5 (Middle)

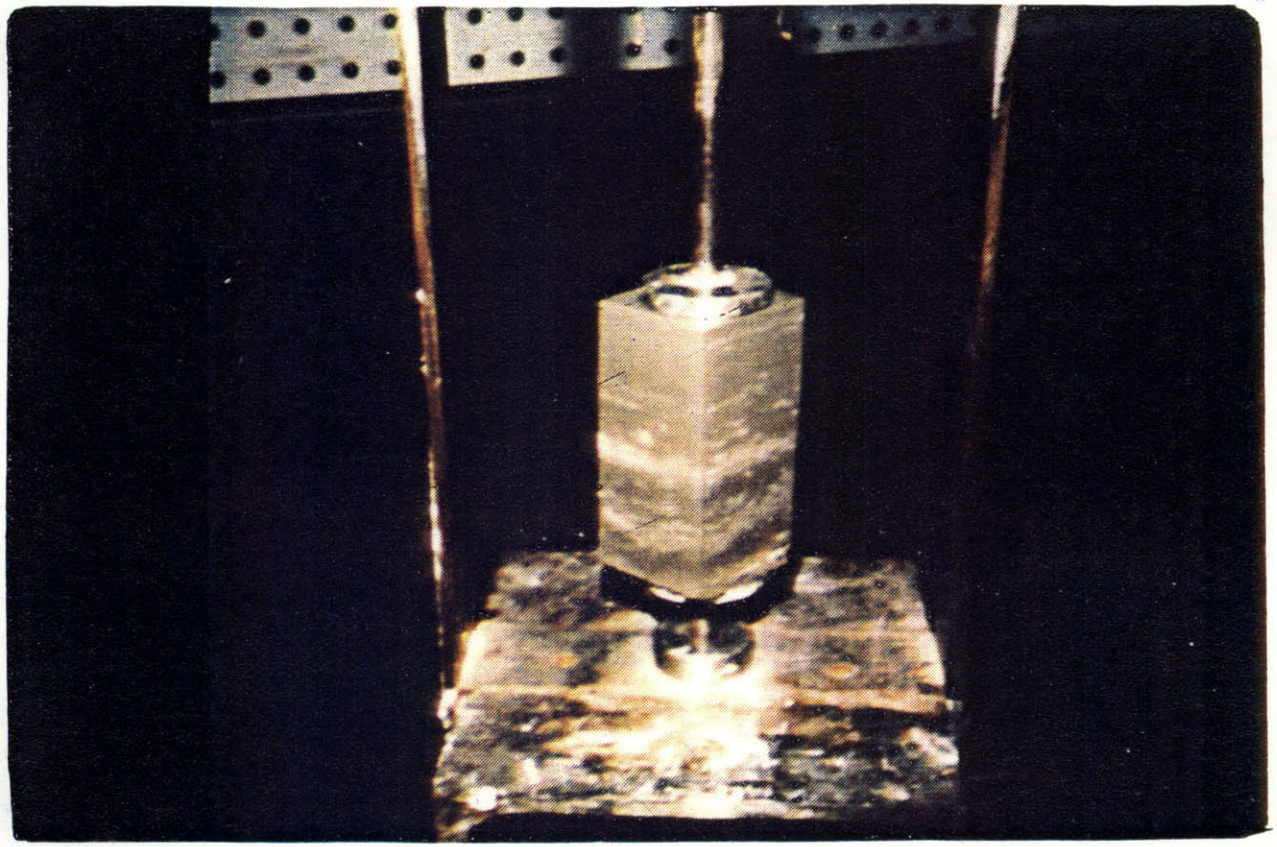

Figure 11.14 Layered nature of sample identified upon extrusion.

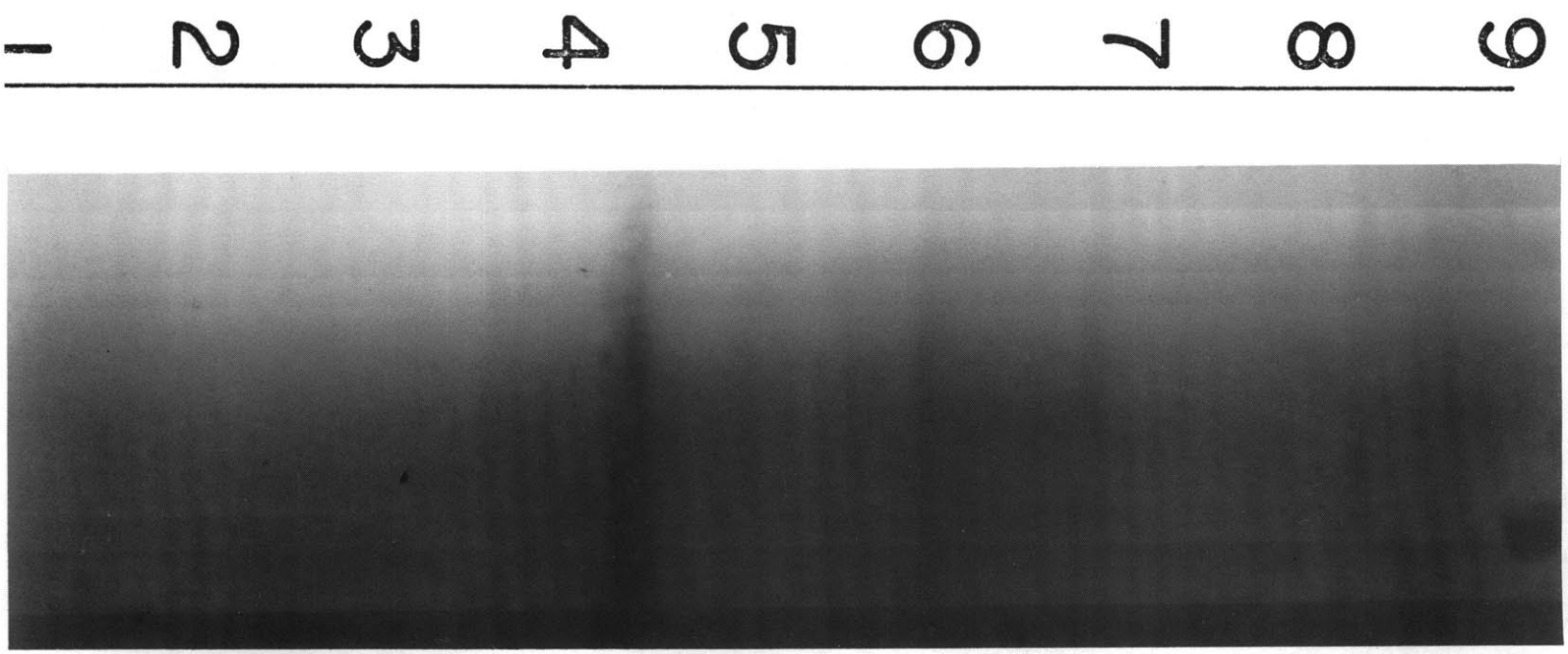

Figure 11.15 Radiograph print: Sample M2-82-84 (Bottom).

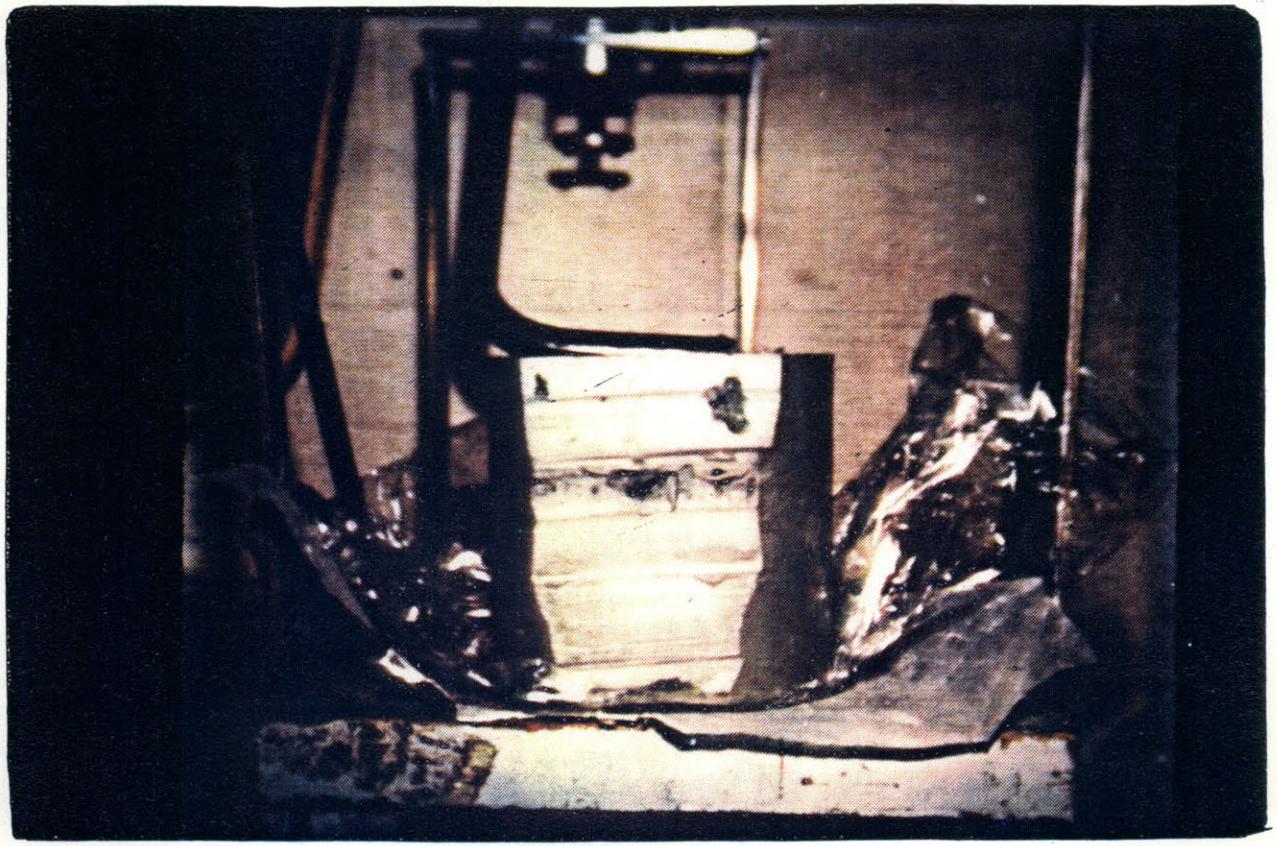

Figure 11.16.a Layer of gravel identified upon extrusion. (M2-82-84, Bottom)

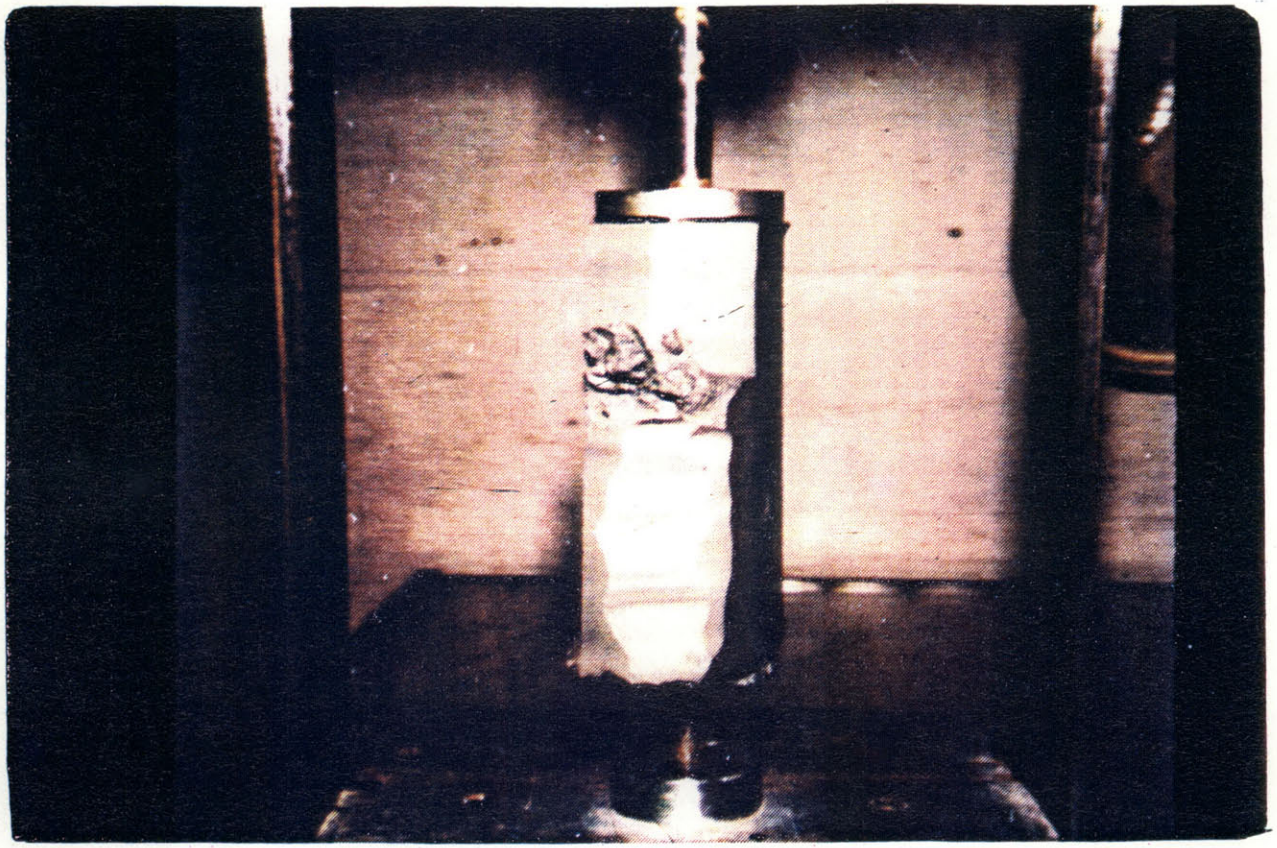

Figure 11.16.b Layer of gravel identified upon extrusion.

Figure 11.17 Radiograph print: Sample M2-82-84 (Middle)

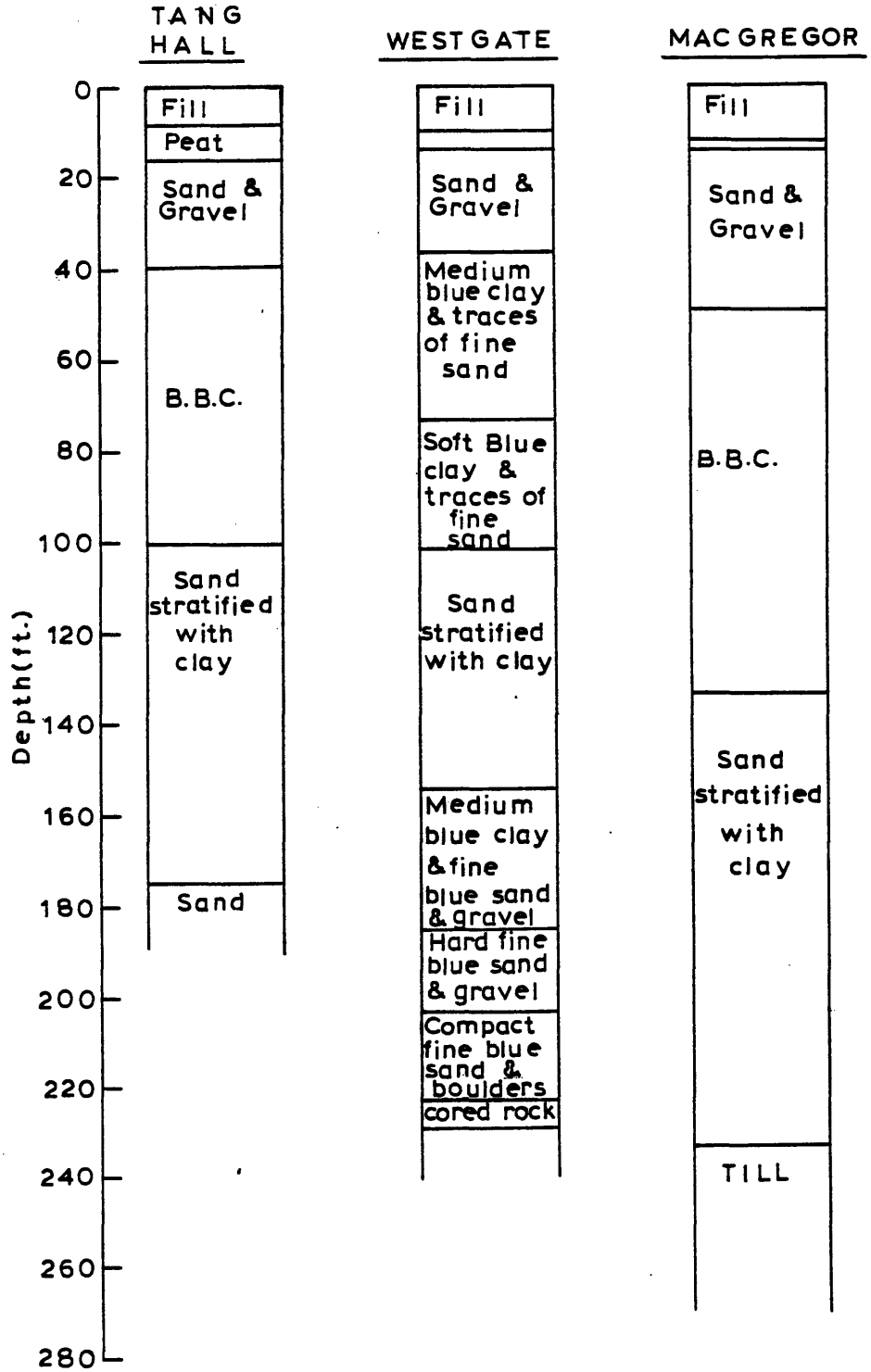

Figure 11.18 Generalized soil profiles at the west side of M.I.T campus.

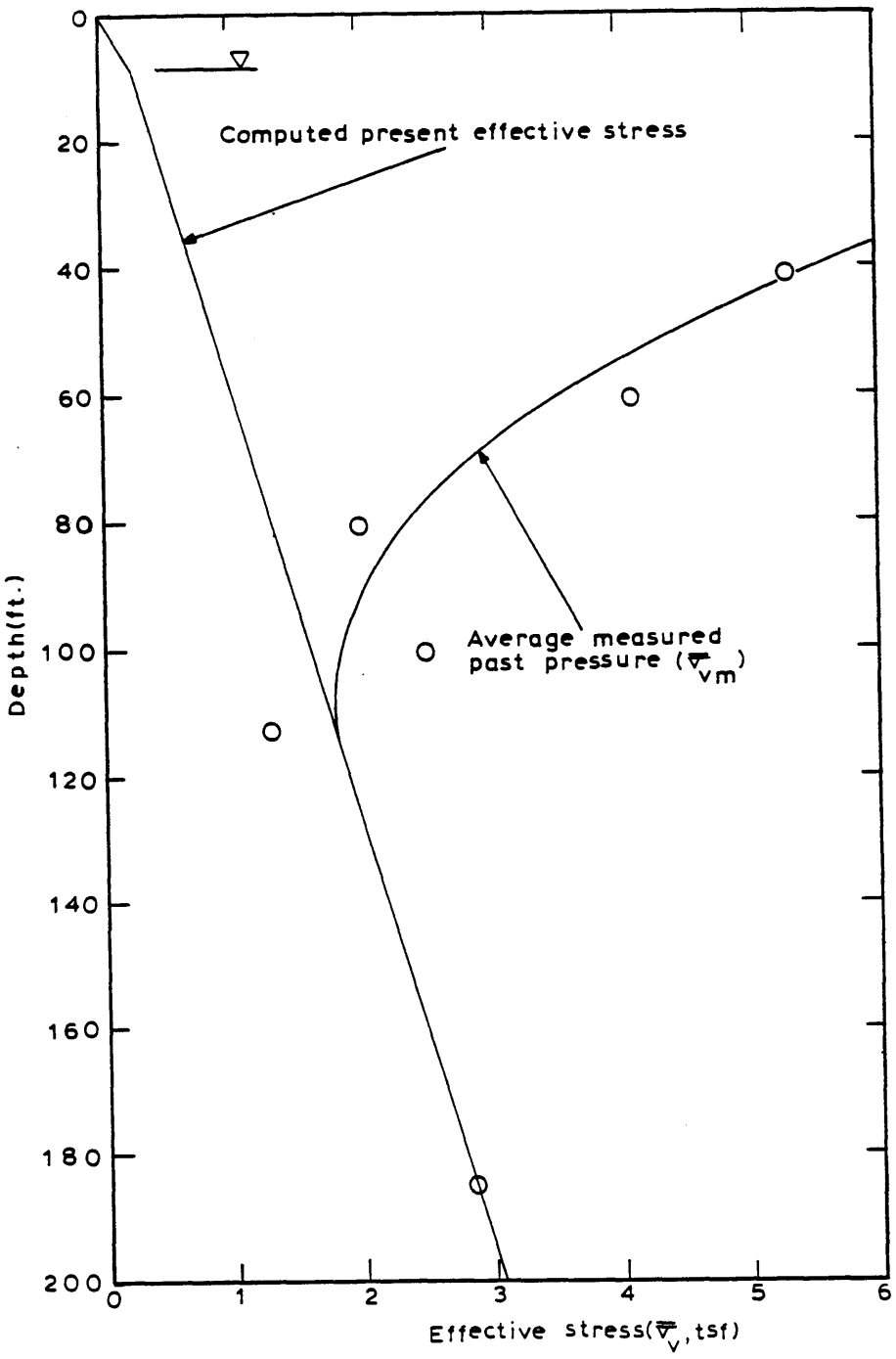

Figure 11.19 In situ effective stress and the stress history at the west side of M.I.T campus.

Figure 11.20 Radiograph print: Sample MUD1-4 (Bottom)

Figure 11.21 Radiograph print: Sample MUD1-9 (Middle).

Figure 11.22 Radiograph print: Sample MUD1-4 (Middle).

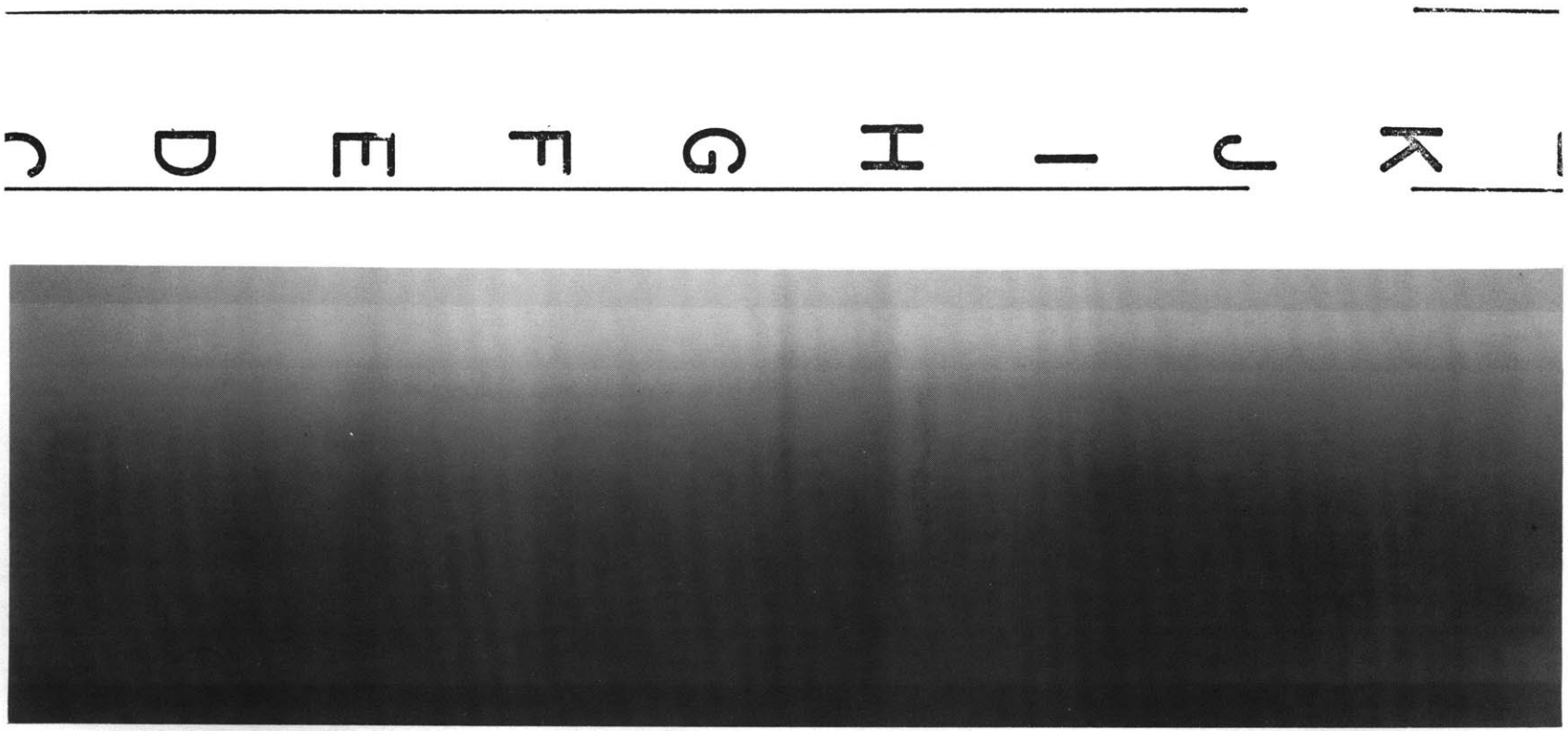

Figure 11.23 Radiograph print: Sample MUD1-6 (Middle)

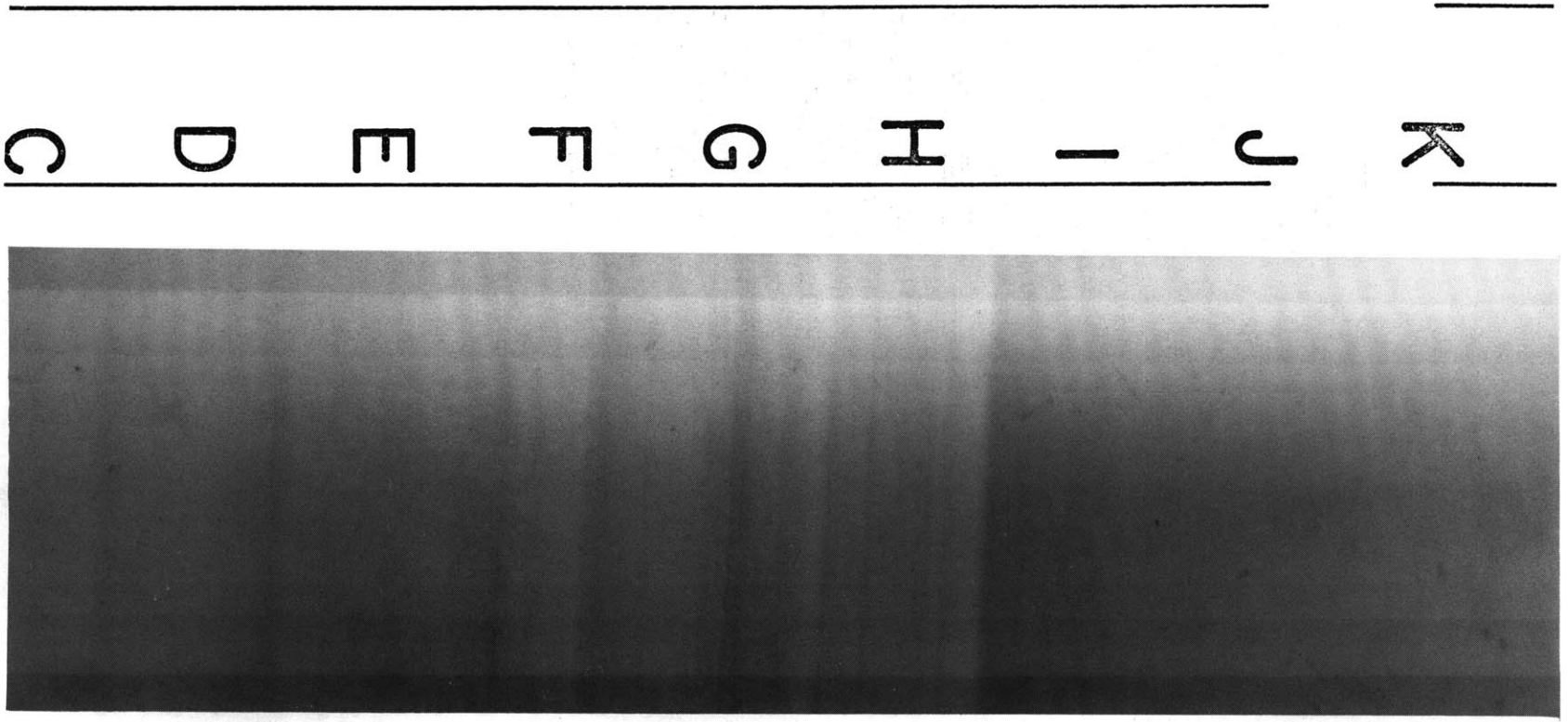

Figure 11.24 Radiograph print: Sample MUD1-7 (Middle)

Figure 11.25 Radiograph print: Sample MUD1-7 (Bottom).

Figure 11.26 Radiograph print: Sample MUD1-9 (Bottom).

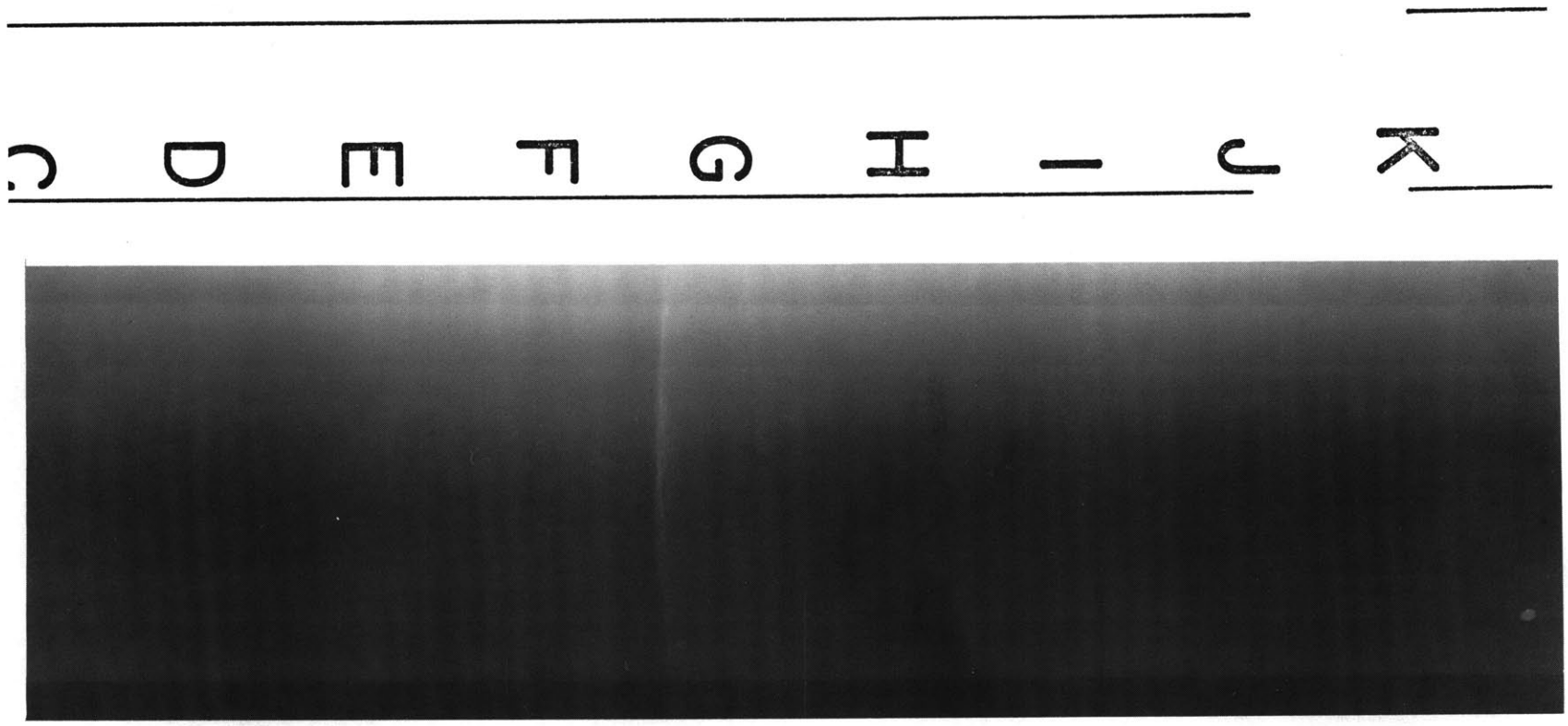

Figure 11.27 Radiograph print: Sample MUD1-10 (Middle).

CHAPTER 12

LABORATORY TESTING PROGRAM, RESULTS AND OBSERVATIONS

12.1 INTRODUCTION

Laboratory test data on undisturbed soil specimens retrieved from the I-95 test site is now used to verify predictions derived from dessipation records of the piezometer probe.

Comparison of the variation of $c_{h(probe)}$ versus depth, reference profile, with laboratory derived $c_{h(O.C)}$ at the in situ $\bar{\sigma}_{vo}$ reveal the fact that the $c_{h(probe)}$ profile is within the expected limits defined by $c_{v(in\ situ)}/c_{v(laboratory)}$, already discussed in Chapter 2, up to a depth of 42 ft. beyond which the $c_{h(probe)}$ grossly overestimates $c_{h(O.C)laboratory}$.

Comparison of $k_{h(probe)}$ with laboratory derived values of $k_{h(O.C)}$ reveals reasonably good agreement.

The severity of the assumptions used in interpreting the C_s profile for the foundation clay under the Student Center is assessed. The assumption of $c_{h(probe)} = c_{v(O.C)} = f(O.C.R)$ is found to be of low severity. The profile of $c_{v(O.C)}$ lies in tolerable limits defined by $c_{v(in\ situ)}/c_{v(laboratory)}$ discussed in Chapter 2.

Interesting soil behavioral aspects are derived and applied to the aforementioned investigation.

12.2 STRESS HISTORY AND CONSOLIDATION PROPERTIES

12.2.1 General

Table 12.1 briefly summarizes the important parameters derived from conventional oedometer tests and the Constant Rate of Strain test (C.R.S.C) conducted on the ten tube samples of Boston Blue Clay retrieved from bore hole M2 at the I-95 test site. To enhance the statistical stability of the results run on B.B.C retrieved from the immediate vacinity of hole M-2 conducted by Germaine (1980) are also included.

Table 12.1 presents the following data:

1. The natural water content for each oedometer and CRSC test as measured from test specimen trimmings.

2. The estimated effective overburden stress, $\bar{\sigma}_{vo}$, obtained from Baligh et. al. (1981).

3. The estimated Atterberg limits for each oedometer and CRSC test obtained from Baligh et. al. (1981).

4. Best estimates of $\bar{\sigma}_{vm}$ values determined with the Casagrande construction technique from compression curves corresponding to the end of primary consolidation.

5. Virgin Compression Ratios, CR, defined as the

slope of the vertical strain vs. log consolidation stress, $_{vc}$, line in the virgin compression region.

6. Recompression ratios, RR, defined as the average slope over the unload reload cycle from a stress $2 \times \bar{\sigma}_{vm}$.

7. Average coefficients of consolidation, c_v, or c_h as determined from dial readings vs. log time and square root of time curves for the normally consolidated region obtained from the conventional oedometer tests, and as supplied by the computer program, CRSCX, for the CRSC tests.

8. Assessment of the "quality" of the test results. The Evaluation criteria included factors like Torvane strength data and the measured strain at $\bar{\sigma}_{vc} = \bar{\sigma}_{vo}$ as they relate to the effects of sample disturbance.

12.2.2 Sample Disturbance and Its Effects on the Compressibility Characteristics

Ladd (1973) discussed the effects of sample disturbance on the compressibility characteristics. This section will attempt to demonstrate those effects with reference to CRSC data.

Figure D.3 and E.17 shown in appendices D and E represent the individual compression curves of samples retrieved from depths within the interval 82.84 ± .65 ft. The effect of depth variation on the in situ stress, $\bar{\sigma}_{vo}$, is negligable. Fig. 12.1 shows that disturbance has the following effects:

1. Increases the overall strain magnitudes. For example, the strain measured during recompression to 1 ksc are the ratio of 1:2.6.

2. Reduces value of the estimated maximum past pressure. Test No. 82-84-O-V yielded a value of $\bar{\sigma}_{vm}$ equal to 2.02-2.14 compared to 1.42-1.47 obtained from SP17VERT.

3. Lowers the compression ratio, CR. The corresponding values of CR obtained from tests are 0.3350 compared to 0.2900-0.1856.

4. Lowers the coefficient of consolidation, c_v, especially during recompression to $\bar{\sigma}_{vo}$.

To judge the quality of the oedometer and CRSC data, the disturbance indices developed by Ladd et. al. (1980) were used, namely:

(a) Ratio of Torvane strength measured directly above the oedometer or CRSC sample prior to extrusion to that measured at the bottom of the tube in the field,
$s_u(T.V)_{laboratory}/s_u(T.V)_{field}$.

(b) Amount of vertical strain, ε_v, at the vertical overburden stress, $\bar{\sigma}_{vo}$.

Classification into Poor, Fair and Good, requires increasing values of $s_u(T.V)_{laboratory}/s_u(T.V)_{field}$ and decreasing values of ε_v at $\bar{\sigma}_{vo}$, in that order.

12.2.3 Stress History

Fig. 12.2 shows the soil profile, the index properties and the stress history at the Saugus site (Baligh and Vivatrat, 1979). The corresponding data from the 33 consolidation tests have also been included. The data for $\bar{\sigma}_{vm}$ and OCR are in good agreement. The stress history of the deposit has already been discussed earlier, and the new data sustains initial conclusions.

12.2.4 Non Homogenity of Boston Blue Clay at Shallow Depths

Radiographs of shallow samples presented in Chapter 11 have indicated the presence of silt seams and extensive layering. This was confirmed upon extrusion and presented severe problems during the process of trimming. Spalling at the silt caly interface necessitated slight patching operations. This, of course, contributes to sample distrubance. Spalling was mostly marked during trimming operation of oedometer samples at very shallow depths. This was mainly due to two factors:

1. Silty nature of the clay sample.
2. The heavy and relatively thick cutting shoe used in conjunction with the restraining ring of the oedometer cell.

Fig. D.1 and Fig. E.3 shown in appendices D and E of the individual compression curves of an oedometer test and a CRSC test on samples retrieved from depths of 26.6 ft. and 27.4 ft., respectively. The effects of disturbance are evident. Furthermore, Fig. D.1 and Fig. E.3 show a large difference in the values of CR and RR of approximately 22.52% and 67.01% , respectively. It is obvious that disturbance is not the sole contributor to this difference as the soil's inherent nonhomogenity is also a significant factor.

Figs. E.1, E.5 and E.25 shown in appendix E , give the individual compression curves of three CRSC tests run on samples retrieved from depths of 22.2', 36.6' and 109.5', respectively. Fig. 12.3 shows the data collectively and the following observations are made:

1. A marked increase in the value of the Compression Ratio in the normally consolidation range, CR, with depth. The parameter CR takes on values of .088, 0.155 to a collapsable clay structure exhibited by the deepest sample.

2. A marked increase in the value of the recompression and swelling ratios, CR and SR respectively with depth.

The parameter RR takes on values of .0064 and .0211.

3. A marked increase in strains at any one particular value of consolidation stress $\bar{\sigma}_{vc}$. For a stress of one ksc, say, the corresponding strains are 1.09, 2.564 and 1.34%.

4. A marked decrease in the values of the coefficient of consolidation in the normally consolidation range, c_{vc}, rebound, c_{vs}, and recompression, c_{vr} with depth. This observation is treated in great detail in the following sections.

Fig. 12.4 exhibits the variation of CR and RR with depth. The values of RR for the top 15 feet are about an order of magnitude less, than the values RR for the bottom 60 feet which range between 2.0×10^{-2} and 3.0×10^{-2}. The values of CR for the top 15 feet are about a third the values of CR for the bottom 60 feet which range between 1.5×10^{-1} to 2.2×10^{-1} with large scatter close to the bottom boundary where the clay exhibits a collapsable structure.

12.2.5 Anisotropic Stress Strain Response of B.B.C.

Anisotropic response of B.B.C., and in fact all clays, is to be expected owing to the inherent anisotropy related to its mode of deposition. Anisotropic response is expected to be more severe as the degree of non homogenity increases. Henceforth, we would expect the shallower samples to exhibit a marked anisotropic behavior.

Figs. E.1 and E.2 from Appendix E show the compression curves for two CRSC tests on samples retrieved from 22.2 and 22.50 ft. trimmed vertically and horizontally, respectively. In both cases, the direction of the soil compression and drainage are identical. To some extent, those tests could shed some light on the possible anisotropic response of the soil to applied loading. Fig. 12.5 collectively incorporates the two compression curves and from which we observe:

1. The vertical sample appears to be less compressible in the normally consolidation range having a value of CR equal to .060 compared to .088 for the horizontal sample.

2. The values of the recompression ratio, RR, are essentially identical and equal to .0064.

3. The strains at a particular value of the consolidation stress are approximately equivalent.

Examination of Fig. 12.4 reveals that the values of CR and RR obtained from vertically and horizontally trimmed samples are almost identical with the exception of those values corresponding to the top 20 feet of the clay layer where a rather slight difference in the values of CR is manifested. At first glance, it would appear that the difference in the RR values is significant, however, remembering that during unloading and subsequent reloading at low values of $\bar{\sigma}_{vc}$ the effects of side

friction could substantially alter the stress strain behavior and since the method of construction is sensitive to such variations in the aforementioned zone, the observed difference in the two values of RR could be in part non-representative of the actual soil behavior. Hence such variations should be treated with due respect to the apparatus induced anomalies. A better method for comparing the compressibilities in the overconsolidated range is suggested in the following section.

12.2.6 Approximate equations for determining in situ values of permeability and coefficient of consolidation.

Cone penetration in clays causes undrained shearing of the soil under constant volume conditions and hence, in medium to soft clays, reduces the effective stresses. When steady penetration is interrupted and pore pressures start to dissipate, effective stresses increase and the soil decreases in volume. Soil compressibility during dissipation is very difficult to predict because of the complicated two dimensional nature of the problem and the variations of the soil compressibility during consolidation. However, knowing that consolidation starts at an effective stress level lower than previously existed before penetration, suggests that soil compressibility corresponds to a reloading (or recompression) mode, at least in the early stages of consolidation. In this mode, the soil compressibility is low and dissipation takes place rapidly because the

coefficient of consolidation is proportional to the ratio of permeability to compressibility. Using one-dimensional consolidation for illustration, this means that the coefficient of consolidation during vertical straining and horizontal water flow, is given by

$$c_h = \frac{k_h}{m_v \gamma_w}$$

In a virgin compression mode (normally consolidated clay)

$$m_{v(N.C)} = \frac{CR}{\Delta\bar{\sigma}_v} \log \left(1 + \frac{\Delta\bar{\sigma}_v}{\bar{\sigma}_{vc}}\right) \qquad 12.1$$

and in a recompression mode (over consolidated)

$$m_{v(O.C)} = \frac{RR}{\Delta\bar{\sigma}_v} \log \left(1 + \frac{\Delta\bar{\sigma}_v}{\bar{\sigma}_{vc}}\right) \qquad 12.2$$

where k_h is the horizontal permeability (cm/sec); m_v is the coefficient of volume charge (cm^2/kg); γ_w is the unit weight of water ($10^{-3} kg/cm^3$); CR and RR are the compression and recompression ratios respectively; and, $\bar{\sigma}_{vc}$ and $\Delta\bar{\sigma}_v$ are the vertical effective stress and its increment at any consolidation level, respectively (kg/cm^2).

For small increments of effective stresses (i.e., $\Delta\bar{\sigma}_v/\bar{\sigma}_{vc} << 1$) Eqs. 12.1 and 12.2 become

$$m_{v\,(N.C)} = \frac{CR}{2.3\bar{\sigma}_{vc}}$$

$$m_{v\,(O.C)} = \frac{RR}{2.3\bar{\sigma}_{vc}}$$

and hence,

$$k_h = \frac{\gamma_w}{2.3\bar{\sigma}_{vc}} \cdot RR \cdot c_{h\,(O.C)} \qquad 12.3$$

and for a fixed value of k_h (small changes in void ratio), we can also write

$$c_{h\,(N.C)} = \frac{RR}{CR}\, c_{h\,(O.C)} \qquad 12.4$$

Eqs. 12.3 and 12.4 provide estimates of the horizontal permeability, k_h, and the normally consolidated coefficient of consolidation, $c_{h\,(N.C)}$ in terms of the over consolidated horizontal coefficient of consolidation, $c_{h\,(O.C)}$ for vertical compression of the clay due to horizontal water flow.

Assuming that early consolidation around cones takes place in a recompression mode, we assume that Eqs. 12.3 and 12.4 can be used approximately for dissipation around conical probes when

$$c_h(\text{probe}) = c_{h\,(O.C)} \qquad 12.5$$

and

$$\bar{\sigma}_{vo} = \bar{\sigma}_{vc}. \qquad 12.6$$

where $c_{h(probe)}$ is estimated from dissipation records as discussed previously; and, $\bar{\sigma}_{vo}$ is the vertical effective stress in the soil prior to cone penetration.

Substituting Eqs. 12.5 into 12.3 and12.4 we get

$$k_{h(probe)} \simeq \frac{\gamma_w}{2.3\bar{\sigma}_{vo}} \cdot RR_{(probe)} \cdot c_{h(probe)} \qquad 12.7$$

$$c_{h(N.C)} = \frac{RR_{(probe)}}{CR} c_{h(probe)} \qquad 12.8$$

and knowing that $c_{v(N.C)} = (k_v/k_h) \cdot c_{h(N.C)}$, we can also write

$$c_{v(N.C)} \simeq \frac{RR_{(probe)}}{CR} \cdot \frac{k_v}{k_h} \cdot c_{h(probe)}. \qquad 12.9$$

Comparison of predicted $c_{h(probe)}$ profile with laboratory values of $c_{h(O.C)}$ assuming that Eqs. 12.5 and 12.6 hold, requires the use of a testing procedure whereby compression is normal to the direction of drainage for horizontally trimmed samples. In a conventional oedometer, or CRSC, compression and drainage take place in the same direction.

Rowe and Barden (1966) described a consolidation cell in which the total stress is applied by means of hydraulic pressure acting across a convoluted rubber jack. They claim that their arrangement improves control of the drainage conditions, allowing the separation of the instant of loading from the commencement of drainage. The soil specimen could be backpressured to insure full saturation. The cell allows both vertical and radial flow tests for consolidation or direct permeability measurements. Radial flow and vertical K_o compression are achieved by the use of a peripheral drain of 1/16 in. thick porous plastic that is in contact with the upper circumferential drain in the cell wall behind the jack, Fig 12.5 a, b and c.

Probably, the biggest disadvantage of the aforementioned apparatus that counter balances the advantages of achieving vertical compression and radial flow is the excessive side friction especially at high values of the over-consolidation ratio. Ladd et. al. (1979) presented a best estimate of the variation of the coefficient of lateral earth pressure (K) based on results from pressuremet tests in Boston Blue Clay indicating that for the top 48 feet K ranges from 1.3 to .7 corresponding to values of OCR ranging between 9 and 1.5. Thus, any attempt to evaluate the insitu values of $c_{h(O.C)}$ would incorporate large errors induced by side friction that is

aggravated by the large values of K and the coarse nature of the peripheral drain. The assumption of no horizontal strain will not hold either because of the compressibility of the drain.

Oedometer and CRSC tests could be used to simulate the required compression-drainage pattern if and only if the value of the coefficient of compressibility m_v or m_h is identical for compression in the vertical and horizontal direction, i.e., any anisotropic behavior is solely due to the permeability.

At first glance, one is tempted to believe that this is not the case for shallow samples due to its nonhomogenous nature. Fig. 12.7 represents the variation of m_v and m_h with the overconsolidation (OCR) for two samples retrieved from depths of 22.43' and 22.24'. The values of $m_{v(swelling)}$ and $m_{h(swelling)}$ from the final unload cycle for vertical and horizontal compression from the same initial consolidation stress, $\bar{\sigma}_{vc}$, appear to be identical with minor scatter. However, a conclusion to the effect that m for horizontal and vertical compression are identical and thus any anisotropy is solely due to the value of the permeability k in the vertical and horizontal direction is fortuitous. The aforementioned values of the coefficient of volume change are derived from the unloading branch after significant compression has taken place due to consolidation stresses

exceeding four times the maximum past pressure. Under such high pressures and strains, it could be argued that for a clay specimen trimmed in the horizontal direction, the clay skeleton exhibits a reorientation of particles so that it could offer better resistance to the applied stress. Fig. 12.8 shows a schematic representation of the aforementioned hypothesis. Hence it could be infered that the clay skeleton at such high strains mimics that of a vertically trimmed sample.

In an attempt to isolate this effect, the values of m_{vs}, m_{hs}, corresponding to the two swelling curves for each of the aforementioned vertical and horizontal samples were normalized with respect to the values of the coefficient of volume change corresponding to the maximum consolidation stress achieved on the virgin compression curve, m_{vo} or m_{ho} and plotted versus corresponding values of OCR. Fig. 12.9 shows that, for that specific depth, the clay exhibits normalized behavior with respect to its values of the coefficient of volume change. That is to say, given the value of m_{vo} corresponding to the last load increment on the virgin compression line before rebound and the value of OCR, we can predict the value of m_{vs} corresponding to the final stress on the rebound branch for that specific OCR. In other words the curve of m_{vs}/m_{vo} vs. OCR is independent

of maximum past pressure and indeed any stress applied in excess of that value. Since the values of m_{vs} and m_{hs} corresponding to the first rebound curve represent the compressibility of the clay at strains less than 5% it is thought highly unlikely that the aforementioned mechanism could have developed. To a good approximation, one can infer that the normalized behavior applies at in situ stresses and hence the assumption of equivalent values of m for compression in the vertical and horizontal direction holds. It also implies that values of $c_{h(O.C)}$ obtained for laboratory tests, oedometer and CRSC tests, could be compared to the predicted profile of $c_{h(probe)}$.

Figs. F.21 through F.26 show the same normalized curves at each depth. We observe the following:

1. At shallow depths the curves exhibit more scatter.

2. Values of m_{vs}/m_{vo} and m_{hs}/m_{ho} are very senstive to OCR in the vicinity of an OCR of one.

3. Beyond a depth of approximately 60 ft. the curves are essentially unique and hence exhibit a true normalized behavior.

4. At any one value of OCR, the values of m_{vs}/m_{vo} and m_{hs}/m_{ho} for deeper samples are higher than those for shallow samples indicating higher compressibility.

Fig. 12.10 shows the data collectively plotted and reveals the aforementioned trend.

12.2.7 Prediction of the In situ Values of $c_{h(O.C)}$ and $c_{v(O.C)}$ from Laboratory Test Data

In Section 12.2.2 we discussed the effects of sample disturbance during first loading from the in situ stress. The increased compressibility of the soil in this disturbed zone tends to reduce the value of c_h or c_v in the vicinity of the in situ stress and renders their prediction impossible.

In Section 12.2.6 we have also assumed that the values of $c_{v(probe)} \tilde{=} c_{v(O.C)}$ for small stress increments decrements, such that $\bar{\sigma}_{vo} \tilde{=} \bar{\sigma}_{vc}$. With conventional oedometer tests, even if we were able to obtain a perfectly undisturbed sample, the values of c_v or c_h obtained cannot be of any use since they would be an average value over a relatively large load increment, decrement, which is primarily due to the fact that for load increment ratios (L.I.R.) of less than 1 it is possible to obtain a type 3 curve of the settlement vs. log time variation that would create problems in interpreting the value of c_v or c_h. Hence it is more appropriate to use the values of c_v or c_h provided by CRSC tests since they relate to much smaller load increment, decrement, ratios.

Gibson, et. al. (1964) and Ladd (1973) suggest that the value of c_v in the normally consolidated range is essentially constant with a slight tendency to increase at high consolidation stresses. This was evidenced from the variation of c_v vs. effective stress plots shown

in Appendix E . Thus if we unload from any one point on the virgin compression line, we know that the initial value of c_v is the same.

If we were to adopt the same notion of normalized behavior and extend it to incorporate the c_v parameter, it suffices to show that $c_{v\,(O.C)}$ is only a function of OCR for any one particular depth*. Fig. 12.11 shows the variation of the coefficient of consolidation c_v during swelling from the two rebound curves for a sample trimmed in the vertical direction. Clearly, the difference between the two sets of data is minimal. Fig. F.1 through F.13 in Appendix F shows similar results for samples taken from different depths. Fig. 12.12 shows the variation of c_{vs} and c_{hs} with OCR collectively throughout the clay stratum at discrete depths. We observe the following:

1. c_{vs} and c_{hs} exhibit more scatter for shallower samples

2. The soil exhibits a marked anisotropic response in terms of the coefficient of consolidation for samples trimmed in the vertical and horizontal direction.

3. This anisotropy tends to diminish with depth but still persists even for very deep samples.

4. The anisotropic behavior increases at high values of OCR.

---

*Same arguement holds for $c_{h\,(O.C)}$.

5. Beyond a depth of 60 ft. the variation of c_{vs} with OCR is essentially unique for samples trimmed in the vertical direction. The same holds true for samples trimmed in the horizontal direction, they in turn define a unique variation.

6. In the vicinity of an OCR of one, the curves are very sensitive to slight variations in OCR.

7. For any one particular value of OCR, the value of c_{vs} and c_{hs} tends to decrease with depth.

12.2.8 Comparison of Laboratory and Field Predicted Values of $c_{h(O.C)}$

Having thus proved that at any one depth the value of $c_{v(swelling)}$, c_{vs}; is only a function of the over consolidation ratio we shall make the assumption that any value of OCR, c_{vs} is approximately equal to $c_{v(reloading)}$, c_{vr}*. Data obtained from the CRSC tests show that this assumption is warranted. Henceforth, given the value of the field OCR at any one depth we can estimate the value of the in situ horizontal coefficeint of consolidation $c_{h(O.C)}$ from the obtained curves. Fig. 12.13 shows the obtained variation of $c_{h(O.C)}$ at the in situ stress, $\bar{\sigma}_{vo}$, with depth. The value of $c_{h(O.C)}$ at any one depth was selected for a range of values of OCR corresponding to an uncertainty in the value of $\bar{\sigma}_{vm}$. We observe:

---

*Same arguement holds true for c_{hr} and c_{hs}.

1. Agreement between $c_{h(probe)}$ and $c_{h(O.C)}$ from laboratory test data is very good for the clay below a depth of 60 ft.

2. Agreement between $c_{h(probe)}$ and $c_{h(O.C)}$ from laboratory test data deteriorates as shallower depths are approached. Within a layer between depths of 42 and 60 ft., $c_{h(probe)}/c_{h(O.C)}$ reaches a maximum of 10 at a depth of 42 ft.

3. In the topmost layer, denoted by A the values of $c_{h(probe)}$ and $c_{h(O.C)}$ deviate such that the values of $c_{h(probe)}/c_{h(O.C)}$ ranges between one and two orders of magnitude.

In Fig. 12.14 the values of $c_{h(O.C)}$ for values of OCR of 1.2 and 2.0 are plotted at each depth. The comparison reveals very good agreement between $c_{h(O.C)}$ for an OCR of 1.2 and $c_{h(probe)}$ at all depth.

12.2.9 Evaluation of c_h Predictions by the Piezometer Probe

Evaluation of the c_h predictions by the piezometer probe incorporates several factors:

1. The predicted $c_{h(probe)}$ profile was derived through the use of field dissipation interpretation technique that utilizes a soil model whose parameters were derived from laboratory test data on normally consolidated resedimented Boston Blue Clay.

Baligh and Levadoux (1980) showed that this interpretation technique yields results that are in good agreement with measurements in the natural deposit having overconsolidation ratios ≤ 3. Attempts to extend this result to the upper clay having an OCR >3 were prevented by the large scatter of measured penetration pore pressure, Δui.

2. Fig. 12.15 shows the cone penetration resistance, q_c obtained by standard Fugro 60^o conical piezometer during steady penetration at a rate of 1 to 2 cm/sec in three different holes. Since cone penetration is continuous and largely independent of testing procedures and human interference, q_c and u_i provide consistant and reliable data for evaluating stratification and variability of the soil.

Thus, observing Fig. 12.15 we can claim that the BBC between 25 and 120 ft. can be divided into an upper overconsolidated clay above 75 ft. and a different lower clay. Further, q_c data suggests that the upper clay could be divided into four (or more) layers, A, B, C, D, within which q_c is more or less continuous, Baligh et. al. (1980).

3. In Chapter 2 we had established that in relatively structureless clays, the most experienced engineer using the best laboratory testing equipment and procedures can, at best, predict field values of k and c_v within a factor of two or three.

With increased nonhomogenity, i.e., presence of silt seams, sand patches, etc., size effects and disturbance during sample preparation become important factors that could increase the margin of error to probably an order of magnitude. This is particularly true as we approach the top boundary of the clay layer where the clay layer exhibits an excessively non-homogenous composition as was previously discussed in 12.2.4.

Keeping the aforementioned factors in mind we can arrive at the following conclusions:

1. Below a depth of 75 ft., $c_{h(probe)}$ is in excellent agreement $c_{h(O.C)}$ at the in situ stress $\bar{\sigma}_{vo}$.

2. Between depths of 60 and 75 ft. corresponding to OCRs of 1.5 and 2.0 agreement is within the accepted tolerance defined by $c_{h(in\ situ)}/c_{h(O.C)_{lab}} \tilde{\sim} 3.0$.

3. Between depths of 42 and 60 corresponding to OCRs of 2.0 and 3.5, $c_{h(probe)}$ exhibits significant scatter as the upper boundary is approached. Furthermore, values of $c_{h(O.C)}$ at the in situ stress are significantly lower than the $c_{h(probe)}$ reference profile. The value of $c_{h(probe)}/c_{h(O.C)}$ in this layer ranges between 3 and 10.

In view of the demonstrated soil nonhomogenity, presence of silt seams, already discussed in Chapter 11, and the expected anisotropic response, Fig. 12.5 and in Appendix E, size and disturbance effects become

important factors in determination of $c_{v(O.C)}$ or $c_{h(O.C)}$ from laboratory tests.

The use of the prediction criteria for $c_{h(probe)}$ in an erratic clay layer having an OCR approaching 3.0 would lead to significant scatter.

Thus we assert that the agreement in this layer is as good as could be expected. Underprediction of the value of $c_{h(O.C)}$ by as much as an order of magnitude from $_{in\ situ}$ laboratory tests is not uncommon. Hence use of the reference profile in this layer should be done with due care to the aforementioned observations.

$c_{h(O.C)}$ exhibits an opposite trend to that given by the reference profile for $c_{h(probe)}$. However, close examination of Fig. 6.14 that contains the actual data points for $c_{h(probe)}$ reveals that such a trend is possible.

4. In the uppermost layer, the clay exhibits an extremely erratic composition with values of OCR ranging from 3.5 to 9.0. The same argument made for layer B applies to this layer with a higher degree of severity. In the absence of a cardinal comparison, since both values are thought to be in error, strictly speaking we cannot qualify either as being more representative.

Thus we claim that the reference profile up to a depth of 42 ft. is a reasonable representation of the in situ profile. Throughout the clay layer the values of $c_{h(probe)}$ are very close to $c_{h(O.C)}$ for values of OCR close to 1.2.

12.3 VARIATION OF COEFFICIENT OF PERMEABILITY WITH DEPTH

Fig. 12.16 shows the variation of the coefficient of permeability k_v and k_h with depth as obtained from direct permeability measurements after isotropic consolidation to the in situ stress, $\bar{\sigma}_{vo}$. To enhance the statistical stability of the aforementioned results obtained from laboratory tests it is desirable to include the values of the coefficient of permeability k_h and k_v obtained from the CRSC tests at the in situ stress, $\bar{\sigma}_{vo}$. However, upon first reload to the in situ stress we would expect that the value of the coefficient of permeability would be lower than the value that could be obtained had we tested a perfectly undisturbed sample. Thus we require to infer the value of the coefficient of permeability from an appropriate model that obtains its parameters from the undisturbed zone, beyond the maximum past pressure, and whose behavior could be extrapolated to predict the values of the coefficient of permeability had the sample been perfectly undisturbed in the vicinity of its in situ effective stress.

The model chosen to achieve this goal assumes the following:

1. At any one depth, the clay exhibits normalized behavior with respect to the variation of $c_{h(O.C)}$ and $c_{v(O.C)}$, i.e.,

2. The rate of change of the constraint modulus D with respect to the consolidation stress increases at shallower depths.

3. The variation of D vs. $\bar{\sigma}_{vc}$ is approximately constant for all samples deeper than 60 feet.

4. With the exception of the shallowest sample there appears to be no anisotropic response of the clay in terms of its coefficient of compressibility in the normally consolidated range.

To obtain the value of the vertical or the horizontal permeability at any depth, the maximum past pressure is first determined. The value of the in situ OCR is then calculated*. The value of $m_{vo(N.C)}$ or $m_{ho(N.C)}$ is calculated using the appropriate variation of D vs. $\bar{\sigma}_{vc}$. For the appropriate value of field OCR the normalized value of $m_{v(O.C)}/m_{vo(N.C)}$ or $m_{h(O.C)}/m_{ho(O.C)}$ is chosen from the variation of $m_{v(O.C)}/m_{v(N.C)}$ or $m_{h(O.C)}/m_{h(N.C)}$ vs. OCR plots shown in Appendix F at the appropriate depth. Thus a value of $m_{vo(O.C)}$ undisturbed, at the field $\bar{\sigma}_{vo}$ or $\bar{\sigma}_{ho}$, could be determined. Using Figs. F.1 through F.13in Appendix F for the variation of $c_{v(O.C)}$ vs. OCR a value of $c_{v(O.C)}$ or $c_{h(O.C)}$ undisturbed, at the field $\bar{\sigma}_{vo}$, is determined. Thus a value of k_h or $k_{v(O.C)}$, at the field $\bar{\sigma}_{vo}$ is determined.

---

*For horizontal samples Fig. 12.18 was used to determine the value of the coefficient of lateral earth pressure, K.

$\frac{c_{h(O.C)}}{c_{n(N.C)}}$ and $\frac{c_{v(O.C)}}{c_{v(N.C)}}$ = f(O.C.R) *depth = z

2. At any one depth, the clay exhibits normalized behavior with respect to the variation of $m_{v(O.C)}$, $m_{h(O.C)}$ to compression in the vertical and horizontal direction, i.e.

$$\frac{m_{v(O.C)}}{m_{vo(N.C)}} = f(O.C.R) \qquad \text{depth} = Z$$

$$\frac{m_{h(O.C)}}{m_{ho(N.C)}} = f(O.C.R) \qquad \text{depth} = z$$

3. It follows that the normalized coefficient of permeability $\frac{k_{(O.C)}}{k_{(N.C)}}$ is also a function of the O.C.R only, at any one particular depth.

4. At any one depth, the variation of the constraint modulus, D, with consolidation stress, $\bar{\sigma}_{vc}$, is linear in the normally consolidated range.

Figs. F.14 through F.20 in Appendix F represent the aforementioned linear variation for various depths along the clay stratum.

Figs. 12.10 and 12.17 summarize the data collectively and from which we observe the following:

1. The rate of change of the constraint modulus $D = \frac{1}{m_{v(N.C)}}$ and $D = \frac{1}{m_{h(N.C)}}$ with respect to the consolidation stress remains approximately constant at any one depth.

---

*Since $c_{v(N.C)}$ and $c_{h(N.C)}$ are approximately constant along the virgin compression line then the following also holds true: $c_{h(O.C)}$ and $c_{v(O.C)}$ = f(OCR)

The values of the vertical and horizontal coefficient of permeability are also shown in Fig. 12.16 and from which we observe:

1. There is good agreement between the values of k_h and k_v obtained from direct permeability measurements and infered values from CRSC tests.

2. The ratio of k_h/k_v ranges from approximately $1.2 \pm .2$ for depths below 60 ft. to approximately $2.4 \pm .3$ for shallower samples.

3. The data exhibits considerable scatter especially at shallow depths*.

4. There appears to be a good overall agreement between the predicted k_n band and the laboratory measured band with restrictions to the top 10 - 20 feet.

Clearly one wonders at this point as to the attenuated magnitude of error corresponding to the comparison between $k_{h(lab)}$ and $k_{h(probe)}$. Although it is difficult to quantitively identify the sources of uncertainties and their interaction we can principally identify them as being:

1. Uncertainty in the value of $RR_{(probe)}$
2. Uncertainty in the value of $c_{h(probe)}$
3. Uncertainty in the value of $\bar{\sigma}_{vc}$ which is assumed to be equal to $\bar{\sigma}_{vo}$ in Equation 12.6

*The values of k_h and k_v at a depth of approximately 21 feet determined from direct permeability measurements are not very reliable since the effective stress declined to zero during backpressuring.

4. Approximate nature of equation 12. 7

It is possible that the interaction of the aforementioned items attenuates the difference between $k_{h(lab)}$ and $k_{h(probe)}$.

12.4 VALIDATION OF MATERIAL PROPERTIES USED AT THE STUDENT CENTER

Prior to the initiation of the analysis of the pore pressure dissipation under the Student Center, the only available information pertaining to the variation of the coefficient of consolidation (c_{vs} and c_{vr}) was derived from CRSC tests run on vertical samples from the I-95 test site, Germaine (1978). The shallowest sample tested was in the vicinity of 41 ft., hence no information pertaining to the upper stiff clay was available.

Values of cone penetration resistance, q_c, obtained by a standard Fugro 60° cone suggests a clear change in the properties below 75 feet. The cone resistance data suggests the possibility of further subdivision of the top layer into four other layers as was discussed earlier.

Observation of Fig. 9.23 of the variation of OCR with elevation at the Student Center reveals that the maximum OCR attained at the top of the clay deposit is approximately 4.0. At an elevation of 60 the OCR is approximately one. This is to be contrasted with Fig. 9.24 corresponding

to the I-95 test site where the maximum OCR attained at the top of the clay layer is approximately 9.0 and at an elevation of approximately 70.0 the OCR is about one.

The effect of the dewatering operation would clearly dominate the values of the pore pressures close to the top boundary where we expect the soil to exhibit most variability.

In view of the aforementioned observations and our lack of knowledge of the exact variation of c_v with depth we assumed that:

1. Based on OCR variation with elevation and the q_c data we shall assume that the clay deposit is divided into two layers:
   a. A homogenous normally consolidated layer extending below a depth of 65 $\pm$ 5 ft. overlain by a homogenous overconsolidated clay layer.
   b. In any one layer
      $$c_{h(probe)} = c_{v(O.C)} = f(OCR)$$
   c. The aforementioned assumptions are true at the I-95 test site and for the foundations of the Student Center.

Thus correlation of $c_h (=c_s)$ with respect to OCR was possible and yielded the dissipation curves given in Fig. 10.30 .

In order to test the severity of the aforementioned assumptions two cases were considered. In one the value of c_{vs} was held constant at a value of 0.04 cm^2/sec which is equal to that of the bottom 40 feet and the corresponding dissipation curve was obtained. In the other case the value of c_{vs} held constant at a value of .15 cm^2/sec equivalent to the value of c_{vs} at an elevation of 12.5 ft. (top boundary) and the corresponding dissipation curve was obtained. The two dissipation curves appear in Fig. 9.33 and from which we observe the following:

1. At piezometer PSC-1 (elevation - 19.4 ft.) the magnitude of the error involved in choosing a constant value of c_{vs} ranges from 5-9% and the two dissipation curves mimic the variation corresponding to change in water table. We conclude that at the top boundary the dissipation curve is strongly correlated to the variation in the water table and less sensitive to choice of c_{vs} value.

2. The magnitude of the error involved in considering a value of c_{vs} equal to 0.04 (equal to that of the lower 40 ft.) is approximately 9, 18, 20 and 19% for PSC-4 through PSC-1, on average. It appears that the value of c_{vs} corresponding to the bottom 40 ft. highly dominates the dissipation curves which is probably due to the low OCR values up to a depth of 45 for which a value of c_{vs} = .04 ft^2/sec was used.

3. The use of a value of c_{vs} equal to .15 ft^2 grossly underpredicts the dissipation curves except for the top piezometer where the value of c_{vs} used was approximately equal to .15 ft^2/sec.

4. The value of the error is magnified with extended time periods.

We thus conclude that the severity of the errors incorporated with the aformentioned assumptions are tolerable, and the use of a variable c_{vs} profiles yields closer answers to the field observed values.

It is of interest at this point to try and assess the reasons that lead to the good agreement between the predicted dissipation curves presented in Fig. 10. and the field observed values. Although we know that for the overconsolidated part of the clay deposit a variable $c_{v(O.C)}$ is preferred to a constant value for matching purposes, we know that the values of $c_{h(probe)}$ beyond 60 ft. are very close to $c_{h(O.C)}$ for values of O.C.R in the close vicinity of 1.2. We have also asserted that the reference profile is a fair representation of the field $c_{v(O.C)}$ up to an elevation of 42 ft. at which the OCR is approximately 3.0.

In the process of obtaining the $c_{v(O.C)}$ profile for the Student Center the only portion of the reference profile used was up to an elevation of 32.5 ft. or a depth of 39.0 ft.

Thus if we assume that the effect of dewatering was dominant to a depth of approximately 31 ft* and if we assume that the overconsolidated layer is roughly homogenous then the assumption (b) is probably not too severe. This of course assumes that in that region $c_h \bar{\sim} c_v$ with no appreciable anisotropy.

Perhaps a more convincing argument to justify the use of the $c_{v(O.C)}$ profile could be derived from observing the relationship between the values of $c_{v(O.C)}$ derived from CRSC tests using the normalized c_v curves at the value of the in situ overburden stress $\bar{\sigma}_{vo}$ and the used profile. It is seen that the used profile lies in the range of twice to three times the values of $c_{v(O.C)}$ derived from laboratory tests. This is in accordance with our previous argument presented in Chapter 2 through the case studies, Fig. 12.19.

12.5 SUMMARY

1. Size effects concerned with CRSC and oedometer tests are negligable.

2. CRSC tests and oedometer tests yield essentially the same compression curve beyond the maximum past pressure.

3. The stress history derived from the new testing

*15% decrease in an assumed triangular variation of the effect of pumping, negative induced pore pressures of 12 ft. of H_2O at the top of the clay layer and zero at the glacial till.

program is in accordance with that already established from previous testing programs.

4. The clay deposit exhibits a marked nonhomogenous nature at shallow depths with the following characteristics:

   a. Increase in RR and CR with depth

   b. Increase in strains for a particular consolidation stress with depth

   c. B.B.C. exhibits a collapsable structure for elevations approximately below 95 ft.

5. The clay deposit exhibits an anisotropic nature at shallow depths. The horizontally trimmed samples appear to be slightly less compressible in the normally consolidated range than the vertically trimmed sample.

6. B.B.C. exhibits normalized behavior with respect to the values of the compressibility m_{vs}.

7. Values of m_{vs} for vertically trimmed samples are almost identical to those obtained for horizontally trimmed samples.

8. B.B.C. exhibits normalized behavior with respect to its value of $c_{v(O.C)}$ and $c_{h(O.C)}$.

9. Degree of anisotropic response concerned with $c_{v(O.C)}$ increases at shallower depths.

10. Beyond 60 ft. the normalized curve of c_{vs} and m_{vs}/m_{vo} vs. OCR is unique.

11. The curves thus mentioned are very sensitive

in the vicinity of an OCR of unity.

12. $c_{h(probe)}$ reference profile could be used to simulate the field variation of $c_{h(O.C)}$ up to a depth of approximately 42 ft. (10 fold deviation from laboratory data at 42 ft.)

13. Throughout the clay deposit the values of $c_{h(probe)}$ are very close to $c_{h(O.C)}$ derived from CRSC tests at an OCR of 1.2.

14. A method for obtaining the value of coefficient of permeability from CRSC tests at the in situ $\bar{\sigma}_{vo}$ simulating zero (or close to zero) disturbance is established.

15. The values of the coefficients of permeability derived from CRSC tests are in good agreement with the values derived from direct measurements in a triaxial cell setup.

16. The anisotropic response of B.B.C. concerned with values of $c_{v(O.C)}$ or $c_{h(O.C)}$ is chiefly due to the anisotropic nature of its permeability characteristics.

17. The ratio of k_h/k_v is approximately 1.2 ± .2 for depths below 60 ft. to approximately 2.4 ± .3 for shallower depths.

18. A good overall agreement between $k_{h(probe)}$ and $k_{h(O.C)}$ from laboratory data with restrictions to the top 10-20 feet.

19. The value of c_{vs} of 0.04 dominates the behavior of the dissipation curves up to a depth of 45 feet.

20. The top 10 feet are highly effected by the

continuous pumping operations which is reflected in the behavior of the dissipation curve at PSC-1.

21. The assumption of

$$c_{v(O.C)} = c_{h(probe)} = f(OCR)$$

does not appear to be very severe.

22. The profile of c_{vs} used to predict the dissipation curves lies in the range of twice to three times the profile of c_{vs} given by laboratory test results.

Depth (ft.)	Oedometer* or CRSC Test. No.	W_N PI	W_L LI	T_v(lab/field) (ε_v at $\bar{\sigma}_{vo}$)	Est. $\bar{\sigma}_{vo}$	Est. $\bar{\sigma}_{vm}$ (Range) (KSC)	CR (RR)	Normally Consolidated C_v(cm^2/sec)	Quality
93.12	SP 19 VERT	48.90 22.61	45.49 115.08	-	2.18	1.30 (1.28-1.33)	0.2256 (0.0218)	$0.87x10^{-3}$	Good
97.83	SP 20 VERT	42.90 23.38	44.50 93.15	-	2.29	1.90 (1.87-1.93)	0.2600	$0.45x10^{-3}$	Good
90.48	SP 13 VERT	38.70 21.02	44.12 74.21	-	2.33	3.26 (3.22-3.30)	0.7524 (0.0344)	$0.31x10^{-3}$	Good+
100.19	100-102-O-V	40.63 24.95	50.19 61.68	1.22	2.35	2.00	0.2190 (0.0225)	$1.22x10^{-3}$	Good°
100.22	100-102-O-H	44.10 24.94	50.70 75.54	1.24	2.35	1.575 (1.51-1.63)	0.1960 (0.0147)	$1.70x10^{-3}$	Good°
109.48	SP 15 VERT	40.70 18.41	40.38 101.72	-	**2.57**	2.98 (2.96-3.00)	0.5066 (0.0225)	$0.65x10^{-3}$	Good+

*C-V = CRSC test using a vertical trimmed sample
C-H = CRSC test using a horizontal trimmed sample
O-V = Oedometer test using a vertical trimmed sample
O-H = Oedometer test using a horizontal trimmed sample

+Based on shape of compression curve using recommendations suggested by Ladd (19).

°Based on ratio of T_v(lab/field)

Table 12.1 (cont.) Summary of pertinent parameters derived from the Oedometer and C.R.S.C tests performed on undisturbed samples of Boston Blue Clay.

Depth (ft.)	Oedometer* or CRSC Test. No.	W_N PL	W_L LI	T_v(lab/field) (ε_v at $\bar{\sigma}_{vo}$)	Est. $\bar{\sigma}_{vo}$	Est. $\bar{\sigma}_{vm}$ (Range) (KSC)	CR (RR)	Normally Consolidated C_v(cm^2/sec)	Quality
83.49	SP 17 VERT	41.10 23.47	46.95 75.07	-	1.947	1.45 (1.42-1.47)	0.2900- 0.1852	$0.42x10^{-3}$	Good+
84.49	SP 10 VERT	49.50 22.89	46.26 92.37	-	1.971	2.15 (2.48-2.55)	0.5600- 0.2260	$1.00x10^{-3}$	Good+
88.49	SP 18 VERT	50.00 79.11	41.69 143.48	-	2.067	1.46 (1.42-1.50)	0.1912 (0.0332)	$1.00x10^{-3}$	Good+
90.98	90-92-C-V	45.80 21.55	33.77 104.27	1.17	2.12	2.28	0.3710- 0.2470 (0.0243)	$0.35x10^{-3}$	Good°
90.25	90-92-C-H	43.05 20.72	43.76 96.57	1.10	2.11	1.77 (1.73-1.82)	0.2525- 0.1702 (0.0205)	$1.78x10^{-3}$	Good°
90.07	90-92-O-V	47.67 20.49	43.47 120.49	1.098	2.11	1.85 (1.81-1.90)	0.2006- 0.3230 (0.0287)	$0.909x10^{-3}$	Good°
90.25	90-92-O-H	45.06 20.72	43.75 106.32	1.098	2.11	1.57 (1.54-1.60)	0.2390 (0.0219)	$1.624x10^{-3}$	Good°

*C-V = CRSC test using vertical trimmed sample
C-H = CRSC test using a horizontal trimmed sample
O-V = Oedometer test using a vertical trimmed sample
O-H = Oedometer test using a horizontal trimmed sample

+Based on shape of compression curve using recommendations suggested by Ladd (19)

°Based on ratio of T_v(lab/field)

Table 12.1 (cont.) Summary of pertinent parameters derived from the Oedometer and C.R.S.C tests performed on undisturbed samples of Boston Blue Clay.

Depth (ft.)	Oedometer* or CRSC Test. No.	W_N PL	W_L LI	T_v(lab/field) (ε_v at $\bar{\sigma}_{vo}$)	Est. $\bar{\sigma}_{vo}$	Est. $\bar{\sigma}_{vm}$ (Range) (KSC)	CR (RR)	Normally Consolidated C_v (cm^2/sec)	Quality
61.47	60-62-C-V	40.20 16.96	38.07 112.55	-	1.419	2.45 (2.40-2.50)	0.205 (0.0250)	0.85×10^{-3}	Good+
61.65	60-62-C-H	40.20 16.93	37.89 113.64	-	1.424	2.05 (2.00-2.10)	0.1987 (0.1225)	1.5×10^{-3}	Good+
67.48	SP 08 VERT	47.10 17.35	38.15 150.16	-	1.563	2.34 (2.29-2.40)	0.2750	1.15×10^{-3}	Good+
73.48	SP 16 VERT	42.70 16.32	36.65 137.07	-	1.707	1.85 (1.81-1.90)	0.2437 (0.0269)	0.62×10^{-3}	Good+
78.48	SP 09 VERT	42.00 19.43	40.72 106.58	-	1.827	2.67 (2.62-2.71)	0.7340- 0.2205 (0.0307)	0.63×10^{-3}	Good+
82.58	82-84-O-H	40.39 19.55	41.71 93.25	1.04	1.92	1.20 (1.15-1.25)	0.1740 (0.0115)		Good°
82.19	82-84-O-V	45.35 18.39	40.16 128.22	1.04	1.92	2.10 (2.07-2.14)	0.3350 (0.0294)		Good°

*C-V = CRSC test using vertical trimmed sample
C-H = ORSC test using a horizontal trimmed sample
O-V = Oedometer test using a vertical trimmed sample
O-H = Oedometer test using a horizontal trimmed sample

+Based on shape of compression curve using recommendations suggested by Ladd (19).

°Based on ratio of T_v(lab/field)

Table 12.1 (cont.) Summary of pertinent parameters derived from the Oedometer and C.R.S.C tests performed on undisturbed samples of Boston Blue Clay.

Depth (ft.)	Oedometer* or CRSC Test. No.	W_N W_L PL LI	T_v(lab/field) (ε_v at $\bar{\sigma}_{vo}$)	Est. $\bar{\sigma}_{vo}$	Est. $\bar{\sigma}_{vm}$ (Range) (KSC)	CR (RR)	Normally Consolidated C_v(cm^2/sec)	Quality
36.59	36.5-38.5-C-V	50.07 31.30 10.48 279.10	-	0.822	2.36 (2.26-2.46)	0.1551 (0.02115)	1.00×10^{-2}	Good
37.18	36.5-38.5-C-H	31.15 31.30 10.40 98.55	-	0.836	2.14 (2.070-2.219)	0.1397 (0.0147)	1.45×10^{-2}	Good
41.00	SP 03 VERT	30.53 41.91 18.94 42.55	-	0.928	3.07 (3.00-3.15)	0.1435 (0.0250)	0.65×10^{-2}	Good
43.12	41.5-43.5-C-H	27.69 48.91 25.39 16.42	1.38	0.978	2.705 (2.63-2.78)	0.1833 (0.0205)	1.35×10^{-2}	Good°
43.31	41.5-43.5-C-V	29.15 48.53 25.29 22.22	1.38	0.983	2.01 (1.93-2.09)	0.1858 (0.01154)	1.75×10^{-3}	Good°
51.95	SP 05 VERT	43.50 44.59 20.58 94.70	-	1.141	3.32 (3.24-3.40)	0.1871 (0.0269)	2.0×10^{-3}	Good
62.31	SP 07 VERT	41.60 37.23 16.86 125.92		1.439	-	0.1400 (0.0268)	1.2×10^{-3}	Good

*C-V = CRSC test using a vertical trimmed sample
C-H = CRSC test using a horizontal trimmed sample
O-V = Oedometer test using a vertical trimmed sample
O-H = Oedometer test using a horizontal trimmed sample

+Based on shape of compression curve using recommendations suggested by Ladd (19).

°Based on ratio of T_v(lab/field)

Table 12.1 (cont.) Summary of pertinent parameters derived from the Oedometer and C.R.S.C tests performed on undisturbed samples of Boston Blue Clay.

Depth (ft.)	Oedometer* or CRSC Test. No.	W_N PI	W_L LI	T_v(lab/field) (ϵ_v at $\bar{\sigma}_{vo}$)	Est. $\bar{\sigma}_{vo}$	Est. $\bar{\sigma}_{vm}$ (Range) (KSC)	CR (RR)	Normally Consolidated C_v (cm^2/sec)	Quality
22.24	21.5-23.5-C-V	19.65 12.36	31.30 5.42	-	0.477	3.58 (3.38-3.78)	0.0060 (0.0064)	1.0×10^{-2}	Fair-Poor +
22.43	21.5-23.5-C-H	22.61 12.34	31.30 29.58	-	0.482	2.22 (2.07-2.37)	0.0884 (0.0069)	1.65×10^{-2}	Fair-Poor +
26.59	26.5-28.5-O-V	30.85 11.80	31.30 96.18	-	0.582	2.83 (2.73-2.93)	0.1390 (0.0194)	1.65×10^{-2}	Fair+
26.77	26.5-28.5-O-H	26.92 11.76	31.30 62.81	-	0.586	2.96 (2.87-3.05)	0.1000 (0.0094)	2.023×10^{-2}	Fair+
27.43	26.5-28.5-C-V	21.12 11.68	31.30 12.84	-	0.602	2.645 (2.37-2.92)	0.1077 (0.0064)	1.70×10^{-2}	Fair+
27.63	26.5-28.5-C-H	21.12 11.62	31.30 12.39	-	0.607	3.00	0.0794 0.0034	6.72×10^{-2}	Fair+

*C-V = CRSC test using a vertical trimmed sample
C-H = CRSC test using a horizontal trimmed sample
O-V = Oedometer test using a vertical trimmed sample
O-H = Oedometer test using a horizontal trimmed sample

+Based on shape of compression curve using recommendations suggested by Ladd (19).

°Based on ratio of T_v(lab/field).

Table 12.1 Summary of pertinent parameters derived from the Oedometer and C.R.S.C tests performed on undisturbed samples of Boston Blue Clay.

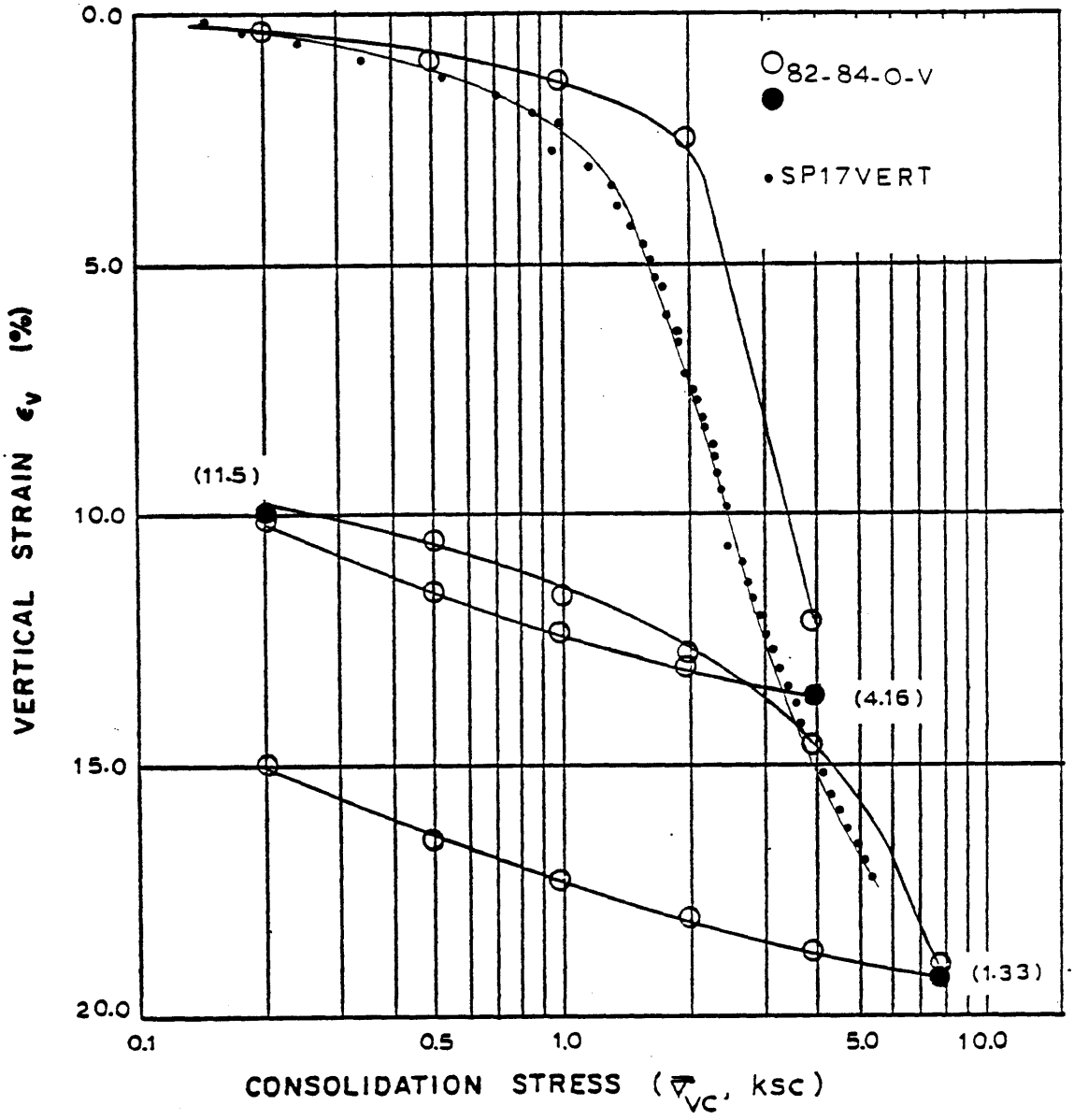

Figure 12.1 Effect of disturbance on the compression curve of two samples of B.B.C.

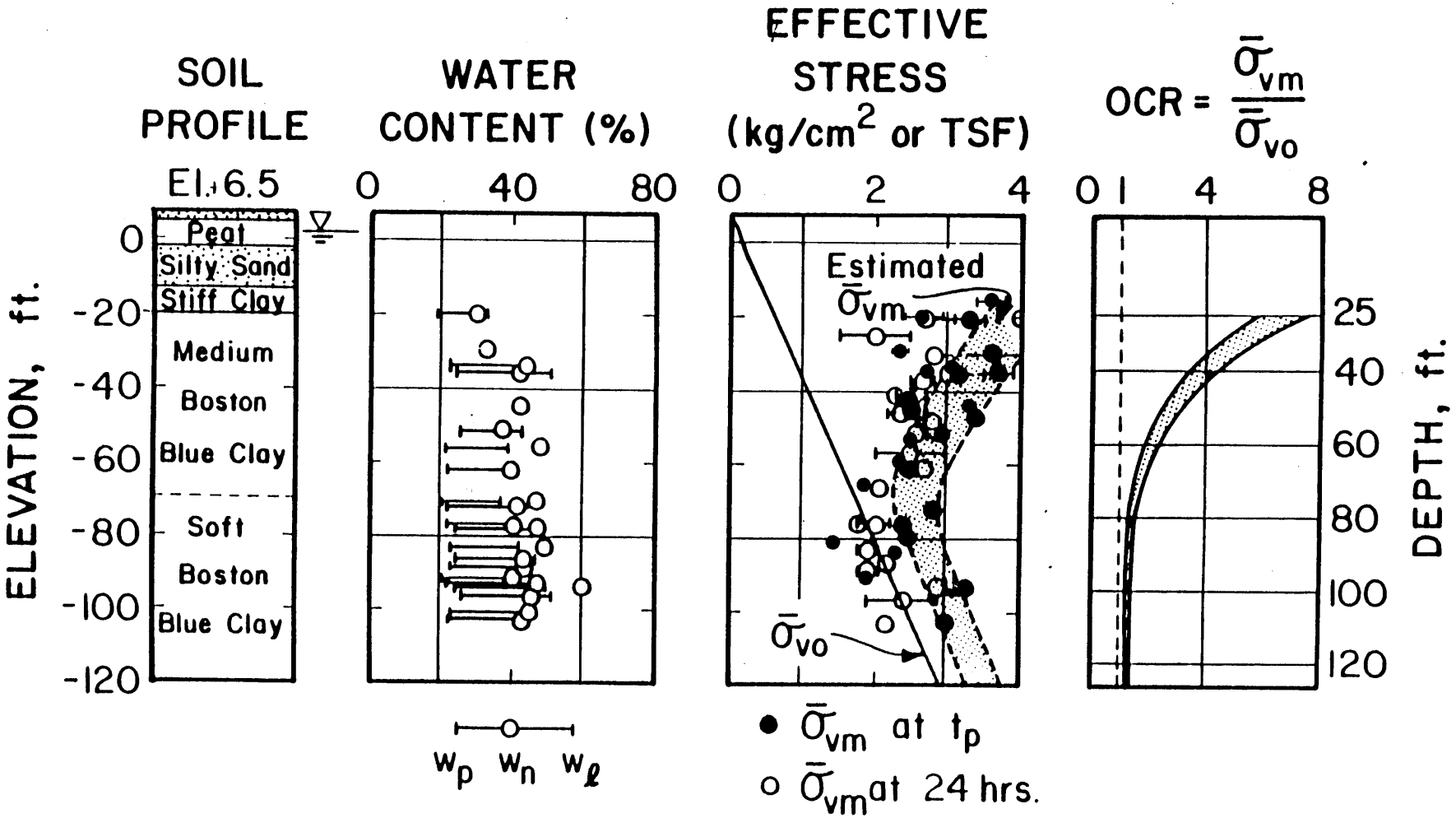

Figure 12.2 Soil profile, index properties and stress history at the Saugus site. Includes data from newly performed CRSC and oedometer tests.

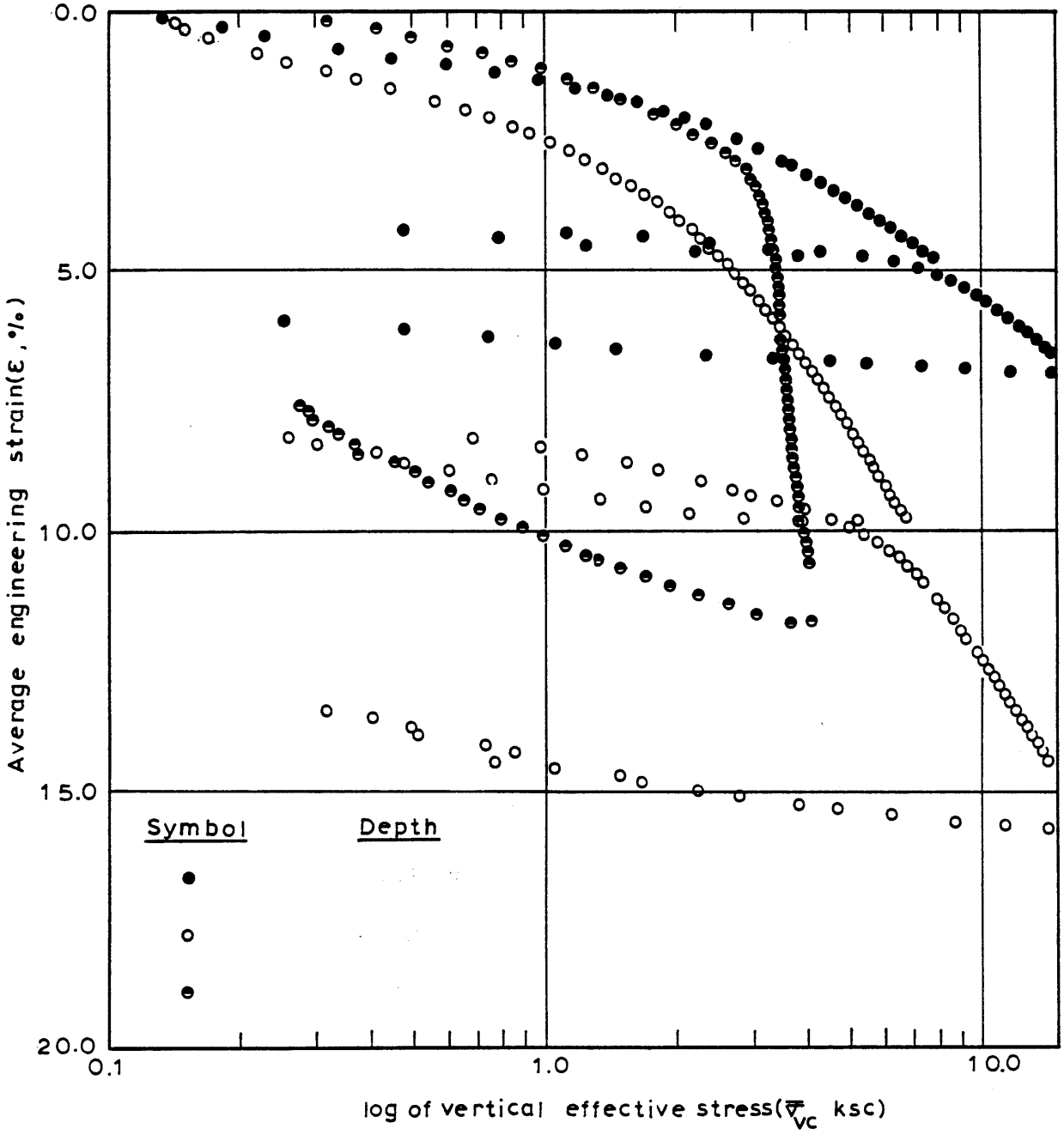

Figure 12.3 Variation in the compressibility properties with depth at the Saugus site.

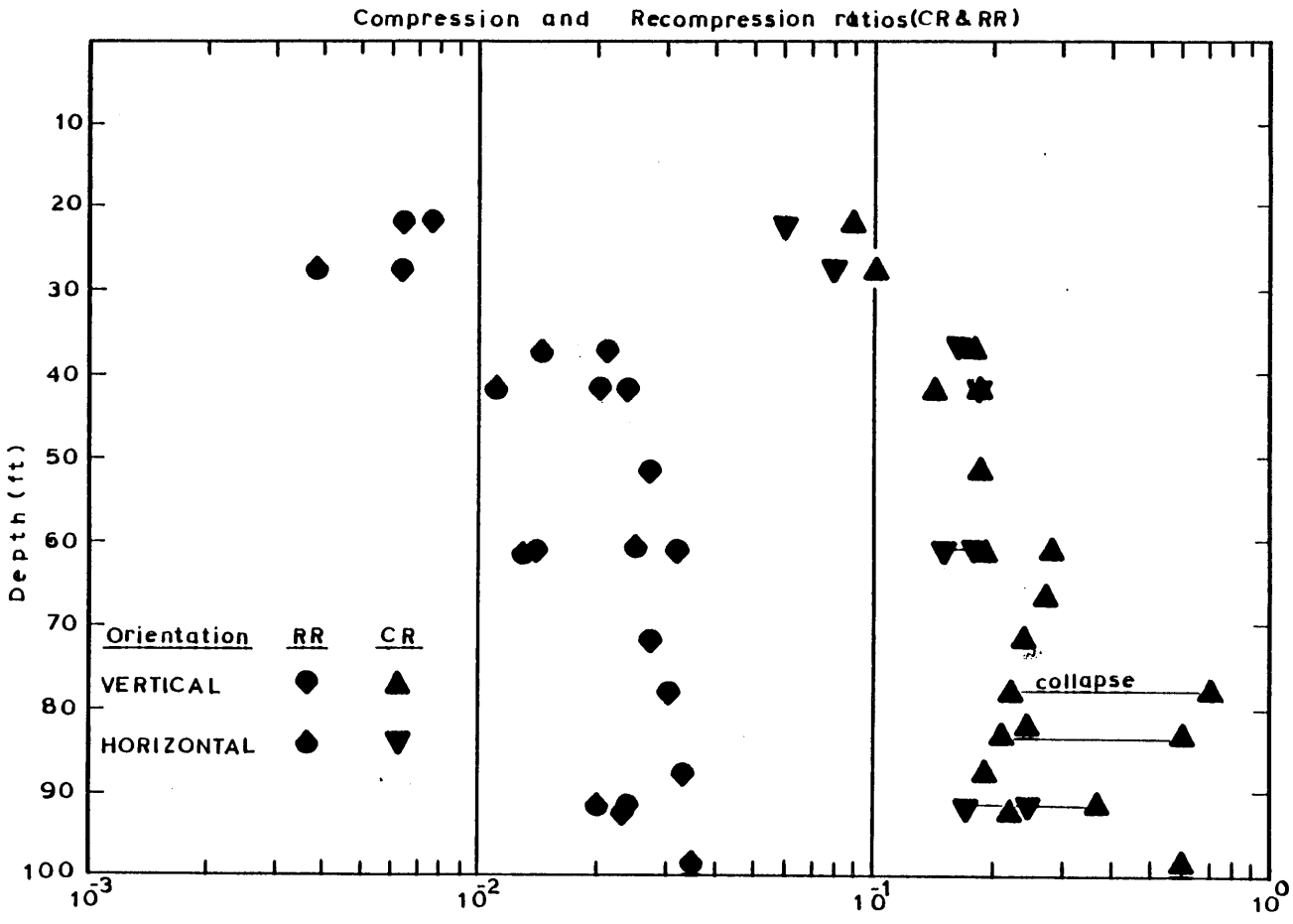

Figure 12.4 Variation of the compression and recompression ratios with depth at the Saugus site.

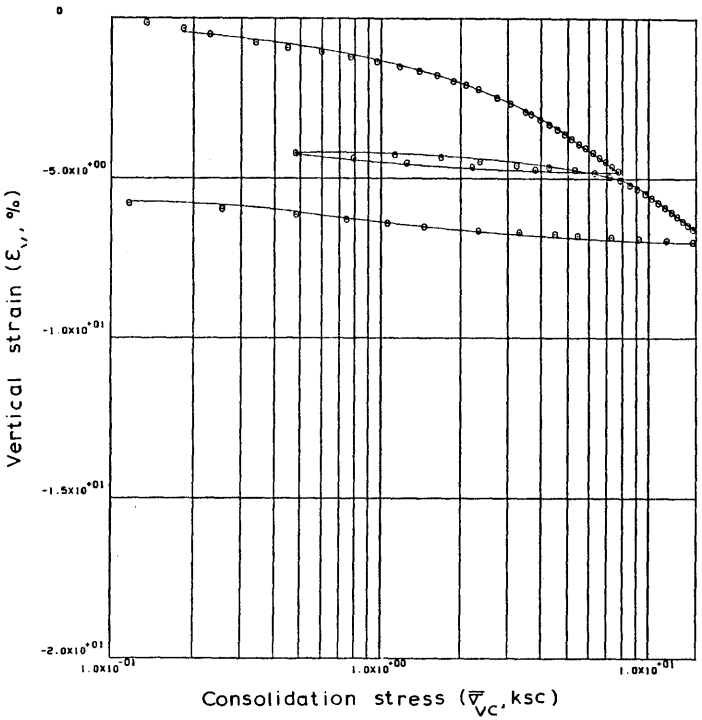

Sample No. 215-235-C.V w_N (%) 19.61 Estimated
Depth 22.24 w_L (%) 31.30 $\bar{\sigma}_{vo}$ 0.48 $\bar{\sigma}_{vm}$ 3.38-3.78
Soil Type Boston w_P (%) 18.94 CR 0.0600 RR 0.0064
Blue Clay P.I.(%) 12.36 G_s 2.77 e_o 0.6155
o At t_p Remarks Data from C.R.S.C test
w_L & w_P estimated from Baligh et al (1980)

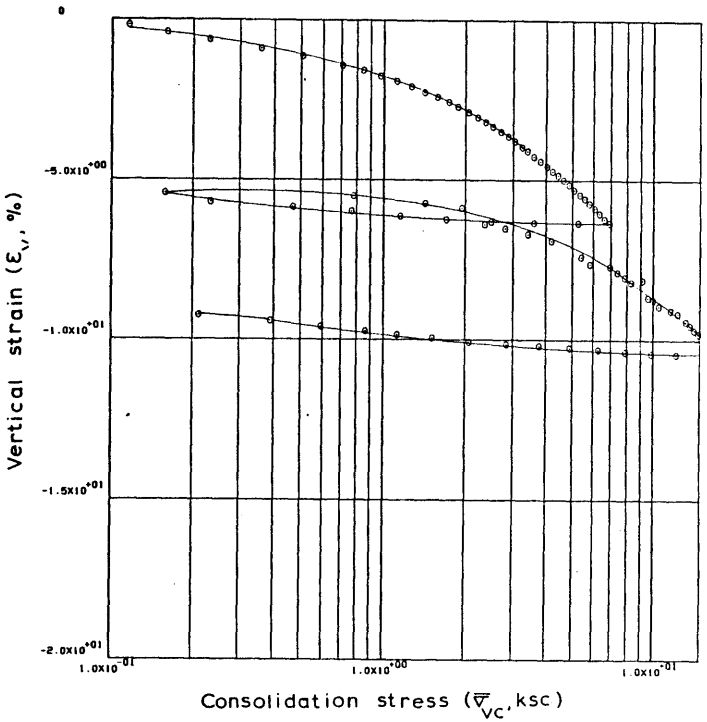

Sample No. 215-235-C.H w_N (%) 22.09 Estimated
Depth 22.43 w_L (%) 31.30 $\bar{\sigma}_{vo}$ 0.48 $\bar{\sigma}_{vm}$ 2.07-2.37
Soil Type Boston w_P (%) 18.96 CR 0.0884 RR 0.0069
Blue Clay P.I.(%) 12.34 G_s 2.77 e_o 0.6937
o At t_p Remarks Data from C.R.S.C test
w_L & w_P estimated from Baligh et al (1980)

Figure 12.5 Anisotropic response in the compressibility charactaristics of B.B.C at shallow depths.

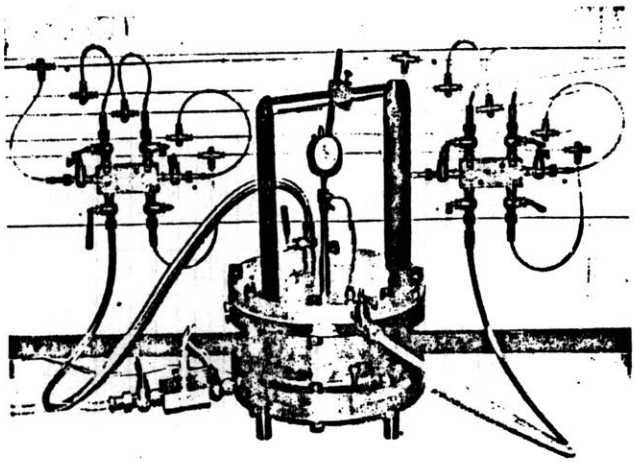

(a)

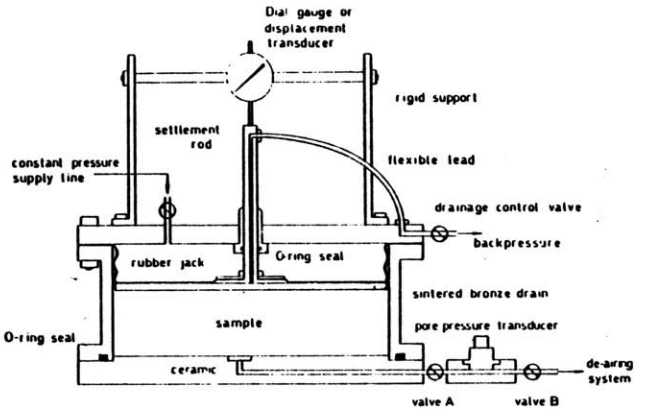

(b)

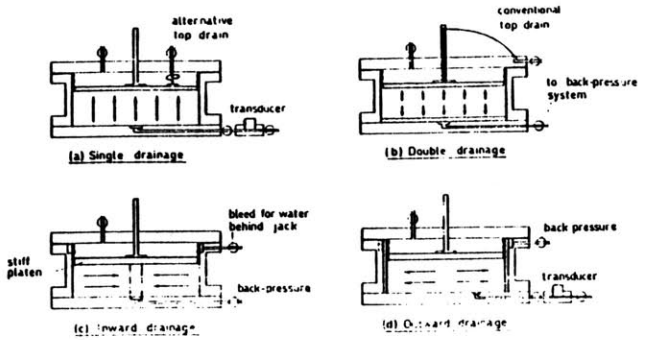

(c)

Figure 12.6 The 10" diameter cell (a), the basic cell construction (b), drainage and pore pressure measurement arrangements for four types of tests.

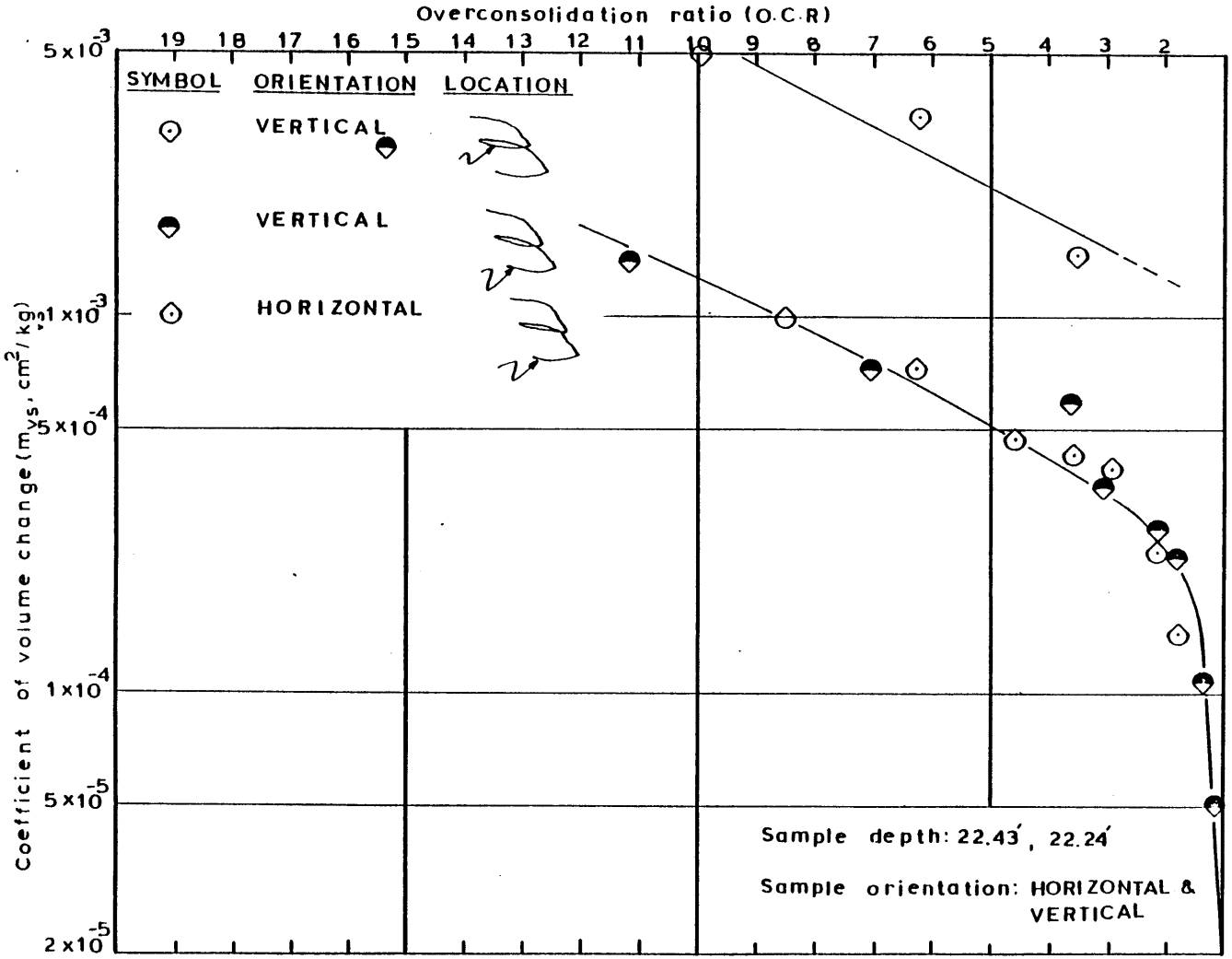

Figure 12.7 Variation of the coefficient of volume change with the overconsolidation ratio.

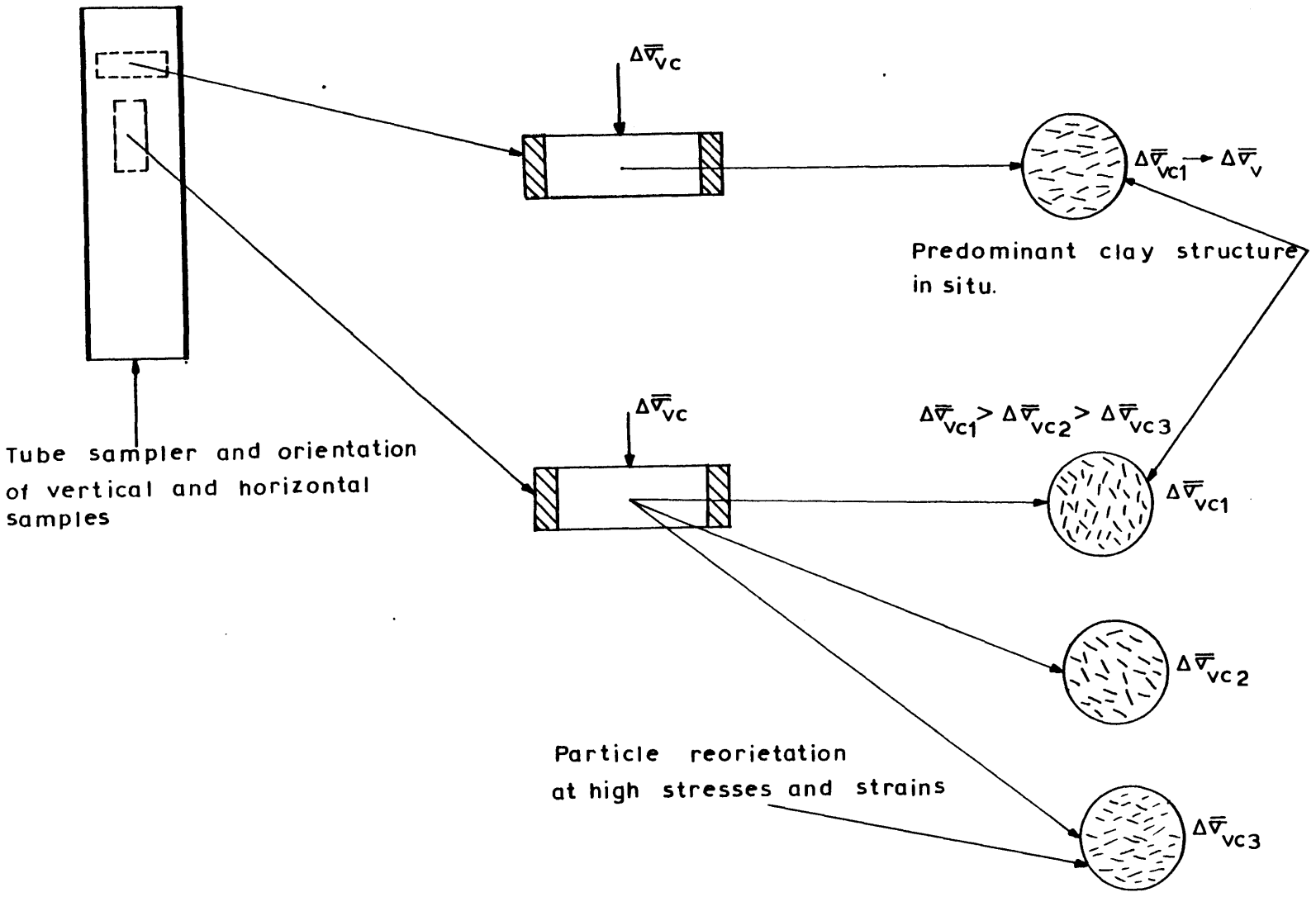

Figure 12.8 Reorientation of clay particals due to a change in direction of major principal stress.

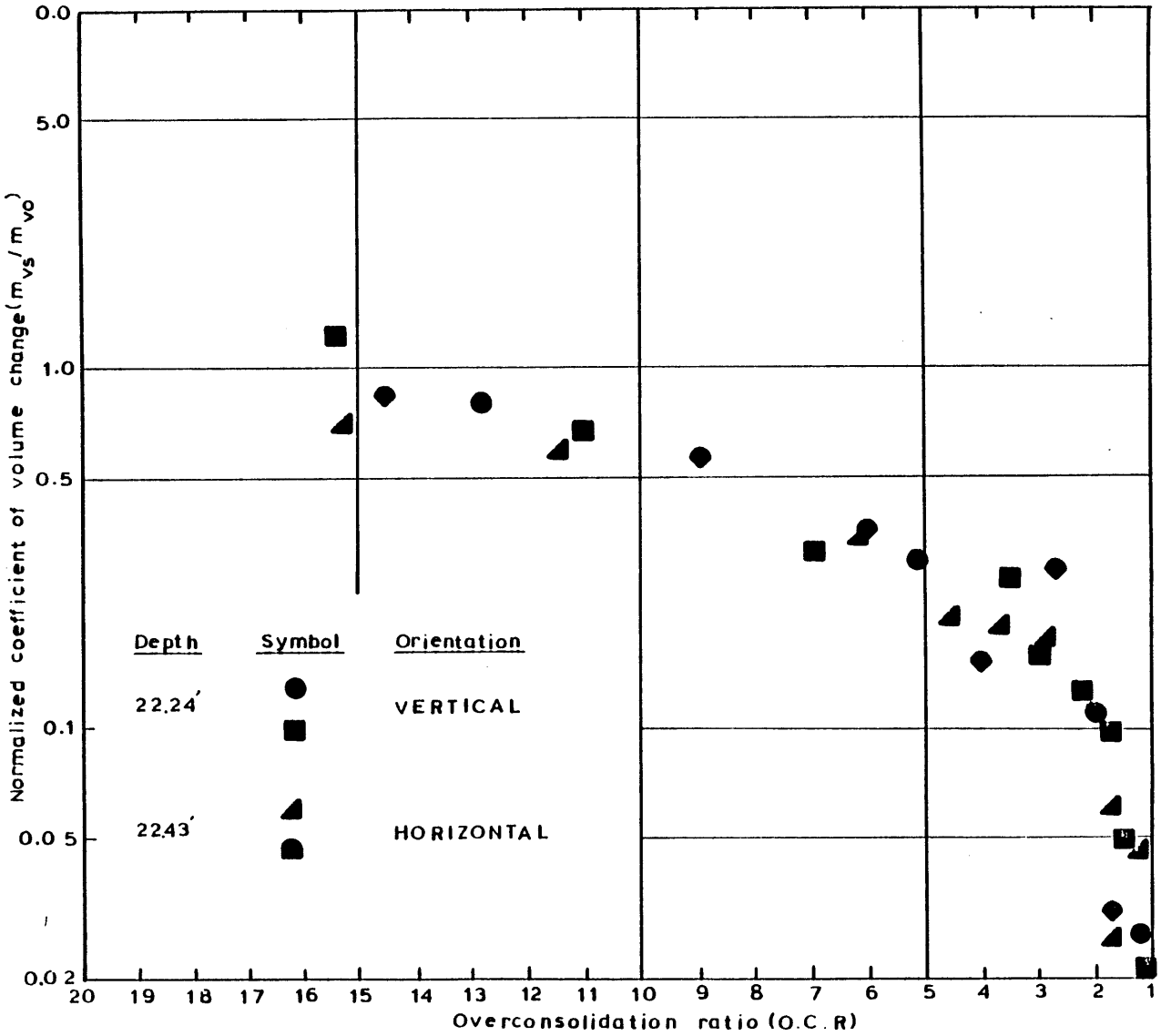
0.0
5.0
1.0
0.5
0.1
0.05
0.02
Normalized coefficient of volume change(m_{vs}/m_{vo})
Depth
Symbol
Orientation
22.24'
VERTICAL
22.43'
HORIZONTAL
20 19 18 17 16 15 14 13 12 11 10 9 8 7 6 5 4 3 2 1
Overconsolidation ratio (O.C.R)

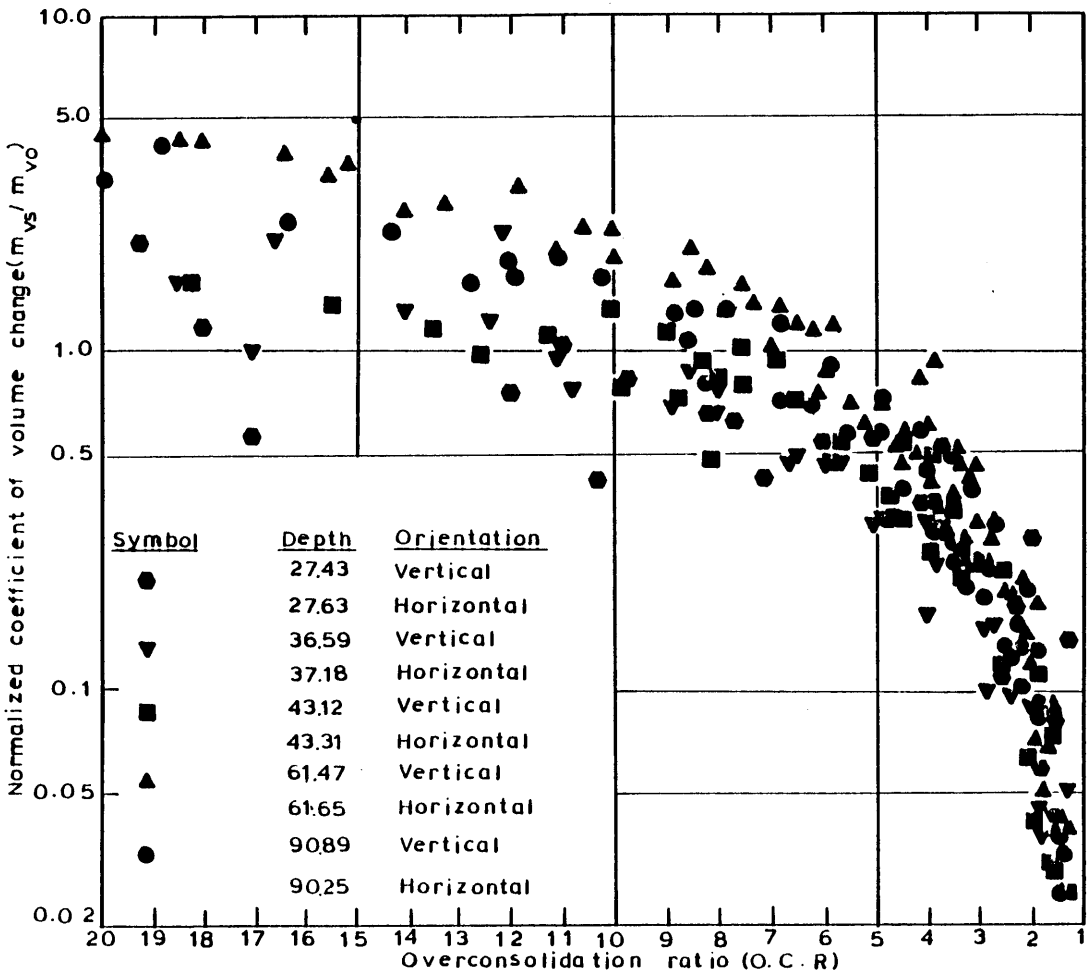

Figure 12.10 Summary of the variation of the normalized coefficient of volume change with the overconsolidation ratio.

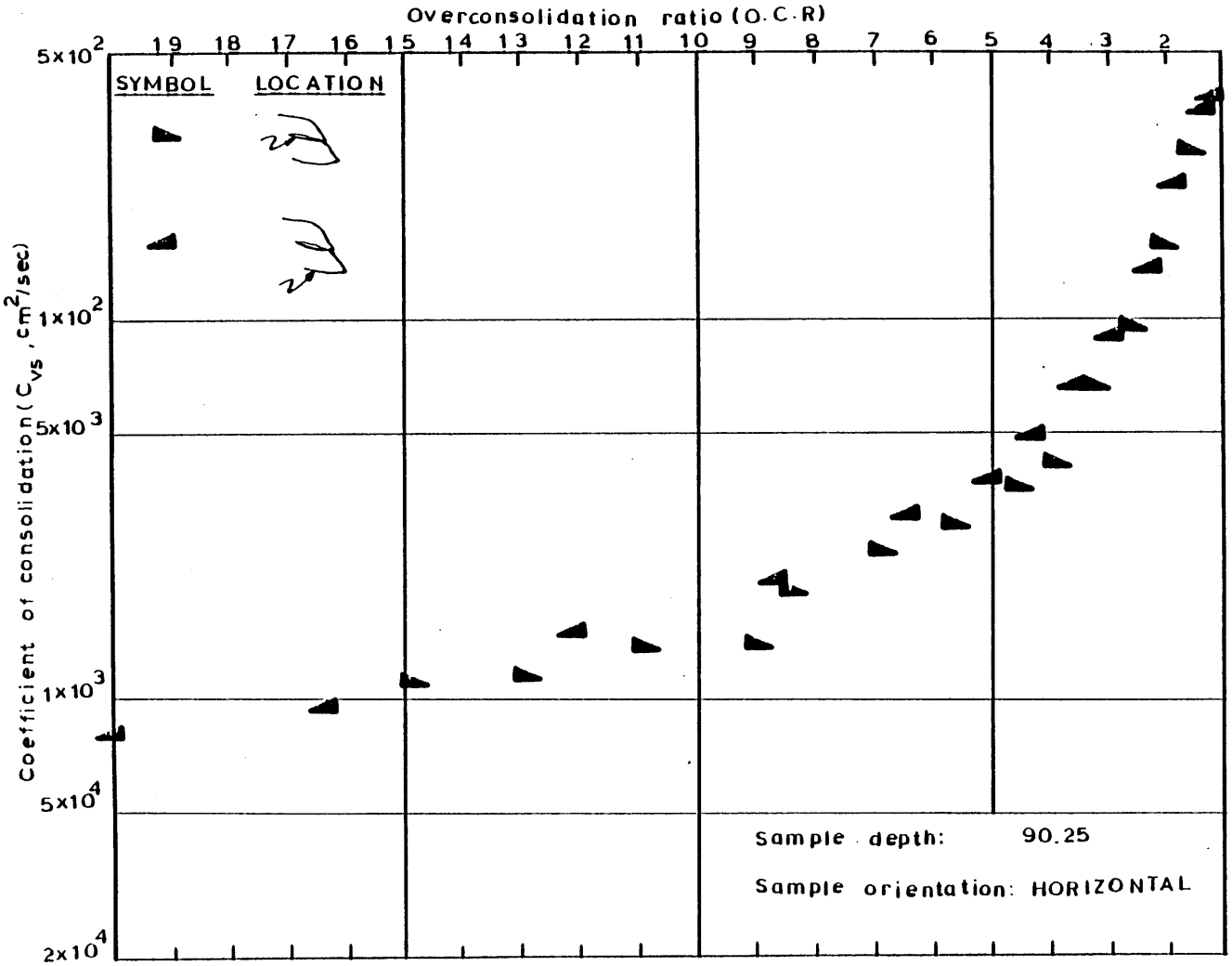
Overconsolidation ratio (O.C.R)
19 18 17 16 15 14 13 12 11 10 9 8 7 6 5 4 3 2
SYMBOL
LOCATION
Coefficient of consolidation (C_{vs}, cm^2/sec)
$5x10^2$
$1x10^2$
$5x10^3$
$1x10^3$
$5x10^4$
$2x10^4$
Sample depth: 90.25
Sample orientation: HORIZONTAL

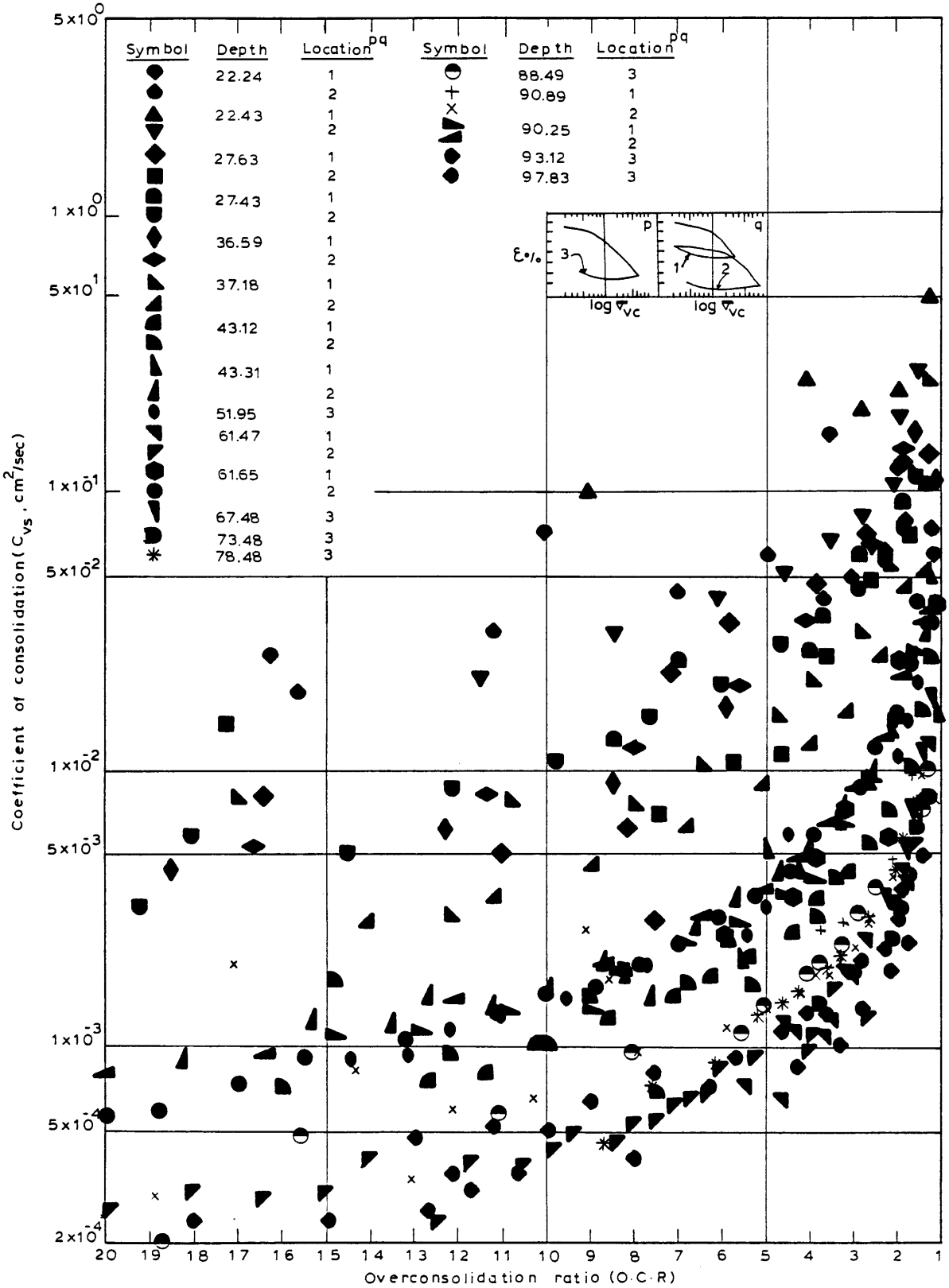

Figure 12.12 Summary of variation of the coefficient of consolidation during rebound

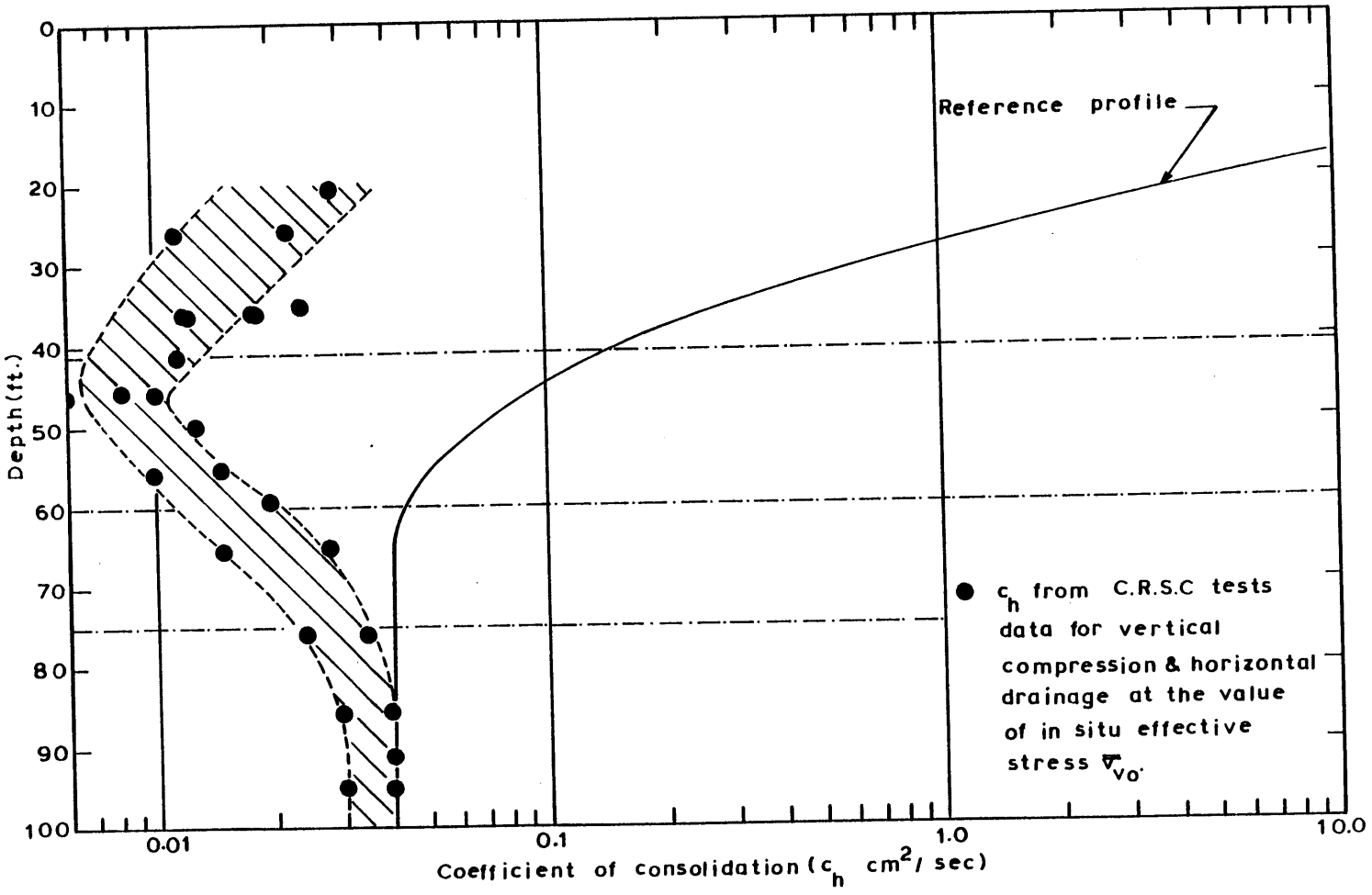

Figure 12.13 Comparison of the variation of the coefficient of consolidation from C.R.S.C data with the reference profile.

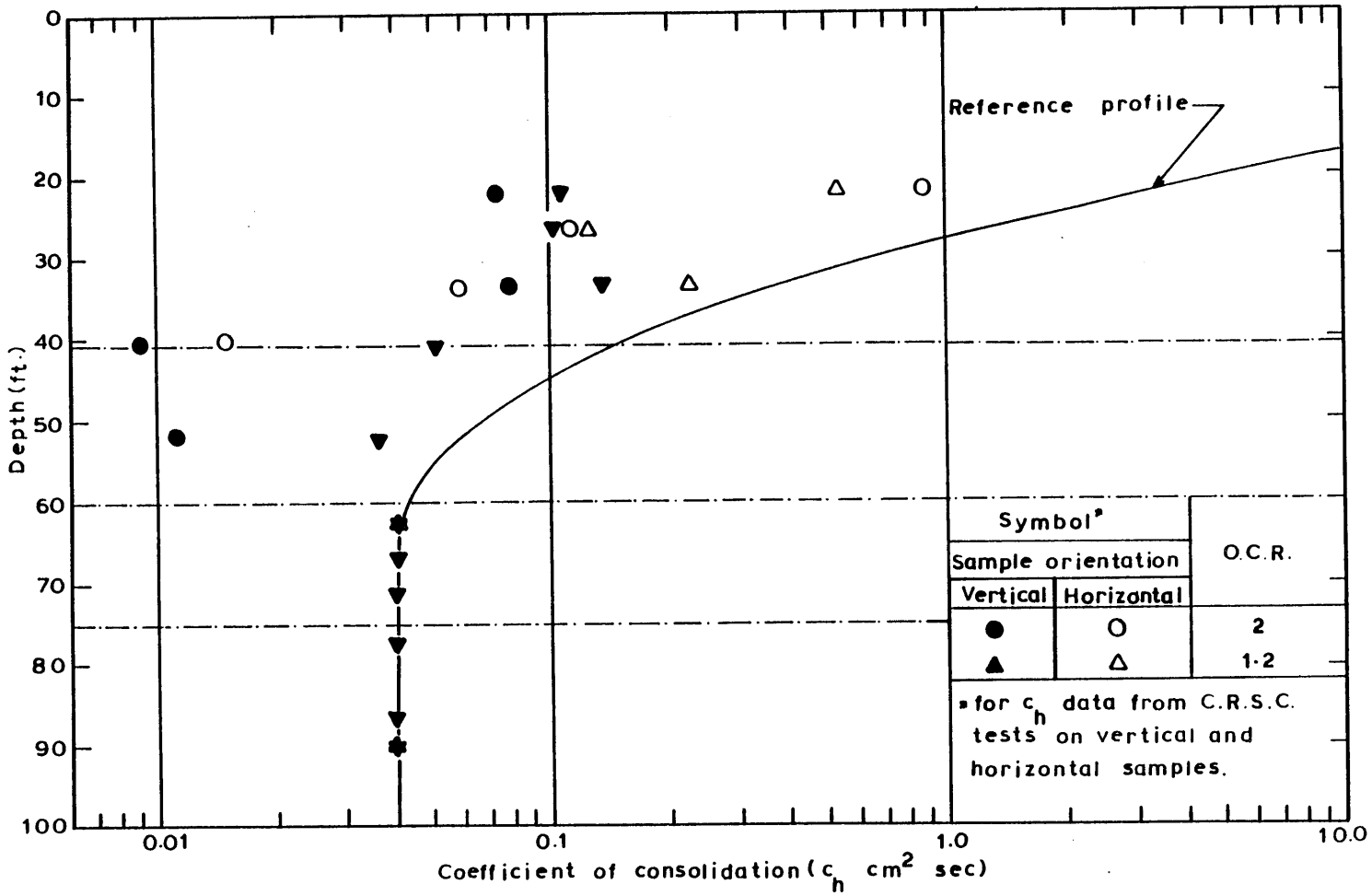

Figure 12.14 Comparison of the variation of the coefficient of consolidation from C.R.S.C data for values of OCR of 1.2 and 2.0 with the reference profile.

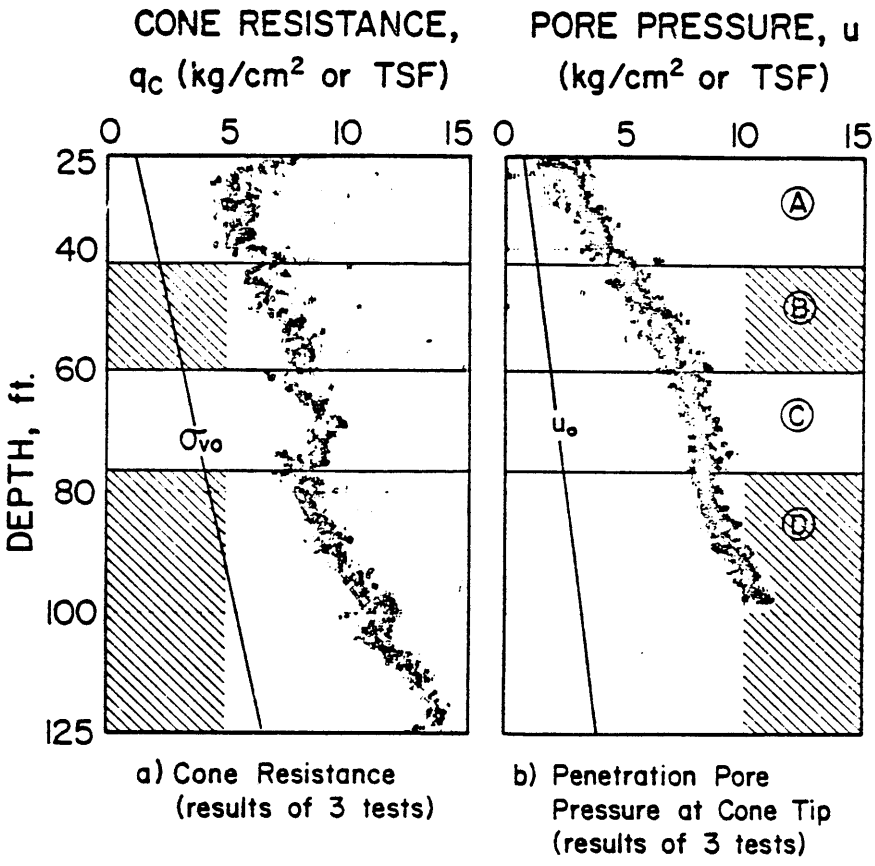

Figure 12.15 Cone resistance and pore pressure during penetration.
(1 ft = 0.305 m; 1 kg/cm² = 98.1 kPa).

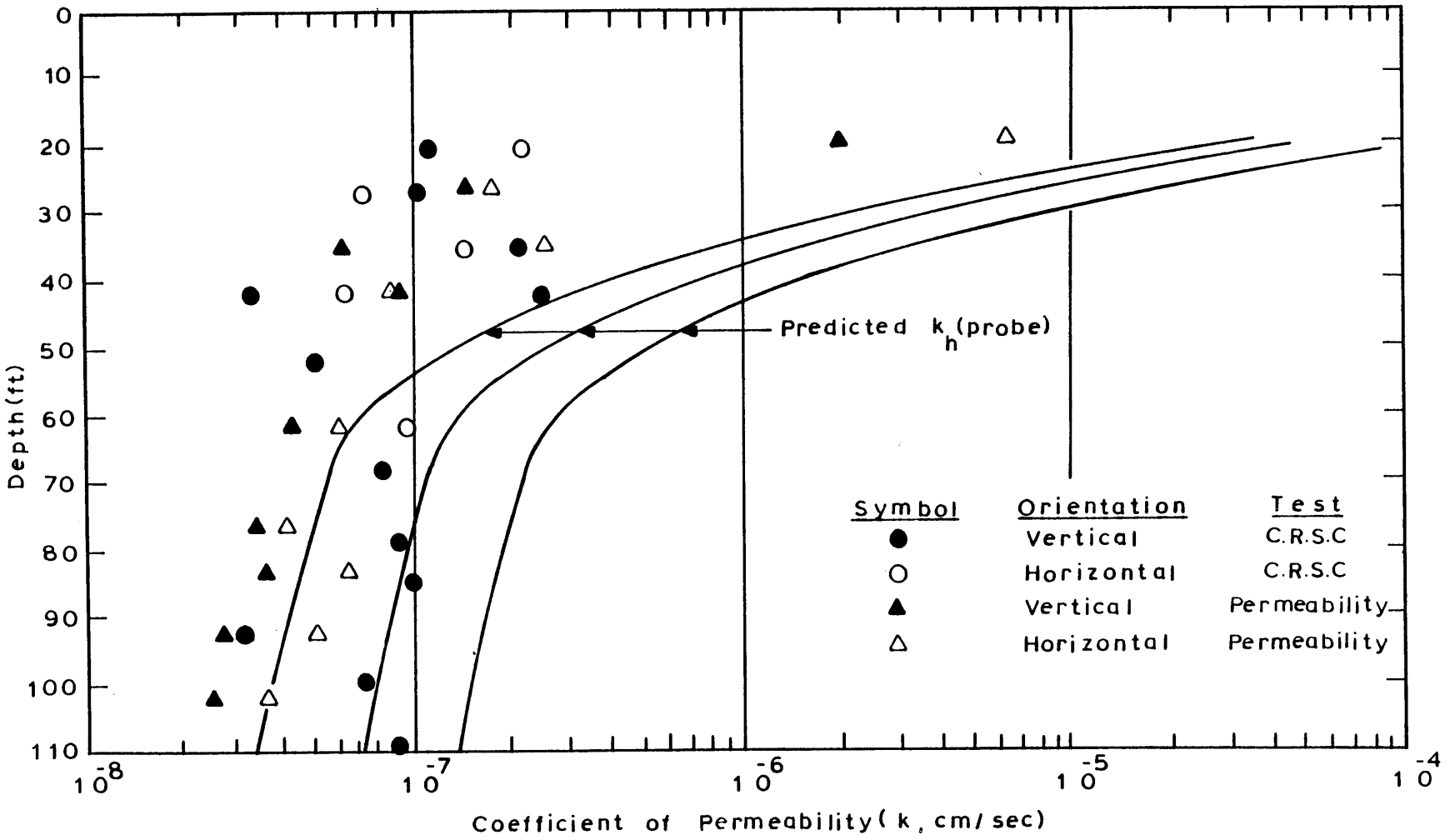

Figure 12.16 Comparison of laboratory and predicted variation of the coefficient of permeability with depth.

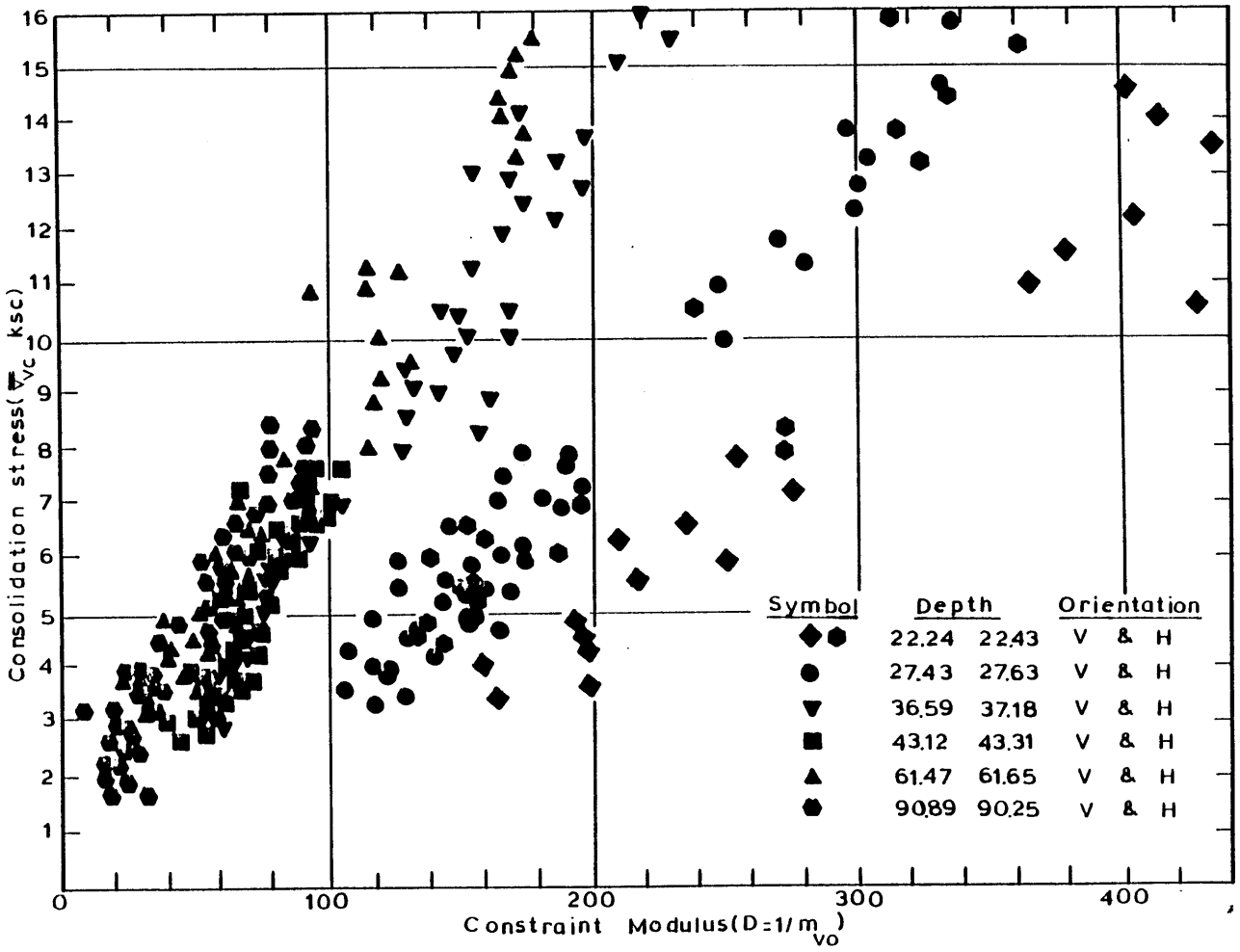

Figure 12.17 Summary of the variation of the constraint modulus with the consolidation stress.

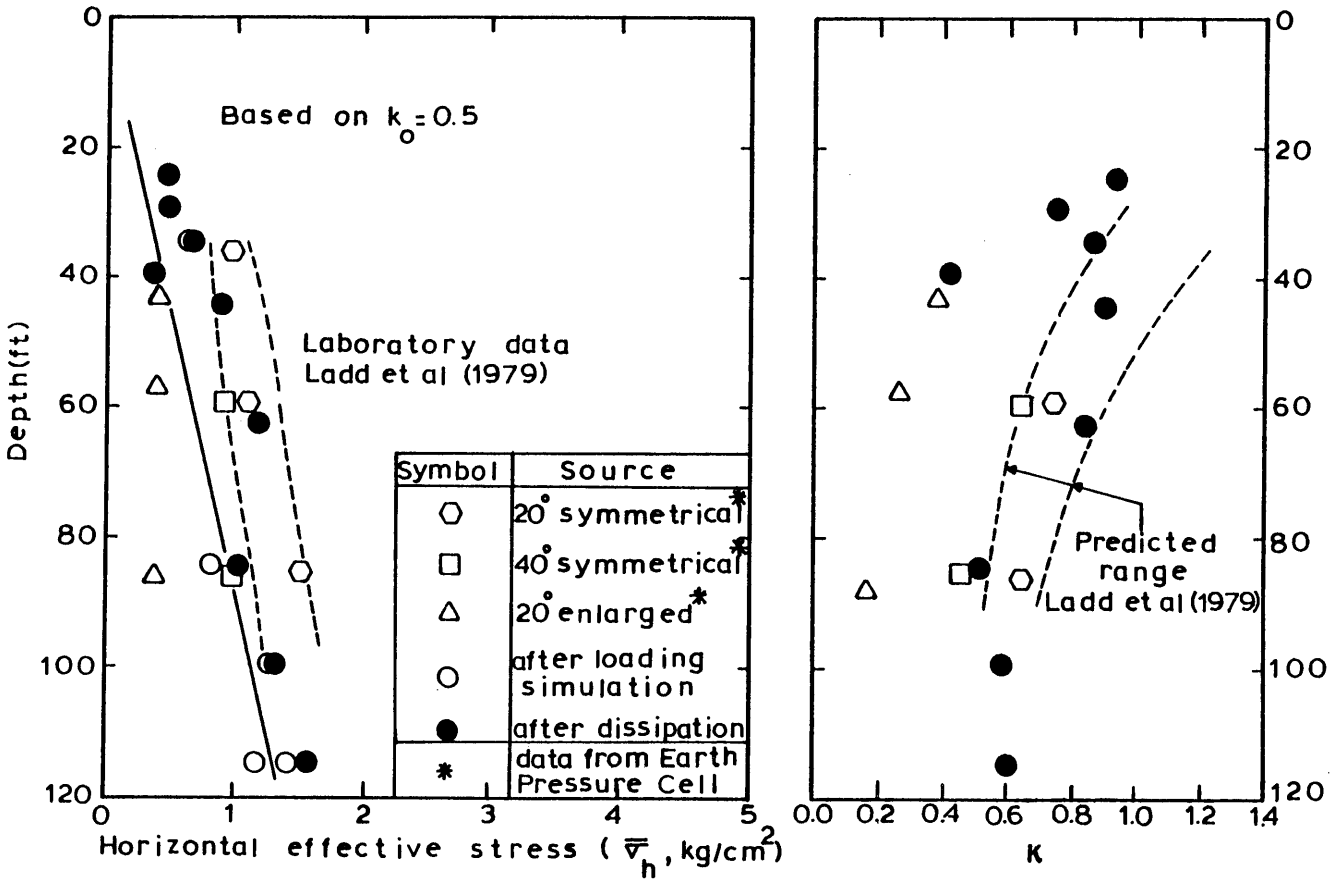

Figure 12.18 Variation of the horizontal effective stress with depth (a) and the derived value of the coefficient of lateral earth pressure.

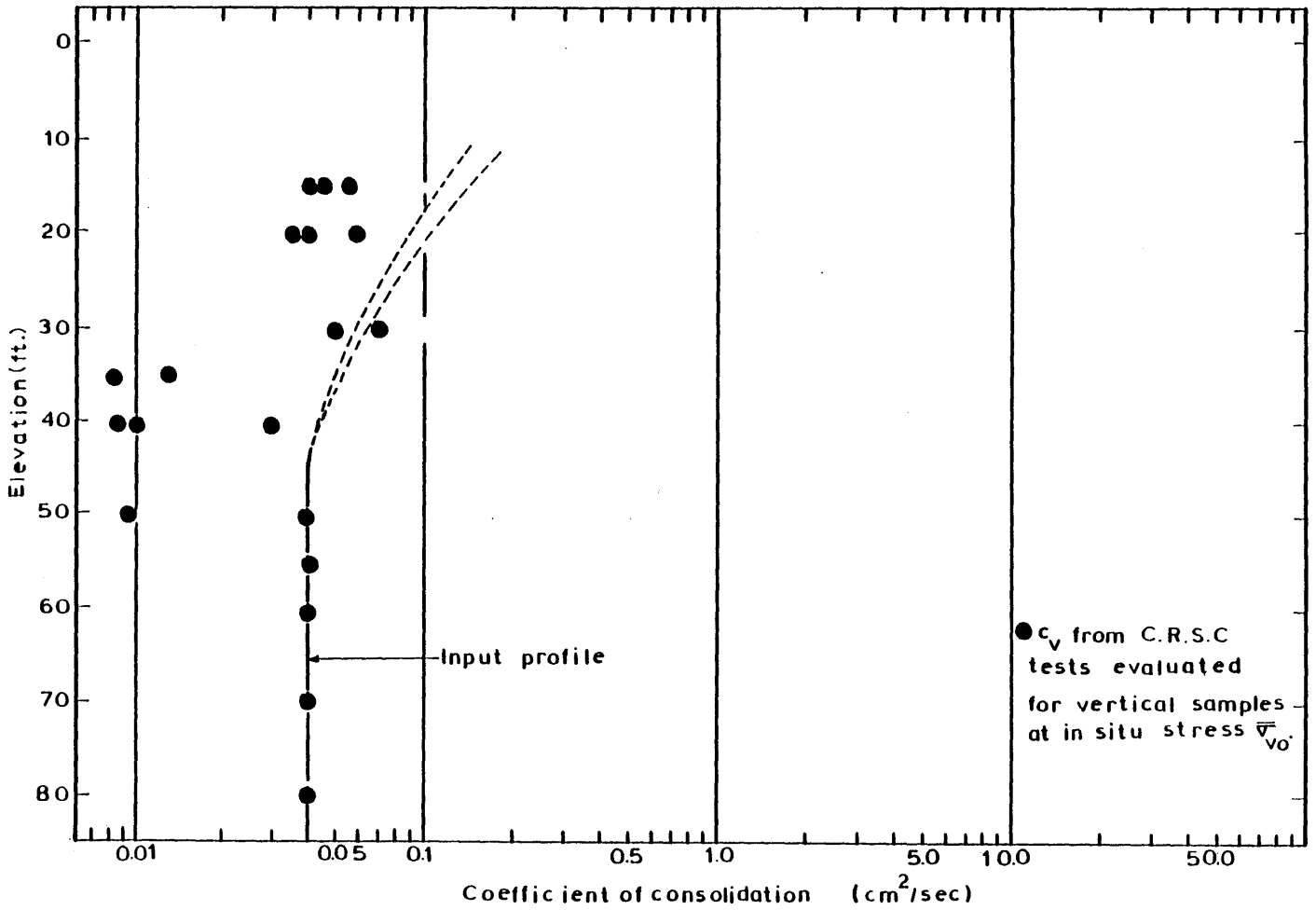

Figure 12.19 Comparison of the ADINAT input profile and values of the coefficient of consolidation derived from laboratory data.

CHAPTER 13

CONCLUSIONS

(1) Geotechnical engineers are usually forced to work with insufficient and inaccurate data to predict the possible behavior of a project at hand. In any one cognitive model formed of various submodels that utilize sophisticated stress or deformation fields, it turns out that the selection of the soil parameter is of critical importance and in some instances highly dominant.

(2) The ability of the current state of the art in predicting soil parameters for later use in behavioral models is best evaluated via 10 case studies on various types of soils under different physical conditions.

(3) A consistent increasing trend in the ratio of $(c_v)_{performance}/(c_v)_{lab}$ is identified when going from the remolded to the undisturbed soil (puddle core to foundation soil). This is to be intuitively yet in no way quantitatively expected since the macrostructure becomes more dominant factor in undisturbed soils. Similarly the trend is more prominent with an increase in sensitivity (puddle core to Leda clay).

(4) No one identifiable trend could be detected in the ratio of $(c_v)_{performance}/(c_v)_{in\ situ}$. It became evident that $(c_v)_{in\ situ}$ derived from constant or falling head tests on piezometer coupled with Gibson's (1963) interpretation

methodology is totally irratic and not much relevance could be attached to it.

(5) $(k_v)_{\text{in situ}}/(k_v)_{\text{lab}}$ has a consistent increase trend when going from remoulded to undisturbed soil. Although the zone surrounding the piezometer is disturbed yet it has the advantage of measuring the average permeability over a larger area of influence hence in comparing the macro structure in the surrounding soil mass. Thus the increasing trend should be expected.

(6) A better measurement tool is required to identify soil parameters so that a more consistant (less guess work) approach could be followed.

(7) In our current endeavor towards achieving a better understanding of the various mechanisms involved with the problem of prediction of in situ soil properties, we are faced with problems characterized by multiplicity of interactions; gaps in our knowledge of the situation and computational limitations. We need a comprehensive, systematic attack with due consideration of multiple iterations. We need a method which accepts complexity and uncertainty as an inherent part of any problem and applies rational procedures to attack it.

(8) A systematic attack strategy devised for such problems could be subdivided into four components:

(a) The problem is defined;

(b) Alternative solutions are generated;

(c) The solutions are evaluated; and

(d) An iterative procedure is followed.

However, we do not follow such a simple linear one-way procedure, we double back and repeat ourselves many times. We usually oscillate from one function to another in an almost random manner until, finally, we exit.

(9) Chapter 3 described the mechanistic properties of a system, e.g., input, output, and feedback. A systems description of reality - a systems model of reality was presented. In the general sense, a model is a description or perception of a thing in existence or being planned. A model is a representation of a real or planned system. In no field is the model used more widely and with greater variety than in systems analysis. The multidisciplinary nature of contemporary problems demands the use of models of all sorts that fit the particular aspect under consideration.

(10) Models are approximate, uncertain and incomplete. If they were not such, they would be the real system. We should accept uncertainty as a fact of life when using system approach and use approximations abundantly. However, we should always determine the sensitivity of the model's output to the uncertainty involved and the approximations used.

(11) We often must force ourselves to quit developing a model that has already provided an answer we need. We should adopt a "sufficientism" philosophy which has a theme,

"precision for decision".

(12) Process involved in the construction of models includes:

1. Identifying the purpose of the model: What are the questions being asked? What processes are to be represented? Why are we producing the model? What would we like to come out of it?
2. Identifying the important parameters: What are the variables? Which parameters will affect our decision.
3. Identifying the relations among the variables: How are the variables related? What are the direct relations? How does a change in each variable affect the other variables?
4. Drawing diagrams: What pictures, sketches, graphs, arrow diagrams, etc. are appropriate?
5. Executing the model sufficiently enough to satisfy the purpose of the model: What idealizations and approximations are sufficient to get a grasp on the questions asked?
6. Testing the model with reality: How do relations check with observation? What is the model's sensitivity to the approximations made.
7. Iterating: Repeat the process. What refinements of the model are necessary to satisfy the purpose of the model? In the process of the iteration we

move from simple to complex, from general to specific. Figure 3.7 gives a schematic presentation of the model building process discussed. The attributes of a good model could be summarized as follows:

(a) Simplicity

(b) Answers the right questions

(c) Versatility

(d) Extendability

(e) Validity

(f) Provide insight into the process modelled

(g) Clarity/understandibility

(h) Completeness

(i) Robustness (not sensitive to assumptions)

(j) Feasibility

(k) Economy

(13) Invoking the first step of our systems perscriptive model, definition of the problem (System definition and description) we address the following issues:

(a) Typical problems encountered by geotechnical engineers almost always require knowledge of consolidation and/or permeability properties of the soil deposit at hand.

(b) In most practical situations involving coarse grained soils (gravels and sands; $k \simeq 10^{-4}$ cm/sec) impose "drained" conditions. Good estimates of the permeability of

gravels is rarely needed since their permeability is often too large. On the other hand, estimates of the permeability of natural deposits could be established by either using empirical correlations with effective grain size, D_{10}, or by in situ testing. Improved estimates of the in situ permeability through laboratory testing is inhibited due to sample disturbance. Errors within an order of magnitude are not uncommon.

(c) "Undrained" conditions are intimately related to the behavior of fine grained soils and would henceforth necessitate knowledge of the coefficient of consolidation. In relatively "structureless" clays, the most experienced engineer using the best laboratory testing equipment and procedures can, at best, predict field values of k and c_v with a factor of two or three. However, the average geotechnical engineer using routine sampling and testing methods can probably estimate k and c_v within a factor of five to ten from laboratory measurements. In "structures" fine grained soils, estimates of k and c_v from laboratory measurements can be several orders of magnitude lower than field value and thus have very limited use in designs.

(d) Reliable in situ tests in fine grained soils are time consuming and require considerable skill and experience. Under ideal conditions, useful permeability data can be obtained. However, direct measurements of the more important

coefficient of consolidation, c_v, are not sufficiently reliable.

(e) Laboratory tests are expensive and time consuming. More importantly, they provide information at discrete locations only and thus reflect local rather than global properties of the soil deposit. Moreover, predictions based on values of the vertical coefficient of consolidation, c_v, measured in the laboratory generally under predict the rate of consolidation observed on full scale structures. On the other hand, large scale field loading tests are seldom available before construction and provide the overall consolidation behavior of the soil mass. Similarly, field pumping tests are difficult to interpret and may lead to erratic results because of their sensitivity to soil nonhomogeneity.

(f) Hence, the need often arises for a more economical in situ test that would provide reliable profiles of consolidation (and/or permeability) coefficients.

(14) Using the piezometer probe as our system, typical records obtained from in situ testing would aid the geotechnical engineer in two aspects:

(a) Provide information on the subsurface stratigraphy (i.e., the extent, thickness, and location of the different soil layers.

(b) Provide estimates of engineering properties of the layers pertinent to foundation design.

(15) A typical dissipation record starts with a value of pore pressure equal to the so-called initial penetration value and later gradually decays until it ultimately reaches the steady state pore pressure. Due to the dependence of the penetration pore pressures on the nature of the soil penetrated, it is usually hard to estimate those values a priori in erratic deposits.

(16) It is usually more meaningful to plot the variation of the ratio $\bar{u}=(\Delta u/\Delta u_i)$ with time. Δu is the pore pressure increment at any one time t and is equal to $u-u_o$ where u is the pore pressure at any time t and u_o is the steady state pore pressure. Δu_i is the initial pore pressure increment and is equal to u_i-u_o where u_i is the initial penetration pore pressures.

(17) The most pertinent objectives of the aforementioned system could be briefly listed as follows:

(a) Provide the measured soil parameters, e.g. vertical or horizontal coefficient of consolidation and/or permeability:

(b) The magnitude of this parameter;

(c) The magnitude of the dessipation period;

(d) The cone angle that provides the most reliable results;

(e) Location for measuring the pore pressures, on the cone; and,

(f) Insight to the mechanism of soil deformation around the cone etc.

(18) Basically, the difficulty in interpreting dissipation records requires the estimation of:

(a) Initial spatial distribution of the penetration pore pressures; and,

(b) The rate of subsequent dissipation of those pore pressures.

(19) Two models were used to determine the initial pore pressure distribution, namely:

(a) The first model assumes that the soil behaves as an elastic perfectly plastic material and the solution is obtained assuming plane stress conditions (Nadai, 1959).

(b) The second model assumes the soil to behave as a "viscous substance" unable to support tensile stresses and the radial stress is evaluated from equilibrium alone.

However, pore pressure spatial variation around the tip of a conical piezometer probe is by far much more complicated since the problem is clearly two dimensional.

(20) Developing an interpretation theory that faithfully incorporates the behavior of a particular soil under specific loading conditions, lacks the generality required to be able to use it for other soils under more versatile loading conditions. Yet to be able to formulate such a universally applicable theory is at the present impossible due to several reasons, namely:

(a) Non-linear behavior of soils.

(b) Soil remolding due to large strain induced by cone penetration.

(c) Soil anisotropy.

(21) Classical approaches towards the problem of pore pressure dessipation around cones involved the use of one dimensional linear solutions (cylindrical or spherical cavity type).

Classical approaches to such problems involved the use of either the Terzaghi-Rendulic uncoupled or unlinked theory, or the Biot coupled or linked theory. Both coupled and uncoupled theories lead to the same governing equation for problems involving one-dimensional rectelinear consolidation and expansion of spherical and cylindrical cavities.

(22) Some important guidelines to evaluate a possible soil model that would explain the soil behavior around cones was presented.

(23) In the second step of our perscriptive model, alternative evaluations, the available alternatives were reduced to two:

(a) Torstenson's interpreation method

(b) Baligh and Levadoux's interpretation method.

(24) Attempts to measure the initial penetration pore pressure and subsequent dissipation records are difficult to conduct because of:

(a) The interaction between the measuring device and the surrounding soil; and,

(b) The difficulties in estimating accurately the relative location of the moving tip with respect to the soil element where pore pressures are measured.

(25) Torstenson (1977) evaluates the pore pressure distribution due to undrained penetration of a conical piezometer probe in clays by means of a model utilizing the classical solution to the expansion of spherical and cylindrical cavities in an infinite medium initially subjected to an isotropic state of stress.

When penetration stops, Torstenson assumes that the consolidation is governed by the Terzaghi-Rendulic (uncoupled) equations.

Torstenson solves these equations with the finite difference technique and provides charts of normalized excess pore pressure at the cavity wall, $\Delta u/\Delta u_i$ vs. the time factor, $T=ct/R^2$, for different values of E_u/S_u.

In order to evaluate the coefficient of consolidation, c, from dissipation records obtained with the piezometer probe, Torstenson proposes the use of the formula:

$$c = \frac{T_{50}}{t_{50}} R^2$$

in which T_{50} is the predicted time factor for a selected value of E_u/S_u and t_{50} is the measured time for 50% dissipation, i.e., $\Delta u/\Delta u_i = 0.5$.

(26) Baligh and Levadoux's method considered a more realistic approach.

1. For the initial pore pressure model they considered the following steps:

(a) Identification of the important parameters:

1. Size of the soil zone affected by cone penetration.
2. The spatial variation of the initial excess pore pressure.
3. Location of boundary drainage.

The relative importance of those variables was assessed through the use of sensitivity analysis involving closed form numerical solutions obtained by Levadoux and Baligh (1980). Results of this sensitivity analysis are stated herein:

1. Dissipation curves (plotted as $\bar{u}$ vs. logt) are very sensitive to the initial distribution of the normalized excess pore pressures $\Delta u_i(r)/(\Delta u)_{sh}$, where $\Delta u_i(r)$ is the excess pore pressure at a radius r and $(\Delta u)_{sh} = u_i(R)$ is the excess pore pressure at the cavity wall (shaft), as characterized by:

(a) The extent (or size or radius) of the soil subjected to excess pore pressures compared to the cavity radius, i.e., the parameter λ.

(b) The spatial variation in the soil, e.g., logarithmic, linear, etc.

2. Analyses performed for a given initial distribution (g and spatial variation) assuming spherical symmetry, lead to slightly faster dissipation than cylindrical symmetry (a factor of 1.5 to 2 in the backfigured coefficient of consolidation at 50% dissipation).

3. Dissipation is mainly controlled by the soil properties within a radius R and is little affected by the outer soil. Furthermore, the soil near the cavity is predominantly subjected to a decrease in volume (compression or recompression) during dissipation.

(b) Identify the relationships among variables

Deep cone penetration in clays is an axisymmetric two-dimensional steady state problem which is essentially strain-controlled, i.e., strains and deformations in the soil are primarily imposed by kinematic requirements. For this type of problem, Baligh (1975) proposes an approximate method of solution called the "strain path method". Levadoux and Baligh, 1980, apply this method to cone penetration in clays and estimate the normalized excess pore pressures on the basis of

laboratory test data on normally consolidated Boston Blue Clay. Linear dissipation analyses are not affected by the absolute value (magnitude) of excess pore pressures $\Delta u_i/(\Delta u)_{sh}$ where $(\Delta u)_{sh}$ is shaft excess pore pressure at sufficiently large distance behind the cone.

(c) Testing the model's sensitivity to assumptions made and compare to reality:

Comparison of $\Delta u_i/(\Delta u)_{sh}$ predicted by the model for various locations of the porous stone (cone & shaft) agree very well with measured values using the piezometer probe in Boston Blue Clay*. The validity of the predicted spatial variation was established through comparison with results of the radial distribution of pore pressure around clyindrical piles jacked into Champlain Clay (O.C.R. ≈ 2). The agreement was extraordinary in view of the various assumptions. Thus the model is not very sensitive to assumptions and the methodology applies equally well to Champlain clay even though it's development employed soil parameters derived from tests on Boston Blue Clay.

*Agreement with field values in Boston Blue Clay deteriorated for OCR > 3.

2. For the subsequent pore pressure dissipation, Baligh and Levadoux used the initial distribution of normalized excess pore pressures obtained from steady state penetration solutions in normally consolidated Boston Blue Clay and utalized a finite element program ADINAT to perform a two dimensional linear isotropic uncoupled consolidation analyses. Sensitivity to coupling was checked by replacing ADINAT with CONSOL that utilizes Biot's coupled/linked theory to perform a two dimensional linear consolidation analysis.

Evidently, the effect of linear coupling between total stresses and pore pressures is reasonably small except at early stages of consolidation especially near the apex of an 18° cone. This suggests that uncoupled solutions can provide reasonably accurate prediction away from apex and after sufficient dissipation has taken place.

Baligh et al. showed that a reduction in the vertical coefficient of consolidation, c_v, from c_h (isotropic case) to 0.1 c_h causes little delay in the uncoupled pore pressure dissipation at 4 selected locations along the tip and the shaft of an 18° piezometer probe in a linear elastic material This suggests that c_h governs consolidation around piezometer probes.

(27) Invoking the last step of our system's approach, alternative evaluation, in which our judgement should be based on how close to reality are the assumptions and system output of a particular approach.

(28) The use of Torstenson's method for evaluating the initial distribution of the pore pressures is highly questionable as it raises serious theoretical and practical problems caused by the severe oversimplifications he introduces.

Torstenson's method for prediction of initial penetration pore pressure distribution and subsequent dissipation mechanism, do not provide the necessary insight into cone penetration mechanism which is essential in understanding and hopefully accounting for soil nonlinearities neglected in conventional consolidation analysis.

(29) Evaluation of Baligh and Levadoux's method was based on comparison of predicted dissipation curves, coefficients of consolidation, c_h and c_v, and coefficients of permeability, k_v and k_h, with dissipation curves obtained from in situ field tests and values of c_v, c_h, k_v and k_h obtained from laboratory tests.

(30) Comparison of predicted dissipation curves with field obtained curves from tests on Boston Blue Clay (OCR<2) indicates that reasonably good dissipation predictions are achieved at four locations on an 18° cone and at the tip of a 60° cone when the horizontal coefficient of consolidation

c_h = 0.04 cm^2/sec.

(21) Profiles of c_h(probe) in the BBC deposit at Saugus are obtained at different dissipation levels for three types of conical probes: a) an 18° cone with the stone at the tip; b) an 18° cone with the cone at mid-height; and c) a 60° cone with the stone at tip.

a) At early dissipation stages ($\bar{u}$=0.8) the scatter of the data is so high that reasonable c_h profiles cannot be established.

b) All three probes provide consistent c_h(probe) profiles after 50% consolidation (± 10%) involving a very moderate degree of scatter.

c) Values of c_h estimated at high levels of consolidation are slightly lower than obtained at 50% dissipation in the lower clay below 40 feet and higher in the upper more pervious clay.

(32) Comparison of the predicted profiles of c_h(probe) at 50% dissipation with laboratory and field measurements of the vertical coefficient of consolidation, c_v, in BBC indicate that

a) The predicted variation of c_h(probe) with depth is consistent with trends of c_v(NC) measured in the laboratory in the normally consolidated range and the profile of c_v(loading) backfigured by Duncan and by Davis and Poulos (MIT, 1975) on the basis of in situ pore pressure measurements conducted in the foundation

clay under the I-95 embankment for a period of 7 days after construction.

b) The predicted magnitude of $c_{h(probe)}$ is: (a) very close to c_v(unloading) backfigured by Bromwell and Lambe (1968) on the basis of in situ pore pressure measurements in a very similar BBC deposit due to a wide excavation and (b) much higher (20 to 40 times) than $c_{v(N.C)}$ or c_v(loading).

c) Profiles of $c_{h(probe)}$ can therefore provide good estimates of the coefficient of consolidation to be used in foundation problems involving unloading and possibly reloading of overconsolidated clays above the maximum past pressure.

(32) Predicted profiles of $k_{h(probe)}$ and $c_{v(N.C)}$ obtained from an approximate method proposed by Baligh and Levadoux are considered very satisfactory especially when compared to other existing in situ permeability testing methods.

(33) The prediction method was then applied to the results of dissipation tests performed on Connecticut Valley Varved Clay. It was found from dissipation records that predictions apply surprisingly well to C.V.V.C. in spite of large differences in behavior. Also a comparison of $k_{h(probe)}$ with laboratory measurements of the horizontal permeability indicate very good agreement.

(34) Testing the model with reality requires its use as a predictive tool to forecast field performance of full scale prototypes. The Student Center case study has been a popular topic for analysis due to the abundance of field observations which are well documented. Several authors attempted to utilize this case study to evaluate their predictions of the in situ coefficient of consolidation by employing se-tlement analysis and prediction of induced pore pressure isocrones. However such analyses were non conclusive and presented severe limitations.

(a) Gass's (1964) explanation of the low tension and the almost instantaneous response to ground water variation as being a direct consequence of faulty sealing of piezometer tip is inaccurate. The high coefficient of consolidation at shallow depths coupled with the short drainage path is responsible for the low tensions registered.

(b) Von Arnim (1967) and Lambe and Bromwell's (1968) methods for prediction of the induced negative tension due to excavation and subsequent reloading suffered from the use of erroneous soil properties as well as inappropriate stress distributions. However the errors thus induced were attenuated by several compensating factors of which:

a) Due to assumption that top 32' have a c_v value

for swelling double that for the lower 34' and the use of the recommended transformation yields a shorter overall drainage path.

b) The value of the backfigured c_v value is low in comparison to that of Lambe et al. (1968), and lower than the in situ value.

c) The predicted initial pore pressure distribution is lower than the actual.

d) The top boundary conditions are lower than anticipated (by use of averages).

Thus any apparent agreement with field data is fruitituous and the analysis depends heavily on compensating errors.

(35) When pore pressure prediction scheme is initiated, it is of utmost importance that the assumed boundary conditions be accurate and duplicate exactly the field conditions, since the pore pressure response to the applied boundary conditions is instantaneous and is reflected in field piezometer readings that would deviate from predicted behavior when we assume some average value of the boundary conditions. However, with regards to heave predictions, since the corresponding field behavior to applied loads is not instantaneous and since sufficient time is available, heave predictions are not very sensitive to averaging boundary conditions.

(36) In the traditional Terzaghi formulation of the governing field equation describing the excess pore pressure isocrones, it is assumed that c_v is constant and furthermore k_v is also constant. Gibson's analysis using polynomial distributions of k_v and m_v show that:

1. The variation of the permeability k is largely responsible for the derivation of the calculated excess pore pressure isocrone at 50% consolidation from that predicted by conventional theory.

2. The variation of the compressibility m_v is largely responsible for the deviation of the calculated time settlement curves from that predicted by conventional theory.

3. The time-settlement curves for similar distributions are proportional to net absolute permeability.

(37) Piezometer PSC-1 readings suggesting a lower value of the excess pore pressure is in perfect agreement with theory and does not reflect any instrument malfunction.

(38) The feasibility of the analytical solution depends heavily on whether the actual variation of k and m_v with depth can be described with sufficient accuracy, by simple functional relationships. Quantitative evaluation of the c_h profile involving comparison of predicted versus field pore pressure dissipation records would involve using a model that can intimately encompass the variation of the soil properties namely c_v, c_h, k_v, k_h, m_v and m_h. Since such variations are

usually by no means easy to express in simple functional relationships we are compelled to use approximate numerical techniques that can accomodate such variations.

(39) The program ADINAT was developed to provide solutions for general linear and nonlinear steady-state and transient heat transfer analysis. A specific feature of a heat transfer analysis program is that the same code can also be used to solve other field problems, such as steady state seepage or transient state seepage problems. The reason for this direct applicability of ADINAT to a number of field problems is the analygy between the various field variables.

(40) The program ADINAT was successfully used to verify Gibson's solutions with no appreciable deviations.

(41) Boston Blue Clay exhibits normalized behavior in as far as compressibility and permeability characteristics are conserned and hence correlation of values of c_v based on equivalent values of O.C.R. is possible.

(42) Predicted dissipation records of excess negative pore pressures using the finite element program ADINAT with a one dimensional soil model utilizing the normalized behavioral characteristics of Boston Blue Clay, agree very well with observed field values.

(43) The loading curves and the dissipation curves reveal the following:

a) All four loading curves are minutely affected by Pour I and no appreciable stress increment is noted.

b) The effect of the stress increment induced by Pour II diminishes at shallower depths.

c) Agreement of predicted excess negative pore pressures with observed field values appears to be poor at the end of stage I of excavation. This could be primarily attributed to the inexact earth work quantities reported or sequence of removal.

d) Agreement is restored at the end of excavation stage II which would suggest that probably the distribution of earthwork removal between stage I and II is not accurate but the total stress release attributed to stages I and II is reasonable.

e) Agreement of predicted excess negative pore pressures with observed field values appears to be excellent after excavation state II. Lack of agreement at the initial dissipation stage at the deepest piezometer (P-4) could be attributed to possible instrumentation error that has been detected in the reported values. Attention is drawn to the corresponding reported observed values of piezometer P-4 between 10/8/63 and 10/21/63 which are believed to be approximate. Perfect agreement resumes after this period which reinforces our hypothesis.

f) The predicted excess negative pore pressure dissipation curve corresponding to the shallowest piezometer agrees very well with field observed values of piezometer

P-1 and also with observed values of well WSC-1. This clearly suggests that the top boundary condition dominates the pore pressure dissipation pattern for the shallow piezometer P-1. This tends to attenuate any possible errors that could be induced by assuming $c_v/c_h = 1.0$ and $k_v/k_h = 1.0$ at very shallow depths.

1) The error induced by using a constant value of $c_v = 0.04\ ft^2/sec$ is an increase of approximately 8% at shallow depths and increase in magnitude to approximately 20% in the vicinity of PSC-2.

2) The error induced by using a constant value of $c_v = 0.04 ft^2/sec$ decreases to approximately 3% as we approach the bottom boundary.

3) The error induced by using a constant value of $c_v = .15 cm^2/sec$ is a decrease of approximately 52%. The magnitude of the error reduces to approximately zero in the close vicinity of PSC-1.

4) Moving away from the centerline of the compressible stratum, the pore pressure isocrone is more dependent on the local value of c_v and the boundary conditions immediately adjacent.

(44) With the current need for high quality representative soil specimens characterized by a high cost of retrieval, a reliable method for planning and locating each specimen in the sampling liner is of essence. Xradiography provides an

excellent non-destructive method that provides a spatial view of the interior of the soil sample.

Xradiography is successful in identifying:

(a) Zones of excess disturbance;

1. possible presence of remoulded soil
2. expansion of gas pockets
3. zones in vicinity of foreign objects (stones, shells, etc.)
4. zones experiencing shoals due to mishandling.

(b) Zones containing large horizontal cracks, possibly due to gas or difficulty in retrieval, especially when sand or silt seams are experienced.

(c) Location of good to excellent quality samples with little or no evidence of disturbance.

(d) Identifying location of foreign objects; stones, shells, gravel layers, etc.

(e) Differences in macroscopic structure, e.g., very uniform and homogeneous to slightly layered.

(f) An estimate of thepossible soil profile in the location.

(45) It is of essence that x-radiography of such samples be executed prior to the initiation of any testing programs to:

(a) Minimize amount of wasted material;

(b) Maximize the reliability of test data;

(c) Ensure representativeness;

(d) Reduce the number of tests run on poor quality material;

(e) Identify the exact location of the soil specimen to be tested.

(46) Preliminary identification of possible locations of good quality samples should be continuously updated, guided by the values of undrained shear strength obtained by the Torvane.

(47) The increased reliability of the laboratory data improves the basis for making engineering judgements regarding design of foundations for public facilities and enhances our ability to perform a proper evaluation of newly developed in situ testing.

(48) The B.B.C. deposit at the I-95 test site exhibits a marked nonhomogeneous nature at shallow depths with the following characteristics:

a. Increase in RR and CR with depth;

b. Increase in strains for a particular consolidation stress with depth;

c. BBC exhibits a collapsable structure for elevations approximately below 95 feet.

(49) The clay deposit exhibits an anisotropic nature at shallow depths. The horizontally trimmed samples appear to be slightly less compressible in the normally consolidated range than the vertically trimmed sample.

(50) Values of m_{vs} for vertically trimmed samples are almost identical to those obtained for horizontally trimmed samples.

(51) B.B.C. exhibits normalized behavior with respect to its value of $c_{v(O.C)}$ and $c_{h(O.C)}$

(52) Degree of anisotropic response concerned with $c_{v(O.C)}$ and $c_{h(O.C)}$ increases at shallower depths.

(53) Beyond 60 ft. the normalized curves of $c_{v(O.C)}$, $c_{h(O.C)}$ and $m_{v(O.C)}/m_{vo}$, $m_{h(O.C)}/m_{ho}$ vs. OCR is unique.

(54) The curves thus mentioned are very senstive in the vicinity of an OCR of unity.

(55) $c_{h(probe)}$ reference profile could be used to simulate the field variation of c_{vs} up to a depth of approximately 42 ft. (10 fold deviation from laboratory data at 42 ft.) Throughout the clay deposit the values of $c_{h(probe)}$ are very close to c_{hs} derived from C.R.S.C. tests at an OCR of 1.2.

(56) A method for obtaining the value of coefficient of permeability from C.R.S.C. tests at the in situ $\bar{\sigma}_{vo}$ simulating zero (or close to zero) disturbance was established. The values of the coefficients of permeability derived from C.R.S.C. tests are in good agreement with the values derived from direct measurements in a triaxial cell set up.

(57) The anisotropic response of B.B.C. concerned with values of c_{vs} and c_{hs} is chiefly due to the anisotropic nature of its permeability characteristics.

(58) The ratio of k_h/k_v is approximately 1.2 ± .2 for depths below 60 ft. to approximately 2.4 ± .3 for shallower depths.

(59) A good overall agreement between $k_{h(probe)}$ and $k_{h(O.C)}$ from laboratory data with restrictions to the top 10-20 feet.

(60) The value of c_{vs} of 0.04 dominates the behavior of the dissipation curves up to a depth of 45 feet.

(61) The top 10 feet are highly affected by the continous pumping operations which is reflected in the behavior of the dissipation curve at PSC-1.

(62) The assumption of

$$c_{v(O.C)} = c_{h(probe)} = f(OCR)$$

does not appear to be very severe.

(63) The profile of c_{vs} used to predict the dissipation curves lies in the range of twice to three times the profile of c_{vs} given by laboratory test results.

REFERENCES AND BIBLIOGRAPHY

Al-Dhahir, Z.A., Kennard, M.F., and Morgenstern, N.R., "Observations on Pore Pressures Beneath the Ash Lagoon Embankments at Fiddler's Ferry Power Station", Proceedings, Conference on In Situ Investigations in Soils and Rocks, British Geotechnical Society London, Paper No. 20, 1970, pp. 265-276.

Al-Dhahir, Z.A.R., Kennard, M.F. and Morgenstern, N.R. Observations on pore pressures beneath the ash lagoon embankments at Fiddler's Ferry Power Station. Proc. Conf. on in situ investigations in soils and rock, Inst. Civ. Eng. London, 1969.

Aldrich, H.P. Jr., "Back Bay Boston, Part I," BSCE/ASCE Journal, Vol. 57, No.1, January 1970, pp. 1-33.

Allen, L.R., Yen, B.C. and McNeill, R.L. "Stenoscopic X-Ray Assessment of Offshore Soil Samples", Offshore Technology Conference, Vol. 3, 1978, pp. 1391-1399.

Arthur, J.R.F. "Industrial Radiography in Soil Mechanics Research" British Journal of Non-Destructive Testing, Jan., 1970, pp. 9-13.

Arthur, J.R.F. and Dunstan, P., "Radiography Measurements in Particle Packing", Nature, Vol. 23,1969,pp. 464-468.

Arthur, J.R.F. and Menzies, B.K. "Inherent Anisotropy in Sands", Geotechnique, Vol. 22, No.1, 1972, pp.115-128.

Arthur, J.R.F. and Phillips, A.B., "Homogeneous and Layered Sand in Triaxial Compression", Geotechnique, Vol. 25, No.4, 1975, pp. 799-815.

Arthur, J.R.F. and Shamash, S.V. "A note on the accuracy of Displacement Measurements in Soils", Civil Engineering and Public Works Review, Vol. 62, 1967, pp. 445-456.

Azzouz, A.S. and Baligh, M.M., "Three-Dimensional Stability of Slopes", Research Report R78-8, No. 595, Department of Civil Engineering, MIT, Cambridge, Mass., June 1978.

Azzouz, A.S., Levadoux, J.N., and Baligh M.M., "Cavity Expansion Approaches in Deep Foundations", Research Report, Department of Civil Engineering, MIT, Cambridge, Mass., 1980.

Baligh, M.M., "Theory of Deep Site Static Cone Penetration Resistance", Research Report R75-56, No. 517, Department of Civil Engineering, MIT, Cambridge, Mass., September, 1975.

Baligh, M.M., Azzouz, A.S. and Martin, R.T., "Cone Penetration Tessts Offshore the Venezuelan Coast", Res. Report R80-31, No. 680, Dept. of Civil Eng, MIT, Cambridge, August, 1980, p. 163.

Baligh, M.M., Azzouz, A.S., Wissa, A.Z.E., Martin, R.T., Morrison, M.J.,"The Piezocone Penetrometer", Report No. MITSG80-10, Index No. 81-310-CIM, MIT, Cambridge, 1981, p. 20.

Baligh, M.M., and Levadoux, J.N., "Pore Pressure Dissipation After Cone Penetration", Research Report, Department of Civil Engineering, MIT, Cambridge, Mass., 1980.

Baligh, M.M. and Vivatrat, V., "In Situ Measurements in a Marine Clay", Proceedings, International conference on the Behavior of Offshore Structures, Paper 14, 1979, pp. 151-174.

Baligh, M.M., Vivatrat, V., and Ladd, C.C., "Cone Penetration in Soil Profiling", Journal of the Geotechnical Division, ASCE, Vol. 106, April, 1980, pp. 447-761.

Baligh, M.M., Vivatrat, V., and Ladd, C.C., "Exploration and Evaluation of Engineering Properties for Foundation Design of Offshore Structures", Research Report R78-40, No. 607, Department of Civil Engineering, MIT, Campbridge, Mass., December, 1978.

Bathe, K.-J., "ADINAT: A Finite Element Program for Automatic Dynamic Incremental Nonlinear Analysis of Temperatures", Research Report 82448-5, Department of Mechanical Engineering, MIT Cambridge, Mass., May 1977 (revised, Dec. 1978).

Beaven, G.C.G. and Strouts, C.B., Discusscion, Session E, Proceedings of the conference organized by the British Geotechnical Society in London on In Situ Investigations in Soils and Rocks, 1970, PP. 307-308.

Bendan, D. and Berhand, R.K., "Pilot Studies of Soil Density Measurements by Means of X-Rays", Proceedings American Society of Testing Materials, Vol.50, 1950, pp. 1328-1339

Biot, M.A., "General Theory of Three-Dimensional Consolidation", Journal of Applied Physics, Vol. 12, 1941, pp. 155-164.

Bishop, A.W. and Al-Dhahir, Z.A., "Some Comparisons Between Laboratory Tests, In Situ Tests, and Full Scale Performance, With Special Reference to Permeability and Coefficient of Consolidation", Proceedings, Conference on In Situ Investigations in Soils and Rocks, British Geotechnical Society, London, Pater No. .9, 1970, pp. 251-264.

Bishop, A.W., Kennard M.F. and Vaughan, P.R., Developements in the measurement and interpretation of pore pressures in earth dams. Trans. 8th Inst. Congr. Large Dams, Edinburgh Vol. 2, 1964, p.47-72.

Bishop, A.W. and Vaughan, P.R., Selset Reservoir: design and performance of the embankment. Proc. Ints. Civ. Eng., Vol. 21, 1962, p. 305-346.

Bjerrum, L., Nash, J.K.T.L., Kennard, R.M., and Gibson, R.E., "Hydraulic fracturing in Field Permeability Testing", Geotechnique Vol. 22, No. 2, 1972, pp. 319-332.

Bromwell, L.G. and Lambe, T. W., "A Comparison of Laboratory and Field Values of c_v for Boston Blue Clay, Professional Paper P68-3, Soils Publication No. 205, Department of Civil Engineering, MIT, Cambridge, Mass., January, 1968.

Carslaw, A.R. and Jaeger, C.J., Conduction of Heat in Solids, Oxford at the Clarendon Press, London, 1959.

Crawford, C.B., "Interpretation of the Consolidation Test", Proceedings, ASCE, 1964, pp. 87-102.

Crawford, C.B., "The Resistance of Soil Structure to Consolidation", Canadian Geotechnical Journal, Vol. II, No. 1965, pp. 90-97.

Chavez, P.S., Jr., "Simple High-Speed Digital Image Processing to Remove Quasi-Coherent Noise Patterns", Proceedings of ASP Convention, Washington, D.C., 1975.

Cryer, C.W., "A Comparison of the Three-Dimensional Consolidation Theories of Biot and Terzaghi", Quarterly Journal of Mechanics and Applied Mathematics, Vol. 16, Part 4, 1963, pp. 401-412.

D'Appolonia, D.J., Lambe, T.W., and Poulos, H.G., "Evaluation of Pore Pressures Beneath an Embankment", Journal of the Soil Mechanics and Foundations Division, ASCE, Vol. 97, No. SM6, 1971, pp. 881-898.

Davis, E.H. and Poulos, H.G., "Discussion of An Analysis of Consolidation Theories by R.L. Schiffman, A.T.F. Chen, and J.C. Jordan, "Journal of the Soil Mechanics and Foundations Division, ASCE, Vol. 96, No. SM1, January 1970, pp. 334-336.

Davis, E.H. and Poulos, H.G., "The Analysis of Settlement under Three-Dimensional Conditions," Symposium on Soft Ground Engineering, Brisbane, Australia, 1965.

Davis, H.E. and Woodward, R.J., "Some Laboratory Studies of factors Pertaining to the bearing Capacity of Soils", Highway Research Board, Proceedings, 29th Annual Meeting, 1949, pp. 467-476.

De Fries, K.C., "The Prediction of Heaves and Pore Pressures Induced by Excavations in Clay", Civil Engineers Thesis in Department of Civil Engineering, MIT, 1967.

Drevich, V.P., Massarsch, K.R., "Sample Disturbance and Stress-Strain Behavior", Proceedings, A.S.C.E., 1979, pp. 1001-1016.

FERMIT, "Second Progress Report on Foundation Evaluation and Research", Research report, Dependent of Civil Engineering, MIT, Cambridge, Mass., 1967.

Gass, A.A., "Comparison of Theoretical and Observed Performance of the M.I.T. Student Center Foundations", M.S. Thesis in the Department of Civil Engineering, M.I.T., 1964.

Germaine, J.T., Unpublished CRSC consolidation results on Boston Blue Clay (Saugus), 1978.

Ghaboussi, J. and Wilson, E.L., "Flow of Compressible Fluid in Porous Elastic Media," UC-SESM Report No. 71-12, Structural Engineering Laboratory, University of California, Berkeley, July, 1971.

Ghaboussi, J. and Wilson, E.L., "Flow of Compressible Fluid in Porous Elastic Media," International Journal for Numerical Methods in Engineering, Vol. 5, 1973, pp. 419-442.

Ghantous, I.B., "Quasi Static Expansion of Cylindrical and Spherical Cavities in Metals and Ideal Soils, BSC. Thesis, University of London, 1978.

Gibson, R.E., "An Analysis of System Flexibility and its Effect on Time-Lag in Pore Water Pressure Measurements", Geotechnique, Vol. 13, 1963, pp.1-11.

Gibson, R.G., "An Extension to the Theory of the Constant Head In Situ Permeability Test", Geotechnique, Volume 20, No.2, 1970, pp. 193-197.

Gibson, R.E., "A Note on the Constant Head Test to Measure Soil Permeability In Situ", Geotechnique, Vol. 16, 1966, pp. 256-257.

Gibson, R.E., "Discussion on the Interpretation of Constant Head In Situ Field Permeability Tests," Proceedings, Conference on In Situ Investigations in Soils and Rocks, British Geotechnical Society, London, 1970, pp. 297-298.

Gibson, R.E. and Anderson, W.F., "In Situ Measurement of Soil Properties with the Pressuremeter," Civil Engineering and Public Works Review, Vol. 56, No 658, May 1961, pp. 615-618.

Gibson, R.E., Schiffman, R.L. and Pu, S.L., "Plane Strain and Axially-Symmetric Consolidation of a Clay Layer of Limited Thickness", University of Ill. (Chicago Circle) MATE report 67-4.

Hill, R., "The Mathematical Theory of Plasticity", Oxford at the Claredon Press, 1950.

Hvorslev, M.J. "Time-lag and soil permeability in ground-water observations" Bulletin No.36, U.S. Waterways Experiment Station, Vicksburg, Mississippi.

Hammond, T.G. and Winder, A.J.H. "Problems affecting the Design and Construction of the Great Ouse Water Supply Scheme", Jr. Inst. Water Engrs. Vol. 21, 1967, p.15-42.

Hedburg, J., Urzua, A., and Marr, W.A., "Exploration Methods for Offshore Foundations", Res. Report R78-42, No. 610, Dept. of Civil Eng. MIT, Cambridge, Mass. July, 1978, p. 278.

Kennard, J. and Kennard, M.F., Selset Reservoir: design and construction. Proc. Inst. Civ. Eng. Vol.21, 1962, p. 277-304.

Kennard, M.F., Penman, A.D.M. and Vaughan, P.R., "Stress and Strain Measurements in the Clay Core at Balderhead Dam". Trans. 9th Int. Cong. Large Dams 3: 129-151 1967.

Kenney, T.C., "Sea Level Movements and Geologic Histories of the Post-Glacial Marine Soils at Boston, Nicolet, Ottawa, and Oslo" Geotechnique, Vol. 14, No.3, 1964 pp. 203-230.

Krinitzsky, E.L., "X-Ray Measurements of Soil Densities in Models", U.S. Army Corps of Engineers, Waterways Experiment Stations, Vicksburg, Misc. Paper S-72-1, 1972.

Krinitzsky, E.L. and Smith, F.L., "Geology of Backswamp Deposits in the Atchafalaya Basin, Louisiana", U.S. Army Corps of Engineers, Waterway Experiment Station, Vicksburg Tech. Report S-69-8, 1969.

Lambe, T.W., "Predictions in Soil Engineering: 13th Rankine Lecture", Geotechnique, Vol. 23, No.2, 1973, pp. 149-202.

Lambe, T.W., "The Stress Path Method", Journal of the Soil Mechanics and Foundations Division, ASCE, Vol. 93, November 1967, pp. 309-331.

Lambe, T.W., "Soil Testing for Engineers", John Wiley and Sons, New York, 1951.

Lambe, T.W. and Whitman, R.V., Soil Mechanics, John Wiley and Sons, New York, 1969.

Ladd, C.C., "Estimating Settlements of Structures Supported on Cohesive Soils", Research Report, MIT, Cambridge, Mass., 1973.

Ladd, C.C., et al., "Evaluation of Self-Boring Pressuremeter Tests in Boston Blue Clay", Research Report No. R79-4, Department of Civil Engineering, MIT, Cambridge, Mass., 1979.

Ladd, C.C., "Stress-Strain Behavior of Saturated Clay and Basic Strength Principles", Research Report, Department of Civil Engineering, MIT, Cambridge, Mass, 1964.

Ladd, C.C., et al., "Stress-Deformation and Strength Characteristics", Proceedings, 9th International Conference on Soil Mechanics and Foundations Engineering, Tokyo, Vol. 2, 1977, pp. 421-494.

Ladd, C.C., Azzouz, A.S., Martin, R.T., Day, W.D., and Malek, A.M., "Evaluation of Compositional and Engineering Properties of Offshore Venezuelan Soils", Research Report, Department of Civil Engineering, MIT, Cambridge, Mass., 1980.

Ladd, C.C. and Arthur, J.R.F. "Radiography for Geotechnical Engineering Research", Engineering Eqipment Grant Request submitted to the National Science Foundation, Washington, D.C. by Department of Civil Engineering, MIT, Cambridge.

Ladd, C.C. and Foott, R., "New Design Procedure for Stability of Soft Clays," Journal of the Geotechnical Division, ASCE, Vol. 100, July, 1974, pp. 763-786.

Ladd, C.C. and Luscher, U., "Engineering Properties of the Soils Underlying the M.I.T. Campus," M.I.T. Department of Civil Engineering Research Report R65-58, December, 1965.

Ladd, C.C., Malik, A.M., Martin, R.T., Mishu, R., "Evaluation of Compositional and Engineering Properties of Offshore Venezuelan Soils", Research Report, Dept. Of Civil Engineering, MIT, Cambridge, Mass, 1981.

Leonards, G.A., and Altschaeffl, A.G.,"Compressibility of Clay", Proceedings, ASCE, 1964, pp. 133-156.

Leonards, G.A. and Girault, P., "A Study of the One-Dimesional Consolidation Test", Proceedings Fifth International Conference of Soil Mechanics and Foundation Engineering, V.1, pp. 213-218

Levadoux, J.N., "Pore Pressures due to Cone Penetration", Ph.D. Thesis, Department of Civil Engineering, MIT, Cambridge, Mass., 1980.

Levadoux, J.N. and Baligh, M.M., "Radial Consolidation in Solutions", Research Report, Department of Civil Engineering, MIT, Cambridge, Mass., 1980.

Lowe III, J., Jonas, E. and Obrician, V., "Controlled Gradient Consolidation Test" IV, ASCE Proceedings, 1969, pp.77-98.

Lumb,P.,"Rate of settlement of a clay layer due to a gradually applied load", Civ. Eng. and Public Works Review, Vol. 58, March, 1963, pp. 315-317.

Lunne, T. and Lacasse, S.M., "Results of In Situ Self-Boring Pressuremeter Dutch Cone and Piezometer Probe Tests in Norwegian Clays", Norwegian Geotechnical Institute, Internal Report 52155-10, Oslo, 1980.

Mandel, J., "Consolidation des Sols (Etude Mathematique)", Geotechnique, Vol. 3,1953, pp. 287-299.

Meyerhof, G.G., "The Ultimate Bearing Capacity of Foundations", Geotechnique, Vol. II, No. 4, 1951, pp. 301-332.

Meyerhof, G.G., "The Ultimate Bearing Capacity of Wedge-Shaped Foundations", Proceedings, 5th International Conference on Soil Mechanics and Foundation Engineering, Vol. 2, 1961, pp. 103-109.

Mesri, G.,Ullrich, C.R., Choi, Y.K., "The Rate of Swelling of Overconsolidated Clays Subjected to Unloading", Geotechnique, Volume 28, No.3, 1978, pp. 281-307.

Mesri, G., Godlewski, P.M., "Time-And-Stress-Compressibility Interrelationship", Proceedings, A.S.C.E., 1977, pp. 417-430.

Mitchell, J.K. and Gardner, W.S., "In Situ Measurement of Volume Change Characteristics", Proceedings, A.S.C.E. Speciality Conference on In situ Measurement of Soil Properties, Raleigh, N.C., 1975, pp. 279-345.

Nadai, "Theory of Flow and Fracture of Solids", McGraw-Hill, New York, 1950.

Randolf, M.F., Steenfelt, J.S., and Wroth, C.P.,"The Effect of Driving Subsequent Consolidation on Behavior of Piles", Proceedings, 7th European Conference on Soil Mechanics and Foundation Engineering, Brighton, England, 1979.

Raymond, G.P. "Construction Method and Performance of an Embankment on a Deep Muskeg". Proc. 3rd Int. Peat Congress (Quebec City), August, 1968 Preprint.

Raymond, G.P. "Construction Method and Stability of Embankments on Muskeg", Proc. 21st. Canadian Soil Mechanics Conf., Winnipeg, September 1968 Preprint.

Raymond, G.P.,"Consolidation of Slightly Overconsolidated Soils", Proc. A.S.C.E., 1966, 92:SM 5:120.

Raymond, G.P. and Azzouz, M.M., "Permeability Determination for Predicting Rates of Consolidation", Proceedings of the conference organized by the British Geotechnical Society in London, Vol.1, 1970, pp. 285-293.

Rendulic, L., "Poreziffer und Poren Wasserdruck in Tonen", Bauingenieur, Vol. 17, 1963, pp. 559-564.

Robertshaw, J.E., Mecca, S.J. and Redrick, M.N., "Problem Solving", PBI-Petrocelli Books, Inc., Princeton, N.J., 1978.

Rowe, P.W. and Barden, L., "A New Consolidation Cell," Geotechnique, Vol. 16, June 1966, pp. 162-170

Roy, M. et al., "Behavior of a Sensitive Clay During Pile Driving", Proceedings, 32nd Canadian Geotechnical Conference, Quebec, Sept. 1979, pp. 4.28-4.49.

Schiffman, R.L., Gibson, R.E. "Consolidation of Nonhomogeneous Clay Layers", IV, A.S.C.E. Proceedings, 1964, pp. 1-30.

Schmertmann, J.H., "The Undisturbed Consolidation Behavior of Clay", Trans. A.S.C.E., Vol. 120, 1965, pp. 1201-1233.

Scrimgeour, J. and Rocke, G., "The Backwater Reservoir for Dundee Corporation Waterworks", J. Inst. Water Engrs., Vol. 20, July, 1966, pp. 325-357.

Sills, G.C., "Some Conditions Under Which Biot's Equation of Consolidation Reduce to Terzaghi's Equation", Geotechnique, Vol. 25, No.1, 1975, pp. 129-132.

Sharma, Y.K., "Particulate Mechanics of Granular Materials", Ph.D. Thesis, London University, 1976.

Small, J.C., Booker, J.R., and Davis, E.H., "Elasto-Plastic Consolidation of Soil", International Journal of Solids and Structures, Vol. 12, 1976, pp. 431-438.

Smith, J.O. and Rennie, A.J. "Civil Engineering Works at Fiddler's Ferry Power Station,", Paper for discussion by Inst. Civ. Eng. North Western Div., 1967.

Smith, R.E. and Wahls, H.E., "Consolidation Under Constant Rates of Strain", A.S.C.E. proceedings, 1969, pp. 519-539.

Soderberg, L.O., "Consolidation Theory Applied to Foundation Pile Time Effects", Geotechnique, Vol. 12, 1962, pp. 217-225.

Taverna, L.M., "The Initial Development of a Radiograph Facility for Geotechnical Engineering Research", S.M. Thesis, Dept. of Civil Engineering, M.I.T, Cambridge, Mass., 1979, p.157.

Taylor, D.W., "Research on Consolidation of Clays", Department of Civil Engineering, M.I.T., Serial 82, August, 1942.

Terzaghi, K., "Die Berechnung der Durchlassigheitsziffer des Tones aus dem Verlaug der Hydrodynamischen Spannungwercheinungen", Akademie der Wissenchaften in Win, Sitzungsberichte Mathematish Naturwissenschaftliche Klass, Part IIa, Vol. 132, No. 3/4, 1923, pp. 125-138.

Terzaghi, K., Theoretical Soil Mechanics, John Wiley and Sons, New York, 1943.

Terzaghi, K. and Peck, R.B., "Soil Mechanics in Engineering Practice", John Wiley and Sons, 2nd ed., New York, p. 729.

Torstenson, B.A., "The Pore Pressure Probe", Nordiske Geotekniske Mte, Oslo, Paper No. 34, 1977, pp. 34.1-34.15.

Torstenson, B.A., "Pore Pressure Sounding Instrument", Proceedings, A.S.C.E. Specialty Conference on In Situ Measurements of Soil Properties, Raleigh, N.C., Volume II, 1975, pp. 48-54.

Tschebotarioff, G.P., Discussion to Paper by D. Berdan and R.K. Bernhard: "Pilot Studies of Soil Density Measurements by Means of X-Rays", Proceedings American Society of Testing Material, Vol. 50, 1950, pp. 1338-1339.

Urzua, A., Hedberg, J., Rodriguez, J. and Marr, W.A., "Foundation Design of Offshore Structures", Research Report R78-41, No. 609, Dept of Civil Engineering, M.I.T., Cambridge, Mass., December, 1978, p.378.

Wilkinson, W.B., "Constant Head In Situ Permeability Tests in Clay Strata", Geotechnique, Vol.18, 1968, pp. 172-194.

Wilkinson, W.B. and Rocke, G., "An Assessment of In Situ and Laboratory Tests in Predicting the Pore Pressure in an Earth Dam", Proceedings, Conference on In Situ Investigations in Soils and Rocks, British Geotechnical Society, London, Paper No. 21, 1970, pp. 277-284.

Wissa, A.E.Z., Christian, J.T., Davis, E.H., and Heiberg,S., "Consolidation at Constant Rate of Strain", Journal of the Soil Mechanics and foundations Division, ASCE, Vol. 97, Oct., 1971, pp. 1393-1412.

Wissa, A.E.Z., Martin, R.T., and Garlanger, J.E., "The Piezometer Probe", Proceedings, ASCE Specialty Conference on In Situ Measurement of soil Properties, Raliegh, N.C., Vol. I, 1975, pp. 536-545.

APPENDIX A

STUDENT CENTER CONCRETE POURING
FROM CONTRACTORS RECORDS (FERMIT FILES)

Date	Quantity (yds^3)	Location
11/23/63	1437.0	*
12/11/63	1224.0	*
1/22/64	1036.5	*
2/5/64	42.0	*
2/7/64	62.0	*
2/13/64	43.0	*
2/14/64	79.0	*
2/15/64	1378.0	*
2/27/64	60.0	*
3/2/64	45.0	*
3/3/64	4.5	*
3/6/64	36.5	*
3/19/64	109.5	*
3/24/64	111.0	*
3/27/64	44.0	*
4/3/64	43.0	*
4/3/64	272.0+	*
4/10/64	225.0	*
4/14 64	404.0	*
4/16/64	9.5	*
4/28/64	179.0	*
4/29/64	25.0	*
4/30/64	15.0	*

*See Pour Location in Figures A1 thru A4 in the FERMIT files

+Light Weight Concrete (γ = 110 lb/ft^3)

Date	Quantity (yds^3)	Location
5/1/64	176.5+	*
5/5/64	54.0	*
5/8/64	37.0	*
5/13/64	86.0	*
5/25/64	376.0	*
5/25/64	46.0	*
6/4/64	11.0	*
6/5/64	143.0+	*
6/13/64	149.0+	*
6/30/64	47.5	*
7/3/64	35.0	*
7/6/64	184.5+	*
7/8/64	33.0	Col. E4,D4,B4,A3,B3 & Final Grading
7/9/64	6.5	Final Grading
7/10/64	224.0+	Slab North End Corner of Main Floor
7/14/64	19.0	Final Grading
7/17/64	201.0+	Slab on Mez. Floor 2-3x Lines North Side
7/21/64	23.0	Main Floor Columns
7/21/64	10.0	Walls on Main Floor
7/23/64	27.0+	Ground Floor, Floor Finish
7/24/64	141.0+/	1st Floor Slab
7/27/64	6.0	Columns on Ground Floor
7/27/64	12.0	Ground Floor Finish
7/28/64	201.0+/	N.W. Mez.
7/29/64	3.0	Office Floor Walls
8/3/64	31.0+	Ground Floor Finish
8/3/64	13.0	Sailors B,D,E, F-2
8/4/64	9.0	Mez. Office Col.
8/7/64	97.0+	Office Floor Slab
8/7/64	56.0	Columns

+ Lightweight Concrete (γ = 110 lb/ft^3)

+/ Lightweight and Regular Concrete

* See Figures B-1 thru B-4 in the FERMIT files

Date	Quantity (yds^3)	Location
8/11/64	151.0+	Office Floor Slab
8/11/64	8/0	Columns
8/12/64	6.0	Wall
8/13/64	22.0	Wolumns
8/13/64	122.0+	Office Floor Slab
8/14/64	11.5	Wind Wall and Sill
8/17/64	7.0	Wind Wall and Sill
8/20/64	150.0+	Office Floor Slab
8/21/64	17.0	Columns A,B,E, F-4
8/25/64	5.0	Columns
8/27/64	150.0+	Office Floor Slab
8/28/64	141.0	Office Floor Slab
9/2/64	25.0	Columns
9/4/64	121.0+	1st Floor Slab
9/9/64	18.0	Columns
9/10/64	163.0+/	Slab and 13 Columns
9/16/64	131.0+	Roof Slab
9/17/64	18.0	Sheer Wall
9/18/64	150.0	Slab
9/22/64	155.0+	Slab and 13 Sheer
9/24/64	29.0	Columns B,C,D, E-3
9/29/64	163.0	Slab and Planter Wall
9/29/64	11.0	Shear Wall
9/30/64	22.0	Roof 6th line A,B,C Columns
10/2/64	151.0	Roof Slab
10/2/64	11.0	Shear Wall
10/6/64	210.0	Office Floor Slab
10/6/64	77.0+	Slab
10/7/64	22.0	Shear Wall & Columns
10/8/64	21.0+	2 Columns and Wall
10/9/64	144.0	Roof Slab

+Lightweight Concrete (γ=110 lb/ft^3)

+/Lightweight and Regular Concrete

Date	Quantity (yds^3)	Location
10/13/64	20.0+	Planter Wall
10/15/64	32.5	Column
10/16/64	256.0	Roof Slab
10/19/64	25.0	2 Columns
10/20/64	287.0+	Office Floor Slab
10/21/64	10.0	Arch Form
10/23/64	146.0	Office Slab
10/28/64	28.0+	4 Columns and Arch
10/29/64	15.0+	Walls
10/30/64	272.0	Roof Slab
10/30/64	15.0	Columns and Walls
11/3/64	39.0+	Arch Forms and Window Walls
11/4/64	12.0+	Arch Forms and Window Walls
11/5/64	24.0+	Arch Forms and Window Walls
11/6/64	15.0+	Arch Forms and Window Walls
11/10/64	3.0+	Arch Forms and Window Walls
11/12/64	30.0+	Parapit Walls North side N.E. Corner
11/13/64	21.0+	Parapit Walls East Side
11/16/64	3.5+	Parapit Walls North Side
11/17/64	5.0+	Topping for Office Floor Slab
11/18/64	24.0+	Parapit Walls (2 East and 1 South Side)
11/19/64	21.0+	Parapit Walls (2 East and 1 South Side)
11/19/64	11.0+	Office Floor Finish Toppings
11/23/64	5.0+	Parapit Wall
11/24/64	7.0+	Parapit Wall South Side
11/25/64	31.0+	Parapit Wall South Side
11/25/64	31.0+	Window Walls
11/27/64	25.0+	Pent House Walls

+Lightweight Concrete (γ=110 lb/ft^3)

APPENDIX B

Appendix B is concerned with the piezometer readings recorded during the construction of the Student Center. The location of those piezometers is shown on Figure 7. 6 and schematic representation of this data appears in Figures 7. 25 through 7. 29 to which the reader is referred. This data was supplied by the FERMIT program and documented in the FERMIT files.

PSC - 1

DATE	READING	ELEVATION	COMMENTS
10-5-63	12'8$\frac{1}{4}$"	8.31'	Elevation Top of Tube - 21.00'
10-7-63	15'9$\frac{1}{4}$"	5.23'	"
10-8-63	17'5$\frac{1}{2}$"	3.54'	"
10-8-63	17'6$\frac{1}{2}$"	3.46'	"
10-8-63	17'8"	3.25'	"
10-9-63	18'6"	2.50'	"
10-9-63	18'7$\frac{1}{4}$"	2.40'	"
10-9-63	18'8$\frac{1}{4}$"	2.32'	"
10-9-63	18'9$\frac{1}{2}$"	2.22'	"
10-10-63	19'8"	1.35'	"
10-10-63	19'10$\frac{1}{4}$"	1.16'	"
10-10-63	20'2"	+0.87'	"
10-10-63	21'1$\frac{1}{4}$"	-0.07'	"
10-11-63	19'4$\frac{1}{2}$"	-0.030'	"
10-11-63	24'6$\frac{1}{2}$"	-3.54'	"
10-12-63	25'1$\frac{1}{2}$"	-4.12'	"
10-14-63	23'1"	-2.08'	"
10-17-63	13'3$\frac{3}{4}$"	-2.31'	Elevation Top of Tube - 11.00'
10-17-63	13'3$\frac{3}{4}$"	-2.21'	"
10-18-63	13'0"	-2.00'	"
10-18-63	12'11$\frac{1}{4}$"	-1.94'	"
10-19-63	12'6$\frac{3}{4}$"	-1.56'	"
10-21-63	11'7$\frac{1}{4}$"	-0.60'	"
10-22-63	11'7$\frac{1}{2}$"	-0.63'	"

Table B.1 Piezometer PSC-1 data (from FERMIT files)

PSC - 1

DATE	READING	ELEVATION	COMMENTS
10-22-63	11'7 1/2"	-0.63'	Elevation Top of Tube - 11.00'
10-23-63	11'7 1/2"	-0.63'	"
10-23-63	11'7"	-0.58'	"
10-24-63	11'8 3/4"	-0.73'	"
10-25-63	11'10 1/2"	-0.87	"
10-25-63	11'10 1/4"	-0.85'	"
10-26-63	12'3 1/2"	-1.29'	"
10-28-63	12'2 3/4"	-1.23'	"
10-28-63	12'1 3/4"	-1.14'	"
10-29-63	12'6 3/4"	-1.56'	"
10-30-63	13'0"	-2.00'	"
10-30-63	13'0"	-2.00'	"
10-31-63	13'2 1/4"	-2.19'	"
10-31-63	13'2 1/2"	-2.21'	"
11-1-63	13'2 1/2"	-2.21'	"
11-3-63	12'11 3/4"	-1.98'	"
11-4-63	13' 1/4"	-2.02'	"
11-4-63	13' 1/4"	-2.02'	"
11-5-63	12'11 3/4"	-1.98'	"
11-6-63	12'10"	-1.83'	"
11-6-63	12'6"	-1.50'	"
11-8-63	12'11 3/4"	-1.98'	"
11-9-63	12'5"	-1.42"	"
11-12-63	12'4 3/4	-1.39'	"

Table B.1 (cont.) Piezometer PSC-1 data (from FERMIT files)

PSC - 1

DATE	READING	ELEVATION	COMMENTS
11-13-63	12'3 3/4"	-1.31'	Elevation Top of Tube-11.00'
11-13-63	12'3 3/4"	-1.31'	"
11-14-63	12'3 3/4"	-1.31'	"
11-16-63	18'6 3/4"	-4.00'	Elevation Top of Tube - 14.50'
11-19-63	16'2"	-1.66'	"
11-21-63	16'7 1/2"	-2.08'	"
11-22-63	16'9"	-2.22'	"
11-23-63	16'6 1/2"	-2.04'	"
11-23-63	16'6"	-2.00'	"
11-23-63	17'2 1/2"	-2.71'	"
11-23-63	16'4 3/4"	-2.06'	"
11-24-63	16'2 1/2"	-1.70'	"
11-25-63	15'9"	-1.25'	"
11-26-63	15'10"	-1.33'	"
12-2-63	16'10 1/4"	-2.35'	"
12-3-63	16'9 1/4"	-2.27'	"
12-5-63	16'6"	-2.00'	"
12-7-63	16'5 1/2"	-1.95'	"
12-10-63	16'2 3/4"	-1.73'	"
12-11-63	16'3"	-1.75'	"
12-11-63	16'0 3/4"	-1.56'	"
12-11-63	15'10 3/4"	-1.39'	"
12-11-63	15'8 1/4"	-1.18'	"
12-11-63	15'6"	-1.00'	"

Table B.1 (cont.) Piezometer PSC-1 data (from FERMIT files)

PSC - 1

DATE	READING	ELEVATION	COMMENTS
12-11-63	15'2$\frac{1}{4}$"	-0.627'	Elevation Top of Tube 14.50'
12-12-63	14'2"	-0.333'	"
12-12-63	14'8$\frac{1}{4}$"	0.187'	"
12-13-63	15'2"	0.666'	"
12-14-63	15'2$\frac{1}{2}$"	0.708'	"
12-17-63		Frozen	"
1-6-64	13'3$\frac{1}{2}$"	+1.29'	"
1-8-64		+1.5'	" Approx. Values
1-9-64		1.6'	" "
1-16-64		1.7'	" "
1-18-64		1.6'	" "
1-21-64		3.4'	" "
1-22-64		+0.1'	" "
1-22-64		0.8'	" "
1-22-64		1.7'	" "
1-22-64		1.6'	" "
1-22-64		4.4'	" "
1-23-64		+2.7'	" "
1-26-64		3.0'	" "
1-28-64		2.6'	" "
1-29-64		2.7'	" "
1-30-64		2.1'	" "
1-31-64		+2.3'	" "
2-3-64		2.3'	" "

Table B-1 (cont.) Piezometer PSC-1 data (from FERMIT files)

PSC - 1

DATE	READING	ELEVATION	COMMENTS
2-5-64		2.8'	Elevation Top of Tube - 14.50' Approx. Values
2-8-64		2.1'	" "
2-12-64	12'7$\frac{1}{4}$	1.90'	"
2-13-64	12'10"	+1.67'	"
2-15-64	13'0$\frac{1}{2}$"	1.46'	"
2-15-64	12'10$\frac{1}{2}$"	1.63'	"
2-15-64	12'6"	2.00'	"
2-15-64	12'4"	2.17'	"
2-18-64	11'11$\frac{1}{4}$"	+2.56'	"
2-19-64	11'7$\frac{3}{4}$"	2.87'	"
2-20-64	11'6$\frac{1}{2}$"	2.96'	"
2-21-64	11'7"	2.92'	"
2-22-64	11'6"	3.00'	"
2-24-64	10'10$\frac{1}{4}$	3.65'	"
2-26-64	11'$\frac{1}{2}$"	3.46'	"
3-2-64	10'1"	4.42'	"
3-6-64	9'9$\frac{1}{2}$"	4.73'	"
3-10-64	8'5$\frac{1}{4}$"	6.06'	"
3-13-64	9'1$\frac{1}{2}$"	+5.37'	"
3-16-64	7'9$\frac{1}{4}$"	6.73'	"
3-20-64	8'1$\frac{3}{4}$"	6.35'	"
3-23-64	7'1$\frac{1}{2}$"	7.37'	"
3-25-64	7'8$\frac{1}{2}$"	6.71'	"
4-3-64	8'3$\frac{3}{4}$"	+6.19'	"

Table B-1 (cont.) Piezometer PSC-1 data (from FERMIT files)

PSC - 1

DATE	READING	ELEVATION	COMMENTS
4-3-64	8'3$\frac{3}{4}$"	+6.19'	Elevation Top of Tube - 14.50'
4-7-64	9'10$\frac{1}{4}$"	4.65'	"
4-10-64	9'1$\frac{1}{2}$"	5.37'	"
4-15-64	8'3$\frac{1}{4}$"	6.23'	"
4-20-64		7.49'	"
4-24-64		+7.13'	"
4-28-64		8.74'	Elevation Top of Tube - 12.11'
5-1-64		8.21'	"
5-5-64		7.53'	"
5-8-64		8.26'	"
5-12-64		+8.61'	
5-15-64		8.17'	"
5-23-64		8.63'	"
5-26-64		8.28'	"
5-29-64		7.73'	"
6-3-64		+7.98'	"
6-5-64		7.48'	"
6-16-64		9.03'	"
6-19-64		8.30	"
6-22-64		9.80'	"
6-26-64		+8.86'	"
6-30-64		8.07	"
7-8-64		8.03'	"
7-10-64		+9.19'	"

Table B-1 (cont.) Piezometer PSC-1 data (from FERMIT files)

PSC - 1

DATE	READING	ELEVATION	COMMENTS
7-20-64		+8.38'	Elevation Top of Tube - 12.11'
7-24-64		+8.40	"
8-11-64		+8.49'	"
8-14-64	3'-5"	+8.69'	"
8-18-64	2'-7"	+9.53'	"
9-1-64	0'-10$\frac{1}{2}$"	+11.23'	"
9-4-64	0'-11"	+11.19'	"
9-21-64	0'-11"	+11.19'	"
10-1-64	0'-10$\frac{1}{2}$"	+11.15'	"
1-11-65		+11.49'	Elevation Top of Tube - 11.60'
1-27-65		+11.60'	"
2-5-65		+11.60'	"
2-9-65	0.3'	+12.3'	"
2-18-65		+12.7'	"
3-4-65		+11.60'	"
3-11-65		+11.60'	"
3-18-65		+11.60'	"
3-25-65		+11.60'	"
4-1-65		12.25'	"
4-6-65		-	No reading taken
4-15-65		+11.62'	"
4-22-65		+11.92'	Since 3-31-65, elev. of the H_2O level has been found by measuring
4-29-65		+12.25'	from the finish slab which has elev. of (π + 10' - 1")
5-13		+11.60'	"

Table B-1 (cont.) Piezometer PSC-1 data (from FERMIT files)

PSC - 1

DATE	READING	ELEVATION	COMMENTS
1-23-67	-3.67	+11.33	Elevation Top of Tube - +15.00'
2-15-67	-3.52	+11.48	"
3-15-67	-2.91	+12.09	"
4-7-67	2.91	12.09	"
4-28-67	2.77	12.23	"
6-2-67	3.08	11.92	"
6-19-67	3.10	11.90	"
8-18-67	2.75	12.25	"
10-10-67	2.90	12.10	"
12-5-67	3.34	11.66	"
12-21-67	3.23	11.77	"
1-15-68	3.11	11.89	"
2-12-69	3.90	11.10	"
3-4-69	3.90	11.10	flushed "
4-5-69	2.47	12.53	checked "
6-19-69	2.91	12.09	"
8-4-69	2.55	12.45	"
10-16-69	3.24	11.76	"
12-2-69	2.65	12.35	"
6-23-70	3.03	11.97	"
9-11-70	-	-	"
10-1-70	3.10	11.90	"
10-27-70	NR	-	"
5-4-71	2.92	12.08	"

Table B-1 (cont.) Piezometer PSC-1 data (from FERMIT files)

PSC -1

DATE	READING	ELEVATION	COMMENTS
5-20-65		+11.92	Since 3-31-65, elev. of the H_2O level has been found by measuring
5-27-65		+11.54	from the finish slab which has elev of (π + 10 - 1")
7-30-64		+11.25'	"
8-17-65		+10.83'	"
9-8-65	5'-17"	+11.41'	(New stand pipe inst.) Elevation top of tube - +15.00'
9-30-65	-3:45	+11.55'	"
10-18-65	-3:64	+11.36'	"
11-2-65	-3.47	+11.53	"
11-17-65	-2.05	12.95	"
12-7-65	-3.58	11.42	"
12-29-65	-3.73	+11.27	"
1-24-66	-3.57	+11.43	"
3-7-66	-3.00	+12.00	"
3-28-66	2.91	12.09	"
4-26-66	3.35	11.65	"
5-16-66	3.31	11.69	"
6-7-66	3.47	11.53	"
9-8-66	-3.67	+11.33	"
10-4-66	-7.42	+7.58	"
11-2-66	-7.20	+7.80	"
11-29-66	-5.85	+9.15	"
12-8-66	-5.10	+9.90	"
12-27-66	-3.69	+11.31	"
1-23-67	-3.67	+11.33	"

Table B-1 (cont.) Piezometer PSC-1 data (from FERMIT files)

PSC - 1

DATE	READING	ELEVATION	COMMENTS
6-23-71	2.71	12.29	Elevation Top of Tube - +15.00
10-15-71	3.24	11.76	"
12-13-71	2.98	12.02	"
4-18-72	2.98	12.02	"
12-18-72	3.02	11.98	"
6-21-73	2.77	12.23	"
3-5-74	3.7	11.3	" Flushed and Hydraulic Fracturing

Table B-1 (cont.) Piezometer PSC-1 data (from FERMIT files)

PIEZOMETER DATA
PIEZOMETER NUMBER - PSC - 2

DATE	READING	ELEVATION	COMMENTS
9-20-63		11.87	Elevation Top of Tube - 26.50'
9-21-63		10.39	"
9-23-63		9.44	"
9-24-63	18'$\frac{1}{4}$"	8.48	"
9-24-63	18'5$\frac{3}{4}$"	8.02	"
9-24-63	18'10$\frac{3}{4}$"	7.65	"
9-25-63	19'5$\frac{1}{2}$"	7.04	"
9-25-63	19'6$\frac{1}{2}$"	6.96	"
9-25-63	15'11$\frac{1}{4}$"	6.56	Elevation Top of Tube - 22.50'
9-26-63	16'7$\frac{1}{2}$"	5.88	"
9-26-63	15'9$\frac{1}{4}$"	5.73	Elevation Top of Tube - 21.50'
9-26-63	16'0"	5.50	"
9-27-63	16'4$\frac{3}{4}$"	5.11	"
9-27-63	16'5$\frac{1}{2}$"	5.05	"
9-27-63	16'8"	4.83	"
9-30-63	16'10$\frac{1}{2}$"	4.62	"
9-30-63	16'11"	4.58	"
10-1-63	16'11$\frac{1}{2}$"	4.54	"
10-1-63	16'11$\frac{1}{4}$"	4.56	"
10-2-63	16'10$\frac{1}{2}$"	4.62	"
10-3-63	16'8$\frac{3}{4}$"	4.77	"
10-3-63	16'8$\frac{1}{2}$"	4.79	"
10-4-63	16'8"	4.83	"
10-4-63	16'7$\frac{3}{4}$"	4.85	"

Table B-2 Piezometer PSC-2 data (from FERMIT files)

PSC-2

DATE	READING	ELEVATION	COMMENTS
10-7-63	17'$\frac{1}{4}$"	4.48	Elevation Top of Tube - 21.50'
10-8-63	17'$\frac{5}{3}$"	4.02	"
10-8-63	17'6$\frac{1}{4}$"	3.98	"
10-8-63	17'6$\frac{1}{2}$"	3.96	"
10-9-63	17'9$\frac{1}{4}$"	3.75	"
10-9-63	17'10$\frac{1}{4}$"	3.67	"
10-9-63	17'10$\frac{1}{2}$"	3.65	"
10-9-63	17'11$\frac{1}{2}$"	3.57	"
10-10-63	18'6"	3.03	"
10-10-63	18'7"	2.95	"
10-10-63	18'10"	2.70	"
10-10-63	19'6$\frac{1}{2}$"	1.99	"
10-11-63	21'4"	0.20	"
10-11-63	23'1"	-1.58	"
10-17-63	20'5$\frac{1}{2}$"	-8.96	Elevation Top of Tube - 11.50' from 10/12/63 to 10/17/63 the water level
10-17-63	20'5$\frac{1}{4}$"	-8.94	was below the limit of the equipment "
10-18-63	20'3$\frac{3}{4}$"	-8.81	"
10-18-63	20'1$\frac{1}{2}$"	-8.62	"
10-19-63	20'2"	-8.67	"
10-21-63	17'11$\frac{1}{2}$"	-6.46	"
10-22-63	18'2$\frac{1}{4}$"	-6.71'	Elevation Top of Tube - 11.50'
10-23-63	18'3$\frac{1}{2}$"	-6.79'	
10-24-63	18'4$\frac{1}{2}$"	-6.87'	
10-25-63	18'5$\frac{3}{4}$"	-6.98'	

Table B-2 (cont.) Piezometer PSC-2 data (from FERMIT files)

PSC-2

DATE	READING	ELEVATION	COMMENTS
10-26-63	18'7 1/2"	-7.12'	
10-28-63	18'6"	-7.00'	
10-29-63	18'4 3/4"	-6.89'	
10-30-63	18'5 1/4"	-6.94'	
10-31-63	18'4"	-6.83'	
11-1-63	18'2 3/4"	-6.73'	
11-3-63	17'10 3/4"	-6.39'	
11-4-63	17'11 1/4"	-6.44'	
11-5-63	17'11 1/2"	-6.46'	
11-6-63	17'9 1/2"	-6.29'	
11-8-63	18'2 3/4"	-6.73'	
11-9-63	17'9 1/2"	-6.29'	
11-12-63	17'9"	-6.25'	
11-13-63	17'9"	-6.25'	
11-13-63	17'9"	-6.25'	
11-14-63	17'8 1/4"	-6.19'	
11-19-63	20'7 1/4"	-6.08'	Elevation Top of Tube 14.5'
11-21-63	20'2 1/2"	-5.70'	
11-22-63	20'2 3/4"	-5.72'	
11-23-63	19'10 1/2"	-5.38'	
11-24-63	19'8"	-5.17'	
11-25-63	19'6"	-5.00'	
11-26-63	19'5 1/4"	-4.94'	
12-2-63	19'8 1/4"	-5.19'	

Table B-2 (cont.) Piezometer PSC-2 data (from FERMIT files)

PSC-2

DATE	READING	ELEVATION	COMMENTS
12-3-63	20'2"	-5.67'	Elevation Top of Tube - 14.5'
12-5-63	19'10$\frac{1}{2}$"	-5.38'	
12-7-63	19'9"	-5.25'	
12-10-63	19'5$\frac{1}{4}$"	-4.94'	
12-11-63	18'5"	-3.92'	
12-12-63	17'8$\frac{3}{4}$"	-3.23'	
12-13-63	17'6"	-3.00'	
12-14-63	17'8"	-3.17'	
12-17-63	17'11$\frac{1}{2}$"	-3.46'	
12-21-63	17'10"	-3.33'	
1-8-64		-1.2'	Approximate Values
1-9-64		-0.9'	"
1-16-64		-0.5'	"
1-18-64		-0.5'	"
1-21-64		-0.5'	"
1-22-64		+2.5'	"
1-23-64		3.3'	"
1-26-64		4.7'	"
1-28-64		5.3'	"
1-29-64		5.1'	"
1-30-64		5.1'	"
1-31-64		6.1'	"
2-3-64		4.6'	"
2-5-64		3.6'	"

Table B-2 (cont.) Piezometer PSC-2 data (from FERMIT files)

PSC-2

DATE	READING	ELEVATION	COMMENTS
2-8-64			Elevation Top of Tube - 14.50' Approximate Values
2-12-64	12'8"	1.83'	"
2-13-64	11'6 1/4"	2.98'	
2-15-64	11' 1/2"	3.46'	
2-18-67	9'11 1/2"	4.56'	
2-19-64	9'6 1/2"	4.96'	
2-20-64	9'5 1/2"	5.04'	
2-21-64	9'3 3/4"	5.19'	
2-22-64	9'11"	5.42	
2-24-64	8'9 1/2"	5.71	
2-26-64	8'8"	5.83'	
3-2-64	9'1"	5.42	
3-6-64	9'11 1/4"	4.56	
3-10-64	9'1 3/4"	5.35	
3-13-64	8'8 3/4"	5.77'	
3-16-64	9'0"	5.50'	
3-20-64	8'4 3/4"	6.10'	
3-23-64	8'7"	5.92'	
3-25-64	8'6 1/2"	5.96'	
4-3-64	7'10 3/4"	6.62'	
4-7-64	8'2 1/2"	6.2 '	
4-10-64	8'3"	6.25'	
4-15-64	7'11 1/2"	6.54'	
4-20-64		6.98'	Readings Cannot be verified

Table B-2 (cont.) Piezometer PSC-2 data (from FERMIT files)

PSC-2

DATE	READING	ELEVATION	COMMENTS
4-24-64		7.40'	Elevation Top of Tube - 14.50' Readings cannot be verified
5-1-64		8.04'	"
5-5-64		8.08'	"
5-8-64		8.04'	"
5-12-64		7.85'	"
5-15-64		8.50'	"
5-23-64		8.02'	"
5-26-64		7.62'	"
5-29-64		8.04'	"
6-3-64		8.75'	"
6-5-64		8.87'	"
6-16-64		8.92'	"
6-19-64	Readings not	9.46'	Elevation Top of Tube - 14.50'
6-22-64	Recorded "	9.83'	
6-26-64	"	9.25'	
6-30-64	"	9.33'	
7-5-64	"	9.19'	
7-10-64	"	9.83'	
7-20-64	"	9.23'	
7-24-64	"	9.65	
8-11-64	"	10.58'	New Elevation 11.46'
8-14-64	"	10.81'	
8-18-64	"	10.79'	
9-1-64	"	11.46'	

Table B-2 (cont.) Piezometer PSC-2 data (from FERMIT files)

PSC-2

DATE	READING	ELEVATION	COMMENTS
9-21-64	Readings not	--	Flow out of Tube
10-1-64	Recorded "	--	
1-11-65	"	12.82'	New Gauges Elev = 11.67'
1-27-65	"	12.37'	
2-5-65	"	12.82'	
2-9-65	"	11.67'	
2-18-65	"	11.67	
3-4-64	"	11.67	Since 3-31-65 Elev of the water level has been found by measuring
3-11-65	"	11.67	from finish slab @ elev. 10'11"
3-18-65	"	11.67'	
3-25-65	"	11.67'	
4-1-65	"	12.25'	
4-6-65	"	11.63'	
4-15-65	"	11.56'	
4-22-65	"	11.67'	
4-29-65	"	12.00'	
5-20-65	"	11.42'	
5-27-65	"	11.33'	
4-30-65	"	11.00'	
8-]7-65	"	10.62'	
9-8-65	-1.8'	11.90'	New Stand Pipe installed Elev+15'
9-30-65	-1.81'	11.59'	
10-18-65	-2.08'	11.32'	
11-2-65	-1.78'	13.22'	

Table B-2 (cont.) Piezometer PSC-2 data (from FERMIT files)

PSC-2

DATE	READING	ELEVATION	COMMENTS
11-17-65	-2.06'	11.34'	New Stand Pipe Installed Elev. +15.00'
12-7-65	-2.35'	12.65'	
12-29-65	-2.45'	12.55'	
1-24-66	-2.42'	12.58'	Questionable
3-7-66	-2.35'	12.65'	"
3-28-66	-1.65'	13.35'	"
4-26-66	-2.27'	12.73'	"
5-16-66	-2.32	12.68'	"
6-7-66	-2.72'	12.28'	
9-8-66	-2.95'	12.05'	
10-4-66	-3.63'	11.37'	
11-2-66	-4.39'	10.61'	
11-29-66	-4.19'	10.81'	
12-8-66	-3.88'	11.12'	
12-22-66	-3.04'	11.96'	
1-23-67	-2.88'	12.17'	
2-15-67	-2.29'	12.71'	
3-15-67	-2.47'	12.53'	
4-7-67	-2.07'	12.93'	
4-28-67	-1.91'	13.09'	
6-2-67	-1.91'	13.00'	
6-19-67	-2.17'	12.83'	
8-18-67	-1.79'	13.21'	
10-10-67	-1.25'	13.75'	

Table B-2 (cont.) Piezometer PSC-2 data (from FERMIT files)

PSC-2

DATE	READING	ELEVATION	COMMENTS
12-5-67	-1.66'	13.34'	Elevation Top of Tube - 15.00'
12-21-67	-1.58'	13.42'	
1-15-68			
-1.76'	13.30'		
2-12-69	-2.00'	11.40'	
3-4-69	-2.10	11.30'	
4-5-69	-2.00	11.40'	
6-14-69	2.42	10.98	
8-4-69	2.65	10.75	*Elevation Top of Tube is 13.4'
10-16-69	2.10	11.30	Not 15.0' since unknown date!
12-2-69	2.65	10-75	

Table B-2 (cont.) Piezometer PSC-2 data (from FERMIT files)

PIEZOMETER DATA

PIEZOMETER NUMBER: PSC - 3

DATE	READING	ELEVATION	COMMENTS
9/21/63	?	10.71'	Elevation Top of Tube - 26.00'
9/23/63	?	9.94'	
9/24/63	18'2 3/4"	7.77'	
9/25/63	14'4"	6.67'	Elevation Top of Tube - 21.00'
9/26/63	14'11"	5.58'	Elevation Top of Tube - 20.50'
9/27/63	15'9 1/2"	4.71'	
9/28/63	16'11 1/4"	3.56'	*Not recorded in office copy?
9/30/63	16'7"	4.08'	
10/1/63	16'6 1/2"	3.96'	
10/2/63	16'7"	3.92'	
10/3/63	16'6 3/4"	3.94'	
10/4/63	16'7"	3.92'	
10/5/63	16'6 1/2"	3.96'	
10/7/63	17'3 1/2"	3.88'	
10/8/63	17'10"	2.72'	
10/9/63	18'4"	2.23'	
10/10/63	20'3 1/4"	0.39'	
10/11/63	23'6"	-3.00'	
10/17/63	21'7 1/4"	-9.10'	Elevation Top of Tube - 12.50'
10/18/63	21'7"	-9.08'	
10/19/63	21'7 3/4"	-9.14'	
10/21/63	18'8 3/4"	-6.23	
10/22/63	19'2 3/4"	-6.73'	
10/23/63	19'5 1/2"	-6.96'	

Table B-3 Piezometer PSC-3 data (from FERMIT files)

PSC - 3

DATE	READING	ELEVATION	COMMENTS
10/24/63	19'8$\frac{3}{4}$"	-7.23'	Elevation Top of Tube - 12.50'
10/25/63	20'0"	-7.50'	
10/26/63	20'3$\frac{1}{2}$"	-7.79'	
10/28/63	20'4$\frac{3}{4}$"	-7.89'	
10/29/63	20'4"	-7.83'	
10/30/63	20'4$\frac{3}{4}$"	-7.89'	
10/31/63	20'5$\frac{1}{2}$"	-7.96'	
11/1/63	20'2$\frac{3}{4}$"	-7.73'	
11/3/63	19'11$\frac{1}{2}$"	-7.46'	
11/4/63	20'0"	-7.50'	
11/5/63	20'0"	-7.50'	
11/6/63	19'9$\frac{1}{2}$"	-7.29'	
11/8/63	20"1$\frac{1}{4}$"	-7.60'	
11/9/63	19'8$\frac{1}{2}$"	-7.21'	
11/12/63	19'7"	-7.08'	
11/13/63	19'7$\frac{3}{4}$"	-7.14'	
11/14/63	19'6$\frac{1}{4}$	-7.02'	
11/16/63	22'7"	-8.00'	Elevation Top of Tube - 14.50'
11/19/63	21'6$\frac{1}{2}$"	-7.02'	
11/21/63	21'2$\frac{3}{4}$"	-6.72'	
11/22/63	21'1$\frac{3}{4}$"	-6.64'	
11/23/63	20'9"	-6.25'	
11/24/63	20'5"	-5.92'	
11/25/63	20'3"	-5.75'	

Table B-3 (cont.) Piezometer PSC-3 data (from FERMIT files)

PSC - 3

DATE	READING	ELEVATION	COMMENTS
11/26/63	20'2 1/2"	-5.73'	Elevation Top of Tube - 14.50'
12/2/63	20'3 3/4"	-5.81'	
12/3/63	20'5 1/2"	-5.96'	
12/5/63	20'2 3/4"	-5.85	
12/7/63	20' 3/4"	-5.58'	
12/10/63	19'9"	-5.25'	
12/11/63	18'5 1/4"	-3.94'	
12/12/63	17'11 1/2"	-3.46'	
12/13/63	17'11"	-3.42'	
12/14/63	18'0 1/4"	-3.52'	
12/17/63	18'0 1/4"	-3.52'	
12/21/63	18'0"	-3.50'	
1/9/64	No readings	-1.7'	Approximate Values
1/21/64	"	-1.7'	"
1/22/64	"	2.4'	"
1/23/64	"	2.8'	"
1/26/64	"	3.9'	"
1/28/64	"	4.2'	"
1/29/64	"	4.4	Elevation Top of Tube - 14.50'
1/30/64	"	4.4	"
1/31/64	"	4.8'	"
2/3/64	"	4.7'	"
2/5/64	"	4.1'	"
2/8/64	"	?	"

Table B-3 (cont.) Piezometer PSC-3 data (from FERMIT files)

PSC -3

DATE	READING	ELEVATION	COMMENTS
2/12/64	10'9"	3.75'	
2/13/64	10'6 1/2"	3.96'	
2/15/64	9'9"	4.75'	
2/18/64	8"3 1/2"	6.23'	
2/19/64	7'11"	6.58'	
2/20/64	7'9"	6.75'	
2/21/64	7'7 1/2"	6.87'	
2/22/64	7'5"	7.08'	
2/24/64	7'3"	7.25'	
2/26/64	7'2 3/4"	7.27'	
3/2/64	7'4 1/2"	7.13'	
3/6/64	8'2 1/4"	6.29'	
3/10/64	7'9 1/2"	6.70'	
3/13/64	7'5 1/2"	7.04'	
3/16/64	7'9 1/2"	6.71'	
3/20/64	7'5"	7.08'	Elevation Top of Tube - 14.50'
3/23/64	7'8 1/4"	6.81'	
3/25/64	7'9 1/4"	6.73'	
4/3/64	7'3 5/4"	7.19'	
4/7/64	7'5 1/4"	7.06'	
4/10/64	7'3"	7.25'	
4/15/64	6'11 1/2"	7.54'	
4/20/64	No readings	7.90'	
4/24/64	"	8.27'	

Table B-3 (cont.) Piezometer PSC-3 data (from FERMIT files)

PSC - 3

DATE	READING	ELEVATION	COMMENTS
4/28/64	No readings	8.29'	
5/1/64	"	8.88'	
5/5/64	"	8.75'	
5/8/64	"	8.60'	
5/12/64	"	8.42'	
5/15/64	"	9.04'	
5/13/64	"	8.67'	
5/26/64	"	8.37'	
5/29/64	"	8.75'	
6/3/64	"	9.27'	
6/5/64	"	9.44'	
6/16/64	"	10.30'	
6/19/64	"	9.80'	Elevation Top of Tube - 14.50'
6/22/64	"	9.58'	
6/26/64	"	9.75	
6/30/64	"	9.71'	
7/8/64	"	9.77'	
7/10/64	"	10.27'	
7/20/64	"	10.00'	
7/24/64	"	10.40'	
8/11/64	"	11.38'	
8/14/64	"	11.52	
8/18/64	"	11.40'	
9/1/64	"	11.48'	

Table B-3 (cont.) Piezometer PSC-3 data (from FERMIT files)

PSC - 3

DATE	READING	ELEVATION	COMMENTS
9/4/64	No Readings	11.67'	Elevation Top of Tube - 14.50'
9/21/64	"	12.02'	
10/1/64	"	11.00'	Questionable
1/11/64	"	14.17'	Elev of Gage - (11.87')
1/27/65	"	14.17'	
2/5/65	"	14.00'	
2/9/65	"	11.87'	
2/18/65	"	11.87'	
3/4/65	"	11.87'	
3/11/65	"	11.87'	
3/18/65	"	11.87'	Elev. of Gage - 11.87'
3/25/65	"	11.87'	
4/1/65	"	12.14'	Since 3/31/65 STAND PIPE has been
4/6/65	"	11.66'	installed, Elev., measured from
4/15/65	"	11.50'	marks on the Stand Pipes.
4/22/65	"	11.81'	
4/29/65	"	12.21'	
5/13/65	"	11.42'	
5/20/65	"	11.67'	
5/27/65	"	11.42'	
7/30/65	"	11.42'	
8/17/65	"	11.14'	
9/8/65	-2.75	12.21'	New Stand Pipe inst. Elev. =15.00'
9/30/65	-2.64'	11.86'	

Table B-3 (cont.) Piezometer PSC-3 data (from FERMIT files)

PSC - 3

DATE	READING	ELEVATION	COMMENTS
10/18/65	-2.95'	11.55'	
11/2/65	-2.59'	12.41'	
11/17/65	-2.84'	12.16'	
12/7/65	-3.10'	11.90'	
12/29/65	-3.35'	11.65'	
1/24/65	-3.20'	11.80'	
3/7/66	-3.40'	11.60'	
3/28/66	-2.70'	12.30'	Elevation of new stand pipe - 15.00'
4/26/66	-3.21'	11.79'	
5/16/66	-3.31'	11.69'	
6/7/66	-3.65'	11.35'	
9/8/66	-3.66'	11.34'	
10/4/66	-3.98'	11.02'	
11/2/66	-4.72'	10.28'	
11/29/66	-4.88'	10.12'	
12/8/66	-4.61'	10.39'	
12/27/66	-4.42'	10.58'	
1/23/67	-4.54'	10.46'	
2/15/67	-3.96'	11.04'	
3/15/67	-4.04'	10.96'	
4/7/67	3.78'	11.22'	
4/28/67	3.71'	11.29'	
6/2/67	3.62	11.38'	
6/19/67	3.61	11.39'	

Table B-3 (cont.) Piezometer PSC-3 data (from FERMIT files)

PSC - 3

DATE	READING	ELEVATION	COMMENTS
8/18/67	3.33'	11.67'	
10/10/67	3.92'	11.08'	
12/5/67	2.78'	12.22'	
12/21/67	3.09'	11.91'	
1/15/68	3.00'	12.00'	Elevation of top of tube is
2/12/69	4.50'	10.50'	14.5 and not 15.0 since unknown
3/4/69	4.50'	10.50'	date!
4/5/69	5.10'	9.90'	
6/19/69	5.31'	9.69'	
8/4/69	5.35'	9.65'	

Table B-3 (cont.) Piezometer PSC-3 data (from FERMIT files)

PIEZOMETER DATA

PIEZOMETER NUMBER: PSC - 4

DATE	READING	ELEVATION	COMMENTS
9/21/63	?	9.58'	Elevation Top of Tube - 25.92'
9/23/63	?	9.29'	
9/24/63	18'11 1/4"	6.99'	
9/25/63	14'10 1/4"	6.07'	Elevation Top of Tube - 20.92'
9/26/63	15'10"	5.09'	
9/27/63	16'7 1/4"	4.32'	
9/30/63	16'10 1/4"	4.07'	
10/1/63	16'10 3/4"	4.03'	
10/2/63	16'10 1/4"	4.07'	
10/3/63	16'9"	4.17'	
10/4/63	16'8 1/2"	4.13'	
10/7/63	17'3 1/2"	3.55'	
10/8/63	17'10"	3.01'	
10/9/63	18'4 1/2"	2.48'	
10/10/63	20'6"	0.36'	Elevation Top of Tube - 11.92'
10/11/63	21'7"	-2.83'	From 10/12/63 to 10/17/63 the
10/17/63	18'6 3/4"	-6.64'	level was below the limit of
10/18/63	18'4"	-6.41'	equipment.
10/19/63	18'3 1/4"	-6.35'	
10/21/63	16'10 1/2"	-4.92'	
10/22/63	17'1 3/4"	-5.23'	
10/22/63	17'1 3/4"	-5.23	Elevation Top of Tube - 11.92'
10/23/63	17'0"	-5.08	
6/24/63	17' 1/4"	-5.10'	

Table B-4 Piezometer PSC-4 data (from FERMIT files)

PSC - 4

DATE	READING	ELEVATION	COMMENTS
10/25/63	16'11$\frac{1}{2}$"	-5.04	
10/26/63	17'1"	-5.16'	
10/28/63	16'8$\frac{1}{2}$"	-4.79'	
10/29/63	16'8$\frac{1}{2}$"	-4.79'	
10/30/63	16'6$\frac{1}{2}$"	-4.62'	
10/31/63	16'5"	-4.50'	
11/1/63	16'4"	-4.41'	
11/3/63	15'10$\frac{1}{2}$"	-3.95'	
11/4/63	15'10$\frac{1}{4}$"	-3.93'	
11/5/63	15'9$\frac{1}{2}$"	-3.87'	
11/6/63	15'6"	-3.58'	
11/8/63	15'9$\frac{1}{2}$"	-3.87'	
11/9/63	15'4$\frac{1}{4}$"	-3.43'	
11/12/63	15'1$\frac{1}{4}$"	-3.08'	
11/13/63	15'1$\frac{3}{4}$"	-3.22'	
11/14/63	?	-	Elevation Top of Table - 14.5',
11/16/63	21'3"	-6.75	Extension added
11/19/63	18'8$\frac{1}{2}$"	-4.20	
11/21/63	18'3$\frac{1}{4}$"	-3.76'	
11/22/63	18'2"	-3.6'	
11/23/63	17'7$\frac{1}{2}$"	-3.13'	
11/24/63	17'5$\frac{1}{2}$"	-2.96'	
11/25/63	17'3"	-2.75'	
11/26/63	17'3"	-2.75'	

Table B-4 (cont.) Piezometer PSC-4 data (from FERMIT files)

PSC - 4

DATE	READING	ELEVATION	COMMENTS
12/2/63	17'2 3/4"	-2.72'	
12/3/63	17'3 3/4"	-2.81'	
12/5/63	17' 1/2"	-2.54'	
12/7/63	16'10 1/4"	-2.35'	
12/10/62	16'5 1/2"	-1.96'	
12/11/63	14'11 1/2"	-0.46'	Elev. top of tube 14.50'
12/12/63	14'6 3/4"	-0.06'	
12/13/63	14'5 3/4"	+0.02'	
12/14/63	14'6 1/2"	-0.04	
12/17/63	14'6"	0.00	
12/21/63	-		FROZEN!
1/6/64	13'7 3/4"	0.85'	
1/21/64		1.80'	
1/22/64		5.00'	Approximate
1/23/64		4.9	Values
1/26/64		+6.0'	Elevation Top of Tube - 14.50'
1/28/64		+7.2'	
1/29/64		6.5'	
1/30/64		6.3'	Approximate Values
1/31/64		7.0'	
2/13/64		6.5'	
2/5/6		6.3'	
2/8/64		-	
2/12/64	8.7"	5.92'	

Table B-4 (cont.) Piezometer PSC-4 data (from FERMIT files)

PSC - 4

DATE	READING	ELEVATION	COMMENTS
2/13/64	8'3 3/4"	6.19'	
2/15/64	7'3"	7.25'	
2/18/64	5'9"	8.75'	
2/19/64	5'3 3/4"	9.19'	
2/20/64	5'2 1/2"	9.29'	
2/21/64	5'1"	9.42'	
2/22/64	4'10 3/4"	9.60'	
2/24/64	4'9 3/4"	9.69'	
2/26/64	4'10 1/4"	9.64'	
3/2/64	5' 3/4"	9.44'	
3/6/64	6' 1/4"	8.48'	
3/10/64	5'7"	8.92'	
3/13/64	5'2 3/4"	9.27'	Elevation Top of Tube - 14.50'
3/16/64	5'7 3/4"	8.85	
3/20/64	5'5"	9.08'	
3/23/64	5'7 1/2"	8.87'	
3/25/64	5'9"	8.75'	
4/3/64	5'5 3/4"	9.02'	
4/7/64	5'7 3/4"	8.85'	
4/10/64	5'5 1/4"	9.06'	
4/15/64	5'2 1/2"	9.29'	
4/20/64	No reading	9.54'	
4/24/	"	9.87'	
4/28/64	"	9.79'	

Table B-4 (cont.) Piezometer PSC-4 data (from FERMIT files)

PSC-4

DATE	READING	ELEVATION	COMMENTS
5/1/64	No readings	10.33'	
5/5/64	"	9.8'	
5/8/64	"	8.67'	
5/12/64	"	10.98'	
5/15/64	"	8.67'	
5/23/64	"	7.52'	
5/26/64	"	7.52'	
5/29/64	"	7.52'	
6/3/64	"	9.83'	
6/5/64	"	10.20'	Elevation Top of Tube - 14.50'
6/16/64	"	9.83'	
6/19/64	"	10.20'	
6/22/64	"	10.06'	
6/26/64	"	10.20'	
6/30/64	"	10.20'	
7/8/64	"	10.52'	
7/10/64	"	11.09'	
7/20/64	"	10.61'	
7/24/64	"	11.11'	
8/11/64	"	11.55'	
8/14/64	"	11.63'	
8/18/64	"	11.71'	
9/1/64	"	11.57'	
9/4/64	"	11.69'	

Table B-4 (cont.) Piezometer PSC-4 data (from FERMIT files)

PSC - 4

DATE	READING	ELEVATION	COMMENTS
10/1/64	No readings	11.48'	
1/11/65	"	13.31'	
1/27/65	"	13.0'	
2/5/65	"	13.20	
2/9/65	"	12.3'	
2/18/65	"	11.6'	
3/4/65	"	11.6'	
3/11/65	"	11.6'	
3/18/65	"	11.6'	
3/25/65	"	11.6'	Since 3-31-65 STAND PIPES were
4/1/65	"	11.58'	installed and elevations are
4/6/65	"	11.66'	found by measuring from A mark
4/15/65	"	11.42'	with known elevations on stand
4/22/65	"	?	pipe
4/29/65	"	?	
5/13/65	"	?	
5/20/65	"	11.52'	
5/27/65	"	11.37'	
7/30/65	"	11.59'	
8/17/65	"	11.27'	
9/8/65	-2.3"	12.18'	New stand pide installed
9/30/65	-2.10'		Elevation 14.10'
10/18/65	-2.35'		
11/2/65	-2.03'		

Table B-4 (cont.) Piezometer PSC-4 data (from FERMIT files)

PSC - 4

DATE	READING	ELEVATION	COMMENTS
11/17/65	-2.32'		
12/7/65	-2.45'		
12/29/65	-2.50'		
1/24/66	-2.35'	11.75'	Elevation Top of Tube - 14.10'
3/7/66	-2.69'	11.41'	
3/28/66	-2.12'	11.98'	
4/26/66	-2.44'	11.66'	
5/16/66	-2.57'	11.53'	
6/7/66	-2.93'	11.17'	
9/8/66	-3.43'	10.67'	
10/4/66	-3.62'	10.98'	
11/2/66	-3.97'	10.63'	
11/29/66	-4.16'	9.96'	
12/8/66	-4.13'	9.97'	
12/27/66	-4.00'	10.10'	
1/23/67	-4.12'	9.98'	
2/15/67	-3.93'	10.17'	
3/15/67	-3.77'	10.33'	
4/7/67	-3.67'	10.43'	
4/28/67	-3.67'	10.43'	
6/2/67	-3.48'	10.62'	
6/19/67	-3.37'	10.73'	
8/18/67	-2.82'	11.28'	
10/10/69	-2.58'	11.52'	

Table B-4 (cont.) Piezometer PSC-4 data (from FERMIT files)

PSC - 4

DATE	READING	ELEVATION	COMMENTS
12/5/67	-2.44'	11.66'	
12/21/67	-2.65'	11.45'	
1/15/68			INACCESSIBLE
2/12/69	-5.10'	9.00'	
3/4/69	-5.50'	8.60'	flushed
4/5/69	-6.20'	7.90'	checked
6/19/69	-6.95'	7.15'	checked
8/4/69	-7.21	6.89'	

Table B-4 (cont.) Piezometer PSC-4 data (from FERMIT files)

APPENDIX C

This appendix includes data from oedometer tests performed by Ladd and Luscher (1965) carried out on "undisturbed" samples of Boston Blue Clay and the top most organic soil. The tests were executed in accordance with procedures and sample specification already stated in Chapter 8 to which the reader is referred to. Figure C.1 through C.5 represent compression curves on Boston Blue Clay and Figs. C.6 through C.9 represent compression curves on the organic soil.

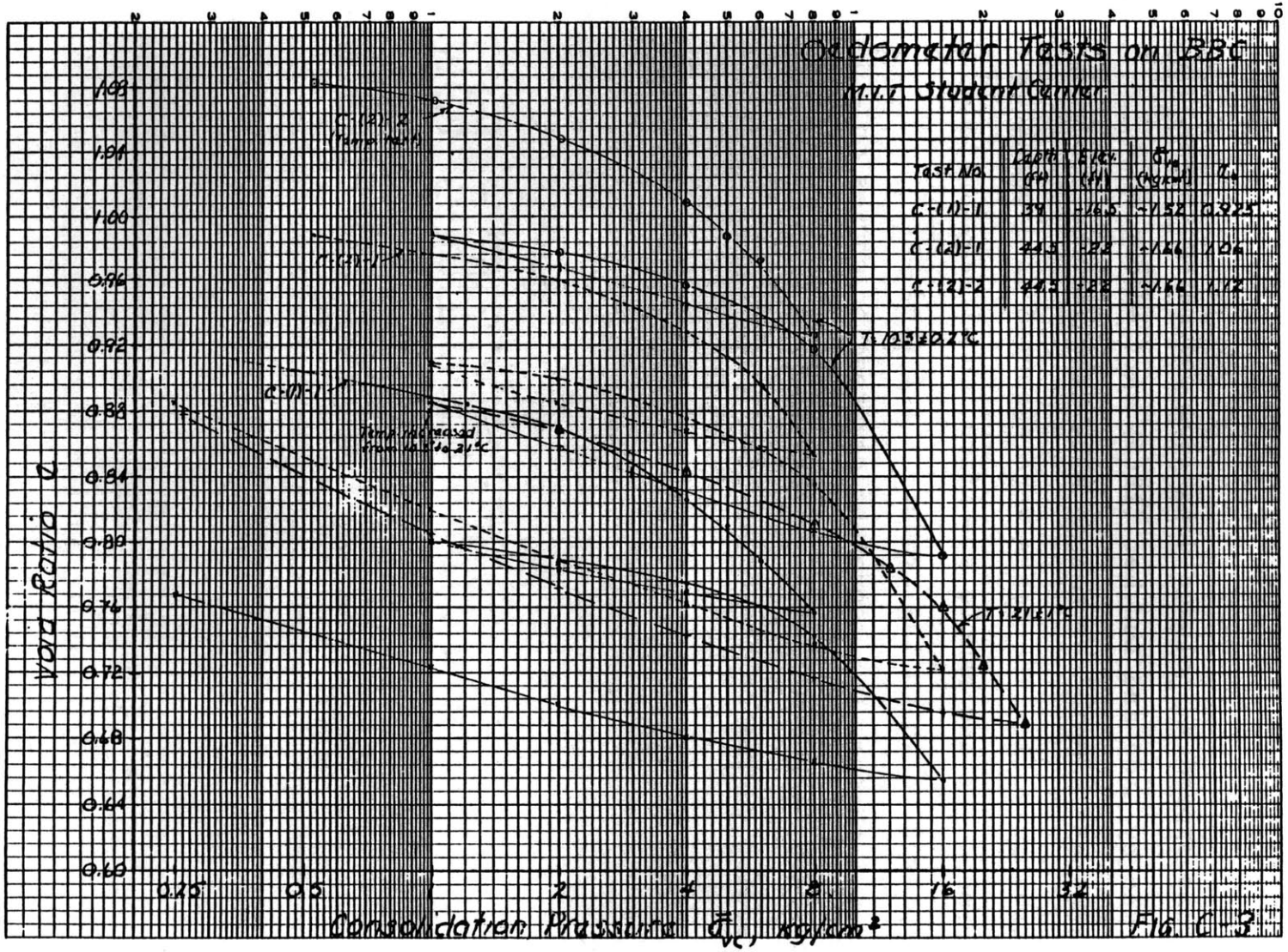

Figure C.1 Compression curves for samples C-(1)-1, C-(2)-1 and C-(2)-2 (from Ladd and Luscher, 1965)

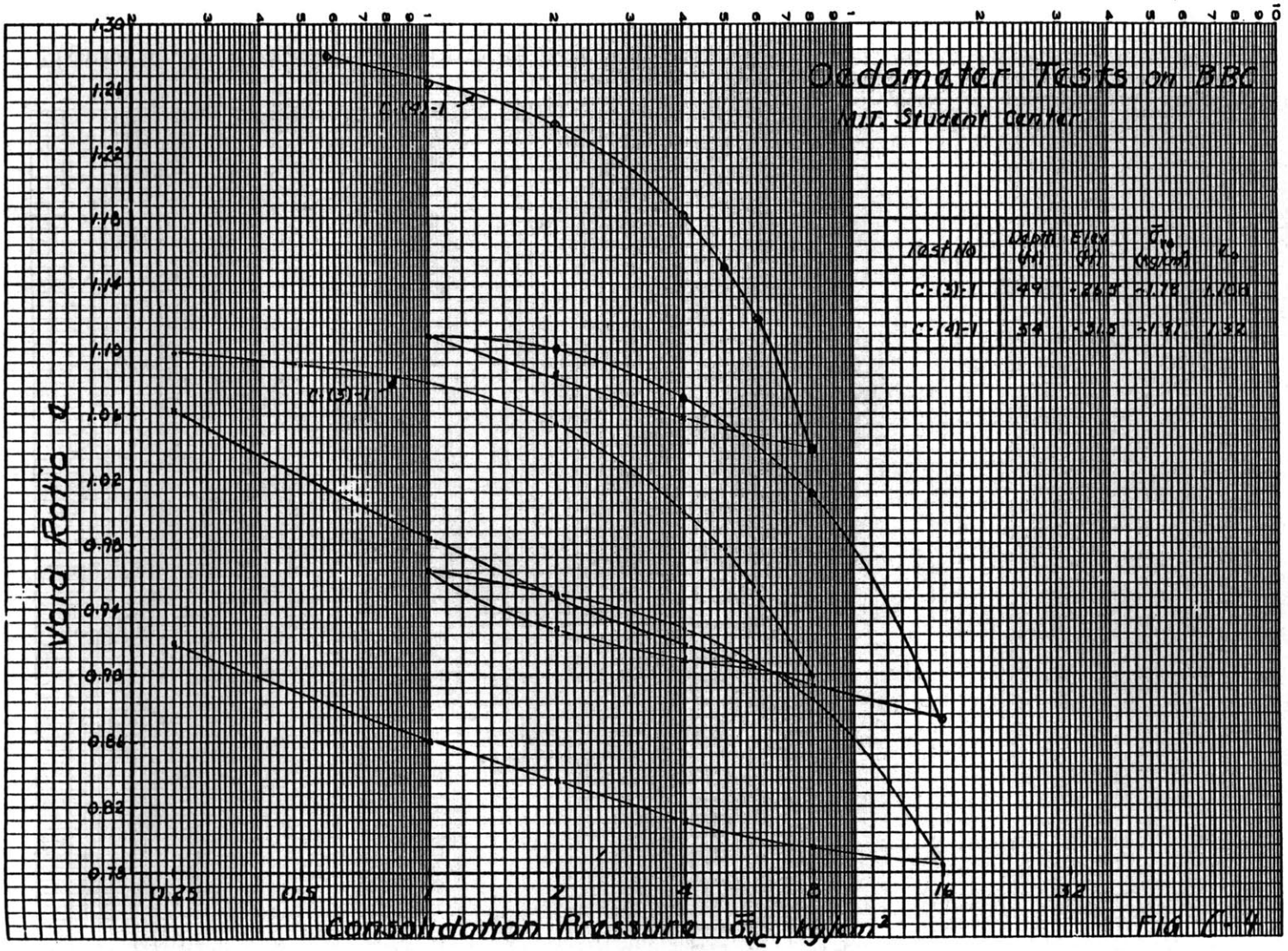

Figure C.2 Compression curves for samples C-(3)-1 and C-(4)-1 (from Ladd and Luscher, 1965)

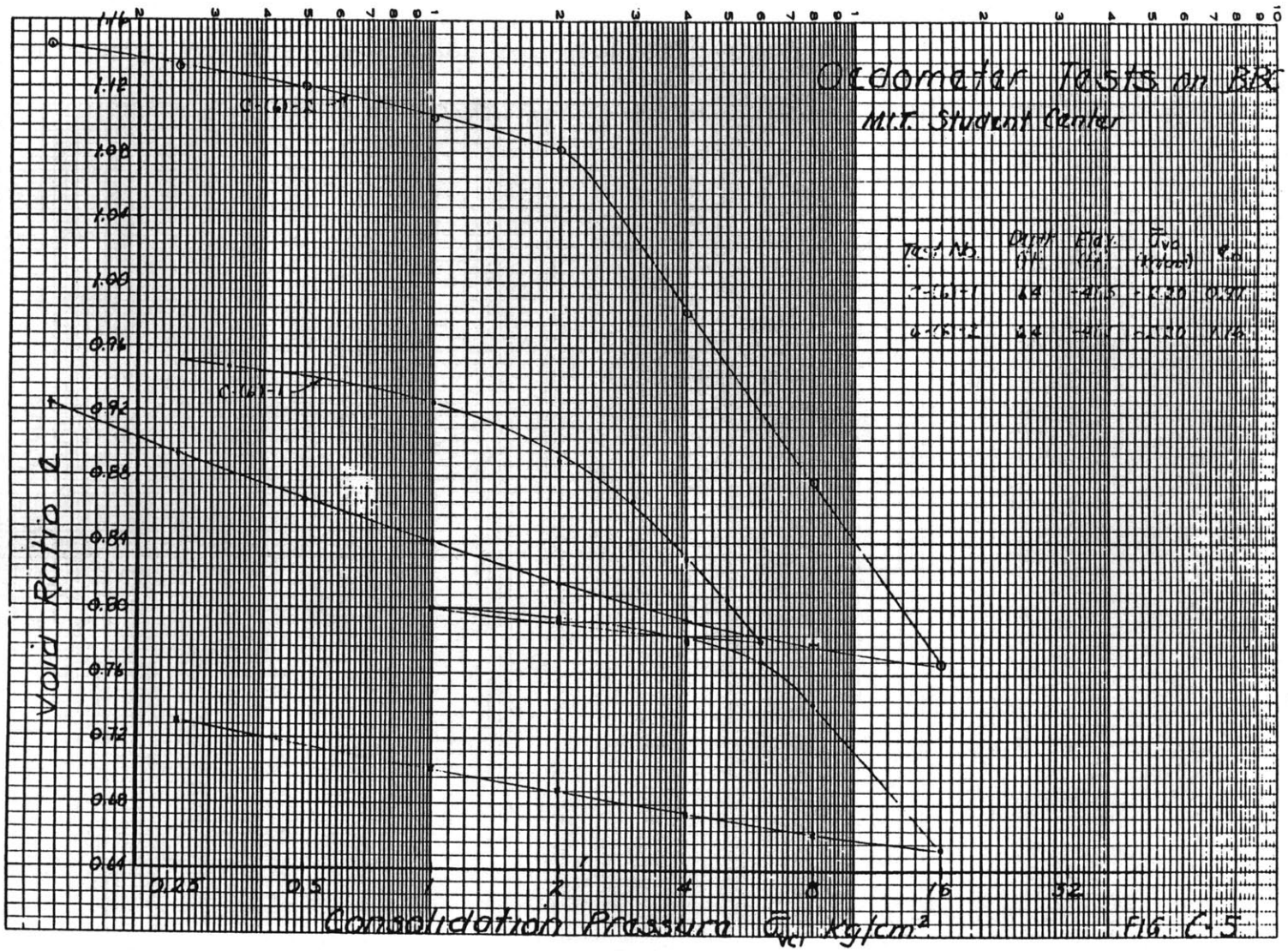

Figure C.3 Compression curves for samples C-(6)-1 and C-(6)-2 (from Ladd and Luscher, 1965)

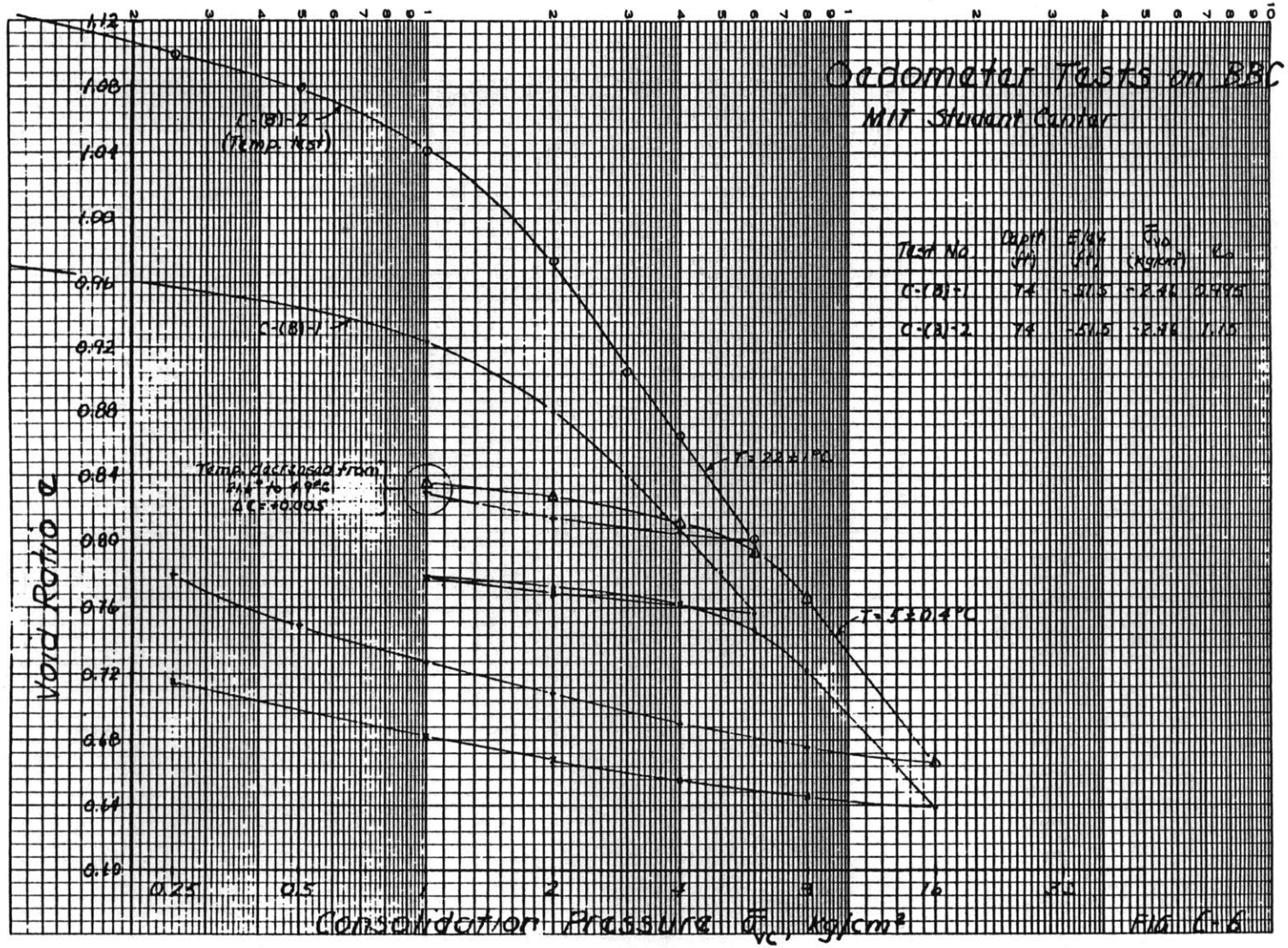

Figure C.4 Compression curves for samples C-(8)-1 and C-(8)-2 (from Ladd and Luscher, 1965)

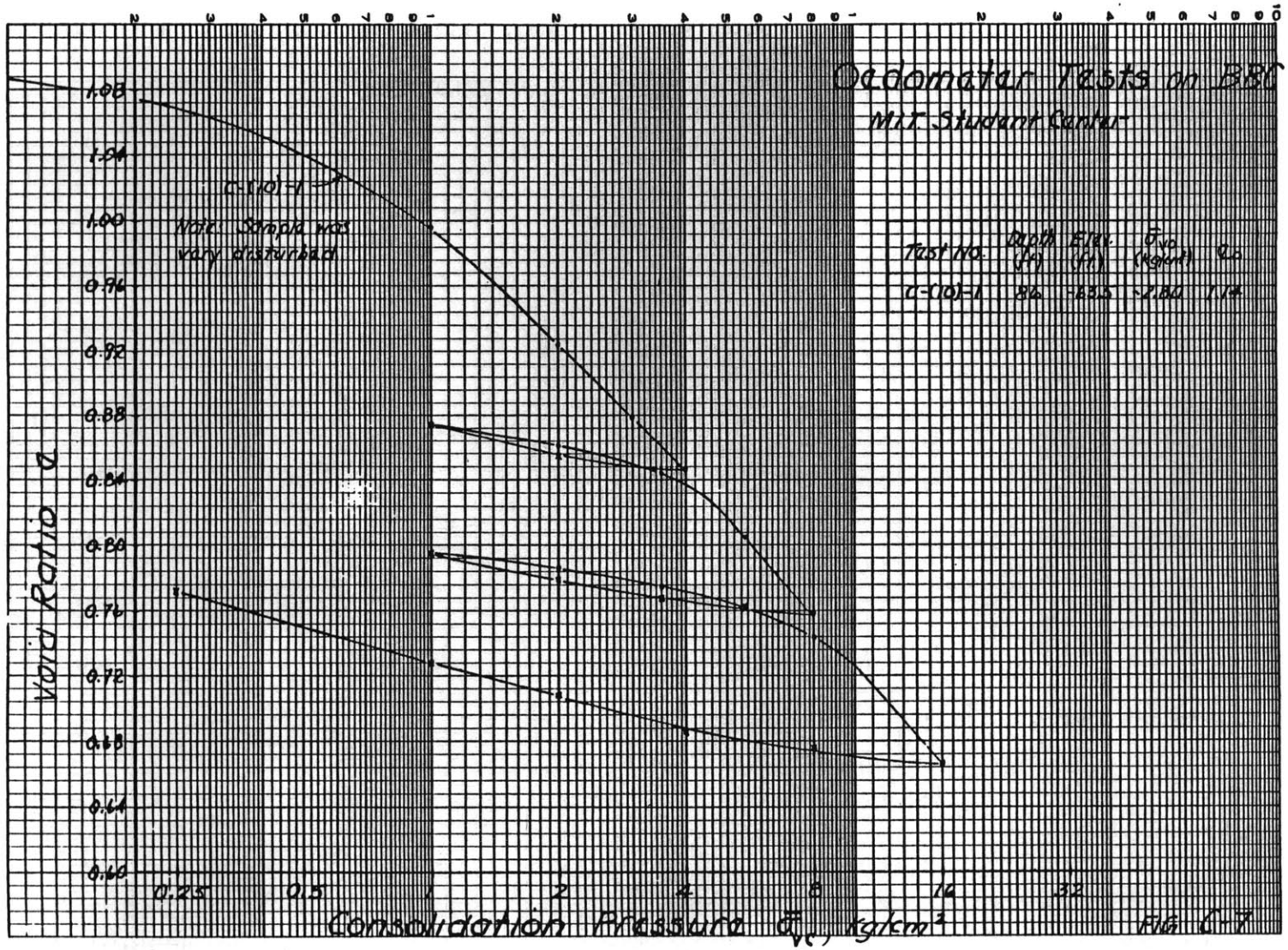

Figure C.5 Compression curve for sample C-(10)-1 (from Ladd and Luscher)

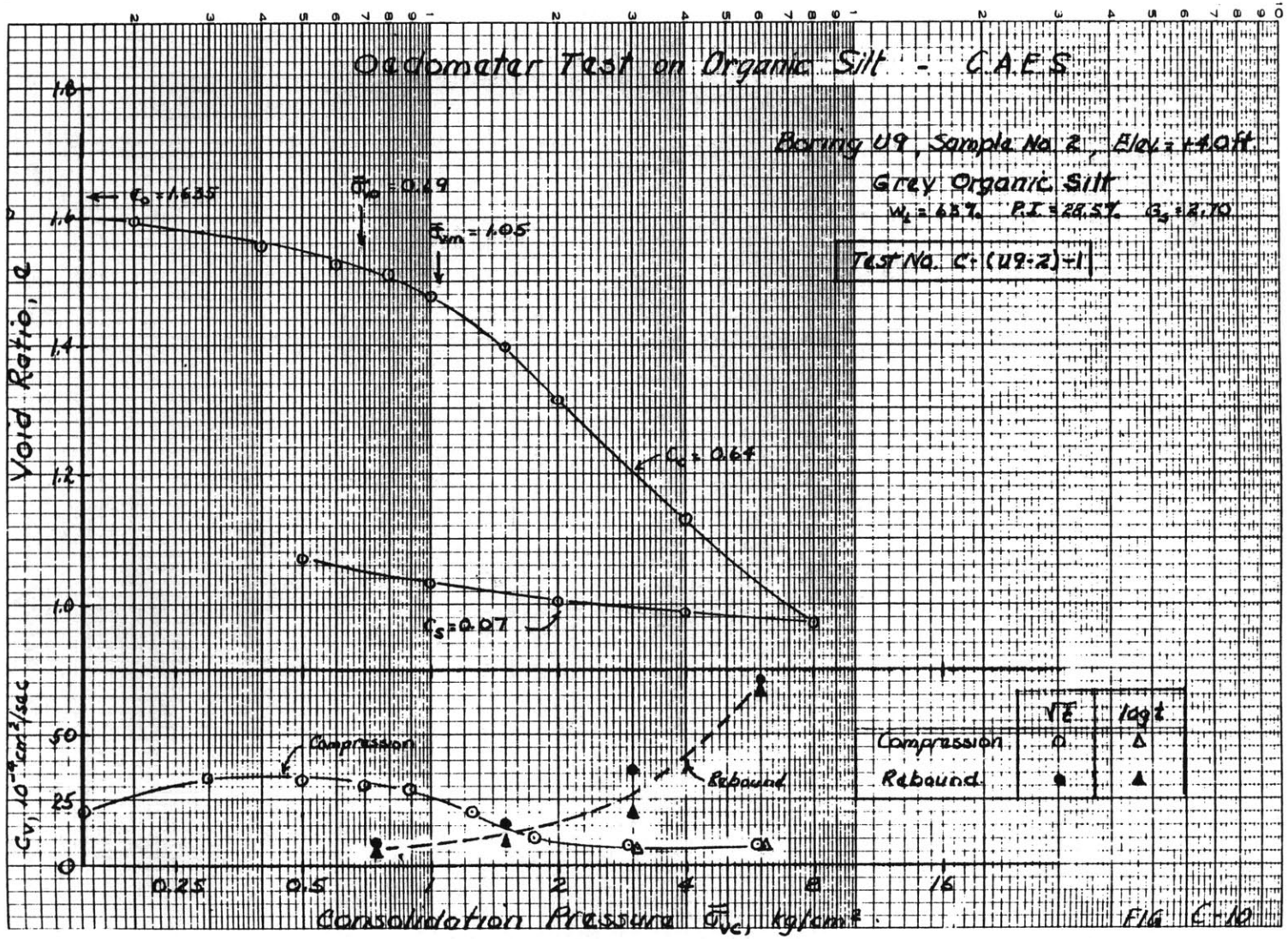

Figure C.6 Compression curve for sample C-(U9-2)-1
(from Ladd and Luscher, 1965)

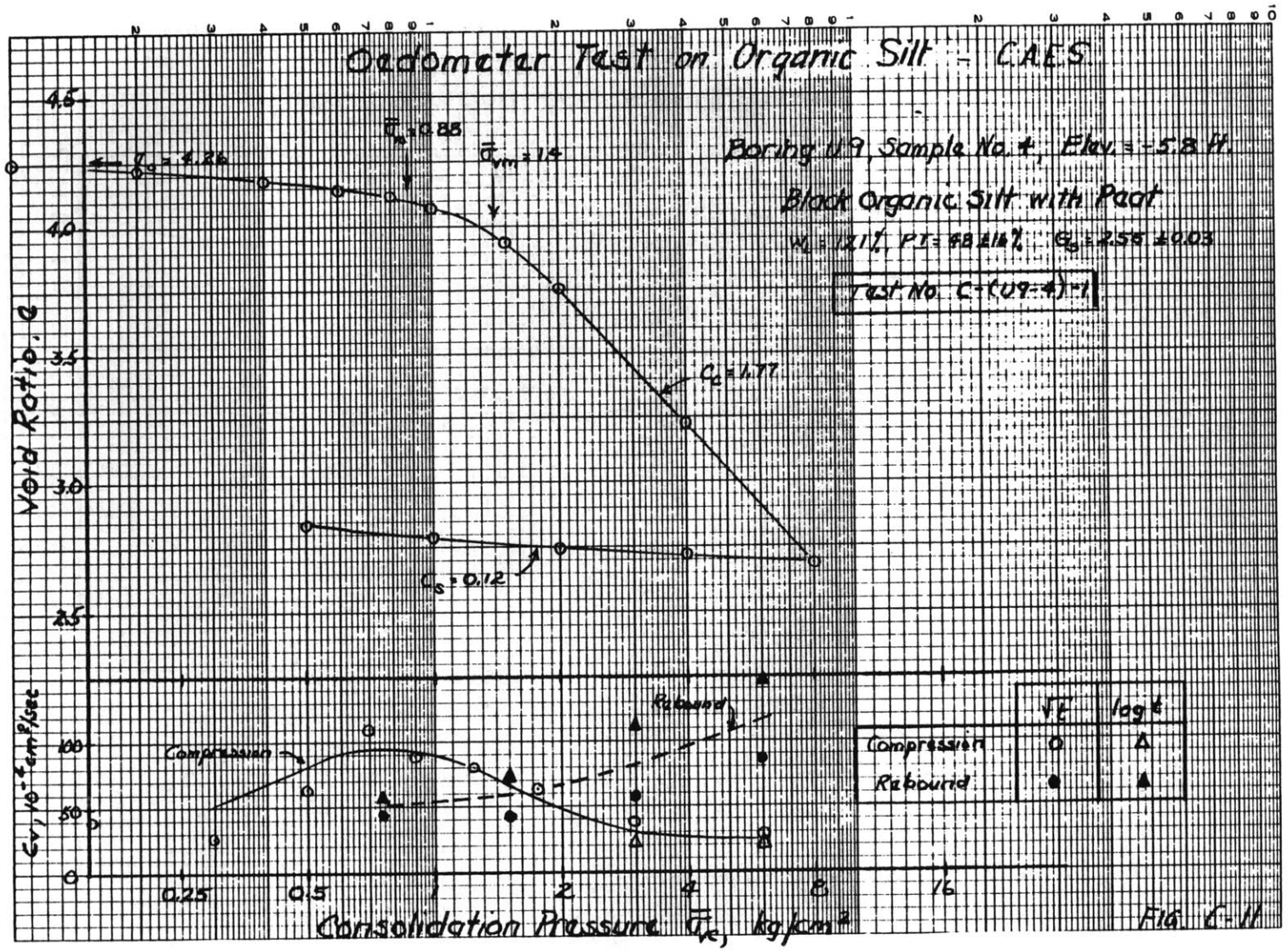

Figure C.7 Compression curve for sample C-(U9-4)-1
(from Ladd and Luscher, 1965)

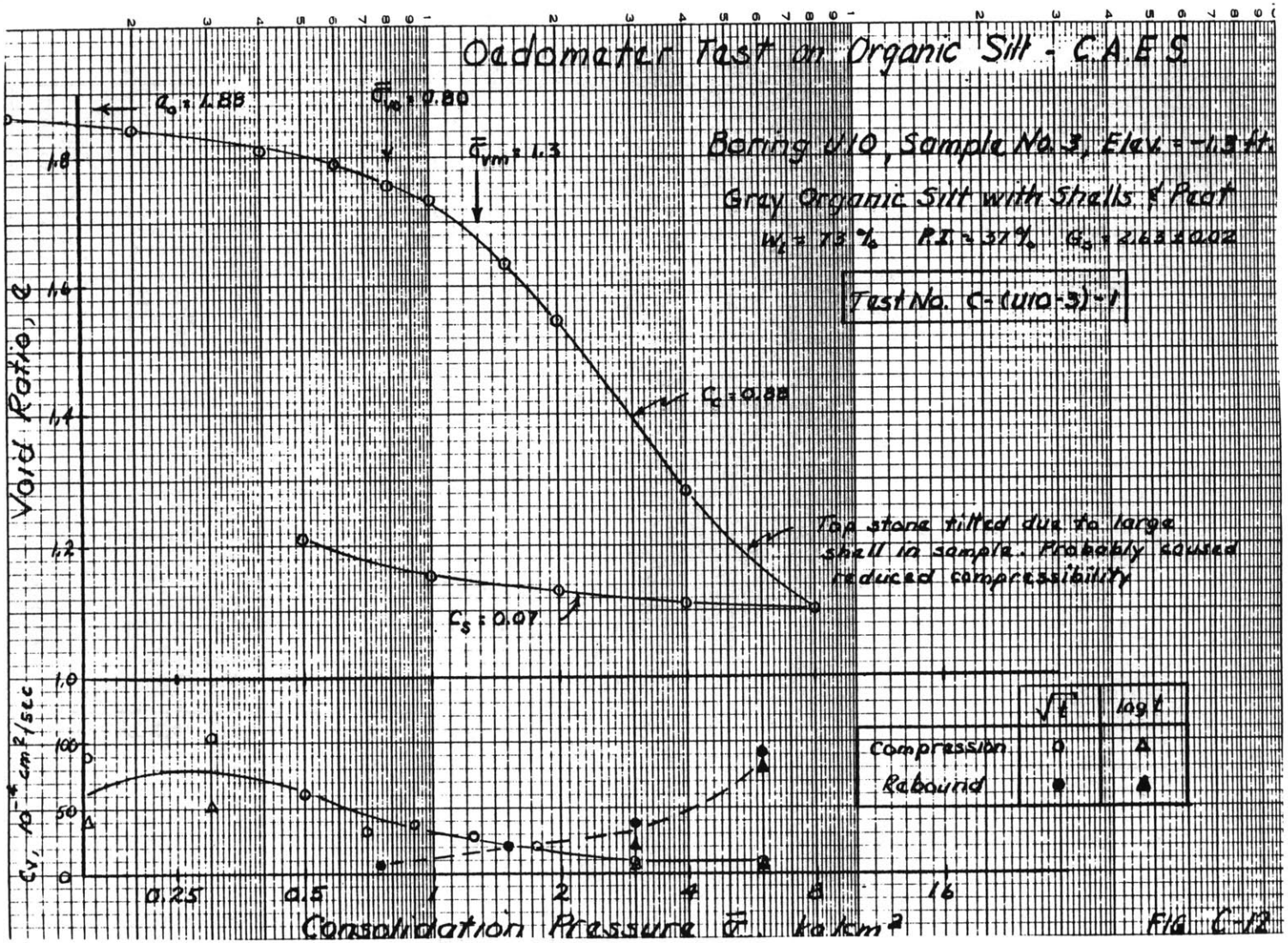

Figure C.8 Compression curve for sample C-(U10-3)-1
(from Ladd and Luscher, 1965)

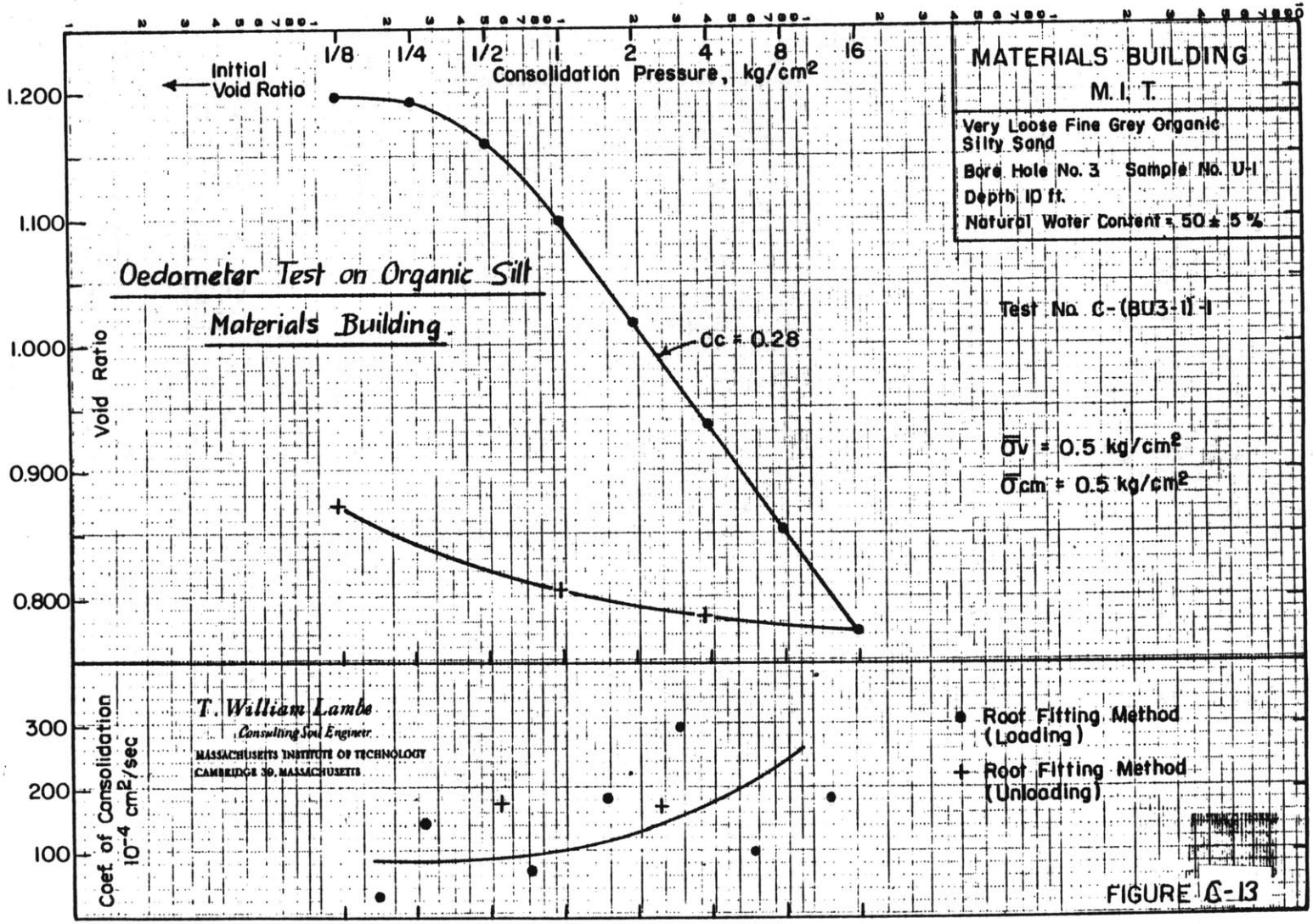

Figure C.9 Compression curve for sample C-(BU3-1)-1
(from Ladd and Luscher, 1965)

APPENDIX D

Appendix D represents data from eight conventional oedometer tests performed on Boston Blue Clay retrieved from the I-95 test site.

The oedometer tests were conducted following the procedures described in Lambe (1951), with the following exceptions:

(1) Load increment ratios less than unity were used near the vicinity of the maximum past pressure, $\bar{\sigma}_{vm}$, in order to obtain a compression curve with a better defined minimum radius of curvature;

(2) Vertical strain, ε_v, rather than void ratio, is used since compression curves based on strain yield more consistant and reliable estimates of compressibility and maximum past pressure (Ladd, 1973);

(3) The maximum past pressure was estimated from compression curves based on strains corresponding to the end of primary consolidation, as recommended by Ladd (1973), such strains being determined from dial readings versus log time data.

The samples were 2.5 inches in diameter and about 0.80 inches in height and were innundated with water after the first load was applied.

The loading program was basically derived from a consideration of the maximum past pressure estimated earlier by Germaine (1978) from conventional oedometer and CRSC tests. An unload-reload cycle emmanating from a consolidation stress equivalent to 2 x $\bar{\sigma}_{vm}$ was performed. Final unloading was initiated from a consolidation stress equivalent to 4 x $\bar{\sigma}_{vm}$. The inclusion of the unload-reload cycle was crucial for observing the variation of the pertinent soil parameters at various stages of overconsolidation and its dependence on the laboratory maximum past pressure.

CONSOLIDATION TEST

Project _____ Type of Test OEDOMETER No. 26-5-28.5ov Tested by IBG Date _____

Soil Type BOSTON BLUE CLAY Location I-95 TEST SITE Sample Height _____

_____ _____ Sample Diameter _____

Initial w(%) 30.85 G_s 2.77 w_N(%) 30.85 w_L(%) 31.30 Corrections APPARATUS COMPRESSIBILITY

Void Ratio e _____ S(%) _____ w_P(%) 19.50 P.I.(%) 11.80 Units: $\bar{\sigma}_{vc}$ KSC c_v cm^2/sec

$\bar{\sigma}_{vc}$	Primary			Coef. of Consol.		Remarks
	t(hr)	ε_v(%)	e	$\sqrt{t}$	log t	
0.02	—	0.000				
0.10	0.11	01.272		8.328×10^{-3}	1.055×10^{-2}	
0.25	0.02	1.749				
0.50	0.02	2.752		2.664×10^{-2}	4.279×10^{-2}	
1.00	0.02	3.848		1.8668×10^{-2}	2.221×10^{-2}	
2.00	0.03	5.357		1.5666×10^{-2}	2.038×10^{-2}	
4.00	0.04	7.975		1.4996×10^{-2}	1.707×10^{-2}	
8.00	0.04	11.838		1.52147×10^{-2}	1.767×10^{-2}	
4.00	0.01	12.963		2.689×10^{-2}	1.85×10^{-2}	
2.00	0.02	12.680		1.407×10^{-2}	1.8911×10^{-2}	
1.00	0.10	12.172		1.320×10^{-2}	1.002×10^{-2}	
0.50	0.18	11.577		6.551×10^{-3}	4.869×10^{-3}	
0.25	0.67	10.650		1.7526×10^{-3}	1.6737×10^{-3}	
0.50	0.07	10.612		1.977×10^{-2}	9.6313×10^{-3}	
1.00	0.08	11.077		1.1919×10^{-2}	1.0930×10^{-2}	
2.00	0.04	11.771		1.2605×10^{-2}	1.4999×10^{-2}	
4.00	0.02	12.374		1.5435×10^{-2}	2.0199×10^{-2}	
				1.4077×10^{-2}	1.984×10^{-2}	

CONSOLIDATION TEST

Project _____ Type of Test OEDOMETER No. 265-28.50V Tested by IBG Date _____

Soil Type _____ Location I-95 TEST SITE Sample Height _____

_____ _____ Sample Diameter _____

Initial w(%) 30.85 G_s 2.77 w_N(%) 30.85 w_L(%) 31.30 Corrections APPARATUS COMPRESSIBILITY

Void Ratio e _____ S(%) _____ w_P(%) 19.50 P.I.(%) 11.80 Units: $\bar{\sigma}_{vc}$ KSC c_v cm^2/sec.

$\bar{\sigma}_{vc}$	Primary			Coef. of Consol.		Remarks
	t (hr)	ε_v(%)	e	$\sqrt{t}$	log t	
8.00	0.02	13.344				
16.00	0.03	15.859		1.7087×10^{-2}	1.633×10^{-2}	
8.00	0.01	16.356		2.9316×10^{-2}	2.5075×10^{-2}	
4.00	0.01	15.971		2.371×10^{-2}	1.5303×10^{-2}	
2.00	0.06	15.467		1.065×10^{-2}	1.237×10^{-2}	
1.00	0.15	14.787		7.1066×10^{-3}	6.273×10^{-2}	
0.50	0.17	14.135		3.9500×10^{-3}	3.823×10^{-2}	

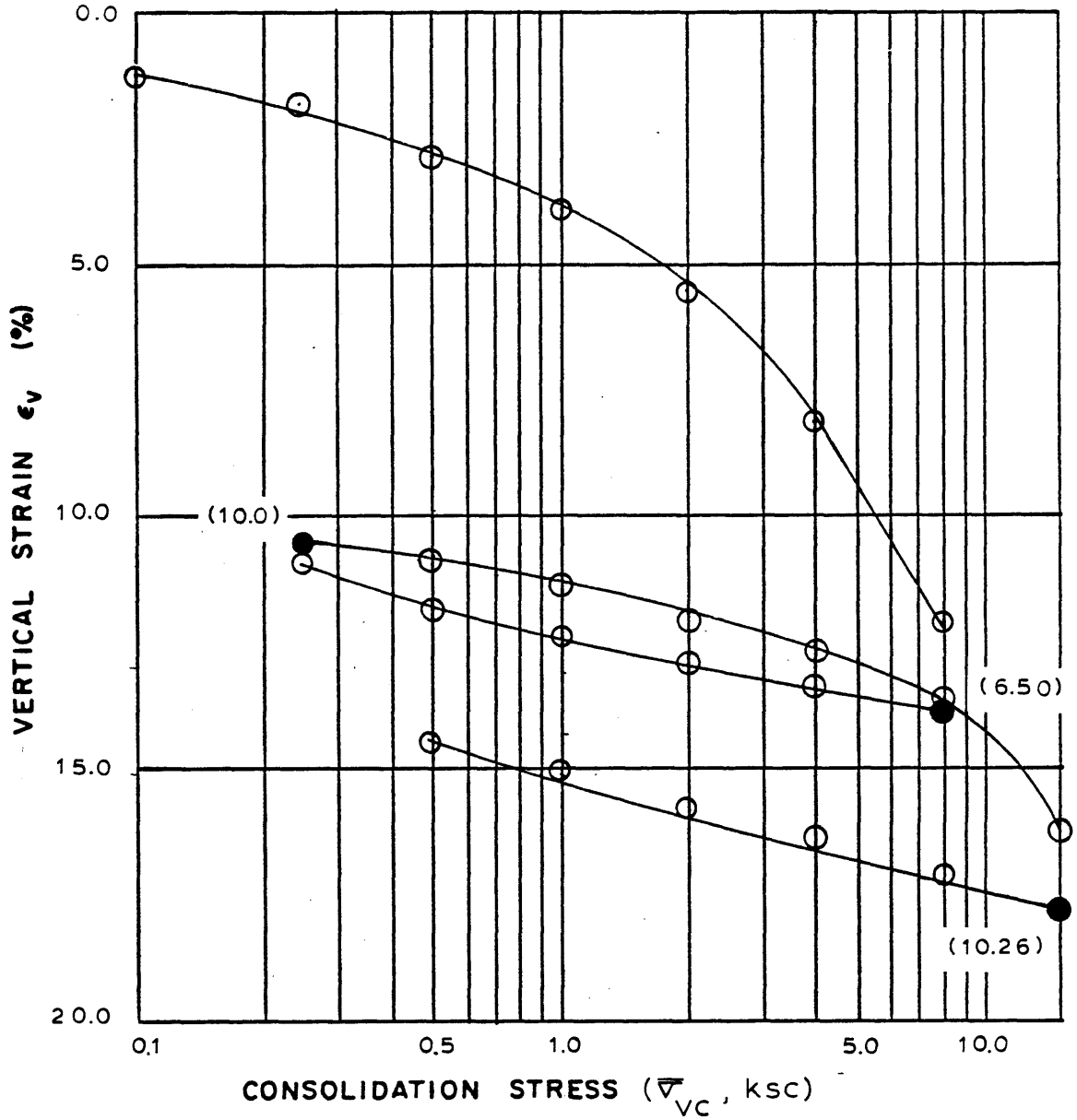

Sample No. 26.5-28.5-O-V w_N (%) 30.85 Estimated

Depth 26.59 w_L (%) 31.30 $\bar{\sigma}_{vo}$ 0.58 $\bar{\sigma}_{vm}$ 2.73-2.93

Soil Type Boston Blue Clay w_P (%) 19.50 CR 0.139 RR 0.0194

P.I.(%) 11.80 G_s 2.77 e_o 0.854

o At t_p

● At ( ) hr

Remarks Data from Oedometer test

w_L & w_P estimated from Baligh et al (1980)

Figure D.1 Compression Curve for Sample No. 26.5-28.5-O-V

CONSOLIDATION TEST

Project _____ Type of Test OEDOMETER No 26.5-28.5-O-H Tested by IBG Date _____

Soil Type BOSTON BLUE CLAY Location I-95 TEST SITE Sample Height _____

_____ _____ Sample Diameter _____

Initial w(%) 26.92 G_s 2.77 w_N(%) 26.92 w_L(%) 31.30 Corrections APPARATUS COMPRESSIBILITY

Void Ratio e _____ S(%) _____ w_P(%) 19.54 P.I.(%) 11.76 Units: $\bar{\sigma}_{vc}$ KSC c_v cm^2/sec

$\bar{\sigma}_{vc}$	Primary			Coef. of Consol.		Remarks
	t (hr)	ε_v(%)	e	$\sqrt{t}$	log t	
0.01	—	0.000				
0.10	0.06	0.718		2.020×10^{-2}	1.878×10^{-2}	
0.25	0.04	1.078		2.062×10^{-2}	2.333×10^{-2}	
0.50	0.05	1.340		1.730×10^{-2}	2.010×10^{-2}	
1.00	0.04	1.973		2.283×10^{-2}	3.585×10^{-2}	
2.00	0.03	2.520		1.945×10^{-2}	2.530×10^{-2}	
4.00	0.03	4.641		2.377×10^{-2}	2.154×10^{-2}	
2.00	0.02	5.733		2.869×10^{-2}	9.615×10^{-2}	
1.00	0.03	5.716		2.536×10^{-2}	2.426×10^{-2}	
0.50	0.05	5.460		1.311×10^{-2}	1.381×10^{-2}	
0.25	0.07	5.171		1.401×10^{-2}	1.191×10^{-2}	
0.50	0.02	5.036		2.978×10^{-2}	3.348×10^{-2}	
1.00	0.02	5.240		2.976×10^{-2}	2.698×10^{-2}	
2.00	0.01	5.578		3.805×10^{-2}	3.327×10^{-2}	
4.00	0.01	6.081		3.549×10^{-2}	3.298×10^{-2}	
8.00	0.04	8.131		2.043×10^{-2}	2.000×10^{-2}	
4.00	0.01	8.696		1.343×10^{-2}	3.899×10^{-2}	
				2.763×10^{-2}	3.236×10^{-2}	

CONSOLIDATION TEST

Project _____ Type of Test OEDOMETER No 26.5-28.5-H Tested by IBG Date _____

Soil Type BOSTON BLUE CLAY Location I-95 TEST SITE Sample Height _____

_____ _____ Sample Diameter _____

Initial w(%) 26.92 G_s 2.77 w_N(%) 26.92 w_L(%) 31.30 Corrections APPARATUS COMPRESSIBILITY

Void Ratio e _____ S(%) _____ w_P(%) 19.54 P.I.(%) 11.76 Units: $\bar{\sigma}_{vc}$ KSC c_v cm^2/sec

$\bar{\sigma}_{vc}$	Primary			Coef. of Consol.		Remarks
	t (hr)	ε_v(%)	e	$\sqrt{t}$	log t	
2.00	0.02	8.490				
1.00	0.03	8.379		1.864×10^{-2}	2.292×10^{-2}	
0.50	0.15	7.945		1.852×10^{-2}	1.045×10^{-2}	
0.25	0.54	7.491		6.442×10^{-3}	3.232×10^{-3}	

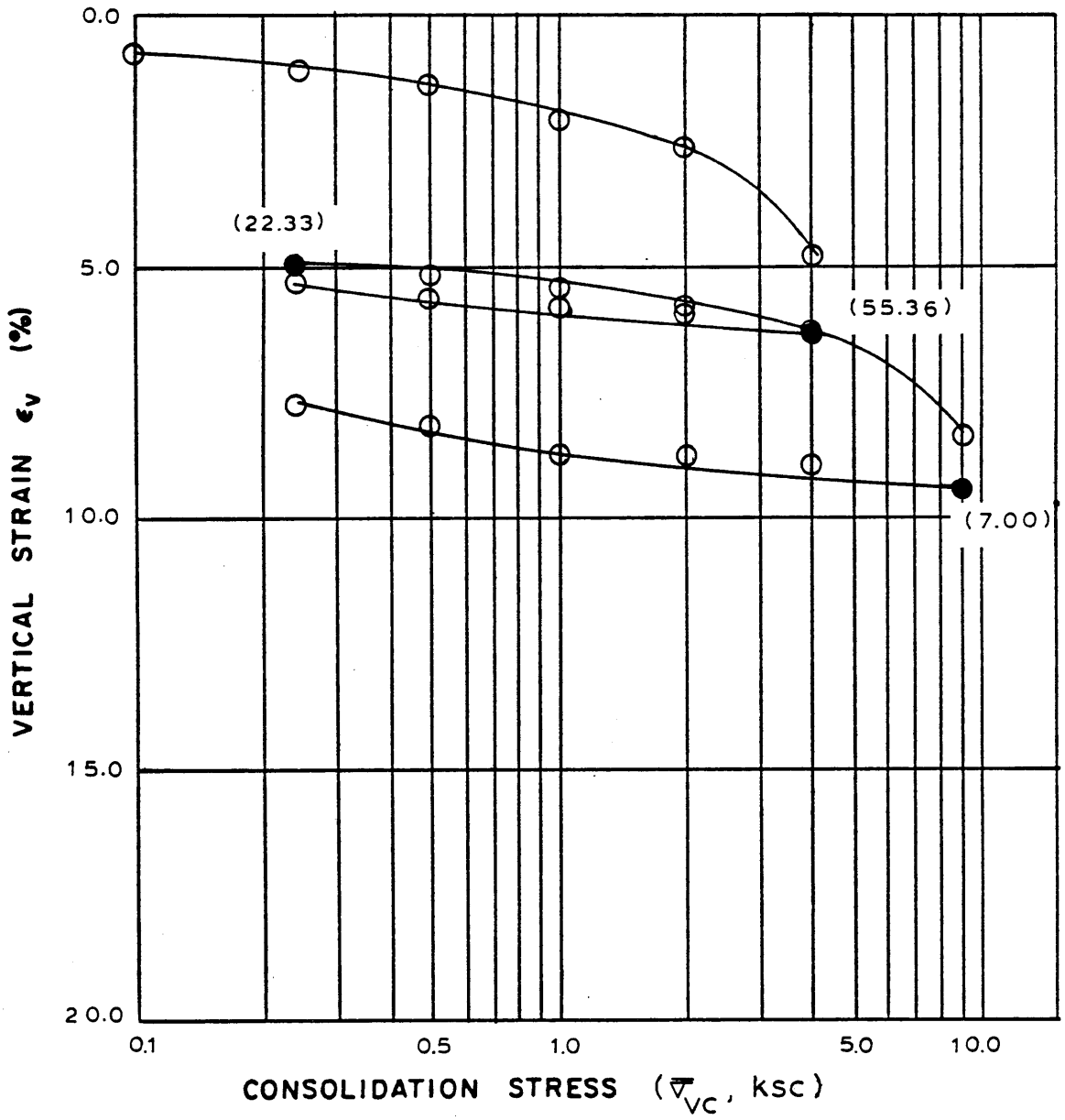

Sample No. 26.5-28.5-O-H w_N (%) 26.92 Estimated

Depth 26.77 w_L (%) 31.30 $\bar{\sigma}_{vo}$ 0.59 $\bar{\sigma}_{vm}$ 287-305

Soil Type Boston Blue Clay w_P (%) 19.54 CR 0.100 RR 0.0094

P.I.(%) 11.76 G_s 2.77 e_o 0.745

o At t_p

● At ( ) hr

Remarks Data from Oedometer test

w&w estimated from Baligh et al (1980)
L P

Figure D. 2 Compression Curve for Sample No. 26.5-28.5-O-H

CONSOLIDATION TEST

Project _____ Type of Test OEDOMETER No. 82-84-0-V Tested by IBG Date _____

Soil Type BOSTON BLUE CLAY Location I-95 TEST SITE Sample Height _____

_____ _____ Sample Diameter _____

Initial w(%) 45.35 G_s 2.77 w_N(%) 45.35 w_L(%) 40.16 Corrections APPARATUS COMPRESSIBILITY

Void Ratio e _____ S(%) _____ w_P(%) 21.77 P.I.(%) 18.39 Units: $\bar{\sigma}_{vc}$ KSC c_v cm²/sec

$\bar{\sigma}_{vc}$	Primary			Coef. of Consol.		Remarks
	t (hr)	ε_v(%)	e	Vf	log t	
0.02	—	0.000				
0.20	0.04	0.170		4.019×10^{-3}	5.187×10^{-3}	
0.50	0.03	0.761		8.241×10^{-3}	6.619×10^{-3}	
1.00	0.05	1.206		4.386×10^{-3}	4.680×10^{-3}	
2.00	0.04	2.161		4.324×10^{-3}	5.948×10^{-3}	
4.00	0.42	12.372		0.776×10^{-3}	0.591×10^{-3}	
2.00	0.03	13.071		4.530×10^{-3}	4.450×10^{-3}	
1.00	0.11	12.364		2.500×10^{-3}	3.563×10^{-3}	
0.50	0.25	11.524		0.753×10^{-3}	0.954×10^{-3}	
0.20	0.75	10.125		0.419×10^{-3}	0.387×10^{-3}	
0.50	0.15	10.554		1.110×10^{-3}	0.709×10^{-3}	
1.00	0.21	11.610		1.016×10^{-3}	1.056×10^{-3}	
2.00	0.16	12.840		1.632×10^{-3}	1.802×10^{-3}	
4.00	0.22	14.713		1.197×10^{-3}	1.337×10^{-3}	
8.00	0.22	19.091		1.263×10^{-3}	1.404×10^{-3}	
4.00	0.06	18.858		1.364×10^{-3}	1.563×10^{-3}	
2.00	0.08	18.165		2.307×10^{-3}	2.582×10^{-3}	
				1.089×10^{-3}	1.265×10^{-3}	

CONSOLIDATION TEST

Project _____ Type of Test OEDOMETER No. B2-84-OV Tested by IBG Date _____

Soil Type BOSTON BLUE CLAY Location I-95 TEST SITE Sample Height _____

_____ _____ Sample Diameter _____

Initial w(%) 45.35 G_s 2.77 w_N(%) 45.35 w_L(%) 40.16 Corrections APPARATUS COMPRESSIBILITY

Void Ratio e _____ S(%) _____ w_P(%) 21.77 P.I.(%) 18.39 Units: $\bar{\sigma}_{vc}$ KSC c_v cm^2/sec

$\bar{\sigma}_{vc}$	Primary			Coef. of Consol.		Remarks
	t(hr)	ε_v(%)	e	$\sqrt{t}$	log t	
1.00	0.21	17.381				
0.50	0.43	16.623		0.462×10^{-3}	0.460×10^{-3}	
0.20	1.25	14.983		0.208×10^{-3}	0.174×10^{-3}	
0.10	0.39	14.426		—	0.340×10^{-3}	

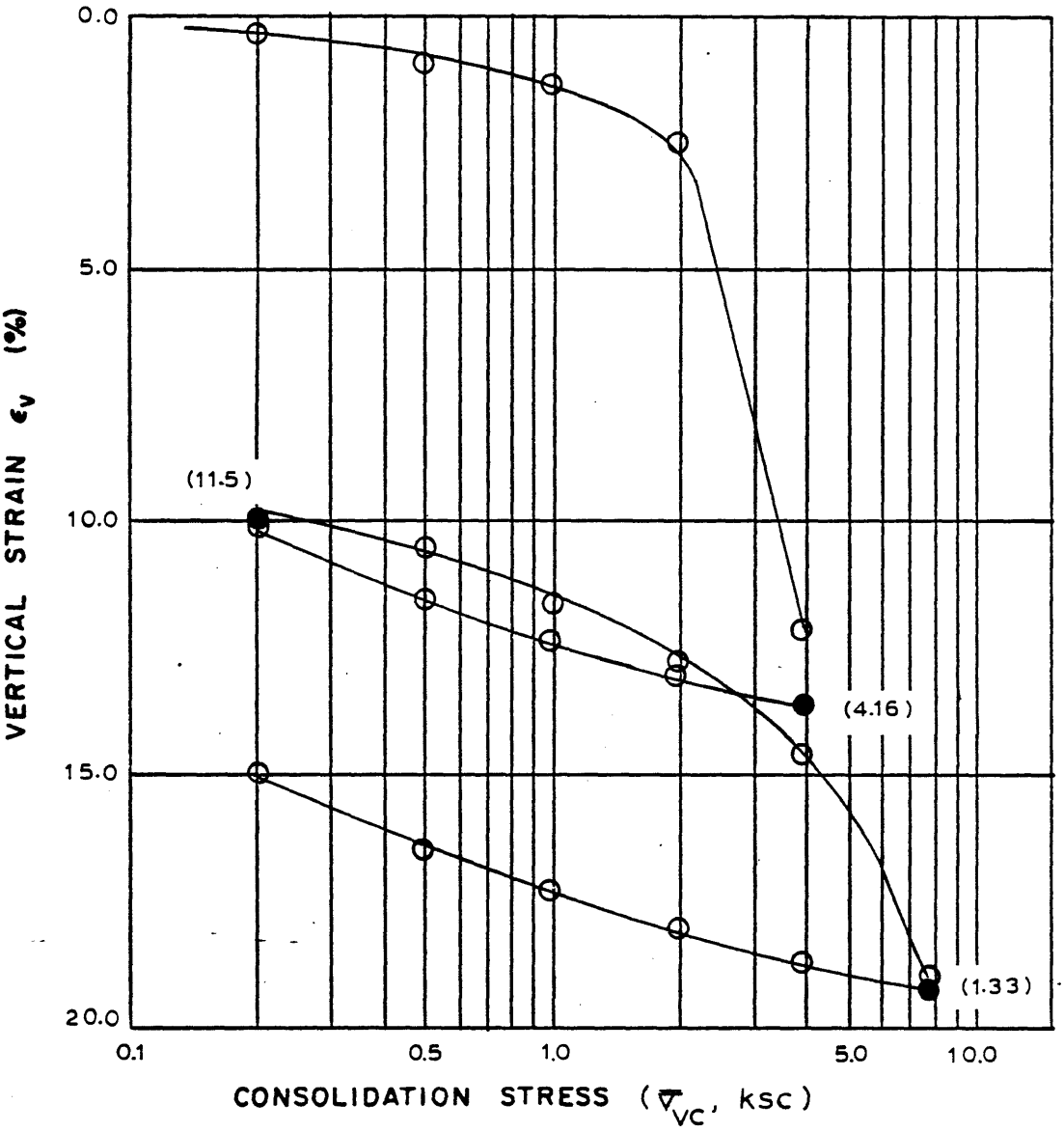

Sample No. 82-84-O-V w_N (%) 45.35 Estimated

Depth 82.19 w_L (%) 40.16 $\bar{\sigma}_{vo}$ 1.92 $\bar{\sigma}_{vm}$ 2.02-2.14

Soil Type Boston Blue Clay w_P (%) 21.77 CR 0.3350 RR 0.0294

P.I.(%) 18.39 G_s 2.77 e_o 1.256

o At t_p

● At ( ) hr

Remarks Data from Oedometer test

w_L & w_P estimated from Baligh et al (1980)

Figure D. 3 Compression Curve for Sample No. 82-84-O-V

CONSOLIDATION TEST

Project _____ Type of Test OEDOMETER No 82-84-O-M Tested by IBG Date _____

Soil Type BOSTON BLUE CLAY Location I-95 TEST SITE Sample Height _____

_____ _____ Sample Diameter _____

Initial w(%) 40.39 G_s 2.77 w_N(%) 40.39 w_L(%) 41.71 Corrections APPARATUS COMPRESSIBILITY

Void Ratio e _____ S(%) _____ w_P(%) 22.16 P.I.(%) 19.55 Units: $\bar{\sigma}_{vc}$ KSC c_v cm^2/sec

$\bar{\sigma}_{vc}$	Primary			Coef. of Consol.		Remarks
	t (hr)	ε_v(%)	e	$\sqrt{t}$	log t	
0.02	—	0.000				
0.10	0.02	0.320		6.022×10^{-2}	3.50×10^{-2}	
0.25	0.07	0.650		4.155×10^{-2}	2.14×10^{-2}	
0.50	0.29	0.761		1.350×10^{-2}	1.153×10^{-2}	
1.00	0.10	1.756		1.631×10^{-2}	1.777×10^{-2}	
2.00	0.53	5.949		6.205×10^{-3}	3.706×10^{-3}	
4.00	0.30	11.576		6.420×10^{-3}	6.676×10^{-3}	
2.00	0.01	12.305		3.604×10^{-2}	4.185×10^{-2}	
1.00	0.08	11.876		1.945×10^{-2}	1.808×10^{-2}	
0.50	0.12	11.652		1.627×10^{-2}	1.214×10^{-2}	
0.25	0.62	10.983		2.720×10^{-3}	3.679×10^{-3}	
0.50	0.03	10.866		2.130×10^{-3}	3.093×10^{-3}	
1.00	0.09	11.317		1.413×10^{-2}	1.707×10^{-2}	
2.00	0.07	11.903		1.844×10^{-2}	1.827×10^{-2}	
4.00	0.08	12.849		2.319×10^{-2}	1.959×10^{-2}	
8.00	0.17	16.355		8.991×10^{-3}	8.900×10^{-3}	
4.00	0.01	16.906		3.817×10^{-2}	3.423×10^{-2}	
				2.138×10^{-2}	2.163×10^{-2}	

CONSOLIDATION TEST

Project _____ Type of Test OEDOMETER No 82-84-0-H Tested by IBG Date _____

Soil Type BOSTON BLUE CLAY Location I-95 TEST SITE Sample Height _____

_____ _____ Sample Diameter _____

Initial w(%) 40.39 G_s 2.77 w_N(%) 40.39 w_L(%) 41.71 Corrections APPARATUS COMPRESSIBILITY

Void Ratio e _____ S(%) _____ w_P(%) 22.16 P.I.(%) 19.55 Units: $\bar{\sigma}_{vc}$ KSC c_v cm²/sec

$\bar{\sigma}_{vc}$	Primary			Coef. of Consol.		Remarks
	t (hr)	ε_v(%)	e	$\sqrt{t}$	log t	
2.00	0.05	16.521				
1.00	0.22	15.995		1.059×10^{-2}	9.113×10^{-3}	
0.50	1.33	15.729		4.176×10^{-3}	2.208×10^{-3}	
0.25	1.42	15.053		1.599×10^{-3}	1.116×10^{-3}	
0.10	1.42	14.057		9.825×10^{-4}	7.318×10^{-4}	

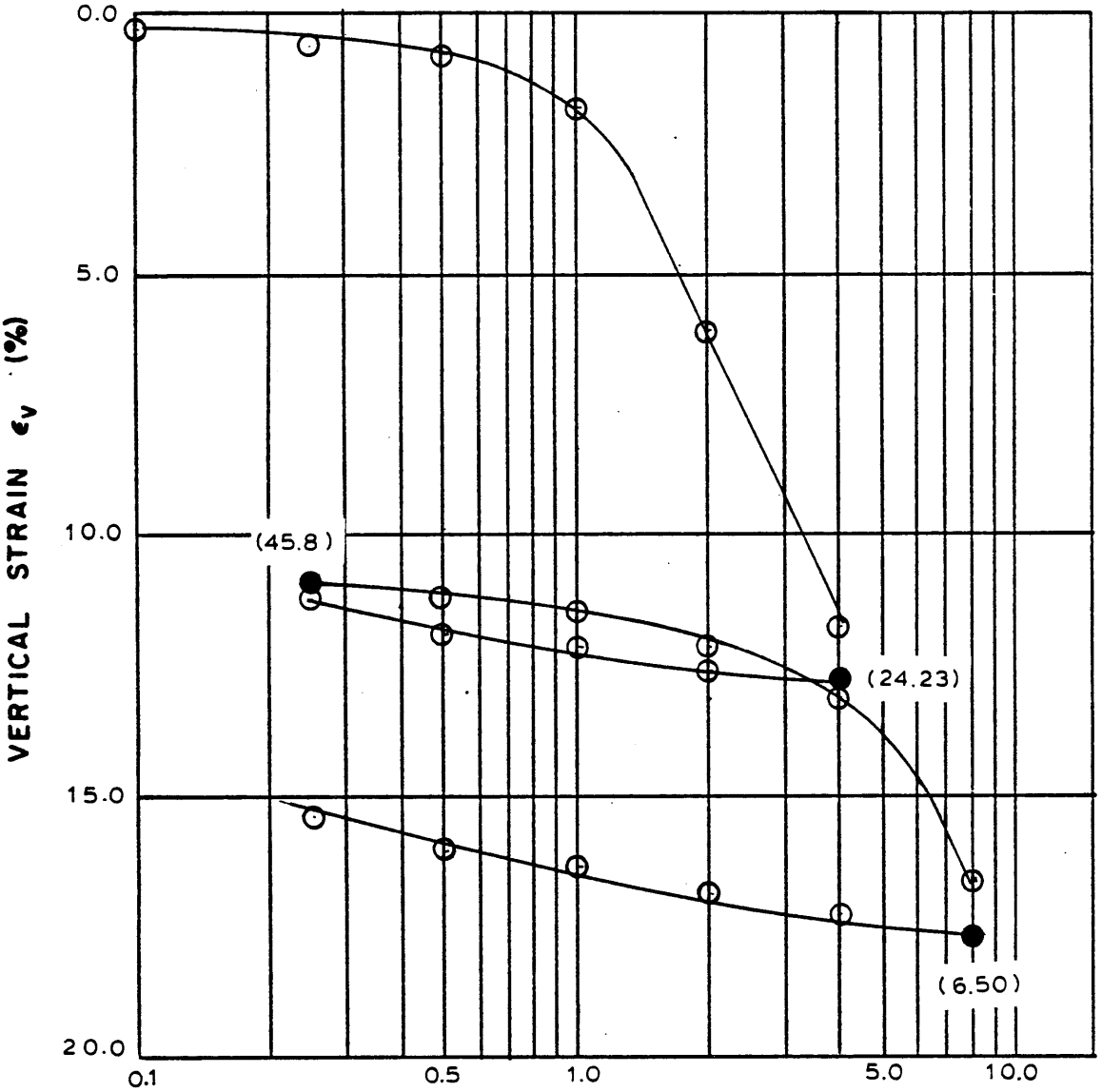

Sample No. 82-84-O-H w_N (%) 40.39 Estimated

Depth 82.58 w_L (%) 41.71 $\bar{\sigma}_{vo}$ 1.92 $\bar{\sigma}_{vm}$ 1.15-1.25

Soil Type Boston Blue Clay w_P (%) 22.16 CR 0.174 RR 0.0115

P.I.(%) 19.55 G_s 2.77 e_0 1.118

o At t_p

● At ( ) hr

Remarks Data from Oedometer test

w_L & w_P estimated from Baligh et al (1980)

Figure D. 4 Compression Curve for Sample No. 82-84-O-H

CONSOLIDATION TEST

Project _____ Type of Test OEDOMETER No. 90-92-0-V Tested by IBG Date _____

Soil Type BOSTON BLUE CLAY Location I-95 TEST SITE Sample Height _____

_____ _____ Sample Diameter _____

Initial w(%) 47.67 G_s 2.77 w_N(%) 47.67 w_L(%) 43.47 Corrections APPARATUS COMPRESSIBILITY

Void Ratio e _____ S(%) _____ w_P(%) 22.98 P.I.(%) 20.49 Units: $\bar{\sigma}_{vc}$ KSC c_v cm²/sec

$\bar{\sigma}_{vc}$	Primary			Coef. of Consol.		Remarks
	t (hr)	ε_v(%)	e	$c_v t$	log t	
0.02	—	0.000				
0.10	0.07	0.211		2.921×10^{-3}	3.951×10^{-3}	
0.25	0.10	0.628		3.626×10^{-3}	3.927×10^{-3}	
0.50	0.10	1.117		2.876×10^{-3}	3.548×10^{-3}	
1.00	0.04	1.631		4.283×10^{-3}	4.593×10^{-3}	
2.00	2.08	4.023		1.038×10^{-3}	0.331×10^{-3}	
4.00	0.47	13.800		0.365×10^{-3}	0.452×10^{-3}	
2.00	0.06	14.622		3.241×10^{-3}	3.804×10^{-3}	
1.00	0.07	14.020		1.865×10^{-3}	2.599×10^{-3}	
0.50	0.29	12.983		0.782×10^{-3}	0.735×10^{-3}	
0.25	0.75	11.977		0.366×10^{-3}	0.324×10^{-3}	
0.50	0.28	12.208		0.750×10^{-3}	0.759×10^{-3}	
1.00	0.22	13.089		0.814×10^{-3}	1.499×10^{-3}	
2.00	0.13	14.249		1.392×10^{-3}	1.046×10^{-3}	
4.00	0.22	16.161		1.377×10^{-3}	1.177×10^{-3}	
8.00	0.21	20.112		0.879×10^{-3}	0.940×10^{-3}	
4.00	0.54	20.224		3.436×10^{-3}	3.477×10^{-3}	
				1.985×10^{-3}	1.577×10^{-3}	

CONSOLIDATION TEST

Project _____ Type of Test OEDOMETER No: 90-92-0-V Tested by IBG Date _____

Soil Type BOSTON BLUE CLAY Location I-95 TEST SITE Sample Height _____

_____ _____ Sample Diameter _____

Initial w(%) 47.67 G_s 2.77 w_N(%) 47.67 w_L(%) 43.47 Corrections APPARATUS COMPRESSIBILITY

Void Ratio e _____ S(%) _____ w_P(%) 22.98 P.I.(%) 20.49 Units: $\bar{\sigma}_{vc}$ KSC c_v cm^2/sec

$\bar{\sigma}_{vc}$	Primary			Coef. of Consol.		Remarks
	t(hr)	ε_v(%)	e	Vt	log t	
2.00	0.17	19.482				
1.00	0.36	18.655		0.720×10^{-3}	0.699×10^{-3}	
0.50	0.87	17.705		0.383×10^{-3}	0.357×10^{-3}	
0.25	5.83	16.833		0.258×10^{-3}	0.112×10^{-3}	

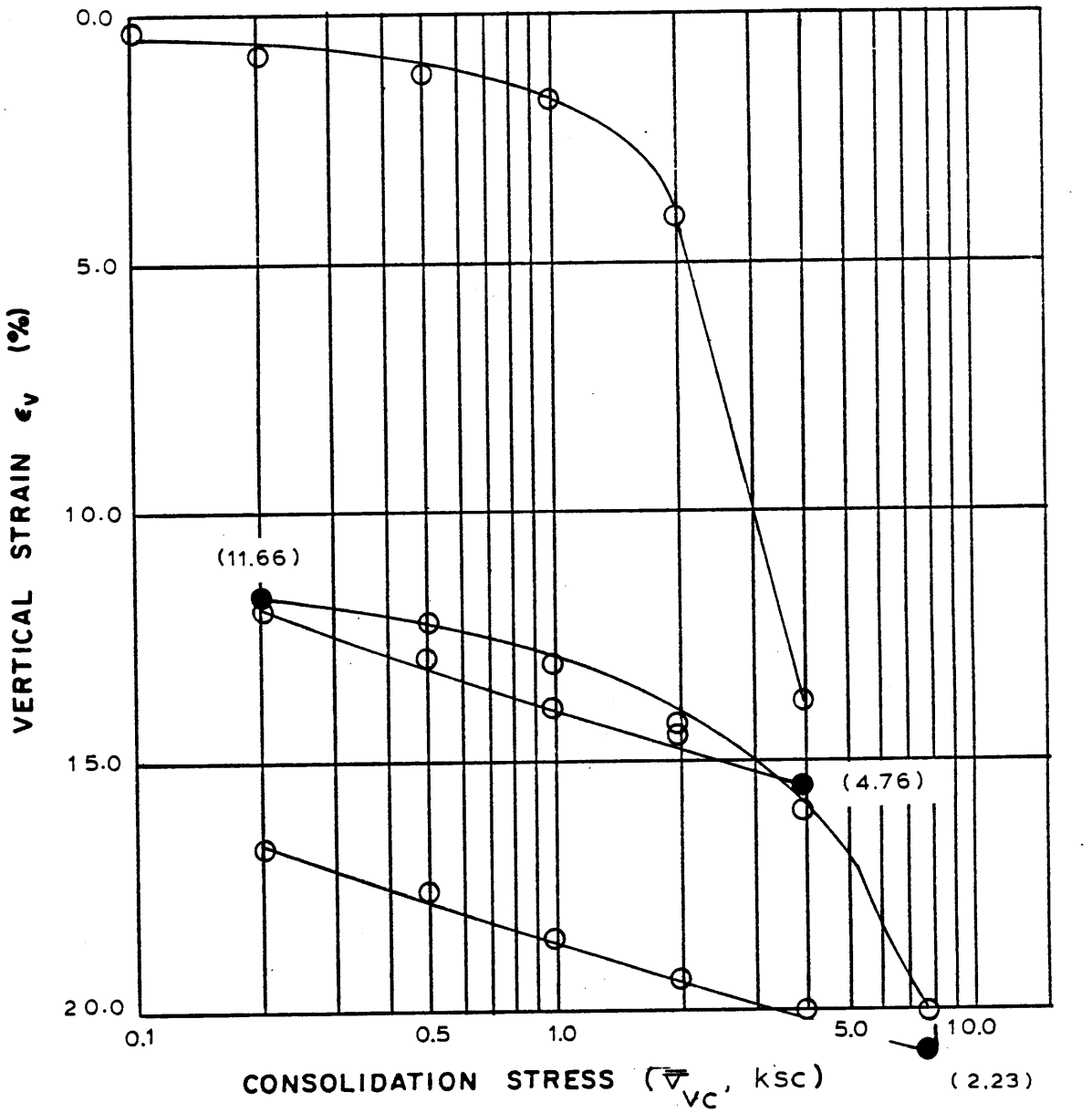

Sample No. 90-92.0.V w_N (%) 47.67 Estimated

Depth 90.07 w_L (%) 43.47 $\bar{\sigma}_{vo}$ 2.11 $\bar{\sigma}_{vm}$ 1.81.1.90

Soil Type Boston w_P (%) 22.98 CR 0.2006-0.3230 RR 0.0287

Blue clay P.I.(%) 20.49 G_s 2.77 e_o 1.320

o At t_p

● At ( ) hr

Remarks Data from Oedometer test

w_L & w_P estimated from Baligh et al (1980)

Figure D.5 Compression Curve for Sample No. 90-92-O-V

CONSOLIDATION TEST

Project _____ Type of Test OEDOMETER No. 90-92-04 Tested by IBG Date _____

Soil Type BOSTON BLUE CLAY Location I-95 TEST SITE Sample Height _____

_____ _____ Sample Diameter _____

Initial w(%) 45.06 G_s 2.77 w_N(%) 45.06 w_L(%) 43.76 Corrections APPARATUS COMPRESSIBILITY

Void Ratio e _____ S(%) _____ w_P(%) 23.04 P.I.(%) 20.72 Units: $\bar{\sigma}_{vc}$ KSC c_v cm^2/sec

$\bar{\sigma}_{vc}$	Primary			Coef. of Consol.		Remarks
	t(hr)	ε_v(%)	e	V_T	log t	
0.01	—	0.000				
0.10	0.07	0.763		3.390×10^{-3}	4.551×10^{-3}	
0.20	0.13	0.972		2.687×10^{-3}	2.817×10^{-3}	
0.50	0.05	1.383		3.336×10^{-3}	3.861×10^{-3}	
1.00	0.06	2.044		2.848×10^{-3}	3.692×10^{-3}	
2.00	0.23	5.797		1.250×10^{-3}	1.176×10^{-3}	
4.00	0.25	13.147		0.899×10^{-3}	0.817×10^{-3}	
2.00	0.03	13.796		5.156×10^{-3}	4.403×10^{-3}	
1.00	0.07	13.479		1.937×10^{-3}	2.280×10^{-3}	
0.50	0.21	12.812		1.191×10^{-3}	1.153×10^{-3}	
0.20	0.40	11.822		0.586×10^{-3}	0.551×10^{-3}	
0.50	0.09	11.845		1.740×10^{-3}	2.228×10^{-3}	
1.00	0.10	12.559		1.725×10^{-3}	1.964×10^{-3}	
2.00	0.08	13.503		2.715×10^{-3}	2.168×10^{-3}	
4.00	0.12	15.126		2.008×10^{-3}	2.105×10^{-3}	
8.00	0.17	19.394		1.689×10^{-3}	1.570×10^{-3}	
4.00	0.03	19.921		3.770×10^{-3}	4.229×10^{-3}	
				3.183×10^{-3}	2.550×10^{-3}	

CONSOLIDATION TEST

Project _____ Type of Test OEDOMETER No: 90-92-O-H Tested by JBG Date _____

Soil Type BOSTON BLUE CLAY Location I-95 TEST SITE Sample Height _____

_____ _____ Sample Diameter _____

Initial w(%) 45.06 G_s 2.77 w_N(%) 45.06 w_L(%) 43.76 Corrections APPARATUS COMPRESSIBILITY

Void Ratio e _____ S(%) _____ w_P(%) 23.04 P.I.(%) 20.72 Units: $\bar{\sigma}_{vc}$ KSC c_v cm^2/sec

$\bar{\sigma}_{vc}$	Primary			Coef. of Consol.		Remarks
	t(hr)	ε_v(%)	e	$\sqrt{t}$	log t	
2.00	0.07	19.466				
1.00	0.22	18.809		1.333×10^{-3}	1.304×10^{-3}	
0.50	0.42	18.031		0.568×10^{-3}	0.555×10^{-3}	
0.20	1.33	16.877		0.187×10^{-3}	0.174×10^{-3}	

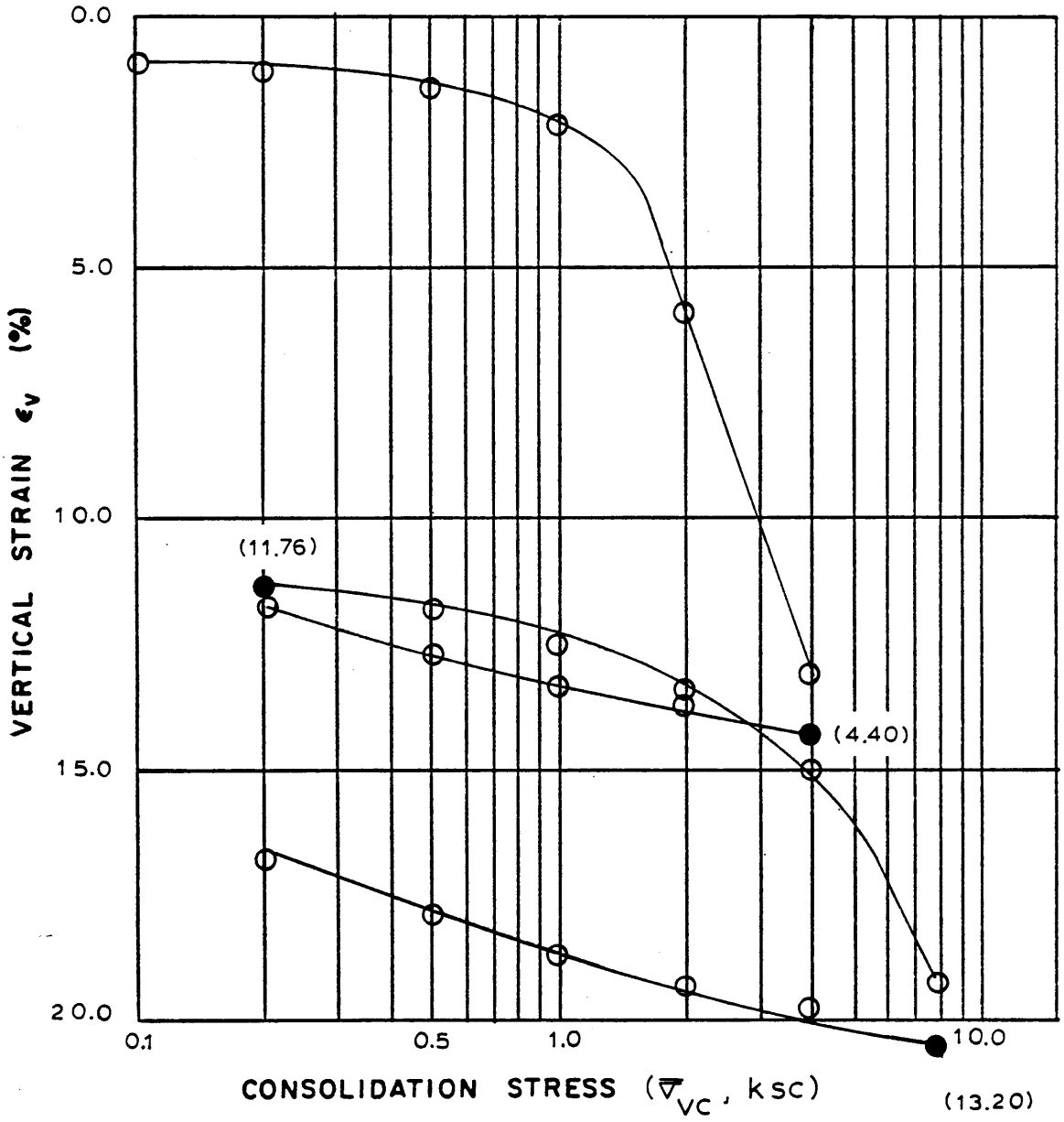

Sample No. 90.92.O.H w_N (%) 45.06 Estimated

Depth 90.25 w_L (%) 43.76 $\bar{\sigma}_{vo}$ 2.11 $\bar{\sigma}_{vm}$ 1.54.1.60

Soil Type Boston w_P (%) 23.04 CR 0.239 RR 0.0219

Blue Clay P.I.(%) 20.72 G_s 2.77 e_o 1.248

o At t_p

● At ( ) hr

Remarks Data from Oedometer test

w_L & w_P estimated from Baligh et al (1980)

Figure D. 6 Compression Curve for Sample No. 90-92-O-H

CONSOLIDATION TEST

Project _____ Type of Test OEDOMETER No. 100-102-0-V Tested by IBG Date _____

Soil Type BOSTON BLUE CLAY Location I-95 TEST SITE Sample Height _____

_____ _____ Sample Diameter _____

Initial w(%) 40.63 G_s 2.77 w_N(%) 40.63 w_L(%) 50.19 Corrections APPARATUS COMPRESSIBILITY

Void Ratio e _____ S(%) _____ w_P(%) 25.24 P.I.(%) 24.95 Units: $\bar{\sigma}_{vc}$ KSC c_v cm^2/sec

$\bar{\sigma}_{vc}$	Primary			Coef. of Consol.		Remarks
	t (hr)	ε_v(%)	e	Tv	log t	
0.02	—	0.000				
0.10	0.07	0.264		2.824×10^{-3}	4.958×10^{-3}	
0.20	0.09	0.497		2.886×10^{-3}	2.763×10^{-3}	
0.35	0.11	0.790		2.366×10^{-3}	4.294×10^{-3}	
0.50	0.09	1.011		3.072×10^{-3}	3.790×10^{-3}	
0.70	0.09	1.140		3.324×10^{-3}	3.870×10^{-3}	
1.00	0.11	1.388		2.886×10^{-3}	3.769×10^{-3}	
1.50	0.18	1.703		1.852×10^{-3}	2.699×10^{-3}	
2.00	0.19	1.978		3.123×10^{-3}	2.230×10^{-3}	
2.50	—	2.100		3.256×10^{-3}	—	
4.00	1.42	9.183		3.066×10^{-3}	0.238×10^{-3}	
2.00	0.054	10.080		4.779×10^{-3}	4.372×10^{-3}	
1.00	0.12	9.644		2.633×10^{-3}	2.260×10^{-3}	
0.50	0.71	8.736		1.114×10^{-3}	0.717×10^{-3}	
0.25	—	8.120		0.545×10^{-3}	—	
0.50	0.21	8.222		1.402×10^{-3}	1.465×10^{-3}	
1.00	0.17	8.776		1.394×10^{-3}	1.665×10^{-3}	
				—	1.910×10^{-3}	

CONSOLIDATION TEST

Project _____ Type of Test OEDOMETER No. 100-102-0-V Tested by IBG Date _____

Soil Type BOSTON BLUE CLAY Location I-95 TEST SITE Sample Height _____

_____ _____ Sample Diameter _____

Initial w(%) 40.63 G_s 2.77 w_N(%) 40.63 w_L(%) 50.19 Corrections APPARATUS COMPRESSIBILITY

Void Ratio e _____ S(%) _____ w_P(%) 25.24 P.I.(%) 24.95 Units: $\bar{\sigma}_{vc}$ KSC c_v cm^2/sec

$\bar{\sigma}_{vc}$	Primary			Coef. of Consol.		Remarks
	t (hr)	ε_v(%)	e	$\sqrt{t}$	log t	
2.00	0.16	9.753				
4.00	0.13	11.104		1.717×10^{-3}	2.428×10^{-3}	
8.00	0.25	15.278		1.175×10^{-3}	1.249×10^{-3}	
16.00	0.25	19.696		1.301×10^{-3}	1.185×10^{-3}	
8.00	0.04	19.909		4.916×10^{-3}	5.596×10^{-3}	
4.00	0.09	19.215		2.423×10^{-3}	3.217×10^{-3}	
2.00	0.20	18.339		1.175×10^{-3}	1.350×10^{-3}	
1.00	0.33	17.400		0.631×10^{-3}	0.757×10^{-3}	
0.50	0.97	16.230		—	0.301×10^{-3}	
0.20	1.50	15.390		0.170×10^{-3}	0.137×10^{-3}	
—						

999

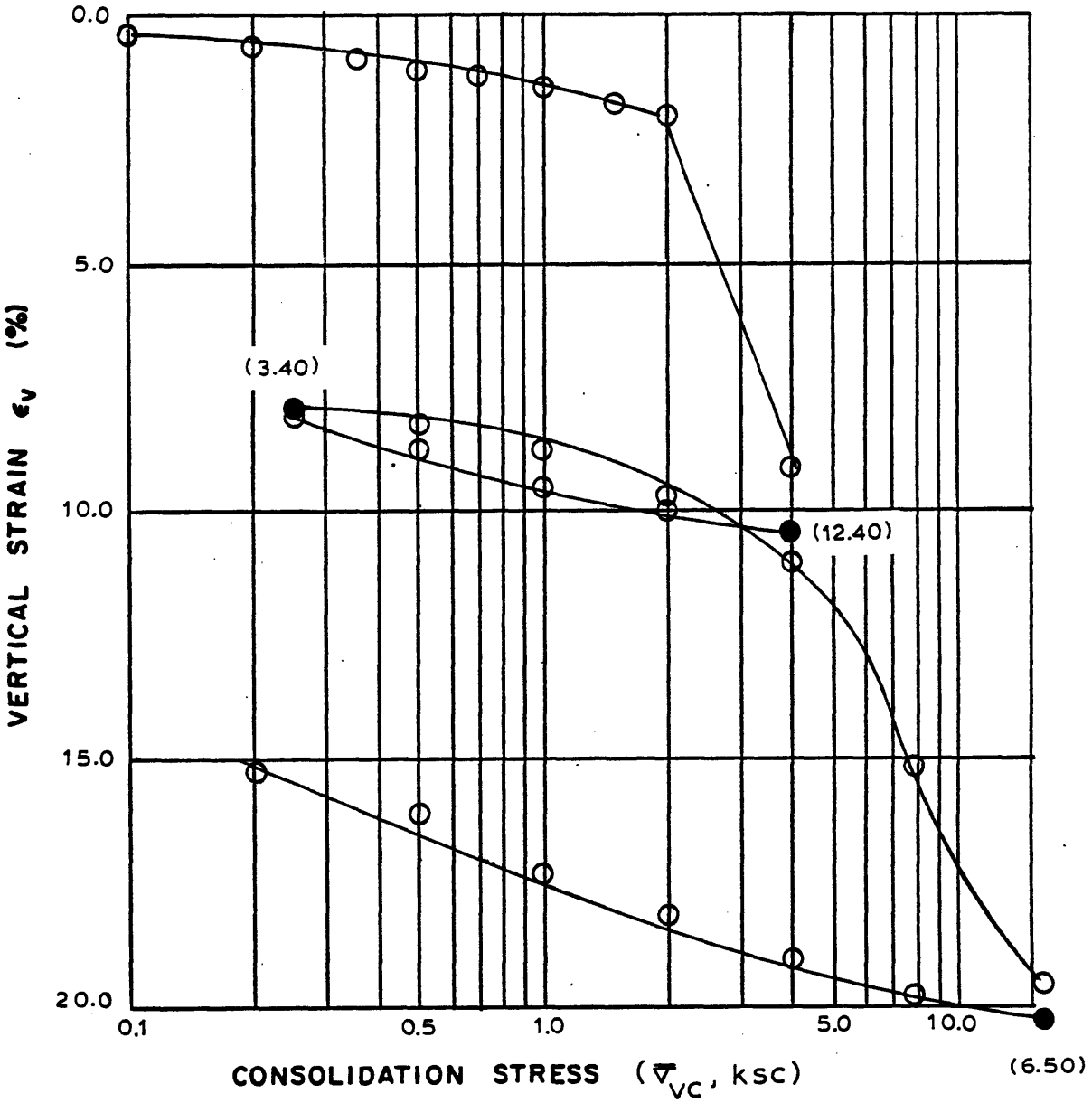

Sample No. 100-102-O-V w_N (%) 40.63 Estimated

Depth 100-19 w_L (%) 50.19 $\bar{\sigma}_{vo}$ 2.35 $\bar{\sigma}_{vm}$ 2.00

Soil Type Boston Blue Clay w_P (%) 25.24 CR 0.219 RR 0.0225

P.I.(%) 24.95 G_s 2.77 e_o 1.125

o At t_p

● At ( ) hr

Remarks _____

Figure D. 7 Compression Curve for Sample No. 100-102-O-V

CONSOLIDATION TEST

Project _____ Type of Test OEDOMETER No 100-102-0-A Tested by IBG Date _____

Soil Type BOSTON BLUE CLAY Location I-95 TEST SITE Sample Height _____

_____ _____ Sample Diameter _____

Initial w(%) 44.10 G_s 2.77 w_N(%) 44.10 w_L(%) 50.20 Corrections APPARATUS COMPRESSIBILITY

Void Ratio e _____ S(%) _____ w_P(%) 25.26 P.I.(%) 24.94 Units: $\bar{\sigma}_{vc}$ KSC c_v cm²/sec

$\bar{\sigma}_{vc}$	Primary			Coef. of Consol.		Remarks
	t (hr)	ε_v(%)	e	$\sqrt{t}$	log t	
0.02	—	0.000				
0.28	0.07	0.670		2.554×10^{-3}	2.373×10^{-3}	
0.60	0.09	1.157		2.952×10^{-3}	2.132×10^{-3}	
1.00	0.12	1.784		1.597×10^{-3}	1.855×10^{-3}	
2.00	0.33	5.203		1.064×10^{-3}	0.988×10^{-3}	
4.00	0.18	10.530		0.970×10^{-3}	1.229×10^{-3}	
2.00	0.04	11.514		3.877×10^{-3}	5.563×10^{-3}	
1.00	0.06	11.140		—	3.415×10^{-3}	
0.56	0.12	10.712		2.040×10^{-3}	2.106×10^{-3}	
0.28	0.21	10.298		1.130×10^{-3}	1.093×10^{-3}	
0.56	0.06	10.320		2.553×10^{-3}	4.270×10^{-3}	
1.00	0.06	10.562		3.222×10^{-3}	3.615×10^{-3}	
2.00	0.05	11.269		3.400×10^{-3}	4.213×10^{-3}	
4.00	0.05	12.530		3.326×10^{-3}	4.120×10^{-3}	
8.00	0.12	16.860		1.697×10^{-3}	1.738×10^{-3}	
4.00	0.08	18.022		2.738×10^{-3}	5.253×10^{-3}	
2.00	0.03	17.706		4.105×10^{-3}	4.605×10^{-3}	
				2.923×10^{-3}	2.328×10^{-3}	

CONSOLIDATION TEST

Project _____ Type of Test OEDOMETER No 100-102-0-H Tested by IBG Date _____

Soil Type BOSTON BLUE CLAY Location I-95 TEST SITE Sample Height _____

_____ _____ Sample Diameter _____

Initial w(%) 44.10 G_s 2.77 w_N(%) 44.10 w_L(%) 50.20 Corrections APPARATUS COMPRESSIBILITY

Void Ratio e _____ S(%) _____ w_P(%) 25.26 P.I.(%) 24.94 Units: $\bar{\sigma}_{vc}$ KSC c_v cm²/sec

$\bar{\sigma}_{vc}$	Primary			Coef. of Consol.		Remarks
	t (hr)	ε_v(%)	e	$\sqrt{t}$	log t	
1.00	0.10	17.103				
0.56	0.18	16.529		0.695×10^{-3}	1.102×10^{-3}	
0.28	0.25	15.898		0.390×10^{-3}	0.559×10^{-3}	

699

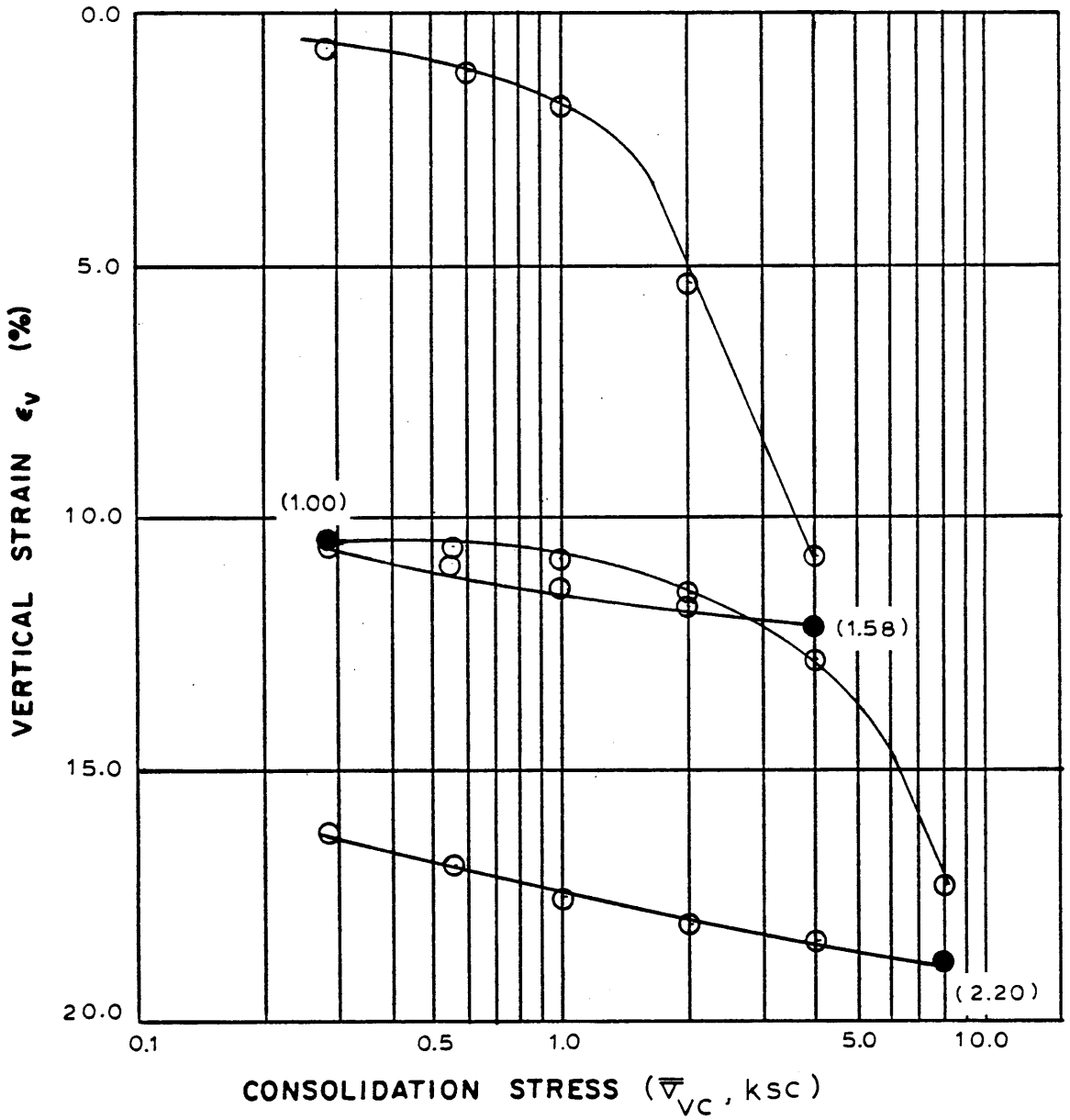

Sample No. 100-102-O-H w_N (%) 44.10 Estimated

Depth 100.22 w_L (%) 50.20 $\bar{\sigma}_{vo}$ 2.35 $\bar{\sigma}_{vm}$ 1.51-1.63

Soil Type Boston Blue Clay w_P (%) 25.26 CR 0.196 RR 0.0147

P.I.(%) 24.94 G_s 2.77 e_o 1.222

o At t_p

● At ( ) hr

Remarks Data from Oedometer test

w_L & w_P estimated from Baligh et al (1980)

Figure D.8 Compression Curve for Sample No. 100-102-O-H

APPENDIX E

Appendix E represents data from thirty five C.R.S.C. tests performed on Boston Blue Clay retrieved from the I-95 test site.

(a) Apparatus Description (Wissa et.al., 197)

Fig. 10.1 shows the basic parts constituting the M.I.T. general purpose consolidation cell. The cell is basically composed of two chambers, an ell chamber and a test specimen chamber hydraulically isolated from each other by means of a rolling diaphram that seals the loading cap to the outer retaining ring. The loading piston uses a rolling diaphram seal and runs in ball bushings. It seals to the loading cap by means of an O-ring to prevent uplift on the piston by the cell pressure.

Top surface drainage from the test specimen occurs through a coarse porous stone located on the underside of the loading cap. Two drainage lines are included to allow for flushing air out from the porous stone after assembly. A back pressure is applied to the test specimen, to ensure 100% saturation, through one of those drainage lines.

The base plate of the cell contains the pore pressure measuring system which uses a high air entry ceramic porous stone, epoxied into a recess in the center of the plate. Two small bone holes connect the stone to a pressure

transducer. The pore pressure measuring system was designed to have a very low volume compressibility in order to minimize hydrodynamic lag during the test.

The test specimen is mounted in a retaining ring using a removable knife-edge shoe cutter. The retaining ring in turn fits tightly into an outer heavy-walled ring that gives it the necessary lateral support to prevent lateral movements during loading. Two O-rings seal the inner ring to the outer ring, which in turn is sealed to the cell base by another O-ring located in the base plate. The test chamber can accomodate two sample sizes, 2.5 and 1.93 in. in diameter.

Vertical deformations of the sample are determined by measuring the movement of the cell piston both with a dial gauge and with an electrical displacement transducer (DCDT). The load applied externally to the piston is monitored with a load cell. The back pressure and cell pressure are monitored with test gauges and pressure transducers and the pore pressure at the impervious surface is measured with a pressure transducer.

(b) Loading

After proper choice of the strain rate compatible with the soil type the clutch is released and the motor is started. Readings initially at 5 to 10 min. are advisable but could be increased to 30 minutes after one hour. A rough estimate of the value of the maximum post pressure could be obtained by

simply plotting the logarithm of the load cell reading versus time during first loading. As soon as the specimen is normally consolidated the logarithm of the load cell reading is linearly related to time, which allows one to predict the value of the maximum past pressure and hence schedule the unload reload cycle ($2 \times \bar{\sigma}_{vm}$) and maximum applied stress before final unloading ($4 \times \bar{\sigma}_{vm}$).

1-D STRAIN CONTROLLED COMPRESSION TEST

COMPUTED RESULTS

INITIAL VOID RATIO= 0.61549
INITIAL HEIGHT= 1.9329

ALL UNITS IN: KG,CM,SEC

LINEAR THEORY

	TIME IN HOURS	VERTICAL STRESS	E	RATE OF STRAIN	EXCESS PORE PRESSURE	C	C/1+E	MV	PERCENT COMPRESSION	K	CV	
1	0.0	0.01626	0.61531	0.0	0.00028	0.0	0.0	0.00678	0.01106	0.0	0.0	1
2	0.33472	0.13496	0.61282	0.12815E-05	0.00424	0.00118	0.00073	0.01301	0.16524	0.563E-06	0.433E-01	2
3	0.65194	0.18375	0.60998	0.15481E-05	0.00819	0.00922	0.00573	0.03623	0.34143	0.351E-06	0.967E-02	3
4	0.98528	0.22943	0.60701	0.15376E-05	0.01271	0.01336	0.00831	0.04039	0.52496	0.224E-06	0.554E-02	4
5	1.45194	0.33942	0.60301	0.14863E-05	0.01582	0.01022	0.00638	0.02270	0.77274	0.173E-06	0.761E-02	5
6	1.78528	0.44785	0.60041	0.13534E-05	0.01915	0.00938	0.00586	0.01498	0.93364	0.130E-06	0.865E-02	6
7	2.11861	0.59611	0.59822	0.11439E-05	0.02396	0.00767	0.00480	0.00926	1.06941	0.873E-07	0.943E-02	7
8	2.45194	0.76998	0.59578	0.12694E-05	0.02989	0.00950	0.00595	0.00876	1.21989	0.774E-07	0.884E-02	8
9	2.78528	0.96757	0.59335	0.12713E-05	0.03469	0.01064	0.00668	0.00772	1.37038	0.666E-07	0.862E-02	9
10	3.11861	1.17153	0.59098	0.12423E-05	0.03611	0.01240	0.00779	0.00731	1.51715	0.623E-07	0.853E-02	10
11	3.43750	1.39342	0.58869	0.12584E-05	0.03249	0.01323	0.00833	0.00651	1.65924	0.700E-07	0.107E-01	11
12	3.77082	1.62801	0.58639	0.12082E-05	0.03639	0.01478	0.00931	0.00618	1.80159	0.598E-07	0.968E-02	12
13	4.12693	1.87631	0.58378	0.12848E-05	0.04119	0.01838	0.01160	0.00663	1.96307	0.560E-07	0.844E-02	13
14	4.43415	2.09785	0.58158	0.12542E-05	0.04346	0.01966	0.01243	0.00626	2.09889	0.517E-07	0.825E-02	14
15	4.76750	2.34663	0.57944	0.11334E-05	0.03362	0.01916	0.01213	0.00547	2.23187	0.602E-07	0.110E-01	15
16	5.32694	2.75491	0.57528	0.13084E-05	0.03701	0.02588	0.01643	0.00645	2.48882	0.628E-07	0.973E-02	16
17	5.75361	3.07715	0.57225	0.12583E-05	0.04063	0.02747	0.01747	0.00600	2.67690	0.548E-07	0.914E-02	17
18	6.30110	3.49433	0.56830	0.12755E-05	0.04543	0.03102	0.01978	0.00603	2.92097	0.494E-07	0.820E-02	18
19	6.53220	3.68548	0.56685	0.11143E-05	0.04600	0.02727	0.01741	0.00485	3.01091	0.426E-07	0.878E-02	19
20	6.86553	3.96534	0.56409	0.14689E-05	0.04712	0.03767	0.02408	0.00630	3.18158	0.546E-07	0.867E-02	20
21	7.21804	4.27376	0.56174	0.11880E-05	0.04170	0.03144	0.02013	0.00489	3.32732	0.497E-07	0.102E-01	21
22	7.55137	4.58290	0.55931	0.12989E-05	0.04452	0.03479	0.02231	0.00504	3.47775	0.508E-07	0.101E-01	22
23	7.88471	4.87616	0.55697	0.12532E-05	0.04396	0.03776	0.02425	0.00513	3.62270	0.495E-07	0.965E-02	23
24	8.21804	5.19266	0.55445	0.13507E-05	0.04396	0.04006	0.02577	0.00512	3.77867	0.531E-07	0.104E-01	24
25	8.55137	5.51682	0.55217	0.12253E-05	0.04480	0.03769	0.02428	0.00454	3.91991	0.472E-07	0.104E-01	25
26	8.88471	5.85331	0.55009	0.11154E-05	0.04566	0.03504	0.02260	0.00398	4.04834	0.420E-07	0.106E-01	26
27	9.21804	6.20756	0.54751	0.13887E-05	0.04453	0.04388	0.02836	0.00470	4.20795	0.535E-07	0.114E-01	27
28	9.55137	6.58564	0.54504	0.13319E-05	0.04390	0.04178	0.02704	0.00423	4.36086	0.518E-07	0.123E-01	28
29	9.88471	6.96156	0.54294	0.11364E-05	0.04305	0.03788	0.02455	0.00363	4.49106	0.450E-07	0.124E-01	29
30	10.19360	7.34735	0.54057	0.13840E-05	0.04587	0.04397	0.02854	0.00399	4.63783	0.513E-07	0.128E-01	30
31	10.53277	7.77797	0.53797	0.13843E-05	0.04311	0.04563	0.02967	0.00393	4.79872	0.544E-07	0.139E-01	31
32	11.34222	3.79395	0.53896	-0.22100E-06	0.02039	0.00138	0.00090	0.00016	4.73740	-0.184E-07	-0.114E+00	32
33	11.82722	2.21347	0.54008	-0.41861E-06	0.00938	0.00209	0.00136	0.00046	4.66774	-0.758E-07	-0.164E+00	33
34	12.28582	1.25195	0.54228	-0.86116E-06	0.00062	0.00385	0.00249	0.00148	4.53201	-0.235E-05	-0.159E+01	34
35	12.69000	0.78449	0.54480	-0.11205E-05	-0.00756	0.00539	0.00349	0.00349	4.37610	0.253E-06	0.725E-01	35
36	13.05528	0.47709	0.54714	-0.11505E-05	-0.01547	0.00471	0.00304	0.00492	4.23120	0.127E-06	0.259E-01	36
37	13.47027	1.12398	0.54642	0.31222E-06	-0.01141	0.00084	0.00054	0.00072	4.27585	-0.468E-07	-0.649E-01	37
38	13.80360	1.68172	0.54499	0.76738E-06	-0.01311	0.00353	0.00229	0.00165	4.36391	-0.100E-06	-0.606E-01	38
39	14.13694	2.37947	0.54308	0.10355E-05	-0.01560	0.00552	0.00358	0.00178	4.48262	-0.113E-06	-0.635E-01	39
40	14.47027	3.24653	0.54118	0.10260E-05	-0.01814	0.00611	0.00396	0.00142	4.60005	-0.962E-07	-0.677E-01	40
41	14.80360	4.26703	0.54020	0.52923E-06	-0.02266	0.00358	0.00232	0.00062	4.66058	-0.397E-07	-0.637E-01	41

42	15.13694	5.33668	0.53895	0.67422E-06	-0.02690	0.00557	0.00362	0.00076	4.73770-0.425E-07-0.562E-01	42
43	15.47027	6.30768	0.53725	0.92333E-06	-0.03189	0.01019	0.00663	0.00114	4.84312-0.490E-07-0.429E-01	43
44	15.80360	7.16777	0.53541	0.99790E-06	-0.03585	0.01438	0.00937	0.00139	4.95691-0.470E-07-0.337E-01	44
45	16.13693	7.88611	0.53354	0.10152E-05	-0.03896	0.01956	0.01276	0.00170	5.07256-0.439E-07-0.259E-01	45
46	16.47026	8.51240	0.53126	0.12429E-05	-0.04433	0.02989	0.01952	0.00238	5.21396-0.471E-07-0.198E-01	46
47	16.80359	9.11028	0.52910	0.11797E-05	-0.04772	0.03188	0.02085	0.00237	5.34790-0.414E-07-0.175E-01	47
48	17.13693	9.71072	0.52681	0.12463E-05	-0.05082	0.03579	0.02344	0.00249	5.48926-0.409E-07-0.164E-01	48
49	17.47026	10.29664	0.52474	0.11315E-05	-0.05558	0.03534	0.02318	0.00232	5.61745-0.339E-07-0.146E-01	49
50	17.80359	10.89152	0.52228	0.13477E-05	-0.05841	0.04382	0.02879	0.00272	5.76981-0.383E-07-0.141E-01	50
51	18.13693	11.49778	0.51985	0.13335E-05	-0.06237	0.04491	0.02955	0.00264	5.92038-0.354E-07-0.134E-01	51
52	18.47026	12.12414	0.51751	0.12844E-05	-0.06289	0.04408	0.02905	0.00246	6.06512-0.337E-07-0.137E-01	52
53	18.80359	12.74880	0.51528	0.12258E-05	-0.06633	0.04436	0.02928	0.00235	6.20314-0.304E-07-0.129E-01	53
54	19.13693	13.42117	0.51294	0.12907E-05	-0.06661	0.04561	0.03015	0.00230	6.34819-0.317E-07-0.138E-01	54
55	19.40582	13.95720	0.51098	0.13384E-05	-0.06802	0.04997	0.03307	0.00242	6.46936-0.322E-07-0.133E-01	55
56	19.70721	14.53822	0.50882	0.13208E-05	-0.04368	0.05303	0.03515	0.00247	6.60321-0.493E-07-0.200E-01	56
57	20.03720	15.22663	0.50653	0.12763E-05	-0.02670	0.04937	0.03277	0.00220	6.74461-0.776E-07-0.353E-01	57
58	20.54248	16.34473	0.50276	0.13790E-05	-0.02505	0.05319	0.03539	0.00224	6.97794-0.890E-07-0.397E-01	58
59	20.85304	14.52655	0.50261	0.88366E-07	-0.03523	-0.00126	-0.00084	-0.00005	6.98711-0.405E-08 0.746E-01	59
60	21.18637	11.68515	0.50309	-0.26213E-06	-0.03472	0.00217	0.00145	0.00011	6.95786 0.122E-07 0.110E+00	60
61	21.54248	9.18591	0.50395	-0.44608E-06	-0.03868	0.00357	0.00238	0.00023	6.90462 0.187E-07 0.816E-01	61
62	21.87582	7.26210	0.50472	-0.42579E-06	-0.04098	0.00327	0.00217	0.00027	6.85701 0.168E-07 0.634E-01	62
63	22.24998	5.45418	0.50567	-0.46777E-06	-0.04296	0.00331	0.00220	0.00035	6.79829 0.177E-07 0.507E-01	63
64	22.48137	4.50626	0.50653	-0.68528E-06	-0.04381	0.00450	0.00299	0.00060	6.74507 0.254E-07 0.422E-01	64
65	22.81471	3.31765	0.50721	-0.37705E-06	-0.02629	0.00223	0.00148	0.00038	6.70284 0.233E-07 0.613E-01	65
66	23.16331	2.34848	0.50827	-0.56236E-06	-0.02775	0.00308	0.00204	0.00073	6.63696 0.330E-07 0.453E-01	66
67	23.59387	1.45796	0.51020	-0.82323E-06	-0.02860	0.00404	0.00268	0.00143	6.51765 0.470E-07 0.328E-01	67
68	23.92720	1.05915	0.51191	-0.94573E-06	-0.02780	0.00537	0.00355	0.00285	6.41148 0.557E-07 0.196E-01	68
69	24.21443	0.74478	0.51393	-0.12876E-05	-0.02893	0.00573	0.00378	0.00424	6.28671 0.730E-07 0.172E-01	69
70	24.54776	0.48289	0.51627	-0.12869E-05	-0.02865	0.00540	0.00356	0.00590	6.14175 0.739E-07 0.125E-01	70
71	24.91914	0.25440	0.51921	-0.14445E-05	-0.03119	0.00458	0.00301	0.00845	5.96014 0.765E-07 0.905E-02	71
72	25.25249	0.11720	0.52181	-0.14283E-05	-0.03091	0.00337	0.00221	0.01249	5.79866 0.766E-07 0.613E-02	72
73	25.58582	0.03674	0.52463	-0.15390E-05	-0.03148	0.00243	0.00159	0.02295	5.62434 0.814E-07 0.354E-02	73

ENGINEERING STRAIN (73)= 5.6243

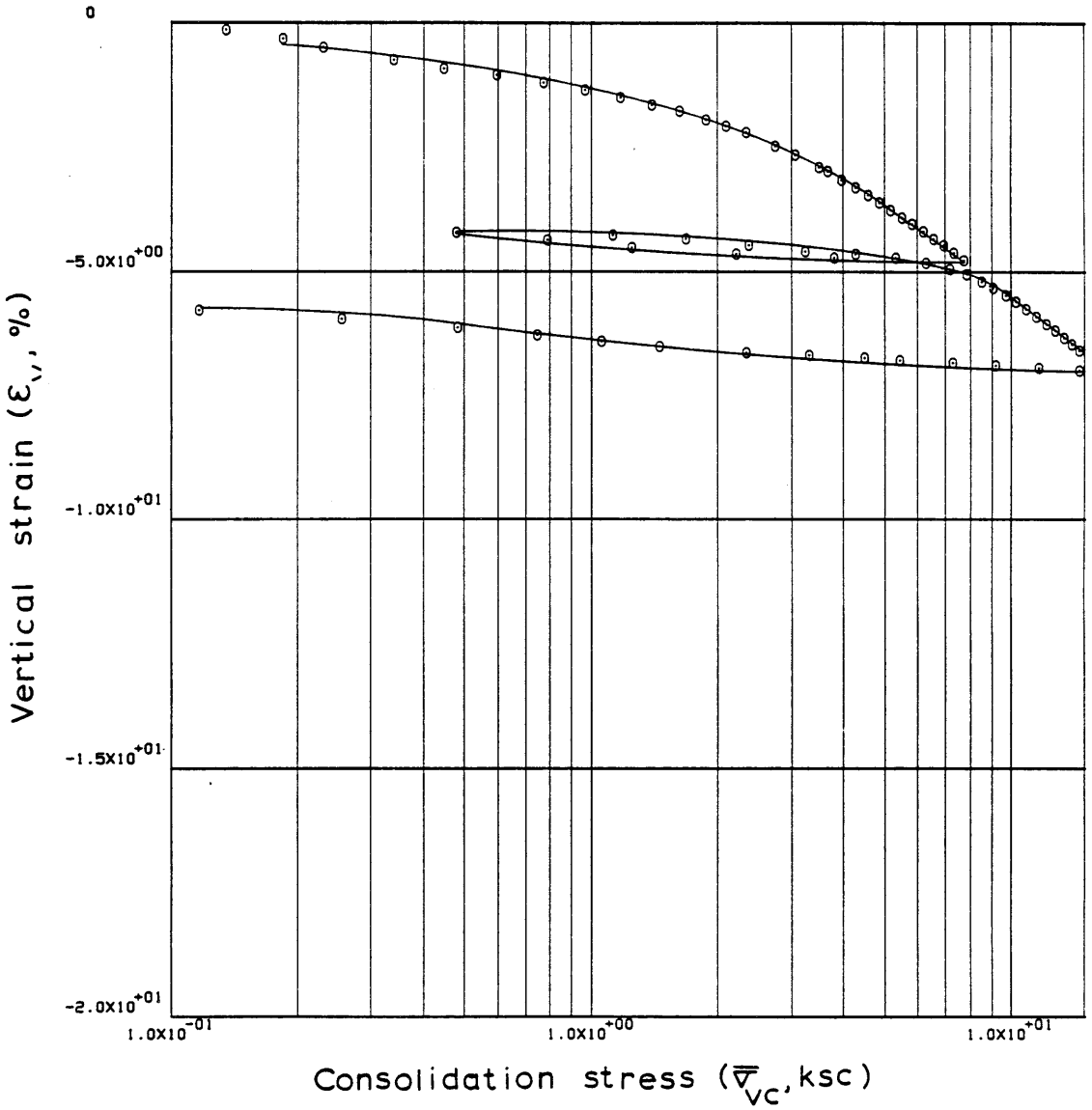

Sample No. 21.5-23.5-C-V w_N (%) 19.61 Estimated

Depth 22.24 w_L (%) 31.30 $\bar{\sigma}_{vo}$ 0.48 $\bar{\sigma}_{vm}$ 3.38-3.78

Soil Type Boston Blue Clay w_P (%) 18.94 CR 0.0600 RR 0.0064

P.I.(%) 12.36 G_s 2.77 e_o 0.6155

o At t_p

Remarks Data from C.R.S.C test

w_L & w_P estimated from Baligh et al (1980)

Figure E.1 Compression Curve for Sample No. 21.5-23.5-C-V

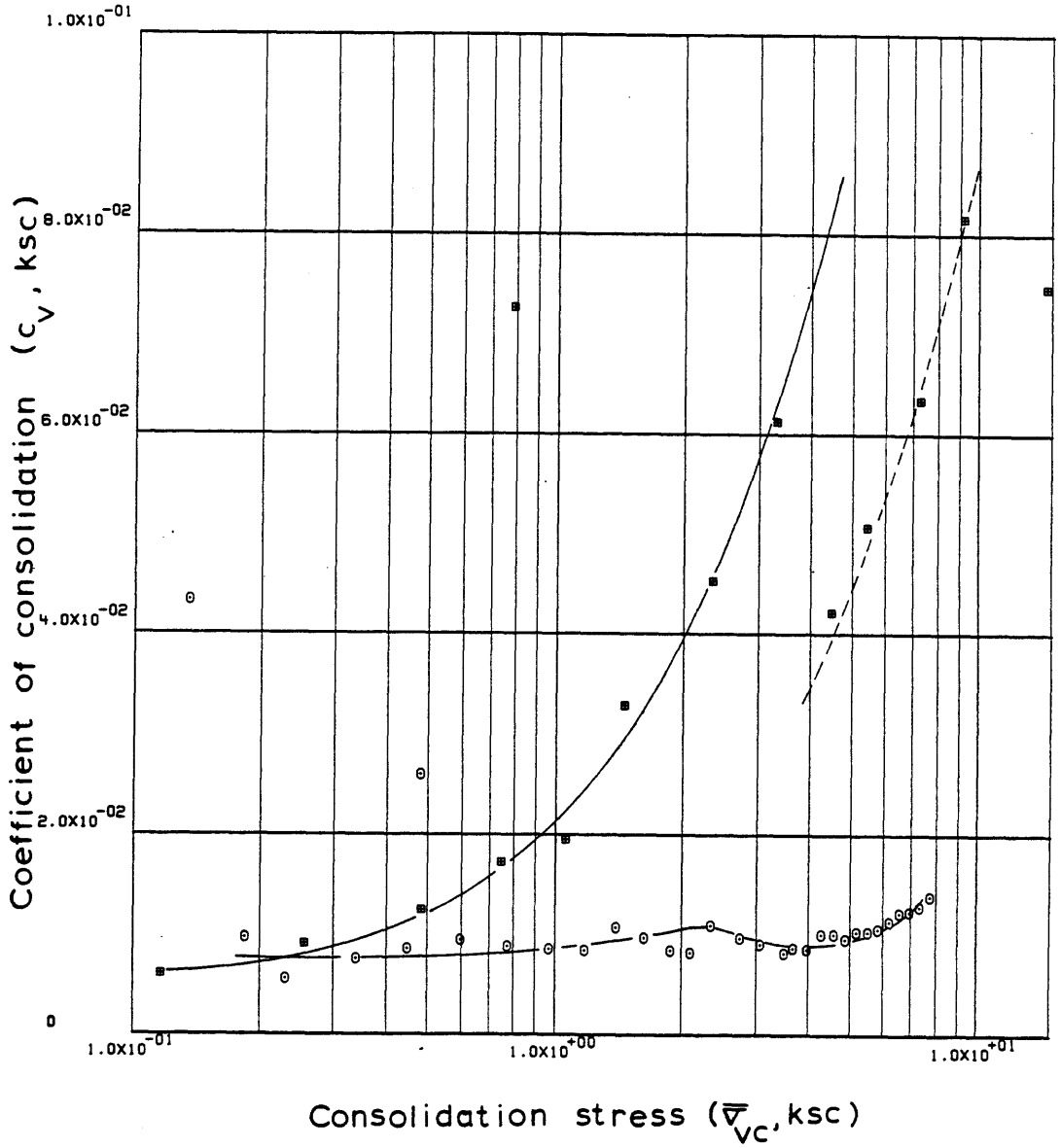

Sample No. 21.5-23.5-C-V w_N (%) 19.61 Estimated

Depth 22.24 w_L (%) 31.30 $\bar{\sigma}_{vo}$ 0.48 $\bar{\sigma}_{vm}$ 3.38, 3.78

Soil Type Boston Blue Clay w_P (%) 18.94 CR 0.0600 RR 0.0064

P.I.(%) 12.36 G_s 2.77 e_o 0.6155

⊙ At t_p

Remarks Data from C.R.S.C test

w_L & w_P estimated from Baligh et al (1980)

Figure E.2 Variation of coefficient of consolidation with consolidation stress for Sample No. 21.5-23.5-C-V

1-D STRAIN CONTROLLED COMPRESSION TEST

COMPUTED RESULTS

INITIAL VOID RATIO= 0.69307
INITIAL HEIGHT= 1.9228

ALL UNITS IN: KG,CM,SEC

LINEAR THEORY

	TIME IN HOURS	VERTICAL STRESS	E	RATE OF STRAIN	EXCESS PORE PRESSURE		C	C/1+E	MV	PERCENT COMPRESSION	K	CV	
1	0.0	0.00744	0.69288	0.0	0.00113	0.0	0.0	0.01482	0.01108	0.0	0.0	1
2	0.37889	0.11639	0.69008	0.12155E-05	0.00113	0.00102	0.00060	0.01522	0.17657	0.199E-05	0.131E+00	2
3	0.85056	0.16082	0.68586	0.14736E-05	0.01092	0.01305	0.00774	0.05633	0.42572	0.247E-06	0.439E-02	3
4	1.26056	0.23040	0.68216	0.14918E-05	0.01825	0.01030	0.00612	0.03164	0.64450	0.149E-06	0.471E-02	4
5	1.79833	0.35793	0.67747	0.14428E-05	0.02731	0.01064	0.00634	0.02190	0.92126	0.959E-07	0.438E-02	5
6	2.18972	0.50557	0.67392	0.15047E-05	0.03182	0.01028	0.00614	0.01436	1.13086	0.854E-07	0.595E-02	6
7	2.79333	0.70630	0.66868	0.14458E-05	0.03795	0.01568	0.00940	0.01565	1.44051	0.684E-07	0.437E-02	7
8	3.12665	0.84085	0.66585	0.14170E-05	0.04049	0.01624	0.00975	0.01264	1.60780	0.626E-07	0.496E-02	8
9	3.45998	0.97620	0.66298	0.14350E-05	0.04387	0.01919	0.01154	0.01272	1.77693	0.583E-07	0.459E-02	9
10	3.79331	1.12267	0.66040	0.12966E-05	0.04696	0.01848	0.01113	0.01062	1.92950	0.491E-07	0.462E-02	10
11	4.12665	1.26640	0.65759	0.14137E-05	0.04718	0.02334	0.01408	0.01180	2.09561	0.531E-07	0.450E-02	11
12	4.45998	1.41961	0.65470	0.14574E-05	0.04831	0.02534	0.01532	0.01141	2.26653	0.533E-07	0.467E-02	12
13	4.79331	1.58084	0.65214	0.12873E-05	0.04971	0.02373	0.01437	0.00958	2.41730	0.456E-07	0.476E-02	13
14	5.12665	1.73971	0.64952	0.13251E-05	0.05162	0.02738	0.01660	0.01001	2.57220	0.450E-07	0.450E-02	14
15	5.45998	1.87604	0.64678	0.13857E-05	0.05190	0.03631	0.02205	0.01220	2.73393	0.467E-07	0.383E-02	15
16	5.79331	2.05846	0.64380	0.15142E-05	0.05218	0.03219	0.01958	0.00996	2.91037	0.506E-07	0.508E-02	16
17	6.12665	2.22130	0.64152	0.11529E-05	0.05162	0.02983	0.01817	0.00850	3.04448	0.388E-07	0.457E-02	17
18	6.45998	2.37904	0.63875	0.14119E-05	0.05296	0.04048	0.02470	0.01074	3.20850	0.462E-07	0.430E-02	18
19	6.79331	2.52493	0.63642	0.11847E-05	0.05078	0.03908	0.02388	0.00974	3.34589	0.403E-07	0.413E-02	19
20	7.12665	2.71201	0.63356	0.14602E-05	0.05275	0.04005	0.02452	0.00937	3.51497	0.476E-07	0.509E-02	20
21	7.45998	2.89169	0.63098	0.13195E-05	0.12320	0.04024	0.02467	0.00881	3.66750	0.184E-07	0.208E-02	21
22	7.79331	3.05133	0.62849	0.12738E-05	0.05162	0.04634	0.02846	0.00958	3.81454	0.422E-07	0.441E-02	22
23	8.12665	3.24254	0.62569	0.14354E-05	0.04993	0.04607	0.02834	0.00901	3.97992	0.490E-07	0.544E-02	23
24	8.42167	3.41258	0.62345	0.12993E-05	0.04880	0.04383	0.02700	0.00812	4.11224	0.453E-07	0.558E-02	24
25	8.75499	3.60290	0.62068	0.14239E-05	0.05049	0.05103	0.03149	0.00898	4.27582	0.478E-07	0.532E-02	25
26	9.08832	3.80035	0.61809	0.13319E-05	0.04874	0.04846	0.02995	0.00809	4.42853	0.461E-07	0.570E-02	26
27	9.42167	4.00932	0.61542	0.13799E-05	0.04902	0.04999	0.03095	0.00792	4.58655	0.474E-07	0.598E-02	27
28	9.75499	4.21002	0.61308	0.12055E-05	0.04846	0.04778	0.02962	0.00721	4.72438	0.417E-07	0.579E-02	28
29	10.08832	4.43542	0.61059	0.12875E-05	0.05071	0.04771	0.02962	0.00685	4.87135	0.425E-07	0.620E-02	29
30	10.42167	4.64849	0.60811	0.12889E-05	0.04712	0.05301	0.03297	0.00726	5.01826	0.456E-07	0.628E-02	30
31	10.75499	4.86987	0.60556	0.13242E-05	0.04571	0.05483	0.03415	0.00718	5.16895	0.482E-07	0.671E-02	31
32	11.08832	5.09901	0.60319	0.12291E-05	0.04036	0.05142	0.03207	0.00644	5.30861	0.505E-07	0.784E-02	32
33	11.42167	5.33970	0.60070	0.12959E-05	0.03867	0.05397	0.03371	0.00646	5.45563	0.554E-07	0.857E-02	33
34	11.75499	5.57864	0.59828	0.12654E-05	0.03501	0.05544	0.03469	0.00635	5.59895	0.595E-07	0.937E-02	34
35	12.08832	5.79766	0.59578	0.13004E-05	0.03204	0.06469	0.04054	0.00712	5.74608	0.666E-07	0.935E-02	35
36	12.42167	6.07384	0.59342	0.12365E-05	0.03255	0.05078	0.03187	0.00537	5.88570	0.622E-07	0.116E-01	36
37	12.75499	6.34324	0.59074	0.14020E-05	0.03085	0.06168	0.03878	0.00624	6.04376	0.742E-07	0.119E-01	37
38	13.08832	6.62215	0.58788	0.15026E-05	0.02720	0.06653	0.04190	0.00646	6.21289	0.898E-07	0.139E-01	38
39	13.41054	6.89570	0.58567	0.12013E-05	0.02495	0.05459	0.03443	0.00509	6.34340	0.781E-07	0.153E-01	39
40	13.76166	5.27694	0.58570	-0.15580E-07	0.00242	0.00012	0.00007	0.00001	6.34155	-0.105E-07	-0.860E+00	40
41	14.09499	3.60722	0.58561	0.49016E-07	-0.00969	-0.00025	-0.00015	-0.00004	6.34706	-0.820E-08	0.233E+00	41

42	14.42832	2.49825	0.58595	-0.17854E-06	-0.00767	0.00093	0.00058	0.00019	6.32698	0.378E-07	0.196E+00	42
43	14.76166	1.70566	0.58723	-0.67015E-06	-0.00429	0.00334	0.00211	0.00101	6.25159	0.254E-06	0.250E+00	43
44	15.09499	1.15761	0.58925	-0.10608E-05	-0.00006	0.00522	0.00328	0.00232	6.13210	0.266E-04	0.115E+02	44
45	15.42832	0.76751	0.59152	-0.11905E-05	0.00522	0.00553	0.00348	0.00366	5.99783	-0.372E-06	-0.102E+00	45
46	15.76166	0.46946	0.59395	-0.12690E-05	0.00016	0.00494	0.00310	0.00511	5.85445	-0.133E-04	-0.260E+01	46
47	16.09499	0.23357	0.59641	-0.12833E-05	0.00325	0.00352	0.00221	0.00653	5.70927	-0.648E-06	-0.993E-01	47
48	16.42831	0.09415	0.59940	-0.15567E-05	-0.00012	0.00329	0.00206	0.01340	5.53279	0.212E-04	0.158E+01	48
49	21.72943	0.15841	0.60114	-0.57052E-07	0.00110	-0.00335	-0.00209	-0.01694	5.42982	-0.858E-07	0.506E-02	49
50	22.14194	0.77488	0.59971	0.60289E-06	0.02949	0.00090	0.00056	0.00145	5.51439	0.337E-07	0.232E-01	50
51	22.72137	1.42360	0.59585	0.11594E-05	0.03512	0.00635	0.00398	0.00373	5.74236	0.542E-07	0.145E-01	51
52	23.12360	1.94143	0.59326	0.11198E-05	0.03681	0.00833	0.00523	0.00313	5.89496	0.498E-07	0.159E-01	52
53	23.48694	2.36243	0.58464	0.41620E-05	0.02596	0.04396	0.02774	0.01293	6.40450	0.260E-06	0.201E-01	53
54	23.77026	2.80481	0.58264	0.12345E-05	0.02596	0.01161	0.00733	0.00285	6.52219	0.768E-07	0.270E-01	54
55	24.17027	3.44152	0.57981	0.12470E-05	0.02490	0.01387	0.00878	0.00282	6.68979	0.806E-07	0.286E-01	55
56	24.68694	4.18843	0.57649	0.11318E-05	0.02985	0.01689	0.01072	0.00282	6.88580	0.608E-07	0.216E-01	56
57	26.02026	5.40351	0.56767	0.11722E-05	0.04087	0.03463	0.02209	0.00463	7.40678	0.455E-07	0.982E-02	57
58	26.42027	5.83864	0.56386	0.16893E-05	0.03019	0.04912	0.03141	0.00559	7.63147	0.883E-07	0.158E-01	58
59	26.58693	6.91877	0.56264	0.13036E-05	0.03003	0.00720	0.00461	0.00072	7.70363	0.684E-07	0.944E-01	59
60	26.93694	7.39482	0.55981	0.14386E-05	0.03250	0.04249	0.02724	0.00381	7.87064	0.694E-07	0.182E-01	60
61	27.33693	7.85940	0.55723	0.11527E-05	0.03250	0.04243	0.02725	0.00357	8.02335	0.555E-07	0.155E-01	61
62	27.68694	8.29666	0.55474	0.12717E-05	0.03250	0.04601	0.02959	0.00366	8.17046	0.610E-07	0.166E-01	62
63	28.38693	9.12229	0.55560	-0.22057E-06	0.02873	-0.00911	-0.00585	-0.00067	8.11943	-0.120E-07	0.178E-01	63
64	28.78693	9.59144	0.54673	0.39855E-05	0.03391	0.17699	0.11443	0.01223	8.64368	0.181E-06	0.148E-01	64
65	29.12027	9.99530	0.54514	0.85308E-06	0.03654	0.03836	0.02483	0.00253	8.73712	0.359E-07	0.142E-01	65
66	29.45360	10.48695	0.54197	0.17158E-05	0.03654	0.06612	0.04288	0.00419	8.92465	0.720E-07	0.172E-01	66
67	30.43193	11.67523	0.53958	0.44060E-06	0.03642	0.02227	0.01446	0.00131	9.06577	0.185E-07	0.142E-01	67
68	30.96359	12.39270	0.53797	0.54690E-06	0.03749	0.02699	0.01755	0.00146	9.16084	0.223E-07	0.153E-01	68
69	31.29692	13.28728	0.53373	0.23029E-05	0.03647	0.06081	0.03965	0.00309	9.41118	0.958E-07	0.310E-01	69
70	31.96359	13.73808	0.53155	0.59350E-06	0.03765	0.06537	0.04268	0.00316	9.54002	0.238E-07	0.755E-02	70
71	32.29692	14.25993	0.52917	0.12977E-05	0.03890	0.06387	0.04177	0.00298	9.68069	0.503E-07	0.169E-01	71
72	32.63026	14.75047	0.52730	0.10204E-05	0.03902	0.05529	0.03620	0.00250	9.79115	0.393E-07	0.158E-01	72
73	32.96359	15.26817	0.52512	0.11922E-05	0.03766	0.06326	0.04148	0.00276	9.92000	0.475E-07	0.172E-01	73
74	33.29692	15.78847	0.52259	0.13819E-05	0.03857	0.07536	0.04950	0.00319	10.06915	0.536E-07	0.168E-01	74
75	33.63026	16.34653	0.52061	0.10839E-05	0.03953	0.05692	0.03743	0.00233	10.18596	0.409E-07	0.175E-01	75
76	33.96359	16.88167	0.51831	0.12663E-05	0.03858	0.07165	0.04719	0.00284	10.32225	0.488E-07	0.172E-01	76
77	34.37692	17.61481	0.51570	0.11540E-05	0.04112	0.06122	0.04039	0.00234	10.47595	0.416E-07	0.178E-01	77
78	34.72830	15.06487	0.51614	-0.22763E-06	-0.00578	0.00279	0.00184	0.00011	10.45016	0.583E-07	0.517E+00	78
79	35.06165	12.21019	0.51642	-0.15421E-06	-0.01267	0.00133	0.00088	0.00006	10.43359	0.180E-07	0.278E+00	79
80	35.39499	9.89435	0.51692	-0.27404E-06	-0.01667	0.00237	0.00156	0.00014	10.40414	0.244E-07	0.172E+00	80
81	35.72832	7.93899	0.51764	-0.39381E-06	-0.02294	0.00326	0.00215	0.00024	10.36177	0.255E-07	0.105E+00	81
82	36.06166	6.28483	0.51867	-0.56465E-06	-0.02565	0.00441	0.00290	0.00041	10.30098	0.327E-07	0.799E-01	82
83	36.39499	4.92641	0.51957	-0.49590E-06	-0.02588	0.00371	0.00244	0.00044	10.24760	0.285E-07	0.651E-01	83
84	36.72832	3.79103	0.52038	-0.44440E-06	-0.02797	0.00310	0.00204	0.00047	10.19969	0.237E-07	0.504E-01	84
85	37.06166	2.84273	0.52150	-0.61476E-06	-0.03028	0.00390	0.00256	0.00078	10.13338	0.303E-07	0.390E-01	85
86	37.39499	2.07732	0.52263	-0.61442E-06	-0.03141	0.00358	0.00235	0.00096	10.06706	0.292E-07	0.304E-01	86
87	37.72832	1.51693	0.52475	-0.11588E-05	-0.03045	0.00674	0.00442	0.00248	9.94188	0.571E-07	0.230E-01	87
88	38.06166	1.12710	0.52652	-0.97027E-06	-0.02289	0.00598	0.00392	0.00299	9.83687	0.637E-07	0.213E-01	88
89	38.39499	0.86066	0.52815	-0.88422E-06	-0.02983	0.00601	0.00393	0.00398	9.74110	0.446E-07	0.112E-01	89
90	38.72832	0.59092	0.53083	-0.14598E-05	-0.02949	0.00713	0.00466	0.00649	9.58273	0.748E-07	0.115E-01	90
91	39.06166	0.38802	0.53357	-0.14911E-05	-0.02808	0.00652	0.00425	0.00882	9.42064	0.805E-07	0.913E-02	91
92	39.39499	0.21114	0.53653	-0.16066E-05	-0.03469	0.00487	0.00317	0.01090	9.24565	0.705E-07	0.647E-02	92
93	39.72832	0.08530	0.53943	-0.15698E-05	-0.03728	0.00320	0.00208	0.01497	9.07439	0.644E-07	0.430E-02	93
94	40.06166	-0.02806	0.54227	-0.15332E-05	-0.02803	0.0	0.0	0.0	8.90680	0.839E-07	0.100E+05	94

ENGINEERING STRAIN (94)= 8.9068

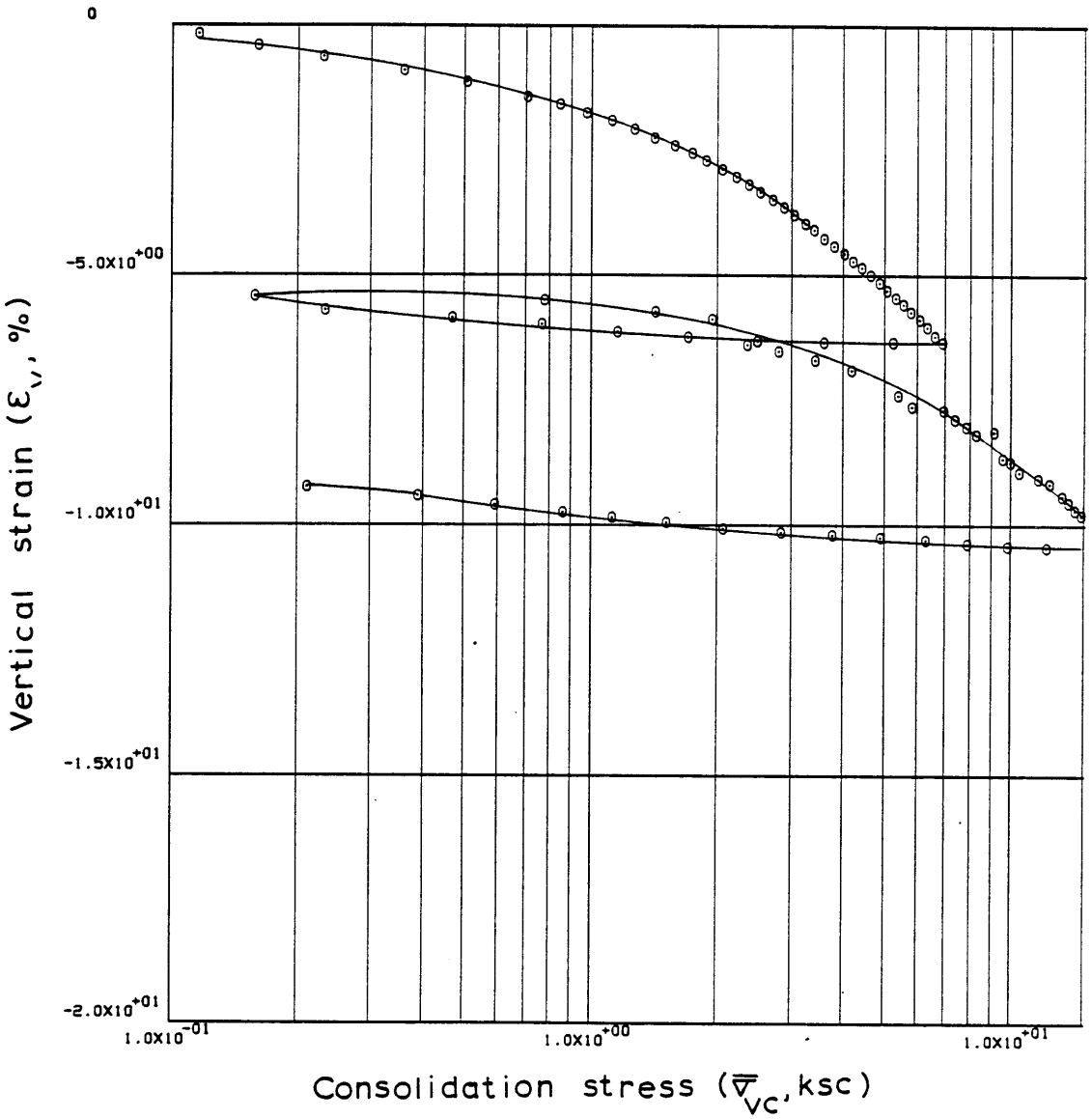

Sample No. 21.5-23.5-C-H w_N (%) 22.09 Estimated

Depth 22.43 w_L (%) 31.30 $\bar{\sigma}_{vo}$ 0.48 $\bar{\sigma}_{vm}$ 207.237

Soil Type Boston w_P (%) 18.96 CR 0.0884 RR 0.0069

Blue Clay P.I.(%) 12.34 G_s 2.77 e_o 0.6937

⊙ At t_p Remarks Data from C.R.S.C test

w_L & w_P estimated from Baligh et al (1980)

Figure E.3 Compression Curve for Sample No. 21.5-23.5-C-H

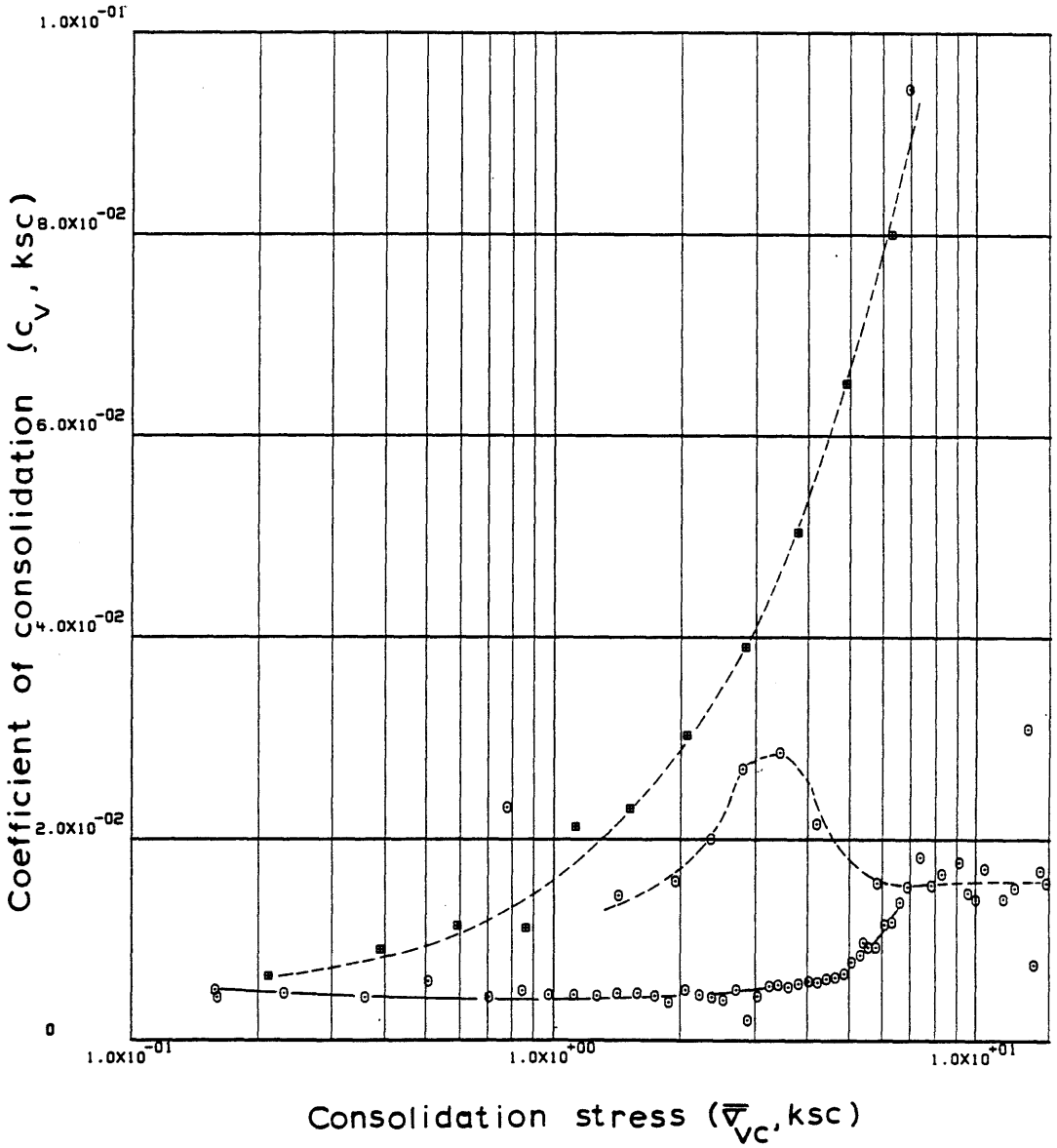

Sample No. 21.5-23.5-C-H w_N (%) 22.09 Estimated

Depth 22.43 w_L (%) 31.30 $\bar{\sigma}_{vo}$ 0.48 $\bar{\sigma}_{vm}$ 207.237

Soil Type Boston w_P (%) 18.96 CR 0.0884 RR 0.0069

Blue Clay P.I.(%) 12.34 G_S 2.77 e_o 0.6937

⊙ At t_p Remarks Data from C.R.S.C test

w_L & w_P estimated from Baligh et al (1980)

Figure E.4 Variation of coeffient of consolidation with consolidation stress for Sample No. 21.5-23.5-C-H

1-D STRAIN CONTROLLED COMPRESSION TEST

COMPUTED RESULTS

INITIAL VOID RATIO= 0.66076
INITIAL HEIGHT= 1.9380

ALL UNITS IN: KG,CM,SEC

LINEAR THEORY

	TIME IN HOURS	VERTICAL STRESS	E	RATE OF STRAIN	EXCESS PORE PRESSURE	C	C/1+E	MV	PERCENT COMPRESSION	K	CV	
1	0.0	0.15112	0.66061	0.0	0.0	0.0	0.0	0.00061	0.00922	0.100E+01	0.165E+07	1
2	0.28473	0.24568	0.65857	0.11972E-05	0.00452	0.00419	0.00253	0.01298	0.13179	0.496E-06	0.382E-01	2
3	0.61806	0.30046	0.65590	0.13455E-05	0.00452	0.01328	0.00802	0.02947	0.29276	0.555E-06	0.188E-01	3
4	0.92111	0.31228	0.65341	0.13809E-05	0.00735	0.06460	0.03907	0.12753	0.44273	0.350E-06	0.274E-02	4
5	1.42111	0.40815	0.64921	0.14122E-05	0.00735	0.01566	0.00949	0.02651	0.69519	0.356E-06	0.134E-01	5
6	1.75446	0.44868	0.64627	0.14916E-05	0.00565	0.03113	0.01891	0.04417	0.87262	0.487E-06	0.110E-01	6
7	2.08778	0.53274	0.64356	0.13710E-05	0.00282	0.01574	0.00958	0.01957	1.03540	0.893E-06	0.456E-01	7
8	2.42111	0.61757	0.64092	0.13403E-05	-0.00033	0.01786	0.01089	0.01896	1.19435	-0.749E-05	-0.395E+00	8
9	2.75446	0.72449	0.63843	0.12689E-05	0.00282	0.01562	0.00954	0.01424	1.34459	0.822E-06	0.577E-01	9
10	3.31195	0.89073	0.63412	0.13154E-05	0.0	0.02088	0.01278	0.01588	1.60431	0.100E+01	0.630E+05	10
11	3.64528	0.92000	0.63308	0.52706E-06	-0.00282	0.03194	0.01956	0.02160	1.66652	-0.339E-06	-0.157E-01	11
12	3.97862	0.94740	0.63241	0.34118E-06	-0.00282	0.02278	0.01396	0.01495	1.70676	-0.219E-06	-0.147E-01	12
13	4.31195	1.00030	0.63126	0.58966E-06	0.0	0.02124	0.01302	0.01338	1.77625	0.100E+01	0.748E+05	13
14	4.64528	1.03027	0.63051	0.38523E-06	-0.00315	0.02555	0.01567	0.01542	1.82167	-0.221E-06	-0.143E-01	14
15	4.97862	1.08248	0.62977	0.37575E-06	0.0	0.01486	0.00912	0.00864	1.86591	0.100E+01	0.116E+06	15
16	5.31195	1.23135	0.62744	0.11946E-05	0.00080	0.01810	0.01112	0.00963	2.00635	0.269E-05	0.280E+00	16
17	5.64528	1.34147	0.62516	0.11682E-05	0.00250	0.02660	0.01637	0.01273	2.14354	0.842E-06	0.661E-01	17
18	5.97862	1.49154	0.62270	0.12634E-05	0.00080	0.02319	0.01429	0.01010	2.29166	0.283E-05	0.280E+00	18
19	6.31195	1.64462	0.62018	0.12967E-05	-0.00033	0.02581	0.01593	0.01016	2.44347	-0.706E-05	-0.695E+00	19
20	6.64528	1.81887	0.61766	0.12987E-05	0.00532	0.02504	0.01548	0.00894	2.59528	0.435E-06	0.486E-01	20
21	6.97862	1.95770	0.61489	0.14263E-05	0.00250	0.03758	0.02327	0.01233	2.76170	0.101E-05	0.823E-01	21
22	7.31195	2.13327	0.61259	0.11929E-05	0.00363	0.02688	0.01667	0.00815	2.90071	0.582E-06	0.714E-01	22
23	7.64528	2.29816	0.60997	0.13521E-05	0.00532	0.03507	0.02178	0.00984	3.05798	0.448E-06	0.455E-01	23
24	7.97862	2.48988	0.60727	0.14015E-05	0.00532	0.03374	0.02099	0.00877	3.22076	0.463E-06	0.528E-01	24
25	8.31195	2.66734	0.60463	0.13724E-05	0.00363	0.03839	0.02392	0.00928	3.37985	0.663E-06	0.714E-01	25
26	8.69139	2.85773	0.60177	0.13049E-05	0.00815	0.04141	0.02585	0.00936	3.55180	0.280E-06	0.299E-01	26
27	9.02473	3.04889	0.59940	0.12343E-05	0.00645	0.03659	0.02288	0.00775	3.69444	0.333E-06	0.430E-01	27
28	9.35806	3.22529	0.59705	0.12266E-05	0.01130	0.04179	0.02617	0.00834	3.83597	0.189E-06	0.226E-01	28
29	9.69139	3.41704	0.59474	0.12065E-05	0.01130	0.03998	0.02507	0.00755	3.97499	0.185E-06	0.245E-01	29
30	10.02473	3.60879	0.59195	0.14629E-05	0.01130	0.05118	0.03215	0.00916	4.14328	0.223E-06	0.244E-01	30
31	10.35806	3.80091	0.58951	0.12812E-05	0.01333	0.04711	0.02964	0.00800	4.29042	0.165E-06	0.207E-01	31
32	10.69139	3.99229	0.58697	0.13330E-05	0.01130	0.05170	0.03258	0.00836	4.44331	0.202E-06	0.242E-01	32
33	11.02473	4.21000	0.58452	0.12856E-05	0.01615	0.04603	0.02905	0.00709	4.59050	0.136E-06	0.192E-01	33
34	11.35806	4.38809	0.58200	0.13285E-05	0.01615	0.06089	0.03849	0.00895	4.74236	0.140E-06	0.157E-01	34
35	11.69139	4.60539	0.57942	0.13627E-05	0.01898	0.05341	0.03382	0.00753	4.89784	0.122E-06	0.162E-01	35
36	11.93251	4.76789	0.57753	0.13757E-05	0.02180	0.05435	0.03445	0.00735	5.01128	0.107E-06	0.145E-01	36
37	12.26584	4.98896	0.57474	0.14793E-05	0.01898	0.06167	0.03916	0.00803	5.17963	0.132E-06	0.164E-01	37
38	12.59917	5.21933	0.57226	0.13119E-05	0.01978	0.05485	0.03488	0.00683	5.32867	0.112E-06	0.163E-01	38
39	13.09222	5.57355	0.56798	0.15391E-05	0.02260	0.06522	0.04160	0.00771	5.58658	0.114E-06	0.148E-01	39
40	13.35890	5.76326	0.56596	0.13422E-05	0.02510	0.06029	0.03850	0.00679	5.70807	0.893E-07	0.131E-01	40
41	13.57028	5.92702	0.56399	0.16589E-05	0.02340	0.07046	0.04505	0.00771	5.82695	0.118E-06	0.153E-01	41

42	13.90390	6.20147	0.56156	0.12956E-05	0.02510	0.05368	0.03438	0.00567	5.97327	0.857E-07	0.151E-01	42
43	14.41196	6.59803	0.55740	0.14608E-05	0.02340	0.06713	0.04310	0.00674	6.22383	0.103E-06	0.153E-01	43
44	14.74529	6.88183	0.55460	0.14979E-05	0.02905	0.06635	0.04268	0.00633	6.39207	0.849E-07	0.134E-01	44
45	15.07861	7.16843	0.55195	0.14245E-05	0.02702	0.06505	0.04192	0.00596	6.55185	0.865E-07	0.145E-01	45
46	15.41196	7.45651	0.54931	0.14210E-05	0.02872	0.06702	0.04326	0.00592	6.71089	0.809E-07	0.137E-01	46
47	15.94528	7.97566	0.54474	0.15390E-05	0.02669	0.06781	0.04390	0.00569	6.98572	0.937E-07	0.165E-01	47
48	16.34723	5.95430	0.54508	-0.14939E-06	-0.02131	0.00114	0.00074	0.00011	6.96565	0.114E-07	0.107E+00	48
49	16.68306	4.31350	0.54629	-0.64967E-06	-0.02414	0.00377	0.00244	0.00048	6.89253	0.438E-07	0.915E-01	49
50	17.16890	2.79439	0.54853	-0.82601E-06	-0.02446	0.00515	0.00333	0.00095	6.75778	0.551E-07	0.580E-01	50
51	17.47250	2.15301	0.54971	-0.69901E-06	-0.02728	0.00454	0.00293	0.00119	6.68649	0.419E-07	0.352E-01	51
52	17.81778	1.60555	0.55120	-0.77143E-06	-0.02728	0.00507	0.00327	0.00175	6.59692	0.463E-07	0.264E-01	52
53	18.34001	1.14637	0.55193	-0.24973E-06	-0.01599	0.00216	0.00139	0.00102	6.55309	0.256E-07	0.250E-01	53
54	18.64557	0.92178	0.55296	-0.60419E-06	-0.02559	0.00473	0.00305	0.00296	6.49094	0.388E-07	0.131E-01	54
55	18.91139	1.29315	0.55290	0.40867E-07	-0.01035	0.00018	0.00011	0.00011	6.49457	-0.649E-08	-0.616E-01	55
56	19.24474	1.89832	0.55229	0.32591E-06	0.00829	0.00158	0.00102	0.00065	6.53114	0.645E-07	0.998E-01	56
57	19.69473	2.83088	0.55090	0.55582E-06	0.00547	0.00350	0.00225	0.00097	6.61523	0.166E-06	0.172E+00	57
58	20.02806	3.52621	0.54957	0.71301E-06	0.00692	0.00604	0.00389	0.00123	6.69505	0.168E-06	0.137E+00	58
59	20.36139	22.27710	0.54853	0.56077E-06	25.52824	0.00056	0.00036	0.00004	6.75778	0.359E-10	0.999E-03	59
60	20.69473	5.20613	0.54677	0.94856E-06	0.01224	-0.00121	-0.00078	-0.00007	6.86383	0.126E-06	-0.189E+01	60
61	21.02806	6.08075	0.54495	0.98253E-06	0.01676	0.01172	0.00759	0.00135	6.97348	0.953E-07	0.707E-01	61
62	21.36139	6.85713	0.54291	0.10985E-05	0.02240	0.01693	0.01097	0.00170	7.09595	0.795E-07	0.468E-01	62
63	21.69473	7.51400	0.54098	0.10461E-05	0.02104	0.02114	0.01372	0.00191	7.21243	0.804E-07	0.421E-01	63
64	22.02806	8.03286	0.53864	0.12662E-05	0.02556	0.03502	0.02276	0.00293	7.35321	0.799E-07	0.273E-01	64
65	22.35944	8.52255	0.53632	0.12632E-05	0.02636	0.03913	0.02547	0.00308	7.49263	0.770E-07	0.250E-01	65
66	22.69305	8.98413	0.53384	0.13513E-05	0.03200	0.04719	0.03077	0.00352	7.64252	0.676E-07	0.192E-01	66
67	23.11417	9.51791	0.53053	0.14261E-05	0.03200	0.05734	0.03746	0.00405	7.84175	0.711E-07	0.175E-01	67
68	23.50307	10.02149	0.52745	0.14365E-05	0.03449	0.05958	0.03901	0.00399	8.02673	0.662E-07	0.166E-01	68
69	23.83640	10.48487	0.52527	0.11940E-05	0.03731	0.04834	0.03169	0.00309	8.15833	0.507E-07	0.164E-01	69
70	24.16972	10.92574	0.52254	0.14924E-05	0.03483	0.06620	0.04348	0.00406	8.32248	0.676E-07	0.167E-01	70
71	24.50307	11.38731	0.52005	0.13646E-05	0.04047	0.06016	0.03957	0.00355	8.47237	0.530E-07	0.150E-01	71
72	24.83640	11.82528	0.51759	0.13503E-05	0.04047	0.06517	0.04294	0.00370	8.62044	0.523E-07	0.141E-01	72
73	25.16972	12.31610	0.51511	0.13692E-05	0.04330	0.06121	0.04040	0.00335	8.77032	0.494E-07	0.148E-01	73
74	25.50307	12.79558	0.51270	0.13229E-05	0.04014	0.06290	0.04158	0.00331	8.91496	0.514E-07	0.155E-01	74
75	25.83640	13.32550	0.51009	0.14405E-05	0.04578	0.06432	0.04260	0.00326	9.07213	0.489E-07	0.150E-01	75
76	26.18304	13.87096	0.50733	0.14683E-05	0.04861	0.06882	0.04566	0.00336	9.23840	0.467E-07	0.139E-01	76
77	26.64667	14.62370	0.50390	0.13670E-05	0.04545	0.06495	0.04319	0.00303	9.44504	0.463E-07	0.153E-01	77
78	26.98000	15.19457	0.50175	0.11956E-05	0.05109	0.05623	0.03745	0.00251	9.57475	0.359E-07	0.143E-01	78
79	27.31334	15.78287	0.49914	0.14507E-05	0.05109	0.06871	0.04584	0.00296	9.73192	0.434E-07	0.147E-01	79
80	27.64667	16.38428	0.49662	0.14025E-05	0.04940	0.06737	0.04502	0.00280	9.88358	0.433E-07	0.155E-01	80
81	27.85973	16.64987	0.49483	0.15615E-05	0.04093	0.11132	0.07447	0.00451	9.99139	0.580E-07	0.129E-01	81
82	28.22278	14.09011	0.49483	0.0	-0.02148	0.0	0.0	0.0	9.99139	0.0	0.100E+05	82
83	28.55612	11.35995	0.49574	-0.50712E-06	-0.02995	0.00423	0.00283	0.00022	9.93657	0.258E-07	0.116E+00	83
84	28.88945	9.12222	0.49656	-0.45615E-06	-0.03841	0.00373	0.00250	0.00024	9.88722	0.181E-07	0.740E-01	84
85	29.22278	7.31745	0.49792	-0.75931E-06	-0.04324	0.00619	0.00413	0.00050	9.80504	0.268E-07	0.531E-01	85
86	29.55612	5.81302	0.49932	-0.77551E-06	-0.04324	0.00606	0.00404	0.00062	9.72104	0.275E-07	0.444E-01	86
87	30.22278	3.54670	0.50229	-0.82419E-06	-0.04920	0.00601	0.00400	0.00087	9.54211	0.257E-07	0.295E-01	87
88	30.55612	2.75360	0.50405	-0.97465E-06	-0.04920	0.00695	0.00462	0.00147	9.43617	0.305E-07	0.207E-01	88
89	30.88945	2.16562	0.50553	-0.82262E-06	-0.04920	0.00619	0.00411	0.00168	9.34671	0.258E-07	0.154E-01	89
90	31.22278	1.70257	0.50711	-0.87206E-06	-0.05202	0.00656	0.00435	0.00226	9.25174	0.259E-07	0.115E-01	90
91	31.52834	1.37439	0.50811	-0.60338E-06	-0.05202	0.00467	0.00310	0.00202	9.19145	0.180E-07	0.888E-02	91
92	31.95334	1.15107	0.50839	-0.12038E-06	-0.04405	0.00157	0.00104	0.00082	9.17473	0.423E-08	0.513E-02	92
93	32.29529	0.92040	0.50954	-0.62045E-06	-0.04688	0.00516	0.00342	0.00331	9.10530	0.205E-07	0.620E-02	93
94	32.69585	0.86300	0.51006	-0.23684E-06	-0.01978	0.00800	0.00530	0.00595	9.07425	0.186E-07	0.312E-02	94
95	33.02917	0.75231	0.51076	-0.38647E-06	-0.03922	0.00511	0.00338	0.00419	9.03207	0.153E-07	0.366E-02	95
96	33.36250	0.62602	0.51276	-0.11051E-05	-0.05583	0.01092	0.00722	0.01050	8.91127	0.308E-07	0.294E-02	96

97	33.69585	0.51278	0.51477	-0.11020E-05	-0.05019	0.01004	0.00663	0.01168	8.79065	0.343E-07	0.294E-02	97
98	34.02917	0.41888	0.51695	-0.12005E-05	-0.05301	0.01080	0.00712	0.01534	8.65907	0.355E-07	0.231E-02	98
99	34.33723	0.34857	0.51865	-0.10092E-05	-0.05019	0.00926	0.00609	0.01592	8.55672	0.316E-07	0.198E-02	99

ENGINEERING STRAIN (99)= 8.5567

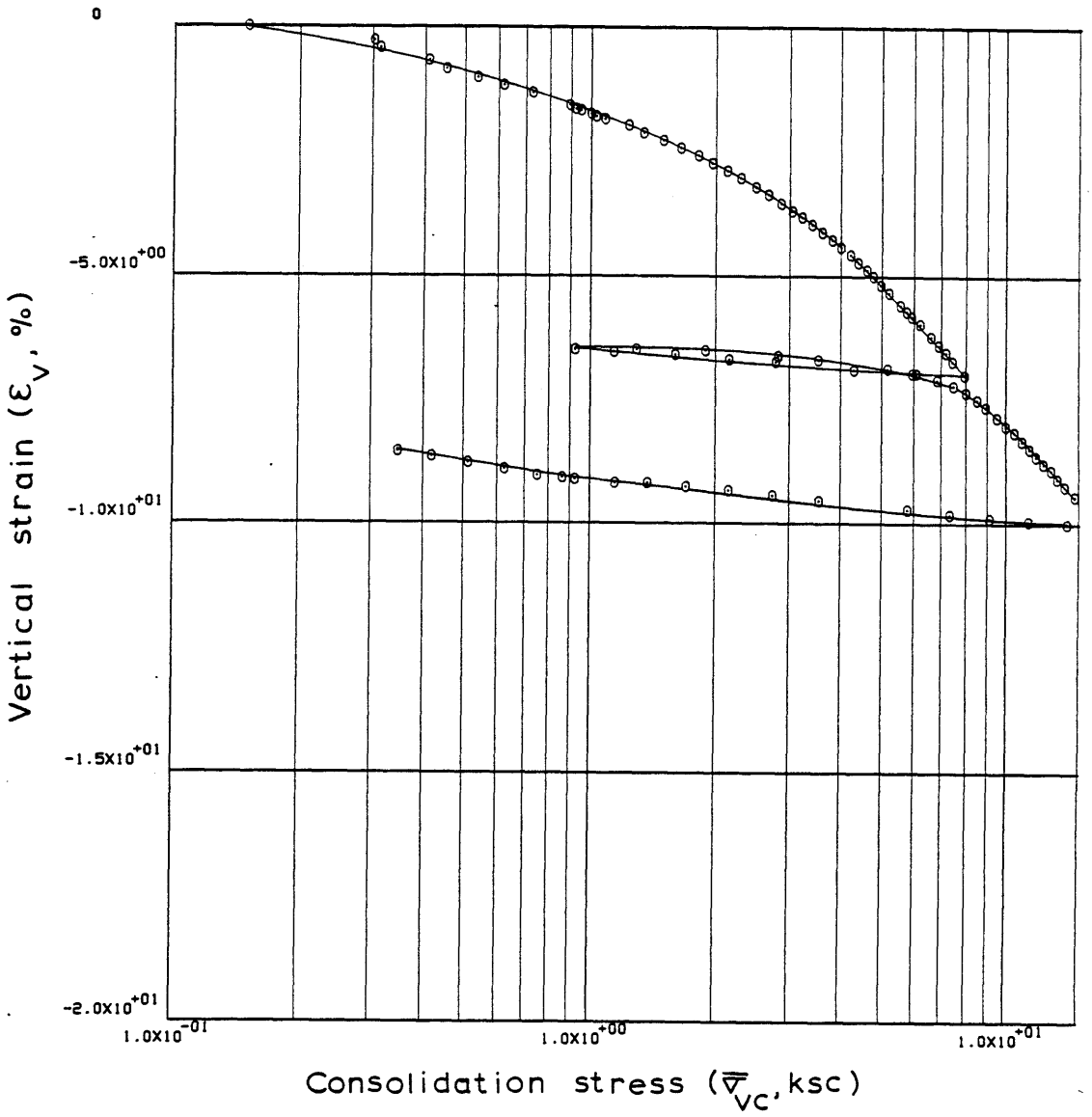

Sample No. 26.5-28.5-C-V w_N (%) 21.12 Estimated

Depth 27.43 w_L (%) 31.30 $\bar{\sigma}_{vo}$ 0.60 $\bar{\sigma}_{vm}$ 237-292

Soil Type Boston Blue Clay w_P (%) 19.62 CR 0.1077 RR 0.0064

P.I.(%) 11.68 G_s 2.77 e_o 0.6608

o At t_p

Remarks Data from C.R.S.C test

w_L & w_P estimated from Baligh et al (1980)

Figure E.5 Compression Curve for Sample No. 26.5-28.5-C-V

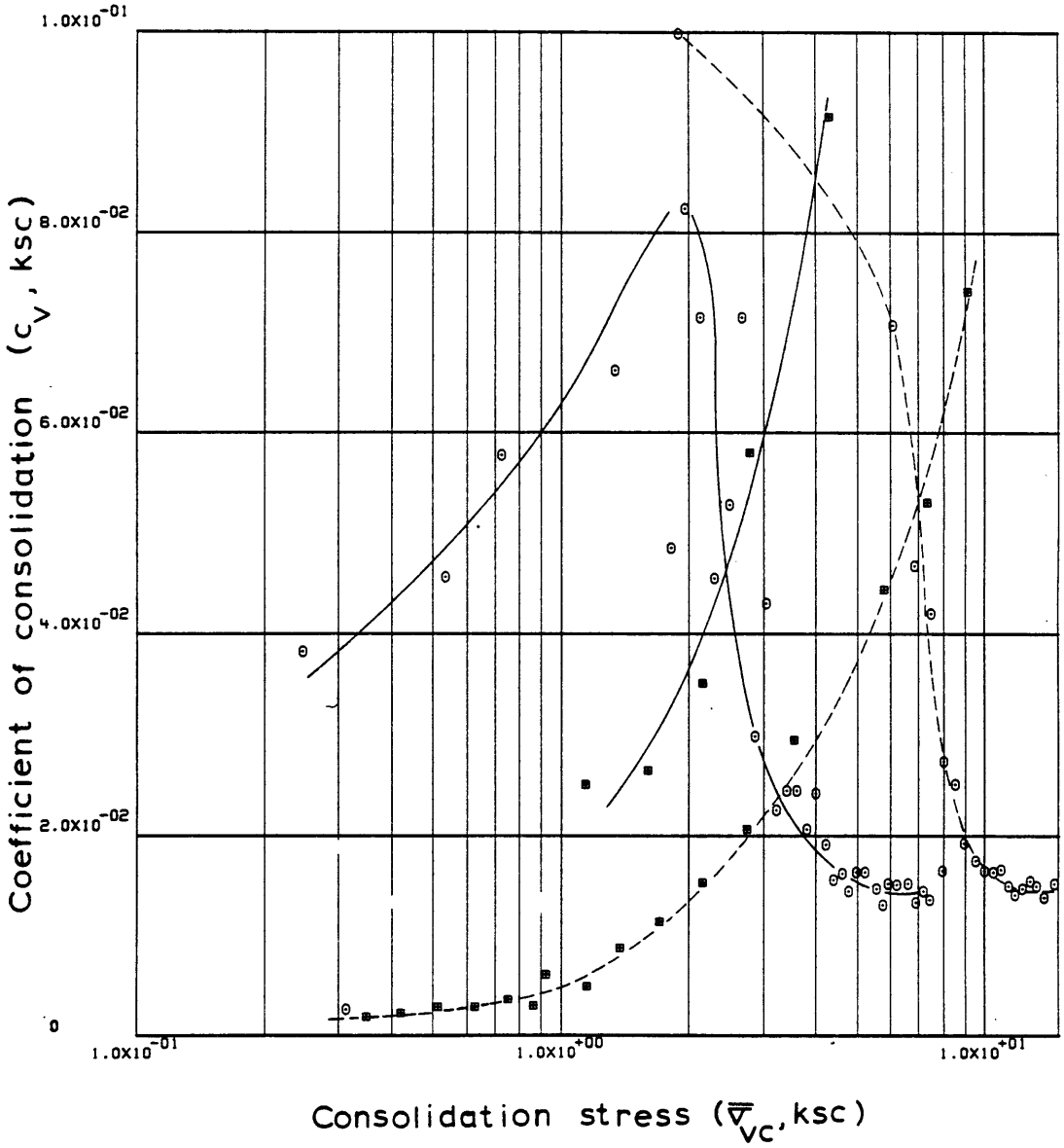

Sample No. 26.5-28.5.C.V w_N (%) 21.12 Estimated

Depth 27.43 w_L (%) 31.30 $\bar{\sigma}_{vo}$ 0.60 $\bar{\sigma}_{vm}$ 237-292

Soil Type Boston w_P (%) 19.62 CR 0.1077 RR 0.0064

Blue Clay P.I.(%) 11.68 G_s 2.77 e_o 0.6608

o At t_p Remarks Data from C.R.S.C test

w_L & w_P estimated from Baligh et al (1980)

Figure E.6 Variation of coefficient of consolidation with consolidation stress for Sample No. 26.5-28.5-C-V

1-D STRAIN CONTROLLED COMPRESSION TEST

COMPUTED RESULTS

INITIAL VOID RATIO= 0.67548
INITIAL HEIGHT= 1.9507

ALL UNITS IN: KG,CM,SEC

LINEAR THEORY

	TIME IN HOURS	VERTICAL STRESS	E	RATE OF STRAIN	EXCESS PORE PRESSURE	C	C/1+E	MV	PERCENT COMPRESSION	K	CV	
1	0.0	0.19980	0.67529	0.0	0.00296	0.0	0.0	0.00056	0.01131	0.0	0.0	1
2	0.33333	0.23045	0.67255	0.13660E-05	0.00014	0.01920	0.01148	0.05347	0.17493	0.190E-04	0.355E+00	2
3	0.72417	0.25181	0.66886	0.15696E-05	-0.00156	0.04159	0.02492	0.10341	0.39493	-0.190E-05	-0.183E-01	3
4	1.07028	0.28247	0.66572	0.15117E-05	-0.00439	0.02731	0.01639	0.06144	0.58217	-0.647E-06	-0.105E-01	4
5	1.40361	0.28880	0.66246	0.16336E-05	-0.00472	0.14703	0.08844	0.30957	0.77670	-0.648E-06	-0.209E-02	5
6	1.85083	0.30849	0.65850	0.14826E-05	-0.00754	0.06002	0.03619	0.12123	1.01299	-0.366E-06	-0.302E-02	6
7	2.18417	0.33537	0.65546	0.15330E-05	-0.00472	0.03644	0.02201	0.06843	1.19475	-0.603E-06	-0.882E-02	7
8	5.40056	0.35420	0.65277	0.14070E-06	2.33174	0.04929	0.02982	0.08653	1.35544	0.112E-09	0.129E-05	8
9	5.73389	0.38710	0.65185	0.46127E-06	2.33118	0.01030	0.00623	0.01682	1.41000	0.366E-09	0.218E-04	9
10	6.40056	0.50913	0.65021	0.41442E-06	2.32910	0.00599	0.00363	0.00815	1.50797	0.328E-09	0.403E-04	10
11	6.73389	0.67229	0.64813	0.10493E-05	2.32816	0.00747	0.00453	0.00772	1.63185	0.830E-09	0.108E-03	11
12	7.06722	0.82387	0.64564	0.12641E-05	2.32740	0.01227	0.00746	0.01001	1.78081	0.997E-09	0.996E-04	12
13	7.53389	1.02951	0.64198	0.13258E-05	2.32740	0.01641	0.01000	0.01083	1.99910	0.104E-08	0.961E-04	13
14	7.90056	1.23457	0.63954	0.11265E-05	2.32571	0.01342	0.00818	0.00725	2.14459	0.882E-09	0.122E-03	14
15	8.43389	1.49504	0.63589	0.11644E-05	2.32571	0.01911	0.01168	0.00858	2.36288	0.908E-09	0.106E-03	15
16	8.71722	1.63213	0.63375	0.12802E-05	2.32571	0.02432	0.01488	0.00953	2.49023	0.996E-09	0.105E-03	16
17	9.05055	1.82275	0.63339	0.18379E-06	2.32778	0.00326	0.00200	0.00116	2.51175	0.143E-09	0.123E-03	17
18	9.56722	2.09683	0.63364	-0.82095E-07	2.32533	-0.00178	-0.00109	-0.00056	2.49684	-0.639E-10	0.115E-03	18
19	9.93498	3.03837	0.62909	0.21101E-05	-0.01607	0.01227	0.00753	0.00297	2.76846	-0.236E-06	-0.796E-01	19
20	10.52387	3.40012	0.62455	0.13173E-05	-0.00759	0.04034	0.02483	0.00772	3.03926	-0.310E-06	-0.402E-01	20
21	10.79138	3.50123	0.62245	0.13447E-05	-0.00928	0.07170	0.04419	0.01281	3.16466	-0.258E-06	-0.202E-01	21
22	11.13165	3.67802	0.61984	0.13156E-05	-0.00990	0.05299	0.03271	0.00912	3.32047	-0.236E-06	-0.259E-01	22
23	11.53138	3.92630	0.61668	0.13609E-05	-0.00849	0.04847	0.02998	0.00789	3.50941	-0.284E-06	-0.360E-01	23
24	11.99915	2.30788	0.61671	-0.11188E-07	-0.02318	0.00006	0.00004	0.00001	3.50760	0.855E-09	0.734E-01	24
25	12.33250	1.47960	0.61781	-0.56887E-06	-0.02492	0.00248	0.00154	0.00082	3.44170	0.405E-07	0.491E-01	25
26	12.66583	1.09573	0.61879	-0.50143E-06	-0.02209	0.00325	0.00200	0.00157	3.38351	0.403E-07	0.257E-01	26
27	12.99915	1.07840	0.61939	-0.30908E-06	-0.02148	0.03769	0.02327	0.02140	3.34769	0.256E-07	0.119E-02	27
28	13.33250	1.02575	0.61963	-0.12530E-06	-0.02007	0.00486	0.00300	0.00286	3.33318	0.111E-07	0.389E-02	28
29	13.66583	0.83984	0.62012	-0.25053E-06	-0.02261	0.00244	0.00150	0.00162	3.30408	0.197E-07	0.122E-01	29
30	13.99915	0.68152	0.62021	-0.47002E-07	-0.01979	0.00043	0.00027	0.00036	3.29865	0.423E-08	0.119E-01	30
31	14.33250	0.53436	0.62019	0.11586E-07	-0.03028	-0.00009	-0.00006	-0.00009	3.29997	-0.681E-09	0.720E-02	31
32	14.69137	0.22740	0.62220	-0.96219E-06	-0.02891	0.00236	0.00146	0.00405	3.17961	0.594E-07	0.147E-01	32
33	14.96333	0.67743	0.62226	-0.38337E-07	-0.01197	-0.00006	-0.00003	-0.00008	3.17599	0.571E-08	-0.685E-01	33
34	15.33138	1.04711	0.62070	0.72640E-06	-0.01899	0.00358	0.00221	0.00260	3.26907	-0.681E-07	-0.262E-01	34
35	15.67220	1.06481	0.62062	0.41992E-07	-0.02016	0.00500	0.00309	0.00291	3.27406	-0.371E-08	-0.127E-02	35
36	16.00552	1.13855	0.62046	0.82328E-07	-0.02266	0.00239	0.00148	0.00134	3.28365	-0.647E-08	-0.483E-02	36
37	16.33887	1.17873	0.62034	0.62556E-07	-0.01927	0.00349	0.00216	0.00187	3.29088	-0.578E-08	-0.309E-02	37
38	16.67221	1.48676	0.62000	0.17225E-06	-0.01306	0.00145	0.00089	0.00067	3.31088	-0.235E-07	-0.350E-01	38
39	17.00554	2.02285	0.61848	0.78365E-06	-0.01419	0.00494	0.00305	0.00175	3.40170	-0.981E-07	-0.559E-01	39
40	17.33887	2.63150	0.61754	0.48609E-06	-0.01531	0.00359	0.00222	0.00096	3.45802	-0.563E-07	-0.587E-01	40
41	17.65082	3.22998	0.61629	0.68754E-06	-0.00939	0.00609	0.00377	0.00129	3.53253	-0.130E-06	-0.101E+00	41

42	17.98415	3.69852	0.61425	0.10528E-05	-0.00826	0.01505	0.00932	0.00270	3.65422-0.225E-06-0.835E-01	42
43	18.31749	3.97877	0.61188	0.12274E-05	-0.00712	0.03251	0.02017	0.00526	3.79594-0.303E-06-0.577E-01	43
44	18.65082	4.30288	0.60956	0.11977E-05	-0.00401	0.02953	0.01835	0.00443	3.93401-0.524E-06-0.118E+00	44
45	18.98415	4.57137	0.60698	0.13417E-05	-0.00882	0.04275	0.02660	0.00600	4.08839-0.266E-06-0.444E-01	45
46	19.31749	4.80935	0.60477	0.11436E-05	-0.00199	0.04339	0.02704	0.00577	4.21986-0.100E-05-0.174E+00	46
47	19.65082	5.06231	0.60216	0.13618E-05	-0.00143	0.05107	0.03188	0.00646	4.37610-0.166E-05-0.257E+00	47
48	19.98415	5.32510	0.59945	0.14117E-05	0.00337	0.05354	0.03347	0.00645	4.53783 0.725E-06 0.113E+00	48
49	20.31749	5.57744	0.59695	0.13027E-05	0.00027	0.05393	0.03377	0.00619	4.68684 0.843E-05 0.136E+01	49
50	20.65082	5.86695	0.59433	0.13685E-05	0.00197	0.05173	0.03245	0.00567	4.84308 0.120E-05 0.211E+00	50
51	20.98415	6.16045	0.59155	0.14575E-05	0.00145	0.05703	0.03583	0.00596	5.00920 0.173E-05 0.290E+00	51
52	21.31749	6.44054	0.58894	0.13661E-05	0.00225	0.05860	0.03688	0.00585	5.16472 0.104E-05 0.178E+00	52
53	21.65082	6.75319	0.58634	0.13668E-05	0.00399	0.05488	0.03460	0.00525	5.31999 0.585E-06 0.111E+00	53
54	21.98415	7.05527	0.58372	0.13779E-05	0.00540	0.05984	0.03779	0.00547	5.47629 0.434E-06 0.792E-01	54
55	22.31749	7.37675	0.58117	0.13480E-05	0.00597	0.05738	0.03629	0.00503	5.62891 0.383E-06 0.760E-01	55
56	22.65082	7.70091	0.57853	0.13907E-05	0.00771	0.06127	0.03882	0.00515	5.78613 0.304E-06 0.591E-01	56
57	22.89304	7.94981	0.57649	0.14843E-05	0.00884	0.06413	0.04068	0.00520	5.90791 0.283E-06 0.544E-01	57
58	23.27081	6.03691	0.57632	0.77802E-07	-0.01664	-0.00061	-0.00038	-0.00006	5.91789-0.788E-08 0.142E+00	58
59	23.60416	4.16053	0.57718	-0.45044E-06	-0.02031	0.00229	0.00145	0.00029	5.86700 0.374E-07 0.130E+00	59
60	23.93748	2.90758	0.57818	-0.53060E-06	-0.02482	0.00281	0.00178	0.00051	5.80701 0.361E-07 0.710E-01	60
61	24.27081	2.05211	0.58059	-0.12683E-05	-0.02568	0.00690	0.00437	0.00178	5.66348 0.836E-07 0.470E-01	61
62	24.70831	1.37066	0.58148	-0.36071E-06	-0.02111	0.00223	0.00141	0.00083	5.60985 0.290E-07 0.347E-01	62
63	24.97916	1.11024	0.58234	-0.55271E-06	-0.01885	0.00405	0.00256	0.00207	5.55896 0.498E-07 0.240E-01	63
64	25.57498	1.06192	0.58296	-0.18372E-06	-0.01550	0.01402	0.00886	0.00816	5.52170 0.201E-07 0.247E-02	64
65	25.93887	0.97570	0.58340	-0.21260E-06	-0.01894	0.00520	0.00329	0.00323	5.49541 0.191E-07 0.591E-02	65
66	26.29166	0.76762	0.58409	-0.34078E-06	-0.02398	0.00286	0.00180	0.00208	5.45448 0.242E-07 0.116E-01	66
67	26.56915	0.71772	0.58451	-0.26934E-06	-0.01692	0.00636	0.00401	0.00539	5.42902 0.271E-07 0.503E-02	67
68	26.97165	0.48508	0.58473	-0.92813E-07	-0.03161	0.00054	0.00034	0.00058	5.41631 0.500E-08 0.865E-02	68
69	27.40027	0.19684	0.58728	-0.10443E-05	-0.03528	0.00283	0.00179	0.00559	5.26367 0.505E-07 0.904E-02	69
70	27.61554	0.11125	0.58888	-0.12970E-05	-0.03278	0.00280	0.00176	0.01174	5.16833 0.677E-07 0.577E-02	70

ENGINEERING STRAIN (70)= 5.1683

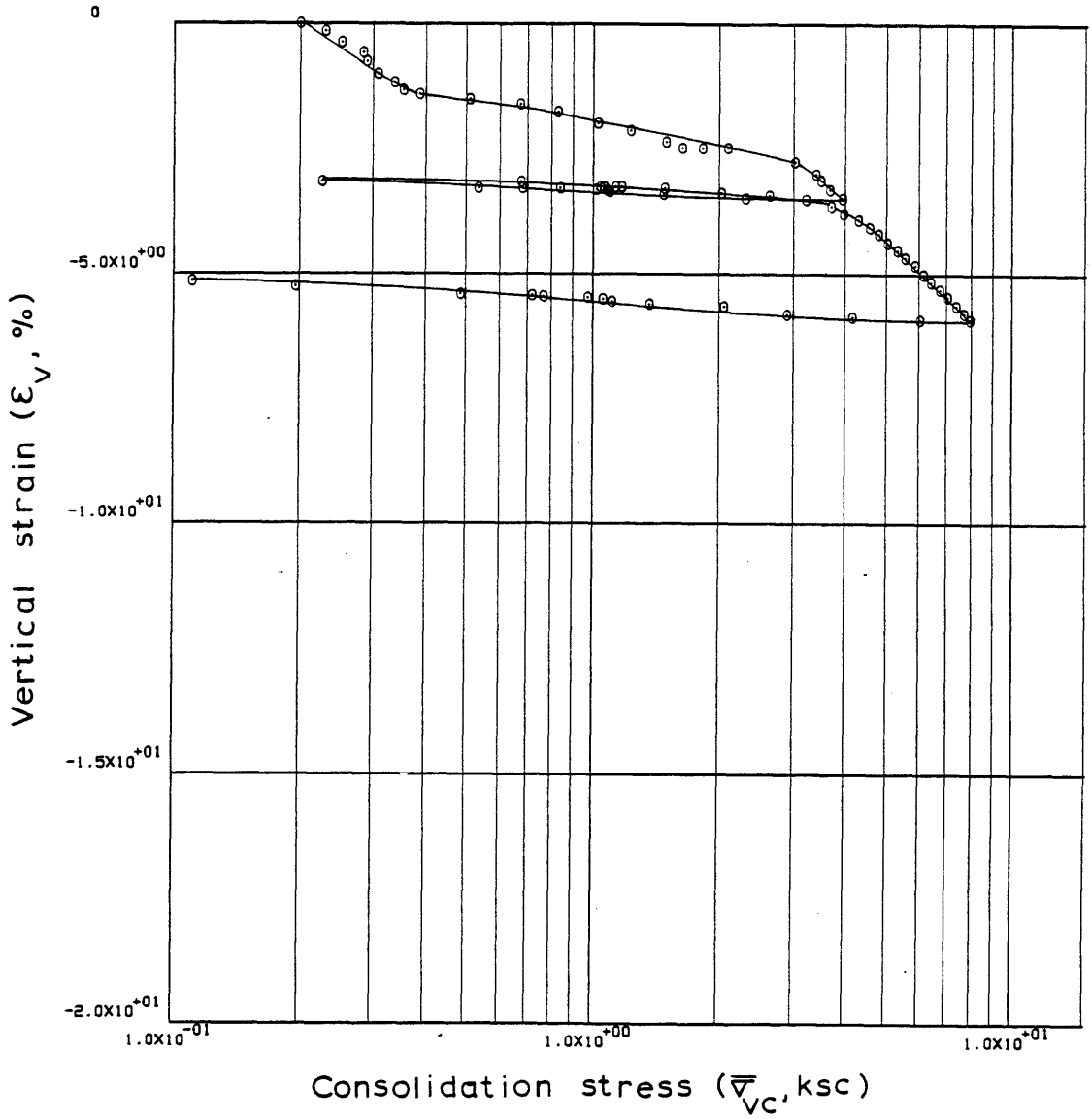

Sample No. 26.5-28.5-C-H w_N (%) 21.46 Estimated

Depth 27.63 w_L (%) 31.30 $\bar{\sigma}_{vo}$ 0.61 $\bar{\sigma}_{vm}$ 3.00

Soil Type Boston w_P (%) 19.68 CR 0.0794 RR 0.0034

Blue Clay P.I.(%) 11.62 G_S 2.77 e_o 0.6755

⊙ At t_p Remarks Data from C.R.S.C test

w_L & w_P estimated from Baligh et al (1980)

Figure E.7 Compression Curve for Sample No. 26.5-28.5-C-H

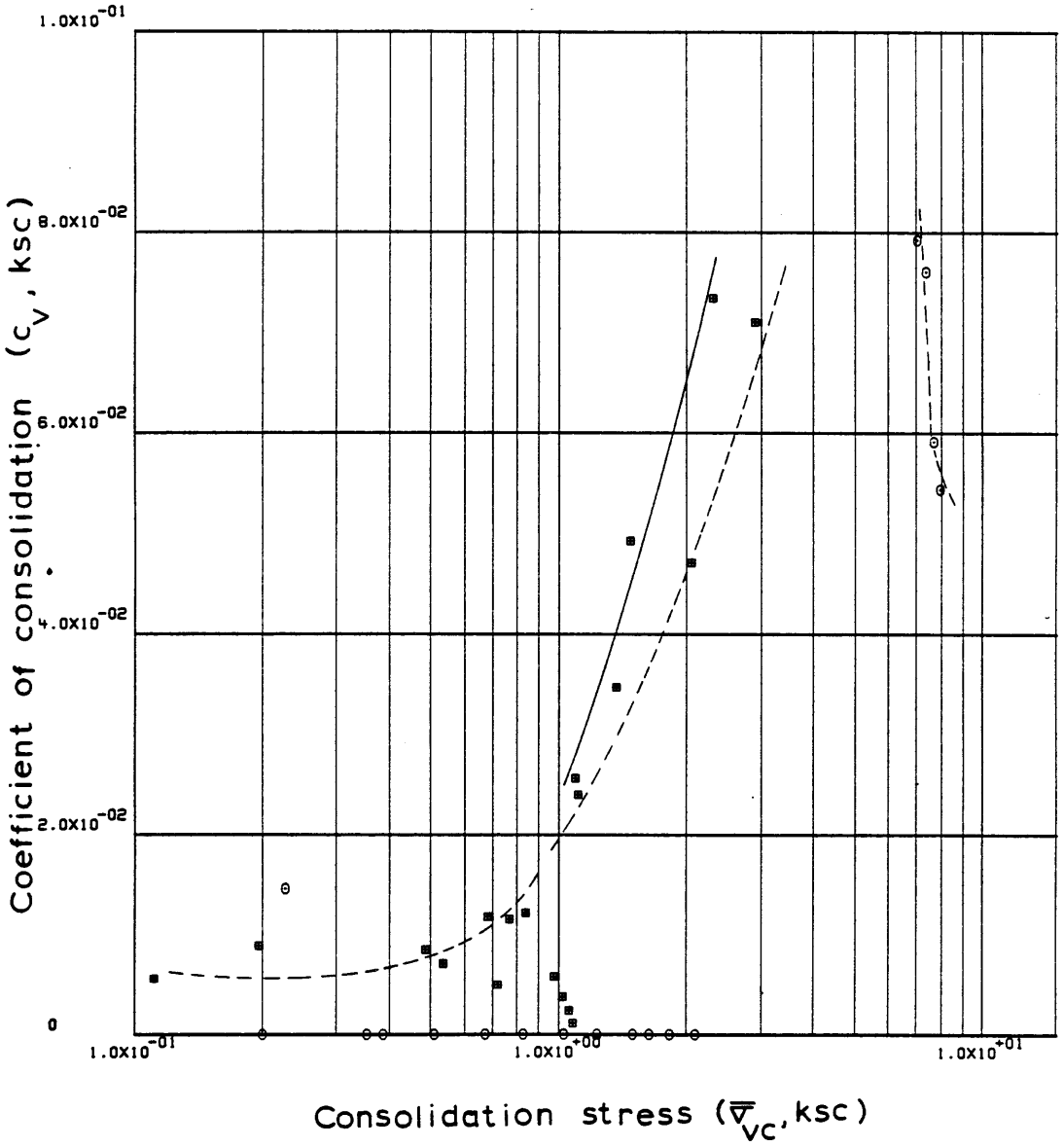

Sample No. 26.5-28.5-C-H w_N (%) 21.46 Estimated

Depth 27.63 w_L (%) 31.30 $\bar{\sigma}_{vo}$ 0.61 $\bar{\sigma}_{vm}$ 3.00

Soil Type Boston w_P (%) 19.68 CR 0.0794 RR 0.0034

Blue Clay P.I.(%) 11.62 G_s 2.77 e_o 0.6755

⊖ At t_p

Remarks Data from C.R.S.C test

w_L & w_P estimated from Baligh et al (1980)

Figure E.8 Variation of coefficient of consolidation with consolidation stress for Sample No. 26.5-28.5-C-H

1-D STRAIN CONTROLLED COMPRESSION TEST

COMPUTED RESULTS

INITIAL VOID RATIO= 0.99534
INITIAL HEIGHT= 1.9050

ALL UNITS IN: KG,CM,SEC

LINEAR THEORY

	TIME IN HOURS	VERTICAL STRESS	E	RATE OF STRAIN	EXCESS PORE PRESSURE	C	C/1+E	MV	PERCENT COMPRESSION	K	CV	
1	0.0	0.00733	0.99498	0.0	-0.01100	0.0	0.0	0.02485	0.01823	0.0	0.0	1
2	0.31889	0.05214	0.98865	0.27736E-05	-0.00873	0.00323	0.00162	0.07108	0.33557	-0.573E-06	-0.806E-02	2
3	0.65222	0.10391	0.98106	0.31914E-05	-0.00310	0.01100	0.00555	0.07397	0.71584	-0.184E-05	-0.249E-01	3
4	1.03611	0.21060	0.97273	0.30550E-05	0.00253	0.01179	0.00598	0.03957	1.13326	0.214E-05	0.542E-01	4
5	1.36944	0.33287	0.96552	0.30565E-05	0.00532	0.01575	0.00801	0.03000	1.49455	0.101E-05	0.337E-01	5
6	0.70278	0.48202	0.95845	0.99000E+02	0.00816	0.01910	0.00975	0.02421	1.84898	0.212E+02	0.876E+06	6
7	2.00583	0.64680	0.95249	0.65030E-06	0.00816	0.02026	0.01038	0.01851	2.14751	0.139E-06	0.748E-02	7
8	2.33917	0.82445	0.94603	0.27662E-05	0.01265	0.02662	0.01368	0.01869	2.47125	0.378E-06	0.202E-01	8
9	2.67250	1.01420	0.93970	0.27184E-05	0.01378	0.03055	0.01575	0.01719	2.78839	0.338E-06	0.197E-01	9
10	2.97806	1.17894	0.93449	0.24488E-05	0.01378	0.03461	0.01789	0.01635	3.04951	0.303E-06	0.185E-01	10
11	3.32528	1.36869	0.92779	0.27801E-05	0.01491	0.04489	0.02329	0.01831	3.38528	0.316E-06	0.172E-01	11
12	3.65889	1.56146	0.92147	0.27419E-05	0.01661	0.04802	0.02499	0.01708	3.70236	0.278E-06	0.163E-01	12
13	3.99222	1.74574	0.91514	0.27533E-05	0.01830	0.05672	0.02962	0.01793	4.01952	0.251E-06	0.140E-01	13
14	4.35028	1.95193	0.90794	0.29259E-05	0.01826	0.06446	0.03379	0.01829	4.38016	0.266E-06	0.145E-01	14
15	5.01692	2.33381	0.89492	0.28640E-05	0.01939	0.07289	0.03847	0.01800	5.03291	0.242E-06	0.134E-01	15
16	5.35026	2.52409	0.88822	0.29561E-05	0.02222	0.08545	0.04526	0.01864	5.36858	0.216E-06	0.116E-01	16
17	5.68359	2.73044	0.88201	0.27485E-05	0.02397	0.07899	0.04197	0.01598	5.67966	0.185E-06	0.116E-01	17
18	6.01692	2.93581	0.87494	0.31432E-05	0.02227	0.09753	0.05202	0.01837	6.03409	0.226E-06	0.123E-01	18
19	6.35026	3.15358	0.86824	0.29882E-05	0.02510	0.09363	0.05011	0.01647	6.36986	0.189E-06	0.115E-01	19
20	6.68359	3.37136	0.86154	0.29993E-05	0.02793	0.10033	0.05390	0.01653	6.70561	0.170E-06	0.103E-01	20
21	7.01692	3.59045	0.85484	0.30099E-05	0.02623	0.10641	0.05737	0.01649	7.04138	0.180E-06	0.109E-01	21
22	7.35026	3.82195	0.84777	0.31893E-05	0.02906	0.11317	0.06125	0.01653	7.39577	0.171E-06	0.103E-01	22
23	7.68359	4.05534	0.84144	0.28635E-05	0.02906	0.10675	0.05797	0.01472	7.71291	0.152E-06	0.103E-01	23
24	8.01692	4.30058	0.83474	0.30429E-05	0.03189	0.11411	0.06219	0.01489	8.04868	0.146E-06	0.983E-02	24
25	8.35026	4.56142	0.82804	0.30541E-05	0.03189	0.11377	0.06224	0.01405	8.38445	0.146E-06	0.104E-01	25
26	8.68359	4.81982	0.82097	0.32363E-05	0.03302	0.12835	0.07049	0.01503	8.73888	0.148E-06	0.985E-02	26
27	9.01692	5.10624	0.81427	0.30773E-05	0.03586	0.11604	0.06396	0.01289	9.07458	0.129E-06	0.999E-02	27
28	9.35026	5.38138	0.80757	0.30885E-05	0.03756	0.12765	0.07062	0.01347	9.41035	0.122E-06	0.909E-02	28
29	9.68359	5.69469	0.80050	0.32731E-05	0.03869	0.12498	0.06941	0.01254	9.76479	0.125E-06	0.997E-02	29
30	10.01692	6.01045	0.79380	0.31126E-05	0.03869	0.12414	0.06921	0.01183	10.10056	0.118E-06	0.997E-02	30
31	10.06944	6.05164	0.79268	0.32935E-05	0.03869	0.16354	0.09122	0.01512	10.15652	0.125E-06	0.825E-02	31
32	10.10277	5.88884	0.79231	0.17313E-05	0.01774	-0.01360	-0.00759	-0.00128	10.17514	0.143E-06	-0.112E+00	32
33	10.16720	5.74726	0.79231	0.0	0.00358	0.0	0.0	0.0	10.17514	0.0	0.100E+05	33
34	10.34833	4.12981	0.79221	0.88150E-07	-0.02365	-0.00031	-0.00017	-0.00004	10.18030	-0.546E-08	0.154E+00	34
35	10.65555	2.51519	0.79630	-0.20604E-05	-0.03384	0.00825	0.00459	0.00141	9.97520	0.895E-07	0.634E-01	35
36	10.97360	1.61303	0.80226	-0.28855E-05	-0.03950	0.01340	0.00744	0.00366	9.67677	0.108E-06	0.295E-01	36
37	11.32111	1.03940	0.80959	-0.32407E-05	-0.04067	0.01669	0.00923	0.00707	9.30907	0.119E-06	0.168E-01	37
38	11.65443	0.71086	0.81751	-0.36318E-05	-0.04517	0.02085	0.01147	0.01327	8.91214	0.121E-06	0.913E-02	38
39	11.98776	0.49176	0.82485	-0.33492E-05	-0.04520	0.01990	0.01091	0.01834	8.54459	0.112E-06	0.613E-02	39
40	12.32111	0.32841	0.83203	-0.32656E-05	-0.04800	0.01778	0.00971	0.02399	8.18474	0.104E-06	0.434E-02	40
41	12.65443	0.23158	0.83936	-0.33213E-05	-0.04350	0.02098	0.01141	0.04116	7.81734	0.118E-06	0.286E-02	41

42	12.99415	0.14808	0.84691	-0.33445E-05	-0.04517	0.01689	0.00915	0.04899	7.43877	0.115E-06	0.235E-02	42
43	13.36444	0.09188	0.85499	-0.32645E-05	-0.04237	0.01692	0.00912	0.07743	7.03418	0.121E-06	0.156E-02	43
44	13.69777	0.04882	0.86243	-0.33297E-05	-0.03954	0.01177	0.00632	0.09279	6.66125	0.133E-06	0.143E-02	44
45	14.03111	0.02137	0.86987	-0.33162E-05	-0.03954	0.00901	0.00482	0.14499	6.28830	0.134E-06	0.922E-03	45
46	22.39192	0.17406	0.90261	-0.57175E-06	0.01198	-0.01561	-0.00821	-0.11271	4.64738	-0.787E-07	0.698E-03	46
47	22.58192	0.21392	0.89839	0.32459E-05	0.01477	0.02044	0.01077	0.05570	4.85864	0.361E-06	0.648E-02	47
48	22.82471	0.25320	0.89356	0.29221E-05	0.01760	0.02869	0.01515	0.06503	5.10100	0.271E-06	0.417E-02	48
49	23.15804	0.31992	0.88538	0.36173E-05	0.02043	0.03499	0.01856	0.06506	5.51115	0.287E-06	0.441E-02	49
50	23.49136	0.40225	0.87868	0.29703E-05	0.02043	0.02924	0.01557	0.04329	5.84676	0.234E-06	0.540E-02	50
51	23.84776	0.51013	0.87124	0.30988E-05	0.02326	0.03131	0.01673	0.03685	6.21962	0.213E-06	0.577E-02	51
52	24.18109	0.63223	0.86368	0.33787E-05	0.02605	0.03521	0.01889	0.03321	6.59828	0.205E-06	0.618E-02	52
53	24.51442	0.78361	0.85650	0.32236E-05	0.02601	0.03345	0.01802	0.02555	6.95818	0.195E-06	0.762E-02	53
54	24.84776	0.97564	0.84906	0.33516E-05	0.02601	0.03393	0.01835	0.02094	7.33089	0.201E-06	0.959E-02	54
55	25.18109	1.19361	0.84189	0.32473E-05	0.02879	0.03560	0.01933	0.01788	7.69063	0.174E-06	0.975E-02	55
56	25.51442	1.46789	0.83482	0.32084E-05	0.02879	0.03415	0.01861	0.01404	8.04466	0.171E-06	0.122E-01	56
57	25.84776	1.78360	0.82765	0.32707E-05	0.02875	0.03682	0.02015	0.01243	8.40416	0.173E-06	0.139E-01	57
58	26.18109	2.16563	0.82059	0.32330E-05	0.03158	0.03639	0.01999	0.01015	8.75815	0.155E-06	0.152E-01	58
59	27.84776	4.62859	0.78639	0.31907E-05	0.04176	0.04503	0.02520	0.00777	10.47206	0.111E-06	0.143E-01	59
60	28.18137	5.11975	0.78007	0.29560E-05	0.04289	0.06267	0.03520	0.00723	10.78880	0.995E-07	0.138E-01	60
61	28.55081	5.68004	0.77301	0.29951E-05	0.04572	0.06800	0.03835	0.00711	11.14273	0.939E-07	0.132E-01	61
62	28.88414	6.17176	0.76631	0.31568E-05	0.04855	0.08059	0.04563	0.00770	11.47804	0.925E-07	0.120E-01	62
63	29.30830	6.78878	0.75814	0.30463E-05	0.04855	0.08583	0.04882	0.00754	11.88795	0.884E-07	0.117E-01	63
64	29.67609	7.32031	0.75107	0.30463E-05	0.05590	0.09368	0.05350	0.00759	12.24188	0.762E-07	0.100E-01	64
65	30.00941	7.82494	0.74429	0.32416E-05	0.05868	0.10179	0.05835	0.00771	12.58195	0.766E-07	0.994E-02	65
66	30.34276	8.33218	0.73760	0.32082E-05	0.05868	0.10652	0.06130	0.00759	12.91722	0.752E-07	0.991E-02	66
67	30.67609	8.86493	0.73128	0.30413E-05	0.06151	0.10194	0.05888	0.00685	13.23386	0.675E-07	0.986E-02	67
68	31.00941	9.38342	0.72459	0.32327E-05	0.06264	0.11771	0.06826	0.00748	13.56917	0.700E-07	0.935E-02	68
69	31.34276	9.95732	0.71827	0.30640E-05	0.06547	0.10643	0.06194	0.00641	13.88582	0.630E-07	0.983E-02	69
70	31.67609	10.52068	0.71167	0.32142E-05	0.06552	0.11995	0.07008	0.00685	14.21667	0.655E-07	0.957E-02	70
71	32.01524	11.13580	0.70498	0.32141E-05	0.06835	0.11775	0.06906	0.00638	14.55197	0.623E-07	0.977E-02	71
72	32.34859	11.76465	0.69866	0.31001E-05	0.07117	0.11503	0.06772	0.00592	14.86867	0.573E-07	0.968E-02	72
73	32.64775	12.38222	0.69271	0.32625E-05	0.07287	0.11626	0.06868	0.00569	15.16679	0.585E-07	0.103E-01	73
74	32.87497	12.83413	0.68825	0.32301E-05	0.07117	0.12443	0.07371	0.00585	15.39032	0.590E-07	0.101E-01	74
75	32.91025	12.90325	0.68751	0.34688E-05	0.07287	0.13850	0.08207	0.00637	15.42761	0.618E-07	0.969E-02	75
76	33.00330	12.31050	0.68705	0.80602E-06	0.01344	-0.00969	-0.00575	-0.00048	15.45044	0.778E-07	-0.171E+00	76
77	32.91997	13.68516	0.68714	0.99000E+02	2.61581	-0.00079	-0.00047	-0.00004	15.44623	0.491E-01	-0.136E+07	77
78	33.33691	7.88576	0.68920	-0.81337E-06	-0.03636	0.00374	0.00222	0.00021	15.34285	0.291E-07	0.138E+00	78
79	33.67024	5.15202	0.69329	-0.20116E-05	-0.04768	0.00960	0.00567	0.00088	15.13800	0.551E-07	0.624E-01	79
80	34.01636	3.42878	0.69849	-0.24582E-05	-0.05333	0.01278	0.00752	0.00178	14.87729	0.606E-07	0.341E-01	80
81	34.32776	2.43215	0.70323	-0.24847E-05	-0.05901	0.01381	0.00811	0.00279	14.63954	0.557E-07	0.199E-01	81
82	34.66109	1.72113	0.70852	-0.25797E-05	-0.06181	0.01530	0.00895	0.00435	14.37447	0.555E-07	0.128E-01	82
83	35.01190	1.20217	0.71521	-0.30877E-05	-0.06464	0.01864	0.01087	0.00751	14.03925	0.640E-07	0.852E-02	83
84	35.39693	0.82028	0.72301	-0.32674E-05	-0.06746	0.02042	0.01185	0.01186	13.64816	0.655E-07	0.553E-02	84
85	35.70636	0.60097	0.73007	-0.36634E-05	-0.06746	0.02269	0.01312	0.01861	13.29433	0.741E-07	0.398E-02	85
86	36.04997	0.43408	0.73760	-0.35009E-05	-0.06461	0.02313	0.01331	0.02595	12.91722	0.746E-07	0.287E-02	86
87	36.36191	0.31315	0.74429	-0.34152E-05	-0.06574	0.02049	0.01175	0.03171	12.58195	0.720E-07	0.227E-02	87
88	36.77887	0.19223	0.75348	-0.34936E-05	-0.06860	0.01884	0.01075	0.04337	12.12109	0.714E-07	0.165E-02	88
89	36.99359	0.14864	0.75804	-0.33524E-05	-0.06574	0.01772	0.01008	0.05945	11.89276	0.718E-07	0.121E-02	89
90	37.44664	0.06510	0.76835	-0.35740E-05	-0.06294	0.01249	0.00706	0.06978	11.37617	0.809E-07	0.116E-02	90

ENGINEERING STRAIN (90)= 11.3762

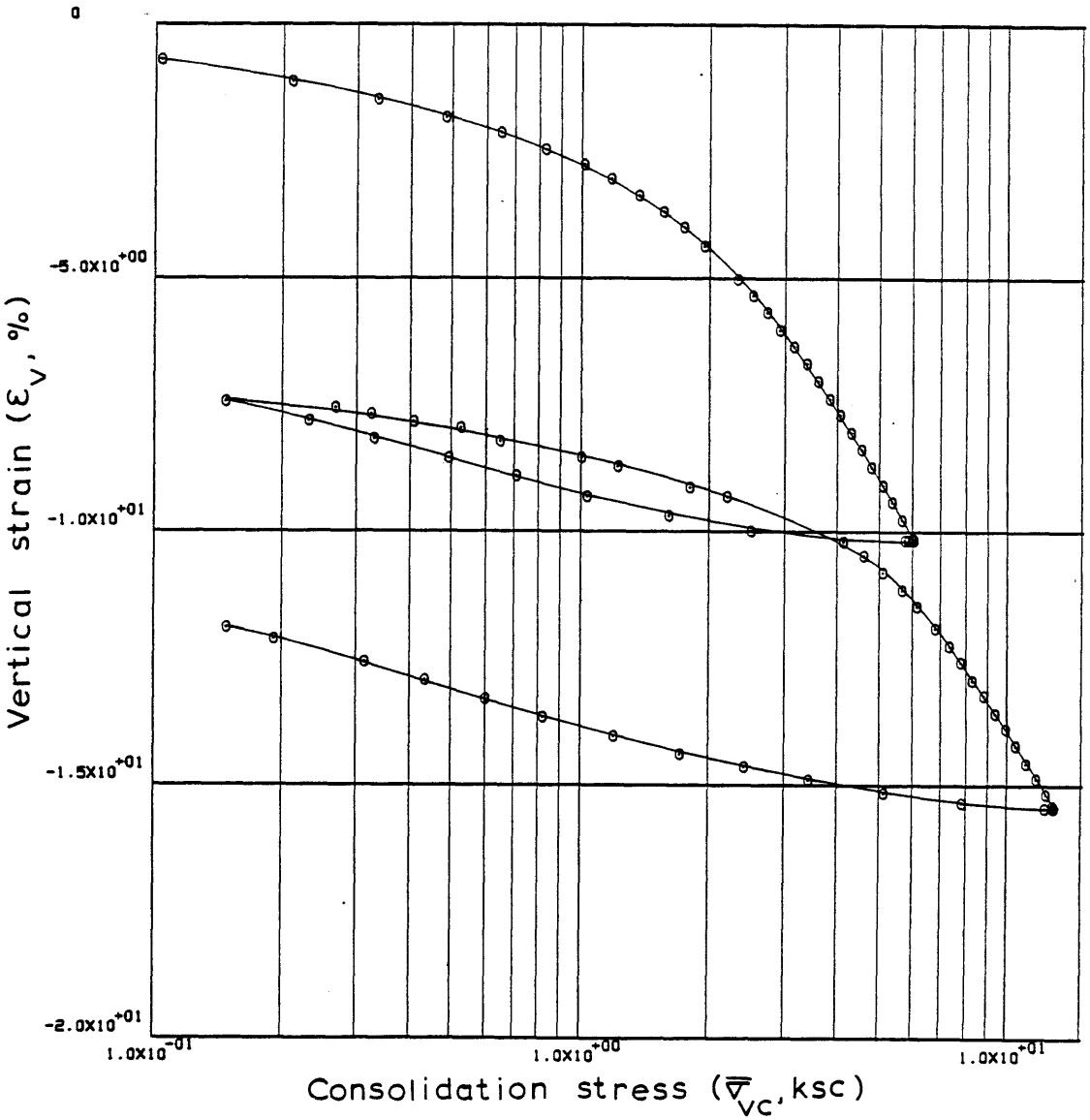

Sample No. 36.5-38.5-C-V w_N (%) 50.07 Estimated

Depth 36.59 w_L (%) 31.30 $\bar{\sigma}_{vo}$ 0.82 $\bar{\sigma}_{vm}$ 2.26-2.46

Boston w_P (%) 20.82 CR 0.1551 RR 0.02115

Blue Clay P.I.(%) 10.48 G_s 2.77 e_o 0.9953

o At t_p Remarks Data from C.R.S.C test

w_L & w_P estimated from Baligh et al (1980)

Figure E.9 Compression Curve for Sample No. 36.5-38.5-C-V

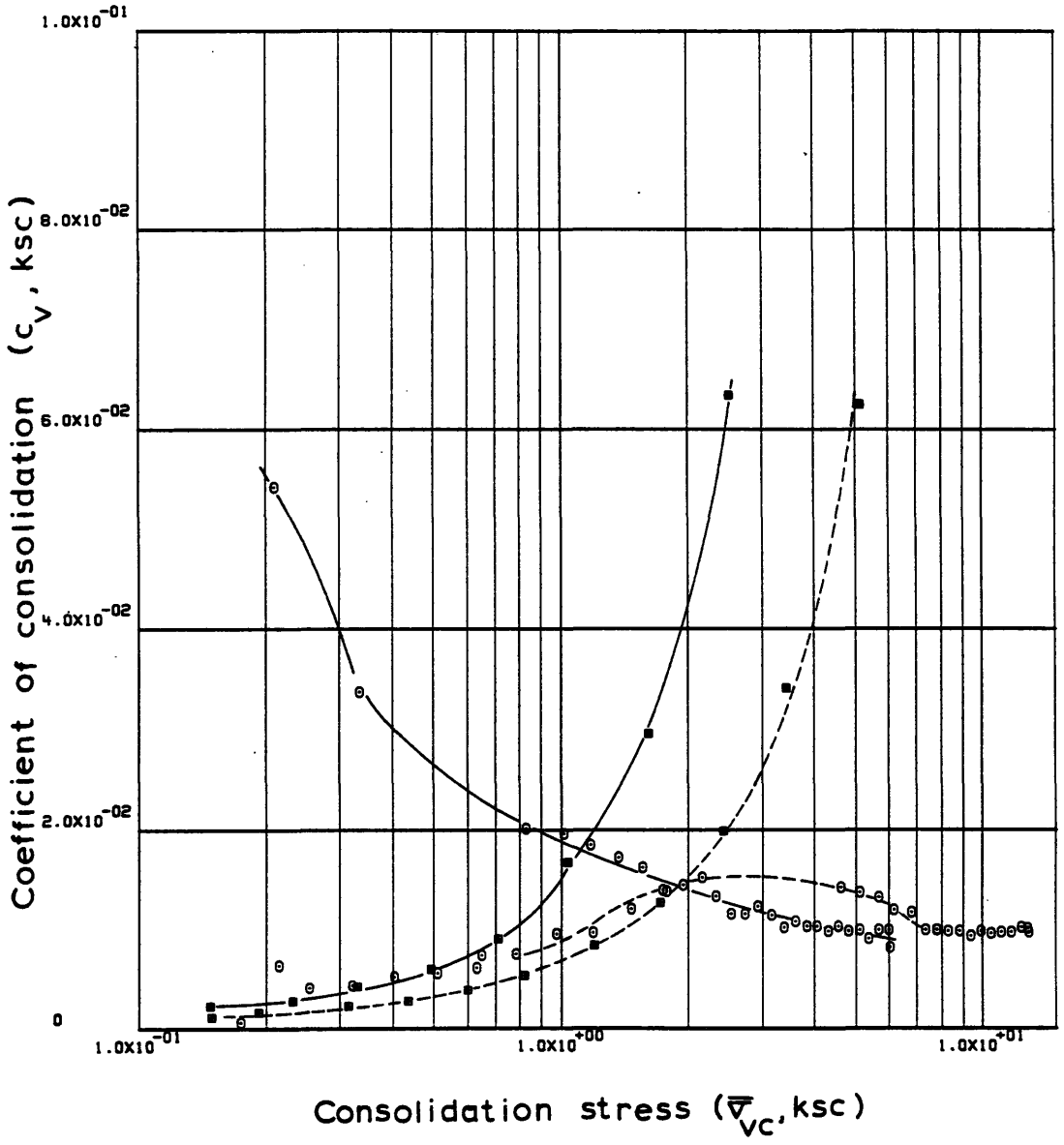

Sample No. 36.5-38.5-C-V w_N (%) 50.07 Estimated

Depth 36.59 w_L (%) 31.30 $\bar{\sigma}_{vo}$ 0.82 $\bar{\sigma}_{vm}$ 226-246

Boston w_P (%) 20.82 CR 01551 RR 002115

Blue Clay P.I.(%) 10.48 G_S 2.77 e_o 0.9953

θ At t_p Remarks Data from C.R.S.C test

w_L & w_P estimated from Baligh et al (1980)

Figure E. 10 Variation of coefficient of consolidation with consolidation stress for Sample No. 36.5-38.5-C-V

1-D STRAIN CONTROLLED COMPRESSION TEST

COMPUTED RESULTS

INITIAL VOID RATIO= 0.94529
INITIAL HEIGHT= 1.9355

ALL UNITS IN: KG,CM,SEC

LINEAR THEORY

	TIME IN HOURS	VERTICAL STRESS	E	RATE OF STRAIN	EXCESS PORE PRESSURE		C	C/1+E	MV	PERCENT COMPRESSION	K	CV	
1	0.0	0.0	0.94529	0.0	0.0	0.0	0.0	0.0	0.00002	0.100E+01	0.100E+05	1
2	0.41056	0.11541	0.94303	0.78731E-06	-0.00768	0.0	0.0	0.0	0.11624	-0.191E-06	0.100E+05	2
3	0.92083	0.12013	0.93735	0.15959E-05	-0.00237	0.14173	0.07316	0.62123	0.40823	-0.125E-05	-0.201E-02	3
4	1.25417	0.12598	0.93382	0.15198E-05	-0.00294	0.07415	0.03834	0.31165	0.58951	-0.958E-06	-0.307E-02	4
5	1.58750	0.14301	0.93025	0.15437E-05	-0.00328	0.02822	0.01462	0.10881	0.77336	-0.869E-06	-0.798E-02	5
6	1.92083	0.14093	0.92686	0.14635E-05	-0.00271	-0.23177	-0.12028	-0.84732	0.94728	-0.992E-06	0.117E-02	6
7	2.25417	0.13728	0.92318	0.15948E-05	-0.00079	-0.14019	-0.07289	-0.52407	1.13649	-0.368E-05	0.701E-02	7
8	2.58750	0.13754	0.91961	0.15509E-05	0.00141	1.87198	0.97519	7.09628	1.32014	0.200E-05	0.282E-03	8
9	3.07695	0.13855	0.91473	0.14459E-05	0.00508	0.66741	0.34857	2.52492	1.57089	0.517E-06	0.205E-03	9
10	3.41028	0.14475	0.91099	0.16303E-05	0.00761	0.08550	0.04474	0.31585	1.76311	0.387E-06	0.123E-02	10
11	3.74361	0.15236	0.90811	0.12595E-05	0.01213	0.05625	0.02948	0.19855	1.91133	0.187E-06	0.943E-03	11
12	4.07694	0.17208	0.90484	0.14293E-05	0.01642	0.02684	0.01409	0.08697	2.07930	0.156E-06	0.180E-02	12
13	4.63304	0.22289	0.89903	0.15288E-05	0.02540	0.02247	0.01183	0.06023	2.37808	0.107E-06	0.178E-02	13
14	4.94444	0.26127	0.89576	0.15413E-05	0.02738	0.02062	0.01088	0.04503	2.54645	0.100E-06	0.222E-02	14
15	5.27777	0.31738	0.89241	0.14739E-05	0.02738	0.01720	0.00909	0.03152	2.71852	0.954E-07	0.303E-02	15
16	5.61110	0.37425	0.88924	0.13977E-05	0.02879	0.01923	0.01018	0.02949	2.88142	0.858E-07	0.291E-02	16
17	5.94444	0.44400	0.88582	0.15103E-05	0.02427	0.02000	0.01061	0.02598	3.05713	0.110E-06	0.422E-02	17
18	6.43889	0.56562	0.88098	0.14463E-05	0.02455	0.02000	0.01063	0.02117	3.30605	0.103E-06	0.487E-02	18
19	6.77138	0.66206	0.87756	0.15225E-05	0.02449	0.02173	0.01158	0.01890	3.48196	0.108E-06	0.574E-02	19
20	7.10498	0.75374	0.87467	0.12808E-05	0.02449	0.02223	0.01186	0.01678	3.63017	0.910E-07	0.542E-02	20
21	7.43831	0.84996	0.87126	0.15219E-05	0.02590	0.02845	0.01520	0.01898	3.80588	0.102E-06	0.536E-02	21
22	7.71388	0.92820	0.86873	0.13633E-05	0.02760	0.02869	0.01535	0.01729	3.93576	0.854E-07	0.494E-02	22
23	8.04721	1.03971	0.86538	0.14950E-05	0.02816	0.02951	0.01582	0.01609	4.10782	0.914E-07	0.568E-02	23
24	8.38056	1.14309	0.86232	0.13698E-05	0.02957	0.03228	0.01734	0.01590	4.26515	0.795E-07	0.500E-02	24
25	8.71388	1.24577	0.85908	0.14524E-05	0.02613	0.03767	0.02026	0.01697	4.43175	0.951E-07	0.560E-02	25
26	9.12389	1.36273	0.85556	0.12865E-05	0.02923	0.03927	0.02116	0.01624	4.61288	0.750E-07	0.462E-02	26
27	9.45722	1.46615	0.85214	0.15380E-05	0.02766	0.04673	0.02523	0.01785	4.78859	0.944E-07	0.529E-02	27
28	9.79054	1.58609	0.84933	0.12675E-05	0.02117	0.03578	0.01935	0.01268	4.93320	0.101E-06	0.799E-02	28
29	10.12389	1.70839	0.84619	0.14151E-05	0.01671	0.04222	0.02287	0.01389	5.09438	0.143E-06	0.103E-01	29
30	10.45722	1.81595	0.84306	0.14171E-05	0.01446	0.05131	0.02784	0.01581	5.25545	0.165E-06	0.104E-01	30
31	10.79054	1.93816	0.83928	0.17103E-05	0.01389	0.05796	0.03151	0.01679	5.44949	0.206E-06	0.123E-01	31
32	11.12389	2.04788	0.83618	0.14077E-05	0.01198	0.05635	0.03069	0.01540	5.60899	0.196E-06	0.127E-01	32
33	11.45722	2.17361	0.83312	0.13925E-05	0.01282	0.05140	0.02804	0.01329	5.76642	0.181E-06	0.136E-01	33
34	11.79054	2.27786	0.82984	0.14945E-05	0.01571	0.07005	0.03828	0.01720	5.93512	0.158E-06	0.917E-02	34
35	12.12389	2.38297	0.82649	0.15278E-05	0.01825	0.07424	0.04065	0.01744	6.10728	0.138E-06	0.792E-02	35
36	12.45722	2.49832	0.82303	0.15825E-05	0.01944	0.07322	0.04016	0.01646	6.28522	0.134E-06	0.813E-02	36
37	12.79054	2.61701	0.81985	0.14521E-05	0.02170	0.06834	0.03755	0.01468	6.44826	0.110E-06	0.747E-02	37
38	13.12389	2.73244	0.81640	0.15856E-05	0.02368	0.08008	0.04408	0.01648	6.62593	0.109E-06	0.663E-02	38
39	13.45722	2.85430	0.81311	0.15103E-05	0.02345	0.07533	0.04154	0.01487	6.79485	0.105E-06	0.705E-02	39
40	13.79054	2.97125	0.81019	0.13453E-05	0.02318	0.07277	0.04020	0.01380	6.94508	0.941E-07	0.682E-02	40
41	14.12389	3.08997	0.80638	0.17591E-05	0.02798	0.09732	0.05387	0.01778	7.14108	0.102E-06	0.571E-02	41

42	14.45722	3.20504	0.80305	0.15363E-05	0.02211	0.09093	0.05043	0.01602	7.31197	0.112E-06	0.698E-02	42
43	14.79054	3.34327	0.79984	0.14853E-05	0.02126	0.07596	0.04220	0.01289	7.47684	0.112E-06	0.869E-02	43
44	15.12389	3.46557	0.79670	0.14598E-05	0.02216	0.08760	0.04875	0.01432	7.63866	0.105E-06	0.735E-02	44
45	15.45722	3.57981	0.79305	0.16954E-05	0.02025	0.11250	0.06274	0.01781	7.82619	0.133E-06	0.748E-02	45
46	15.79054	3.70781	0.79009	0.13777E-05	0.02562	0.08423	0.04706	0.01292	7.97835	0.853E-07	0.660E-02	46
47	16.12389	3.84407	0.78663	0.16132E-05	0.02477	0.09585	0.05365	0.01421	8.15611	0.103E-06	0.724E-02	47
48	16.45721	3.96805	0.78321	0.15997E-05	0.02590	0.10783	0.06047	0.01548	8.33208	0.972E-07	0.628E-02	48
49	16.79054	4.09717	0.77963	0.16763E-05	0.02964	0.11180	0.06282	0.01558	8.51611	0.887E-07	0.569E-02	49
50	17.12389	4.22476	0.77669	0.13784E-05	0.02800	0.09581	0.05393	0.01296	8.66718	0.769E-07	0.593E-02	50
51	17.45721	4.35653	0.77350	0.14988E-05	0.02948	0.10387	0.05857	0.01365	8.83116	0.792E-07	0.580E-02	51
52	17.79054	4.49090	0.77011	0.15937E-05	0.02875	0.11142	0.06295	0.01423	9.00514	0.860E-07	0.604E-02	52
53	18.12389	4.63461	0.76682	0.15564E-05	0.02995	0.10476	0.05929	0.01300	9.17480	0.803E-07	0.618E-02	53
54	18.45721	4.78305	0.76366	0.14922E-05	0.03030	0.10019	0.05681	0.01206	9.33714	0.758E-07	0.629E-02	54
55	18.79054	4.94204	0.76055	0.14702E-05	0.02747	0.09499	0.05395	0.01110	9.49680	0.821E-07	0.740E-02	55
56	19.12389	5.07765	0.75675	0.18038E-05	0.02612	0.14050	0.07998	0.01596	9.69231	0.106E-06	0.661E-02	56
57	19.45721	5.23845	0.75384	0.13832E-05	0.02872	0.09336	0.05323	0.01032	9.84196	0.733E-07	0.710E-02	57
58	19.79054	5.39031	0.75069	0.14961E-05	0.02589	0.11000	0.06283	0.01182	10.00352	0.876E-07	0.741E-02	58
59	20.12389	5.54322	0.74742	0.15593E-05	0.03643	0.11687	0.06688	0.01224	10.17160	0.647E-07	0.529E-02	59
60	20.45721	5.69312	0.74403	0.16216E-05	0.03247	0.12721	0.07294	0.01298	10.34607	0.752E-07	0.579E-02	60
61	20.79054	5.86294	0.74065	0.16177E-05	0.03621	0.11496	0.06604	0.01143	10.51976	0.670E-07	0.586E-02	61
62	21.12389	6.02658	0.73741	0.15527E-05	0.03854	0.11759	0.06768	0.01139	10.68816	0.602E-07	0.529E-02	62
63	21.45721	6.19899	0.73432	0.14874E-05	0.03860	0.10975	0.06328	0.01035	10.84531	0.574E-07	0.554E-02	63
64	21.79054	6.36240	0.73104	0.15768E-05	0.03782	0.12590	0.07273	0.01158	11.01367	0.618E-07	0.534E-02	64
65	22.12389	6.55583	0.72826	0.13444E-05	0.03782	0.09308	0.05386	0.00834	11.15701	0.526E-07	0.630E-02	65
66	22.46555	6.75097	0.72507	0.14995E-05	0.04348	0.10846	0.06288	0.00945	11.32056	0.508E-07	0.537E-02	66
67	22.82999	5.23233	0.72390	0.52111E-06	-0.03348	-0.00463	-0.00268	-0.00045	11.38115	-0.229E-07	0.509E-01	67
68	23.16333	3.76697	0.72450	-0.29353E-06	-0.03914	0.00185	0.00107	0.00024	11.34991	0.110E-07	0.459E-01	68
69	23.47916	2.84513	0.72542	-0.46750E-06	-0.04713	0.00327	0.00189	0.00058	11.30276	0.146E-07	0.254E-01	69
70	23.81248	2.14871	0.72724	-0.87895E-06	-0.05138	0.00648	0.00375	0.00151	11.20914	0.253E-07	0.167E-01	70
71	24.11055	1.70581	0.72946	-0.11935E-05	-0.05025	0.00960	0.00555	0.00289	11.09528	0.352E-07	0.122E-01	71
72	24.44388	1.34249	0.73212	-0.12827E-05	-0.05086	0.01113	0.00642	0.00424	10.95824	0.375E-07	0.884E-02	72
73	24.88222	0.99590	0.73591	-0.13820E-05	-0.05199	0.01268	0.00730	0.00629	10.76361	0.396E-07	0.630E-02	73
74	25.27499	0.75834	0.73955	-0.14810E-05	-0.05398	0.01337	0.00768	0.00882	10.57632	0.411E-07	0.466E-02	74
75	25.60832	0.60813	0.74269	-0.15029E-05	-0.05313	0.01424	0.00817	0.01201	10.41476	0.425E-07	0.354E-02	75
76	25.94167	0.48016	0.74587	-0.15172E-05	-0.05680	0.01345	0.00771	0.01423	10.25137	0.403E-07	0.283E-02	76
77	26.27499	0.37884	0.74923	-0.15994E-05	-0.06134	0.01416	0.00810	0.01894	10.07881	0.395E-07	0.208E-02	77
78	26.60832	0.30829	0.75264	-0.16224E-05	-0.06110	0.01656	0.00945	0.02759	9.90340	0.404E-07	0.146E-02	78
79	26.85971	0.26273	0.75523	-0.16294E-05	-0.07408	0.01618	0.00922	0.03237	9.77036	0.335E-07	0.104E-02	79
80	27.19333	0.68382	0.75482	0.19525E-06	0.02141	0.00043	0.00024	0.00056	9.79150	0.139E-07	0.250E-01	80
81	27.52666	0.98361	0.75210	0.12912E-05	0.03105	0.00747	0.00426	0.00517	9.93105	0.632E-07	0.122E-01	81
82	27.85999	1.22694	0.74889	0.15320E-05	0.02396	0.01454	0.00832	0.00756	10.09630	0.968E-07	0.128E-01	82
83	28.22137	1.53531	0.74592	0.13053E-05	0.03926	0.01323	0.00758	0.00551	10.24876	0.502E-07	0.911E-02	83
84	28.53638	1.81372	0.74321	0.13733E-05	0.04181	0.01629	0.00934	0.00559	10.38831	0.494E-07	0.883E-02	84
85	28.99498	2.27529	0.73917	0.14058E-05	0.03897	0.01781	0.01024	0.00503	10.59578	0.540E-07	0.107E-01	85
86	29.34166	2.66134	0.73589	0.15169E-05	0.04435	0.02097	0.01208	0.00490	10.76476	0.510E-07	0.104E-01	86
87	29.58388	2.96771	0.73378	0.13941E-05	0.04775	0.01934	0.01116	0.00397	10.87309	0.434E-07	0.109E-01	87
88	29.91721	3.39949	0.73142	0.11347E-05	0.04888	0.01736	0.01002	0.00315	10.99426	0.344E-07	0.109E-01	88
89	30.30304	3.94263	0.72831	0.12946E-05	0.04775	0.02097	0.01213	0.00331	11.15405	0.401E-07	0.121E-01	89
90	30.71860	4.53418	0.72463	0.14260E-05	0.05228	0.02632	0.01526	0.00361	11.34317	0.402E-07	0.111E-01	90
91	31.05220	4.99077	0.72216	0.11971E-05	0.05505	0.02580	0.01498	0.00315	11.47044	0.319E-07	0.101E-01	91
92	31.38554	5.38876	0.71923	0.14195E-05	0.05477	0.03817	0.02220	0.00428	11.62102	0.379E-07	0.886E-02	92
93	31.71887	5.77751	0.71624	0.14518E-05	0.06163	0.04292	0.02501	0.00448	11.77470	0.343E-07	0.766E-02	93
94	32.05220	6.12858	0.71316	0.14990E-05	0.06326	0.05223	0.03049	0.00512	11.93312	0.344E-07	0.672E-02	94
95	32.38554	6.46973	0.71076	0.11656E-05	0.06637	0.04419	0.02583	0.00410	12.05615	0.254E-07	0.620E-02	95
96	32.71887	6.75927	0.70734	0.16735E-05	0.06609	0.07831	0.04587	0.00694	12.23241	0.365E-07	0.527E-02	96

97	33.05220	7.07576	0.70473	0.12745E-05	0.07118	0.05698	0.03342	0.00483	12.36642	0.258E-07	0.533E-02 97
98	33.38554	7.34513	0.70144	0.16093E-05	0.07486	0.08793	0.05168	0.00717	12.53534	0.308E-07	0.430E-02 98
99	34.05220	7.90989	0.69544	0.14762E-05	0.07508	0.08108	0.04782	0.00627	12.84409	0.280E-07	0.446E-02 99
100	34.38554	8.19822	0.69226	0.15621E-05	0.08025	0.08862	0.05237	0.00650	13.00717	0.276E-07	0.424E-02100
101	34.84665	8.57900	0.68830	0.14145E-05	0.08110	0.08732	0.05172	0.00617	13.21097	0.246E-07	0.399E-02101
102	35.29637	8.94396	0.68373	0.16770E-05	0.08506	0.10972	0.06516	0.00744	13.44595	0.277E-07	0.372E-02102
103	35.62971	9.24323	0.68065	0.15247E-05	0.08725	0.09345	0.05560	0.00611	13.60408	0.244E-07	0.400E-02103
104	60.20444	9.74025	0.67508	0.37572E-07	0.09072	0.10632	0.06347	0.00669	13.89030	0.575E-09	0.860E-04104
105	60.53777	10.03465	0.67219	0.14427E-05	0.09433	0.09720	0.05813	0.00588	14.03911	0.212E-07	0.360E-02105
106	60.91110	10.38733	0.66873	0.15438E-05	0.09780	0.10022	0.06006	0.00588	14.21709	0.218E-07	0.370E-02106
107	61.21944	10.65415	0.66576	0.16032E-05	0.10120	0.11691	0.07018	0.00667	14.36948	0.218E-07	0.326E-02107
108	61.55276	10.98367	0.66294	0.14140E-05	0.09752	0.09261	0.05569	0.00515	14.51450	0.198E-07	0.385E-02108
109	61.88611	11.32197	0.65986	0.16498E-05	0.09922	0.10830	0.06526	0.00585	14.68341	0.227E-07	0.387E-02109
110	62.21944	11.66739	0.65683	0.14195E-05	0.09335	0.09393	0.05669	0.00493	14.82851	0.207E-07	0.419E-02110
111	62.55276	12.00006	0.65380	0.15300E-05	0.09279	0.10798	0.06529	0.00552	14.98456	0.223E-07	0.404E-02111
112	62.88611	12.36721	0.65051	0.16592E-05	0.09250	0.10908	0.06609	0.00542	15.15352	0.242E-07	0.446E-02112
113	63.21944	12.70912	0.64776	0.13911E-05	0.09505	0.10085	0.06121	0.00488	15.29494	0.197E-07	0.403E-02113
114	63.55276	13.08997	0.64444	0.16835E-05	0.08911	0.11253	0.06843	0.00530	15.46571	0.253E-07	0.477E-02114
115	63.88611	13.45305	0.64143	0.15251E-05	0.09088	0.10980	0.06689	0.00504	15.62015	0.224E-07	0.444E-02115
116	64.21944	13.84043	0.63879	0.13424E-05	0.09420	0.09299	0.05674	0.00416	15.75583	0.189E-07	0.456E-02116
117	64.55276	14.23308	0.63511	0.18752E-05	0.09477	0.13152	0.08044	0.00573	15.94499	0.262E-07	0.457E-02117
118	64.88611	14.64598	0.63257	0.12971E-05	0.10306	0.08888	0.05444	0.00377	16.07562	0.166E-07	0.440E-02118
119	65.21944	15.05870	0.62939	0.16263E-05	0.10249	0.11438	0.07020	0.00473	16.23906	0.209E-07	0.441E-02119
120	65.55276	15.49523	0.62632	0.15744E-05	0.10533	0.10756	0.06614	0.00433	16.39703	0.196E-07	0.452E-02120
121	65.88611	15.92325	0.62318	0.16141E-05	0.10192	0.11536	0.07107	0.00453	16.55864	0.207E-07	0.456E-02121
122	66.21944	16.38475	0.62031	0.14738E-05	0.10370	0.10031	0.06191	0.00383	16.70598	0.185E-07	0.482E-02122
123	66.55276	16.82991	0.61738	0.15098E-05	0.11446	0.10933	0.06760	0.00407	16.85660	0.171E-07	0.420E-02123
124	66.88611	17.31479	0.61438	0.15494E-05	0.11702	0.10566	0.06545	0.00383	17.01088	0.171E-07	0.445E-02124
125	67.36722	18.01114	0.60981	0.16405E-05	0.12438	0.11600	0.07206	0.00408	17.24600	0.169E-07	0.415E-02125
126	67.86583	14.24613	0.60992	-0.40279E-07	-0.01253	0.00050	0.00031	0.00002	17.24005	0.413E-08	0.215E+00126
127	68.23637	11.35757	0.61067	-0.34922E-06	-0.02330	0.00331	0.00206	0.00016	17.20146	0.192E-07	0.119E+00127
128	68.68054	8.67550	0.61225	-0.61322E-06	-0.03865	0.00587	0.00364	0.00037	17.12021	0.204E-07	0.558E-01128
129	69.20888	6.26950	0.61458	-0.75881E-06	-0.05172	0.00717	0.00444	0.00060	17.00043	0.189E-07	0.316E-01129
130	69.67583	4.67951	0.61694	-0.86720E-06	-0.05654	0.00806	0.00498	0.00092	16.87927	0.198E-07	0.216E-01130
131	69.99611	3.81742	0.61869	-0.93768E-06	-0.06079	0.00859	0.00531	0.00125	16.78929	0.200E-07	0.160E-01131
132	70.49472	2.79120	0.62187	-0.10918E-05	-0.06390	0.01015	0.00626	0.00191	16.62590	0.222E-07	0.116E-01132
133	70.84721	2.23836	0.62413	-0.10949E-05	-0.06820	0.01023	0.00630	0.00251	16.50987	0.210E-07	0.834E-02133
134	71.19666	1.66469	0.62684	-0.13261E-05	-0.06990	0.00916	0.00563	0.00291	16.37038	0.249E-07	0.855E-02134
135	71.53000	1.48530	0.62966	-0.14425E-05	-0.06848	0.02474	0.01518	0.00965	16.22536	0.277E-07	0.287E-02135
136	71.86333	1.05525	0.63241	-0.14036E-05	-0.05913	0.00805	0.00493	0.00392	16.08400	0.313E-07	0.799E-02136
137	72.19666	0.77084	0.63487	-0.12560E-05	-0.05460	0.00784	0.00480	0.00530	15.95737	0.304E-07	0.574E-02137
138	72.53000	0.85718	0.63791	-0.15442E-05	-0.07244	-0.02859	-0.01746	-0.02146	15.80132	0.283E-07	-0.132E-02138
139	72.86333	0.73378	0.64119	-0.16681E-05	-0.07470	0.02113	0.01288	0.01622	15.63246	0.298E-07	0.184E-02139
140	73.24638	0.51467	0.64473	-0.15599E-05	-0.07814	0.00998	0.00607	0.00982	15.45059	0.267E-07	0.272E-02140
141	73.57971	0.49497	0.64787	-0.15889E-05	-0.07899	0.08051	0.04886	0.09681	15.28908	0.270E-07	0.279E-03141
142	73.91306	0.40637	0.65109	-0.16217E-05	-0.08607	0.01629	0.00987	0.02196	15.12386	0.254E-07	0.116E-02142
143	74.24638	0.31812	0.65419	-0.15648E-05	-0.08182	0.01269	0.00767	0.02128	14.96422	0.259E-07	0.122E-02143
144	74.57971	0.11666	0.65748	-0.16514E-05	-0.08380	0.00327	0.00198	0.00984	14.79535	0.268E-07	0.272E-02144
145	74.91306	-0.08897	0.66076	-0.16481E-05	-0.08777	0.0	0.0	0.0	14.62650	0.256E-07	0.100E+05145

ENGINEERING STRAIN (145)= 14.6265

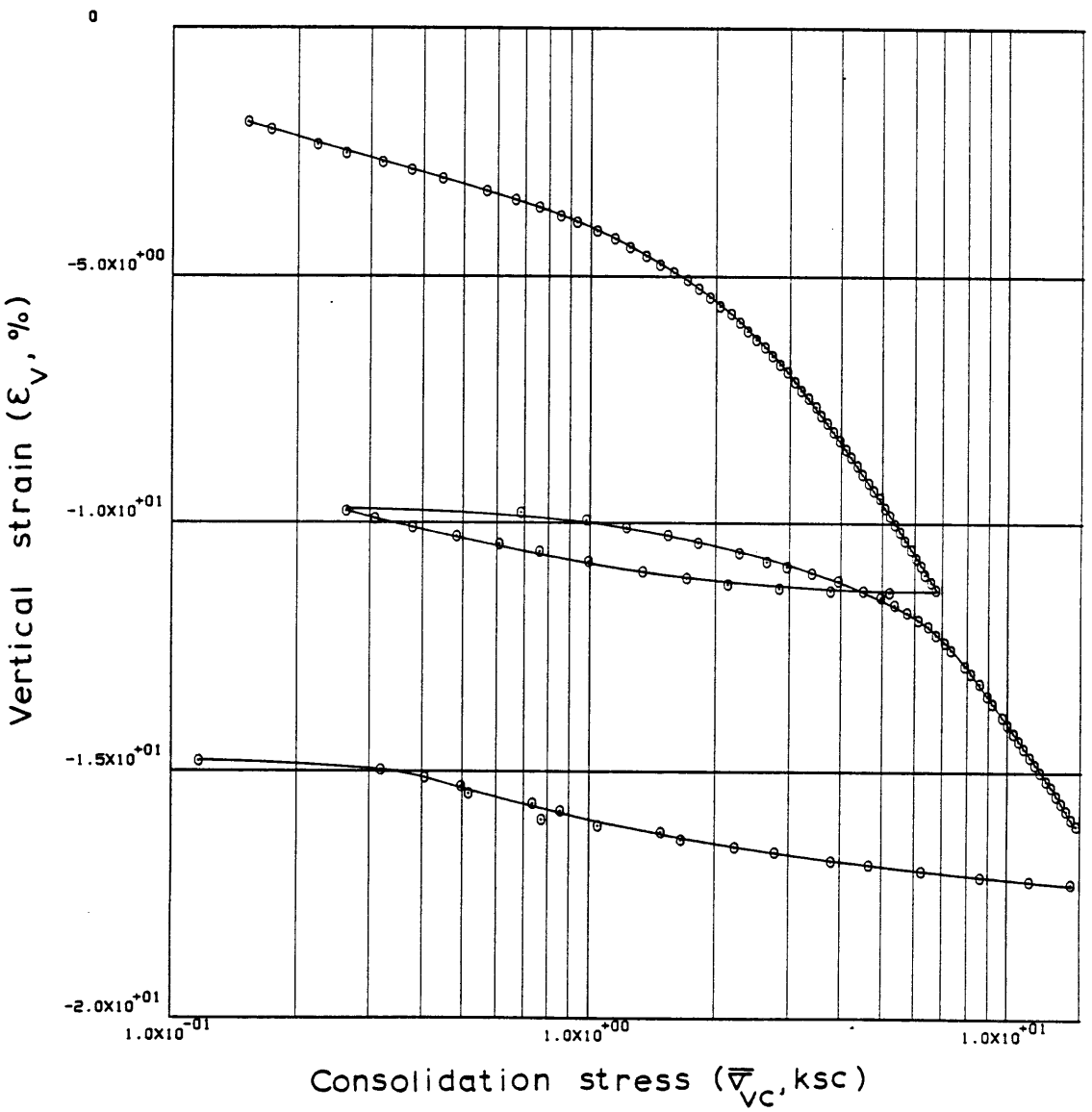

Sample No. 36.5-38.5-C-H w_N (%) 31.15 Estimated

Depth 37.18 w_L (%) 31.30 $\bar{\sigma}_{vo}$ 0.84 $\bar{\sigma}_{vm}$ 207-222

Soil Type Boston w_P (%) 20.90 CR 0.1397 RR 0.0147

Blue Clay P.I.(%) 10.40 G_s 2.77 e_o 0.9453

o At t_p Remarks Data from C.R.S.C test

$\bar{w}_L$ & $\bar{w}_P$ estimated from Baligh et al (1980)

Figure E.11 Compression curve for Sample No. 36.5-38.5-C-H

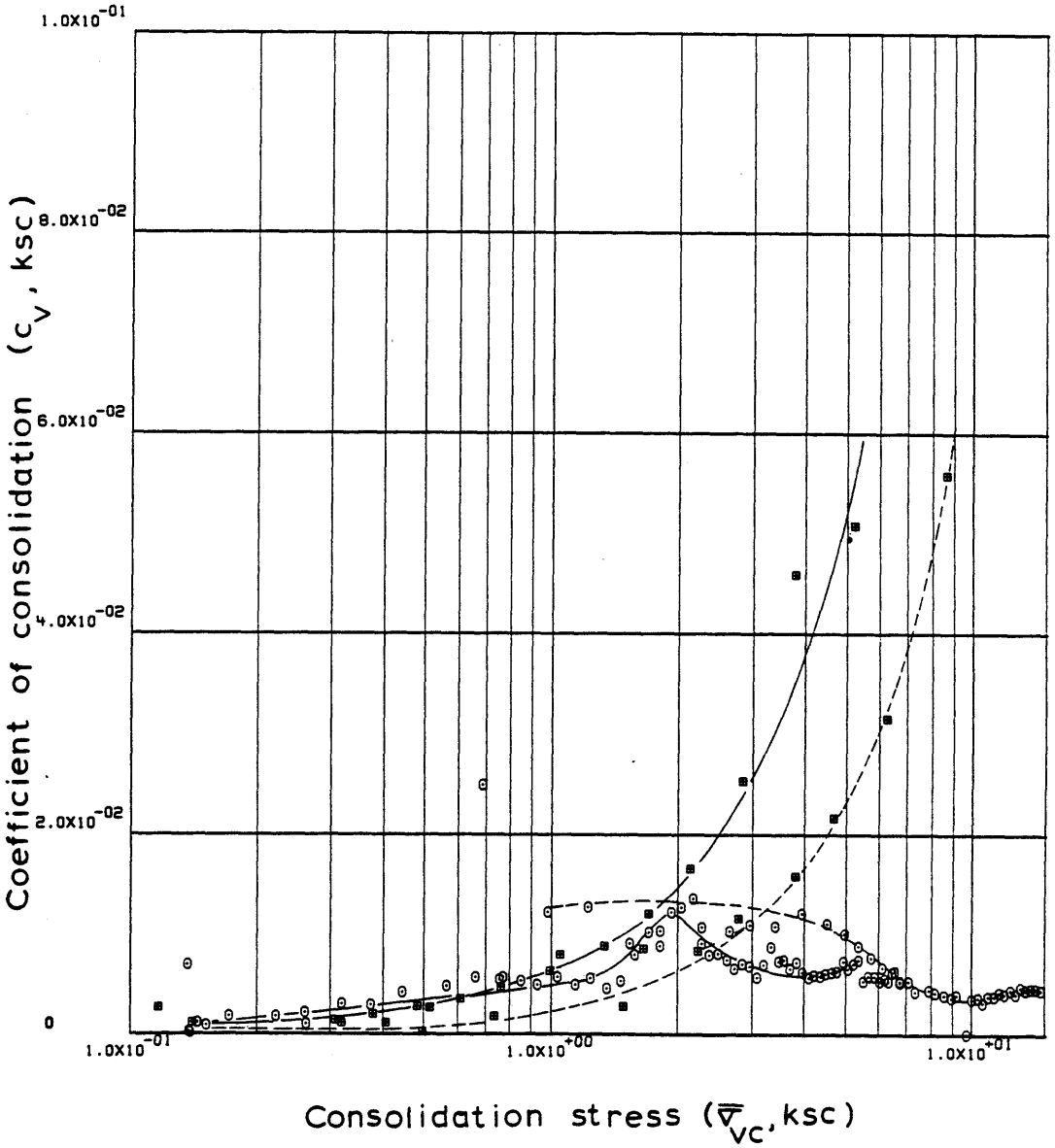

Sample No. 36.5-38.5-C-H w_N (%) 31.15 Estimated

Depth 37.18 w_L (%) 31.30 $\bar{\sigma}_{vo}$ 0.84 $\bar{\sigma}_{vm}$ 207-222

Soil Type Boston w_P (%) 20.90 CR 0.1397 RR 0.0147

Blue Clay P.I.(%) 10.40 G_S 2.77 e_o 0.9453

o At t_p Remarks Data from C.R.S.C test

$\bar{w}_L$ & $\bar{w}_P$ estimated from Baligh et al (1980)

Figure E.12 Variation of coefficient of consolidation with consolidation stress for Sample No. 36.5-38.5-C-H

1-D STRAIN CONTROLLED COMPRESSION TEST

COMPUTED RESULTS

INITIAL VOID RATIO= 0.84595
INITIAL HEIGHT= 2.3368

ALL UNITS IN: KG,CM,SEC

LINEAR THEORY

	TIME IN HOURS	VERTICAL STRESS	E	RATE OF STRAIN	EXCESS PORE PRESSURE	C	C/1+E	MV	PERCENT COMPRESSION	K	CV	
1	0.0	0.35529	0.84584	0.0	0.00014	0.0	0.0	0.00017	0.00597	0.0	0.0	1
2	0.34167	0.41332	0.84440	0.63195E-06	0.01425	0.00947	0.00514	0.01339	0.08363	0.121E-06	0.902E-02	2
3	0.67500	0.48683	0.84311	0.58529E-06	0.01371	0.00791	0.00429	0.00955	0.15378	0.116E-06	0.122E-01	3
4	1.00833	0.55939	0.84044	0.12109E-05	0.01147	0.01925	0.01046	0.02003	0.29866	0.286E-06	0.143E-01	4
5	1.34167	0.65443	0.83725	0.14453E-05	0.01825	0.02030	0.01105	0.01825	0.47125	0.214E-06	0.117E-01	5
6	1.67500	0.74060	0.83391	0.15168E-05	0.01543	0.02699	0.01471	0.02112	0.65208	0.265E-06	0.125E-01	6
7	2.00833	0.87504	0.83074	0.14427E-05	0.01374	0.01900	0.01038	0.01288	0.82379	0.282E-06	0.219E-01	7
8	2.34167	0.98770	0.82732	0.15597E-05	0.02221	0.02824	0.01546	0.01661	1.00906	0.188E-06	0.113E-01	8
9	2.67500	1.12454	0.82392	0.15546E-05	0.02727	0.02623	0.01438	0.01363	1.19341	0.152E-06	0.111E-01	9
10	3.00833	1.25438	0.82036	0.16274E-05	0.01993	0.03253	0.01787	0.01504	1.38596	0.217E-06	0.144E-01	10
11	3.34167	1.42071	0.81674	0.16645E-05	0.02895	0.02914	0.01604	0.01201	1.58255	0.152E-06	0.127E-01	11
12	3.67500	1.55883	0.81355	0.14648E-05	0.02950	0.03436	0.01895	0.01273	1.75526	0.131E-06	0.103E-01	12
13	4.00833	1.72843	0.81010	0.15878E-05	0.03119	0.03340	0.01845	0.01123	1.94209	0.134E-06	0.119E-01	13
14	4.34167	1.86930	0.80700	0.14312E-05	0.03061	0.03967	0.02196	0.01222	2.11018	0.122E-06	0.100E-01	14
15	4.67500	1.96634	0.80459	0.11128E-05	0.03171	0.04654	0.02579	0.01344	2.24075	0.916E-07	0.681E-02	15
16	5.00833	2.10731	0.80127	0.15321E-05	0.03567	0.04855	0.02695	0.01323	2.42015	0.112E-06	0.844E-02	16
17	5.34167	2.24555	0.79788	0.15724E-05	0.03622	0.05339	0.02970	0.01365	2.60393	0.112E-06	0.824E-02	17
18	5.67500	2.38739	0.79456	0.15438E-05	0.03904	0.05427	0.03024	0.01306	2.78403	0.102E-06	0.781E-02	18
19	6.00833	2.53821	0.79125	0.15368E-05	0.04355	0.05399	0.03014	0.01224	2.96318	0.908E-07	0.742E-02	19
20	6.34167	2.67821	0.78754	0.17289E-05	0.04920	0.06908	0.03865	0.01482	3.16409	0.900E-07	0.607E-02	20
21	6.67500	2.81331	0.78505	0.11635E-05	0.03963	0.05064	0.02837	0.01033	3.29910	0.750E-07	0.725E-02	21
22	7.00833	2.94993	0.78254	0.11732E-05	0.03515	0.05291	0.02968	0.01030	3.43504	0.850E-07	0.825E-02	22
23	7.34165	3.04097	0.77931	0.15144E-05	0.03738	0.10640	0.05980	0.01996	3.61020	0.101E-06	0.507E-02	23
24	7.67498	3.15827	0.77610	0.15017E-05	0.02668	0.08456	0.04761	0.01536	3.78362	0.142E-06	0.926E-02	24
25	8.00833	3.29937	0.77263	0.16312E-05	0.03574	0.07941	0.04480	0.01387	3.97159	0.115E-06	0.828E-02	25
26	8.34165	3.38376	0.76916	0.16385E-05	0.03570	0.13771	0.07784	0.02330	4.16002	0.115E-06	0.494E-02	26
27	8.67498	3.51658	0.76553	0.17100E-05	0.03684	0.09410	0.05330	0.01545	4.35628	0.116E-06	0.750E-02	27
28	9.00833	3.62750	0.76199	0.16744E-05	0.04021	0.11402	0.06471	0.01811	4.54808	0.104E-06	0.572E-02	28
29	9.34165	3.75147	0.75835	0.17281E-05	0.03174	0.10850	0.06171	0.01673	4.74561	0.135E-06	0.806E-02	29
30	9.67498	3.82239	0.75488	0.16470E-05	0.04187	0.18515	0.10551	0.02787	4.93347	0.971E-07	0.348E-02	30
31	10.00833	3.98416	0.75157	0.15718E-05	0.04527	0.07972	0.04551	0.01166	5.11246	0.853E-07	0.732E-02	31
32	10.34165	4.08199	0.74822	0.16015E-05	0.04300	0.13847	0.07920	0.01964	5.29443	0.912E-07	0.464E-02	32
33	10.67498	4.19807	0.74471	0.16741E-05	0.03622	0.12503	0.07166	0.01731	5.48433	0.113E-06	0.651E-02	33
34	11.00833	4.28426	0.74112	0.17163E-05	0.04128	0.17645	0.10134	0.02390	5.67859	0.101E-06	0.423E-02	34
35	11.34165	4.46231	0.73776	0.16150E-05	0.04300	0.08270	0.04759	0.01088	5.86102	0.909E-07	0.835E-02	35
36	11.67498	4.57988	0.73435	0.16376E-05	0.04920	0.13107	0.07557	0.01671	6.04565	0.802E-07	0.480E-02	36
37	12.00833	4.73144	0.73092	0.16526E-05	0.04751	0.10545	0.06092	0.01308	6.23163	0.835E-07	0.638E-02	37
38	12.34165	4.85613	0.72761	0.15953E-05	0.05822	0.12711	0.07357	0.01535	6.41078	0.655E-07	0.427E-02	38
39	12.67498	4.99399	0.72410	0.16959E-05	0.04920	0.12534	0.07270	0.01476	6.60085	0.821E-07	0.556E-02	39
40	13.00833	5.12489	0.72067	0.16624E-05	0.05316	0.13266	0.07710	0.01524	6.78677	0.742E-07	0.487E-02	40
41	13.34165	5.30702	0.71723	0.16689E-05	0.05830	0.09848	0.05735	0.01100	6.97308	0.671E-07	0.610E-02	41

42	13.67498	5.42610	-0.15260	0.85541E-03	0.05257	39.20087	0.0	8.62042	54.09422	0.936E-05	0.109E-02	42
43	14.00833	5.56305	0.70806	-0.41989E-03	0.05033	-30.18347	-17.67116	-3.21040	7.46954	-0.195E-04	0.607E-02	43
44	14.34165	5.76646	0.70470	0.16448E-05	0.05147	0.10409	0.06106	0.01076	7.65181	0.744E-07	0.691E-02	44
45	14.67498	5.90661	0.70137	0.16303E-05	0.04920	0.13861	0.08147	0.01396	7.83211	0.769E-07	0.551E-02	45
46	15.00833	6.11950	0.69788	0.17156E-05	0.05429	0.09871	0.05814	0.00967	8.02148	0.730E-07	0.755E-02	46
47	15.34165	6.30299	0.69444	0.16897E-05	0.05543	0.11631	0.06864	0.01105	8.20761	0.701E-07	0.635E-02	47
48	15.67500	6.48401	0.69112	0.16337E-05	0.05770	0.11711	0.06925	0.01083	8.38724	0.649E-07	0.599E-02	48
49	16.00832	6.62916	0.68775	0.16667E-05	0.05316	0.15245	0.09033	0.01378	8.57007	0.716E-07	0.519E-02	49
50	16.34164	6.89932	0.68447	0.16215E-05	0.06107	0.08206	0.04872	0.00720	8.74763	0.604E-07	0.838E-02	50
51	16.67499	7.08270	0.68115	0.16457E-05	0.06221	0.12655	0.07528	0.01077	8.92749	0.599E-07	0.556E-02	51
52	17.00832	7.28993	0.67779	0.16698E-05	0.05825	0.11660	0.06950	0.00967	9.10962	0.647E-07	0.669E-02	52
53	17.34164	7.52162	0.67454	0.16165E-05	0.06052	0.10379	0.06198	0.00837	9.28557	0.600E-07	0.717E-02	53
54	17.67499	7.74891	0.67124	0.16481E-05	0.06676	0.11103	0.06644	0.00870	9.46465	0.553E-07	0.635E-02	54
55	18.00832	7.98658	0.66778	0.17283E-05	0.06731	0.11355	0.06809	0.00865	9.65201	0.572E-07	0.661E-02	55
56	18.34164	8.22287	0.66465	0.15658E-05	0.06844	0.10822	0.06501	0.00802	9.82146	0.508E-07	0.633E-02	56
57	18.67499	8.44827	0.66131	0.16728E-05	0.06958	0.12333	0.07424	0.00891	10.00212	0.532E-07	0.597E-02	57
58	19.00832	8.71036	0.65803	0.16515E-05	0.06958	0.10754	0.06486	0.00756	10.18010	0.523E-07	0.691E-02	58
59	19.34164	8.96394	0.65489	0.15825E-05	0.06958	0.10954	0.06619	0.00749	10.35036	0.499E-07	0.666E-02	59
60	19.67499	9.24001	0.65160	0.16588E-05	0.07973	0.10611	0.06424	0.00706	10.52846	0.455E-07	0.644E-02	60
61	20.00832	9.51821	0.64847	0.15803E-05	0.07691	0.10775	0.06536	0.00697	10.69783	0.447E-07	0.642E-02	61
62	20.34164	9.80973	0.64528	0.16190E-05	0.08087	0.10593	0.06439	0.00666	10.87096	0.434E-07	0.652E-02	62
63	20.67499	10.10644	0.64205	0.16392E-05	0.07467	0.10840	0.06602	0.00663	11.04594	0.474E-07	0.715E-02	63
64	21.00832	10.40944	0.63883	0.16326E-05	0.07918	0.10870	0.06633	0.00647	11.21989	0.444E-07	0.686E-02	64
65	21.34164	10.71599	0.63573	0.15796E-05	0.07804	0.10682	0.06530	0.00618	11.38783	0.434E-07	0.702E-02	65
66	21.67499	11.03723	0.63256	0.16201E-05	0.07805	0.10749	0.06584	0.00605	11.55980	0.443E-07	0.732E-02	66
67	22.00832	11.37172	0.62955	0.15381E-05	0.08369	0.10072	0.06181	0.00552	11.72272	0.391E-07	0.709E-02	67
68	22.34164	11.69110	0.62667	0.14742E-05	0.08652	0.10391	0.06388	0.00554	11.87862	0.361E-07	0.652E-02	68
69	22.67499	12.05493	0.62346	0.16495E-05	0.08820	0.10484	0.06458	0.00544	12.05267	0.395E-07	0.726E-02	69
70	23.00832	12.39636	0.62042	0.15630E-05	0.08876	0.10882	0.06716	0.00549	12.21735	0.370E-07	0.674E-02	70
71	23.34164	12.79786	0.61712	0.17002E-05	0.09272	0.10352	0.06402	0.00508	12.39607	0.384E-07	0.756E-02	71
72	23.67499	13.22034	0.61400	0.16136E-05	0.10235	0.09619	0.05960	0.00458	12.56535	0.329E-07	0.718E-02	72
73	24.00832	13.60496	0.61103	0.15337E-05	0.09839	0.10339	0.06418	0.00478	12.72598	0.324E-07	0.677E-02	73
74	24.34164	14.01914	0.60808	0.15320E-05	0.10460	0.09858	0.06130	0.00444	12.88612	0.303E-07	0.684E-02	74
75	24.67499	14.39870	0.60479	0.17062E-05	0.10119	0.12302	0.07666	0.00539	13.06413	0.348E-07	0.645E-02	75
76	25.00832	14.84081	0.60182	0.15478E-05	0.10798	0.09836	0.06140	0.00420	13.22531	0.295E-07	0.702E-02	76
77	25.34164	15.29273	0.59881	0.15665E-05	0.11362	0.10021	0.06268	0.00416	13.38811	0.282E-07	0.679E-02	77
78	47.94998	15.51206	0.59086	0.61435E-07	0.00756	0.55859	0.35113	0.02280	13.81903	0.165E-07	0.722E-03	78
79	48.29164	13.55659	0.58891	0.99543E-06	-0.01444	-0.01443	-0.00908	-0.00063	13.92439	-0.139E-06	0.223E+00	79
80	48.62498	11.27417	0.58967	-0.39775E-06	-0.03004	0.00411	0.00259	0.00021	13.88330	0.268E-07	0.128E+00	80
81	48.95831	9.47326	0.59054	-0.45717E-06	-0.04072	0.00501	0.00315	0.00030	13.83604	0.228E-07	0.747E-01	81
82	49.29164	8.02367	0.59212	-0.82898E-06	-0.03924	0.00953	0.00599	0.00069	13.75026	0.429E-07	0.625E-01	82
83	49.62498	6.82270	0.59367	-0.80583E-06	-0.03978	0.00951	0.00597	0.00081	13.66676	0.412E-07	0.512E-01	83
84	49.95831	5.80199	0.59577	-0.10999E-05	-0.03979	0.01299	0.00814	0.00129	13.55266	0.564E-07	0.436E-01	84
85	50.29164	4.95034	0.59826	-0.12970E-05	-0.05557	0.01567	0.00981	0.00183	13.41789	0.478E-07	0.261E-01	85
86	50.62498	4.25460	0.60086	-0.13549E-05	-0.04202	0.01718	0.01073	0.00234	13.27689	0.662E-07	0.283E-01	86
87	50.95831	3.67983	0.60315	-0.11868E-05	-0.04539	0.01573	0.00981	0.00248	13.15320	0.538E-07	0.217E-01	87
88	51.29164	3.18907	0.60575	-0.13488E-05	-0.05842	0.01816	0.01131	0.00330	13.01244	0.477E-07	0.145E-01	88
89	51.62498	2.79101	0.60811	-0.12264E-05	-0.04598	0.01775	0.01104	0.00370	12.88420	0.553E-07	0.149E-01	89
90	51.95831	2.47171	0.61137	-0.16851E-05	-0.05048	0.02681	0.01664	0.00633	12.70770	0.695E-07	0.110E-01	90
91	52.29164	2.16043	0.61425	-0.14840E-05	-0.06457	0.02136	0.01323	0.00572	12.55196	0.480E-07	0.839E-02	91
92	52.62498	1.91943	0.61725	-0.15489E-05	-0.06230	0.02541	0.01571	0.00771	12.38913	0.521E-07	0.676E-02	92
93	52.95831	1.69027	0.61991	-0.13686E-05	-0.05780	0.02092	0.01291	0.00717	12.24503	0.498E-07	0.695E-02	93
94	53.29164	1.51699	0.62255	-0.13566E-05	-0.02061	0.02442	0.01505	0.00939	12.10194	0.139E-06	0.148E-01	94
95	53.62498	1.42004	0.62535	-0.14339E-05	-0.05614	0.04235	0.02606	0.01775	11.95041	0.541E-07	0.305E-02	95
96	53.95831	1.25796	0.62935	-0.20444E-05	-0.07074	0.03297	0.02024	0.01514	11.73390	0.615E-07	0.406E-02	96

97	54.29164	1.09758	0.63277	-0.17485E-05	-0.07074	0.02512	0.01539	0.01308	11.54829	0.528E-07	0.404E-02 97
98	54.62498	0.94909	0.63591	-0.16001E-05	-0.09388	0.02161	0.01321	0.01293	11.37814	0.365E-07	0.283E-02 98
99	54.95831	0.84169	0.63906	-0.15988E-05	-0.09499	0.02619	0.01598	0.01786	11.20781	0.362E-07	0.203E-02 99
100	55.29164	0.79954	0.64218	-0.15854E-05	-0.08120	0.06082	0.03704	0.04514	11.03853	0.422E-07	0.935E-03100
101	55.62498	0.68942	0.64527	-0.15614E-05	-0.08124	0.02081	0.01265	0.01701	10.87152	0.417E-07	0.245E-02101
102	55.95831	0.65485	0.64857	-0.16727E-05	-0.07559	0.04012	0.02434	0.03678	10.69228	0.482E-07	0.131E-02102
103	56.29164	0.60396	0.65165	-0.15526E-05	-0.07504	0.06170	0.03736	0.06032	10.52557	0.452E-07	0.750E-03103
104	56.62498	0.55221	0.65497	-0.16711E-05	-0.07052	0.03705	0.02238	0.03875	10.34579	0.520E-07	0.134E-02104
105	56.95831	0.49408	0.65836	-0.17015E-05	-0.07671	0.03045	0.01836	0.03513	10.16235	0.489E-07	0.139E-02105

ENGINEERING STRAIN (105)= 10.1624

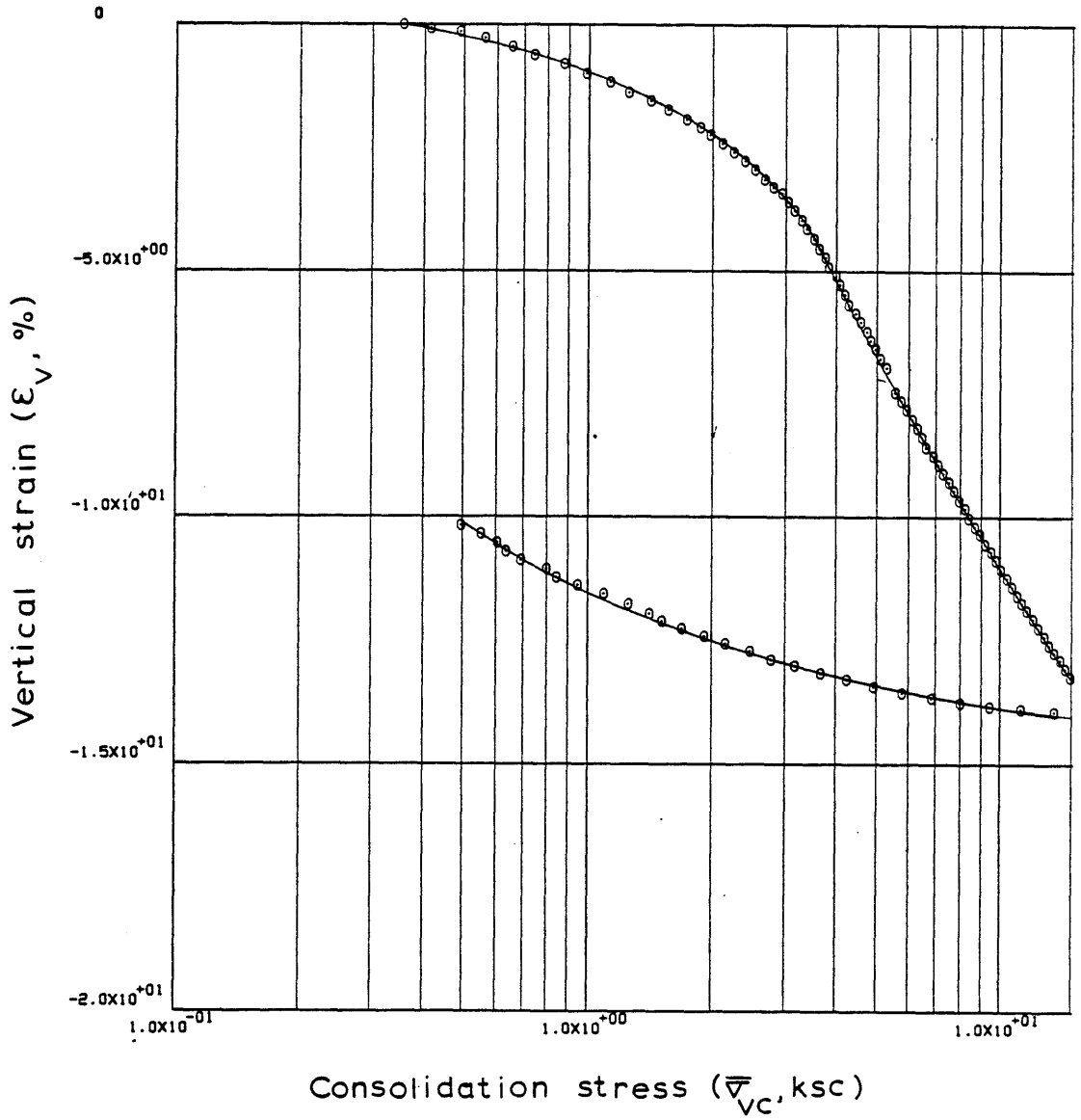

Sample No. SP03VERT w_N (%) 30.53 Estimated

Depth 41.00 w_L (%) 41.41 $\bar{\sigma}_{vo}$ 0.93 $\bar{\sigma}_{vm}$ 300.315

Soil Type Boston w_P (%) 22.47 CR 01435 RR 0.0250

Blue Clay P.I.(%) 18.94 G_S 2.77 e_o 0.8459

⊙ At t_p Remarks Data from C.R.S.C test

w_L & w_P estimated from Baligh et al (1980)

Figure E.13 Compression Curve for Sample No. SP03VERT

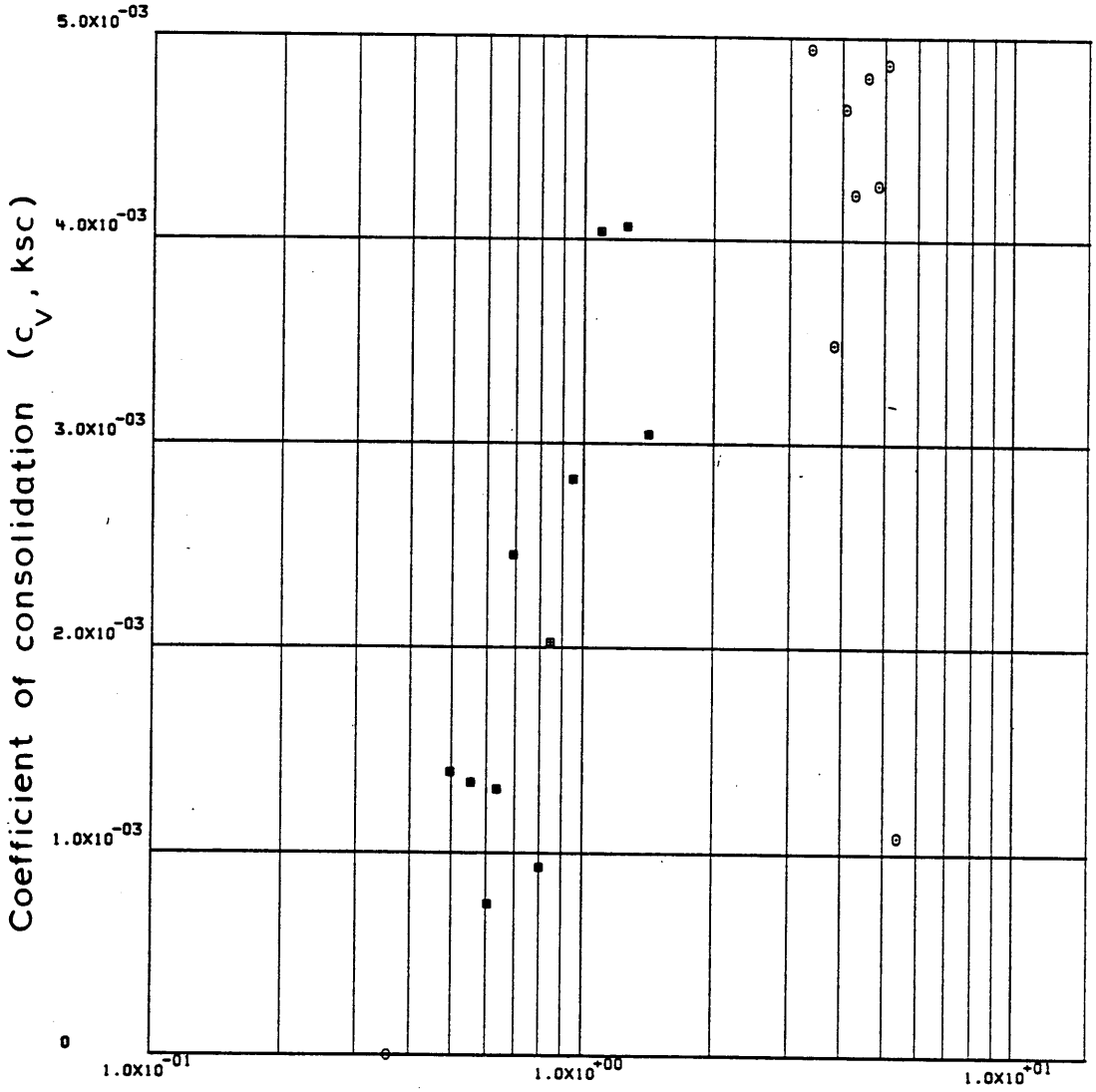

Sample No. SP03VERT w_N (%) 30.53 Estimated

Depth 41.00 w_L (%) 41.41 $\bar{\sigma}_{vo}$ 0.93 $\bar{\sigma}_{vm}$ 300.315

Soil Type Boston w_P (%) 22.47 CR 0.1435 RR 0.0250

Blue Clay P.I.(%) 18.94 G_S 2.77 e_o 0.8459

o At t_p Remarks Data from C.R.S.C test

w_L & w_P estimated from Baligh et al (1980)

Figure E.14 Variation of coefficient of consolidation with consolidation stress for Sample No. SP03VERT

1-D STRAIN CONTROLLED COMPRESSION TEST

COMPUTED RESULTS

INITIAL VOID RATIO= 0.96812
INITIAL HEIGHT= 1.9406

ALL UNITS IN: KG,CM,SEC

LINEAR THEORY

	TIME IN HOURS	VERTICAL STRESS	E	RATE OF STRAIN	EXCESS PORE PRESSURE	C	C/1+E	MV	PERCENT COMPRESSION	K	CV	
1	0.0	0.00137	0.96787	0.0	0.0	0.0	0.0	0.09257	0.01274	0.100E+01	0.108E+05	1
2	0.44585	0.06224	0.96333	0.14418E-05	-0.00363	0.00119	0.00061	0.03802	0.24362	-0.743E-06	-0.195E-01	2
3	0.77917	0.06612	0.95994	0.14419E-05	-0.00278	0.05602	0.02858	0.44545	0.41592	-0.967E-06	-0.217E-02	3
4	1.11250	0.06887	0.95687	0.13060E-05	-0.00278	0.07526	0.03846	0.57000	0.57172	-0.873E-06	-0.153E-02	4
5	1.44585	0.06167	0.95380	0.13080E-05	-0.00023	-0.02778	-0.01422	-0.21805	0.72754	-0.104E-04	0.476E-01	5
6	1.77917	0.07042	0.95016	0.15572E-05	0.00884	0.02749	0.01410	0.21371	0.91272	0.326E-06	0.152E-02	6
7	2.11250	0.08803	0.94695	0.13744E-05	0.02415	0.01438	0.00739	0.09366	1.07582	0.105E-06	0.112E-02	7
8	2.44585	0.09587	0.94367	0.14076E-05	0.03662	0.03844	0.01978	0.21521	1.24268	0.706E-07	0.328E-03	8
9	2.77917	0.12054	0.94038	0.14101E-05	0.04909	0.01434	0.00739	0.06859	1.40947	0.526E-07	0.766E-03	9
10	3.41556	0.16797	0.93410	0.14176E-05	0.06617	0.01893	0.00979	0.06848	1.72865	0.390E-07	0.569E-03	10
11	3.74916	0.19792	0.93082	0.14142E-05	0.06752	0.01999	0.01035	0.05671	1.89526	0.380E-07	0.669E-03	11
12	4.08250	0.24168	0.92771	0.13435E-05	0.06900	0.01556	0.00807	0.03684	2.05321	0.352E-07	0.955E-03	12
13	4.41585	0.29411	0.92439	0.14376E-05	0.06872	0.01691	0.00879	0.03291	2.22188	0.377E-07	0.114E-02	13
14	4.74918	0.36152	0.92144	0.12833E-05	0.07070	0.01434	0.00746	0.02285	2.37221	0.326E-07	0.143E-02	14
15	5.08250	0.41229	0.91840	0.13167E-05	0.07496	0.02307	0.01203	0.03112	2.52621	0.314E-07	0.101E-02	15
16	5.41585	0.49122	0.91562	0.12087E-05	0.07410	0.01587	0.00828	0.01838	2.66742	0.291E-07	0.158E-02	16
17	5.74918	0.56976	0.91285	0.12105E-05	0.07382	0.01874	0.00979	0.01849	2.80861	0.292E-07	0.158E-02	17
18	6.41585	0.74533	0.90754	0.11587E-05	0.07439	0.01974	0.01035	0.01584	3.07811	0.276E-07	0.174E-02	18
19	6.74918	0.09374	0.90509	0.10734E-05	0.06617	-0.00118	-0.00062	-0.00198	3.20279	0.286E-07	-0.145E-01	19
20	7.08250	0.89352	0.90343	0.72673E-06	0.03356	0.00074	0.00039	0.00109	3.28712	0.381E-07	0.350E-01	20
21	7.41862	0.90993	0.90292	0.21940E-06	0.01513	0.02772	0.01457	0.01618	3.31277	0.255E-07	0.158E-02	21
22	7.74918	0.94392	0.90255	0.16357E-06	0.03560	0.01012	0.00532	0.00573	3.33160	0.808E-08	0.141E-02	22
23	8.08250	0.98243	0.90165	0.39538E-06	0.01858	0.02256	0.01186	0.01232	3.37746	0.374E-07	0.304E-02	23
24	8.41585	1.00882	0.90115	0.21725E-06	0.01938	0.01871	0.00984	0.00988	3.40266	0.197E-07	0.199E-02	24
25	8.74918	1.04440	0.90035	0.35247E-06	0.04780	0.02319	0.01220	0.01189	3.44351	0.129E-07	0.109E-02	25
26	9.08250	1.15754	0.89822	0.93481E-06	0.07814	0.02070	0.01090	0.00992	3.55167	0.210E-07	0.211E-02	26
27	9.41585	1.26057	0.89548	0.12059E-05	0.08239	0.03218	0.01698	0.01405	3.69104	0.256E-07	0.182E-02	27
28	9.74918	1.37991	0.89255	0.12873E-05	0.08693	0.03233	0.01708	0.01294	3.83961	0.258E-07	0.199E-02	28
29	10.08250	1.50204	0.88974	0.12415E-05	0.08523	0.03319	0.01756	0.01220	3.98262	0.253E-07	0.207E-02	29
30	10.41585	1.61744	0.88667	0.13550E-05	0.08949	0.04145	0.02197	0.01409	4.13850	0.262E-07	0.186E-02	30
31	10.74918	1.72738	0.88406	0.11551E-05	0.08700	0.03971	0.02107	0.01261	4.27119	0.229E-07	0.182E-02	31
32	11.08250	1.84087	0.88092	0.13914E-05	0.09210	0.04936	0.02624	0.01471	4.43077	0.260E-07	0.177E-02	32
33	11.41585	1.94041	0.87783	0.13714E-05	0.09998	0.05869	0.03125	0.01653	4.58778	0.235E-07	0.142E-02	33
34	11.68806	2.02173	0.87558	0.12253E-05	0.09721	0.05487	0.02926	0.01477	4.70224	0.216E-07	0.146E-02	34
35	12.02168	2.14122	0.87234	0.14381E-05	0.11019	0.05630	0.03007	0.01445	4.86653	0.222E-07	0.154E-02	35
36	12.35501	2.25391	0.86889	0.15380E-05	0.11267	0.06727	0.03599	0.01638	5.04182	0.232E-07	0.142E-02	36
37	12.68834	2.36617	0.86576	0.14022E-05	0.11494	0.06457	0.03461	0.01499	5.20129	0.206E-07	0.138E-02	37
38	13.35501	2.57748	0.85892	0.15329E-05	0.12195	0.07996	0.04301	0.01741	5.54880	0.211E-07	0.121E-02	38
39	13.68834	2.69326	0.85551	0.15312E-05	0.12741	0.07759	0.04182	0.01587	5.72203	0.201E-07	0.127E-02	39
40	14.02168	2.79360	0.85228	0.14527E-05	0.12762	0.08825	0.04765	0.01737	5.88608	0.190E-07	0.109E-02	40
41	14.35501	2.90185	0.84993	0.10564E-05	0.13017	0.06169	0.03334	0.01171	6.00525	0.135E-07	0.115E-02	41

42	14.68834	3.00471	0.84531	0.20855E-05	0.13670	0.13260	0.07186	0.02433	6.23991	0.253E-07	0.104E-02	42
43	14.99446	3.10409	0.84218	0.15461E-05	0.13811	0.09645	0.05236	0.01714	6.39938	0.185E-07	0.108E-02	43
44	15.36890	3.22105	0.83824	0.15871E-05	0.13585	0.10634	0.05785	0.01829	6.59921	0.192E-07	0.105E-02	44
45	15.56918	3.28855	0.83619	0.15533E-05	0.14180	0.09914	0.05399	0.01659	6.70369	0.180E-07	0.108E-02	45
46	15.90279	3.39429	0.83272	0.15736E-05	0.14605	0.10945	0.05972	0.01787	6.87967	0.176E-07	0.984E-03	46
47	16.23611	3.50495	0.82922	0.15944E-05	0.14038	0.10910	0.05964	0.01729	7.05748	0.185E-07	0.107E-02	47
48	16.48723	3.59267	0.82683	0.14496E-05	0.14739	0.09688	0.05303	0.01494	7.17915	0.160E-07	0.107E-02	48
49	16.82085	3.70217	0.82327	0.16252E-05	0.15172	0.11851	0.06500	0.01783	7.35995	0.173E-07	0.971E-03	49
50	17.15417	3.82853	0.82013	0.14371E-05	0.15597	0.09352	0.05138	0.01365	7.51942	0.148E-07	0.109E-02	50
51	17.48752	3.92557	0.81673	0.15607E-05	0.15873	0.13595	0.07483	0.01930	7.69232	0.158E-07	0.817E-03	51
52	17.98611	4.11037	0.81146	0.16197E-05	0.16185	0.11448	0.06320	0.01573	7.95992	0.160E-07	0.101E-02	52
53	18.31946	4.23742	0.80832	0.14462E-05	0.16298	0.10314	0.05704	0.01366	8.11938	0.141E-07	0.103E-02	53
54	18.65279	4.35697	0.80493	0.15656E-05	0.16298	0.12186	0.06751	0.01571	8.29169	0.152E-07	0.968E-03	54
55	19.05779	4.50808	0.80082	0.15662E-05	0.16922	0.12061	0.06698	0.01511	8.50060	0.146E-07	0.966E-03	55
56	19.40028	4.64593	0.79873	0.94334E-06	0.17063	0.06944	0.03860	0.00844	8.60690	0.869E-08	0.103E-02	56
57	19.73363	4.75754	0.79378	0.22990E-05	0.17140	0.20850	0.11623	0.02472	8.85837	0.210E-07	0.849E-03	57
58	19.96834	4.85314	0.79154	0.14772E-05	0.17225	0.11240	0.06274	0.01306	8.97198	0.134E-07	0.102E-02	58
59	20.32196	4.99201	0.78812	0.15052E-05	0.17622	0.12143	0.06791	0.01380	9.14606	0.133E-07	0.962E-03	59
60	20.53084	5.07738	0.78588	0.16691E-05	0.17756	0.13216	0.07400	0.01470	9.25993	0.146E-07	0.991E-03	60
61	20.86417	5.22171	0.78263	0.15172E-05	0.18153	0.11582	0.06497	0.01261	9.42485	0.129E-07	0.102E-02	61
62	21.19751	5.34658	0.77931	0.15537E-05	0.18379	0.14041	0.07891	0.01493	9.59343	0.130E-07	0.871E-03	62
63	21.62000	5.52421	0.77502	0.15895E-05	0.18521	0.13128	0.07396	0.01361	9.81143	0.131E-07	0.966E-03	63
64	22.00557	5.69233	0.77113	0.15841E-05	0.19059	0.12992	0.07335	0.01308	10.00932	0.127E-07	0.969E-03	64
65	22.33890	5.82985	0.76814	0.14096E-05	0.18274	0.12528	0.07085	0.01230	10.16129	0.117E-07	0.953E-03	65
66	22.82028	6.06183	0.76359	0.14869E-05	0.19748	0.11643	0.06602	0.01111	10.39217	0.114E-07	0.102E-02	66
67	23.15363	6.19765	0.76017	0.16224E-05	0.19909	0.15469	0.08788	0.01434	10.56628	0.123E-07	0.856E-03	67
68	23.48695	6.36841	0.75674	0.16251E-05	0.20051	0.12603	0.07174	0.01142	10.74034	0.122E-07	0.106E-02	68
69	24.48695	6.85076	0.74693	0.15598E-05	0.20938	0.13436	0.07691	0.01164	11.23877	0.111E-07	0.949E-03	69
70	24.82028	7.02197	0.74372	0.15341E-05	0.21221	0.13004	0.07458	0.01075	11.40187	0.107E-07	0.994E-03	70
71	25.15363	7.19993	0.74047	0.15541E-05	0.21732	0.12972	0.07453	0.01048	11.56680	0.105E-07	0.100E-02	71
72	25.48695	7.39270	0.73723	0.15571E-05	0.21873	0.12287	0.07073	0.00969	11.73174	0.104E-07	0.108E-02	72
73	25.96945	7.66918	0.73268	0.15128E-05	0.22259	0.12398	0.07155	0.00950	11.96306	0.992E-08	0.104E-02	73
74	26.20723	7.73767	0.73016	0.16956E-05	0.21326	0.28244	0.16324	0.02119	12.09064	0.116E-07	0.546E-03	74
75	26.54056	6.47418	0.73017	-0.22711E-08	-0.07891	0.00003	0.00002	0.00000	12.09039	0.419E-10	0.100E+05	75
76	26.78612	5.49495	0.73133	-0.75673E-06	-0.11236	0.00706	0.00408	0.00068	12.03157	0.981E-08	0.144E-01	76
77	27.11945	4.48184	0.73331	-0.95321E-06	-0.12511	0.00973	0.00561	0.00113	11.93082	0.111E-07	0.986E-02	77
78	27.56694	3.49649	0.73584	-0.90366E-06	-0.13052	0.01018	0.00586	0.00148	11.80246	0.101E-07	0.686E-02	78
79	27.85556	2.99008	0.73778	-0.10778E-05	-0.13080	0.01245	0.00716	0.00221	11.70354	0.121E-07	0.547E-02	79
80	28.42641	2.22104	0.74218	-0.12281E-05	-0.14694	0.01478	0.00849	0.00328	11.48016	0.123E-07	0.376E-02	80
81	28.61612	2.02211	0.74384	-0.13920E-05	-0.14921	0.01766	0.01013	0.00478	11.39594	0.138E-07	0.289E-02	81
82	28.94946	1.72325	0.74676	-0.13926E-05	-0.14779	0.01826	0.01045	0.00559	11.24756	0.140E-07	0.250E-02	82
83	29.35335	1.48085	0.75032	-0.14020E-05	-0.13222	0.02353	0.01345	0.00841	11.06631	0.158E-07	0.188E-02	83
84	29.57028	1.31457	0.75158	-0.92092E-06	-0.13641	0.01058	0.00604	0.00433	11.00229	0.101E-07	0.233E-02	84
85	29.90417	1.13534	0.75443	-0.13505E-05	-0.15029	0.01943	0.01107	0.00906	10.85760	0.134E-07	0.148E-02	85
86	30.23752	1.02303	0.75652	-0.99205E-06	-0.07041	0.02008	0.01143	0.01060	10.75136	0.211E-07	0.199E-02	86
87	30.57085	0.98095	0.75710	-0.27357E-06	-0.03613	0.01374	0.00782	0.00780	10.72202	0.114E-07	0.146E-02	87
88	30.90417	0.92411	0.75797	-0.41001E-06	-0.06138	0.01449	0.00824	0.00866	10.67809	0.100E-07	0.116E-02	88
89	31.23752	0.85293	0.75934	-0.64905E-06	-0.08769	0.01710	0.00972	0.01094	10.60844	0.111E-07	0.102E-02	89
90	31.57085	0.78109	0.76110	-0.83553E-06	-0.07753	0.02006	0.01139	0.01395	10.51875	0.162E-07	0.116E-02	90
91	31.90417	0.71061	0.76301	-0.90306E-06	-0.11236	0.02021	0.01146	0.01538	10.42165	0.121E-07	0.790E-03	91
92	32.23752	0.62948	0.76481	-0.85100E-06	-0.10188	0.01487	0.00842	0.01259	10.33009	0.126E-07	0.100E-02	92
93	32.57085	0.60073	0.76510	-0.13611E-06	-0.06082	0.00616	0.00349	0.00568	10.31544	0.339E-08	0.597E-03	93
94	32.90417	0.52451	0.76845	-0.15787E-05	-0.15572	0.02470	0.01396	0.02486	10.14522	0.154E-07	0.620E-03	94
95	33.08446	0.48673	0.77011	-0.14430E-05	-0.16082	0.02217	0.01252	0.02478	10.06097	0.137E-07	0.551E-03	95
96	33.11362	0.51723	0.77011	-0.13989E-07	-0.11888	-0.00003	-0.00002	-0.00005	10.06088	0.179E-09	-0.372E-02	96

M241-43V LINEAR THEORY

97	33.44696	0.81055	0.76968	0.20370E-06	0.04257	0.00096	0.00054	0.00083	10.08284	0.728E-08	0.874E-02	97
98	33.78029	0.89911	0.76925	0.20265E-06	0.03101	0.00415	0.00234	0.00275	10.10472	0.994E-08	0.362E-02	98
99	34.11362	0.93570	0.76932	-0.35078E-07	0.00217	-0.00186	-0.00105	-0.00115	10.10094	-0.246E-07	0.214E-01	99
100	34.44696	0.99303	0.76893	0.18687E-06	0.03617	0.00667	0.00377	0.00391	10.12108	0.786E-08	0.201E-02	100
101	34.78029	1.03383	0.76871	0.10083E-06	0.00930	0.00531	0.00300	0.00297	10.13194	0.165E-07	0.556E-02	101
102	35.11362	1.08465	0.76857	0.67992E-07	0.04642	0.00300	0.00170	0.00161	10.13927	0.223E-08	0.139E-02	102
103	35.44696	1.29688	0.76561	0.13950E-05	0.12982	0.01654	0.00937	0.00789	10.28944	0.163E-07	0.206E-02	103
104	35.78029	1.53753	0.76302	0.12271E-05	0.13726	0.01525	0.00865	0.00612	10.42136	0.135E-07	0.221E-02	104
105	36.07196	1.73019	0.76064	0.12880E-05	0.11628	0.02017	0.01146	0.00702	10.54234	0.167E-07	0.238E-02	105
106	36.40529	1.99953	0.75804	0.12314E-05	0.14520	0.01796	0.01021	0.00549	10.67435	0.127E-07	0.232E-02	106
107	36.73862	2.28853	0.75515	0.13703E-05	0.14909	0.02138	0.01218	0.00569	10.82100	0.138E-07	0.242E-02	107
108	37.07196	2.61611	0.75223	0.13896E-05	0.15448	0.02184	0.01247	0.00509	10.96947	0.134E-07	0.264E-02	108
109	37.40529	2.95021	0.74942	0.13403E-05	0.15420	0.02342	0.01338	0.00481	11.11243	0.129E-07	0.269E-02	109
110	37.73862	3.33811	0.74826	0.55089E-06	0.15512	0.00936	0.00535	0.00170	11.17116	0.528E-08	0.310E-02	110
111	38.07196	3.73481	0.74823	0.16568E-07	0.16043	0.00030	0.00017	0.00005	11.17287	0.153E-09	0.306E-02	111
112	38.40529	4.16109	0.74830	-0.33713E-07	0.16221	-0.00065	-0.00037	-0.00009	11.16928	-0.309E-09	0.325E-02	112
113	38.73862	4.58020	0.74826	0.17145E-07	0.16646	0.00039	0.00022	0.00005	11.17116	0.153E-09	0.312E-02	113
114	39.07196	5.03622	0.74815	0.51609E-07	0.17100	0.00113	0.00064	0.00014	11.17661	0.448E-09	0.330E-02	114
115	39.40529	5.48054	0.74801	0.68792E-07	0.17865	0.00171	0.00098	0.00019	11.18398	0.572E-09	0.308E-02	115
116	39.73862	5.93363	0.74808	-0.34380E-07	0.18347	-0.00091	-0.00052	-0.00009	11.18028	-0.278E-09	0.306E-02	116
117	40.07196	6.34355	0.72726	0.10043E-04	0.19736	0.31163	0.18042	0.02940	12.23802	0.738E-07	0.251E-02	117
118	40.40529	6.74877	0.72423	0.14648E-05	0.20389	0.04895	0.02839	0.00434	12.39204	0.104E-07	0.239E-02	118
119	40.73862	7.11888	0.72124	0.14498E-05	0.21154	0.05609	0.03259	0.00470	12.54419	0.987E-08	0.210E-02	119
120	41.07196	7.45737	0.71824	0.14523E-05	0.21664	0.06446	0.03752	0.00515	12.69633	0.962E-08	0.187E-02	120
121	41.40529	7.78956	0.71543	0.13671E-05	0.22345	0.06458	0.03764	0.00494	12.83931	0.875E-08	0.177E-02	121
122	41.73862	8.11655	0.71225	0.15452E-05	0.23648	0.07721	0.04509	0.00567	13.00064	0.931E-08	0.164E-02	122
123	42.19807	8.53998	0.70828	0.14077E-05	0.24594	0.07822	0.04579	0.00550	13.20273	0.812E-08	0.148E-02	123
124	42.53140	8.83221	0.70515	0.15297E-05	0.25151	0.09303	0.05456	0.00628	13.36176	0.860E-08	0.137E-02	124
125	42.86473	9.13840	0.70193	0.15772E-05	0.25558	0.09450	0.05553	0.00618	13.52541	0.869E-08	0.141E-02	125
126	43.19807	9.42321	0.69883	0.15171E-05	0.25973	0.10077	0.05932	0.00639	13.68257	0.819E-08	0.128E-02	126
127	43.53140	9.73037	0.69774	0.53651E-06	0.26664	0.03407	0.02007	0.00210	13.73810	0.282E-08	0.135E-02	127
128	44.02724	10.16529	0.69763	0.35729E-07	0.27202	0.00249	0.00146	0.00015	13.74361	0.184E-09	0.125E-02	128
129	44.36055	10.45024	0.69757	0.30182E-07	0.27363	0.00224	0.00132	0.00013	13.74675	0.155E-09	0.122E-02	129
130	44.69389	10.78043	0.69750	0.35433E-07	0.27930	0.00230	0.00135	0.00013	13.75038	0.178E-09	0.138E-02	130
131	45.02722	11.07253	0.69774	-0.11875E-06	0.28648	-0.00906	-0.00534	-0.00049	13.73810	-0.581E-09	0.119E-02	131
132	45.36055	11.39986	0.69768	0.28220E-07	0.28697	0.00200	0.00118	0.00010	13.74106	0.138E-09	0.133E-02	132
133	45.95473	11.98391	0.69755	0.36809E-07	0.29708	0.00267	0.00157	0.00013	13.74783	0.174E-09	0.129E-02	133
134	46.48695	12.50898	0.69769	-0.44398E-07	0.30190	-0.00338	-0.00199	-0.00016	13.74046	-0.206E-09	0.127E-02	134
135	46.82028	12.85298	0.69780	-0.53142E-07	0.30304	-0.00394	-0.00232	-0.00019	13.73500	-0.246E-09	0.133E-02	135
136	47.15363	13.19056	0.69778	0.12462E-07	0.31370	0.00096	0.00056	0.00004	13.73628	0.557E-10	0.126E-02	136
137	47.48695	13.55986	0.69763	0.70893E-07	0.31852	0.00522	0.00307	0.00023	13.74361	0.312E-09	0.135E-02	137
138	47.82028	13.90501	0.69763	0.0	0.32249	0.0	0.0	0.0	13.74361	0.0	0.100E+05	138
139	48.15363	14.27594	0.69763	0.0	0.32902	0.0	0.0	0.0	13.74361	0.0	0.100E+05	139
140	48.48695	14.65081	0.69774	-0.53144E-07	0.33582	-0.00419	-0.00247	-0.00017	13.73810	-0.222E-09	0.130E-02	140
141	48.82028	15.04779	0.69770	0.17745E-07	0.34036	0.00139	0.00082	0.00005	13.73997	0.730E-10	0.136E-02	141
142	49.08751	15.35215	0.69760	0.66258E-07	0.33951	0.00538	0.00317	0.00021	13.74542	0.273E-09	0.131E-02	142
143	49.37946	13.79032	0.69781	-0.12131E-06	-0.04159	0.00202	0.00119	0.00008	13.73447	0.409E-08	0.501E-01	143
144	50.03500	9.94286	0.69779	0.63367E-08	-0.16722	-0.00008	-0.00005	-0.00000	13.73575	-0.531E-10	0.100E+05	144
145	50.40224	8.35550	0.69779	0.0	-0.18791	0.0	0.0	0.0	13.73575	0.0	0.100E+05	145
146	51.51279	5.06179	0.69775	0.53170E-08	-0.21371	-0.00007	-0.00004	-0.00001	13.73756	-0.349E-10	0.100E+05	146
147	52.01279	4.06691	0.69782	-0.23638E-07	-0.22222	0.00033	0.00020	0.00004	13.73387	0.149E-09	0.349E-02	147
148	52.39473	3.45696	0.69779	0.15485E-07	-0.22676	-0.00023	-0.00013	-0.00003	13.73575	-0.957E-10	0.274E-02	148
149	52.84891	2.86996	0.69781	-0.91461E-08	-0.23298	0.00014	0.00008	0.00003	13.73447	0.550E-10	0.216E-02	149
150	53.18224	2.50360	0.69775	0.30177E-07	-0.23157	-0.00045	-0.00026	-0.00010	13.73756	-0.183E-09	0.185E-02	150
151	53.51556	2.20123	0.69782	-0.35457E-07	-0.23157	0.00056	0.00033	0.00014	13.73387	0.215E-09	0.152E-02	151

152	54.05084	1.80503	0.69779	0.11049E-07	-0.23101	-0.00019	-0.00011	-0.00005	13.73575	-0.670E-10	0.125E-02152
153	54.55724	1.49804	0.69775	0.11660E-07	-0.22250	-0.00019	-0.00011	-0.00007	13.73756	-0.734E-10	0.106E-02153
154	54.87335	1.34994	0.69779	-0.18679E-07	-0.22250	0.00034	0.00020	0.00014	13.73575	0.118E-09	0.820E-03154
155	55.20668	1.20882	0.69775	0.17715E-07	-0.21541	-0.00032	-0.00019	-0.00015	13.73756	-0.115E-09	0.765E-03155
156	55.54001	1.13117	0.69775	0.0	-0.10513	0.0	0.0	0.0	13.73756	0.0	0.100E+05156
157	55.87335	1.09173	0.69779	-0.17713E-07	-0.06658	0.00099	0.00059	0.00054	13.73575	0.373E-09	0.692E-03157
158	57.09612	0.88233	0.69782	-0.48369E-08	-0.10088	0.00017	0.00010	0.00010	13.73387	0.672E-10	0.661E-03158

ENGINEERING STRAIN (158)= 13.7339

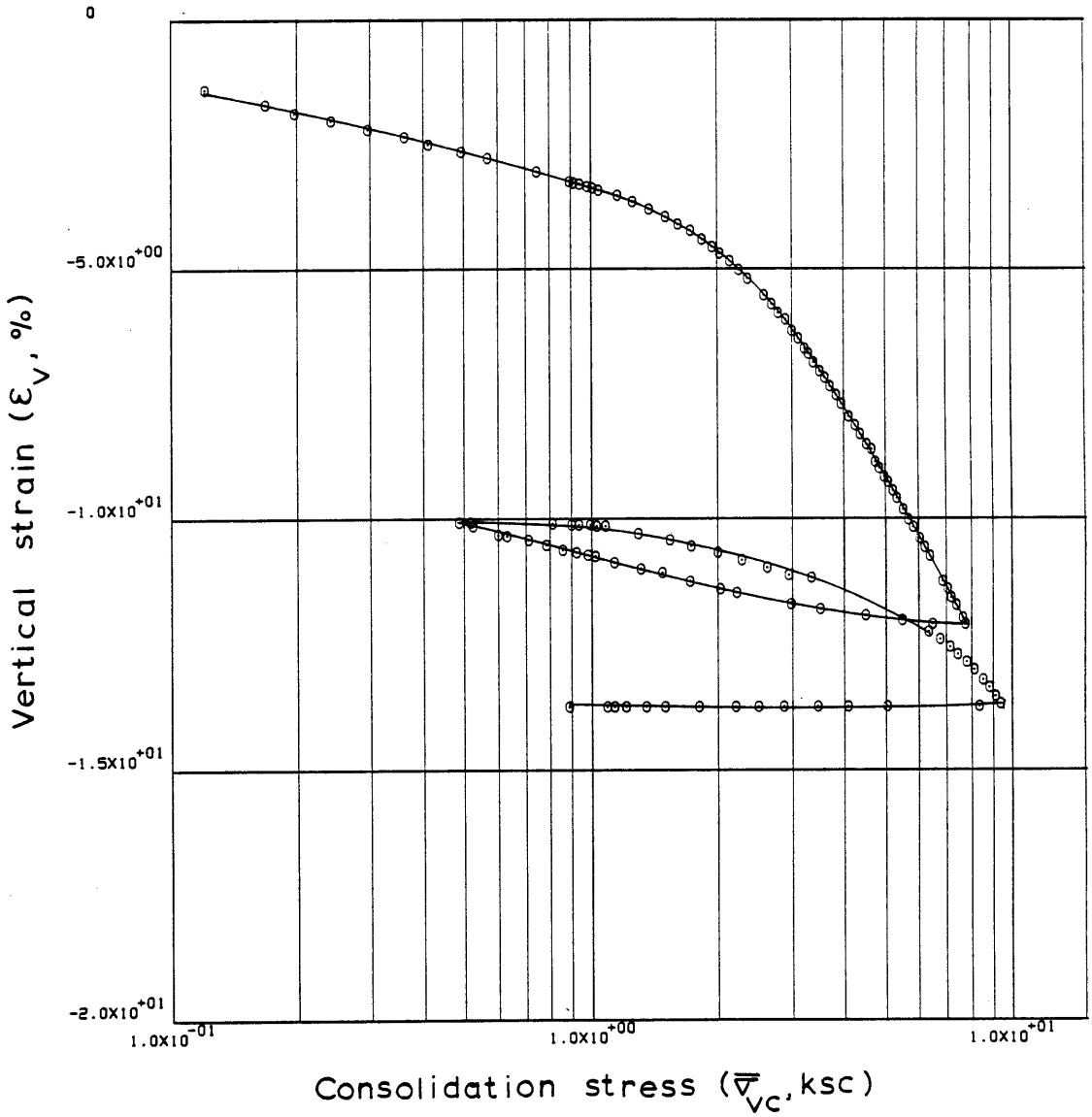

Sample No. 415-435-C-V w_N (%) 27.69 Estimated

Depth 43.12 w_L (%) 48.91 $\bar{\sigma}_{vo}$ 0.98 $\bar{\sigma}_{vm}$ 263-278

Soil Type Boston w_P (%) 23.52 CR 0.1833 RR 0.0205

Blue Clay P.I.(%) 25.39 G_s 2.77 e_o 0.9681

⊙ At t_p Remarks Data from C.R.S.C test

w_L & w_P estimated from Baligh et al (1980)

Figure E.15 Compression Curve for Sample No. 41.5-43.5-C-V

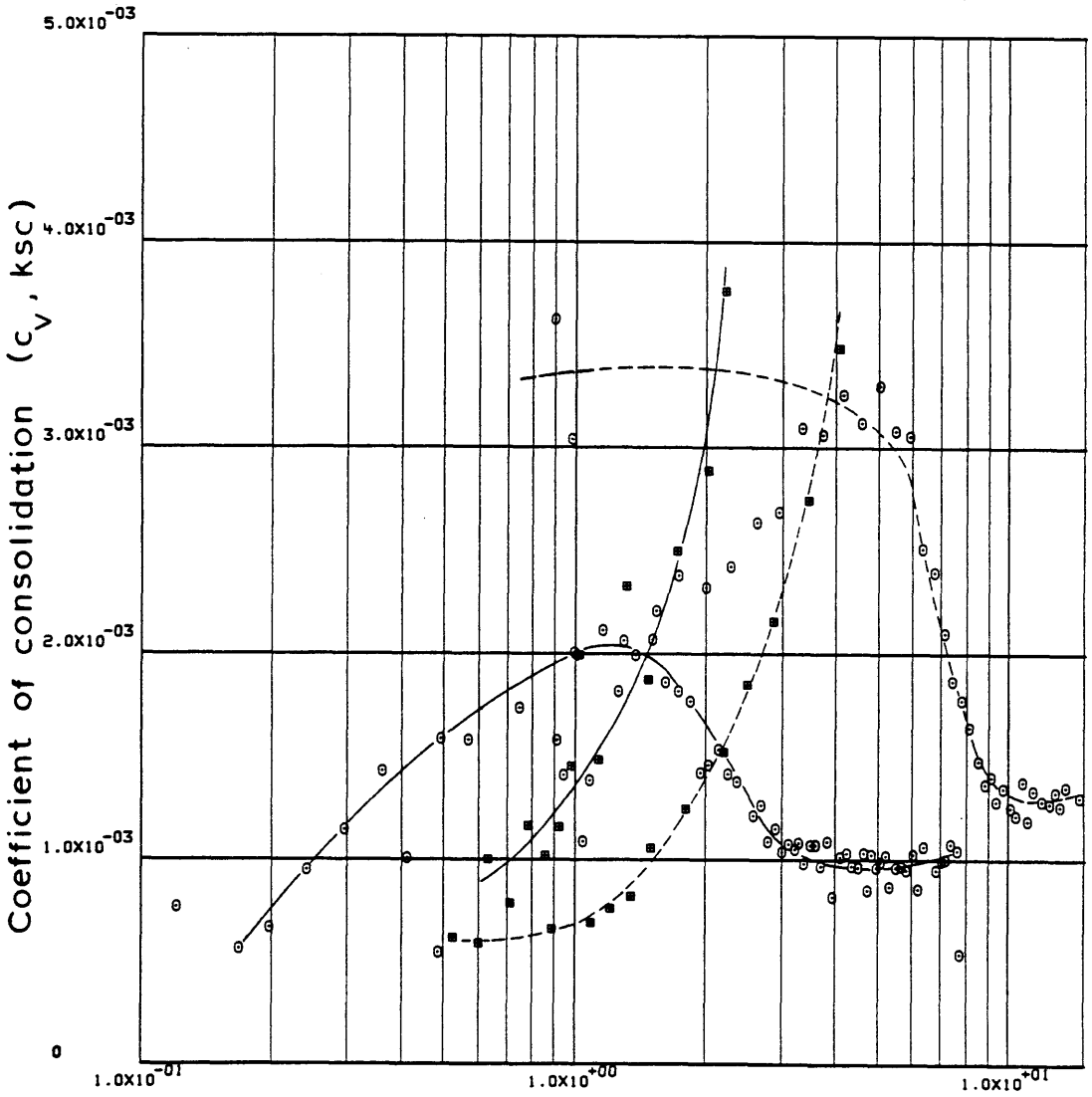

Sample No. 41.5-43.5-C.V w_N (%) 27.69 Estimated

Depth 43.12 w_L (%) 48.91 $\bar{\sigma}_{vo}$ 0.98 $\bar{\sigma}_{vm}$ 263-278

Soil Type Boston w_P (%) 23.52 CR 0.1833 RR 0.0205

Blue Clay P.I.(%) 25.39 G_s 2.77 e_o 0.9681

o At t_p Remarks Data from C.R.S.C test

w_L & w_P estimated from Baligh et al (1980)

Figure E.16 Variation of coefficient of consolidation with consolidation stress for Sample No. 41.5-43.5-C-V

1-D STRAIN CONTROLLED COMPRESSION TEST

COMPUTED RESULTS

INITIAL VOID RATIO= 1.19336
INITIAL HEIGHT= 1.9406

ALL UNITS IN: KG,CM,SEC

LINEAR THEORY

	TIME IN HOURS	VERTICAL STRESS	E	RATE OF STRAIN	EXCESS PORE PRESSURE	C	C/1+E	MV	PERCENT COMPRESSION	K	CV	
1	0.0	0.03233	1.19336	0.0	0.00089	0.0	0.0	0.0	0.0	0.0	0.100E+05	1
2	0.33333	0.20929	1.19029	0.11656E-05	-0.00284	0.00164	0.00075	0.00790	0.13972	-0.772E-06	-0.977E-01	2
3	0.66667	0.21969	1.18628	0.15290E-05	-0.00198	0.08270	0.03783	0.17642	0.32259	-0.144E-05	-0.818E-02	3
4	1.00000	1.21642	1.18238	0.14908E-05	-0.00373	0.00228	0.00105	0.00179	0.50060	-0.745E-06	-0.415E+00	4
5	1.33333	0.23808	1.17835	0.15390E-05	-0.00350	-0.00247	-0.00113	-0.00189	0.68401	-0.816E-06	0.433E+00	5
6	1.66667	0.23615	1.17438	0.15214E-05	-0.00520	-0.48633	-0.22366	-0.94320	0.86501	-0.542E-06	0.574E-03	6
7	2.10695	0.23770	1.16913	0.15278E-05	-0.00547	0.80019	0.36890	1.55685	1.10448	-0.514E-06	-0.330E-03	7
8	2.44028	0.25122	1.16520	0.15124E-05	-0.00520	0.07104	0.03281	0.13422	1.28366	-0.534E-06	-0.398E-02	8
9	2.77361	0.25953	1.16254	0.10235E-05	-0.00439	0.08163	0.03775	0.14782	1.40475	-0.426E-06	-0.288E-02	9
10	3.10695	0.26345	1.16251	0.15515E-07	-0.00411	0.00261	0.00121	0.00475	1.40657	-0.691E-08	-0.146E-02	10
11	3.44028	0.27140	1.16246	0.15465E-07	0.00041	0.00138	0.00064	0.00233	1.40843	0.687E-07	0.294E-01	11
12	3.66306	0.29201	1.16238	0.46050E-07	0.00239	0.00109	0.00051	0.00179	1.41208	0.353E-07	0.197E-01	12
13	4.18167	0.34934	1.14458	0.44458E-05	0.00889	0.09929	0.04630	0.14477	2.22365	0.900E-06	0.622E-02	13
14	4.51500	0.39111	1.14094	0.14179E-05	0.01318	0.03225	0.01506	0.04074	2.38971	0.193E-06	0.474E-02	14
15	4.89193	0.43626	1.13653	0.15214E-05	0.01742	0.04038	0.01890	0.04573	2.59081	0.156E-06	0.341E-02	15
16	5.22526	0.49685	1.13364	0.11293E-05	0.01992	0.02223	0.01042	0.02237	2.72260	0.101E-06	0.452E-02	16
17	5.55999	0.56413	1.13380	-0.62326E-07	0.01766	-0.00125	-0.00059	-0.00112	2.71533	-0.629E-08	0.564E-02	17
18	5.89332	0.61889	1.12558	0.32210E-05	0.02308	0.08869	0.04172	0.07059	3.08990	0.247E-06	0.350E-02	18
19	6.22664	0.68799	1.12197	0.14174E-05	0.02223	0.03409	0.01607	0.02461	3.25444	0.112E-06	0.457E-02	19
20	6.61249	0.77066	1.11792	0.13765E-05	0.02364	0.03569	0.01685	0.02313	3.43907	0.102E-06	0.442E-02	20
21	6.93276	0.83893	1.11452	0.13983E-05	0.02274	0.04017	0.01900	0.02361	3.59453	0.108E-06	0.456E-02	21
22	7.26609	0.91293	1.11127	0.12819E-05	0.02274	0.03841	0.01819	0.02079	3.74255	0.983E-07	0.473E-02	22
23	7.59943	0.98363	1.10758	0.14584E-05	0.02359	0.04944	0.02346	0.02475	3.91072	0.107E-06	0.434E-02	23
24	7.93276	1.06311	1.10377	0.15086E-05	0.02359	0.04903	0.02331	0.02278	4.08440	0.111E-06	0.486E-02	24
25	8.26609	1.10416	1.10165	0.84259E-06	0.01341	0.05607	0.02668	0.02464	4.18126	0.109E-06	0.441E-02	25
26	8.59943	1.13456	1.10012	0.60440E-06	0.00069	0.05610	0.02671	0.02385	4.25070	0.151E-05	0.634E-01	26
27	8.93276	1.13658	1.09968	0.17511E-06	-0.00439	0.24794	0.11809	0.10408	4.27080	-0.688E-07	-0.661E-03	27
28	9.26609	1.17695	1.09848	0.47838E-06	0.00838	0.03451	0.01645	0.01422	4.32574	0.984E-07	0.692E-02	28
29	9.66639	1.20340	1.09655	0.63708E-06	0.00159	0.08663	0.04132	0.03471	4.41351	0.688E-06	0.198E-01	29
30	10.08220	1.22676	1.09571	0.26841E-06	0.00357	0.04381	0.02091	0.01720	4.45189	0.129E-06	0.751E-02	30
31	10.32248	1.24945	1.09523	0.26403E-06	0.00720	0.02612	0.01247	0.01006	4.47371	0.630E-07	0.626E-02	31
32	10.65581	1.33106	1.09266	0.10230E-05	0.02393	0.04059	0.01940	0.01504	4.59082	0.733E-07	0.487E-02	32
33	10.98916	1.38688	1.08978	0.11513E-05	0.02449	0.07027	0.03363	0.02475	4.72244	0.804E-07	0.325E-02	33
34	11.27303	1.45178	1.08685	0.13726E-05	0.02789	0.06403	0.03068	0.02162	4.85591	0.839E-07	0.388E-02	34
35	11.76526	1.55189	1.08188	0.13477E-05	0.02987	0.07457	0.03582	0.02386	5.08261	0.766E-07	0.321E-02	35
36	12.09861	1.61827	1.07886	0.12078E-05	0.03303	0.07193	0.03460	0.02184	5.21997	0.618E-07	0.283E-02	36
37	12.43194	1.70057	1.07521	0.14655E-05	0.03501	0.07357	0.03545	0.02137	5.38637	0.706E-07	0.330E-02	37
38	12.76526	1.76642	1.07172	0.14065E-05	0.03648	0.09205	0.04443	0.02563	5.54579	0.648E-07	0.253E-02	38
39	13.09861	1.85594	1.06842	0.13281E-05	0.03795	0.06668	0.03223	0.01780	5.69609	0.586E-07	0.329E-02	39
40	13.43194	1.92418	1.06481	0.14573E-05	0.04050	0.09999	0.04842	0.02562	5.86072	0.600E-07	0.234E-02	40
41	13.76528	2.01450	1.06140	0.13786E-05	0.04078	0.07435	0.03607	0.01832	6.01620	0.562E-07	0.307E-02	41

42	14.09861	2.08780	1.05779	0.14623E-05	0.04191	0.10102	0.04909	0.02394	6.18079	0.578E-07	0.242E-02	42
43	14.43194	2.16186	1.05446	0.13507E-05	0.04191	0.09554	0.04651	0.02189	6.33264	0.532E-07	0.243E-02	43
44	14.76526	2.24070	1.05085	0.14672E-05	0.04503	0.10081	0.04915	0.02233	6.49722	0.536E-07	0.240E-02	44
45	15.09861	2.32237	1.04739	0.14090E-05	0.04763	0.09669	0.04723	0.02070	6.65508	0.485E-07	0.234E-02	45
46	15.43194	2.40886	1.04359	0.15495E-05	0.04786	0.10391	0.05085	0.02150	6.82831	0.529E-07	0.246E-02	46
47	15.76526	2.50074	1.04028	0.13490E-05	0.04961	0.08823	0.04324	0.01762	6.97890	0.443E-07	0.251E-02	47
48	16.09860	2.60092	1.03655	0.15270E-05	0.05414	0.09501	0.04665	0.01829	7.14903	0.458E-07	0.250E-02	48
49	16.43193	2.67423	1.03334	0.13156E-05	0.05527	0.11548	0.05679	0.02153	7.29538	0.385E-07	0.179E-02	49
50	16.76526	2.77498	1.02965	0.15158E-05	0.05640	0.09982	0.04918	0.01805	7.46370	0.433E-07	0.240E-02	50
51	17.09860	2.85520	1.02608	0.14689E-05	0.05951	0.12536	0.06187	0.02197	7.62657	0.397E-07	0.180E-02	51
52	17.43193	2.96848	1.02227	0.15709E-05	0.06036	0.09797	0.04845	0.01664	7.80034	0.417E-07	0.250E-02	52
53	17.76526	3.05911	1.01876	0.14480E-05	0.06212	0.11664	0.05778	0.01917	7.96027	0.372E-07	0.194E-02	53
54	18.09860	3.15756	1.01503	0.15436E-05	0.06467	0.11784	0.05848	0.01881	8.13045	0.379E-07	0.202E-02	54
55	18.43193	3.23874	1.01125	0.15632E-05	0.06637	0.14863	0.07390	0.02311	8.30244	0.373E-07	0.161E-02	55
56	18.76526	3.35029	1.00752	0.15494E-05	0.06778	0.11023	0.05491	0.01667	8.47264	0.361E-07	0.216E-02	56
57	19.09860	3.45231	1.00417	0.13930E-05	0.06954	0.11170	0.05573	0.01639	8.62538	0.315E-07	0.192E-02	57
58	19.76526	3.65014	0.99688	0.15204E-05	0.07329	0.13075	0.06548	0.01844	8.95760	0.324E-07	0.176E-02	58
59	20.09860	3.75350	0.99371	0.13257E-05	0.07470	0.11360	0.05698	0.01539	9.10217	0.276E-07	0.179E-02	59
60	20.43193	3.85417	0.98944	0.17904E-05	0.07549	0.16151	0.08118	0.02134	9.29707	0.367E-07	0.172E-02	60
61	20.76526	3.94852	0.98563	0.16005E-05	0.07803	0.15765	0.07940	0.02036	9.47090	0.317E-07	0.155E-02	61
62	21.09860	4.07571	0.98171	0.16444E-05	0.07854	0.12336	0.06225	0.01551	9.64920	0.322E-07	0.207E-02	62
63	21.43193	4.17335	0.97798	0.15726E-05	0.08023	0.15767	0.07971	0.01933	9.81938	0.300E-07	0.155E-02	63
64	21.76526	4.33420	0.97400	0.16800E-05	0.08541	0.10523	0.05331	0.01253	10.00082	0.300E-07	0.239E-02	64
65	22.09860	4.39272	0.97074	0.13783E-05	0.08385	0.24304	0.12333	0.02826	10.14944	0.250E-07	0.884E-03	65
66	22.43193	4.50769	0.96712	0.15359E-05	0.08350	0.14035	0.07135	0.01603	10.31476	0.279E-07	0.174E-02	66
67	22.76526	4.62143	0.96325	0.16406E-05	0.08541	0.15507	0.07899	0.01731	10.49094	0.290E-07	0.167E-02	67
68	23.09860	4.74036	0.95957	0.15639E-05	0.08830	0.14473	0.07386	0.01578	10.65862	0.266E-07	0.169E-02	68
69	23.43193	4.87131	0.95580	0.16069E-05	0.09142	0.13842	0.07077	0.01473	10.83058	0.263E-07	0.179E-02	69
70	23.76526	4.98513	0.95207	0.15928E-05	0.09142	0.16153	0.08275	0.01679	11.00067	0.260E-07	0.155E-02	70
71	24.09860	5.11137	0.94845	0.15489E-05	0.09248	0.14485	0.07434	0.01472	11.16579	0.249E-07	0.169E-02	71
72	24.43193	5.22336	0.94490	0.15210E-05	0.09657	0.16378	0.08421	0.01630	11.32762	0.233E-07	0.143E-02	72
73	24.94693	5.41250	0.93890	0.16683E-05	0.09531	0.16861	0.08696	0.01635	11.60106	0.258E-07	0.157E-02	73
74	24.95610	5.37890	0.93886	0.76622E-06	0.09382	-0.00766	-0.00395	-0.00075	11.60327	0.120E-07	-0.160E-01	74
75	25.19638	4.65403	0.93829	0.33495E-06	-0.02183	-0.00388	-0.00200	-0.00040	11.62888	-0.226E-07	0.564E-01	75
76	25.52971	3.35941	0.93962	-0.56862E-06	-0.05605	0.00405	0.00209	0.00053	11.56857	0.149E-07	0.283E-01	76
77	25.86638	2.54531	0.94135	-0.73696E-06	-0.06902	0.00625	0.00322	0.00110	11.48950	0.158E-07	0.144E-01	77
78	26.17943	2.01850	0.94336	-0.91580E-06	-0.07269	0.00865	0.00445	0.00196	11.39806	0.186E-07	0.951E-02	78
79	26.51277	1.61751	0.94656	-0.13737E-05	-0.07382	0.01449	0.00744	0.00411	11.25175	0.276E-07	0.671E-02	79
80	26.94527	1.27624	0.94980	-0.10667E-05	-0.07132	0.01367	0.00701	0.00487	11.10413	0.223E-07	0.457E-02	80
81	27.42387	1.09740	0.95225	-0.72731E-06	-0.02721	0.01620	0.00830	0.00701	10.99255	0.399E-07	0.569E-02	81
82	27.55138	1.09027	0.95253	-0.31323E-06	-0.02268	0.04300	0.02202	0.02016	10.97978	0.206E-07	0.102E-02	82
83	28.06610	0.98624	0.95385	-0.36557E-06	-0.03936	0.01320	0.00676	0.00651	10.91943	0.139E-07	0.213E-02	83
84	28.41360	1.11637	0.95350	0.14296E-06	-0.00905	0.00282	0.00144	0.00137	10.93535	-0.236E-07	-0.172E-01	84
85	28.74693	1.15270	0.95349	0.49719E-08	-0.00939	0.00036	0.00018	0.00016	10.93590	-0.791E-09	-0.482E-02	85
86	29.08026	1.58413	0.95318	0.13193E-06	0.02149	0.00097	0.00050	0.00037	10.95000	0.917E-08	0.250E-01	86
87	29.41360	2.11613	0.95150	0.71941E-06	0.04412	0.00582	0.00298	0.00162	11.02681	0.243E-07	0.150E-01	87
88	29.74693	2.62457	0.94917	0.99465E-06	0.05684	0.01081	0.00554	0.00235	11.13287	0.260E-07	0.111E-01	88
89	30.08275	3.12102	0.94656	0.11080E-05	0.06080	0.01505	0.00773	0.00270	11.25175	0.270E-07	0.100E-01	89
90	30.41360	3.62221	0.94404	0.10914E-05	0.06589	0.01697	0.00873	0.00259	11.36699	0.245E-07	0.945E-02	90
91	30.74693	4.09630	0.94122	0.12095E-05	0.07035	0.02290	0.01180	0.00306	11.49541	0.254E-07	0.828E-02	91
92	31.08026	4.52947	0.93821	0.12933E-05	0.07658	0.02992	0.01544	0.00358	11.63257	0.248E-07	0.693E-02	92
93	31.41360	4.85987	0.93500	0.13817E-05	0.08478	0.04557	0.02355	0.00502	11.77882	0.239E-07	0.476E-02	93
94	31.74693	5.12905	0.93175	0.14047E-05	0.08981	0.06040	0.03127	0.00626	11.92728	0.228E-07	0.365E-02	94
95	32.08026	5.36736	0.92815	0.15567E-05	0.09468	0.07934	0.04115	0.00784	12.09152	0.239E-07	0.305E-02	95
96	32.41360	5.55754	0.92462	0.15281E-05	0.09524	0.10134	0.05265	0.00964	12.25243	0.233E-07	0.241E-02	96

97	32.74693	5.76077	0.92121	0.14787E-05	0.10090	0.09490	0.04940	0.00873	12.40782	0.212E-07	0.242E-02 97
98	33.08026	5.88418	0.91760	0.15686E-05	0.09468	0.17029	0.08880	0.01525	12.57240	0.238E-07	0.156E-02 98
99	33.41360	6.09542	0.91435	0.14141E-05	0.10684	0.09213	0.04812	0.00803	12.72052	0.190E-07	0.236E-02 99
100	33.74693	6.25530	0.91054	0.16618E-05	0.10711	0.14719	0.07704	0.01247	12.89424	0.222E-07	0.178E-02100
101	34.08026	6.43125	0.90673	0.16652E-05	0.11051	0.13731	0.07201	0.01136	13.06793	0.214E-07	0.189E-02101
102	34.41360	6.59421	0.90332	0.14925E-05	0.11333	0.13626	0.07159	0.01099	13.22336	0.187E-07	0.170E-02102
103	34.62859	6.70255	0.90099	0.15810E-05	0.11277	0.14273	0.07508	0.01129	13.32942	0.198E-07	0.176E-02103
104	34.96164	6.86862	0.89722	0.16573E-05	0.11249	0.15404	0.08119	0.01197	13.50128	0.208E-07	0.173E-02104
105	35.23637	6.99409	0.89430	0.15627E-05	0.11758	0.16169	0.08535	0.01232	13.63475	0.187E-07	0.152E-02105
106	35.56970	7.18739	0.89069	0.15909E-05	0.11758	0.13244	0.07005	0.00988	13.79933	0.189E-07	0.192E-02106
107	35.78722	7.29786	0.88836	0.15731E-05	0.11843	0.15249	0.08075	0.01115	13.90540	0.185E-07	0.166E-02107
108	36.12025	7.46809	0.88455	0.16863E-05	0.12012	0.16524	0.08768	0.01188	14.07912	0.195E-07	0.164E-02108
109	36.21414	7.51140	0.88371	0.13228E-05	0.12097	0.14565	0.07732	0.01032	14.11749	0.152E-07	0.147E-02109
110	36.48943	7.66316	0.88070	0.16131E-05	0.12458	0.15028	0.07990	0.01053	14.25456	0.179E-07	0.170E-02110
111	36.82277	7.84895	0.87958	0.49772E-06	0.12345	0.04690	0.02495	0.00321	14.30577	0.557E-08	0.173E-02111
112	37.25693	6.36217	0.88002	-0.14955E-06	-0.03880	0.00209	0.00111	0.00016	14.28572	0.533E-08	0.339E-01112
113	37.59305	4.84549	0.88010	-0.35210E-07	-0.06481	0.00029	0.00016	0.00003	14.28207	0.752E-09	0.268E-01113
114	37.92360	3.78891	0.88018	-0.35109E-07	-0.07722	0.00032	0.00017	0.00004	14.27849	0.629E-09	0.159E-01114
115	38.25693	3.01832	0.88210	-0.85252E-06	-0.08542	0.00847	0.00450	0.00133	14.19072	0.138E-07	0.104E-01115
116	38.59027	2.44446	0.88443	-0.10288E-05	-0.08797	0.01103	0.00586	0.00215	14.08463	0.163E-07	0.756E-02116
117	38.92360	2.00346	0.88652	-0.92145E-06	-0.09079	0.01048	0.00556	0.00251	13.98953	0.141E-07	0.564E-02117
118	39.25693	1.66087	0.88936	-0.12562E-05	-0.09108	0.01518	0.00804	0.00440	13.85968	0.193E-07	0.438E-02118
119	39.59027	1.40013	0.89221	-0.12542E-05	-0.08457	0.01667	0.00881	0.00577	13.72984	0.208E-07	0.360E-02119
120	39.92360	1.19943	0.89502	-0.12348E-05	-0.08175	0.01815	0.00958	0.00738	13.60182	0.212E-07	0.288E-02120
121	40.25693	1.05831	0.89751	-0.10929E-05	-0.05794	0.01988	0.01048	0.00929	13.48834	0.266E-07	0.286E-02121
122	40.59027	1.02944	0.89819	-0.29939E-06	-0.02287	0.02465	0.01299	0.01245	13.45724	0.185E-07	0.148E-02122
123	40.92360	0.96022	0.89883	-0.28171E-06	-0.04295	0.00922	0.00486	0.00488	13.42799	0.925E-08	0.190E-02123
124	41.25693	0.89369	0.89980	-0.42241E-06	-0.03730	0.01341	0.00706	0.00762	13.38406	0.160E-07	0.210E-02124
125	41.59027	0.79930	0.90120	-0.61638E-06	-0.06724	0.01259	0.00662	0.00784	13.31998	0.130E-07	0.165E-02125
126	41.92360	0.70104	0.90337	-0.94877E-06	-0.07828	0.01653	0.00868	0.01159	13.22115	0.172E-07	0.148E-02126
127	42.25693	0.62133	0.90481	-0.63198E-06	-0.05904	0.01196	0.00628	0.00951	13.15530	0.152E-07	0.160E-02127
128	42.59027	0.58373	0.90570	-0.38603E-06	-0.03556	0.01415	0.00742	0.01232	13.11505	0.154E-07	0.125E-02128
129	42.92360	0.51226	0.90759	-0.82542E-06	-0.06551	0.01446	0.00758	0.01386	13.02890	0.179E-07	0.129E-02129
130	43.25693	0.43129	0.91031	-0.11888E-05	-0.10318	0.01584	0.00829	0.01762	12.90466	0.165E-07	0.934E-03130
131	43.59027	0.35393	0.91320	-0.12603E-05	-0.10739	0.01463	0.00765	0.01955	12.77277	0.168E-07	0.860E-03131
132	43.92360	0.29223	0.91689	-0.16030E-05	-0.10855	0.01925	0.01004	0.03118	12.60464	0.212E-07	0.681E-03132
133	44.25693	0.23396	0.92031	-0.14827E-05	-0.10852	0.01537	0.00800	0.03053	12.44885	0.197E-07	0.646E-03133
134	44.59027	0.18632	0.92428	-0.17206E-05	-0.10909	0.01745	0.00907	0.04334	12.26770	0.229E-07	0.527E-03134
135	44.92360	0.14472	0.92826	-0.17203E-05	-0.10736	0.01576	0.00817	0.04963	12.08621	0.233E-07	0.470E-03135
136	45.25693	0.11100	0.93199	-0.16103E-05	-0.10000	0.01407	0.00728	0.05730	11.91603	0.235E-07	0.411E-03136
137	45.59027	0.08051	0.93592	-0.16897E-05	-0.10060	0.01222	0.00631	0.06650	11.73705	0.246E-07	0.371E-03137

ENGINEERING STRAIN (137)= 11.7370

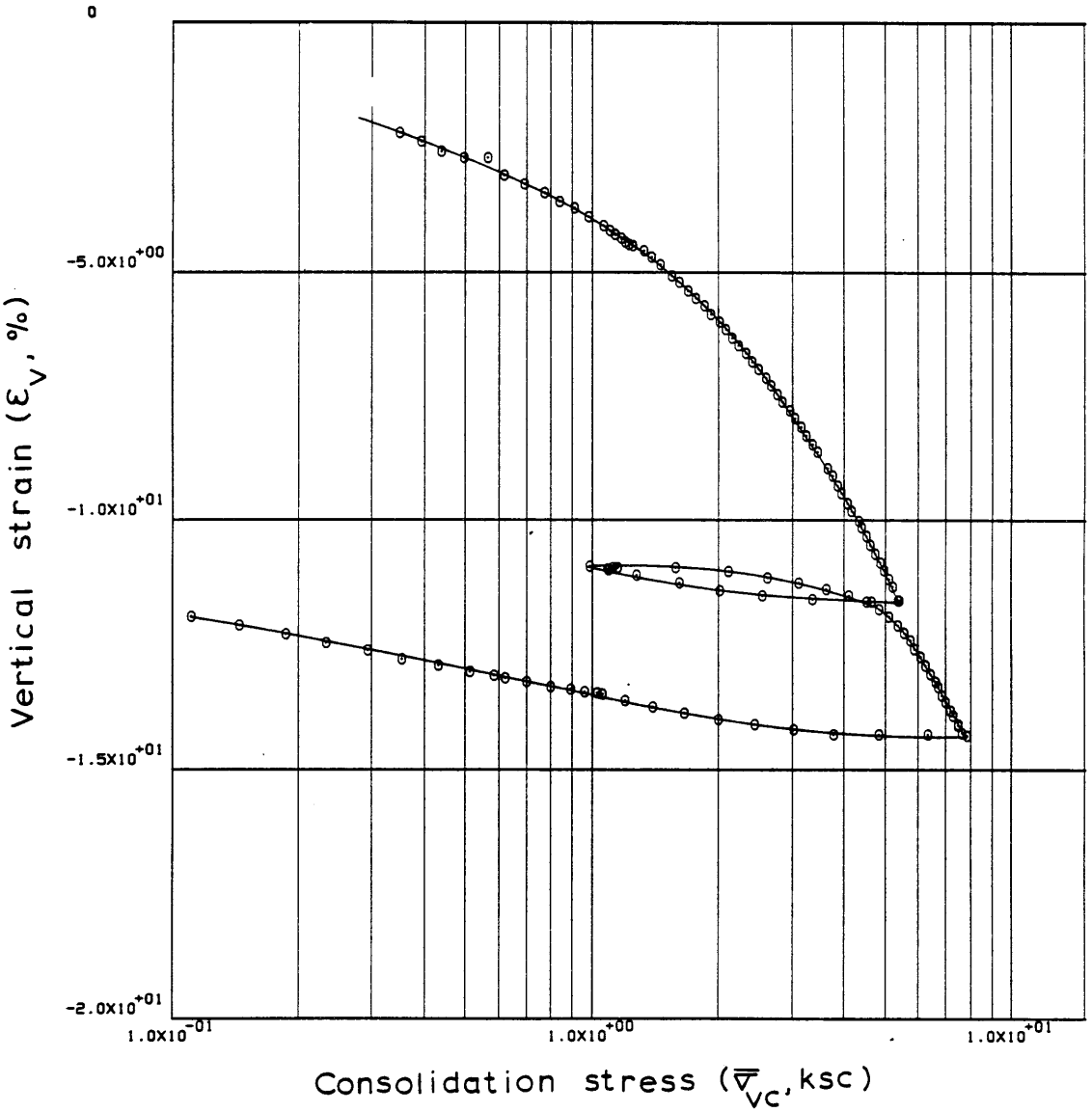

Sample No. 41.5-43.5-C-H w_N (%) 29.15 Estimated

Depth 43.31 w_L (%) 48.82 $\bar{\sigma}_{vo}$ 0.98 $\bar{\sigma}_{vm}$ 193.209

Soil Type Boston w_P (%) 23.53 CR 0.1858 RR 0.0115

Blue Clay P.I.(%) 25.29 G_s 2.77 e_o 1.1934

o At t_p Remarks Data from C.R.S.C test

w_L & w_P estimated from Baligh et al (1980)

Figure E.17 Compression Curve for Sample No. 41.5-43.5-C-H

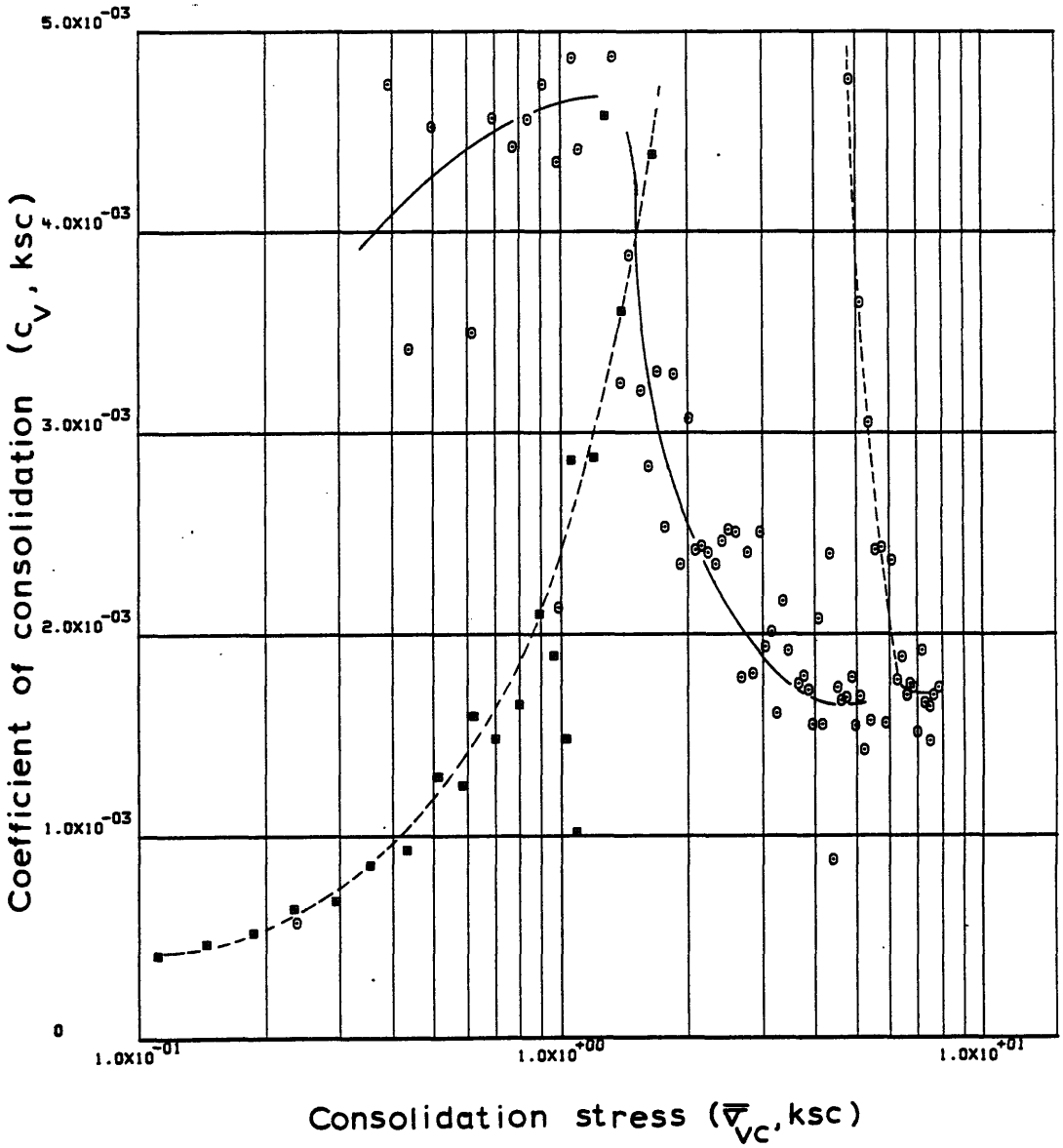

Sample No. 415.435.C.H w_N (%) 29.15 Estimated

Depth 43.31 w_L (%) 48.82 $\bar{\sigma}_{vo}$ 0.98 $\bar{\sigma}_{vm}$ 193.209

Soil Type Boston w_P (%) 23.53 CR 0.1858 RR 0.0115

Blue Clay P.I.(%) 25.29 G_s 2.77 e_o 1.1934

• At t_p Remarks Data from C.R.S.C test

w_L & w_P estimated from Baligh et al (1980)

Figure E.18 Variation of coefficient of consolidation with consolidation stress for Sample No. 41.5-43.5-C-H

1-D STRAIN CONTROLLED COMPRESSION TEST

COMPUTED RESULTS

INITIAL VOID RATIO= 0.93225
INITIAL HEIGHT= 2.3368

ALL UNITS IN: KG,CM,SEC

LINEAR THEORY

	TIME IN HOURS	VERTICAL STRESS	E	RATE OF STRAIN	EXCESS PORE PRESSURE	C	C/1+E	MV	PERCENT COMPRESSION	K	CV	
1	0.0	0.43047	0.93219	0.0	0.01169	0.0	0.0	0.00007	0.00311	0.0	0.0	1
2	0.34167	0.53592	0.93221	-0.79865E-08	0.03310	-0.00009	-0.00005	-0.00009	0.00209	-0.659E-09	0.707E-02	2
3	0.67500	0.66296	0.92915	0.13203E-05	0.05847	0.01437	0.00745	0.01247	0.16028	0.615E-07	0.493E-02	3
4	1.00833	0.78072	0.92541	0.16223E-05	0.05675	0.02293	0.01191	0.01653	0.35429	0.775E-07	0.469E-02	4
5	1.34167	0.90635	0.92183	0.15483E-05	0.05334	0.02393	0.01245	0.01479	0.53909	0.784E-07	0.530E-02	5
6	1.67500	1.05638	0.91848	0.14577E-05	0.05616	0.02191	0.01142	0.01166	0.71278	0.699E-07	0.599E-02	6
7	2.00833	1.21296	0.91509	0.14731E-05	0.06180	0.02449	0.01279	0.01129	0.88799	0.639E-07	0.566E-02	7
8	2.34165	1.38965	0.91151	0.15612E-05	0.06011	0.02633	0.01378	0.01060	1.07330	0.694E-07	0.655E-02	8
9	2.67498	1.57872	0.90805	0.15138E-05	0.06238	0.02717	0.01424	0.00961	1.25267	0.646E-07	0.672E-02	9
10	3.00833	1.79234	0.90464	0.14906E-05	0.07083	0.02684	0.01409	0.00837	1.42897	0.558E-07	0.667E-02	10
11	3.34165	1.97598	0.90133	0.14483E-05	0.06578	0.03389	0.01782	0.00946	1.60001	0.582E-07	0.615E-02	11
12	3.67498	2.09753	0.89965	0.74030E-06	0.08159	0.02826	0.01488	0.00731	1.68735	0.239E-07	0.328E-02	12
13	4.00833	2.29138	0.89611	0.15554E-05	0.07991	0.04004	0.02112	0.00963	1.87051	0.512E-07	0.531E-02	13
14	4.34165	2.47301	0.89269	0.15061E-05	0.08386	0.04485	0.02369	0.00995	2.04755	0.470E-07	0.473E-02	14
15	4.67498	2.60923	0.88916	0.15551E-05	0.08724	0.06574	0.03480	0.01370	2.22998	0.465E-07	0.340E-02	15
16	5.00833	2.76435	0.88561	0.15690E-05	0.08779	0.06150	0.03261	0.01214	2.41374	0.465E-07	0.383E-02	16
17	5.34165	2.92600	0.88187	0.16559E-05	0.09120	0.06580	0.03496	0.01229	2.60727	0.470E-07	0.383E-02	17
18	5.67498	3.06369	0.87825	0.16094E-05	0.09006	0.07887	0.04199	0.01403	2.79500	0.461E-07	0.329E-02	18
19	6.00833	3.17942	0.87463	0.16073E-05	0.09908	0.09753	0.05203	0.01667	2.98212	0.417E-07	0.250E-02	19
20	6.34165	3.29562	0.87102	0.16079E-05	0.09229	0.10056	0.05375	0.01661	3.16896	0.446E-07	0.269E-02	20
21	6.67498	3.39110	0.86746	0.15895E-05	0.09115	0.12471	0.06678	0.01997	3.35330	0.445E-07	0.223E-02	21
22	7.00833	3.43480	0.86373	0.16665E-05	0.08657	0.29113	0.15621	0.04577	3.54617	0.489E-07	0.107E-02	22
23	7.34165	3.56490	0.86013	0.16112E-05	0.09676	0.09673	0.05200	0.01486	3.73232	0.421E-07	0.284E-02	23
24	7.67498	3.69271	0.85647	0.16440E-05	0.10017	0.10397	0.05600	0.01544	3.92184	0.414E-07	0.268E-02	24
25	8.00833	3.79873	0.85277	0.16658E-05	0.10582	0.13086	0.07063	0.01886	4.11353	0.395E-07	0.210E-02	25
26	8.34165	3.90799	0.84912	0.16451E-05	0.10413	0.12874	0.06962	0.01807	4.30244	0.395E-07	0.219E-02	26
27	8.67498	3.99303	0.84547	0.16484E-05	0.10582	0.16954	0.09187	0.02326	4.49135	0.388E-07	0.167E-02	27
28	9.00833	4.10269	0.84188	0.16217E-05	0.11373	0.13232	0.07184	0.01775	4.67688	0.354E-07	0.199E-02	28
29	9.34165	4.20555	0.83816	0.16875E-05	0.12671	0.15032	0.08178	0.01969	4.86951	0.329E-07	0.167E-02	29
30	9.67498	4.29513	0.83440	0.17067E-05	0.11656	0.17828	0.09719	0.02286	5.06393	0.360E-07	0.158E-02	30
31	10.00833	4.41191	0.83085	0.16178E-05	0.12898	0.13250	0.07237	0.01662	5.24791	0.307E-07	0.185E-02	31
32	10.34165	4.50861	0.82743	0.15570E-05	0.12334	0.15747	0.08617	0.01932	5.42459	0.308E-07	0.160E-02	32
33	10.67500	4.60268	0.82375	0.16837E-05	0.12671	0.17846	0.09785	0.02148	5.61530	0.323E-07	0.150E-02	33
34	11.00833	4.68905	0.82028	0.15863E-05	0.12388	0.18636	0.10238	0.02204	5.79462	0.310E-07	0.141E-02	34
35	11.34165	4.79700	0.81685	0.15757E-05	0.12670	0.15097	0.08309	0.01752	5.97243	0.300E-07	0.171E-02	35
36	11.67500	4.87136	0.81314	0.17052E-05	0.12161	0.24118	0.13302	0.02752	6.16444	0.337E-07	0.122E-02	36
37	12.00833	4.98210	0.80960	0.16304E-05	0.13289	0.15749	0.08703	0.01767	6.34766	0.294E-07	0.166E-02	37
38	12.34165	5.07410	0.80618	0.15771E-05	0.12160	0.18686	0.10346	0.02057	6.52457	0.309E-07	0.150E-02	38
39	12.67500	5.18202	0.80276	0.15817E-05	0.12442	0.16254	0.09016	0.01759	6.70164	0.302E-07	0.172E-02	39
40	13.00833	5.27419	0.79924	0.16301E-05	0.13062	0.19967	0.11098	0.02122	6.88379	0.295E-07	0.139E-02	40
41	13.34165	5.40145	0.79576	0.16133E-05	0.13230	0.14584	0.08121	0.01521	7.06372	0.288E-07	0.189E-02	41

$POSVERT LINEAR THEORY

42	13.67500	5.50094	0.79195	0.17742E-05	0.13512	0.20902	0.11664	0.02140	7.26117	0.308E-07	0.144E-02	42
43	14.00833	5.62293	0.78863	0.15448E-05	0.12947	0.15114	0.08450	0.01520	7.43274	0.279E-07	0.184E-02	43
44	14.34165	5.74177	0.78501	0.16905E-05	0.13116	0.17314	0.09700	0.01707	7.62015	0.300E-07	0.176E-02	44
45	14.67500	5.86660	0.77866	0.29762E-05	0.13399	0.29541	0.16609	0.02861	7.94891	0.514E-07	0.180E-02	45
46	15.00833	5.99981	0.77520	0.16235E-05	0.13680	0.15402	0.08676	0.01462	8.12791	0.273E-07	0.187E-02	46
47	15.34165	6.12841	0.77155	0.17174E-05	0.13398	0.17213	0.09717	0.01602	8.31683	0.294E-07	0.184E-02	47
48	15.67500	6.25436	0.76876	0.13125E-05	0.14018	0.13693	0.07742	0.01251	8.46101	0.214E-07	0.171E-02	48
49	16.00832	6.38710	0.76878	-0.90331E-08	0.14131	-0.00091	-0.00051	-0.00008	8.46004	-0.146E-09	0.179E-02	49
50	16.34164	6.48853	0.76882	-0.15093E-07	0.14132	-0.00206	-0.00116	-0.00018	8.45836	-0.244E-09	0.137E-02	50
51	16.67499	6.68335	0.76880	0.47599E-08	0.14300	0.00035	0.00020	0.00003	8.45889	0.762E-10	0.260E-02	51
52	17.00832	6.83715	0.76882	-0.94506E-08	0.14810	-0.00084	-0.00047	-0.00007	8.45787	-0.146E-09	0.198E-02	52
53	17.34164	6.99958	0.76883	-0.47601E-08	0.14528	-0.00045	-0.00025	-0.00004	8.45734	-0.750E-10	0.213E-02	53
54	17.67499	7.15012	0.76882	0.83821E-08	0.15770	0.00081	0.00046	0.00007	8.45824	0.122E-09	0.182E-02	54
55	18.00832	7.30884	0.76871	0.49067E-07	0.16053	0.00473	0.00268	0.00037	8.46362	0.699E-09	0.188E-02	55
56	18.34164	7.48390	0.76861	0.50278E-07	0.16167	0.00455	0.00257	0.00034	8.46918	0.711E-09	0.206E-02	56
57	18.67499	7.70030	0.76856	0.21504E-07	0.16903	0.00161	0.00091	0.00012	8.47154	0.291E-09	0.244E-02	57
58	19.00832	7.86194	0.76859	-0.13957E-07	0.17240	-0.00147	-0.00083	-0.00010	8.47000	-0.185E-09	0.179E-02	58
59	19.34164	8.02746	0.76859	0.16256E-08	0.17013	0.00014	0.00008	0.00001	8.47015	0.219E-10	0.185E-02	59
60	19.67499	8.21213	0.76835	0.11044E-06	0.17465	0.01036	0.00586	0.00072	8.48232	0.145E-08	0.201E-02	60
61	20.00832	8.41625	0.76820	0.70730E-07	0.18762	0.00610	0.00345	0.00042	8.49008	0.862E-09	0.207E-02	61
62	20.34164	8.59213	0.71787	0.24417E-04	0.18253	2.43367	1.41668	0.16659	11.09492	0.289E-06	0.173E-02	62
63	20.67499	8.82234	0.71506	0.13641E-05	0.18931	0.10619	0.06192	0.00711	11.24020	0.155E-07	0.218E-02	63
64	21.00832	9.01935	0.71199	0.14950E-05	0.18988	0.13909	0.08124	0.00911	11.39917	0.169E-07	0.185E-02	64
65	21.34164	9.23671	0.70874	0.15835E-05	0.19099	0.13636	0.07980	0.00874	11.56723	0.177E-07	0.203E-02	65
66	21.67499	9.42386	0.70516	0.17532E-05	0.19440	0.17882	0.10487	0.01124	11.75288	0.192E-07	0.171E-02	66
67	22.00832	9.67337	0.70170	0.16948E-05	0.20004	0.13244	0.07783	0.00815	11.93201	0.179E-07	0.220E-02	67
68	22.34164	9.91049	0.69879	0.14233E-05	0.20172	0.11980	0.07052	0.00720	12.08215	0.149E-07	0.207E-02	68
69	22.67499	10.13644	0.69508	0.18248E-05	0.19495	0.16469	0.09716	0.00969	12.27425	0.197E-07	0.203E-02	69
70	23.00832	10.37336	0.69222	0.14115E-05	0.20452	0.12404	0.07330	0.00715	12.42259	0.145E-07	0.202E-02	70
71	23.34164	10.61571	0.68850	0.18332E-05	0.20564	0.16085	0.09526	0.00908	12.61481	0.186E-07	0.205E-02	71
72	23.67499	10.86572	0.68458	0.19405E-05	0.21130	0.16855	0.10006	0.00931	12.81786	0.191E-07	0.205E-02	72
73	24.00832	11.15627	0.68114	0.17030E-05	0.20564	0.13018	0.07743	0.00703	12.99567	0.171E-07	0.243E-02	73
74	24.34164	11.42176	0.67910	0.10118E-05	0.21580	0.08670	0.05163	0.00457	13.10115	0.967E-08	0.211E-02	74
75	24.67499	11.71824	0.67430	0.23889E-05	0.22709	0.18730	0.11187	0.00967	13.34958	0.216E-07	0.223E-02	75
76	25.00832	12.00016	0.67119	0.15533E-05	0.22764	0.13102	0.07840	0.00661	13.51077	0.139E-07	0.211E-02	76
77	25.34164	12.28411	0.66794	0.16231E-05	0.22537	0.13890	0.08327	0.00686	13.67888	0.147E-07	0.214E-02	77
78	25.67499	12.57847	0.66439	0.17788E-05	0.23159	0.15006	0.09016	0.00725	13.86278	0.156E-07	0.215E-02	78
79	26.00832	12.92408	0.66135	0.15252E-05	0.23782	0.11217	0.06752	0.00530	14.02010	0.129E-07	0.244E-02	79
80	26.34164	13.25482	0.65886	0.12499E-05	0.24120	0.09847	0.05936	0.00453	14.14890	0.104E-07	0.230E-02	80
81	45.00832	13.73756	0.64577	0.11839E-06	0.04933	0.36604	0.22241	0.01648	14.82652	0.475E-08	0.266E-03	81
82	45.34164	12.19069	0.64481	0.48343E-06	-0.07315	-0.00798	-0.00485	-0.00038	14.87592	-0.131E-07	0.349E-01	82
83	45.67499	-10.25232	0.64631	-0.75597E-06	-0.09294	0.00862	0.00524	0.00047	14.79861	0.161E-07	0.344E-01	83
84	46.00832	8.80599	0.64814	-0.92651E-06	-0.11375	0.01205	0.00731	0.00077	14.70377	0.162E-07	0.210E-01	84
85	46.34164	7.63081	0.65028	-0.10803E-05	-0.12503	0.01493	0.00905	0.00110	14.59305	0.172E-07	0.156E-01	85
86	46.67499	6.66166	0.65249	-0.11181E-05	-0.14365	0.01632	0.00988	0.00138	14.47829	0.155E-07	0.112E-01	86
87	48.67499	3.05927	0.66995	-0.14434E-05	-0.16341	0.02230	0.01335	0.00288	13.58015	0.180E-07	0.624E-02	87
88	49.00832	2.74291	0.67313	-0.16320E-05	-0.15777	0.03002	0.01794	0.00619	13.41058	0.212E-07	0.342E-02	88
89	49.34164	2.47406	0.67631	-0.15829E-05	-0.16226	0.03087	0.01841	0.00707	13.24579	0.200E-07	0.284E-02	89
90	49.67499	2.21475	0.67939	-0.15288E-05	-0.17128	0.02782	0.01657	0.00707	13.08633	0.184E-07	0.260E-02	90
91	50.34164	1.77513	0.68618	-0.16779E-05	-0.18088	0.03069	0.01820	0.00916	12.73492	0.193E-07	0.211E-02	91
92	50.67497	1.58866	0.68923	-0.15172E-05	-0.18257	0.02771	0.01640	0.00976	12.57576	0.173E-07	0.178E-02	92
93	51.00832	1.45714	0.69208	-0.13894E-05	-0.13743	0.03264	0.01929	0.01268	12.42978	0.212E-07	0.167E-02	93
94	51.34164	1.36064	0.69468	-0.12799E-05	-0.16451	0.04828	0.02849	0.02008	12.29506	0.163E-07	0.814E-03	94
95	51.67497	1.25330	0.69793	-0.15938E-05	-0.16620	0.03356	0.01976	0.01502	12.12700	0.202E-07	0.135E-02	95
96	52.00832	1.13748	0.70147	-0.17353E-05	-0.16733	0.03654	0.02147	0.01798	11.94363	0.220E-07	0.122E-02	96

97	52.34164	1.04405	0.70494	-0.16941E-05	-0.16902	0.04044	0.02372	0.02176	11.76427	0.213E-07	0.979E-03	97
98	52.67497	0.95288	0.70792	-0.14577E-05	-0.17184	0.03270	0.01914	0.01919	11.60963	0.181E-07	0.943E-03	98

ENGINEERING STRAIN (98)= 11.6096

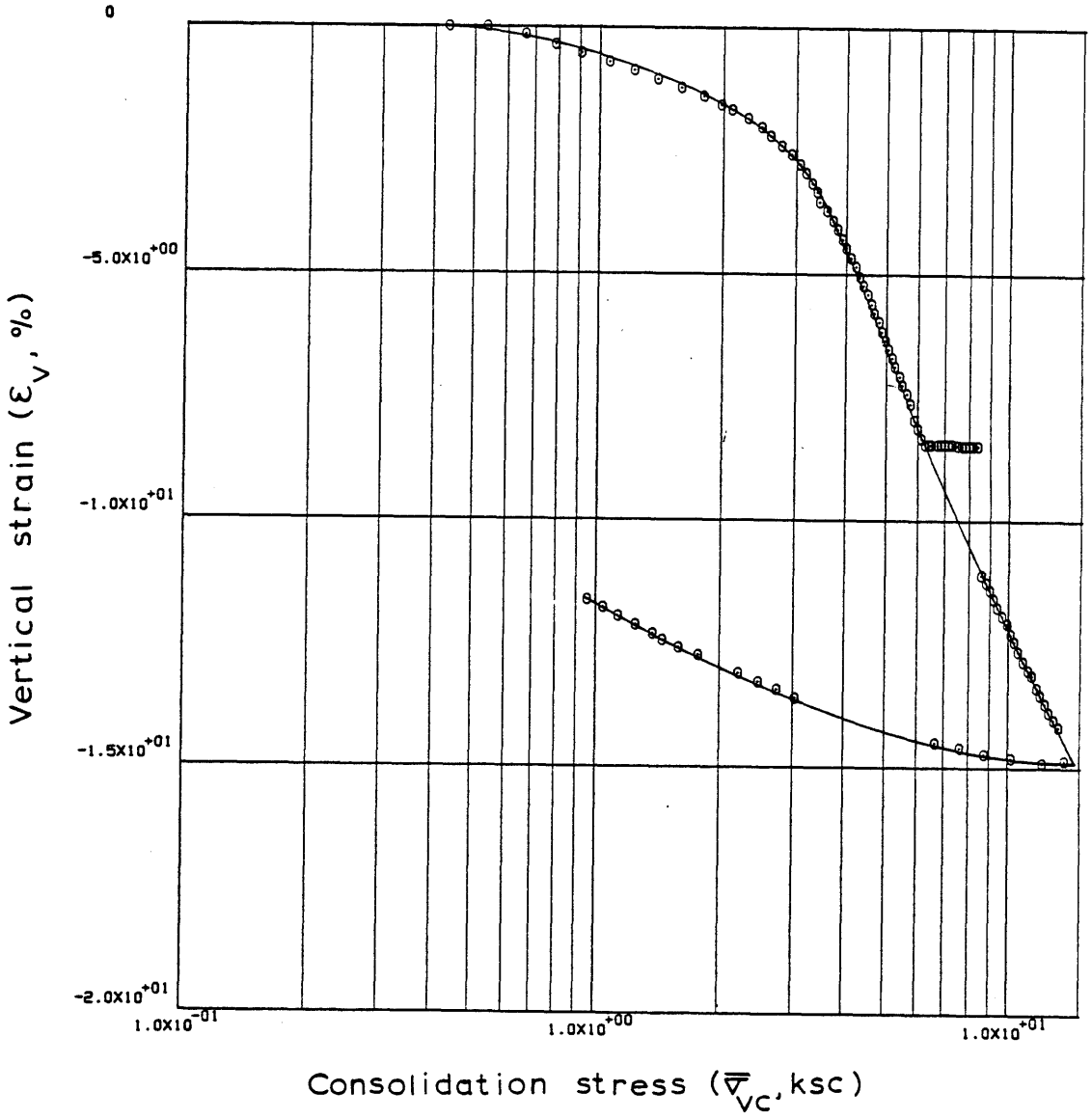

Sample No. SP05VERT w_N (%) 43.50 Estimated

Depth 51.95 w_L (%) 44.59 $\bar{\sigma}_{vo}$ 1.19 $\bar{\sigma}_{vm}$ 3.24-3.40

Soil Type Boston w_P (%) 24.01 CR 0.1871 RR 0.0269

Blue Clay P.I.(%) 20.58 G_s 2.77 e_o 0.9322

o At t_p Remarks Data from C.R.S.C test

w_L & w_P estimated from Baligh et al (1980)

Figure E.19 Compression Curve for Sample No. SP05VERT

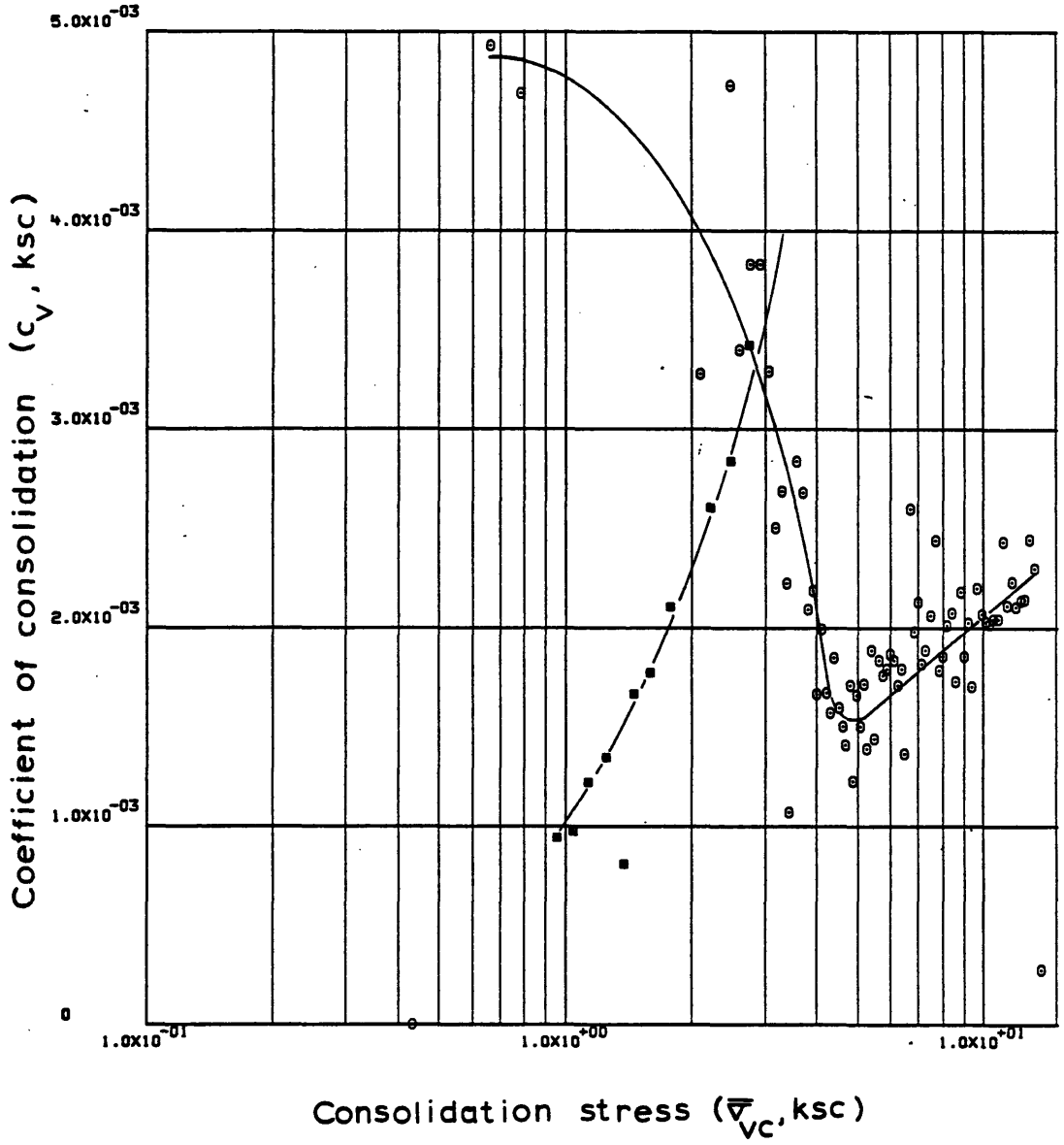

Sample No. SP05VERT w_N (%) 43.50 Estimated

Depth 51.95 w_L (%) 44.59 $\bar{\sigma}_{vo}$ ~ 1.19 $\bar{\sigma}_{vm}$ 324-340

Soil Type Boston Blue Clay w_P (%) 24.01 CR 0.1871 RR 0.0269

P.I.(%) 20.58 G_s 2.77 e_o 0.9322

o At t_p Remarks Data from C.R.S.C test

w_L & w_P estimated from Baligh et al (1980)

Figure E.20 Variation of coefficient of consolidation with consolidation stress for Sample No. SP05VERT

1-D STRAIN CONTROLLED COMPRESSION TEST

COMPUTED RESULTS

INITIAL VOID RATIO= 1.16753
INITIAL HEIGHT= 1.9355

ALL UNITS IN: KG,CM,SEC

LINEAR THEORY

	TIME IN HOURS	VERTICAL STRESS	E	RATE OF STRAIN	EXCESS PORE PRESSURE	C	C/1+E	MV	PERCENT COMPRESSION	K	CV	
1	0.0	0.11214	1.16555	0.0	-0.00113	0.0	0.0	0.00813	0.09106	0.0	0.0	1
2	0.33333	0.17863	1.16212	0.13225E-05	-0.00215	0.00737	0.00341	0.02387	0.24937	-0.115E-05	-0.480E-01	2
3	0.66667	0.18555	1.15829	0.14779E-05	0.00571	0.10074	0.04668	0.25640	0.42598	0.480E-06	0.187E-02	3
4	1.00000	0.19311	1.15448	0.14752E-05	0.02804	0.09545	0.04430	0.23404	0.60193	0.973E-07	0.416E-03	4
5	1.33333	0.21160	1.15063	0.14932E-05	0.04297	0.04214	0.01959	0.09689	0.77971	0.641E-07	0.661E-03	5
6	1.76250	0.23421	1.14470	0.17896E-05	0.06197	0.05842	0.02724	0.12229	1.05327	0.530E-07	0.433E-03	6
7	2.19083	0.25777	1.14052	0.12636E-05	0.07186	0.04352	0.02033	0.08273	1.24568	0.321E-07	0.388E-03	7
8	2.52415	0.29145	1.13690	0.14132E-05	0.07575	0.02950	0.01381	0.05035	1.41287	0.340E-07	0.675E-03	8
9	2.85749	0.33087	1.13334	0.13930E-05	0.07887	0.02812	0.01318	0.04241	1.57739	0.320E-07	0.756E-03	9
10	3.08111	0.35346	1.13071	0.15285E-05	0.08198	0.03969	0.01863	0.05446	1.69836	0.337E-07	0.620E-03	10
11	3.41444	0.39753	1.12682	0.15254E-05	0.08627	0.03313	0.01558	0.04153	1.87796	0.319E-07	0.768E-03	11
12	3.74777	0.43789	1.12313	0.14500E-05	0.08741	0.03821	0.01800	0.04312	2.04840	0.298E-07	0.691E-03	12
13	4.08111	0.49003	1.11943	0.14525E-05	0.08860	0.03284	0.01549	0.03343	2.21884	0.294E-07	0.878E-03	13
14	4.41444	0.53329	1.11561	0.15039E-05	0.08807	0.04513	0.02133	0.04172	2.39499	0.305E-07	0.730E-03	14
15	4.74777	0.59646	1.11331	0.90841E-06	0.08581	0.02058	0.00974	0.01726	2.50127	0.188E-07	0.109E-02	15
16	5.08111	0.63234	1.10874	0.18062E-05	0.08733	0.07824	0.03711	0.06041	2.71216	0.367E-07	0.607E-03	16
17	5.41444	0.71657	1.10521	0.13978E-05	0.07083	0.02823	0.01341	0.01991	2.87506	0.349E-07	0.175E-02	17
18	5.74777	0.77966	1.10175	0.13701E-05	0.08281	0.04096	0.01949	0.02606	3.03450	0.291E-07	0.112E-02	18
19	6.08111	0.85809	1.09810	0.14518E-05	0.08648	0.03814	0.01818	0.02222	3.20313	0.295E-07	0.133E-02	19
20	6.41444	0.93744	1.09460	0.13901E-05	0.08432	0.03951	0.01886	0.02102	3.36435	0.288E-07	0.137E-02	20
21	6.74777	1.01061	1.09186	0.10915E-05	0.06087	0.03644	0.01742	0.01790	3.49072	0.313E-07	0.175E-02	21
22	7.08111	1.06054	1.08992	0.77581E-06	0.03940	0.04036	0.01931	0.01864	3.58051	0.343E-07	0.184E-02	22
23	7.41444	1.08835	1.08924	0.26923E-06	0.01900	0.02609	0.01249	0.01162	3.61165	0.247E-07	0.212E-02	23
24	7.74777	1.11024	1.08877	0.19017E-06	0.01442	0.02389	0.01144	0.01042	3.63362	0.229E-07	0.220E-02	24
25	8.08111	1.17121	1.08678	0.79284E-06	0.03753	0.03714	0.01780	0.01561	3.72522	0.367E-07	0.235E-02	25
26	8.41444	1.19498	1.08615	0.25382E-06	0.01651	0.03161	0.01515	0.01281	3.75455	0.267E-07	0.208E-02	26
27	8.74777	1.22270	1.08563	0.20628E-06	0.01577	0.02254	0.01081	0.00893	3.77838	0.227E-07	0.254E-02	27
28	9.08111	1.30342	1.08503	0.23804E-06	0.05703	0.00931	0.00446	0.00354	3.80583	0.723E-08	0.204E-02	28
29	9.41444	1.38496	1.08495	0.31776E-07	0.06393	0.00132	0.00063	0.00047	3.80952	0.861E-09	0.184E-02	29
30	9.74777	1.48409	1.08491	0.15741E-07	0.08088	0.00057	0.00027	0.00019	3.81136	0.337E-09	0.177E-02	30
31	10.63916	1.74004	1.08499	-0.11832E-07	0.08919	-0.00049	-0.00024	-0.00015	3.80769	-0.230E-09	0.155E-02	31
32	10.97250	1.83641	1.08495	0.15901E-07	0.08179	0.00073	0.00035	0.00020	3.80952	0.337E-09	0.170E-02	32
33	11.30583	1.93399	1.08499	-0.15901E-07	0.08286	-0.00076	-0.00036	-0.00020	3.80769	-0.333E-09	0.170E-02	33
34	11.63916	2.00854	1.08495	0.15901E-07	0.09202	0.00103	0.00050	0.00026	3.80952	0.299E-09	0.117E-02	34
35	11.97250	2.12050	1.08499	-0.15900E-07	0.09258	-0.00072	-0.00035	-0.00017	3.80769	-0.298E-09	0.175E-02	35
36	12.30583	2.20329	1.08511	-0.47673E-07	0.09450	-0.00314	-0.00150	-0.00069	3.80219	-0.874E-09	0.127E-02	36
37	12.63916	2.29831	1.08519	-0.31772E-07	0.09964	-0.00190	-0.00091	-0.00040	3.79849	-0.553E-09	0.138E-02	37
38	12.97250	2.37466	1.08531	-0.47187E-07	0.09954	-0.00359	-0.00172	-0.00074	3.79306	-0.822E-09	0.111E-02	38
39	13.63916	2.54513	1.08535	-0.79491E-08	0.09508	-0.00056	-0.00027	-0.00011	3.79124	-0.145E-09	0.130E-02	39
40	14.30583	2.70077	1.08551	-0.31807E-07	0.11673	-0.00268	-0.00129	-0.00049	3.78391	-0.472E-09	0.963E-03	40
41	14.63916	2.77991	1.08543	0.31849E-07	0.11927	0.00274	0.00131	0.00048	3.78755	0.463E-09	0.959E-03	41

42	14.97250	2.86082	1.08559	-0.63289E-07	0.12303	-0.00552	-0.00265	-0.00094	3.78026	-0.892E-09 0.950E-03 42
43	15.30583	2.93605	1.08551	0.31447E-07	0.12628	0.00305	0.00146	0.00050	3.78391	0.432E-09 0.861E-03 43
44	15.63916	3.00765	1.08567	-0.63076E-07	0.12631	-0.00657	-0.00315	-0.00106	3.77661	-0.866E-09 0.819E-03 44
45	15.97250	2.00412	1.15034	-0.25061E-04	0.41987	0.15930	0.07408	0.02997	0.79306	-0.110E-06 -0.367E-02 45
46	16.30582	3.15261	1.08559	0.25872E-04	0.13524	0.14293	0.06853	0.02703	3.78026	0.332E-06 0.123E-01 46
47	16.63914	3.21812	1.00336	0.34204E-04	0.13795	3.99820	1.99574	0.62655	7.57381	0.397E-06 0.633E-03 47
48	16.97249	3.29835	0.99963	0.15561E-05	0.13863	0.15166	0.07584	0.02327	7.74612	0.179E-07 0.769E-03 48
49	17.30582	3.36204	0.99596	0.15329E-05	0.14216	0.19199	0.09619	0.02888	7.91547	0.171E-07 0.593E-03 49
50	17.63914	2.88286	0.93194	0.27612E-04	-0.21874	-0.41630	-0.21548	-0.06915	10.86871	-0.188E-06 0.272E-02 50
51	17.97249	3.47972	0.98817	-0.23566E-04	0.14606	-0.29880	-0.15029	-0.04738	8.27472	-0.254E-06 0.537E-02 51
52	18.30582	3.58174	0.98440	0.15851E-05	0.14979	0.13059	0.06581	0.01864	8.44885	0.166E-07 0.891E-03 52
53	18.63914	3.64928	0.98064	0.15796E-05	0.15405	0.20102	0.10149	0.02806	8.62210	0.160E-07 0.571E-03 53
54	18.97249	3.73768	0.97686	0.15913E-05	0.15434	0.15771	0.07978	0.02160	8.79623	0.161E-07 0.744E-03 54
55	19.30582	3.78636	0.97321	0.15440E-05	0.15123	0.28247	0.14315	0.03805	8.96489	0.158E-07 0.416E-03 55
56	19.63914	3.87925	0.96931	0.16479E-05	0.15558	0.16071	0.08161	0.02129	9.14459	0.164E-07 0.769E-03 56
57	19.97249	3.95247	0.96572	0.15256E-05	0.16121	0.19243	0.09789	0.02500	9.31059	0.146E-07 0.583E-03 57
58	20.30582	4.03268	0.96192	0.16108E-05	0.16062	0.18878	0.09622	0.02410	9.48557	0.154E-07 0.639E-03 58
59	20.63914	4.10417	0.95823	0.15727E-05	0.16136	0.21031	0.10740	0.02640	9.65605	0.149E-07 0.564E-03 59
60	21.27748	4.26001	0.95115	0.15775E-05	0.16356	0.18980	0.09727	0.02326	9.98239	0.146E-07 0.629E-03 60
61	21.29109	4.23606	0.95112	0.41613E-06	0.16684	-0.00694	-0.00355	-0.00085	9.98421	0.379E-08 -0.445E-02 61
62	21.62442	3.43175	0.94981	0.55577E-06	-0.07971	-0.00618	-0.00317	-0.00083	10.04422	-0.106E-07 0.127E-01 62
63	21.95776	2.81171	0.95176	-0.83101E-06	-0.11244	0.00976	0.00500	0.00161	9.95444	0.112E-07 0.698E-02 63
64	22.29109	2.36614	0.95461	-0.12129E-05	-0.12944	0.01649	0.00844	0.00327	9.82318	0.143E-07 0.437E-02 64
65	22.62442	2.02488	0.95753	-0.12444E-05	-0.13003	0.01877	0.00959	0.00438	9.68832	0.146E-07 0.334E-02 65
66	22.95776	1.76013	0.96070	-0.13501E-05	-0.13026	0.02266	0.01156	0.00612	9.54179	0.159E-07 0.260E-02 66
67	23.29109	1.55907	0.96356	-0.12134E-05	-0.10477	0.02357	0.01200	0.00724	9.40988	0.178E-07 0.246E-02 67
68	23.62442	1.40564	0.96649	-0.12378E-05	-0.10819	0.02820	0.01434	0.00968	9.27512	0.176E-07 0.182E-02 68
69	23.95776	1.29800	0.96879	-0.97467E-06	-0.07283	0.02891	0.01468	0.01087	9.16888	0.207E-07 0.190E-02 69
70	24.29109	1.26028	0.96895	-0.67183E-07	-0.03909	0.00540	0.00274	0.00214	9.16154	0.266E-08 0.124E-02 70
71	24.62442	1.20932	0.96980	-0.36186E-06	-0.06077	0.02072	0.01052	0.00852	9.12207	0.921E-08 0.108E-02 71
72	24.95776	1.15524	0.97183	-0.85553E-06	-0.08467	0.04423	0.02243	0.01898	9.02870	0.157E-07 0.825E-03 72
73	25.29109	1.07338	0.97373	-0.80444E-06	-0.09360	0.02593	0.01314	0.01179	8.94080	0.133E-07 0.113E-02 73
74	25.62442	0.98781	0.97645	-0.11462E-05	-0.09752	0.03273	0.01656	0.01607	8.81535	0.183E-07 0.114E-02 74
75	25.95776	0.93896	0.97758	-0.47698E-06	-0.05270	0.02232	0.01129	0.01172	8.76312	0.141E-07 0.120E-02 75
76	26.29109	0.91798	0.97806	-0.20062E-06	-0.04151	0.02106	0.01065	0.01147	8.74113	0.754E-08 0.657E-03 76
77	26.62442	0.85977	0.97985	-0.75186E-06	-0.11518	0.02727	0.01377	0.01550	8.65875	0.102E-07 0.658E-03 77
78	26.95775	0.78332	0.98302	-0.13345E-05	-0.13608	0.03409	0.01719	0.02095	8.51227	0.154E-07 0.734E-03 78
79	27.12025	0.82499	0.98403	-0.87143E-06	-0.05472	-0.01952	-0.00984	-0.01223	8.46561	0.250E-07 -0.204E-02 79
80	27.45358	1.08882	0.98290	0.47513E-06	0.07865	0.00407	0.00205	0.00216	8.51773	0.947E-08 0.438E-02 80
81	27.78693	1.18136	0.98187	0.43393E-06	0.02611	0.01265	0.00638	0.00563	8.56534	0.260E-07 0.463E-02 81
82	28.12025	1.21797	0.98167	0.83453E-07	0.00046	0.00650	0.00328	0.00274	8.57449	0.282E-06 0.103E+00 82
83	28.43886	1.22055	0.98163	0.17504E-07	-0.00186	0.01897	0.00957	0.00780	8.57632	-0.148E-07 -0.189E-02 83
84	28.77219	1.28616	0.98094	0.29229E-06	0.02137	0.01328	0.00670	0.00535	8.60840	0.214E-07 0.400E-02 84
85	29.10553	1.31950	0.98100	-0.25102E-07	0.00301	-0.00235	-0.00118	-0.00090	8.60564	-0.131E-07 0.145E-01 85
86	29.43886	1.40879	0.98000	0.41765E-06	0.06447	0.01515	0.00765	0.00561	8.65141	0.101E-07 0.180E-02 86
87	29.92108	1.64969	0.97587	0.12035E-05	0.10752	0.02616	0.01324	0.00867	8.84190	0.174E-07 0.201E-02 87
88	30.25441	1.84802	0.97238	0.14758E-05	0.11763	0.03076	0.01560	0.00893	9.00302	0.195E-07 0.218E-02 88
89	30.58775	2.05818	0.96939	0.12673E-05	0.11304	0.02780	0.01412	0.00724	9.14119	0.173E-07 0.240E-02 89
90	30.92108	2.27626	0.96629	0.13120E-05	0.12428	0.03075	0.01564	0.00722	9.28404	0.163E-07 0.225E-02 90
91	31.25441	2.51190	0.96300	0.13984E-05	0.13021	0.03343	0.01703	0.00712	9.43599	0.165E-07 0.232E-02 91
92	31.58775	2.35919	0.96504	-0.86429E-06	0.16220	0.03248	0.01653	0.00679	9.34198	-0.820E-08 -0.121E-02 92
93	31.92108	2.98074	0.95645	0.36574E-05	0.12676	0.03672	0.01877	0.00706	9.73814	0.440E-07 0.624E-02 93
94	32.25441	3.23129	0.95324	0.13715E-05	0.11677	0.03982	0.02039	0.00657	9.88640	0.179E-07 0.272E-02 94
95	32.58775	3.41757	0.95010	0.13398E-05	0.13512	0.05594	0.02869	0.00863	10.03107	0.150E-07 0.174E-02 95
96	32.92108	3.67380	0.94653	0.15292E-05	0.14665	0.04940	0.02538	0.00716	10.19583	0.158E-07 0.220E-02 96

97	33.25441	3.84886	0.94288	0.15660E-05	0.14693	0.07845	0.04038	0.01073	10.36430	0.160E-07	0.149E-02 97
98	33.58775	4.03060	0.93946	0.14665E-05	0.15569	0.07398	0.03814	0.00968	10.52177	0.141E-07	0.146E-02 98
99	33.92108	4.18373	0.93581	0.15718E-05	0.15856	0.09793	0.05059	0.01232	10.69025	0.148E-07	0.120E-02 99
100	34.25441	4.32811	0.93228	0.15233E-05	0.15970	0.10412	0.05389	0.01266	10.85320	0.142E-07	0.112E-02100
101	34.58775	4.45585	0.92855	0.16119E-05	0.16653	0.12823	0.06649	0.01514	11.02531	0.144E-07	0.948E-03101
102	34.92110	4.53302	0.92494	0.15635E-05	0.16450	0.21035	0.10927	0.02431	11.19189	0.140E-07	0.577E-03102
103	35.25443	4.70963	0.92113	0.16527E-05	0.16992	0.09968	0.05189	0.01123	11.36771	0.143E-07	0.127E-02103
104	35.58775	4.83330	0.91784	0.14276E-05	0.17108	0.12675	0.06609	0.01385	11.51927	0.122E-07	0.883E-03104
105	35.92110	4.94081	0.91406	0.16452E-05	0.17562	0.17176	0.08973	0.01836	11.69359	0.137E-07	0.745E-03105
106	36.25443	5.05909	0.91041	0.15926E-05	0.17918	0.15435	0.08079	0.01616	11.86206	0.129E-07	0.800E-03106
107	36.58775	5.16429	0.90652	0.17029E-05	0.18169	0.18933	0.09931	0.01942	12.04181	0.136E-07	0.699E-03107
108	36.92110	5.28891	0.90295	0.15612E-05	0.18127	0.14951	0.07857	0.01503	12.20628	0.124E-07	0.827E-03108
109	37.25443	5.38320	0.89934	0.15846E-05	0.18692	0.20434	0.10758	0.02017	12.37288	0.122E-07	0.605E-03109
110	37.58775	5.51097	0.89609	0.14303E-05	0.17935	0.13876	0.07318	0.01343	12.52303	0.114E-07	0.851E-03110
111	37.92110	5.63478	0.89224	0.16936E-05	0.19130	0.17307	0.09147	0.01642	12.70045	0.126E-07	0.770E-03111
112	38.25443	5.76183	0.88855	0.16303E-05	0.19121	0.16574	0.08776	0.01540	12.87094	0.121E-07	0.787E-03112
113	38.58775	5.87232	0.88501	0.15615E-05	0.19619	0.18597	0.09865	0.01696	13.03389	0.113E-07	0.665E-03113
114	38.92110	6.00706	0.88144	0.15820E-05	0.19714	0.15744	0.08368	0.01409	13.19865	0.113E-07	0.804E-03114
115	39.25443	6.11200	0.87783	0.16021E-05	0.19260	0.20848	0.11102	0.01832	13.36525	0.117E-07	0.638E-03115
116	39.58775	6.26411	0.87418	0.16232E-05	0.20589	0.14851	0.07924	0.01281	13.53366	0.110E-07	0.862E-03116
117	39.92110	6.39341	0.87029	0.17338E-05	0.20571	0.19040	0.10180	0.01609	13.71317	0.118E-07	0.730E-03117
118	40.25443	6.52479	0.86692	0.15060E-05	0.20633	0.16588	0.08885	0.01376	13.86882	0.101E-07	0.737E-03118
119	40.58775	6.67574	0.86338	0.15794E-05	0.21149	0.15446	0.08289	0.01256	14.03177	0.103E-07	0.823E-03119
120	40.92110	6.81102	0.85961	0.16904E-05	0.21272	0.18801	0.10110	0.01499	14.20580	0.110E-07	0.731E-03120
121	41.25443	6.95941	0.85608	0.15861E-05	0.15831	0.16395	0.08833	0.01283	14.36879	0.138E-07	0.107E-02121
122	41.58775	7.08667	0.85255	0.15892E-05	0.20954	0.19493	0.10522	0.01498	14.53178	0.104E-07	0.692E-03122
123	41.92110	7.27186	0.84894	0.16263E-05	0.21787	0.13986	0.07564	0.01054	14.69823	0.102E-07	0.965E-03123
124	42.25443	7.40859	0.84521	0.16848E-05	0.21454	0.20028	0.10854	0.01479	14.87035	0.107E-07	0.721E-03124
125	42.92110	7.73738	0.83826	0.15742E-05	0.22069	0.15995	0.08701	0.01149	15.19077	0.961E-08	0.836E-03125
126	43.18471	7.80065	0.83544	0.16177E-05	0.22437	0.34594	0.18848	0.02426	15.32076	0.968E-08	0.399E-03126
127	43.51888	8.04710	0.83163	0.17291E-05	0.23154	0.12252	0.06689	0.00844	15.49657	0.999E-08	0.118E-02127
128	43.87970	6.74849	0.83120	0.18355E-06	-0.08426	-0.00248	-0.00135	-0.00018	15.51666	-0.291E-08	0.159E-01128
129	44.21304	5.66154	0.83318	-0.90206E-06	-0.15792	0.01130	0.00616	0.00100	15.42511	0.765E-08	0.768E-02129
130	44.50415	4.95617	0.83505	-0.96990E-06	-0.16780	0.01401	0.00764	0.00144	15.33908	0.776E-08	0.538E-02130
131	44.83748	4.28348	0.83770	-0.12032E-05	-0.18377	0.01819	0.00990	0.00215	15.21669	0.882E-08	0.411E-02131
132	45.17082	3.69231	0.84033	-0.11887E-05	-0.18814	0.01768	0.00961	0.00241	15.09557	0.853E-08	0.354E-02132
133	45.44554	2.75994	0.83145	0.48984E-05	-0.28659	-0.03048	-0.01664	-0.00520	15.50488	-0.229E-07	0.440E-02133
134	45.77554	2.97387	0.84545	-0.63820E-05	-0.19661	-0.18743	-0.10156	-0.03544	14.85936	0.441E-07	-0.124E-02134
135	46.24359	2.52746	0.84957	-0.13244E-05	-0.19706	0.02537	0.01372	0.00500	14.66898	0.917E-08	0.183E-02135
136	46.57692	2.25429	0.85259	-0.13568E-05	-0.19214	0.02638	0.01424	0.00596	14.52977	0.966E-08	0.162E-02136
137	46.91026	2.03767	0.85545	-0.12833E-05	-0.21660	0.02827	0.01524	0.00711	14.39796	0.813E-08	0.114E-02137
138	47.06943	1.94582	0.85707	-0.15292E-05	-0.22875	0.03530	0.01901	0.00954	14.32288	0.919E-08	0.963E-03138
139	47.59221	1.64367	0.86144	-0.12461E-05	-0.17034	0.02587	0.01390	0.00776	14.12149	0.101E-07	0.130E-02139
140	47.92554	1.49653	0.86501	-0.15960E-05	-0.17785	0.03809	0.02043	0.01302	13.95668	0.124E-07	0.956E-03140
141	48.25887	1.37778	0.86795	-0.13102E-05	-0.16402	0.03551	0.01901	0.01324	13.82121	0.111E-07	0.839E-03141
142	48.64249	1.30669	0.86977	-0.70703E-06	-0.08311	0.03447	0.01844	0.01374	13.73697	0.119E-07	0.863E-03142
143	48.97581	1.26649	0.87120	-0.63614E-06	-0.07029	0.04569	0.02442	0.01899	13.67108	0.126E-07	0.665E-03143
144	49.17831	1.23152	0.87208	-0.63966E-06	-0.09356	0.03120	0.01667	0.01334	13.63078	0.955E-08	0.716E-03144
145	49.51164	1.17321	0.87374	-0.74150E-06	-0.09900	0.03437	0.01834	0.01526	13.55386	0.105E-07	0.687E-03145
146	49.90303	1.09817	0.87584	-0.79581E-06	-0.11352	0.03181	0.01696	0.01494	13.45685	0.983E-08	0.658E-03146
147	50.14886	1.04779	0.87751	-0.10031E-05	-0.14063	0.03550	0.01891	0.01762	13.37993	0.100E-07	0.569E-03147
148	50.48219	0.97107	0.88041	-0.12847E-05	-0.16783	0.03813	0.02028	0.02010	13.24620	0.108E-07	0.537E-03148
149	50.81552	0.93019	0.88216	-0.77333E-06	-0.10394	0.04061	0.02158	0.02270	13.16559	0.105E-07	0.463E-03149
150	51.37608	0.85541	0.88391	-0.46005E-06	-0.10560	0.02086	0.01107	0.01242	13.08493	0.616E-08	0.496E-03150
151	51.70941	0.81212	0.88609	-0.96354E-06	-0.11761	0.04199	0.02226	0.02671	12.98431	0.116E-07	0.435E-03151

152	52.04387	0.75703	0.88883	-0.12043E-05	-0.17106	0.03898	0.02064	0.02632	12.85797	0.100E-07	0.380E-03152
153	52.47247	0.68379	0.89347	-0.15896E-05	-0.17597	0.04565	0.02411	0.03349	12.64369	0.129E-07	0.386E-03153
154	52.80580	0.64312	0.89716	-0.16216E-05	-0.20716	0.06021	0.03174	0.04785	12.47336	0.112E-07	0.235E-03154
155	53.13913	0.57923	0.90070	-0.15513E-05	-0.18826	0.03380	0.01778	0.02913	12.31015	0.119E-07	0.407E-03155
156	53.47247	0.53174	0.90432	-0.15836E-05	-0.18372	0.04232	0.02222	0.04002	12.14316	0.125E-07	0.311E-03156
157	53.80580	0.48832	0.90789	-0.15580E-05	-0.18544	0.04187	0.02194	0.04306	11.97859	0.122E-07	0.283E-03157
158	54.13913	0.44478	0.91186	-0.17338E-05	-0.16965	0.04260	0.02228	0.04779	11.79510	0.149E-07	0.312E-03158
159	54.47247	0.40633	0.91536	-0.15203E-05	-0.17542	0.03864	0.02018	0.04744	11.63388	0.127E-07	0.267E-03159
160	54.80580	0.38429	0.91909	-0.16209E-05	-0.18757	0.06694	0.03488	0.08827	11.46167	0.127E-07	0.144E-03160
161	55.13913	0.35185	0.92286	-0.16348E-05	-0.17615	0.04277	0.02224	0.06048	11.28764	0.137E-07	0.226E-03161
162	55.47247	0.32502	0.92683	-0.17173E-05	-0.17700	0.05006	0.02598	0.07680	11.10443	0.144E-07	0.187E-03162
163	55.80580	0.30546	0.93088	-0.17481E-05	-0.17643	0.06526	0.03380	0.10726	10.91759	0.147E-07	0.137E-03163
164	56.13913	0.28581	0.93487	-0.17153E-05	-0.17031	0.05988	0.03095	0.10472	10.73386	0.150E-07	0.144E-03164

ENGINEERING STRAIN (164)= 10.7339

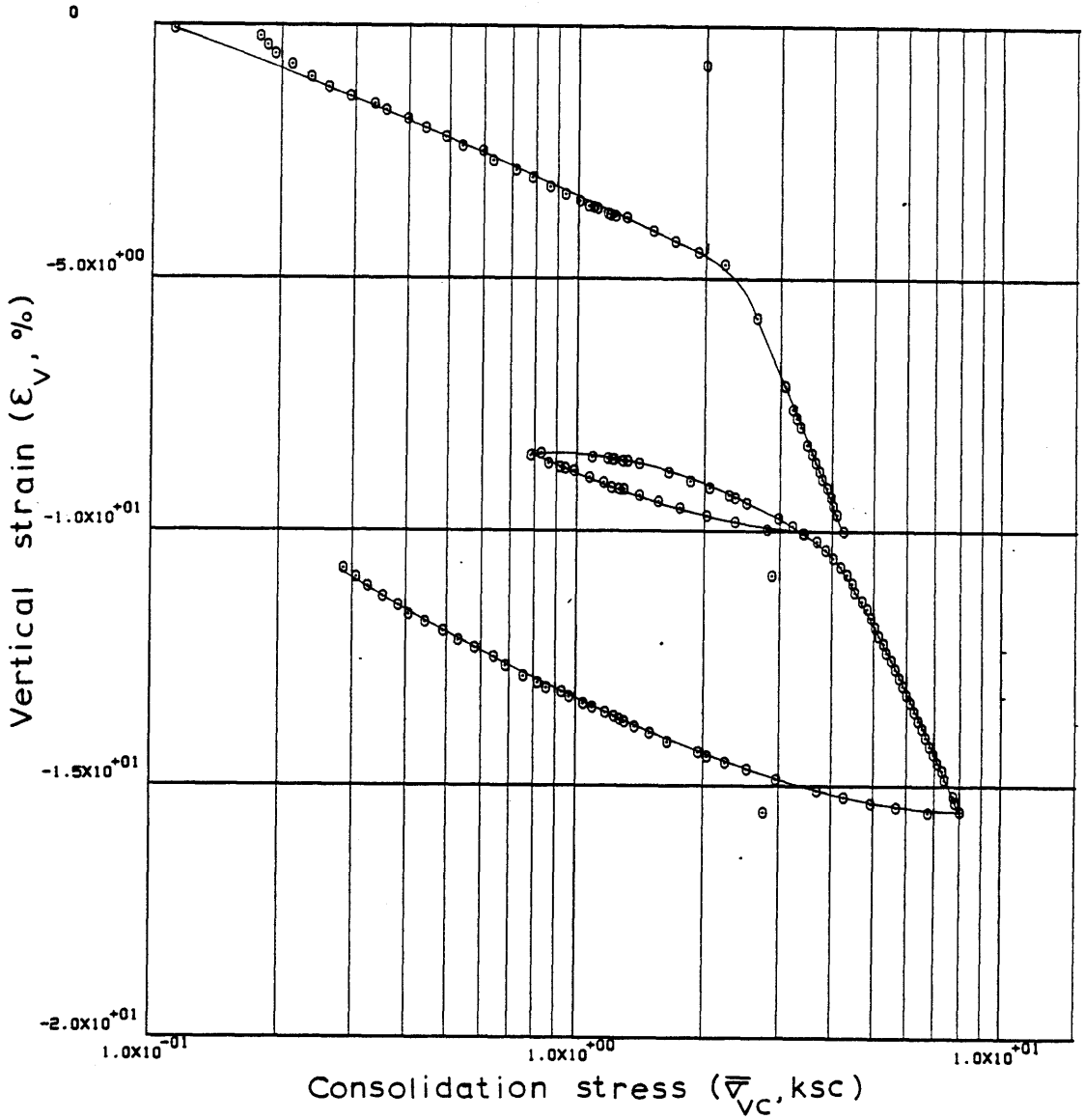

Sample No. 60-62-C-V w_N (%) 43.20 Estimated

Depth 61.47 w_L (%) 38.07 $\bar{\sigma}_{vo}$ 1.42 $\bar{\sigma}_{vm}$ 240-250

Soil Type Boston w_P (%) 21.11 CR 0.2050 RR 0.0250

Blue Clay P.I.(%) 16.96 G_s 2.77 e_o 1.1675

⊙ At t_p Remarks Data from C.R.S.C test

w_L & w_P estimated from Baligh et al (1980)

Figure E.21 Compression Curve for Sample No. 60-62-C-V

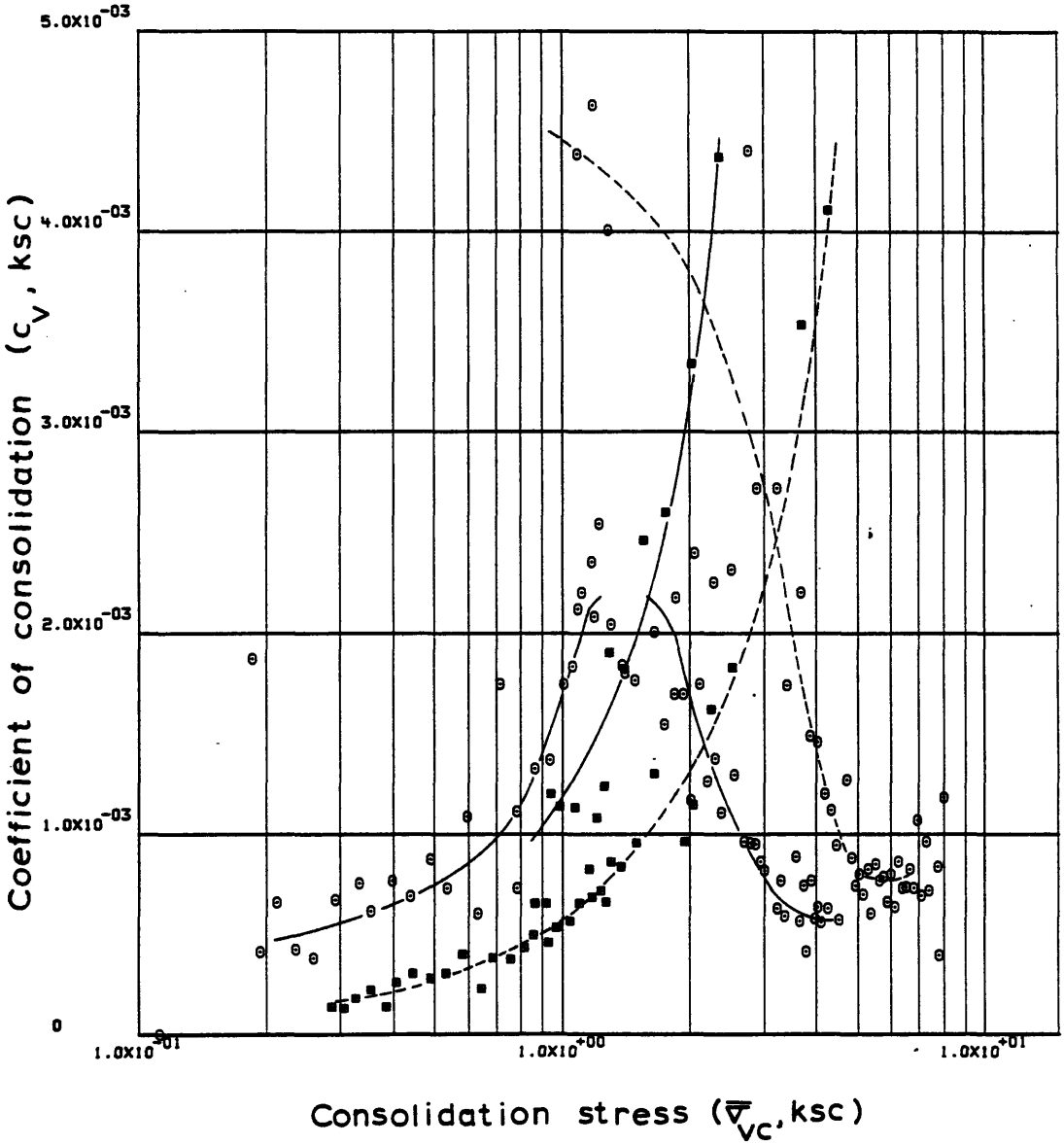

Sample No. 60-62-C-V w_N (%) 43.20 Estimated

Depth 61.47 w_L (%) 38.07 $\bar{\sigma}_{vo}$ 1.42 $\bar{\sigma}_{vm}$ 240-250

Soil Type Boston Blue Clay w_P (%) 21.11 CR 0.2050 RR 0.0250

P.I.(%) 16.96 G_S 2.77 e_o 1.1675

θ At t_p

Remarks Data from C.R.S.C test

w_L & w_P estimated from Baligh et al (1980)

Figure E.22 Variation of coefficient of consolidation with consolidation stress for Sample No. 60-62-C-V

1-D STRAIN CONTROLLED COMPRESSION TEST

COMPUTED RESULTS

INITIAL VOID RATIO= 1.14981
INITIAL HEIGHT= 1.9279

ALL UNITS IN: KG,CM,SEC

LINEAR THEORY

	TIME IN HOURS	VERTICAL STRESS	E	RATE OF STRAIN	EXCESS PORE PRESSURE	C	C/1+E	MV	PERCENT COMPRESSION	K	CV	
1	0.0	0.00137	1.14981	0.0	0.0	0.0	0.0	0.0	0.00002	0.100E+01	0.100E+05	1
2	0.33361	0.15406	1.14685	0.11489E-05	0.01071	0.00063	0.00029	0.00904	0.13783	0.199E-06	0.220E-01	2
3	1.33361	0.28839	1.13564	0.14577E-05	0.01185	0.01787	0.00837	0.03906	0.65912	0.226E-06	0.578E-02	3
4	1.66692	0.38309	1.13196	0.14375E-05	0.05141	0.01295	0.00607	0.01821	0.83018	0.511E-07	0.281E-02	4
5	2.00027	0.30994	1.12840	0.13932E-05	0.03739	-0.01680	-0.00789	-0.02286	0.99571	0.679E-07	-0.297E-02	5
6	2.66692	0.53757	1.12120	0.14161E-05	-0.01103	0.01309	0.00617	0.01493	1.33104	-0.232E-06	-0.155E-01	6
7	3.66692	0.62326	1.10984	0.14951E-05	0.17389	0.07678	0.03639	0.06282	1.85927	0.154E-07	0.245E-03	7
8	4.00027	0.75473	1.10622	0.14308E-05	-0.00488	0.01889	0.00897	0.01306	2.02751	-0.523E-06	-0.400E-01	8
9	4.66692	0.99174	1.09911	0.14110E-05	0.19979	0.02603	0.01240	0.01429	2.35815	0.125E-07	0.876E-03	9
10	5.00027	1.11412	1.09571	0.13555E-05	0.07096	0.02930	0.01398	0.01329	2.51675	0.337E-07	0.254E-02	10
11	5.66692	1.13367	1.08796	0.15466E-05	0.06711	0.44547	0.21335	0.18984	2.87721	0.404E-07	0.213E-03	11
12	6.00027	1.27278	1.08491	0.12169E-05	0.06209	0.02630	0.01261	0.01050	3.01884	0.343E-07	0.326E-02	12
13	6.33359	1.40834	1.08131	0.14406E-05	0.02931	0.03556	0.01709	0.01275	3.18625	0.856E-07	0.671E-02	13
14	6.66692	1.56621	1.07800	0.13299E-05	0.06463	0.03121	0.01502	0.01011	3.34048	0.357E-07	0.353E-02	14
15	7.00027	1.67657	1.07432	0.14792E-05	0.06135	0.05406	0.02606	0.01608	3.51175	0.417E-07	0.259E-02	15
16	7.66692	1.92317	1.06779	0.13141E-05	0.12494	0.04752	0.02298	0.01279	3.81508	0.181E-07	0.141E-02	16
17	7.86999	1.97499	1.06546	0.15470E-05	0.09045	0.08789	0.04255	0.02183	3.92377	0.293E-07	0.134E-02	17
18	8.84914	1.98531	1.05522	0.14131E-05	0.09750	1.96406	0.95564	0.48257	4.39995	0.246E-07	0.510E-04	18
19	9.27082	2.13058	1.05039	0.15513E-05	0.08937	0.06836	0.03334	0.01621	4.62453	0.293E-07	0.181E-02	19
20	9.60416	2.24259	1.04707	0.13535E-05	0.09982	0.06490	0.03171	0.01450	4.77922	0.228E-07	0.158E-02	20
21	9.93749	2.34345	1.04346	0.14689E-05	0.10124	0.08188	0.04007	0.01748	4.94676	0.244E-07	0.139E-02	21
22	10.27082	2.42698	1.03935	0.16822E-05	0.10351	0.11756	0.05765	0.02417	5.13826	0.272E-07	0.112E-02	22
23	10.60416	2.50945	1.03563	0.15231E-05	0.10322	0.11133	0.05469	0.02216	5.31129	0.246E-07	0.111E-02	23
24	10.93749	2.58947	1.03203	0.14772E-05	0.10662	0.11472	0.05646	0.02215	5.47884	0.230E-07	0.104E-02	24
25	11.27082	2.67766	1.02826	0.15451E-05	0.10804	0.11231	0.05537	0.02102	5.65376	0.237E-07	0.113E-02	25
26	11.60416	2.74973	1.02462	0.14989E-05	0.10690	0.13714	0.06773	0.02496	5.82320	0.231E-07	0.926E-03	26
27	11.93749	2.84186	1.02078	0.15833E-05	0.10860	0.11648	0.05764	0.02062	6.00177	0.239E-07	0.116E-02	27
28	12.27082	2.91889	1.01706	0.15373E-05	0.11030	0.13913	0.06898	0.02395	6.17487	0.228E-07	0.952E-03	28
29	14.27082	3.39563	0.99477	0.15523E-05	0.11913	0.14737	0.07388	0.02344	7.21191	0.208E-07	0.889E-03	29
30	14.60416	3.46079	0.99088	0.16285E-05	0.10817	0.20472	0.10283	0.02999	7.39291	0.240E-07	0.800E-03	30
31	14.93749	3.54968	0.98748	0.14230E-05	0.12310	0.13379	0.06732	0.01921	7.55077	0.184E-07	0.956E-03	31
32	15.27082	3.63515	0.98400	0.14634E-05	0.12451	0.14646	0.07382	0.02055	7.71281	0.186E-07	0.905E-03	32
33	15.60416	3.71320	0.98008	0.16494E-05	0.12677	0.18451	0.09319	0.02536	7.89516	0.205E-07	0.809E-03	33
34	15.93749	3.79909	0.97652	0.15023E-05	0.12706	0.15580	0.07883	0.02099	8.06088	0.186E-07	0.885E-03	34
35	16.27081	3.86886	0.97291	0.15217E-05	0.12734	0.19799	0.10036	0.02617	8.22847	0.187E-07	0.715E-03	35
36	16.60416	3.94515	0.96925	0.15517E-05	0.12812	0.18779	0.09536	0.02441	8.39903	0.189E-07	0.774E-03	36
37	16.93748	4.01926	0.96557	0.15607E-05	0.13010	0.19775	0.10061	0.02527	8.57025	0.186E-07	0.737E-03	37
38	17.27081	4.10585	0.96208	0.14795E-05	0.12981	0.16345	0.08331	0.02050	8.73232	0.176E-07	0.860E-03	38
39	17.60416	4.18624	0.95811	0.16917E-05	0.13272	0.20505	0.10472	0.02525	8.91722	0.197E-07	0.778E-03	39
40	17.93748	4.29090	0.95448	0.15454E-05	0.13406	0.14676	0.07509	0.01772	9.08580	0.177E-07	0.999E-03	40
41	18.27081	4.37525	0.95090	0.15296E-05	0.13724	0.18394	0.09429	0.02176	9.25237	0.171E-07	0.784E-03	41

42	18.60416	4.47950	0.94718	0.15927E-05	0.13724	0.15808	0.08118	0.01833	9.42551	0.177E-07	0.965E-03	42
43	18.93748	4.56137	0.94334	0.16468E-05	0.13583	0.21200	0.10909	0.02414	9.60414	0.184E-07	0.763E-03	43
44	19.27081	4.65713	0.93962	0.15985E-05	0.13738	0.17908	0.09232	0.02003	9.77718	0.176E-07	0.879E-03	44
45	19.60416	4.73845	0.93590	0.16013E-05	0.13880	0.21491	0.11101	0.02363	9.95021	0.174E-07	0.736E-03	45
46	19.93748	4.81094	0.93228	0.15609E-05	0.12854	0.23839	0.12337	0.02584	10.11855	0.182E-07	0.706E-03	46
47	20.27081	4.91044	0.92872	0.15387E-05	0.14127	0.17398	0.09020	0.01856	10.28423	0.163E-07	0.878E-03	47
48	20.60416	5.02871	0.92520	0.15243E-05	0.14070	0.14794	0.07684	0.01547	10.44800	0.161E-07	0.104E-02	48
49	20.93748	5.12966	0.92130	0.16888E-05	0.14317	0.19596	0.10199	0.02007	10.62917	0.175E-07	0.872E-03	49
50	21.27081	5.25463	0.91790	0.14783E-05	0.14487	0.14133	0.07369	0.01420	10.78741	0.151E-07	0.106E-02	50
51	21.60416	5.37624	0.91391	0.17397E-05	0.14544	0.17465	0.09125	0.01717	10.97327	0.176E-07	0.103E-02	51
52	21.93748	5.52182	0.91031	0.15705E-05	0.14656	0.13471	0.07052	0.01294	11.14070	0.157E-07	0.121E-02	52
53	22.27081	5.62194	0.90657	0.16312E-05	0.14395	0.20778	0.10898	0.01955	11.31435	0.166E-07	0.847E-03	53
54	22.60416	5.76343	0.90326	0.14492E-05	0.14600	0.13314	0.06995	0.01229	11.46829	0.145E-07	0.118E-02	54
55	22.93748	5.88828	0.89953	0.16367E-05	0.14734	0.17409	0.09165	0.01573	11.64183	0.161E-07	0.102E-02	55
56	23.27081	6.03614	0.89574	0.16692E-05	0.14960	0.15313	0.08077	0.01355	11.81847	0.161E-07	0.119E-02	56
57	23.60416	6.16751	0.89218	0.15678E-05	0.14989	0.16531	0.08736	0.01432	11.98404	0.151E-07	0.105E-02	57
58	23.80777	5.82950	0.89205	0.94509E-07	0.01640	-0.00232	-0.00123	-0.00020	11.99013	0.830E-08	-0.405E-01	58
59	24.14110	4.13713	0.89260	-0.24458E-06	-0.03644	0.00162	0.00086	0.00017	11.96429	0.967E-08	0.557E-01	59
60	24.47443	3.15854	0.89382	-0.53465E-06	-0.04807	0.00450	0.00238	0.00066	11.90776	0.160E-07	0.245E-01	60
61	24.88832	2.74619	0.89002	0.13479E-05	-0.06869	-0.02714	-0.01436	-0.00487	12.08437	-0.282E-07	0.579E-02	61
62	25.45499	1.96911	0.89457	-0.11765E-05	-0.07435	0.01367	0.00722	0.00309	11.87283	0.228E-07	0.739E-02	62
63	25.82166	1.62787	0.89766	-0.12359E-05	-0.07686	0.01627	0.00857	0.00478	11.72884	0.233E-07	0.487E-02	63
64	26.15498	1.40619	0.90087	-0.14043E-05	-0.07572	0.02188	0.01151	0.00760	11.57983	0.269E-07	0.354E-02	64
65	26.82166	1.04436	0.90921	-0.18210E-05	-0.08533	0.02805	0.01469	0.01208	11.19171	0.313E-07	0.259E-02	65
66	27.28831	1.64204	0.90955	-0.10666E-06	0.06694	-0.00076	-0.00040	-0.00030	11.17578	-0.234E-08	0.779E-02	66
67	27.90498	2.47875	0.90441	0.12158E-05	0.08842	0.01248	0.00655	0.00323	11.41487	0.201E-07	0.622E-02	67
68	28.23833	2.87140	0.90135	0.13408E-05	0.09477	0.02081	0.01094	0.00410	11.55717	0.206E-07	0.502E-02	68
69	28.57166	3.33670	0.89769	0.16083E-05	0.09860	0.02438	0.01285	0.00415	11.72755	0.236E-07	0.569E-02	69
70	28.90498	3.80002	0.89492	0.12172E-05	0.09972	0.02129	0.01123	0.00315	11.85626	0.176E-07	0.559E-02	70
71	29.23833	4.26936	0.89295	0.87030E-06	0.10199	0.01698	0.00897	0.00223	11.94823	0.123E-07	0.552E-02	71
72	29.62166	4.76967	0.88959	0.12884E-05	0.11017	0.03033	0.01605	0.00355	12.10454	0.168E-07	0.472E-02	72
73	29.90498	5.17961	0.88726	0.12077E-05	0.11504	0.02819	0.01494	0.00300	12.21268	0.150E-07	0.500E-02	73
74	30.23833	5.53172	0.88405	0.14219E-05	0.11865	0.04888	0.02594	0.00485	12.36221	0.171E-07	0.353E-02	74
75	30.57166	5.85752	0.88088	0.14025E-05	0.12600	0.05531	0.02941	0.00517	12.50943	0.158E-07	0.307E-02	75
76	30.93832	6.10557	0.87737	0.14178E-05	0.12975	0.08471	0.04512	0.00754	12.67288	0.155E-07	0.205E-02	76
77	31.27165	6.28797	0.87538	0.88272E-06	0.12544	0.06749	0.03599	0.00581	12.76529	0.995E-08	0.171E-02	77
78	31.82166	6.79751	0.86850	0.18592E-05	0.13314	0.08828	0.04725	0.00722	13.08525	0.196E-07	0.271E-02	78
79	32.73833	7.30011	0.85881	0.15799E-05	0.14368	0.13586	0.07309	0.01037	13.53606	0.153E-07	0.147E-02	79
80	33.07166	7.35154	0.85428	0.20347E-05	0.14509	0.64488	0.34778	0.04747	13.74664	0.194E-07	0.408E-03	80
81	33.43719	7.38550	0.85534	-0.43258E-06	0.15728	-0.22910	-0.12348	-0.01676	13.69753	-0.381E-08	0.227E-03	81
82	33.87665	7.62294	0.85044	0.16745E-05	0.16124	0.15494	0.08373	0.01116	13.92557	0.143E-07	0.128E-02	82
83	34.14221	7.96733	0.84869	0.98730E-06	0.13906	0.03950	0.02137	0.00274	14.00673	0.976E-08	0.356E-02	83
84	34.47554	8.19465	0.84573	0.13382E-05	0.16363	0.10529	0.05705	0.00706	14.14456	0.112E-07	0.159E-02	84
85	34.80887	8.41741	0.84237	0.15186E-05	0.16597	0.12520	0.06796	0.00818	14.30072	0.125E-07	0.153E-02	85
86	35.14221	8.65536	0.83905	0.15044E-05	0.16851	0.11909	0.06476	0.00759	14.45517	0.121E-07	0.160E-02	86
87	35.47554	8.87419	0.83549	0.16149E-05	0.17028	0.14247	0.07762	0.00886	14.62064	0.128E-07	0.145E-02	87
88	35.80887	9.11052	0.83202	0.15825E-05	0.17170	0.13237	0.07225	0.00804	14.78246	0.124E-07	0.155E-02	88
89	36.14221	9.33145	0.82858	0.15678E-05	0.17460	0.14356	0.07851	0.00852	14.94247	0.121E-07	0.142E-02	89
90	36.47554	9.58569	0.82510	0.15888E-05	0.17544	0.12946	0.07093	0.00750	15.10434	0.121E-07	0.162E-02	90
91	36.80887	9.81120	0.82162	0.15917E-05	0.17827	0.14966	0.08216	0.00847	15.26619	0.119E-07	0.141E-02	91
92	37.14221	10.06227	0.81826	0.15403E-05	0.17771	0.13301	0.07315	0.00736	15.42252	0.115E-07	0.157E-02	92
93	37.47554	10.31453	0.81482	0.15796E-05	0.18562	0.13892	0.07655	0.00751	15.58255	0.113E-07	0.150E-02	93
94	37.80887	10.57666	0.81122	0.16555E-05	0.18901	0.14338	0.07916	0.00758	15.74989	0.116E-07	0.152E-02	94
95	38.14221	10.82575	0.80778	0.15857E-05	0.18731	0.14778	0.08175	0.00764	15.90993	0.111E-07	0.146E-02	95
96	38.47554	11.07716	0.80434	0.15888E-05	0.19495	0.14984	0.08304	0.00758	16.06995	0.107E-07	0.141E-02	96

97	38.80887	11.30300	0.80090	0.15918E-05	0.19523	0.17044	0.09464	0.00846	16.22993	0.106E-07	0.126E-02 97
98	39.14221	11.59344	0.79749	0.15794E-05	0.19729	0.13430	0.07472	0.00653	16.38843	0.104E-07	0.159E-02 98
99	39.47554	11.77965	0.79401	0.16165E-05	0.19955	0.21835	0.12171	0.01042	16.55029	0.105E-07	0.101E-02 99
100	39.80887	8.40059	0.79061	0.15829E-05	0.20408	-0.01006	-0.00562	-0.00056	16.70848	0.100E-07	-0.178E-01100
101	40.14221	12.24178	0.78717	0.16042E-05	0.20718	0.00914	0.00511	0.00050	16.86856	0.994E-08	0.198E-01101
102	40.47554	12.80085	0.78365	0.16444E-05	0.20916	0.07880	0.04418	0.00353	17.03226	0.101E-07	0.285E-02102
103	40.80887	13.14366	0.78025	0.15921E-05	0.21284	0.12868	0.07228	0.00557	17.19044	0.953E-08	0.171E-02103
104	41.14221	13.48489	0.77681	0.16135E-05	0.21481	0.13425	0.07556	0.00567	17.35048	0.953E-08	0.168E-02104
105	41.47554	13.81178	0.77341	0.15982E-05	0.21566	0.14199	0.08007	0.00587	17.50868	0.937E-08	0.160E-02105
106	41.80887	14.14028	0.76997	0.16199E-05	0.21821	0.14639	0.08271	0.00592	17.66876	0.935E-08	0.158E-02106
107	42.47554	14.80995	0.76318	0.16041E-05	0.22517	0.14671	0.08321	0.00575	17.98451	0.891E-08	0.155E-02107
108	42.80887	15.15224	0.75974	0.16299E-05	0.22573	0.15064	0.08560	0.00571	18.14459	0.899E-08	0.157E-02108
109	43.14221	15.50421	0.75629	0.16331E-05	0.23026	0.14993	0.08537	0.00557	18.30472	0.880E-08	0.158E-02109
110	43.67249	16.11548	0.75084	0.16334E-05	0.23648	0.14115	0.08062	0.00510	18.55864	0.851E-08	0.167E-02110
111	44.03665	13.86182	0.75084	-0.24324E-08	-0.01671	0.00003	0.00002	0.00000	18.55840	0.179E-09	0.100E+05111
112	44.36998	11.42994	0.75151	-0.31978E-06	-0.05937	0.00349	0.00199	0.00016	18.52713	0.664E-08	0.421E-01112
113	44.70332	9.51247	0.75266	-0.54510E-06	-0.08254	0.00624	0.00356	0.00034	18.47380	0.816E-08	0.239E-01113
114	45.03665	7.97452	0.75441	-0.83154E-06	-0.09548	0.00992	0.00566	0.00065	18.39238	0.108E-07	0.166E-01114
115	45.36998	6.71033	0.75663	-0.10519E-05	-0.10687	0.01285	0.00732	0.00100	18.28923	0.122E-07	0.122E-01115
116	45.70332	5.66472	0.75881	-0.10366E-05	-0.12131	0.01292	0.00734	0.00119	18.18744	0.106E-07	0.893E-02116
117	46.03665	4.82420	0.76092	-0.99760E-06	-0.13065	0.01313	0.00746	0.00142	18.08939	0.952E-08	0.668E-02117
118	46.36998	4.14194	0.76341	-0.11765E-05	-0.13206	0.01632	0.00926	0.00207	17.97359	0.111E-07	0.538E-02118
119	46.70332	3.55904	0.76578	-0.11190E-05	-0.14082	0.01564	0.00886	0.00230	17.86327	0.996E-08	0.432E-02119
120	47.03665	3.06568	0.76836	-0.12161E-05	-0.14395	0.01729	0.00978	0.00296	17.74326	0.106E-07	0.359E-02120
121	47.36998	2.64873	0.77109	-0.12828E-05	-0.14480	0.01865	0.01053	0.00369	17.61642	0.112E-07	0.303E-02121
122	47.70332	2.32449	0.77405	-0.13920E-05	-0.14507	0.02269	0.01279	0.00515	17.47861	0.121E-07	0.236E-02122
123	48.03665	2.04547	0.77725	-0.15006E-05	-0.14592	0.02503	0.01408	0.00645	17.32976	0.131E-07	0.202E-02123
124	48.36998	1.82089	0.78043	-0.14840E-05	-0.14312	0.02727	0.01531	0.00793	17.18225	0.132E-07	0.167E-02124
125	48.70332	1.61475	0.78377	-0.15644E-05	-0.14000	0.02787	0.01562	0.00911	17.02646	0.143E-07	0.157E-02125
126	49.01721	1.45065	0.78655	-0.13742E-05	-0.14002	0.02589	0.01449	0.00946	16.89745	0.126E-07	0.133E-02126
127	49.57582	1.21742	0.79217	-0.15606E-05	-0.13809	0.03209	0.01791	0.01346	16.63582	0.146E-07	0.108E-02127
128	50.03775	1.04432	0.79715	-0.16649E-05	-0.14316	0.03244	0.01805	0.01599	16.40436	0.151E-07	0.944E-03128
129	50.35081	0.95152	0.80043	-0.16152E-05	-0.14147	0.03522	0.01956	0.01962	16.25189	0.149E-07	0.759E-03129
130	50.68414	0.85575	0.80398	-0.16418E-05	-0.14147	0.03351	0.01857	0.02057	16.08658	0.152E-07	0.738E-03130
131	50.96860	0.79112	0.80718	-0.17284E-05	-0.13893	0.04073	0.02254	0.02739	15.93777	0.163E-07	0.597E-03131
132	51.31471	0.71574	0.81097	-0.16801E-05	-0.13668	0.03787	0.02091	0.02777	15.76141	0.162E-07	0.584E-03132
133	51.64832	0.65927	0.81476	-0.17394E-05	-0.13611	0.04612	0.02541	0.03699	15.58511	0.169E-07	0.457E-03133
134	51.97470	0.60504	0.81832	-0.16648E-05	-0.14206	0.04144	0.02279	0.03607	15.41965	0.156E-07	0.432E-03134
135	52.33748	0.55215	0.82233	-0.16870E-05	-0.13939	0.04389	0.02409	0.04166	15.23291	0.162E-07	0.388E-03135
136	52.67081	0.51235	0.82605	-0.16962E-05	-0.13828	0.04968	0.02721	0.05114	15.06001	0.164E-07	0.322E-03136
137	53.00415	0.47362	0.82976	-0.16921E-05	-0.13463	0.04726	0.02583	0.05242	14.88718	0.169E-07	0.323E-03137
138	53.33748	0.43657	0.83344	-0.16701E-05	-0.13039	0.04511	0.02461	0.05410	14.71626	0.173E-07	0.320E-03138
139	53.67081	0.41609	0.83719	-0.17026E-05	-0.12842	0.07809	0.04251	0.09975	14.54169	0.180E-07	0.180E-03139
140	53.93137	0.39268	0.84019	-0.17396E-05	-0.12616	0.05187	0.02819	0.06971	14.40199	0.188E-07	0.269E-03140

ENGINEERING STRAIN (140)= 14.4020

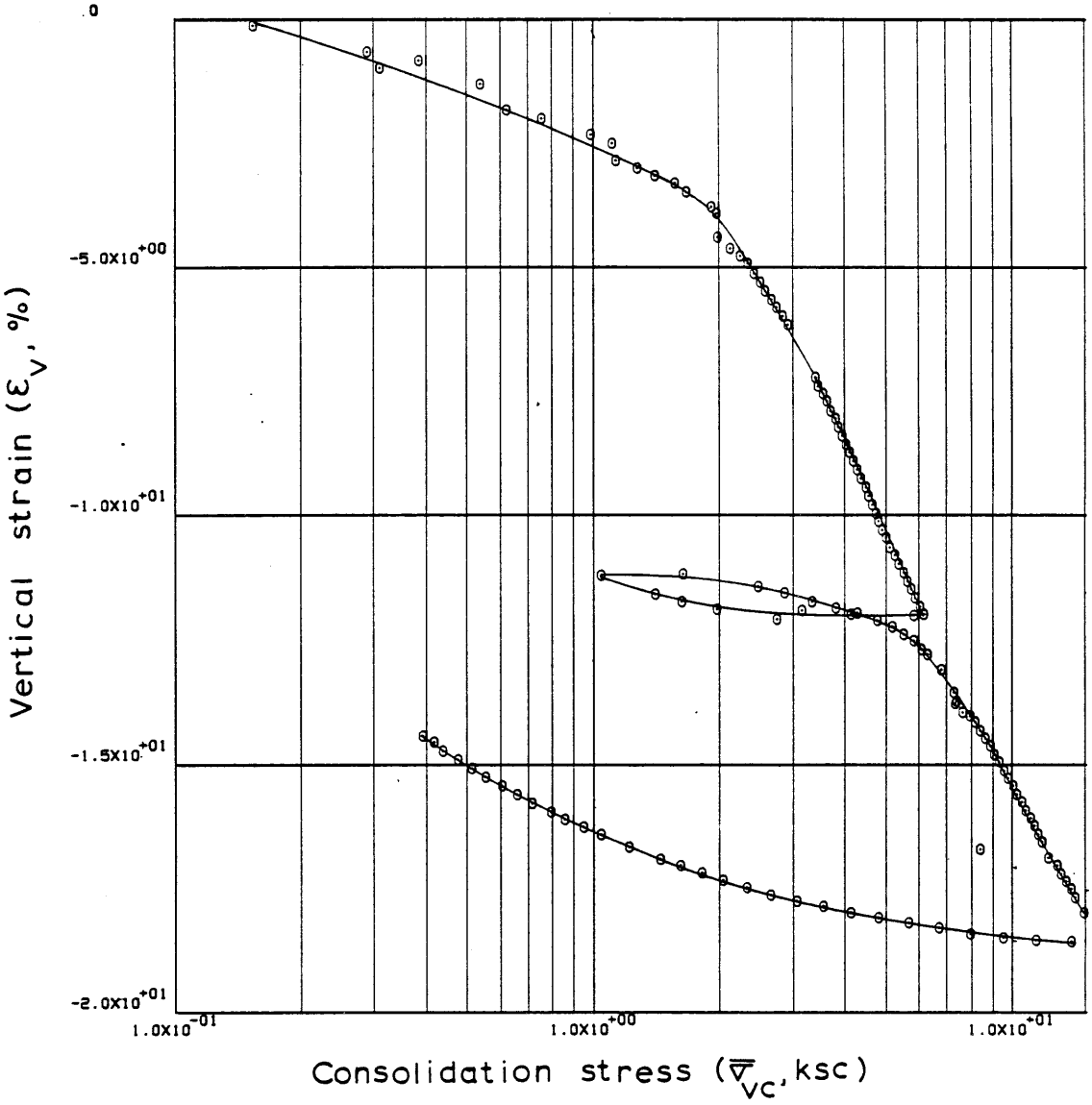

Sample No. 60-62-C-H w_N (%) 40.18 Estimated

Depth 61.65 w_L (%) 37.89 $\bar{\sigma}_{vo}$ 1.42 $\bar{\sigma}_{vm}$ 200-210

Soil Type Boston w_P (%) 20.96 CR 0.1987 RR 0.0122

Blue Clay P.I.(%) 16.93 G_S 2.77 e_o 1.1498

o At t_p Remarks Data from C.R.S.C test

w_L & w_P estimated from Baligh et al (1980)

Figure E.23 Compression Curve for Sample No. 60-62-C-H

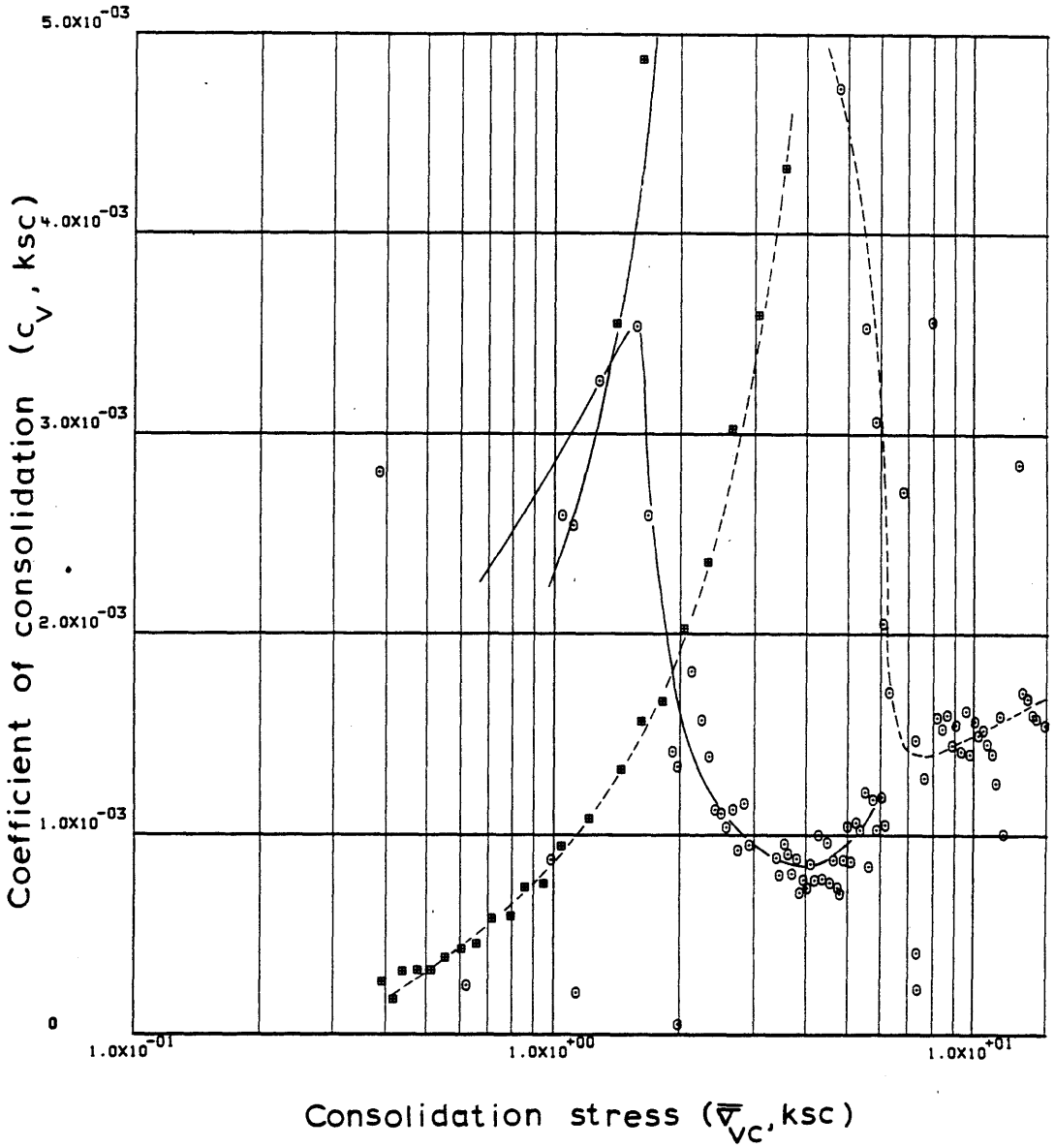

Sample No. 60.62.C.H w_N (%) 40.18 Estimated

Depth 61.65 w_L (%) 37.89 $\bar{\sigma}_{vo}$ 1.42 $\bar{\sigma}_{vm}$ 200.210

Soil Type Boston w_P (%) 20.96 CR 0.1987 RR 0.0122

Blue Clay P.I.(%) 16.93 G_s 2.77 e_o 1.1498

⊙ At t_p Remarks Data from C.R.S.C test

w_L & w_P estimated from Baligh et al (1980)

Figure E.24 Variation of coefficient of consolidation with consolidation stress for Sample No. 60-62-C-H

1-D STRAIN CONTROLLED COMPRESSION TEST

COMPUTED RESULTS

INITIAL VOID RATIO= 1.10876
INITIAL HEIGHT= 2.3368

ALL UNITS IN: KG,CM,SEC

LINEAR THEORY

	TIME IN HOURS	VERTICAL STRESS	E	RATE OF STRAIN	EXCESS PORE PRESSURE	C	C/1+E	MV	PERCENT COMPRESSION	K	CV	
1	0.0	0.40023	1.10628	0.0	0.03041	0.0	0.0	0.00294	0.11754	0.0	0.0	1
2	0.34167	0.45548	1.10537	0.35027E-06	0.04232	0.00701	0.00333	0.00780	0.16057	0.225E-07	0.289E-02	2
3	0.67500	0.47742	1.10421	0.46251E-06	0.07338	0.02481	0.01179	0.02530	0.21594	0.171E-07	0.677E-03	3
4	1.00833	0.48327	1.10134	0.11361E-05	0.07451	0.23520	0.11193	0.23301	0.35176	0.413E-07	0.177E-03	4
5	1.34167	0.51086	1.09731	0.16036E-05	0.08130	0.07268	0.03466	0.06974	0.54317	0.533E-07	0.764E-03	5
6	1.67500	0.53426	1.09316	0.16502E-05	0.08412	0.09257	0.04422	0.08465	0.73972	0.528E-07	0.623E-03	6
7	2.00833	0.57629	1.08918	0.15857E-05	0.08412	0.05250	0.02513	0.04528	0.92827	0.505E-07	0.112E-02	7
8	2.34167	0.59152	1.08500	0.16747E-05	0.09651	0.16056	0.07701	0.13190	1.12694	0.463E-07	0.351E-03	8
9	2.67500	0.61841	1.08087	0.16520E-05	0.10158	0.09279	0.04459	0.07372	1.32257	0.432E-07	0.587E-03	9
10	3.00833	0.63993	1.07695	0.15728E-05	0.10722	0.11463	0.05519	0.08772	1.50847	0.389E-07	0.443E-03	10
11	3.34167	0.67437	1.07276	0.16827E-05	0.10891	0.07982	0.03851	0.05862	1.70694	0.408E-07	0.695E-03	11
12	3.67500	0.68556	1.06872	0.16312E-05	0.11738	0.24618	0.11900	0.17501	1.89896	0.365E-07	0.209E-03	12
13	4.00833	0.72056	1.06492	0.15328E-05	0.12075	0.07626	0.03693	0.05255	2.07906	0.332E-07	0.632E-03	13
14	4.34167	0.75793	1.06078	0.16715E-05	0.12302	0.08176	0.03968	0.05367	2.27507	0.354E-07	0.660E-03	14
15	4.67500	0.78510	1.05670	0.16537E-05	0.12020	0.11591	0.05636	0.07305	2.46864	0.357E-07	0.489E-03	15
16	5.00833	0.81515	1.05396	0.11117E-05	0.12415	0.07294	0.03551	0.04439	2.59859	0.232E-07	0.522E-03	16
17	5.34167	0.82533	1.05058	0.13753E-05	0.11176	0.27265	0.13296	0.16213	2.75905	0.318E-07	0.196E-03	17
18	5.67500	0.85523	1.04687	0.15090E-05	0.11741	0.10418	0.05090	0.06057	2.93481	0.331E-07	0.546E-03	18
19	6.00833	0.86165	1.04291	0.16174E-05	0.12023	0.52945	0.25917	0.30193	3.12283	0.345E-07	0.114E-03	19
20	6.67499	0.90453	1.03481	0.16583E-05	0.11400	0.16676	0.08195	0.09282	3.50687	0.370E-07	0.398E-03	20
21	7.00832	0.96244	1.03062	0.17174E-05	0.11851	0.06745	0.03322	0.03559	3.70534	0.367E-07	0.103E-02	21
22	7.34166	0.97915	1.02646	0.17129E-05	0.12639	0.24201	0.11942	0.12304	3.90286	0.342E-07	0.270E-03	22
23	7.67499	1.04745	1.02232	0.17055E-05	0.12812	0.06138	0.03035	0.02997	4.09912	0.334E-07	0.112E-02	23
24	8.00832	1.06771	1.01808	0.17499E-05	0.13035	0.22108	0.10955	0.10360	4.30008	0.336E-07	0.324E-03	24
25	8.34166	1.10020	1.01401	0.16834E-05	0.13487	0.13577	0.06741	0.06218	4.49303	0.311E-07	0.500E-03	25
26	8.67499	1.14127	1.00984	0.17293E-05	0.13937	0.11380	0.05662	0.05053	4.69080	0.308E-07	0.609E-03	26
27	9.00832	1.18458	1.00566	0.17364E-05	0.14275	0.11219	0.05593	0.04810	4.88898	0.300E-07	0.625E-03	27
28	9.34166	1.21845	1.00145	0.17554E-05	0.14275	0.14957	0.07473	0.06220	5.08891	0.302E-07	0.486E-03	28
29	10.00832	1.25290	0.99525	0.12948E-05	0.13485	0.22240	0.11147	0.09022	5.38292	0.235E-07	0.260E-03	29
30	10.34166	1.28745	0.99153	0.15535E-05	0.12866	0.13649	0.06854	0.05395	5.55902	0.294E-07	0.545E-03	30
31	10.67499	1.32469	0.98773	0.15953E-05	0.13094	0.13346	0.06714	0.05141	5.73944	0.296E-07	0.575E-03	31
32	11.00832	1.38886	0.98378	0.16606E-05	0.12078	0.08354	0.04211	0.03105	5.92688	0.332E-07	0.107E-02	32
33	11.34166	1.41383	0.97968	0.17219E-05	0.11909	0.22960	0.11598	0.08275	6.12086	0.348E-07	0.420E-03	33
34	11.67499	1.45559	0.97548	0.17730E-05	0.12694	0.14438	0.07309	0.05094	6.32018	0.335E-07	0.657E-03	34
35	12.00832	1.52061	0.97140	0.17274E-05	0.13600	0.09352	0.04744	0.03188	6.51395	0.303E-07	0.951E-03	35
36	12.34166	1.57480	0.96726	0.17523E-05	0.14615	0.11815	0.06006	0.03881	6.71013	0.285E-07	0.734E-03	36
37	12.67499	1.61101	0.96283	0.18610E-05	0.13710	0.19278	0.09821	0.06166	6.91798	0.321E-07	0.521E-03	37
38	13.00832	1.65619	0.95893	0.16773E-05	0.14557	0.14256	0.07278	0.04456	7.10498	0.271E-07	0.609E-03	38
39	13.34166	1.70619	0.95485	0.17418E-05	0.15176	0.13740	0.07029	0.04181	7.29875	0.269E-07	0.644E-03	39
40	14.00832	1.77127	0.94575	0.19489E-05	0.14499	0.24309	0.12493	0.07186	7.73033	0.312E-07	0.435E-03	40
41	14.34166	1.83874	0.94162	0.17717E-05	0.15297	0.11042	0.05687	0.03151	7.92607	0.268E-07	0.851E-03	41

42	14.67499	1.90671	0.93745	0.17930E-05	0.16247	0.11484	0.05928	0.03166	8.12375	0.254E-07	0.803E-03	42
43	15.00833	1.95435	0.93389	0.15338E-05	0.15234	0.14426	0.07460	0.03864	8.29254	0.231E-07	0.598E-03	43
44	15.34166	2.01313	0.93074	0.13608E-05	0.15065	0.10638	0.05510	0.02778	8.44208	0.207E-07	0.744E-03	44
45	15.67499	2.09091	0.92699	0.16214E-05	0.15575	0.09890	0.05133	0.02502	8.61986	0.237E-07	0.949E-03	45
46	16.00832	2.11748	0.92294	0.17549E-05	0.15124	0.32067	0.16676	0.07925	8.81187	0.263E-07	0.332E-03	46
47	16.34166	2.20784	0.91883	0.17821E-05	0.15238	0.09820	0.05118	0.02367	9.00645	0.264E-07	0.112E-02	47
48	16.67499	2.27755	0.91468	0.18073E-05	0.15913	0.13357	0.06976	0.03111	9.20337	0.256E-07	0.822E-03	48
49	17.00832	2.34937	0.91038	0.18768E-05	0.16309	0.13861	0.07255	0.03136	9.40742	0.258E-07	0.822E-03	49
50	17.34166	2.42834	0.90623	0.18143E-05	0.16364	0.12551	0.06584	0.02757	9.60422	0.247E-07	0.897E-03	50
51	17.67499	2.49406	0.90219	0.17681E-05	0.16646	0.15117	0.07947	0.03228	9.79562	0.236E-07	0.731E-03	51
52	18.00832	2.56880	0.89821	0.17492E-05	0.17097	0.13495	0.07109	0.02809	9.98457	0.226E-07	0.806E-03	52
53	18.34166	2.65987	0.89431	0.17143E-05	0.17380	0.11185	0.05904	0.02259	10.16937	0.217E-07	0.962E-03	53
54	18.67499	2.75071	0.89036	0.17406E-05	0.18450	0.11757	0.06220	0.02299	10.35661	0.207E-07	0.900E-03	54
55	19.00832	2.82420	0.88622	0.18292E-05	0.19352	0.15706	0.08327	0.02987	10.55295	0.206E-07	0.691E-03	55
56	19.34166	2.92039	0.88235	0.17153E-05	0.18618	0.11567	0.06145	0.02140	10.73668	0.200E-07	0.937E-03	56
57	19.67499	2.99673	0.87838	0.17615E-05	0.19579	0.15384	0.08190	0.02769	10.92494	0.195E-07	0.704E-03	57
58	20.00832	3.10115	0.87434	0.17959E-05	0.19634	0.11796	0.06293	0.02064	11.11652	0.197E-07	0.956E-03	58
59	20.34166	3.19281	0.87071	0.16181E-05	0.20085	0.12470	0.06666	0.02118	11.28877	0.173E-07	0.817E-03	59
60	20.67499	3.27820	0.86761	0.13833E-05	0.19468	0.11747	0.06290	0.01944	11.43578	0.152E-07	0.783E-03	60
61	21.00832	3.38218	0.86393	0.16426E-05	0.18566	0.11765	0.06312	0.01896	11.61000	0.189E-07	0.996E-03	61
62	21.34166	3.45372	0.86032	0.16197E-05	0.17210	0.17277	0.09287	0.02717	11.78149	0.200E-07	0.736E-03	62
63	21.67499	3.56279	0.85649	0.17189E-05	0.17834	0.12316	0.06634	0.01891	11.96306	0.204E-07	0.108E-02	63
64	22.00832	3.67919	0.85244	0.18186E-05	0.18116	0.12575	0.06788	0.01875	12.15475	0.212E-07	0.113E-02	64
65	22.34166	3.76777	0.84861	0.17293E-05	0.18509	0.16128	0.08724	0.02343	12.33669	0.196E-07	0.837E-03	65
66	22.67499	3.86418	0.84479	0.17236E-05	0.18734	0.15098	0.08184	0.02145	12.51759	0.192E-07	0.896E-03	66
67	23.00832	3.99664	0.84076	0.18264E-05	0.20430	0.11969	0.06502	0.01654	12.70892	0.186E-07	0.112E-02	67
68	23.34166	4.11511	0.83692	0.17425E-05	0.19639	0.13151	0.07159	0.01765	12.89107	0.184E-07	0.104E-02	68
69	23.67499	4.27062	0.83291	0.18242E-05	0.20661	0.10816	0.05901	0.01408	13.08133	0.182E-07	0.129E-02	69
70	24.00832	4.37387	0.82922	0.16802E-05	0.20400	0.15441	0.08442	0.01953	13.25624	0.169E-07	0.867E-03	70
71	24.34166	4.50342	0.82535	0.17660E-05	0.21257	0.13252	0.07260	0.01636	13.43968	0.170E-07	0.104E-02	71
72	24.67499	4.62661	0.82159	0.17219E-05	0.21034	0.13945	0.07655	0.01677	13.61815	0.167E-07	0.994E-03	72
73	25.00832	4.75074	0.81768	0.17908E-05	0.21936	0.14754	0.08117	0.01731	13.80339	0.166E-07	0.957E-03	73
74	25.34166	4.93626	0.81438	0.15166E-05	0.23518	0.08621	0.04752	0.00981	13.95999	0.130E-07	0.133E-02	74
75	25.67499	5.08911	0.81130	0.14163E-05	0.22901	0.10095	0.05573	0.01112	14.10597	0.125E-07	0.112E-02	75
76	26.00832	5.24385	0.80771	0.16562E-05	0.21999	0.11994	0.06635	0.01284	14.27635	0.151E-07	0.118E-02	76
77	26.34166	5.39051	0.80379	0.18108E-05	0.22054	0.14210	0.07878	0.01482	14.46222	0.164E-07	0.111E-02	77
78	26.67499	5.54265	0.80039	0.15716E-05	0.22051	0.12199	0.06776	0.01240	14.62321	0.142E-07	0.114E-02	78
79	27.00832	5.71584	0.79674	0.16940E-05	0.22441	0.11871	0.06607	0.01174	14.79642	0.150E-07	0.127E-02	79
80	27.34166	5.85520	0.79284	0.18129E-05	0.22826	0.16193	0.09032	0.01561	14.98137	0.157E-07	0.100E-02	80
81	27.67499	6.04807	0.78934	0.16287E-05	0.24059	0.10791	0.06031	0.01013	15.14723	0.133E-07	0.131E-02	81
82	28.00832	6.21211	0.78516	0.19523E-05	0.25062	0.15627	0.08754	0.01428	15.34554	0.152E-07	0.107E-02	82
83	28.34166	6.41722	0.78150	0.17114E-05	0.25722	0.11265	0.06323	0.01001	15.51906	0.130E-07	0.129E-02	83
84	28.67499	6.59390	0.77763	0.18152E-05	0.26328	0.14256	0.08020	0.01233	15.70267	0.134E-07	0.109E-02	84
85	29.00832	6.77123	0.77400	0.17026E-05	0.27106	0.13656	0.07698	0.01152	15.87451	0.121E-07	0.105E-02	85
86	29.34166	6.98545	0.76999	0.18881E-05	0.27153	0.12875	0.07274	0.01058	16.06470	0.134E-07	0.126E-02	86
87	29.67499	7.18564	0.76640	0.16970E-05	0.28052	0.12731	0.07208	0.01017	16.23529	0.116E-07	0.114E-02	87
88	30.00832	7.41148	0.76242	0.18816E-05	0.27446	0.12860	0.07297	0.01000	16.42400	0.131E-07	0.131E-02	88
89	30.34166	7.61586	0.75856	0.18268E-05	0.27165	0.14171	0.08058	0.01073	16.60680	0.128E-07	0.119E-02	89
90	30.67499	7.84599	0.75481	0.17805E-05	0.28803	0.12596	0.07178	0.00928	16.78461	0.117E-07	0.126E-02	90
91	31.00832	8.10155	0.75093	0.18478E-05	0.29650	0.12113	0.06918	0.00868	16.96870	0.117E-07	0.135E-02	91
92	31.34166	8.34079	0.74772	0.15316E-05	0.29878	0.11037	0.06315	0.00768	17.12105	0.961E-08	0.125E-02	92
93	31.67499	8.62218	0.74453	0.15212E-05	0.30106	0.09597	0.05501	0.00649	17.27205	0.944E-08	0.146E-02	93
94	32.00832	8.89987	0.74099	0.16968E-05	0.29938	0.11183	0.06423	0.00733	17.44016	0.105E-07	0.144E-02	94
95	32.34166	9.15806	0.73733	0.17551E-05	0.28923	0.12795	0.07365	0.00816	17.61369	0.112E-07	0.138E-02	95
96	32.67499	9.41387	0.73373	0.17298E-05	0.28974	0.13065	0.07535	0.00811	17.78435	0.110E-07	0.136E-02	96

97	33.00832	9.68221	0.73009	0.17525E-05	0.29244	0.12945	0.07482	0.00784	17.95686	0.110E-07	0.141E-02 97
98	33.34166	9.97682	0.72630	0.18296E-05	0.30022	0.12644	0.07324	0.00745	18.13660	0.112E-07	0.150E-02 98
99	33.67499	10.27238	0.72259	0.17942E-05	0.30801	0.12704	0.07375	0.00728	18.31250	0.106E-07	0.146E-02 99
100	34.00832	10.56317	0.71864	0.19182E-05	0.31186	0.14175	0.08248	0.00792	18.50011	0.112E-07	0.141E-02100
101	34.34166	10.89160	0.71483	0.18486E-05	0.32755	0.12422	0.07244	0.00675	18.68050	0.102E-07	0.151E-02101
102	34.67499	11.24096	0.71130	0.17231E-05	0.33939	0.11207	0.06549	0.00592	18.84827	0.913E-08	0.154E-02102
103	49.08333	10.42292	0.69848	0.14542E-06	-0.09313	-0.16956	-0.09983	-0.00922	19.45581	-0.277E-08	0.300E-03103
104	49.41666	8.65228	0.70000	-0.74345E-06	-0.13595	0.00814	0.00479	0.00050	19.38391	0.970E-08	0.193E-01104
105	49.74998	7.36850	0.70233	-0.11406E-05	-0.15231	0.01450	0.00852	0.00107	19.27344	0.133E-07	0.125E-01105
106	50.08333	6.32602	0.70455	-0.10860E-05	-0.15175	0.01457	0.00855	0.00125	19.16806	0.128E-07	0.102E-01106
107	50.41666	5.47790	0.70774	-0.15582E-05	-0.16694	0.02218	0.01299	0.00220	19.01665	0.167E-07	0.758E-02107
108	50.74998	4.72453	0.71113	-0.16496E-05	-0.18506	0.02290	0.01338	0.00263	18.85602	0.160E-07	0.610E-02108
109	51.08333	4.16973	0.71454	-0.16592E-05	-0.19739	0.02732	0.01594	0.00359	18.69417	0.152E-07	0.423E-02109
110	51.41666	3.65703	0.71783	-0.15927E-05	-0.20983	0.02503	0.01457	0.00373	18.53847	0.138E-07	0.369E-02110
111	51.74998	3.20746	0.72113	-0.15971E-05	-0.21835	0.02515	0.01461	0.00426	18.38203	0.133E-07	0.312E-02111
112	52.08333	2.85015	0.72463	-0.16908E-05	-0.21105	0.02963	0.01718	0.00568	18.21609	0.146E-07	0.258E-02112
113	52.41666	2.53397	0.72851	-0.18707E-05	-0.20709	0.03300	0.01909	0.00710	18.03209	0.166E-07	0.233E-02113
114	52.74998	2.22976	0.73165	-0.15114E-05	-0.22615	0.02456	0.01418	0.00596	17.88316	0.123E-07	0.206E-02114
115	53.08333	1.98502	0.73554	-0.18691E-05	-0.24350	0.03348	0.01929	0.00916	17.69858	0.142E-07	0.155E-02115
116	53.41666	1.74763	0.73897	-0.16454E-05	-0.24677	0.02698	0.01551	0.00832	17.53574	0.124E-07	0.149E-02116
117	53.74998	1.54304	0.74220	-0.15453E-05	-0.22810	0.02593	0.01488	0.00906	17.38254	0.126E-07	0.139E-02117
118	54.08333	1.41325	0.74462	-0.11558E-05	-0.17007	0.02755	0.01579	0.01069	17.26778	0.127E-07	0.119E-02118
119	54.41666	1.29291	0.74822	-0.17161E-05	-0.21959	0.04044	0.02313	0.01711	17.09706	0.147E-07	0.857E-03119
120	54.74998	1.18256	0.75139	-0.15067E-05	-0.21340	0.03550	0.02027	0.01638	16.94687	0.133E-07	0.812E-03120
121	55.08331	1.06274	0.75501	-0.17185E-05	-0.21065	0.03388	0.01930	0.01721	16.77527	0.154E-07	0.896E-03121
122	55.41666	0.97742	0.75815	-0.14892E-05	-0.19665	0.03755	0.02136	0.02095	16.62627	0.144E-07	0.686E-03122
123	55.74998	0.91056	0.76136	-0.15204E-05	-0.18712	0.04534	0.02574	0.02729	16.47388	0.155E-07	0.567E-03123

ENGINEERING STRAIN (123)= 16.4739

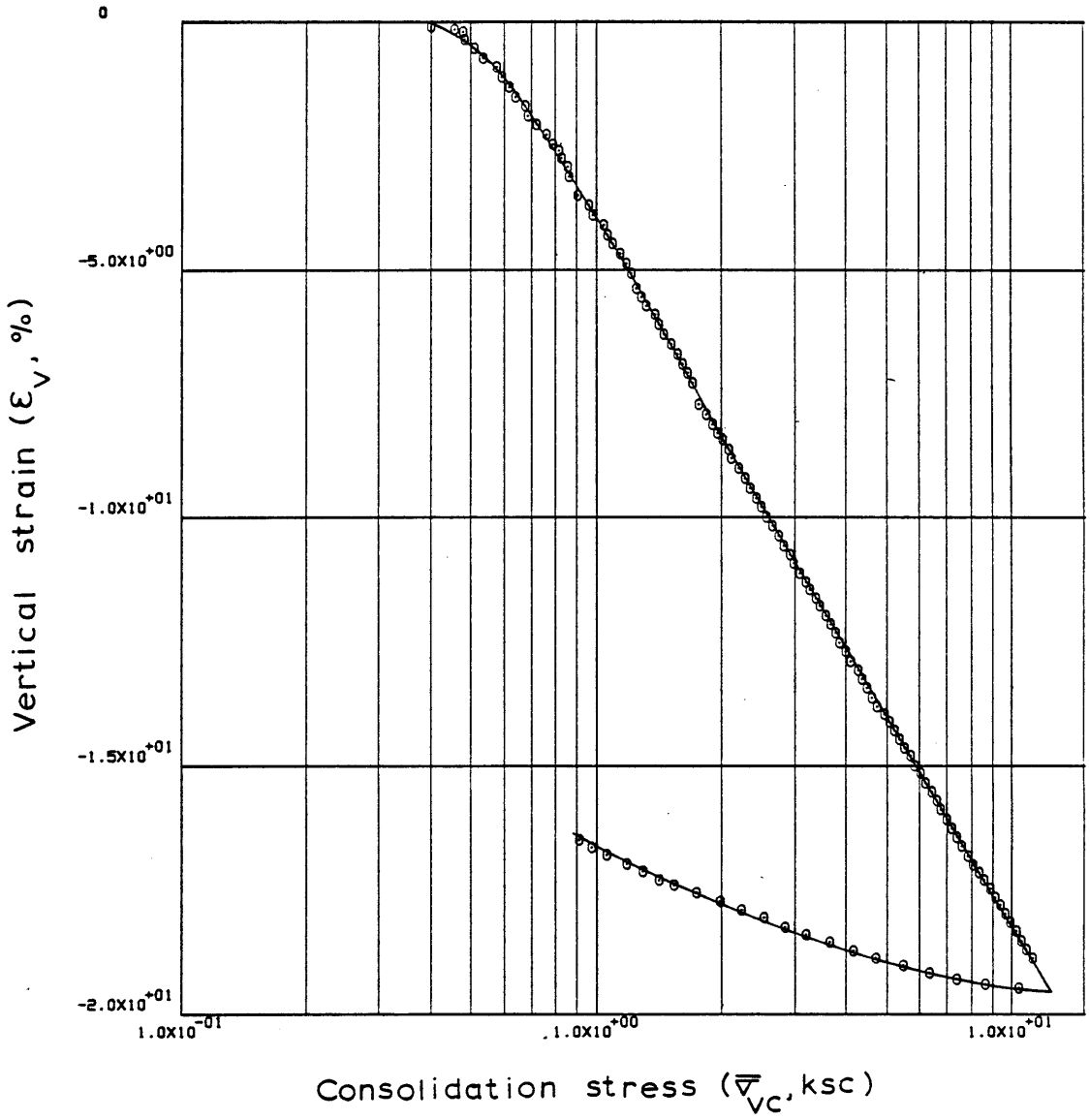

Sample No. SP07VERT w_N (%) 41.61 Estimated

Depth 62.31 w_L (%) 37.23 $\bar{\sigma}_{vo}$ 1.44 $\bar{\sigma}_{vm}$ -

Soil Type Boston Blue Clay w_P (%) 20.37 CR 0.1400 RR 0.0268

P.I.(%) 16.86 G_s 2.77 e_o 1.1080

⊙ At t_p

Remarks Data from C.R.S.C test

w_L & w_P estimated from Baligh et al (1980)

Figure E.25 Compression Curve for Sample No. SP07VERT

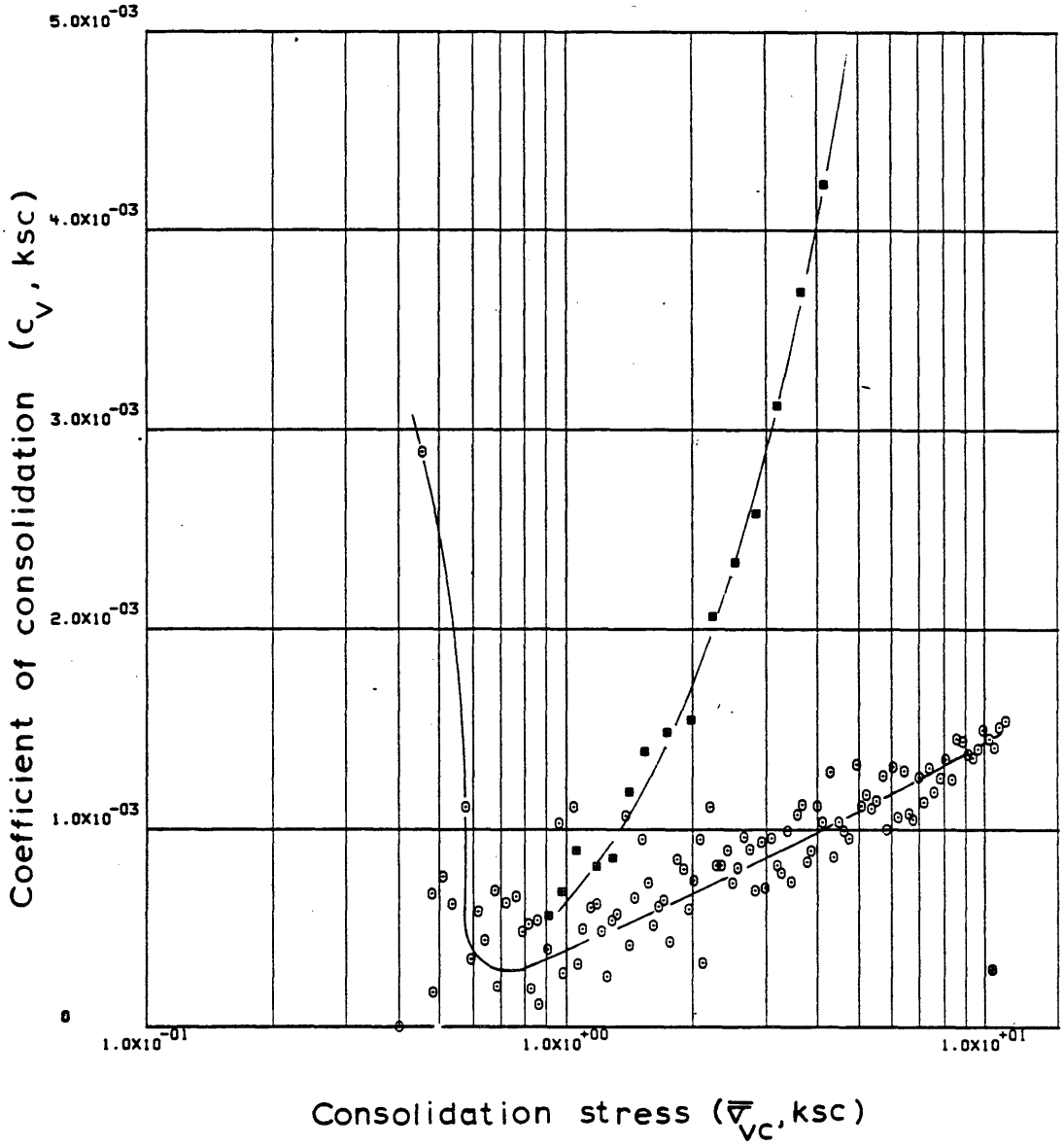

Sample No. SP07VERT w_N (%) 41.61 Estimated

Depth 62.31 w_L (%) 37.23 $\bar{\sigma}_{vo}$ 1.44 $\bar{\sigma}_{vm}$ -

Soil Type Boston w_P (%) 20.37 CR 0.1400 RR 0.0268

Blue Clay P.I.(%) 16.86 G_S 2.77 e_o 1.1080

⊙ At t_p Remarks Data from C.R.S.C test

w_L & w_P estimated from Baligh et al (1980)

Figure E.26 Variation of coefficient of consolidation With consolidation stress for Sample No. SP07VERT

1-D STRAIN CONTROLLED COMPRESSION TEST

COMPUTED RESULTS

INITIAL VOID RATIO= 1.41879
INITIAL HEIGHT= 2.3368

ALL UNITS IN: KG,CM,SEC

LINEAR THEORY

	TIME IN HOURS	VERTICAL STRESS	E	RATE OF STRAIN	EXCESS PORE PRESSURE	C	C/1+E	MV	PERCENT COMPRESSION	K	CV	
1	0.0	0.01845	1.41592	0.0	-0.02257	0.0	0.0	0.06439	0.11865	0.0	0.0	1
2	0.33333	0.03308	1.41506	0.29732E-06	-0.02143	0.00148	0.00061	0.02439	0.15427	-0.378E-07	-0.155E-02	2
3	0.66667	0.09718	1.41484	0.75324E-07	-0.01579	0.00020	0.00008	0.00141	0.16330	-0.130E-07	-0.921E-02	3
4	1.00000	0.13516	1.41433	0.17762E-06	-0.00390	0.00156	0.00065	0.00561	0.18456	-0.124E-06	-0.221E-01	4
5	1.33333	0.17937	1.41231	0.69555E-06	0.01076	0.00712	0.00295	0.01888	0.26781	0.176E-06	0.930E-02	5
6	2.00000	0.24138	1.40559	0.11651E-05	0.04460	0.02265	0.00942	0.04509	0.54590	0.705E-07	0.156E-02	6
7	2.33333	0.35103	1.40183	0.13026E-05	0.05087	0.01003	0.00417	0.01426	0.70114	0.689E-07	0.484E-02	7
8	2.66667	0.38287	1.39767	0.14463E-05	0.05369	0.04793	0.01999	0.05452	0.87317	0.723E-07	0.133E-02	8
9	3.00000	0.42320	1.39326	0.15363E-05	0.04860	0.04406	0.01841	0.04571	1.05559	0.845E-07	0.185E-02	9
10	4.00000	0.60855	1.37981	0.15691E-05	0.04688	0.03701	0.01555	0.03048	1.61136	0.885E-07	0.290E-02	10
11	4.33333	0.68704	1.37515	0.16372E-05	0.04574	0.03845	0.01619	0.02503	1.80428	0.942E-07	0.376E-02	11
12	4.66667	0.72592	1.37136	0.13297E-05	0.02763	0.06876	0.02899	0.04105	1.96069	0.126E-06	0.308E-02	12
13	5.00000	0.81831	1.36725	0.14471E-05	0.02594	0.03431	0.01449	0.01879	2.13063	0.146E-06	0.776E-02	13
14	5.33333	0.93180	1.36297	0.15099E-05	0.02822	0.03297	0.01395	0.01596	2.30768	0.139E-06	0.873E-02	14
15	5.66667	1.05506	1.35865	0.15258E-05	0.02598	0.03476	0.01474	0.01485	2.48618	0.152E-06	0.103E-01	15
16	5.99999	1.17992	1.35425	0.15574E-05	0.03672	0.03934	0.01671	0.01497	2.66812	0.110E-06	0.733E-02	16
17	6.33333	1.30436	1.34968	0.16207E-05	0.02994	0.04558	0.01940	0.01563	2.85704	0.139E-06	0.892E-02	17
18	6.66666	1.42002	1.34454	0.18296E-05	0.03900	0.06060	0.02585	0.01898	3.06987	0.120E-06	0.634E-02	18
19	6.99999	1.48235	1.34044	0.14586E-05	0.02367	0.09533	0.04073	0.02808	3.23920	0.158E-06	0.561E-02	19
20	7.33333	1.58047	1.33752	0.10426E-05	0.02144	0.04563	0.01952	0.01275	3.36012	0.124E-06	0.972E-02	20
21	7.66666	1.72027	1.33318	0.15498E-05	0.03500	0.05120	0.02194	0.01330	3.53952	0.112E-06	0.845E-02	21
22	7.99999	1.79163	1.32858	0.16434E-05	0.02932	0.11299	0.04852	0.02763	3.72937	0.142E-06	0.513E-02	22
23	8.33333	1.85098	1.32426	0.15518E-05	0.03097	0.13278	0.05713	0.03138	3.90829	0.126E-06	0.403E-02	23
24	8.66666	1.98811	1.31996	0.15422E-05	0.03610	0.06009	0.02590	0.01350	4.08582	0.107E-06	0.795E-02	24
25	8.99999	2.08097	1.31539	0.16460E-05	0.02818	0.10020	0.04327	0.02127	4.27489	0.146E-06	0.687E-02	25
26	9.33333	2.15885	1.31081	0.16527E-05	0.03328	0.12472	0.05397	0.02547	4.46439	0.124E-06	0.486E-02	26
27	9.66666	2.26902	1.30620	0.16650E-05	0.04298	0.09259	0.04015	0.01814	4.65489	0.964E-07	0.531E-02	27
28	9.99999	2.34206	1.30161	0.16627E-05	0.04233	0.14493	0.06297	0.02731	4.84474	0.971E-07	0.356E-02	28
29	10.33333	2.41127	1.29698	0.16776E-05	0.04739	0.15880	0.06913	0.02909	5.03590	0.872E-07	0.300E-02	29
30	10.66666	2.48545	1.29228	0.17098E-05	0.05021	0.15521	0.06771	0.02766	5.23032	0.835E-07	0.302E-02	30
31	10.99999	2.52169	1.28780	0.16324E-05	0.04908	0.30952	0.13529	0.05404	5.41560	0.812E-07	0.150E-02	31
32	24.99998	4.73833	1.09743	0.18008E-05	0.11627	0.30181	0.14390	0.04095	13.28604	0.318E-07	0.777E-03	32
33	25.33333	4.81907	1.09306	0.17390E-05	0.12192	0.25852	0.12351	0.02585	13.46663	0.292E-07	0.113E-02	33
34	25.66666	4.89324	1.08834	0.18842E-05	0.12474	0.30913	0.14803	0.03048	13.66182	0.307E-07	0.101E-02	34
35	25.99998	5.00011	1.08403	0.17212E-05	0.12416	0.19921	0.09559	0.01933	13.83977	0.281E-07	0.145E-02	35
36	26.33333	5.07671	1.07944	0.18405E-05	0.12585	0.30207	0.14527	0.02883	14.02965	0.295E-07	0.102E-02	36
37	26.66666	5.17247	1.07535	0.16427E-05	0.13431	0.21890	0.10547	0.02059	14.19878	0.246E-07	0.119E-02	37
38	26.99998	5.25753	1.07101	0.17465E-05	0.13604	0.26616	0.12851	0.02464	14.37822	0.257E-07	0.104E-02	38
39	27.33333	5.36078	1.06664	0.17630E-05	0.13321	0.22480	0.10878	0.02049	14.55898	0.264E-07	0.129E-02	39
40	27.66666	5.44470	1.06246	0.16886E-05	0.13152	0.26910	0.13047	0.02415	14.73177	0.255E-07	0.106E-02	40
41	28.33333	5.64375	1.05400	0.17153E-05	0.13717	0.23549	0.11465	0.02068	15.08136	0.246E-07	0.119E-02	41

SPOBVERT LINEAR THEORY

42	28.66666	5.72307	1.04963	0.17795E-05	0.12980	0.31364	0.15303	0.02692	15.26231	0.269E-07	0.998E-03	42
43	28.99998	5.82075	1.04535	0.17428E-05	0.13545	0.25275	0.12357	0.02141	15.43915	0.251E-07	0.117E-02	43
44	29.33333	5.93247	1.04077	0.18713E-05	0.13263	0.24108	0.11813	0.02010	15.62863	0.274E-07	0.136E-02	44
45	29.66666	6.02998	1.03631	0.18227E-05	0.14616	0.27318	0.13415	0.02243	15.81277	0.241E-07	0.108E-02	45
46	29.99998	6.17182	1.03203	0.17576E-05	0.14898	0.18430	0.09070	0.01487	15.98993	0.227E-07	0.153E-02	46
47	79.66666	6.67739	0.97006	0.17593E-06	-0.00832	0.78708	0.39952	0.06222	18.55193	-0.383E-07	-0.616E-03	47
48	79.99998	6.00263	0.99486	-0.10362E-04	-0.11440	0.23284	0.11672	0.01843	17.52647	0.168E-06	0.913E-02	48
49	80.33333	5.04008	0.99788	-0.12607E-05	-0.14606	0.01729	0.00866	0.00157	17.40150	0.161E-07	0.102E-01	49
50	80.66666	4.30936	1.00116	-0.13646E-05	-0.15793	0.02092	0.01045	0.00224	17.26605	0.161E-07	0.721E-02	50
51	80.99998	3.77150	1.00503	-0.16085E-05	-0.15738	0.02903	0.01448	0.00359	17.10603	0.192E-07	0.534E-02	51
52	81.33333	3.32896	1.00878	-0.15549E-05	-0.15798	0.03003	0.01495	0.00422	16.95108	0.185E-07	0.440E-02	52
53	81.66666	2.97456	1.01260	-0.15843E-05	-0.15629	0.03399	0.01689	0.00536	16.79289	0.192E-07	0.357E-02	53

ENGINEERING STRAIN (53)= 16.7929

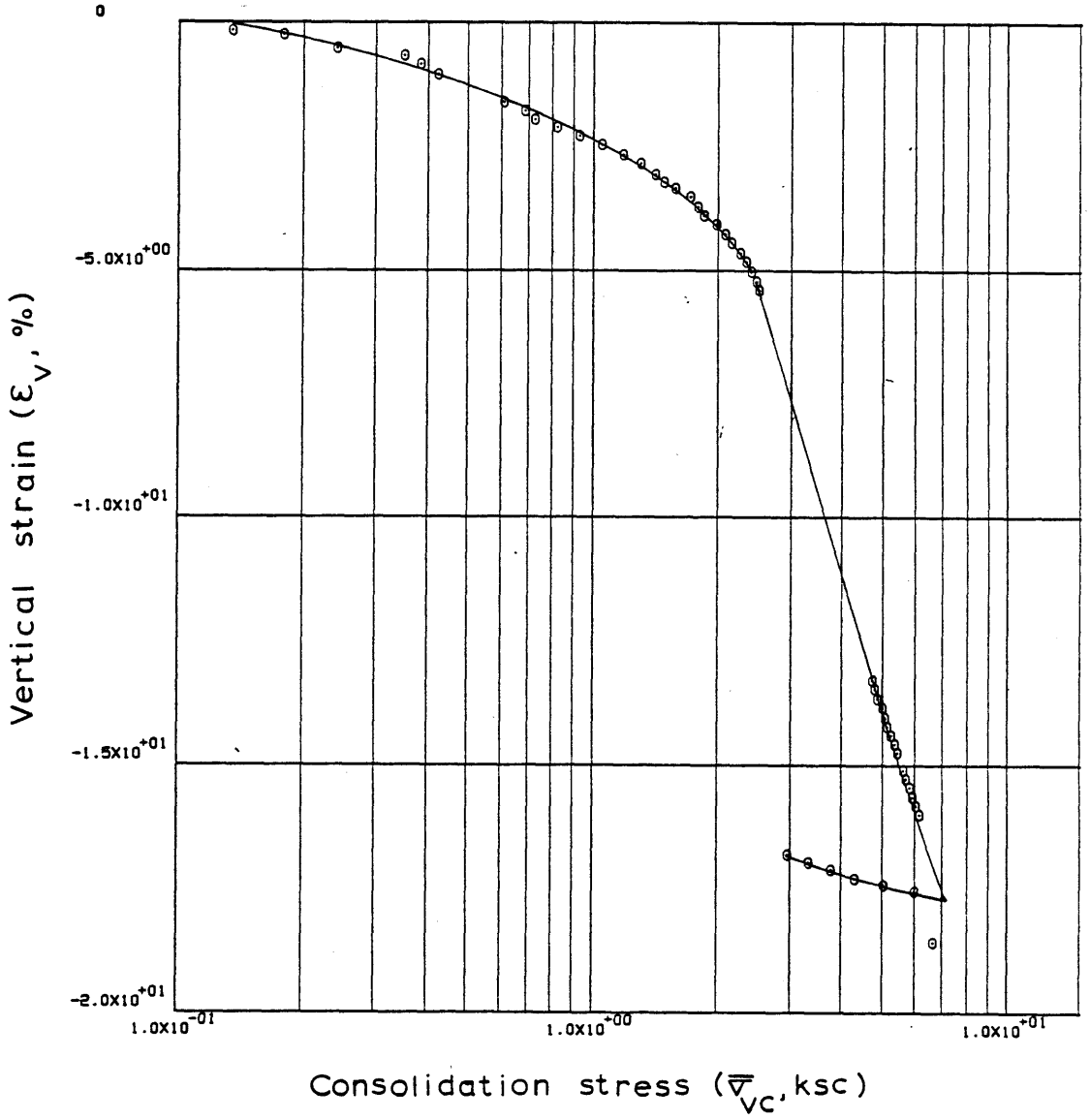

Sample No. SP08 VERT w_N (%) 47.10 Estimated

Depth 67.48 w_L (%) 38.15 $\bar{\sigma}_{vo}$ 1.56 $\bar{\sigma}_{vm}$ 2.29.240

Soil Type Boston w_P (%) 20.80 CR 0.2750 RR -

Blue Clay P.I.(%) 17.35 G_s 2.77 e_o 1.4188

o At t_p Remarks Data from C.R.S.C test

w_L & w_P estimated from Baligh et al (1980)

Figure E.27 Compression Curve for Sample No. SP08VERT

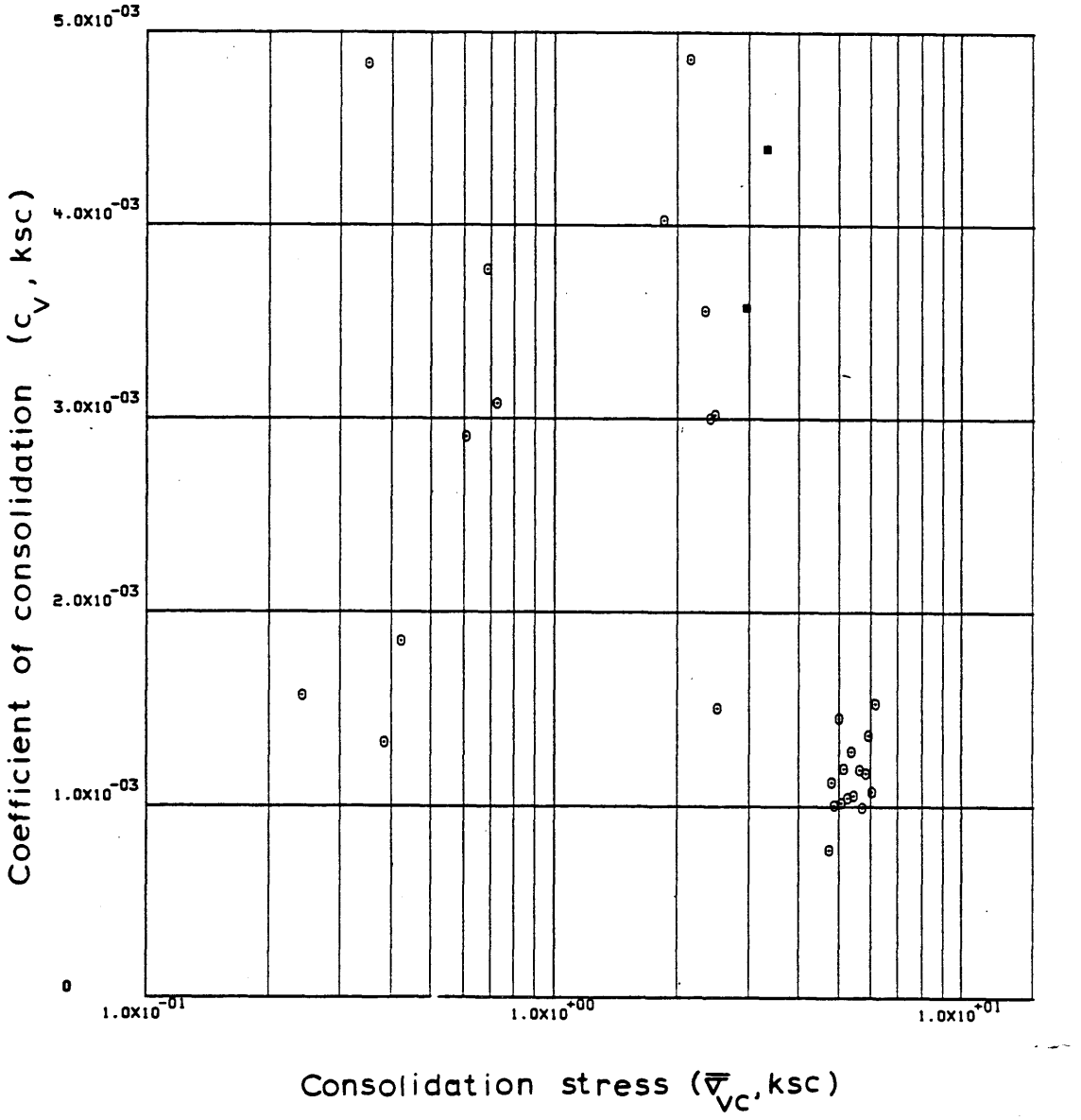

Sample No. SP08 VERT w_N (%) 47.10 Estimated

Depth 67.48 w_L (%) 38.15 $\bar{\sigma}_{vo}$ 1.56 $\bar{\sigma}_{vm}$ 2.29.240

Soil Type Boston w_P (%) 20.80 CR 0.2750 RR -

Blue Clay P.I.(%) 17.35 G_S 2.77 e_o 1.4188

θ At t_p Remarks Data from C.R.S.C test

w_L & w_P estimated from Baligh et al (1980)

Figure E.28 Variation of coefficient of consolidation with consolidation stress for Sample No. SP08VERT

1-D STRAIN CONTROLLED COMPRESSION TEST

COMPUTED RESULTS

INITIAL VOID RATIO= 1.31499
INITIAL HEIGHT= 2.3368

ALL UNITS IN: KG,CM,SEC

LINEAR THEORY

	TIME IN HOURS	VERTICAL STRESS	E	RATE OF STRAIN	EXCESS PORE PRESSURE	C	C/1+E	MV	PERCENT COMPRESSION	K	CV	
1	0.0	0.15894	1.30780	0.0	-0.00705	0.0	0.0	0.01961	0.31067	0.0	0.0	1
2	0.83333	0.27692	1.30359	0.60881E-06	0.05960	0.00758	0.00329	0.01548	0.49243	0.276E-07	0.178E-02	2
3	1.17500	0.35924	1.29907	0.15984E-05	0.08784	0.01737	0.00755	0.02388	0.68768	0.490E-07	0.205E-02	3
4	1.50833	0.39493	1.29552	0.12898E-05	0.10082	0.03750	0.01634	0.04336	0.84113	0.343E-07	0.792E-03	4
5	1.84444	0.46208	1.29181	0.13380E-05	0.09914	0.02363	0.01031	0.02411	1.00143	0.361E-07	0.150E-02	5
6	2.17500	0.53727	1.28766	0.15227E-05	0.09576	0.02749	0.01202	0.02410	1.18048	0.424E-07	0.176E-02	6
7	2.50833	0.61343	1.28363	0.14703E-05	0.09576	0.03040	0.01331	0.02317	1.35454	0.408E-07	0.176E-02	7
8	2.84417	0.69999	1.28012	0.12767E-05	0.09297	0.02666	0.01169	0.01783	1.50655	0.364E-07	0.204E-02	8
9	3.17500	0.78753	1.27604	0.15043E-05	0.09352	0.03460	0.01520	0.02047	1.68269	0.425E-07	0.207E-02	9
10	3.84167	0.94551	1.26755	0.15590E-05	0.08670	0.04642	0.02047	0.02368	2.04921	0.471E-07	0.199E-02	10
11	4.17500	1.04796	1.26295	0.16946E-05	0.09008	0.04473	0.01977	0.01985	2.24800	0.491E-07	0.247E-02	11
12	4.50833	1.12855	1.25841	0.16770E-05	0.09573	0.06134	0.02716	0.02497	2.44432	0,455E-07	0.182E-02	12
13	4.84167	1.22331	1.25395	0.16470E-05	0.10079	0.05525	0.02451	0.02086	2.63673	0.423E-07	0.203E-02	13
14	5.50833	1.38965	1.24488	0.16837E-05	0.10982	0.07116	0.03170	0.02429	3.02861	0.394E-07	0.162E-02	14
15	5.84167	1.47044	1.24048	0.16357E-05	0.11547	0.07782	0.03473	0.02430	3.21858	0.362E-07	0.149E-02	15
16	6.17500	1.55070	1.23568	0.17901E-05	0.12731	0.09037	0.04042	0.02677	3.42603	0.358E-07	0.134E-02	16
17	6.50833	1.61549	1.23189	0.14143E-05	0.12676	0.09252	0.04145	0.02619	3.58963	0.283E-07	0.108E-02	17
18	6.84167	1.69851	1.22810	0.14165E-05	0.12169	0.07559	0.03393	0.02047	3.75325	0.294E-07	0.144E-02	18
19	7.17499	1.75112	1.22381	0.16079E-05	0.11887	0.14070	0.06327	0.03668	3.93861	0.341E-07	0.929E-03	19
20	7.50833	1.80046	1.22007	0.14053E-05	0.11380	0.13469	0.06067	0.03417	4.10031	0.310E-07	0.907E-03	20
21	8.17499	1.83122	1.21372	0.11948E-05	0.10530	0.37478	0.16930	0.09323	4.37451	0.283E-07	0.304E-03	21
22	8.50833	1.87893	1.20936	0.16449E-05	0.10474	0.16955	0.07674	0.04137	4.56290	0.391E-07	0.944E-03	22
23	8.84166	1.93705	1.20469	0.17651E-05	0.11315	0.15332	0.06954	0.03645	4.76462	0.386E-07	0.106E-02	23
24	9.17499	2.00990	1.19998	0.17858E-05	0.12047	0.12768	0.05804	0.02941	4.96828	0.366E-07	0.124E-02	24
25	9.50833	2.05013	1.19538	0.17446E-05	0.12329	0.23199	0.10567	0.05205	5.16682	0.347E-07	0.668E-03	25
26	9.84166	2.10778	1.19077	0.17527E-05	0.13570	0.16613	0.07583	0.03648	5.36586	0.316E-07	0.866E-03	26
27	10.17499	2.13914	1.18615	0.17621E-05	0.13684	0.31297	0.14316	0.06742	5.56551	0.314E-07	0.465E-03	27
28	10.50833	2.19269	1.18166	0.17151E-05	0.13739	0.18160	0.08324	0.03844	5.75948	0.303E-07	0.788E-03	28
29	10.84166	2.22385	1.17704	0.17693E-05	0.14639	0.32752	0.15044	0.06812	5.95914	0.292E-07	0.428E-03	29
30	11.17499	2.26610	1.17259	0.17050E-05	0.14639	0.23624	0.10873	0.04843	6.15114	0.280E-07	0.578E-03	30
31	11.50833	2.29972	1.16826	0.16637E-05	0.14640	0.29387	0.13553	0.05937	6.33813	0.272E-07	0.458E-03	31
32	11.84166	2.35893	1.16374	0.17411E-05	0.14639	0.17785	0.08219	0.03529	6.53343	0.284E-07	0.804E-03	32
33	12.17499	2.38101	1.15920	0.17546E-05	0.15372	0.48800	0.22601	0.09536	6.72981	0.271E-07	0.284E-03	33
34	12.50833	2.42260	1.15486	0.16761E-05	0.15203	0.25035	0.11618	0.04836	6.91705	0.261E-07	0.539E-03	34
35	12.84166	2.46832	1.15047	0.17042E-05	0.16217	0.23520	0.10937	0.04473	7.10703	0.248E-07	0.554E-03	35
36	13.17499	2.52867	1.14592	0.17657E-05	0.15767	0.18820	0.08770	0.03511	7.30341	0.263E-07	0.748E-03	36
37	13.50833	2.57258	1.14140	0.17570E-05	0.16275	0.26230	0.12249	0.04802	7.49844	0.252E-07	0.525E-03	37
38	13.84166	2.58582	1.13734	0.15825E-05	0.16839	0.79105	0.37011	0.14348	7.67377	0.219E-07	0.152E-03	38
39	14.17499	2.64436	1.13379	0.13900E-05	0.16670	0.15894	0.07449	0.02849	7.82750	0.193E-07	0.679E-03	39
40	14.50833	2.68925	1.13010	0.14414E-05	0.15772	0.21890	0.10277	0.03853	7.98666	0.211E-07	0.548E-03	40
41	15.17499	2.76269	1.11949	0.20861E-05	0.15896	0.39390	0.18585	0.06818	8.44505	0.301E-07	0.441E-03	41

42	15.50833	2.79532	1.11502	0.17590E-05	0.14756	0.38024	0.17978	0.06468	8.63792	0.272E-07	0.420E-03	42
43	15.84166	2.82723	1.11047	0.17967E-05	0.15038	0.40088	0.18995	0.06757	8.83447	0.271E-07	0.401E-03	43
44	16.17497	2.85094	1.10590	0.18110E-05	0.16276	0.54812	0.26028	0.09166	9.03217	0.251E-07	0.274E-03	44
45	16.50832	2.90675	1.10142	0.17775E-05	0.17009	0.23118	0.11001	0.03822	9.22577	0.235E-07	0.615E-03	45
46	16.84164	2.97001	1.09683	0.18244E-05	0.17404	0.21320	0.10168	0.03461	9.42407	0.235E-07	0.679E-03	46
47	17.17497	3.03321	1.09235	0.17835E-05	0.17799	0.21271	0.10166	0.03387	9.61752	0.223E-07	0.660E-03	47
48	17.50832	3.10246	1.08788	0.17838E-05	0.18307	0.19797	0.09482	0.03091	9.81056	0.216E-07	0.700E-03	48
49	17.84164	3.13129	1.08339	0.17933E-05	0.18531	0.48489	0.23274	0.07465	10.00424	0.214E-07	0.287E-03	49
50	18.17497	3.19561	1.07913	0.17097E-05	0.19264	0.20975	0.10088	0.03190	10.18851	0.195E-07	0.613E-03	50
51	18.50832	3.26912	1.07454	0.18428E-05	0.19377	0.20173	0.09724	0.03008	10.38669	0.209E-07	0.693E-03	51
52	18.84164	3.31544	1.07013	0.17740E-05	0.19772	0.31325	0.15132	0.04596	10.57703	0.196E-07	0.426E-03	52
53	19.17497	3.36832	1.06579	0.17522E-05	0.20446	0.27451	0.13289	0.03976	10.76468	0.186E-07	0.469E-03	53
54	19.50832	3.42681	1.06131	0.18101E-05	0.20278	0.26002	0.12614	0.03714	10.95808	0.193E-07	0.520E-03	54
55	19.84164	3.48829	1.05714	0.16889E-05	0.20165	0.23450	0.11399	0.03297	11.13818	0.181E-07	0.548E-03	55
56	20.17497	3.53331	1.05251	0.18831E-05	0.21011	0.36173	0.17624	0.05019	11.33853	0.192E-07	0.383E-03	56
57	20.50832	3.60981	1.04807	0.18046E-05	0.21179	0.20703	0.10108	0.02831	11.53009	0.182E-07	0.643E-03	57
58	20.84164	3.68821	1.04370	0.17814E-05	0.21070	0.20334	0.09950	0.02727	11.71880	0.180E-07	0.660E-03	58
59	21.17497	3.75441	1.03933	0.17851E-05	0.21520	0.24552	0.12039	0.03236	11.90752	0.176E-07	0.543E-03	59
60	21.50832	3.82528	1.03511	0.17309E-05	0.22535	0.22614	0.11112	0.02931	12.09015	0.162E-07	0.553E-03	60
61	21.84164	3.88981	1.03063	0.18363E-05	0.22479	0.26742	0.13169	0.03414	12.28343	0.172E-07	0.503E-03	61
62	22.17497	3.96821	1.02644	0.17237E-05	0.22366	0.21005	0.10365	0.02638	12.46446	0.161E-07	0.611E-03	62
63	22.50832	4.03439	1.02201	0.18254E-05	0.22817	0.26778	0.13243	0.03310	12.65579	0.167E-07	0.503E-03	63
64	26.09164	4.96226	0.97754	0.17434E-05	0.25196	0.21485	0.10864	0.02424	14.57692	0.138E-07	0.569E-03	64
65	26.12498	4.97014	0.97727	0.11077E-05	0.25028	0.16530	0.08360	0.01687	14.58827	0.882E-08	0.523E-03	65
66	26.32498	5.03167	0.97444	0.19971E-05	0.24914	0.23075	0.11687	0.02337	14.71091	0.159E-07	0.681E-03	66
67	32.07498	5.03199	0.95698	0.43097E-06	0.06969	9999.00000	5109.41016	28.09111	15.46506	0.121E-07	0.430E-06	67
68	32.42497	4.23722	0.95785	-0.35199E-06	-0.15119	0.00505	0.00258	0.00056	15.42755	0.455E-08	0.815E-02	68
69	32.75932	3.57805	0.96109	-0.13765E-05	-0.16700	0.01916	0.00977	0.00251	15.28761	0.161E-07	0.644E-02	69
70	33.09164	3.06833	0.96479	-0.15701E-05	-0.19127	0.02408	0.01226	0.00370	15.12772	0.161E-07	0.437E-02	70
71	33.42497	2.69142	0.96857	-0.16025E-05	-0.18900	0.02889	0.01467	0.00510	14.96419	0.167E-07	0.328E-02	71
72	33.75832	2.37643	0.97328	-0.19865E-05	-0.20368	0.03779	0.01915	0.00757	14.76099	0.193E-07	0.256E-02	72
73	34.61664	1.70412	0.98386	-0.17260E-05	-0.22514	0.03182	0.01604	0.00793	14.30394	0.154E-07	0.194E-02	73
74	35.28331	1.35660	0.99107	-0.15091E-05	-0.20142	0.03162	0.01588	0.01042	13.99243	0.151E-07	0.145E-02	74

ENGINEERING STRAIN (74)= 13.9924

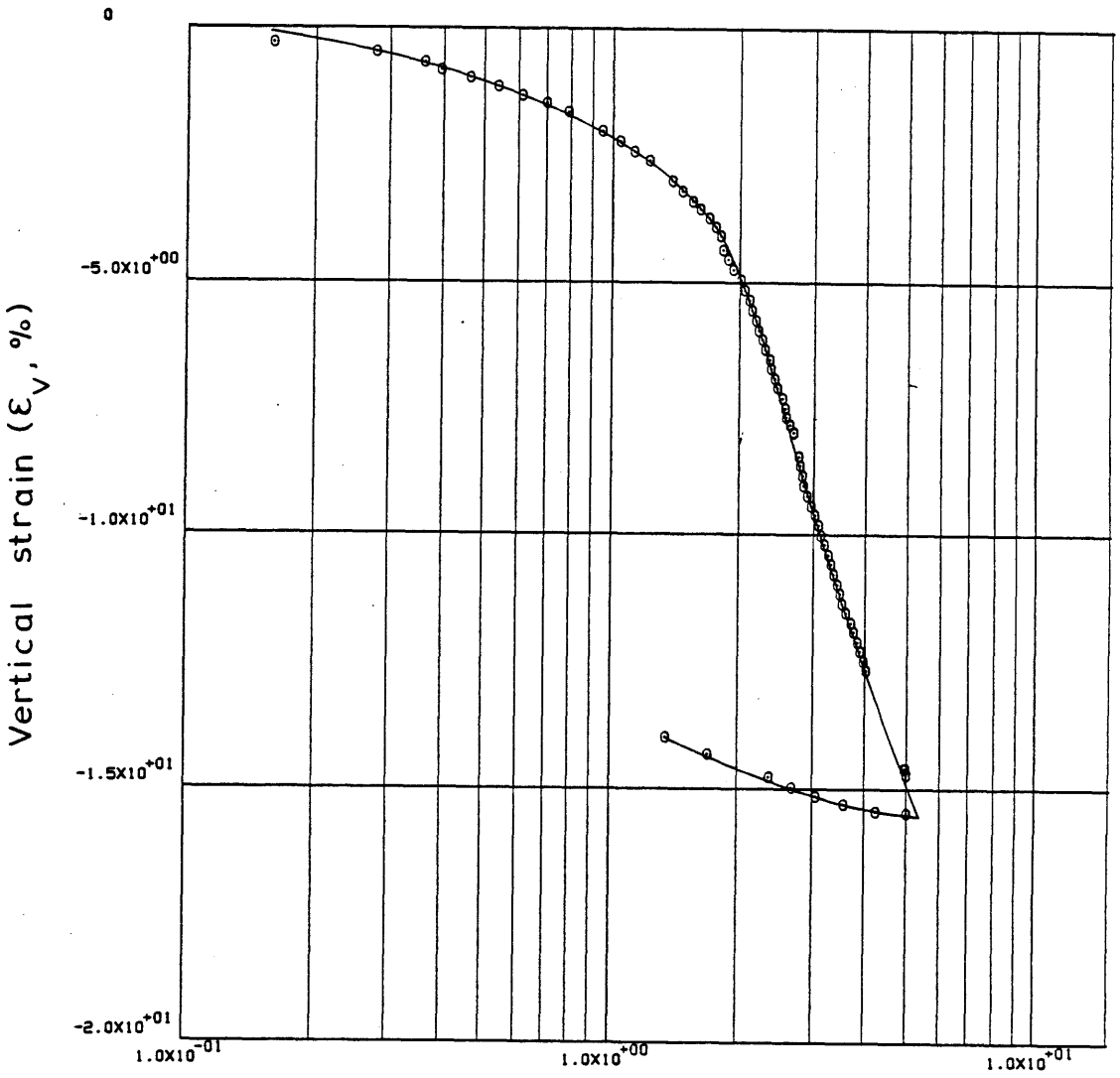

Sample No. SP16VERT w_N (%) 42.70 Estimated

Depth 73.48 w_L (%) 36.65 $\bar{\sigma}_{vo}$ 1.71 $\bar{\sigma}_{vm}$ 1.81-1.90

Soil Type Boston Blue Clay w_P (%) 20.33 CR 0.2437 RR 0.0269

P.I.(%) 16.32 G_s 2.77 e_o 1.3150

⊙ At t_p

Remarks Data from C.R.S.C test

w_L & w_P estimated from Baligh et al (1980)

Figure E.29 Compression Curve for Sample No. SP16VERT

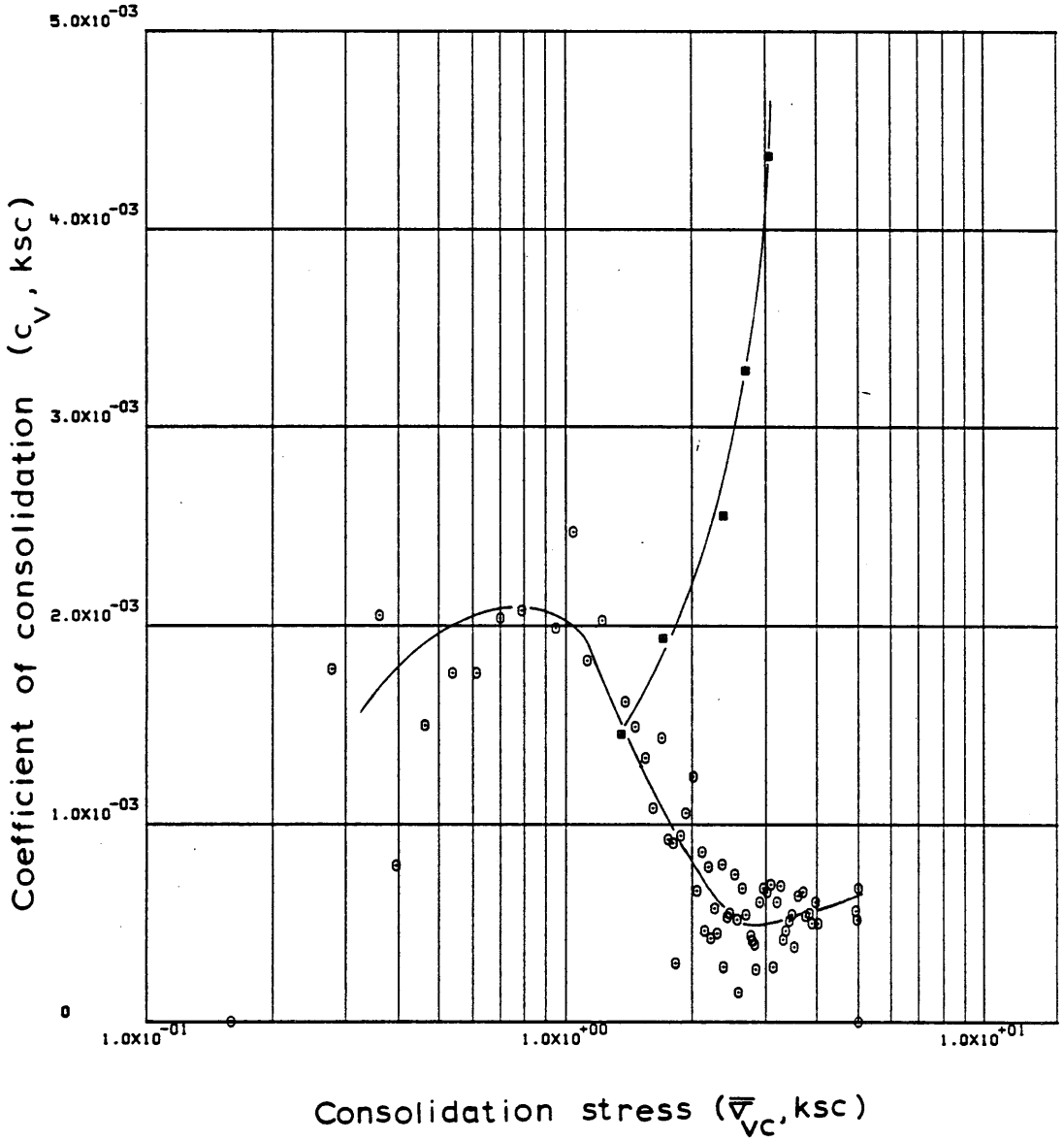

Sample No. SP16VERT w_N (%) 42.70 Estimated

Depth 73.48 w_L (%) 36.65 $\bar{\sigma}_{vo}$ 1.71 $\bar{\sigma}_{vm}$ 1.81-1.90

Soil Type Boston w_P (%) 20.33 CR 0.2437 RR 0.0269

Blue Clay P.I.(%) 16.32 G_s 2.77 e_o 1.3150

o At t_p Remarks Data from C.R.S.C test

w_L & w_P estimated from Baligh et al (1980)

Figure E.30 Variation of coefficient of consolidation with consolidation stress for Sample No. SP16VERT

1-D STRAIN CONTROLLED COMPRESSION TEST

COMPUTED RESULTS

INITIAL VOID RATIO= 1.26611
INITIAL HEIGHT= 2.3368

ALL UNITS IN: KG,CM,SEC

LINEAR THEORY

	TIME IN HOURS	VERTICAL STRESS	E	RATE OF STRAIN	EXCESS PORE PRESSURE	C	C/1+E	MV	PERCENT COMPRESSION	K	CV	
1	0.0	0.01111	1.26766	0.0	-0.03083	0.0	0.0	-0.06163	-0.06851	0.0	0.0	1
2	0.34167	0.12138	1.26572	0.69671E-06	0.02163	0.00081	0.00036	0.00777	0.01715	0.879E-07	0.113E+01	2
3	0.67500	0.18955	1.26135	0.16120E-05	0.02496	0.00981	0.00434	0.02838	0.21019	0.176E-06	0.619E-02	3
4	1.00833	0.32680	1.25769	0.13521E-05	0.03965	0.00672	0.00298	0.01182	0.37184	0.924E-07	0.782E-02	4
5	1.34167	0.42618	1.25320	0.16591E-05	0.04247	0.01690	0.00750	0.02003	0.56981	0.105E-06	0.526E-02	5
6	1.67500	0.56647	1.24927	0.14564E-05	0.04980	0.01381	0.00614	0.01246	0.74326	0.787E-07	0.632E-02	6
7	2.00833	0.73575	1.24528	0.14820E-05	0.04983	0.01527	0.00680	0.01051	0.91948	0.797E-07	0.759E-02	7
8	2.34167	0.87686	1.24187	0.12665E-05	0.03346	0.01942	0.00866	0.01077	1.06984	0.101E-06	0.939E-02	8
9	2.67500	1.02228	1.23816	0.13827E-05	0.02273	0.02420	0.01081	0.01141	1.23373	0.162E-06	0.142E-01	9
10	3.00833	1.20325	1.23391	0.15845E-05	0.03291	0.02606	0.01167	0.01051	1.42114	0.128E-06	0.122E-01	10
11	3.34167	1.30357	1.22989	0.15002E-05	0.02323	0.05012	0.02248	0.01794	1.59830	0.171E-06	0.952E-02	11
12	3.67500	1.45863	1.22691	0.11159E-05	-0.00158	0.02653	0.01192	0.00864	1.72987	-0.187E-05	-0.216E+00	12
13	4.00833	1.63470	1.22353	0.12687E-05	0.02832	0.02971	0.01336	0.00865	1.87927	0.118E-06	0.136E-01	13
14	4.34167	1.81845	1.21919	0.16296E-05	0.03114	0.04073	0.01836	0.01064	2.07077	0.137E-06	0.129E-01	14
15	4.67500	2.01140	1.21487	0.16240E-05	0.04357	0.04280	0.01932	0.01010	2.26123	0.972E-07	0.963E-02	15
16	5.00833	2.15808	1.21070	0.15715E-05	0.04415	0.05923	0.02679	0.01286	2.44521	0.925E-07	0.719E-02	16
17	5.34167	2.30084	1.20649	0.15897E-05	0.05035	0.06573	0.02979	0.01336	2.63098	0.817E-07	0.612E-02	17
18	5.67500	2.33791	1.20221	0.16185E-05	0.05254	0.26763	0.12153	0.05239	2.81973	0.794E-07	0.152E-02	18
19	6.00833	2.44661	1.19795	0.16178E-05	0.05709	0.09386	0.04270	0.01786	3.00800	0.728E-07	0.408E-02	19
20	6.34166	2.54921	1.19386	0.15517E-05	0.06050	0.09946	0.04534	0.01815	3.18826	0.656E-07	0.362E-02	20
21	6.67499	2.61445	1.18988	0.15150E-05	0.06958	0.15751	0.07193	0.02786	3.36395	0.555E-07	0.199E-02	21
22	7.00833	2.68012	1.18628	0.13744E-05	0.07244	0.14540	0.06651	0.02512	3.52307	0.482E-07	0.192E-02	22
23	7.34166	2.72097	1.18189	0.16736E-05	0.08490	0.28962	0.13274	0.04916	3.71643	0.499E-07	0.102E-02	23
24	7.67499	2.79096	1.17760	0.16450E-05	0.08380	0.16930	0.07775	0.02821	3.90613	0.495E-07	0.175E-02	24
25	8.00833	2.81672	1.17329	0.16508E-05	0.09339	0.46847	0.21556	0.07688	4.09610	0.444E-07	0.577E-03	25
26	8.34166	2.82513	1.16887	0.16970E-05	0.09340	1.48271	0.68363	0.24228	4.29102	0.454E-07	0.188E-03	26
27	8.67499	2.78097	1.16451	0.16809E-05	0.08031	-0.27721	-0.12807	-0.04568	4.48369	0.521E-07	-0.114E-02	27
28	9.00833	2.80250	1.16026	0.16372E-05	0.08595	0.55028	0.25473	0.09125	4.67097	0.473E-07	0.518E-03	28
29	9.34166	2.81804	1.15557	0.18153E-05	0.09046	0.84953	0.39411	0.14023	4.87816	0.496E-07	0.354E-03	29
30	9.67499	2.87113	1.15134	0.16375E-05	0.09727	0.22649	0.10528	0.03701	5.06471	0.414E-07	0.112E-02	30
31	10.00833	2.90646	1.14700	0.16842E-05	0.11028	0.35482	0.16526	0.05721	5.25620	0.374E-07	0.654E-03	31
32	10.34166	2.94143	1.14270	0.16742E-05	0.11368	0.35998	0.16800	0.05745	5.44617	0.359E-07	0.626E-03	32
33	10.67499	2.96132	1.13829	0.17159E-05	0.11423	0.65316	0.30546	0.10351	5.64043	0.365E-07	0.353E-03	33
34	11.00833	2.98075	1.13439	0.15259E-05	0.11314	0.59759	0.27998	0.09424	5.81290	0.327E-07	0.347E-03	34
35	11.34166	3.01456	1.13007	0.16894E-05	0.11317	0.38303	0.17982	0.05997	6.00349	0.360E-07	0.600E-03	35
36	11.67499	3.02488	1.12573	0.16988E-05	0.11035	1.26762	0.59632	0.19748	6.19469	0.370E-07	0.187E-03	36
37	12.00833	3.04694	1.12130	0.17414E-05	0.11768	0.61016	0.28764	0.09473	6.39034	0.354E-07	0.374E-03	37
38	12.34166	3.05723	1.11709	0.16571E-05	0.11485	1.24928	0.59009	0.19326	6.57611	0.344E-07	0.178E-03	38
39	12.67499	3.12098	1.11287	0.16657E-05	0.12844	0.20462	0.09684	0.03135	6.76245	0.308E-07	0.982E-03	39
40	13.00833	3.10350	1.10836	0.17822E-05	0.11881	-0.80289	-0.38081	-0.12236	6.96146	0.355E-07	-0.290E-03	40
41	13.34166	3.11172	1.10366	0.18602E-05	0.12669	1.77640	0.84443	0.27173	7.16866	0.345E-07	0.127E-03	41

42	13.67499	3.09309	1.09909	0.18154E-05	0.12156	-0.76169	-0.36287	-0.11694	7.37045	0.350E-07	-0.299E-03	42
43	14.00833	3.12712	1.09465	0.17656E-05	0.12328	0.40211	0.19197	0.06171	7.56631	0.334E-07	0.541E-03	43
44	14.34166	3.15285	1.09078	0.15429E-05	0.12328	0.47783	0.22854	0.07280	7.73711	0.291E-07	0.400E-03	44
45	14.67499	3.15641	1.08672	0.16201E-05	0.12555	3.59797	1.72422	0.54622	7.91615	0.299E-07	0.547E-04	45
46	15.00833	3.17943	1.08266	0.16256E-05	0.12669	0.55924	0.26852	0.08474	8.09543	0.296E-07	0.349E-03	46
47	15.34166	3.20875	1.07771	0.19876E-05	0.11317	0.53976	0.25979	0.08135	8.31410	0.403E-07	0.495E-03	47
48	15.67499	3.23438	1.07342	0.17238E-05	0.12277	0.53916	0.26003	0.08072	8.50334	0.321E-07	0.398E-03	48
49	16.00832	3.26027	1.06890	0.18196E-05	0.12445	0.56659	0.27386	0.08433	8.70270	0.333E-07	0.395E-03	49
50	16.34164	3.29889	1.06438	0.18230E-05	0.12222	0.38354	0.18579	0.05664	8.90198	0.338E-07	0.597E-03	50
51	16.67497	3.33956	1.05979	0.18581E-05	0.13463	0.37480	0.18196	0.05483	9.10464	0.311E-07	0.568E-03	51
52	17.00832	3.38195	1.05525	0.18423E-05	0.12672	0.36027	0.17529	0.05215	9.30516	0.327E-07	0.626E-03	52
53	17.34164	3.42456	1.05078	0.18164E-05	0.13632	0.35711	0.17414	0.05116	9.50243	0.298E-07	0.582E-03	53
54	17.67497	3.46608	1.04631	0.18207E-05	0.14251	0.37094	0.18127	0.05262	9.69972	0.284E-07	0.541E-03	54
55	18.00832	3.51949	1.04176	0.18542E-05	0.15097	0.29710	0.14551	0.04166	9.90018	0.272E-07	0.653E-03	55
56	18.34164	3.54487	1.03734	0.18073E-05	0.15097	0.61479	0.30176	0.08544	10.09517	0.264E-07	0.309E-03	56
57	18.67497	3.57727	1.03305	0.17601E-05	0.15548	0.47199	0.23216	0.06518	10.28467	0.249E-07	0.382E-03	57
58	19.00832	3.63576	1.02900	0.16619E-05	0.16170	0.24951	0.12297	0.03410	10.46321	0.225E-07	0.660E-03	58
59	19.34164	3.67551	1.02517	0.15775E-05	0.16284	0.35249	0.17405	0.04762	10.63237	0.211E-07	0.444E-03	59
60	19.67497	3.73058	1.02115	0.16588E-05	0.15891	0.27066	0.13391	0.03615	10.80994	0.227E-07	0.627E-03	60
61	20.00832	3.77463	1.01720	0.16321E-05	0.15609	0.33652	0.16682	0.04446	10.98428	0.226E-07	0.509E-03	61
62	20.34164	3.83196	1.01298	0.17445E-05	0.15104	0.27951	0.13885	0.03651	11.17023	0.249E-07	0.681E-03	62
63	20.67497	3.90196	1.00864	0.18023E-05	0.14994	0.23996	0.11947	0.03090	11.36191	0.258E-07	0.835E-03	63
64	21.00832	3.93924	1.00434	0.17884E-05	0.15218	0.45254	0.22578	0.05757	11.55176	0.251E-07	0.436E-03	64
65	21.34164	4.05106	0.99984	0.18723E-05	0.16686	0.16050	0.08026	0.02009	11.75002	0.239E-07	0.119E-02	65
66	21.67497	4.12084	0.99520	0.19402E-05	0.17364	0.27204	0.13635	0.03337	11.95502	0.237E-07	0.709E-03	66
67	24.34164	4.72477	0.96152	0.17883E-05	0.20466	0.24623	0.12553	0.02843	13.44107	0.179E-07	0.629E-03	67
68	24.67497	4.82506	0.95758	0.16773E-05	0.20128	0.18756	0.09581	0.02007	13.61493	0.170E-07	0.846E-03	68
69	25.00832	4.89679	0.95334	0.18103E-05	0.20524	0.28761	0.14724	0.03029	13.80217	0.179E-07	0.591E-03	69
70	25.34164	5.01697	0.94983	0.14983E-05	0.20246	0.14459	0.07415	0.01496	13.95688	0.150E-07	0.100E-02	70
71	25.67497	5.10601	0.94549	0.18592E-05	0.19062	0.24672	0.12682	0.02506	14.14841	0.196E-07	0.783E-03	71
72	26.00832	5.22882	0.94142	0.17480E-05	0.20418	0.17138	0.08828	0.01708	14.32814	0.172E-07	0.100E-02	72
73	26.34164	5.31990	0.93769	0.16059E-05	0.20701	0.21621	0.11158	0.02116	14.49290	0.155E-07	0.732E-03	73
74	26.67497	5.40199	0.93302	0.20130E-05	0.20811	0.30492	0.15775	0.02943	14.69896	0.192E-07	0.653E-03	74
75	35.79997	5.53240	0.91375	0.30650E-06	0.01507	0.80777	0.42209	0.07721	15.54926	0.396E-07	0.513E-03	75
76	36.14165	4.97457	0.91233	0.60430E-06	-0.10405	-0.01337	-0.00699	-0.00133	15.61198	-0.113E-07	0.847E-02	76
77	36.47498	4.13660	0.91510	-0.12087E-05	-0.12495	0.01505	0.00786	0.00173	15.48943	0.189E-07	0.109E-01	77
78	36.80830	3.53052	0.91811	-0.13064E-05	-0.12609	0.01899	0.00990	0.00259	15.35670	0.203E-07	0.784E-02	78
79	37.14165	3.06028	0.92113	-0.13086E-05	-0.12553	0.02110	0.01098	0.00334	15.22359	0.205E-07	0.613E-02	79
80	37.47498	2.69331	0.92493	-0.16450E-05	-0.12781	0.02975	0.01546	0.00538	15.05589	0.254E-07	0.471E-02	80
81	37.80830	2.39677	0.92824	-0.14332E-05	-0.12955	0.02842	0.01474	0.00580	14.90958	0.219E-07	0.377E-02	81
82	38.14165	2.15237	0.93195	-0.16000E-05	-0.12781	0.03449	0.01785	0.00786	14.74588	0.248E-07	0.316E-02	82
83	38.47498	1.90570	0.93536	-0.14682E-05	-0.13290	0.02801	0.01447	0.00714	14.59541	0.220E-07	0.308E-02	83
84	38.80832	1.70658	0.93915	-0.16279E-05	-0.13855	0.03432	0.01770	0.00981	14.42825	0.235E-07	0.239E-02	84
85	39.14165	1.54649	0.94255	-0.14567E-05	-0.12894	0.03448	0.01775	0.01092	14.27840	0.227E-07	0.208E-02	85
86	39.47498	1.43695	0.94565	-0.13286E-05	-0.09392	0.04223	0.02170	0.01456	14.14151	0.285E-07	0.196E-02	86
87	39.80832	1.32787	0.94907	-0.14619E-05	-0.10936	0.04331	0.02222	0.01608	13.99063	0.269E-07	0.167E-02	87
88	40.14165	1.21597	0.95392	-0.20672E-05	-0.12433	0.05506	0.02818	0.02217	13.77675	0.337E-07	0.152E-02	88
89	40.47498	1.09903	0.95790	-0.16948E-05	-0.14631	0.03937	0.02011	0.01739	13.60104	0.236E-07	0.136E-02	89
90	40.80832	1.00013	0.96189	-0.16955E-05	-0.15534	0.04234	0.02158	0.02057	13.42487	0.223E-07	0.109E-02	90
91	41.14165	0.91310	0.96599	-0.17390E-05	-0.16214	0.04506	0.02292	0.02398	13.24384	0.220E-07	0.919E-03	91
92	41.47498	0.80548	0.96984	-0.16293E-05	-0.15536	0.03071	0.01559	0.01817	13.07390	0.216E-07	0.119E-02	92
93	41.80832	0.74061	0.97385	-0.16918E-05	-0.14693	0.04773	0.02418	0.03130	12.89702	0.239E-07	0.762E-03	93
94	42.14165	0.67870	0.97773	-0.16355E-05	-0.14581	0.04446	0.02248	0.03170	12.72574	0.233E-07	0.736E-03	94
95	42.47498	0.63793	0.98165	-0.16490E-05	-0.15035	0.06329	0.03194	0.04853	12.55269	0.229E-07	0.472E-03	95

ENGINEERING STRAIN (95)= 12.5527

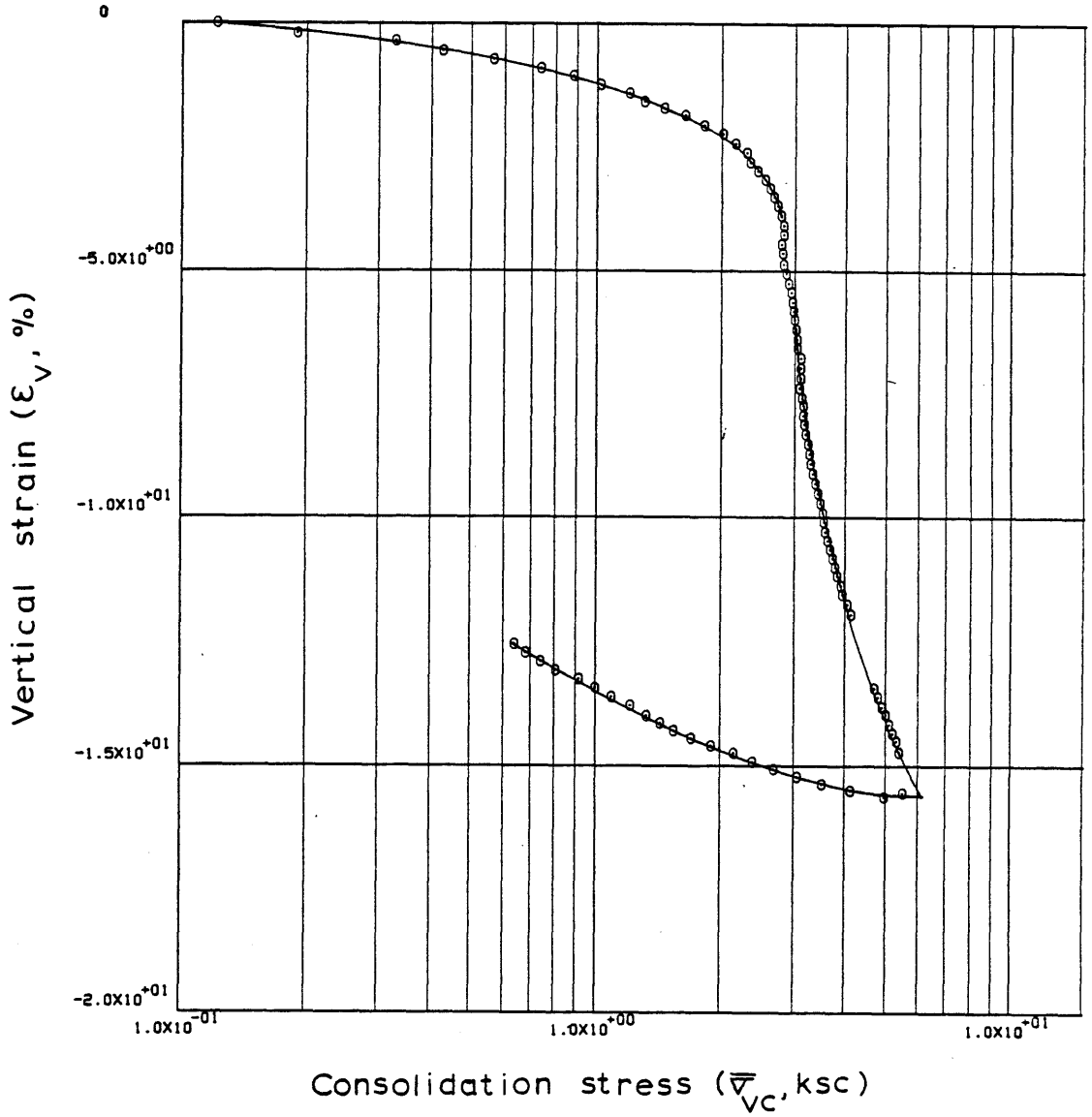

Sample No. SP09VERT w_N (%) 42.00 Estimated

Depth 78.48 w_L (%) 40.72 $\bar{\sigma}_{vo}$ 1.83 $\bar{\sigma}_{vm}$ 2.62-2.71

Soil Type Boston Blue Clay w_P (%) 21.29 CR 0.7340-0.2205 RR 0.0307

P.I.(%) 19.43 G_s 2.77 e_o 1.2661

⊙ At t_p Remarks Data from C.R.S.C test

w_L & w_P estimated from Baligh et al (1980)

Figure E.31 Compression Curve for Sample No. SP09VERT

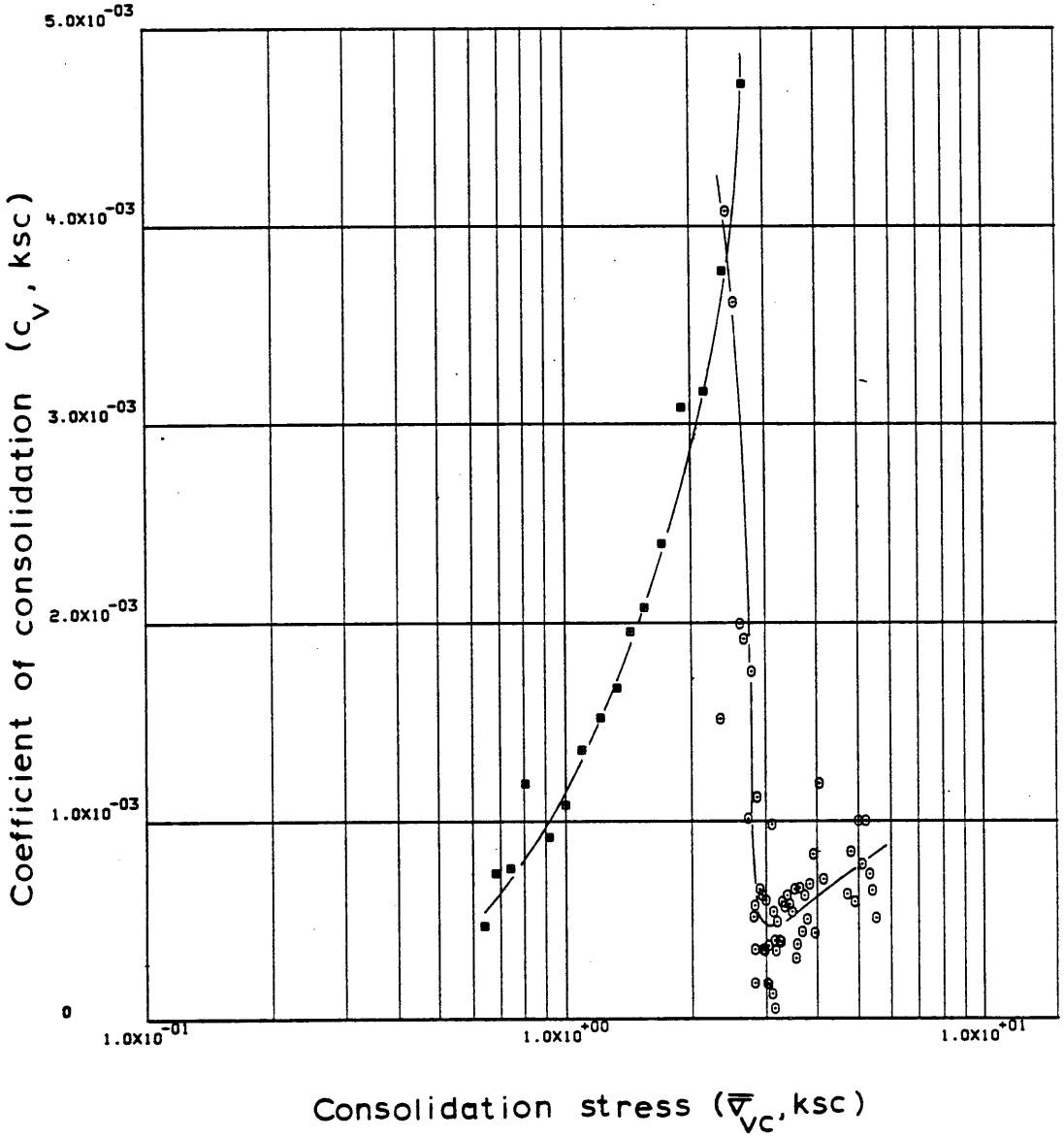

Sample No. SP09VERT w_N (%) 42.00 Estimated

Depth 78.48 w_L (%) 40.72 $\bar{\sigma}_{vo}$ 1.83 $\bar{\sigma}_{vm}$ 262.271

Soil Type Boston w_P (%) 21.29 CR 0.7340-0.2205 RR 0.0307

Blue Clay P.I.(%) 19.43 G_s 2.77 e_o 1.2661

⊙ At t_p Remarks Data from C.R.S.C test

w_L & w_P estimated from Baligh et al (1980)

Figure E.32 Variation of coefficient of consolidation with consolidation stress for Sample No. SP09VERT

1-D STRAIN CONTROLLED COMPRESSION TEST

COMPUTED RESULTS

INITIAL VOID RATIO= 1.42050
INITIAL HEIGHT= 2.3368

ALL UNITS IN: KG,CM,SEC

LINEAR THEORY

	TIME IN HOURS	VERTICAL STRESS	E	RATE OF STRAIN	EXCESS PORE PRESSURE	C	C/1+E	MV	PERCENT COMPRESSION	K	CV	
1	0.0	-0.10172	1.42157	0.0	-0.04315	0.0	0.0	0.00435	-0.04419	0.0	0.0	1
2	0.34166	-0.08298	1.42050	0.35960E-06	0.01724	0.0	0.0	0.0	0.0	0.569E-07	0.100E+05	2
3	0.59166	-0.04160	1.41780	0.12418E-05	0.03437	0.0	0.0	0.0	0.11166	0.984E-07	0.100E+05	3
4	0.94167	-0.02968	1.41489	0.95754E-06	0.04214	0.0	0.0	0.0	0.23203	0.617E-07	0.100E+05	4
5	1.28027	-0.06867	1.41185	0.10326E-05	0.11184	0.0	0.0	0.0	0.35747	0.250E-07	0.100E+05	5
6	1.60834	-0.01511	1.40772	0.14523E-05	0.07634	0.0	0.0	0.0	0.52806	0.514E-07	0.100E+05	6
7	1.94167	0.02352	1.40339	0.15023E-05	0.04848	0.0	0.0	0.0	0.70706	0.834E-07	0.100E+05	7
8	2.44167	0.03397	1.39708	0.14630E-05	0.05471	0.01718	0.00717	0.25206	0.96788	0.716E-07	0.284E-03	8
9	2.77499	0.05863	1.39286	0.14683E-05	0.08871	0.00772	0.00323	0.07145	1.14206	0.442E-07	0.618E-03	9
10	3.10834	0.09715	1.38855	0.15027E-05	0.09786	0.00853	0.00357	0.04682	1.32001	0.408E-07	0.872E-03	10
11	3.44167	0.13861	1.38421	0.15172E-05	0.09471	0.01221	0.00512	0.04391	1.49933	0.424E-07	0.967E-03	11
12	3.77501	0.16808	1.37974	0.15646E-05	0.12260	0.02318	0.00974	0.06371	1.68391	0.337E-07	0.529E-03	12
13	4.28334	0.23217	1.37325	0.14947E-05	0.11460	0.02010	0.00847	0.04268	1.95213	0.342E-07	0.802E-03	13
14	4.95000	0.33071	1.36437	0.15650E-05	0.12710	0.02510	0.01062	0.03812	2.31898	0.321E-07	0.842E-03	14
15	5.61667	0.52303	1.35545	0.15787E-05	0.11939	0.01947	0.00827	0.01970	2.68771	0.342E-07	0.174E-02	15
16	6.28334	0.70611	1.34638	0.16094E-05	0.18906	0.03020	0.01287	0.02110	3.06215	0.218E-07	0.104E-02	16
17	6.95000	0.86316	1.33749	0.15846E-05	0.21564	0.04426	0.01894	0.02422	3.42941	0.187E-07	0.773E-03	17
18	7.28334	1.00336	1.33326	0.15116E-05	0.11030	0.02813	0.01205	0.01294	3.60428	0.348E-07	0.269E-02	18
19	8.28334	0.96881	1.31985	0.16064E-05	0.30030	-0.38288	-0.16504	-0.16740	4.15854	0.134E-07	-0.801E-04	19
20	8.95000	1.17873	1.31057	0.16731E-05	0.17497	0.04731	0.02047	0.01913	4.54184	0.238E-07	0.124E-02	20
21	9.61667	1.34479	1.30100	0.17332E-05	0.22610	0.07262	0.03156	0.02505	4.93726	0.189E-07	0.755E-03	21
22	10.28334	1.39658	1.29148	0.17308E-05	0.22600	0.25193	0.10994	0.08021	5.33055	0.187E-07	0.234E-03	22
23	10.95000	1.49713	1.28156	0.18110E-05	0.24476	0.14262	0.06251	0.04322	5.74022	0.179E-07	0.415E-03	23
24	11.61667	1.60147	1.27264	0.16365E-05	0.23082	0.13250	0.05830	0.03764	6.10899	0.171E-07	0.453E-03	24
25	12.28334	1.60925	1.26348	0.16856E-05	0.24949	1.88934	0.83471	0.51998	6.48726	0.161E-07	0.310E-04	25
26	12.95000	1.66359	1.25427	0.17013E-05	0.31773	0.27728	0.12300	0.07517	6.86766	0.127E-07	0.169E-03	26
27	13.28334	1.72959	1.25003	0.15703E-05	0.23242	0.10900	0.04844	0.02855	7.04286	0.159E-07	0.558E-03	27
28	14.28334	1.76299	1.23588	0.17578E-05	0.20736	0.73973	0.33084	0.18946	7.62741	0.197E-07	0.104E-03	28
29	14.95000	1.86297	1.22658	0.17417E-05	0.22452	0.16870	0.07577	0.04181	8.01189	0.179E-07	0.429E-03	29
30	15.28334	1.89334	1.22200	0.17160E-05	0.25549	0.28298	0.12735	0.06781	8.20093	0.155E-07	0.228E-03	30
31	16.28334	1.97172	1.20828	0.17261E-05	0.25857	0.33830	0.15320	0.07928	8.76784	0.152E-07	0.191E-03	31
32	16.95000	2.04471	1.19852	0.18496E-05	0.25069	0.26853	0.12214	0.06082	9.17105	0.166E-07	0.273E-03	32
33	17.28334	2.08236	1.19393	0.17435E-05	0.26168	0.25152	0.11465	0.05557	9.36066	0.149E-07	0.269E-03	33
34	17.95000	2.15394	1.18444	0.18095E-05	0.25103	0.28069	0.12849	0.06066	9.75261	0.160E-07	0.264E-03	34
35	18.28334	2.17778	1.17996	0.17143E-05	0.22768	0.40756	0.18696	0.08631	9.93790	0.167E-07	0.193E-03	35
36	18.95000	2.25833	1.17059	0.17979E-05	0.23712	0.25785	0.11879	0.05357	10.32481	0.166E-07	0.311E-03	36
37	19.28333	2.28868	1.16628	0.16569E-05	0.24953	0.32269	0.14896	0.06551	10.50276	0.145E-07	0.222E-03	37
38	19.95000	2.30756	1.15694	0.18046E-05	0.17843	1.13677	0.52703	0.22934	10.88870	0.219E-07	0.956E-04	38
39	20.61667	2.37608	1.14758	0.18162E-05	0.21708	0.31993	0.14897	0.06362	11.27544	0.180E-07	0.283E-03	39
40	21.28333	2.44462	1.13841	0.17868E-05	0.23719	0.32251	0.15082	0.06257	11.65433	0.161E-07	0.257E-03	40
41	22.61667	2.46913	1.12073	0.17371E-05	0.26633	1.77245	0.83577	0.34018	12.38484	0.137E-07	0.402E-04	41

42	23.28333	2.64495	1.11178	0.17659E-05	0.24465	0.13012	0.06162	0.02411	12.75459	0.150E-07	0.622E-03	42
43	23.95000	2.72952	1.10292	0.17542E-05	0.26169	0.28131	0.13377	0.04978	13.12038	0.138E-07	0.278E-03	43
44	24.61667	2.80370	1.09430	0.17156E-05	0.29417	0.32159	0.15355	0.05551	13.47662	0.119E-07	0.215E-03	44
45	25.28333	2.92319	1.08531	0.17970E-05	0.27709	0.21550	0.10334	0.03609	13.84821	0.131E-07	0.364E-03	45
46	25.95000	3.02940	1.07619	0.18289E-05	0.30823	0.25533	0.12298	0.04133	14.22469	0.119E-07	0.288E-03	46
47	26.61667	3.13563	1.06741	0.17701E-05	0.22310	0.25486	0.12327	0.03999	14.58754	0.158E-07	0.395E-03	47
48	27.28334	3.26572	1.05897	0.17085E-05	0.32377	0.20770	0.10088	0.03152	14.93636	0.104E-07	0.331E-03	48
49	27.95000	3.40606	1.04955	0.19155E-05	0.31114	0.22394	0.10926	0.03276	15.32561	0.121E-07	0.368E-03	49
50	28.61667	3.54257	1.04068	0.18094E-05	0.34982	0.22551	0.11051	0.03181	15.69173	0.100E-07	0.316E-03	50
51	29.28334	3.68425	1.03176	0.18300E-05	0.34351	0.22759	0.11202	0.03100	16.06041	0.102E-07	0.331E-03	51
52	29.95000	3.82628	1.02258	0.18910E-05	0.35915	0.24264	0.11997	0.03195	16.43964	0.100E-07	0.314E-03	52
53	30.61667	4.01828	1.01355	0.18678E-05	0.37165	0.18438	0.09157	0.02335	16.81256	0.950E-08	0.407E-03	53
54	31.28334	4.19575	1.00547	0.16802E-05	0.38706	0.18711	0.09330	0.02272	17.14664	0.814E-08	0.358E-03	54
55	31.95000	4.33508	0.99643	0.18855E-05	0.41339	0.27657	0.13853	0.03248	17.51990	0.847E-08	0.261E-03	55
56	32.61667	4.52396	0.98801	0.17654E-05	0.39787	0.19750	0.09935	0.02243	17.86790	0.817E-08	0.364E-03	56
57	33.28334	4.71737	0.97913	0.18700E-05	0.41008	0.21218	0.10721	0.02320	18.23486	0.832E-08	0.359E-03	57
58	33.95000	4.91843	0.97050	0.18251E-05	0.42400	0.20679	0.10494	0.02179	18.59143	0.779E-08	0.358E-03	58
59	34.61667	5.15149	0.96217	0.17683E-05	0.39470	0.17988	0.09167	0.01821	18.93547	0.804E-08	0.441E-03	59
60	35.28334	5.39378	0.95351	0.18470E-05	0.42575	0.18842	0.09645	0.01830	19.29323	0.772E-08	0.422E-03	60
61	35.95000	6.97733	0.94529	0.17612E-05	4.46295	0.03194	0.01642	0.00267	19.63293	0.696E-09	0.261E-03	61
62	37.28334	6.14887	0.92912	0.17461E-05	0.45654	-0.12792	-0.06631	-0.01012	20.30093	0.663E-08	-0.656E-03	62
63	38.95000	6.83455	0.90797	0.18475E-05	0.39480	0.20005	0.10485	0.01617	21.17470	0.794E-08	0.491E-03	63
64	40.28334	7.46590	0.89105	0.18634E-05	0.39034	0.18582	0.09826	0.01373	21.87352	0.796E-08	0.579E-03	64
65	41.95000	8.33178	0.86688	0.19777E-05	0.35939	0.20714	0.11084	0.01403	22.78967	0.896E-08	0.638E-03	65

ENGINEERING STRAIN (65)= 22.7897

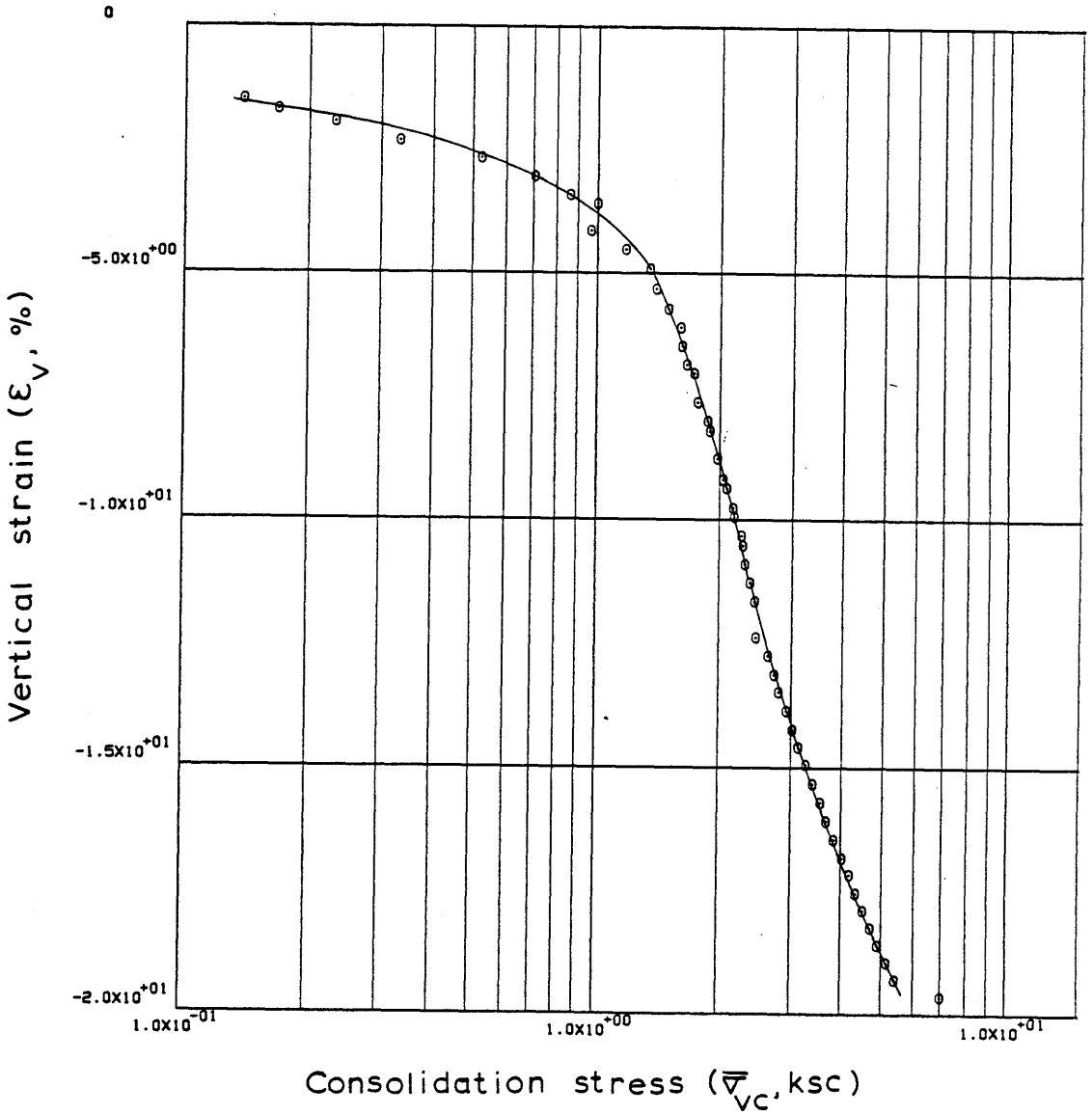

Sample No. SP17VERT w_N (%) 41.10 Estimated

Depth 83.49 w_L (%) 46.95 $\bar{\sigma}_{vo}$ 1.95 $\bar{\sigma}_{vm}$ 1.42-1.47

Soil Type Boston w_P (%) 23.48 CR 0.2900 0.1856 RR -

Blue Clay P.I.(%) 23.47 G_S 2.77 e_o 1.4205

⊙ At t_p Remarks Data from C.R.S.C test

w_L & w_P estimated from Baligh et al (1980)

Figure E.33 Compression Curve for Sample No. SP17VERT

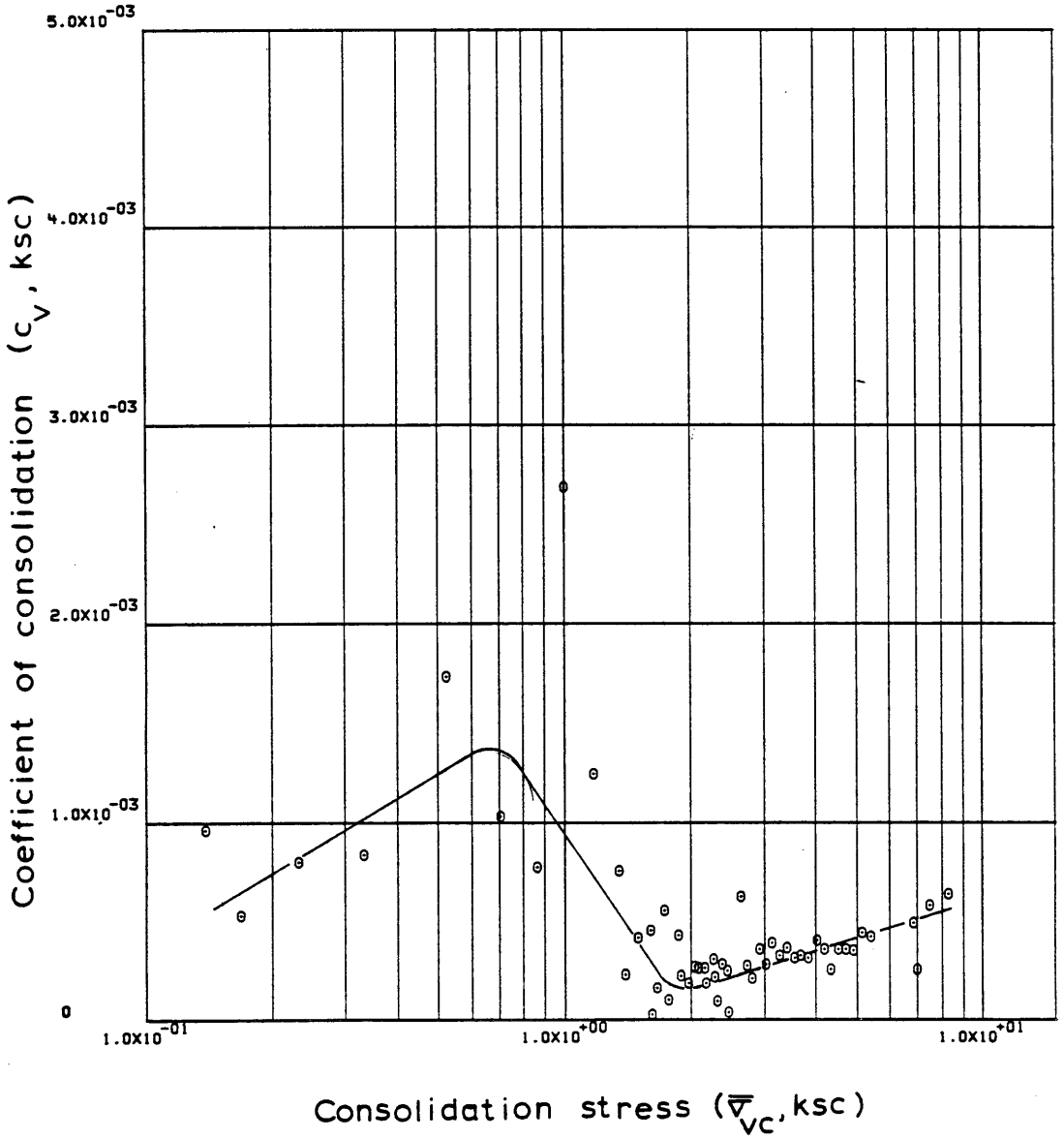

Sample No. SP17VERT w_N (%) 41.10 Estimated

Depth 83.49 w_L (%) 46.95 $\bar{\sigma}_{vo}$ 1.95 $\bar{\sigma}_{vm}$ 142-147

Soil Type Boston w_P (%) 23.48 CR 0.2900 0.1856 RR -

Blue Clay P.I.(%) 23.47 G_s 2.77 e_o 1.4205

o At t_p Remarks Data from C.R.S.C test

w_L & w_P estimated from Baligh et al (1980)

Figure E.34 Variation of coefficient of consolidation with consolidation stress for Sample No. SP17VERT

SP10VERT LINEAR THEORY

1-D STRAIN CONTROLLED COMPRESSION TEST

COMPUTED RESULTS

INITIAL VOID RATIO= 1.15555
INITIAL HEIGHT= 2.3368

ALL UNITS IN; KG,CM,SEC

LINEAR THEORY

	TIME IN HOURS	VERTICAL STRESS	E	RATE OF STRAIN	EXCESS PORE PRESSURE	C	C/1+E	MV	PERCENT COMPRESSION	K	CV	
1	0.0	0.03774	1.15588	0.0	-0.01801	0.0	0.0	-0.00411	-0.01550	0.0	0.0	1
2	0.33334	0.14384	1.15326	0.10153E-05	0.02093	0.00196	0.00091	0.01148	0.10620	0.132E-06	0.115E-01	2
3	0.66667	0.25066	1.14941	0.14914E-05	0.04573	0.00693	0.00322	0.01675	0.28467	0.885E-07	0.528E-02	3
4	1.00002	0.34013	1.14551	0.15148E-05	0.04350	0.01278	0.00596	0.02032	0.46558	0.942E-07	0.464E-02	4
5	1.33334	0.40638	1.14172	0.14735E-05	0.03218	0.02128	0.00993	0.02669	0.64128	0.123E-06	0.463E-02	5
6	1.66667	0.53600	1.13769	0.15719E-05	0.04064	0.01457	0.00681	0.01455	0.82835	0.104E-06	0.714E-02	6
7	2.00002	0.65253	1.13403	0.14294E-05	0.03558	0.01861	0.00872	0.01472	0.99817	0.107E-06	0.730E-02	7
8	2.33334	0.76976	1.13109	0.11494E-05	0.04013	0.01779	0.00835	0.01177	1.13452	0.764E-07	0.650E-02	8
9	2.66667	0.92770	1.12792	0.12430E-05	0.02379	0.01701	0.00799	0.00944	1.28177	0.139E-06	0.147E-01	9
10	3.00002	1.04515	1.12409	0.15024E-05	0.02210	0.03213	0.01513	0.01535	1.45941	0.180E-06	0.117E-01	10
11	3.33334	1.20545	1.12011	0.15652E-05	0.02210	0.02791	0.01316	0.01172	1.64417	0.187E-06	0.160E-01	11
12	3.66667	1.32879	1.11622	0.15294E-05	0.02943	0.03986	0.01884	0.01488	1.82436	0.137E-06	0.919E-02	12
13	4.00002	1.49299	1.11197	0.16785E-05	0.02379	0.03652	0.01729	0.01227	2.02171	0.185E-06	0.151E-01	13
14	4.33334	1.54826	1.10963	0.92194E-06	0.00404	0.06420	0.03043	0.02002	2.12999	0.597E-06	0.298E-01	14
15	4.66667	1.73666	1.10602	0.14304E-05	0.04576	0.03148	0.01495	0.00911	2.29767	0.815E-07	0.894E-02	15
16	5.00002	1.85375	1.10200	0.15951E-05	0.04240	0.06166	0.02934	0.01635	2.48434	0.977E-07	0.598E-02	16
17	5.33334	1.99730	1.09807	0.15588E-05	0.04240	0.05262	0.02508	0.01303	2.66640	0.951E-07	0.730E-02	17
18	5.66667	2.10545	1.09404	0.16040E-05	0.06269	0.07643	0.03650	0.01780	2.85341	0.659E-07	0.370E-02	18
19	6.00002	2.20382	1.08960	0.17702E-05	0.06210	0.09720	0.04652	0.02160	3.05930	0.731E-07	0.339E-02	19
20	6.33334	2.26828	1.08585	0.14992E-05	0.06155	0.13017	0.06241	0.02791	3.23340	0.623E-07	0.223E-02	20
21	6.66667	2.32347	1.08151	0.17376E-05	0.07511	0.18055	0.08674	0.03778	3.43475	0.589E-07	0.156E-02	21
22	7.00002	2.39646	1.07735	0.16668E-05	0.07452	0.13433	0.06466	0.02740	3.62750	0.567E-07	0.207E-02	22
23	7.33334	2.44709	1.07315	0.16890E-05	0.07452	0.20106	0.09698	0.04003	3.82246	0.572E-07	0.143E-02	23
24	7.66667	2.50843	1.06906	0.16470E-05	0.08130	0.16511	0.07980	0.03221	4.01215	0.510E-07	0.158E-02	24
25	8.00002	2.57222	1.06487	0.16902E-05	0.08694	0.16680	0.08078	0.03180	4.20645	0.487E-07	0.153E-02	25
26	8.33334	2.57892	1.06063	0.17181E-05	0.08185	1.63482	0.79336	0.30803	4.40353	0.524E-07	0.170E-03	26
27	8.66667	2.58132	1.05632	0.17432E-05	0.08072	4.61462	2.24411	0.86935	4.60310	0.537E-07	0.617E-04	27
28	9.00002	2.64924	1.05220	0.16740E-05	0.09031	0.15871	0.07734	0.02958	4.79434	0.459E-07	0.155E-02	28
29	9.33334	2.65683	1.04807	0.16830E-05	0.08691	1.50519	0.73493	0.27693	4.98624	0.477E-07	0.172E-03	29
30	9.66667	2.69543	1.04447	0.14660E-05	0.08467	0.24745	0.12103	0.04523	5.15308	0.425E-07	0.940E-03	30
31	10.00002	2.69377	1.04142	0.12462E-05	0.07961	-4.97960	-2.43929	-0.90540	5.29472	0.383E-07	-0.423E-04	31
32	10.33334	2.71680	1.03760	0.15624E-05	0.07284	0.44891	0.22031	0.08143	5.47192	0.523E-07	0.643E-03	32
33	10.66667	2.73833	1.03356	0.16546E-05	0.07851	0.51158	0.25157	0.09222	5.65926	0.512E-07	0.555E-03	33
34	11.00002	2.76416	1.02924	0.17721E-05	0.08020	0.45959	0.22648	0.08233	5.85942	0.535E-07	0.649E-03	34
35	11.33334	2.78962	1.02499	0.17489E-05	0.07229	0.46336	0.22882	0.08240	6.05659	0.583E-07	0.707E-03	35
36	11.66667	2.80626	1.02045	0.18755E-05	0.08017	0.76519	0.37872	0.13532	6.26753	0.561E-07	0.415E-03	36
37	12.00002	2.82853	1.01597	0.18523E-05	0.07958	0.56677	0.28114	0.09980	6.47543	0.556E-07	0.557E-03	37
38	12.66667	2.88016	1.00731	0.17976E-05	0.09083	0.47879	0.23853	0.08356	6.87717	0.469E-07	0.561E-03	38
39	13.00002	2.90249	1.00322	0.17013E-05	0.09025	0.52941	0.26428	0.09140	7.06691	0.445E-07	0.486E-03	39
40	13.33334	2.91185	0.99943	0.15777E-05	0.08405	1.17685	0.58859	0.20245	7.24251	0.441E-07	0.218E-03	40
41	13.66667	2.94004	0.99564	0.15852E-05	0.09251	0.39403	0.19745	0.06747	7.41861	0.401E-07	0.594E-03	41

42	14.33334	2.96389	0.98579	0.20647E-05	0.07955	1.21820	0.61346	0.20779	7.87517	0.601E-07	0.289E-03	42
43	14.66667	2.99430	0.98180	0.16780E-05	0.06940	0.39091	0.19725	0.06621	8.06029	0.558E-07	0.843E-03	43
44	15.00002	3.01281	0.97750	0.18151E-05	0.07445	0.69890	0.35343	0.11764	8.26010	0.560E-07	0.476E-03	44
45	15.33334	3.03192	0.97317	0.18282E-05	0.08120	0.68472	0.34701	0.11481	8.46094	0.515E-07	0.449E-03	45
46	15.66667	3.02901	0.96901	0.17608E-05	0.07270	-4.33525	-2.20174	-0.72665	8.65393	0.552E-07	-0.759E-04	46
47	16.00002	3.09036	0.96460	0.18696E-05	0.08117	0.21774	0.11083	0.03622	8.85843	0.522E-07	0.144E-02	47
48	17.66667	3.31650	0.94480	0.16970E-05	0.09021	0.28115	0.14457	0.04514	9.77705	0.418E-07	0.926E-03	48
49	18.00000	3.37077	0.94058	0.18104E-05	0.09247	0.25986	0.13391	0.04004	9.97266	0.433E-07	0.108E-02	49
50	18.33334	3.43825	0.93671	0.16649E-05	0.09248	0.19518	0.10078	0.02961	10.15219	0.397E-07	0.134E-02	50
51	18.66667	3.48237	0.93249	0.18218E-05	0.08966	0.33135	0.17146	0.04955	10.34816	0.446E-07	0.900E-03	51
52	19.00000	3.54970	0.92845	0.17440E-05	0.09753	0.21075	0.10929	0.03108	10.53540	0.391E-07	0.126E-02	52
53	19.33334	3.61782	0.92391	0.19683E-05	0.09922	0.23911	0.12428	0.03468	10.74623	0.431E-07	0.124E-02	53
54	19.66667	3.68461	0.91973	0.18152E-05	0.10541	0.22861	0.11908	0.03261	10.94022	0.373E-07	0.114E-02	54
55	20.00000	3.74463	0.91549	0.18436E-05	0.11669	0.26221	0.13689	0.03685	11.13680	0.341E-07	0.924E-03	55
56	20.33334	3.79224	0.91139	0.17866E-05	0.11611	0.32440	0.16972	0.04504	11.32689	0.330E-07	0.733E-03	56
57	20.66667	3.89173	0.90728	0.17957E-05	0.11893	0.15869	0.08320	0.02166	11.51756	0.323E-07	0.149E-02	57
58	21.00000	3.97244	0.90341	0.16952E-05	0.12457	0.18863	0.09910	0.02520	11.69717	0.290E-07	0.115E-02	58
59	21.33334	4.05634	0.89985	0.15621E-05	0.12291	0.17042	0.08970	0.02234	11.86241	0.270E-07	0.121E-02	59
60	21.66667	4.13289	0.89625	0.15810E-05	0.12463	0.19242	0.10148	0.02479	12.02930	0.268E-07	0.108E-02	60
61	22.00000	4.20382	0.89220	0.17833E-05	0.10939	0.23797	0.12577	0.03017	12.21715	0.343E-07	0.114E-02	61
62	22.33334	4.28861	0.88823	0.17507E-05	0.11899	0.19868	0.10522	0.02478	12.40120	0.308E-07	0.124E-02	62

ENGINEERING STRAIN (62)= 12.4012

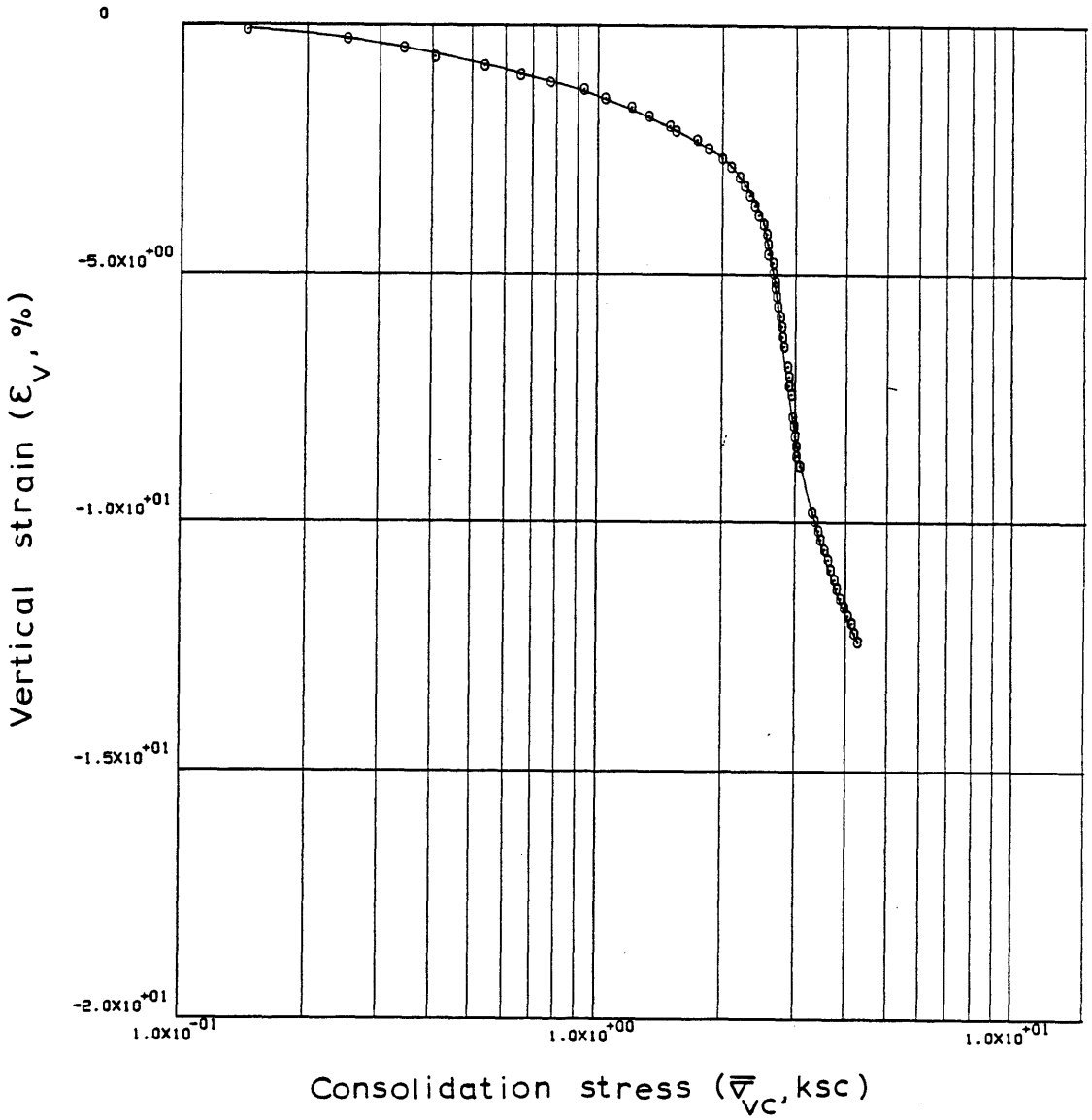

Sample No. SP10 VERT w_N (%) 44.50 Estimated

Depth 84.49 w_L (%) 46.26 $\bar{\sigma}_{vo}$ 1.97 $\bar{\sigma}_{vm}$ 248-255
0.5600

Soil Type Boston w_P (%) 23.37 CR 0.2260 RR -

Blue Clay P.I.(%) 22.89 G_s 2.77 e_o 1.1555

⊙ At t_p Remarks Data from C.R.S.C test

w_L & w_P estimated from Baligh et al (1980)

Figure E.35 Compression Curve for Sample No. SP10VERT

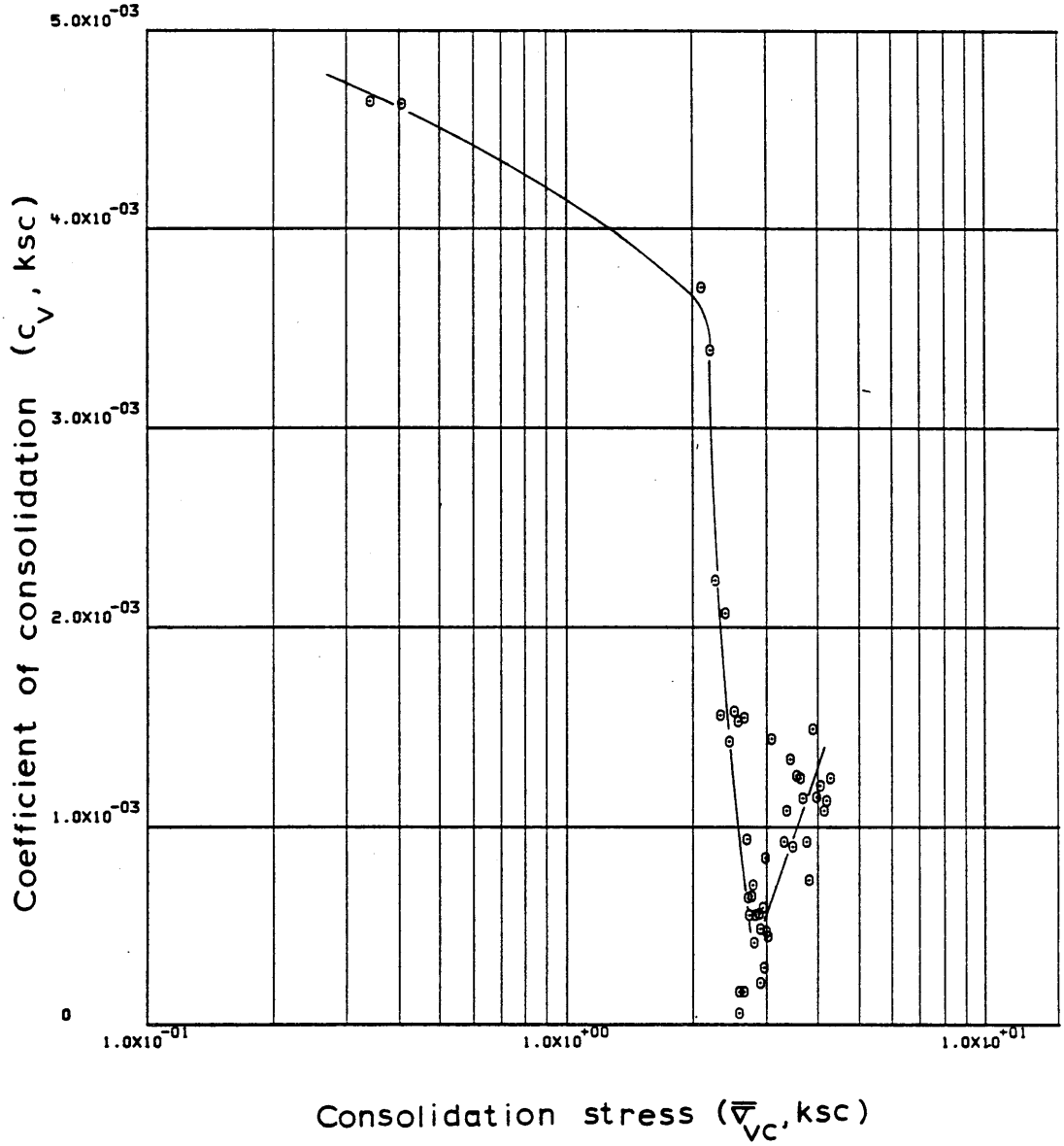

Sample No. SP10VERT w_N (%) 44.50 Estimated

Depth 84.49 w_L (%) 46.26 $\bar{\sigma}_{vo}$ 1.97 / 0.5600 $\bar{\sigma}_{vm}$ 248.255

Soil Type Boston Blue Clay w_P (%) 23.37 CR 0.2260 RR -

P.I.(%) 22.89 G_s 2.77 e_o 1.1555

⊖ At t_p

Remarks Data from C.R.S.C test

w_L & w_P estimated from Baligh et al (1980)

Figure E.36 Variation of coefficient of consolidation with consolidation stress for Sample No. SP10VERT

1-D STRAIN CONTROLLED COMPRESSION TEST

COMPUTED RESULTS

INITIAL VOID RATIO= 1.18124
INITIAL HEIGHT= 2.3368

ALL UNITS IN: KG,CM,SEC

LINEAR THEORY

	TIME IN HOURS	VERTICAL STRESS	E	RATE OF STRAIN	EXCESS PORE PRESSURE	C	C/1+E	MV	PERCENT COMPRESSION	K	CV	
1	0.0	0.15995	1.16656	0.0	-0.00203	0.0	0.0	0.04234	0.67262	0.0	0.0	1
2	0.83333	0.19513	1.16580	0.11846E-06	0.00305	0.00387	0.00179	0.01010	0.70792	0.104E-06	0.103E-01	2
3	1.57500	0.23117	1.16064	0.89398E-06	0.03520	0.03043	0.01408	0.06623	0.94434	0.680E-07	0.103E-02	3
4	1.91083	0.24940	1.15662	0.15410E-05	0.04025	0.05293	0.02454	0.10219	1.12856	0.102E-06	0.100E-02	4
5	2.24167	0.30828	1.15255	0.15871E-05	0.04815	0.01920	0.00892	0.03211	1.31511	0.876E-07	0.273E-02	5
6	2.57500	0.37763	1.14811	0.17242E-05	0.05324	0.02191	0.01020	0.02983	1.51888	0.858E-07	0.287E-02	6
7	2.90833	0.43639	1.14399	0.16010E-05	0.05324	0.02848	0.01328	0.03270	1.70770	0.793E-07	0.243E-02	7
8	3.24167	0.48556	1.13953	0.17375E-05	0.05771	0.04178	0.01953	0.04241	1.91222	0.791E-07	0.187E-02	8
9	3.57500	0.53800	1.13478	0.18539E-05	0.05486	0.04630	0.02169	0.04242	2.12994	0.884E-07	0.208E-02	9
10	3.90833	0.61557	1.13026	0.17666E-05	0.05991	0.03353	0.01574	0.02733	2.33698	0.768E-07	0.281E-02	10
11	4.24167	0.68073	1.12687	0.13279E-05	0.06105	0.03369	0.01584	0.02446	2.49234	0.565E-07	0.231E-02	11
12	4.57500	0.76890	1.12321	0.14382E-05	0.06331	0.03009	0.01417	0.01957	2.66037	0.588E-07	0.300E-02	12
13	4.90833	0.84283	1.11911	0.16112E-05	0.05658	0.04462	0.02106	0.02616	2.84818	0.734E-07	0.281E-02	13
14	5.24167	0.92283	1.11513	0.15688E-05	0.06053	0.04392	0.02076	0.02353	3.03073	0.665E-07	0.283E-02	14
15	5.57500	0.97478	1.11133	0.15006E-05	0.05603	0.06941	0.03287	0.03466	3.20503	0.685E-07	0.198E-02	15
16	5.90833	1.03594	1.10783	0.13822E-05	0.05321	0.05747	0.02726	0.02712	3.36534	0.662E-07	0.244E-02	16
17	6.24167	1.10312	1.10394	0.15428E-05	0.06112	0.06199	0.02946	0.02756	3.54393	0.641E-07	0.233E-02	17
18	6.57500	1.15095	1.09973	0.16678E-05	0.05266	0.09899	0.04714	0.04184	3.73656	0.801E-07	0.192E-02	18
19	6.90832	1.20702	1.09573	0.15915E-05	0.05211	0.08415	0.04015	0.03406	3.92004	0.770E-07	0.226E-02	19
20	7.24166	1.26952	1.09141	0.17221E-05	0.06225	0.08563	0.04094	0.03306	4.11823	0.694E-07	0.210E-02	20
21	7.57499	1.32946	1.08702	0.17529E-05	0.06562	0.09513	0.04558	0.03509	4.31946	0.668E-07	0.190E-02	21
22	7.90832	1.42328	1.08276	0.17028E-05	0.07689	0.06242	0.02997	0.02178	4.51459	0.551E-07	0.253E-02	22
23	8.24166	1.48977	1.07806	0.18853E-05	0.08143	0.10297	0.04955	0.03403	4.73010	0.574E-07	0.169E-02	23
24	8.57499	1.51027	1.07434	0.14951E-05	0.08367	0.27228	0.13126	0.08751	4.90073	0.441E-07	0.504E-03	24
25	8.90832	1.55746	1.07047	0.15593E-05	0.08143	0.12592	0.06082	0.03966	5.07834	0.471E-07	0.119E-02	25
26	9.24166	1.57504	1.06645	0.16194E-05	0.07521	0.35778	0.17314	0.11054	5.26244	0.528E-07	0.477E-03	26
27	9.57499	1.62735	1.06242	0.16305E-05	0.08030	0.12351	0.05988	0.03741	5.44743	0.496E-07	0.133E-02	27
28	9.90832	1.67172	1.05840	0.16259E-05	0.08707	0.14931	0.07254	0.04397	5.63158	0.454E-07	0.103E-02	28
29	10.24166	1.73660	1.05431	0.16604E-05	0.07861	0.10751	0.05234	0.03071	5.81923	0.512E-07	0.167E-02	29
30	10.57499	1.75826	1.05037	0.16013E-05	0.08425	0.31774	0.15497	0.08869	5.99986	0.459E-07	0.517E-03	30
31	10.90832	1.79917	1.04682	0.14430E-05	0.08088	0.15410	0.07529	0.04233	6.16232	0.429E-07	0.101E-02	31
32	11.24166	1.82025	1.04256	0.17395E-05	0.07693	0.36592	0.17915	0.09899	6.35782	0.541E-07	0.547E-03	32
33	11.57499	1.85274	1.03827	0.17531E-05	0.08143	0.24241	0.11893	0.06475	6.55440	0.513E-07	0.793E-03	33
34	11.90832	1.85029	1.03565	0.10708E-05	0.05720	-1.97002	-0.96776	-0.52284	6.67430	0.445E-07	-0.851E-04	34
35	12.24166	1.96219	1.03135	0.17648E-05	0.08934	0.07326	0.03607	0.01893	6.87155	0.468E-07	0.247E-02	35
36	12.57499	1.99153	1.02705	0.17670E-05	0.09326	0.28962	0.14288	0.07227	7.06857	0.447E-07	0.618E-03	36
37	12.90832	2.05335	1.02254	0.18611E-05	0.10172	0.14775	0.07305	0.03612	7.27565	0.430E-07	0.119E-02	37
38	13.24166	2.08630	1.01789	0.19206E-05	0.10790	0.29215	0.14478	0.06995	7.48889	0.416E-07	0.595E-03	38
39	13.57499	2.17814	1.01429	0.14888E-05	0.11244	0.08353	0.04147	0.01945	7.65385	0.308E-07	0.158E-02	39
40	13.90832	2.16066	1.01057	0.15404E-05	0.11072	-0.46126	-0.22942	-0.10575	7.82423	0.323E-07	-0.305E-03	40
41	14.24166	2.19869	1.00655	0.16681E-05	0.10677	0.23026	0.11475	0.05264	8.00838	0.361E-07	0.686E-03	41

42	14.57499	2.24332	1.00225	0.17906E-05	0.10563	0.21408	0.10692	0.04814	8.20561	0.390E-07	0.810E-03	42
43	14.90833	2.28504	0.99616	0.25421E-05	0.10395	0.33051	0.16557	0.07312	8.48480	0.559E-07	0.765E-03	43
44	15.24166	2.34912	0.99260	0.14913E-05	0.10171	0.12894	0.06471	0.02793	8.64830	0.334E-07	0.120E-02	44
45	15.57499	2.39361	0.98868	0.16416E-05	0.10058	0.20873	0.10496	0.04427	8.82787	0.370E-07	0.837E-03	45
46	15.90833	2.44884	0.98457	0.17254E-05	0.10622	0.18017	0.09079	0.03749	9.01625	0.367E-07	0.979E-03	46
47	16.24165	2.47668	0.98055	0.16934E-05	0.10508	0.35601	0.17975	0.07299	9.20076	0.363E-07	0.497E-03	47
48	16.57498	2.53495	0.97620	0.18318E-05	0.11127	0.18681	0.09453	0.03772	9.39992	0.369E-07	0.978E-03	48
49	16.90833	2.58658	0.97202	0.17671E-05	0.11464	0.20741	0.10518	0.04107	9.59164	0.344E-07	0.838E-03	49
50	17.24165	2.66728	0.96751	0.19078E-05	0.12027	0.14663	0.07453	0.02837	9.79816	0.352E-07	0.124E-02	50
51	17.57498	2.71964	0.96320	0.18336E-05	0.12533	0.22221	0.11319	0.04203	9.99620	0.324E-07	0.770E-03	51
52	17.90833	2.77577	0.95954	0.15551E-05	0.12477	0.17901	0.09135	0.03324	10.16386	0.275E-07	0.826E-03	52
53	18.24165	2.84799	0.95567	0.16500E-05	0.13041	0.15071	0.07706	0.02742	10.34134	0.278E-07	0.101E-02	53
54	18.57498	2.90706	0.95167	0.17058E-05	0.13041	0.19467	0.09975	0.03466	10.52451	0.286E-07	0.825E-03	54
55	18.90833	2.97941	0.94767	0.17133E-05	0.12815	0.16289	0.08364	0.02842	10.70811	0.291E-07	0.102E-02	55
56	19.24165	3.04404	0.94408	0.15392E-05	0.12759	0.16732	0.08607	0.02858	10.87271	0.262E-07	0.915E-03	56
57	19.57498	3.10442	0.94018	0.16715E-05	0.12309	0.19815	0.10213	0.03322	11.05113	0.293E-07	0.883E-03	57
58	19.90833	3.14889	0.93619	0.17183E-05	0.12196	0.28067	0.14496	0.04637	11.23416	0.303E-07	0.654E-03	58
59	20.24165	3.23496	0.93218	0.17317E-05	0.12701	0.14890	0.07706	0.02414	11.41823	0.292E-07	0.121E-02	59
60	20.57498	3.30025	0.92812	0.17542E-05	0.12024	0.20313	0.10535	0.03224	11.60432	0.311E-07	0.965E-03	60
61	20.90833	3.36633	0.92394	0.18079E-05	0.12474	0.21056	0.10944	0.03283	11.79568	0.308E-07	0.938E-03	61
62	21.24165	3.42950	0.91976	0.18182E-05	0.12867	0.22530	0.11736	0.03454	11.98770	0.299E-07	0.865E-03	62
63	21.57498	3.57472	0.91550	0.18516E-05	0.13378	0.10263	0.05358	0.01530	12.18283	0.291E-07	0.190E-02	63
64	21.90833	3.63162	0.91134	0.18144E-05	0.14448	0.26347	0.13785	0.03826	12.37361	0.263E-07	0.688E-03	64
65	22.24165	3.70463	0.90744	0.17018E-05	0.14389	0.19572	0.10261	0.02797	12.55220	0.247E-07	0.883E-03	65
66	22.57498	3.77997	0.90348	0.17362E-05	0.14218	0.19703	0.10351	0.02766	12.73402	0.254E-07	0.918E-03	66
67	22.90833	3.81909	0.89956	0.17179E-05	0.14159	0.38028	0.20020	0.05269	12.91354	0.251E-07	0.477E-03	67
68	23.24165	3.94593	0.89598	0.15726E-05	0.13368	0.10949	0.05775	0.01488	13.07758	0.243E-07	0.163E-02	68
69	23.57498	4.07180	0.89259	0.14959E-05	0.13993	0.10819	0.05716	0.01426	13.23331	0.220E-07	0.154E-02	69
70	23.90833	4.15744	0.88876	0.16870E-05	0.13541	0.18372	0.09727	0.02364	13.40863	0.255E-07	0.108E-02	70
71	24.24165	4.22190	0.88457	0.18549E-05	0.13483	0.27262	0.14466	0.03453	13.60094	0.280E-07	0.812E-03	71
72	24.57498	4.32733	0.88043	0.18338E-05	0.13878	0.16778	0.08922	0.02087	13.79062	0.268E-07	0.128E-02	72
73	24.90833	4.47902	0.87645	0.17660E-05	0.14669	0.11546	0.06153	0.01397	13.97296	0.243E-07	0.174E-02	73
74	25.24165	4.57506	0.87249	0.17644E-05	0.13936	0.18682	0.09977	0.02204	14.15469	0.255E-07	0.116E-02	74
75	25.57498	4.67013	0.86868	0.16993E-05	0.14610	0.18529	0.09916	0.02145	14.32941	0.233E-07	0.109E-02	75
76	25.90833	4.79317	0.86485	0.17102E-05	0.14384	0.14717	0.07892	0.01668	14.50485	0.237E-07	0.142E-02	76
77	26.24165	4.96063	0.86088	0.17804E-05	0.15639	0.11577	0.06222	0.01276	14.68712	0.226E-07	0.177E-02	77
78	26.57498	5.07276	0.85699	0.17442E-05	0.16317	0.17386	0.09363	0.01867	14.86530	0.212E-07	0.113E-02	78
79	26.90833	5.23126	0.85324	0.16867E-05	0.17390	0.12191	0.06578	0.01277	15.03728	0.191E-07	0.150E-02	79
80	27.24165	5.34472	0.84957	0.16515E-05	0.17614	0.17085	0.09237	0.01747	15.20534	0.184E-07	0.105E-02	80
81	32.08331	4.79437	0.83597	0.42516E-06	-0.09886	-0.12521	-0.06820	-0.01347	15.82910	-0.832E-08	0.618E-03	81
82	32.41664	3.95599	0.83843	-0.11161E-05	-0.12933	0.01281	0.00697	0.00160	15.71622	0.167E-07	0.105E-01	82
83	32.74998	3.34331	0.84193	-0.15861E-05	-0.13330	0.02083	0.01131	0.00311	15.55550	0.232E-07	0.746E-02	83
84	33.08331	2.86654	0.84482	-0.13054E-05	-0.13552	0.01879	0.01018	0.00329	15.42299	0.188E-07	0.573E-02	84
85	33.41664	2.49467	0.84830	-0.15662E-05	-0.13552	0.02500	0.01352	0.00505	15.26375	0.227E-07	0.448E-02	85
86	33.74998	2.16023	0.85179	-0.15722E-05	-0.14118	0.02428	0.01311	0.00564	15.10355	0.219E-07	0.388E-02	86
87	34.08331	1.87617	0.85543	-0.16347E-05	-0.14851	0.02581	0.01391	0.00691	14.93672	0.217E-07	0.315E-02	87
88	34.41664	1.64786	0.85899	-0.15953E-05	-0.14851	0.02742	0.01475	0.00838	14.77356	0.213E-07	0.254E-02	88
89	34.74998	1.44565	0.86284	-0.17207E-05	-0.15472	0.02939	0.01577	0.01021	14.59721	0.221E-07	0.217E-02	89
90	35.08331	1.28997	0.86616	-0.14860E-05	-0.13158	0.02920	0.01565	0.01145	14.44466	0.226E-07	0.197E-02	90
91	35.41664	1.20762	0.86899	-0.12578E-05	-0.11687	0.04276	0.02288	0.01833	14.31534	0.216E-07	0.118E-02	91
92	35.74998	1.07768	0.87287	-0.17285E-05	-0.13494	0.03412	0.01822	0.01596	14.13724	0.258E-07	0.162E-02	92
93	36.08331	0.97059	0.87619	-0.14767E-05	-0.14396	0.03177	0.01693	0.01655	13.98480	0.207E-07	0.125E-02	93
94	37.17499	0.67121	0.88944	-0.17840E-05	-0.14620	0.03592	0.01901	0.02342	13.37749	0.250E-07	0.107E-02	94
95	38.17499	0.48473	0.90110	-0.17031E-05	-0.16374	0.03581	0.01884	0.03288	12.84306	0.216E-07	0.656E-03	95
96	39.17499	0.34425	0.91294	-0.17200E-05	-0.15363	0.03461	0.01810	0.04408	12.30003	0.235E-07	0.533E-03	96

97	40.17499	0.31402	0.92274	-0.14160E-05	-0.10053	0.10661	0.05545	0.16858	11.85071	0.299E-07	0.177E-03 97
98	41.17499	0.28558	0.93084	-0.11652E-05	-0.08523	0.08532	0.04419	0.14749	11.47935	0.292E-07	0.198E-03 98
99	42.17499	0.25349	0.93823	-0.10582E-05	-0.07217	0.06195	0.03196	0.11872	11.14088	0.316E-07	0.266E-03 99
100	43.17499	0.25408	0.94244	-0.60265E-06	-0.06089	-1.80064	-0.92700	-3.65157	10.94768	0.214E-07	-0.587E-05100
101	44.17499	0.24923	0.94658	-0.59096E-06	-0.04905	0.21480	0.11034	0.43853	10.75783	0.262E-07	0.597E-04101
102	45.17499	0.25204	0.95244	-0.83363E-06	-0.04058	-0.52347	-0.26811	-1.06974	10.48921	0.449E-07	-0.420E-04102
103	46.17499	0.26001	0.95609	-0.51864E-06	-0.02478	-0.11729	-0.05996	-0.23419	10.32176	0.460E-07	-0.196E-03103
104	47.17499	0.21502	0.96044	-0.61518E-06	-0.03321	0.02285	0.01165	0.04922	10.12273	0.409E-07	0.830E-03104

ENGINEERING STRAIN (%104)= 10.1227

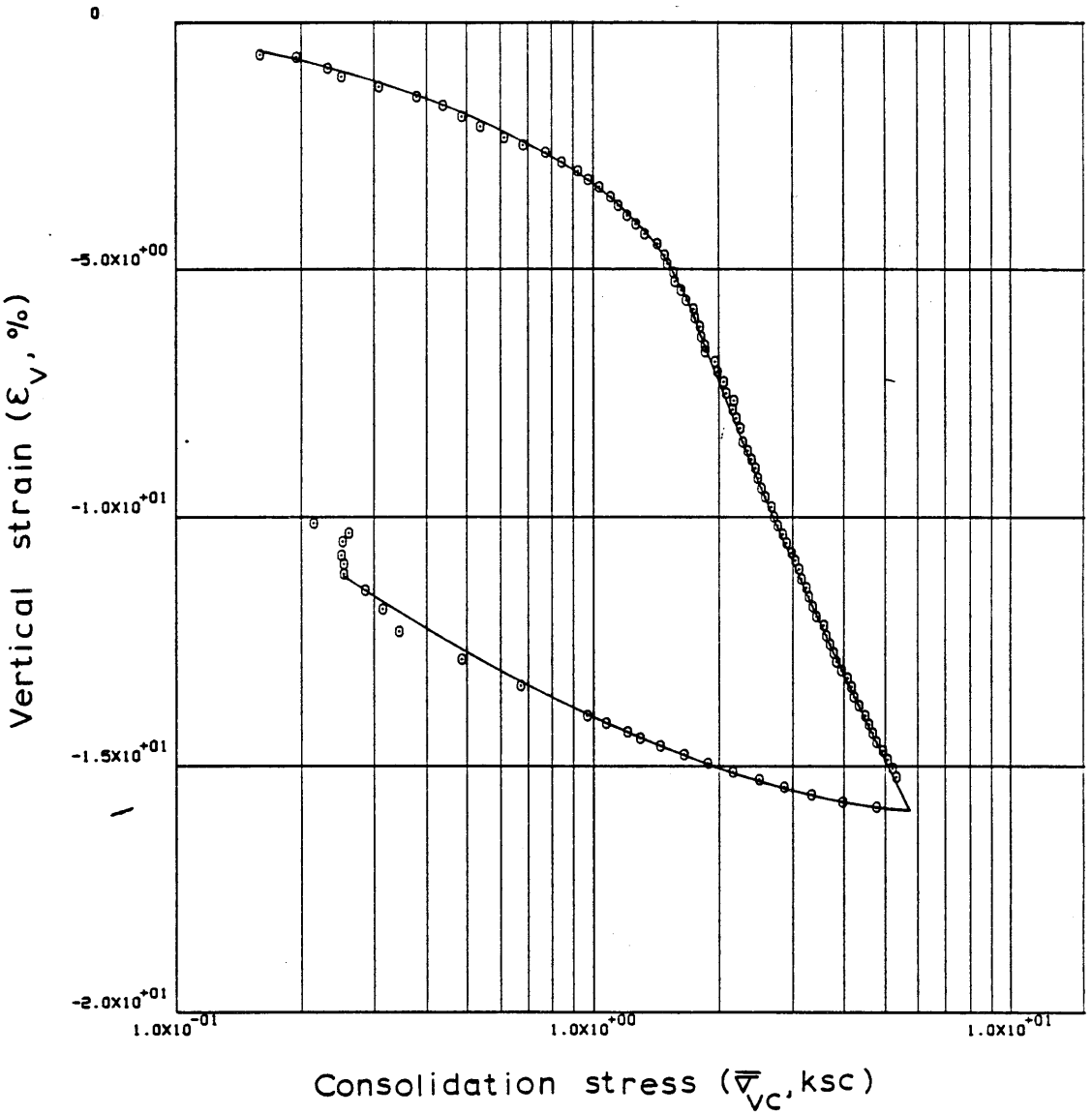

Sample No. SP18VERT w_N (%) 50.00 Estimated

Depth 88.49 w_L (%) 41.69 $\bar{\sigma}_{vo}$ 2.07 $\bar{\sigma}_{vm}$ 1.42-1.50

Soil Type Boston Blue Clay w_P (%) 22.58 CR 0.1912 RR 0.0332

P.I.(%) 19.11 G_s 2.77 e_o 1.1812

o At t_p

Remarks Data from C.R.S.C test

w_L & w_P estimated from Baligh et al (1980)

Figure E.37 Compression Curve for Sample No. SP18VERT

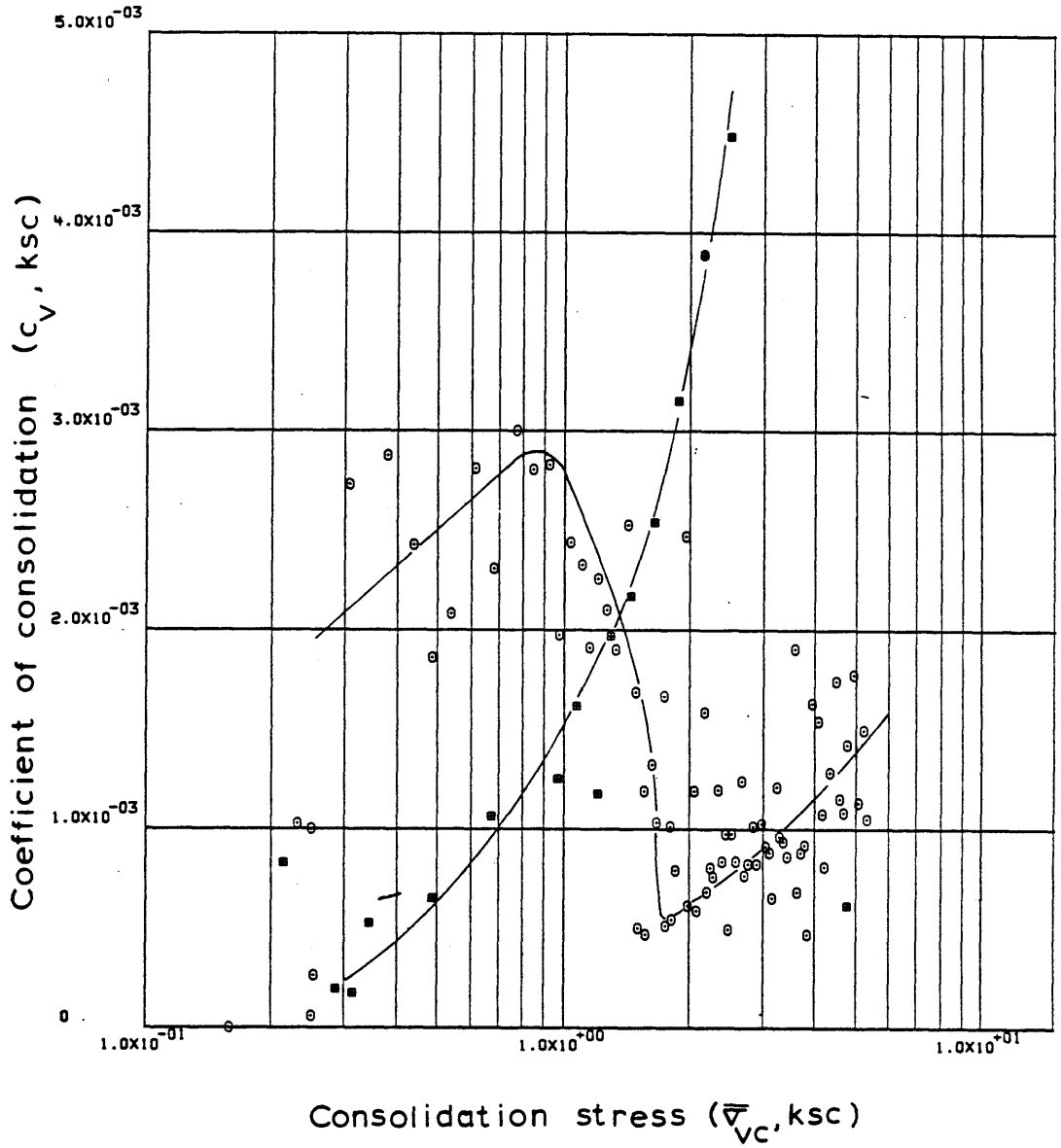

Sample No. SP18VERT w_N (%) 50.00 Estimated

Depth 88.49 w_L (%) 41.69 $\bar{\sigma}_{vo}$ 2.07 $\bar{\sigma}_{vm}$ 1.42-1.50

Soil Type Boston Blue Clay w_P (%) 22.58 CR 0.1912 RR 0.0332

P.I.(%) 19.11 G_s 2.77 e_o 1.1812

° At t_p

Remarks Data from C.R.S.C test

w_L & w_P estimated from Baligh et al (1980)

Figure E.38 Variation of coefficient of consolidation with consolidation stress for Sample No. SP18VERT

1-D STRAIN CONTROLLED COMPRESSION TEST

COMPUTED RESULTS

INITIAL VOID RATIO= 1.43823
INITIAL HEIGHT= 1.9406

ALL UNITS IN: KG,CM,SEC

LINEAR THEORY

	TIME IN HOURS	VERTICAL STRESS	E	RATE OF STRAIN	EXCESS PORE PRESSURE	C	C/1+E	MV	PERCENT COMPRESSION	K	CV	
1	0.0	0.00099	1.43769	0.0	0.00056	0.0	0.0	0.22049	0.02193	0.0	0.0	1
2	0.35833	0.01940	1.43302	0.14896E-05	0.01920	0.00157	0.00065	0.10438	0.21368	0.145E-06	0.139E-02	2
3	0.69167	0.01357	1.42879	0.14514E-05	0.02541	-0.01183	-0.00487	-0.29854	0.38718	0.107E-06	-0.357E-03	3
4	1.03056	0.01247	1.42441	0.14789E-05	0.03224	-0.05179	-0.02136	-1.64137	0.56660	0.854E-07	-0.520E-04	4
5	1.44304	0.00710	1.41862	0.16120E-05	0.03620	-0.01027	-0.00424	-0.44531	0.80406	0.825E-07	-0.185E-03	5
6	1.84165	0.00722	1.41302	0.16185E-05	0.04305	0.31470	0.13042	18.21933	1.03391	0.693E-07	0.381E-05	6
7	2.17499	0.00938	1.40844	0.15859E-05	0.05829	0.01754	0.00728	0.88224	1.22188	0.500E-07	0.567E-04	7
8	2.56028	0.02084	1.40359	0.14549E-05	0.07805	0.00608	0.00253	0.17612	1.42082	0.341E-07	0.194E-03	8
9	2.98082	0.03531	1.39802	0.15323E-05	0.09329	0.01055	0.00440	0.16034	1.64900	0.299E-07	0.187E-03	9
10	3.44388	0.06446	1.39199	0.15137E-05	0.10644	0.01003	0.00419	0.08656	1.89653	0.258E-07	0.298E-03	10
11	3.77721	0.08602	1.38802	0.13839E-05	0.11266	0.01375	0.00576	0.07702	2.05920	0.222E-07	0.288E-03	11
12	4.11055	0.10979	1.38334	0.16359E-05	0.11859	0.01917	0.00804	0.08258	2.25107	0.248E-07	0.301E-03	12
13	4.44388	0.13786	1.37933	0.14045E-05	0.12170	0.01761	0.00740	0.06004	2.41554	0.207E-07	0.345E-03	13
14	4.77721	0.16640	1.37566	0.12886E-05	0.12318	0.01953	0.00822	0.05418	2.56622	0.187E-07	0.345E-03	14
15	5.11055	0.20265	1.37165	0.14093E-05	0.12432	0.02035	0.00858	0.04666	2.73071	0.202E-07	0.433E-03	15
16	5.44388	0.24301	1.36706	0.16162E-05	0.12545	0.02527	0.01068	0.04805	2.91898	0.229E-07	0.476E-03	16
17	5.77721	0.28866	1.36309	0.13987E-05	0.12685	0.02304	0.00975	0.03676	3.08165	0.195E-07	0.530E-03	17
18	6.11055	0.32629	1.35875	0.15349E-05	0.12679	0.03546	0.01503	0.04895	3.25984	0.213E-07	0.436E-03	18
19	6.44388	0.37425	1.35429	0.15773E-05	0.12679	0.03250	0.01380	0.03947	3.44261	0.218E-07	0.553E-03	19
20	6.77721	0.42183	1.35019	0.14536E-05	0.12481	0.03425	0.01457	0.03666	3.61073	0.204E-07	0.556E-03	20
21	7.11055	0.48206	1.34640	0.13451E-05	0.12283	0.02838	0.01210	0.02680	3.76608	0.191E-07	0.713E-03	21
22	7.44388	0.53762	1.34226	0.14744E-05	0.12170	0.03799	0.01622	0.03184	3.93602	0.211E-07	0.661E-03	22
23	7.77721	0.60140	1.33834	0.13974E-05	0.12057	0.03498	0.01496	0.02629	4.09688	0.201E-07	0.763E-03	23
24	8.11055	0.66655	1.33451	0.13679E-05	0.11944	0.03725	0.01596	0.02520	4.25404	0.198E-07	0.785E-03	24
25	8.44388	0.74148	1.33027	0.15138E-05	0.11803	0.03973	0.01705	0.02424	4.42761	0.221E-07	0.910E-03	25
26	8.77721	0.79560	1.32733	0.10531E-05	0.08666	0.04176	0.01794	0.02335	4.54826	0.208E-07	0.893E-03	26
27	9.11055	0.83802	1.32515	0.78249E-06	0.08214	0.04202	0.01807	0.02214	4.63780	0.163E-07	0.737E-03	27
28	9.44388	0.86687	1.32390	0.44739E-06	0.06970	0.03686	0.01586	0.01861	4.68896	0.110E-07	0.590E-03	28
29	9.77721	0.87583	1.32390	0.0	0.06292	0.0	0.0	0.0	4.68896	0.0	0.100E+05	29
30	10.22583	0.92859	1.32334	0.15031E-06	0.07965	0.00965	0.00415	0.00460	4.71211	0.323E-08	0.701E-03	30
31	10.55916	0.94873	1.32267	0.23987E-06	0.06382	0.03115	0.01341	0.01429	4.73953	0.642E-08	0.449E-03	31
32	10.89249	0.97436	1.32258	0.32030E-07	0.07315	0.00333	0.00143	0.00150	4.74316	0.748E-09	0.499E-03	32
33	18.43388	2.60735	1.23576	0.14303E-05	0.17655	0.08820	0.03945	0.02378	8.30388	0.128E-07	0.539E-03	33
34	18.88165	2.67629	1.23532	0.12325E-06	0.18028	0.01703	0.00762	0.00288	8.32210	0.108E-08	0.375E-03	34
35	19.21500	2.71511	1.23527	0.16668E-07	0.18989	0.00311	0.00139	0.00052	8.32393	0.139E-09	0.270E-03	35
36	19.51555	2.75046	1.23527	-0.27869E-09	0.19208	0.0	0.0	-0.00001	8.32393	-0.230E-11	0.100E+05	36
37	20.83333	2.88942	1.23474	0.50339E-07	0.20782	0.01082	0.00484	0.00172	8.34579	0.383E-09	0.223E-03	37
38	21.10693	2.92060	1.23478	-0.20073E-07	0.21036	-0.00418	-0.00187	-0.00063	8.34398	-0.151E-09	0.238E-03	38
39	21.44026	2.94754	1.23465	0.49740E-07	0.21516	0.01454	0.00651	0.00222	8.34943	0.366E-09	0.165E-03	39
40	21.77361	2.98024	1.23461	0.16254E-07	0.21508	0.00398	0.00178	0.00060	8.35126	0.120E-09	0.200E-03	40
41	22.07166	3.01071	1.23452	0.37233E-07	0.22327	0.00872	0.00390	0.00131	8.35489	0.264E-09	0.201E-03	41

42	22.40498	3.04353	1.23452	0.0	0.22130	0.0	0.0	0.0	8.35489	0.0	0.100E+05	42
43	22.73833	3.06654	1.23461	-0.33290E-07	0.22582	-0.01178	-0.00527	-0.00174	8.35126	-0.233E-09	0.134E-03	43
44	23.07166	3.10849	1.17358	0.23396E-04	0.22864	4.49202	2.06664	0.66933	10.85402	0.153E-06	0.229E-03	44
45	23.40498	3.13374	1.16910	0.17235E-05	0.23195	0.55448	0.25563	0.08190	11.03801	0.111E-07	0.135E-03	45
46	23.73833	3.17216	1.16472	0.16853E-05	0.22921	0.35935	0.16600	0.05264	11.21759	0.109E-07	0.207E-03	46
47	24.07166	3.20833	1.16049	0.16322E-05	0.22836	0.37316	0.17272	0.05414	11.39113	0.106E-07	0.195E-03	47
48	24.42055	3.25151	1.15578	0.17381E-05	0.22941	0.35210	0.16333	0.05057	11.58417	0.112E-07	0.221E-03	48
49	25.33916	3.35797	1.14374	0.16986E-05	0.23147	0.37375	0.17434	0.05276	12.07800	0.107E-07	0.202E-03	49
50	25.66666	2.68857	1.14344	0.11649E-06	-0.01946	-0.00133	-0.00062	-0.00021	12.09009	-0.871E-08	0.425E-01	50
51	25.99637	2.17996	1.14558	-0.83935E-06	-0.06380	0.01019	0.00475	0.00196	12.00243	0.192E-07	0.979E-02	51
52	26.34998	1.81456	1.14901	-0.12535E-05	-0.07030	0.01869	0.00870	0.00437	11.86177	0.261E-07	0.597E-02	52
53	26.67610	1.54449	1.15217	-0.12514E-05	-0.07143	0.01962	0.00912	0.00544	11.73209	0.257E-07	0.472E-02	53
54	27.00943	1.33160	1.15548	-0.12800E-05	-0.06779	0.02233	0.01036	0.00721	11.59630	0.278E-07	0.385E-02	54
55	27.34276	1.17198	1.15894	-0.13350E-05	-0.06521	0.02708	0.01254	0.01004	11.45447	0.302E-07	0.301E-02	55
56	27.63416	1.04384	1.16193	-0.13157E-05	-0.06042	0.02576	0.01192	0.01077	11.33209	0.322E-07	0.299E-02	56
57	27.96748	0.95815	1.16420	-0.87452E-06	-0.00787	0.02653	0.01226	0.01225	11.23892	0.165E-06	0.135E-01	57
58	28.21748	0.93401	1.16501	-0.41832E-06	0.01468	0.03192	0.01475	0.01560	11.20549	-0.423E-07	-0.271E-02	58
59	28.57248	0.97864	1.16627	-0.45508E-06	0.04908	-0.02697	-0.01245	-0.01303	11.15385	-0.138E-07	0.106E-02	59
60	28.90581	1.24790	1.16568	0.22777E-06	0.11889	0.00243	0.00112	0.00102	11.17813	0.285E-08	0.280E-02	60
61	29.23915	1.51367	1.16247	0.12354E-05	0.16746	0.01660	0.00768	0.00558	11.30959	0.109E-07	0.196E-02	61
62	29.57248	1.75377	1.15893	0.13694E-05	0.16768	0.02410	0.01116	0.00684	11.45511	0.121E-07	0.176E-02	62
63	29.90581	1.99146	1.15584	0.11932E-05	0.17368	0.02428	0.01126	0.00602	11.58170	0.101E-07	0.168E-02	63
64	30.23915	2.25186	1.15201	0.14828E-05	0.18357	0.03117	0.01448	0.00683	11.73877	0.118E-07	0.173E-02	64
65	30.57248	2.48146	1.14842	0.13926E-05	0.18857	0.03697	0.01721	0.00728	11.88600	0.108E-07	0.148E-02	65
66	30.90581	2.71640	1.14504	0.13144E-05	0.19393	0.03741	0.01744	0.00671	12.02478	0.988E-08	0.147E-02	66
67	31.23915	2.88951	1.14103	0.15595E-05	0.20071	0.06485	0.03029	0.01081	12.18907	0.113E-07	0.104E-02	67
68	31.58192	3.05710	1.13680	0.16040E-05	0.20805	0.07502	0.03511	0.01181	12.36255	0.111E-07	0.944E-03	68
69	31.91527	3.16620	1.13324	0.13912E-05	0.21483	0.10155	0.04761	0.01530	12.50861	0.933E-08	0.610E-03	69
70	32.24860	3.27525	1.12910	0.16205E-05	0.21963	0.12226	0.05742	0.01783	12.67841	0.106E-07	0.594E-03	70
71	32.58192	3.36167	1.12498	0.16155E-05	0.22604	0.15819	0.07444	0.02243	12.84737	0.102E-07	0.456E-03	71
72	32.91527	3.43872	1.12066	0.16960E-05	0.22903	0.19048	0.08982	0.02642	13.02438	0.105E-07	0.399E-03	72
73	33.24860	3.50610	1.11650	0.16393E-05	0.23064	0.21457	0.10138	0.02919	13.19516	0.101E-07	0.345E-03	73
74	33.58194	3.58301	1.11238	0.16247E-05	0.23440	0.18978	0.08984	0.02535	13.36406	0.980E-08	0.386E-03	74
75	33.91527	3.64451	1.10835	0.15922E-05	0.23911	0.23676	0.11229	0.03106	13.52930	0.937E-08	0.302E-03	75
76	34.24860	3.71419	1.10395	0.17457E-05	0.23883	0.23272	0.11061	0.03007	13.71004	0.102E-07	0.341E-03	76
77	34.58194	3.77735	1.09952	0.17569E-05	0.23846	0.26248	0.12502	0.03338	13.89159	0.103E-07	0.308E-03	77
78	34.91527	3.84508	1.09538	0.16463E-05	0.24157	0.23296	0.11118	0.02917	14.06137	0.948E-08	0.325E-03	78
79	35.24860	3.92395	1.09120	0.16673E-05	0.24439	0.20606	0.09853	0.02537	14.23294	0.945E-08	0.372E-03	79
80	35.58194	3.98573	1.08706	0.16528E-05	0.24411	0.26503	0.12699	0.03211	14.40273	0.934E-08	0.291E-03	80
81	35.91527	4.06624	1.08290	0.16626E-05	0.24430	0.20776	0.09975	0.02478	14.57317	0.935E-08	0.377E-03	81
82	36.24860	4.13892	1.07858	0.17307E-05	0.24769	0.24372	0.11725	0.02858	14.75023	0.956E-08	0.335E-03	82
83	36.58194	4.21002	1.07431	0.17162E-05	0.24571	0.25077	0.12089	0.02896	14.92543	0.952E-08	0.329E-03	83
84	36.91527	4.27980	1.07050	0.15348E-05	0.24185	0.23194	0.11202	0.02639	15.08180	0.862E-08	0.326E-03	84
85	37.24860	4.36962	1.06648	0.16208E-05	0.24854	0.19360	0.09369	0.02166	15.24669	0.882E-08	0.407E-03	85
86	37.58194	4.44609	1.06240	0.16492E-05	0.25314	0.23521	0.11405	0.02588	15.41408	0.878E-08	0.339E-03	86
87	37.91527	4.53774	1.05812	0.17302E-05	0.25116	0.20945	0.10177	0.02265	15.58932	0.924E-08	0.408E-03	87
88	38.24860	4.61180	1.05403	0.16613E-05	0.25709	0.25290	0.12313	0.02692	15.75725	0.863E-08	0.321E-03	88
89	38.58194	4.70954	1.04993	0.16646E-05	0.25879	0.19532	0.09528	0.02044	15.92522	0.856E-08	0.419E-03	89
90	38.91527	4.78232	1.04593	0.16317E-05	0.26048	0.26121	0.12767	0.02690	16.08951	0.830E-08	0.309E-03	90
91	39.24860	4.88086	1.04152	0.17987E-05	0.26048	0.21602	0.10582	0.02190	16.27022	0.912E-08	0.416E-03	91
92	39.58194	4.97285	1.03743	0.16749E-05	0.26415	0.21932	0.10764	0.02185	16.43819	0.834E-08	0.382E-03	92
93	39.91527	5.07947	1.03338	0.16600E-05	0.26641	0.19094	0.09390	0.01868	16.60429	0.816E-08	0.437E-03	93
94	40.24860	5.17211	1.02928	0.16817E-05	0.26500	0.22663	0.11168	0.02178	16.77228	0.828E-08	0.380E-03	94
95	40.58194	5.26536	1.02519	0.16826E-05	0.26933	0.22880	0.11298	0.02165	16.93996	0.812E-08	0.375E-03	95
96	40.91527	5.36293	1.02100	0.17276E-05	0.27234	0.22823	0.11293	0.02125	17.11182	0.821E-08	0.386E-03	96

97	41.24860	5.47851	1.01704	0.16367E-05	0.27347	0.18580	0.09211	0.01699	17.27428	0.771E-08	0.454E-03	97
98	41.58194	5.57365	1.01273	0.17861E-05	0.27299	0.25054	0.12448	0.02253	17.45120	0.839E-08	0.373E-03	98
99	41.93748	5.69172	1.00850	0.16451E-05	0.27864	0.20177	0.10046	0.01783	17.62468	0.754E-08	0.423E-03	99
100	42.35416	5.84687	1.00360	0.16288E-05	0.27705	0.18203	0.09085	0.01575	17.82542	0.748E-08	0.475E-03	100
101	42.85416	6.01531	0.99737	0.17340E-05	0.28655	0.21950	0.10990	0.01853	18.08113	0.765E-08	0.413E-03	101
102	43.18748	6.14046	0.99327	0.17124E-05	0.29135	0.19891	0.09979	0.01642	18.24911	0.740E-08	0.450E-03	102
103	43.52083	6.26527	0.98909	0.17531E-05	0.29305	0.20792	0.10453	0.01686	18.42072	0.750E-08	0.445E-03	103
104	44.07054	6.47409	0.98223	0.17472E-05	0.29521	0.20906	0.10547	0.01656	18.70183	0.737E-08	0.445E-03	104
105	44.57971	6.69327	0.97632	0.16333E-05	0.30019	0.17774	0.08994	0.01366	18.94450	0.673E-08	0.493E-03	105
106	45.07639	6.89329	0.96978	0.18574E-05	0.30189	0.22217	0.11279	0.01660	19.21283	0.756E-08	0.455E-03	106
107	45.45055	7.06259	0.96559	0.15819E-05	0.30706	0.17259	0.08781	0.01259	19.38458	0.630E-08	0.501E-03	107
108	45.95055	7.26266	0.95913	0.18302E-05	0.30875	0.23103	0.11793	0.01647	19.64928	0.721E-08	0.438E-03	108
109	46.31166	7.42761	0.95473	0.17312E-05	0.31120	0.19594	0.10024	0.01364	19.82973	0.673E-08	0.493E-03	109
110	46.74500	7.64472	0.94962	0.16827E-05	0.31346	0.17762	0.09110	0.01209	20.03963	0.646E-08	0.535E-03	110
111	47.12360	6.21187	0.95011	-0.18416E-06	-0.03119	0.00236	0.00121	0.00018	20.01953	0.711E-08	0.406E-01	111
112	47.37360	5.44003	0.95166	-0.88675E-06	-0.10910	0.01174	0.00601	0.00103	19.95564	0.981E-08	0.948E-02	112
113	47.62360	4.82108	0.95367	-0.11389E-05	-0.13309	0.01657	0.00848	0.00166	19.87352	0.103E-07	0.625E-02	113
114	48.22276	3.72401	0.95910	-0.12848E-05	-0.14805	0.02103	0.01073	0.00253	19.65085	0.105E-07	0.418E-02	114
115	48.85944	2.88096	0.96550	-0.14225E-05	-0.16018	0.02497	0.01270	0.00387	19.38803	0.109E-07	0.281E-02	115
116	49.10944	2.61586	0.96808	-0.14572E-05	-0.16075	0.02673	0.01358	0.00495	19.28217	0.111E-07	0.225E-02	116
117	49.35944	2.38361	0.97067	-0.14554E-05	-0.16132	0.02777	0.01409	0.00564	19.17632	0.111E-07	0.197E-02	117
118	49.60942	2.16985	0.97316	-0.14034E-05	-0.16499	0.02652	0.01344	0.00591	19.07410	0.105E-07	0.178E-02	118
119	50.03415	1.85866	0.97752	-0.14423E-05	-0.16414	0.02818	0.01425	0.00709	18.89520	0.109E-07	0.154E-02	119
120	50.53415	1.56486	0.98255	-0.14092E-05	-0.14833	0.02922	0.01474	0.00863	18.68900	0.118E-07	0.137E-02	120
121	51.03415	1.31598	0.98798	-0.15172E-05	-0.15426	0.03134	0.01577	0.01097	18.46632	0.123E-07	0.112E-02	121
122	51.51997	1.12879	0.99345	-0.15700E-05	-0.14718	0.03568	0.01790	0.01467	18.24178	0.134E-07	0.915E-03	122
123	52.01997	0.97533	0.99835	-0.13611E-05	-0.11613	0.03350	0.01676	0.01597	18.04099	0.148E-07	0.929E-03	123
124	52.48804	0.89494	1.00088	-0.75254E-06	-0.03454	0.02949	0.01474	0.01577	17.93695	0.276E-07	0.175E-02	124
125	52.98804	0.84105	1.00262	-0.48110E-06	-0.01453	0.02792	0.01394	0.01607	17.86583	0.420E-07	0.262E-02	125
126	53.48804	0.74896	1.00631	-0.10228E-05	-0.10063	0.03186	0.01588	0.01999	17.71432	0.130E-07	0.648E-03	126
127	53.82582	0.68812	1.00925	-0.12021E-05	-0.10994	0.03467	0.01725	0.02402	17.59386	0.140E-07	0.582E-03	127
128	54.08359	0.63847	1.01147	-0.11903E-05	-0.11674	0.02966	0.01475	0.02225	17.50275	0.131E-07	0.587E-03	128
129	54.58359	0.59583	1.01587	-0.12128E-05	-0.09504	0.06368	0.03159	0.05120	17.32225	0.164E-07	0.321E-03	129
130	55.08359	0.53613	1.01912	-0.89481E-06	-0.05352	0.03080	0.01525	0.02698	17.18887	0.216E-07	0.800E-03	130
131	55.40414	0.45310	1.01921	-0.36221E-07	-0.04764	0.00050	0.00025	0.00050	17.18538	0.982E-09	0.195E-02	131
132	55.90414	0.40746	1.02383	-0.12685E-05	-0.11369	0.04351	0.02150	0.05002	16.99588	0.145E-07	0.289E-03	132

ENGINEERING STRAIN (132)= 16.9959

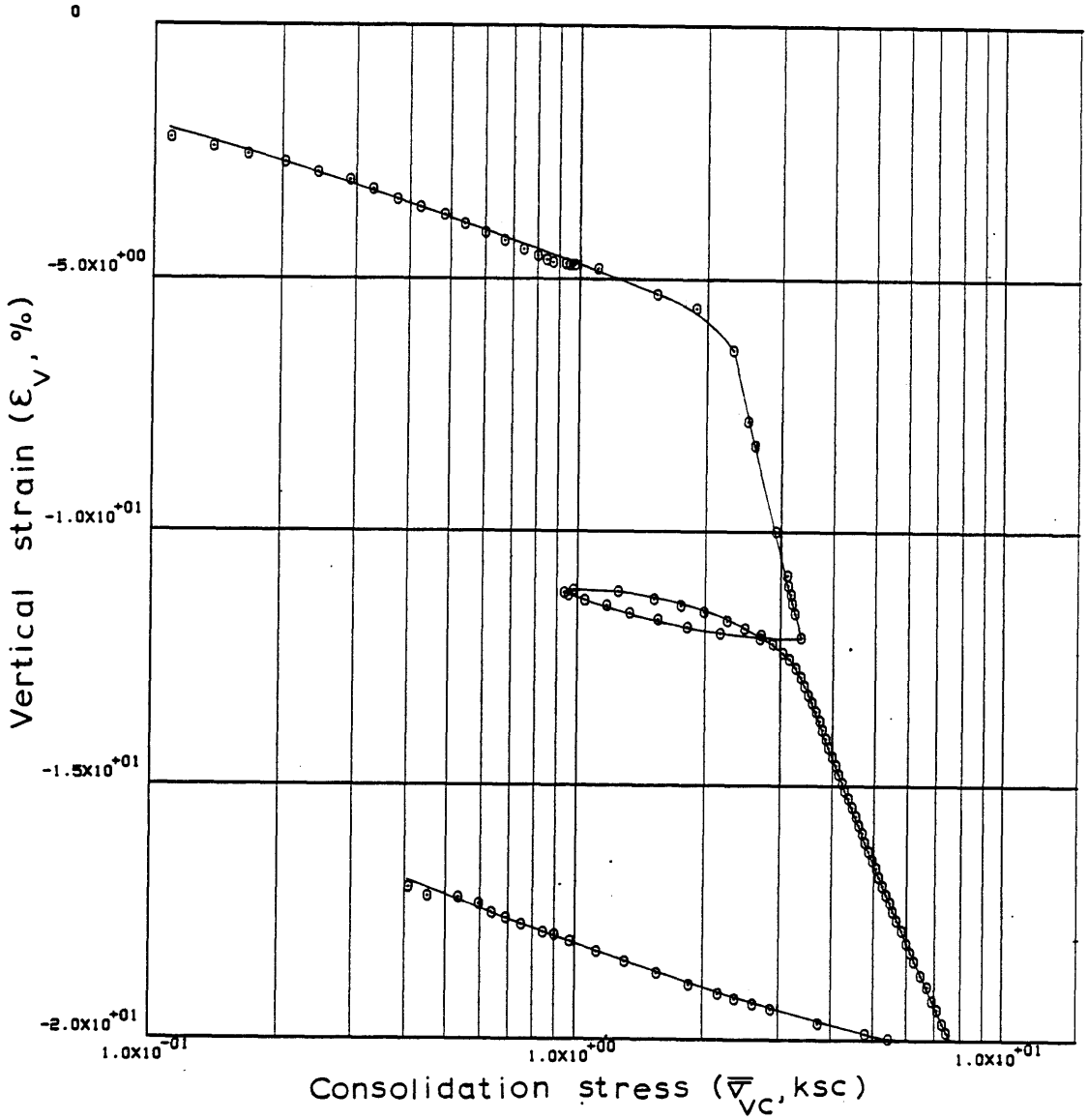

Sample No. 90-92-C-V w_N (%) 45.80 Estimated

Depth 90.89 w_L (%) 44.77 $\bar{\sigma}_{vo}$ 2.12 $\bar{\sigma}_{vm}$ 2.28

Soil Type Boston w_P (%) 23.22 CR 0.2470 RR 0.0243

Blue Clay P.I.(%) 21.55 G_s 2.77 e_o 1.4832

o At t_p Remarks Data from C.R.S.C test

w_L & w_P estimated from Baligh et al (1980)

Figure E.39 Compression Curve for Sample No. 90-92-C-V

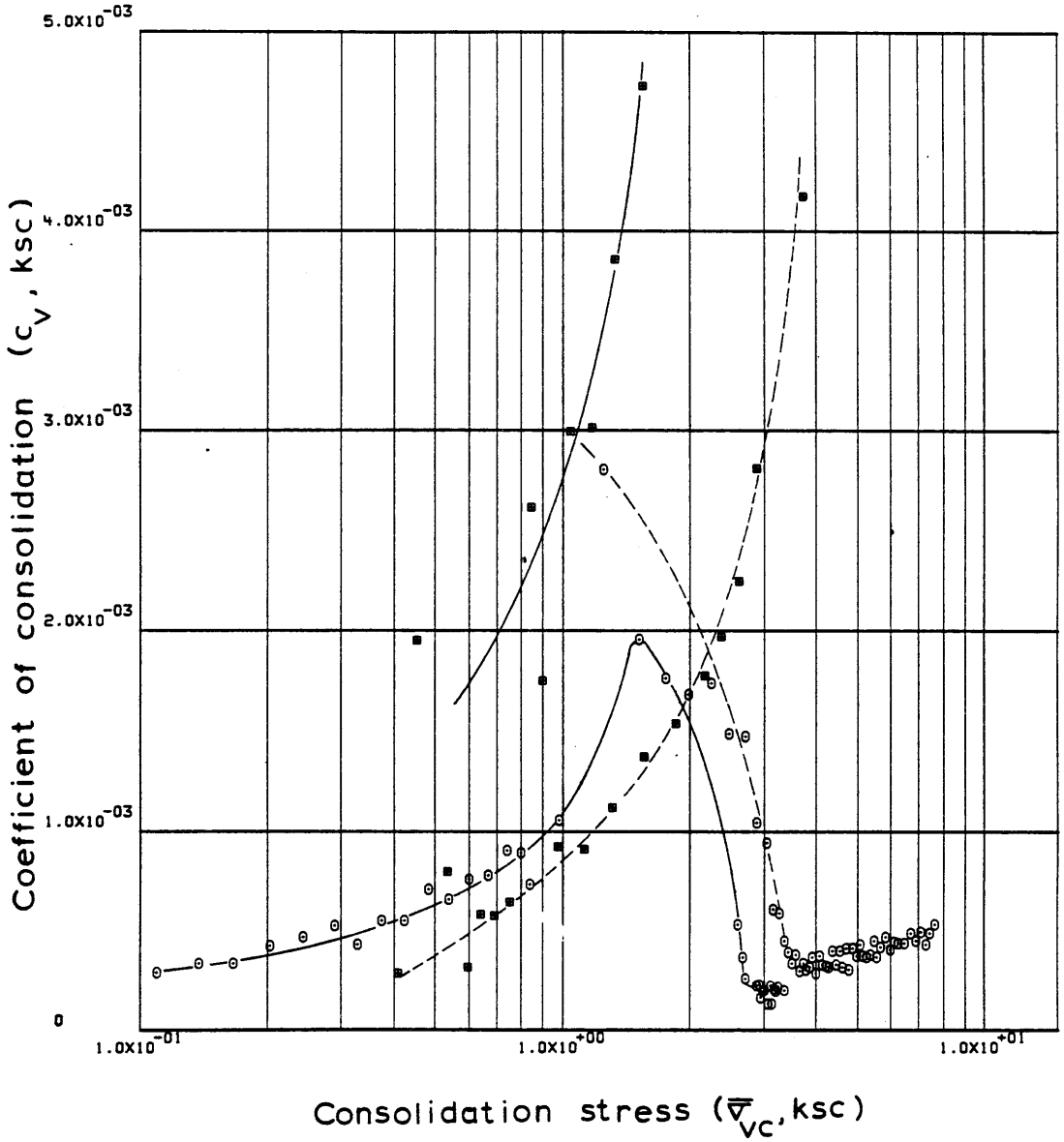

Sample No. 90-92-C.V w_N (%) 45.80 Estimated

Depth 90.89 w_L (%) 44.77 $\bar{\sigma}_{vo}$ 2.12 $\bar{\sigma}_{vm}$ 2.28

Soil Type Boston Blue Clay w_P (%) 23.22 CR 0.2470 RR 0.0243

P.I.(%) 21.55 G_s 2.77 e_o 1.4832

o At t_p

Remarks Data from C.R.S.C test

w_L & w_P estimated from Baligh et al (1980)

Figure E.40 Variation of coefficient of consolidation with consolidation stress for Sample No. 90-92-C-V

1-D STRAIN CONTROLLED COMPRESSION TEST

COMPUTED RESULTS

INITIAL VOID RATIO= 1.35573
INITIAL HEIGHT= 1.9050

ALL UNITS IN: KG,CM,SEC

LINEAR THEORY

	TIME IN HOURS	VERTICAL STRESS	E	RATE OF STRAIN	EXCESS PORE PRESSURE	C	C/1+E	MV	PERCENT COMPRESSION	K	CV	
1	0.0	0.00569	1.35546	0.0	-0.01808	0.0	0.0	0.02055	0.01173	0.0	0.0	1
2	0.66667	0.20166	1.34623	0.16391E-05	0.01989	0.00259	0.00110	0.02007	0.40350	0.148E-06	0.739E-02	2
3	1.00000	0.28572	1.34087	0.19065E-05	0.02325	0.01537	0.00657	0.02722	0.63083	0.147E-06	0.540E-02	3
4	1.66667	0.45676	1.32981	0.19788E-05	0.02490	0.02359	0.01012	0.02777	1.10057	0.141E-06	0.508E-02	4
5	2.00000	0.56951	1.32446	0.19182E-05	0.02373	0.02425	0.01043	0.02042	1.32770	0.143E-06	0.699E-02	5
6	2.33334	0.67987	1.31875	0.20522E-05	0.02543	0.03224	0.01390	0.02232	1.57010	0.142E-06	0.636E-02	6
7	2.66667	0.80338	1.31304	0.20574E-05	0.02543	0.03420	0.01479	0.01999	1.81248	0.142E-06	0.708E-02	7
8	3.00000	0.92788	1.30725	0.20896E-05	0.02709	0.04016	0.01741	0.02014	2.05809	0.134E-06	0.667E-02	8
9	3.33334	1.05137	1.30198	0.19078E-05	0.02709	0.04218	0.01833	0.01854	2.28181	0.122E-06	0.658E-02	9
10	3.66667	1.16171	1.29671	0.19122E-05	0.02879	0.05281	0.02299	0.02080	2.50554	0.115E-06	0.551E-02	10
11	4.00000	1.27205	1.29188	0.17566E-05	0.03049	0.05324	0.02323	0.01910	2.71060	0.989E-07	0.518E-02	11
12	4.33336	1.35740	1.28705	0.17601E-05	0.03106	0.07441	0.03254	0.02475	2.91571	0.969E-07	0.392E-02	12
13	4.66669	1.44886	1.28215	0.17898E-05	0.03328	0.07516	0.03293	0.02348	3.12376	0.916E-07	0.390E-02	13
14	5.00002	1.53200	1.27695	0.19031E-05	0.03672	0.09319	0.04093	0.02747	3.34448	0.879E-07	0.320E-02	14
15	5.33336	1.60608	1.27212	0.17718E-05	0.03615	0.10229	0.04502	0.02870	3.54953	0.827E-07	0.288E-02	15
16	5.66669	1.67582	1.26685	0.19375E-05	0.03956	0.12400	0.05470	0.03334	3.77325	0.823E-07	0.247E-02	16
17	6.00002	1.73922	1.26107	0.21288E-05	0.04007	0.15553	0.06879	0.04029	4.01846	0.888E-07	0.220E-02	17
18	6.33336	1.78503	1.25718	0.14347E-05	0.03786	0.14949	0.06623	0.03759	4.18341	0.631E-07	0.168E-02	18
19	6.66669	1.84897	1.25191	0.19503E-05	0.03956	0.14974	0.06649	0.03660	4.40714	0.817E-07	0.223E-02	19
20	7.00002	1.89323	1.24627	0.20944E-05	0.04243	0.23864	0.10624	0.05678	4.64677	0.814E-07	0.143E-02	20
21	7.33336	1.95304	1.24144	0.17964E-05	0.04017	0.15542	0.06934	0.03605	4.85194	0.735E-07	0.204E-02	21
22	7.66669	1.98401	1.23617	0.19644E-05	0.03506	0.33488	0.14976	0.07609	5.07565	0.916E-07	0.120E-02	22
23	8.00002	2.03538	1.23089	0.19691E-05	0.04017	0.20626	0.09246	0.04600	5.29944	0.798E-07	0.173E-02	23
24	8.33336	2.08101	1.22568	0.19510E-05	0.03851	0.23504	0.10560	0.05131	5.52066	0.821E-07	0.160E-02	24
25	8.66669	2.13125	1.22041	0.19787E-05	0.04021	0.22099	0.09952	0.04726	5.74443	0.793E-07	0.168E-02	25
26	9.00002	2.16695	1.21558	0.18178E-05	0.04078	0.29094	0.13131	0.06110	5.94958	0.716E-07	0.117E-02	26
27	9.33336	2.20795	1.21036	0.19660E-05	0.04082	0.27825	0.12588	0.05755	6.17096	0.769E-07	0.134E-02	27
28	9.66669	2.24498	1.20509	0.19928E-05	0.03685	0.31703	0.14377	0.06458	6.39479	0.860E-07	0.133E-02	28
29	10.00002	2.30707	1.20026	0.18308E-05	0.04139	0.17719	0.08053	0.03538	6.59999	0.700E-07	0.198E-02	29
30	10.33336	2.32833	1.19548	0.18139E-05	0.04030	0.52107	0.23734	0.10242	6.80284	0.709E-07	0.693E-03	30
31	10.66669	2.38858	1.19026	0.19862E-05	0.03978	0.20438	0.09331	0.03956	7.02446	0.783E-07	0.198E-02	31
32	11.00002	2.43615	1.18542	0.18439E-05	0.04317	0.24520	0.11220	0.04651	7.22971	0.667E-07	0.143E-02	32
33	11.33336	2.48283	1.18015	0.20162E-05	0.04261	0.27793	0.12748	0.05183	7.45364	0.735E-07	0.142E-02	33
34	11.66669	2.51320	1.17482	0.20408E-05	0.04369	0.43803	0.20141	0.08063	7.67972	0.722E-07	0.896E-03	34
35	12.00002	2.58545	1.16911	0.21951E-05	0.04596	0.20160	0.09294	0.03646	7.92227	0.735E-07	0.202E-02	35
36	12.33336	2.63269	1.16383	0.20311E-05	0.04710	0.29127	0.13461	0.05160	8.14615	0.660E-07	0.128E-02	36
37	12.66669	2.67420	1.15856	0.20361E-05	0.04935	0.33709	0.15617	0.05886	8.37003	0.629E-07	0.107E-02	37
38	13.00002	2.73517	1.15329	0.20411E-05	0.05049	0.23394	0.10864	0.04017	8.59390	0.613E-07	0.153E-02	38
39	13.33336	2.78707	1.14801	0.20461E-05	0.04992	0.28066	0.13066	0.04731	8.81783	0.618E-07	0.131E-02	39
40	13.66669	2.84622	1.14269	0.20687E-05	0.05385	0.25327	0.11820	0.04197	9.04359	0.577E-07	0.137E-02	40
41	14.00002	2.90391	1.13698	0.22277E-05	0.05497	0.28468	0.13321	0.04634	9.28609	0.605E-07	0.131E-02	41

42	14.33336	2.88892	1.13171	0.20613E-05	0.04138	-1.01839	-0.47773	-0.16495	9.50992	0.740E-07	-0.449E-03	42
43	14.66669	3.01242	1.12731	0.17214E-05	0.05950	0.10495	0.04934	0.01672	9.69646	0.428E-07	0.256E-02	43
44	15.00002	3.09725	1.12204	0.20708E-05	0.05838	0.18995	0.08951	0.02929	9.92033	0.522E-07	0.178E-02	44
45	15.33336	3.16401	1.11677	0.20759E-05	0.06121	0.24723	0.11680	0.03732	10.14415	0.497E-07	0.133E-02	45
46	15.66669	3.21647	1.11105	0.22550E-05	0.06234	0.34740	0.16456	0.05158	10.38664	0.527E-07	0.102E-02	46
47	16.00002	3.29694	1.10530	0.22764E-05	0.06512	0.23273	0.11054	0.03395	10.63075	0.507E-07	0.149E-02	47
48	16.33336	3.36614	1.10003	0.20921E-05	0.06682	0.25385	0.12088	0.03628	10.85458	0.451E-07	0.124E-02	48
49	16.66669	3.44906	1.09476	0.20974E-05	0.06852	0.21667	0.10343	0.03035	11.07840	0.439E-07	0.145E-02	49
50	17.00002	3.52953	1.08949	0.21026E-05	0.07135	0.22859	0.10940	0.03135	11.30217	0.421E-07	0.134E-02	50
51	17.33336	3.62316	1.08421	0.21079E-05	0.07248	0.20132	0.09659	0.02702	11.52596	0.413E-07	0.153E-02	51
52	17.66669	3.69236	1.07850	0.22900E-05	0.07418	0.30196	0.14528	0.03971	11.76845	0.436E-07	0.110E-02	52
53	18.00002	3.77273	1.07320	0.21322E-05	0.07696	0.24639	0.11884	0.03184	11.99362	0.389E-07	0.122E-02	53
54	18.33336	3.86937	1.06793	0.21242E-05	0.07866	0.20838	0.10077	0.02638	12.21736	0.378E-07	0.143E-02	54
55	18.42001	3.88453	1.06664	0.19955E-05	0.07418	0.32895	0.15917	0.04105	12.27197	0.376E-07	0.915E-03	55
56	18.58336	3.92313	1.06397	0.21972E-05	0.07526	0.26983	0.13074	0.03348	12.38521	0.407E-07	0.121E-02	56
57	18.65585	3.92369	1.06222	0.32648E-05	0.07696	12.19955	5.91575	1.50411	12.45975	0.590E-07	0.392E-04	57
58	19.05252	2.62954	1.06438	-0.73456E-06	-0.04536	0.00541	0.00262	0.00081	12.36784	0.226E-07	0.278E-01	58
59	19.38585	1.92820	1.06871	-0.17437E-05	-0.05277	0.01395	0.00674	0.00298	12.18411	0.462E-07	0.155E-01	59
60	19.71919	1.49173	1.07266	-0.15886E-05	-0.05390	0.01540	0.00743	0.00437	12.01636	0.414E-07	0.948E-02	60
61	20.05252	1.20457	1.07705	-0.17615E-05	-0.04995	0.02053	0.00988	0.00736	11.83003	0.497E-07	0.676E-02	61
62	20.38585	1.03532	1.08056	-0.14068E-05	-0.04824	0.02320	0.01115	0.00997	11.68089	0.413E-07	0.414E-02	62
63	20.71918	0.84781	1.08539	-0.19299E-05	-0.06013	0.02417	0.01159	0.01235	11.47589	0.456E-07	0.370E-02	63
64	21.05251	0.70286	1.09063	-0.20858E-05	-0.06071	0.02791	0.01335	0.01727	11.25377	0.491E-07	0.284E-02	64
65	21.38585	0.57642	1.09589	-0.20943E-05	-0.06129	0.02656	0.01267	0.01988	11.03020	0.491E-07	0.247E-02	65
66	21.71918	0.47382	1.10116	-0.20891E-05	-0.06412	0.02688	0.01279	0.02443	10.80656	0.470E-07	0.192E-02	66
67	21.83195	0.44941	1.10336	-0.25700E-05	-0.06355	0.04149	0.01973	0.04275	10.71341	0.585E-07	0.137E-02	67
68	21.89029	0.43815	1.10423	-0.19869E-05	-0.06468	0.03457	0.01643	0.03705	10.67616	0.445E-07	0.120E-02	68
69	22.22362	0.36462	1.10902	-0.18924E-05	-0.06415	0.02607	0.01236	0.03089	10.47285	0.429E-07	0.139E-02	69
70	22.55696	0.30736	1.11477	-0.22639E-05	-0.06129	0.03363	0.01590	0.04745	10.22896	0.540E-07	0.114E-02	70
71	22.80196	0.26676	1.11824	-0.18579E-05	-0.06132	0.02449	0.01156	0.04035	10.08162	0.445E-07	0.110E-02	71
72	22.81308	0.26676	1.11868	-0.51734E-05	-0.06132	0.0	0.0	0.0	10.06300	0.124E-06	0.100E+05	72
73	22.92140	0.34067	1.11916	-0.58038E-06	-0.00585	-0.00196	-0.00093	-0.00306	10.04262	0.146E-06	-0.476E-01	73
74	23.25475	0.60550	1.11437	0.18872E-05	0.04625	0.00832	0.00394	0.00855	10.24588	0.597E-07	0.698E-02	74
75	23.58807	0.76701	1.10914	0.20662E-05	0.05535	0.02212	0.01049	0.01535	10.46790	0.543E-07	0.354E-02	75
76	23.92140	0.94291	1.10387	0.20872E-05	0.05648	0.02552	0.01213	0.01424	10.69157	0.535E-07	0.376E-02	76
77	24.25475	1.12200	1.09904	0.19175E-05	0.05025	0.02778	0.01323	0.01285	10.89662	0.550E-07	0.428E-02	77
78	24.58807	1.30547	1.09424	0.19076E-05	0.04974	0.03166	0.01512	0.01248	11.10013	0.550E-07	0.441E-02	78
79	24.85806	1.44962	1.09073	0.17289E-05	0.05483	0.03354	0.01604	0.01166	11.24927	0.451E-07	0.387E-02	79
80	25.19141	2.43534	1.07188	0.75826E-05	0.06564	0.03634	0.01754	0.00923	12.04955	0.162E-06	0.176E-01	80
81	26.52473	2.69364	1.06661	0.53139E-06	0.06677	0.05229	0.02530	0.00987	12.27333	0.111E-07	0.113E-02	81
82	26.85806	2.92633	1.06181	0.19407E-05	0.06512	0.05795	0.02811	0.01001	12.47713	0.414E-07	0.414E-02	82
83	27.08113	3.08425	1.05829	0.21264E-05	0.07021	0.06688	0.03249	0.01081	12.62636	0.420E-07	0.388E-02	83
84	27.41473	3.30442	1.05343	0.19714E-05	0.07187	0.07050	0.03433	0.01075	12.83272	0.378E-07	0.352E-02	84
85	27.74806	3.51198	0.74177	0.14911E-03	0.07696	5.11606	2.93728	0.86209	26.06256	0.192E-05	0.223E-02	85
86	28.08141	3.69780	1.04242	-0.12267E-03	0.08370	-5.83137	-2.85513	-0.79219	13.30003	-0.200E-05	0.252E-02	86
87	28.41473	3.87674	1.03715	0.21559E-05	0.08540	0.11150	0.05473	0.01446	13.52371	0.343E-07	0.237E-02	87
88	28.74808	4.05195	1.03142	0.23523E-05	0.08478	0.12975	0.06387	0.01611	13.76717	0.374E-07	0.232E-02	88
89	29.08141	4.20360	1.02617	0.21574E-05	0.08653	0.14276	0.07046	0.01707	13.98984	0.335E-07	0.196E-02	89
90	29.41473	4.35152	1.02134	0.19918E-05	0.08597	0.13968	0.06910	0.01616	14.19489	0.310E-07	0.192E-02	90
91	29.74808	4.50792	1.01607	0.21783E-05	0.08540	0.14927	0.07404	0.01671	14.41861	0.339E-07	0.203E-02	91
92	30.08141	4.65535	1.01082	0.21754E-05	0.09112	0.16312	0.08112	0.01771	14.64143	0.316E-07	0.178E-02	92
93	30.41473	4.80386	1.00599	0.20074E-05	0.09225	0.15385	0.07670	0.01622	14.84654	0.286E-07	0.177E-02	93
94	30.74808	4.95237	1.00072	0.21955E-05	0.09338	0.17316	0.08655	0.01774	15.07033	0.308E-07	0.173E-02	94
95	31.08141	5.08749	0.99590	0.20098E-05	0.09456	0.17884	0.08960	0.01785	15.27467	0.277E-07	0.155E-02	95
96	31.41473	5.25410	0.99063	0.22071E-05	0.09173	0.16358	0.08217	0.01590	15.49844	0.312E-07	0.196E-02	96

97	31.74808	5.42353	0.98580	0.20280E-05	0.09740	0.15228	0.07669	0.01436	15.70360	0.268E-07	0.187E-02 97
98	32.08141	5.56962	0.98097	0.20331E-05	0.09966	0.18185	0.09180	0.01670	15.90875	0.262E-07	0.157E-02 98
99	32.41473	5.73479	0.97571	0.22176E-05	0.09972	0.17987	0.09104	0.01611	16.13193	0.284E-07	0.176E-02 99
100	32.74808	5.91081	0.97088	0.20438E-05	0.10085	0.15990	0.08113	0.01393	16.33713	0.257E-07	0.185E-02100
101	33.08141	6.08872	0.96560	0.22356E-05	0.09915	0.17781	0.09046	0.01508	16.56096	0.285E-07	0.189E-02101
102	33.41473	6.25403	0.96033	0.22417E-05	0.10085	0.19683	0.10041	0.01627	16.78479	0.279E-07	0.172E-02102
103	33.74808	6.45621	0.95551	0.20551E-05	0.10487	0.15161	0.07753	0.01220	16.98953	0.245E-07	0.201E-02103
104	34.08141	6.63529	0.95023	0.22536E-05	0.10657	0.19276	0.09884	0.01510	17.21341	0.263E-07	0.174E-02104
105	34.41473	6.82752	0.94540	0.20710E-05	0.10657	0.16927	0.08701	0.01293	17.41861	0.240E-07	0.186E-02105
106	34.74808	7.04402	0.94012	0.22653E-05	0.11394	0.16897	0.08709	0.01256	17.64253	0.245E-07	0.195E-02106
107	35.08141	7.22442	0.93529	0.20818E-05	0.11111	0.19117	0.09878	0.01385	17.84775	0.229E-07	0.166E-02107
108	35.41473	7.42604	0.93002	0.22772E-05	0.11507	0.19159	0.09927	0.01355	18.07161	0.241E-07	0.178E-02108
109	35.74808	7.66061	0.92518	0.20926E-05	0.11847	0.15548	0.08076	0.01071	18.27687	0.214E-07	0.200E-02109
110	36.08141	7.88088	0.91991	0.22892E-05	0.12017	0.18604	0.09690	0.01247	18.50075	0.230E-07	0.184E-02110
111	36.41473	8.12370	0.91507	0.21038E-05	0.12414	0.15931	0.08319	0.01040	18.70595	0.203E-07	0.195E-02111
112	36.74808	8.36992	0.91024	0.21078E-05	0.12703	0.16181	0.08471	0.01027	18.91106	0.198E-07	0.193E-02112
113	36.82974	8.42674	0.90892	0.23497E-05	0.12420	0.19510	0.10220	0.01216	18.96707	0.225E-07	0.185E-02113
114	36.85419	8.19190	0.90848	0.26324E-05	0.08618	-0.01562	-0.00819	-0.00099	18.98579	0.364E-07	-0.369E-01114
115	37.18752	6.41390	0.90979	-0.57298E-06	-0.04983	0.00537	0.00281	0.00039	18.93007	0.137E-07	0.355E-01115
116	37.52086	4.83154	0.91286	-0.13383E-05	-0.07024	0.01084	0.00567	0.00101	18.79967	0.228E-07	0.225E-01116
117	37.85419	3.75480	0.91681	-0.17171E-05	-0.08159	0.01566	0.00817	0.00191	18.63200	0.253E-07	0.132E-01117
118	38.18752	3.00202	0.92077	-0.17149E-05	-0.08442	0.01767	0.00920	0.00273	18.46420	0.245E-07	0.896E-02118
119	38.52086	2.44435	0.92516	-0.19011E-05	-0.08668	0.02137	0.01110	0.00409	18.27777	0.266E-07	0.650E-02119
120	38.85419	2.01920	0.92954	-0.18941E-05	-0.08670	0.02294	0.01189	0.00535	18.09164	0.266E-07	0.497E-02120
121	39.18752	1.68938	0.93394	-0.18921E-05	-0.08840	0.02463	0.01274	0.00688	17.90521	0.262E-07	0.380E-02121
122	39.66446	1.33080	0.93964	-0.17141E-05	-0.08557	0.02392	0.01233	0.00821	17.66292	0.246E-07	0.300E-02122
123	40.33113	0.97788	0.94843	-0.18780E-05	-0.09123	0.02850	0.01463	0.01277	17.29010	0.256E-07	0.200E-02123
124	40.99780	0.70642	0.95895	-0.22390E-05	-0.09238	0.03237	0.01652	0.01980	16.84326	0.304E-07	0.154E-02124
125	41.66446	0.52193	0.96993	-0.23215E-05	-0.10370	0.03626	0.01841	0.03020	16.37733	0.284E-07	0.941E-03125
126	42.14058	0.42026	0.97783	-0.23311E-05	-0.09521	0.03647	0.01844	0.03930	16.04187	0.313E-07	0.797E-03126
127	42.77252	0.30562	0.98793	-0.22327E-05	-0.09295	0.03170	0.01595	0.04431	15.61324	0.310E-07	0.700E-03127
128	43.43918	0.22200	0.99890	-0.22879E-05	-0.08842	0.03434	0.01718	0.06566	15.14731	0.338E-07	0.515E-03128
129	44.10583	0.16392	1.01030	-0.23616E-05	-0.08279	0.03756	0.01869	0.09758	14.66367	0.377E-07	0.386E-03129
130	44.59334	0.13461	1.01864	-0.23541E-05	-0.07996	0.04233	0.02097	0.14094	14.30963	0.392E-07	0.278E-03130
131	45.12807	0.11410	1.02786	-0.23613E-05	-0.07487	0.05578	0.02751	0.22169	13.91835	0.424E-07	0.191E-03131
132	45.63335	0.09775	1.03705	-0.24807E-05	-0.06753	0.05943	0.02917	0.27595	13.52812	0.498E-07	0.181E-03132
133	45.75278	0.09775	1.03836	-0.15022E-05	-0.06753	0.0	0.0	0.0	13.47224	0.302E-07	0.100E+05133

ENGINEERING STRAIN (133)= 13.4722

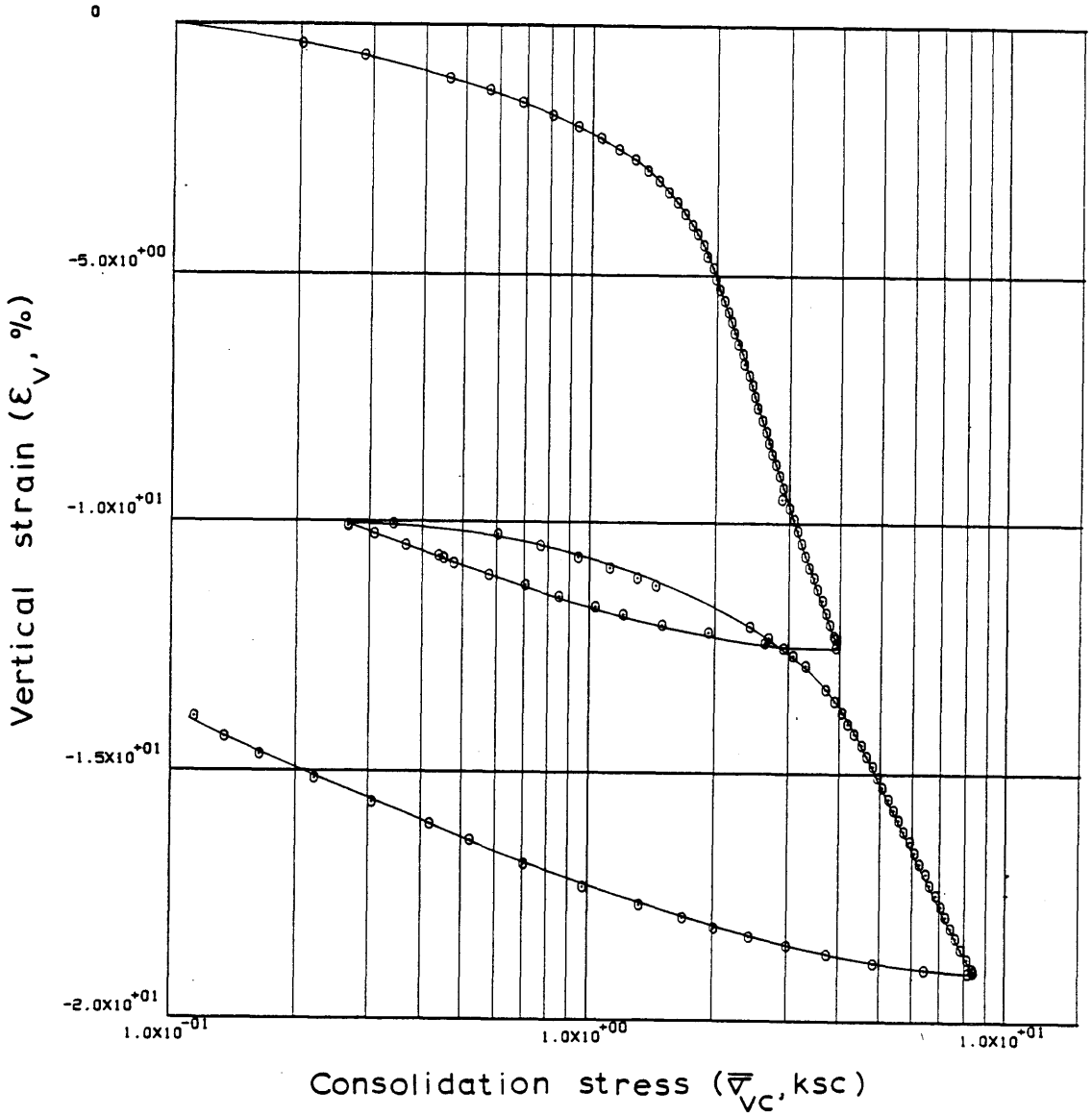

Sample No. 90-92-C-H w_N (%) 43.05 Estimated

Depth 90.25 w_L (%) 43.76 $\bar{\sigma}_{vo}$ 2.11 / 0.2525 $\bar{\sigma}_{vm}$ 1.73-1.82

Soil Type Boston Blue Clay w_P (%) 23.04 CR 0.1702 RR 0.0205

P.I.(%) 20.72 G_s 2.77 e_o 1.3557

⊙ At t_p Remarks Data from C.R.S.C test

w_L & w_P estimated from Baligh et al (1980)

Figure E.41 Compression Curve for Sample No. 90-92-C-H

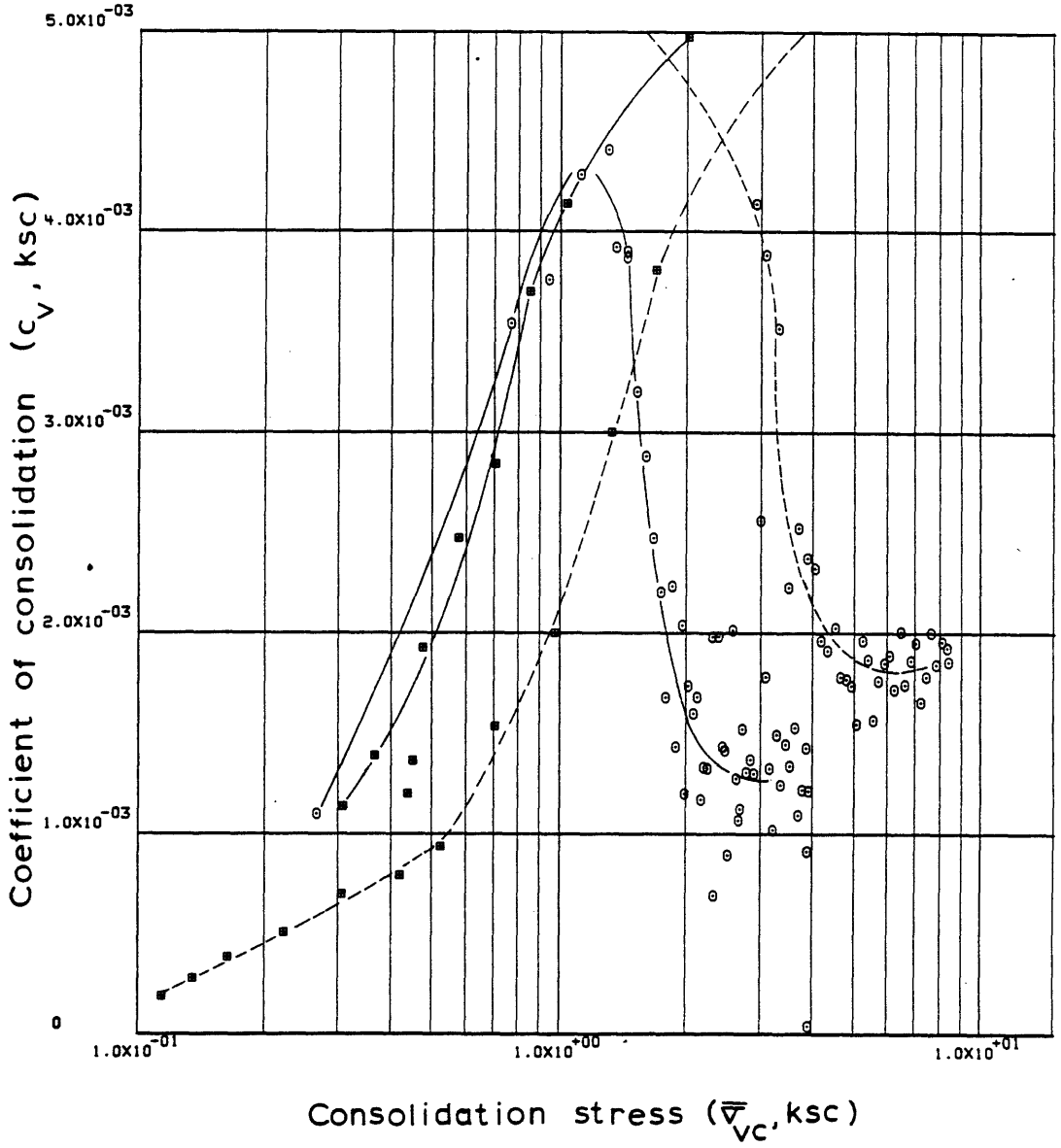

Sample No. 90-92-C-H w_N (%) 43.05 Estimated

Depth 90.25 w_L (%) 43.76 $\bar{\sigma}_{vo}$ 2.11 / 0.2525 $\bar{\sigma}_{vm}$ 1.73-1.82

Soil Type Boston Blue Clay w_P (%) 23.04 CR 0.170.2 RR 0.0205

P.I.(%) 20.72 G_s 2.77 e_o 1.3557

⊙ At t_p

Remarks Data from C.R.S.C test

w_L & w_P estimated from Baligh et al (1980)

Figure E.42 Variation of coefficient of consolidation with consolidation stress for Sample No. 90-92-C-H

1-D STRAIN CONTROLLED COMPRESSION TEST

COMPUTED RESULTS

INITIAL VOID RATIO= 1.30251
INITIAL HEIGHT= 2.3368

ALL UNITS IN: KG,CM,SEC

LINEAR THEORY

	TIME IN HOURS	VERTICAL STRESS	E	RATE OF STRAIN	EXCESS PORE PRESSURE	C	C/1+E	MV	PERCENT COMPRESSION	K	CV	
1	0.0	0.04142	1.30292	0.0	-0.04324	0.0	0.0	-0.00431	-0.01782	0.0	0.0	1
2	0.36667	0.04543	1.30030	0.86420E-06	-0.03249	0.02840	0.01235	0.28460	0.09612	-0.725E-07	-0.255E-03	2
3	0.73861	0.05181	1.29570	0.14972E-05	-0.01850	0.03501	0.01525	0.31410	0.29602	-0.220E-06	-0.699E-03	3
4	1.24000	0.07253	1.28928	0.15517E-05	-0.00924	0.01907	0.00833	0.13522	0.57451	-0.453E-06	-0.335E-02	4
5	2.15000	0.13265	1.27707	0.16367E-05	-0.06182	0.02022	0.00888	0.08918	1.10474	-0.707E-07	-0.793E-03	5
6	2.48333	0.16087	1.27292	0.15235E-05	-0.03539	0.02155	0.00948	0.06478	1.28523	-0.115E-06	-0.177E-02	6
7	2.81667	0.18939	1.26876	0.15264E-05	-0.04767	0.02546	0.01122	0.06422	1.46570	-0.849E-07	-0.132E-02	7
8	3.15000	0.23525	1.26452	0.15607E-05	-0.02140	0.01956	0.00864	0.04084	1.64989	-0.193E-06	-0.472E-02	8
9	3.48333	0.24449	1.26024	0.15787E-05	-0.01974	0.11111	0.04916	0.20496	1.83586	-0.210E-06	-0.103E-02	9
10	3.81666	0.29202	1.25618	0.14988E-05	-0.00901	0.02284	0.01012	0.03784	2.01208	-0.436E-06	-0.115E-01	10
11	4.14999	0.35947	1.25193	0.15727E-05	-0.04764	0.02045	0.00908	0.02798	2.19662	-0.862E-07	-0.308E-02	11
12	4.48333	0.38073	1.24817	0.13953E-05	-0.05847	0.06556	0.02916	0.07879	2.36015	-0.621E-07	-0.788E-03	12
13	5.14999	0.47315	1.24026	0.14717E-05	-0.00606	0.03640	0.01625	0.03822	2.70378	-0.627E-06	-0.164E-01	13
14	5.48333	0.56298	1.23608	0.15554E-05	-0.01529	0.02401	0.01074	0.02078	2.88507	-0.262E-06	-0.126E-01	14
15	5.81666	0.59934	1.23177	0.16096E-05	-0.01067	0.06890	0.03087	0.05313	3.07231	-0.387E-06	-0.728E-02	15
16	6.14999	0.67001	1.22751	0.15960E-05	-0.02309	0.03826	0.01718	0.02710	3.25755	-0.177E-06	-0.652E-02	16
17	6.48333	0.73260	1.22346	0.15149E-05	0.00485	0.04527	0.02036	0.02904	3.43312	0.795E-06	0.274E-01	17
18	7.14999	0.83183	1.21519	0.15571E-05	-0.03834	0.06517	0.02942	0.03766	3.79263	-0.103E-06	-0.273E-02	18
19	7.48333	0.90277	1.21103	0.15652E-05	-0.03211	0.05075	0.02295	0.02648	3.97301	-0.123E-06	-0.463E-02	19
20	7.81666	0.93421	1.20683	0.15874E-05	-0.03996	0.12281	0.05565	0.06059	4.15561	-0.996E-07	-0.164E-02	20
21	8.14999	0.98703	1.20269	0.15635E-05	-0.03691	0.07515	0.03412	0.03552	4.33508	-0.106E-06	-0.298E-02	21
22	8.48333	1.07091	1.19711	0.21176E-05	-0.04009	0.06843	0.03115	0.03029	4.57755	-0.131E-06	-0.433E-02	22
23	8.81666	1.09125	1.19279	0.16440E-05	-0.03235	0.22997	0.10488	0.09699	4.76544	-0.126E-06	-0.130E-02	23
24	9.14999	1.11846	1.18846	0.16461E-05	-0.04788	0.17552	0.08020	0.07261	4.95317	-0.848E-07	-0.117E-02	24
25	9.94999	1.31388	1.17754	0.17415E-05	-0.02449	0.06782	0.03115	0.02566	5.42749	-0.174E-06	-0.677E-02	25
26	10.28332	1.32619	1.17288	0.17861E-05	-0.03373	0.49937	0.22982	0.17407	5.62978	-0.129E-06	-0.740E-03	26
27	10.94999	1.43059	1.16447	0.16197E-05	-0.02908	0.11104	0.05130	0.03723	5.99521	-0.134E-06	-0.361E-02	27
28	11.61666	1.48011	1.15605	0.16279E-05	0.02183	0.24755	0.11482	0.07891	6.36104	0.178E-06	0.226E-02	28
29	11.94999	1.58078	1.15171	0.16806E-05	-0.01980	0.06594	0.03065	0.02003	6.54950	-0.202E-06	-0.101E-01	29
30	12.28333	1.56826	1.14768	0.15639E-05	0.00785	-0.50677	-0.23596	-0.14988	6.72453	0.473E-06	-0.316E-02	30
31	12.61666	1.59652	1.14338	0.16695E-05	0.03251	0.24048	0.11220	0.07090	6.91106	0.121E-06	0.171E-02	31
32	12.94999	1.65320	1.13886	0.17042E-05	0.02635	0.12980	0.06068	0.03735	7.10768	0.158E-06	0.422E-02	32
33	13.28333	1.68476	1.13432	0.17703E-05	0.04020	0.23976	0.11233	0.06731	7.30460	0.103E-06	0.153E-02	33
34	13.61666	1.72321	1.12985	0.17488E-05	0.03078	0.19809	0.09301	0.05458	7.49873	0.133E-06	0.243E-02	34
35	13.94999	1.76388	1.12511	0.18611E-05	0.04807	0.20344	0.09573	0.05491	7.70482	0.900E-07	0.164E-02	35
36	14.28333	1.81535	1.12061	0.17653E-05	0.04962	0.15618	0.07365	0.04115	7.89995	0.824E-07	0.200E-02	36
37	14.61666	1.85532	1.11599	0.18210E-05	0.06523	0.21238	0.10037	0.05468	8.10077	0.644E-07	0.118E-02	37
38	14.94999	1.92570	1.11117	0.19038E-05	0.05135	0.12950	0.06134	0.03246	8.31021	0.851E-07	0.262E-02	38
39	15.28333	1.90356	1.10747	0.14609E-05	0.09616	-0.31955	-0.15163	-0.07918	8.47069	0.347E-07	-0.439E-03	39
40	15.61666	1.96911	1.10343	0.16028E-05	0.06987	0.11950	0.05681	0.02934	8.64638	0.523E-07	0.178E-02	40
41	15.94999	1.99383	1.09907	0.17299E-05	0.08850	0.34923	0.16637	0.08397	8.83566	0.444E-07	0.528E-03	41

42	16.28333	2.03023	1.09490	0.16586E-05	0.09134	0.23049	0.11002	0.05469	9.01674	0.410E-07	0.751E-03	42
43	16.61665	2.08134	1.09084	0.16165E-05	0.09142	0.16313	0.07802	0.03795	9.19289	0.398E-07	0.105E-02	43
44	17.28333	2.13959	1.08217	0.17365E-05	0.08814	0.31442	0.15101	0.07155	9.56978	0.440E-07	0.615E-03	44
45	17.61665	2.20374	1.07772	0.17843E-05	0.09737	0.15057	0.07247	0.03338	9.76297	0.407E-07	0.122E-02	45
46	18.28333	2.31522	1.06658	0.18409E-05	0.08195	0.18519	0.08952	0.03963	10.15990	0.495E-07	0.125E-02	46
47	18.61665	2.33300	1.06377	0.19426E-05	0.12382	0.62903	0.30480	0.13112	10.36885	0.344E-07	0.262E-03	47
48	18.94998	2.39080	1.05927	0.18216E-05	0.12085	0.18394	0.08932	0.03782	10.56433	0.329E-07	0.870E-03	48
49	19.28333	2.42678	1.05464	0.18771E-05	0.10852	0.30979	0.15078	0.06260	10.76534	0.376E-07	0.601E-03	49
50	19.61665	2.47267	1.05073	0.15865E-05	0.09777	0.20842	0.10163	0.04148	10.93491	0.351E-07	0.847E-03	50
51	20.28333	2.56743	1.04203	0.17755E-05	0.06213	0.23138	0.11331	0.04497	11.31282	0.614E-07	0.136E-02	51
52	20.61665	2.62583	1.03785	0.17096E-05	0.07748	0.18591	0.09123	0.03513	11.49438	0.472E-07	0.134E-02	52
53	20.94998	2.65003	1.03343	0.18104E-05	0.07599	0.48166	0.23687	0.08977	11.68628	0.507E-07	0.565E-03	53
54	21.28333	2.71861	1.02886	0.18803E-05	0.11581	0.17913	0.08829	0.03290	11.88507	0.344E-07	0.105E-02	54
55	21.61665	2.79701	1.02454	0.17769E-05	0.08182	0.15186	0.07501	0.02720	12.07256	0.458E-07	0.169E-02	55
56	21.94998	2.83193	1.02025	0.17708E-05	0.10339	0.34599	0.17126	0.06084	12.25902	0.360E-07	0.592E-03	56
57	22.28333	2.89477	1.01587	0.18072E-05	0.11111	0.19916	0.09880	0.03451	12.44887	0.340E-07	0.986E-03	57
58	22.61665	2.93385	1.01153	0.17986E-05	0.10326	0.32384	0.16099	0.05523	12.63742	0.363E-07	0.657E-03	58
59	22.94998	2.99529	1.00714	0.18221E-05	0.08788	0.21176	0.10550	0.03559	12.82805	0.430E-07	0.121E-02	59
60	23.28333	3.09141	1.00294	0.17514E-05	0.15142	0.13325	0.06652	0.02187	13.01085	0.239E-07	0.109E-02	60
61	23.61165	3.15064	0.99895	0.16858E-05	0.11106	0.20989	0.10500	0.03364	13.18384	0.312E-07	0.929E-03	61
62	24.15833	3.16792	0.99310	0.14917E-05	0.07232	1.06950	0.53660	0.16983	13.43797	0.422E-07	0.248E-03	62
63	24.85832	3.17185	0.98854	0.90920E-06	-0.01599	3.68255	1.85188	0.58426	13.63582	-0.116E-06	-0.198E-03	63
64	25.87498	3.22681	0.98333	0.71798E-06	-0.04374	0.30340	0.15298	0.04781	13.86220	-0.333E-07	-0.695E-03	64
65	26.87498	3.28404	0.98077	0.35916E-06	-0.07168	0.14564	0.07353	0.02259	13.97342	-0.101E-07	-0.448E-03	65
66	28.54166	3.23319	0.97702	0.31637E-06	-0.03148	-0.24053	-0.12166	-0.03733	14.13641	-0.202E-07	0.542E-03	66
67	28.67499	3.29993	0.97487	0.22662E-05	-0.20787	0.10512	0.05323	0.01630	14.22971	-0.219E-07	-0.134E-02	67
68	29.09998	2.64252	0.97656	-0.56004E-06	-0.15812	0.00762	0.00385	0.00130	14.15617	0.713E-08	0.547E-02	68
69	29.59998	1.99240	0.98140	-0.13570E-05	-0.28554	0.01714	0.00865	0.00376	13.94595	0.961E-08	0.256E-02	69
70	30.09998	1.62723	0.98550	-0.11472E-05	-0.22468	0.02025	0.01020	0.00565	13.76788	0.104E-07	0.183E-02	70
71	30.59998	1.30816	0.99027	-0.13299E-05	-0.25418	0.02183	0.01097	0.00750	13.56097	0.107E-07	0.142E-02	71
72	31.09998	1.06892	0.99541	-0.14319E-05	-0.25739	0.02546	0.01276	0.01077	13.33762	0.114E-07	0.106E-02	72
73	31.76665	0.80304	1.00167	-0.13018E-05	-0.26198	0.02187	0.01092	0.01175	13.06598	0.103E-07	0.873E-03	73
74	32.69165	0.61094	1.01035	-0.12977E-05	-0.26960	0.03178	0.01581	0.02249	12.68867	0.100E-07	0.445E-03	74
75	33.69165	0.47252	1.01964	-0.12769E-05	-0.21996	0.03613	0.01789	0.03321	12.28546	0.122E-07	0.367E-03	75
76	34.69165	0.28922	1.02981	-0.13922E-05	-0.34533	0.02072	0.01021	0.02734	11.84364	0.855E-08	0.313E-03	76
77	35.69165	0.18563	1.03941	-0.13075E-05	-0.25739	0.02165	0.01062	0.04544	11.42671	0.109E-07	0.239E-03	77
78	36.69165	0.09738	1.04926	-0.13357E-05	-0.30080	0.01527	0.00745	0.05449	10.99876	0.960E-08	0.176E-03	78
79	37.69165	0.07185	1.05844	-0.12389E-05	-0.27731	0.03035	0.01474	0.17544	10.60001	0.975E-08	0.556E-04	79
80	38.69165	0.04527	1.06890	-0.14032E-05	-0.26333	0.02255	0.01090	0.18930	10.14615	0.117E-07	0.621E-04	80

ENGINEERING STRAIN (80)= 10.1461

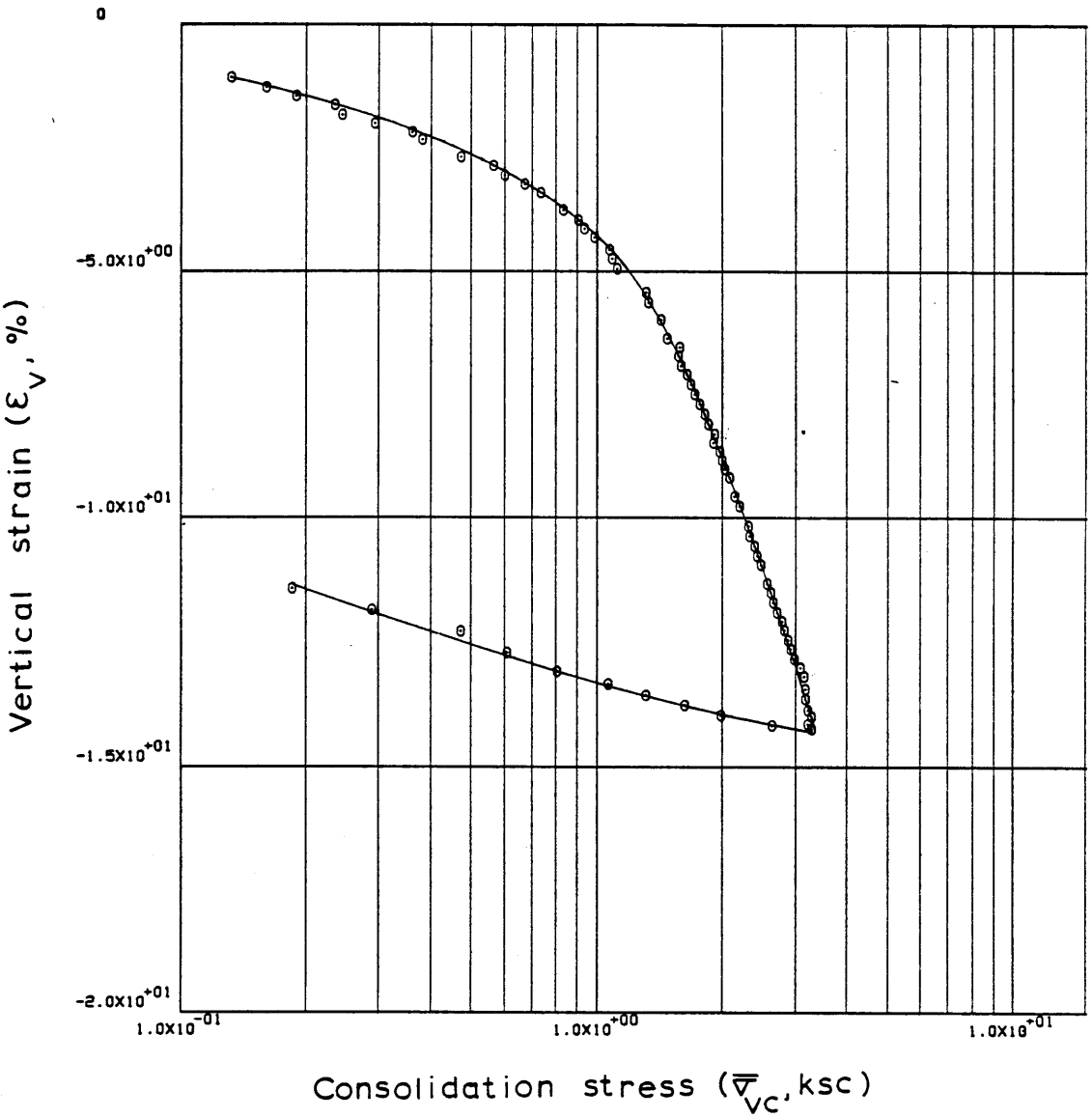

Sample No. SP19VERT w_N (%) 48.90 Estimated

Depth 93.12 w_L (%) 45.49 $\bar{\sigma}_{vo}$ 2.18 $\bar{\sigma}_{vm}$ 1.28-1.33

Soil Type Boston Blue Clay w_P (%) 22.88 CR 0.2256 RR 0.0218

P.I.(%) 22.61 G_s 2.77 e_o 1.3025

⊙ At t_p

Remarks Data from C.R.S.C test

w_L & w_P estimated from Baligh et al (1980)

Figure E.43 Compression Curve for Sample No. SP19VERT

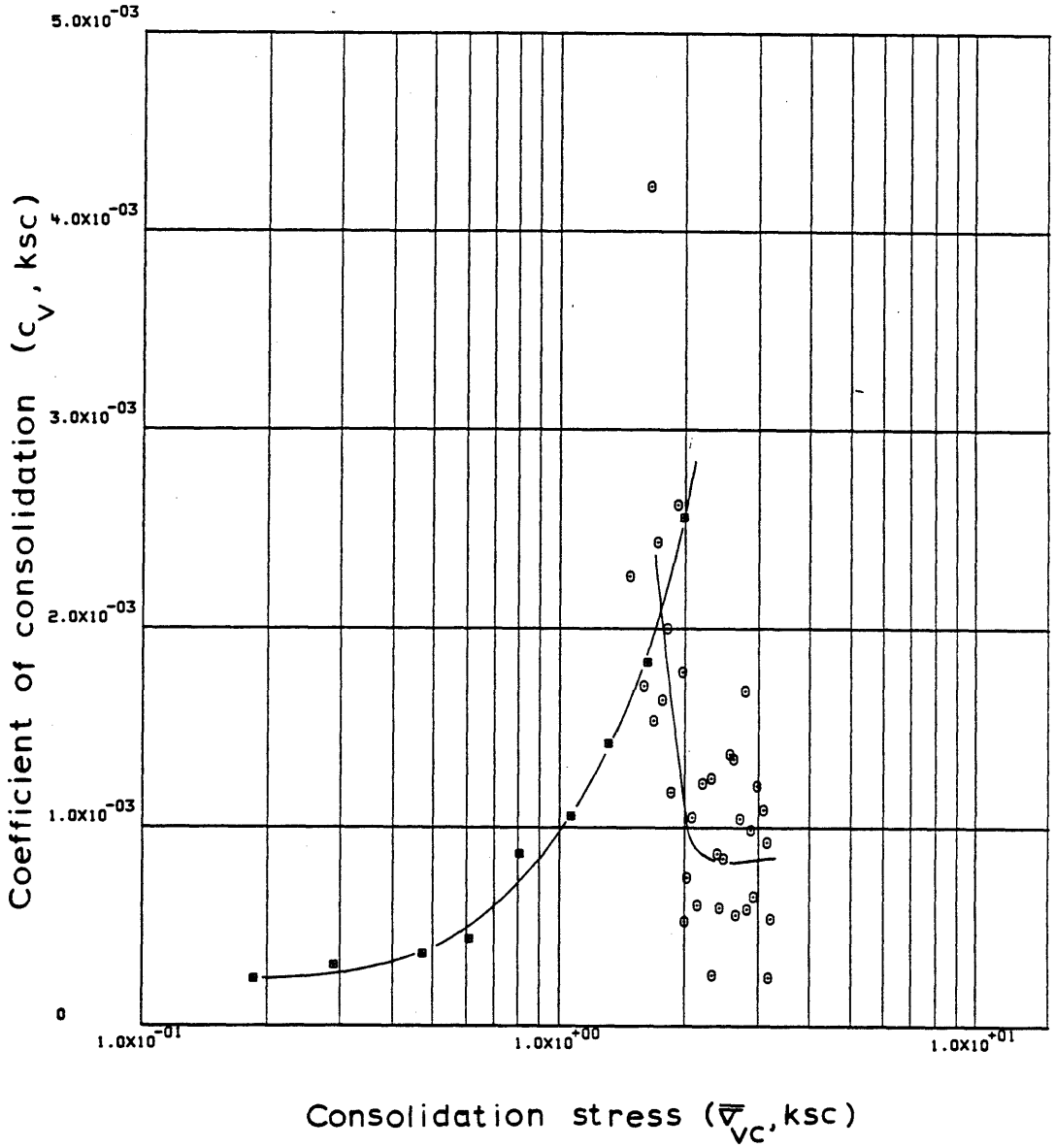

Sample No. SP19 VERT w_N (%) 48.90 Estimated

Depth 93.12 w_L (%) 45.49 $\bar{\sigma}_{vo}$ 2.18 $\bar{\sigma}_{vm}$ 1.28,1.33

Soil Type Boston w_p (%) 22.88 CR 0.2256 RR 0.0218

Blue Clay P.I.(%) 22.61 G_s 2.77 e_o 1.3025

o At t_p Remarks Data from C.R.S.C test

w_L & w_p estimated from Baligh et al (1980)

Figure E.44 Variation of coefficient of consolidation with consolidation stress for Sample No. SP19VERT

1-D STRAIN CONTROLLED COMPRESSION TEST

COMPUTED RESULTS

INITIAL VOID RATIO= 1.31369
INITIAL HEIGHT= 2.3368

ALL UNITS IN: KG,CM,SEC

LINEAR THEORY

	TIME IN HOURS	VERTICAL STRESS	E	RATE OF STRAIN	EXCESS PORE PRESSURE	C	C/1+E	MV	PERCENT COMPRESSION	K	CV	
1	0.0	0.15397	1.30921	0.0	0.00354	0.0	0.0	0.01259	0.19345	0.0	0.0	1
2	1.04556	0.15634	1.30999	-0.89592E-07	-0.01016	-0.05100	-0.02208	-0.14226	0.15979	0.240E-07	-0.169E-03	2
	ENGINEERING STRAIN (2)= 0.1598											
3	0.0	0.13876	1.31019	0.99000E+02	-0.02994	0.00166	0.00072	0.00486	0.15126	-0.900E+01	-0.185E+07	3
4	0.16667	0.17431	1.31009	0.67629E-07	-0.02487	0.00041	0.00018	0.00114	0.15530	-0.740E-08	-0.649E-02	4
5	0.25000	0.19943	1.31005	0.54376E-07	-0.02493	0.00028	0.00012	0.00065	0.15694	-0.594E-08	-0.914E-02	5
6	0.64305	0.22195	1.30787	0.66921E-06	0.02719	0.02042	0.00885	0.04204	0.25136	0.669E-07	0.159E-02	6
7	0.97639	0.25876	1.30401	0.13942E-05	0.05134	0.02513	0.01091	0.04546	0.41800	0.735E-07	0.162E-02	7
8	1.30972	0.29586	1.29973	0.15525E-05	0.05903	0.03197	0.01390	0.05021	0.60315	0.709E-07	0.141E-02	8
9	1.64305	0.33223	1.29542	0.15661E-05	0.04692	0.03721	0.01621	0.05168	0.78958	0.897E-07	0.174E-02	9
10	1.97639	0.37845	1.29115	0.15525E-05	0.07440	0.03277	0.01430	0.04031	0.97409	0.559E-07	0.139E-02	10
11	2.30972	0.42393	1.28671	0.16178E-05	0.08207	0.03911	0.01710	0.04268	1.16594	0.526E-07	0.123E-02	11
12	2.64305	0.51265	1.28243	0.15609E-05	0.09067	0.02250	0.00986	0.02111	1.35074	0.457E-07	0.217E-02	12
13	2.97639	0.55986	1.27809	0.15901E-05	0.08141	0.04934	0.02166	0.04042	1.53859	0.517E-07	0.128E-02	13
14	3.30972	0.63714	1.27407	0.14711E-05	0.12248	0.03105	0.01365	0.02284	1.71211	0.317E-07	0.139E-02	14
15	3.64305	0.69605	1.26889	0.19023E-05	0.10435	0.05857	0.02581	0.03875	1.93597	0.479E-07	0.124E-02	15
16	3.97639	0.77620	1.26522	0.13499E-05	0.09573	0.03366	0.01486	0.02021	2.09456	0.369E-07	0.183E-02	16
17	4.30972	0.84564	1.26081	0.16285E-05	0.06228	0.05157	0.02281	0.02814	2.28552	0.682E-07	0.242E-02	17
18	4.64305	0.94102	1.25675	0.14988E-05	0.10435	0.03798	0.01683	0.01886	2.46092	0.373E-07	0.198E-02	18
19	4.97639	1.02066	1.25253	0.15620E-05	0.09406	0.05197	0.02307	0.02354	2.64343	0.430E-07	0.183E-02	19
20	5.30972	1.10750	1.24824	0.15882E-05	0.08036	0.05247	0.02334	0.02195	2.82863	0.510E-07	0.232E-02	20
21	5.64305	1.23786	1.24392	0.16037E-05	0.07454	0.03881	0.01729	0.01476	3.01526	0.553E-07	0.371E-02	21
22	5.97639	1.27295	1.23966	0.15843E-05	0.09514	0.15231	0.06801	0.05417	3.19928	0.426E-07	0.786E-03	22
23	6.64778	1.43244	1.23093	0.16191E-05	0.10987	0.07396	0.03315	0.02454	3.57661	0.374E-07	0.152E-02	23
24	6.97639	1.51945	1.22694	0.15143E-05	0.11431	0.06765	0.03038	0.02059	3.74904	0.335E-07	0.163E-02	24
25	7.30832	1.59426	1.22282	0.15521E-05	0.14949	0.08577	0.03859	0.02479	3.92723	0.262E-07	0.106E-02	25
26	7.64165	1.68661	1.21865	0.15672E-05	0.16588	0.07412	0.03341	0.02037	4.10756	0.237E-07	0.116E-02	26
27	7.97500	1.71041	1.21418	0.16838E-05	0.16181	0.31926	0.14419	0.08489	4.30093	0.260E-07	0.306E-03	27
28	8.30832	1.78079	1.20969	0.16906E-05	0.16784	0.11118	0.05032	0.02882	4.49471	0.251E-07	0.870E-03	28
29	8.64165	1.84448	1.20512	0.17263E-05	0.15846	0.12997	0.05894	0.03253	4.69211	0.270E-07	0.831E-03	29
30	9.30832	1.92950	1.19609	0.17142E-05	0.12634	0.20051	0.09130	0.04839	5.08263	0.334E-07	0.690E-03	30
31	9.64165	2.00136	1.19166	0.16824E-05	0.14541	0.12101	0.05521	0.02809	5.27386	0.283E-07	0.101E-02	31
32	9.97500	2.03231	1.18744	0.16084E-05	0.13940	0.27517	0.12580	0.06238	5.45634	0.282E-07	0.451E-03	32
33	10.30832	2.09400	1.18312	0.16485E-05	0.16342	0.14441	0.06615	0.03207	5.64301	0.245E-07	0.765E-03	33
34	10.64165	2.13557	1.17894	0.16013E-05	0.16172	0.21302	0.09776	0.04622	5.82396	0.240E-07	0.519E-03	34
35	10.97500	2.17777	1.17443	0.17285E-05	0.16174	0.23046	0.10599	0.04915	6.01892	0.258E-07	0.524E-03	35
36	11.30832	2.22267	1.17017	0.16332E-05	0.18579	0.20845	0.09605	0.04365	6.20273	0.211E-07	0.484E-03	36
37	11.64165	2.25078	1.16610	0.15680E-05	0.17375	0.32416	0.14965	0.06691	6.37888	0.216E-07	0.323E-03	37
38	11.97500	2.28103	1.16271	0.13077E-05	0.18406	0.25423	0.11755	0.05189	6.52554	0.169E-07	0.327E-03	38
39	12.30832	2.32817	1.15841	0.16594E-05	0.19439	0.21011	0.09734	0.04224	6.71132	0.203E-07	0.480E-03	39
40	12.64165	2.36285	1.15402	0.16959E-05	0.21574	0.29659	0.13769	0.05868	6.90080	0.186E-07	0.317E-03	40

41	12.97500	2.40178	1.14949	0.17588E-05	0.19002	0.27756	0.12913	0.05422	7.09686	0.218E-07	0.402E-03	41
42	13.30832	2.44490	1.14485	0.17994E-05	0.21138	0.26034	0.12138	0.05008	7.29704	0.200E-07	0.399E-03	42
43	13.64165	2.51015	1.14024	0.17957E-05	0.20705	0.17508	0.08180	0.03302	7.49635	0.203E-07	0.614E-03	43
44	13.97500	2.53358	1.13544	0.18750E-05	0.22238	0.51721	0.24220	0.09602	7.70406	0.196E-07	0.204E-03	44
45	14.64165	2.59137	1.12676	0.17010E-05	0.18378	0.38494	0.18100	0.07064	8.07930	0.214E-07	0.302E-03	45
46	14.97500	2.63573	1.12258	0.16379E-05	0.18809	0.24576	0.11578	0.04431	8.25961	0.200E-07	0.452E-03	46
47	15.30832	2.68293	1.11701	0.21926E-05	0.19845	0.31383	0.14824	0.05574	8.50037	0.253E-07	0.453E-03	47
48	15.64165	2.71211	1.11275	0.16803E-05	0.20782	0.39390	0.18644	0.06912	8.68449	0.184E-07	0.266E-03	48
49	15.97500	2.75877	1.10854	0.16637E-05	0.21651	0.24678	0.11704	0.04279	8.86642	0.174E-07	0.407E-03	49
50	16.64165	2.81731	1.10019	0.16577E-05	0.19677	0.39794	0.18948	0.06796	9.22757	0.190E-07	0.279E-03	50
51	17.30832	2.90535	1.09147	0.17369E-05	0.22413	0.28332	0.13547	0.04735	9.60439	0.173E-07	0.365E-03	51
52	17.97499	3.00258	1.08236	0.18230E-05	0.21469	0.27678	0.13292	0.04500	9.99817	0.188E-07	0.417E-03	52
53	18.64165	3.10658	1.07324	0.18325E-05	0.22310	0.26777	0.12916	0.04229	10.39224	0.180E-07	0.426E-03	53
54	19.30832	3.23633	1.06453	0.17583E-05	0.24885	0.21293	0.10314	0.03252	10.76880	0.154E-07	0.472E-03	54
55	19.97499	3.33406	1.05615	0.16973E-05	0.25918	0.28152	0.13691	0.04168	11.13080	0.141E-07	0.339E-03	55
56	20.64165	3.44578	1.04760	0.17414E-05	0.28156	0.25965	0.12681	0.03741	11.50067	0.132E-07	0.354E-03	56
57	21.30832	3.57209	1.03930	0.16959E-05	0.29953	0.23057	0.11306	0.03223	11.85939	0.120E-07	0.373E-03	57
58	21.97499	3.68733	1.03054	0.17961E-05	0.29344	0.27566	0.13576	0.03741	12.23772	0.129E-07	0.344E-03	58
59	22.64165	3.82101	1.02164	0.18356E-05	0.31045	0.25010	0.12371	0.03295	12.62265	0.123E-07	0.374E-03	59
60	23.30832	3.95032	1.01267	0.18563E-05	0.31886	0.26944	0.13387	0.03445	13.01022	0.120E-07	0.349E-03	60
61	23.97499	4.10821	1.00465	0.16679E-05	0.33258	0.20474	0.10214	0.02535	13.35704	0.103E-07	0.405E-03	61
62	24.64165	4.27189	0.99658	0.16829E-05	0.31986	0.20641	0.10338	0.02468	13.70561	0.107E-07	0.434E-03	62
63	25.30832	4.42588	0.98862	0.16672E-05	0.32421	0.22468	0.11298	0.02598	14.04948	0.104E-07	0.399E-03	63
64	25.97499	4.57476	0.97934	0.19553E-05	0.33619	0.28077	0.14185	0.03152	14.45094	0.116E-07	0.369E-03	64

ENGINEERING STRAIN (64)= 14.4509

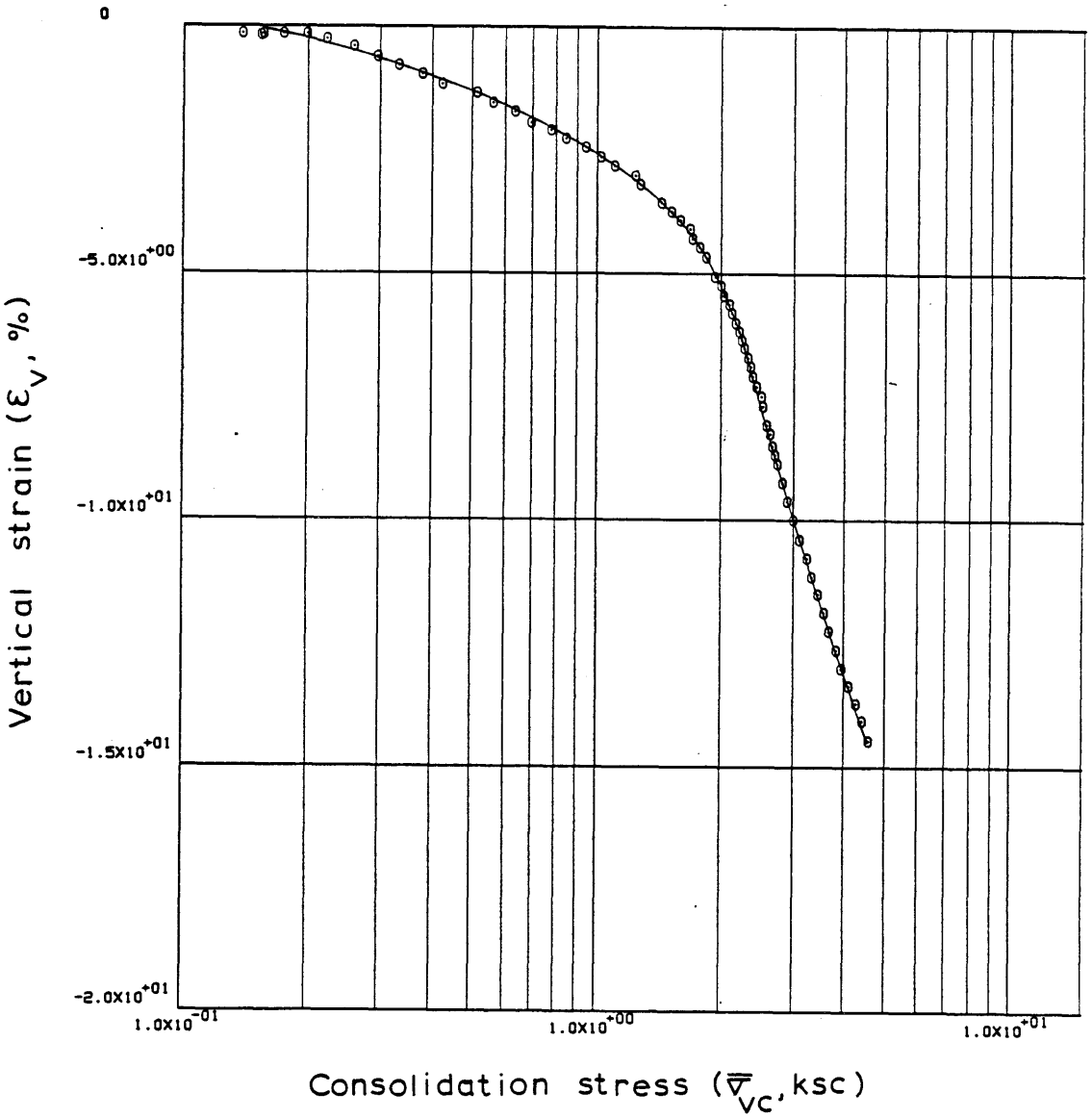

Sample No. SP20VERT w_N (%) 42.90 Estimated

Depth 97.83 w_L (%) 44.50 $\bar{\sigma}_{vo}$ 2.29 $\bar{\sigma}_{vm}$ 1.87-1.93

Soil Type Boston w_P (%) 21.12 CR 0.2600 RR -

Blue Clay P.I.(%) 23.38 G_s 2.77 e_o 1.3137

⊙ At t_p Remarks Data from C.R.S.C test

w_L & w_P estimated from Baligh et al (1980)

Figure E.45 Compression Curve for Sample No. SP20VERT

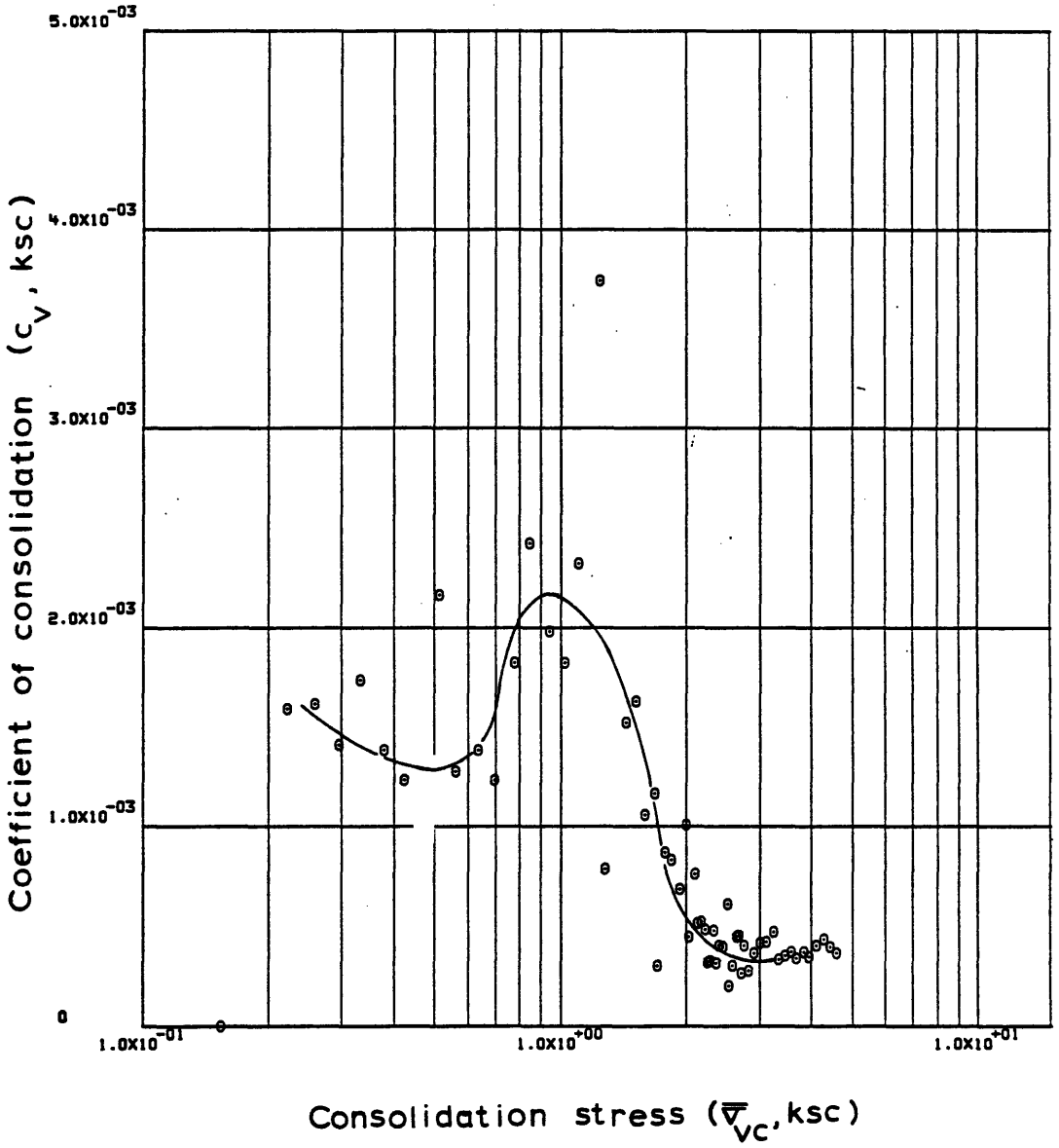

Sample No. SP20VERT w_N (%) 42.90 Estimated

Depth 97.83 w_L (%) 44.50 $\bar{\sigma}_{vo}$ 2.29 $\bar{\sigma}_{vm}$ 1.87-1.93

Soil Type Boston Blue Clay w_P (%) 21.12 CR 0.2600 RR -

P.I.(%) 23.38 G_s 2.77 e_o 1.3137

o At t_p

Remarks Data from C.R.S.C test

w_L & w_P estimated from Baligh et al (1980)

Figure E.46 Variation of coefficient of consolidation with consolidation stress for Sample No. SP20VERT

1-D STRAIN CONTROLLED COMPRESSION TEST

COMPUTED RESULTS

INITIAL VOID RATIO= 0.42378
INITIAL HEIGHT= 2.3368

ALL UNITS IN: KG,CM,SEC

LINEAR THEORY

	TIME IN HOURS	VERTICAL STRESS	E	RATE OF STRAIN	EXCESS PORE PRESSURE	C	C/1+E	MV	PERCENT COMPRESSION	K	CV	
1	0.0	0.15093	0.42467	0.0	-0.00992	0.0	0.0	-0.00415	-0.06259	0.0	0.0	1
2	0.34418	0.17990	0.42451	0.94186E-07	-0.00765	0.00095	0.00067	0.00403	-0.05092	-0.337E-07	-0.835E-02	2
3	0.67500	0.24264	0.42389	0.36639E-06	0.02788	0.00208	0.00146	0.00695	-0.00729	0.359E-07	0.516E-02	3
4	1.01085	0.31902	0.42148	0.14018E-05	0.06285	0.00880	0.00619	0.02219	0.16191	0.607E-07	0.274E-02	4
5	1.34418	0.41517	0.41899	0.14628E-05	0.07300	0.00946	0.00666	0.01826	0.33687	0.543E-07	0.298E-02	5
6	1.67500	0.50008	0.41678	0.13101E-05	0.06509	0.01188	0.00838	0.01837	0.49211	0.544E-07	0.296E-02	6
7	2.01085	0.60272	0.41443	0.13736E-05	0.06849	0.01258	0.00890	0.01618	0.65712	0.540E-07	0.334E-02	7
8	2.34418	0.72345	0.41235	0.12254E-05	0.05948	0.01138	0.00805	0.01218	0.80296	0.553E-07	0.454E-02	8
9	2.67502	0.84796	0.41017	0.12997E-05	0.05274	0.01375	0.00975	0.01243	0.95630	0.660E-07	0.531E-02	9
10	3.01085	0.97863	0.40774	0.14269E-05	0.04879	0.01694	0.01203	0.01320	1.12685	0.781E-07	0.591E-02	10
11	3.34418	1.13233	0.40513	0.15467E-05	0.04597	0.01788	0.01273	0.01208	1.31001	0.895E-07	0.741E-02	11
12	3.67502	1.30034	0.40244	0.16087E-05	0.05216	0.01942	0.01385	0.01140	1.49875	0.817E-07	0.717E-02	12
13	4.01085	1.50295	0.39963	0.16601E-05	0.05216	0.01940	0.01386	0.00991	1.69604	0.840E-07	0.848E-02	13
14	4.34418	1.63382	0.39759	0.12178E-05	0.02282	0.02445	0.01750	0.01117	1.83949	0.140E-06	0.126E-01	14
15	4.67502	1.79526	0.39542	0.13081E-05	0.05948	0.02308	0.01654	0.00965	1.99220	0.577E-07	0.598E-02	15
16	5.01085	2.02151	0.39270	0.16167E-05	0.05443	0.02293	0.01647	0.00864	2.18336	0.776E-07	0.898E-02	16
17	5.34418	2.20525	0.39013	0.15378E-05	0.05725	0.02949	0.02121	0.01004	2.36354	0.699E-07	0.696E-02	17
18	5.67502	2.40878	0.38754	0.15682E-05	0.06853	0.02936	0.02116	0.00918	2.54556	0.593E-07	0.647E-02	18
19	6.01085	2.59686	0.38469	0.17016E-05	0.07527	0.03789	0.02736	0.01094	2.74567	0.584E-07	0.534E-02	19
20	6.34418	2.75916	0.38233	0.14256E-05	0.07248	0.03900	0.02821	0.01054	2.91173	0.506E-07	0.480E-02	20
21	6.67502	2.90107	0.37994	0.14546E-05	0.06742	0.04767	0.03455	0.01221	3.07967	0.553E-07	0.453E-02	21
22	7.01085	2.98798	0.37758	0.14146E-05	0.06632	0.07984	0.05796	0.01968	3.24510	0.545E-07	0.277E-02	22
23	7.34418	3.06798	0.37518	0.14544E-05	0.07028	0.09081	0.06604	0.02182	3.41370	0.527E-07	0.242E-02	23
24	7.67502	3.15421	0.37251	0.16361E-05	0.06746	0.09647	0.07028	0.02260	3.60150	0.615E-07	0.272E-02	24
25	8.01085	3.20352	0.36958	0.17678E-05	0.07196	0.18877	0.13783	0.04335	3.80711	0.621E-07	0.143E-02	25
26	8.34418	3.23960	0.36683	0.16740E-05	0.07083	0.24515	0.17935	0.05567	3.99995	0.595E-07	0.107E-02	26
27	8.67502	3.29042	0.36374	0.19039E-05	0.08830	0.19871	0.14571	0.04462	4.21715	0.540E-07	0.121E-02	27
28	9.01085	3.33822	0.36082	0.17717E-05	0.07984	0.20206	0.14848	0.04481	4.42189	0.553E-07	0.124E-02	28
29	9.34418	3.38960	0.35815	0.16438E-05	0.09903	0.17541	0.12915	0.03839	4.61003	0.412E-07	0.107E-02	29
30	9.67502	3.41493	0.35523	0.18079E-05	0.09903	0.39201	0.28926	0.08502	4.81499	0.452E-07	0.531E-03	30
31	10.01085	3.43159	0.35234	0.17642E-05	0.10691	0.59230	0.43798	0.12795	5.01758	0.406E-07	0.318E-03	31
32	10.34418	3.44757	0.34951	0.17484E-05	0.11311	0.60990	0.45194	0.13133	5.21645	0.379E-07	0.289E-03	32
33	10.67502	3.46692	0.34669	0.17596E-05	0.11197	0.50421	0.37441	0.10830	5.41466	0.384E-07	0.354E-03	33
34	11.01085	3.48547	0.34380	0.17756E-05	0.11703	0.54056	0.40226	0.11571	5.61729	0.369E-07	0.319E-03	34
35	11.34418	3.48599	0.34098	0.17580E-05	0.11872	19.01422	14.17939	4.05139	5.81596	0.359E-07	0.885E-05	35
36	11.67502	3.51547	0.33802	0.18531E-05	0.12268	0.35083	0.26220	0.07488	6.02341	0.364E-07	0.486E-03	36
37	12.01085	3.53046	0.33522	0.17332E-05	0.12550	0.65777	0.49263	0.13981	6.21991	0.332E-07	0.237E-03	37
38	12.34418	3.55096	0.33294	0.14255E-05	0.12776	0.39375	0.29540	0.08342	6.38005	0.267E-07	0.320E-03	38
39	12.67502	3.56605	0.33046	0.15700E-05	0.13058	0.58678	0.44104	0.12396	6.55476	0.287E-07	0.231E-03	39
40	13.01085	3.55410	0.32798	0.15420E-05	0.12834	-0.73764	-0.55546	-0.15602	6.72867	0.285E-07	-0.183E-03	40
41	13.34418	3.57414	0.32552	0.15459E-05	0.12101	0.43714	0.32979	0.09254	6.90134	0.302E-07	0.327E-03	41

SP13VERT LINEAR THEORY

42	13.67502	3.58237	0.32139	0.26233E-05	0.12893	1.79725	1.36012	0.37998	7.19135	0.479E-07	0.126E-03	42
43	14.01085	3.61368	0.31848	0.18261E-05	0.13006	0.33439	0.25361	0.07051	7.39577	0.329E-07	0.466E-03	43
44	14.34418	3.62968	0.31577	0.17189E-05	0.13627	0.61445	0.46699	0.12892	7.58640	0.294E-07	0.228E-03	44
45	14.67502	3.63406	0.31298	0.17834E-05	0.13230	2.31548	1.76353	0.48513	7.78229	0.313E-07	0.645E-04	45
46	15.01085	3.65782	0.30999	0.18882E-05	0.14469	0.45869	0.35015	0.09605	7.99229	0.302E-07	0.314E-03	46
47	15.34418	3.66323	0.30730	0.17168E-05	0.14411	1.62393	1.39519	0.38079	8.18146	0.274E-07	0.720E-04	47
48	15.67502	3.67748	0.30450	0.18017E-05	0.15313	0.72094	0.55266	0.15057	8.37808	0.270E-07	0.179E-03	48
49	16.01085	3.70395	0.30171	0.17722E-05	0.15653	0.38902	0.29885	0.08095	8.57397	0.258E-07	0.319E-03	49
50	16.34418	3.74913	0.29892	0.17864E-05	0.15709	0.22963	0.17679	0.04745	8.76955	0.258E-07	0.545E-03	50
51	16.67502	3.76813	0.29605	0.18643E-05	0.17173	0.56937	0.43931	0.11685	8.97165	0.246E-07	0.210E-03	51
52	17.01085	3.77766	0.29327	0.17757E-05	0.17511	1.09864	0.84950	0.22516	9.16664	0.228E-07	0.101E-03	52
53	17.34418	3.80715	0.29084	0.15673E-05	0.17906	0.31235	0.24197	0.06379	9.33719	0.196E-07	0.308E-03	53
54	17.67502	3.85246	0.28829	0.16598E-05	0.17963	0.21523	0.16707	0.04363	9.51607	0.207E-07	0.473E-03	54
55	18.01085	3.88216	0.28582	0.15913E-05	0.17570	0.32212	0.25051	0.06478	9.68980	0.202E-07	0.311E-03	55
56	18.34418	3.91287	0.28339	0.15788E-05	0.17516	0.30863	0.24048	0.06168	9.86060	0.200E-07	0.324E-03	56
57	18.67500	3.96847	0.28075	0.17317E-05	0.17291	0.18717	0.14614	0.03709	10.04608	0.221E-07	0.596E-03	57
58	19.01085	3.99265	0.27802	0.17686E-05	0.16954	0.44995	0.35207	0.08843	10.23801	0.229E-07	0.260E-03	58
59	19.67500	4.05978	0.27240	0.18456E-05	0.18530	0.33678	0.26468	0.06573	10.63242	0.217E-07	0.330E-03	59
60	25.64307	4.08669	0.25727	0.56008E-06	0.00308	2.29080	1.82204	0.44730	11.69501	0.387E-06	0.866E-03	60
61	25.98334	3.65782	0.25655	0.47069E-06	-0.11079	-0.00653	-0.00520	-0.00134	11.74586	-0.903E-08	0.672E-02	61
62	26.31668	3.04041	0.25883	-0.15083E-05	-0.13161	0.01232	0.00979	0.00293	11.58585	0.245E-07	0.834E-02	62
63	26.65001	2.63194	0.26147	-0.17450E-05	-0.14964	0.01831	0.01452	0.00513	11.40031	0.250E-07	0.488E-02	63
64	26.98335	2.25681	0.26416	-0.17730E-05	-0.16938	0.01749	0.01384	0.00567	11.21140	0.225E-07	0.397E-02	64
65	27.31668	1.95240	0.26659	-0.16005E-05	-0.17898	0.01679	0.01326	0.00631	11.04056	0.193E-07	0.306E-02	65
66	27.65001	1.70686	0.26893	-0.15378E-05	-0.18068	0.01742	0.01373	0.00752	10.87610	0.185E-07	0.246E-02	66
67	27.98334	1.50103	0.27121	-0.14934E-05	-0.17336	0.01773	0.01395	0.00871	10.71608	0.188E-07	0.215E-02	67
68	28.31668	1.32766	0.27335	-0.14010E-05	-0.16152	0.01744	0.01370	0.00970	10.56573	0.189E-07	0.195E-02	68
69	28.65001	1.24260	0.27474	-0.90709E-06	-0.11245	0.02096	0.01644	0.01280	10.46828	0.177E-07	0.138E-02	69
70	28.98334	1.12253	0.27741	-0.17435E-05	-0.16039	0.02630	0.02059	0.01742	10.28058	0.239E-07	0.137E-02	70
71	29.31668	0.99777	0.27970	-0.14907E-05	-0.16321	0.01943	0.01518	0.01434	10.11978	0.201E-07	0.140E-02	71
72	29.65001	0.89045	0.28213	-0.15798E-05	-0.16435	0.02136	0.01666	0.01767	9.94907	0.213E-07	0.120E-02	72
73	29.98334	0.79570	0.28445	-0.15077E-05	-0.16153	0.02066	0.01608	0.01909	9.78586	0.207E-07	0.109E-02	73
74	30.31668	0.71464	0.28716	-0.17499E-05	-0.15138	0.02515	0.01954	0.02590	9.59601	0.258E-07	0.996E-03	74
75	30.65001	0.65616	0.28968	-0.16294E-05	-0.14966	0.02954	0.02290	0.03344	9.41888	0.244E-07	0.729E-03	75
76	30.98334	0.61249	0.29235	-0.17254E-05	-0.14516	0.03885	0.03006	0.04740	9.23096	0.267E-07	0.564E-03	76
77	31.31668	0.54221	0.29487	-0.16185E-05	-0.15362	0.02064	0.01594	0.02764	9.05432	0.238E-07	0.861E-03	77
78	31.65001	0.50942	0.29730	-0.15595E-05	-0.15026	0.03892	0.03000	0.05706	8.88382	0.235E-07	0.412E-03	78
79	31.98334	0.45639	0.30004	-0.17559E-05	-0.14911	0.02492	0.01917	0.03974	8.69144	0.268E-07	0.675E-03	79
80	32.31668	0.41417	0.30259	-0.16317E-05	-0.14911	0.02628	0.02018	0.04638	8.51227	0.250E-07	0.539E-03	80
81	32.65001	0.36768	0.30493	-0.14989E-05	-0.15308	0.01971	0.01511	0.03869	8.34744	0.225E-07	0.500E-03	81
82	32.98334	0.34083	0.30761	-0.17047E-05	-0.14056	0.03528	0.02698	0.07618	8.15955	0.279E-07	0.366E-03	82
83	33.31668	0.32307	0.30989	-0.14544E-05	-0.12656	0.04270	0.03260	0.09823	7.99899	0.266E-07	0.270E-03	83
84	33.65001	0.29523	0.31201	-0.13450E-05	-0.10796	0.02349	0.01791	0.05797	7.85028	0.289E-07	0.498E-03	84
85	33.98334	0.28867	0.31392	-0.12099E-05	-0.09331	0.08501	0.06470	0.22154	7.71625	0.302E-07	0.136E-03	85
86	34.31668	0.27700	0.31563	-0.10861E-05	-0.09390	0.04153	0.03158	0.11162	7.59583	0.270E-07	0.242E-03	86

ENGINEERING STRAIN (86)= 7.5958

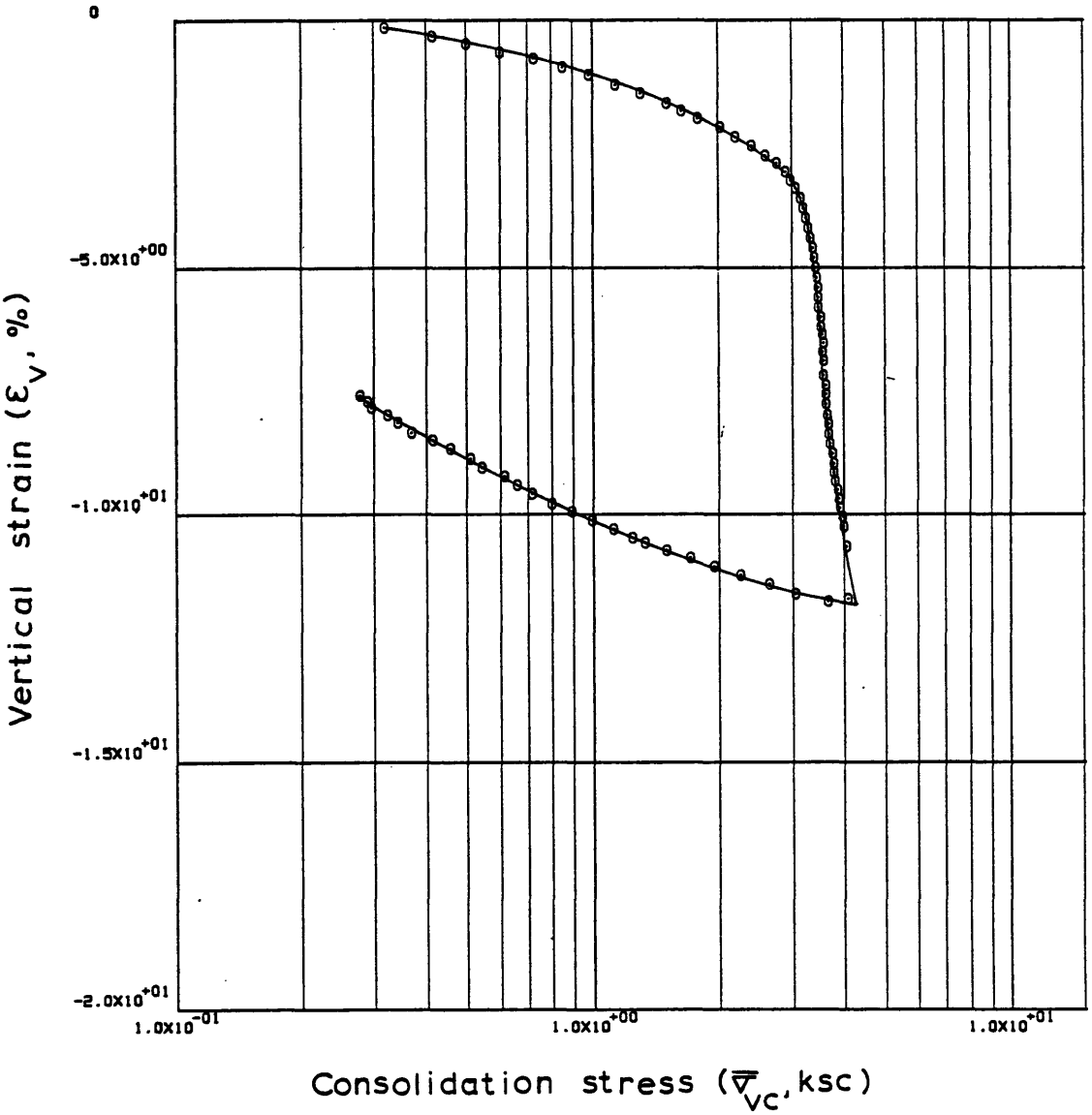

Sample No. SP13VERT w_N (%) 38.70 Estimated

Depth 99.48 w_L (%) 44.12 $\bar{\sigma}_{vo}$ 2.33 $\bar{\sigma}_{vm}$ 3.22-3.30

Soil Type Boston Blue Clay w_P (%) 23.10 CR 0.7524 RR 0.3437

P.I.(%) 21.02 G_s 2.77 e_o 1.0720

o At t_p

Remarks Data from C.R.S.C test

w_L & w_P estimated from Baligh et al (1980)

Figure E.47 Compression Curve for Sample No. SP13VERT

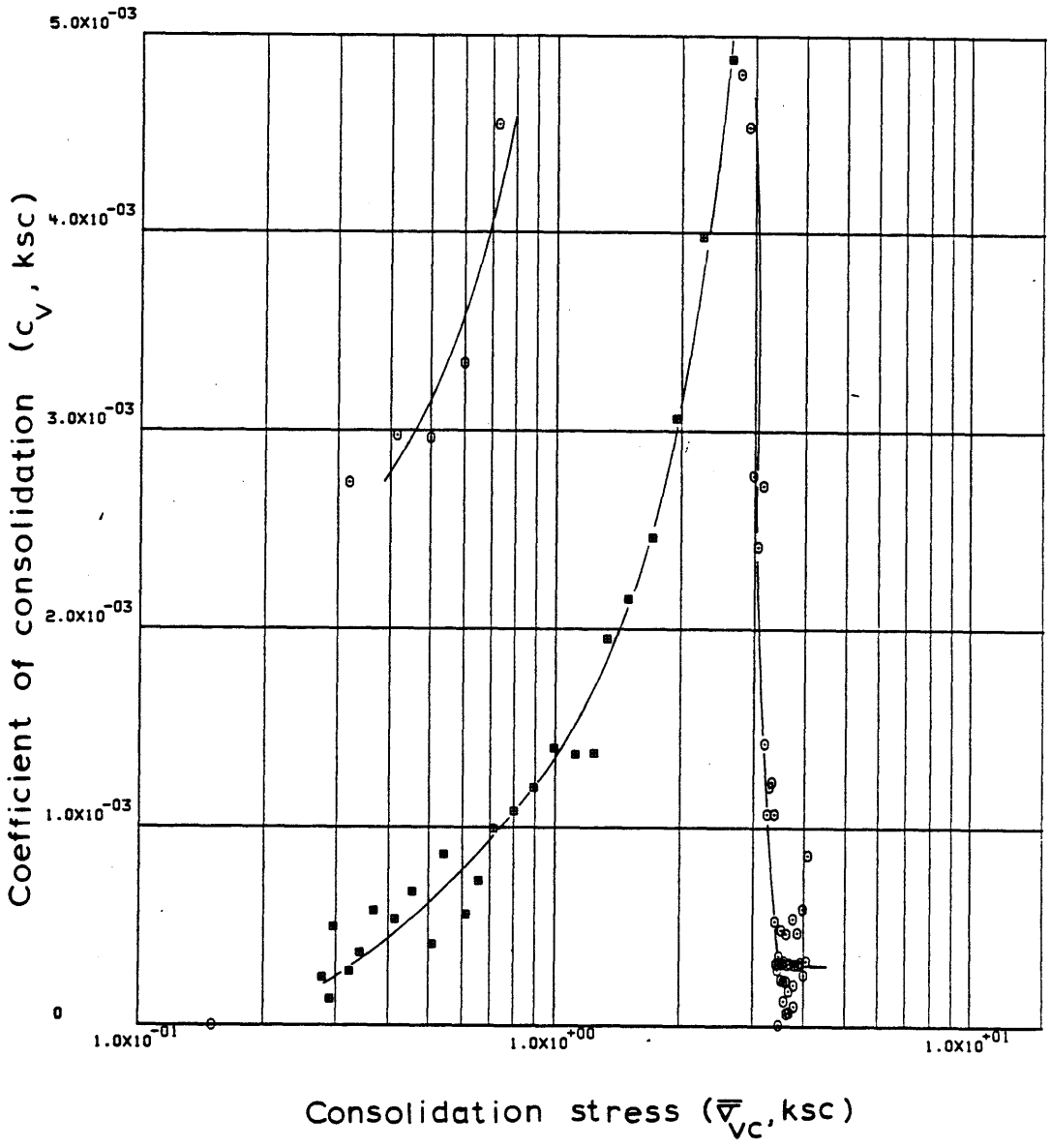

Sample No. SP13VERT w_N (%) 38.70 Estimated

Depth 99.48 w_L (%) 44.12 $\bar{\sigma}_{vo}$ 2.33 $\bar{\sigma}_{vm}$ 322.330

Soil Type Boston Blue Clay w_P (%) 23.10 CR 0.7524 RR 0.3437

P.I.(%) 21.02 G_S 2.77 e_o 1.0720

o At t_p

Remarks Data from C.R.S.C test

w_L & w_P estimated from Baligh et al (1980)

Figure E.48 Variation of coefficient of consolidation with consolidation stress for Sample No. SP13VERT

1-D STRAIN CONTROLLED COMPRESSION TEST

COMPUTED RESULTS

INITIAL VOID RATIO= 1.12582
INITIAL HEIGHT= 2.3368

ALL UNITS IN: KG,CM,SEC

LINEAR THEORY

	TIME IN HOURS	VERTICAL STRESS	E	RATE OF STRAIN	EXCESS PORE PRESSURE	C	C/1+E	MV	PERCENT COMPRESSION	K	CV	
1	0.0	0.13396	1.12132	0.0	-0.02398	0.0	0.0	0.01583	0.21162	0.0	0.0	1
2	0.08305	0.16695	1.12143	-0.17621E-06	-0.00197	-0.00051	-0.00024	-0.00160	0.20634	0.244E-06	-0.152E+00	2
3	0.16777	0.21886	1.12057	0.13314E-05	0.01102	0.00318	0.00150	0.00782	0.24687	0.328E-06	0.420E-01	3
4	0.50806	0.30975	1.11714	0.13222E-05	0.02969	0.00987	0.00466	0.01782	0.40816	0.121E-06	0.677E-02	4
5	0.84138	0.41320	1.11342	0.14687E-05	0.04436	0.01293	0.00612	0.01704	0.58340	0.893E-07	0.524E-02	5
6	1.17471	0.51047	1.10950	0.15488E-05	0.04040	0.01854	0.00879	0.01911	0.76784	0.103E-06	0.539E-02	6
7	1.50806	0.61922	1.10564	0.15258E-05	0.03699	0.01997	0.00948	0.01684	0.94920	0.110E-06	0.656E-02	7
8	1.84138	0.76230	1.10171	0.15580E-05	0.04319	0.01890	0.00899	0.01307	1.13403	0.963E-07	0.737E-02	8
9	2.17471	0.91299	1.09796	0.14893E-05	0.04771	0.02079	0.00991	0.01186	1.31041	0.830E-07	0.700E-02	9
10	2.50806	1.07946	1.09417	0.15070E-05	0.03923	0.02261	0.01080	0.01086	1.48856	0.102E-06	0.937E-02	10
11	2.84138	1.25272	1.09059	0.14282E-05	0.04319	0.02407	0.01151	0.00989	1.65710	0.873E-07	0.883E-02	11
12	3.17473	1.45586	1.08675	0.15333E-05	0.04319	0.02554	0.01224	0.00906	1.83769	0.934E-07	0.103E-01	12
13	3.50806	1.60873	1.08298	0.15084E-05	0.03696	0.03777	0.01813	0.01184	2.01506	0.107E-06	0.904E-02	13
14	3.84138	1.72130	1.08064	0.93936E-06	0.02793	0.03467	0.01666	0.01001	2.12537	0.880E-07	0.878E-02	14
15	4.17473	1.92978	1.07696	0.14737E-05	0.04488	0.03213	0.01547	0.00848	2.29816	0.856E-07	0.101E-01	15
16	4.50806	2.10920	1.07306	0.15693E-05	0.04995	0.04392	0.02118	0.01050	2.48181	0.816E-07	0.777E-02	16
17	4.84138	2.28470	1.06931	0.15086E-05	0.06069	0.04687	0.02265	0.01031	2.65804	0.643E-07	0.623E-02	17
18	5.17473	2.43263	1.06516	0.16771E-05	0.06466	0.06623	0.03207	0.01360	2.85352	0.668E-07	0.491E-02	18
19	5.50806	2.59571	1.06120	0.15986E-05	0.06352	0.06095	0.02957	0.01176	3.03954	0.646E-07	0.549E-02	19
20	5.84138	2.70865	1.05723	0.16098E-05	0.06410	0.09331	0.04536	0.01710	3.22650	0.642E-07	0.375E-02	20
21	6.17473	2.81538	1.05335	0.15730E-05	0.07144	0.10029	0.04884	0.01769	3.40880	0.561E-07	0.317E-02	21
22	6.50806	2.90655	1.04929	0.16504E-05	0.07427	0.12733	0.06213	0.02172	3.59972	0.564E-07	0.260E-02	22
23	6.84138	2.97232	1.04545	0.15658E-05	0.07709	0.17176	0.08397	0.02857	3.78050	0.513E-07	0.180E-02	23
24	7.17473	3.03432	1.04135	0.16753E-05	0.08556	0.19883	0.09740	0.03243	3.97359	0.493E-07	0.152E-02	24
25	7.50806	3.08918	1.03727	0.16656E-05	0.08953	0.22724	0.11154	0.03643	4.16512	0.467E-07	0.128E-02	25
26	7.84138	3.11458	1.03296	0.17703E-05	0.08953	0.52745	0.25945	0.08365	4.36827	0.494E-07	0.590E-03	26
27	8.17473	3.17184	1.02883	0.16966E-05	0.09235	0.22674	0.11176	0.03556	4.56258	0.457E-07	0.128E-02	27
28	8.50806	3.19589	1.02485	0.16354E-05	0.09686	0.52620	0.25987	0.08161	4.74950	0.418E-07	0.512E-03	28
29	8.84138	3.23438	1.02077	0.16846E-05	0.10252	0.34126	0.16888	0.05252	4.94167	0.405E-07	0.772E-03	29
30	9.17473	3.25445	1.01680	0.16397E-05	0.09518	0.64164	0.31815	0.09805	5.12834	0.423E-07	0.432E-03	30
31	9.50806	3.29936	1.01277	0.16667E-05	0.11158	0.29372	0.14593	0.04453	5.31770	0.366E-07	0.821E-03	31
32	9.84138	3.32004	1.00867	0.17027E-05	0.10593	0.65680	0.32698	0.09880	5.51074	0.392E-07	0.397E-03	32
33	10.17473	3.34835	1.00472	0.16420E-05	0.10648	0.46523	0.23207	0.06961	5.69659	0.374E-07	0.538E-03	33
34	10.84138	3.39763	0.99612	0.17951E-05	0.11097	0.58870	0.29492	0.08743	6.10110	0.389E-07	0.445E-03	34
35	11.17473	3.42300	0.99179	0.18128E-05	0.11097	0.58229	0.29235	0.08573	6.30492	0.392E-07	0.457E-03	35
36	11.50806	3.44756	0.98764	0.17387E-05	0.11718	0.58019	0.29190	0.08497	6.50000	0.354E-07	0.417E-03	36
37	11.84138	3.48556	0.98353	0.17265E-05	0.12114	0.37483	0.18897	0.05451	6.69331	0.339E-07	0.621E-03	37
38	12.17473	3.49894	0.97984	0.15512E-05	0.11889	0.96185	0.48582	0.13909	6.86668	0.309E-07	0.222E-03	38
39	12.50806	3.54748	0.97687	0.12532E-05	0.11486	0.21578	0.10915	0.03098	7.00655	0.258E-07	0.831E-03	39
40	12.84138	3.55908	0.97297	0.16466E-05	0.10754	1.19413	0.60524	0.17029	7.18991	0.360E-07	0.211E-03	40
41	13.17473	3.57648	0.96903	0.16699E-05	0.10922	0.80951	0.41112	0.11523	7.37552	0.358E-07	0.311E-03	41

42	13.50806	3.61683	0.96465	0.18563E-05	0.11205	0.39012	0.19857	0.05519	7.58141	0.386E-07	0.700E-03	42
43	13.84138	3.64980	0.96044	0.17880E-05	0.11824	0.46359	0.23647	0.06509	7.77927	0.351E-07	0.539E-03	43
44	14.17473	3.68600	0.95610	0.18490E-05	0.11711	0.43976	0.22482	0.06129	7.98344	0.365E-07	0.596E-03	44
45	14.50806	3.70100	0.94970	0.27380E-05	0.11989	1.57774	0.80922	0.21906	8.28474	0.524E-07	0.239E-03	45
46	14.84138	3.73534	0.94553	0.17848E-05	0.12158	0.45120	0.23191	0.06237	8.48077	0.336E-07	0.538E-03	46
47	15.17473	3.75467	0.94140	0.17744E-05	0.12045	0.80100	0.41259	0.11015	8.67523	0.335E-07	0.305E-03	47
48	15.50806	3.79611	0.93730	0.17646E-05	0.12664	0.37375	0.19292	0.05110	8.86819	0.316E-07	0.618E-03	48
49	15.84138	3.86415	0.93376	0.15220E-05	0.13625	0.19877	0.10279	0.02684	9.03433	0.252E-07	0.940E-03	49
50	16.63306	3.96833	0.92510	0.15789E-05	0.11933	0.32565	0.16916	0.04319	9.44183	0.296E-07	0.686E-03	50
51	17.29973	4.03944	0.91742	0.16691E-05	0.12160	0.43251	0.22557	0.05634	9.80316	0.305E-07	0.541E-03	51
52	17.96638	4.15218	0.90914	0.18081E-05	0.12215	0.30095	0.15764	0.03849	10.19287	0.326E-07	0.847E-03	52
53	18.63306	4.28595	0.90069	0.18520E-05	0.12663	0.26644	0.14018	0.03323	10.59029	0.319E-07	0.961E-03	53
54	19.29971	4.41837	0.89220	0.18683E-05	0.13732	0.27759	0.14670	0.03371	10.98938	0.294E-07	0.873E-03	54
55	25.49138	4.52047	0.87330	0.45270E-06	0.01044	0.83234	0.44432	0.09941	11.87859	0.919E-07	0.925E-03	55
56	25.66777	4.16510	0.87323	0.54929E-07	-0.07698	-0.00080	-0.00043	-0.00010	11.88168	-0.151E-08	0.154E-01	56
57	25.83305	3.68220	0.87374	-0.45240E-06	-0.10746	0.00409	0.00218	0.00056	11.85793	0.893E-08	0.160E-01	57
58	26.17471	2.97034	0.87665	-0.12591E-05	-0.11591	0.01353	0.00721	0.00218	11.72121	0.231E-07	0.106E-01	58
59	26.50806	2.49710	0.88090	-0.18839E-05	-0.11759	0.02450	0.01302	0.00478	11.52119	0.342E-07	0.717E-02	59
60	26.84138	2.09263	0.88515	-0.18809E-05	-0.14124	0.02409	0.01278	0.00558	11.32101	0.286E-07	0.512E-02	60
61	27.17473	1.75065	0.88915	-0.17649E-05	-0.15474	0.02242	0.01187	0.00619	11.13280	0.246E-07	0.397E-02	61
62	27.50806	1.49813	0.89295	-0.16691E-05	-0.16093	0.02434	0.01286	0.00793	10.95445	0.225E-07	0.283E-02	62
63	27.84138	1.25342	0.89657	-0.15905E-05	-0.16885	0.02029	0.01070	0.00780	10.78419	0.205E-07	0.262E-02	63
64	28.17473	1.10290	0.89904	-0.10880E-05	-0.11301	0.01938	0.01021	0.00867	10.66754	0.210E-07	0.242E-02	64
65	28.50806	0.96520	0.90187	-0.12384E-05	-0.15476	0.02120	0.01114	0.01079	10.53459	0.175E-07	0.162E-02	65
66	28.84138	0.82314	0.90530	-0.15021E-05	-0.16718	0.02156	0.01132	0.01269	10.37305	0.197E-07	0.155E-02	66
67	29.17473	0.68382	0.90866	-0.14647E-05	-0.16322	0.01809	0.00948	0.01262	10.21524	0.198E-07	0.157E-02	67
68	29.50806	0.58761	0.91277	-0.17900E-05	-0.15591	0.02710	0.01417	0.02233	10.02196	0.254E-07	0.114E-02	68
69	29.84138	0.51186	0.91640	-0.15810E-05	-0.15590	0.02634	0.01374	0.02504	9.85092	0.225E-07	0.899E-03	69
70	30.17473	0.43581	0.91994	-0.15344E-05	-0.15590	0.02198	0.01145	0.02421	9.68462	0.219E-07	0.905E-03	70
71	30.50806	0.37596	0.92396	-0.17408E-05	-0.14971	0.02721	0.01414	0.03490	9.49557	0.260E-07	0.745E-03	71
72	30.84138	0.31470	0.92798	-0.17393E-05	-0.15648	0.02262	0.01173	0.03407	9.30629	0.250E-07	0.733E-03	72
73	31.17473	0.27841	0.93167	-0.15912E-05	-0.15535	0.03011	0.01559	0.05262	9.13277	0.231E-07	0.439E-03	73
74	31.50806	0.21020	0.93550	-0.16472E-05	-0.14915	0.01361	0.00703	0.02898	8.95279	0.250E-07	0.863E-03	74
75	31.84138	0.18859	0.93934	-0.16531E-05	-0.14688	0.03546	0.01829	0.09180	8.77184	0.256E-07	0.279E-03	75
76	32.17473	0.15991	0.94292	-0.15351E-05	-0.13956	0.02170	0.01117	0.06423	8.60344	0.251E-07	0.391E-03	76
77	32.50806	0.12143	0.94600	-0.13158E-05	-0.11982	0.01116	0.00574	0.04103	8.45894	0.251E-07	0.612E-03	77
78	32.84138	0.13023	-0.04344	0.86199E-03	-0.11023	14.13809	0.0	117.50941	55.00269	-0.432E-05	-0.368E-04	78
79	33.17473	0.09667	0.95366	-0.42530E-03	-0.10067	3.34560	1.71248	15.20633	8.09857	0.974E-05	0.641E-03	79
80	33.50806	0.08431	0.95594	-0.97108E-06	-0.09504	0.01666	0.00852	0.09426	7.99132	0.236E-07	0.251E-03	80
81	33.84138	0.08370	0.95814	-0.93964E-06	-0.08881	0.30770	0.15714	1.87077	7.88745	0.245E-07	0.131E-04	81
82	34.17473	0.05998	0.95998	-0.78184E-06	-0.08376	0.00552	0.00281	0.03955	7.80098	0.217E-07	0.548E-03	82
83	34.50806	0.04325	0.96186	-0.79787E-06	-0.08208	0.00574	0.00293	0.05722	7.71262	0.226E-07	0.395E-03	83
84	34.84138	0.02496	0.96344	-0.67014E-06	-0.07758	0.00287	0.00146	0.04398	7.63834	0.201E-07	0.458E-03	84
85	35.17473	0.01004	0.96550	-0.87477E-06	-0.08040	0.00227	0.00115	0.07034	7.54129	0.254E-07	0.361E-03	85
86	35.50806	0.01172	0.96752	-0.85396E-06	-0.07530	-0.01303	-0.00662	-0.61005	7.44646	0.265E-07	-0.435E-04	86
87	35.84138	-0.00556	0.96973	-0.93400E-06	-0.07698	0.0	0.0	0.0	7.34259	0.284E-07	0.100E+05	87

ENGINEERING STRAIN (87)= 7.3426

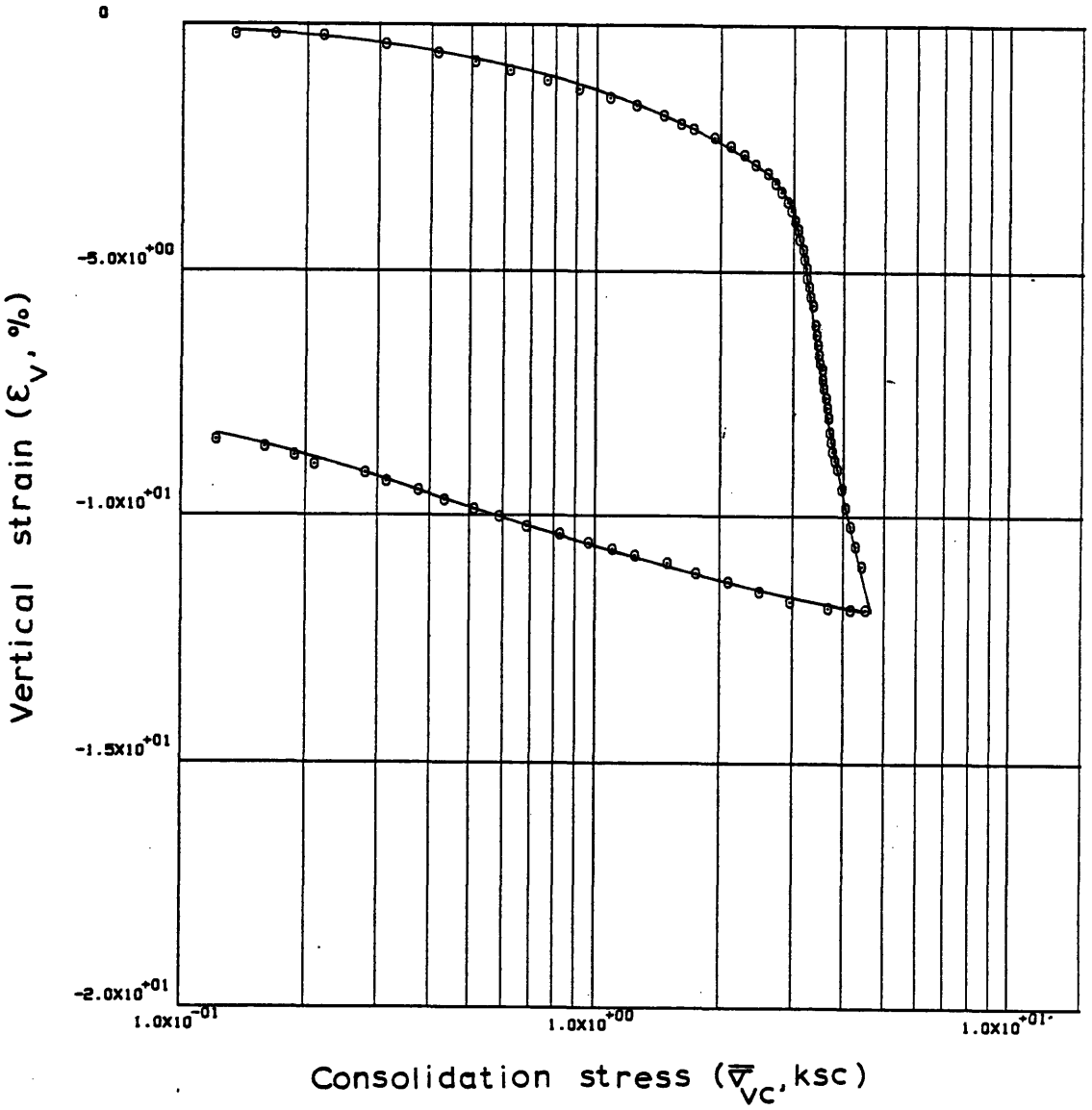

Sample No. SP15VERT w_N (%) 40.70 Estimated

Depth 109.48 w_L (%) 40.38 $\bar{\sigma}_{vo}$ 2.57 $\bar{\sigma}_{vm}$ 2.96-3.00

Soil Type Boston Blue Clay w_P (%) 21.97 CR 0.5066 RR 0.0225

P.I.(%) 18.41 G_s 2.77 e_o 1.1274

o At t_p

Remarks Data from C.R.S.C test

w_L & w_P estimated from Baligh et al (1980)

Figure E.49 Compression Curve for Sample No. SP15VERT

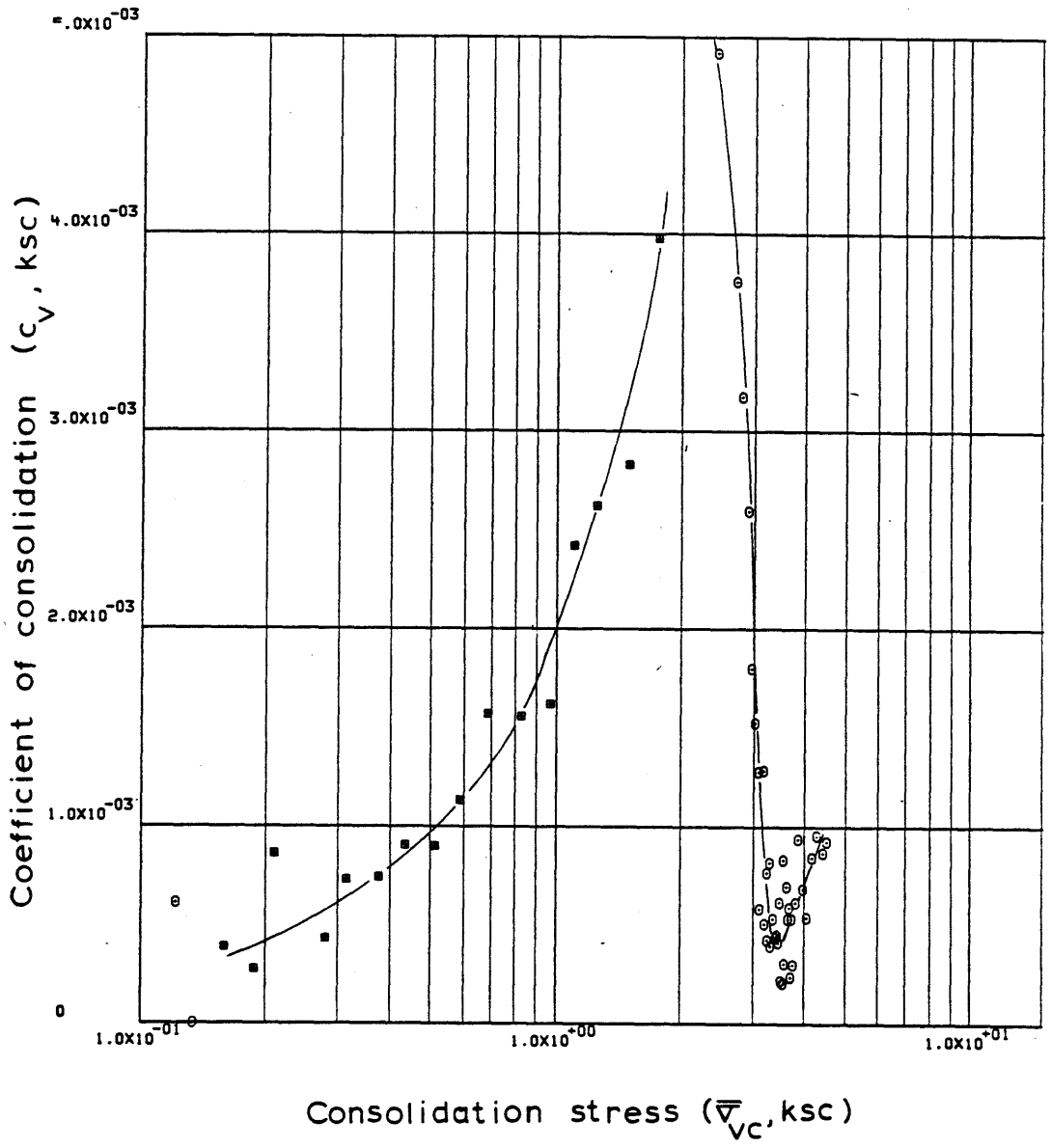

Sample No. SP15VERT w_N (%) 40.70 Estimated

Depth 109.48 w_L (%) 40.38 $\bar{\sigma}_{vo}$ 2.57 $\bar{\sigma}_{vm}$ 2.96-3.00

Soil Type Boston Blue Clay w_P (%) 21.97 CR 0.5066 RR 0.0225

P.I.(%) 18.41 G_s 2.77 e_o 1.1274

⊙ At t_p

Remarks Data from C.R.S.C test

w_L & w_P estimated from Baligh et al (1980)

Figure E.50 Variation of coefficient of consolidation with consolidation stress for Sample No. SP15VERT

APPENDIX F

This Appendix represents data derived from C.R.S.C. tests on Boston Blue Clay samples retrieved from the I-95 test site. Figs. F.1 to F.13 represent the variation of coefficient of consolidation corresponding to different values fo the overconsolidation ratio during gradual load removal starting from stresses in the virgin compression range. For tests performed with a load-reload cycle, data from the first unload branch (corresponding to the load-unload cycle) and the second unload branch (corresponding to final unload) are plotted simultaneously. Of interest is the normalized behavior of the soil specimens.

Figs. F.14 to F.20 represent the variation of the constraint modulus $D = \frac{1}{m_v}$ ' ($= \frac{1}{m_h}$) with the consolidation effective stress, restricted in the normally consolidated range. The data appears to follow a linear trend with appreciable scatter. This data is used to estimate the value of the coefficient of volume change m_{vo}, m_{ho} in the normally consolidated range upon first reloading.

Figs. F.21 through F.26 represent the variation of the normalized parameters (m_{vs}/m_{vo}),(m_{hs}/m_{ho}) with the overconsolidation ratio (OCR), where m_{vs} is the value of the coefficient of volume change corresponding to the two swelling curves (for the unload-reload

cycle and final unloading). The curves exhibit reasonable scatter and manifest normalized behavior. Those curves are later used to derive the value of the in situ m_{vs}, m_{hs} (which is assumed to be equal to m_v, m_{hs} reloading, m_{vr} or m_{hr}, in situ, in the overconsolidated range corresponding to small load increments (or decrements).

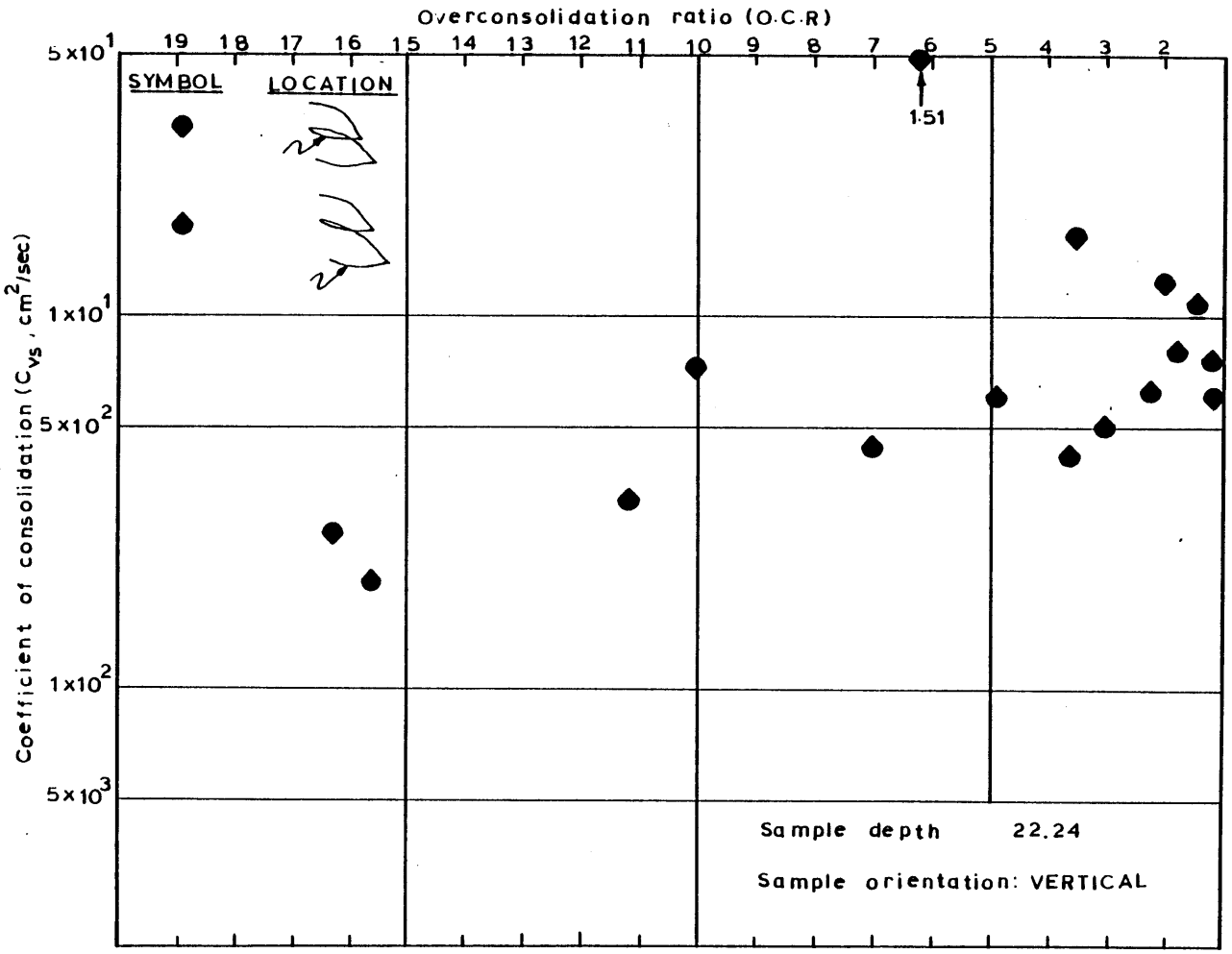

Figure F.1 Variation of the coefficient of consolidation for rebound with the overconsolidation ratio from C.R.S.C. tests.

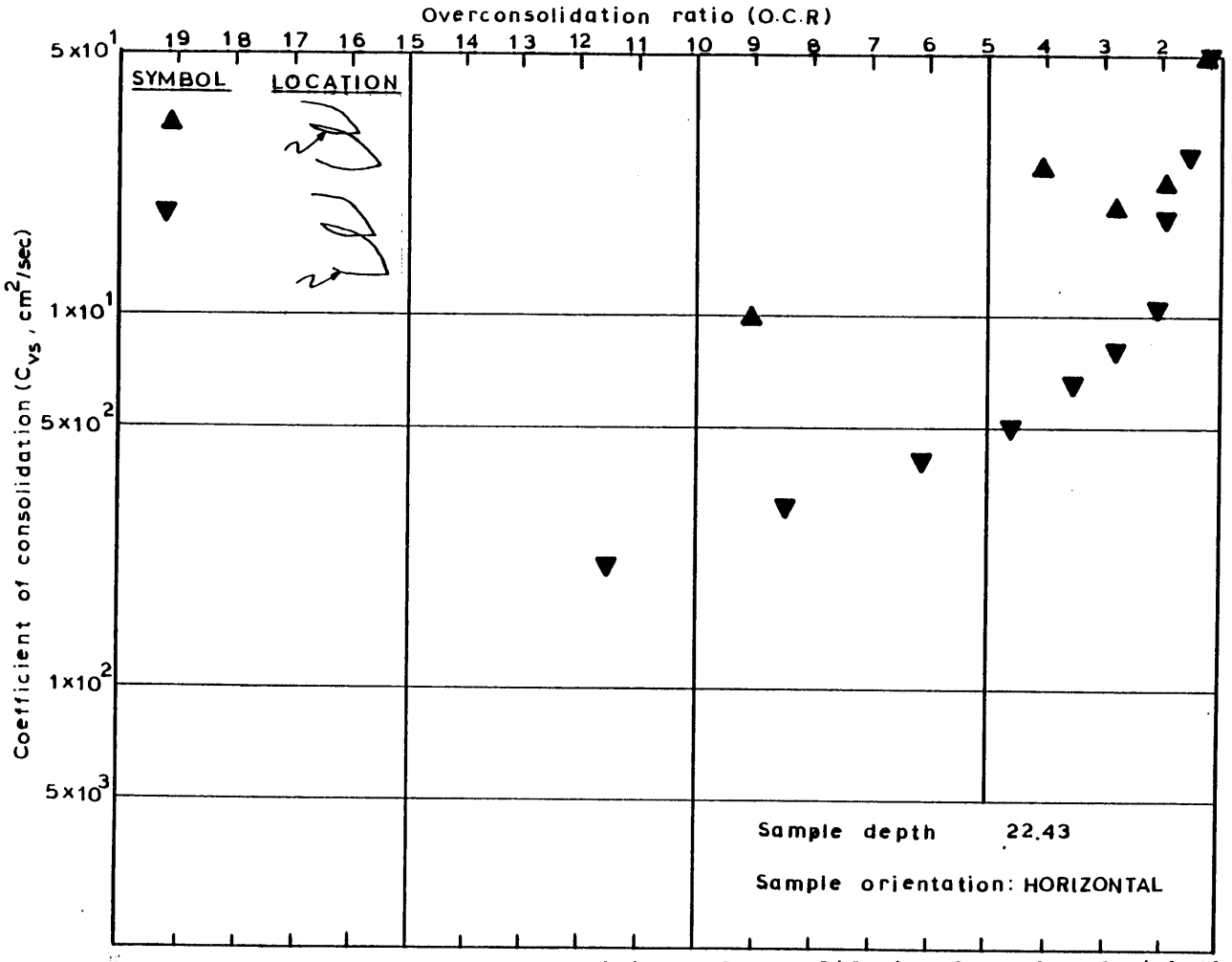

Figure F.2 Variation of the coefficient of consolidation for rebound with the overconsolidation ratio from C.R.S.C. tests.

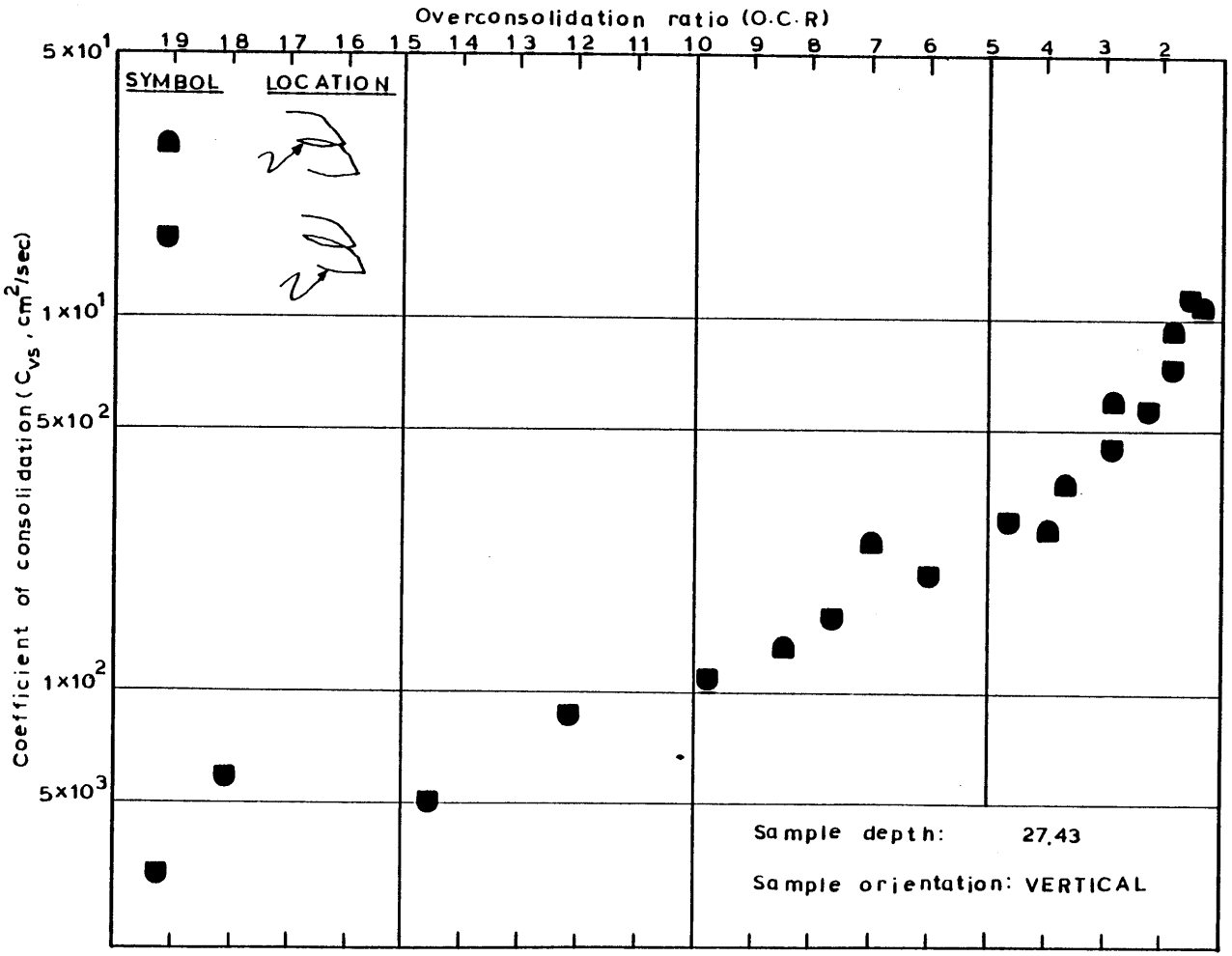

Figure F.3 Variation of the coefficient of consolidation for rebound with the overconsolidation ratio from C.R.S.C. tests.

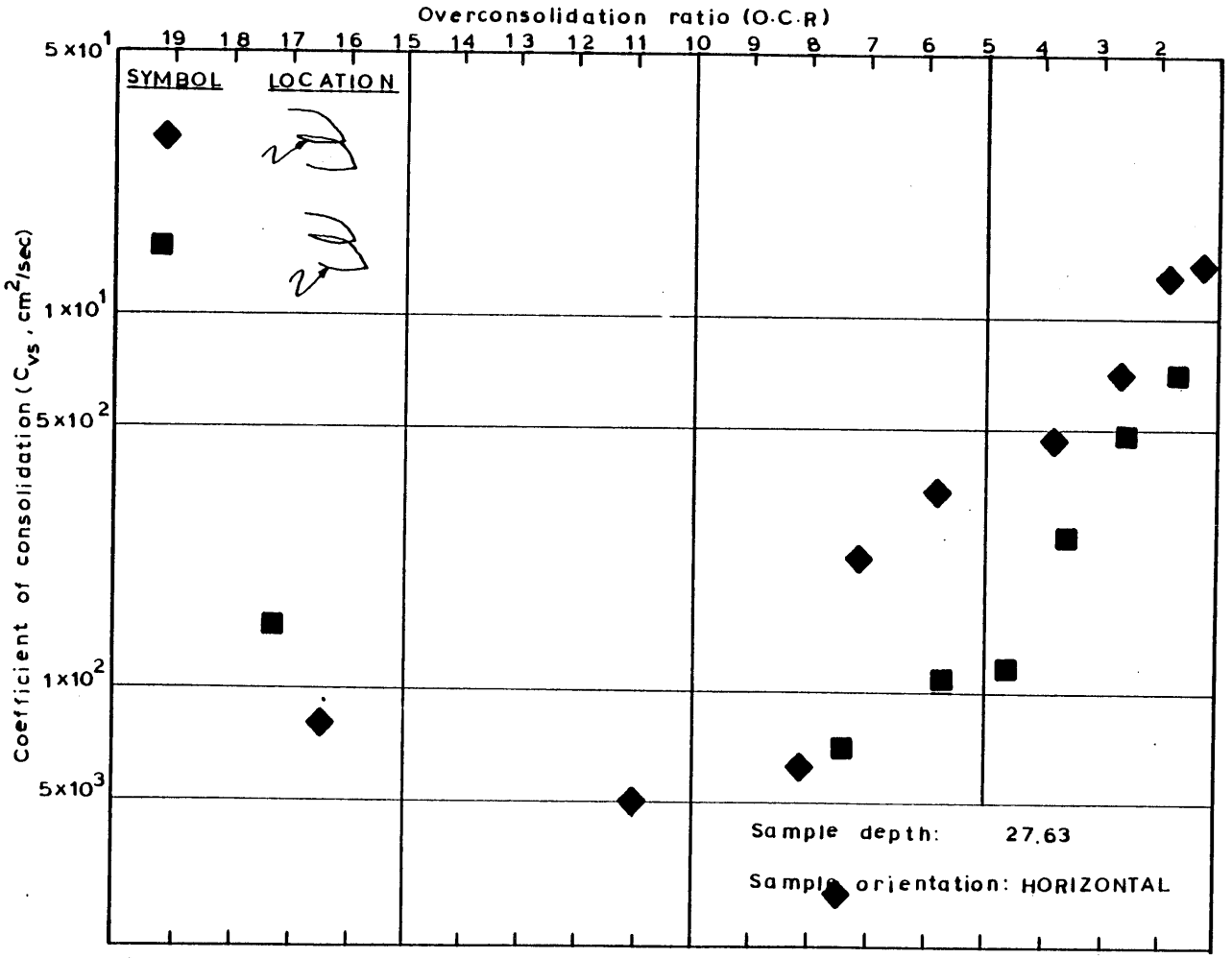

Figure F.4 Variation of the coefficient of consolidation for rebound with the overconsolidation ratio from C.R.S.C. tests.

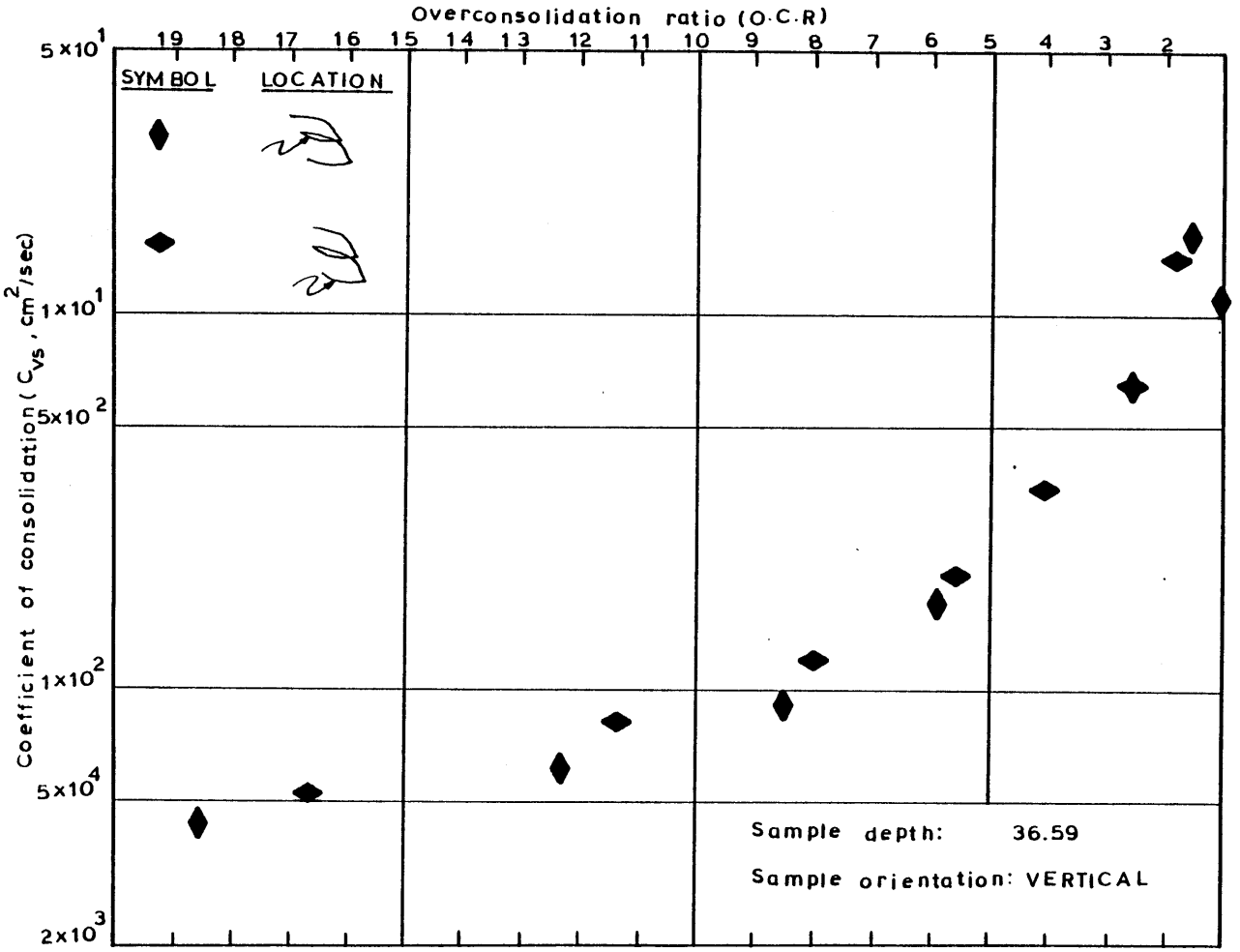

Figure F.5 Variation of the coefficient of consolidation for rebound with the overconsolidation ratio from C.R.S.C. tests.

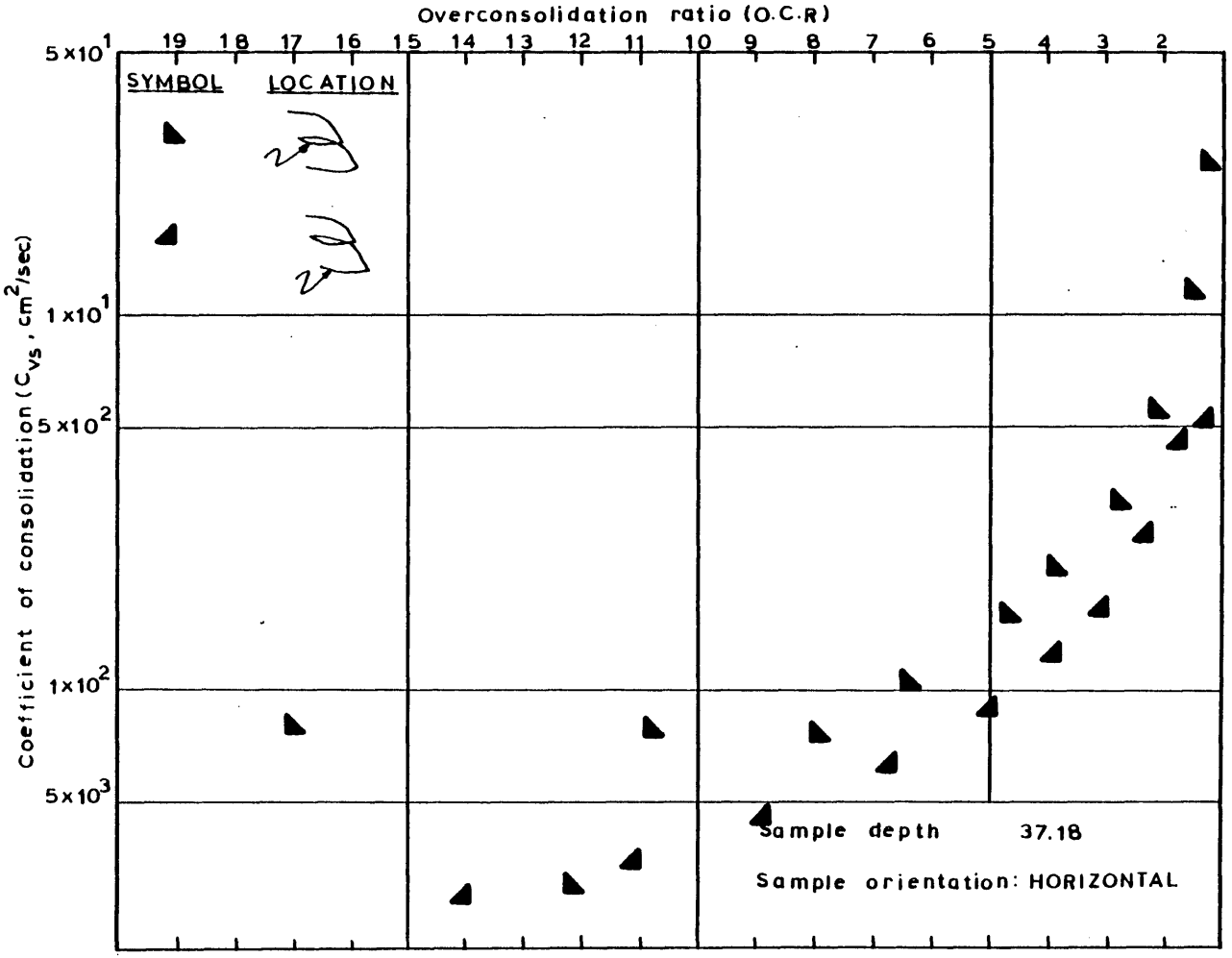

Figure F.6 Variation of the coefficient of consolidation for rebound with the overconsolidation ratio from C.R.S.C. tests.

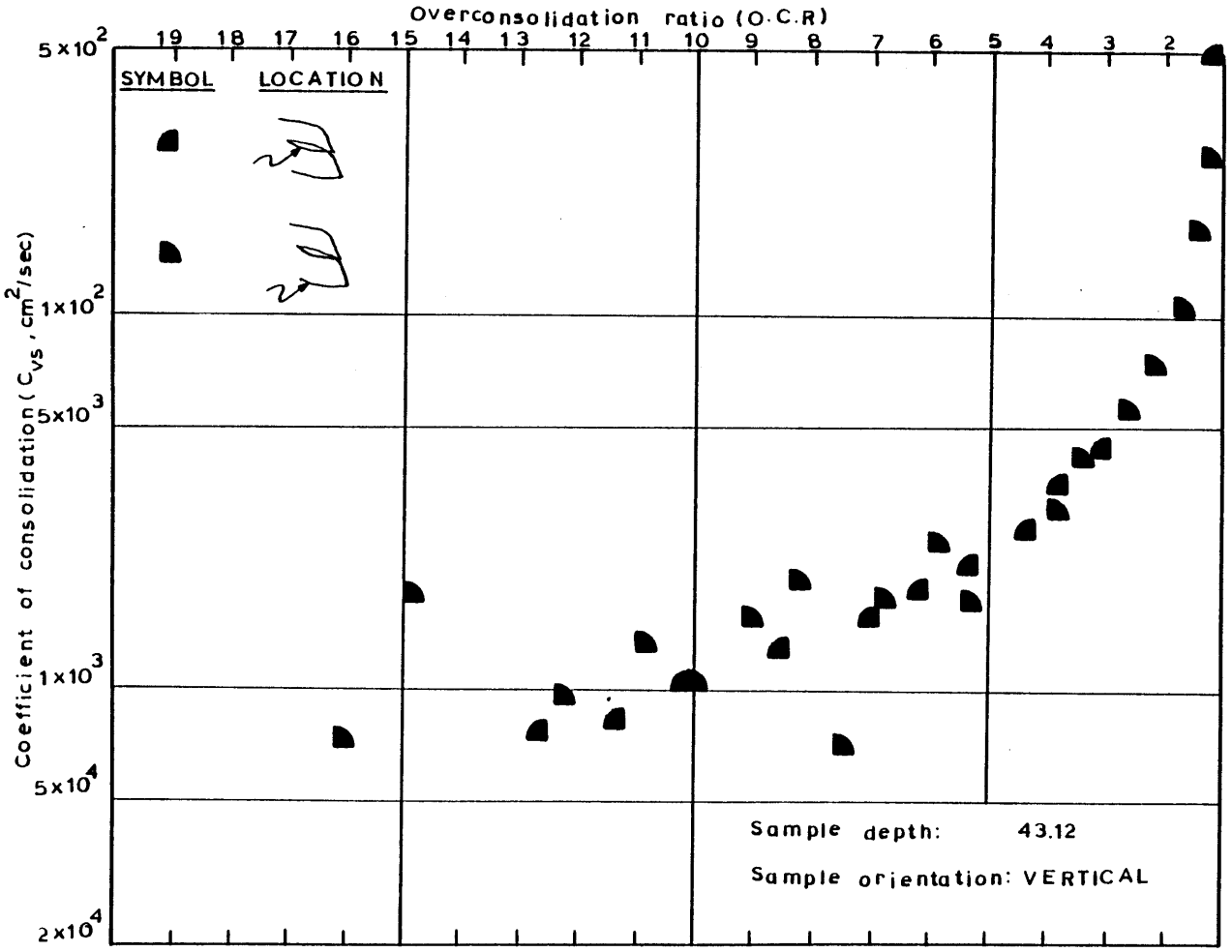

Figure F.7 Variation of the coefficient of consolidation for rebound with the overconsolidation ratio from C.R.S.C. tests.

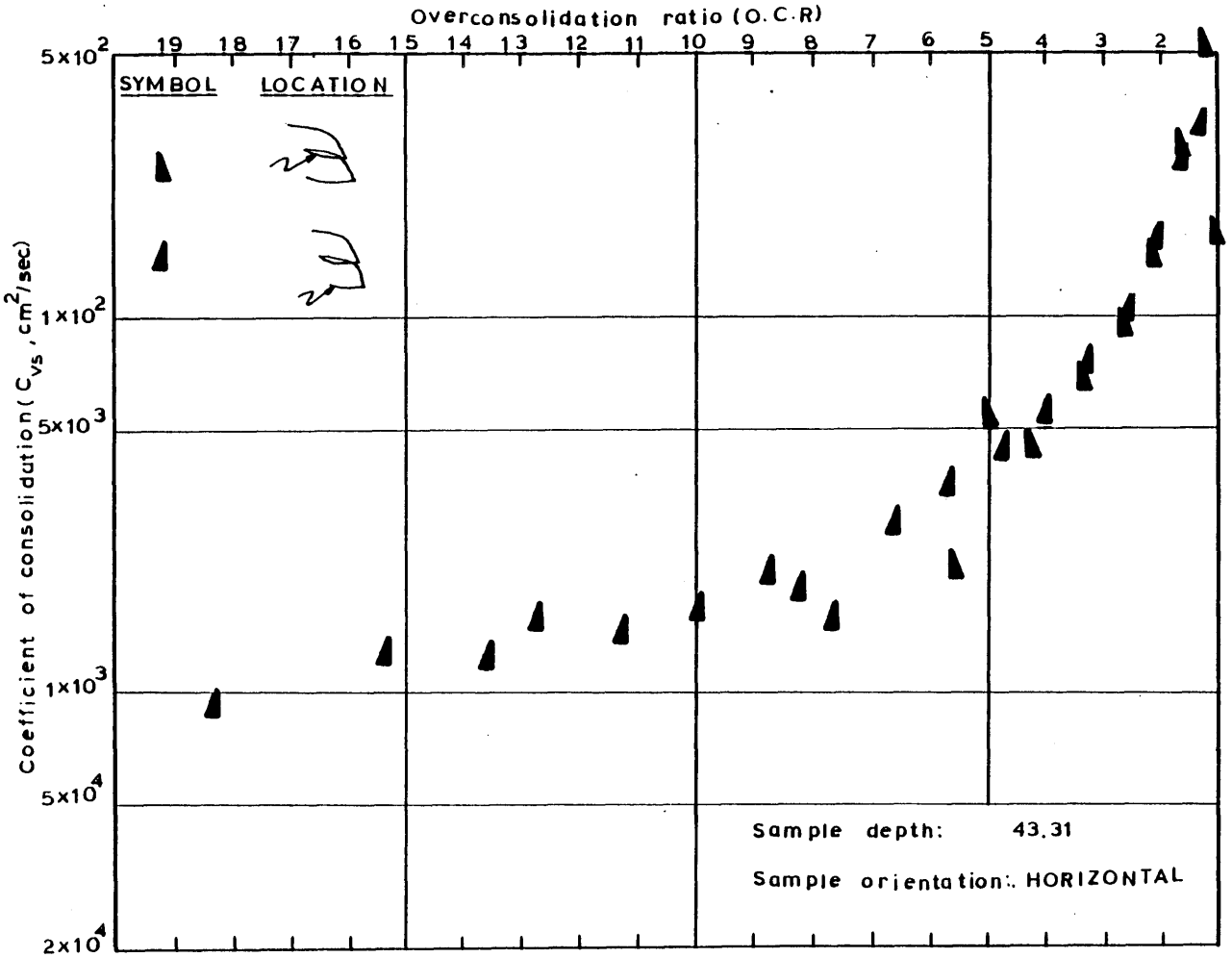

Figure F.8 Variation of the coefficient of consolidation for rebound with the overconsolidation ratio from C.R.S.C. tests.

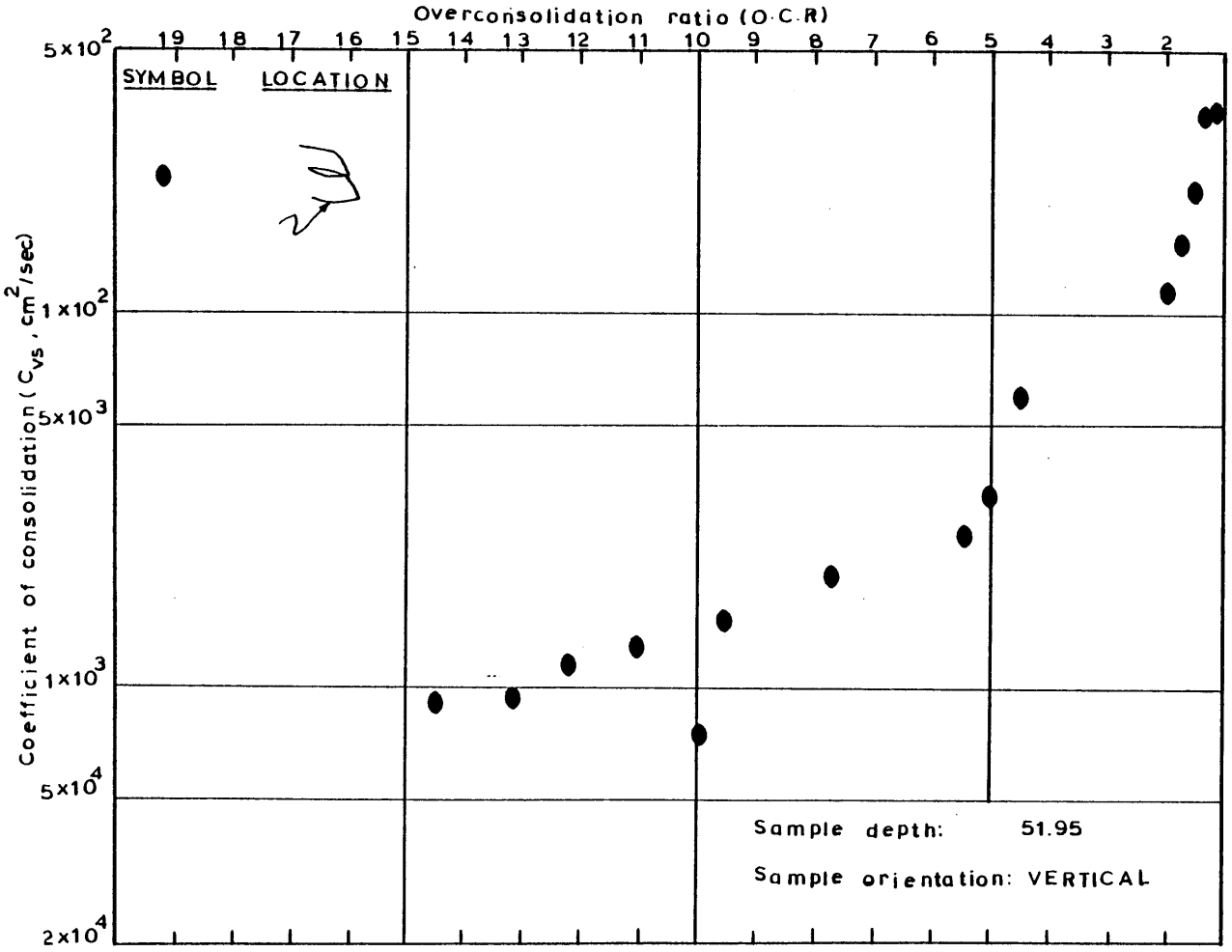

Figure F.9 Variation of the coefficient of consolidation for rebound with the overconsolidation ratio from C.R.S.C. tests.

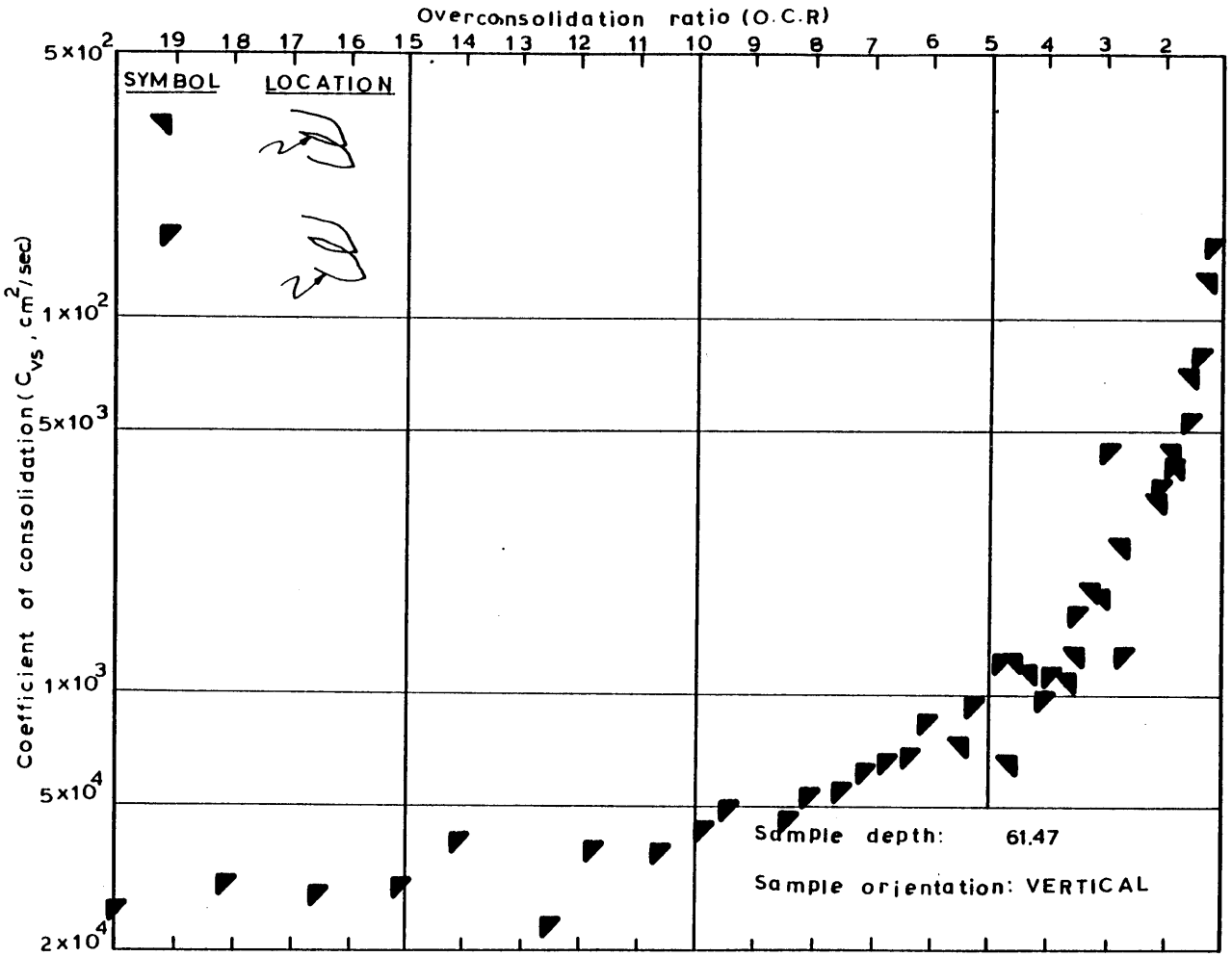

Figure F.10 Variation of the coefficient of consolidation for rebound with the overconsolidation ratio from C.R.S.C. tests.

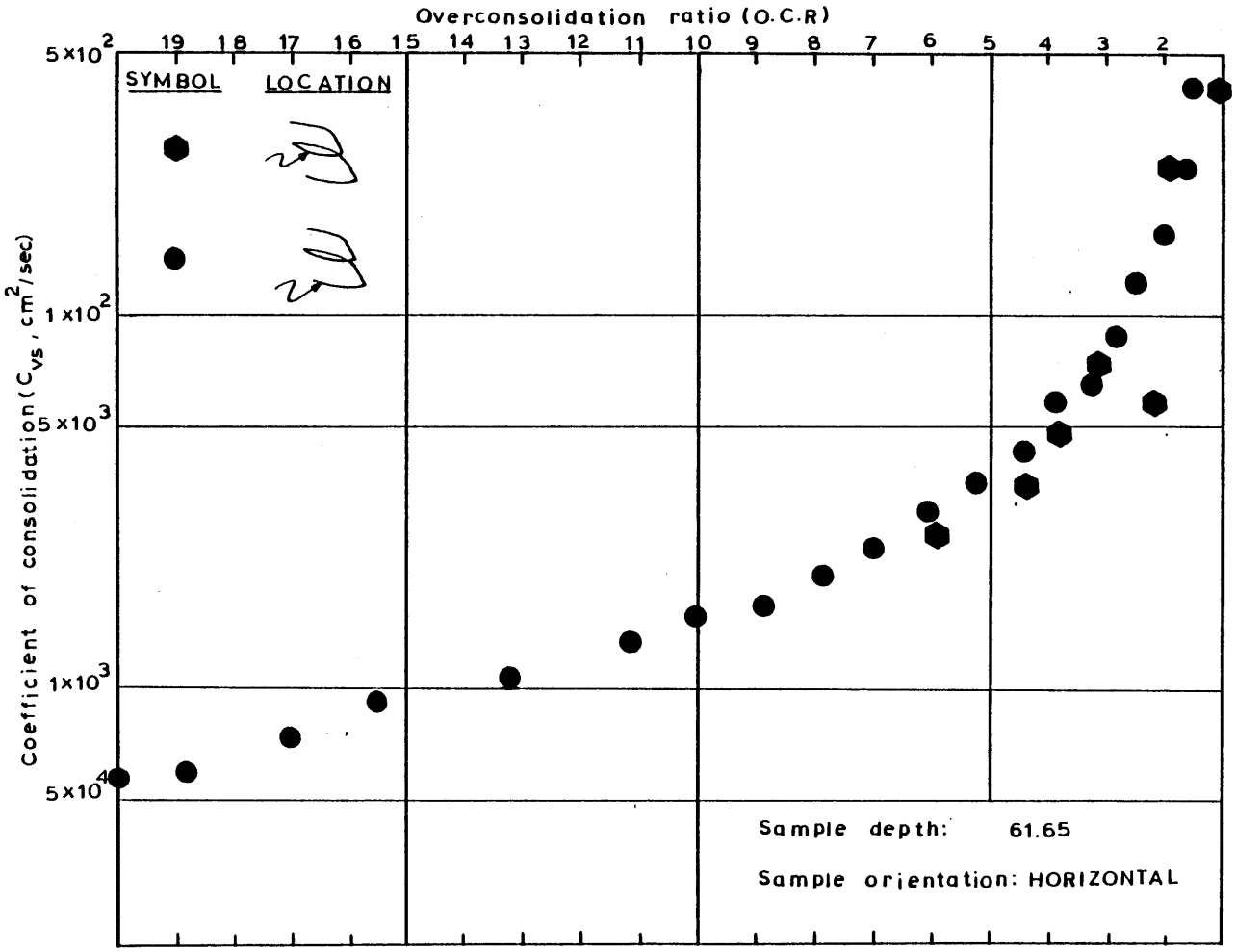

Figure F.11 Variation of the coefficient of consolidation for rebound with the overconsolidation ratio from C.R.S.C. tests.

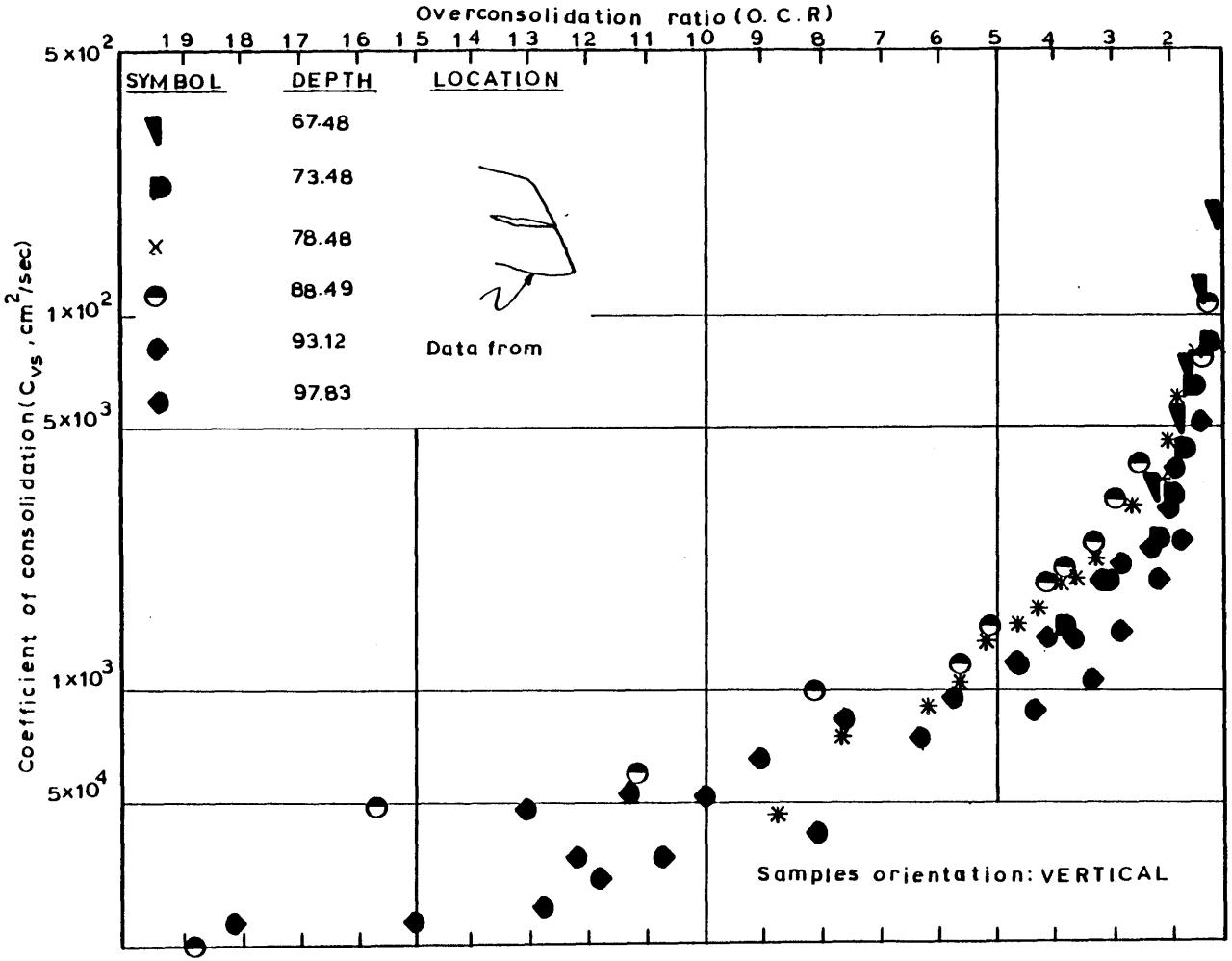

Figure F.12 Variation of the coefficient of consolidation for rebound with the overconsolidation ratio from C.R.S.C. tests.

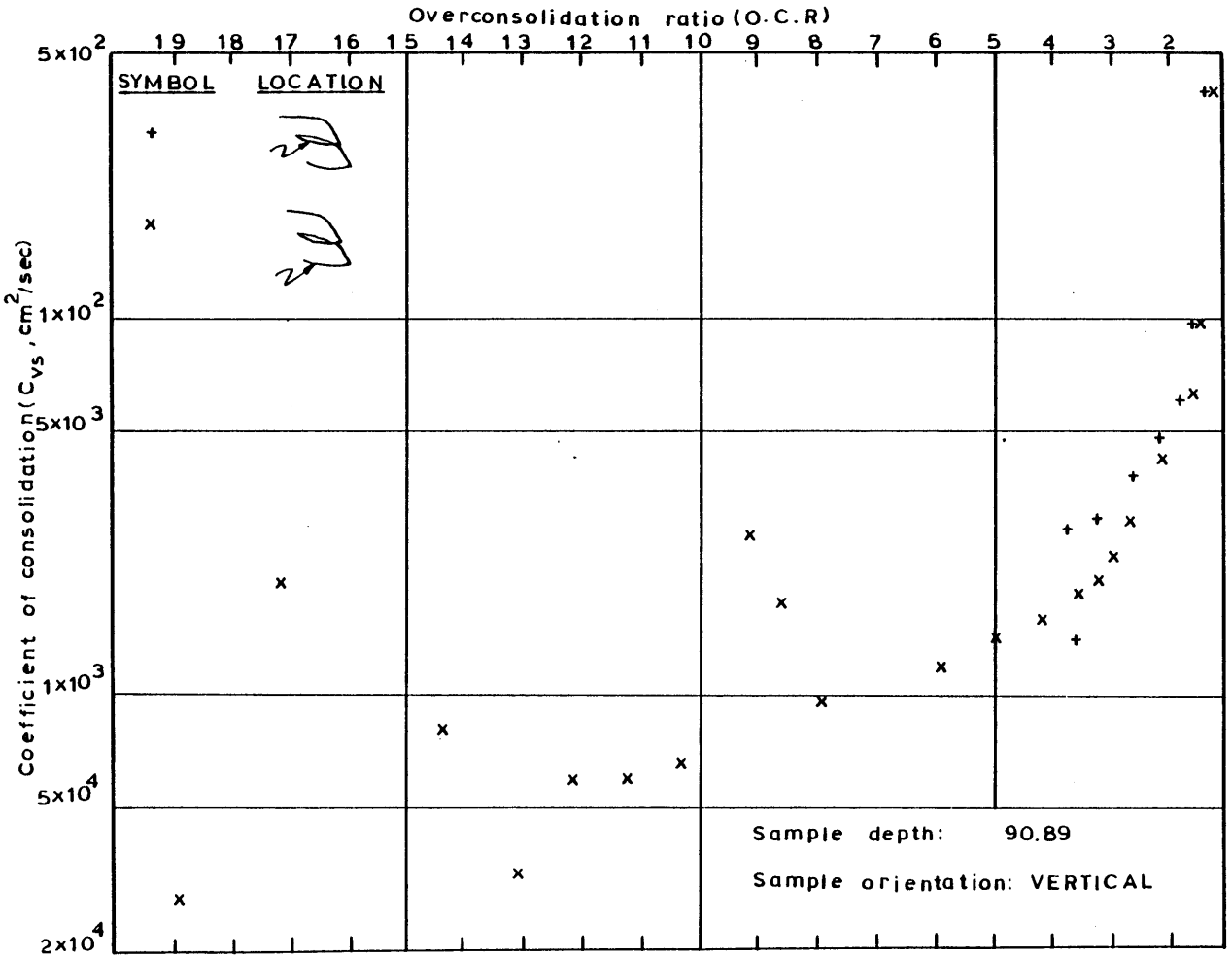

Figure F.13 Variation of the coefficient of consolidation for rebound with the overconsolidation ratio from C.R.S.C. tests.

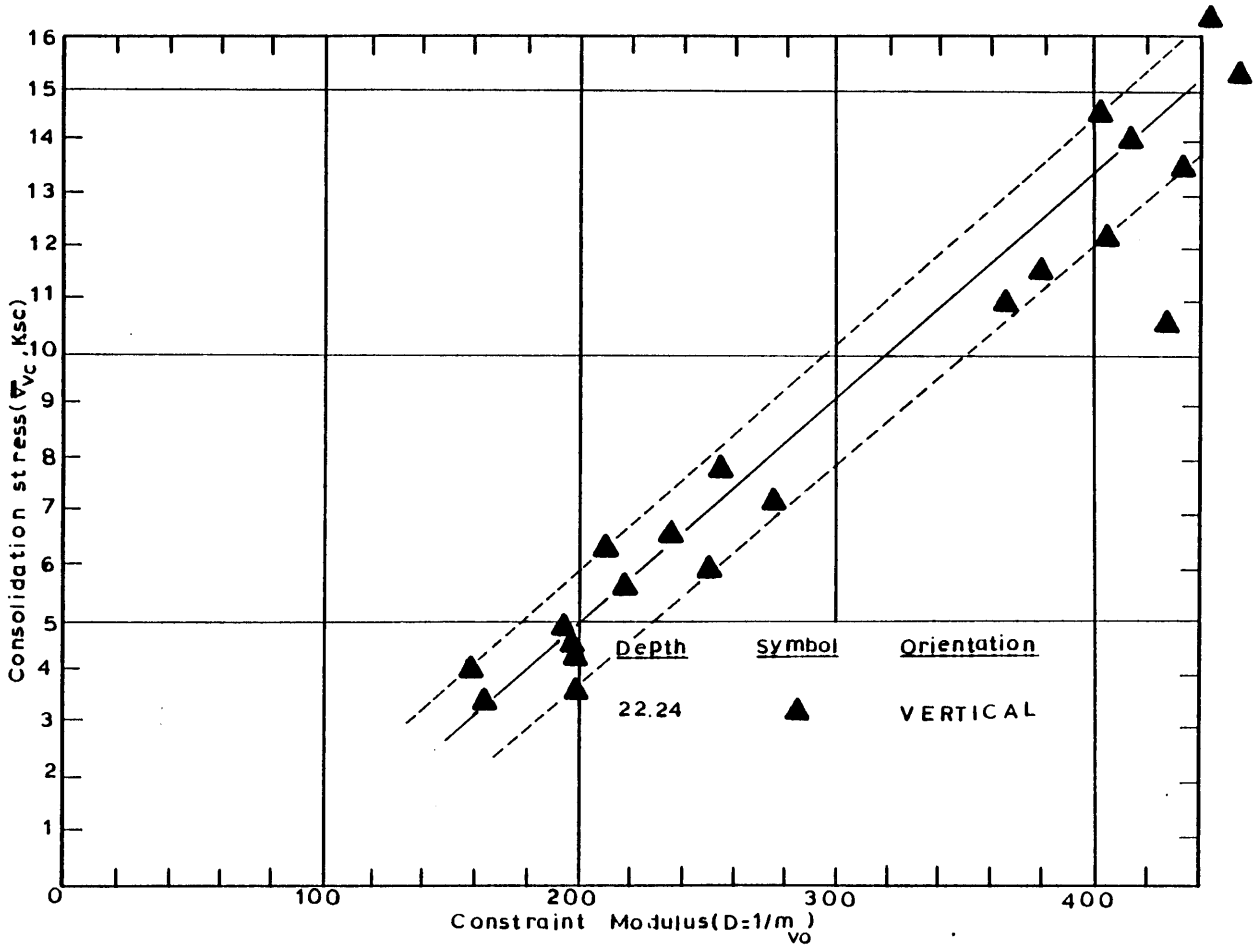

Figure F.14 Variation of the constraint modulus with consolidation stress.

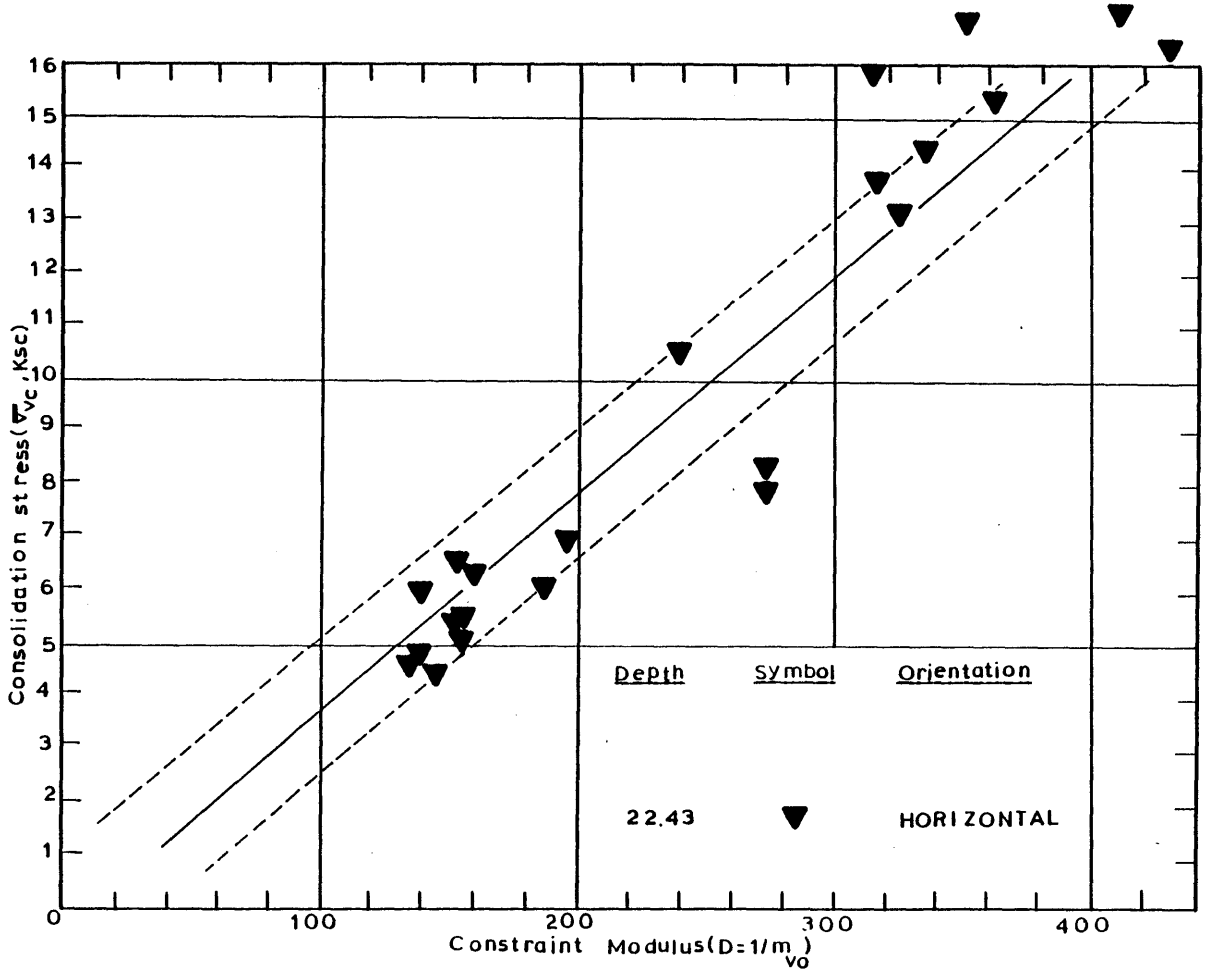

Figure F.15 Variaton of the constraint modulus with consolidation stress.

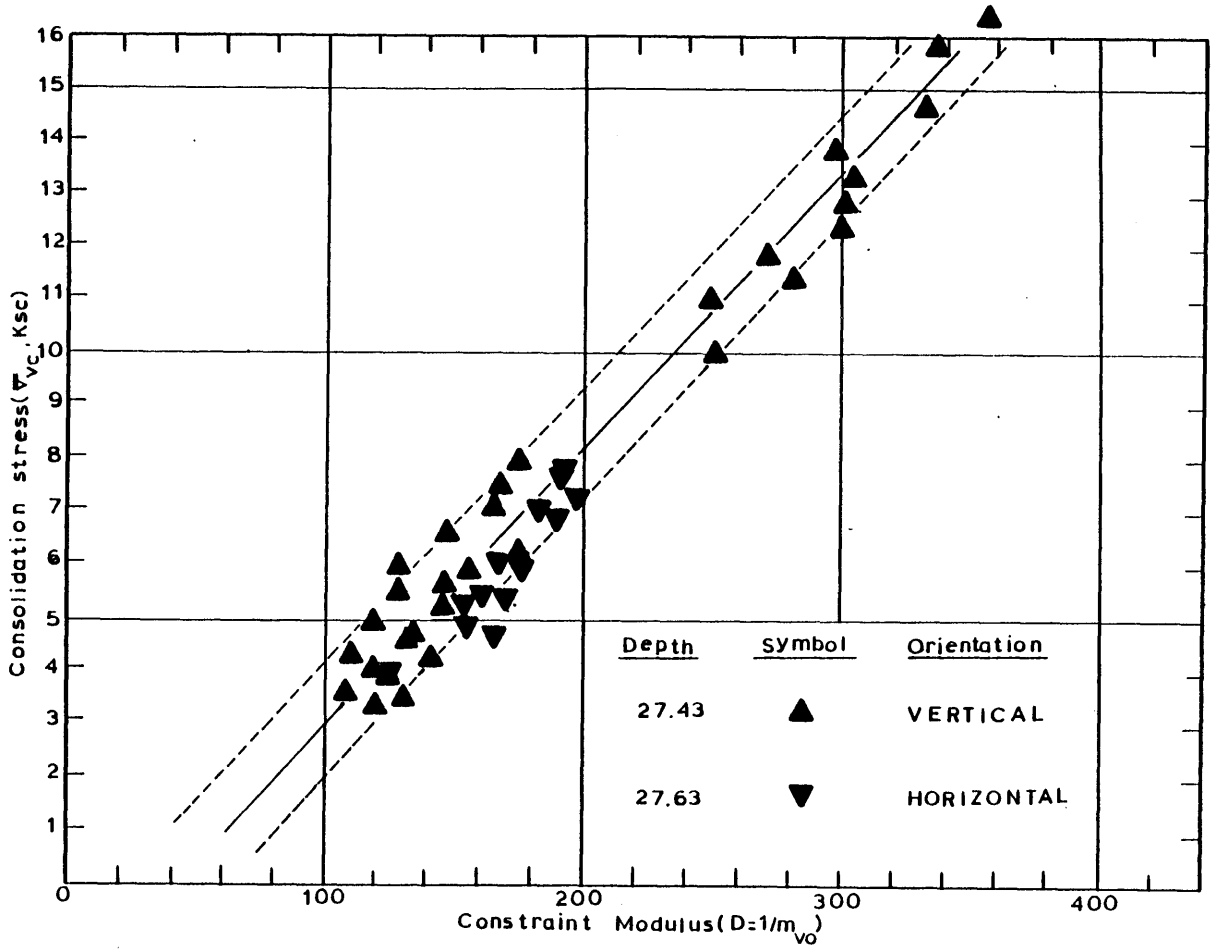

Figure F.16 Variation of the constraint modulus with consolidation stress.

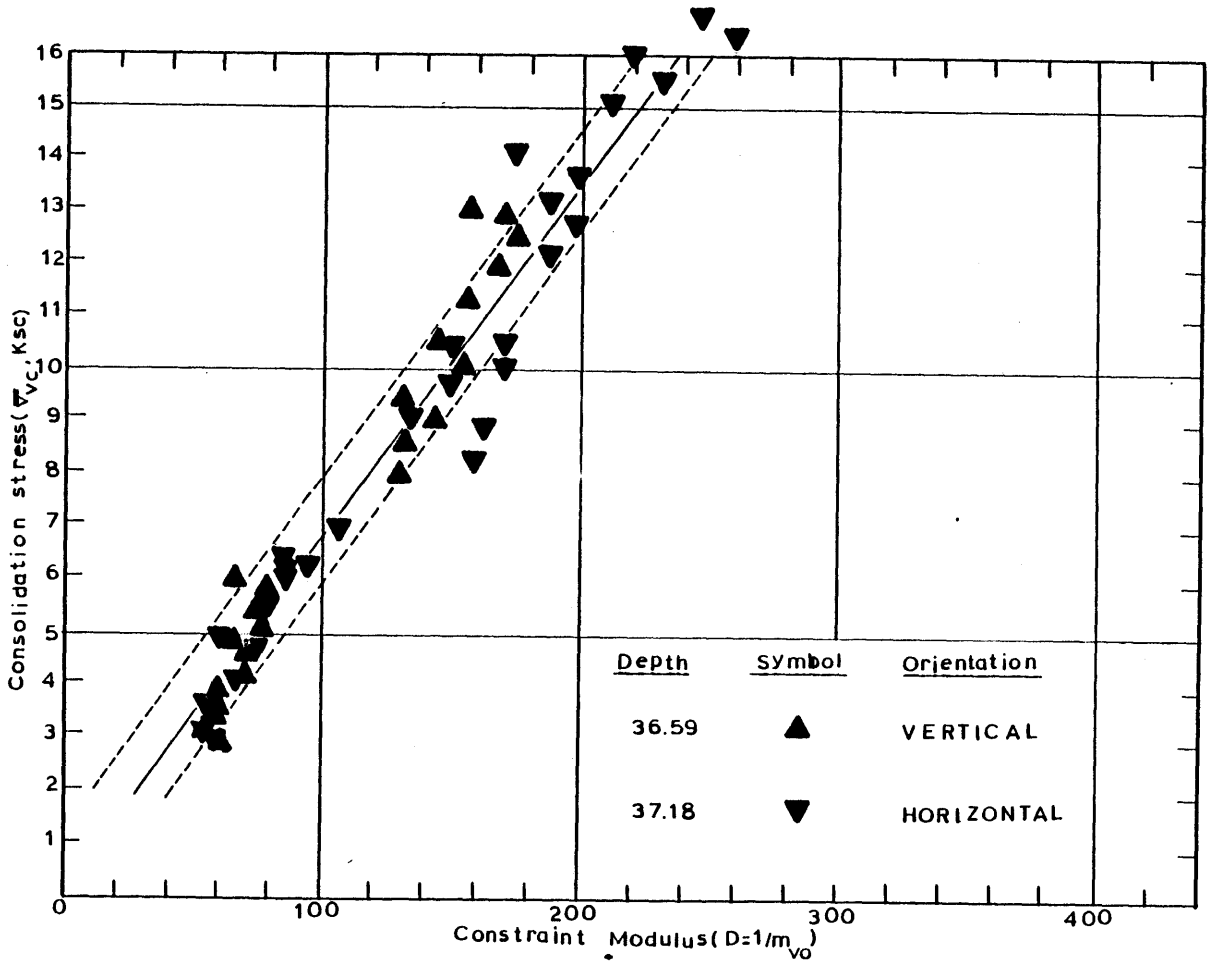

Figure F.17 Variation of the constraint modulus with consolidation stress.

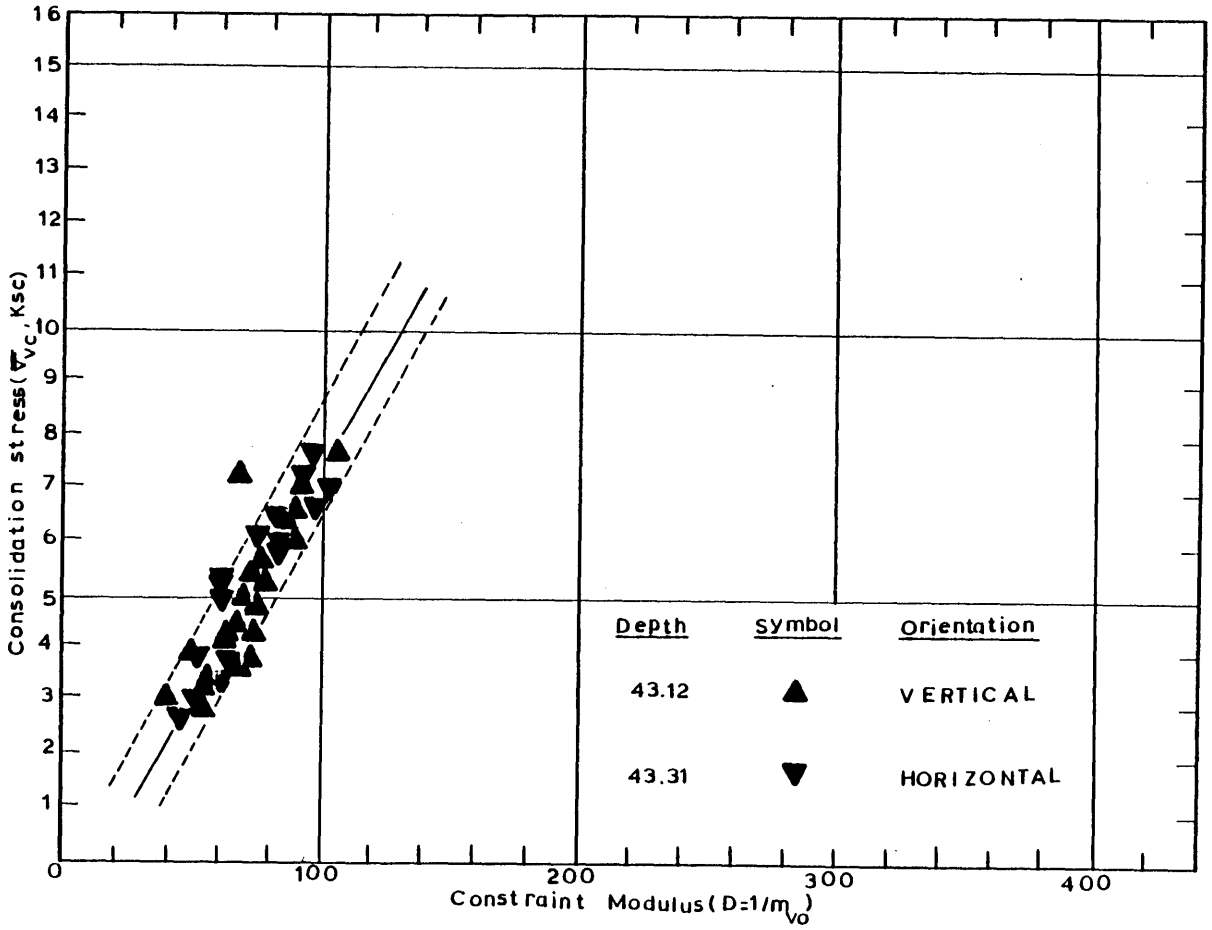

Figure F.18 Variation of the constraint modulus with consolidation stress.

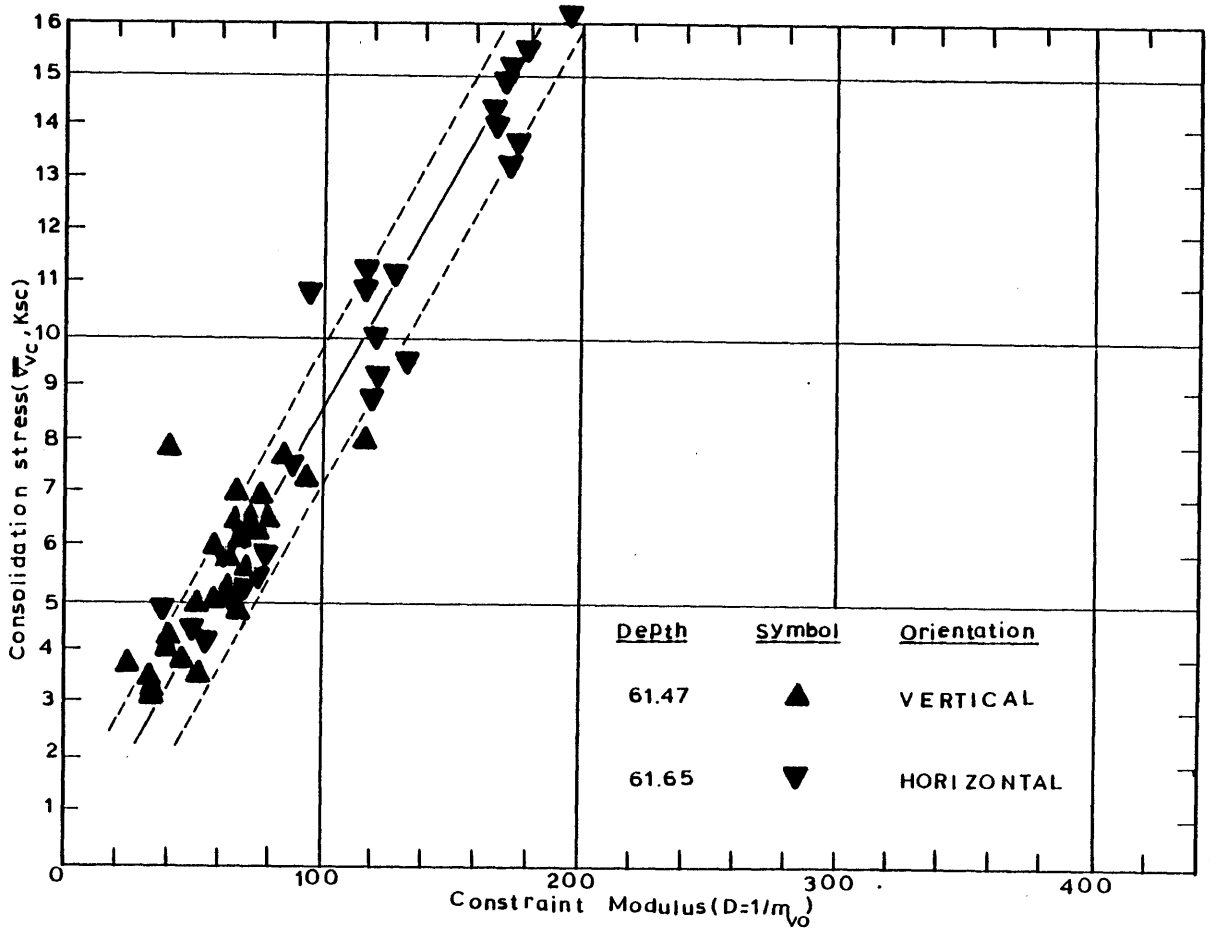

Figure F.19 Variation of the constraint modulus with consolidation stress.

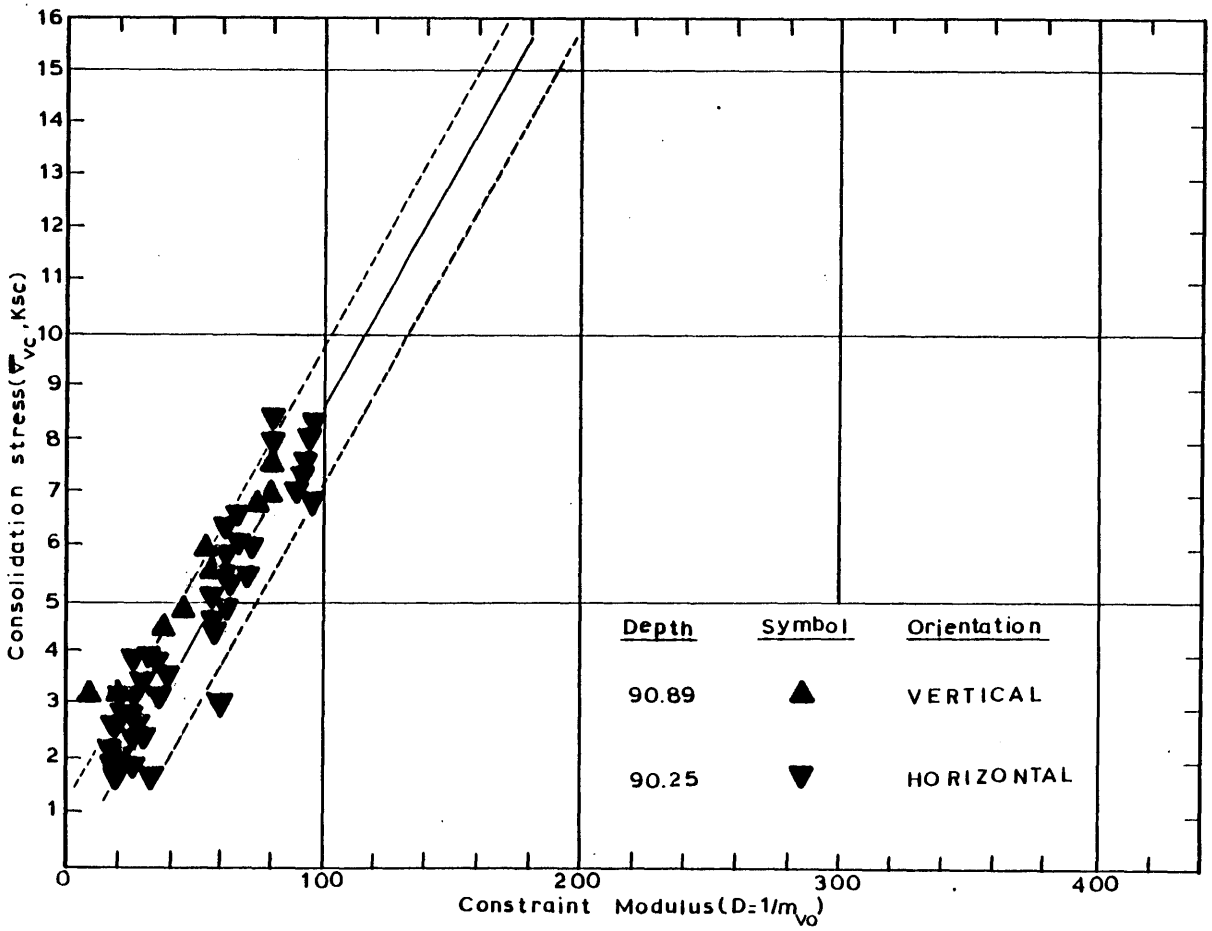

Figure F.20 Variation of the constraint modulus with consolidation stress.

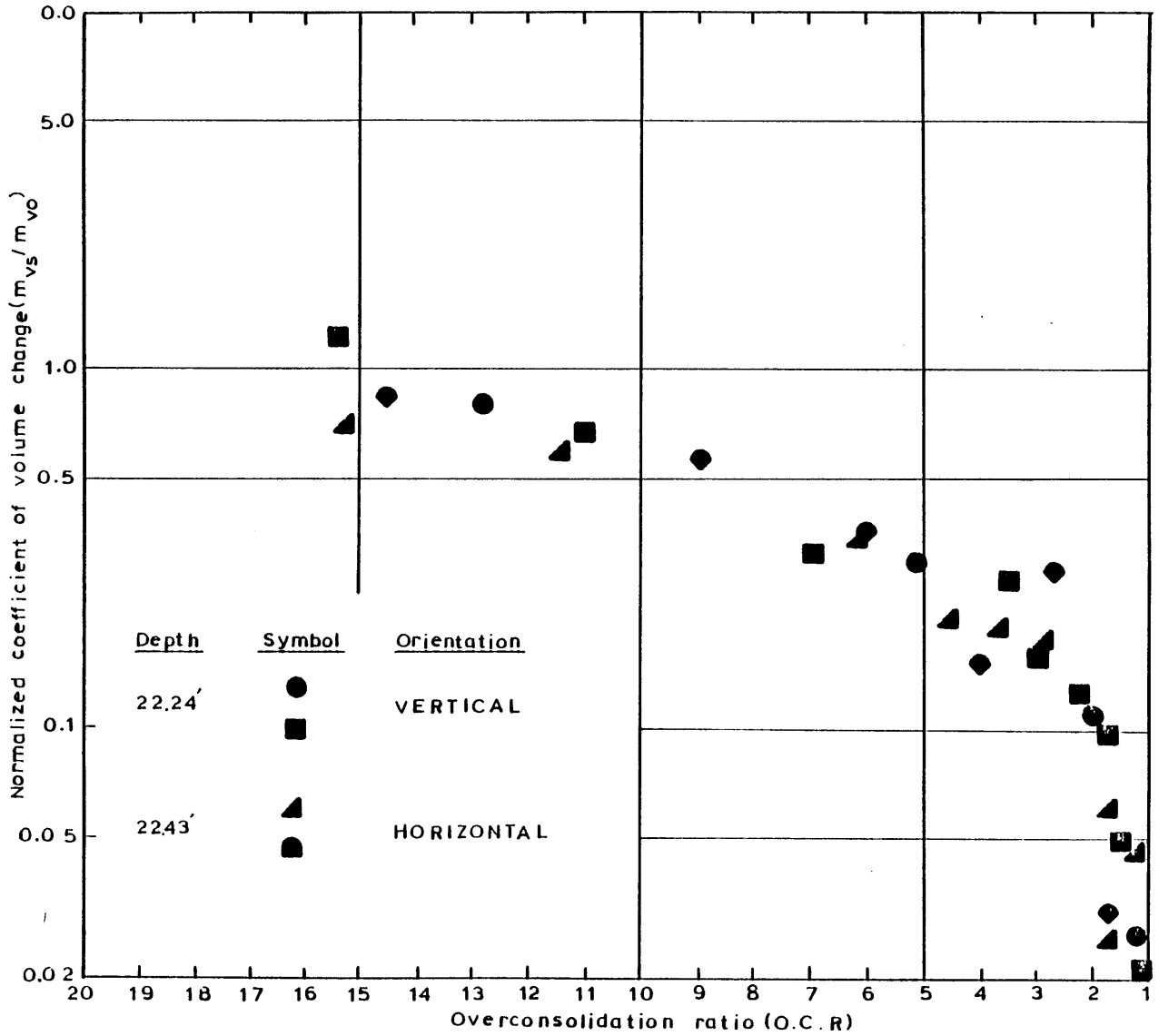

Figure 21 Variation of the normalized coefficient of volume change with overconsolidation ratio.

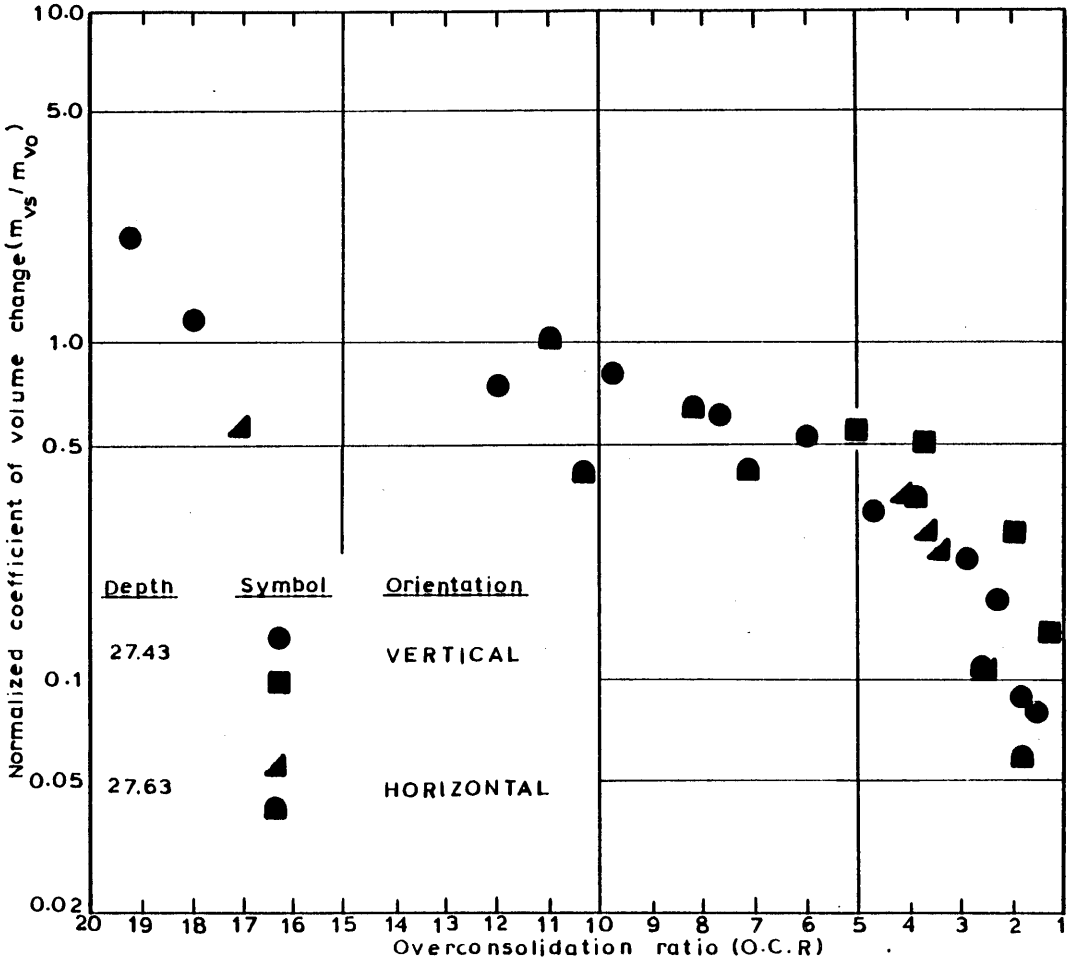

Figure F.22 Variation of the normalized coefficient of volume change with overconsolidation ratio.

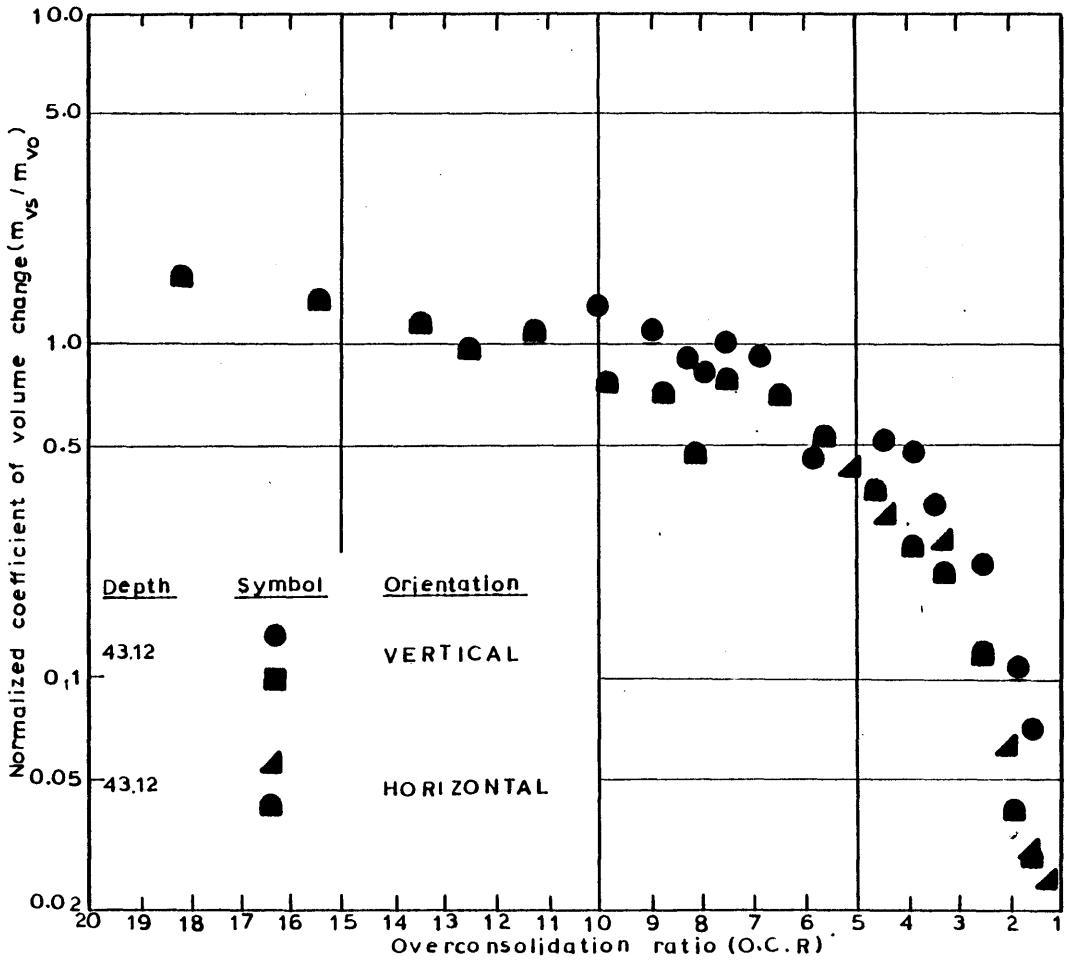

Figure F.23 Variation of the normalized coefficient of volume change with overconsolidation ratio.

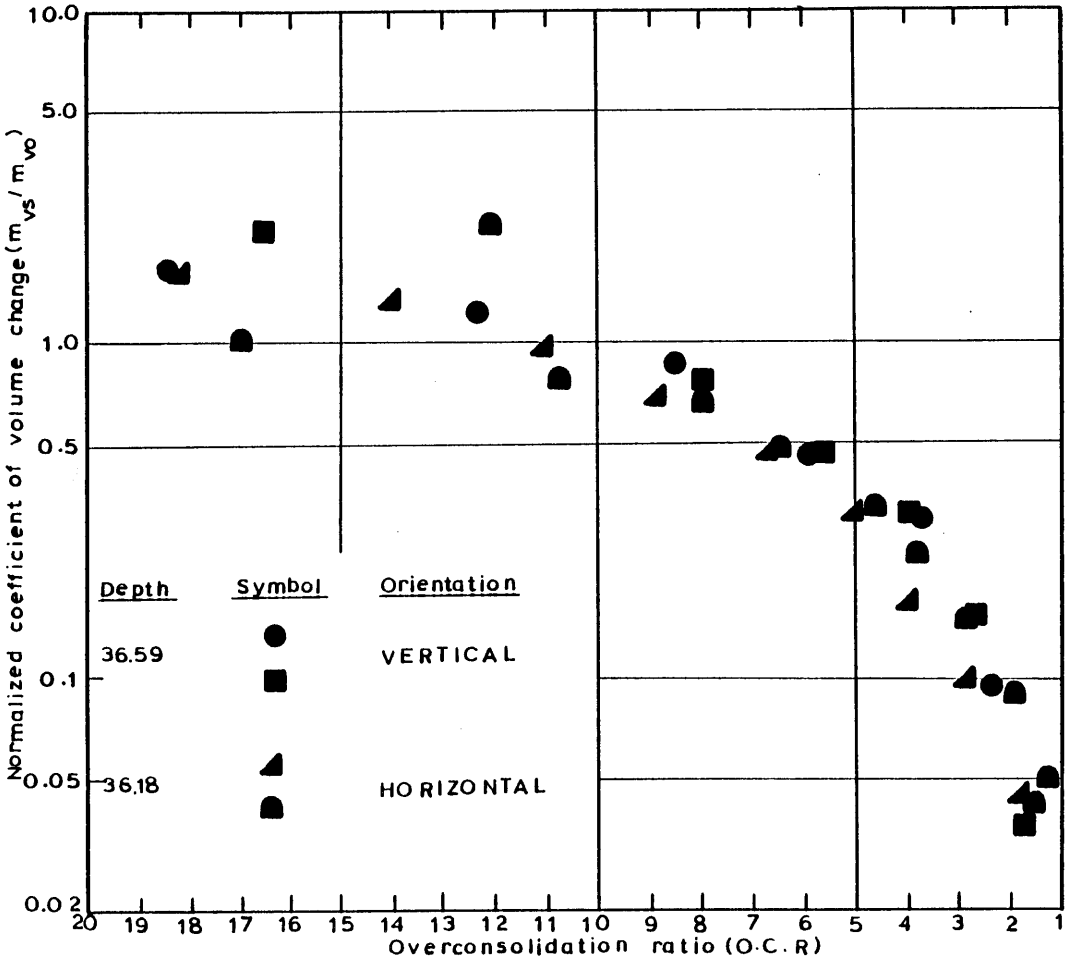

Figure F.24 Variation of the normalized coefficient of volume change with overconsolidation ratio.

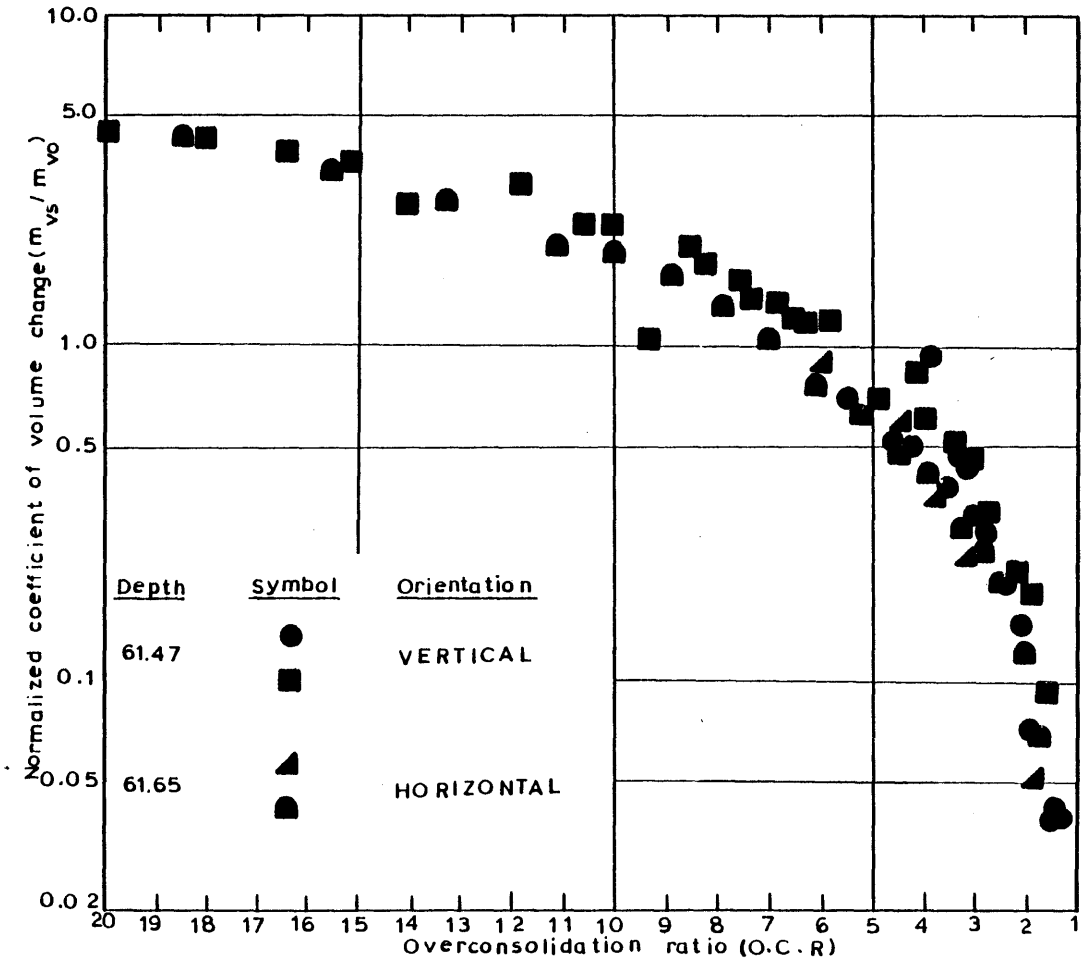

Figure F.25 Variation of the normalized coefficient of volume change with overconsolidation ratio.

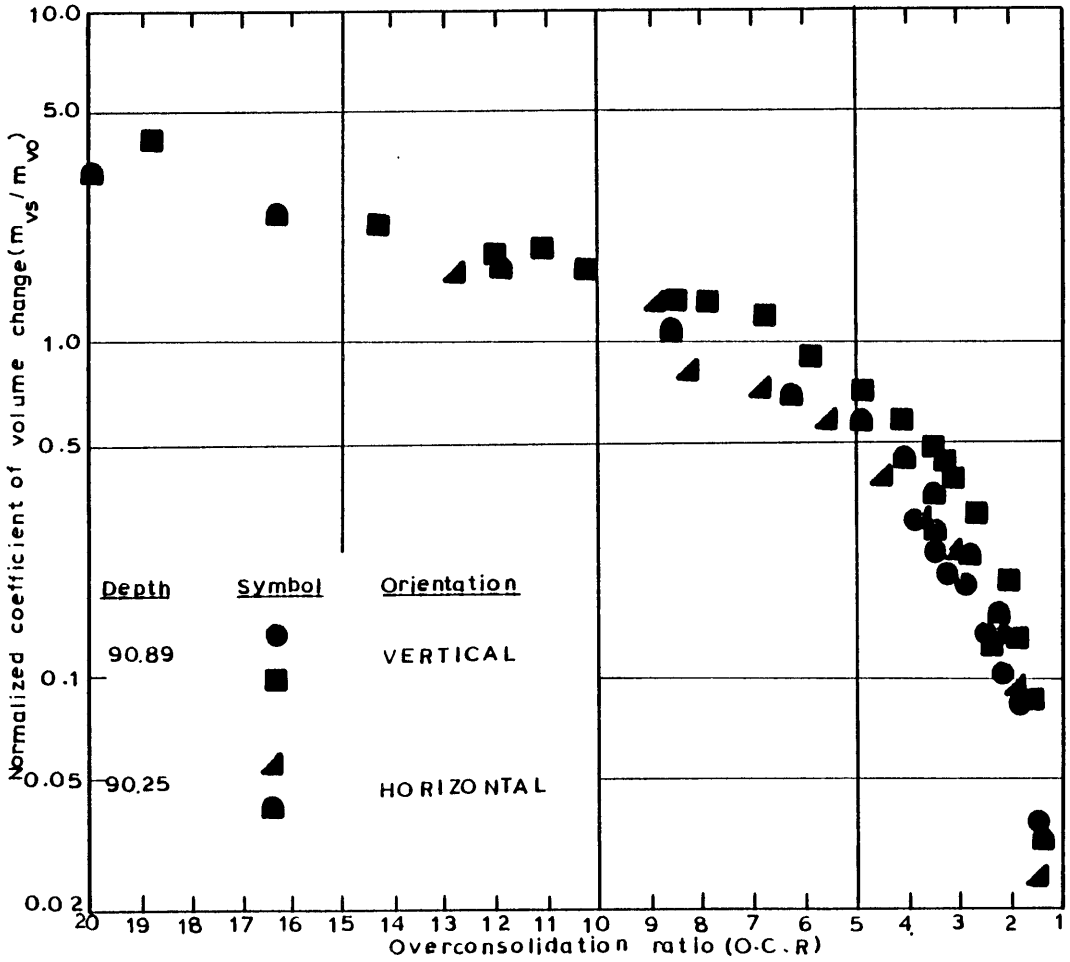

Figure F.26 Variation of the normalized coefficient of volume change with overconsolidation ratio.

APPENDIX G

Appendix G is concerned with the constant head permeability tests. Eighteen tests were performed on undisturbed samples retrieved from the I-95 test site. Description of the apparatus and the test procedure were given earlier in Chapter 10 to which the reader is referred. The results together with a summary of the soil properties are tabulated herein.

Sample No.	Sample Depth (ft.)	Effective Stress (ksc)	w_N(%)	w_L	w_p	P.I.	Gradient i	Q/At	$k_{cm/sec}$	k_{av}
21.5-23.5-P-V	22.70	0.489	29.25	31.30	18.99	12.21	10.00 65.57	2.2×10^{-6} 3.22×10^{-5}	2.2×10^{-6} 1.95×10^{-6}	2.07×10^{-6}
21.5-23.5-H	22.95	0.495	26.56	31.30	19.02	12.28	91.15 60.00	5.837×10^{-5} 3.78×10^{-4}	6.39×10^{-6} 9.3×10^{-6}	6.34×10^{-6}
26.5-28.5-P-V	27.04	0.603	25.42	31.30	19.45	11.85	10 70 50	1.6600×10^{-6} 9.527×10^{-6} 7.25×10^{-6}	1.66×10^{-7} 1.361×10^{-7} 1.45×10^{-7}	1.49×10^{-7}
26.5-28.5-P-H	27.25	0.609	25.88	31.30	19.47	11.83	12.2 50.0 72.0	2.440×10^{-6} 9.75×10^{-6} 1.354×10^{-5}	2.00×10^{-7} 1.95×10^{-7} 1.88×10^{-7}	1.94×10^{-7}
36.5-38.5P-V	37.06	0.867	35.09	31.30	20.89	10.41	17.22 34.40 51.68	9.316×10^{-7} 1.799×10^{-6} 2.909×10^{-6}	5.41×10^{-8} 5.23×10^{-8} 5.63×10^{-8}	5.4×10^{-8}
36.5-38.5-P-H	37.08	0.867	35.09	31.30	20.89	10.41	28.30 42.64	6.707×10^{-6} 1.117×10^{-5}	2.37×10^{-7} 2.56×10^{-7}	2.46×10^{-7}
41.5-43.5-P-V	42.25	1.00	34.52	45.83	23.09	22.74	21.28 30.39 39.54 50.41	1.830×10^{-6} 2.826×10^{-6} 3.87×10^{-6} 5.041×10^{-6}	8.0×10^{-8} 9.30×10^{-8} 9.80×10^{-8} 100×10^{-7}	9.42×10^{-8}
41.5-43.5-P-H	42.47	1.009	42.87	46.61	23.20	23.41	16.17 30.63 42.99	$1.164\text{-}\times10^{-6}$ 2.695×10^{-6} 4.299×10^{-6}	7.20×10^{-8} 8.80×10^{-8} 10.00×10^{-8}	

Table G.1 Summary of constant head tests performed on "undisturbed" samples of Boston Blue Clay retrieved from the I-95 test site.

Sample No.	Sample Depth (ft)	Effective Stress $\bar{\sigma}_{vo}$(ksc)	w_N(%)	w_L(%)	w_p(%)	P.I.	Gradient i	Q/At	k cm/sec	k_{av}
60-62-P-V	60.53	1.484	40.79	39.01	21.90	17.11	1.96	3.72×10^{-7}	2.90×10^{-7}	4.29×10^{-8}
							10.31	3.71×10^{-7}	3.60×10^{-8}	
							20.43	8.58×10^{-7}	4.2×10^{-8}	
							21.58	1.177×10^{-6}	5.45×10^{-8}	
							30.18	1.177×10^{-6}	3.9×10^{-8}	
60-62-P-H	60.53	1.484	40.12	39.01	21.90	17.11	10.83	6.389×10^{-7}	5.9×10^{-8}	5.95×10^{-8}
							21.83	1.22×10^{-6}	5.6×10^{-8}	
							30.40	1.82×10^{-6}	6.01×10^{-8}	
							30.13	1.89×10^{-6}	6.3×10^{-8}	
75-77-V	75.17	1.870	38.81	38.02	20.65	17.37	34.37	1.196×10^{-6}	3.48×10^{-8}	3.13×10^{-8}
							44.91	1.450×10^{-6}	3.23×10^{-8}	
							25.19	7.05×10^{-7}	2.80×10^{-8}	
75-77-P-H	75.50	1.878	36.87	38.29	20.72	17.57	39.59	1.741×10^{-6}	4.40×10^{-8}	4.00×10^{-8}
							51.69	2.067×10^{-6}	4.00×10^{-8}	
							29.02	1.044×10^{-6}	3.60×10^{-8}	
82-84-P-V	83.77	2.096	45.89	46.75	23.06	23.69	18.84	6.405×10^{-7}	3.40×10^{-8}	3.01×10^{-8}
							18.66	5.971×10^{-7}	3.20×10^{-8}	
							37.07	1.093×10^{-6}	2.95×10^{-8}	
							37.22	1.019×10^{-6}	2.74×10^{-8}	
							28.92	8.445×10^{-7}	2.92×10^{-8}	
							28.80	8.32×10^{-7}	2.89×10^{-8}	
82-84-P-V	83.77	2.096	41.12	46.75	23.06	23.69	17.28	1.062×10^{-6}	6.15×10^{-8}	6.04×10^{-8}
							34.10	2.00×10^{-6}	5.87×10^{-8}	
							31.36	1.919×10^{-6}	6.12×10^{-8}	

Table G.1 (cont.) Summary of constant head tests performed on "undisturbed" samples of Boston Blue Clay retrieved from the I-95 test site.

Sample No.	Sample Depth (ft)	Effective Stress $\bar{\sigma}_{vo}$ (ksc)	w_N(%)	w_L(%)	w_o(%)	P.I.	Gradient i	Q/At	k cm/sec	b_{av}
90-92-P-V	90.50	2.273	48.70	44.15	23.11	21.40	18.72	5.108×10^{-7}	2.70×10^{-8}	2.71×10^{-8}
							28.49	7.83×10^{-7}	2.75×10^{-8}	
							28.15	7.910×10^{-7}	2.81×10^{-8}	
							29.63	7.644×10^{-7}	2.58×10^{-8}	
90-92-P-H	90.50	2.273	48.80	44.15	23.11	21.04	15.14	7.615×10^{-7}	5.03×10^{-8}	5.04×10^{-8}
							30.28	1.480×10^{-6}	4.89×10^{-8}	
							45.60	2.389×10^{-6}	5.24×10^{-8}	
							47.42	2.371×10^{-6}	5.0×10^{-8}	
100-102-P-V	100.64	2.540	42.87	50.34	25.54	24.80	9.77	2.639×10^{-7}	2.70×10^{-8}	2.48×10^{-8}
							18.86	4.526×10^{-7}	2.40×10^{-8}	
							28.10	7.025×10^{-7}	2.50×10^{-8}	
							38.07	9.517×10^{-7}	2.50×10^{-8}	
							47.14	1.131×10^{-6}	2.40×10^{-8}	
							58.10	1.45×10^{-6}	2.50×10^{-8}	
							51.62	1.238×10^{-6}	2.40×10^{-8}	
100-102-P-H	100.72	2.542	40.42	50.36	25.59	24.77	22.68	8.164×10^{-7}	3.60×10^{-8}	3.78×10^{-8}
							35.3	1.370×10^{-6}	3.90×10^{-8}	
							47.4	1.750×10^{-6}	3.70×10^{-8}	
							57.6	2.188×10^{-6}	3.8×10^{-8}	
							66.0	2.690×10^{-6}	3.9×10^{-8}	

Table G.1 (cont.) Summary of constant head tests performed on "undisturbed" samples of Boston Blue Clay retrieved from the I-95 test site.